University of New Mexico
UNM Digital Repository

Civil Engineering ETDs | Engineering ETDs

Fall 12-15-2017

Characterization and Modeling of Asphalt Concrete for Dynamic Properties and Performances

A S M A. Rahman
University of New Mexico - Main Campus

Follow this and additional works at: https://digitalrepository.unm.edu/ce_etds

Part of the Civil Engineering Commons, Engineering Mechanics Commons, Geotechnical Engineering Commons, Mechanics of Materials Commons, Polymer and Organic Materials Commons, Structural Engineering Commons, Structural Materials Commons, and the Transportation Engineering Commons

Recommended Citation
Rahman, A S M A.. "Characterization and Modeling of Asphalt Concrete for Dynamic Properties and Performances." (2017).
https://digitalrepository.unm.edu/ce_etds/193

This Dissertation is brought to you for free and open access by the Engineering ETDs at UNM Digital Repository. It has been accepted for inclusion in Civil Engineering ETDs by an authorized administrator of UNM Digital Repository. For more information, please contact disc@unm.edu.

A. S. M. Asifur Rahman

Candidate

Civil Engineering

Department

This dissertation is approved, and it is acceptable in quality and form for publication:

Approved by the Dissertation Committee:

Dr. Rafiqul A. Tarefder, Chairperson

Dr. Arup K. Maji

Dr. Tang-Tat “Percy” Ng

Dr. Tariq Khraishi

Characterization and Modeling of Asphalt Concrete for Dynamic Properties and Performances

BY

A. S. M. ASIFUR RAHMAN

B. Sc., Civil Engineering, Bangladesh University of Engineering & Technology, 2007
M. S., Civil Engineering, University of New Mexico, 2012

DISSERTATION

Submitted in Partial Fulfillment of the
Requirements for the Degree of

Doctor of Philosophy
in
Engineering

The University of New Mexico
Albuquerque, New Mexico, USA

December 2017

DEDICATION

This dissertation is dedicated to

my mother, Tahamina Begum,

my father, A. S. M. Shamsur Rahman,

my brother, A. S. M. Arifur Rahman,

my sister, Shahanaz Rahman,

my wife, Mehnaj Tabassum Rahman,

and lastly,

to my daughter Aubani Tabassum Rahman.

ACKNOWLEDGMENTS

I would like to thank my advisor Dr. Rafiqul A. Tarefder for his continuous support throughout my pursuit of Ph.D., continuous guidance, and time. I would also like to express my sincere gratitude to my Ph.D. committee members, Drs. Arup K. Maji, Percy Ng, and Tariq Khraishi for their valuable time, suggestions and willingness to guide through my research work.

Funding for this study came from the New Mexico State Department of Transportation. My special thank goes to Jeff Mann (Head of Pavement Design, NMDOT), Virgil Valdez (Research Bureau, NMDOT), Parveez Anwar (State Asphalt Engineer, NMDOT), and James Gallegos (State Materials Manager) for their valuable suggestions and continuous support.

I would also like to thank undergraduate student, Shaikh Ahmad, for helping me in material collection and sample preparation throughout this study. Also, I would like to extend my wholehearted gratitude to my colleagues and friends at the Department of Civil Engineering, University of New Mexico.

Characterization and Modeling of Asphalt Concrete for Dynamic Properties and Performances

BY

A. S. M. ASIFUR RAHMAN

B. Sc., Civil Engineering, Bangladesh University of Engineering & Technology (BUET), Dhaka, Bangladesh, 2007

M. S., Civil Engineering (Structural Mechanics & Materials), University of New Mexico, Albuquerque, New Mexico, USA, 2012

Ph.D. in Engineering (Civil), University of New Mexico, Albuquerque, New Mexico, USA, 2017

ABSTRACT

The recently developed mechanistic-empirical pavement design guide (MEPDG, also known as Pavement M-E design method) uses the nationally calibrated, binder viscosity-based dynamic modulus predictive model for the design and analysis of asphalt pavements. In this study, this model is assessed for its appropriateness for asphalt-aggregate mixtures typically used in New Mexico. In essence, this study investigates the predictability issue of complex modulus of New Mexico mixes. A total of 54 Superpave mixes with different aggregate gradations, air voids, and binder grades were collected from the mixing plants and from the pavement construction sites. The loose asphalt mixtures were then compacted, cored, and sawed to cylindrical specimens and tested for dynamic modulus and phase angle in the laboratory. Independence assurance testing was performed to assess the precision and accuracy of the test results. The time-temperature superposition principle was applied

to develop mastercurves of complex modulus and phase angle functions of the asphalt concrete samples. The evaluated complex modulus mastercurve parameters were then used to calibrate the viscosity-based Witczak model for predicting dynamic or complex modulus of local asphalt concrete materials. The assessment of this model indicated significant underprediction and bias of the model in its current form for predicting complex modulus of the Superpave asphalt-aggregate mixes of New Mexico.

To this end, a new set of regression-based models for predicting dynamic modulus and phase angle functions of local asphalt mixtures were developed and validated in this study. Material properties such as mix volumetrics, aggregate gradations, and asphalt binder characteristics are the main factors that affect the viscoelastic material functions, such as the complex modulus of asphalt concrete. A goal is to examine the effects of these mixture variables on the complex modulus of asphalt concrete and thus modify existing predictive models or develop a new model to predict the complex modulus of asphalt concrete more accurately. With the aim at hand, the effects of aggregate gradation parameters on the complex modulus function of asphalt concrete were determined. To characterize various aggregate gradations, the two well-known gradation parameters of the aggregate blend, namely, the fineness modulus and the uniformity coefficient, were considered. Next, the effects of these two parameters on the complex modulus and phase angle functions were determined, and used in developing new predictive models. Statistical evaluation showed that fairly accurate estimations of dynamic modulus and phase angle of the local mixes can be possible by using these new predictive models.

While the above models use binder's viscosity, a new set of models were developed using binder's shear modulus. Indeed, M-E design has a binder shear modulus based

dynamic modulus model. Various researcher claimed that the binder shear modulus based model is more biased and inaccurate when compared to the tested data or the predicted data from viscosity based model. The new binder shear modulus based model also uses gradation parameters and mixture volumetrics. To develop this model, asphalt binders were tested for complex shear modulus and phase angle using dynamic shear rheometer. Dynamic shear modulus and phase angle functions were generated by applying time-temperature superposition principle. Non-linear optimization technique was used to correlate the model parameters to the material properties to develop the final form of the model. Statistical evaluation showed good accuracy of the predictions made by these models.

Apart from the regression-based modeling and to improve the accuracy of the characterization problem, an advanced dynamic modulus and phase angle predictive model is developed in this study based on the artificial neural network methodology. A database containing 1,620 dynamic moduli with phase angle were used to develop this artificial neural network. A neural architecture with two hidden layers, each with 12 nodes was found to be suitable for predicting the dynamic modulus and phase angle of asphalt concrete. Statistical evaluation showed an excellent prediction ability of this model.

It is known that viscoelastic time-domain material functions, such as, relaxation modulus and creep compliance, or frequency domain function, such as, complex modulus can be used to characterize the linear viscoelastic behavior of asphalt concrete in modeling of pavement structure. Among these, the complex modulus has been adopted in the recent pavement M-E design method. However, for advanced analysis of pavement, such as, use of finite element method requires that the complex modulus function to be converted into

relaxation modulus or creep compliance functions. There are a number of exact or approximate methods available in the literature to convert one linear viscoelastic material function to another. All these methods (i.e. exact or approximate methods) are applicable for any linear viscoelastic material up to a certain level of accuracy. However, the applicability and accuracy of these interconversion methods for asphalt concrete material were not studied very much in the past. Thus, a question arises if these methods are even applicable in case of asphalt concrete, and if so, what is the precision level of the interconversion method being used. To investigate these facts, this study has undertaken an effort to validate a numerical interconversion technique by conducting representative laboratory tests. The method was previously used in asphalt industry with adopting a simplification of considering time constants to be identical in generalized Maxwell and generalized Voigt model. However, in the present context, the assumption is regarded as over-simplification and therefore, an exact approach to estimate the time constants in these two mechanical models is developed. For validation, cylindrical asphalt concrete specimens were tested for complex modulus, relaxation modulus, and creep compliance at different test temperatures and loading rates. The time-temperature superposition principle was applied to develop linear viscoelastic material functions. The numerical interconversion technique was used to convert one material function to another, and hence, were compared to the laboratory tested material functions. The conversion showed good agreement with the laboratory test data. A statistical evaluation was conducted to determine if the interconverted material functions are similar to the laboratory tested material functions. Besides finite element modeling technique was also used to validate the interconversion method.

TABLE OF CONTENTS

CONTENTS

LIST OF FIGURES

LIST OF TABLES

Chapter 1

Introduction

1.1 Introduction

Asphalt's complex modulus (E^*) is a complex number that relates applied stress to the strain subjected to sinusoidal loading. The two viscoelastic material properties that can be determined from a E^*-test are the dynamic modulus ($|E^*|$), and the phase angle (ϕ). The norm of the complex modulus is referred to as dynamic modulus ($|E^*|$), and calculated by dividing the stress amplitude by the recoverable strain under cyclic loading. The phase angle, ϕ is the phase difference between the applied stress and the strain response, determined from the time lag between the applied stress and corresponding strain response (Meyers and Chawla 1999). In the case of asphalt concrete (AC), laboratory determination of $|E^*|$ involves application of sinusoidal loading at different frequencies and temperatures, and monitoring resulting strain history.

To improve the current practice of designing asphalt mix as well as design and analysis of pavement structure, or simply to implement mechanistic-empirical (M-E) design of pavements, determination of $|E^*|$ of the AC mixture is crucial (ARA Inc. 2004). The $|E^*|$ is used in M-E design method to determine the stress state of AC and the empirical relationships for predicting pavement distresses such as, rutting and cracking. In the past only three of New Mexico AC mixes were tested for $|E^*|$. Therefore, a wide-spread evaluation of $|E^*|$ from all over the regions in the state of New Mexico was not possible.

Determination of the |E^*| of locally produced AC by laboratory test enables the state engineers to implement the recently developed M-E design method on a site-specific level. This also improves the capability of material engineer to assess local mix design mechanistically. However, a wide-spread evaluation of dynamic modulus representing all over the state requires extensive laboratory testing program and enormous amount of time. In these circumstances, a relatively accurate prediction model for |E^*| estimation is appreciated for cost savings and timeliness. There are some empirical and semi-empirical models available in literature for predicting |E^*| of AC mixtures. Each of these predictive models has certain level of accuracy for New Mexico's regional use. One way to increase the level of accuracy is to calibrate these predictive models for local or regional application. The other way is to develop alternative models based on comprehensive laboratory testing program. Currently, a |E^*| predictive model specific to New Mexico AC mixtures is not available. Thus, predictive models for estimating |E^*|, specific to New Mexico AC mixes are needed to be developed for the implementation of M-E design method.

1.1.1 Problem Statement Related to Hypothesis 1

Several empirical and semi-empirical predictive models are available to estimate |E^*| of AC. Of all these models, the most commonly used are the viscosity (η) based Witczak model, the binder shear modulus (|G_b^*|) based Witczak model, and the Hirsch model (Weldegiorgis 2014). The η-based Witczak model is the primary |E^*| predictive model used in the recently developed mechanistic-empirical (M-E) pavement design software (Rahman and Tarefder 2016). This model uses the viscosity (η) of the asphalt binder to capture binder effects on |E^*| of the AC mixture. The other parameters included in this

model are the aggregate gradation parameters, the air void content, and the effective asphalt content.

The accuracy as well as the performance of the η-based Witczak model for predicting $|E^*|$ of AC are evaluated by several researchers. Clyne et al., Christensen et al., Tran and Hall, Mohammad et al., Schwartz, and Rahman et al. reported that the η-based Witczak model produces significantly less value of $|E^*|$ compared to the measured value (Clyne et al. 2003, Christensen et al. 2003, Tran and Hall 2005, Mohammad et al. 2005, Schwartz 2005, and Rahman et al. 2016). Lee et al. (2007) found that the $|E^*|$ predicted by the η-based Witczak model estimates lower $|E^*|$ values at higher temperatures and higher $|E^*|$ values at lower temperatures. Hossain and Zaman (2013) studied the η-based Witczak model and reported that the η-based Witczak model significantly underestimates $|E^*|$ values when the Dynamic Shear Rheometer (DSR) test data is used. In addition, they also found that the η-based Witczak model overestimates $|E^*|$ values when rotational viscosity (RV) test data is used. Birgisson et al. (2005) showed an over-prediction of $|E^*|$ value by the η-based Witczak model. Kim et al. (2005) reported that the η-based Witczak equation predicts better at low temperature. Dongré et al. (2005) implemented the η-based Witczak model for unaged, Rolling Thin Film Oven (RTFO) and Pressure Aging Vessel (PAV) aged binders. They reported that the η-based Witczak model produces unreasonable estimates of modulus below 700 MPa (100,000 psi) and underpredicts measured $|E^*|$ for air void and binder content higher than those of the mix design. They recommended to improve the η-based Witczak model by revising the coefficients of volumetric variables, such as the percentage of voids in mineral aggregate (VMA), the percentage of voids filled

with asphalt (VFA), AC percentage, and V_a. Rahman et al. (2016) evaluated η-based Witczak model for 21 AC mixtures typically produced in New Mexico and reported that the model produces significantly lower $|E^*|$ values when compared to the tested data. They suggested a calibrated version of η-based Witczak model for predicting $|E^*|$ values of local AC mixtures with a higher prediction accuracy.

The $|G_b^*|$-based Witczak model was developed using the Bari (2005) database of 7400 measured $|E^*|$ values obtained from 346 different AC mixtures (Bari and Witczak 2006). The η of the asphalt binder was determined from the viscosity-temperature relationship suggested by American Society for Testing and Materials (ASTM) (ASTM 1998). However, to convert conventional viscosity-temperature susceptibility parameters, identified as, *A* and *VTS* to $|G_b^*|$ and binder phase angle (δ_b), empirical relationships were used due to unavailability of test data (Ceylan et al. 2009). Some issues have been raised by Christiansen (2006) regarding the use of inconsistent treatment of loading frequency in case of AC mixture and asphalt binder. Singh et al. (2011) reported that the accuracy of the $|G_b^*|$-based Witczak model is poor when compared to the other available $|E^*|$ models. El-Badawy et al. (2012) concluded that the $|G_b^*|$-based $|E^*|$ model produces less accurate and relatively higher biased estimates of $|E^*|$ than the η-based Witczak model. Therefore, it is clear that the model possesses significant error.

Christensen et al. (2003) found the simplest and most effective version of Hirsch model in which $|E^*|$ is directly estimated from binder $|G_b^*|$, voids in mineral aggregate (VMA), and voids filled with asphalt binder (VFA). Singh et al. (2011) investigated that Hirsch model predicted $|E^*|$ values are dispersed around the line of equality (LOE) while

compared to the observed |E^*| data, indicating that the model exhibits significant error. Bari and Witczak (2006), Obulareddy (2006), King et al. (2005), and Ceylan et al. (2009) concluded that the Hirsch model underpredicts |E^*|. However, the fundamental weakness of this model includes strong dependence on volumetric parameters, particularly under low air void and volume-filled-with-asphalt (VFA) conditions (Al-Khateeb et al. 2006, Soleymani et al. 2004).

Zeng and Huang (2006) established a relationship between the complex shear modulus and phase angle of asphalt binder and AC mixture. In their study, DSR testing was used for characterizing the asphalt binders and Simple Shear Testing (SST) was used for characterizing the AC mixtures. Their results indicated that the complex shear modulus and phase angle (in shear) of the AC mixture can be represented by the same parameters obtained from the asphalt binder under the condition of material linearity. However, their study had not indicated how the |E^*| of the AC mixture can be evaluated from |G_b^*|, and δ_b of the asphalt binder.

Ceylan et al. (2008) developed a simplified |E^*| predictive model employing artificial neural network (ANN) methodology. The |E^*| databased that was used is available to the researchers form National Cooperative Highway Research Program (NCHRP) Report 547, which contains 7400 data points from 346 hot-mix asphalt (HMA) mixtures (Bari and Witczak 2006, Bari 2005). The ANN-based |E^*| predictions showed significantly higher accuracy when compared to the simplified Hirsch model proposed by Christensen et al. (2003). In their other studies, Ceylan et al. (2007, 2009a, 2009b) developed another ANN-based |E^*| predictive model which uses the same input parameters as in η and

dynamic shear modulus ($|G_b^*|$) based Witczak model. This time also the ANN-based $|E^*|$ model showed higher prediction accuracy when compared to the $|E^*|$-values predicted from η or $|G_b^*|$-based Witczak model. Similar type of ANN-based $|E^*|$ predictive model was also developed by Far et al. (2009), in which, ANN methodology showed better accuracy over the other available $|E^*|$-predictive models. However, all these studies used the same $|E^*|$ databased which is available to the researchers from NCHRP Report 547, fully or partially. This database contains $|E^*|$ data of the AC mixtures designed based on previous mix-design scheme, other than the recent Superpave mix-design approach. Therefore, it is logical to assume that the NCHRPT Report 547 database may be obsolete considering the recent advancement in asphalt mix-design method.

On the other hand, phase angle, ϕ is an important parameter needed to separate the complex modulus (E^*) in its two inherent parts: storage and loss modulus. Storage modulus is required to determine the relaxation modulus or creep compliance which are needed for viscoelastic analysis of AC using finite element method (FEM) (Ahmed et al. 2015). Therefore, determination of ϕ-value is important for advanced analysis of pavements. Unfortunately, there are very few models available in the literature to determine the ϕ-function of AC. Therefore, this study also attempted to develop a regression-based ϕ-model to determine the ϕ-value of AC mixtures in New Mexico.

1.1.2 Problem Statement Related to Hypothesis 2

The linear viscoelastic (LVE) material functions commonly used in characterizing materials are creep compliance $D(t)$, dynamic modulus $|E^*|$ and relaxation modulus $E(t)$. Once the $|E^*|$ function of an asphalt-aggregate mixture is known, the $D(t)$ or $E(t)$ function

can be obtained by applying an appropriate interconversion technique. This is because these functions are mathematically equivalent and inter-convertible from any function as a source to a target function. The |*E**|-function can be directly used in modern M-E design and analysis technique. However, for advanced level analysis, such as constitutive modeling or Finite Element Method (FEM) application as in Ahmed et al. (2015), *D*(*t*) or *E*(*t*) functions are the most usable data-formats for any material showing LVE behavior. There are a number of interconversion methods available to convert one LVE material function to another, of which, most of these methods have various levels of approximation. The most recent interconversion method in asphalt area is given by Kim (2009). However, this method still has some approximations regarding the issue of time constants in relaxation modulus and creep compliance functions. According to his method, the time constants for *D*(*t*) (called retardation times) and for *E*(*t*) (called relaxation times) are assumed to be the same. This assumption therefore makes his method of interconversion to be highly approximate. To generate reliable data by interconversion, the drawback of assuming the time constants to be the same needs to be eliminated.

1.2 Hypotheses

1.2.1 Hypothesis One

Previous studies showed that the predicted |*E**| from viscosity based Witczak model is not good enough to claim its validity. The inherent cause of the substandard performance of the viscosity based Witczak model is not known for New Mexico AC mixtures. Therefore, it is hypothesized that a recalibration of the viscosity based Witczak model is possible by optimizing the mixture and binder variables using New Mexico Superpave AC mixes. The

recalibration will require a comprehensive dynamic modulus testing program incorporating asphalt concrete mixtures from all over the state.

It is also hypothesized that a completely new and regression based accurate predictive models of $|E^*|$ and ϕ can be developed based on the mixture properties of AC. These models will incorporate all the contributing parameters: such as aggregate gradation, mixture volumetric, and binder property used in the AC mix.

Simultaneously, it is hypothesized that an Artificial Neural Network (ANN) model of $|E^*|$ and ϕ can be developed. It is expected that ANN model will have better predictability than regression models. Previous studies have not predicted phase angle using ANN, nor they have predicted $|E^*|$ for Superpave mixes. Prediction of phase angle is important for estimating the two parts, storage and loss modulus of the material. It is also important to know how ANN performs in predicting $|E^*|$ of Superpave mixes, which is the current trend.

1.2.2 Hypothesis Two

Previous studies have shown that dynamic modulus and creep compliance obtained from uniaxial loading mode are related and available mathematical interconversion procedures are applicable. However, the applicability of these interconversion procedures is not experimentally verified for dynamic modulus, creep compliance or relaxation modulus in uniaxial compression-only mode. Also, previous studies in asphalt concrete industry develop interconversion techniques which can fairly interconvert one material function to other. Most of these methods have a certain level of approximation. A fully exact method

is not yet developed for the AC material for interconversion of asphalt concrete material properties. Therefore, it is hypothesized that a numerical exact interconversion technique can be developed to convert one material function to another in case of asphalt concrete material in compression.

1.3 Dissertation Organization

Chapter 1 discusses a brief introduction of the current state of the art and practice of asphalt concrete mix design and pavement design. In addition, fundamental problems associated with asphalt concrete industry are identified. Besides, current research hypotheses and objectives are documented. A brief review of relevant definitions, terms and literature are documented in Chapter 2. Chapter 3 is dedicated to present detailed description of the dynamic modulus testing conducted in this study and presented the test results. Chapter 4 presents the analyses of dynamic modulus and phase angle test data and the method of development of dynamic modulus mastercurves. Chapter 5 presents analyses on dynamic modulus test results from two independent sources to determine accuracy and bias of the test results. Chapter 6 presents a study on the effect of different aggregate parameters on the dynamic modulus of asphalt concrete. Chapters 7 and 9 are related to hypothesis one. Chapter 7 presents the development and assessment of viscosity-based dynamic modulus predictive model. Chapter 8 presents the development and assessment of binder dynamic shear modulus based dynamic modulus predictive model. Chapter 9 presents the development and assessment of artificial neural network based dynamic modulus predictive model. Chapter 10 documents the method of interconversion of different LVE material functions developed in this study and discussion on their accuracy with respected

to laboratory tested data. Finally, Chapter 11 presents conclusions of this study and the recommendations for future research.

Chapter 2

Literature Review

2.1 General

Dynamic modulus (|*E**|) is an important viscoelastic property. While AC exhibits viscoelasticity under cyclic loading, the dynamic modulus can be defined as the ratio of applied stress amplitude to the recoverable strain amplitude.

2.2 Viscoelasticity

Viscoelasticity of a material is the property that exhibit both viscous and elastic characteristics when subjected to deformation. Viscous materials resist shear flow and strain with time when a stress is applied. On the other hand, when an elastic material is stretched, it strains instantaneously, and returns to their original state once the stress is removed. Both of these properties exhibit in a viscoelastic material. Due to the viscous part, these materials show time dependent deformation. Some common characteristics of viscoelastic materials can be: (i) if the stress is held constant, the strain increases with time (creep); (ii) if the strain is held constant, the stress decreases with time (relaxation); (iii) the effective stiffness depends on the rate of application of the load; (iv) if cyclic loading is applied, hysteresis occurs, leading to a dissipation of mechanical energy. Synthetic polymer, asphalt concrete, and human tissue at high temperature show significant viscoelasticity.

Strain due to loading of a viscoelastic material has an elastic component and a viscous component. Purely elastic materials do not dissipate energy (heat) when a load is applied and removed. A viscoelastic substance loses energy when a load is applied and then removed. Hysteresis is observed in the stress-strain curve, with the area of the loop being equal to the energy lost during the loading cycle. There are three types of viscoelasticity: linear, non-linear and anelastic. Linear viscoelasticity is when the function is separable in both creep response and load, and applicable only for small deformations. All linear viscoelastic models can be represented by a Volterra equation relating stress and strain -

$$\varepsilon(t) = \frac{\sigma(t)}{E_{inst,\,creep}} + \int_0^t K(t-t')\,\dot{\sigma}(t')\,dt', \tag{2.1}$$

and,

$$\sigma(t) = E_{inst,\,relax}\;\varepsilon(t) + \int_0^t F(t-t')\,\dot{\varepsilon}(t')\,dt' \tag{2.2}$$

where, t is the time, $\sigma(t)$ is the applied stress, $E_{inst,\,creep}$ and $E_{inst,\,relax}$ are instantaneous elastic moduli for creep and relaxation, $K(t)$ is the creep function, and $F(t)$ is the relaxation function. Linear viscoelasticity is usually applicable only for small deformations.

Nonlinear viscoelasticity is when the function is not separable. It usually occurs when the deformations are large or if the material changes its properties under deformation. An anelastic material is a special case of viscoelastic material. This type of material is fully recovered to its original state with time on the removal of load. Viscoelastic materials can be modeled in order to determine their stress or strain interaction as well as time dependencies. Three of the most popular viscoelastic models are: Maxwell model, Kelvin-

Voigt model and the standard linear solid model. The elastic and viscous components of viscoelastic behavior can be modeled as linear combinations of springs and dashpots, respectively. Each model differs in the arrangement of these elements.

2.3 Asphalt Concrete

Asphalt concrete (AC) is a composite material with two main components. These are asphalt binder and aggregates. Asphalt binder is a dark brown-to-black, highly viscous hydrocarbon produced from petroleum distillation residue, whereas, aggregate is a collective term for the mineral materials such as sand, gravel and crushed stone (Brown et al. 2009). Currently, the Superpave® mix design procedure, a product of Strategic Highway Research Program (SHRP) is used to produce AC. This mix design procedure involves volumetric calculations to assess the performance of the asphalt-aggregate mixture which are highly dependent on experience and subjective to local environmental conditions. Recently, researchers have found that the $|E^*|$ of asphalt concrete to be useful for determining the performance of the mixture. Furthermore, the mechanistic-empirical design and analysis of pavement (MEPDG 2008) uses $|E^*|$ for analyzing and designing new pavement structures. In essence, MEPDG (2008) uses mechanistic methods to determine the stress and strains in pavement structures, and empirical models to predict pavement distresses. This is obviously an improvement over traditional practice which is purely empirical. Therefore, either analyzing asphalt concrete with a constitutive relation, or using MEPDG for design and analysis of pavement structures, determination of dynamic modulus ($|E^*|$) as well as the phase angle (ϕ) properties of the material is an important issue. The most direct way to determine the $|E^*|$ of asphalt concrete is laboratory testing,

which requires expensive laboratory equipment, may or may not be always accessible. The only other way is to use predictive models, which can significantly reduce the cost and time of investigation.

Because of a number of variability associated with asphalt-aggregate mixtures, mechanical characterization of AC is quite a bit challenging. The selection of binder for a certain AC mix depends greatly on the climatic condition of the region. Moreover, the distribution of air voids, aggregate packing, and binder coating always varies even for mixtures that are produced in laboratory under controlled conditions. On the other hand, asphalt ages over time as it is exposed to high temperature and pressure. Aging causes stiffer binder which in turn contributes to less resistance to fatigue distress of asphalt pavement. In recent years, the dynamic modulus ($|E^*|$) or complex modulus (E^*) has got a wide range of acceptance for mechanistic characterization of AC in small strain range. Also, there is numerous research going on to assess the capability of the use of $|E^*|$ in predicting the performance of AC.

Like any other material property of a viscoelastic solid, $|E^*|$ depends on temperature and loading-frequency or loading-time. For AC, the effect of loading-time or loading-frequency and temperature can be combined by applying time-temperature superposition principle (TTSP). On the other hand, a material can be referred as thermo-rheologically simple if it obeys the time-temperature superposition principle. The TTSP is used to determine temperature-dependent mechanical properties of linear viscoelastic (LVE) materials from known properties at a reference temperature. Application of TTSP allows the test data collected from laboratory tests conducted at different loading frequencies and

temperatures to be shifted horizontally toward reference temperature to form a single curve on a $|E^*|$ versus loading-frequency plot. The TTSP is a very powerful concept in reducing the required number of tests and time. When TTSP is applied, the material property can be thought to be as simplified from being dependent on both the temperature and loading frequency to the loading frequency only. In essence, TTSP allows expressing the material property at hand in terms of loading frequency only and allows for predicting the material properties over a wide frequency range often impossible to test (Gibson 2002).

Similar to $|E^*|$, creep compliance ($D(t)$) can be also used to characterize asphalt concrete. In a creep test, the specimen is held under constant stress, and the resulting strain is monitored. The $|E^*|$ and $D(t)$ functions are mathematically equivalent and one can be derived from other with numerical or analytical methods. One advantage of $|E^*|$ testing over $D(t)$ is its ability to capture material characteristics at a very short loading time which in turn eliminates the ramp effect of loading as in the creep test. This made this $|E^*|$ test more involved than creep test. However, once the $|E^*|$ function of the AC material is known, one can easily convert the $|E^*|$-function to $D(t)$-function by adopting an appropriate interconversion technique.

Relaxation modulus ($E(t)$) test is another way to characterize any viscoelastic material. In a relaxation test, the specimen is held under constant applied strain and the resulting stress history is monitored. The $E(t)$ function is also mathematically equivalent to the $|E^*|$-function. However, conducting $E(t)$ test is extremely difficult as because of the requirement of test equipment of more robust nature. Therefore, $E(t)$ function is often derived from the interconversion of $|E^*|$ or $D(t)$-function. Therefore, selecting an

appropriate interconversion technique is very important in both complimenting the test results and elimination of the need of very difficult tests.

2.4 Dynamic Modulus

The dynamic modulus ($|E^*|$) is one of the two material properties that can be determined from complex modulus (E^*) testing. The other property is the phase angle (ϕ). The complex modulus (E^*) is a complex number that relates stress to strain for a linear viscoelastic material subjected to sinusoidal or cyclic loading. The absolute value of E^* is commonly referred to as the dynamic modulus ($|E^*|$). Studying viscoelasticity by conducting the dynamic modulus analysis involves application of an oscillatory load to a material. The resulting strain is then measured. In purely elastic materials the stress and strain are in phase. In purely viscous materials, there is a phase difference between stress and strain. A 90-degree phase lag is observed for the strain in purely viscous material (Figure 2.1). In viscoelastic materials, the behavior is somewhere in between that of purely elastic and purely viscous materials, exhibiting some phase lag less than that for purely viscous materials. For example, asphalt typically shows 10 to 60° phase lag.

Stress and strain in a viscoelastic material under sinusoidal loading condition can be expressed using the following expressions:

$$\varepsilon = \varepsilon_0 \sin(\omega t) \tag{2.3}$$

$$\sigma = \sigma_0 \sin(\omega t + \phi) \tag{2.4}$$

where σ is the stress, ε is the strain, ω is the frequency of strain oscillation, t is the time of loading, and ϕ is the phase lag between stress and strain. Equations 2.3 and 2.4 are parametric equations for an elliptic Lissajous curve (Figure 2.2). In the elliptic Lissajous curve the stress and strains are related to the components of dynamic modulus. The width of the ellipse is directly proportional to the phase angle. As the material gets more viscous the phase angle increases. When the material is purely elastic the phase angle is zero (Lakes 2009).

For any viscoelastic material, complex modulus (E^*) or dynamic modulus ($|E^*|$) is an important parameter. Because, this property represents the frequency, and therefore time-dependent stiffness characteristic of the material. This parameter is the main input property of AC in the M-E design and analysis of pavements. The M-E design method uses the $|E^*|$ to determine the temperature- and rate-dependent behavior of an AC layer.

In mathematical context, $|E^*|$ is the ratio of stress to strain under oscillatory loading in shear, compression, or elongation. This parameter can be decomposed in to storage (E') and loss moduli (E''). The storage modulus (E') measures the stored energy representing the elastic portion of the response. On the other hand, the loss modulus (E'') represents the viscous response measuring the energy dissipated as heat (Figure 2.3). The storage modulus, loss modulus, and the phase angle can be mathematically expressed as:

Storage Modulus: $$E' = \frac{\sigma_0}{\varepsilon_0} \cos \phi \qquad (2.5)$$

Loss Modulus: $$E'' = \frac{\sigma_0}{\varepsilon_0} \sin \phi \quad (2.6)$$

Phase angle (tangent): $$\tan \phi = \frac{E''}{E'} \quad (2.7)$$

The complex modulus is then expressed as:

$$E^* = E' + i\, E'' \quad (2.8)$$

The absolute value of this complex modulus (E^*), called the dynamic modulus ($|E^*|$) is thus:

$$|E^*| = \sqrt{(E')^2 + (E'')^2} = \left[\left(\frac{\sigma_0}{\varepsilon_0}\right)^2 \left(\sin^2 \phi + \cos^2 \phi\right)\right]^{\frac{1}{2}} = \frac{\sigma_0}{\varepsilon_0} \quad (2.9)$$

where $|E^*|$ is the dynamic modulus, σ_0 is the peak dynamic stress and ε_0 is the peak recoverable strain.

Equation 2.9 represents the definition of dynamic modulus. For instance, the dynamic modulus is defined mathematically as the ratio of peak dynamic stress (σ_0) and the peak recoverable axial strain (ε_0) (Tashman and Elangovan 2004). The phase angle (ϕ) is the phase lag between a sinusoidal applied peak stress and the resulting peak strain in a controlled stress test. The phase angle can also be determined as (Brown et al. 2009):

$$\phi = 2\pi\ f\ \Delta t \quad (2.10)$$

where, ϕ is the phase angle in radians, f is the frequency in Hz, and Δt is the time lag between stress and strain in seconds. The storage modulus is related to the applied maximum strain. This portion of the stiffness modulus is in phase with the applied strain. However, the loss modulus is out of phase by 90 degrees.

2.5 Factors Affecting Dynamic Modulus

This section represents a brief description of the factors that affect dynamic modulus as well as the performance of asphalt concrete.

2.5.1 Rate of Loading

The $|E^*|$ of asphalt concrete gets higher as the rate of loading increases and it decreases as the rate of loading decreases (Kim 2009). At any given temperature, asphalt concrete will deform slowly and permanently if it is loaded slowly, while if it is loading at a higher rate, it will be much stiffer and will be subject to fracture.

2.5.2 Temperature

The $|E^*|$ of asphalt concrete decreases as the temperature increases (Kim 2009). At any given strain rate of loading, there is a temperature above which the material will relax quickly enough that no stress will accumulate in the test sample.

2.5.3 Age

Aging results in an increase in |*E**| of asphalt concrete. The brittle fracture susceptibility increases with aging (Kim 2009). Aging results in stiffer binder which ultimately increases the stiffness of the AC mixture.

2.5.4 Moisture

High moisture results in plastic flow of asphalt concrete which is accompanied with decrease in |*E**| of the mix (Kim 2009).

2.5.5 Binder Stiffness

Dynamic or complex shear modulus (|*G**|) of the binder has a direct impact on the dynamic modulus of asphalt mix. The dynamic modulus increases with increasing binder stiffness (Kim 2009).

2.5.6 Aggregate Stiffness

Shu and Huang (2008) showed that the value of |*E**| continually increases with increasing binder stiffness. However, the increase in the |*E**| is limited for increase in aggregate stiffness. Even if the aggregate modulus is increased, the |*E**| of the AC is found to be reduced beyond a threshold aggregate modulus of 5000 MPa.

2.5.7 Asphalt Content

The |*E**| of AC found to be decreasing with increasing binder content. The cause of this phenomenon is seen as an increasing lubrication effect of higher binder content. This

phenomenon indicates that lowering asphalt content is an effective way of increasing the |*E**| (Shu and Huang 2008).

2.5.8 Air Voids

Kim (2009) observed that higher air void results in lower value of |*E**|. It was also observed that not only the amount of air voids but also their size and distribution have significant effect on the |*E**|. Kim (2009) described the effect of small well-dispersed air voids in the mix as "micro crack arresters". Well-dispersed air voids provide enough volume for the asphalt to expand into at high temperatures and too much air will accelerate the growth of micro cracks. On the other hand, too little air will cause bleeding and promote large plastic deformations. Again, too much air provides suitable access for both air and water into the interior of an asphalt concrete layer, and thus can cause aging and moisture damage. The author recommended for thoroughly distributed air voids to enhance the stiffness of asphalt concrete mix.

2.6 Laboratory Dynamic Modulus Test Methods

Dynamic modulus tests are conducted by applying sinusoidal load on an asphalt concrete mix specimen. These tests methods can vary based on the application of resonances, control methods, and type of load application. Forced and free resonances are the two types of resonances. In the free resonance type, the sample is suspended and oscillation of the free end is measured. In forced resonance type, the material is forced to oscillate at a specified frequency. There are two types of test control types: stress-controlled and strain-controlled. In the stress-controlled test, a specified load is applied and the resulting displacement is

measured. In the strain controlled test a specified strain is applied and resulting stress is measured. Types of load application can be axial force, torsion or shear (Menard 1999).

Based on the changing of test variables, such as, temperature, load frequency etc., testing procedure can be classified as: temperature sweep, frequency sweep and stress amplitude sweep procedures. In the temperature sweep test procedure, the $|E^*|$ is measured by changing the sample temperature and keeping the loading-frequency constant. For frequency sweep test, the temperature is kept constant and the loading-frequency is varied. Stress sweep testing procedure is performed by gradually increasing the load amplitude. Some of the universally used test methods are described in the following sections.

2.6.1 AASHTO TP-62 / AASHTO T 342 – Standard Method of Test for Determining Dynamic Modulus of Hot-Mix Asphalt (HMA) Concrete Mixtures

The AASHTO TP 62 (2010)/T 342 (2011) test protocol is a stress controlled $|E^*|$ test method. The test series consists of testing at five different temperatures and six frequency sweeps. The five test temperatures are: -10, 4.4, 21.1, 37.8, and 54.4 °C (14, 40, 70, 100, and 130 °F) and the six loading-frequencies are 0.1, 0.5, 1, 5, 10, and 25 Hz at each test-temperature. The AASHTO TP-62 / T 342 can be used to determine both the dynamic modulus and phase angle of the AC material.

2.6.2 ASTM D 3497-79 – Standard Test Method for Dynamic Modulus of Asphalt Mixtures

This test method was adopted as a standard by American Society of Testing and Materials (ASTM) in 1979 (ASTM 2003). This is a stress controlled testing. The load is kept constant

throughout the frequency sweep. The procedure is performed over a range of test temperature and loading frequencies. The test procedure includes a temperature sweep of 41, 77, and 104 °F (5, 25, and 40 °C) and loading frequencies of 1, 4, and 16 Hz for each temperature. Uniaxial compressive haversine load between 0 to 241 kPa is applied. As the temperature is increased, the load level is decreased to avoid damage of the specimen. The specimen prepared should have a height to diameter ratio greater than two.

2.6.3 Confined Dynamic Modulus Testing Protocol

Confined dynamic modulus test follows the same test procedure as that of AASHTO T 342, except a confinement pressure is applied to the specimen. The confining pressure applied on the order of 138 kPa and 206 kPa. Confined dynamic modulus testing is more complex than unconfined dynamic modulus test. Nevertheless, confined dynamic modulus test is found to be better to categorize and contrast the field performance of the different mixtures of dense-graded, gap-graded, and open-graded mixtures (Sotil et al. 2004, Sotil 2003, and Pellinen 2001). Sotil et al. (2004) found that the unconfined and confined $|E^*|$ test results shows a linear relationship with the applied bulk stress.

2.6.4 Simplified Dynamic Modulus Testing Protocol

The AASHTO T 342 test requires that at least two replicate specimens should be tested at five temperatures and six loading frequencies to develop a mastercurve at a reference temperature. Bonaquist and Christensen (2005) observed that there is a large amount of overlap in the measured data that is not needed for the development of the $|E^*|$ mastercurve. They came up with an alternative testing protocol which requires testing at only three

temperatures 40, 70, and 115˚F (4.4, 21.1, and 46.1˚C), and four rates of loading 10, 1, 0.1, and 0.01 Hz. The |*E**| mastercurve obtained from this procedure was shown to be similar to that of the AASHTO T 342 standard test.

2.6.5 Dynamic Shear Modulus Test / Simple Shear Test

The Strategic Highway Research Program (SHRP) developed shear frequency sweep test. Simple Shear Tester (SST) is used to perform this test. This test protocol was first introduced as SHRP designation M-003: "Standard Method of Test for Determining the Shear Stiffness Behavior of Modified and Unmodified Hot Mix Asphalt (HMA) with Superpave Shear Test Device" (SHRP 1994). The test protocol was later adopted by American Association of State Highway Transportation Officials (AASHTO) as a provisional standard as AASHTO TP7-94 test protocol (AASHTO 1994, Kim 2009). In a simple shear test, a shear load is applied to an asphalt concrete specimen with a diameter of 150 mm and a height of 50 mm glued at the top and bottom platens. The test is a strain-controlled test with the maximum applied strain of 100 microstrains. This test is conducted at temperatures of 4, 20 and 40˚C. At each temperature, a sinusoidal shear strain is applied with maximum and minimum loading frequencies of 10 Hz and 0.1 Hz (Kim 2009).

2.6.6 Resilient Modulus Test in Indirect Tensile Test Mode

Kim (2009) proposed a relationship to evaluate uniaxial |*E**| from repeated resilient modulus test in an indirect tensile test mode. The AASHTO T 342 test requires a sample height to be 150 mm. This height of specimen is often impossible to get as most pavements are constructed as layers and each layer thickness is less than 150 mm. This greatly reduces

the use of |*E**| testing for investigating pavement condition, which ultimately is eliminated with this proposed relationship by Kim (2009).

2.6.7 Hollow Cylinder Tensile Test (HCT)

Buttlar et al. (2002) explored the adoptability of using the hollow cylinder test (HCT) to obtain the |*E**| of AC and found that the HCT device established a good agreement with |*E**| measurements obtained with uniaxial compression testing apparatus at 0°C and 20°C. The Witczak dynamic modulus predictive equation results are found to be reasonably in good agreement with the test results of the HCT. The hollow cylinder tester is essentially developed with a desire to have alternative test for IDT. The test is conducted by applying pressure to the internal wall of a hollow cylindrical specimen using flexible membrane. The applied pressure produces hoop stress on the wall of hollow cylindrical specimen. By implementing closed form solutions for thick-walled cylinder, the tensile strength and creep compliance is calculated. The strain is either measured by the use of strain gauges or directly calculated from the volume change of the cavity. The size of the specimen used is of 115mm height, 150mm outside diameter, and 106mm inside diameter.

2.7 Dynamic Modulus Predictive Models

Many researchers have developed predictive equations for evaluating dynamic modulus of hot-mix asphalt concrete using information from mix design and volumetric. These predictive models provide a fast and simple means to determine the dynamic modulus value with a certain degree of accuracy. Some of these are discussed in the following sections.

2.7.1 Viscosity-Based Witczak Predictive Model

This model is based on data from 205 different asphalt mixtures with 2,750 data points, tested over the last 30 years in the laboratories of the Asphalt Institute, the University of Maryland, and the Federal Highway Administration. According to the developers, the model can predict the dynamic modulus of asphalt concrete mixes of modified and conventional asphalt cements (Garcia and Thompson 2007). The equation is given as:

$$\log|E^*| = -1.249937 + 0.029232\,\rho_{200} - 0.001767\,(\rho_{200})^2 - 0.002841\,\rho_4 - 0.058097\,V_a - 0.802208\left(\frac{V_{beff}}{V_{beff}+V_a}\right) + \frac{3.871977 - 0.0021\,\rho_4 + 0.003958\,\rho_{3/8} - 0.000017(\rho_{3/8})^2 + 0.00547\,\rho_{3/4}}{1+e^{(-603313-0.313351\log(f)-0.393532\log(\eta))}} \quad (2.11)$$

where, $|E^*|$ is the dynamic modulus, 10^5 psi; η is the bitumen viscosity, 10^6 poise; f is the loading frequency, Hz; V_a is the air void content, % by volume; V_{beff} is the effective bitumen content, % by volume; $\rho_{3/4}$ is the cumulative percentage retained of the aggregate material on 19-mm (3/4-in) sieve; $\rho_{3/8}$ is the cumulative percentage retained on 9.5-mm (3/8-in) sieve; ρ_4 is the cumulative percentage retained on 4.76-mm (No. 4) sieve; ρ_{200} is the percentage passing the 0.075-mm (No. 200) sieve. The binder viscosity can be determined as:

$$\eta = \left(\frac{G^*}{\omega}\right)\left(\frac{1}{\sin(\delta)}\right)^{a_0+a_1*\omega+a_2*\omega^2} \quad (2.12)$$

where, η is the binder viscosity, cP; G^* is the binder shear modulus, Pa; ω is the angular frequency used to measure G^* and δ, rad/sec; δ is the binder phase angle, degree; a_0 = 3.639216, a_1 = 0.131373, and a_2 = -0.000901.

One of the limitations of the viscosity-based Witczak model is its reliance on other models to translate the currently used binder's dynamic shear modulus, $|G^*|$ measurements into binder viscosity.

2.7.2 Binder Shear Modulus Based Witczak Model

This model uses dynamic shear modulus as a parameter instead of viscosity. A database containing 7400 data point from 346 hot-mix asphalt mixtures was used to develop $|G^*|$-based Witczak model. This database is the combination of that used to develop the viscosity-based Witczak model plus additional new data points. The model is given below (Garcia and Thompson 2007).

$$\log|E^*| = -0.349 + 0.754\left(|G_b^*|^{-0.0052}\right) * \begin{pmatrix} 6.65 - 0.032\rho_{200} + 0.0027(\rho_{200})^2 - 0.011\rho_4 \\ -0.0001(\rho_4)^2 + 0.006\rho_{38} - 0.00014(\rho_{38})^2 \\ -0.08V_a - 1.06\left(\dfrac{V_{b\,eff}}{V_{b\,eff}+V_a}\right) \end{pmatrix} + \frac{2.558 + 0.032V_a + 0.713\left(\dfrac{V_{b\,eff}}{V_{b\,eff}+V_a}\right) + 0.0124\ \rho_{38} + 0.0001\ (\rho_{38})^2 + 0.00 - 0.0098\rho_{34}}{1+e^{\left(-0.7814-0.5785\log|G^*|-0.8834\log(\delta_b)\right)}} \quad (2.13)$$

where, $|E^*|$ is dynamic modulus in psi; ρ_{200} is percentage (by weight of total aggregate) passing the 0.075-mm (No. 200) sieve; ρ_4 is cumulative percentage (by weight) retained on the 4.76-mm (No. 4) sieve; $\rho_{3/4}$ is cumulative percentage (by weight) retained on the 19-

mm (3/4-in) sieve; ρ_{38} is cumulative percentage (by weight) retained on the 9.5-mm (3/8-in) sieve; V_a is air void content (by volume of the mix), %; V_{beff} is effective binder content (by volume of the mix), %; $|G_b^*|$ is dynamic shear modulus of the binder in psi; δ_b is the phase angle of binder associated with the $|G_b^*|$ in degrees.

2.7.3 Hirsch Model

Hirsch model for predicting asphalt concrete modulus is as follows (Garcia and Thompson 2007).

$$\left|E^*\right| = P_c\left[4{,}200{,}000 * \left(1 - \frac{VMA}{100}\right) + 3\left|G_b^*\right|\left(\frac{VFA * VMA}{10{,}000}\right)\right] + \frac{\left(1 - P_c\right)}{\frac{\left(1 - \frac{VMA}{100}\right)}{4{,}200{,}000} + \frac{VMA}{3\left|G_b^*(VFA)\right|}}} \tag{2.14}$$

$$P_c = \frac{\left(20 + \frac{3\left|G_b^*\right|\left(VFA\right)}{VMA}\right)^{0.58}}{650 + \left(\frac{3\left|G_b^*\right|\left(VFA\right)}{VMA}\right)^{0.58}}$$

(2.15)

$$\phi = -21\left(\log\ P_c\right)^2 - 55\log\ P_c$$

(2.16)

where, $|E^*|$ is dynamic modulus in psi; $|G_b^*|$ is binder dynamic modulus in psi; *VMA* is voids in the mineral aggregate in %; *VFA* is voids filled with asphalt in %; P_c is aggregate contact factor; and ϕ is the phase angle.

The strength of this model is the empirical phase angle equation, which is important for interconversion of the $|G_b^*|$ to relaxation modulus or creep compliance. The weakness of the model includes strong dependence on volumetric parameters, particularly under low air void and *VFA* conditions, and questions regarding the ability of the $|G_b^*|$ parameters to account for the possible beneficial effects of modifiers (Al-Khateeb et al. 2006, Soleymani et al. 2004).

2.7.4 Stress-Dependent Stiffness Predictive Equation

To incorporate the effect of nonlinearity, Kim (2009) presented a model for $|E^*|$ prediction. This model can predict the $|E^*|$ beyond the linear viscoelastic (LVE) limit of the material. The model expects a minimum bulk stress value of 21 kPa and octahedral shear stress value of 9.9 kPa for unconfined linear viscoelastic stress case prediction. The proposed model is given below.

$$\log\left(\left|E^*\right|\right) = \delta + A + \frac{\alpha - (\delta + A) + a_4 G_a + a_5\, VFA}{1 + e^{\beta + \gamma \log(f) - c \log(\eta)}} \tag{2.17}$$

$$A = a_0 + a_1 G_a + a_2\, VFA + a_3 \log(\eta) \tag{2.18}$$

$$\delta = \left[(k_1 p_a) \left(\frac{\theta}{p_a} \right)^{k_2} \left(\frac{\tau_{oct}}{p_a} \right)^{k_3} \right] \tag{2.19}$$

$$G_a = \frac{p200 + p4 + p3/8 + p3/4}{4} \quad (2.20)$$

where, log |*E**| is the logarithm of stress-dependent |*E**|, δ is the equilibrium modulus, G_a is the average gradation (passing %), *VFA* is the voids filled with asphalt (volume %), η is the binder viscosity (10^6 P), *F* is the frequency (Hz), a_i are the regression coefficients, θ is the bulk stress (kPa), τ_{oct} is the octahedral shear stress (kPa), P_a is the atmospheric pressure (103.3 KPa), k_i are the regression coefficients, p_{200} is the percentage of materials passing 0.074 mm sieve (%), p_4 is the percentage of materials passing 4.36 mm sieve (%), $p_{3/8}$ is the percentage of materials passing 9.5 mm sieve (%), $p_{3/4}$ is the percentage of materials passing 19 mm sieve (%).

2.7.5 Neural-Network Models

Ceylan et al. (2007) developed a new method of predicting HMA dynamic modulus by means of artificial neural network (ANN). They reported that the ANN model's predictions using the same input variables used in η or $|G_b^*|$-based Witczak model show significantly better overall prediction accuracy, better local accuracy at high and low temperature extremes, less prediction bias, and better balance between temperature and mixture influences. The ANN model developed by Ceylan et al. (2007) is a four-layered feed-forward back propagation model. The ANN architecture has one input, two hidden and one output layer. All input variables used for the development of the Witczak models are used as an input in the ANN model and the sole out of the ANN model is the |*E**|. Input database used for the ANN models is also the same as that used by Witczak. However, instead of using all the data for prediction as in the regression analysis, input data were divided in to

training and testing sets. The training data subset was used to train the back-propagation ANN model, and the testing data subset was used to examine the statistical accuracy of the developed ANN model. Finally, after a lot of trials for the best network architecture, the 8-30-30-1 architecture (eight inputs, 30 and 30 hidden neurons, and one output neuron, respectively), was chosen as the best architecture.

2.7.6 Visco-Elasto-Plastic Continuum Damage (VEPCD) Model

The visco-elasto-plastic model is developed by Kim (2009) to model AC under a wide verity of loading conditions. This model can predict the mechanical behavior of asphalt mixtures in both linear viscoelastic and visco-plastic conditions. The model is developed using three modified and one original binder asphalt mixtures. The concept of elastic-visco-elastic correspondence principle is used to model the first stage of the response of asphalt concrete which is without any damage. Then continuum damage mechanics is applied to predict the behavior of asphalt with micro cracking. The plastic and visco-plastic responses are captured with time and stress dependent visco-plastic model. In all stages, the time temperature superposition principle is applied to capture the effect of temperature. Finally, the strain components are superimposed to give the final form of the VEPCD model.

2.8 Constitutive Models for Linear Viscoelastic Materials

Viscoelastic materials can be modeled in order to relate their time-dependent stress and strain. These models include the Maxwell model, the Kelvin–Voigt model, and the Standard Linear Solid Model. These models are used to predict the response of a material under variety of loading conditions. The elastic and viscous components of a

viscoelastic behavior can be modeled as linear combinations of springs and dashpots, respectively. Each model differs in the arrangement of these elements.

The elastic components can be modeled as springs obeying Hooke's law as:

$$\sigma_e = E\varepsilon \tag{2.21}$$

where, σ_e is the elastic stress component; E is the elastic modulus of the material; and ε is the strain that occurs under the applied stress. On the other hand, the viscous components can be modeled as dashpots, for which the stress-strain relationship can be given as:

$$\sigma_v = \eta \frac{d\varepsilon}{dt} \tag{2.22}$$

In Equation 2.22, σ_v is the viscous stress component, η is the viscosity of the material, and $d\varepsilon/dt$ is the time derivative of strain due to the applied stress.

2.8.1 Maxwell Model

The Maxwell material can be represented by a purely viscous damper and a purely elastic spring connected in series, as shown in Figure 2.4. Since both elements are connected in series, the total elongation for the applied stress σ would be:

$$\varepsilon_{total} = \varepsilon_D + \varepsilon_S \tag{2.23}$$

where, where subscript D and S refer to dashpot and spring, respectively. Differentiating Equation 2.23 and substituting Equations 2.2 and2.3, we have:

$$\frac{d\varepsilon_{total}}{dt} = \frac{d\varepsilon_D}{dt} + \frac{d\varepsilon_S}{dt} = \frac{\sigma}{\eta} + \frac{1}{E}\frac{d\sigma}{dt} \tag{2.24}$$

According to this model, if a Maxwell material is held under a constant strain, the stress gradually relaxes. On the other hand, when a constant stress is applied, the resulting strain has two components. The first one is the elastic one corresponding to the spring, which occurs instantaneously and relaxes immediately upon removal. The second one is the viscous component which increases with time, as long as the stress is applied.

The Maxwell model can predict the decay in stress with time, which is accurate for most polymers. However, it does not predict creep accurately. The Maxwell model for creep or constant-stress condition postulates that strain will increase linearly with time, whereas, most of the polymers show the strain rate to be decreasing with time.

2.8.2 Kelvin-Voigt Model

The Kelvin-Voigt model, also known as the Voigt Model, consists of a Hookean elastic spring and a Newtonian damper connected in parallel. Figure 2.5 shows Kelvin-Voigt model. This model is used to illustrate creep behavior of the material. The constitutive expression for this model can be given as:

$$\sigma(t) = E\ \varepsilon(t) + \eta\ \frac{d\varepsilon(t)}{dt} \tag{2.25}$$

According to this model, if a constant stress is applied to a material, the material deforms at a decreasing rate, asymptotically approaching the steady-state strain. When the stress is

released, the material gradually relaxes to its un-deformed state. At constant stress (creep), the model is quite realistic as it predicts strain to tend to σ/E as time continues to infinity.

This model is accurate for modeling creep in materials, but with regards to relaxation, this model is less accurate.

2.8.3 Standard Solid Model

The Standard Linear Solid Model combines the Maxwell model and a Hookean spring in parallel, shown in Figure 2.6. The governing constitutive relation for this model can be given as:

$$\frac{d\varepsilon}{dt} = \frac{\frac{E_2}{\eta}\left(\frac{\eta}{E_2}\frac{d\sigma}{dt} + \sigma - E_1\varepsilon\right)}{E_1 + E_2} \tag{2.26}$$

According to this constitutive relation, the material under concern will instantaneously deform to some strain, which is the elastic portion of the total strain. After that, the material will continue to deform and asymptotically approach a steady-state strain due to viscous behavior.

The Standard Linear Solid Model is more accurate than the Maxwell and Kelvin-Voigt models. However, for some specific loading conditions, this model returns inaccurate results.

2.8.4 Generalized Maxwell Model

The Generalized also known as the Maxwell-Wiechert model is the most general form of the linear model for viscoelasticity. The model accounts that the relaxation does not occur at a single time, but at a distribution of times. Due to molecular segments of different lengths with shorter ones contributing less than the longer ones, there is a varying time distribution. This model allows this by having as many Maxwell elements as are necessary to accurately represent the distribution. Figure 2.7 shows the Generalized Maxwell or Wiechert model.

2.8.5 Generalized Voigt Model

The Generalized Voight model consists of a spring and a dashpot and *n* Voigt elements connected in series, as shown in Figure 2.8. This model has similar advantages as in Generalized Maxwell model. Generally, creep behavior of a material is expressed with this model.

2.9 Interconversions of Linear Viscoelastic Material Functions

Several researchers have tried to develop interrelationships between linear viscoelastic materials functions based on the theory of linear integral and differential equations (Birgisson et al. 2005). Based on these relationships, a given material function (source) can be converted into another function (target) as long as the given function is known over a wide-enough range of time or frequency. The interconversion makes it possible to predict one viscoelastic property from another and therefore eliminates the need to do more than one test to calculate all needed material properties.

2.9.1 Basis of Interconversion of Material Functions and Its Importance

All linear viscoelastic material functions are mathematically equivalent for each mode of loading such as uniaxial load or shear. The interrelationships between linear viscoelastic material functions have a basis in the theory of linear differential and integral equations. Thus, a given (or source) material function can be converted into other (or target) material functions as long as the given function is known over a wide-enough range of time or frequency (Park and Schapery 1999).

Interconversion is required for various reasons. The response of a material under a certain excitation condition inaccessible to direct experiment may be calculated from measurements under other readily realizable conditions. For example, the response of a very stiff material subjected to a specified deformation is usually difficult to obtain from a constant-strain, relaxation test because of the requirement of a robust testing device. However, the required response may be obtained from an easily-realizable, constant-stress, creep test and through an interconversion between the relaxation modulus and creep compliance (Park and Schapery 1999). Weldegiorgis and Tarefder (2012) applied material function interconversion technique to convert dynamic modulus data to estimate creep compliance and relaxation modulus mastercurves.

2.9.2 Conversion of Creep Compliance into Dynamic Modulus

Jeong et al. (2007) validated the interconversion between dynamic moduli and creep compliances obtained from two typical mixes used in Virginia. The measured dynamic modulus was successfully converted into creep compliance, and the measured creep

compliance was successfully converted into dynamic modulus. Jeong et al. (2007) used a Prony series model to fit the creep compliance master curve in their study. The following equation represents the model:

$$D(t_r) = D_g + \sum_{i=1}^{n} D_i\left(1 - e^{-t_r/\tau_i}\right) \tag{2.27}$$

where, $D(t_r)$ is the creep compliance at reduced time t_r, $D_g = \lim_{t_r \to 0} D(t_r)$ is the equilibrium creep compliance, D_i and τ_i are the Prony series parameters, and n is the number of terms used in the series. The real and imaginary parts of the complex compliance are then, respectively:

$$D'(\omega) = D_g + \sum_{j=1}^{n}\left(\frac{D_j}{\omega^2\ \tau_j{}^2 + 1}\right) \tag{2.28}$$

and,

$$D''(\omega) = \sum_{j=1}^{n}\left(\frac{\omega\ \tau_j D_j}{\omega^2\ \tau_j{}^2 + 1}\right) \tag{2.29}$$

where, ω is the angular frequency. The complex compliance and the dynamic modulus then determined as:

$$|D^*(\omega)| = \sqrt{[D'(\omega)]^2 + [D''(\omega)]^2} \tag{2.30}$$

$$E^*(\omega) = \frac{1}{D^*(\omega)} \tag{2.31}$$

2.9.3 Conversion of Dynamic Modulus into Creep Compliance

Jeong et al. (2007) suggested calculation of creep compliance from the dynamic modulus in two steps. First, the dynamic modulus is converted into relaxation modulus, and then the relaxation modulus is converted in creep compliance. Schapery and Park (1999) proposed an approximate interconversion method to convert dynamic modulus data to relaxation modulus and verified the method using polymeric material. Following are the proposed equations by these researchers using the real and the imaginary part of the dynamic modulus respectively for relaxation modulus.

$$E(t) \cong \frac{1}{\lambda'} E'(\omega)|_{\omega=1/t} \tag{2.32}$$

$$E(t) \cong \frac{1}{\lambda''} E''(\omega)|_{\omega=1/t} \tag{2.33}$$

where, λ' is the adjust function $\left[\Gamma(1-n)\cos\left(\frac{n\pi}{2}\right)\right]$, λ'' is the adjust function $\left[\Gamma(1-n)\sin\left(\frac{n\pi}{2}\right)\right]$, Γ is the gamma function $\left[\Gamma(n) = \int_0^\infty u^{n-1}e^{-u}\ du\right]$, and n is the local log-log slope of the storage modulus $\left[\frac{d\log E'(\omega)}{d\log \omega}\right]$. Jeong et al. (2007) used the storage modulus data to calculate the relaxation modulus.

Ferry (1980) given an exact relationship between the creep compliance and relaxation modulus using the convolution integral as:

$$\int_0^t E(t-\tau)\, D(\tau)\, d\tau = t$$

(2.34)

where, $E(t)$ is the relaxation modulus, $D(t)$ is the creep compliance, t is the time, and τ is an integral variable. The integral above can be solved numerically (Park and Kim 1999). Leaderman (1958) showed that if both the creep compliance and the relaxation modulus are modeled using a power law, the following equation can be used to relate the relaxation modulus and the creep compliance.

$$E(t)\, D(t) = \frac{\sin n\pi}{n\pi} \qquad (2.35)$$

where, $E(t) = E_1\, t^{-n}$, and $D(t) = D_1\, t^{n}$.

2.9.4 Numerical Method of Interconversion between LVE Material Functions

The uniaxial, non-aging, isothermal stress-strain equation for a linear viscoelastic material can be represented by a Boltzmann superposition integral (Park and Schapery 1999),

$$\sigma(t) = \int_0^t E(t-\tau)\frac{d\varepsilon(t)}{d\tau}\, d\tau\,. \qquad (2.36)$$

Here, E is the relaxation modulus, t is the time, and ε is the strain response. The lower limit in this and all succeeding integrals over time should be interpreted as 0^- whenever the integrand contains the derivative of a step function at the origin, such as when ε is that for

a stress relaxation test. Equation 2.36 is based on the mathematical properties governing all linear, non-aging systems. The stress-strain expression can be expressed in a differential form based on a mechanical model consisting of linear springs and dashpots,

$$\sum_{n=0}^{N} a_n \frac{d^n \sigma}{dt^n} = \sum_{m=0}^{M} b_m \frac{d^m \varepsilon}{dt^m}. \tag{2.37}$$

Mechanical models with different arrangement of springs and dashpots provide different mechanical interpretations of the constants a_n and b_m in Equation 2.37.

The generalized Maxwell model (or Wiechert model) consists of a spring and m Maxwell elements connected in parallel. The relaxation modulus derived from this model is given by -

$$E(t) = E_e + \sum_{i=1}^{m} E_i e^{-(t/\rho_i)} \tag{2.38}$$

where E_e (the equilibrium modulus), E_i (relaxation strengths), and ρ_i (relaxation times) are all positive constants. The series expression in Equation 2.38 is often referred to as a Prony or Dirichlet series. The creep compliance can be characterized more easily using the generalized Voigt model (or Kelvin model) which consists of a spring and a dashpot and n Voigt elements connected in series, and is given by –

$$D(t) = D_g + \frac{1}{\eta_0} + \sum_{j=1}^{n} D_j (1 - e^{-(t/\tau_j)}) \tag{2.39}$$

where D_g (the glassy compliance), η_0 (the zero-shear or long-time viscosity), D_j (retardation strengths), and τ_j (retardation times) are positive constants. The constants in the generalized Maxwell and generalized Voigt models can be chosen so that the models are mathematically equivalent, and thus a viscoelastic material depicted by one model also can be depicted by the other.

The constants in Equations 2.38 and 2.39 can be obtained by fitting these expressions to the available experimental data. Note that, when for viscoelastic solids $\eta_0 \to \infty$ and $E_e > 0$, Equation 2.39 has the same form as Equation 2.38 in which $(D_g + \sum D_j)$ and $-D_j$ are compared, respectively, with E_e and E_i when $n = m$. Further, in Equation 2.38, the constant E_e may be viewed as a term arising from one of the Maxwell units from which $\rho_i \to \infty$. The principle advantage of using the series representation Equation 2.38 or 2.39 is the remarkable computational efficiency associated with these expressions. For example, once a material function is defined in the time domain by Equation 2.38 or 2.39, the corresponding function in the frequency or Laplace-transform domain can be readily obtained in terms of the constants involved in Equation 2.38 and 2.39.

From Equation 2.36, the following integral relationship between the uniaxial relaxation modulus $E(t)$ and creep compliance $D(t)$ can be found:

$$\int_0^t E(t-\tau)\frac{dD(\tau)}{d\tau}\,d\tau = 1 \qquad (t > 0)\,. \tag{2.40}$$

The operational modulus and the compliance are defined as follows:

$$\tilde{E}(s) \equiv s\int_0^\infty E(t)\,e^{-st}dt \tag{2.41}$$

$$\tilde{D}(s) \equiv s\int_0^{\infty} D(t)\, e^{-st} dt \tag{2.42}$$

where the integrals in Equation 2.41 and 2.42 are the Laplace transforms of $E(t)$ and $D(t)$, respectively; the *s*-multiplied Laplace transform is called Carson transform. From Equations 2.40 to 2.42, one can obtain the following familiar relationship between the two operational functions:

$$\tilde{E}(s)\,\tilde{D}(s) = 1 \tag{2.43}$$

Complex material functions arise from the response to a steady-state sinusoidal loading, and are related to the operational functions as follows:

$$E^*(\omega) = \tilde{E}(s)\big|_{s \to i\omega} \tag{2.44}$$

$$D^*(\omega) = \tilde{D}(s)\big|_{s \to i\omega}\,. \tag{2.45}$$

The real and imaginary parts, denoted with primes and double primes, are –

$$E^*(\omega) = E'(\omega) + iE''(\omega) \tag{2.46}$$

$$D^*(\omega) = D'(\omega) - iD''(\omega)\,. \tag{2.47}$$

The minus sign is used in Equation 2.47 so that *D"* will be positive. The real and imaginary parts are commonly called the storage and loss functions, respectively. The following relationship between the complex functions from Equation 2.43 to 2.47:

$$E^*(\omega)\, D^*(\omega) = 1\,. \tag{2.48}$$

The operation and the components of complex material functions, based on Equations 2.41 to 2.47 and the Prony series representations Equation 2.37 and Equation 2.38, are given, respectively, by –

$$\tilde{E}(s) = E_e + \sum_{i=1}^{m} \frac{s\rho_i E_i}{s\rho_i + 1} \tag{2.49}$$

$$\tilde{D}(s) = D_g + \frac{1}{\eta_0 s} + \sum_{j=1}^{n} \frac{D_j}{s\tau_j + 1} \tag{2.50}$$

$$E'(\omega) = E_e + \sum_{i=1}^{m} \frac{\omega^2 \rho_i^2 E_i}{\omega^2 \rho_i^2 + 1} \tag{2.51}$$

$$E''(\omega) = \sum_{i=1}^{m} \frac{\omega \rho_i E_i}{\omega^2 \rho_i^2 + 1} \tag{2.52}$$

$$D'(\omega) = D_g + \sum_{j=1}^{n} \frac{D_j}{\omega^2 \tau_j^2 + 1} \tag{2.53}$$

$$D''(\omega) = \frac{1}{\eta_0 \omega} + \sum_{j=1}^{n} \frac{\omega \tau_j D_j}{\omega^2 \tau_j^2 + 1} \tag{2.54}$$

2.9.4.1 Prony Series Fit of Wiechert Model

Park and Schapery (1999) developed Prony series expression for Wiechert model as given in the previous section. This expression with decaying exponential terms can be used to model the dynamic modulus mastercurves. Fitting the dynamic modulus data to Prony

series expression as in Equations 2.50 and 2.51 is important to derive relaxation modulus and creep compliance curves.

Storage modulus data from dynamic modulus test can be pre-smoothened with sigmoidal function. After that, using the expression in Equation 2.51 a Prony series with definite number of terms can be fitted with acceptable precision. As stated earlier, this Prony series fit of storage modulus data can be used to derive relaxation modulus and creep compliance.

Park and Schapery (1999) presented a method of numerical interconversion between the modulus and compliance functions in time, Laplace-transform, and frequency domains when the transient material functions involved are represented by Prony series. Although the theory considered a viscoelastic solid with $E_e > 0$ and $\eta_0 \to \infty$, the authors recommended the theory to be equally valid for viscoelastic liquids for which $E_e = 0$ and η_0 is finite.

2.9.4.2 Relationships between Relaxation Modulus and Creep Compliance

Equation 2.39 can be used to determine the relaxation modulus from a known creep compliance or vice versa; except for very special cases, this must be done by approximate analytical or numerical methods. A common numerical approach normally requires that the integral be decomposed into a great number of intervals because of the spread of the function over many decades of time. This may render inaccurate results and cause computational difficulties unless one is very careful in the choice of the intervals. However, by substituting the series representations in Equations 2.37 and 2.38 into Equation 2.39,

one may readily carry out the integration analytically and then easily derive the target function.

When one set of constants, either $\{\rho_i,\ E_i\ (i = 1,\ 2,\ ...,\ m)\ and\ E_e\}$ or, $\{\tau_j,\ D_j\ (j = 1,\ 2,\ ...,\ n),\ D_g\ and\ \eta_0\}$, is known and the target time constants are specified, the other (unknown) set of constants can be determined simply by solving the resulting system of linear algebraic equations. For example, if one seeks to find $D(t)$ from known $E(t)$, the following system of equations for unknown constants $D_j\ (j = 1, 2, ..., n)$ results:

$$[\mathbf{A}]\{\mathbf{D}\} = \{\mathbf{B}\} \tag{2.54}$$

or $A_{kj} D_j = B_k$ (summed on j; $j = 1,\ 2,\ ...,\ n$); $k = 1,\ ...,\ p$) where,

$$A_{kj} = \begin{cases} E_e(1 - e^{-(t_k/\tau_j)}) + \sum_{i=1}^{m} \dfrac{\rho_i\ E_i}{\rho_i - \tau_j}\left(e^{-(t_k/\rho_i)} - e^{-(t_k/\tau_j)}\right) & when \quad \rho_i \neq \tau_j \\ or & \\ E_e(1 - e^{-(t_k/\tau_j)}) + \sum_{i=1}^{m} \dfrac{t_k\ E_i}{\tau_j}\ e^{-(t_k/\rho_i)} & when \quad \rho_i = \tau_j \end{cases} \tag{2.55}$$

and,

$$B_k = 1 - \left(E_e + \sum_{i=1}^{m} E_i\ e^{-(t_k/\rho_i)}\right) \Bigg/ \left(E_e + \sum_{i=1}^{m} E_i\right). \tag{2.56}$$

The symbol $t_k\ (k = 1, ..., p)$ denotes a discrete time corresponding to the upper limit of integration in Equation 2.39.

In Equation 2.54, E_e, E_i, and ρ_i (where $i = 1, 2, \ldots, m$) together with τ_j (where $j = 1, 2, \ldots, n$) and t_k (where $k = 1, 2, \ldots, p$) are known or specified, and D_j (where $i = 1, 2, \ldots, n$) are the unknowns. For the system of linear algebraic equations (Equation 2.54), the collocation method is effected when $p = n$ (in which Equation 5 is satisfied exactly at times t_k), and the least squares method may be used when $p > n$ (when the number of available equations in Equation 2.54 is greater than the number of unknowns). In the case of the least squares method, a minimization of the square error $\|\{\mathbf{B}\} - [\mathbf{A}]\{\mathbf{D}\}\|^2$ with respect to D_j (where $j = 1, 2, \ldots, n$) leads to the replacement of Equations 2.54 with $[\mathbf{A}]^T[\mathbf{A}]\{\mathbf{D}\} = [\mathbf{A}]^T\{\mathbf{B}\}$ in which the product $[\mathbf{A}]^T[\mathbf{A}]$ is a square matrix.

The time constants τ_j (where $j = 1, 2, \ldots, n$) are usually specified appropriately rather than being calculated by solving a nonlinear system of equations with *2n* unknowns. Selection of the sampling points t_k (where $k = 1, 2, \ldots, p$) depends on the method of solution. For the collocation method (where $p = n$), t_k may conveniently be taken to be $t_k = a\tau_k$ (where $k = 1, 2, \ldots, n$) where typically $a = 1$ or ½ is used. For the least-squares method, one may take t_k (where k = 1, 2, …., p) with equidistant intervals (on the *log-t* axis) which are smaller than the intervals of τ_j (where $j = 1, 2, \ldots, n$) so that $p > n$. The glassy compliance D_g can be obtained from the following expression:

$$D_g = \frac{1}{E_e + \sum_{i=1}^{m} E_i} \tag{2.57}$$

Once the model constants D_g, D_j, and τ_j are known, functions $D(t)$, $\tilde{D}(s)$, $D'(\omega)$, and $D''(\omega)$ can be readily determined form Equations 2.38, 2.49, 2.52, and 2.53, respectively. A similar set of equations may be formulated for unknown constants E_i (where $i = 1, 2, \ldots, m$) when one seeks to find the modulus function from a known compliance function.

2.9.4.3 Relationship between Operational Functions

The relation in Equation 2.8 is very useful in directly evaluating one function when other is known at a particular value of the argument. However, if both the source and the target functions are represented in Prony series, the complete target function can be determined by solving a system of linear algebraic equations using collocation of Equation 2.8 or a least-squares method. For example, if one seeks to find $\tilde{D}(s)$ from known $\tilde{E}(s)$, the same form of equation as that of Equation 2.54 is obtained, but with the following definitions of A_{jk} and B_k,

$$A_{jk} = \left(E_e + \sum_{i=1}^{m} E_i \frac{s_k}{s_k + 1/\rho_i} \right) \left(\frac{1}{s_k \tau_j + 1} \right) \tag{2.58}$$

and,

$$B_k = 1 - \left(E_e + \sum_{i=1}^{m} E_i \frac{s_k}{s_k + 1/\rho_i} \right) \Big/ \left(E_e + \sum_{i=1}^{m} E_i \right). \tag{2.59}$$

Equation 2.54, with Equations 2.58 and 2.59, were obtained by substituting Equations 2.48 and 2.49 with $\eta_0 \to \infty$ into Equation 2.42 and rearranging terms. The symbol s_k (where k = 1, 2, …., p) denotes a discrete value of the transform variable at which the

interrelationship in Equation 2.43 is satisfied, and its selection is analogous to that of t_k discussed earlier except that $s_k = 1/t_k$. The glassy compliance D_g is represented in terms of E_e and E_i according to Equation 2.57. The number of sampling points (or number of equations) should not be less than the number of the unknowns (i.e., $p \geq n$).

2.9.4.4 Relationship between Complex Functions

Using the relationship in the Equation 2.47 between the complex modulus and compliance functions together with the definitions in Equations 2.45 and 2.46, one may readily obtain interrelationships between the components (real and imaginary) of the complex modulus and compliance functions. It can be seen, from Equations 2.50 to 2.53, that if the Prony series coefficients for either the real or the imaginary component of a complex function are known, the series representation of other component is automatically known. Therefore, if both the source and the target functions are representable in Prony series, one can determine the target function by solving a system of linear algebraic equations in terms of the model constants of the source function.

For example, if one seeks to find *D'* from *E'* and *E"*, the following relationship, derived from Equations 2.45 to 2.47, can be used:

$$D' = \frac{E'}{(E')^2 + (E'')^2}. \tag{2.60}$$

Once *D'* is determined, *D"* is readily established in terms of the same set of constants. Now substituting Equations 2.50 to 2.53 into Equation 60, one may obtain the same form of equation as Equation 2.54 with the following A_{jk} and B_k:

$$A_{jk} = \frac{1}{\omega_k^2 \tau_j^2 + 1} \tag{2.61}$$

and,

$$B_k = \frac{E_e + \sum_{i=1}^{m} \frac{\omega_k^2 \rho_i^2 E_i}{\omega_k^2 \rho_i^2 + 1}}{\left(E_e + \sum_{i=1}^{m} \frac{\omega_k^2 \rho_i^2 E_i}{\omega_k^2 \rho_i^2 + 1} \right)^2 + \left(\sum_{i=1}^{m} \frac{\omega_k \rho_i E_i}{\omega_k^2 \rho_i^2 + 1} \right)^2} - \frac{1}{E_e + \sum_{i=1}^{m} E_i}. \tag{2.62}$$

The symbol ω_k (where $k = 1, 2, \ldots, p$) denotes a discrete value of the angular frequency at which the interrelationship in Equation 2.60 is established and can be selected in the same manner as that of s_k discussed in the previous section. Again, the glassy compliance D_g can be computed from E_e and E_i according to Equation 2.57.

2.9.5 Approximate Analytical Method of Interconversion between Linear Viscoelastic Material Functions

Analysis of a viscoelastic continuum using the elastic-viscoelastic correspondence principle requires the use of Laplace or Fourier transforms of related material functions to derive transformed response functions. Again, these transformed response functions require transform inversion to predict time-dependent response. There are a number of analytical and approximate interconversion methods with different bases and accuracies. Some of these methods are discussed in the following sections.

2.9.5.1 Common Approximate Analytical Methods of Interconversion

Schapery (1962) proposed two approximate methods of Laplace transform inversion; the direct method and the collocation method. As a special application of direct method which can be defined as the Carson transform or the *s*-multiplied Laplace transform, the relation between the uniaxial relaxation modulus $E(t)$ and the operational modulus,

$$\tilde{E}(s) \equiv s\int_0^\infty E(t)\, e^{-st} dt = s\int_{-\infty}^{\infty} E(t)\, t\, e^{-st}\, d(\ln t) \tag{2.63}$$

have the following approximate interconversion:

$$E(t) \cong \tilde{E}(s)\big|_{s=(\alpha/t)} \quad or \quad \tilde{E}(s) \cong E(t)\big|_{t=(\alpha/s)} \tag{2.64}$$

where, $\tilde{E}(s) \equiv s\bar{E}(s)$ and $\tilde{E}(s)$ is the Laplace transform of the function $E(t)$. Also, $\alpha = e^{-C}$ in which C = 0.5772… as Euler's constant, resulting in $\alpha \cong 0.56$. The relationship in Equation 2.64 gives good results, especially, when the derivative of $E(t)$ with respect to log-t is a slowly varying. For this type of slowly varying $E(t)$ with respect to log-t Schapery (1962) also proposed an improved relationship as:

$$E(t) \cong \tilde{E}(s)\big|_{s=(\beta/t)} \quad or \quad \tilde{E}(s) \cong E(t)\big|_{t=(\beta/s)}. \tag{2.65}$$

In Equation 65, $\beta = \{\Gamma(1-n)\}^{-(1/n)}$. Also, $\Gamma(\cdot)$ denotes the Gamma function and n is the local log-log slope of the source function defined by either, $n \equiv \dfrac{-d\log E}{d\log t}$ or, $n \equiv \dfrac{d\log \tilde{E}}{d\log s}$. It can be easily shown by using Equation 2.63 that Equation 2.65 is exact

for all $t > 0$ if $E(t) \sim t^{-n}$, where n is constant. When the moduli in Equations 2.64 and 2.65 are replaced by compliances, denoted by *D*'s, one can obtain analogous relationships between the creep compliance $D(t)$ and the operational compliance $\tilde{D}(s)$.

Christensen (1982) proposed an approximate interconversion between the $E(t)$ and the $E'(\omega)$ of the following form:

$$E(t) \cong E'(\omega)\big|_{\omega=(2/\pi t)} \quad or \quad E'(\omega) \cong E(t)\big|_{t=(2/\pi\omega)}. \tag{2.66}$$

Similar relationship holds for compliance functions when *E*'s in Equation 2.66 are replaced by *D*'s. Staverman and Schwarzl (1955) presented approximate conversion from $E'(\omega)$ to the loss modulus $E''(\omega)$:

$$E''(\omega) \cong \frac{\pi}{2}\frac{dE'(\omega)}{d\ln\omega} \tag{2.67}$$

Booij and Thoone (1982) proposed the following conversion from $E''(\omega)$ to $E'(\omega)$:

$$E'(\omega) \cong E_e - \frac{\pi\omega}{2}\frac{d\left[E''(\omega)/\omega\right]}{d\ln\omega}. \tag{2.68}$$

Equation 2.68 may also be rewritten as:

$$E'(\omega) \cong E_e + \frac{\pi}{2}\left(1 - \frac{d\ln E''}{d\ln\omega}\right)E''(\omega) \tag{2.69}$$

where E_e is the equilibrium (or rubbery) modulus. Equations 2.67 to 2.69 also apply to compliances when *E'* and *E"* are replaced by *D'* and -*D"*, respectively.

2.9.5.2 Basis of Approximate Analytical Method Proposed by Schapery and Park

Following exact relations between two material functions may be obtained from the theory of viscoelasticity.

$$E(t) = \frac{2}{\pi}\int_0^\infty E'(\omega)\frac{\sin \omega t}{\omega}d\omega \tag{2.70}$$

$$E(t) = E_e + \frac{2}{\pi}\int_0^\infty E''(\omega)\frac{\cos \omega t}{\omega}d\omega \tag{2.71}$$

$$E'(\omega) = E_e + \frac{2\omega^2}{\pi}\int_0^\infty E''(\lambda)\frac{1}{\lambda(\omega^2 - \lambda^2)}d\lambda \tag{2.72}$$

$$E''(\omega) = \frac{2\omega}{\pi}\int_0^\infty [E'(\lambda) - E_e]\frac{1}{\lambda^2 - \omega^2)}d\lambda \tag{2.73}$$

Equations 2.72 and 2.73 are known as Kronig-Kramers relations; the integrals are to be interpreted as Cauchy principal values. The Carson transforms of Equations 2.70 and 2.71 are,

$$\tilde{E}(s) = \frac{2s}{\pi}\int_0^\infty E'(\omega)\frac{1}{s^2 + \omega^2}d\omega \tag{2.74}$$

$$\tilde{E}(s) = E_e + \frac{2s^2}{\pi}\int_0^\infty E''(\omega)\frac{1}{\omega(s^2 + \omega^2)}d\omega \tag{2.75}$$

Schapery (1982) presented the relationship between a viscoelastic transient function $\psi(t)$ and its corresponding Carson transform $s\overline{\psi}$. The following relationship

between this transform and the transient function with logarithmic independent variables is derived.

$$\hat{f}(u) = \int_{-\infty}^{\infty} g(w)\ f(w-u)\ dw \qquad (2.76)$$

Here, $\hat{f}(u) \equiv s\overline{\psi}(s)$, $f(v) \equiv \psi(t)$, $\overline{\psi}(s) \equiv \int_0^{\infty} \psi(t) e^{-st} dt$, $g(w) \equiv (\ln 10) 10^{w} \exp(-10^{w})$, $u \equiv \log s$, $v \equiv \log t$, and $w = u + v$. The weight function $g(w)$ is small outside of a roughly two-decade range $-1.25 \le w \le 0.75$ centered at the centroid $w_c \equiv \log(e^{-C}) \cong -0.25$. This indicates, the value of a Carson transform at a particular *s*-value is dictated primarily by the variation of the corresponding transient function within the *t*-range of $-\log s - 1 < \log(t/\alpha) < -\log s + 1$, where $\alpha = e^{-C} \cong 0.56$. If the weight function is replaced by a Dirac delta function $\delta(w - w_c)$, an approximate inversion formula, $f(w_c - u) \cong \hat{f}(u)$, is obtained. Equivalently, $\psi(t) \equiv s\overline{\psi}(s)|_{s=(\alpha/t)}$ in terms of original function can be obtained. This result is easily shown to be exact when $s\overline{\psi}$ is linear in $\log s$ for all $s > 0$.

In view of the narrow-band character of the weight function, the relationship will be a good approximation for a function $\psi(t)$, that can be approximated on a logarithmic time scale by piecewise straight lines that are two decades wide. An improved approximation that accounts for curvature was given later by Schapery. Equation 65 follows from a similar argument if $\psi \sim t^{n}$ and n is a slowly varying function of $\log t$. Schapery also observed that integrals like that in Equation 74 may be approximated in a

similar fashion (if *n* is not close to -1) because they too can be expressed in terms of a narrow band weight function.

In deriving Equation 66, Christensen (1982) used an approximation of the weight function, $(\sin \omega t)/\omega$, in Equation 70 by replacing it with $(\pi/2)\delta(\omega-\omega_0)$ where $\delta(\cdot)$ is the Dirac delta function. The parameter ω_0 was determined by assuming that $E'(\omega)$ is a linear function of ω in the neighborhood of ω_0, and $\omega_0 = 1/(\pi t)$ resulted. The definite integral $\int_0^\infty (\sin \eta/\eta)\, d\eta = \pi/2$ was used to determine the normalizing factor $\pi/2$.

2.9.5.3 Expanded Theory Proposed by Schapery and Park

Schapery and Park (1999) expanded the above ideas discussed in the previous section by placing emphasis on material functions of the power law type, t^n or ω^n, where *n* is a slowly varying function of log*t* or $\log \omega$ and in the range of $-1 < n < 1$; this latter restriction assures convergence of the relevant integrals and covers almost all cases of practical interest.

The relaxation modulus can be written in the following form –

$$E(t) = E_n \left(\frac{t}{t_n} \right)^{-n} [1 + F(t)] \tag{2.77}$$

where $E(t) \equiv E(t_n)$. For a pure power law representation $F \equiv 0$. The function F accounts for an arbitrary departure from a power law; the time t_n is the time at which the negative of

the slope, $n \equiv -d \log E / d \log t$, is evaluated. Considering the definition of E_n and *n*, it follows form of Equation 77 that –

$$F(t_n) = \frac{dF}{dt}(t_n) = 0 \tag{2.78}$$

The Carson transform of Equation 77 is –

$$\tilde{E}(s) = E_n \, \Gamma(1-n)(st_n)^n \left[1 + c_n\right] \tag{2.79}$$

where

$$c_n \equiv s^{1-n} \int_{-\infty}^{\infty} F \, t^{1-n} \, e^{-st} \, d(\ln t) / \Gamma(1-n) . \tag{2.80}$$

c_n is the relative correction due to the departure from a pure power law. If c_n is neglected, and we choose $t_n = 1/s$, then Equation 79 may be written in the form,

$$\tilde{E}(s) = \Gamma(1-n) \, E(t) \quad \text{with} \quad t = 1/s . \tag{2.81}$$

Equation 2.81 is equivalent to Equation 2.65 if *n* is constant. Both of the Equations 2.65 and 2.81 produce essentially the same results when *n* varies slowly. Equation 81 is better for its simplicity when two conversion steps are used as discussed below.

A better choice for t_n is a value that minimizes the correction c_n, given s. This choice depends on the value of *n* at the initially unknown time t_n. The value of $\log(s\,t_n)$ for the optimum t_n is estimated to be only a fraction of a decade in most cases (i.e., when

$n \le 0.5$), and the result depends on the initially unknown value of *n*. Motivated by these facts, Schapery and Park (1999) used $\log(s\,t_n) = 0$, although it is recognized that an iterative process could be used to reduce the error through a better choice of t_n.

The Carson transform $\tilde{E}$ in terms of E' is given in Equation 2.74. This integral may be approximated using arguments similar to those leading to Equation 2.81. The counterpart to Equation 2.76 is given as:

$$\hat{f}(u) = \int_{-\infty}^{\infty} h(w)\, f(w+u)\, dw \tag{2.82}$$

where $\hat{f}$ and *u* are as before; but here $f(v) \equiv E'(\omega)$, $v \equiv \log \omega$, $w \equiv v - u = \log(\omega / s)$, and the weight function $h(w)$ is:

$$h(w) \equiv \frac{2}{\pi} \frac{\ln 10}{(10^{-w} + 10^{w})} \tag{2.83}$$

The function $h(w)$ is symmetric with respect to $w = 0$, and is small outside a roughly two-decade range. A representation for E', analogous to that in Equation 2.77 is given as:

$$E'(\omega) = E'_n \left(\frac{\omega}{\omega_n} \right)^n \left[1 + F' \left(\frac{\omega}{\omega_n} \right) \right] \tag{2.84}$$

where $E'_n \equiv E'(\omega_n)$ and $n \equiv d \log E' / d \log \omega$. Neglecting the contribution of F' to the integral, together with selecting $\omega_n = s$, we find:

$$\tilde{E}(s) = \frac{E'(\omega)}{\cos(n\pi/2)} \quad \text{with} \quad \omega = s \,. \tag{2.85}$$

Equations 2.81 and 2.85 may be used to eliminate $\tilde{E}$, so that

$$E'(\omega) = \Gamma(1-n)\cos\left(\frac{n\pi}{2}\right)E(t) \qquad \text{with} \quad t = 1/\omega \,. \tag{2.86}$$

It has been assumed *n* in Equation 2.81 is essentially the same as *n* in Equation 2.85. This assumption depends on *n* varying slowly with log*t* or $\log\omega$.

Considering next the Carson-transform in terms of E'', as in Equation 85, it is seen that $(\tilde{E} - E_e)/s$ in terms of E''/ω is analogous to Equation 2.74. E''/ω is a monotone, decreasing function of ω. However, the magnitude of the log-log slope approaches two at high frequencies, which is far greater than that for E'; in fact, for a pure power law $(E''/\omega) \sim \omega^{-2}$, and the integral Equation 2.85 does not converge. Moreover, the optimum point of evaluation for ω_n is not close to *s* at intermediate frequencies near the point where the slope of E'' vanishes.

While recognizing the resulting approximations will be good over only a limited frequency range, Schapery and Park (1999) used Equation 2.85. Results like Equations 2.85 and 86 are found, but with the changes $E' \to E''$, $\tilde{E} \to \tilde{E} - E_e$, and $\cos \to \sin$. By combining these results, we find

$$E''(\omega) = \tan\left(\frac{n\pi}{2}\right)\left[E'(\omega) - E_e\right] \tag{2.87}$$

where the local slope is now

$$n \equiv \frac{d \log\left[E'(\omega) - E_e\right]}{d \log \omega} \tag{2.88}$$

Clearly, when $n \geq 1$, this result is not valid. Equation 52 will not be valid at very low frequencies.

As an alternative approach, Schapery and Park (1999) used a modified form of Equation 73,

$$E''(\omega) = \frac{2\omega}{\pi} \int_0^\infty E'(\lambda) \frac{1}{\lambda^2 - \omega^2} d\lambda \tag{2.89}$$

which also has a narrow band weight function. This form is obtained by recognizing that the part of the integral in Equation 2.73 involving E_e vanishes. Using Equation 84 but neglecting F'; then

$$E''(\omega) = \tan\left(\frac{n\pi}{2}\right) E'(\omega) \tag{2.90}$$

where now

$$n \equiv \frac{d \log E'(\omega)}{d \log \omega} \tag{2.91}$$

Equation 2.90 is not also valid for low frequency behavior. Also, Equations 2.87 and 2.90 do not predict the correct limiting behavior for $\omega \to 0$. However, simple exact

expressions may be derived from Equation 2.73 for the low and high frequency limits. The authors found:

$$E''(\omega) \to c_1 \omega \qquad \text{as} \qquad \omega \to 0 \tag{2.92}$$

and

$$E''(\omega) \to \frac{c_2}{\omega} \qquad \text{as} \qquad \omega \to \infty \tag{2.93}$$

where

$$c_1 \equiv \frac{2}{\pi}\int_0^\infty \left[E'(\lambda) - E_e\right]\frac{d\lambda}{\lambda^2} \tag{2.94}$$

and

$$c_2 \equiv \frac{2}{\pi}\int_0^\infty \left[E_g - E'(\lambda)\right]d\lambda \tag{2.95}$$

where, E_g is the glassy modulus. The result in Equation 2.95 was obtained from Equation 2.73 by adding $E_e - E_g$ to the integrand; the step of adding a constant has no effect on the integral, but is needed to achieve convergence when $\omega \to \infty$. Equations 2.93 to 2.95 may be used with experimental data to complete the prediction of E'' when combined with Equations 2.87 or 2.90. If the Prony series constants are available, the following expression may be used to obtain c_1 and c_2 more simply.

$$E'(\omega) = E_e + \sum_{i=1}^{m} \frac{\omega^2 \rho_i^2 E_i}{\omega^2 \rho_i^2 + 1} \tag{2.96}$$

and

$$c_1 = \sum_{i=1}^{m} \rho_i E_i, \qquad c_2 = \sum_{i=1}^{m} E_i / \rho_i \tag{2.97}$$

2.9.5.4 New Approximate Interconversion Method Proposed by Schapery and Park

Equations 2.81, 2.85 and 2.90 may be combined and rearranged to summarize the set of approximate interconversions:

$$\tilde{E}(s) \cong \tilde{\lambda}\, E(t)\,|_{t=(1/s)} \qquad \text{or} \qquad E(t) \cong \frac{1}{\tilde{\lambda}} \tilde{E}(s)\,|_{s=(1/t)} \tag{2.98}$$

$$E'(\omega) \cong \lambda'\, E(t)\,|_{t=(1/\omega)} \qquad \text{or} \qquad E(t) \cong \frac{1}{\lambda'} E'(\omega)\,|_{\omega=(1/t)} \tag{2.99}$$

$$E''(\omega) \cong \lambda''\, E(t)\,|_{t=(1/\omega)} \qquad \text{or} \qquad E(t) \cong \frac{1}{\lambda''} E''(\omega)\,|_{\omega=(1/t)} \tag{2.100}$$

$$E'(\omega) \cong \hat{\lambda}\, \tilde{E}(s)\,|_{s=\omega} \qquad \text{or} \qquad \tilde{E}(s) \cong \frac{1}{\hat{\lambda}} E'(\omega)\,|_{\omega=s} \tag{2.101}$$

$$E''(\omega) \cong \bar{\lambda}\, \tilde{E}(s)\,|_{s=\omega} \qquad \text{or} \qquad \tilde{E}(s) \cong \frac{1}{\bar{\lambda}} E''(\omega)\,|_{\omega=s} \tag{2.102}$$

$$E''(\omega) \cong \lambda^*\, E'(\hat{\omega})\,|_{\hat{\omega}=\omega} \qquad \text{or} \qquad E'(\omega) \cong \frac{1}{\lambda^*} E''(\hat{\omega})\,|_{\hat{\omega}=\omega} \tag{2.103}$$

where the adjustment factors, $\tilde{\lambda}, \lambda', \lambda'', \hat{\lambda}, \bar{\lambda}$ and λ^* are given in Table 2.1 as functions of *n*. Relations in Equations 2.98 to 2.103 are exact when the material functions are described by pure power laws; however, these are shown as approximate relationships allowing for behavior which does not exactly obey a power law over $0 < t, s, \omega < \infty$. One should interpret *n* as the local, log-log slope of the source function at the specified position. For instance, for the case of Equation 98, $n = -d \log E(t) / d \log t$ at $t = 1/s$ when $E(t)$ is the source function, and $n = d \log \tilde{E}(s) / d \log s$ at $s = 1/t$ when $\tilde{E}(s)$ is the source function.

It is emphasized by Schapery and Park (1999) that the equations with E'' as the source function have a limited range of validity, but are given here for completeness. Also, they assumed that the *n*-value may be taken as the log-log slope of the source function, regardless of which function was used in the original development of the equation; e.g., $E(t)$ is the source function in Equation 81, but $\tilde{E}(s)$ is the source function in the second part of Equation 2.98. This procedure is valid for a slowly varying slope.

Now if we consider a power-law creep compliance,

$$D(t) = D_1 \, t^n \tag{2.104}$$

relations similar to Equations 2.77 to 2.103 hold for compliance functions when appropriate changes of parameters are made; i.e., $E_1 \to D_1$, $n \to -n$, $\tilde{E} \to \tilde{D}$, $E' \to D'$, and $E'' \to -D''$. It is noted that the sign change in $E'' \to -D''$ requires that the sign of *n* be

used because the argument of the trigonometric functions that appear in the λ -function definitions should not change when modulus and compliance are interchanged.

It is of interest to apply Equation 2.98 to both the modulus and compliance functions and use the exact relationship, $\tilde{E}(s)\,\tilde{D}(s)=1$. Assuming, as before, a local power law behavior, the process yields Ferry's (1980) equation,

$$E(t)\,D(t)=\Gamma(1-n)\,\Gamma(1+n)=\frac{\sin n\pi}{n\pi} \tag{2.105}$$

where *n* is again the local log-log slope. This equation has been found to be very accurate for broadband functions, as reported by Ferry (1980).

Finally, for viscoelastic solids, Schapery and Park noted that the nonzero equilibrium modulus E_e must be explicitly added to the far right-hand sides of Equations 2.100, 2.102 and 2.103 to obtain good results as $t\to\infty$ and $s,\omega\to 0$ if *E"* is the source function. This is certainly clear because *E"* is independent of E_e. More generally, the exact interrelationships in Equations 2.71, 2.72 and 2.75 show that E_e is to be added to the integrals containing *E"*. In this context, the Equations 2.100, 2.102 and 2.103 can be improved as:

$$E''(\omega)\cong\lambda''\left[E(t)-E_e\right]|_{t=(1/\omega)} \quad \text{or} \quad E(t)\cong E_e+\frac{1}{\lambda''}E''(\omega)\,|_{\omega=(1/t)} \tag{2.106}$$

$$E''(\omega)\cong\bar{\lambda}\left[\tilde{E}(s)-E_e\right]|_{s=\omega} \quad \text{or} \quad \tilde{E}(s)\cong E_e+\frac{1}{\bar{\lambda}}E''(\omega)\,|_{\omega=s} \tag{2.107}$$

$$E''(\omega) \cong \lambda * [E'(\hat{\omega}) - E_e]|_{\hat{\omega}=\omega} \quad \text{or} \qquad E'(\omega) \cong E_e + \frac{1}{\lambda *} E''(\hat{\omega})|_{\hat{\omega}=\omega} \tag{2.108}$$

where the adjustment factors λ'', $\bar{\lambda}$ and $\lambda*$ are as defined above as functions of *n*; however, the log-log slope *n* in this cases is defined as $d\log E''/d\log\omega$ when E'' is the source function, or as $-d\log(E-E_e)/\log t$, $d\log\left(\tilde{E}-E_e\right)/\log s$ or $d\log(E'-E_e)/\log\omega$ when $E, \tilde{E}$ or E' are the source functions, respectively. Equations 2.106, 2.107 and 2.108 can be shown to be exact when *n* is constant.

As mentioned above, the modified Equations 2.106, 2.107 and 2.108 must be used to obtain $E, \tilde{E}$ or E' from E'' when $t \to \infty$ and $s, \omega \to 0$. However, when E'' is to be predicted, the modified equations are found to offer only a small improvement over Equations 2.100, 2.102 and 2.103.

2.10 Dynamic Modulus from Falling Weight Deflections

Falling weight deflection test is a popular test for evaluating pavement properties. A process of back calculation can be used to determine *E** from FWD test data. Varma et al. (2013) used a viscoelastic genetic algorithm for inverse analysis of asphalt layer properties such as relaxation modulus, dynamic modulus from falling weigh deflections. Most back calculation methods assume the pavement to be layered elastic half-space. However, asphalt pavements behave more like multilayered visco-elastic systems in response to small or short duration load applications. According to Varma et al. (2013) the elastic analysis cannot produce the viscoelastic properties of the asphalt concrete layer. In their study, the

FWD load-response history of a single FWD drop and variation in temperature along the depth of AC layer during the drop are used to perform analysis. Varma et al. offered a genetic algorithm based optimization scheme to search for the pavement properties. A brief picture of the study by Varma et al. (2013) is given in the following paragraphs.

In Varma et al. (2013) proposed approach the asphalt pavement system is modeled as a layered half-space, with the top layer being linear visco-elastic solid. The base, sub-base, sub-grade, and bed rock are assumed linear elastic. The visco-elastic properties to be back calculated from FWD data include two functions: a time function and a temperature function. The time function refers to the relaxation modulus $E(t, T_0)$. The temperature function refers to the time-temperature shift factor a_T. The shift factor a_T allows applying $E(t, T_0)$ for any temperature level T by simply replacing physical time with a reduced time $t_R = \frac{t}{a_T}$; therefore a_T is a function of both T and T_0 such that when $a_T = 1, T = T_0$.

The primary component of Varma et al. (2013) proposed back calculation procedure is a layered viscoelastic forward solution. The authors used layered viscoelastic algorithm called LAVA to support the back-calculation algorithm called BACKLAVA. The forward solution, LAVA, assumes that the viscoelastic response due to a Heaviside function, at any time t, can be approximated by a corresponding elastic solution calculated using the relaxed modulus at that time.

$$R_H^{ve}(t, r, z) \cong R_H^e(E(t), r, z) \tag{2.109}$$

where, $R_H^{ve}(t, r, z)$ denotes a visco-elastic response at time t for a point located at coordinates r, z and, $R_H^e(E(t), r, z)$ is the corresponding elastic response for the same point

and for the same problem configuration. The time argument is inserted into the elastic solution via the viscoelastic material property $E(t)$. The 'response' refers to a surface deflection due to a unit FWD stress that is applied as a step function. Consequently, the viscoelastic deflection history due to a time-varying FWD stress $\sigma(t)$ can be obtained from Equation 109 using the convolution integral. Equation 110 is a discrete form of the convolution integral, in which the varying FWD stress is approximated by M stress-steps. The coordinate dependency omitted for clarity.

$$R^{ve}(t_i) = \sum_{j=0}^{M} R_H^{ve}\left(t_i - \tau_j\right) \Delta\sigma\ (\tau_j) \qquad i = 1,2,3, \dots N \qquad (2.110)$$

where, t_i are the times for which the surface deflection history R^{ve} at a point is calculated; τ_j are the timing of the discrete stress-steps. The response obtained from the forward analysis is then matched with response obtained from the FWD test. The difference between these two is then minimized by manipulating the layer properties of the system until best match is achieved.

In the study by Varma et al. (2013) the asphalt concrete properties are represented by a sigmoid function containing four parameters for $E(t)$ and by a polynomial containing two parameters for a_T. Hence, it is naturally expected that the probability of multiple local solutions will increase. Among various optimization techniques, Genetic Algorithm was chosen because of its capability to converge to a unique global minimum solution, irrespective of the presence of local solutions. The genetic algorithm performs: the initialization, selection, generation of offspring, and termination. In initialization, the genetic algorithm generates a pool of solutions using a subset of the feasible search space,

so-called ‘population’. Each solution is a vector of feasible variable values. In selection process, each solution is evaluated using an objective function, and the best fitted solutions are selected. The selected solutions are then used to generate next generation population (offspring). This process mainly involves two operators: crossover and mutation. In crossover, a new solution is formed by exchanging information between two parent solutions, which is done by swapping a portion of parent vectors. In mutation, a new solution is formed by randomly changing a portion of parent solution vector. The newly generated population is evaluated using the objective function. This process is repeated until a termination criterion is reached. Through guided random search from one ‘generation’ to another, genetic algorithm minimizes the desired objective function. The formulation of the optimization model using genetic algorithm is given as:

$$Minimize \qquad Er = \sum_{k=1}^{m} 100 \sum_{i,o=1}^{n} \frac{\left|d_i^k - d_0^k\right|}{(d^k)_{max}}$$

$$Subject\ to$$

$$c_1^l \leq c_1 \leq c_1^u, c_2^l \leq c_2 \leq c_2^u, c_3^l \leq c_3 \leq c_3^u, c_4^l \leq c_4 \leq c_4^u \tag{2.111}$$

$$E_b^l \leq E_b \leq E_b^u, E_s^l \leq E_s \leq E_s^u$$

$$d_s^l \leq d_s \leq d_s^u$$

$$a_1^l \leq a_1 \leq a_1^u, a_2^l \leq a_2 \leq a_2^u$$

where, Er is the error to be minimized, m is the number of FWD sensors, d_i is the input deflection information obtained from field at sensor k, d_0^k is the output deflection

information obtained from forward analysis at sensor k, $(d^k)_{max}$ is the peak response at sensor k, n is the total number of deflection data points recorded by a sensor, and c_i and a_i are values of sigmoid and shift factor coefficients, E_b is base modulus, E_s is subgrade modulus, d_s is depth to stiff layer, and the superscripts l and u represent lower and upper limits of the parameter.

The relaxation modulus is assumed to follow a sigmoid shape with the following equation:

$$\log\big(E(t)\big) = c_1 + \frac{c_2}{1+\exp(-c_3-c_4\log(t_R))} \tag{2.112}$$

where, t_R is reduced time, defined as $t_R = t/a_T(T)$. The logarithm of the shift factor is computed using a second order polynomial given by the following expression:

$$\log\big(a_T(T)\big) = a_1(T - T_0)^2 + a_2(T - T_0). \tag{2.113}$$

Therefore, six coefficients are needed to represent the relaxation properties of the asphalt concrete layer, including the temperature dependency. Also, the theory of viscoelasticity states that if one of the following linear viscoelastic properties is known: complex modulus (*E**), creep compliance (*D(t)*), or relaxation modulus (*E(t)*), the others can be calculated through numerical interconversion procedures.

Table 2.1 Adjustment functions used in new approximate interconversion method

Ratios	Adjustment Functions
$\tilde{\lambda} = \tilde{E}(s)/E(t)$	$\tilde{\lambda} = \Gamma(1-n)$
$\lambda' = E'(\omega)/E(t)$	$\lambda' = \Gamma(1-n)\cos(n\pi/2)$
$\lambda'' = E''(\omega)/E(t)$	$\lambda'' = \Gamma(1-n)\sin(n\pi/2)$
$\hat{\lambda} = E'(\omega)/\tilde{E}(s)$	$\hat{\lambda} = \cos(n\pi/2)$
$\bar{\lambda} = E''(\omega)/\tilde{E}(s)$	$\bar{\lambda} = \sin(n\pi/2)$
$\lambda^* = E''(\omega)/E'(\omega)$	$\lambda^* = \tan(n\pi/2)$

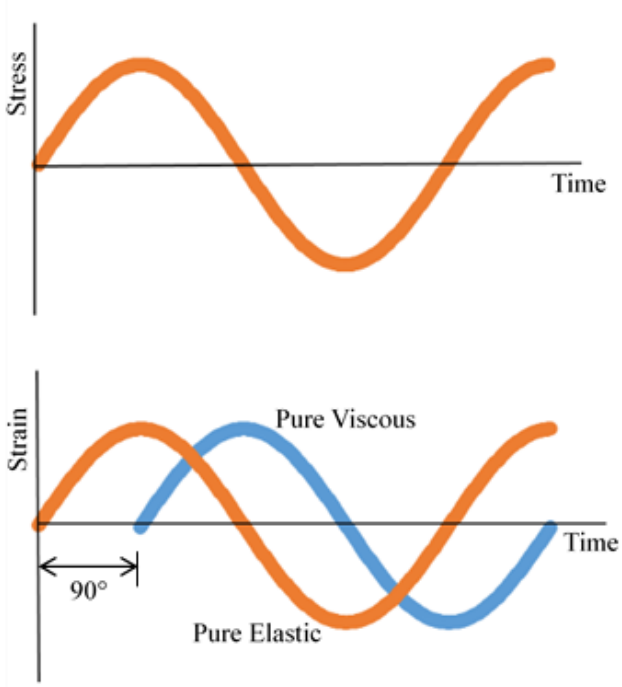

Figure 2.1 Elastic and viscous material response with time due to sinusoidal applied stress.

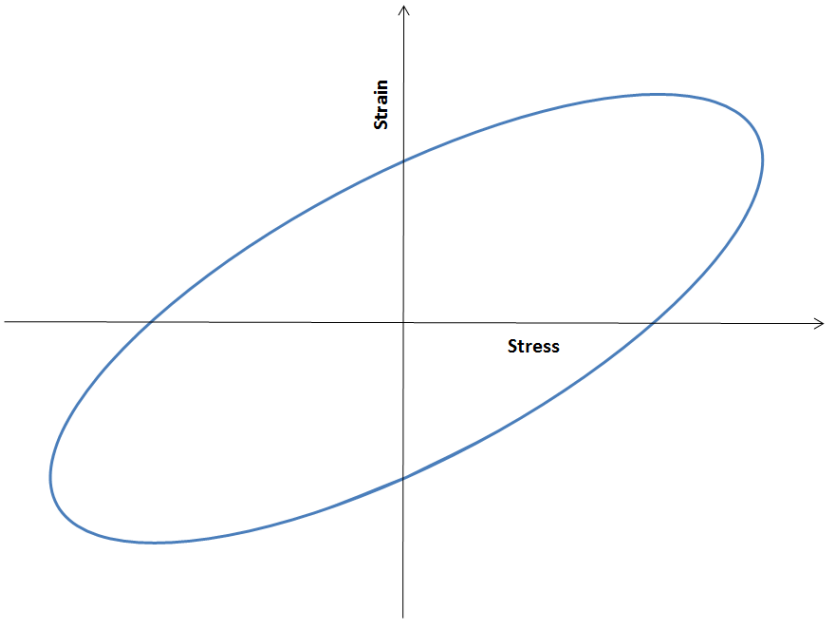

Figure 2.2 Stress versus strain plot for viscoelastic material (Lissajous curve).

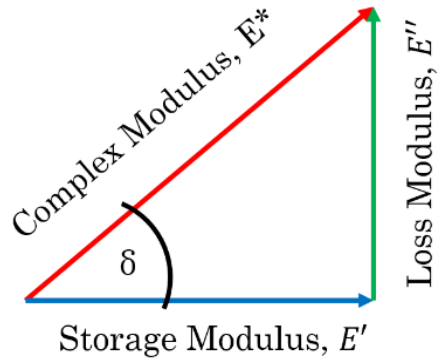

Figure 2.3 Relationship among complex, storage, and loss moduli.

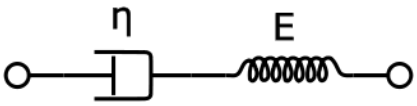

Figure 2.4 Spring and dashpot in series: Maxwell Material.

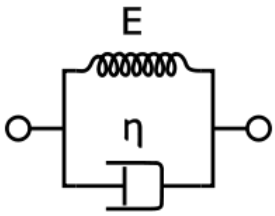

Figure 2.5 Spring and dashpot in parallel: Kelvin material.

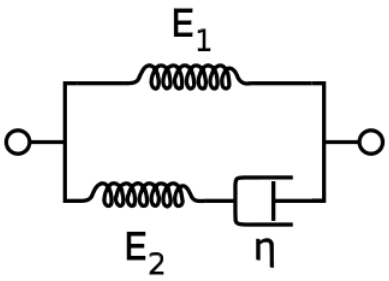

Figure 2.6 Standard Linear Solid model.

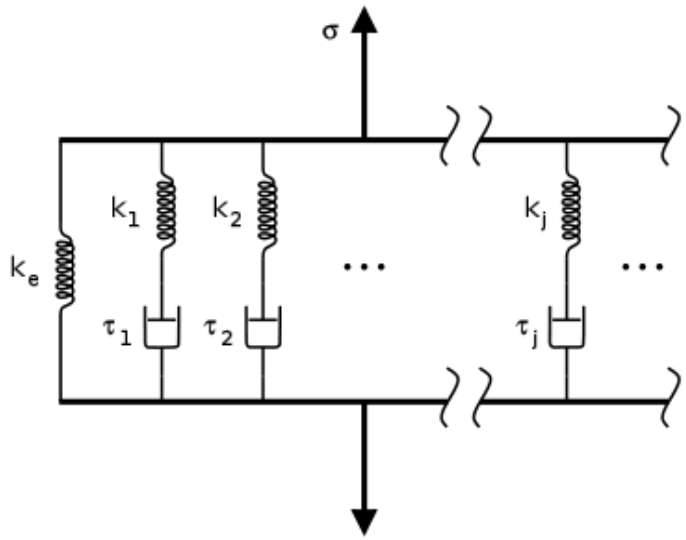

Figure 2.7 Generalized Maxwell or Maxwell-Wiechert model.

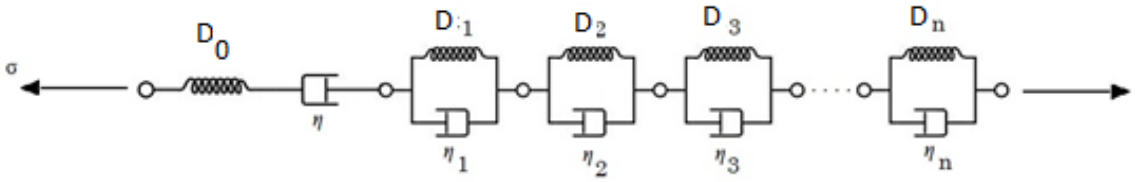

Figure 2.8 Generalized Voigt model.

Chapter 3

Dynamic Modulus Testing for New Mexico Superpave Mixes

3.1 Introduction

This chapter presents a brief summary of the materials used in this study. Besides, a detail depiction of test specimen preparation and hence, dynamic modulus ($|E^*|$) testing of New Mexico's asphalt concrete mixes are also presented in this chapter. The use of $|E^*|$ is pretty common for quantifying mechanical behavior of any viscoelastic material. However, its use for characterizing asphalt concrete (AC) is relatively new. The standard test protocol, designated as, AASHTO T 342 "Standard Method of Test for Determining Dynamic Modulus of Hot-Mix Asphalt (HMA)" published by the American Association of State Highway and Transportation Officials (AASHTO) is used to conduct $|E^*|$ tests on New Mexico's Superpave AC mixtures.

3.2 Selection of Materials

Tables A-1 through A-6 in Appendix A summarize the information regarding AC mixtures from the six regional districts of New Mexico Department of Transportation (NMDOT) used in this study for $|E^*|$ testing. Figure 3.1 shows the New Mexico counties and the boundaries of the regional districts. A total of 54 AC mixtures from six districts are selected for this study. All the AC mixtures are plant mixed Superpave mixes. Figure 3.2 shows the material matrix tested for this study. Three types of aggregate gradations according to AASHTO MP 2 (2001), defined by the 12.5 mm (SP IV) and 19.0 mm (SP III) nominal

maximum aggregate sizes (NMAS) were considered. Also, two types of materials with 19.0 mm NMAS, coarse and fine gradations, were considered for this study. In case of AC binders, three grades of binders, namely, PG 64-22 or lower, PG 70-22, and PG 76-22 or higher grades were considered for each of the NMDOT districts. For each of the individual AC mix three replicate specimens were tested for developing average |*E**| mastercurves. The target air void content was set to 5.5±0.5% for each specimen. This range of air void content is believed to be most representative of the field compaction level and therefore used in this study.

3.2.1 Materials from NMDOT District 1

Table A-1 summarizes the plant produced AC materials used in this study from the NMDOT district 1. In general, a total of 8 AC mixtures collected and used in this study from this district. Four of these AC mixtures are Superpave mixtures with 12.5 mm nominal maximum aggregate size (NMAS), widely known as SP IV mixtures. The other four mixtures are Superpave mixtures with 19.0 mm NMAS, widely known as SP III mixtures.

3.2.2 Materials from NMDOT District 2

Table A-2 summarizes the plant produced AC materials used in this study from the NMDOT district 2. In general, a total of 9 AC mixtures used in this study from this district. Three of these AC mixtures are SP IV mixtures and six of these mixtures are SP III mixtures.

3.2.3 Materials from NMDOT District 3

Table A-3 summarizes the plant produced AC materials used in this study from the NMDOT district 3. In general, a total of 11 AC mixtures used in this study from this district. Three of these AC mixtures are SP IV mixtures and other eight of these mixtures are SP III mixtures.

3.2.4 Materials from NMDOT District 4

Table A-4 summarizes the plant produced AC materials used in this study from the NMDOT district 4. In general, a total of 11 AC mixtures used in this study from this district. All of these mixtures are SP III mixtures.

3.2.5 Materials from NMDOT District 5

Table A-5 summarizes the plant produced AC materials used in this study from the NMDOT district 5. A total of 5 AC mixtures used in this study from this district. Two of these AC mixtures are SP IV mixtures and other three of these mixtures are SP III mixtures.

3.2.6 Materials from NMDOT District 6

Table A-6 summarizes the plant produced AC materials used in this study from the NMDOT district 6. A total of 10 AC mixtures used in this study from this district. Only one of these AC mixtures is SP IV mixture and all others are SP III mixtures.

3.3 Mix Collection and Sample Preparation

3.3.1 Mix Collection

The AC mixtures of different Superpave gradation with different performance grades (PG) from various NMDOT districts are collected directly from the plant or from the paving sites in cooperation with the New Mexico Department of Transportation (NMDOT) research bureau. The sampling was performed as per the requirements of AASHTO T-168: "Standard Method of Test for Sampling Bituminous Paving Mixtures". For each mix, approximately 20 bags of sample (10-12 kg each) were collected from the plant or from on-going construction site of NMDOT projects. Approximately, 1080 (54 mixes x 20 bags) bags of AC materials were collected for this study. In addition to the mix collection, virgin aggregates, binders and recycled asphalt samples for most of the AC mixtures considered in this study are also collected. Sampling of aggregates and reclaimed asphalt pavement (RAP) were done according to AASHTO T-2: "Standard Method of Test for Sampling of Aggregates" (2011). Also, binder samples for most of the AC mixtures considered in this study were collected either from the mixing plant or from the manufacturing plant in paint cans.

3.3.2 Sieve Analysis Test

For every 6 AC samples, one sieve analysis test was conducted according to the AASHTO T-27: "Standard Method of Test for Sieve Analysis of Fine and Coarse Aggregates" standard specification. These tests were conducted to check if the aggregate gradations of the AC mixtures are in accordance to the mix designs.

3.3.3 Asphalt Content Test

One asphalt content test for every 6 AC mixtures are also conducted to ensure the presence of specified amount of asphalt in the mix designs of the AC mixtures. The tests were conducted in accordance to the AASHTO T 308: "Standard Method of Test for Determining the Asphalt Binder Content of Hot Mix Asphalt (HMA) by the Ignition Method" standard specification.

3.3.4 Theoretical Maximum Specific Gravity (G_{mm})

The theoretical maximum specific gravity (G_{mm}) of the AC mixtures is determined according to the AASHTO T-209: "Standard Method of Test for Theoretical Maximum Specific Gravity (G_{mm}) and Density of Hot-Mix Asphalt (HMA)" standard specification.

3.3.5 Sample Preparation

A Superpave Gyratory Compactor (SGC) is used to compact AC sample in accordance to the standard specification provided by AASHTO T 312: "Standard Method of Test for Preparing and Determining the Density of Asphalt Mixture Specimens by Means of the Superpave Gyratory Compactor". Figure 3.3 shows a picture of the SGC used in this study to compact AC mixtures. The use of SGC for compacting |E^*| test specimen preparation is a popular method as it produces AC specimens with similar characteristics as in the field. The compactor is equipped to set the maximum number of gyration of the mold or a minimum height requirement for the sample inside the mold. Any of these criteria can rule out further compaction of the specimen, allowing a good control over the air void requirement of the sample.

The SGC is used to compact AC samples with 150 mm in diameter and 170 mm in height. Figure 3.4 shows a picture of a typical compacted sample. The compaction temperature used to achieve viscosity of 280±30 is selected per the recommendation provided by the binder manufacturer. Several trial specimens are prepared with the aim of achieving 5.5±0.5% air void for the inside core. The material weight used for compaction is approximately 6500 gm. Compacted samples were cooled off and left for about 16 hours to be hardened.

3.3.6 Coring and Trimming

Asphalt samples with 100 mm in diameter were cored out of the 150 mm in diameter SGC compacted samples using GCTS core-drill equipment. Figure 3.5 shows the core-drill equipment used in this study. The core-drill equipment is cooled down by flowing water. A diamond edged drilling barrel is used for drilling out 100 mm diameter AC samples. The rate of coring is controlled by a hydraulic press system and a 1.5 HP electric motor with adjustable spindle speed control the drilling process. Figure 3.6 shows a typical AC specimen cored out of a compacted specimen.

The GCTS Lab Specimen Saw (RLS-3HA) is used to trimmed off the edges of core-drilled asphalt samples using a diamond cutting edge wet saw. The device is built with stainless steel bearing guide rollers to guide the vise carriage smoothly on precision ground. This machine has a mechanism to use water to cool down the blade without affecting the asphalt sample. A hydraulic feed allows control of cutting speed without slowing down the blade RPM for better cuts. The whole assembly is completely covered with a rectangular

hood for safety. Figure 3.7 presents a picture of this saw currently housed in UNM laboratory. Figure 3.8 shows a typical AC specimen after coring and trimming.

3.3.7 Determining Bulk Specific Gravity (G_{mb})

The bulk specific gravity of the AC specimens was determined according to the standard specification designated by AASHTO T 166: "Standard Method of Test for Bulk Specific Gravity (G_{mb}) of Compacted Hot Mix Asphalt (HMA) Using Saturated Surface-Dry Specimens". The G_{mb} and G_{mm} are required to determine the air void content of the finished AC specimens.

3.3.8 Determining Air Void Content

To determine the air void contents of the AC specimens, the theoretical maximum specific gravities (G_{mm}) of the AC mixtures and bulk specific gravities (G_{mb}) of the AC specimens were utilized. The following equation is used to estimate the air void content of each AC specimens considered in this study.

$$A_v\,(\%) = \left(1 - \frac{G_{mb}}{G_{mm}}\right) \times 100 \qquad (3.1)$$

3.3.9 Geometric Requirements for the Test Specimens

In addition to the target air void content, the AC test specimens prepared in the earlier steps should meet the geometric requirements suggested by the test protocol AASHTO T 342: "Standard Method of Test for Determining Dynamic Modulus of Hot-Mix Asphalt Concrete Mixtures". The geometric requirement which should be checked according to

AASHTO T 342 are the diameter, height, end perpendicularity and waviness of the AC specimens.

3.3.9.1 Diameter Requirements

The diameters of each of the specimens are measured at the top, middle and bottom sections along two 90-degree apart axes. The means and standard deviations of these six measurements were then compared with the AASHTO T 342 diameter requirements. The average diameter, as per the AASHTO T 342 requirements, should be between 100 and 104 mm. The standard deviation, for the average of the six measurements recorded to the nearest 1.00 mm, should be less than 2.5 mm. An electronic slide calipers is used in this purpose.

3.3.9.2 Height Requirements

The heights of each AC specimens are measured at locations 120° apart around the centroidal axis and recorded. According to AASHTO T 342, the average height at locations 120° apart of the cored and sawed cylindrical specimen for dynamic modulus test should be between 147.5 and 152.5 mm. An electronic slide calipers is used for measuring heights.

3.3.9.3 Waviness and Perpendicularity Requirements

The ends of all AC specimens are checked for perpendicularity and waviness requirements as suggested by the AASHTO T 342 test protocol. The required waviness requirement according to AASHTO T 342 for any sample should be checked on three different axes which are 120° apart. The maximum differential height across any diameter on these axes

is 0.05 mm. This is checked using a straight edge and feeler gauges. A picture showing the straight edge and feeler gauges is presented in Figure 3.9. Again, according to AASHTO T 342 standard, the specimen edge should not deviate from 90° by more than one degree. This need to be checked on three axes which are 120° apart. A device called rock flatness gauge is used for this purpose which is shown in Figure 3.10.

3.3.10 Fixing LVDT Mounting Buttons

All the AC specimens meeting target air void and geometry requirements were supplied to the GCTS Automatic Positioning Fixture (GPF-100) fix loading buttons to mount the Linear Variable Different Transducers (LVDTs). Polymer epoxy was used to glue the loading buttons on the AC specimens. The gauge length was maintained 100 mm (50 mm away from the mid-section of the specimen) as per AASHTO T 342 specification. The device used for fixing loading buttons allows easy specimen preparation for dynamic modulus testing. Figure 3.11 presents a picture of the automatic loading button positioning fixture.

3.4 Dynamic Modulus Testing System

The pavement laboratory at University of New Mexico, is equipped with GCTS ATM-025 (GCTS 2013) Servo-Hydraulic testing system capable for performing Dynamic modulus test. Figure 3.12 shows a picture of the testing system. The GCTS ATM-025 is a modular system thus can be configured to test asphalt concrete in a variety of testing modes. The machine is capable of producing controlled sinusoidal compressive loading up to 100 Hz frequency. The top actuator has a dynamic load capacity of 25 kN and a stock of the top actuator 100mm. The system is also equipped with an environmental chamber capable of

controlling temperature ranging between -30 °C to +150 °C. The system has its own air conditioning unit and the temperature in the chamber can be controlled with an accuracy of ±0.5°C. A picture of the environmental chamber and the conditioning unit is presented in Figure 3.13.

The GCTS ATM-025 is controlled with a digital servo controller SCON-2000. It has a capacity of controlling up to 24 sensors within its reach. The control system has a maximum of 6 Hz loop rate and 300 kHz conversion rate between channels. It provides automatic dynamic control mode switching between any connected transducer. Adaptive controller system in GCTS ATM-025 allows the system to precisely match the desired cyclic stress amplitudes throughout the tests. Figure 3.14 presents the pictures of the SCON-2000 controller.

The GCTS ATM-025 system can be connected to two load cells. For dynamic modulus testing top actuator is connected with a load cell that is capable of measuring loads up to 25 kN. The bottom actuator is used with a load cell that has a maximum capacity of 100kN. The resolution of the top actuator load cell is 5 N. Spring loaded LVDTs are used for conducting the dynamic modulus testing in this study. The range of these LVDTs is ± 0.5mm and the resolution is 0.0025mm. A picture of the top actuator and the load cell is given in Figure 3.15.

3.5 Test Setup

Currently the use of spring loaded LVDTs are recommended in the AASHTO T 342. This instrumentation can be used for both confined and unconfined conditions. AASHTO T 342 recommends measuring deformations at a minimum of two locations 180° apart. By

increasing the LVDTs to three locations located 120° apart the required number of replicates for testing can be reduced. LVDT mounting buttons are glued to the specimen using epoxy. The gauge length is maintained to be 100 mm and the Automatic Positioning Fixture is used to fix LVDT mounting buttons 50 mm away from the mid height of the specimen. Figure 3.16 shows a picture of the LVDTs mounted on an asphalt concrete test specimen. End treatments are used instead of capping between specimen ends and platens. Even though, Capping is recommended in the ASTM test standard for dynamic modulus, Witczak et al. (2000) recommends avoiding capping and using friction-reducing treatments between the specimen ends and the platens. The recommended end treatments in the AASHTO T 342 test standard is to use a sandwich of two 0.5-mm-thick latex sheets separated with silicone paper or vacuum grease.

3.6 Test Procedure

The axial LVDTs (LVDT attached to extensometer) are attached to the specimen and adjusted to extend up to at least the middle of the linear range to make sure that enough of the range is available for the accumulation of permanent deformation. The specimen is then conditioned to reach the desired temperature. This is achieved by keeping the specimen in the environmental chamber and allowing it to equilibrate to the specified testing temperature. AASHTO T 342 specification recommended the minimum time to reach equilibrium for each of the test temperatures. A dummy specimen with a thermocouple cored in to the center is also used to monitor and justify the specimen temperature. The specimen is then placed on the base platen. While placing caution need to be taken to avoid eccentric loading on the sample. For this reason, it is needed to be ensured that the sample

and the top platen and concentric with the top actuator loading point. A contact load equal to 5 percent of the dynamic load is then applied. The uniformity of the load over the specimen is then checked at the conditioning stage by applying approximately 50 percent of the required load and observing the response from the LVDTs. The position of the specimen is moved and adjusted very carefully to balance the LVDT measurements until the AASHTO T 342 recommended uniformity is reached. Once the deformations are uniform, the full haversine loading is applied to the specimen. The full dynamic load is adjusted to produce axial strains of about 55-60 micro-strains. The AASHTO recommended stain range is 50 to 150 micro-strains. This is to avoid excessive damage of the sample by producing more permanent deformation. The dynamic load increases as the stiffness increases which in turn increases as the temperature decreases. The general range recommended for the entire dynamic modulus test over all temperatures is between 15 and 2800 kPa. A two-minute rest period between frequencies in the frequency sweep is applied during testing. This is mainly because the controller used cannot produce continuous frequency sweeps and each frequency is programmed separately in such a manner that there will be some time-lag or rest period between each loading frequency. According to Kim (2009), even though applying rest period helps to prevent specimen from heating up too much during cyclic testing the application of rest period allows some of the transient strains to recover during testing which may have some effect on the measured modulus values and selection of suitable data analysis methods.

Dynamic modulus testing was conducted at -10, 4.4, 21.1, 37.8, and 54.4 °C (14, 40, 70, 100 and 130°F) at loading frequencies of 0.1, 0.5, 1, 5, 10, and 25 Hz at each

temperature. Testing is conducted starting from the lowest to the highest temperature. Within each temperature testing is conducted staring at the highest frequency and proceeding to the lowest frequency. This combination of test temperature and frequency is recommended in the AASHTO T 342 for constructing the mastercurve.

3.7 Test Results

3.7.1 Raw Data

The displacements of the three LVDTs is recorded and stored separately. However, for the calculation of strain the average of all the LVDT-deformations is taken into account. Before the tests are performed, the AASHTO requirements for specimen geometry are checked for the perpendicularity, waviness and accuracy of dimensions. The displacement data collected from the LVDTs are divided by the axial gage length to get the actual axial strain. For each test temperature and frequency combination data points are collected and stored for the last five cycles. To store data in a systematic manner, the GCTS software called CATS provides a data organization scheme by generating individual folders for project. In the project folder, it generates sample folder for each mix sample. Again, in the sample folder it generates specimen folder for each of the test specimen. This is done to ease test data retrieving afterward. Within each sample folder, data files are named by specimen type and number. It is important to note that the specimen names are test data files. Therefore, with in each sample folder the data files are created for each test sample-temperature combination. Each data file collects the required data for all frequencies under the test temperature. The data is arranged from 25 Hz and ends at 0.1 Hz for each of the test temperatures.

3.7.2 Stress-Strain Data

The stress and strain data obtained from feedback signal is not perfectly sinusoidal. This is because of the test equipment limitations. The noise in the feedback signal accompanied with the recoverable deformation and permanent deformation affect the computed modulus and phase angle values. Kim (2009) introduced many analysis methods to deal with these discrepancies. However, to conduct the analysis, the GCTS software can be used. The GCTS CATS software uses the AASHTO T 342 analysis method. The AASHTO T 342 employs a method to transform and fit the discrete time-stress data and time strain data to a sinusoidal function. Then dynamic modulus values are calculated by determining the stress amplitude and strain amplitude from the fitted sinusoidal curve. The phase angle is determined by determining the difference of the phase angles of the strain and stress sinusoidal fit curves. All calculations are made from the last five loading cycles.

The peak stress (σ_o) is defined as:

$$\sigma_o = \frac{\bar{P}}{A} \tag{3.2}$$

where, $\bar{P}$ is average of the load amplitudes for the last five loading cycles; A is the cross-sectional area of the specimen.

Recoverable axial strain (ε_o) is defined as:

$$\varepsilon_o = \frac{\bar{\Delta}}{GL} \tag{3.5}$$

where, $\bar{\Delta}$ is average of the deformation amplitudes for the last five loading cycles; GL is the gauge length.

Dynamic Modulus $|E^*|$ is defined as:

$$|E^*| = \frac{\sigma_o}{\varepsilon_o} \tag{3.6}$$

Phase angle (ϕ) is defined as:

$$\phi = \frac{t_i}{t_p} * 360 \tag{3.7}$$

where, t_i is the average phase lag between a cycle of stress and strain (sec); t_p is the average time for stress cycle (sec). Schematics of the |*E**|-testing are provided in Figure 3.17 and Figure 3.18.

3.7.3 Dynamic Modulus Test Data Points

For dynamic modulus (|*E**|) test, combinations of six frequencies: 25, 10, 5, 1, 0.5, and 0.1 Hz with corresponding cycles of 200, 200, 100, 20, 15, and 15 and five temperatures: 14, 40, 70, 100, and 130 °F (-10, 4.4, 21.1, 37.8, and 54.4 °C) are required to be considered. The total number of data points per sample test are then:

6 frequencies x 5 temperatures = **30 data points for each specimen**

The total number of data points for the target number of samples is then:

54 target samples x 30 test data per sample = **1620 data points**.

3.7.4 Summary of Tested Mixes and Specimens

Table A-7 in Appendix A summarizes the AC mixtures on which the dynamic modulus tests have been conducted. This table provides information about the serial number on which the test had been conducted, associated NMDOT district, Superpave gradation of the mix, specified and used Performance Grade (PG) of the binder, mix type, Reclaimed Asphalt Pavement (RAP) fraction, number and ID of the specimen tested, theoretical maximum specific gravity of the mix, bulk specific gravity of the specimen, air void content, the asphalt content, and the NMDOT project information. For brevity in mentioning a specific AC mixture, the collected samples are numbered in the order these are tested and used throughout this document.

3.7.5 The Dynamic Modulus and Phase Angle Test Results

The specimen-wise $|E^*|$ and ϕ test results for all the 54-AC mixtures mentioned in Table A-7 are presented in the Tables B-1 through B-165 in APPENDIX B. The tables in APPENDIX B listed the test-temperature (°C), loading frequency (Hz), applied stress amplitude (kPa), standard error of the applied stress ($se(\sigma)$ in %), calculated dynamic modulus (MPa), calculated phase angle (°), uniformity coefficient for the phase angle measurement (°), recoverable strain ($\mu\varepsilon$), accumulated residual strain ($\mu\varepsilon$), average standard effort of the measured strain ($se(\varepsilon)$ in %), and uniformity coefficient for the measured strain (%). The definition of standard errors and uniformity coefficients are calculated in accordance to the AASHTO T 342 standard specification.

Graphical presentation of the $|E^*|$ with ϕ test data are presented in Figure C-1 to C-165 in APPENDIX C of this document. Each of these figures presents the isothermal

thermal curves at top-left corner, isochronal curves at top right corner, cole-cole or complex plane plot at bottom-left corner, and the black space plot at bottom-right corner.

Isothermal curves are the $|E^*|$ or $\log(|E^*|)$ versus f or $\log(f)$ plots, in which, each of the lines presents the test data of a certain test temperature. The plot is important to follow changes in $|E^*|$ values with f at a defined temperature of interest. In general, $|E^*|$ increases as the f increases. Again, the highest value of $|E^*|$ can be obtained at lowest temparture, whereas, the lowest value of $|E^*|$ can be obtained at the highest temperature. Therefore, in general, the highest value of $|E^*|$ can be seen at the lowest temperature and at highest loading frequency, whereas, the lowest $|E^*|$ is observed at the highest temperature and at lowest loading frequency.

Isochronal curves are the $|E^*|$ versus temperature (T) plots, in which, each of the lines presents the test data of a certain loading frequency f. The plot is important to follow changes in $|E^*|$ values with T at a defined frequency of loading. In general, $|E^*|$ decreases as the T increases. Again, the highest value of $|E^*|$ can be obtained at highest loading frequency, whereas, the lowest value of $|E^*|$ can be obtained at the lowest loading frequency. Therefore, similar to isothermal curves, the highest value of $|E^*|$ can be expected at the lowest temperature and at highest loading frequency, whereas, the lowest value of $|E^*|$ can be expected at the highest temperature and at lowest loading frequency.

Cole-Cole or complex plane plot are the loss modulus versus storage modulus plots, essentially, showing the imaginary and real part of the complex modulus. The plot is generally used to identify the maximum loss modulus which essentially results from the viscous behavior of the material. The curve can also be used for modeling purpose. In general, data points in a cole-cole plot is expected to form an arc which can be used to

characterize the material. Also, the curve can be used to identify any discrepancy in the laboratory test results.

Lastly, the black space plot is the phase angle versus $|E^*|$ or $\log(|E^*|)$ plot. Generally, the black space plot is used to characterize the high-temperature behavior of AC materials. The plot can identify the maximum attainable phase angle by the material. A material with higher peak phase angle value shows more viscous behavior than the material with lower peak phase angle value.

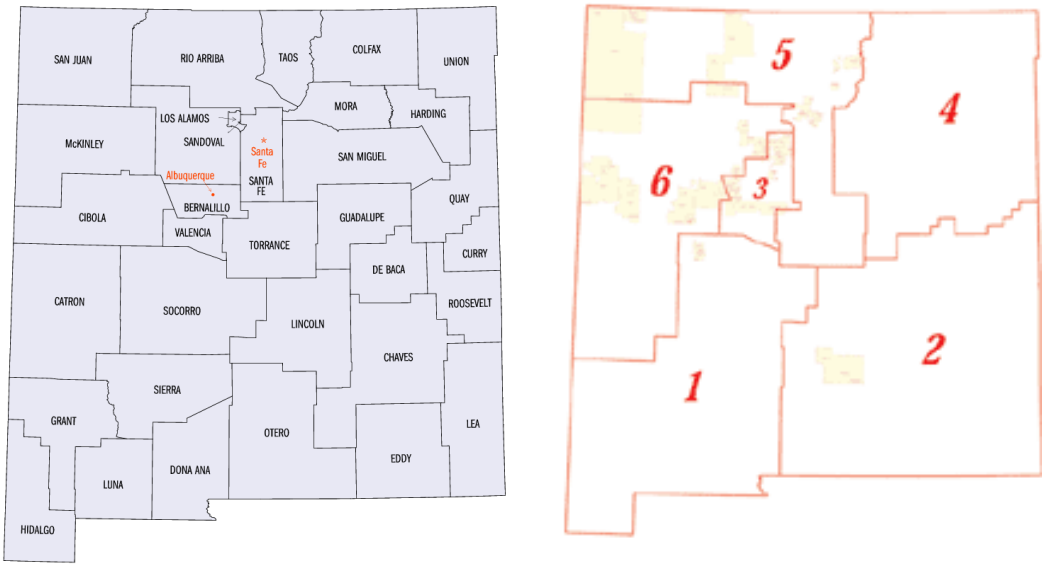

Figure 3.1 Maps showing New Mexico Counties and NMDOT districts.

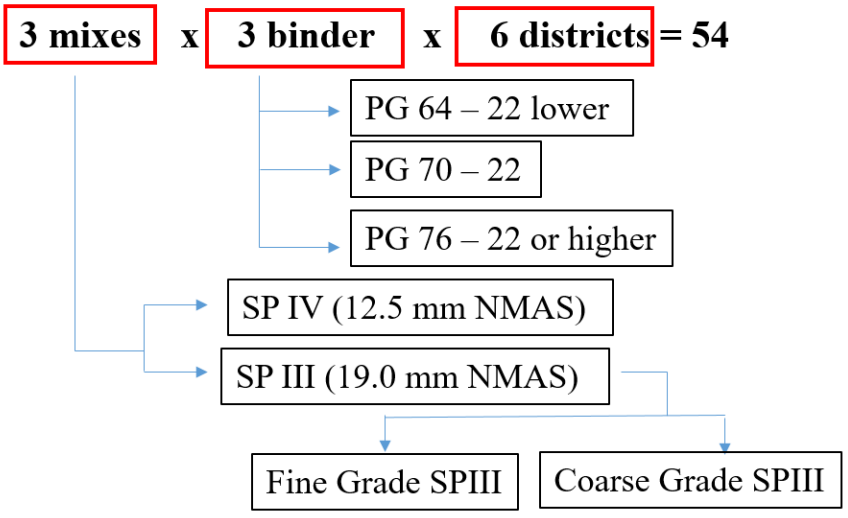

Figure 3.2 Test materials matrix.

Figure 3.3 Superpave Gyratory Compactor.

Figure 3.4 Compacted Asphalt Concrete Specimen.

Figure 3.5 Asphalt Coring Machine GCTS SCD 150.

Figure 3.6 100mm specimen cored out of a 150mm compacted specimen.

Figure 3.7 Lab Specimen Saw GCTS RLS-3HA.

Figure 3.8 Typical core-drilled and sawed AC specimen.

Figure 3.9 Straight edge and feeler gauge for Waviness check.

Figure 3.10 Rock Flatness Gauge RFG-100.

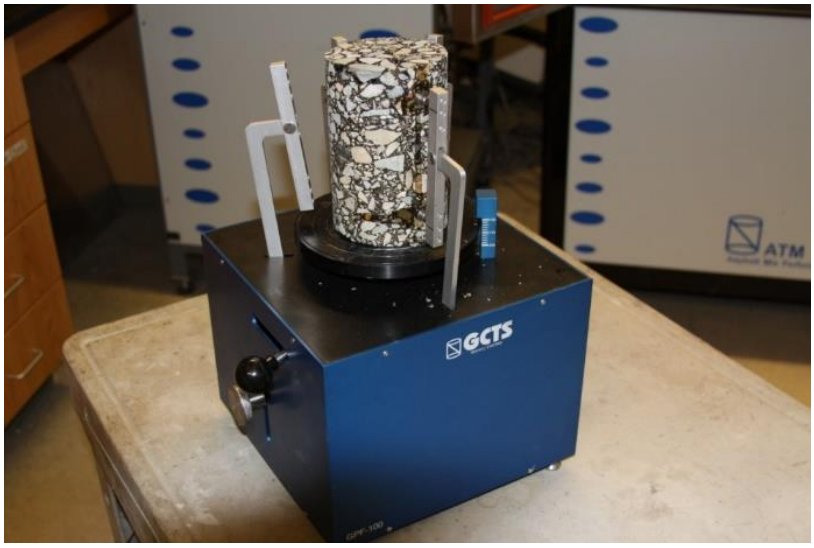

Figure 3.11 Automatic Positioning Fixture GCTS GPF 100.

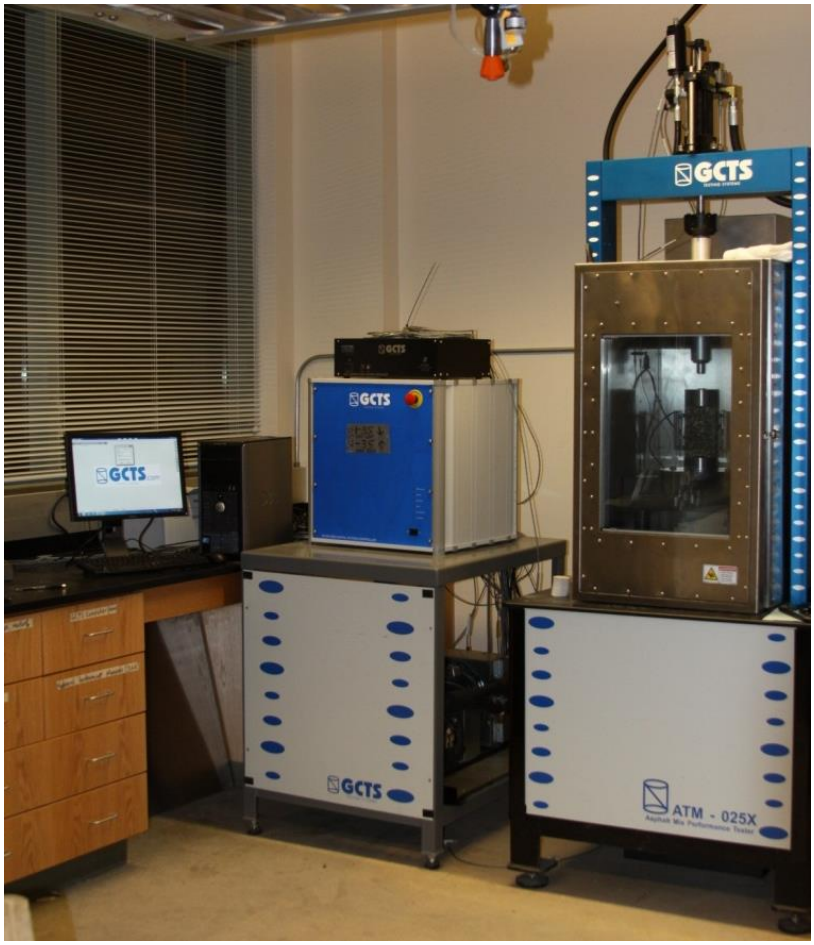

Figure 3.12 Servo-Hydraulic Testing System

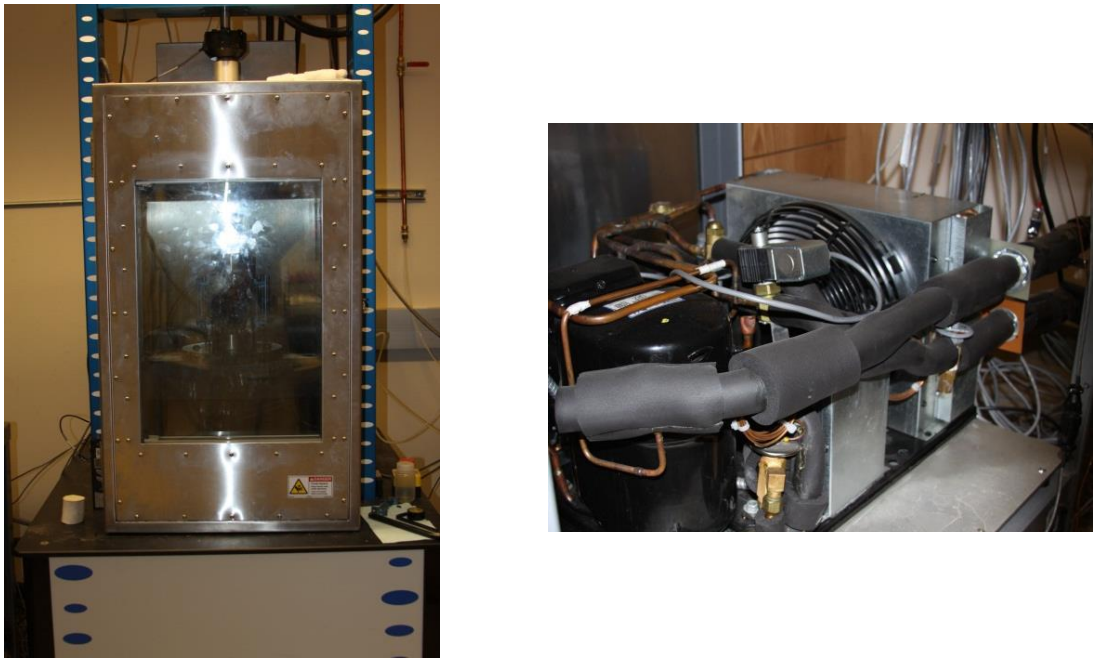

Figure 3.13 Environmental Chamber GCTS (ECH-30CS/CH) (Left) and Air Conditioning Unit (Right).

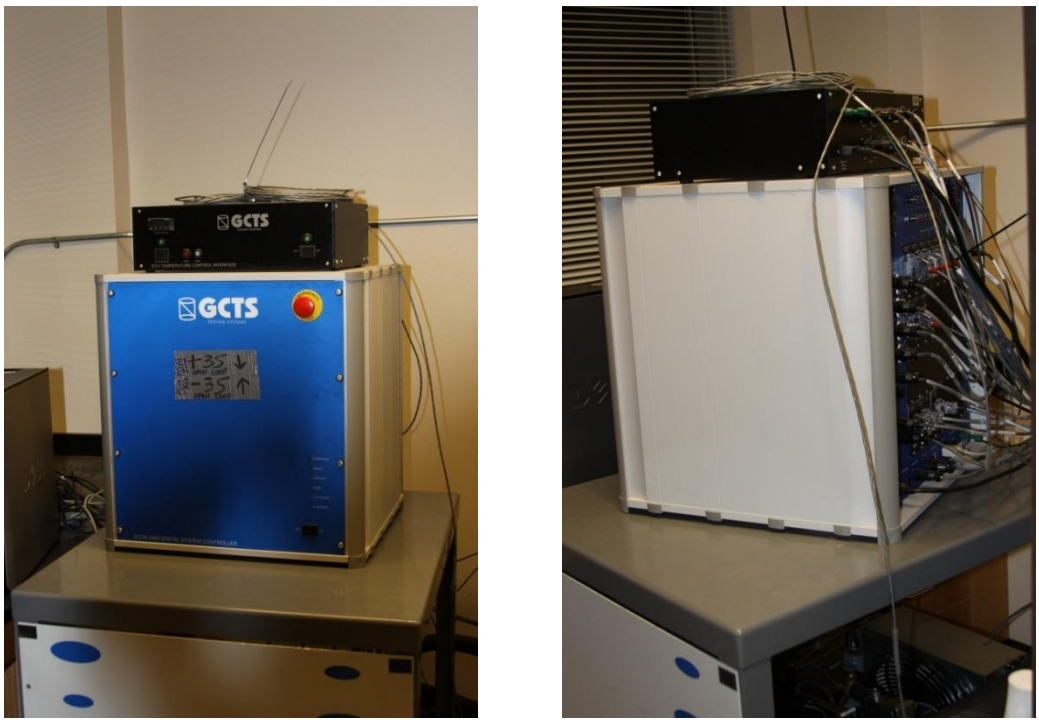

Figure 3.14 Control System GCTS SCON 2000.

Figure 3.15 25kN Load Cell Connected to a 25 kN Actuator.

Figure 3.16 Linear variable differential transformers (LVDTs) mounted on specimen.

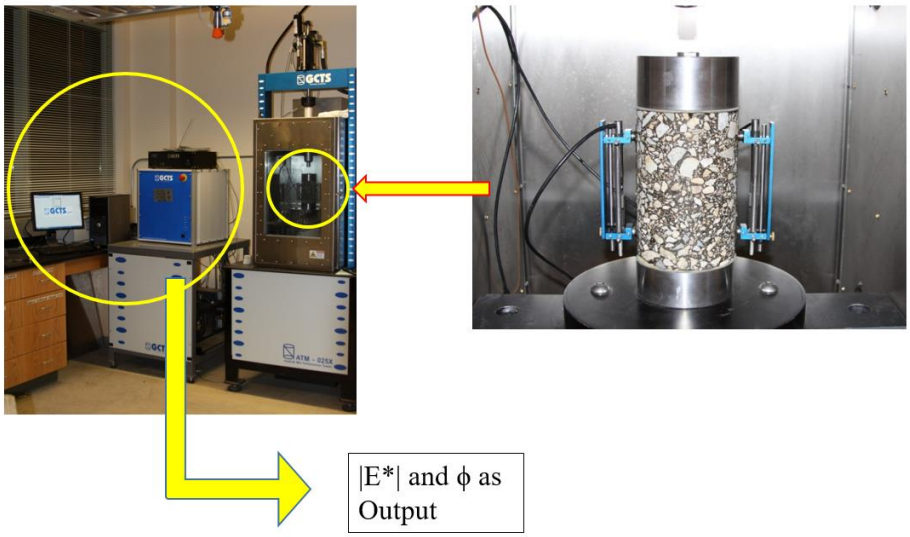

Figure 3.17 |E*| test setup.

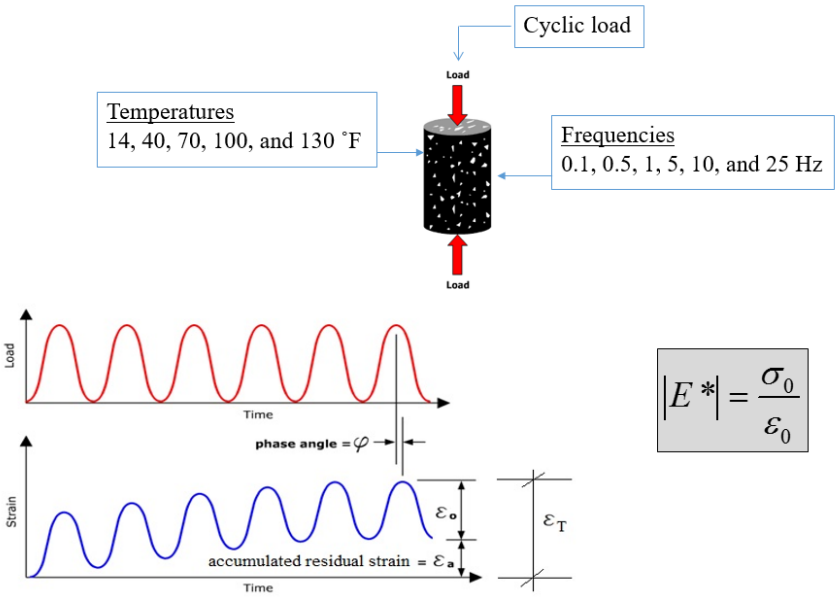

Figure 3.18 Schematic of |E*| testing.

Chapter 4

Analysis of Dynamic Modulus Test Results

4.1 Introduction

In this chapter, average $|E^*|$ and ϕ values are determined from three replicate samples Next, dynamic modulus ($|E^*|$) mastercurves at 70 °F (21.1 °C) and the frequency-temperature shift factor functions were determined. Following sections presents a brief overview on time-temperature superposition principle (TTSP) and the processes involved for developing mastercurves for the asphalt concrete mixtures by applying this principle.

4.2 Objective

The objectives of this study are to develop average $|E^*|$ and ϕ mastercurves at 21.1 °C (70 °F) reference temperature for all the AC materials.

4.3 Developments of Mastercurves for the New Mexico Superpave Mixtures

4.3.1 Time-Temperature Superposition Principle (TTSP)

The time-temperature superposition is a concept typically used to determine temperature-dependent mechanical properties of linear viscoelastic materials like asphalt concrete from known properties at a reference temperature. The elastic moduli of asphaltic materials increase with loading rate or frequency but decrease when the temperature is increased. As a fundamental property of linear viscoelastic material, the curves of the instantaneous

modulus as a function of time or loading frequency for asphalt concrete do not change shape as the temperature is changed but appear only to shift left or right in a modulus versus loading-frequency or loading-time plot. This behavior of linear viscoelastic asphaltic material facilitates the idea that a mastercurve at a given temperature, also called reference temperature, can be used as the reference to predict the modulus versus loading time or frequency curves at various temperatures by applying only a shift operation. The time-temperature superposition principle of linear viscoelasticity is based on the above observation (Christensen 1971, Rongzhi 2000, Van Gurp and Palmen 1998).

The application of the time-temperature superposition principle typically involves, firstly, the experimental determination of loading frequency-dependent curves of isothermal viscoelastic mechanical properties such as the dynamic moduli, at several temperatures for a small range of selected frequencies. The second step is the computation of a translation factor to correlate these properties for the temperature and frequency range involved in the experimental determination and development of a mastercurve based on experimental data showing the effect of frequency for a wide range of frequencies. The final step is the application of the translation factor to determine temperature-dependent moduli over the whole range of frequencies involved in the experimental mastercurve.

4.3.2 Construction of Mastercurves: An Application of TTSP

The time-temperature superposition principle is applied on the dynamic modulus test results conducted at different temperatures and loading frequencies. This principle allows us to move horizontally the dynamic modulus data at different temperatures on the loading time scale or loading frequency scale to produce one smooth curve dependent only on

loading frequency or time. The amount by which dynamic modulus data is shifted to fit in a smooth curve at a reference temperature is referred to as shift factor, $a(T)$. Shifting is achieved by dividing the loading time in the time domain or multiplying the loading frequency in the frequency domain by the shift factor to get the reduced time or reduced frequency. The smooth curve that is developed by shifting the dynamic modulus data is referred to as the mastercurve. The mastercurve can be developed for any reference temperature chosen arbitrarily. At the reference temperature, the shift factor is 1 and its logarithm is zero (Kim 2009).

Reduced frequency:

$$f_r = f * a(T) \tag{4.1}$$

and,

$$\log(f_r) = \log(f) + \log[a(T)]. \tag{4.2}$$

Otherwise, reduced time:

$$t_r = \frac{t}{a(T)} \tag{4.3}$$

and,

$$\log(t_r) = \log(t) - \log[a(T)]. \tag{4.4}$$

The use of time-temperature superposition principle (TTSP) to develop mastercurve has two advantages other than characterizing the linear viscoelastic behavior

of a material over a wide range (broadband) loading frequency or loading time domain. The first and the foremost is it reduces the three-dimensional data (dynamic modulus, loading time/frequency and temperature) in to two-dimensional data by eliminating the temperature variable. This makes it easy to compare test results conducted at different conditions. The other advantage is the possibility of interpolation to get intermediate data within the test data range.

4.3.3 Fitting Frequency-Temperature Shift Factor Functions

There are a number of expression can be found to fit the time-temperature or frequency-temperature shift factor functions. Among these, the Arrhenius equation and the Williams, Landel, and Ferry (WLF) equation are often used and shown good performance over the years. Beside these, a second-order polynomial fit can also be used to fit the frequency-temperature shift factor function. Brief descriptions of these shift-factor fitting functions are presented in the following sections.

4.3.3.1 Arrhenius Equation

The basic form of Arrhenius equation can be presented by the following expression –

$$\log a_t = C\left(\frac{1}{T} - \frac{1}{T_{ref}}\right) = \frac{E_a}{2.203 * R}\left(\frac{1}{T} - \frac{1}{T_{ref}}\right) \tag{4.5}$$

Here, C is a material constant (K); E_a is the activation energy (J/mol); R is the ideal gas constant (8.314 $\frac{J}{mol} * K$); T is the experimental temperature (K); T_{ref} is the reference temperature and the value 2.303 is the natural logarithm of 10. Different values ranging

from 44 kJ/mol to 205 kJ/mol are reported in the literature for the activation energy of asphalt binders. The material constant, *C* is reported to have values of 10920 K, 13060 K, and 7680 K (Rowe and Sharrock 2010).

4.3.3.2 Williams, Landel, and Ferry (WLF) Equation

The Williams, Landel, and Ferry (WLF) equation for fitting frequency-temperature shift factor function can be given by the following expression –

$$\log a_t = \frac{-C_1\left(T - T_{ref}\right)}{C_2 + \left(T - T_{ref}\right)} \tag{4.6}$$

where, C_1 and C_2 are constants that depend on the material properties and reference temperature. The negative sign in the WLF expression is omitted in case of time-temperature shift factor or time-domain material functions. Rowe and Sharrock (2010) recommended using the WLF equation near the glassy temperature (T_g) of the material.

4.3.3.3 Second Degree Polynomial

Expression of a second-degree polynomial can be also used to fit the frequency-temperature shift factor function. This can be given as –

$$\log a_t = aT^2 + bT + C \tag{4.7}$$

4.3.4 Fitting Experimental Dynamic Modulus Mastercurve

The function that is predominantly used for developing mastercurve for dynamic modulus data is the sigmoid function (Kim 2009) and can be given as:

$$\log\left(|E^*|\right) = \delta + \frac{\alpha}{1 + e^{\beta + \gamma \log(f_r)}}. \quad (4.8)$$

Here, $|E^*|$ is the dynamic modulus; f_r is the reduced frequency; δ is the minimum modulus value; α is the vertical span of modulus function; β and γ are the shape parameters. The parameter, γ indicates how steep the function is i.e. how fast the modulus is changing from the minimum to the maximum value. The parameter, β represents the horizontal position at which the rate of change of modulus changes from positive to negative. On the other hand, δ is associated with the minimum value of the modulus generally caused by high-temperature, also called rubbery modulus. At high-temperatures, the modulus of the binder becomes insignificant and aggregate interlock plays a significant role in determining compressive stiffness. This behavior of asphalt mix is captured by the parameter δ. The largest modulus which is associated with binder modulus at very low temperature is represented in the sigmoidal function by the sum of parameters δ and α (i.e. $\alpha+\delta$). This highest modulus is also referred to as glassy modulus.

There are different methods that can be used to fit the horizontally shifted dynamic modulus data by the sigmoidal function. Witczak and Sotil (2004) have investigated a variety of methods and recommended to optimize all four parameters of the sigmoidal function together with the three coefficients of the polynomial shift factor function. The

sigmoidal function of the mastercurve can be fitted using Solver Function in the Excel spreadsheets program. However, Kim (2009) recommends being cautious about fitting data with insufficient temperature range. The method recommended to avoid bias is to confine the asymptotic high and low modulus values to assumed proper modulus values.

4.3.5 The Dynamic Modulus Mastercurve Fitting Steps

The procedure proposed by Witczak and Sotil (2004) to develop dynamic modulus mastercurve includes the following steps.

Step 1: Determination of the logarithm of test frequencies and dynamic moduli for all the temperature considered in the experiments.

Step 2: Selection of the reference temperature. For example, 21.1°C (70 °F) reference temperature can be chosen.

Step 3: Approximation of initial estimate of shift factors for each temperature case and program excel with if statement to change the values for each temperature in the iteration process. Dynamic modulus test is conducted at five temperatures, -10, 4.4, 21.1, 37.8, 54.4 °C, with loading frequencies of 25, 10, 5, 1, 0.5, and 0.1 Hz at each test temperature. The log-reduced frequency can be found as follows:

$$a(T) = \frac{f_r}{f} \tag{4.9}$$

$$f_r = a(T) * f \tag{4.10}$$

$$\log(f_r) = \log[a(T)] + \log(f) \tag{4.11}$$

Step 4: Approximation of the initial values for the mastercurve parameters. A symmetrical sigmoid function is expected for the mastercurve fitting and initial value of 1 is used for the parameters α, β, γ and δ.

Step 5: Computation of the coefficient of determination. To evaluate the goodness of fit for the iteration results of the solver function it is required to minimize the sum of error squared values and the final result goodness of fit can be evaluated by the coefficient of determination given as follows:

$$R^2 = 1 - \frac{SS_{err}}{SS_{tot}} = \frac{\sum_{i=1}^{n}(y_i - \bar{y})^2}{\sum_{i=1}^{n}(y_i - f_i)^2} \tag{4.12}$$

where, R^2 is the Coefficient of determination; y_i are the dataset values; f_i are the modeled values; and, $\bar{y}$ is the dataset mean, i.e. $\bar{y} = \frac{\sum_{i=1}^{n} y_i}{n}$.

To represent a typical work involved in developing |*E**| mastercurves, Figure 4.1 shows the tested average |*E**| values versus loading frequencies at different test temperatures for one of the AC sample (AC Mix 22). The figure also shows TTSP applied horizontally shifted |*E**| data along the frequency axis to construct mastercurve. The horizontally shifted |*E**| data were then fitted by the sigmoidal expression. Figure 4.2 shows

the shift factor versus temperature plot with the fitted shift factor function fitted by the second-degree polynomial.

4.3.6 Development of Experimental Phase Angle Mastercurve

The ϕ of asphalt-aggregate mixture is an important parameter for understanding the extent of loss or viscous modulus as well as the storage modulus. The higher the ϕ, the more viscous is the material. Thus, a lower value of ϕ indicates that the material behavior will be more elastic in nature. Also, to separate the complex modulus (E^*) into its two parts: storage and loss modulus, the δ of the material is required. The ϕ of an AC material can be found from the $|E^*|$ test at a given temperature and loading frequency. It is the time lag at which the strain lags the stress (Witczak 2005, Bonaquist et al. 2003). In a $|E^*|$ test, ϕ can be mathematically expressed as:

$$\delta = \left(t_i \Big/ t_p \right) \times 360^{\circ} \tag{4.13}$$

Here, t_i is the time-lag between a cycle of stress and a cycle of strain in seconds; t_p is the time for a stress cycle in seconds. For a purely elastic material, $\phi = 0°$; and for a purely viscous material, $\phi = 90°$.

The same temperature shift factors for $|E^*|$ mastercurve can be used to develop ϕ mastercurve. The resulting ϕ mastercurve should be a single smooth curve if the assumption that AC material to be thermo-rheologically simple is valid. Figure 4.3 shows a typical ϕ versus f_r plot (or simply ϕ mastercurve) for a typical AC sample (AC Mix 22). The plot also includes the tested ϕ data which were horizontally shifted afterward. The shifted ϕ data in Figure 4.3 form a single curve except some deviating outliers.

4.3.7 Fitting Experimental Phase Angle Mastercurve

Fitting δ mastercurve has long been an issue because of the existence of very few models to accurately fit this behavior. Booij and Thoone (1982) presented a simplified and approximated relation between $|E^*|$ and δ. This can be expressed as:

$$\phi(\omega) \approx \frac{\pi}{2} \frac{d \log \left(|E^*(\omega)|\right)}{d \log (\omega)}. \tag{4.14}$$

In Equation 5, $\phi(\omega)$ is the phase angle function expressed in the angular frequency (rad/sec) domain; $|E^*(\omega)|$ is the dynamic modulus also in angular frequency space. The relationship between angular and ordinary frequency can be given as:

$$f_r = \frac{\omega}{2\pi} \tag{4.15}$$

Substituting, Equation 4.15 into Equation 4.8, and differentiating with respect to *log* (ω), we have the following expression for the ϕ function in radian in ordinary frequency space as:

$$\phi(f_r) \approx -\frac{\pi}{2} \alpha\gamma \frac{e^{\beta+\gamma \log(f_r)}}{\left(1+e^{\beta+\gamma \log(f_r)}\right)^2}. \tag{4.16}$$

In Equation 4.16, $\phi(f_r)$ is the phase angle in radians; f_r is the reduced frequency in Hz; and α, β, and γ are the regression coefficients, which can be found by fitting $|E^*|$ function by Equation 4.8. Therefore, if the $|E^*|$ function of an AC material is known, the ϕ function can be easily found by using Equation 4.16. Figure 4.4 shows the ϕ-function found by using Equation 4.16 with the actual tested data for the AC Mix 22. The coefficient of determination, R^2 for the fitting is found to be 0.84, and the test-data actually seemed a bit apart from the fitted function. The study by Yang and You (2015) found that Equation 4.16

is less accurate and once again as Equation 4.14 itself is an approximate relation, therefore, they proposed for a modified version of Equation 4.14 given as:

$$\phi(\omega) = c\frac{\pi}{2}\frac{d\log\left(|E^*(\omega)|\right)}{d\log\left(\omega\right)} \tag{4.17}$$

where, c is a fitting coefficient. Again, using Equation 4.8 and the relationship between angular and ordinary frequencies, one can obtain:

$$\phi(f_r) = -c\ \frac{\pi}{2}\alpha\gamma\frac{e^{\beta+\gamma\log(f_r)}}{\left(1+e^{\beta+\gamma\log(f_r)}\right)^2}. \tag{4.18}$$

Figure 4.5 shows the ϕ mastercurve fit by Equation 4.18 for the AC Mix 22. The value of c is found to be 1.119 for an optimized coefficient of determination (R^2) of 0.92. Observation of Figure 4.5 indicates that, Equation 4.18 gives fairly good estimation of ϕ at mid-frequency range. However, at lower and higher end of the frequency band, the fitted ϕ function deviates from the measured data. Therefore, to reduce this deviation, a new model is proposed in this study to have a better fit of the tested ϕ of AC. Thus, Equation 4.18 is modified as:

$$\phi(f_r) = \xi_1 + \xi_2\log\left(f_r\right) - \xi_3\ \frac{\pi}{2}\alpha\gamma\frac{e^{\beta+\gamma\log(f_r)}}{\left(1+e^{\beta+\gamma\log(f_r)}\right)^2} \tag{4.19}$$

where, ξ_1, ξ_2, and ξ_3 are the fitting parameters. Figure 4.6 shows the ϕ function fitted by the Equation 4.19. The R^2 of this fitting is found to be 0.95, which is very close to 1. Thus, Equation 4.19 is used in this study to fit the phase angle mastercurves of the AC samples.

4.4 Dynamic Modulus and Phase Angle Data Summary

The $|E^*|$ and ϕ data summaries for the all the AC samples tested in this study are presented in Table D-1 through Table D-54 in Appendix D of this document. The tables in Appendix

D listed the tested $|E^*|$ and ϕ values at various temperatures and loading frequencies of three replicate test specimens of all 54-AC samples, the average $|E^*|$ and ϕ of the AC samples, the coefficient of variation of the modulus values obtained from the replicate specimens, and the standard deviations of the phase angles of the replicate specimens. In general, a coefficient of variation value of 30% or lower and a standard deviation value of 5 degrees or lower indicate good repeatability of the testing on replicate specimens of an AC sample.

The graphical data summaries for all 54-AC samples are presented in Figure E-1 through Figure E-54 in Appendix E of this document. Each of the figures in Appendix E shows the average log-$|E^*|$ versus log-f plot, average $|E^*|$ versus frequency plot, ϕ versus log-f plot, $|E^*|$ versus temperature plot (also called isochronal curves), the complex plane plot (also called cole-cole plot), and the ϕ versus log-$|E^*|$ plot (also called black space plot).

4.5 Average |E*| and ϕ Mastercurves

The average $|E^*|$ and ϕ mastercurves at 70 °F reference temperature with frequency-temperature shift factor as functions of temperature are presented in Figure F-1 through Figure F-54 in Appendix F for all 54-AC samples considered in this study. These figures also present the fitted or smoothened curves for the mastercurves and the shift factor functions. It should be noted that, in the case of fitting ϕ-mastercurves both the Equations 4.16 and 4.19 are used to study their relative fitting accuracy. It is clear from these figures that performance of Equation 4.19 is better for fitting phase angle mastercurves.

Table 4.1 shows the fitted parameters, i.e. α, β, δ, and γ for the $|E^*|$-mastercurves of all 54-AC mixtures, for which, Equation 4.8 is used. Table 4.2 presents the frequency-

temperature shift factors at different temperatures and the fitted parameters, i.e. a, b, and c in Equation 4.7 for the shift factor functions of all 54-AC mixtures. Lastly, Table 4.3 presents the fitted parameters, i.e. ξ_1, ξ_2, and ξ_3 for the phase angle mastercurves of all 54-AC mixtures, for which, expression given in Equation 4.19 is used.

4.6 Program Codes for Test Data Processing and Mastercurve Development

Throughout this study, from processing of the data from the machine generated file to the development of mastercurves and shift factor functions, a set of computer program codes was written to facilitate the study in a time-effective manner. Appendix G presents some example of these codes. The Code G-1 is especially used for processing data from the machine generated ".csv" files for 5 test-temperatures in case of a AC test-specimen. After, test data at different temperatures of a AC specimen is processed, Code G-2 was used to summarize and averaging the $|E^*|$ and ϕ data from replicate specimens. Code G-3 was developed to generate $|E^*|$ and ϕ-mastercurves as well as the frequency-temperature shift factor functions for the AC samples.

4.7 Conclusions

In this chapter, the $|E^*|$ with ϕ test results are analyzed and the mastercurve was generated for a broad range of frequency band. All the mastercurves generated in this chapter showed good fitting characteristics.

Table 4.1 Summary of Fitted |E*|-Mastercurve Parameters

AC Mix ID	***When |E*| is determined in pound per square inch (psi)***			
	α	β	δ	γ
1	2.839303244	-1.048751938	4.133886227	-0.437782231
2	2.459344705	-0.436846842	4.505228728	-0.55049812
3	2.247746053	-0.41632694	4.661230636	-0.491805449
4	2.585522607	-0.734952139	4.342716697	-0.383808791
5	1.622805168	-0.598974063	5.043399799	-0.695693351
6	2.284721349	-0.45689395	4.55411541	-0.439786925
7	2.284721349	-0.45689395	4.55411541	-0.439786925
8	2.691299692	-0.667504372	4.293204159	-0.440394315
9	2.701502081	-0.874784293	4.242484422	-0.429151245
10	2.214802854	-0.106554409	4.622881894	-0.571171533
11	2.527764646	-0.493144808	4.338058416	-0.484500504
12	2.291879441	-0.257920453	4.49911462	-0.49987719
13	2.649555738	-0.823587523	4.2155804	-0.514447999
14	2.800228245	-0.851717102	4.236109287	-0.403479578
15	2.31509833	0.055918054	4.610468432	-0.371384452
16	2.767362819	-0.801847671	4.291299723	-0.351897188
17	3.413556143	-1.504323908	3.607679444	-0.397262518
18	2.551111567	-1.01739384	4.281325159	-0.505102372
19	2.436933225	-0.759979273	4.390760219	-0.551191577
20	2.686067636	-0.600143006	4.250369163	-0.512096712
21	2.738708557	-1.124195567	4.141928726	-0.431511168
22	2.884813753	-0.64332726	4.140482227	-0.405916725
23	2.301203258	-0.740427301	4.46583167	-0.547486572
24	2.557892121	-0.788310629	4.431513611	-0.510396326
25	2.907337617	-0.276821117	4.153709438	-0.404748302
26	2.059454199	-0.726629718	4.64034634	-0.657146686
27	2.335366739	-0.522624539	4.529269405	-0.523456996
28	2.335366739	-0.522624539	4.529269405	-0.523456996
29	2.610029251	-0.860504009	4.264249836	-0.516214129
30	3.117883561	-0.920429032	3.839799854	-0.279002141
31	3.293401819	-0.932121292	3.736001149	-0.338835223
32	2.563177712	-0.565334964	4.348652445	-0.426352028
33	2.857205494	-0.632807791	4.137740831	-0.409202661
34	2.763698908	-0.538327311	4.216999982	-0.373138638
35	2.719719033	-1.042352759	4.168097191	-0.47155231
36	2.767173301	-0.782738284	4.134174429	-0.344259115
37	2.655072902	-0.801472607	4.22454721	-0.330605484
38	2.63847552	-0.776085103	4.251330787	-0.482647489
39	2.343361861	-0.522675948	4.514486812	-0.515138087
40	2.639254595	-0.608906484	4.228001242	-0.401734883
41	3.362614507	-1.668249292	3.539548025	-0.380116212
42	2.249438172	-0.280583608	4.59514898	-0.563644247
43	2.430942898	-0.508527091	4.506314056	-0.502260025
44	2.402087067	-0.495778089	4.534389191	-0.492695284
45	2.639898217	-0.959524123	4.378341657	-0.465790677
46	2.699468332	-0.845617247	4.242251681	-0.469999158
47	2.71077166	-0.720914466	4.19833146	-0.464202666
48	3.075554392	-0.988920653	3.828968197	-0.435922001
49	2.932455644	-1.039746066	4.068217916	-0.432228919
50	2.414905262	-0.935343241	4.386437595	-0.54199424
51	2.537755102	-0.704272587	4.350231247	-0.502546155
52	2.593695436	0.043792625	4.467817419	-0.567737766
53	2.739752962	-0.782628092	4.326926182	-0.487316192
54	2.477357469	-0.557365204	5.358851408	-0.537726433

Table 4.2 Summary of Frequency-Temperature Shift Factors at Different Temperature and Fitted Shift Factor Function Parameters

AC Mix ID	Temperatures (°F)					a_T parameters (when temperature is in °F)		
	14	40	70	100	130	*a*	*b*	*c*
1	4.6600	2.6600	0.0000	-2.0500	-3.8600	0.00013972	-0.09452802	6.03575541
2	4.5000	2.2500	0.0000	-1.6300	-3.2900	0.00019903	-0.09512773	5.76370033
3	5.5300	2.1000	0.0000	-1.6300	-2.3000	0.00055414	-0.14568542	7.33115540
4	4.3200	1.7400	0.0000	-1.9500	-3.7000	0.00016473	-0.09109152	5.42439829
5	4.0600	1.7700	0.0000	-1.9100	-3.4400	0.00015903	-0.08670671	5.16630932
6	4.4200	2.2800	0.0000	-1.8900	-3.6500	0.00014644	-0.09052171	5.65694581
7	4.4200	2.2800	0.0000	-1.8900	-3.6500	0.00014644	-0.09052171	5.65694581
8	4.7500	2.0500	0.0000	-2.1500	-4.0800	0.00017002	-0.09915493	5.99175100
9	4.1500	2.1900	0.0000	-1.7100	-3.0700	0.00018893	-0.08987410	5.40565053
10	4.0600	2.0900	0.0000	-1.4500	-3.1100	0.00014915	-0.08257685	5.16226352
11	4.3100	2.1900	0.0000	-1.7500	-3.0800	0.00021824	-0.09536456	5.61941325
12	4.4400	2.2200	0.0000	-1.6900	-3.2700	0.00020006	-0.09483446	5.71003461
13	4.0800	2.2400	0.0000	-1.7800	-3.1900	0.00015961	-0.08644181	5.31759527
14	4.3000	2.4400	0.0000	-1.8600	-3.3100	0.00017000	-0.09122905	5.63076257
15	4.4000	2.2900	0.0000	-2.0100	-3.3100	0.00021186	-0.09789127	5.78119752
16	4.8800	2.5300	0.0000	-1.8400	-3.3400	0.00025530	-0.10783215	6.36510350
17	4.9400	2.6600	0.0000	-1.8800	-3.4500	0.00024132	-0.10758817	6.44978772
18	4.3000	2.3500	0.0000	-1.7700	-3.1700	0.00019175	-0.09275504	5.62067763
19	4.3000	2.3600	0.0000	-1.7300	-3.2000	0.00018211	-0.09147579	5.59883743
20	4.0600	2.1900	0.0000	-2.0800	-3.5100	0.00013353	-0.08561978	5.29669875
21	4.9500	2.2900	0.0000	-1.8900	-3.4000	0.00027866	-0.11138130	6.40343009
22	4.6200	2.2300	0.0000	-2.2700	-3.7100	0.00020983	-0.10251310	6.02200674
23	4.0800	1.8700	0.0000	-1.4900	-2.9700	0.00019583	-0.08780027	5.19842683
24	3.6800	2.1200	0.0000	-2.0100	-3.8100	0.00001588	-0.06774619	4.68574178
25	4.3800	2.2800	0.0000	-1.5400	-3.7200	0.00009444	-0.08205765	5.45514614
26	3.6400	1.9000	0.0000	-1.6900	-3.1500	0.00010706	-0.07413624	4.66946488
27	4.8300	2.0400	0.0000	-1.6900	-3.0400	0.00031846	-0.11222653	6.23384869
28	4.8300	2.0400	0.0000	-1.6900	-3.0400	0.00031846	-0.11222653	6.23384869
29	4.3500	2.0500	0.0000	-1.9100	-3.6700	0.00014927	-0.08983870	5.52163719
30	5.1300	2.4700	0.0000	-1.9800	-3.6500	0.00026237	-0.11292783	6.62634316
31	4.3100	2.1500	0.0000	-1.9700	-3.2600	0.00021118	-0.09620632	5.63841853
32	4.3900	2.5300	0.0000	-1.6500	-3.0200	0.00020859	-0.09497697	5.77281019
33	5.2000	2.7500	0.0000	-1.7200	-3.5900	0.00024007	-0.10988806	6.69499880
34	5.3300	2.6700	0.0000	-1.7600	-3.6000	0.00026993	-0.11496892	6.85408034
35	4.4400	2.1600	0.0000	-2.1200	-3.6500	0.00018017	-0.09586250	5.74248730
36	5.0300	2.3400	0.0000	-2.1400	-3.6600	0.00026803	-0.11322360	6.52929450
37	4.9600	2.3200	0.0000	-1.8700	-3.5200	0.00025583	-0.10903393	6.37865216
38	4.3000	2.1200	0.0000	-2.1800	-4.1000	0.00008794	-0.08483877	5.44371499
39	4.3000	2.1900	0.0000	-2.1000	-3.7000	0.00014378	-0.09007986	5.54957603
40	6.0800	2.5900	0.0000	-1.8900	-3.3800	0.00045315	-0.14496293	7.89854366
41	5.3200	2.7700	0.0000	-2.2600	-4.0200	0.00023684	-0.11512537	6.92150418
42	4.8200	2.4000	0.0000	-1.9300	-3.4100	0.00025086	-0.10711742	6.27436489
43	3.9600	2.0700	0.0000	-1.9700	-3.3200	0.00014703	-0.08476950	5.16178558
44	4.9000	2.2900	0.0000	-1.9900	-3.6800	0.00023178	-0.10658567	6.29289881
45	5.1300	2.5500	0.0000	-2.0600	-3.4700	0.00029509	-0.11695053	6.72732052
46	4.5800	2.4600	0.0000	-2.1300	-3.6200	0.00018887	-0.09895596	5.99503084
47	4.6400	2.2700	0.0000	-2.0100	-3.6400	0.00019769	-0.09966714	5.98011838
48	4.4000	2.2300	0.0000	-2.0700	-4.6300	-0.00000387	-0.07598759	5.39194751
49	6.1600	2.4400	0.0000	-2.5900	-4.3300	0.00038142	-0.14361622	7.94116607
50	3.8400	2.0000	0.0000	-2.0900	-3.4600	0.00011901	-0.08106819	4.99794940
51	4.6600	2.3100	0.0000	-2.0600	-3.7300	0.00018763	-0.09929197	6.00516288
52	4.9900	2.5900	0.0000	-1.8500	-3.2700	0.00028269	-0.11227243	6.54140863
53	5.3100	2.4700	0.0000	-2.1100	-4.3700	0.00018226	-0.10803452	6.68423080
54	5.5100	2.7900	0.0000	-1.8300	-3.6900	0.00028334	-0.11939427	7.10529508

Table 4.3 Summary of Fitted ϕ-Mastercurve Parameters

AC Mix ID	***When ϕ is determined in degrees***		
	ξ_1	ξ_2	ξ_3
1	2.839303244	-1.048751938	4.133886227
2	2.459344705	-0.436846842	4.505228728
3	2.247746053	-0.41632694	4.661230636
4	2.585522607	-0.734952139	4.342716697
5	1.622805168	-0.598974063	5.043399799
6	2.284721349	-0.45689395	4.55411541
7	2.284721349	-0.45689395	4.55411541
8	2.691299692	-0.667504372	4.293204159
9	2.701502081	-0.874784293	4.242484422
10	2.214802854	-0.106554409	4.622881894
11	2.527764646	-0.493144808	4.338058416
12	2.291879441	-0.257920453	4.49911462
13	2.649555738	-0.823587523	4.2155804
14	2.800228245	-0.851717102	4.236109287
15	2.31509833	0.055918054	4.610468432
16	2.767362819	-0.801847671	4.291299723
17	3.413556143	-1.504323908	3.607679444
18	2.551111567	-1.01739384	4.281325159
19	2.436933225	-0.759979273	4.390760219
20	2.686067636	-0.600143006	4.250369163
21	2.738708557	-1.124195567	4.141928726
22	2.884813753	-0.64332726	4.140482227
23	2.301203258	-0.740427301	4.46583167
24	2.557892121	-0.788310629	4.431513611
25	2.907337617	-0.276821117	4.153709438
26	2.059454199	-0.726629718	4.64034634
27	2.335366739	-0.522624539	4.529269405
28	2.335366739	-0.522624539	4.529269405
29	2.610029251	-0.860504009	4.264249836
30	3.117883561	-0.920429032	3.839799854
31	3.293401819	-0.932121292	3.736001149
32	2.563177712	-0.565334964	4.348652445
33	2.857205494	-0.632807791	4.137740831
34	2.763698908	-0.538327311	4.216999982
35	2.719719033	-1.042352759	4.168097191
36	2.767173301	-0.782738284	4.134174429
37	2.655072902	-0.801472607	4.22454721
38	2.63847552	-0.776085103	4.251330787
39	2.343361861	-0.522675948	4.514486812
40	2.639254595	-0.608906484	4.228001242
41	3.362614507	-1.668249292	3.539548025
42	2.249438172	-0.280583608	4.59514898
43	2.430942898	-0.508527091	4.506314056
44	2.402087067	-0.495778089	4.534389191
45	2.639898217	-0.959524123	4.378341657
46	2.699468332	-0.845617247	4.242251681
47	2.71077166	-0.720914466	4.19833146
48	3.075554392	-0.988920653	3.828968197
49	2.932455644	-1.039746066	4.068217916
50	2.414905262	-0.935343241	4.386437595
51	2.537755102	-0.704272587	4.350231247
52	2.593695436	0.043792625	4.467817419
53	2.739752962	-0.782628092	4.326926182
54	2.477357469	-0.557365204	5.358851408

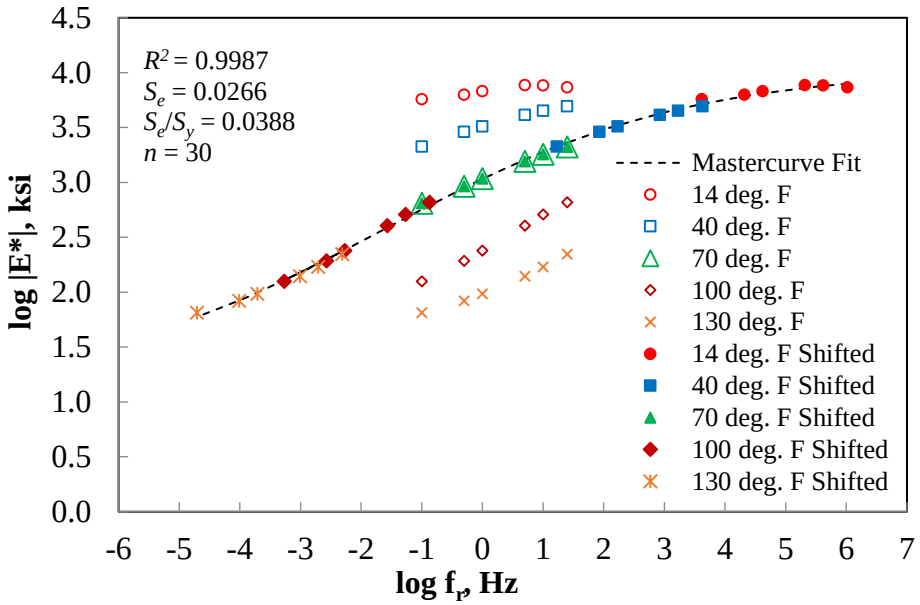

Figure 4.1 Typical development of dynamic modulus mastercurve at 70 °F reference temperature in log-log space.

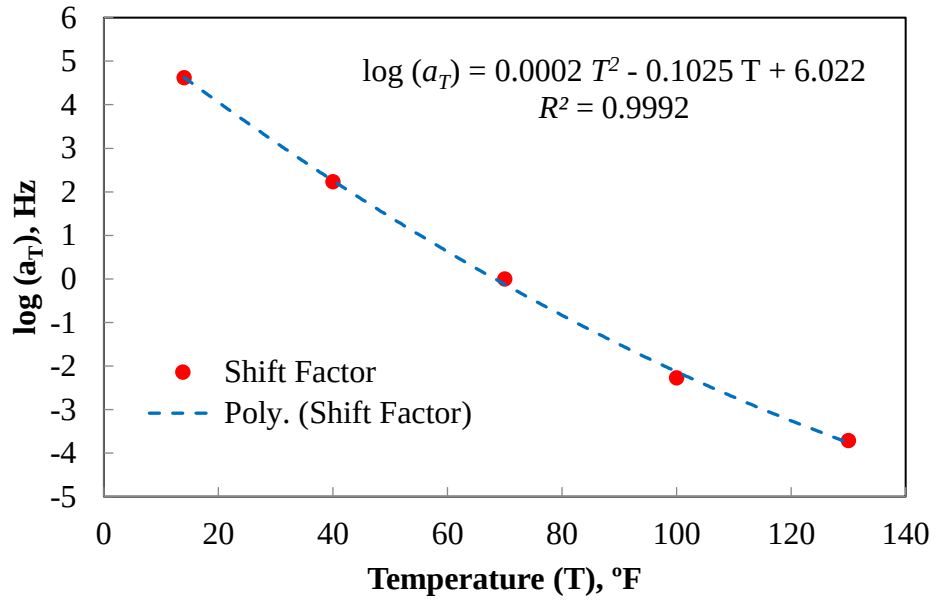

Figure 4.2 Typical development of frequency-temperature shift factor function.

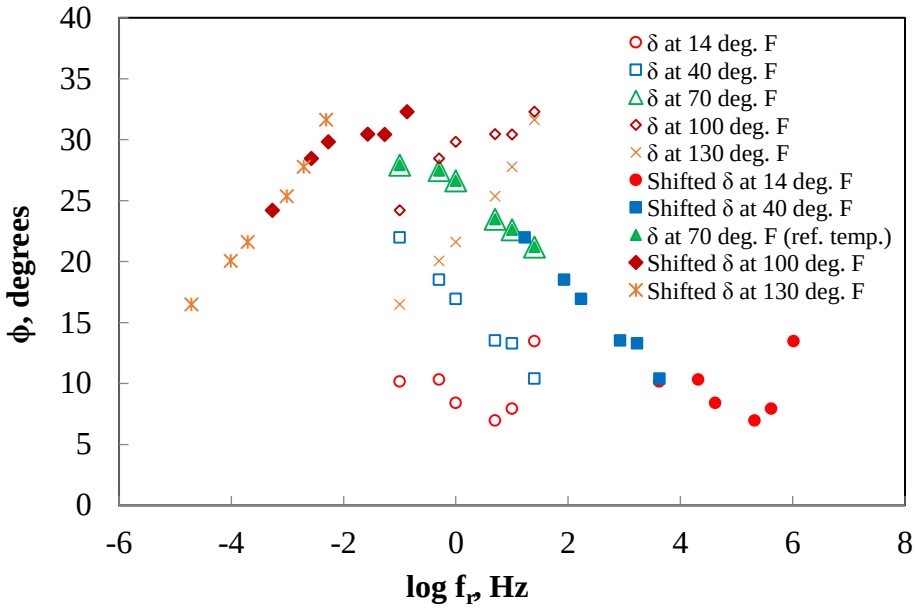

Figure 4.3 Typical development of phase angle mastercurve at 70 °F reference temperature.

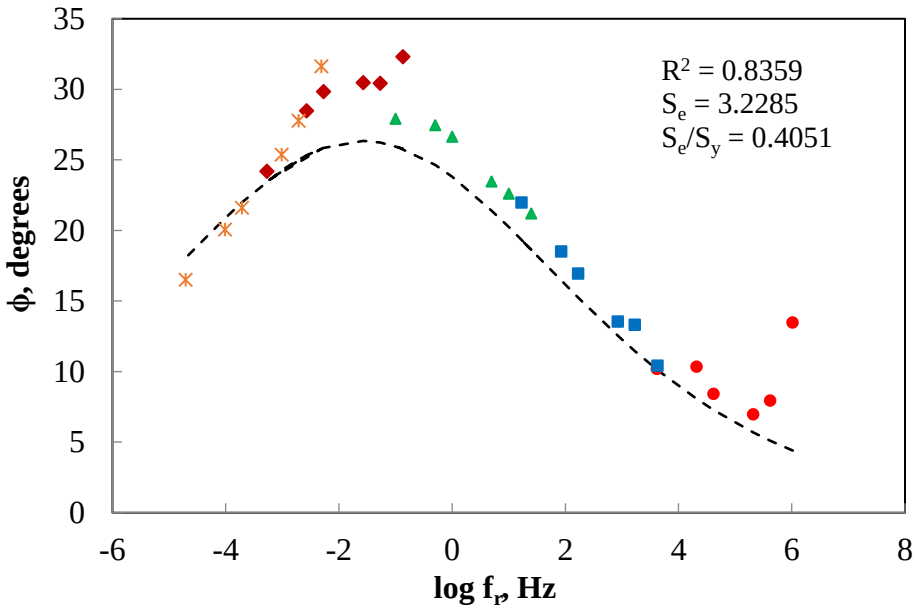

Figure 4.4 Phase angle mastercurve fitted by expression given in Equation 4.16.

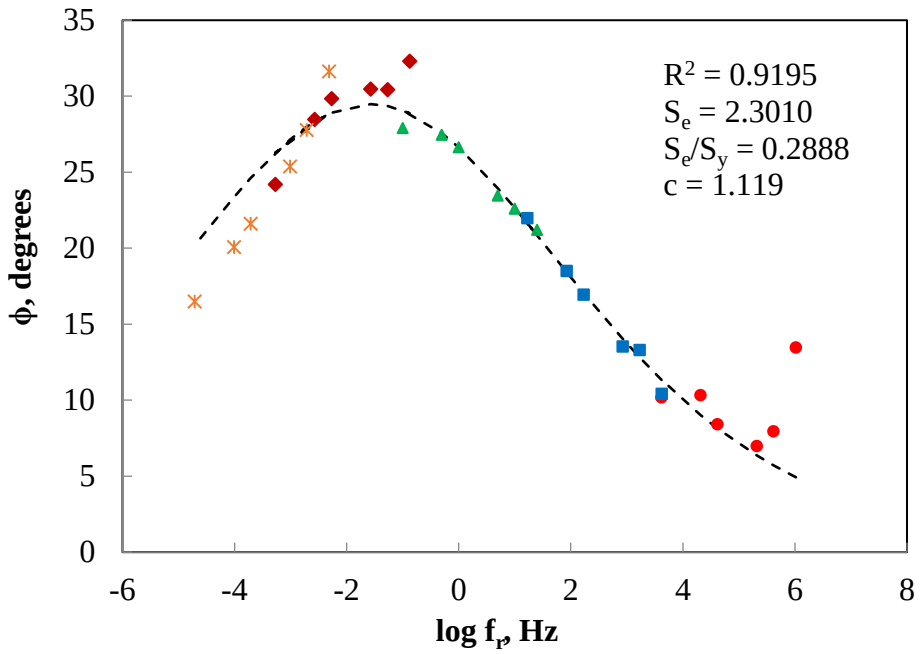

Figure 4.5 Phase angle mastercurve fitted by expression given in Equation 4.18.

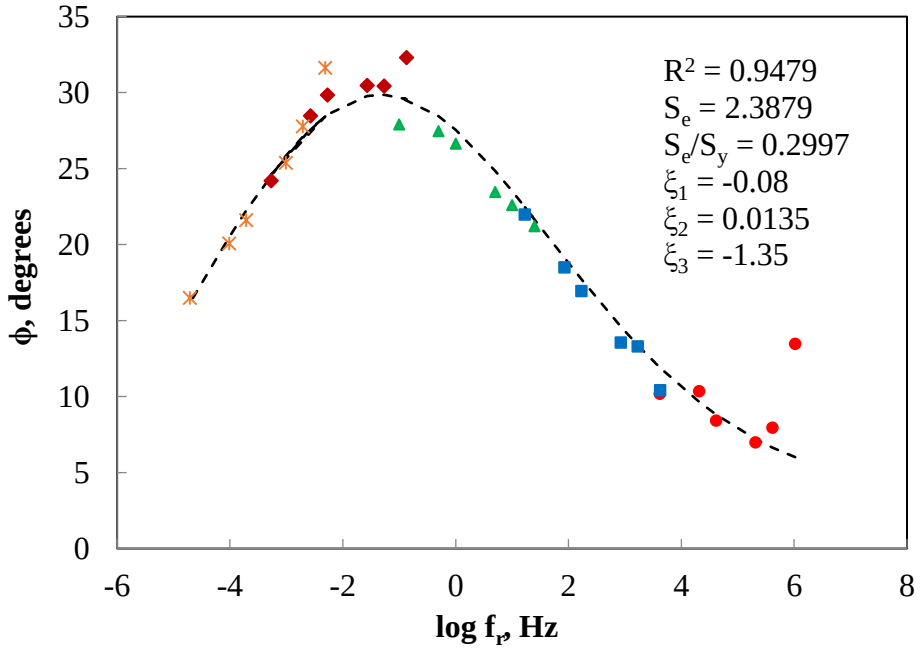

Figure 4.6 Phase angle mastercurve fitted by expression given in Equation 4.19.

Chapter 5

Independent Assurance Testing

5.1 Introduction

The |*E**| with ϕ testing is conducted over five test-temperatures and six loading frequencies in each test temperature, producing a total of 30 data points per AC specimen. Therefore, test results may vary depending on the equipment used or operatory bias. An independent assurance (IA) testing can help understand any bias, and thus precision level of the test results, and thus, the probable cause of variations can be identified.

In this study, A total of 5 (five) asphalt concrete (AC) samples were tested by the AMEC Foster Wheeler for Dynamic Modulus (|*E**|). The UNM Civil Engineering also performed |*E**| tests on the same AC samples. This study presents the comparison of |*E**| test results by the two independent laboratories. Statistical tests are done to determine whether the testing by the two independent laboratories are significantly different or not.

5.2 Objective

The specific objectives of this study are to –

- Graphical comparison of |E*|-test data obtained from the two sources, namely, the UNM |E*| testing program and test results from AMEC Foster Wheeler, and evaluate if there are any significant variations in these test results.

- Conduct statistical tests to determine the accuracy of the |*E**| testing program. Statistical tests include t-tests and single factor analysis of variance (ANOVA).

5.3 Materials

Table 5.1 gives a summary of the AC sample selected for IA testing. Four out of five of these AC samples has aggregates with Nominal Maximum Aggregate Size (NMAS) of 19mm (SP III), and the remaining AC sample has NMAS of 12.5mm. A varieties of Performance Grade (PG) binders are used in these mixtures depending upon the climatic region of the operation site. The first column of Table 5.1 shows the sample ID assigned in a chronological order by which the materials are provided to the IA testing organization. The second column presents the AC Mix ID used in this document. Elaborate descriptions of the AC samples supplied for IA testing are given in Table 5.2.

5.4 Preparation of IA Test Specimens

A Superpave® gyratory compactor was used to compact loose AC mixture. Cylindrical AC cores of 150 mm in diameter and 170 mm in height were compacted using Superpave gyratory compactor. The target air void was set at 5.5±0.5% for the finished specimen to avoid possible deviation in test results due to large air void variation. Also, most of the field cores from different regions of New Mexico showed the air void content to be in between 5 and 6%. Several trial mixes were compacted at the beginning with different weights of loose AC material. The required number of gyrations to reach 170 mm overall height was then noted for each trial AC cores. The compacted samples were then core-drilled and sawed to finished specimens of diameter 100 mm and of height 150 mm. The

theoretical maximum specific gravity (G_{mm}) was determined by AASHTO T 209. The bulk specific gravity (G_{mb}) was determined according to the AASHTO T 166 protocol. The air void (AV%) contents of the specimens were found by using Equation 5.1:

$$AV\ (\%) = \left(1 - \frac{G_{mb}}{G_{mm}}\right) \times 100 \tag{5.1}$$

The loose mix weights corresponding to the air void content of 5.5±0.5 were then used to compact further AC cores. The finished specimens were checked for *AV* at the end. For each AC mixture, 4-5 cylindrical specimens were prepared for IA testing. Several extra specimens were prepared for each of the AC mixtures for possible contingency use. Figure 5.1 shows a picture of the prepared AC specimens for IA testing.

5.5 Comparison and Statistical Analyses

The comparison and statistical analyses results are presented in the following order for each of the AC sample supplied for IA testing:

1. Comparison of $|E^*|$ mastercurves of individual test specimens
2. Two sample t-test, assuming equal variance for average $|E^*|$ and ϕ test data
3. Two sample t-test, assuming unequal variance for average $|E^*|$ and ϕ test data
4. Single factor analysis of variance (ANOVA) for $|E^*|$ and ϕ test data of individual test-specimen

5.5.1 Analyses of IA Sample 1 (AC Mix 27)

5.5.1.1 Description of the Test Specimens

Table 5.3 listed the G_{mm}, G_{mb} and the air void contents (AV%) of each of the cylindrical test-specimens tested by UNM Pavement Laboratory and AMEC Foster Wheeler Laboratory for the IA Sample 1. A difference in average air void content of 0.05% can be observed between IA specimens and UNM specimens.

5.5.1.2 Comparison of |E| Mastercurves of Individual Specimens*

Figure 5.2 shows the comparison of the |*E**| mastercurves of the individual AC specimens reported by UNM and AMEC laboratories. The mastercurves from the two laboratories shows good agreement. The |*E**|-mastercurves of all the specimens seems to be close enough. The maximum deviations in test results can be seen at the lower frequency domain which also corresponds to the high-temperature |*E**| values.

5.5.1.3 Two Sample T-test: Assuming Equal Variance for Average |E| and ϕ*

The results of the two-sample t-test assuming equal variance for the average |*E**| and ϕ are presented in Table 5.4. It can be observed from Table 5.4 that for both the average |*E**| and average ϕ, the two-tail *p*-value is found to be greater than α (alpha) which is assumed to be, $\alpha = 0.05$. This indicates the null hypothesis is true, and therefore there is no difference in population means of the two average test data from the two sources.

5.5.1.4 Two Sample T-test: Assuming Unequal Variance for Average |E| and ϕ*

The results of the two-sample *t*-test assuming unequal variance for the average |*E**| and ϕ are presented in Table 5.5. In this case, the two-tail *p*-values for both the average |*E**| and the average ϕ, found to be greater than $\alpha = 0.05$, indicating the null hypothesis to be true, and thus, there is no difference in population means of the two average test data from the two laboratories.

5.5.1.5 Single Factor ANOVA Results for the |E| and ϕ of Induvial Test Specimen*

A total of 3 replicate test-specimens were tested by UNM laboratory and 2 replicate specimens were tested by AMEC laboratory. In this Analysis of Variance (ANOVA) analysis single factor is assumed as all the 5 specimens were made from the same AC mixtures. The result of single factor ANOVA for |*E**| is presented in Table 5.6. In the case of |*E**|, the values of *F* between the groups (each of the 5-specimen data) is less than the critical *F*-value (F_{crit}). Also, the *p*-value is found to be $p = 0.76$ which is greater than $\alpha = 0.05$. This indicates that the null hypothesis is true i.e. there is no significant difference in the |*E**| data of all the five specimens. In the case of ϕ, the values of *F* between the groups is less than F_{crit}. The *p*-value is $p = 0.50$ which is greater than $\alpha = 0.05$. This indicates that the null hypothesis is true i.e. there is no significant difference in the ϕ data of all the five specimens.

5.5.2 Analyses of IA Sample 2 (AC Mix 28)

5.5.2.1 Description of the Test Specimens

Table 5.7 listed the G_{mm}, G_{mb} and the air void contents (AV%) of each of the cylindrical test-specimens tested by UNM Pavement Laboratory and AMEC Foster Wheeler Laboratory for the IA Sample 2. A difference in average air void content of 0.37% can be observed between IA specimens and UNM specimens.

5.5.2.2 Comparison of |E| Mastercurves of Individual Specimens*

Figure 5.3 shows the comparison of the |*E**| mastercurves of the individual AC specimens reported by UNM and AMEC laboratories. The mastercurves from the two laboratories shows good agreement, except one of the UNM specimen showing higher modulus values for the entire loading frequency domain considered. Otherwise, the dynamic modulus mastercurves of all other specimens seemed to be close enough.

5.5.2.3 Two Sample T-test: Assuming Equal Variance for Average |E| and ϕ*

The results of the two-sample t-test assuming equal variance for the average |*E**| and ϕ are presented in Table 5.8. It can be observed from Table 5.4 that for both the average |*E**| and average ϕ, the two-tail *p*-value is found to be greater than $\alpha = 0.05$. This indicates the null hypothesis is true, and therefore there is no difference in population means of the two average test data from the two sources.

5.5.2.4 Two Sample T-test: Assuming Unequal Variance for Average |E| and φ*

The results of the two-sample *t*-test assuming unequal variance for the average |*E**| and ϕ are presented in Table 5.9. Also in this case, the two-tail *p*-value of both the average |*E**| and the average φ, found to be greater than $\alpha = 0.05$, the null hypothesis to be true, and there is no difference in population means of the two average test data from the two laboratories.

5.5.2.5 Single Factor ANOVA Results for the |E| and ϕ of Induvial Test Specimen*

Also, for this AC sample, 3 replicate specimens were tested by UNM laboratory and 2 replicate specimens were tested by AMEC laboratory. The result of single factor ANOVA for |*E**| and ϕ is presented in Table 5.10. In the case of |*E**|, the values of *F* between the groups is less than F_{crit}. Also, the *p*-value is found to be $p = 0.20$ which is greater than $\alpha = 0.05$. This indicates that the null hypothesis is true i.e. there is no significant difference in the |*E**| data of all the five specimens. Also, in the case of ϕ, the values of *F* between the groups is less than F_{crit}. The *p*-value is found to be $p = 0.11$ which is greater than $\alpha = 0.05$. Thus, there is no significant difference in the ϕ data of all the five specimens.

5.5.3 Analyses of IA Sample 3 (AC Mix 25)

5.5.3.1 Description of the Test Specimens

Table 5.11 listed the G_{mm}, G_{mb} and the air void contents (AV%) of each of the cylindrical test-specimens tested by UNM Pavement Laboratory and AMEC Foster Wheeler

Laboratory for the IA Sample 3. A difference in average air void content of 0.07% can be observed between IA specimens and UNM specimens.

5.5.3.2 Comparison of |E| Mastercurves of Individual Specimens*

Figure 5.4 shows the comparison of the |*E**| mastercurves of the individual AC specimens reported by UNM and AMEC laboratories. The mastercurves from the two laboratories shows good agreement, except one of the UNM specimen showing higher modulus values for the entire loading frequency domain considered. Otherwise, the dynamic modulus mastercurves of all other specimens seemed to be close enough.

5.5.3.3 Two Sample T-test: Assuming Equal Variance for Average |E| and ϕ*

The results of the two-sample t-test assuming equal variance for average |*E**| and ϕ are given in Table 5.12. For both average |*E**| and average ϕ, the two-tail *p*-value is found to be greater than $\alpha = 0.05$. This indicates the null hypothesis is true, and therefore there is no difference in population means of the two average test data from the two sources.

5.5.3.4 Two Sample T-test: Assuming Unequal Variance for Average |E| and ϕ*

The results of the two-sample t-test assuming equal variance for average |*E**| and ϕ are given in Table 5.13. Also in this case, the two-tail *p*-value of both the average |*E**| and the average ϕ, found to be greater than $\alpha = 0.05$. This indicates the null hypothesis is true, and therefore there is no difference in population means of the two average test data from the two sources.

5.5.3.5 Single Factor ANOVA Results for the |E| and ϕ of Induvial Test Specimen*

For this IA sample, also a total of 3 replicate specimens were tested by UNM laboratory and 2 replicate specimens were tested by AMEC laboratory. The result of single factor ANOVA for |*E**| and ϕ is given in Table 5.14. In the case of |*E**|, the value of *F* between the groups is less than F_{crit}. Also, the *p*-value is found to be $p = 0.09$ which is greater than $\alpha = 0.05$. This indicates that the null hypothesis is true i.e. there is no significant difference in the |*E**| data of all the five specimens. In the case of ϕ, the value of *F* is less than F_{crit}. The *p*-value is also found to be $p = 0.94$ which is greater than $\alpha = 0.05$. This indicates that the null hypothesis is true i.e. there is no significant difference in the ϕ data of all the five specimens.

5.5.4 Analyses of IA Sample 4 (AC Mix 26)

5.5.4.1 Description of the Test Specimens

Table 5.15 listed the G_{mm}, G_{mb} and the air void contents (AV%) of each of the cylindrical test-specimens tested by UNM Pavement Laboratory and AMEC Foster Wheeler Laboratory for the IA Sample 4. A difference in average air void content of 0.02% can be observed between IA specimens and UNM specimens.

5.5.4.2 Comparison of |E| Mastercurves of Individual Specimens*

Figure 5.5 shows the comparison of the |*E**| mastercurves of the individual AC specimens reported by UNM and AMEC laboratories. The mastercurves from the two laboratories shows good agreement, except one of the UNM specimen showing lower modulus values

for the entire loading frequency domain considered. Otherwise, the dynamic modulus mastercurves of all other specimens seemed to be close enough.

5.5.4.3 Two Sample T-test: Assuming Equal Variance for Average |E| and ϕ*

The results of the two-sample t-test assuming equal variance for the average |*E**| and ϕ are given in Table 5.16. For both the average |*E**| and average φ, the two-tail *p*-value is found to be greater than $\alpha = 0.05$. This indicates the null hypothesis is true, and therefore there is no difference in population means of the two average test data from the two sources.

5.5.4.4 Two Sample T-test: Assuming Unequal Variance for Average |E| and ϕ*

The results of the two-sample t-test assuming equal variance for average |*E**| and ϕ are given in Table 5.17. Also in this case, the two-tail *p*-value of both the average |*E**| and the average ϕ, found to be greater than $\alpha = 0.05$. This indicates the null hypothesis is true, and therefore there is no difference in population means of the two average test data from the two sources.

5.5.4.5 Single Factor ANOVA Results for the |E| and ϕ of Induvial Test Specimen*

A total of 3 replicate specimens were tested by UNM laboratory and 2 replicate specimens were tested by AMEC laboratory. The result of single factor ANOVA for |*E**| and ϕ is given in Table 5.18. In the case of |*E**|, the value of *F* between the groups is less than F_{crit}. Also, the *p*-value is found to be $p = 0.43$ which is greater than $\alpha = 0.05$. This indicates that the null hypothesis is true i.e. there is no significant difference in the |*E**| data of all the five specimens. Again, in the case of ϕ, the values of *F* between the groups is less than the

critical *F*-value, and the *p*-value is found to be $p = 0.31$ which is greater than $\alpha = 0.05$. This indicates that the null hypothesis is true i.e. there is no significant difference in the ϕ data of all the five specimens.

5.5.5 Analyses of IA Sample 5 (AC Mix 27)

5.5.5.1 Description of the Test Specimens

Table 5.19 listed the G_{mm}, G_{mb} and the air void contents (AV%) of each of the cylindrical test-specimens tested by UNM Pavement Laboratory and AMEC Foster Wheeler Laboratory for the IA Sample 5. A difference in average air void content of 0.07% can be observed between IA specimens and UNM specimens.

5.5.5.2 Comparison of |E| Mastercurves of Individual Specimens*

Figure 5.6 shows the comparison of the |*E**| mastercurves of the individual AC specimens reported by UNM and AMEC laboratories. The two of the UNM specimen showing higher modulus values for the entire reduced frequency domain considered.

5.5.5.3 Two Sample T-test: Assuming Equal Variance for Average |E| and ϕ*

The results of the two-sample t-test assuming equal variance for average |*E**| and ϕ are given in Table 5.20. For both the average |*E**| and average ϕ, the two-tail *p*-value is found to be greater than $\alpha = 0.05$. This indicates the null hypothesis is true, and therefore there is no difference in population means of the two average test data from the two sources.

5.5.5.4 Two Sample T-test: Assuming Unequal Variance for Average |E| and ϕ*

The results of the two-sample t-test assuming equal variance for average |*E**| and ϕ are given in Table 5.21. Also in this case, the two-tail *p*-value of both the average |*E**| and the average ϕ, found to be greater than $\alpha = 0.05$. This indicates the null hypothesis is true, and therefore there is no difference in population means of the two average test data from the two sources.

5.5.5.5 Single Factor ANOVA Results for the |E| and ϕ of Induvial Test Specimen*

A total of 3 replicate specimens were tested by UNM and 2 replicate specimens are tested by AMEC. The result of single factor ANOVA for |*E**| and ϕ is given in Table 2.22. In the case of |*E**|, the value of *F* between the groups is greater than F_{crit}, and the *p*-value is found to be $p = 0.03$ which is less than $\alpha = 0.05$. This indicates that the null hypothesis can be rejected i.e. there is significant difference in the |*E**| data of all the five specimens. Again, in the case of ϕ, the values of *F* between the groups is less than the critical *F*-value, and the *p*-value is found to be $p = 0.056$ which is greater than $\alpha = 0.05$. This indicates that the null hypothesis is true i.e. there is no significant difference in the ϕ data of all the five specimens.

5.6 Findings

Table 5.23 gives a summary of the statistical analysis of IA test data. Only in case of ANOVA analysis of |E*| data for the IA sample 5 infers significant difference between the test data from two laboratories, whereas, the t-statistics infers the |*E**| data are not different.

All the other IA samples showed no difference in |E*| and ϕ data from the two laboratories considering all the statistical test considered in this study.

Table 5.1 AC Samples Selected for IA Testing

IA Sample ID	AC Mix ID (AC mixes in current study)	NMDOT District	Superpave Gradation	Specified/Used Binder PG
1	27	5	SP-III	64-28/58-28
2	28	3	SP-III	70-22/64-22
3	25	4	SP-III	76-22/70-28
4	26	4	SP-III	76-22/70-28+
5	29	3	SP-IV	76-22/70-22

Table 5.2 Description of the IA Test Samples

Info	**IA Sample 1**	**IA Sample 2**	**IA Sample 3**	**IA Sample 4**	**IA Sample 5**
Sample Identification	AC Mix 27	AC Mix 28	AC Mix 25	AC Mix 26	AC Mix 29
NMDOT District	District 5	District 3	District 4	District 4	District 3
SP Gradation	SP-III	SP-III	SP-III	SP-III	SP-IV
Specified Binder	PG 64-28	PG 70-22	PG 76-22	PG 76-22	PG 76-22
Used Binder	PG 58-28	PG 64-22	PG 70-28	PG 70-28+	PG 70-22
Mix Type	HMA	HMA	WMA (Cecabase RT)	WMA (Cecabase RT)	WMA (Maxam Aqua-Black)
RAP Content	35%	35%	20%	20%	15%
NMDOT Project No.	5100411	A300411	4100600-SPS10-TS-4	4100600-SPS10-TS-5	A301010/ A301610
Location	I-40 & US 285 Intersection	NM 333	I-40	I-40	I-25
Mile Post	248.84 – 250.46	0.000-4.425	239.179-243.000	239.179-243.000	216.25-220.00
County	Torrance	Bernalillo	Guadalupe	Guadalupe	Bernalillo
Contractor	Mountain States Constructions	Mountain States Constructors	Fisher Sand & Gravel NM, Inc.	Fisher Sand & Gravel NM, Inc.	Mountain States Constructors
SML Mix Design No.	2014-HMA-D5-10-60	2014-SMA-D3-05-35	2014-WMA-D4-08-48 TS-4	2014-WMA-D4-08-49 TS-5	2015-WMA-D3-02-32
Asphalt Source	Western Refining	Western Refining	HollyFrontier Ref. & Marketing LLC	HollyFrontier Ref. & Marketing LLC	Western Refining
Aggregate Source	Davis Pit, Moriarty, NM	Davis Pit, Moriarty, NM	Moon Pit, Guadalupe, NM	Moon Pit, Guadalupe, NM	Los Lunas Pit, Los Lunas, NM

Table 5.3 G_{mm}, G_{mb}, and AV% of IA Sample 1 Test-Specimens

Laboratory	Specimen ID	G_{mm}	G_{mb}	Individual AV%	Average AV%
UNM Pavement Laboratory	US-285-1	2.522	2.372	6.0	6.00
	US-285-2		2.370	6.0	
	US-285-4		2.371	6.0	
AMEC Foster Wheeler Laboratory	US-285-5		2.370	6.0	5.95
	US-285-6		2.373	5.9	

Table 5.4 T-Test Results Assuming Equal Variance for the Average |E^*| and ϕ of IA Sample 1

Dynamic Modulus (|E^*|)			**Phase Angle (ϕ)**		
	UNM	**IA**		**UNM**	**IA**
Mean	2221.61288	1794.995	Mean	21.01	21.40166667
Variance	5138273.333	3007306.114	Variance	68.35181226	152.0790489
Observations	30	30	Observations	30	30
Pooled Variance	4072789.723		Pooled Variance	110.2154306	
Hypothesized Mean Difference	0		Hypothesized Mean Difference	0	
df	58		df	58	
t Stat	0.8187262		t Stat	-0.144491081	
P(T<=t) one-tail	0.208146976		P(T<=t) one-tail	0.442806806	
t Critical one-tail	1.671552762		t Critical one-tail	1.671552762	
P(T<=t) two-tail	0.416293951		P(T<=t) two-tail	0.885613612	
t Critical two-tail	2.001717484		t Critical two-tail	2.001717484	

Table 5.5 T-Test Results Assuming Unequal Variance for the Average |E^*| and ϕ of IA Sample 1

Dynamic Modulus (|E^*|)			**Phase Angle (ϕ)**		
	UNM	**IA**		**UNM**	**IA**
Mean	2221.61288	1794.995	Mean	21.01	21.40166667
Variance	5138273.333	3007306.114	Variance	68.35181226	152.0790489
Observations	30	30	Observations	30	30
Hypothesized Mean Difference	0		Hypothesized Mean Difference	0	
df	54		df	51	
t Stat	0.8187262		t Stat	-0.144491081	
P(T<=t) one-tail	0.208270597		P(T<=t) one-tail	0.442841093	
t Critical one-tail	1.673564906		t Critical one-tail	1.67528495	
P(T<=t) two-tail	0.416541195		P(T<=t) two-tail	0.885682186	
t Critical two-tail	2.004879288		t Critical two-tail	2.00758377	

Table 5.6 Single Factor ANOVA Results for $|E^*|$ and ϕ of IA Sample 1

(a) Dynamic Modulus ($|E^*|$)

Groups	Count	Sum	Average	Variance		
Column 1	30	69621.87371	2320.729124	5771540.297		
Column 2	30	66003.43315	2200.114438	5042441.179		
Column 3	30	64319.85232	2143.995077	4801506.985		
Column 4	30	49598.6	1653.286667	2270871.194		
Column 5	30	58101.1	1936.703333	3970577.725		

ANOVA

Source of Variation	SS	df	MS	F	P-value	F crit
Between Groups	8246298.536	4	2061574.634	0.471606474	0.75650919	2.434065136
Within Groups	633851184	145	4371387.476			
Total	642097482.6	149				

(b) Phase Angle (ϕ)

Groups	Count	Sum	Average	Variance		
Column 1	30	591.7	19.72333333	68.23702299		
Column 2	30	674.8	22.49333333	71.92822989		
Column 3	30	624.4	20.81333333	71.67498851		
Column 4	30	706.9	23.56333333	304.1755057		
Column 5	30	577.2	19.24	79.83351724		

ANOVA

Source of Variation	SS	df	MS	F	P-value	F crit
Between Groups	402.7246667	4	100.6811667	0.844854334	0.49892613	2.434065136
Within Groups	17279.62867	145	119.1698529			
Total	17682.35333	149				

Table 5.7 G_{mm}, G_{mb}, and AV% of IA Sample 2 Test-Specimens

Laboratory	**Specimen ID**	G_{mm}	G_{mb}	**Individual AV%**	**Average AV%**
UNM Pavement Laboratory	NM-333-7	2.518	2.367	6.0	5.97
	NM-333-12		2.366	6.0	
	NM-333-13		2.369	5.9	
AMEC Foster Wheeler Laboratory	NM-333-11		2.387	5.2	5.60
	NM-333-14		2.366	6.0	

Table 5.8 T-Test Results Assuming Equal Variance for the Average $|E^*|$ and ϕ of IA Sample 2

Dynamic Modulus ($\|E^*\|$)			**Phase Angle (ϕ)**		
	UNM	**IA**		**UNM**	**IA**
Mean	2261.97056	1870.411667	Mean	21.29888889	21.77666667
Variance	5416626.927	3280957.947	Variance	49.04800639	187.0782299
Observations	30	30	Observations	30	30
Pooled Variance	4348792.437		Pooled Variance	118.0631181	
Hypothesized Mean Difference	0		Hypothesized Mean Difference	0	
df	58		df	58	
t Stat	0.727207554		t Stat	-0.170299923	
P(T<=t) one-tail	0.235012026		P(T<=t) one-tail	0.432683468	
t Critical one-tail	1.671552762		t Critical one-tail	1.671552762	
P(T<=t) two-tail	0.470024053		P(T<=t) two-tail	0.865366937	
t Critical two-tail	2.001717484		t Critical two-tail	2.001717484	

Table 5.9 T-Test Results Assuming Unequal Variance for the Average $|E^*|$ and ϕ of IA Sample 2

Dynamic Modulus ($\|E^*\|$)			**Phase Angle (ϕ)**		
	UNM	**IA**		**UNM**	**IA**
Mean	2261.97056	1870.411667	Mean	21.29888889	21.77666667
Variance	5416626.927	3280957.947	Variance	49.04800639	187.0782299
Observations	30	30	Observations	30	30
Hypothesized Mean Difference	0		Hypothesized Mean Difference	0	
df	55		df	43	
t Stat	0.727207554		t Stat	-0.170299923	
P(T<=t) one-tail	0.235091517		P(T<=t) one-tail	0.432786518	
t Critical one-tail	1.673033965		t Critical one-tail	1.681070703	
P(T<=t) two-tail	0.470183034		P(T<=t) two-tail	0.865573036	
t Critical two-tail	2.004044783		t Critical two-tail	2.016692199	

Table 5.10 Single Factor ANOVA Results for |*E**| and ϕ of IA Sample 2

(a) Dynamic Modulus (|*E|)**

Groups	Count	Sum	Average	Variance		
Column 1	30	54223.69796	1807.456599	3343319.232		
Column 2	30	89166.77263	2972.225754	9521075.021		
Column 3	30	60186.87977	2006.229326	4448083.449		
Column 4	30	53138.1	1771.27	2690577.818		
Column 5	30	59086.6	1969.553333	3937981.191		

ANOVA

Source of Variation	SS	df	MS	F	P-value	F crit
Between Groups	29402674.24	4	7350668.56	1.535160872	0.195051375	2.434065136
Within Groups	694290064.6	145	4788207.342			
Total	723692738.8	149				

(b) Phase Angle (*ϕ*)

Groups	Count	Sum	Average	Variance		
Column 1	30	688	22.93333333	55.7954023	30	688
Column 2	30	549.2	18.30666667	65.45926437	30	549.2
Column 3	30	679.7	22.65666667	37.00391954	30	679.7
Column 4	30	558.2	18.60666667	69.92891954	30	558.2
Column 5	30	748.4	24.94666667	430.1108506	30	748.4

ANOVA

Source of Variation	SS	df	MS	F	P-value	F crit
Between Groups	1015.202667	4	253.8006667	1.927702418	0.108911935	2.434065136
Within Groups	19090.65233	145	131.6596713			
Total	20105.855	149				

Table 5.11 G_{mm}, G_{mb}, and AV% of IA Sample 3 Test-Specimens

Laboratory	**Specimen ID**	***Gmm***	***Gmb***	**Individual AV%**	**Average AV%**
UNM Pavement Laboratory	TS-4-1	2.470	2.322	6.0	5.93
	TS-4-2		2.327	5.8	
	TS-4-3		2.321	6.0	
AMEC Foster Wheeler Laboratory	TS-4-7		2.323	6.0	6.00
	TS-4-12		2.321	6.0	

Table 5.12 T-Test Results Assuming Equal Variance for the Average $|E^*|$ and ϕ of IA Sample 3

Dynamic Modulus ($\|E^*\|$)			**Phase Angle (ϕ)**		
	UNM	**IA**		**UNM**	**IA**
Mean	1987.880644	1099.976667	Mean	20.82111111	21.95166667
Variance	5099618.235	1129929.587	Variance	76.11766156	110.267842
Observations	30	30	Observations	30	30
Pooled Variance	3114773.911		Pooled Variance	93.19275176	
Hypothesized			Hypothesized		
Mean Difference	0		Mean Difference	0	
df	58		df	58	
t Stat	1.948490832		t Stat	-0.453572244	
P(T<=t) one-tail	0.02809987		P(T<=t) one-tail	0.325914647	
t Critical one-tail	1.671552762		t Critical one-tail	1.671552762	
P(T<=t) two-tail	0.05619974		P(T<=t) two-tail	0.651829294	
t Critical two-tail	2.001717484		t Critical two-tail	2.001717484	

Table 5.13 T-Test Results Assuming Unequal Variance for the Average $|E^*|$ and ϕ of IA Sample 3

Dynamic Modulus ($\|E^*\|$)			**Phase Angle (ϕ)**		
	UNM	**IA**		**UNM**	**IA**
Mean	1987.880644	1099.976667	Mean	20.82111111	21.95166667
Variance	5099618.235	1129929.587	Variance	76.11766156	110.267842
Observations	30	30	Observations	30	30
Hypothesized			Hypothesized		
Mean Difference	0		Mean Difference	0	
df	41		df	56	
t Stat	1.948490832		t Stat	-0.453572244	
P(T<=t) one-tail	0.029111349		P(T<=t) one-tail	0.325944788	
t Critical one-tail	1.682878002		t Critical one-tail	1.672522303	
P(T<=t) two-tail	0.058222698		P(T<=t) two-tail	0.651889577	
t Critical two-tail	2.01954097		t Critical two-tail	2.003240719	

Table 5.14 Single Factor ANOVA Results for $|E^*|$ and ϕ of IA Sample 3

(a) Dynamic Modulus ($\|E^*\|$)						
Groups	Count	Sum	Average	Variance		
Column 1	30	61059.71417	2035.323806	5076555.87		
Column 2	30	57888.52053	1929.617351	4784349.02		
Column 3	30	59961.02325	1998.700775	5495532.643		
Column 4	30	34076.7	1135.89	1178393.342		
Column 5	30	31921.9	1064.063333	1086393.417		
ANOVA						
Source of Variation	SS	df	MS	F	P-value	F crit
Between Groups	28631707.27	4	7157926.818	2.031052638	0.093097054	2.434065136
Within Groups	511015504.5	145	3524244.859			
Total	539647211.8	149				
(b) Phase Angle (ϕ)						
Groups	Count	Sum	Average	Variance		
Column 1	30	627.2	20.90666667	79.97236782	30	627.2
Column 2	30	626.8	20.89333333	79.40409195	30	626.8
Column 3	30	619.9	20.66333333	71.84378161	30	619.9
Column 4	30	639.2	21.30666667	84.3096092	30	639.2
Column 5	30	677.9	22.59666667	160.5844713	30	677.9
ANOVA						
Source of Variation	SS	df	MS	F	P-value	F crit
Between Groups	72.098	4	18.0245	0.189287522	0.9436809	2.434065136
Within Groups	13807.31533	145	95.22286437			
Total	13879.41333	149				

Table 5.15 G_{mm}, G_{mb}, and AV% of IA Sample 4 Test-Specimens

Laboratory	**Specimen ID**	G_{mm}	G_{mb}	**Individual AV%**	**Average AV%**
UNM Pavement Laboratory	TS-5-4	2.475	2.331	5.8	5.4
	TS-5-5		2.341	5.4	
	TS-5-6		2.352	5.0	
AMEC Foster Wheeler Laboratory	TS-5-9		2.341	5.4	5.2
	TS-5-10		2.352	5.0	

Table 5.16 T-Test Results Assuming Equal Variance for the Average |E^*| and ϕ of IA Sample 4

Dynamic Modulus (|E^*|)			**Phase Angle (ϕ)**		
	UNM	**IA**		**UNM**	**IA**
Mean	1839.380778	1367.951667	Mean	17.75444444	21.16166667
Variance	2679802.301	1669954.91	Variance	77.77038186	110.0692557
Observations	30	30	Observations	30	30
Pooled Variance	2174878.605		Pooled Variance	93.91981881	
Hypothesized Mean Difference	0		Hypothesized Mean Difference	0	
df	58		df	58	
t Stat	1.238068049		t Stat	-1.361656194	
P(T<=t) one-tail	0.110339472		P(T<=t) one-tail	0.089286208	
t Critical one-tail	1.671552762		t Critical one-tail	1.671552762	
P(T<=t) two-tail	0.220678945		P(T<=t) two-tail	0.178572415	
t Critical two-tail	2.001717484		t Critical two-tail	2.001717484	

Table 5.17 T-Test Results Assuming Unequal Variance for the Average |E^*| and ϕ of IA Sample 4

Dynamic Modulus (|E^*|)			**Phase Angle (ϕ)**		
	UNM	**IA**		**UNM**	**IA**
Mean	1839.380778	1367.951667	Mean	17.75444444	21.16166667
Variance	2679802.301	1669954.91	Variance	77.77038186	110.0692557
Observations	30	30	Observations	30	30
Hypothesized Mean Difference	0		Hypothesized Mean Difference	0	
df	55		df	56	
t Stat	1.238068049		t Stat	-1.361656194	
P(T<=t) one-tail	0.110474843		P(T<=t) one-tail	0.089379816	
t Critical one-tail	1.673033965		t Critical one-tail	1.672522303	
P(T<=t) two-tail	0.220949685		P(T<=t) two-tail	0.178759631	
t Critical two-tail	2.004044783		t Critical two-tail	2.003240719	

Table 5.18 Single Factor ANOVA Results for $|E^*|$ and ϕ of IA Sample 4

(a) Dynamic Modulus ($\|E^*\|$)						
Groups	Count	Sum	Average	Variance		
Column 1	30	57696.67603	1923.222534	3023770.32		
Column 2	30	54762.95702	1825.431901	2624850.964		
Column 3	30	53084.63693	1769.487898	2454901.053		
Column 4	30	38614.5	1287.15	1624417.692		
Column 5	30	43462.6	1448.753333	1737920.912		
ANOVA						
Source of Variation	SS	df	MS	F	P-value	F crit
Between Groups	8755839.977	4	2188959.994	0.954555443	0.434507958	2.434065136
Within Groups	332509967.3	145	2293172.188			
Total	341265807.3	149				
(b) Phase Angle (ϕ)						
Groups	Count	Sum	Average	Variance		
Column 1	30	539.5	17.98333333	83.50143678		
Column 2	30	539.4	17.98	78.56372414		
Column 3	30	519	17.3	77.28965517		
Column 4	30	607.9	20.26333333	88.00585057		
Column 5	30	661.8	22.06	169.2183448		
ANOVA						
Source of Variation	SS	df	MS	F	P-value	F crit
Between Groups	475.6436	4	118.9109	1.197300905	0.314575275	2.434065136
Within Groups	14400.79133	145	99.3158023			
Total	14876.43493	149				

Table 5.19 G_{mm}, G_{mb}, and AV% of IA Sample 5 Test-Specimens

Laboratory	**Specimen ID**	G_{mm}	G_{mb}	**Individual AV%**	**Average AV%**
UNM Pavement Laboratory	RB-2	2.580	2.425	6.0	5.53
	RB-6		2.436	5.6	
	RB-10		2.451	5.0	
AMEC Foster Wheeler Laboratory	RB-1		2.454	5.5	5.60
	RB-5		2.448	5.7	

Table 5.20 T-Test Results Assuming Equal Variance for the Average $|E^*|$ and ϕ of IA Sample 5

Dynamic Modulus ($\|E^*\|$)			**Phase Angle (ϕ)**		
	UNM	**IA**		**UNM**	**IA**
Mean	2387.134068	1470.166667	Mean	19.83111111	23.74333333
Variance	5431655.146	2251768.085	Variance	84.47853895	198.4747816
Observations	30	30	Observations	30	30
Pooled Variance	3841711.615		Pooled Variance	141.4766603	
Hypothesized			Hypothesized		
Mean Difference	0		Mean Difference	0	
df	58		df	58	
t Stat	1.811912186		t Stat	-1.273874797	
P(T<=t) one-tail	0.037588823		P(T<=t) one-tail	0.103894462	
t Critical one-tail	1.671552762		t Critical one-tail	1.671552762	
P(T<=t) two-tail	0.075177647		P(T<=t) two-tail	0.207788925	
t Critical two-tail	2.001717484		t Critical two-tail	2.001717484	

Table 5.21 T-Test Results Assuming Unequal Variance for the Average $|E^*|$ and ϕ of IA Sample 5

Dynamic Modulus ($\|E^*\|$)			**Phase Angle (ϕ)**		
	UNM	**IA**		**UNM**	**IA**
Mean	2387.134068	1470.166667	Mean	19.83111111	23.74333333
Variance	5431655.146	2251768.085	Variance	84.47853895	198.4747816
Observations	30	30	Observations	30	30
Hypothesized			Hypothesized		
Mean Difference	0		Mean Difference	0	
df	50		df	50	
t Stat	1.811912186		t Stat	-1.273874797	
P(T<=t) one-tail	0.038003705		P(T<=t) one-tail	0.104298772	
t Critical one-tail	1.675905025		t Critical one-tail	1.675905025	
P(T<=t) two-tail	0.076007411		P(T<=t) two-tail	0.208597543	
t Critical two-tail	2.008559112		t Critical two-tail	2.008559112	

Table 5.22 Single Factor ANOVA Results for |*E**| and ϕ of IA Sample 5

(a) Dynamic Modulus (|*E|)**						
Groups	Count	Sum	Average	Variance		
Column 1	30	53795.52679	1793.184226	3561459.468		
Column 2	30	75724.90974	2524.163658	5779942.281		
Column 3	30	85321.6296	2844.05432	7368508.496		
Column 4	30	48054.3	1601.81	2699115.308		
Column 5	30	40155.7	1338.523333	1846934.379		
ANOVA						
Source of Variation	SS	df	MS	F	P-value	F crit
Between Groups	48719538.98	4	12179884.74	2.86505168	0.025407021	2.434065136
Within Groups	616422838	145	4251191.986			
Total	665142377	149				
(b) Phase Angle (*ϕ*)						
Groups	Count	Sum	Average	Variance		
Column 1	30	656.5	21.88333333	101.5421264		
Column 2	30	583.4	19.44666667	81.4336092		
Column 3	30	544.9	18.16333333	76.47964368		
Column 4	30	814.6	27.15333333	395.2653333		
Column 5	30	610	20.33333333	120.4022989		
ANOVA						
Source of Variation	SS	df	MS	F	P-value	F crit
Between Groups	1462.910267	4	365.7275667	2.359158232	0.056180073	2.434065136
Within Groups	22478.56733	145	155.0246023			
Total	23941.4776	149				

Table 5.23 Summary of Statistical Analyses of IA Test Results

ID	AC MIX	Dynamic Modulus $\|E^*\|$		
		t-Test: Two Sample		ANOVA: Single Factor Analysis
		Assuming Equal Variance	Assuming Unequal Variance	
1	D5 SP-III PG 64-28/58-28 HMA 35% RAP	$p = 0.42 > \alpha = 0.05$ No significant difference in test results	$p = 0.42 > \alpha = 0.05$ No significant difference in test results	$F = 0.47$, $F_{critical} = 2.43$ $p = 0.76 > \alpha = 0.05$ $F < F_{critical}$ No significant difference in test results
2	D3 SP-III PG 70-22/64-22 HMA 35% RAP	$p = 0.47 > \alpha = 0.05$ No significant difference in test results	$p = 0.47 > \alpha = 0.05$ No significant difference in test results	$F = 1.54$, $F_{critical} = 2.43$ $p = 0.20 > \alpha = 0.05$ $F < F_{critical}$ No significant difference in test results
3	D4 SP-III PG 76-22/70-28 WMA (Cecabase RT) 20% RAP	$p = 0.06 > \alpha = 0.05$ No significant difference in test results	$p = 0.06 > \alpha = 0.05$ No significant difference in test results	$F = 2.03$, $F_{critical} = 2.43$ $p = 0.09 > \alpha = 0.05$ $F < F_{critical}$ No significant difference in test results
4	D4 SP-III PG 76-22/70-28+ WMA (Cecabase RT) 20% RAP	$p = 0.22 > \alpha = 0.05$ No significant difference in test results	$p = 0.22 > \alpha = 0.05$ No significant difference in test results	$F = 0.95$, $F_{critical} = 2.43$ $p = 0.43 > \alpha = 0.05$ $F < F_{critical}$ No significant difference in test results
5	D3 SP-IV PG 76-22/70-22 WMA (Maxam Aqua-Black) 15% RAP	$p = 0.08 > \alpha = 0.05$ No significant difference in test results	$p = 0.08 > \alpha = 0.05$ No significant difference in test results	$F = 2.87$, $F_{critical} = 2.43$ $p = 0.03 < \alpha = 0.05$ $F > F_{critical}$ Significant difference in test results

Figure 5.1 AC specimens prepared for IA testing.

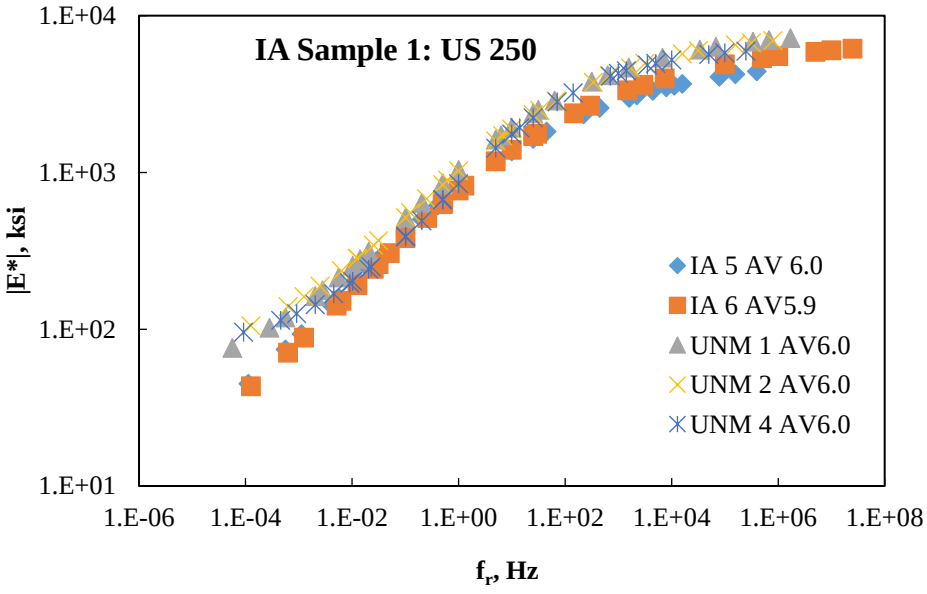

Figure 5.2 |*E**|-mastercurves of induvial test-specimen for the IA Sample 1.

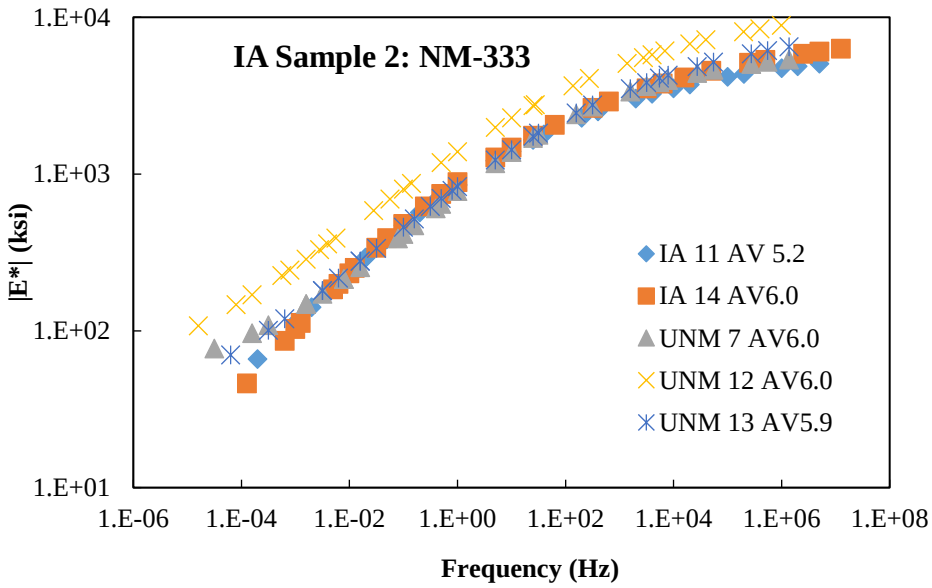

Figure 5.3 |*E**|-mastercurves of induvial test-specimen for the IA Sample 2.

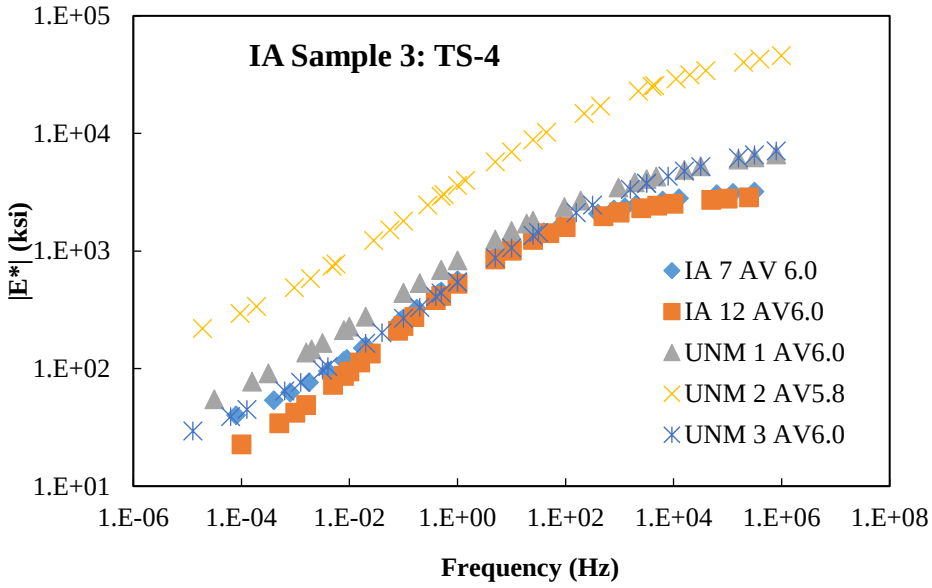

Figure 5.4 |*E**|-mastercurves of induvial test-specimen for the IA Sample 3.

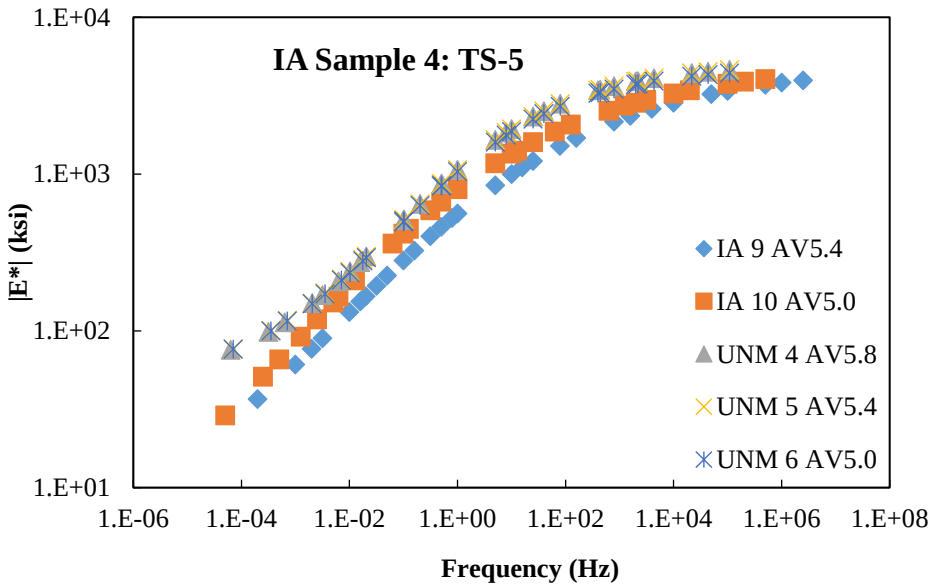

Figure 5.5 |*E**|-mastercurves of induvial test-specimen for the IA Sample 4.

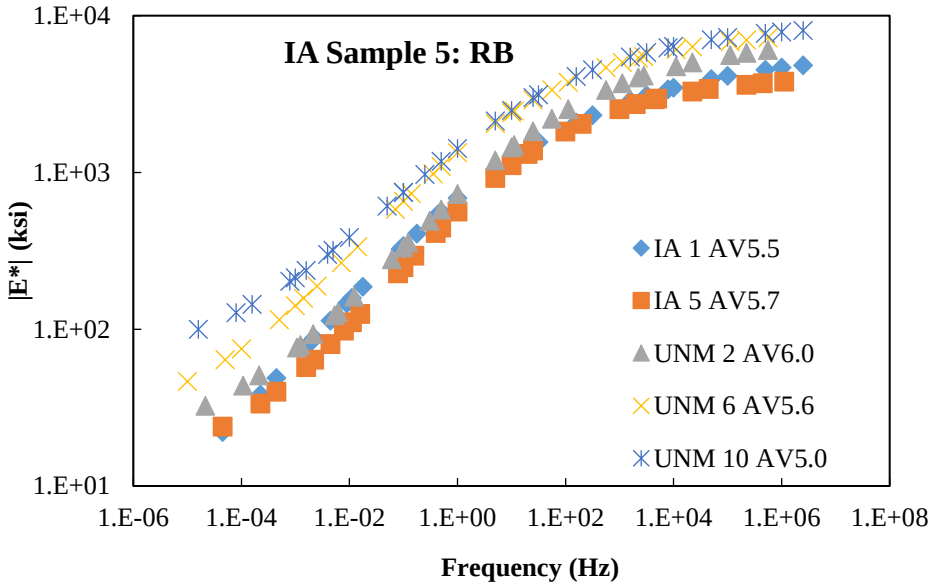

Figure 5.6 |*E**|-mastercurves of induvial test-specimen for the IA Sample 5.

Chapter 6

Effect of Fineness Modulus and Uniformity Coefficient on Dynamic Modulus of Asphalt Concrete

6.1 General

The $|E^*|$ of AC depends on many factors such as aggregate gradation, binder property, mixture volumetrics, etc. (Weldegiorgis, 2014). Several empirical and semi-empirical models are available in the literature addressing these factors to determine $|E^*|$ of AC; of which the most commonly used are the viscosity (η) based Witczak model (MEPDG 2008), the binder shear modulus ($|G_b^*|$) based Witczak model (Bari and Witczak 2006), and the Hirsch model (Christiansen et al. 2003). The η and $|G_b^*|$-based Witczak models for predicting $|E^*|$ uses four gradations parameters, namely, the percentages materials retained on the ¾ inch, 3/8 inch, No. 4 sieves ($\rho_{3/4}$, $\rho_{3/8}$, and, ρ_{200}) and the percentage passing No. 200 sieve (ρ_{200}). Significant relationships between these aggregate parameters and the $|E^*|$ of AC were found in these studies, and therefore, these parameters were included in the $|E^*|$ predictive models. On the other hand, Hirsch model indicates that there are strong relationships between $|E^*|$ and AC volumetrics, which is actually a result of aggregate packing or gradation inside the AC material. Birgisson and Roque (2005) identified and evaluated relationships between aggregate gradation and the dynamic modulus at higher temperature. In their study, power law-based gradation factors were used to identify fine and coarse graded aggregates.

From all these studies, it is clear that $|E^*|$ of AC is significantly related the aggregate gradation used in the AC mixture. However, there are a number of ways to classify, and hence, identify aggregate gradation. Some of these classification uses specific gradation parameters, such as, in Witczak's models, and some of these classification uses volumetrics, such as, in Hirsch model. In this study, the well-known fineness modulus (F_m) and the uniformity coefficient (C_u) of the aggregate blend used in the AC mixture are considered to be the parameters affecting the stiffness of AC. This study has borrowed the idea from soil mechanics to use F_m and C_u parameters for predicting $|E^*|$ of AC.

6.2 Objective

The primary objective of this study is to assess the effect of aggregate gradation on $|E^*|$ of asphalt concrete. To classify among various aggregate gradations, two universally known gradation parameters, i.e., the uniformity coefficient (C_u) and the fineness modulus (F_m) are considered, instead of using directly the percentage of material retained or passing on a particular sieve which is very common in current practice. It should be noted that, the F_m which is an empirical figure, introduced in this study is slightly different than the conventional F_m. In determining the conventional F_m, the sieve-size increases in the ratio of 2:1. However, in the current study, all the sieves used for Superpave gradation analysis are considered for determining the relative F_m of the aggregates. The deviation from the standard definition of F_m is introduced to incorporate all the sieves used in the Superpave gradation analysis and also to attain considerable ease while determining F_m. The alternative definition of F_m is also consistent with the fundamental concept regarding F_m that a smaller value indicating relatively finer aggregate type.

6.3 Materials

All 54 AC mixtures with different aggregate gradations and binder performance grades (PG) tested in this study were considered. According to AASHTO MP-2 specification, 13 of these asphalt-aggregate mixtures are Type IV Superpave aggregate blend (SP 4) with the nominal maximum aggregate size (NMAS) being 12.5 mm. The remaining 41 mixtures are Type III Superpave blend (SP 3) with the NMAS being 19 mm. A variety of binder performance grades are used in these mixtures depending on the regional climate associated with the pavement operation sites.

6.4 Determination of F_m and C_u

The definitions of F_m and C_u can be given by the following expressions:

$$F_m = \frac{\sum_{i=1}^{n} CPR_i}{100}, \text{ and} \tag{6.1}$$

$$C_u = \frac{D_{60}}{D_{10}} \tag{6.2}$$

In the above expressions, CPR_i is the cumulative percentage of aggregate retained at i^{th} sieve used in Superpave gradation analysis, D_{60} is the sieve size corresponding to 60% material passing, D_{10} is the sieve size corresponding to 10% material passing, and n is the number of sieves used in the sieve analysis.

Sieve analyses were conducted on aggregate samples corresponding to all the asphalt-aggregate mixtures considered in this study according to AASHTO T-27 (2011)

standard specification. A total of 13 standard sieves were used for sieve analyses of the aggregate blends. The designation and the opening sizes of the sieves are presented in Table 6.1.

6.5 Results and Discussion

As stated earlier, for fitting |*E**| mastercurves the following sigmoid expression is used:

$$\log\left(|E^*|\right) = \delta + \frac{\alpha}{1 + e^{\beta + \gamma \log(f_r)}} \tag{6.3}$$

In Equation 6.3, δ is the minimum modulus value; α is the vertical span of the |*E**| function, thus $\alpha + \delta$ is the maximum value of |*E**|; β and γ are the shape parameters. The parameters (e.g. α, β, δ, and γ) can be found by fitting laboratory tested |*E**| mastercurve. Table 6.2 gives a summary of the |*E**|-mastercurve parameters and F_m and C_u values for the aggregate corresponding to all 54 AC mixtures. All four |*E**| mastercurve parameters, i.e., α, β, δ, and γ were studied against the gradation variables F_m, and C_u. The effect study showed that the mastercurve parameters α, β, γ, and δ are inter-related in various trends and degrees to the F_m, and C_u of the aggregate samples corresponding to the AC mixtures. The study and discussions are presented in the following sections.

6.5.1 Effect of F_m and C_u on α

Figures 6.1 shows the |*E**|-mastercurve parameter, α versus F_m plot for all 54 AC mixtures considered in this study. The figure also presents the best suited data-trend and the corresponding coefficient of determination (R^2), which can also be interpreted as the degree of correlation between the two datasets. The value R^2 ranges between 0 to 1, and a relatively

higher value of R^2 indicates stronger correlation between the dependent and independent variables, i.e. the α and F_m, respectively, for the current case. A square root of R^2 gives the correlation coefficient (r), for which, the numerical values ranges between +1.0 to -1.0, giving an indication of the strength of the relationship. Again, when $r > 0$, a positive relationship exists between the two datasets, i.e., the dependent variable increases as the independent variable increases. On the other hand, when $r < 0$, a negative relationship exists between the two datasets, means, the dependent variable increases as the independent variable decreases. As a rule of thumb, guideline given in Table 6.3, can be used to evaluate the strength of the relationship, which can be found in any standard statistics book.

It can be observed from the Figure 6.1 that there is some non-linear relationship existing between α and F_m, for which R^2 can be estimated as 0.07. A square root of R^2 gives the correlation coefficient which can be calculated as ±0.26. Therefore, with the help of Table 6.3, it can be said that the α which is actually can be seen as the vertical span of the $|E^*|$-function, can be "weakly" correlated to the F_m of the aggregate blend, i.e., F_m has a "weak" effect on the range of $|E^*|$ found over a wide-range of frequency or temperature band.

Figure 6.2 shows the α versus C_u plot for the AC mixtures. The trend between α and C_u can be best approximated by a linear relationship. The value of estimated R^2 is found as 0.07, for which $r = 0.26$, and thus, C_u has a "weak" effect on the range of $|E^*|$ found over a wide-range of frequency or temperature band.

6.5.2 Effect of F_m and C_u on β

The |*E**|-mastercurve parameter, β is one of the two shape parameters, defining the curvature at upper portion of the |*E**|-mastercurve. As the parameter, β increases, the curvature at the upper portion decreases. Figure 6.3 shows the β versus F_m plot for the AC mixtures. In this case, also, some non-linear relationship can be established. The trend between β and F_m can be best approximated by a second-order polynomial, for which, R^2 value is found to 0.09. The correlation coefficient can be calculated as ±0.30, indicating a "moderate" strength relationship between β and F_m, according to the information provided in Table 6.3. Therefore, it can be said that, the upper curvature of the |*E**|-mastercurve is "moderately" influenced by the F_m of the aggregate blend used in the AC mixture.

Figure 6.4 presents the β versus C_u plot. A linear relationship can be approximated in this case. The R^2 value is found to be 0.003, for which, r can be calculated as -0.05. Thus, according to the information provided in Table 6.3, the strength of this relationship can be considered negligible or "very week". Correspondingly, it can be concluded that the gradation parameter, C_u has none or negligible effect on the upper limb curvature of the |*E**|-function.

6.5.3 Effect of F_m and C_u on δ

As mentioned earlier, the parameter, δ indicates the minimum modulus value possible in the |*E**|-mastercurve of a certain AC sample, which also corresponds to the high-temperature or low-frequency modulus of the material. Figure 6.5 shows the δ versus F_m

plot for all the AC mixtures. In this case, a non-linear relationship can be approximated observing the trend between these two datasets. The trend between δ and F_m is therefore, can be best approximated by a second-order polynomial, for which, R^2 value is 0.05. The correlation coefficient can be calculated, and found as ±0.22, indicating a "weak" relationship between δ and F_m, according to Table 6.3. Therefore, it can be said that, the minimum |*E**| of an AC material is "weakly" influenced by the F_m of the aggregate blend used in the AC mixture.

Figure 6.6 presents the δ versus C_u plot. A linear relationship can be approximated in this case. The R^2 value is found to be 0.04, for which, *r* can be calculated as -0.20. Thus, according to Table 6.3, the strength of this relationship can be considered "weak". Correspondingly, it can be concluded that the gradation parameter, C_u has a weak effect on the possible minimum |*E**| value.

6.5.4 Effect of F_m and C_u on γ

The parameter γ is one of the two shape parameters in a |*E**|-mastercurve, defining the slope of the transition zone in a |*E**|-mastercurve. As the parameter, γ increases, the slope at the transition zone decreases. Figure 6.7 shows the γ versus F_m plot. A linear relationship can be approximated in this case, for which, R^2 value is found to be 0.08. The correlation coefficient can be calculated as -0.28, indicating a "weak" strength relationship between γ and F_m, according to Table 6.3. Therefore, it can be said that, the slope of the transition zone in a |*E**|-mastercurve is "weakly" influenced by the F_m of the aggregate blend used in the AC mixture.

Figure 6.8 presents the γ versus C_u plot. A non-linear relationship can be approximated in this case. The R^2 value is found to be 0.02, for which, r can be calculated as ±0.14. Thus, in this case, also, the strength of the relationship can be considered "week", as mentioned in Table 6.3. Correspondingly, it can be concluded that the gradation parameter, C_u has "weak" effect on the slope at transition zone of a $|E^*|$-function.

6.5.5 General Assessment

The correlation study conducted in the earlier section can be summarized as in Table 6.4. It can be observed in Table 6.4 that all the $|E^*|$-mastercurve parameters, i.e., α, β, δ, and, γ have relatively strong relationships with the F_m of the aggregate blend. However, only the parameters α, and δ have relatively strong relationship with C_u of the aggregate blend, while effect of C_u on β and γ parameters can be neglected. In other words, the shape parameters of the $|E^*|$-mastercurve do not affected by the C_u of the aggregate blend used in the AC mixture. Thus, all the attributes of a $|E^*|$-mastercurve, such as, minimum modulus value, vertical span, upper limb curvature, and the transition zone slope are affected by the F_m, while, only minimum modulus and the vertical span is affected by the C_u of the aggregate blend used in the AC mixture.

6.6 Remarks

In this study, the effects of fineness modulus and uniformity coefficient on the dynamic modulus of asphalt concrete was evaluated. Based on the findings of this study, the following conclusions can be made:

- The fineness modulus of the aggregate blend has effect on the minimum |*E**|, the maximum |*E**|, and the overall shape of the |*E**|-function. Therefore, a change in fineness modulus, can cause changes in overall |*E**|-function of an asphalt concrete material.

- The uniformity coefficient has a trivial effect on the shape of the |*E**|-mastercurve.

Table 6.1 Standard Sieves and Opening Sizes

Sieve Designation	Sieve Opening (mm)
2 inch	50.00
1.5 inch	37.50
1 inch	25.00
3/4 inch	19.00
1/2 inch	12.50
3/8 inch	9.50
No. 4	4.75
No. 8	2.36
No. 16	1.18
No. 30	0.60
No. 50	0.30
No. 100	0.15
No. 200	0.075

Table 6.2 |*E**| Mastercurve and Gradation Parameters

AC Mix ID	When |E*| is in psi				F_m	C_u
	α	β	δ	γ		
1	2.8393	-1.0488	4.1339	-0.4378	5.5700	40.2041
2	2.4593	-0.4368	4.5052	-0.5505	6.5260	38.2931
3	2.2477	-0.4163	4.6612	-0.4918	6.3950	24.9577
4	2.5855	-0.7350	4.3427	-0.3838	6.1410	30.9424
5	1.6228	-0.5990	5.0434	-0.6957	6.6850	19.5680
6	2.2847	-0.4569	4.5541	-0.4398	5.0390	40.5145
7	2.2847	-0.4569	4.5541	-0.4398	5.0390	40.5145
8	2.6913	-0.6675	4.2932	-0.4404	6.1430	55.7617
9	2.7015	-0.8748	4.2425	-0.4292	6.2640	34.1142
10	2.2148	-0.1066	4.6229	-0.5712	5.9950	28.2259
11	2.5278	-0.4931	4.3381	-0.4845	6.5850	29.8732
12	2.2919	-0.2579	4.4991	-0.4999	6.0600	25.2685
13	2.6496	-0.8236	4.2156	-0.5144	6.0220	16.7356
14	2.8002	-0.8517	4.2361	-0.4035	6.5350	29.7956
15	2.3151	0.0559	4.6105	-0.3714	5.7770	34.2346
16	2.7674	-0.8018	4.2913	-0.3519	5.9630	39.5004
17	3.4136	-1.5043	3.6077	-0.3973	5.9630	39.5004
18	2.5511	-1.0174	4.2813	-0.5051	6.1210	37.2496
19	2.4369	-0.7600	4.3908	-0.5512	6.3920	39.2736
20	2.6861	-0.6001	4.2504	-0.5121	6.2520	55.4358
21	2.7387	-1.1242	4.1419	-0.4315	5.7670	26.6533
22	2.8848	-0.6433	4.1405	-0.4059	6.3800	36.4426
23	2.3012	-0.7404	4.4658	-0.5475	6.3800	36.4426
24	2.5579	-0.7883	4.4315	-0.5104	6.3800	36.4426
25	2.9073	-0.2768	4.1537	-0.4047	6.3800	36.4426
26	2.0595	-0.7266	4.6403	-0.6571	6.3800	36.4426
27	2.3354	-0.5226	4.5293	-0.5235	6.0790	26.9132
28	2.3354	-0.5226	4.5293	-0.5235	5.9050	32.6700
29	2.6100	-0.8605	4.2642	-0.5162	5.6350	36.3767
30	3.1179	-0.9204	3.8398	-0.2790	6.1490	18.4130
31	3.2934	-0.9321	3.7360	-0.3388	5.1390	42.5597
32	2.5632	-0.5653	4.3487	-0.4264	5.4760	45.3653
33	2.8572	-0.6328	4.1377	-0.4092	5.4760	45.3653
34	2.7637	-0.5383	4.2170	-0.3731	5.3190	62.1797
35	2.7197	-1.0424	4.1681	-0.4716	5.5910	32.6301
36	2.7672	-0.7827	4.1342	-0.3443	6.6410	31.9961
37	2.6551	-0.8015	4.2245	-0.3306	6.1460	18.8490
38	2.6385	-0.7761	4.2513	-0.4826	5.8300	23.8928
39	2.3434	-0.5227	4.5145	-0.5151	6.8030	21.3369
40	2.6393	-0.6089	4.2280	-0.4017	6.5680	26.5988
41	3.3626	-1.6682	3.5395	-0.3801	5.9560	49.0980
42	2.2494	-0.2806	4.5951	-0.5636	5.6000	49.6334
43	2.4309	-0.5085	4.5063	-0.5023	5.9830	15.1050
44	2.4021	-0.4958	4.5344	-0.4927	6.8700	17.5438
45	2.6399	-0.9595	4.3783	-0.4658	5.5340	31.6039
46	2.6995	-0.8456	4.2423	-0.4700	5.6750	31.9135
47	2.7108	-0.7209	4.1983	-0.4642	5.8330	24.0097
48	3.0756	-0.9889	3.8290	-0.4359	6.2080	39.4487
49	2.9325	-1.0397	4.0682	-0.4322	5.9440	24.8972
50	2.4149	-0.9353	4.3864	-0.5420	5.9680	29.0607
51	2.5378	-0.7043	4.3502	-0.5025	5.9810	41.5609
52	2.5937	0.0438	4.4678	-0.5677	6.6610	37.7431
53	2.7398	-0.7826	4.3269	-0.4873	6.5020	37.2268
54	2.4774	-0.5574	5.3589	-0.5377	5.9460	33.1510

Table 6.3 Thumb Rule for Strength of Relationships

Value of *r*		**Strength of Relationship**
If negatively related	**If positively related**	
-1.0 to -0.5	0.5 to 1.0	Strong
-0.5 to -0.3	0.3 to 0.5	Moderate
-0.3 to -0.1	0.1 to 0.3	Weak
-0.1 to 0.1		None or very weak

Table 6.4 Effect Study Summary

|E*|-Mastercurve Parameters	**Correlation (r) with**			
	F_m	***r***	C_u	***r***
α	Weak	±0.26	Weak	+0.26
β	Moderate	±0.30	None or Very Weak	-0.05
δ	Weak	±0.22	Weak	-0.20
γ	Weak	-0.28	Weak	±0.14

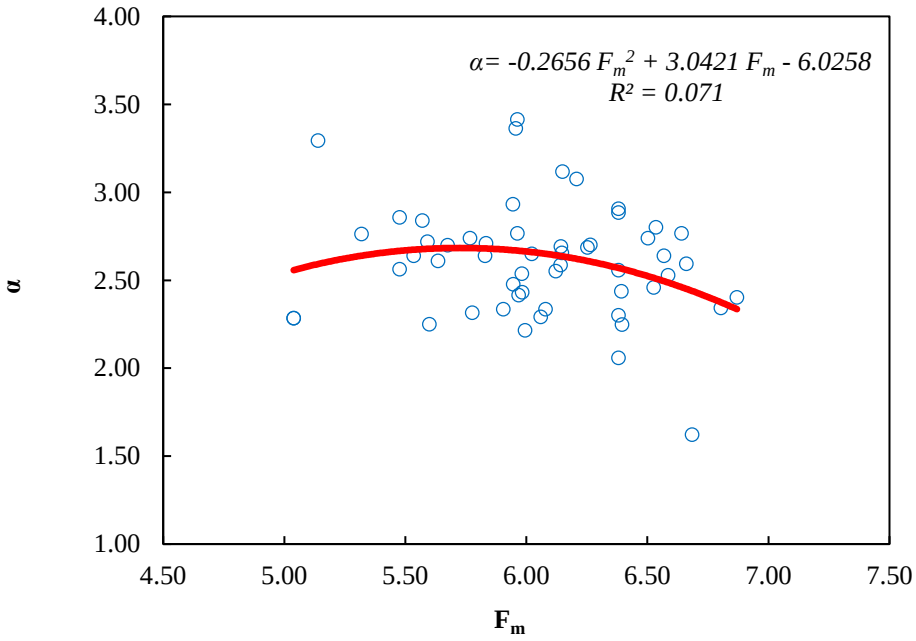

Figure 6.1 α versus F_m plot.

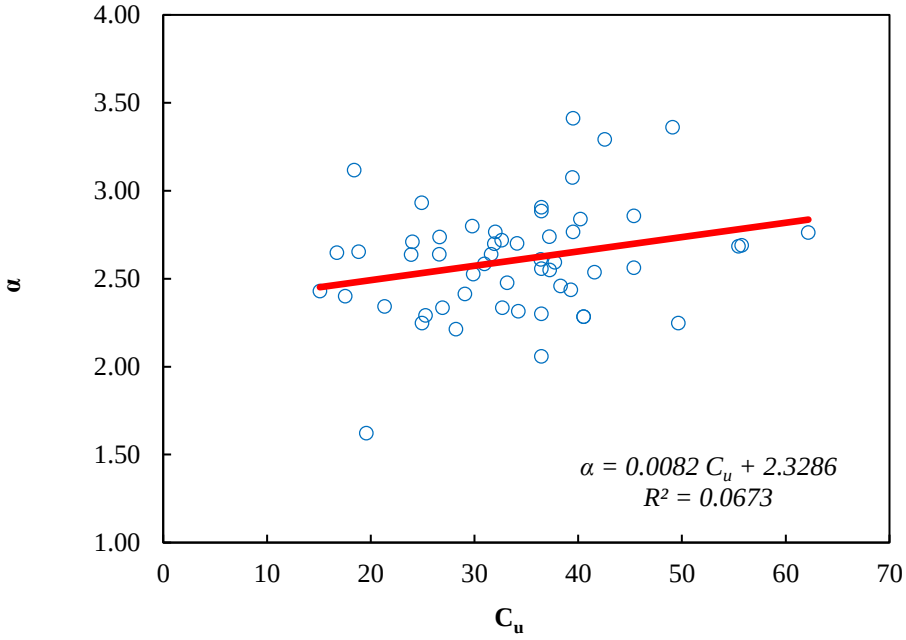

Figure 6.2 α versus C_u plot.

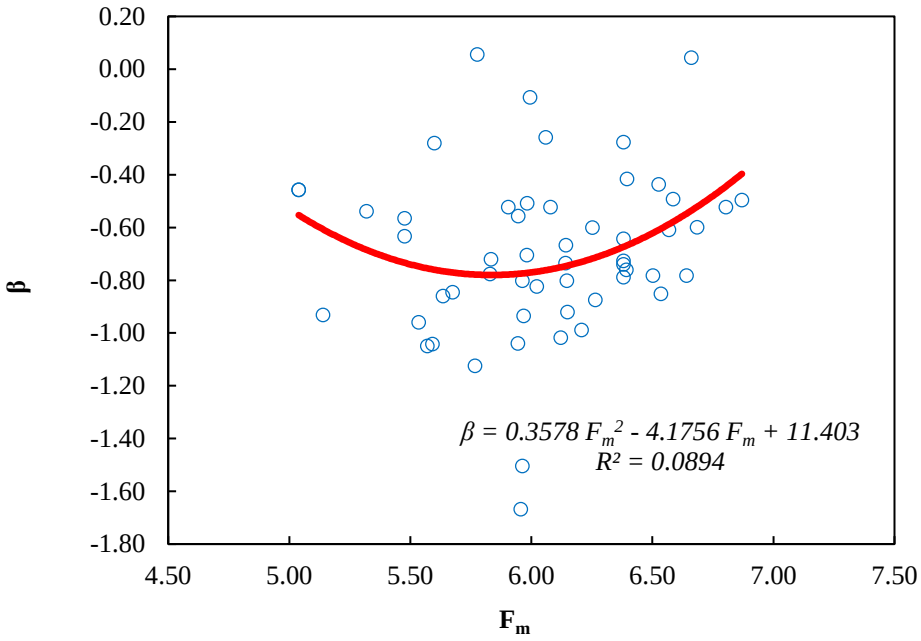

Figure 6.3 β versus F_m plot.

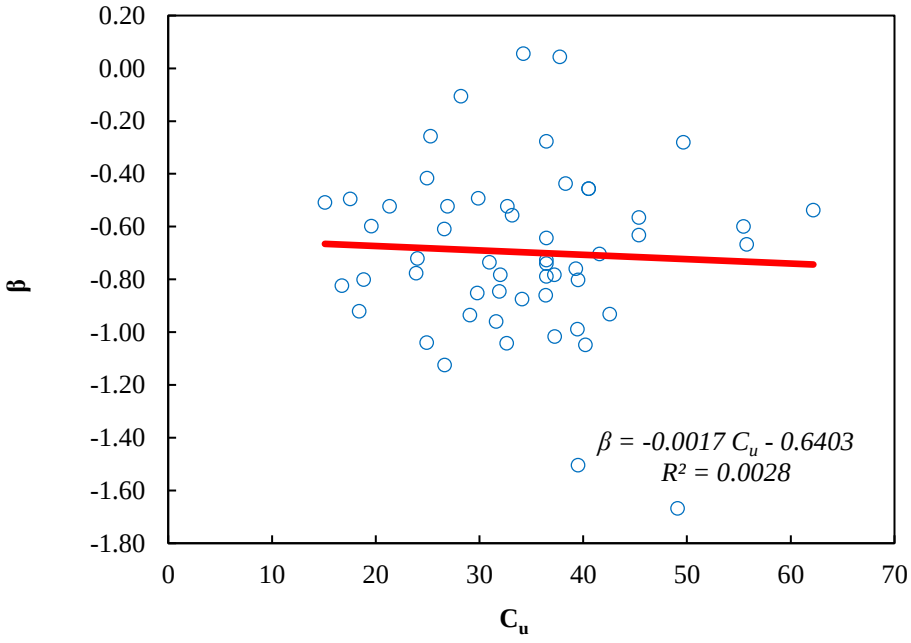

Figure 6.4 β versus C_u plot.

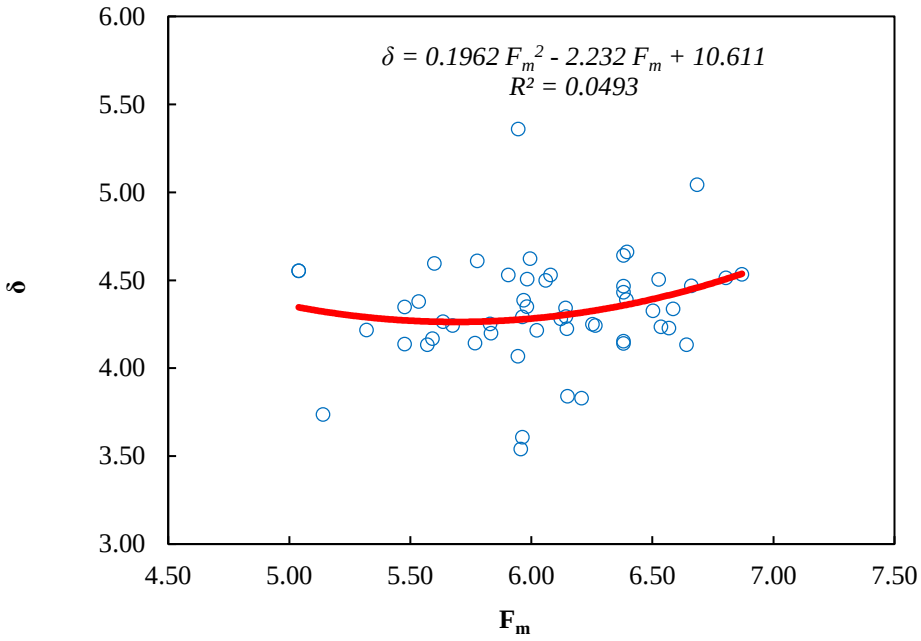

Figure 6.5 δ versus F_m plot.

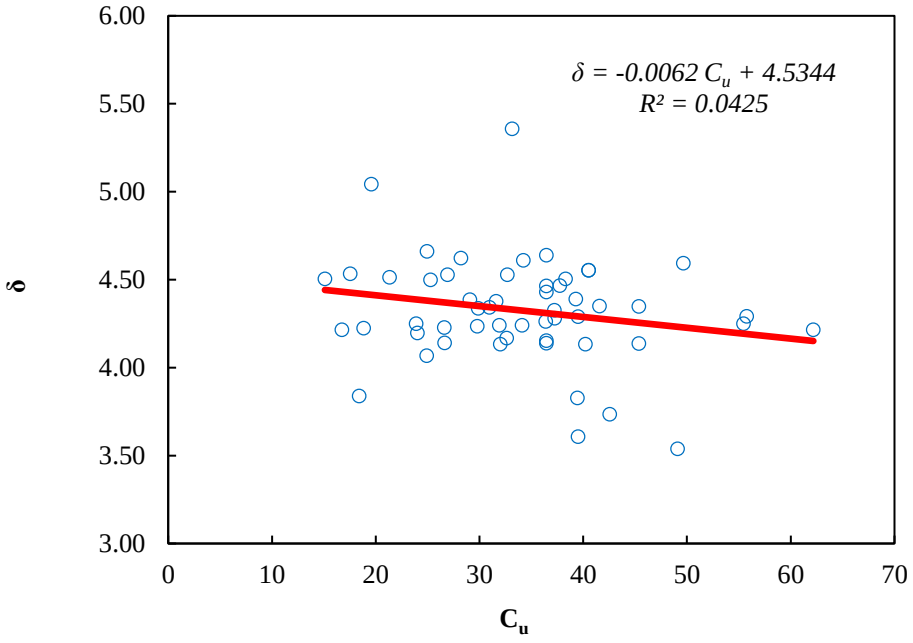

Figure 6.6 δ versus C_u plot.

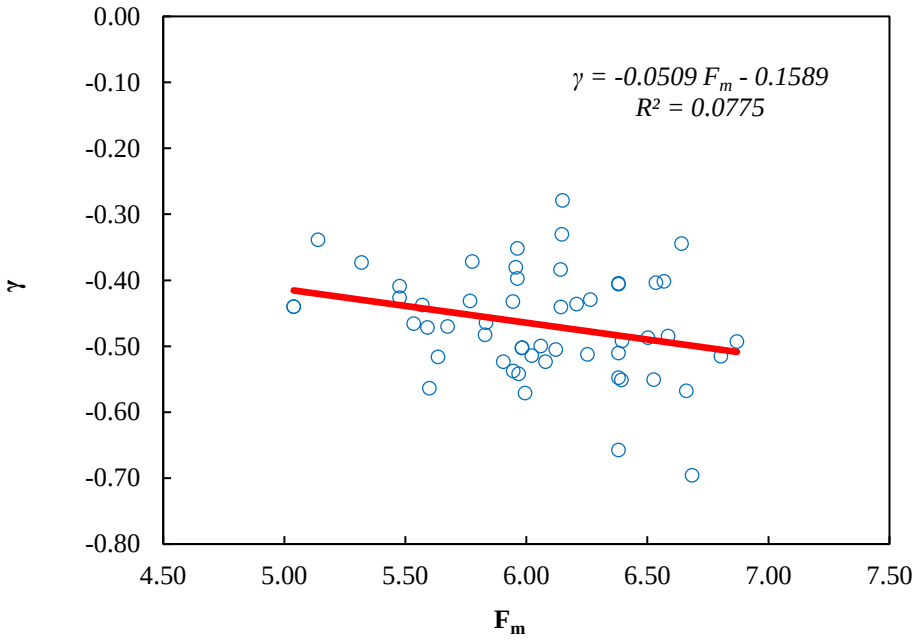

Figure 6.8 γ versus F_m plot.

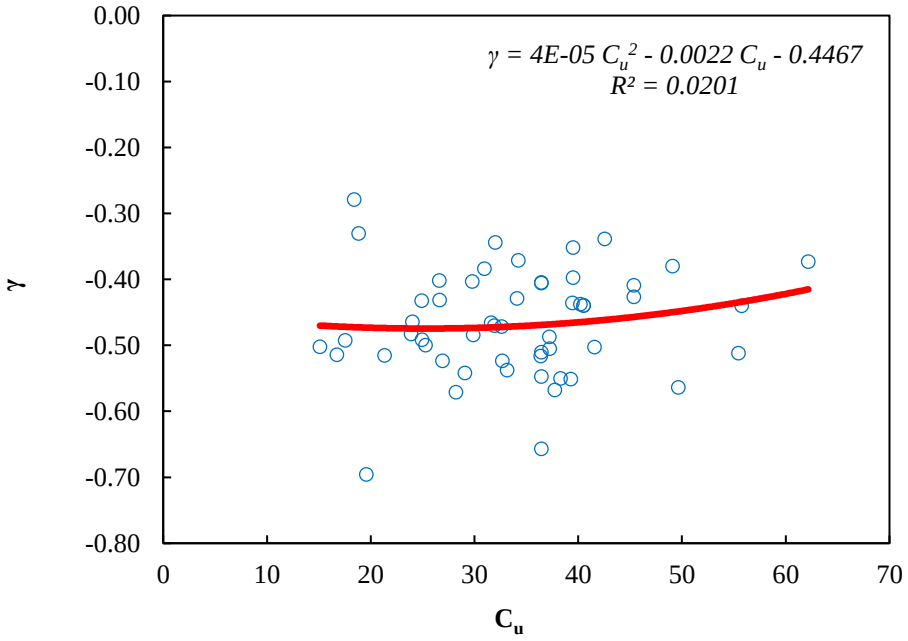

Figure 6.9 γ versus C_u plot.

Chapter 7

Binder Viscosity Based Modeling of Dynamic Modulus

7.1 Background

The most commonly used |*E**| models are the viscosity (η) based Witczak model, the binder shear modulus (|G_b*|) based Witczak model, and the Hirsch model (Weldegiorgis 2014). The nationally calibrated η-based Witczak model is the primary |*E**| predictive model in the recently developed pavement design software AASHTOWare-ME (AASHTO 2008).

The nationally calibrated η-based Witczak model for predicting |*E**| of asphalt concrete can be given as:

$$\log\left|E^*\right| = 3.750063 + 0.02932\,\rho_{200} - 0.001767\left(\rho_{200}\right)^2 - 0.002841\,\rho_4 - 0.058097\,V_a - 0.802208\left(\frac{V_{beff}}{V_{beff}+V_a}\right) + \frac{3.871977 - 0.0021\,\rho_4 + 0.003958\,\rho_{38} - 0.000017\left(\rho_{38}\right)^2 + 0.00547\,\rho_{34}}{1+e^{\left[-0.603313-0.313351\log\left(f_r\right)-0.393532\log\left(\eta\right)\right]}} \quad , \qquad (7.1)$$

where,

|*E**| = dynamic modulus in psi

ρ_{34} = cumulative % retained on the ¾ in sieve

ρ_{38} = cumulative % retained on the 3/8 in sieve

ρ_4 = cumulative % retained on the No. 4 sieve

ρ_{200} = percentage passing through the No. 200 sieve

η = viscosity of binder at the temperature of interest, 10^6 Poise

V_{beff} = effective binder content, percentage by volume

V_a = air void content, percentage by volume

f_r = a(T)*f

= reduced frequency at the reference temperature, Hz

f = frequency at a given temperature of interest, Hz

$a(T)$ = shift factor as a function of temperature

T = temperature of interest, °F

$\log f_r$ = $\log f + \log[a(T)]$

= $\log f + c(\log \eta - \log \eta_{T_r})$

η_{Tr} = viscosity at the reference temperature, 10^6 Poise

c = 1.255882, a constant.

Equation 1 can be expressed as the sigmoidal function, given as:

$$\log(|E^*|) = \delta + \frac{\alpha}{1 + e^{\beta + \gamma \log(f_r)}}. \qquad (7.2)$$

where,

$$\delta = 3.750063 + 0.02932\ \rho_{200} - 0.001767\ (\rho_{200})^2 - 0.002841\ \rho_4 - 0.058097\ V_a - 0.802208\left(\frac{V_{beff}}{V_{beff} + V_a}\right), \quad (7.3)$$

$$\alpha = 3.871977 - 0.0021\ \rho_4 + 0.003958\ \rho_{38} - 0.000017\ (\rho_{38})^2 + 0.00547\ \rho_{34}, \quad (7.4)$$

$$\beta = -0.603313 - 0.393532\ \log(\eta), \quad (7.5)$$

$$\gamma = -0.313351. \quad (7.6)$$

Thus, the η-based Witczak model uses the viscosity, η of the binder as an input parameter to capture the effect of binder on the $|E^*|$ of the AC mixture. The other parameters included in this model are the aggregate gradation parameters, the air void content, and the effective asphalt content.

7.2 Objective

The objective of this study is to develop an alternative, more accurate, regression-based $|E^*|$ and ϕ predictive models based on binder viscosity for the AC mixtures typically used in New Mexico. To incorporate the aggregate gradation, the uniformity coefficient (C_u) and the fineness modulus (F_m) are introduced instead of using directly the percentage of material retained or passing on a particular sieve as in η-based Witczak model (Equation 7.1).

7.3 Materials, Preparation of Test Specimens, and Complex Modulus Test

All 54 AC mixtures with different aggregate gradations and binder performance grades (PG) tested in this study were considered model development. According to AASHTO MP2 (AASHTO 2011) specification, 13 of these asphalt-aggregate mixtures are Type IV Superpave® aggregate blend (SP 4) with the nominal maximum aggregate size (NMAS) being 12.5 mm. The remaining 41 mixtures are Type III Superpave blend (SP 3) with the NMAS being 19 mm. A variety of binder performance grades are used in these mixtures depending on the regional climate associated with the pavement operation sites. Detail descriptions of the AC materials used in this study can be found in New Mexico Department of Transportation (NMDOT) research report conducted and authored by Tarefder and Rahman (2016).

Figure 7.1(a) shows the gyratory compactor and a typical compacted sample prepared in this study. Figure 7.1(b) shows a typical core-drilled cylindrical AC specimen, while Figure 7.1(c) shows a typical edge-cut test specimen. For each AC mixture, three replicate cylindrical specimens were prepared for $|E^*|$ with ϕ testing. The AC specimens were tested for $|E^*|$ and ϕ at loading frequencies of 25, 10, 5, 1, 0.5, and 0.1 Hz at five different test temperatures of -10, 4.4, 21.1, 37.8, and 54.4 °C (14, 40, 70, 100, and 130 °F). The load levels in these tests were kept low enough to keep the material response in the linear viscoelastic range as suggested by the specification. Figure 7.1(d) shows a typical setup for $|E^*|$ testing while the Linear Variable Differential Transducers (LVDT) are mounted on the test specimen and placed under the loading actuators. Three replicate specimens from each of the 54 AC mixtures were tested. The average $|E^*|$ and ϕ at different

test temperatures and loading frequencies of the three replicate specimens were then determined.

7.4 The Mastercurves

Figure 7.2(a) and 7.2(b) presents a typical work involved in developing and fitting the |*E**|-mastercurve, and the frequency-temperature shift factor function for one of the AC mixtures considered in this study (to be specific, AC Mix 1 in Tarefder and Rahman 2016). Figure 7.2(a) shows the average |*E**| versus loading frequency plots at different test temperatures. The figure also shows the TTSP applied horizontally shifted |*E**| data along the frequency space to construct |*E**| mastercurve at 70 °F (21.1 °C) reference temperature. After a smoother representation of |*E**| data was found by applying TTSP, the generated |*E**|-mastercurve (discrete data points) were fitted. Figure 2(b) shows a typical frequency-temperature shift factor versus temperature plot. The figure also shows the fitted shift factor function.

The ϕ-mastercurves at 21.1 °C (70 °F) reference temperature were generated by using the same frequency-temperature shift factors obtained while developing |*E**|-mastercurves. Figure 7.3 shows the average ϕ versus loading frequency plots at different test temperatures. The figure also shows the TTSP applied horizontally shifted ϕ data along the frequency space to construct ϕ-mastercurve at 70 °F (21.1 °C) reference temperature by applying the same frequency-temperature shift factors found while generating |*E**|-mastercurve. The figure also shows the fitted ϕ-mastercurve. For all 54-AC mixtures the smoothened ϕ-functions were generated.

7.5 Assessment of Viscosity-based Witczak Model

The assessment and development of a regression-based model depends on the statistical analysis and optimization process used. The fundamental aim of this type of model development process is to reduce the error from the prediction by comparing the predicted data with the observed data. The optimization process involves the determination of regression coefficients in such a way that the developed equation provides minimum error when the predicted and observed data are compared. To determine the level of accuracy, "goodness of fit" is used in this study. To determine "goodness of fit", the estimated values by the predictive model are compared to the tested or observed data at the identical input conditions. Generally, two statistical parameters are required to be evaluated to determine the "goodness of fit". The first one is the coefficient of determination (R^2), and the second one is the ratio of the standard error (S_e) to the standard deviation (S_y). The mathematical form of R^2, S_e, and S_y can be given as:

$$R^2 = 1 - \frac{(n - p - 1)S_e^{\ 2}}{(n-1)S_y^{\ 2}}, \tag{7.9}$$

$$S_e = \left[\frac{1}{(n - p - 1)}\sum_{1}^{n}(\hat{x}_i - x_i)^2\right]^{\frac{1}{2}}, \text{ and} \tag{7.10}$$

$$S_y = \left[\frac{1}{(n-1)}\sum_{1}^{n}(x_i - \bar{x})^2\right]^{\frac{1}{2}}. \tag{7.11}$$

In the above expressions, $\hat{x}_i$ are the predicted data, x_i are the observed data, $\bar{x}$ is the average of the observed data, *n* is the number of data points used for fitting, and *p* is the number of fitting parameters. A relatively good predictive model would have a higher R^2, close to 1 and a smaller S_e/S_y close to zero.

In this study, the nationally calibrated η-based Witczak model is assessed to understand its performance for the AC mixtures of New Mexico. Figures 7.4(a) and 7.4(b) show the observed $|E^*|$ versus $|E^*|$ predicted by the η-based Witczak model in arithmetic and logarithmic scales respectively. To facilitate comparison of predicted and observed data, a Line of Equality (LOE) is included in these plots. Both of the plots show that most of the $|E^*|$ data points are significantly below the LOE which confirms that a significant amount of bias exists in the current nationally calibrated η-based Witczak model in case of the AC mixtures of New Mexico. The "goodness of fit" of the nationally calibrated η-based Witczak model, given in Equation 7.1, is evaluated in two ways, i.e., in logarithmic scale and in normal or arithmetic scale. The model has a smaller coefficient of determination, R^2 of 0.32 and a larger S_e/S_y value of 0.83 in normal or arithmetic scale. Again, in logarithmic scale, these are: $R^2 = 0.71$, and $S_e/S_y = 0.54$. Therefore, considering both of the scales used in this study, the nationally calibrated η-based Witczak model proved to be less accurate for estimating $|E^*|$ of AC mixtures typically produced in New Mexico.

7.6 Calibration of Viscosity-based Witczak Model

As a first attempt, calibration of the η-based Witczak model given in Equation 7.1 was conducted by non-liner regression technique correlating the material attributes to the

observed |*E**|. The best fit modified η-based Witczak model for the AC mixtures of New Mexico can be given by the following expression:

$$\log\left|E^*\right| = 5.77883709 \;-0.24410256\;\rho_{200} + 0.02694553\;(\rho_{200})^2 + 0.00318312\;\rho_4 + 0.09337565\;V_a - 2.46522049\left(\frac{V_{beff}}{V_{beff}+V_a}\right) + \frac{2.34570698 \;-0.00278047\;\rho_4 + 0.03484798\;\rho_{38} - 0.00063488\;(\rho_{38})^2 - 0.00478981\;\rho_{34}}{1+e^{\left(-0.58064918-0.08256248\log(\eta)-0.37840512\log(f_r)\right)}} \quad . \tag{7.12}$$

Again, as Equation 7.12 is analogous to Equation 7.2, one can find:

$$\delta = 5.77883709 \;-0.24410256\;\rho_{200} + 0.02694553\;(\rho_{200})^2 + 0.00318312\;\rho_4 + 0.09337565\;V_a - 2.46522049\left(\frac{V_{beff}}{V_{beff}+V_a}\right) \quad , \tag{7.13}$$

$$\alpha = 2.34570698 - 0.00278047\rho_4 + 0.03484798\rho_{38} - 0.00063488(\rho_{38})^2 - 0.00478981\rho_{34} \, , \tag{7.14}$$

$$\beta = -0.58064918 \;-0.08256248\;\log(\eta), \text{ and,} \tag{7.15}$$

$$\gamma = -0.37840512 \quad . \tag{7.16}$$

The reduced frequency function associated with η-based Witczak model can be given as -

$$\log\, f_r = \log\, f + c(\log \eta - \log \eta_{T_r}). \tag{7.17}$$

Here, the parameters *c* is a constant, which is optimized in this study and found to be *c* = 1.32306387, with R^2 value of 0.98, which is very close to unity, and S_e/S_y value of 0.15, which is small enough to claim its validity. Figure 7.5(a) and 7.5(b) show the |*E**| values predicted by the calibrated η-based Witczak model versus the observed |*E**|-values for all 54-AC mixtures in arithmetic and logarithmic scales respectively. The predicted |*E**|

matches well with the measured data. The R^2 in case of arithmetic and log scale are found to be 0.87 and 0.94, respectively, which are close to unity. The ratios of S_e and S_y for the arithmetic and log scale data are found to be 0.37 and 0.24 respectively. These values are low enough to claim that the predicted data fit well with the measured data.

7.7 The New Predictive Models

Although the calibrated η-based Witczak model given in Equation 7.12 gives a fairly accurate prediction of $|E^*|$ for the AC mixtures of New Mexico, a second attempt was taken into account for developing new models which can predict $|E^*|$ as well as the ϕ of the New Mexico AC mixtures with better accuracy. To develop the new $|E^*|$- and ϕ-predictive models nonlinear regression-optimization technique was used. A two-step modeling approach was adopted while developing the $|E^*|$ and the ϕ predictive models. In the first step, the first 50 AC mixtures were used to develop the models, and the modulus and phase angle data of remaining 4 AC mixtures were used for the validation of the models. In the second step, all 54-AC mixtures are used to obtain the final forms of the predictive models. As the differences between the models developed using 50-AC mixtures at the first step and 54-AC mixtures in the second step were very small, thus, only the final forms of this new predictive models for estimating $|E^*|$ and ϕ of AC mixtures developed in the second step are discussed in the following sections.

7.7.1 Model Variables

For the model development, the variables affecting $|E^*|$ of AC mixtures considered are: the fineness modulus (F_m), and uniformity coefficient (C_u) for the aggregate blend used in the

AC mixture; effective binder content (V_{beff}), air void content (V_a), the viscosity of the binder (η), and the loading frequency (f). The definitions of F_m, and C_u can be given as:

$$F_m = \frac{\sum_{i=1}^{N} CPR_i}{100}, \text{ and} \tag{7.18}$$

$$C_u = \frac{D_{60}}{D_{10}}. \tag{7.19}$$

In Equations 7.18 and 7.19, the parameters CPR_i is the cumulative percentage of aggregate retained at i^{th} sieve, D_{60} is the sieve size corresponding to 60% material passing, D_{10} is the sieve size corresponding to 10% material passing, and N is the number of sieves used in the sieve analysis. A total of 13 standard sieves are used for sieve analysis of the aggregate blends of the AC mixtures. These are: 2 inch (50 mm), 1.5 inch (37.5 mm), 1 inch (25 mm), ¾ inch (19 mm), ½ inch (12.5 mm), 3/8 inch (9.5 mm), No. 4 (4.75 mm), No. 8 (2.36 mm), No. 16 (1.18 mm), No. 30 (0.6 mm), No. 50 (0.3 mm), No. 100 (0.15 mm), and No. 200 (0.075 mm) standard sieves. The viscosities (η) of the asphalt binders associated with the AC mixtures are determined from the ASTM viscosity-temperature relationship (ASTM 1998) given as -

$$\log\log(\eta) = A + VTS * \log(T_R). \tag{7.20}$$

Note that, in Equation 2.20, the viscosity η is in centi-poise (cP), with a maximum limiting value of 2.7×10^{10} poise; T_R is the temperature in Rankine scale; A is the regression intercept; and VTS is the regression slope. The parameters A and VTS are called viscosity-

temperature susceptibility parameters. The values of *A* and *VTS* for a certain PG binder were taken from ASTM chart (ASTM 1998) for Rolling Thin-Film Oven (RTFO) aged binder.

7.7.2 Effect of Mixture Attributes on the Mastercurve Parameters

The effects of different mix-variables on the $|E^*|$ and ϕ mastercurve parameters of AC are evaluated in this study to establish their inter-relationships. Subsequently, the initial form of the $|E^*|$ and ϕ-predictive models were formulated. As stated earlier, in Equation 7.2, the parameters δ is the minimum $|E^*|$-value, α is the vertical span of the $|E^*|$-function, and therefore, $\alpha+\delta$ is the maximum $|E^*|$-value, and finally, β and γ are the shape parameters for the $|E^*|$-function. In case of ϕ-function, ξ_1, ξ_2, and ξ_3 are the regression coefficients and considered to be dependent on the material attributes. All seven model parameters, i.e., α, β, δ, and γ for $|E^*|$-model, and ξ_1, ξ_2, and ξ_3 for ϕ-model, were studied against the variables F_m, C_u, V_{beff}, and V_a to identify the behavior of these variables in the final $|E^*|$ and ϕ predictive models. The effect study showed that the parameters α, β, γ, and δ in Equation 2 are inter-related in various trends and degrees to the F_m, C_u, V_{beff}, and V_a of the AC sample. An example of this study is shown in Figures 7.6(a), 7.6(b), 7.6(c) and 7.6(d) in case of minimum $\log|E^*|$ identified as δ in Equation 2. The Figure 7.6(a) shows an increasing trend of δ with increasing F_m of the aggregate blend. Figure 7.6(b) shows that with increasing C_u, the parameter δ decreases. Again, in Figure 7.6(c) a positive decreasing trend of δ with increasing V_a can be observed. Lastly, in Figure 7.6(d), δ decreases with increasing V_{beff}. In a similar way, the effects of these variables on the other parameters of $|E^*|$ and ϕ

functions are identified and correlated. The correlations with higher R^2 values were considered to be the strongest factors affecting $|E^*|$ and ϕ of the AC mixtures.

7.7.3 Formulation of Initial Models

After evaluating the significant factors or mix-variables affecting each of the mastercurve parameters of $|E^*|$ and ϕ, the trends of these variables with respect to each of the individual mastercurve parameters were superimposed and hence, the initial expressions of the models were formulated. The initial formulation of the $|E^*|$-model was considered to be analogous to Equation 2, where, the model parameters can be given as:

$$\delta = a_0 + a_1 (F_m)^2 + a_2 (F_m) + a_3 (C_u) + a_4 (V_a)^2 + a_5 (V_a) + a_6 (V_{beff})^2 + a_7 (V_{beff}), \quad (7.21)$$

$$\alpha = b_0 + b_1 (F_m)^2 + b_2 (F_m) + b_3 (C_u) + b_4 (V_a)^2 + b_5 (V_a) + b_6 (V_{beff})^2 + b_7 (V_{beff}), \quad (7.22)$$

$$\beta = c_0 (F_m)^2 + c_1 (F_m) + c_2 (V_a)^2 + c_3 (V_a) + c_4 (V_{beff})^2 + c_5 (V_{beff}) + c_6 \log \eta, \text{ and} \quad (7.23)$$

$$\gamma = d_0 + d_1 (F_m) + d_2 (C_u)^2 + d_3 (C_u) + d_4 (V_a)^2 + d_5 (V_a). \quad (7.24)$$

In Equations 18, 19, 20, and 21, coefficients a_0, a_1, a_2, …, b_0, b_1, b_2, …, c_0, c_1, c_2, …, and d_0, d_1, d_2, … are the regression coefficients, which can be determined by fitting actual δ, α, β, and γ to the initial formulations.

On the other hand, the effect study showed that the parameters ξ_1 and ξ_2 can be correlated to the F_m of the AC mixtures, whereas, parameter ξ_3 can be correlated to both

the F_m and C_u of the AC mixtures. Thus, the initial formulation of the ϕ-model was considered as in Equation 7.8, where-

$$\xi_1 = p_0 + p_1 F_m + p_2 \left(F_m\right)^2, \tag{7.25}$$

$$\xi_2 = q_0 + q_1 F_m + q_2 \left(F_m\right)^2, \text{ and} \tag{7.26}$$

$$\xi_3 = r_0 + r_1 \left(F_m\right) + r_2 \left(F_m\right)^2 + r_3 \left(C_u\right) + r_4 \left(C_u\right)^2. \tag{7.27}$$

Also, in Equations 22, 23, and 24, the coefficients p_0, p_1, …, q_0, q_1, …, and, r_0, r_1, … are the regression coefficients, and can be determined by fitting actual ξ_1, ξ_2, and ξ_3 to the initial formulations.

The regression coefficients in Equations 7.21, 7.22, 7.23, 7.24, 7.25, 7.26, and 7.27 were found by non-linear least squares regression analyses. Several computer programs in MATLAB® were coded for this purpose, and the best estimated regression coefficients producing minimum errors between observed and estimated data were evaluated.

7.7.4 Dynamic Modulus Predictive Model

The final form of the $|E^*|$ predictive model can be presented by the expression similar to the Equation 2. The new $|E^*|$ predictive model can be given as -

$$\log\left|E^*\right| = \delta_{E^*} + \frac{\alpha_{E^*}}{1 + e^{\beta_{E^*} + \gamma_{E^*} \log(f)}}, \tag{7.28}$$

where,

$$\delta_{E^*} = -3.31676767 + 0.15223521\ (F_m)^2 - 1.78427544\ (F_m) - 0.00508589\ (C_u) - 0.50580886\ (V_a)^2 + 5.791483\ (V_a) + 0.02629492\ (V_{beff})^2 - 0.61189577\ (V_{beff}), \quad (7.29)$$

$$\alpha_{E^*} = -0.81621932 - 0.26422402\ (F_m)^2 + 3.07887763\ (F_m) + 0.00633059\ (C_u) + 0.28170835\ (V_a)^2 - 3.2881344\ (V_a) - 0.03350841\ (V_{beff})^2 + 0.72041062\ (V_{beff}), \quad (7.30)$$

$$\beta_{E^*} = 0.26881379\ (F_m)^2 - 3.16127514\ (F_m) - 0.43917071\ (V_a)^2 + 5.14118364\ (V_a) + 0.05136617\ (V_{beff})^2 - 1.15376261\ (V_{beff}) + 0.01434329\ \log\eta, \text{ and} \quad (7.31)$$

$$\gamma_{E^*} = -1.39453189 - 0.0512783\ (F_m) + 0.00003869\ (C_u)^2 - 0.00290191\ (C_u) - 0.05321409\ (V_a)^2 + 0.5285461\ (V_a). \quad (7.32)$$

In Equation 7.31, the unit of the viscosity of binder η is in mega-poise, i.e., 10^6 Poise, which is consistent with the nationally calibrated η-based Witczak model.

The "goodness of fit" of the new |*E**| model given by the Equations 7.28, 7.29, 7.30, 7.31, and 7.32 is evaluated also in two ways, i.e., in logarithmic scale and in normal or arithmetic scale. The developed |*E**| model has a good coefficient of determination (R^2 = 0.93) and a small S_e/S_y (S_e/S_y = 0.27) in normal or arithmetic scale. Again, in logarithmic scale, these are: R^2 = 0.96, and S_e/S_y = 0.20, which are excellent for this type of models where numerous complexities are involved. Also, in terms of "goodness of fit", the new η-based |*E**| model shows better performance than the nationally calibrated η-based Witczak model as well as the locally calibrated η-based Witczak model for New Mexico developed earlier in this study. Figures 7.7(a) and 7.7(b) show the |*E**| data predicted from the new |*E**| model versus observed |*E**| data in arithmetic and logarithmic scales, respectively. Both of the plots show that all the |*E**| data points are around the line of equality (LOE)

without any significant bias. Therefore, it can be said that the proposed |*E**| model gives a fairly good estimation of |*E**| of the AC mixture of New Mexico.

7.7.5 Phase Angle Predictive Model

The expression given in Equation 7.8 was used to develop the ϕ predictive model for asphalt concrete. The final form of the ϕ predictive model can be given as -

$$\phi = \xi_{\phi_1} + \xi_{\phi_2} \log\left(f_r\right) - \xi_{\phi_3} \frac{\pi}{2} \alpha_{E^*} \gamma_{E^*} \frac{e^{\beta_{E^*} + \gamma_{E^*} \log(f)}}{\left(1 + e^{\beta_{E^*} + \gamma_{E^*} \log(f)}\right)^2}, \qquad (7.33)$$

where,

$$\xi_{\phi_1} = 2.21608382 - 0.75568954\, F_m + 0.06437214 \left(F_m\right)^2, \qquad (7.34)$$

$$\xi_{\phi_2} = -0.34763481 + 0.12199569\, F_m - 0.01049798 \left(F_m\right)^2, \text{ and} \qquad (7.35)$$

$$\xi_{\phi_3} = -4.07898971 + 1.89863056 \left(F_m\right) - 0.16375571 \left(F_m\right)^2 - 0.01494262 \left(C_u\right) + 0.0001655 \left(C_u\right)^2. \qquad (7.36)$$

In Equation 7.33, the values of α_{E^*}, β_{E^*}, and γ_{E^*} can be found from Equations 7.30, 7.31, and 7.32, respectively.

The "goodness of fit" is also evaluated for the new ϕ model. The developed ϕ-model produced a fairly good R^2 values of 0.81 with a small S_e/S_y value of 0.44. Figure 7.8 shows the ϕ-values predicted from the new ϕ-model given in Equation 7.33 versus the observed

ϕ-values. The plot shows that all the ϕ-data points are around the LOE without any significant bias. Therefore, it can be said that the proposed ϕ model gives a fairly good prediction of ϕ in case of the AC mixtures of New Mexico.

7.7.6 Validation of the Models

As mentioned earlier, the new $|E^*|$ and ϕ models found at the first step where a total of 50-AC mixtures were used, were validated for four independent AC-mixtures. As each of the AC mixtures has 30 data-points (5 temperatures and 6 loading frequencies), a total of 120 data-points were available for the validations of these models.

Figure 7.9(a) and 7.9(b) show the $|E^*|$ values predicted by the New $|E^*|$-model versus the observed $|E^*|$-values for all 4 independent AC mixtures in arithmetic and log scales respectively. The predicted $|E^*|$ matches well with the measured data. The R^2 in case of arithmetic and log scale are found to be 0.90 and 0.97, respectively, which are close to unity. The ratios of S_e and S_y for the arithmetic and log scale data are found to be 0.34 and 0.18 respectively. These values are low enough to claim the validity of the developed $|E^*|$ model.

On the other hand, the developed ϕ-model from 50-AC mixtures produced a fairly good R^2 values of 0.84 with a small S_e/S_y value of 0.41 for the 4 independent AC mixtures. Figure 7.10 shows the ϕ-values of the 4 independent AC mixtures predicted from the new ϕ-model versus the observed ϕ-values. The plot shows that all the ϕ-data points are around the LOE without any significant bias. Therefore, it can be said that the proposed ϕ model

gives a fairly good prediction of ϕ in case of the 4 independent AC mixtures used for validation of the models.

7.8 Conclusions

In this study, new predictive models for dynamic modulus and phase angle of asphalt concrete are developed based on observed data of 54 asphalt concrete mixtures typically used in New Mexico. The developed models use two fundamental aggregate gradation parameters: the fineness modulus and the uniformity coefficient, mix volumetric parameters (air void content and effective binder volume), binder viscosity, and loading frequency as direct input. The developed models possess fairly good statistics, considering "goodness of fit" between predicted and observed data.

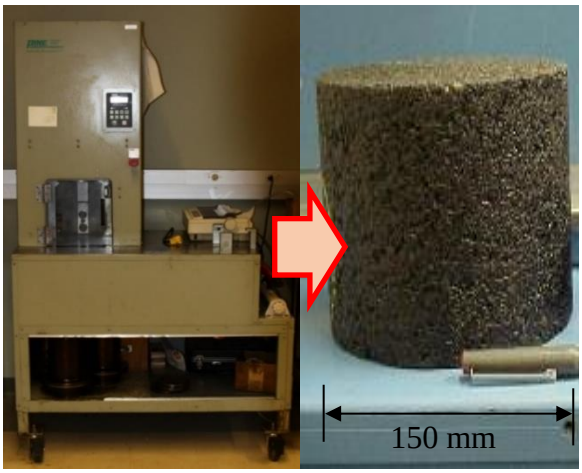

(a) SGC compacted sample

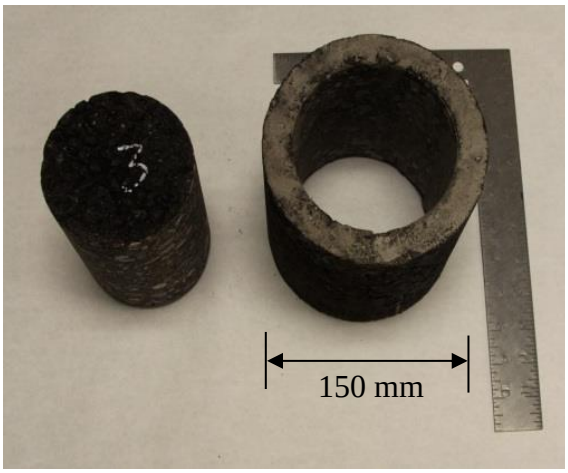

(b) Cored sample

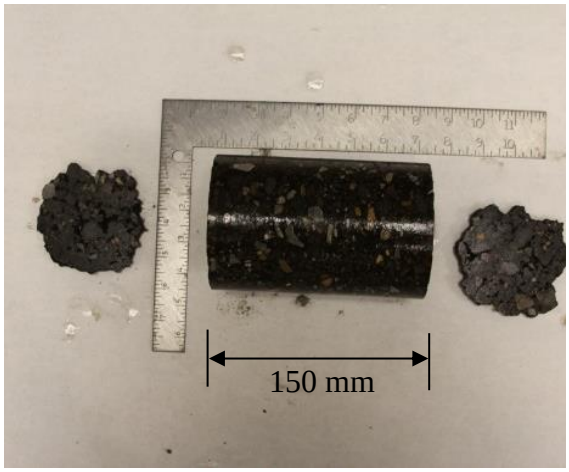

(c) Edge-cut sample

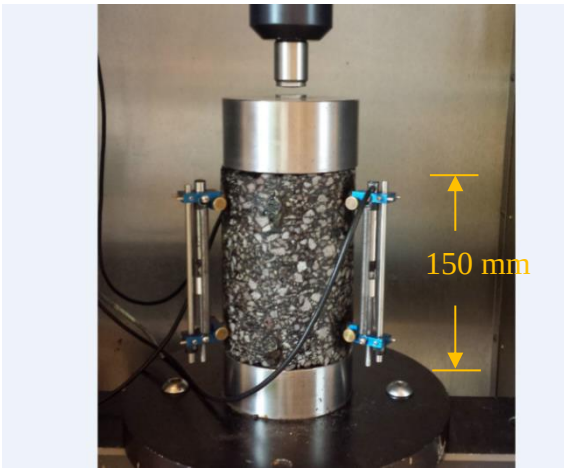

(d) |E*| test setup

Figure 7.1 Dynamic modulus sample preparation and test setup.

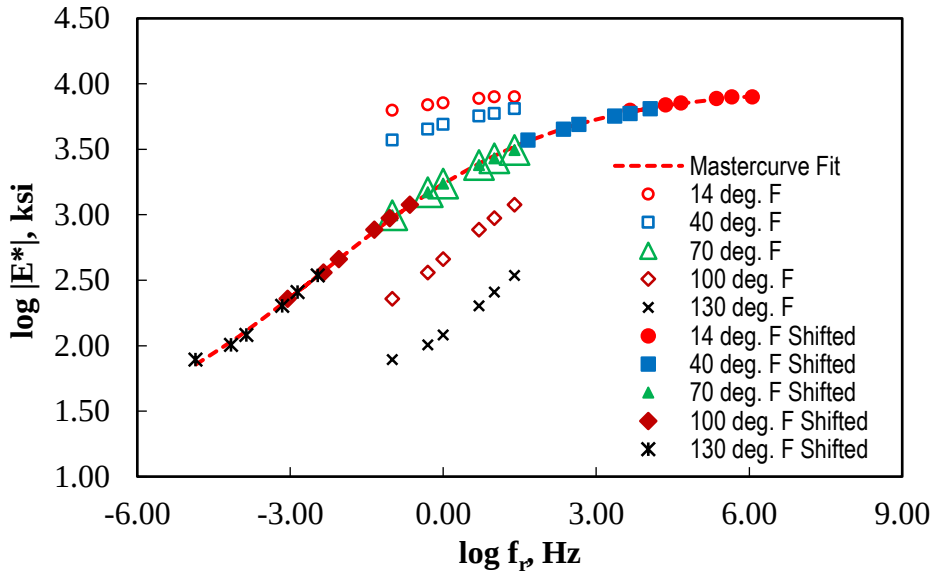

(a) |E*| Mastercurve Fit

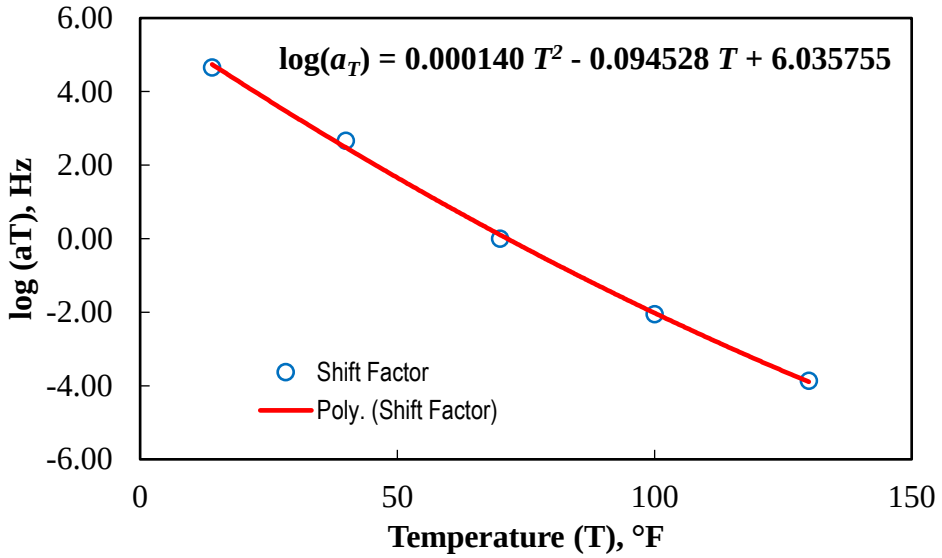

(b) Shift Factor Fit

Figure 7.2 Typical development of (a) |*E**| mastercurve, and (b) frequency-temperature shift factor function [for AC Mix 1 in Tarefder and Rahman (2016)].

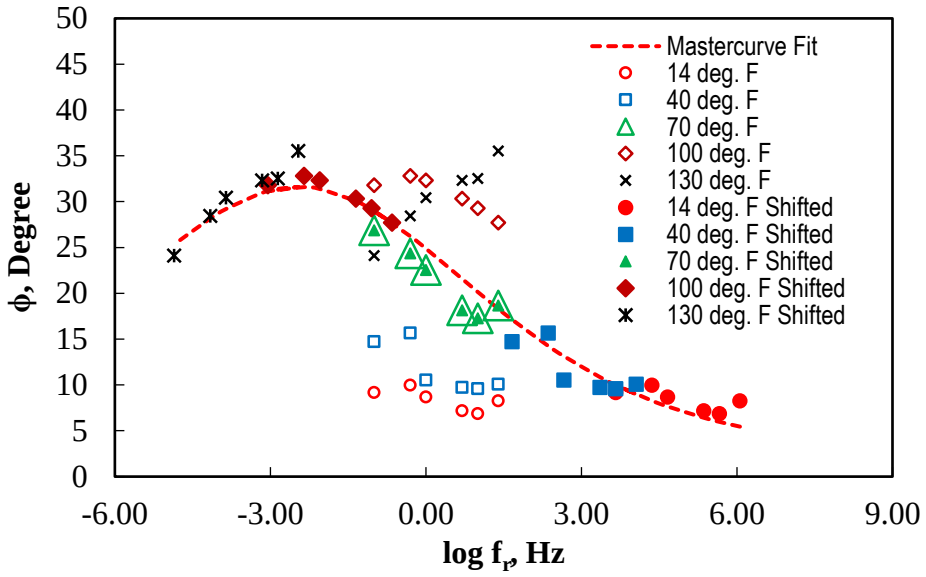

Figure 7.3 Typical development of ϕ-mastercurve [for AC Mix 1 in Tarefder and Rahman (2016)].

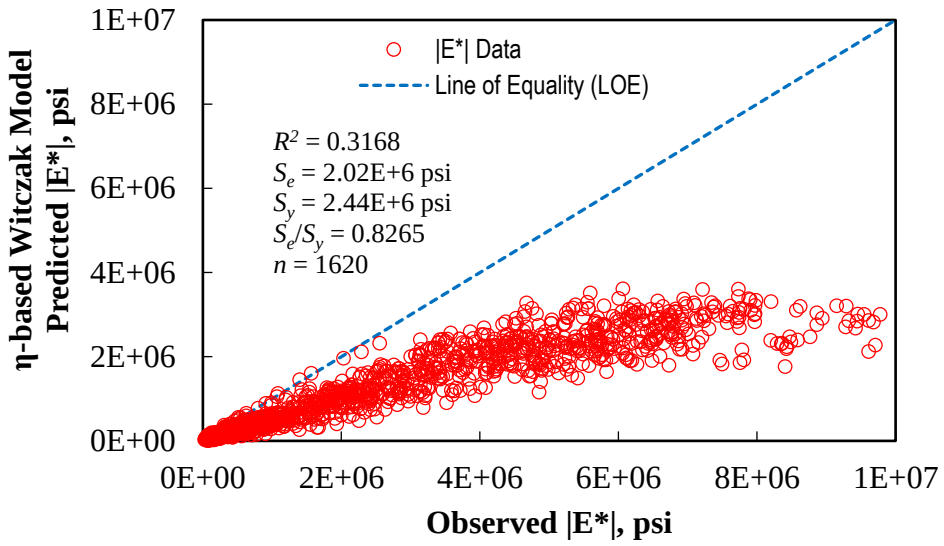

(a) Arithmetic Scale

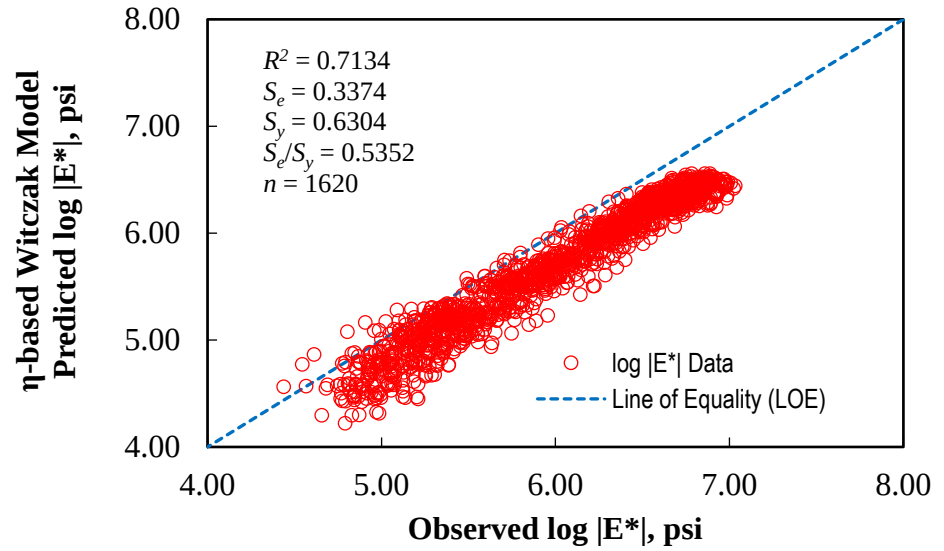

(b) Logarithmic Scale

Figure 7.4 |*E**| predicted by *η*-based Witczak model versus Observed |*E**|.

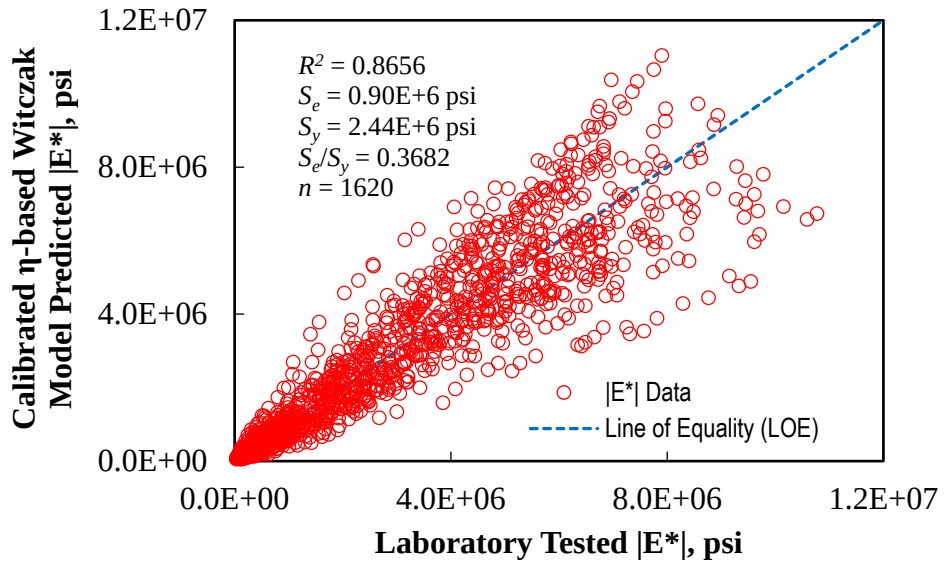

(a) Arithmetic Scale

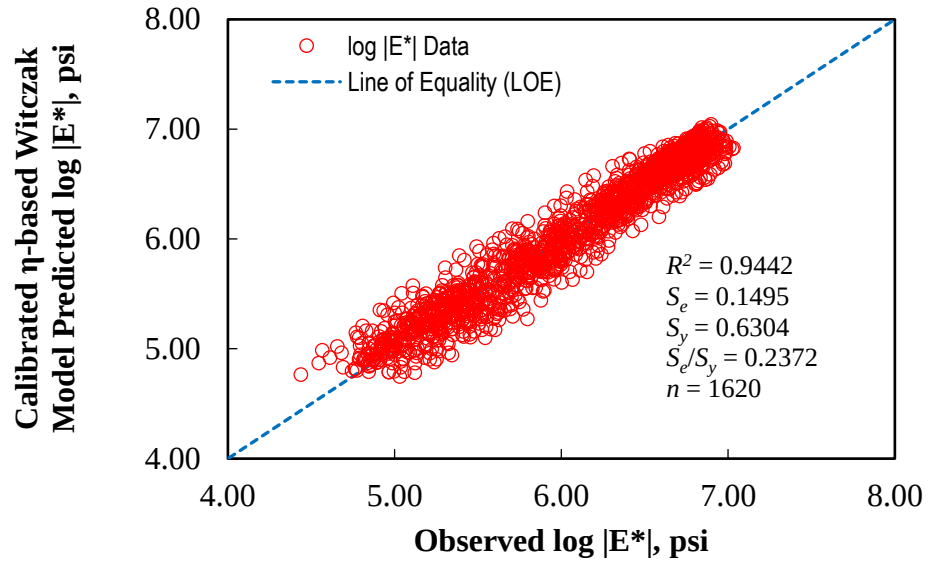

(b) Logarithmic Scale

Figure 7.5 |*E**| predicted by calibrated *η*-based Witczak model versus Observed |*E**|.

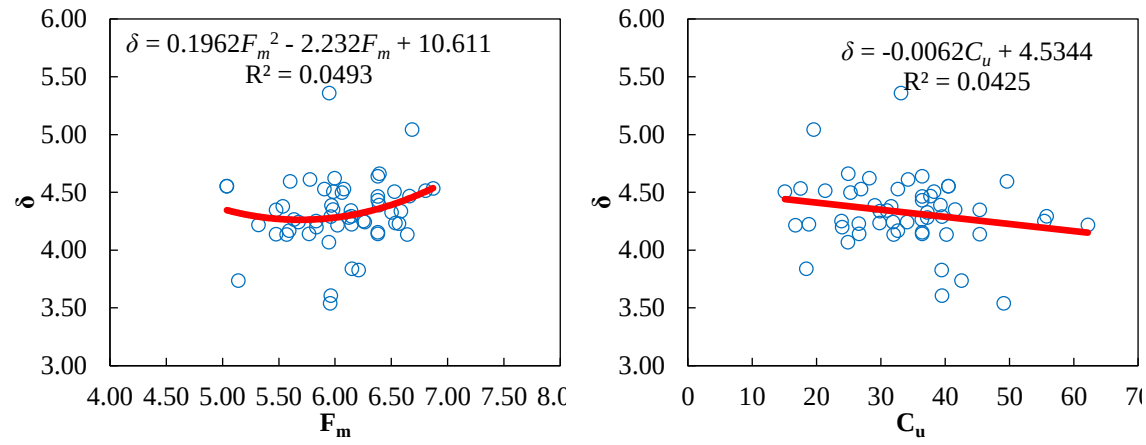

(a) δ versus F_m (b) δ versus C_u

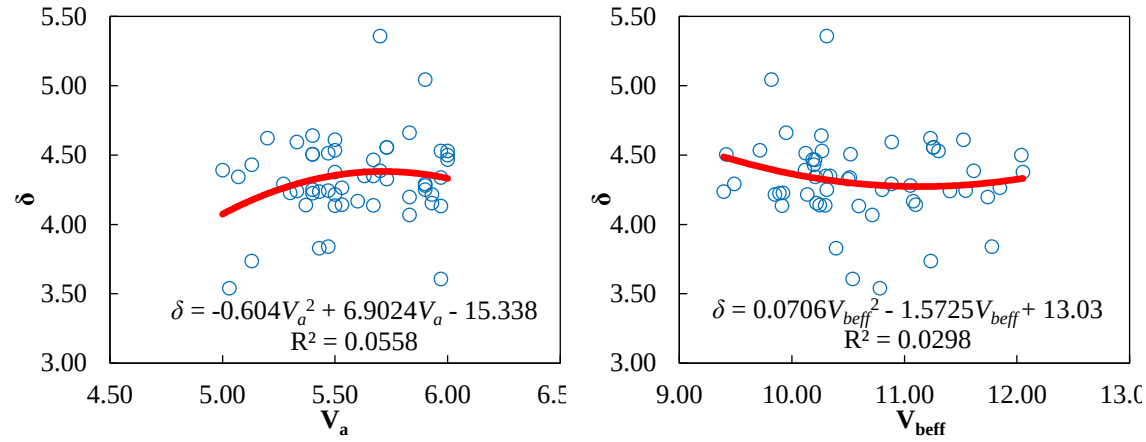

(c) δ versus V_a (d) δ versus V_{beff}

Figure 7.6 (a) δ versus F_m, (b) δ versus C_u, (c) δ versus V_a, and (d) (d) δ versus V_{beff} plots.

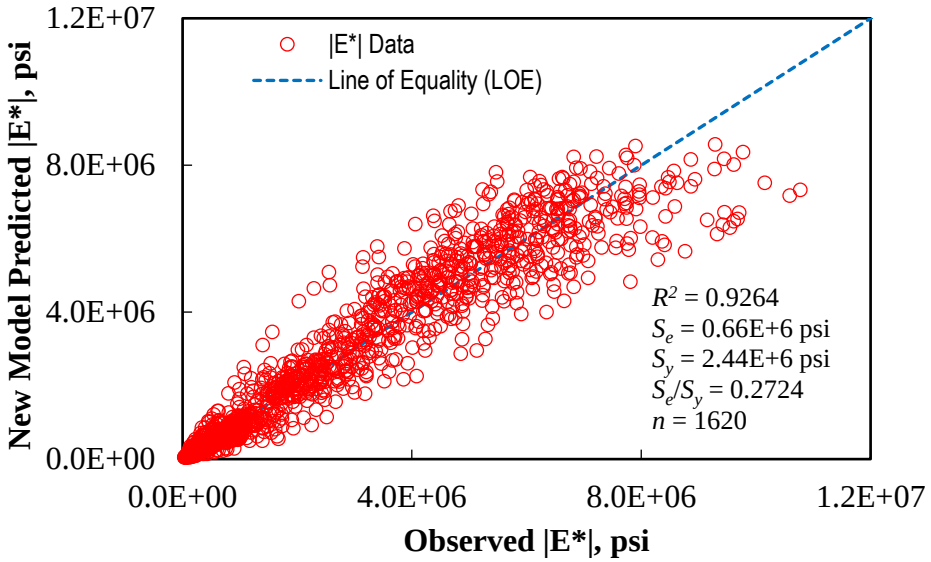

(a) Arithmetic Scale

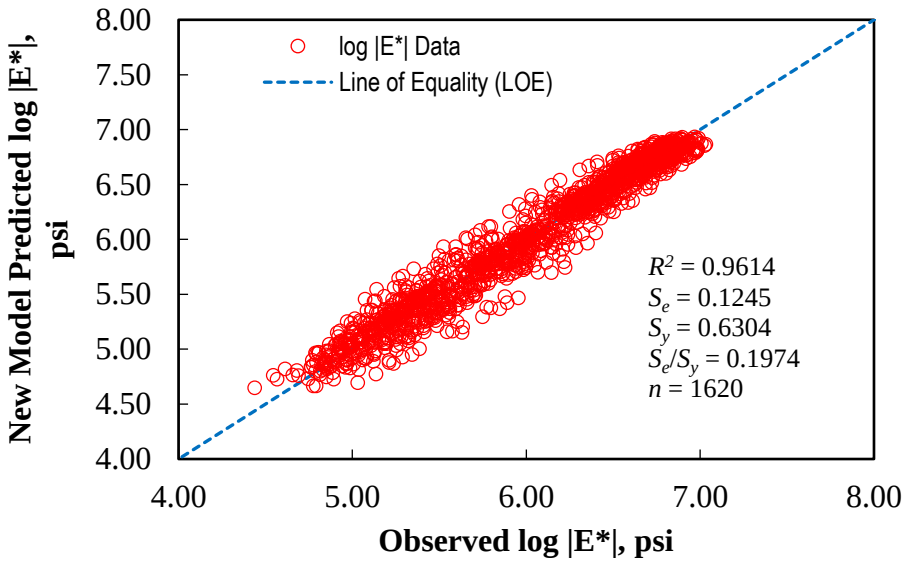

(b) Logarithmic Scale

Figure 7.7 |E^*| predicted by the new η-based model versus Observed |E^*|.

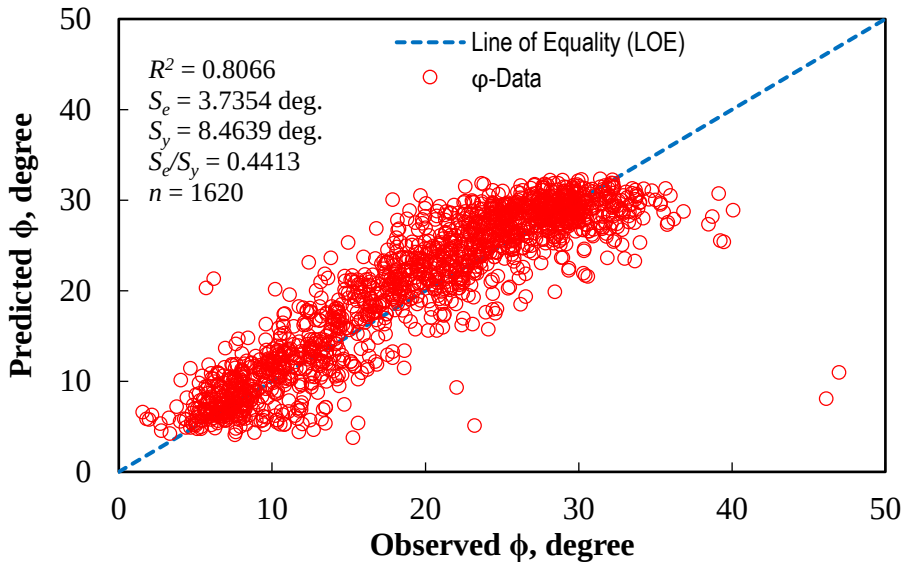

Figure 7.8 Predicted ϕ versus observed ϕ plot.

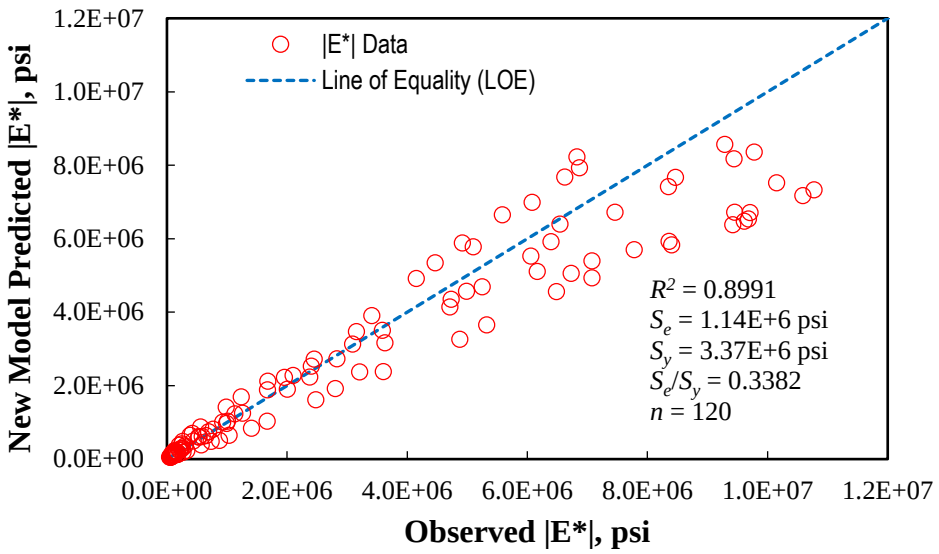

(a) Arithmetic Scale

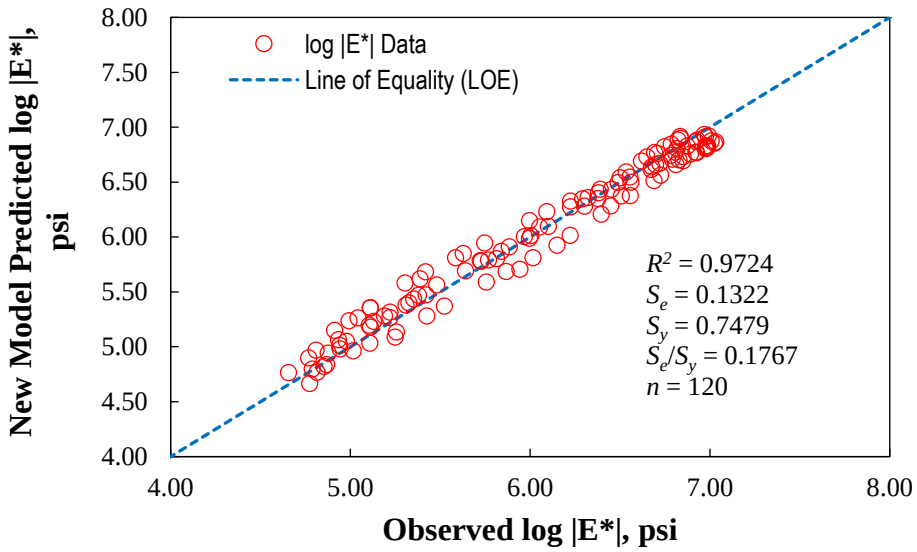

(b) Logarithmic Scale

Figure 7.9 |*E**| predicted by the new η-based model (based on 50 AC mixtures) versus Observed |*E**|.

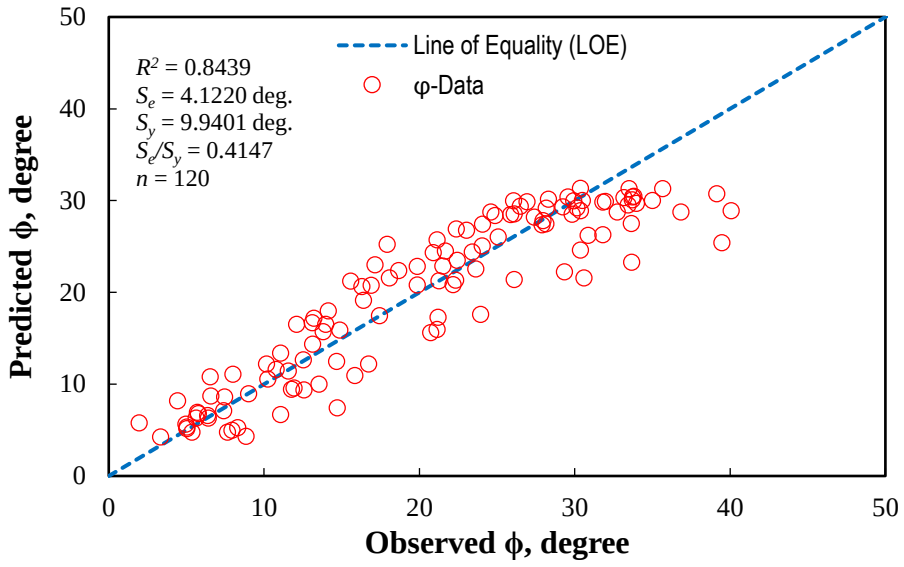

Figure 7.10 Predicted ϕ (from model based on 50 AC mixtures) versus observed ϕ plot.

Chapter 8

Binder Shear Modulus Based Modeling of Dynamic Modulus

8.1 Background

The $|G_b^*|$-based Witczak model was developed using the Bari (2005) database (Bari and Witczak 2006). The η of the asphalt binder was determined from the viscosity-temperature relationship suggested by ASTM (1998). However, to convert conventional viscosity-temperature susceptibility parameters, identified as, *A* and *VTS* to $|G_b^*|$ and binder phase angle (δ_b), empirical relationships are also provided due to unavailability of test data (2009). Also, some issues have been raised by Christiansen (2006) regarding the use of inconsistent treatment of loading frequency in case of AC mixture and asphalt binder. Singh et al. (2011) reported that the accuracy of the $|G_b^*|$-based Witczak model is poor when compared to other available $|E^*|$ models. El-Badawy et al. (2012) concluded that the $|G_b^*|$-based $|E^*|$ model produces less accurate and relatively higher biased estimates of $|E^*|$ than the η-based Witczak model.

Christensen et al. (2003) found the simplest and most effective version of Hirsch model in which $|E^*|$ is directly estimated from binder $|G_b^*|$, voids in mineral aggregate (VMA), and voids filled with asphalt binder (VFA). Singh et al. (2011) investigated this Hirsch model and reported that the predicted $|E^*|$ values are dispersed around the Line of Equality (LOE) while compared to the observed $|E^*|$ data, indicating that the model exhibits significant error. Bari and Witczak (2006), Obulareddy (2006), King et al. (2005),

and Ceylan et al. (2007) concluded that the Hirsch model underpredicts $|E^*|$. However, the fundamental weakness of this model includes strong dependence on volumetric parameters, particularly under low air void and VFA conditions (Al-Khateeb et al. 2006, Soleymani et al. 2004).

Zeng and Huang (2006) established a relationship between the complex shear modulus and phase angle of asphalt binder and AC mixture. In their study, DSR testing was used for characterizing the asphalt binders and Simple Shear Testing (SST) was used for characterizing the AC mixtures. Their results indicated that the complex shear modulus and phase angle (in shear) of the AC mixture can be represented by the same parameters obtained from the asphalt binder under the condition of material linearity. However, their study had not indicated how the $|E^*|$ of the AC mixture can be evaluated from $|G_b^*|$, and δ_b of the asphalt binder.

8.2 Objective

The objective of this study is to develop an alternative regression-based $|E^*|$ and ϕ predictive models based on binder $|G_b^*|$ for the AC mixtures typically used in New Mexico. The model should be capable of reflecting changes in $|E^*|$ of AC as a function of aggregate gradation parameters, mixture volumetrics, binder rheological properties, temperature and loading frequency.

8.3 Materials

A total of ten loose AC mixtures (referred as AC Mix-1 through AC Mix-10) using four asphalt binders of different performance grades (PG) were selected for this study. Liquid

asphalt binders corresponding to each of these AC mixtures were collected from the manufacturing plants for dynamic shear rheometer (DSR) testing. A summary of the selected AC mixtures and binders used in these mixes and the AC sample ID used in this document is listed in Table 8.1. Sieve analyses were conducted on aggregate samples corresponding to the selected AC mixtures. Figure 8.1 presents the gradation curves for the aggregate samples of all 10-AC mixtures used in this study. The gradation parameters evaluated in this step were used later for establishing the model parameters. Figure 8.2 shows the typical pictures of the final AC specimen tested in this study for complex modulus, and Figure 8.3 shows a typical test setup for the complex modulus testing.

8.4 Frequency Sweep Complex Shear Modulus Test

The AASHTO T 315 (2012) standard specification was employed as a guideline for conducting $|G_b^*|$ and δ_b testing on the asphalt binders using a DSR equipment setup. The $|G_b^*|$ with δ_b tests were conducted at test temperatures of 54.4 °C, 46.1 °C, 37.8 °C, 29.4 °C, 21.1 °C, 12.8 °C, and 4.4 °C (130 °F, 115 °F, 100 °F, 85 °F, 70 °F, 55 °F, and 40 °F). However, instead of testing only at one angular frequency of loading of 10 rad/sec as specified in AASHTO T 315, $|G_b^*|$ tests were conducted at 11 frequencies ranging between 1.0 and 100 rad/sec at each test temperature. Test specimens with 8 mm of diameter and 2 mm of height were used for $|G_b^*|$ testing. Three replicate binder specimens from each of the asphalt binders were tested for $|G_b^*|$ and δ_b, and at the end average $|G_b^*|$ and δ_b were determined. The tests were conducted in a strain-controlled mechanism. The applied strain level was 1.0% as suggested by Weldegiorgis et al. (2014). Figure 8.4(a) shows a typical

binder specimen in the silicon mold. Figure 8.4(b) shows a schematic of DSR testing on a binder specimen.

8.5 The Modulus Mastercurves

The time-temperature superposition principal (TTSP) was applied to develop the $|E^*|$-mastercurves for each of the cylindrical AC specimens and the $|G_b^*|$-mastercurves for the associated asphalt binders at 21.1 °C (70 °F) reference temperature. The developed mastercurves were used later in non-linear optimization of the model parameters. As both the $|E^*|$ and $|G_b^*|$ functions follow sigmoid shape, the following sigmoid expression was used to smoothen these functions:

$$\log|F(\lambda)| = \delta_{MC} + \frac{\alpha}{1+e^{\beta+\gamma\log(\lambda_r)}}. \qquad (8.1)$$

In Equation 1, $F(\lambda)$ is the material function, i.e. $|E^*|$ for AC specimens, and $|G_b^*|$ for the asphalt binders; λ_r is the reduced ordinary frequency (f_r) in the case of $|E^*|$, and reduced angular frequency (ω_r) in case of $|G_b^*|$. Note that, the $|E^*|$ and $|G_b^*|$ functions are determined in two different frequency spaces in current practice, and therefore, it is necessary to transform these functions in identical frequency space to establish a valid relationship. The other parameters in Equation 8.1, such as, δ_{MC} is the minimum modulus value; α is the vertical span of the modulus function, which indicates $\alpha+\delta_{MC}$ to be the maximum modulus value; β and γ are the shape parameters for the modulus function.

Figure 8.5 shows a typical tested $|E^*|$ at different temperature versus loading frequency (in Hertz) plot for one of the AC specimens. The figure also shows TTSP applied

|E^*| data horizontally shifted along the ordinary frequency space to construct |E^*|-mastercurve. After a smooth representation of |E^*| mastercurve was found by applying TTSP, the discrete |E^*|-function was fitted by the expression given in Equation 1. Once the |E^*|-function was fitted, the relationship, $\omega_r = 2\pi f_r$, was used to transform ordinary frequency space in Hertz (Hz) into angular frequency space in radian per second (rad/sec).

Similarly, Figure 8.6 shows the |G_b^*| or, |$G_b^*(\omega)$| versus angular loading frequency (in rad/sec) plots at different test temperatures for the PG 64-22 binder. Note that, the |$G_b^*(\omega)$| data is already in angular frequency space, and therefore, no transformation is necessary. The figure also shows TTSP applied horizontally shifted |$G_b^*(\omega)$| data. Finally, the generated |$G_b^*(\omega)$| mastercurve was fitted by the expression given in Equation 1.

8.6 The Phase Angle Mastercurves

The phase angle mastercurves at 21.1 °C (70 °F) reference temperature for the AC specimens and for the asphalt binders were generated by using the same frequency-temperature shift factors obtained while developing |$E^*(\omega)$| or, |$G_b^*(\omega)$|- mastercurves. The ϕ-mastercurves of the AC specimens and the δ_b-mastercurves of the asphalt binders were then fitted by the expression suggested by Rahman et al. (2016). The expression suggested by Rahman et al. (2016) can be given as –

$$\theta(\lambda) = \xi_1 + \xi_2 \log(\lambda_r) - \xi_3 \frac{\pi}{2} \alpha\gamma \frac{e^{\beta+\gamma\log(\lambda_r)}}{\left(1+e^{\beta+\gamma\log(\lambda_r)}\right)^2}. \quad (8.2)$$

Here, $\theta(\lambda)$ is the phase angle function, i.e. $\phi(f_r)$ for the AC specimens, or, $\delta_b(\omega_r)$ for the binders; ξ_1, ξ_2, and ξ_3 are the regression constants; and α, β, and γ are the |$E^*(f_r)$| or,

$|G_b^*(\omega_r)|$-mastercurve fitting parameters. Figure 8.7 shows a typical curve fitting of the ϕ-mastercurve for one of the AC specimens, while Figure 8.8 shows a typical curve fitting of δ_b-mastercurve of PG 64-22 binder by the expression given in Equation 8.2.

8.7 The Mastercurve Parameters

Table 8.2 presents the |E*| and ϕ-mastercurve fitting parameters for the AC mixtures and their test specimens considered in this study. Table 8.3 presents the |Gb*| and δb-mastercurve fitting parameters for the asphalt binders used in the AC mixtures. These smoothened mastercurve parameters are letter used for least-square, non-linear regression to obtain the model coefficients.

8.8 Model Variables

The variables affecting $|E^*|$ of AC mixtures considered in this study are: the fineness modulus (F_m), and uniformity coefficient (C_u) for the aggregate used in the AC mixture; voids filled with asphalt (*VFA*); the dynamic shear modulus ($|G_b^*(\omega)|$) and the associated phase angle (δ_b) of the binder at a given angular frequency of loading. The definitions of F_m, C_u, and *VFA* can be given as-

$$F_m = \frac{\sum_{i=1}^{N} CPR_i}{100}, \tag{8.3}$$

$$C_u = \frac{D_{60}}{D_{10}}, \text{ and} \tag{8.4}$$

$$VFA = \frac{V_{beff}}{V_{beff} + V_a}. \tag{8.5}$$

Here, CPR_i is the cumulative percentage of aggregate retained at i^{th} sieve, D_{60} and D_{10} are the sieve sizes corresponding to 60% and 10% material passing, and N is the number of sieves used in the sieve analysis. The variable V_{beff} is the effective percent volume of the asphalt binder, and V_a is the percent air void content of AC specimen. A total of 13 standard sieves were used for sieve analyses of the aggregate blends. The designations and the opening sizes of the sieves are presented in Table 8.4. The analyses on aggregate blends were conducted to establish the model parameters. Table 8.5 summarizes the gradation parameters (i.e. CPR_i, D_{60}, D_{10}, F_m and C_u), V_{beff}, and V_a of individual cylindrical AC specimens for the 10 asphalt-aggregate mixtures considered in this study.

8.9 Effect Study

The effects of F_m, C_u, and *VFA* on the $|E^*|$ and ϕ of AC were studied in this research work to understand their trends in the predictive models and subsequently, the initial form of the $|E^*|$ and ϕ-predictive models were formulated. All seven model parameters, i.e., α, β, δ_{MC}, and γ for $|E^*|$-model, and ξ_1, ξ_2, and ξ_3 for ϕ-model, were studied against the variables F_m, C_u, and *VFA* to identify initial tendency of the variables in the $|E^*|$ and ϕ predictive models. To simplify the analysis in its initial stage, linear relationships were considered. Brief discussions on these studies are presented in the following sections.

8.9.1 Dynamic Modulus

8.9.1.1 The Fineness Modulus (F_m)

Figure 8.9 shows the variations of α, β, δ_{MC}, and γ with the F_m of the AC mixtures. Weak correlations can be observed between the mastercurve parameters and F_m. In general, the

parameters δ_{MC}, β, and γ are decreasing with increasing F_m. However, the parameter α is found to be increasing with increasing F_m. Also, relatively stronger relationships exist between α and F_m, and, β and F_m.

8.9.1.2 The Uniformity Coefficient (C_u)

Figure 8.10 shows the variations of α, β, δ_{MC}, and γ with the C_u of the AC mixtures. In this case, strong correlations are found in the case of α, β, and δ_{MC}, whereas, weak correlation exits between γ and C_u. In general, α, and γ are found to be increasing with the increasing C_u, whereas, β, and δ_{MC} are found to be decreasing with the increasing C_u.

8.9.1.3 The Voids Filled with Asphalt (VFA)

Figure 8.11 shows the variation of α, β, δ_{MC}, and γ with the *VFA* of the of the AC specimens. In general, the δ_{MC}, and β are found to be increasing with increasing *VFA*. However, the parameters α and γ are found to be decreasing with increasing *VFA*. Also, the strengths of these correlations are found to be similar.

8.9.2 Phase Angle

8.9.2.1 The Fineness Modulus (F_m)

Figure 8.12 shows the variations of ξ_1, ξ_2, and ξ_3 with the F_m of the AC mixtures. Weak relationships of these parameters with F_m of the AC mixtures are observed in these figures. Correlations between ξ_1 and F_m and, ξ_3 and F_m are relatively stronger than the correlation between ξ_2 and F_m. In general, the parameter ξ_1 has a decreasing trend with increasing F_m, whereas, ξ_2, and ξ_3 increases as the F_m increases.

8.9.2.2 The Uniformity Coefficient (C_u)

Figure 8.13 shows the variations of ξ_1, ξ_2, and ξ_3 with the C_u of the AC mixtures. Strong and similar correlations between the mastercurve parameters and C_u can be observed. In general, the parameter ξ_1 has a decreasing trend with increasing C_u, whereas, ξ_2, and ξ_3 increases as the C_u increases.

8.9.2.3 The Voids Filled with Asphalt (VFA)

Figure 8.14 shows the variation of ξ_1, ξ_2, and ξ_3 with the *VFA* of the AC mixtures. Weak correlations between the mastercurve parameters and the *VFA* of the AC mixture can be observed in these figures. In general, the parameter ξ_1 has an increasing trend with increasing F_m, whereas, ξ_2, and ξ_3 decreases as the F_m increases.

8.10 The New Predictive Models

In current practice $|E^*|$ or, $|E^*(f)|$ is determined in ordinary frequency space in Hz, while $|G_b^*|$ or, $|G_b^*(\omega)|$ is determined in angular frequency space in rad/sec. Therefore, to study the effect of binder rheological properties on the proposed models, it was necessary to transform either the ordinary frequency space to angular frequency space in case of $|E^*|$ functions of the AC mixtures, or, the angular frequency space to ordinary frequency space in case of $|G_b^*|$ function by the relation $\omega = 2\pi f$. In this study, the ordinary frequency space was transformed into angular frequency space in case of $|E^*|$, and therefore designated as $|E^*(\omega)|$ later on. As the $|G_b^*(\omega)|$ and δ_b-mastercurves are already fitted by the expression given in Equation 1 and Equation 2, respectively, the values of these two binder parameters are calculated for the reduced angular frequencies associated with the $|E^*(\omega)|$-functions.

To develop the new dynamic modulus and phase angle predictive models for AC nonlinear regression-optimization technique was used. A two-step modeling approach was adopted while developing the $|E^*(\omega)|$ as well as the $\phi(\omega)$ predictive models. In the first step, the first seven AC mixtures (21 cylindrical AC specimens) and associated binders were used to develop the initial models, and the modulus and phase angle data of remaining AC mixtures and binders were tested. In the second step, all 10-AC mixtures (30 cylindrical AC specimens) were used to obtain the final forms of the predictive models. The final forms of this new predictive models for estimating $|E^*(\omega)|$ and $\phi(\omega)$ of AC mixtures are discussed in the following sections.

8.10.1 Dynamic Modulus Predictive Model

An effect study showed that the parameters α, β, γ, and δ_{MC} in Equation 8.1 for the AC mixtures are related in various scales to the F_m, C_u, VFA of the AC sample. After a considerable amount of trials, the final form of the $|E^*(\omega)|$ predictive model can be presented by the following expression -

$$\log|E^*(\omega)| = \delta_{|E^*(\omega)|} + \frac{\alpha_{|E^*(\omega)|}}{1 + e^{\beta_{|E^*(\omega)|} + \gamma_{|E^*(\omega)|} * \{1.24058 \log|G_b^*(\omega)| - 1.18561 \log\delta_b(\omega)\}}} . \qquad (8.4)$$

Note that, the $|E^*(\omega)|$ is kept in angular frequency space ($|E^*(\omega)|$) so that the angular loading frequency associated with a certain pair of $|G_b^*|$ and δ_b can be readily used in the equation to estimate the $|E^*(\omega)|$ of the AC mix for that particular angular frequency of loading. In Equation 8.4, both the $|E^*(\omega)|$ and $|G_b^*(\omega)|$ are in pound per square inch (psi) unit. Equation 8.4 is analogous to Equation 8.1, where –

$$\delta_{|E^*(\omega)|} = 2.98344 - 0.36204\ (F_m)^{0.5879} - 0.00291\ (C_u)^{1.6006} + 4.47476\left(\frac{V_{beff}}{V_{beff}+V_a}\right)^{0.78665}, \quad (8.5)$$

$$\alpha_{|E^*(\omega)|} = 4.118646\ (F_m)^{0.161757} + 0.308047\ (C_u)^{0.608689} - 7.137353\left(\frac{V_{beff}}{V_{beff}+V_a}\right)^{0.588208}, \quad (8.6)$$

$$\beta_{|E^*(\omega)|} = -1.935020\ (F_m)^{0.304465} - 0.947132\ (C_u)^{0.436790} + 8.367143\left(\frac{V_{beff}}{V_{beff}+V_a}\right)^{0.376962}, \text{ and} \quad (8.7)$$

$$\gamma_{|E^*(\omega)|} = -0.00438\ (F_m)^{1.58911} + 1.00862\ (C_u)^{0.08551} - 2.05138\left(\frac{V_{beff}}{V_{beff}+V_a}\right)^{0.38889}. \quad (8.10)$$

8.10.2 Phase Angle Predictive Model

The expression given in Equation 8.2 was used to develop the ϕ predictive model for AC. The effect study earlier showed that the parameters ξ_1, ξ_2 and ξ_3 can be correlated to the F_m, C_u, and *VFA* of the AC samples. After a considerable amount of trials the final form of the ϕ-predictive model for AC mix is found as –

$$\phi(\omega) = \xi_1 + \xi_2 \log(\omega) - \xi_3 \frac{\pi}{2} \alpha_{|E^*(\omega)|}\ \gamma_{|E^*(\omega)|} \frac{e^{\beta_{|E^*(\omega)|}+\gamma_{|E^*(\omega)|}\log(\omega)}}{\left(1+e^{\beta_{|E^*(\omega)|}+\gamma_{|E^*(\omega)|}\log(\omega)}\right)^2}. \quad (8.9)$$

Equation 8.9 is analogous to Equation 8.2, where –

$$\xi_1 = -0.75729 - 0.04673\,F_m - 0.000051\,(C_u)^{2.4065} + 2.00944\left(\frac{V_{beff}}{V_{beff}+V_a}\right), \quad (8.10)$$

$$\xi_2 = 0.43604 + 0.03399\,(C_u)^{0.53471} - 0.74847\left(\frac{V_{beff}}{V_{beff}+V_a}\right)^{0.30623}, \text{ and} \quad (8.11)$$

$$\xi_3 = 3.53402 + 0.1047\ F_m + 0.00064\ (C_u)^{2.04946} - 6.12145\left(\frac{V_{beff}}{V_{beff} + V_a}\right). \quad (8.12)$$

In Equation 8.9, the values of $\alpha_{|E^*(\omega)|}$, $\beta_{|E^*(\omega)|}$, and $\gamma_{|E^*(\omega)|}$ can be found from Equations 8.6, 8.7, and 8.8 respectively.

8.11 Model Evaluation

The development of a regression-based model greatly depends on the statistical analysis and optimization process used. The fundamental aim of this type of model development process is to reduce the error from the prediction by comparing the predicted data with the observed data for the identical input conditions. The optimization process involves the determination of regression coefficients in such a way that the developed equation provides minimum error when the predicted and observed data are compared. To determine the level of accuracy of the model, a statistical evaluation called "goodness of fit" is used. To determine "goodness of fit", the estimated values by the developed models are compared with the tested or observed values at the same input conditions. Generally, two statistical parameters are required to be evaluated to determine the "goodness of fit" of the model. The first one is the coefficient of determination (R^2), and the second one is the ratio of the standard error (S_e) to the standard deviation (S_y). The mathematical forms of R^2, S_e, and S_y can be presented by the following expressions:

$$R^2 = 1 - \frac{(n - p - 1)S_e^{\ 2}}{(n-1)S_y^{\ 2}}, \quad (8.13)$$

$$S_e = \left[\frac{1}{(n - p - 1)} \sum_{1}^{n} (\hat{x}_i - x_i)^2 \right]^{\frac{1}{2}}, \text{ and} \tag{8.14}$$

$$S_y = \left[\frac{1}{(n - 1)} \sum_{1}^{n} (x_i - \bar{x})^2 \right]^{\frac{1}{2}}. \tag{8.15}$$

In the above expressions, $\hat{x}_i$ are the predicted data, x_i are the observed data, $\bar{x}$ is the average of the observed data, *n* is the number of data points used in the model, and *p* is the number of fitting parameters used in the model. A relatively good predictive model would have a higher R^2, close to 1 and a smaller S_e/S_y close to zero.

8.11.1 Model Parameters

Figure 8.15 shows all the predicted (or also can be called as optimized) versus observed parameters related to the new $|E^*(\omega)|$ and $\phi(\omega)$ predictive models. The R^2, S_e, S_y, and S_e/S_y values are also included in the plots to identify how well the predicted parameters fit observed data. All the predicted parameters show good coefficient of determination, R^2-value greater than 0.3 with a S_e/S_y-value less than 0.85, except for the parameter $\gamma_{|E^*(\omega)|}$, for which, the R^2-value is found to be 0.14 with a slightly larger S_e/S_y-value of 0.93. This indicates that for the parameter $\gamma_{|E^*(\omega)|}$, a higher degree of "goodness of fit" was not attainable by the non-linear optimization process. However, the "goodness of fit" for $\gamma_{|E^*(\omega)|}$ is still fairly good considering numerous complexities involved in this type of prediction. Another study showed that, instead of using Equation 8, use of an average $\gamma_{|E^*(\omega)|}$ which is found as, $\gamma_{|E^*(\omega)|}$= -0.45236, does not change significantly the output of these models. This also indicates the value of $\gamma_{|E^*(\omega)|}$ is loosely dependent on the variables F_m, C_u, and *VFA* of

the AC mixture, and if desired, a constant value of $\gamma_{|E^*(\omega)|}$ = -0.45236, independent of any mixture attributes, can be used for all AC mixtures.

8.11.2 Dynamic Modulus Model

The goodness of fit of the proposed $|E^*(\omega)|$ model given in Equation 8.4 is evaluated in two ways, i.e., in logarithmic scale and in normal or arithmetic scale. The developed $|E^*(\omega)|$ model has a fairly good coefficient of determination (R^2 = 0.84) and a small S_e/S_y (S_e/S_y = 0.41) in normal or arithmetic scale. Again, in logarithmic scale, these are: R^2 = 0.91, and S_e/S_y = 0.30, which are fairly good for this type of models where numerous complexities are involved.

Figures 8.16(a) and 8.16(b) show the observed $|E^*(\omega)|$ data versus the $|E^*(\omega)|$ data predicted from the model in arithmetic and logarithmic scales respectively. Both of the plots show that all the $|E^*(\omega)|$ data points are around the LOE without any significant bias. Therefore, it can be said that the proposed dynamic modulus model based on $|G_b^*(\omega)|$ gives a fairly good prediction of $|E^*(\omega)|$ of the AC mixture typically used in New Mexico.

8.11.3 Phase Angle Model

In case of proposed ϕ model, the goodness of fit is also evaluated. The developed ϕ-model has a fairly good R^2 = 0.73 and a small S_e/S_y = 0.52. Figure 8.16(c) shows the observed ϕ-values versus the ϕ-values predicted from the model given in Equation 8.9. In this case, the plot shows that all the ϕ-data points are around the LOE without any significant bias. Therefore, it can be said that the proposed phase angle model for AC based on $|G_b^*(\omega)|$ of

the used binder gives a fairly good prediction of ϕ of the AC mixture typically used in New Mexico.

8.12 Conclusions

In this study, new predictive models for dynamic modulus and phase angle of AC are developed based on observed data of 10 asphalt concrete mixtures typically used in New Mexico. The developed models use two fundamental aggregate gradation parameters: the fineness modulus and the uniformity coefficient, mix volumetric parameters (air void content and effective binder volume), and binder rheological properties (dynamic shear modulus and binder phase angle) as direct input. The developed $|E^*(\omega)|$ and $\phi(\omega)$ models possesses fairly good statistics, considering goodness of fit of the data.

Table 8.1 Summary of Selected Asphalt Concrete Mixtures and Binders

Mix ID used in this chapter	AC Mix ID	Superpave Gradation	Nominal Maximum Aggregate Size (NMAS), mm	Asphalt Binder Performance Grade (PG)	Type of Aggregate Material
Mix 1	6	SP IV	12.5	PG 64-22	Alluvial Limestone
Mix 2	9	SP III	19.0	PG 64-28	Sand & Gravel
Mix 3	10	SP III	19.0	PG 76-28	Dacite
Mix 4	11	SP III	19.0	PG 76-28	Basalt
Mix 5	14	SP III	19.0	PG 76-22	Sand & Gravel
Mix 6	12	SP III	19.0	PG 64-28	Basalt
Mix 7	16	SP III	19.0	PG 64-22	Limestone (Source 1)
Mix 8	17	SP III	19.0	PG 64-22	Limestone (Source 2)
Mix 9	18	SP III	19.0	PG 64-22	River Deposits
Mix 10	19	SP III	19.0	PG 64-28	River Deposits

Table 8.2 |E*| and ϕ-Mastercurve Fitting Parameters in case of Asphalt Concretes

Mix ID used in this chapter	AC Mix ID	Test Specimen ID	Parameters of the Fitted |E*|-Mastercurve (When |E*| is measured in psi)				Parameters of the Fitted ϕ-Mastercurve (When ϕ is measured in Degrees)		
			α	β	δ	γ	ξ_1	ξ_2	ξ_3
1	6	1	2.093803	-0.439430	4.630672	-0.471133	0.146988	-0.009953	0.766151
		2	2.341267	-0.427220	4.560573	-0.406556	0.073982	0.002103	0.913147
		3	2.443948	-0.537820	4.422175	-0.435130	0.102853	-0.011449	0.870669
2	9	1	2.512331	-0.720857	4.398010	-0.469215	0.065624	-0.007118	0.899463
		2	2.720948	-1.001125	4.241432	-0.418658	-0.098478	0.019667	1.370354
		3	2.696008	-0.937278	4.171732	-0.424492	-0.093793	0.025394	1.363759
3	10	1	2.157695	0.062459	4.683677	-0.573106	0.149871	-0.023793	0.819400
		2	2.319916	-0.062671	4.519527	-0.555567	0.083570	-0.001842	0.827412
		3	2.140978	-0.353913	4.643369	-0.563617	0.124151	-0.004023	0.813003
4	11	1	2.373514	-0.557944	4.434320	-0.515756	0.039791	-0.005993	0.949108
		2	2.486698	-0.375507	4.369586	-0.464755	0.150231	-0.024847	0.734936
		3	2.737394	-0.598750	4.172102	-0.438263	-0.007545	0.001334	1.045620
5	14	1	2.300968	-0.421243	4.555751	-0.460374	0.138925	-0.009020	0.699044
		2	2.624587	-0.206232	4.239956	-0.432937	-0.040121	0.000275	1.149471
		3	2.088267	-0.168149	4.548541	-0.616549	0.135589	-0.009747	0.740034
6	12	1	2.815853	-0.854161	4.241701	-0.390771	-0.033913	0.000042	1.202484
		2	2.772544	-0.762042	4.230183	-0.395098	-0.124684	0.014375	1.470256
		3	2.856943	-0.958318	4.190851	-0.362256	0.028082	0.003852	1.084668
7	16	1	3.644620	-1.263216	3.415983	-0.290736	0.004293	0.008278	1.115898
		2	2.611705	-0.805432	4.436904	-0.381204	0.073199	-0.010009	0.742677
		3	2.475351	-0.415688	4.573543	-0.407110	0.102896	-0.008516	0.822654
8	17	1	4.092691	-1.559659	3.006473	-0.329657	-0.623235	0.115979	3.089551
		2	4.370580	-1.548764	2.698798	-0.339709	-0.649177	0.111479	2.793961
		3	2.846760	-1.633314	4.128127	-0.452196	-0.138708	0.039263	1.564348
9	18	1	2.429417	-1.104553	4.263919	-0.495106	0.064337	-0.006439	0.899132
		2	2.783488	-0.962327	4.135592	-0.445871	-0.169382	0.027208	1.617240
		3	2.487294	-0.979357	4.418204	-0.502170	0.103696	-0.016056	0.742776
10	19	1	2.404182	-0.560408	4.515656	-0.446836	-0.098629	0.008777	1.596412
		2	2.732213	-1.038204	4.007651	-0.508053	-0.069842	0.017288	1.256755
		3	2.509936	-0.872765	4.344383	-0.577950	0.031112	0.010543	0.979627

Table 8.3 $|G_b^*|$ and δ_b-Mastercurve Fitting Parameters in case of Asphalt Binders

Asphalt Binder Performance Grade	**Parameters of the Fitted $\|G_b^*\|$-Mastercurve (When $\|G_b^*\|$ is measured in psi)**				**Parameters of the Fitted δ_b-Mastercurve (When ϕ is measured in Degrees)**		
	α	β	δ	γ	ξ_1	ξ_2	ξ_3
PG 64-22	11.323256	-0.479263	-5.874146	-0.290429	0.207308	-0.013160	0.806487
PG 64-28	13.975432	-0.714728	-8.065467	-0.260670	0.674454	-0.062991	0.445871
PG 76-22	11.337356	-0.470740	-5.852800	-0.288641	0.202996	-0.014533	0.811842
PG 76-28	14.627483	-0.770618	-8.455716	-0.212341	0.425500	-0.032159	0.589191

Table 8.4 Standard Sieves Used in this Study

Sieve Designation	Sieve Opening (mm)
2 inch	50.00
1.5 inch	37.50
1 inch	25.00
3/4 inch	19.00
1/2 inch	12.50
3/8 inch	9.50
No. 4	4.75
No. 8	2.36
No. 16	1.18
No. 30	0.60
No. 50	0.30
No. 100	0.15
No. 200	0.075

Table 8.5 Summary of AC Volumetric and Aggregate Gradation Parameters

Mix ID	$\sum_{i=1}^{n} CPR_i$	D_{60}	D_{10}	F_m	C_u	V_{beff}	V_a		
							Specimen 1	*Specimen 2*	*Specimen 3*
Mix 1	503.90	4.10	0.11	5.039	37.27	11.26	6.0	6.0	5.2
Mix 2	626.40	8.10	0.22	6.264	36.82	11.54	5.6	5.1	5.7
Mix 3	598.50	6.80	0.23	5.985	29.57	11.23	5.6	5.0	5.0
Mix 4	658.50	10.0	0.30	6.585	33.33	10.52	6.0	5.9	6.0
Mix 5	606.00	6.50	0.22	6.060	29.55	12.04	6.0	6.0	6.0
Mix 6	653.50	10.00	0.22	6.535	31.25	9.39	5.7	5.3	5.3
Mix 7	596.30	6.60	0.18	5.963	36.67	10.88	5.0	5.0	5.8
Mix 8	597.10	6.90	0.15	5.971	46.00	10.54	6.0	5.9	6.0
Mix 9	612.10	6.70	0.18	6.121	37.22	11.05	6.0	5.7	6.0
Mix 10	639.20	10.00	0.22	6.392	45.46	10.12	5.0	5.0	5.0

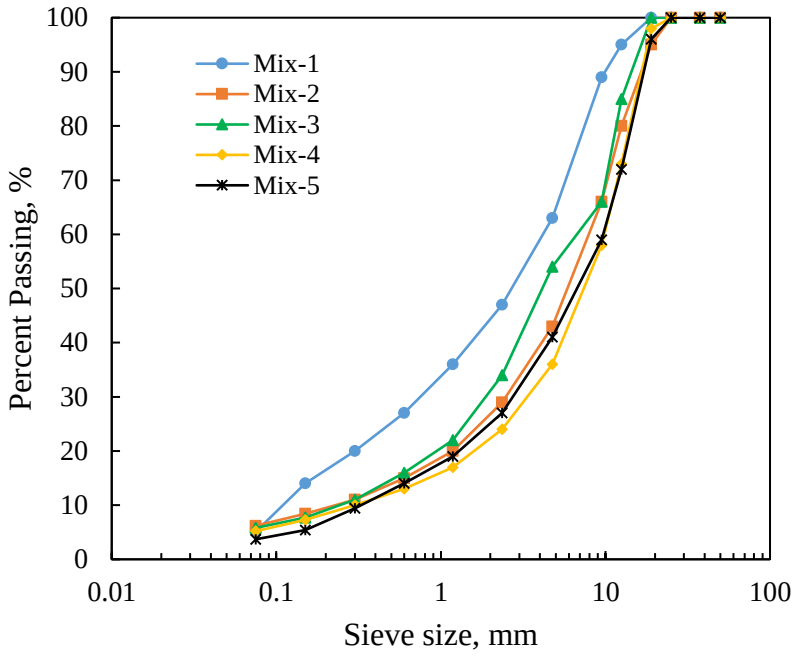

(a)

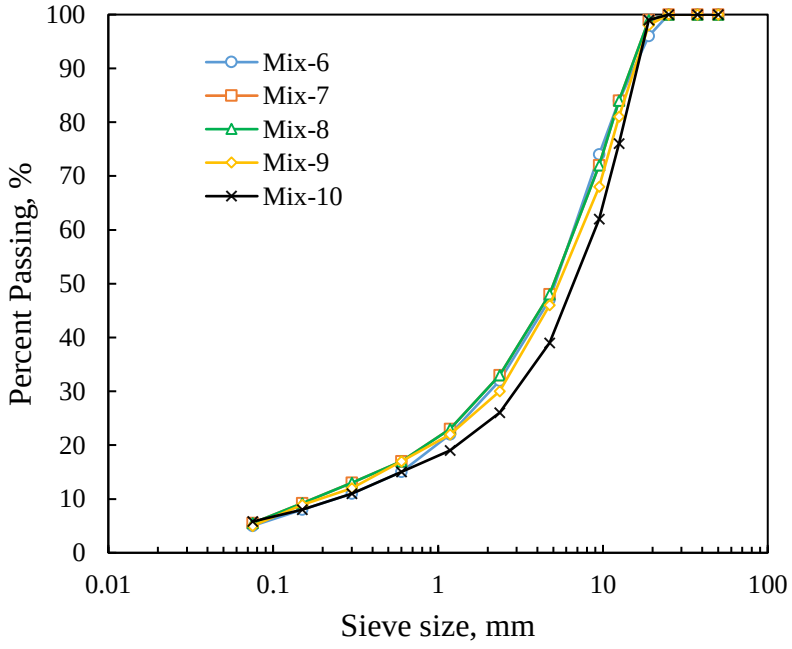

(b)

Figure 8.1 (a) Sieve analysis results for aggregate samples of (a) Mix 1 through Mix 5, and (b) Mix 6 through Mix 10.

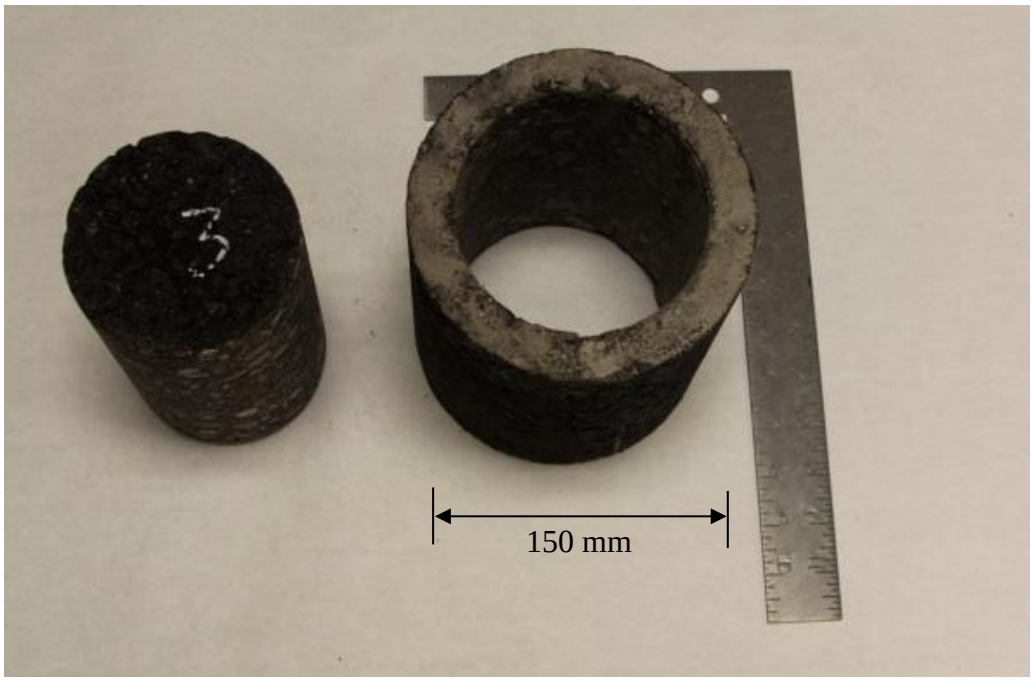

(a) Cored sample

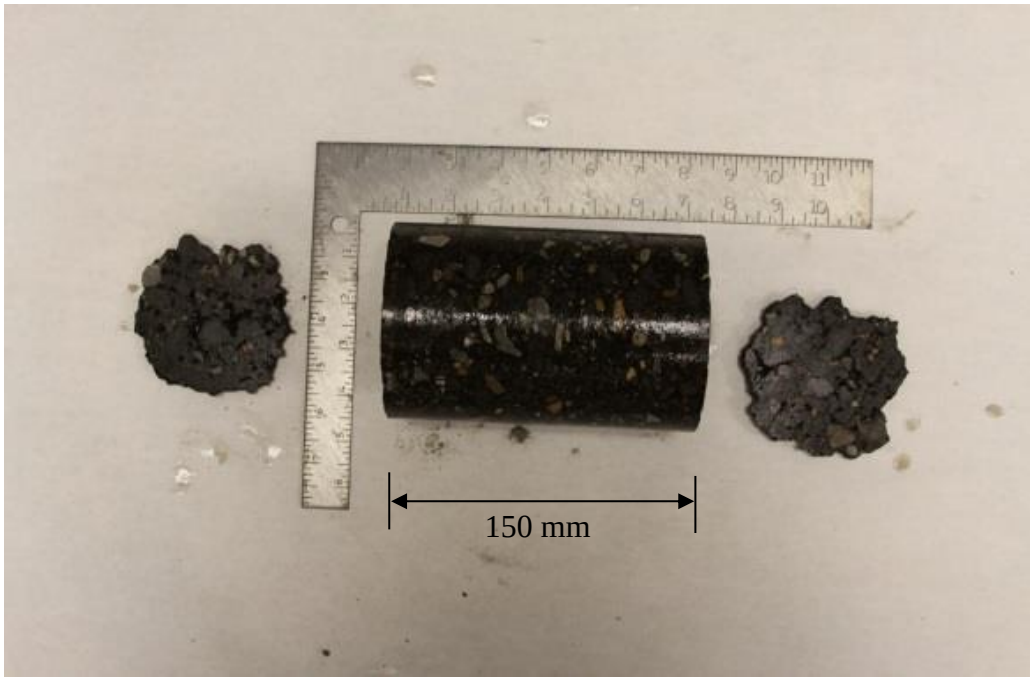

(b) Edge-cut sample

Figure 8.2 Preparation of |E^*| test specimens; (a) typical core-drilled specimen, and after that, (b) edge-sawed specimen.

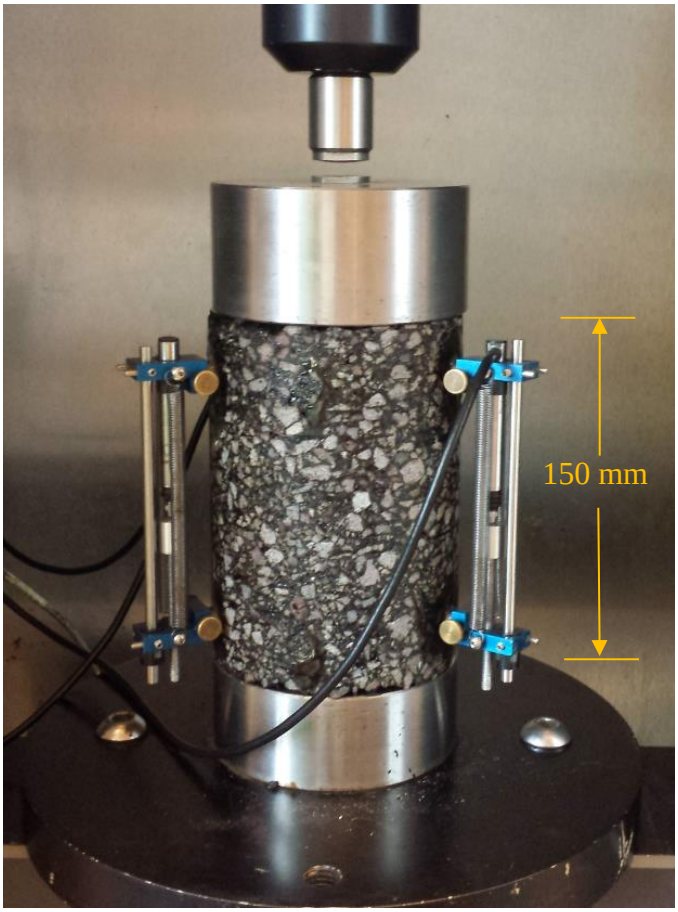

Figure 8.3 Dynamic modulus test setup.

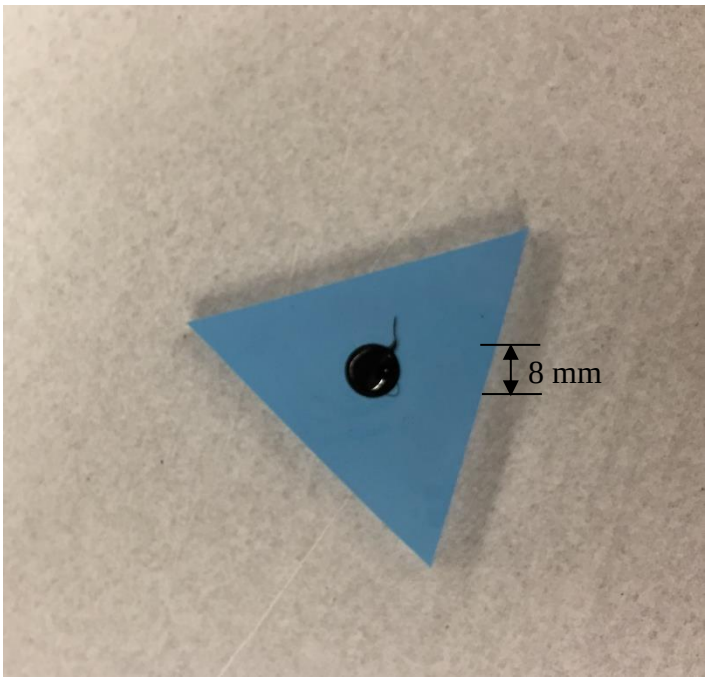

(a) Binder sample in silicon mold

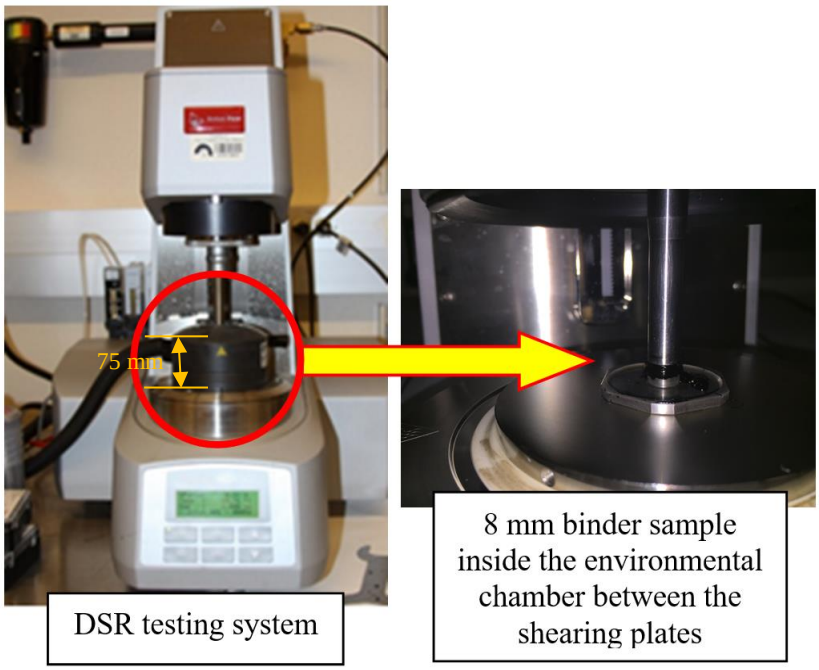

(b) DSR testing on binder sample

Figure 8.4 (a) Preparation of DSR test sample, and (b) DSR testing on binder sample.

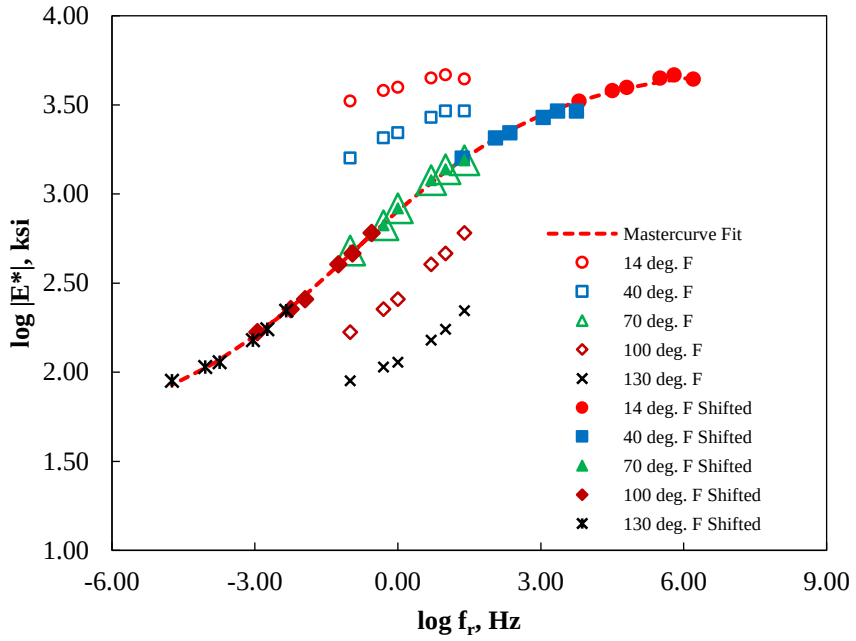

Figure 8.5 Typical development of |*E**|-mastercurve for the AC specimens.

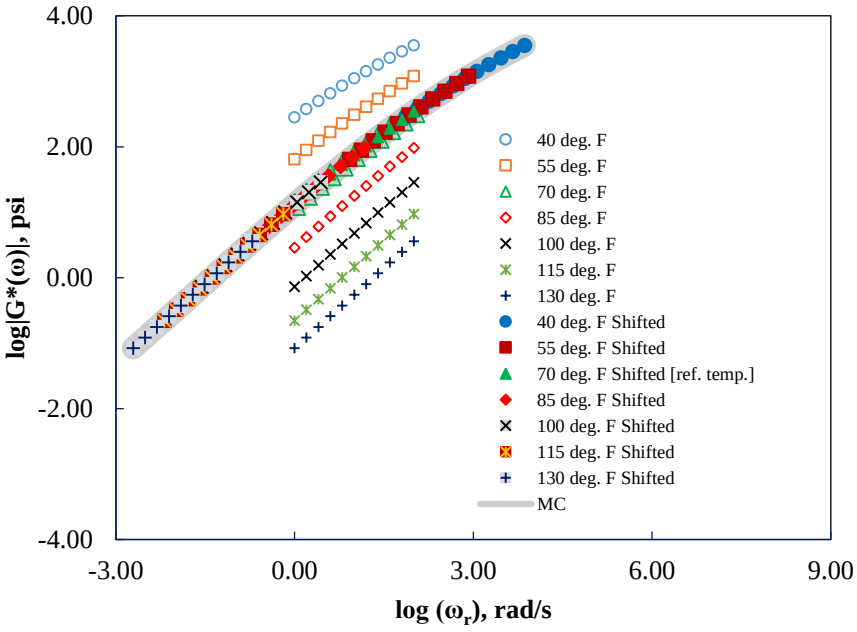

Figure 8.6 Typical development of |G_b*(ω)|-mastercurve at 70°F reference temperature.

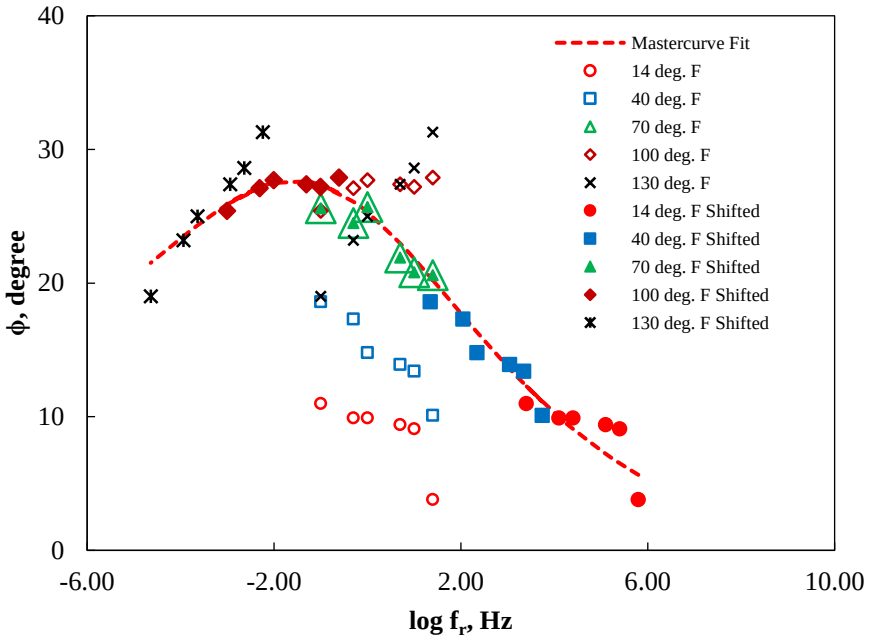

Figure 8.7 Typical development of ϕ-mastercurve for the AC specimens at 21.1 °C (70 °F) reference temperature.

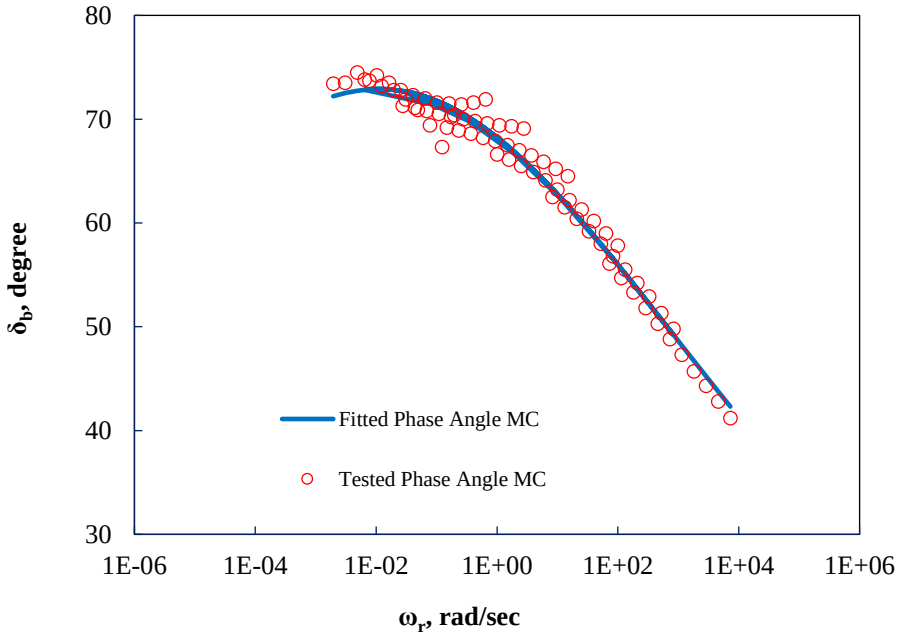

Figure 8.8 Typical development of δ_b-mastercurve for the binders at 21.1 °C (70 °F) reference temperature.

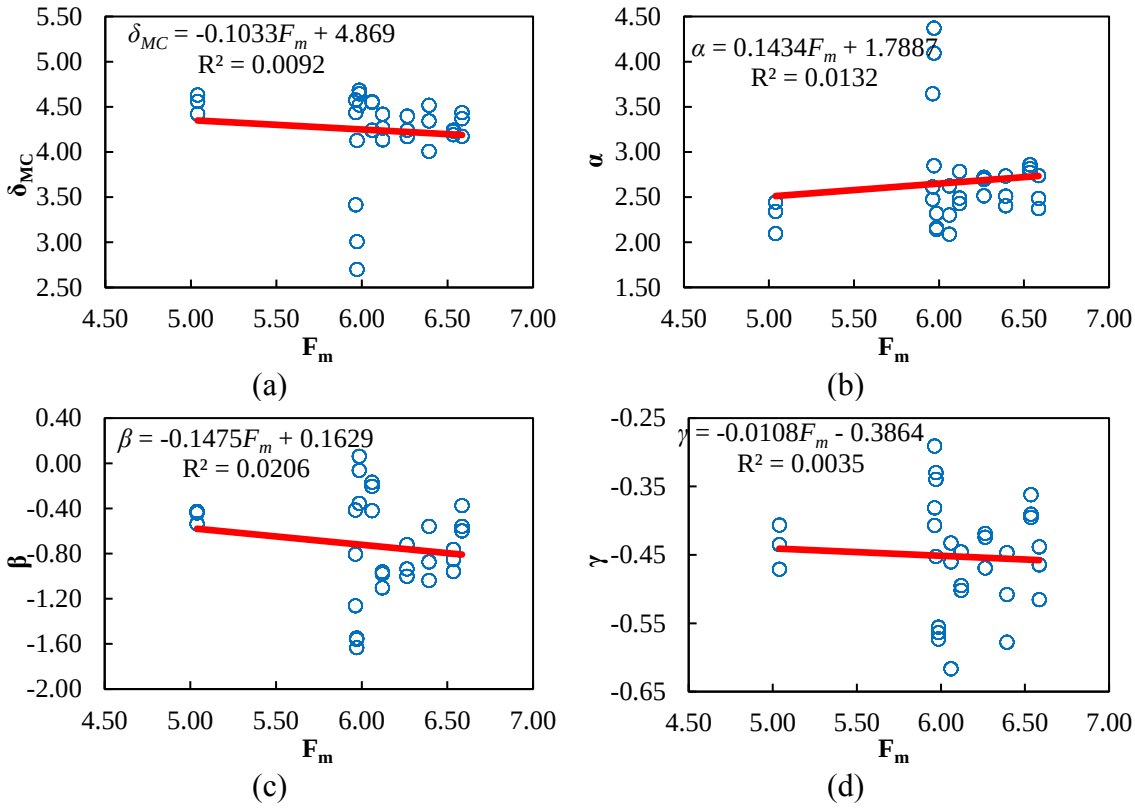

Figure 8.9 Parameters α, β, δ_{MC}, and γ versus F_m plots.

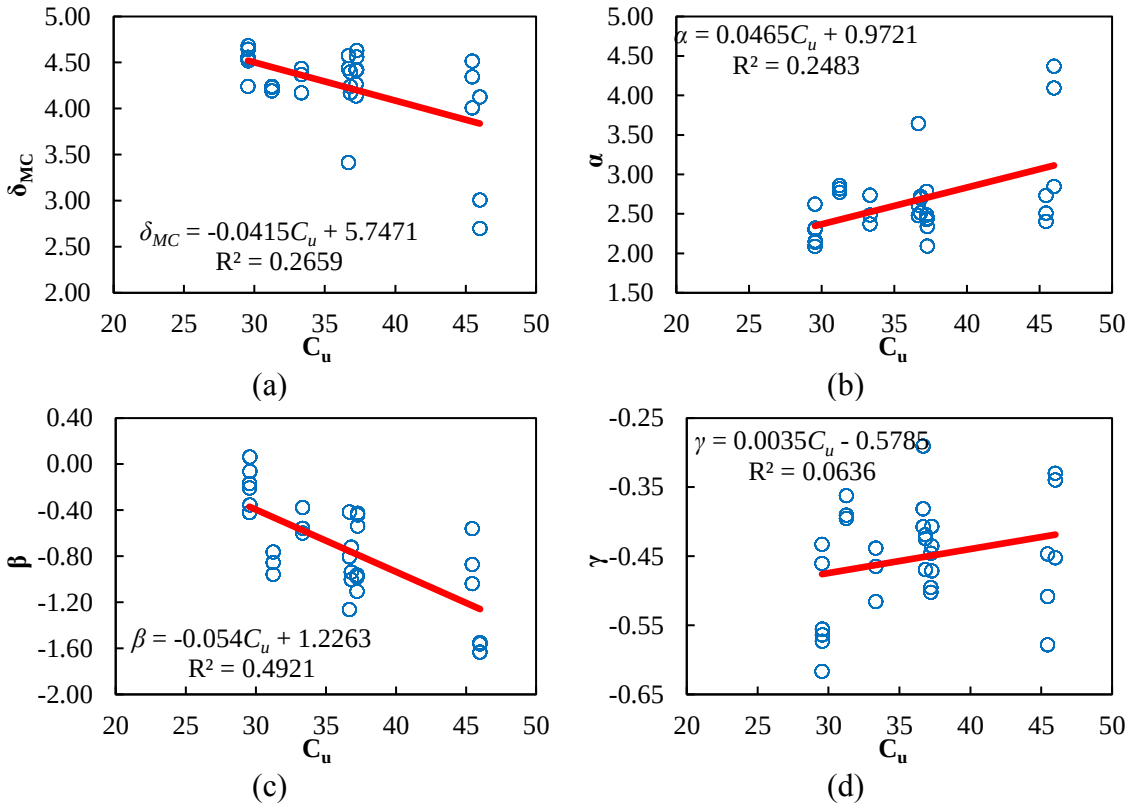

Figure 8.10 Parameters α, β, δ_{MC}, and γ versus C_u plots.

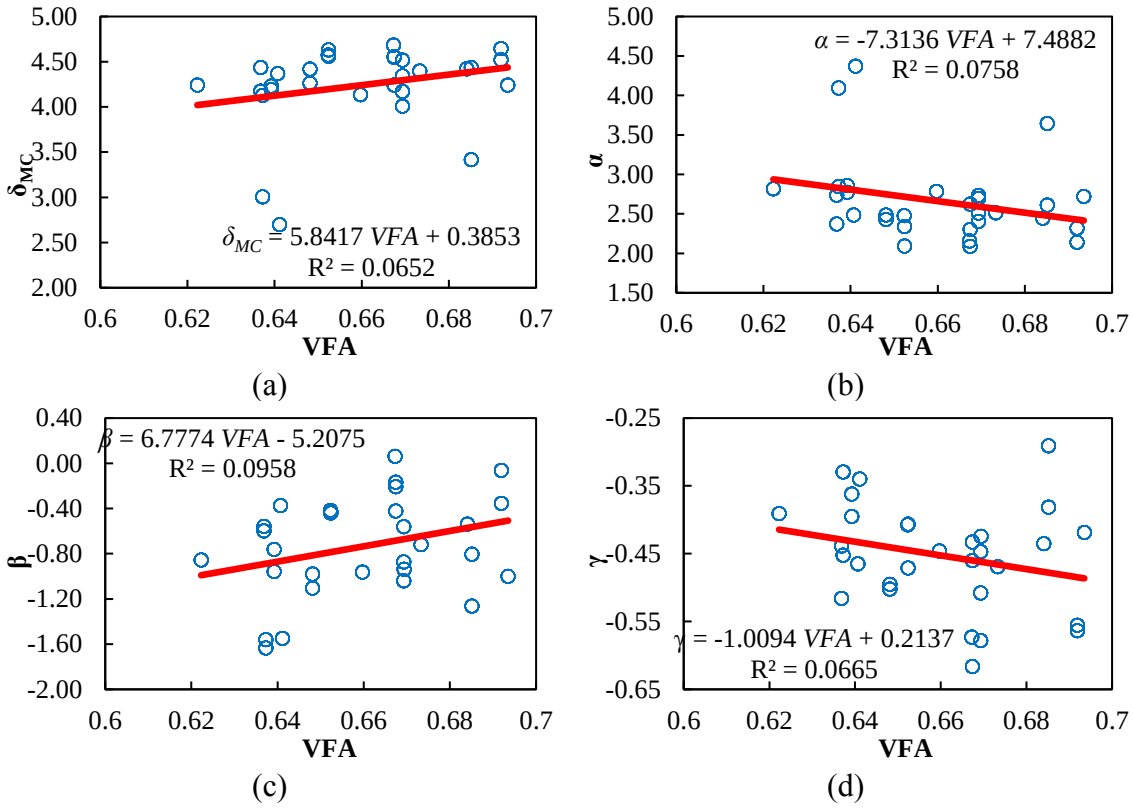

Figure 8.11 Relationships of α, β, δ_{MC}, and γ with the *VFA* of the AC mixtures.

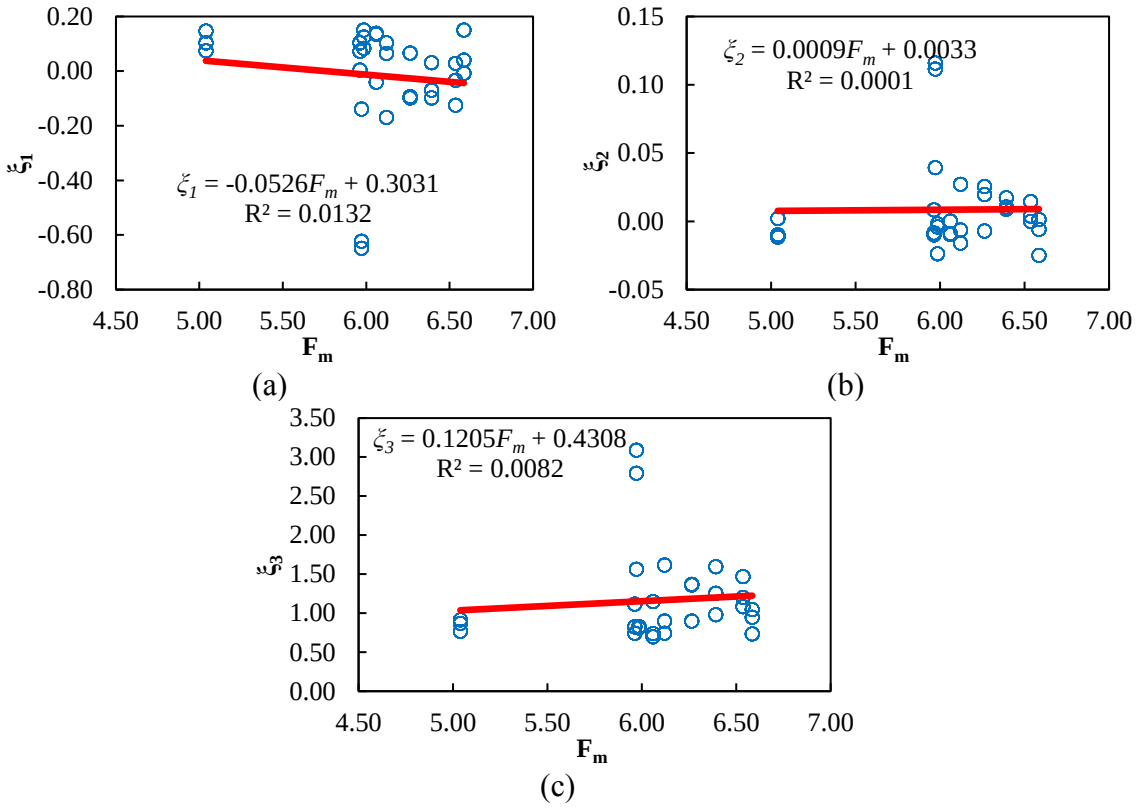

Figure 8.12 Parameters ξ_1, ξ_2, and ξ_3 versus F_m plots.

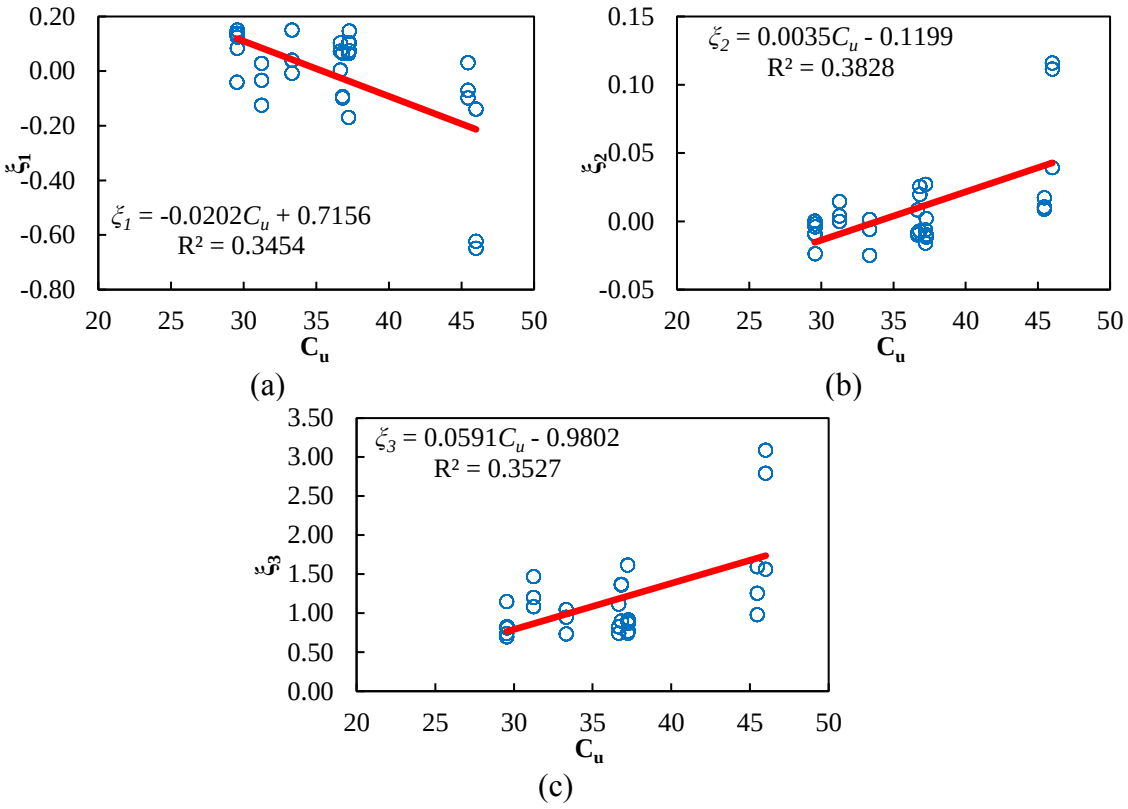

Figure 8.13 Parameters ξ_1, ξ_2, and ξ_3 versus C_u plots.

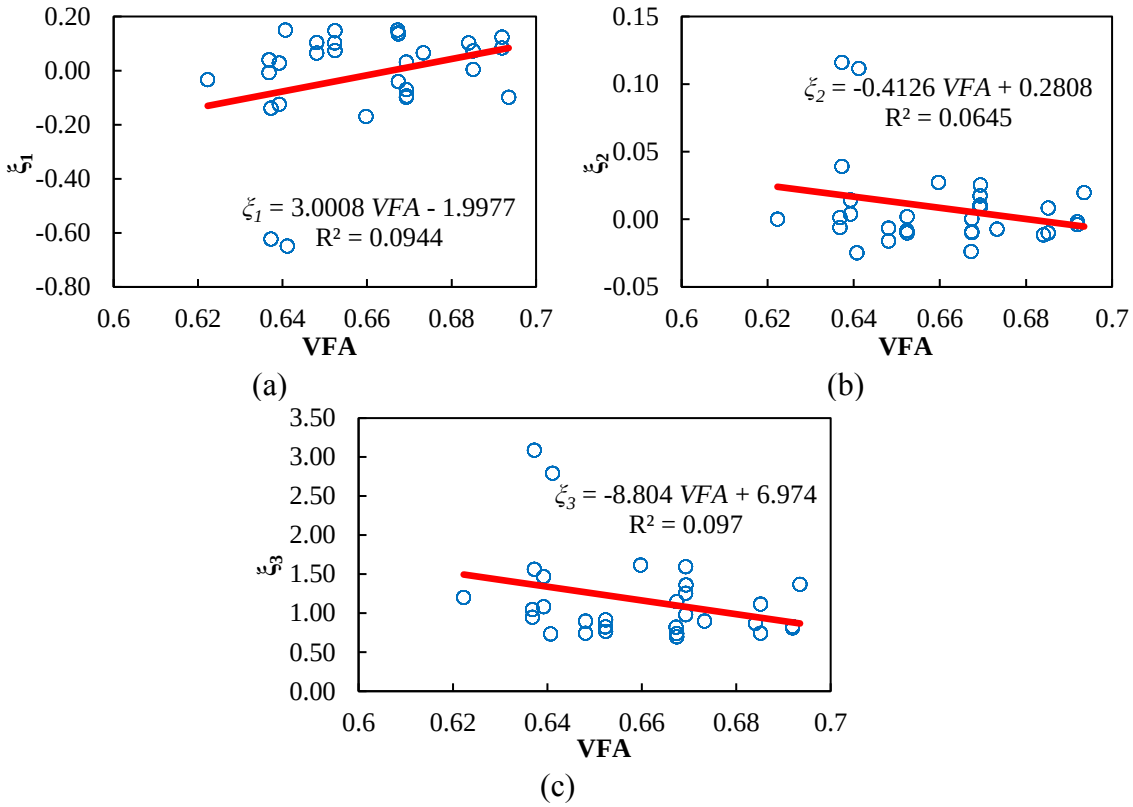

Figure 8.14 Parameters ξ_1, ξ_2, and ξ_3 versus *VFA* plots.

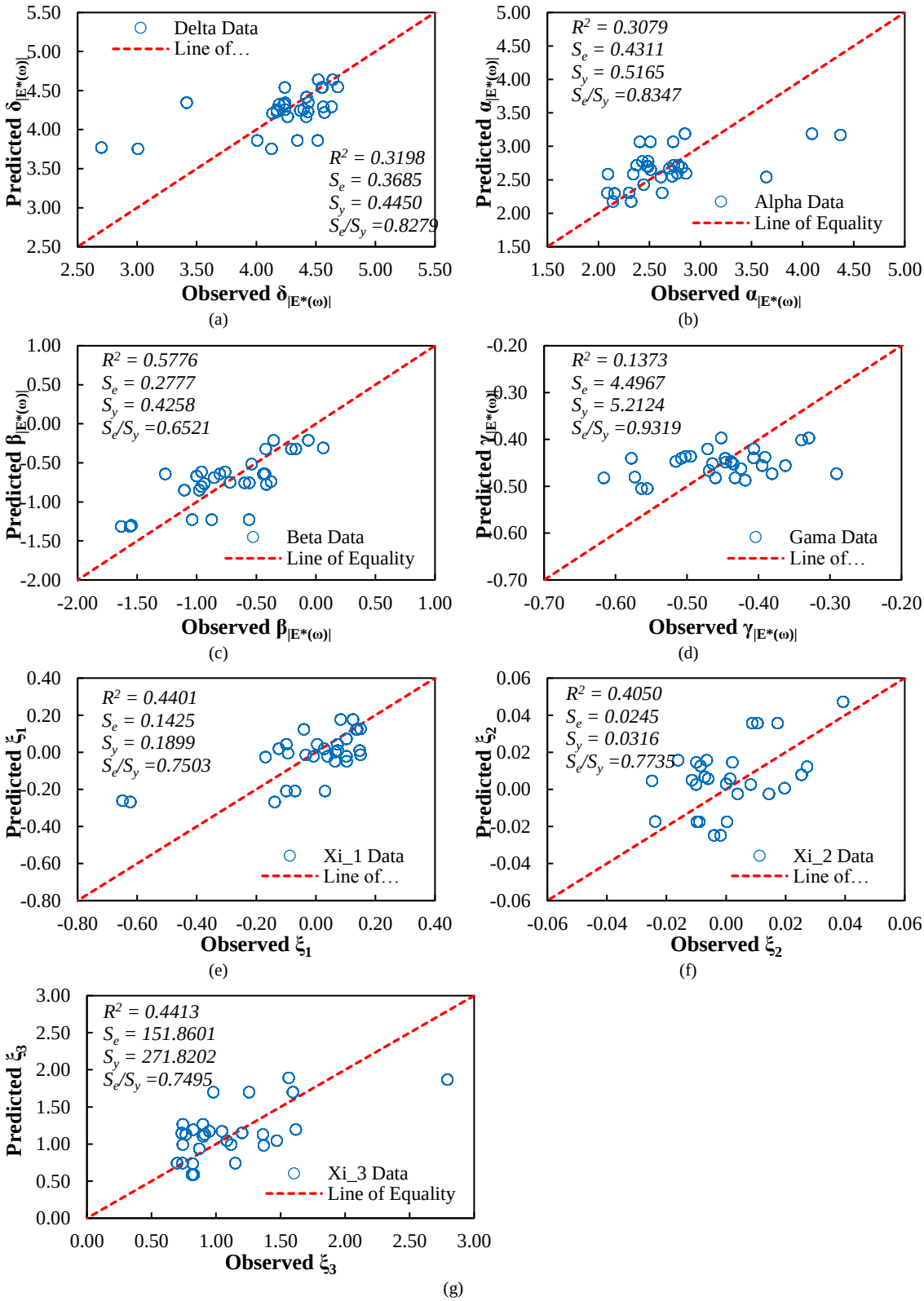

Figure 8.15 Predicted versus observed model parameters.

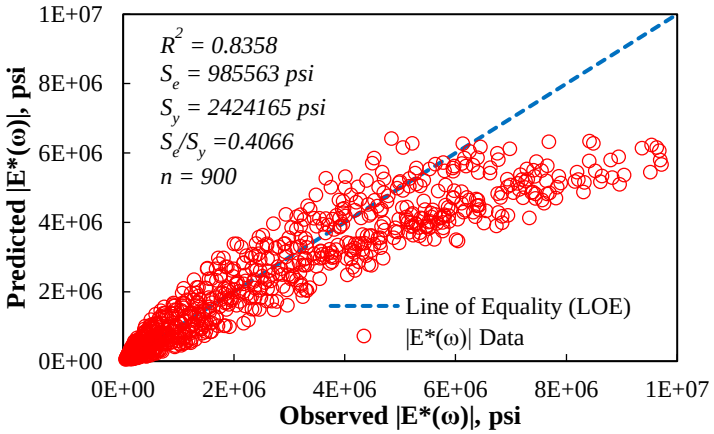

(a) Predicted versus observed $|E^*(\omega)|$

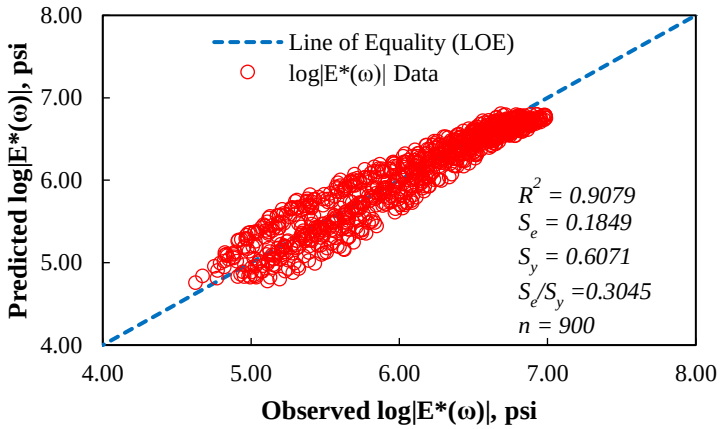

(b) Predicted versus observed log $|E^*(\omega)|$

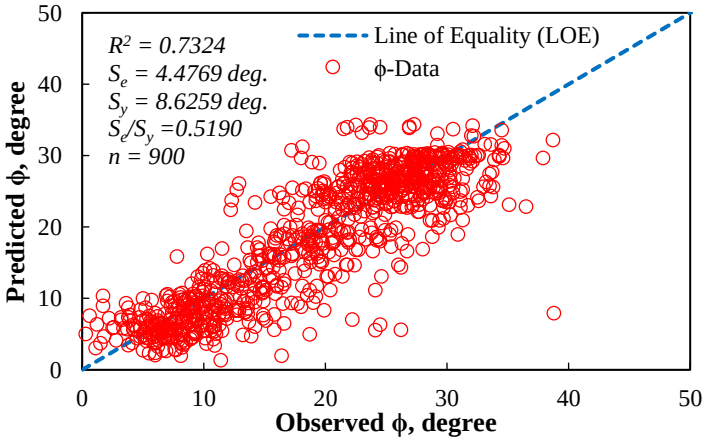

(c) Predicted versus observed ϕ

Figure 8.16 (a) Predicted $|E^*(\omega)|$ versus observed $|E^*(\omega)|$, (b) predicted log $|E^*(\omega)|$ versus observed log $|E^*(\omega)|$, and (c) predicted ϕ versus observed ϕ plot.

Chapter 9

Artificial Neural Network Based Modeling of Dynamic Modulus

9.1 Background

Past studies regarding ANN-based |E^*| predictive model used the |E^*| databased which is available to the researchers from NCHRP Report 547, fully or partially. This database contains dynamic modulus data of the AC mixtures designed based on previous mix design approach (starting from the year 1975 to 2002) other than the recent Superpave mix design approach. Therefore, it is logical to assume that the NCHRPT Report 547 database may be obsolete considering the recent approach of Superpave design. Also, any of ANN-based studies did not attempt to develop a phase angle predictive model which is important for advanced analysis of pavements. With the |E^*| of asphalt concrete, the phase angle (ϕ) is important to determine storage or loss modulus of asphalt concrete. Loss modulus is an indicator of permanent deformation of asphalt concrete, whereas, the storage modulus is used to estimate the relaxation modulus or creep compliance of asphalt concrete, which may be required for advanced analysis of pavement such as application of finite element method for pavement analysis (Ahmed et al. 2016). Therefore, this study is the first time which actually conducted laboratory |E^*| and ϕ testing on Superpave samples and after that used the test data to develop a ANN-based predictive model which can predict both the |E^*| and ϕ of asphalt concrete for the identical input conditions.

9.2 Objective

The objective of this study is to develop an alternative, more accurate, ANN-based $|E^*|$ and ϕ predictive models for the AC mixtures typically used in New Mexico. The model should be capable of reflecting changes in $|E^*|$ and ϕ of AC as a function of aggregate gradation parameters, mixture volumetrics, binder viscosity, temperature and loading frequency.

9.3 Neural Network Approach for Modeling

Application of neural networks (NN) has grown rapidly in the past several decades in different executive sectors and field of studies. The most common topic of these attempts is the modeling of complex systems to understand and simulate its behavior. A model that can transform a set of inputs to a set of output for a complex system is always appreciated in terms of cost and study-time. Such a model can be obtained by training an artificial neural network, in which, the network is repeatedly presented with input/output pairs which have to be correlated to understand the system. Generally, a neural network model is developed from an available dataset. The dataset is believed to be containing a number of interesting relationships, feature correlations, and other information that cannot be deduced in a straightforward manner from the first principles, theoretical knowledge, or even with numerical methods.

ANN-based approaches have several advantages over the conventional approaches based on principles, which include the self-learning capacity and the ability to model complex systems without the necessity of detailed understanding of the underlying phenomena (Haykin 1999, Bose and Liang 1996, Hagan et al. 1996). An ANN is a relatively complex computational model inspired by the biological recognizing process,

formed from a number of artificial neurons (or processing elements), connected with synapses like connections known as weights, constituting the neural structure. Each neuron has weighted inputs, a transfer function, and outputs. The network development consists of three stages. The first one is the selection of data and choosing their variables that are to be used as input to the network. The second stage is the design of the network and implementation of algorithms. The third and final stage is the evaluation of the predictability of the model. Figure 9.1 shows the schematic of a simple neuron. The input to the neuron *i* multiplied by its weight *w* and summed with the bias value *b* goes to the transfer function *f*. The output of the neuron is calculated as,

$$O = f\ (w.i + b). \tag{9.1}$$

One of the vast application of neural network is the data modeling. When neural networks are used for data analysis, it is important to distinguish between artificial neural network models and neural network algorithms. The neural network models are the arrangement of the network elements, whereas, ANN algorithms are computations that eventually produce the network outputs. The structure of a neural network (also called neural architecture) depends on its application. A neural architecture can be considered ready to be trained when the network is structured according to its application.

The ANN architecture chosen in this study for predicting $|E^*|$ and ϕ of AC is a supervised, multilayered, feedforward-backpropagation network. The basis of supervised learning in ANN is that it takes numerical input (the training data) and transform it into the desired output. A feedforward neural network is an artificial neural network in which

connections (weights) between the units do not form a cycle. The feedforward neural network is the first and simplest type of artificial neural network devised. In this network, the information moves only in forward direction, from the input nodes, through the hidden nodes (if any) and to the output nodes. There are no loops in the network. Mathematically, feed-forward neural network is a computational graph whose nodes are computing units and whose directed edges transmit numerical information from one node to another node. Each computing unit is capable of evaluating a single primitive function of its input. The network as a whole represents a chain of functions which transform the input vector to an output vector (called a pattern). The network is a particular implementation of a composite function from input to output space, which we call the network function. The learning problem consists of finding the optimal combination of weights so that the network function approximates a given function as closely as possible. However, we are not given the function explicitly but only implicitly through some examples. Lastly, the feedforward-backpropagation artificial neural networks are multilayer feedforward networks with an essential capability to propagate the error in its output, defined by the difference between the output and the desired output, backward to update network function. These feedforward networks generally use an error backpropagation (EBP) algorithm to update its weights in order to minimize error between the actual and desired output. With given input vectors and targets (desired output), such network can approximate a function or classify input vectors in an appropriate way, as defined by the user. A typical feedforward neural network with backpropagation rule or algorithm has three layers, called as the input, the hidden, and the output layers, respectively. The neurons in the input layer receive input data from a data file and the neurons in the output layer provide the ANN's response to the

input data. The neurons in the hidden layer communicate only with other neurons in the network. These are the parts of the large internal pattern that determines a solution to the problem. As the information passed from one processing element to another, is continued within a set of weights, some of the interconnections are strengthened and some are weakened, so that, a more accurate answer can be generated by the network function. The activation of the neurons, defined as the sum of the weighted input signals, is transformed with a transfer function which is used to get to the output level. Several functions can be used as the transfer function in each neuron for this purpose, but the sigmoid function is most often applied. To train the network using the backpropagation algorithm, the differences between the ANN output and its desired value are calculated after each iteration. The changes in the weights can then be made. The goal of training a network is to change the weights between the layers in a direction that minimizes the error. In backpropagation learning, the error in prediction is fed backward through the network to adjust the weights and minimize the error, preventing the same error happening again. The process is continued with multiple training sets until the error is minimized across many sets.

9.4 ANN for Predicting Dynamic Modulus and Phase Angle of Asphalt Concrete

9.4.1 Network Architecture

A typical four-layered, i.e. one input, two hidden, and one output layer, and feedforward error back propagation ANN architecture was used in this study for $|E^*|$ and ϕ prediction model. Figure 9.2 shows the supervised feedforward ANN with a backpropagation learning rule used in this study. The number of the neurons in the hidden layer influences the number

of connections. During the training phase, inputs are adjusted (transformed) by the connection weights. Therefore, the number of connections has a significant effect on the network performance and should be optimized. Too few hidden neurons hinder the learning process and too many depress the process's abilities through overtraining. When the ANN is trained to a satisfactory level, the weighted links between the units are saved. These weights are then used as an analytical tool to predict results for a new set of input data. This is a prediction phase when the network works only by forward propagation of data and there is no backward propagation of error. The output of a forward propagation is then considered as results predicted by the model.

9.4.2 Activation Function

In general, the backpropagation algorithms look for the minimum of the error function in weight space using the method of gradient descent. The overall weight vector which minimizes the error function is considered to be a solution of the learning problem. This method requires computation of the gradient of the error function at each iteration step. Therefore, one need to make sure that the error function is continuous and differentiable. This can be ensured by choosing a differentiable activation function so that the composite function produced by interconnected neurons is continuous and thus the error function is also continuous. There are several activation functions available to be known. One of the most popular activation functions for backpropagation networks is the sigmoid function, a real function $s_c = \mathbf{IR} \rightarrow (0,1)$ can be defined as

$$s_c(x) = \frac{1}{1+e^{-cx}}. \tag{9.2}$$

The constant c ban be selected arbitrarily and its reciprocal $1/c$ is called the temperature parameter in stochastic neural networks. The shape of the sigmoid changes with the value of c. Figure 9.3 shows the shape of the sigmoid function for $c = 1$, $c = 2$, and $c = 3$. As the value of c increases, the shape of the sigmoid function gradually takes the shape of a step function. At $c \to \infty$ the sigmoid converges to a step function at the origin. The derivative of the sigmoid with respect to x, when $c = 1$ is then

$$\frac{d}{dx} s_1(x) = \frac{e^{-x}}{\left(1+e^{-x}\right)^2} = s_1(x)\left\{1 - s_1(x)\right\}. \tag{9.3}$$

Equation 9.3 is a function of the sigmoid itself and therefore vary handy to use as an activation function.

The symmetrical sigmoid $S_c(x)$ is an alternative to the sigmoid function which can be defined as,

$$S_c(x) = \frac{2}{1+e^{-cx}} - 1 = \frac{1-e^{-cx}}{1+e^{-cx}}. \tag{9.4}$$

when c = 1,

$$S_1(x) = \frac{2}{1+e^{-x}} - 1 = \frac{1-e^{-x}}{1+e^{-x}} = \boldsymbol{tanh}\left(\frac{x}{2}\right) \tag{9.5}$$

This is nothing but the hyperbolic tangent for the argument $x/2$. For simplifying purpose, the hyperbolic tangent for the argument x, the c value is often taken to be $c = 2$, for which the symmetrical sigmoid function becomes

$$S_2(x) = \frac{2}{1+e^{-2x}} - 1 = \frac{1-e^{-2x}}{1+e^{-2x}} = \boldsymbol{tanh}(x). \tag{9.6}$$

Equation 9.6 is used as the activation functions for all the neurons in the neural network used in this study. Figure 9.4 shows the shapes of the symmetrical sigmoid function for *c* = 1, *c* = 2, and *c* = 3. In this case, also the shape of the symmetrical sigmoid function gradually takes the shape of a step function as the value of *c* increases. The derivative of the symmetric sigmoid function in Equation 9.6 is then

$$\frac{d}{dx} S_2(x) = \frac{d}{dx}\left(\frac{2}{1+e^{-2x}} - 1\right) = \frac{d}{dx}\left(\frac{1-e^{-2x}}{1+e^{-2x}}\right) = \frac{d}{dx}\boldsymbol{tanh}(x) = 1 - \{S_2(x)\}^2. \tag{9.7}$$

Equation 9.7 is also a function of the symmetrical sigmoid itself.

Many other activation functions have been proposed in literature. A differentiable activation function makes the function computed by a neural network differentiable, since the network itself computes only function compositions. The error function also becomes differentiable. It is important that the error function not to be completely flat in any region as the gradient direction is followed to find the minimum. The sigmoid function always has a positive derivative, for which, the slope of the error function provides a greater or lesser descent direction. Both extreme values for sigmoid or symmetrical sigmoid activation functions can only be reached asymptotically. The computing units evaluate the activation function using the net amount of excitation. The only problem is that, the local minima appear in the error function under some circumstances, and, therefore, require attention of the modeler as training process progresses.

9.4.3 Backpropagation Algorithm

The backpropagation algorithm used in this study for updating the neuron weights in the ANN model is the Levenberg-Marquardt algorithm (Levenberg 1944, Marquardt 1963). It provides a numerical solution to the problem of minimizing non-linear error function. The algorithm itself is fast and has a stable convergence. It is suitable for training small to medium-sized problems. Many other methods have already been developed for neural-networks training. The steepest descent algorithm, also known as the error backpropagation algorithm (EBP) (Rumelhart 1986, Werbos 1988) could be regarded as one of the most significant breakthroughs for neural network training. Many improvements have been made to EBP (Wilamowski and Torvik 1993, Andersen and Wilamowski 1995, Wilamowski 1996, Wilamowski and Jaeger 1996, Wilamowski et al. 1999). However, these improvements are relatively minor (Wilamowski 2002, Wilamowski et al. 2003, Yu and Wilamowski 2009, Wilamowski 2009, Wilamowski and Yu 2010). Although still widely used, the EBP algorithm in proved to be an inefficient algorithm because of its slow convergence. The two principal reasons for this are, firstly, its step sizes should be appropriate to the gradients. Especially, where the gradient is steeper small step sizes should be taken to avoid rattle out of the minima. As the step size is constant and required to be small, the training processes would be very slow where the gradient is mild. Secondly, the curvature of the error surface may not be the same in all directions, therefore the classic "error valley" problem (Osborne 1992) may exist and may result in slow convergence. The slow convergence of steepest decent method can be greatly improved by the Gauss–Newton algorithm. Using second-order derivatives of error function to "naturally" evaluate

the curvature of error surface, the Gauss–Newton algorithm can find proper step sizes for each direction and converge very fast; especially, if the error function has a quadratic surface, it can converge directly in the first iteration. But this improvement only happens when the quadratic approximation of error function is reasonable. Otherwise, the Gauss–Newton algorithm would be mostly divergent.

The Levenberg–Marquardt algorithm merges the steepest descent method and the Gauss–Newton algorithm. Fortunately, it inherits the speed advantage of the Gauss–Newton algorithm and the stability of the steepest descent method. It's more robust than the Gauss–Newton algorithm, because in many cases it can converge well even if the error surface is much more complex than the quadratic situation. Although the Levenberg–Marquardt algorithm tends to be a bit slower than Gauss–Newton algorithm (in convergent situation), it converges much faster than the steepest descent method. The basic idea of the Levenberg–Marquardt algorithm is that it performs a combined training process: around the area with complex curvature, the Levenberg–Marquardt algorithm switches to the steepest descent algorithm, until the local curvature is proper to make a quadratic approximation; then it approximately becomes the Gauss–Newton algorithm, which can speed up the convergence significantly (Yu and Wilamowski 2011).

9.4.3.1 The Levenberg–Marquardt Algorithm

The derivation of the Levenberg–Marquardt algorithm will be presented in five parts: (1) steepest descent algorithm, (2) steepest descent algorithm with momentum term, (3) Newton's method, (4) Gauss–Newton's algorithm, and (5) Levenberg–Marquardt algorithm. Before the derivation, let us introduce some commonly used indices:

p is the index of patterns, from *1* to *P*, where *P* is the number of patterns.

m is the index of outputs, from *1* to *M*, where *M* is the number of outputs.

i and *j* are the indices of weights, from *1* to *N*, where *N* is the number of weights.

k is the index of iterations.

Let us consider a feed-forward network with *n* input and *m* output neurons. The network can be consisted of any number of hidden neurons with any feedforward connection pattern. The training set, $A = \{(\boldsymbol{x}_1, \boldsymbol{d}_1), (\boldsymbol{x}_2, \boldsymbol{d}_2), ..., (\boldsymbol{x}_p, \boldsymbol{d}_p)\}$ consists of *p* ordered pairs of *n*- and *m*-dimensional vectors, which are called the input and output patterns. Let the primitive functions or activation functions at nodes are continuous and differentiable. The initial weights are real numbers and selected at random. When the input pattern is presented to this network, it produces an output different from the target. We want is to make the output and the target identical by using a learning algorithm. The error function for all training patterns and network outputs can be defined as

$$E(\boldsymbol{x},\boldsymbol{w}) = \frac{1}{2}\sum_{p=1}^{P}\sum_{m=1}^{M}\boldsymbol{e}_{p,m}^{\ 2} \tag{9.8}$$

where, $\boldsymbol{x}$ is the input vector, $\boldsymbol{w}$ is the weight vector, and $\boldsymbol{e}_{p,m}$ is the error at output *m* when applying pattern *p* and it is defined as

$$\boldsymbol{e}_{p,m} = \boldsymbol{d}_{p,m} - \boldsymbol{o}_{p,m} \tag{9.9}$$

where, $\boldsymbol{d}$ is the desired output vector, and $\boldsymbol{o}$ is the actual output vector.

Steepest Descent Algorithm

The steepest descent algorithm uses the first-order derivative of total error function to find the minima in error space. Normally, gradient g is defined as the first-order derivative of total error function (Equation 9.8):

$$\boldsymbol{g} = \frac{\partial E(\boldsymbol{x}, \boldsymbol{w})}{\partial \boldsymbol{w}} = \left[\frac{\partial E}{\partial w_1} \quad \frac{\partial E}{\partial w_2} \quad \cdots \quad \frac{\partial E}{\partial w_N} \right]^T . \tag{9.10}$$

Therefore, the update rule of the steepest descent algorithm can be written as

$$\boldsymbol{w}_{k+1} = \boldsymbol{w}_k - \alpha \, \boldsymbol{g}_k \tag{9.11}$$

where, α is the learning constant (step size). The training process of the steepest descent algorithm is asymptotic convergence. Therefore, all the elements of gradient vector would be very small around the solution and there would be a very tiny weight change.

Steepest Descent Algorithm with Momentum term

When the minimum of the error function for a given learning task, lies in a narrow "valley, i.e. the width of the minimum error surface is very narrow, wide oscillations of the search process by gradient decent can occur. The case can be best solved by orienting the search process towards the center of the valley. However, the error surface is such that the gradient does not point in this direction. A simple solution of this problem is to introduce a momentum term. The gradient of the error function is computed for each new combination of weights, but instead of just following the negative gradient direction a weighted average of the current gradient and the previous correction direction is computed at each step.

Theoretically, this approach should provide the search process with a kind of inertia and could help to avoid excessive oscillations in narrow valleys of the error function. As mentioned earlier, in case of standard backpropagation, the input-output patterns are fed into the network and the error function E is determined at the output. When using backpropagation with momentum the update rule can be written as

$$\boldsymbol{w}_{k+1} = \boldsymbol{w}_k - \alpha\, \boldsymbol{g}_k + \gamma \left[\boldsymbol{w}_k - \boldsymbol{w}_{k-1}\right] \tag{9.12}$$

or,

$$\Delta \boldsymbol{w}_{k+1} = -\alpha\, \boldsymbol{g}_k + \gamma \Delta \boldsymbol{w}_k \tag{9.13}$$

where, α and γ are the learning and momentum rate respectively. Therefore, if someone is interested in accelerating convergence to a minimum of the error function, this can be done by increasing the learning rate up to an optimal value. The momentum rate allows the attenuation of oscillations in the iteration process. These learning parameters are normally selected by trial and error or even by some kind of random search to obtain the best possible convergence.

Newton's Method

The assumption in Newton's method is that all the gradient components $g_1, g_2, \ldots, g_N$ are functions of the weights and all weights are linearly independent:

$$\begin{cases} g_1 = F_1(w_1, w_2, \cdots w_N) \\ g_2 = F_2(w_1, w_2, \cdots w_N) \\ \\ g_N = F_N(w_1, w_2, \cdots w_N) \end{cases} \tag{9.14}$$

where F_1, F_2, …, F_N are the nonlinear relationships between weights and related gradient components. Unfolding each g_i (i = 1, 2, …, N) in Equations 9.14 by Taylor series and taking the first-order approximation:

$$\begin{cases} g_1 \approx g_{1,0} + \dfrac{\partial g_1}{\partial w_1}\Delta w_1 + \dfrac{\partial g_1}{\partial w_2}\Delta w_2 + \cdots + \dfrac{\partial g_1}{\partial w_N}\Delta w_N \\ g_2 \approx g_{2,0} + \dfrac{\partial g_2}{\partial w_1}\Delta w_1 + \dfrac{\partial g_2}{\partial w_2}\Delta w_2 + \cdots + \dfrac{\partial g_2}{\partial w_N}\Delta w_N \\ \\ g_N \approx g_{N,0} + \dfrac{\partial g_N}{\partial w_1}\Delta w_1 + \dfrac{\partial g_N}{\partial w_2}\Delta w_2 + \cdots + \dfrac{\partial g_N}{\partial w_N}\Delta w_N \end{cases} \tag{9.15}$$

By the definition of gradient vector $\boldsymbol{g}$ in Equation 9.10, we obtain

$$\frac{\partial g_i}{\partial w_j} = \frac{\partial\left(\dfrac{\partial E}{\partial w_i}\right)}{\partial w_j} = \frac{\partial^2 E}{\partial w_i \partial w_j} \tag{9.16}$$

By inserting Equation 9.16 to Equation 9.15, we have

$$\begin{cases} g_1 \approx g_{1,0} + \dfrac{\partial^2 E}{\partial w_1^{\,2}}\Delta w_1 + \dfrac{\partial^2 E}{\partial w_1 \partial w_2}\Delta w_2 + \cdots + \dfrac{\partial^2 E}{\partial w_1 \partial w_N}\Delta w_N \\ g_2 \approx g_{2,0} + \dfrac{\partial^2 E}{\partial w_2 \partial w_1}\Delta w_1 + \dfrac{\partial^2 E}{\partial w_2^{\,2}}\Delta w_2 + \cdots + \dfrac{\partial^2 E}{\partial w_2 \partial w_N}\Delta w_N \\ \\ g_N \approx g_{N,0} + \dfrac{\partial^2 E}{\partial w_N \partial w_1}\Delta w_1 + \dfrac{\partial^2 E}{\partial w_N \partial w_2}\Delta w_2 + \cdots + \dfrac{\partial^2 E}{\partial w_N^{\,2}}\Delta w_N \end{cases} \tag{9.17}$$

Comparing with the steepest descent method, the second-order derivatives of the total error function need to be calculated for each component of gradient vector.

In order to get the minima of total error function E, each element of the gradient vector should be zero. Therefore, left sides of the Equations 9.17 are all zero, therefore

$$\begin{cases} 0 \approx g_{1,0} + \dfrac{\partial^2 E}{\partial w_1^{\,2}} \Delta w_1 + \dfrac{\partial^2 E}{\partial w_1 \partial w_2} \Delta w_2 + \cdots + \dfrac{\partial^2 E}{\partial w_1 \partial w_N} \Delta w_N \\ 0 \approx g_{2,0} + \dfrac{\partial^2 E}{\partial w_2 \partial w_1} \Delta w_1 + \dfrac{\partial^2 E}{\partial w_2^{\,2}} \Delta w_2 + \cdots + \dfrac{\partial^2 E}{\partial w_2 \partial w_N} \Delta w_N \\ 0 \approx g_{N,0} + \dfrac{\partial^2 E}{\partial w_N \partial w_1} \Delta w_1 + \dfrac{\partial^2 E}{\partial w_N \partial w_2} \Delta w_2 + \cdots + \dfrac{\partial^2 E}{\partial w_N^{\,2}} \Delta w_N \end{cases} \tag{9.18}$$

By combining Equation 9.10 with Equation 9.18

$$\begin{cases} -\dfrac{\partial E}{\partial w_1} = -g_{1,0} \approx \dfrac{\partial^2 E}{\partial w_1^{\,2}} \Delta w_1 + \dfrac{\partial^2 E}{\partial w_1 \partial w_2} \Delta w_2 + \cdots + \dfrac{\partial^2 E}{\partial w_1 \partial w_N} \Delta w_N \\ -\dfrac{\partial E}{\partial w_2} = -g_{2,0} \approx \dfrac{\partial^2 E}{\partial w_2 \partial w_1} \Delta w_1 + \dfrac{\partial^2 E}{\partial w_2^{\,2}} \Delta w_2 + \cdots + \dfrac{\partial^2 E}{\partial w_2 \partial w_N} \Delta w_N \\ -\dfrac{\partial E}{\partial w_N} = -g_{N,0} \approx \dfrac{\partial^2 E}{\partial w_N \partial w_1} \Delta w_1 + \dfrac{\partial^2 E}{\partial w_N \partial w_2} \Delta w_2 + \cdots + \dfrac{\partial^2 E}{\partial w_N^{\,2}} \Delta w_N \end{cases} \tag{9.19}$$

There are N equations for N parameters so that all Δw_i can be calculated. With the solutions, the weight space can be updated iteratively. Equations 9.19 can also be written in matrix form as

$$\begin{bmatrix} -g_1 \\ -g_2 \\ \\ -g_N \end{bmatrix} = \begin{bmatrix} -\dfrac{\partial E}{\partial w_1} \\ -\dfrac{\partial E}{\partial w_2} \\ \\ -\dfrac{\partial E}{\partial w_N} \end{bmatrix} = \begin{bmatrix} \dfrac{\partial^2 E}{\partial w_1^{\,2}} & \dfrac{\partial^2 E}{\partial w_1 \partial w_2} & \cdots & \dfrac{\partial^2 E}{\partial w_1 \partial w_N} \\ \dfrac{\partial^2 E}{\partial w_2 \partial w_1} & \dfrac{\partial^2 E}{\partial w_2^{\,2}} & \cdots & \dfrac{\partial^2 E}{\partial w_2 \partial w_N} \\ \cdots & \cdots & \cdots & \cdots \\ \dfrac{\partial^2 E}{\partial w_N \partial w_1} & \dfrac{\partial^2 E}{\partial w_N \partial w_2} & \cdots & \dfrac{\partial^2 E}{\partial w_N^{\,2}} \end{bmatrix} \times \begin{bmatrix} \Delta w_1 \\ \Delta w_2 \\ \\ \Delta w_N \end{bmatrix}$$

(9.20)

where the square matrix is Hessian matrix:

$$\boldsymbol{H} = \begin{bmatrix} \dfrac{\partial^2 E}{\partial w_1^{\,2}} & \dfrac{\partial^2 E}{\partial w_1 \partial w_2} & \cdots & \dfrac{\partial^2 E}{\partial w_1 \partial w_N} \\ \dfrac{\partial^2 E}{\partial w_2 \partial w_1} & \dfrac{\partial^2 E}{\partial w_2^{\,2}} & \cdots & \dfrac{\partial^2 E}{\partial w_2 \partial w_N} \\ \cdots & \cdots & \cdots & \cdots \\ \dfrac{\partial^2 E}{\partial w_N \partial w_1} & \dfrac{\partial^2 E}{\partial w_N \partial w_2} & \cdots & \dfrac{\partial^2 E}{\partial w_N^{\,2}} \end{bmatrix} \tag{9.21}$$

By combining Equations 9.10 and 9.21 with Equation 9.20, we have

$$-\boldsymbol{g} = \boldsymbol{H}\Delta\boldsymbol{w}\,. \tag{9.22}$$

Or,

$$\Delta\boldsymbol{w} = -\boldsymbol{H}^{-1}\boldsymbol{g}\,. \tag{9.23}$$

Therefore, the update rule for Newton's method can be given as

$$\boldsymbol{w}_{k+1} = \boldsymbol{w}_k - \boldsymbol{H}_k^{\,-1}\boldsymbol{g}_k \tag{9.24}$$

As the second-order derivatives of total error function, Hessian matrix $\boldsymbol{H}$ gives the proper evaluation on the change of gradient vector. By comparing Equations 9.12 and 9.24, one may notice that well-matched step sizes are given by the inverted Hessian matrix.

Gauss-Newton Algorithm

In order to get Hessian matrix, $\boldsymbol{H}$, Newton's method the second-order derivatives of total error function have to be calculated and it could be very complicated. In order to simplify the calculation process, Jacobian matrix $\boldsymbol{J}$ is introduced as

$$\boldsymbol{J} = \begin{bmatrix} \frac{\partial e_{1,1}}{\partial w_1} & \frac{\partial e_{1,1}}{\partial w_2} & \cdots & \frac{\partial e_{1,1}}{\partial w_N} \\ \frac{\partial e_{1,2}}{\partial w_1} & \frac{\partial e_{1,2}}{\partial w_2} & \cdots & \frac{\partial e_{1,2}}{\partial w_N} \\ \cdots & \cdots & \cdots & \cdots \\ \frac{\partial e_{1,M}}{\partial w_1} & \frac{\partial e_{1,M}}{\partial w_2} & \cdots & \frac{\partial e_{1,M}}{\partial w_N} \\ \cdots & \cdots & \cdots & \cdots \\ \frac{\partial e_{P,1}}{\partial w_1} & \frac{\partial e_{P,1}}{\partial w_2} & \cdots & \frac{\partial e_{P,1}}{\partial w_N} \\ \frac{\partial e_{P,2}}{\partial w_1} & \frac{\partial e_{P,2}}{\partial w_2} & \cdots & \frac{\partial e_{P,2}}{\partial w_N} \\ \cdots & \cdots & \cdots & \cdots \\ \frac{\partial e_{P,M}}{\partial w_1} & \frac{\partial e_{P,M}}{\partial w_2} & \cdots & \frac{\partial e_{P,M}}{\partial w_N} \end{bmatrix} \tag{9.25}$$

By integrating Equations 9.8 and 9.10, the elements of gradient vector can be calculated as

$$g_i = \frac{\partial E}{\partial w_i} = \frac{\partial\left(\frac{1}{2}\sum_{p=1}^{P}\sum_{m=1}^{M} e_{p,m}{}^2\right)}{\partial w_i} = \sum_{p=1}^{P}\sum_{m=1}^{M}\left(\frac{\partial e_{p,m}}{\partial w_i}\right) e_{p,m} \tag{9.26}$$

Combining Equations 9.25 and 9.26, the relationship between Jacobian matrix $\boldsymbol{J}$ and gradient vector **g** would be

$$\boldsymbol{g} = \boldsymbol{J}\boldsymbol{e} \tag{9.27}$$

where error vector $\boldsymbol{e}$ has the form

$$\boldsymbol{e} = \begin{bmatrix} e_{1,1} \\ e_{1,2} \\ \cdots \\ e_{1,M} \\ \cdots \\ e_{P,1} \\ e_{P,2} \\ \cdots \\ e_{P,M} \end{bmatrix} \tag{9.28}$$

Inserting Equation 9.8 into Equation 21, the element at *i*th row and *j*th column of Hessian matrix can be calculated as

$$h_{i,j} = \frac{\partial^2 E}{\partial w_i \partial w_j} = \frac{\partial^2 \left(\frac{1}{2} \sum_{p=1}^{P} \sum_{m=1}^{M} e_{p,m}{}^2 \right)}{\partial w_i \partial w_j} = \sum_{p=1}^{P} \sum_{m=1}^{M} \frac{\partial e_{p,m}}{\partial w_i} \frac{\partial e_{p,m}}{\partial w_j} + S_{i,j} \tag{9.29}$$

where $S_{i,j}$ is equal to

$$S_{i,j} = \sum_{p=1}^{P} \sum_{m=1}^{M} \frac{\partial^2 e_{p,m}}{\partial w_i \partial w_j} e_{p,m} \tag{9.30}$$

As the basic assumption of Newton's method is that $S_{i,j}$ is closed to zero (Hagan and Menhaj 1994), the relationship between Hessian matrix, $\boldsymbol{H}$ and Jacobian matrix $\boldsymbol{J}$ can be rewritten as

$$\boldsymbol{H} \approx \boldsymbol{J}^T \boldsymbol{J} \tag{9.31}$$

By combining Equations 9.24, 9.27, and 9.31, the update rule of the Gauss–Newton algorithm can be presented as

$$\boldsymbol{w}_{k+1} = \boldsymbol{w}_k - \left(\boldsymbol{J}_k{}^T \boldsymbol{J}_k\right)^{-1} \boldsymbol{J}_k \boldsymbol{e}_k \tag{9.32}$$

Obviously, the advantage of the Gauss–Newton algorithm over the standard Newton's method (Equation 9.24) is that the former does not require the calculation of second-order derivatives of the total error function, by introducing Jacobian matrix $\boldsymbol{J}$ instead. However, the Gauss–Newton algorithm still faces the same convergent problem, like the Newton algorithm for complex error space optimization. Mathematically, the problem can be interpreted as the matrix $\boldsymbol{J^T J}$ may not be invertible.

Levenberg-Marquardt Algorithm

In order to make sure that the approximated Hessian matrix $\boldsymbol{J^T J}$ is invertible, Levenberg–Marquardt algorithm introduces another approximation to Hessian matrix:

$$\boldsymbol{H} \approx \boldsymbol{J}^T \boldsymbol{J} + \mu \boldsymbol{I} \tag{9.33}$$

where μ is always positive, called combination coefficient, and $\boldsymbol{I}$ is the identity matrix. From Equation 9.33, one may notice that the elements on the main diagonal of the approximated Hessian matrix will be larger than zero. Therefore, with this approximation, it can be ensured that matrix $\boldsymbol{H}$ is always invertible. By combining Equations 9.32 and 9.33, the update rule of Levenberg–Marquardt algorithm can be presented as

$$\boldsymbol{w}_{k+1} = \boldsymbol{w}_k - \left(\boldsymbol{J}_k{}^T \boldsymbol{J}_k + \mu \boldsymbol{I}\right)^{-1} \boldsymbol{J}_k \boldsymbol{e}_k \tag{9.34}$$

As the combination of the steepest descent algorithm and the Gauss–Newton algorithm, the Levenberg–Marquardt algorithm switches between the two algorithms during the

training process. When the combination coefficient μ is very small (nearly zero), Equation 9.34 is approaching to Equation 9.32 and Gauss–Newton algorithm is used. When combination coefficient μ is very large, Equation 9.34 approximates to Equation 9.11 and the steepest descent method is used. If the combination coefficient μ in Equation 9.34 is very big, it can be interpreted as the learning coefficient in the steepest descent method (Equation 9.11):

$$\alpha = \frac{1}{\mu} \tag{9.35}$$

Table 1 summarizes the update rules for various algorithms.

9.4.3.2 Implementation of Levenberg–Marquardt Algorithm

In order to implement the Levenberg–Marquardt algorithm for neural network training, two problems have to be solved: (1) calculation of Jacobian matrix, and (2) the training process design. The solution of these problem is described in the following sections.

Calculation of Jacobian Matrix

Different from the earlier section, in this section *j* and *k* are used as the indices of neurons, from 1 to *nn*, where *nn* is the number of neurons contained in a topology; *i* is the index of neuron inputs, from 1 to *ni*, where *ni* is the number of inputs and it may vary for different neurons. As an introduction of basic concepts of neural network training, let us consider a neuron *j* with *ni* inputs, as shown in Figure 9.5. If neuron *j* is in the first layer, all its inputs would be connected to the inputs of the network, otherwise, its inputs can be connected to outputs of other neurons or to networks inputs if connections across layers are allowed.

Node y is an important and flexible concept. It can be $y_{j,i}$, meaning the ith input of neuron j. It also can be used as y_j to define the output of neuron j. In the following derivation, if node y has one index then it is used as a neuron output node, but if it has two indices (neuron and input), it is a neuron input node. The output node of neuron j is calculated using

$$y_j = f_j\left(net_j\right) \tag{9.36}$$

where f_j is the activation function of neuron j and net value net_j is the sum of weighted input nodes of neuron j:

$$net_j = \sum_{i=1}^{ni} w_{j,i} y_{j,i} + w_{j,0} \tag{9.37}$$

where $y_{j,i}$ is the ith input node of neuron j, weighted by $w_{j,i}$, and $w_{j,0}$ is the bias weight of neuron j. Using Equation 9.37, one may notice that derivative of net_j is

$$\frac{\partial net_j}{\partial w_{j,i}} = y_{j,i} \tag{9.38}$$

and slope s_j of the activation function f_j is

$$s_j = \frac{\partial y_j}{\partial net_j} = \frac{\partial f_j\left(net_j\right)}{\partial net_j} \tag{9.39}$$

Between the output node y_j of a hidden neuron j and network output o_m, there is a complex nonlinear relationship (Figure 9.5):

$$o_m = F_{m,j}\left(y_j\right) \tag{9.40}$$

where o_m is the m^{th} output of the network. The complexity of this nonlinear function $F_{mj}(y_j)$ depends on how many other neurons are between neuron j and network output m. If neuron j is at network output m, then $o_m = y_j$ and $F_{mj}'(y_j) = 1$, where F_{mj}' is the derivative of nonlinear relationship between neuron j and output m. The elements of Jacobian matrix in Equation 9.25 can be calculated as

$$\frac{\partial e_{p,m}}{\partial w_{j,i}} = \frac{\partial\left(d_{p,m} - o_{p,m}\right)}{\partial w_{j,i}} = -\frac{\partial o_{p,m}}{\partial w_{j,i}} = -\frac{\partial o_{p,m}}{\partial y_j}\frac{\partial y_j}{\partial net_j}\frac{\partial net_j}{\partial w_{j,i}} \tag{9.41}$$

Combining with Equations 9.37, 9.38, and 9.39, Equation 9.41 can be rewritten as

$$\frac{\partial e_{p,m}}{\partial w_{j,i}} = -F_{mj}{}' s_j y_{j,i} \tag{9.42}$$

where F_{mj}' is the derivative of nonlinear function between neuron j and output m.

The computation process for Jacobian matrix can be organized according to the traditional backpropagation computation in first-order algorithms (like the EBP algorithm). But there are also differences between them. First of all, for every pattern, in the EBP algorithm, only one backpropagation process is needed, while in the Levenberg–Marquardt algorithm the backpropagation process has to be repeated for every output separately in order to obtain consecutive rows of the Jacobian matrix (Equation 9.25). Another

difference is that the concept of backpropagation of δ parameter (Nielsen 1989) has to be modified. In the EBP algorithm, output errors are parts of the δ parameter:

$$\delta_j = s_j \sum_{m=1}^{M} F_{mj}' e_m \tag{9.43}$$

In the Levenberg–Marquardt algorithm, the δ parameters are calculated for each neuron j and each output m, separately. Also, in the backpropagation process, the error is replaced by a unit value (Hagan and Menhaj 1994):

$$\delta_{m,j} = s_j F_{mj}' \tag{9.44}$$

By combining Equations 9.42 and 9.44, elements of the Jacobian matrix can be calculated by

$$\frac{\partial e_{p,m}}{\partial w_{j,i}} = -\delta_{m,j} y_{j,i} \tag{9.45}$$

There are two unknowns in Equation 9.45 for the Jacobian matrix computation. The input node, $y_{j,i}$, can be calculated in the forward computation (signal propagating from inputs to outputs); while $\delta_{m,j}$ is obtained in the backward computation, which is organized as errors backpropagating from output neurons (output layer) to network inputs (input layer). At output neuron m ($j = m$), $\delta_{m,j} = s_m$. For better interpretation of forward computation and backward computation, let us consider the three-layer multilayer perceptron network (Figure 9.6) as an example. For a given pattern, the forward computation can be organized in the following steps:

a. Calculate net values, slopes, and outputs for all neurons in the first layer:

$$net_j^1 = \sum_{i=1}^{ni} I_i w_{j,i}^1 + w_{j,0}^1 \tag{9.46}$$

$$y_j^1 = f_j^1\left(net_j^1\right) \tag{9.47}$$

$$s_j^1 = \frac{\partial f_j^1}{\partial net_j^1} \tag{9.48}$$

where I_i are the network inputs; the superscript "1" means the first layer, j is the index of neurons in the first layer.

b. Use the outputs of the first layer neurons as the inputs of all neurons in the second layer, do a similar calculation for net values, slopes, and outputs.

$$net_j^2 = \sum_{i=1}^{n1} y_i^1 w_{j,i}^2 + w_{j,0}^2 \tag{9.49}$$

$$y_j^2 = f_j^2\left(net_j^2\right) \tag{9.50}$$

$$s_j^2 = \frac{\partial f_j^2}{\partial net_j^2} \tag{9.51}$$

c. Use the outputs of the second layer neurons as the inputs of all neurons in the output layer (third layer), do a similar calculation for net values, slopes, and outputs.

$$net_j^3 = \sum_{i=1}^{n2} y_i^2 w_{j,i}^3 + w_{j,0}^3 \tag{9.52}$$

$$o_j = f_j^3\left(net_j^3\right) \tag{9.53}$$

$$s_j^3 = \frac{\partial f_j^3}{\partial net_j^3} \tag{9.54}$$

After the forward calculation, node array ***y*** and slope array ***s*** can be obtained for all neurons with the given pattern. With the results from the forward computation, for a given output *j*, the backward computation can be organized as -

d. Calculate error at the output *j* and initial δ as the slope of output *j*.

$$e_j = d_j - o_j \tag{9.55}$$

$$\delta_{j,j}^3 = s_j^3 \tag{9.56}$$

$$\delta_{j,k}^3 = 0 \tag{9.57}$$

where d_j is the desired output at output *j*, o_j is the actual output at output *j* obtained in the forward computation, $\delta_{j,j}^3$ is the self-backpropagation, $\delta_{j,k}^3$ is the backpropagation from other neurons in the same layer (output layer).

e. Backpropagate δ from the inputs of the third layer to the outputs of the second layer.

$$\delta_{j,k}^{2} = w_{j,k}^{3}\delta_{j,j}^{3} \tag{9.58}$$

where k is the index of neurons in the second layer, from 1 to n_2.

f. Backpropagate δ from the outputs of the second layer to the inputs of the second layer.

$$\delta_{j,k}^{2} = \delta_{j,k}^{2} s_{k}^{2} \tag{9.59}$$

where k is the index of neurons in the second layer, from 1 to n_2.

g. Backpropagate δ from the inputs of the second layer to the outputs of the first layer.

$$\delta_{j,k}^{1} = \sum_{i=1}^{n_2} w_{j,i}^{2}\delta_{j,i}^{2} \tag{9.60}$$

where k is the index of neurons in the first layer, from 1 to n_1.

h. Backpropagate δ from the outputs of the first layer to the inputs of the first layer.

$$\delta_{j,k}^{1} = \delta_{j,k}^{1} s_{k}^{1} \tag{9.61}$$

where k is the index of neurons in the second layer, from 1 to n_1.

For the backpropagation process of other outputs, the steps (d) – (h) are repeated. By performing the forward computation and backward computation, the whole **δ** array and y array can be obtained for the given pattern. Then related row elements (no rows) of

Jacobian matrix can be calculated by using Equation 9.45. For other patterns, by repeating the forward and backward computation, the whole Jacobian matrix can be calculated. The pseudo code of the forward computation and backward computation for Jacobian matrix in the Levenberg–Marquardt algorithm is shown in Figure 9.7.

Training Process Design

With the update rule of the Levenberg–Marquardt algorithm (Equation 9.34) and the computation of Jacobian matrix, the next step is to organize the training process. According to the update rule, if the error goes down, which means it is smaller than the last error, it implies that the quadratic approximation on total error function is working and the combination coefficient μ could be changed smaller to reduce the influence of gradient descent part (ready to speed up). On the other hand, if the error goes up, which means it's larger than the last error, it shows that it's necessary to follow the gradient more to look for a proper curvature for quadratic approximation and the combination coefficient μ is increased. Therefore, the training process using Levenberg–Marquardt algorithm could be designed as follows:

1. With the initial weights (randomly generated), evaluate the total error (SSE).

2. Do an update as directed by Equation 9.34 to adjust weights.

3. With the new weights, evaluate the total error.

4. If the current total error is increased as a result of the update, then retract the step (such as reset the weight vector to the precious value) and increase combination coefficient μ by a factor of 10 or by some other factors. Then go to step-ii and try an update again.

5. If the current total error is decreased as a result of the update, then accept the step (such as keep the new weight vector as the current one) and decrease the combination coefficient μ by a factor of 10 or by the same factor as step iv.

6. Go to step ii with the new weights until the current total error is smaller than the required value.

The flowchart of the above procedure is shown in Figure 9.8.

9.5 Preparation of ANN Database

The eight input variables of the nationally calibrated η-based Witczak predictive equation used while developing the ANN model. A total of 1620 test data was used. Table 9.2 shows the ranges of values for all input and output variables used in the ANN model. The overall dataset was divided randomly into two different subsets: the training data subset of 1500 data points and the testing data subset of 120 data points. Both datasets were normalized within the range of -1 to +1 for input and target values to satisfy the transfer function (symmetrical sigmoid) range and to prevent network saturation which is responsible for impeding the performance of the network. The training data subset was used to train the model, while the testing data subset was used to assess the accuracy and generalization of the developed ANN model. Consequently, the trained ANN model was also finally evaluated using all the 1620 data points to obtain the overall prediction accuracy.

9.6 Development of ANN Model

There are two major processes involved in developing prediction models using ANN. These are: the learning or the training processes, and the testing process. The initial connection weights and node biases were selected randomly at the beginning of training. The network was considered to be well trained when the error reaches a minimum. The network performance is verified by testing datasets unknown to the ANN the training process. A number of network architectures with one and two hidden layers were examined to determine the optimum number of hidden layers and number of nodes in each layer through a parametric study. Figures 9.9 and 9.10 presents the training and testing performances with increasing neuron number of 1-hidden layer and 2-hidden layers ANNs, respectively. For each network architecture, the model was repeatedly run for 20 times, with randomly selected training and testing datasets. In case of 1-hidden layer ANN (Figure 9.9), it can be observed that with a choice of 16 to 18 neurons, the minimum MSE (best performance) can be reached. However, beyond 18 neurons, the training and testing performances degrade and deviate, indicating lack of sufficient generalization of the model. In case of 2-hidden layers ANN (Figure 9.10), it can be observed that with a choice of 24 to 28 neurons, the minimum MSE (best performance) can be increased. However, beyond 18 neurons, the training and testing performances degrade and deviate, indicating lack of sufficient generalization of the model. Overall, the training and testing mean squared errors (MSE) decreased as the networks grew in size with increasing number of neurons in the hidden layers. Also, at a certain number of nodes the decrease in MSE becomes insignificant. The error levels for both the training and testing sets matched closely when

the number of hidden nodes approached 12 as in the case of 8-12-12-2 architecture (8 input neurons, 12 neurons in each of the hidden layers, and 2 output neurons, respectively). Figure 9.11 shows the training and testing MSE progress curves for the 8-12-12-2 network for 25,000 learning cycles or training epochs. The 8-12-12-2 architecture was chosen as the best architecture for the ANN model based on its lowest training and testing mean squared errors (MSE). Both the training and testing curves for the output are in the same order of magnitude, thus depicting proper training and generalization. The almost constant MSEs obtained for the last several thousand epochs also provided a good indication of adequate training for this network.

It should be noted that despite their superior performance, ANNs sometimes suffer from a number of shortcomings. For instance, ANNs sometimes cannot explain the results while data modeling. Again, the ANNs may seem to converge on some solution for any given training dataset. However, there is no assurance that this solution provides the best solution. Therefore, one need to check an ANN model with independent testing and validation datasets and assure that the achieved solution corresponds to the global minimum.

9.7 Formulation of the ANN Model

The basic form of the ANN model developed in this study can be given by the Equation 9.62 through 21. For these equations, it should be understood that, when a single index is used, it indicates an array; when dual indices are used they represent a matrix, with the first letter indicating the values in the row and the second letter indicating the values in the column. The index *i* represents the number of input parameters, the index *k* represents the

number of nodes in the first hidden layer, *j* subscript represents the number of nodes in the second hidden layer and the *o* subscript represents the number of nodes in the output layer.

$$f(T) = \frac{2}{1+e^{-2T}} - 1 \tag{9.62}$$

$$H_k^1 = B_k^1 + \sum_{i=1}^{M} W_{ik}^1 P_i \tag{9.63}$$

$$\hat{H}_k^1 = f\left(H_k^1\right) \tag{9.64}$$

$$H_j^2 = B_j^2 + \sum_{k=1}^{N} \hat{H}_k^1 W_{kj}^2 \tag{9.65}$$

$$\hat{H}_j^2 = f\left(H_j^2\right) \tag{9.66}$$

$$H_o^3 = B_o + \sum_{j=1}^{N} \hat{H}_j^2 W_{jo}^3 \tag{9.67}$$

$$\hat{H}_o^3 = f\left(H_o^3\right) \tag{9.68}$$

$$\left|E^*\right|_{Output} = \left(\hat{H}_1^3 + 1\right)\left(\frac{|E^*|_{\max} - |E^*|_{\min}}{2}\right) + |E^*|_{\min} \tag{9.69}$$

$$\phi_{Output} = \left(\hat{H}_2^3 + 1\right)\left(\frac{\phi_{\max} - \phi_{\min}}{2}\right) + \phi_{\min} \tag{9.70}$$

where

T = placeholder variable, also called any excitation to the activation function,

H_k^1 = input excitation values at nodes of first hidden layer,

$\hat{H}_k^1$ = transferred output of nodes at first hidden layer,

H_j^2 = input excitation values at nodes of second hidden layer,

$\hat{H}_j^2$ = transferred output of nodes at second hidden layer,

H_o^3 = input excitation values at nodes of output layer,

$\hat{H}_o^3$ = transferred output of nodes at output layer, normalized overall output,

P_{i} = input vector, representing input variables,

W_{ik}^1 = weights of first hidden layer from the input layer,

W_{kj}^2 = weights of second hidden layer from the first hidden layer,

W_{jo}^3 = weights of output layer from the second hidden layer,

B_k^1 = bias for first hidden layer,

B_j^2 = bias for second hidden layer,

B_o = bias for output layer,

M = number of input nodes, or number of input variables,

N = number of neurons in both of the hidden layers,

$|E^*|_{max}$ = maximum $|E^*|$ observed in the dataset,

$|E^*|_{min}$ = minimum $|E^*|$ observed in the dataset,

ϕ_{max} = maximum ϕ observed in the dataset, and

ϕ_{min} = minimum ϕ observed in the dataset.

The values of weights and biases of the trained network is shown in Table 9.3. Also, A MATLAB® code for deploying the model in direct application is given in Appendix H of this document. The model accuracy is evaluated by the "goodness-of-fit" statistics presented in the next section.

9.8 Results and Discussion

9.8.1 Goodness-of-Fit

The 'goodness-of-fit' statistics for the ANN model predictions in arithmetic scale were performed using statistical parameters: the coefficient of determination (R^2), and the standard error of estimate (SE) of the predicted values divided by the standard deviation (SD) of the observed values (S_e/S_y). The coefficient of determination (R^2) is a measure of correlation between the predicted and the measured values and, therefore determines the accuracy of the fitted model. A higher value of R^2, close to unity indicates higher accuracy of the predictive model. The S_e/S_y indicates the relative improvement in accuracy of the model. A smaller value of S_e/S_y is indicative of better accuracy. In this case, also a set of

criteria originally developed by Pellinen (2001) in Table 9.4, were also adopted for the evaluation.

Figure 9.12 present the results of statistical analysis for the 120 $|E^*|$ test data while Figure 9.13 presents the 120-test data for ϕ prediction. As mentioned earlier, these test data form an independent dataset that was not used in the training phase of the ANN model, rather it was used to test the accuracy of the trained network. The R^2 and S_e/S_y values are found to be $R^2 = 0.99$ and $S_e/S_y = 0.11$ for $|E^*|$ prediction and $R^2 = 0.93$ and $S_e/S_y = 0.26$ for ϕ prediction. Figure 9.14 presents the results of statistical analysis for the 1500 $|E^*|$ training data while Figure 9.15 presents the results of statistical analysis for the 1500 ϕ training data. In this case, the R^2 and S_e/S_y values are found to be $R^2 = 0.99$ and $S_e/S_y = 0.09$ for $|E^*|$ prediction and $R^2 = 0.96$ and $S_e/S_y = 0.20$ for ϕ prediction for the training dataset. Lastly, Figure 9.16 presents the results of statistical analysis for the all 1620 |E*| data while Figure 9.17 presents the results of statistical analysis for all the 1620 ϕ data. In this case, the R^2 and S_e/S_y values are found to be $R^2 = 0.99$ and $S_e/S_y = 0.09$ for $|E^*|$ prediction and $R^2 = 0.96$ and $S_e/S_y = 0.21$ for ϕ prediction for the overall dataset. Therefore, in all three cases, the testing, training, and overall data, the "goodness-of-fit" indicates that the ANN model developed in this study is "excellent" for predicting $|E^*|$ and ϕ of the Superpave AC mixtures of New Mexico, according to Table 9.4.

9.8.2 Sensitivity Analysis

The sensitivity of the ANN model predictions to the input variables was examined by studying the effect of different combinations of input parameters on $|E^*|$ and ϕ prediction. Table 9.5 and 9.6 list the different input variable combinations and the goodness of fit

statistics for $|E^*|$ and ϕ respectively, corresponding to each ANN models for the all the $|E^*|$ and ϕ data.

The rational influence of the asphalt binder η and loading frequency (f) on the ANN model can be observed from the goodness-of-fit statistics results in Tables 9.5 and 9.6. The ANN model with the asphalt binder η showed better goodness-of-fits for the $|E^*|$ and ϕ, while the ANN model with only the loading frequency (f) input showed little or no correlations to $|E^*|$ and ϕ.

The effect of asphalt mastic properties, including ρ_{200}, η, and f can be observed form the goodness-of-fit statistics in Tables 9.5 and 9.6, which ensures that the inclusion of ρ_{200} with the binder η and loading frequency, can improve the accuracy of the ANN model (R^2 = 0.97 for $|E^*|$ and R^2 = 0.93 for ϕ). This indicates that the asphalt mastic properties are sensitive variables.

The effect of volumetric properties (V_a, V_{beff}) and/or effect of aggregate gradation properties ($\rho_{3/4}$, $\rho_{3/8}$, ρ_4, and ρ_{200}) on $|E^*|$ and ϕ predictions can be observed in Tables 9.5 and 9.6. It can be observed that the ANN model using only asphalt volumetric properties and/or aggregate gradations show very poor goodness-of-fit statistics. This poor behavior of the model is due to exclusion of time and temperature effects represented by the η and f. These results indicate that the asphalt binder input parameters are critical input variables in the ANN predictive model, which is rational and concurrent with the literature.

9.9 Comparison of the Models Developed

Table 9.7 presents a summary of the statistics of all the $|E^*|$ and ϕ-models evaluated in this study. Considering the "goodness of fit" of the models, it can be concluded that the ANN-based model produces significantly accurate estimations of $|E^*|$ and ϕ of asphalt concrete.

9.10 Conclusions

In this study, an artificial neural network model is developed for predicting dynamic modulus and phase angle of Superpave asphalt concrete based on the laboratory tested data of 54 asphalt concrete mixtures. Considering goodness-of-fit statistics, the model can be considered as an excellent option for predicting dynamic modulus and phase angle of asphalt concrete. As such, the artificial neural network methodology is proven to be a promising modeling technique, especially for data sets having the kind of nonlinear relationships frequently encountered in characterization problem.

Table 9.1 Update Rules for Various Backpropagation Algorithms.

Algorithms	**Update Rules**	**Convergence**	**Computation Complexity**
EBP algorithm	$\boldsymbol{w}_{k+1} = \boldsymbol{w}_k - \alpha\, \boldsymbol{g}_k$	Stable, slow	Gradient
Newton algorithm	$\boldsymbol{w}_{k+1} = \boldsymbol{w}_k - \boldsymbol{H}_k^{-1}\boldsymbol{g}_k$	Unstable, fast	Gradient and Hessian
Gauss-Newton algorithm	$\boldsymbol{w}_{k+1} = \boldsymbol{w}_k - \left(\boldsymbol{J}_k^{T}\boldsymbol{J}_k\right)^{-1}\boldsymbol{J}_k\boldsymbol{e}_k$	Unstable, fast	Jacobian
Levenberg-Marquardt algorithm	$\boldsymbol{w}_{k+1} = \boldsymbol{w}_k - \left(\boldsymbol{J}_k^{T}\boldsymbol{J}_k + \mu\boldsymbol{I}\right)^{-1}\boldsymbol{J}_k\boldsymbol{e}_k$	Stable, fast	Jacobian

Table 9.2 Definitions and ranges of values for input and output variables used in ANN model developement.

Variable	**Range**		**Mean**	**SD**
	Min	**Max**		
Aggregate Gradataion				
$\rho_{3/4}$	0.00	7.00	2.09	2.08
$\rho_{3/8}$	11.00	46.00	29.43	9.41
ρ_{4}	37.00	69.00	53.65	8.18
ρ_{200}	3.60	6.40	5.20	0.58
Mixture Volumetric				
V_a	5.00	6.00	5.59	0.28
V_{beff}	7.52	11.42	9.95	0.62
Binder				
η (Poise)	5.03E+03	2.70E+10	5.81E+09	1.06E+10
Loading Frequency				
F (Hz)	0.1	25	6.93	8.78
Dynamic Modulus				
|E| (psi)*	2.74E+04	1.08E+07	2.41E+06	2.44E+06
Phase Angle				
Φ (Degree)	1.57	46.97	19.62	8.47

Table 9.3 Weights, Biases, and Mapping Data for the ANN model Developed in this Study.

B_k^1
1.82279758
-2.83972297
-31.25259489
78.77927717
-4.07645427
2.07261166
-0.44163939
-1.11106186
10.40245044
-4.32202242
1.39621846
6.55941078

B_j^2
-58.88242311
-8.36820149
22.40784549
6.68927024
178.75231105
6.09260744
-11.24847615
181.95765499
10.48420244
-8.26659190
-3.19263957
1508.41824034

B_o
221.21822769
-76.20647264

W_{ik}^1							
0.25131945	0.40431435	-1.99173633	-1.35822167	-0.61980268	-1.93668362	-0.04111902	0.06111864
3.53513651	-4.13636762	4.61420995	-1.45578929	2.82839655	1.94335105	-3.38540833	-0.03132789
114.96158162	7.10062471	-75.45060711	-43.06204722	33.25937940	-66.42066395	2.17210237	-0.03091165
0.00619664	0.00041623	-0.01010699	0.00658305	0.02302434	-0.00905831	78.85597998	0.00252495
-7.78924650	11.59180907	-9.26643066	0.73924650	-2.34222049	4.87384454	0.25183398	0.01124050
-1.58689023	0.56103918	-5.93410067	0.19645504	-6.70520968	-2.33370861	0.08088704	-0.01475391
0.09488271	0.27396653	-0.34388359	-0.69874143	-0.61377885	0.30427684	-0.65259446	-0.12673724
0.10773192	0.30069595	-0.38599388	-0.76926705	-0.61742935	0.32275273	-1.33341262	-0.13727932
0.02437085	-0.02303326	-0.01516404	0.06842658	0.01152215	-0.00634441	0.05852864	6.83803637
-2.05740412	1.46506388	-0.32360930	-0.49363863	2.18825093	2.99825817	0.02612375	-0.00701185
0.46171648	-2.76974566	5.02614145	-0.53337011	-1.31654142	1.71245607	0.43521167	0.02329511
-5.71299003	-13.42861614	13.16798023	3.70116186	2.42949510	-17.13993626	0.28573807	0.01452210

W_{kj}^2											
-11.96544446	-0.10752220	6.20076037	0.35410101	-6.58370803	-21.82603986	-5.79880975	3.72394878	55.33306321	4.17984218	1.14474972	-4.42952509
6.49970645	-2.32653186	-0.17626995	-2.38519575	-0.68772025	-7.71227589	-2.60142116	2.64910901	5.34497077	2.73411175	-1.91900798	-5.87936853
0.01683488	0.08505213	0.27172080	-0.02248698	-0.12474786	0.57703641	-0.60690913	0.53193730	-22.07284816	0.22098877	-0.01746493	0.34613806
-0.43959400	0.00040171	0.54552131	-0.06785999	0.14730480	0.02798216	0.97916391	-0.83082082	-5.20427876	1.15141689	-0.11993833	0.02004100
-0.30842355	1.23096224	0.03819675	-131.46057261	0.32498981	0.80435539	-54.93989144	49.15516571	-189.72136698	-1.51262869	-0.67075338	-0.23315416
-0.44610879	0.00143398	0.56722917	-0.06436013	0.15903584	0.01953806	0.95681906	-0.81218316	-4.59041846	1.14991285	-0.12192438	0.01985498
0.25332956	0.07041868	0.01991235	0.05034741	-0.26744486	0.82962451	-0.51003337	0.35818033	10.95192366	0.22019578	0.07377254	0.37918942
-0.32017298	1.23501919	0.04424277	-131.93348779	0.32461502	0.81045028	-55.26942347	49.46960766	-192.96433595	-1.52099632	-0.67572502	-0.23129181
-0.03525357	-0.04943273	-0.26294285	-0.10482667	-0.14376286	0.09665367	1.05632872	-0.90779076	-9.56641567	0.51950642	0.00156237	-0.04526523
6.54208646	-2.34662418	-0.20489228	-2.39035291	-0.67821617	-7.77818316	-2.66833053	2.71930522	5.17709083	2.72392579	-1.92609703	-5.92007895
-2.15691102	30.16927738	-17.37750573	55.81237832	10.04497969	8.88023433	4.28941203	-2.92235439	11.13616546	3.76339170	-4.26140916	7.81753589
0.32206358	-0.13979444	1484.78617149	-0.15676782	0.81294668	-0.22418425	2.44321974	-2.04643528	-18.79696689	-0.85403525	-0.09033494	-1.48414618

W_{jo}^3											
-0.30310149	28.49533179	-6.55836455	-77.41088566	-20.46062342	77.71502603	4.84984042	18.81988544	-0.89401000	-28.42379035	0.59390252	-222.43620136
-0.13361150	-92.82233855	3.31687012	221.52265037	103.96087607	-219.03220619	-3.43124640	-104.43311346	-8.74912907	92.54249759	-2.12994300	81.52728717

Maximum and Minimum Values of $\|E^*\|$ and ϕ for Data Mapping	
$\|E^*\|_{max}$	10770747.65 psi
$\|E^*\|_{min}$	27386.23878 psi
ϕ_{max}	46.96666667 deg.
ϕ_{min}	1.566666667 deg.

Table 9.4 Statistical criteria for correlation between the observed and the predicted data (Pellinen 2001).

Overall Correlation	**Statistical Criteria**	
	R^2	S_e/S_y
Excellent	≥ 0.90	≤ 0.35
Good	0.79 – 0.89	0.36 – 0.55
Fair	0.40 – 0.69	0.56 – 0.75
Poor	0.20 – 0.39	0.76 – 0.90
Very Poor	≤ 0.19	≥ 0.90

Table 9.5 Sensitivity Analysis Results for $|E^*|$

Predictive Model	**ANN Architecture**	**Input Parameter**		**Goodness-of-fit**	
		Property	**Parameter**	R^2	S_e/S_y
ANN-NM-$\|E^*\|$-1.1	1-12-12-2	Binder Viscosity, and Loading Frequency	η	0.90	0.32
ANN-NM-$\|E^*\|$-1.2	1-12-12-2		f	0.04	0.98
ANN-NM-$\|E^*\|$-1.3	2-12-12-2		η, f	0.95	0.23
ANN-NM-$\|E^*\|$-2	3-12-12-2	Asphalt Mastic	ρ_{200}, η, f	0.97	0.16
ANN-NM-$\|E^*\|$-3.1	1-12-12-2	Air Void, and Effective Asphalt Content	V_a	0.01	1.00
ANN-NM-$\|E^*\|$-3.2	1-12-12-2		V_{beff}	0.02	0.99
ANN-NM-$\|E^*\|$-3.3	2-12-12-2		V_a, V_{beff}	0.02	0.99
ANN-NM-$\|E^*\|$-4	4-12-12-2	Binder Viscosity, Loading Frequency, Air Void, Effective Asphalt Content	η, f, V_a, V_{beff}	0.98	0.15
ANN-NM-$\|E^*\|$-5	5-12-12-2	Asphalt Mastic, Air Void, Effective Asphalt Content	$\rho_{200}, \eta, f, V_a, V_{beff}$	0.99	0.10
ANN-NM-$\|E^*\|$-6.1	1-12-12-2	Aggregate Gradation Variables	$\rho_{3/4}$	0.00	1.00
ANN-NM-$\|E^*\|$-6.2	1-12-12-2		$\rho_{3/8}$	0.00	1.00
ANN-NM-$\|E^*\|$-6.3	1-12-12-2		ρ_4	0.00	1.00
ANN-NM-$\|E^*\|$-6.4	1-12-12-2		ρ_{200}	0.02	1.00
ANN-NM-$\|E^*\|$-6.5	2-12-12-2		$\rho_{3/4}, \rho_{3/8}$	0.00	1.00
ANN-NM-$\|E^*\|$-6.6	2-12-12-2		$\rho_{3/4}, \rho_4$	0.01	1.00
ANN-NM-$\|E^*\|$-6.7	2-12-12-2		$\rho_{3/4}, \rho_{200}$	0.02	0.99
ANN-NM-$\|E^*\|$-6.8	2-12-12-2		$\rho_{3/8}, \rho_4$	0.02	0.99
ANN-NM-$\|E^*\|$-6.9	2-12-12-2		$\rho_{3/8}, \rho_{200}$	0.02	0.99
ANN-NM-$\|E^*\|$-6.10	2-12-12-2		ρ_4, ρ_{200}	0.02	0.99
ANN-NM-$\|E^*\|$-6.11	3-12-12-2		$\rho_{3/4}, \rho_{3/8}, \rho_4$	0.02	0.99
ANN-NM-$\|E^*\|$-6.12	3-12-12-2		$\rho_{3/4}, \rho_{3/8}, \rho_{200}$	0.02	0.99
ANN-NM-$\|E^*\|$-6.13	3-12-12-2		$\rho_{3/4}, \rho_4, \rho_{200}$	0.02	0.99
ANN-NM-$\|E^*\|$-6.14	3-12-12-2		$\rho_{3/8}, \rho_4, \rho_{200}$	0.02	0.99
ANN-NM-$\|E^*\|$-6.15	3-12-12-2		$\rho_{3/4}, \rho_{3/8}, \rho_4, \rho_{200}$	0.02	0.99
ANN-NM-$\|E^*\|$-6.16	8-12-12-2	Witczak's Parameters	$\rho_{3/4}, \rho_{3/8}, \rho_4, \rho_{200}, \eta, f, V_a, V_{beff}$	0.99	0.09

Table 9.6 Sensitivity Analysis Results for ϕ

Predictive Model	ANN Architecture	Input Parameter		Goodness-of-fit	
		Property	Parameter	R^2	S_e/S_y
ANN-NM-ϕ-1.1	1-12-12-2	Binder Viscosity, and	η	0.77	0.48
ANN-NM-ϕ-1.2	1-12-12-2	Loading Frequency	f	0.00	1.00
ANN-NM-ϕ-1.3	2-12-12-2		η, f	0.89	0.34
ANN-NM-ϕ-2	3-12-12-2	Asphalt Mastic	ρ_{200}, η, f	0.93	0.26
ANN-NM-ϕ-3.1	1-12-12-2	Air Void, and	V_a	0.00	1.00
ANN-NM-ϕ-3.2	1-12-12-2	Effective Asphalt	V_{beff}	0.01	1.00
ANN-NM-ϕ-3.3	2-12-12-2	Content	V_a, V_{beff}	0.03	0.99
ANN-NM-ϕ-4	4-12-12-2	Binder Viscosity, Loading Frequency, Air Void, Effective Asphalt Content	η, f, V_a, V_{beff}	0.93	0.26
ANN-NM-ϕ-5	5-12-12-2	Asphalt Mastic, Air Void, Effective Asphalt Content	$\rho_{200}, \eta, f, V_a, V_{beff}$	0.90	0.32
ANN-NM-ϕ-6.1	1-12-12-2	Aggregate Gradation	$\rho_{3/4}$	0.00	1.00
ANN-NM-ϕ-6.2	1-12-12-2		$\rho_{3/8}$	0.02	1.00
ANN-NM-ϕ-6.3	1-12-12-2		ρ_4	0.02	1.00
ANN-NM-ϕ-6.4	1-12-12-2		ρ_{200}	0.02	1.00
ANN-NM-ϕ-6.5	2-12-12-2		$\rho_{3/4}, \rho_{3/8}$	0.02	0.99
ANN-NM-ϕ-6.6	2-12-12-2		$\rho_{3/4}, \rho_4$	0.03	0.99
ANN-NM-ϕ-6.7	2-12-12-2		$\rho_{3/4}, \rho_{200}$	0.03	0.99
ANN-NM-ϕ-6.8	2-12-12-2		$\rho_{3/8}, \rho_4$	0.03	0.99
ANN-NM-ϕ-6.9	2-12-12-2		$\rho_{3/8}, \rho_{200}$	0.03	0.99
ANN-NM-ϕ-6.10	2-12-12-2		ρ_4, ρ_{200}	0.03	0.99
ANN-NM-ϕ-6.11	3-12-12-2		$\rho_{3/4}, \rho_{3/8}, \rho_4$	0.03	0.99
ANN-NM-ϕ-6.12	3-12-12-2		$\rho_{3/4}, \rho_{3/8}, \rho_{200}$	0.03	0.99
ANN-NM-ϕ-6.13	3-12-12-2		$\rho_{3/4}, \rho_4, \rho_{200}$	0.03	0.99
ANN-NM-ϕ-6.14	3-12-12-2		$\rho_{3/8}, \rho_4, \rho_{200}$	0.03	0.99
ANN-NM-ϕ-6.15	4-12-12-2		$\rho_{3/4}, \rho_{3/8}, \rho_4, \rho_{200}$	0.03	0.99
ANN-NM-ϕ-6.16	8-12-12-2	Witczak's Parameters	$\rho_{3/4}, \rho_{3/8}, \rho_4, \rho_{200}, \eta, f, V_a, V_{beff}$	0.96	0.20

Table 9.7 Summary of the Statistics of the Evaluated Models

Models	**Material Property**		**R^2**	**Se**	**S_e/S_y**	***n***	***p***
Nationally Calibrated η-based Witczak's Model	Dynamic Modulus, psi	log-|E*|	0.7134	0.3374	0.5352	1620	8
		|E*|	0.3168	2.02×10^6	0.8265	1620	8
Revised η-based Witczak's Model	Dynamic Modulus, psi	log-|E*|	0.9442	0.1495	0.2372	1620	8
		|E*|	0.8656	0.90×10^6	0.3682	1620	8
New η-based models	Dynamic Modulus, psi	log-|E*|	0.9614	0.1245	0.1974	1620	6
		|E*|	0.9264	0.66×10^6	0.2724	1620	6
	Phase Angle, deg.	ϕ	0.8066	3.7354	0.4413	1620	6
New $\|G_b^*\|$-based models	Dynamic Modulus, psi	log-|E*|	0.9079	0.1849	0.3045	900	6
		|E*|	0.8358	985563	0.4066	900	6
	Phase Angle, deg.	ϕ	0.7324	4.4769	0.5190	900	6
New ANN-based Models	Dynamic Modulus, psi	|E*|	0.9916	235594.06	0.0920	1620	8
	Phase Angle, deg.	ϕ	0.9576	1.8819	0.2068	1620	8

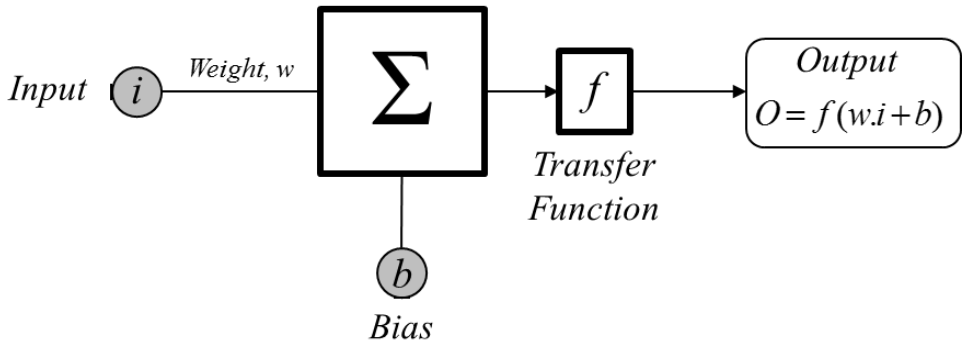

Figure 9.1 A simple neuron model.

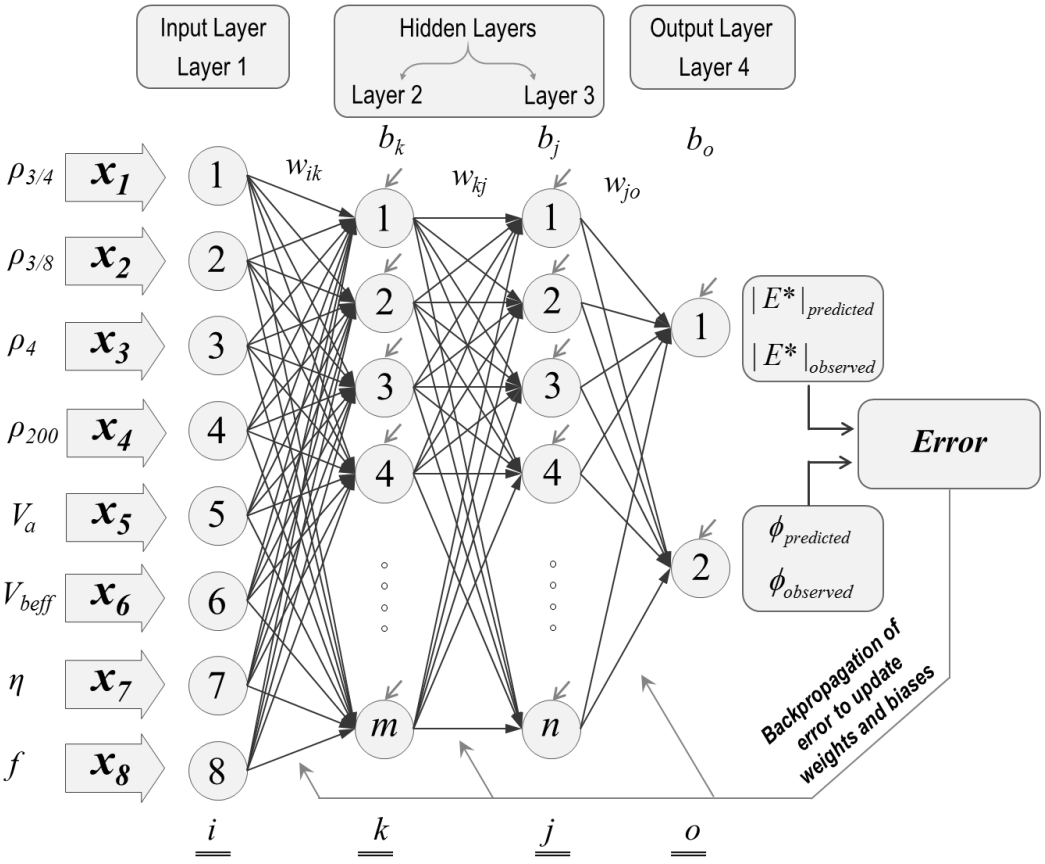

Figure 9.2 Pictoral representation of four-layered neural network architecture.

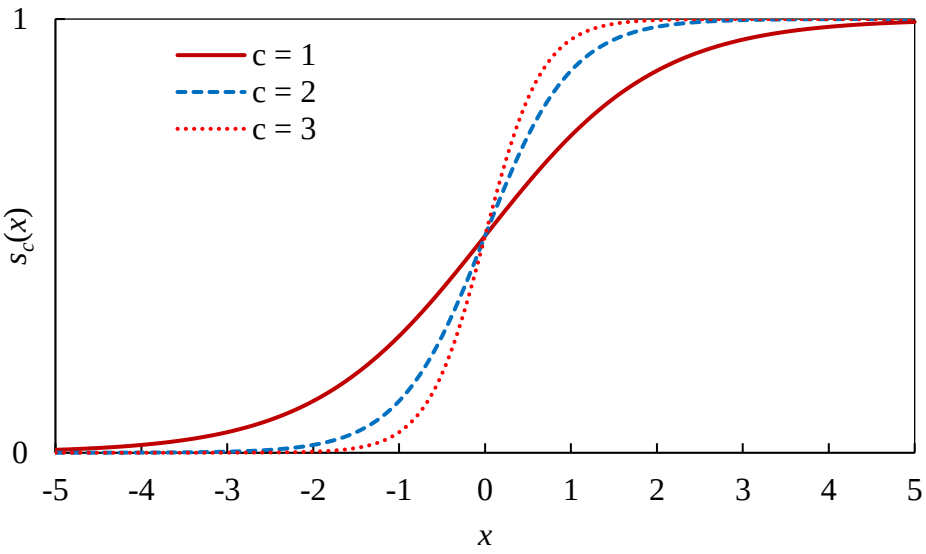

Figure 9.3 Three sigmoids (for c = 1, c = 2, and c = 3).

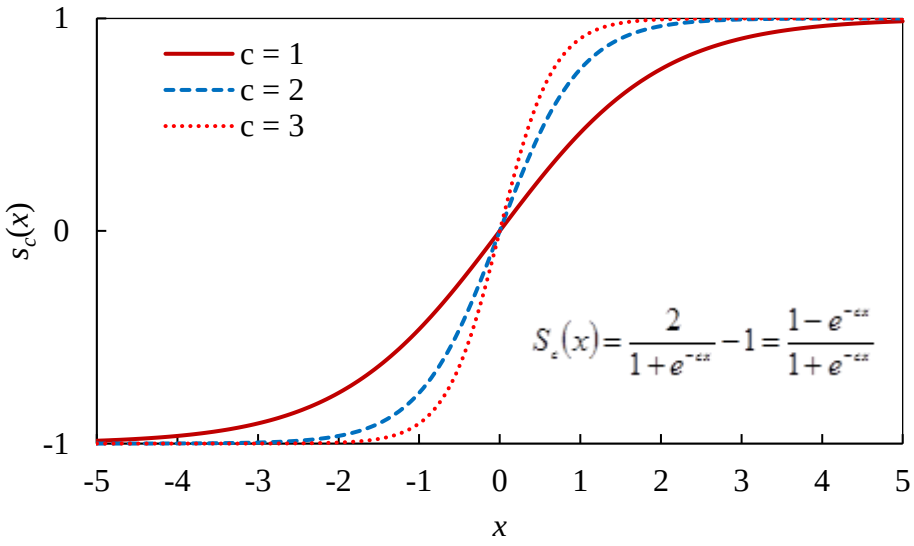

Figure 9.4 Three symetrical sigmoids (for c = 1, c = 2, and c = 3).

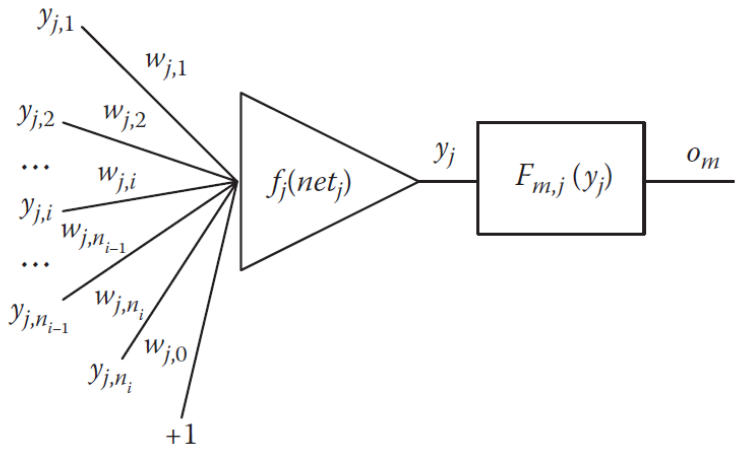

Figure 9.5 Connection of a neuron j with the rest of the network. Nodes yj,i could represent network inputs or outputs of other neurons. Fm,j(yj) is the nonlinear relationship between the neuron output node yj and the network output om.

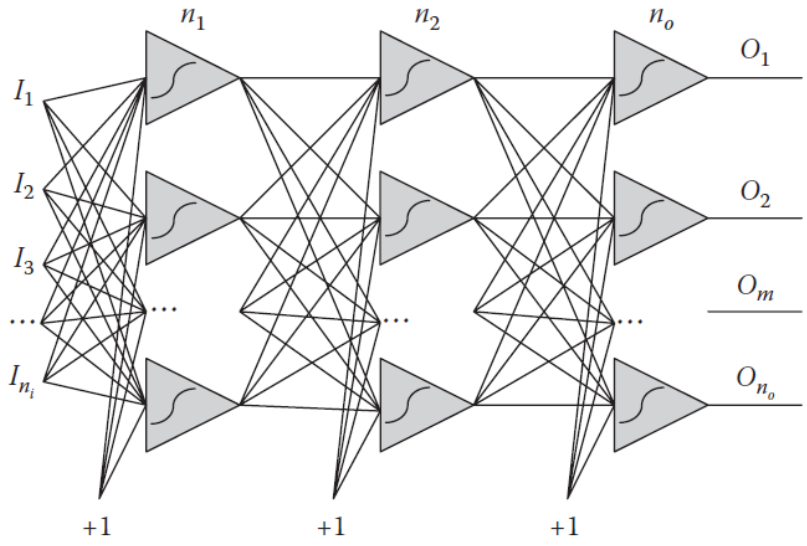

Figure 9.6. Three-layer multilayer perceptron network: the number of inputs is n_i, the number of outputs is n_o, and n_1 and n_2 are the numbers of neurons in the first and second layers separately.

```
for all patterns
% Forward Computation
    for all layers
        for all neurons in the layer
            calculate net;          % Equation 28
            calculate output;       % Equation 27
            calculate slope;        % Equation 30
        end;
    end;
% Backward Computation
    Initial delta as slope;
    for all outputs
        calculate error;
        for all layers
            for all neurons in the previous layer
                for all neurons in the current layer
                    multiply delta through weights
                    sum the backpropagated delta at proper nodes
                end;
                multiply delta by slope;
            end;
        end;
    end;
end;
```

Figure 9.7 Pseudo code of forward computation and backward computation implementing Levenberg–Marquardt algorithm.

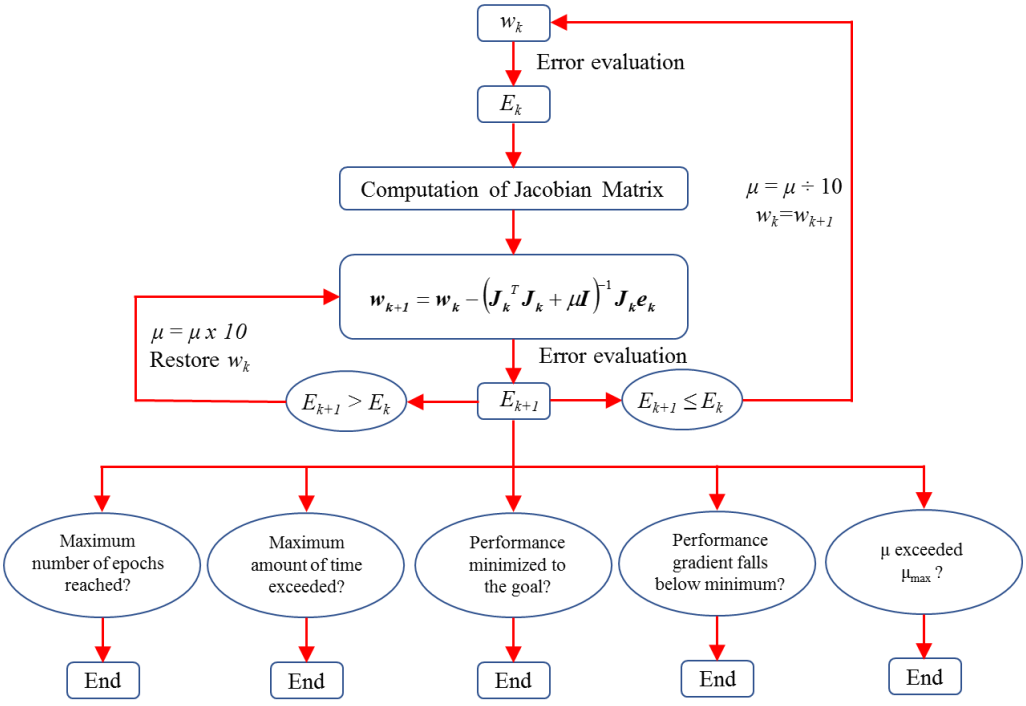

Figure 9.8 Block diagram for training using Levenberg–Marquardt algorithm: wk is the current weight, wk+1 is the next weight, Ek+1 is the current total error, and Ek is the last total error.

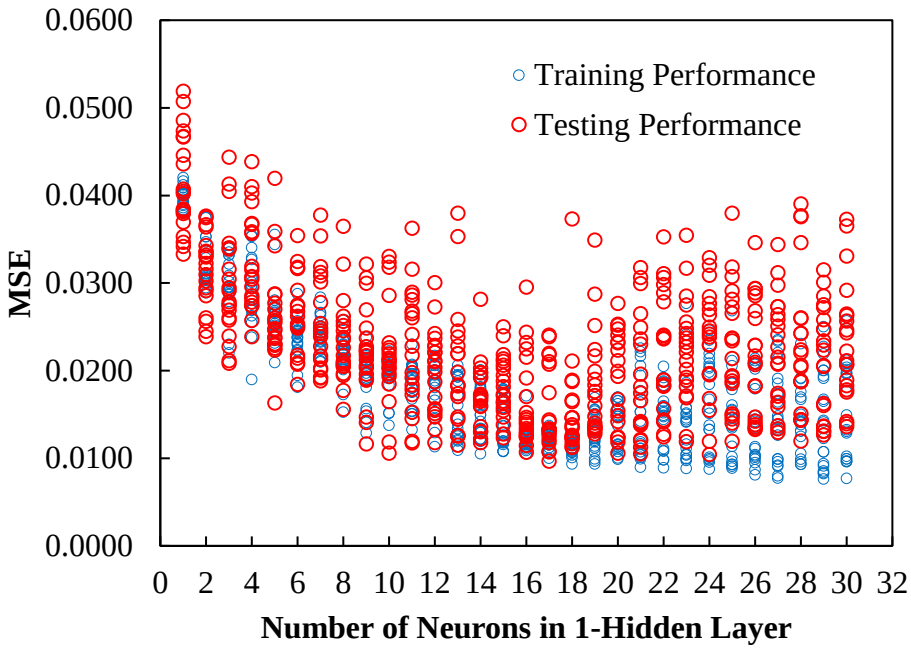

(a) Training and testing performances with increasing number of neurons

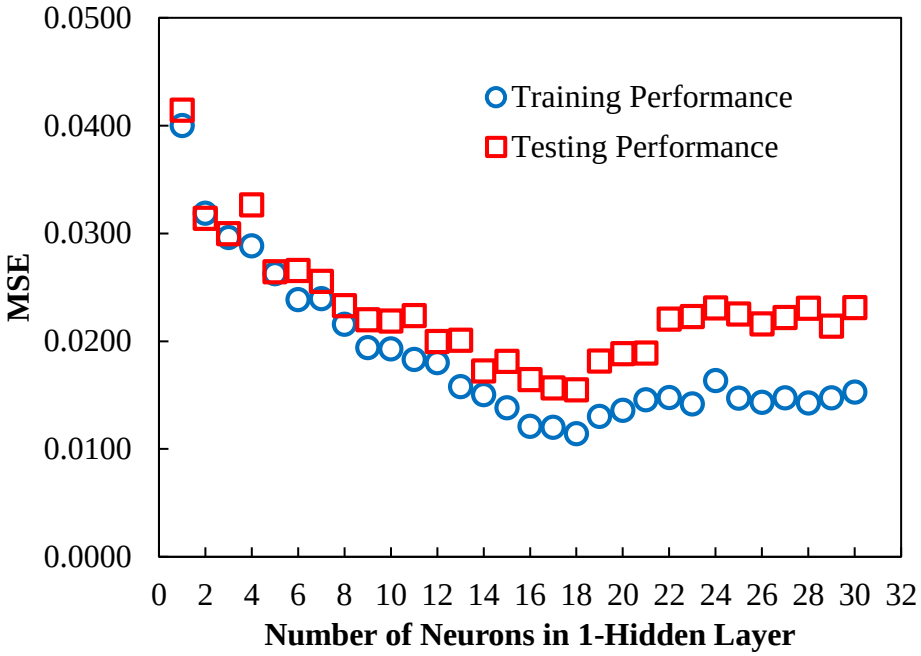

(b) Average training and testing performances with increasing number of neurons

Figure 9.9. Training and testing performance of a 1-hidden layer network with increasing number of neurons, (a) performances for individual run, (b) Average performances of the 20 runs.

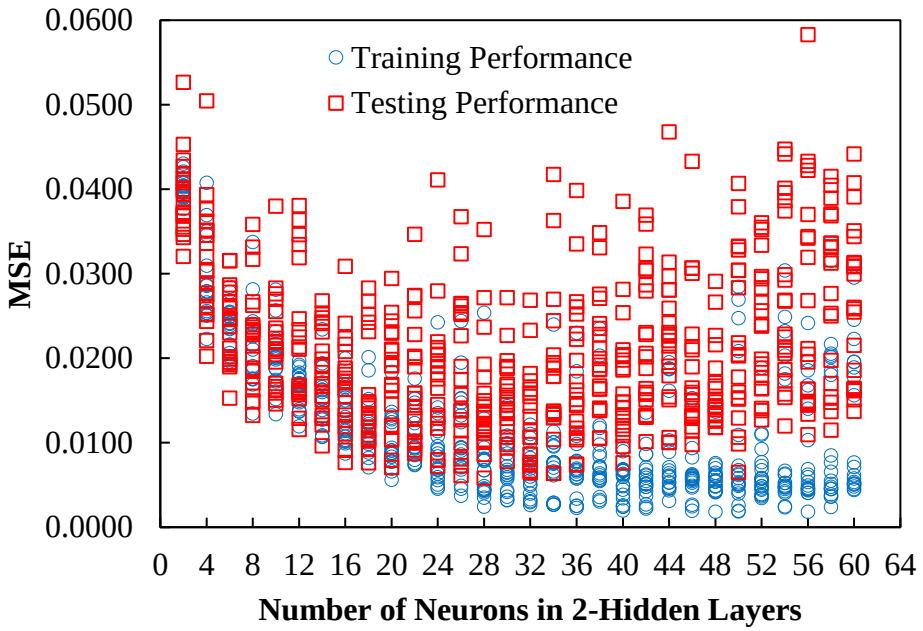

(a) Training and testing performances with increasing number of neurons

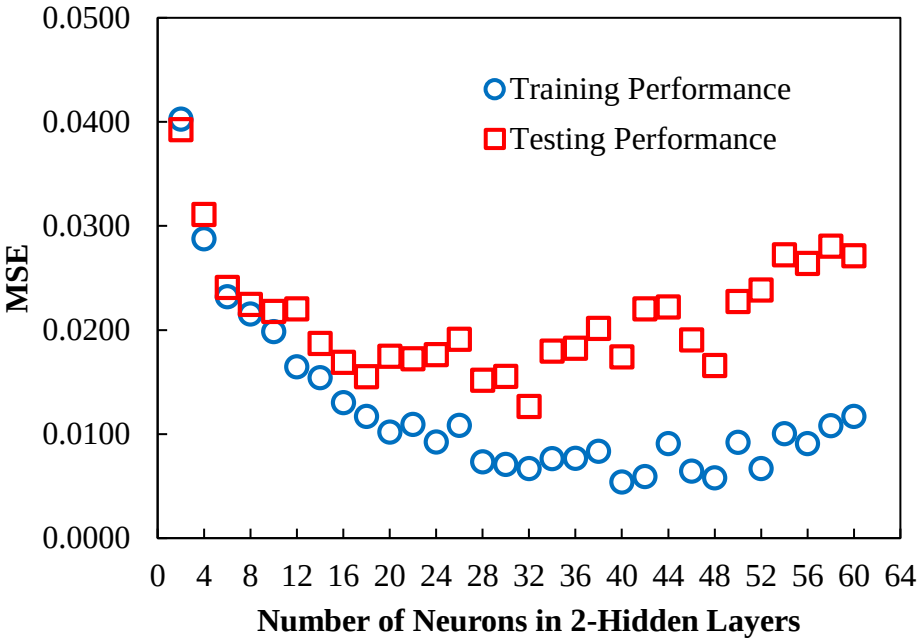

(b) Average training and testing performances with increasing number of neurons

Figure 9.10 Training and testing performance of a 2-hidden layers network with increasing number of neurons, (a) performances for individual run, (b) Average performances of the 20 runs.

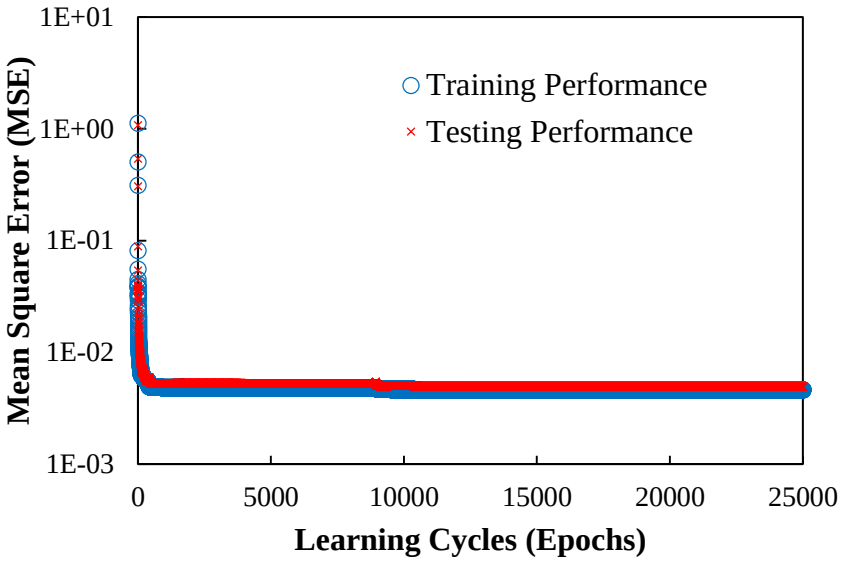

Figure 9.11 Training and testing progresses of the |E*| ANN model.

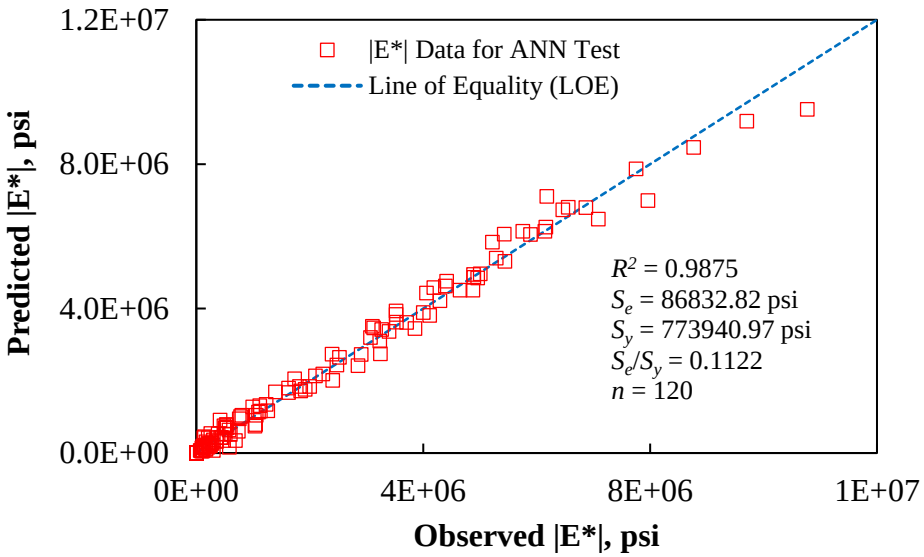

Figure 9.12 Predicted versus observed |E*| using 120 ANN testing data.

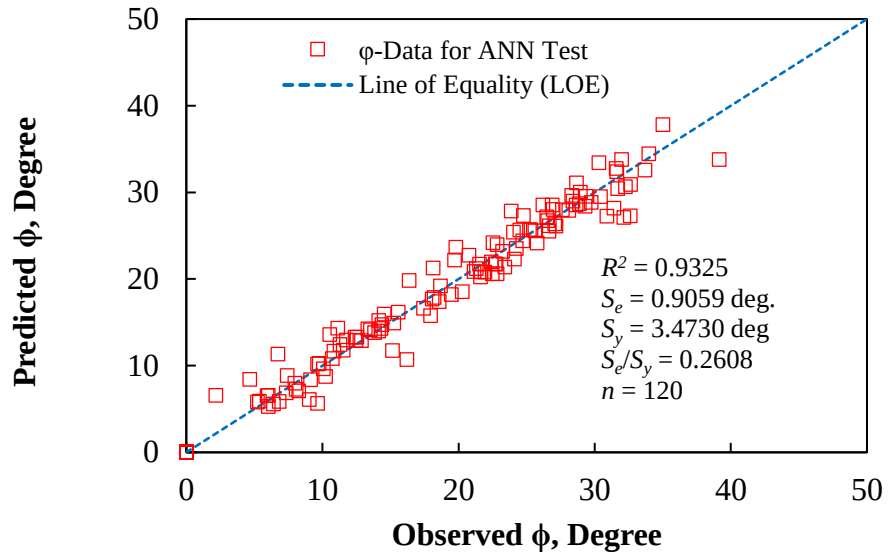

Figure 9.13 Predicted versus observed ϕ using 120 ANN testing data.

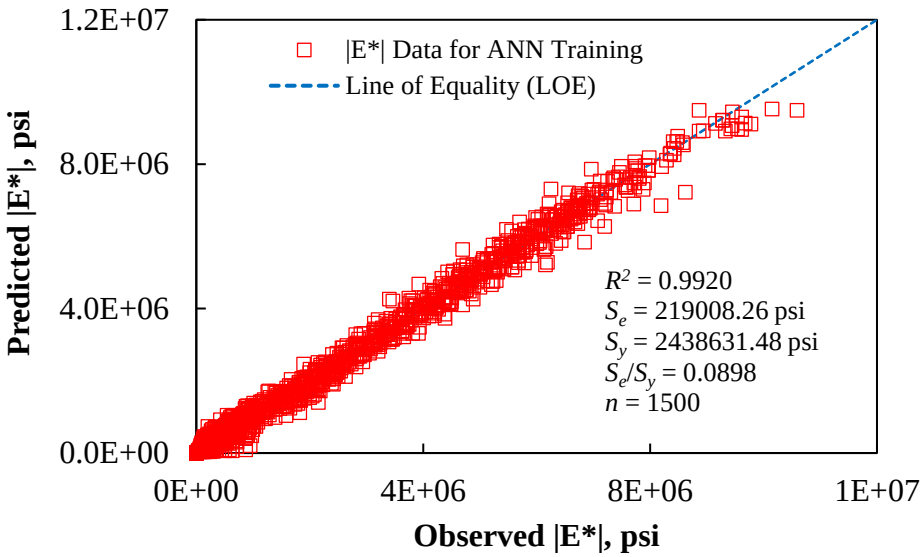

Figure 9.14 Predicted versus observed |E*| using training set of 1500 data.

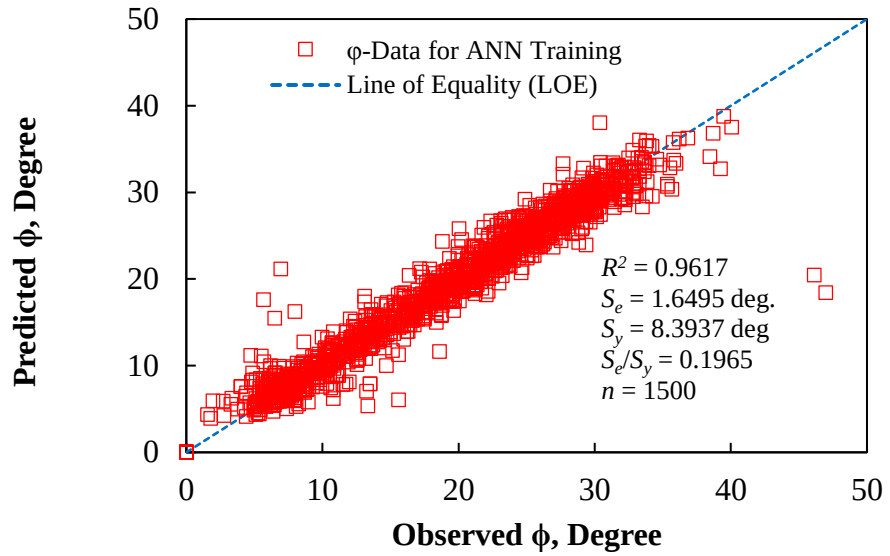

Figure 9.15 Predicted versus observed ϕ using training set of 1500 data.

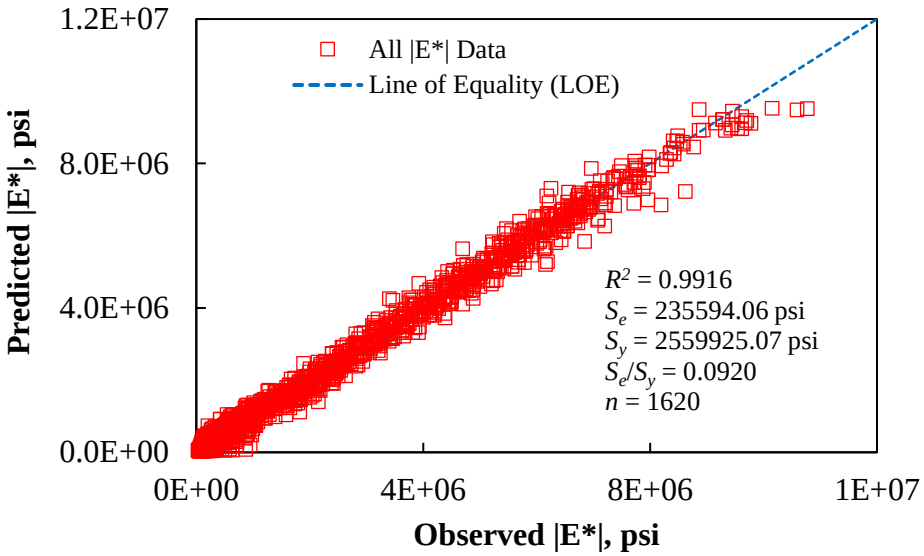

Figure 9.16 Predicted versus observed |E*| using all 1620 data.

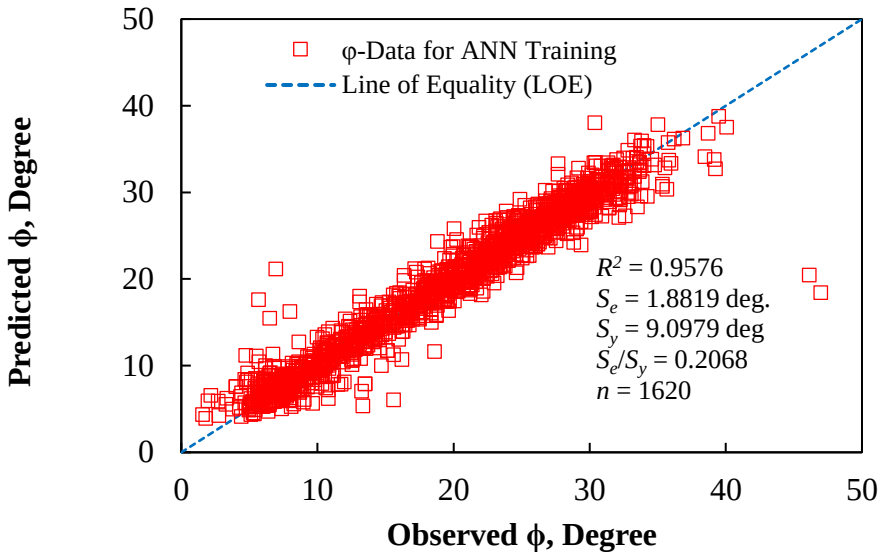

Figure 9.17 Predicted versus observed ϕ using all 1620 data.

Chapter 10

Interconversion of Linear Viscoelastic Material Functions: Numerical Modeling and Laboratory Validation

10.1 Introduction

In this study, a procedure is derived to interconvert one function from another. Cylindrical specimens of asphalt concrete were prepared in the laboratory for conducting complex modulus, relaxation modulus, and creep compliance tests at different test temperatures and loading rates. The time-temperature superposition principle was applied to develop broadband linear viscoelastic material functions. A numerical interconversion technique was used to interconvert one material function to another, and hence, the converted material functions are compared to the laboratory tested material functions. The comparison showed good agreement with the laboratory test data. Toward the end, a statistical assessment is conducted to determine if the interconverted material functions are similar to the laboratory tested material functions.

10.2 Background

There are a number of viscoelastic material functions available to characterize the linear viscoelastic (LVE) behavior of asphalt concrete (AC). Some of these are expressed in time domain, such as, relaxation modulus, $E(t)$ or creep compliance, $D(t)$ and some are expressed in frequency domain, such as, dynamic or complex modulus ($|E^*|$, or E^*). The E^* of AC material is useful for the implementation of mechanistic-empirical (M-E)

analysis and design of pavement (MEPDG 2004). However, time domain LVE material functions of AC may be required for constitutive modeling or finite element application as in the work of Ahmed et al. (2016).

The interrelationships between linear viscoelastic (LVE) material functions have a basis in the theory of linear differential and integral equations. Therefore, a given or source LVE function can be converted into a target LVE material functions as long as the given function is known over a wide-enough range of time or frequency. Researchers like Hopkins and Hamming (1957), Knoff and Hopkins (1972), Baumgaertel and Winter (1989), Mead (1998), Schapery and Park (1998), Ramkumar et al. (1997), Park and Schapery (1999) presented different approaches of certain accuracy levels to convert one linear viscoelastic function to another for polymer materials. Mun et al. (2007) demonstrated an interconversion technique to convert frequency-domain LVE material functions of asphalt concrete to time-domain LVE material functions. Their work involved pre-smoothing of raw data, refinement of phase angle data, Prony series representation of the material function, and interconversion by exact and approximate techniques. However, in their exact method of interconversion, the details about calculating the time constants (e.g. calculation of retardation times from the relaxation times) are missing. Park and Kim (1999) proposed a new approximate interconversion method between $E(t)$ and $D(t)$ of asphalt concrete. Their scheme is based on the concept of equivalent time which can be determined by rescaling the physical time. The rescaling factor is governed by the local slope of the source function expressed in logarithmic scale. However, to study the effect of any physical or environmental factors to the linear viscoelastic material functions of asphalt concrete, application of a valid interconversion technique is always helpful in terms of cost

and time. An appropriate interconversion technique can reduce the cost of testing for all the material functions and thus can reduce the study time. Danial et al. (1998) studied the effect of asphalt-aging on viscoelastic properties of AC. They found the aging of the asphalt concrete mixture results in a decrease in the slope of the linear portion of the creep and relaxation curves. The dynamic modulus increases and phase angles decrease with higher level of aging. In their study, the creep compliance testing was performed and the relaxation modulus is predicted through the procedure based on theory of linear viscoelasticity suggested by Kim and Lee (1995).

10.3 Objective

The main objective of this study is to perform representative laboratory tests on various LVE material functions of the AC specimens to evaluate the validity of the numerical method employed herein for interconversion. The linear viscoelastic material functions considered in this study are: time-domain functions such as $E(t)$, and $D(t)$; and frequency-domain function as E^* of asphalt concrete. Toward the end, a statistical evaluation was conducted in this study to determine if the interconverted LVE material functions are similar to the laboratory tested LVE functions.

10.4 Preparation of Test Specimens for Laboratory Tests

10.4.1 Materials

Two asphalt-aggregate mixtures with different binder performance grades (PG) used in this study were collected from a manufacturing plant in New Mexico. Both of these mixtures have the same aggregate materials mostly consisting of dacite materials. According to AASHTO MP 2 (2002), the aggregate used in the AC mixtures is a Type III Superpave

blend with the nominal maximum aggregate size (NMAS) of 19mm. The aggregate blend consists of 35% coarse fraction, 10% intermediate fraction, 54% crushed fines, and 1% hydrated lime. The combined aggregate specific gravity was found to be 2.521. The first AC mixtures contains 5.8% PG 70-22 asphalt binder (AC sample 1), while, the second AC mixtures contains 5.8% PG 76-22 asphalt binder (AC sample 2).

10.4.2 Compaction and Fabrication of Test Specimens

A Superpave gyratory compactor was used to compact the collected asphalt-aggregate mixtures. Before compaction, the AC mixture was preheated by the recommended temperatures provided by the manufacturer. The initial dimensions of the cylindrical specimens were 150 mm in diameter and around 170 mm in height. These specimens are then cored and sawed to have finished specimens of diameter 100 mm and of height 150 mm. To achieve consistency in the test results the target air void was set at 5.5±0.5 for the finished specimens, and therefore, several trial mixes were compacted at the beginning to reach the target air void condition. The bulk specific gravity and the air void content of the finished cylindrical specimens were determined per AASHTO T 166 (2010).

10.4.3 Laboratory Tests

A Material Testing System (MTS) (GCTS 2012) was used for testing different LVE material functions at various test-temperatures and loading frequencies or time period. The system can control cyclic or static stress or strain on a cylindrical AC specimen helpful to conduct uniaxial E^* with phase angle (ϕ), $D(t)$ and $E(t)$ tests. Stresses can be controlled by the load cells, and the strains can be controlled by the linear variable displacement transducers (LVDTs) attached to the specimen. The average of the displacements from all

the LVDTs is the feedback strain from the equipment. To keep the stress uniform over the specimen or to keep the difference in displacements of the three LVDTs under permissible limit, several trial tests were needed to make. The uniformity coefficients (UC) for three LVDTs were kept within 35% for all the tests. The AASHTO T 342 (2011) standard for testing $|E^*|$ also recommends a 35% uniformity coefficient among the LVDTs. Each of the specimens was tested for $|E^*|$ with ϕ, $E(t)$ and $D(t)$ under uniaxial compression at different temperatures and loading rates to develop mastercurves for the material functions. The load or strain levels in these tests were kept low enough to avoid risk of inducing any damage to the specimen, hence, material response was considered in the linear viscoelastic range as suggested by Daniel et al. (2007).

10.4.3.1 Complex Modulus with Phase Angle Test

Complex modulus, E^* with phase angle, ϕ tests were conducted on the AC specimens according to standard specification provided by AASHTO T 342 (2011). Each of the test specimens was tested for $|E^*|$ and ϕ at five different test-temperatures (T) of, 14, 40, 70, 100, and 130 °F, starting at the lowest temperature and proceeding to the highest temperature. At each test-temperature, tests were conducted for six loading frequencies (f) of 25, 10, 5, 1, 0.5, and 0.1 Hz, from the highest toward the lowest frequency. For testing at a specific test-temperature, conditioning was done according AASHTO T 342 recommended conditioning time to reach equilibrium condition with a precision tolerance of ±0.5 °C. During each test, the recoverable strain was kept in between 50 and 150 με, and the accumulated permanent strain from all the loading frequencies at a specific test temperature were kept below 1500 με. These two provisions were implemented by AASHTO T 342 to keep the material response in LVE range and to avoid any damage to

the specimen due to excessive permanent deformation. To keep the loading uniform over the specimen, several trial tests were needed to make with lower load level at the beginning of a test cycle. The uniformity coefficients (UC) for three LVDTs were kept within 35% as recommended by AASHTO T 342. Next, averages of the $|E^*|$ and ϕ for three replicate specimens were determined. Figures 10.1(a) and 10.1(b) show the average log-$|E^*|$ and average ϕ versus log(f) plots for the AC sample 1, respectively.

10.4.3.2 Creep Compliance Test

Creep tests were conducted for 1000 seconds on each specimen at five different temperatures of 14, 40, 70, 100, and 130 °F, starting at the lowest temperature and proceeding to the highest temperature as suggested by Park and Kim (2001). The applied stresses at each temperature level were approximated by trial to limit the total strain within 200 με after 1000 seconds of test period. The creep compliance $D(t)$ was found by dividing the creep strain by the input stress. A typical $D(t)$-test conducted on 14 °F temperature is shown in Figure 10.2. The figure shows the applied and feedback stress on the specimen, and the creep strain due to the applied stress.

10.4.3.3 Relaxation Modulus Test

Similar to the creep compliance test, relaxation tests were conducted for 1000 seconds on each of the specimens at five different temperatures 14, 40, 70, 100, and 130 °F, starting from the lowest temperature and proceeding to the highest temperature. The applied total strains were 50, 50, 75, 100, and 150 με at temperatures 14, 40, 70, 100, and 130 °F, respectively. The maximum total strain limit was set to 150 με to avoid any possibility of leaving the LVE range of the material. Finally, the $E(t)$ was found by dividing the relaxed

stress by the input strain. Figure 10.3 shows a typical $E(t)$ test at 14 °F test-temperature. The figure shows the input and feedback strains and the relaxed stress varying with time.

10.5 The Mastercurves

10.5.1 Dynamic or Complex Modulus Mastercurve

The time-temperature superposition principal (TTSP) was applied to develop $|E^*|$ mastercurves at 70 °F reference temperature. For fitting $|E^*|$ mastercurves the following sigmoid expression was used:

$$\log\left(|E^*|\right) = \delta_{MC} + \frac{\alpha}{1 + e^{\beta + \gamma \log(f_r)}}. \qquad (10.1)$$

In Equation 10.1, f_r is the reduced loading-frequency (Hz); δ_{MC} is the minimum attainable $|E^*|$-value; α is the vertical span of the $|E^*|$ function; $\alpha + \delta_{MC}$ is the maximum attainable value of $|E^*|$; β and γ are the shape parameters. The parameters (e.g. α, β, δ_{MC}, and γ) can be found by fitting laboratory tested $|E^*|$ mastercurve. For fitting frequency-temperature shift factor (a_T) functions following second degree polynomial expression is used:

$$\log\left[a_T\right] = aT_i^2 + bT_i + c. \qquad (10.2)$$

In Equation 10.2, a, b, and, c are fitting parameters. Figure 10.4(a) shows the fitting of the laboratory tested $|E^*|$ mastercurve by the Equation 1. The figure shows the development of $|E^*|$-mastercurve by horizontally shifting the tested $|E^*|$ at different temperatures and frequencies. The figure also shows the sigmoidal fitting of the $|E^*|$-mastercurve by the expression given in Equation 10.1 in case of AC sample 1. The fitting statistics are also included in this figure showing the value of coefficient of determination (R^2) to be very

close to unity. Figure 10.4(b) shows the frequency-temperature (a_T) various test-temperatures of the AC sample 1 and a_T-function fitted by the expression given in Equation 10.2. Figure 10.5 shows the tested mastercurve, fitted mastercurve, and after that 30 smoothened |E^*|-data points evaluated for later use in case of the AC sample 1.

10.5.2 Phase Angle Mastercurve

The same temperature shift factors for |E^*|-mastercurve is used to develop ϕ-mastercurve. The resulting ϕ-mastercurve is expected to be a single smooth curve. For fitting ϕ-mastercurve, following expression suggested by Rahman et al. (2016) is used:

$$\phi(f_r) = \xi_1 + \xi_2 \log(f_r) - \xi_3 \frac{\pi}{2} \alpha\gamma \frac{e^{\beta+\gamma\log(f_r)}}{\left(1+e^{\beta+\gamma\log(f_r)}\right)^2}. \quad (10.3)$$

In Equation 10.3, $\phi(f_r)$ is the phase angle; f_r is the reduced frequency in Hz; and α, β, and γ are the regression coefficients found by fitting |E^*|-function by Equation 10.1, and ξ_1, ξ_2, and ξ_3 are the fitting parameters. Figure 10.6(a) shows the development of ϕ-mastercurve for the AC sample 1 by horizontally shifting the tested ϕ at different test-temperatures and loading-frequencies. The same frequency-temperature shift factors which were found while generating |E^*|-mastercurve were used for generating ϕ-mastercurve. The figure also shows the fitted ϕ-mastercurve by the expression given in Equation 10.3. Figure 10.6(b) shows the tested, fitted ϕ-mastercurves, and after that 30 smoothened ϕ-data points for the AC sample 1. These 30 smoothened ϕ-data points were evaluated for later use in this study.

10.5.3 Creep Compliance Mastercurve

Similar to the $|E^*|$-function, the TTSP was applied to develop $D(t)$ mastercurves at 70 °F reference temperature. To have a smoother representation of $D(t)$ function, the developed mastercurve was pre-smoothened using piecewise-polynomial fit. Figure 10.7(a) shows the $D(t)$ at different temperatures and the developed mastercurve by shifting the creep compliance data along the time space in case of AC sample 1. Figure 10.7(b) shows the unsmooth and smoothened $D(t)$ function for the AC sample 1.

10.5.4 Relaxation Modulus Mastercurve

In this case, also, the TTSP was applied to develop the $E(t)$ mastercurves at 70 °F reference temperature. Again, to have a smoother representation of $E(t)$, the developed mastercurves were smoothened using piecewise-polynomial fit. Figure 10.8(a) shows the $E(t)$ at different temperatures and the developed mastercurve by shifting the $E(t)$ data along the time space for the AC sample 1. Figure 10.8(b) shows the unsmooth and smoothened $E(t)$ function for the AC sample 1.

10.6 Numerical of Interconversion

All LVE material functions are known to be mathematically equivalent for a certain mode of loading. The relationships among LVE material functions are based on the theory of linear differential and integral equations. Therefore, a given or source function, expressed in loading-time or loading-frequency domain, can be converted into a target function as long as the source function is known over a broadband loading-time or loading-frequency space. The numerical interconversion method used in this study was developed by Park

and Schapery (1999) for polymer materials, and therefore, never been applied in case of AC. Kim (2009) suggested similar method for AC with a simplified approach to consider time constant in the model. However, the approach may be considered as logically incorrect and as over-simplification of the method and thus, can result in erroneous target function.

10.6.1 Case 1: Relaxation Modulus as Source LVE Function

10.6.1.1 Complex Modulus from Relaxation Modulus

The relaxation behavior of a LVE material can be best represented by the generalized Maxwell model (also called Wiechert model) in Figure 10.9(a). When a LVE material is represented by the generalized Maxwell model, consisting of a spring and *m*-Maxwell elements as in Figure 10.9(b) connected in parallel, the $E(t)$ can be derived and given as -

$$E(t) = E_e + \sum_{i=1}^{m} E_i e^{-(t/\rho_i)} \tag{10.4}$$

where E_e is the equilibrium modulus or long-time modulus; E_i are the relaxation strengths; and ρ_i are the relaxation times. The parameters, E_e, E_i, and ρ_i are positive constants. The Equation 10.4 is also known as Prony series representation of $E(t)$. If η the viscosity of the dashpot, and E is the elastic modulus in the Maxwell material in Figure 10.9(b), the relaxation time (also called characteristic time) can be given as –

$$\rho = \frac{\eta}{E} \tag{10.5}$$

The creep behavior of a LVE material can be best represented by the generalized Voigt model (also called Kelvin model) in Figure 10.10(a). When a LVE material is

represented by the generalized Voigt model, consisting of a spring, a dashpot and *n* Voigt elements as in Figure 10.10(b) connected in series, $D(t)$ can be derived and given as -

$$D(t) = D_g + \frac{1}{\eta_0} + \sum_{j=1}^{n} D_j (1 - e^{-(t/\tau_j)}) \tag{10.6}$$

where D_g is the glassy compliance; η_0 is the zero-shear or long-time viscosity; D_j are the retardation strengths; and τ_j are the retardation times; all are positive constants. If η the viscosity of the dashpot, and D is the elastic compliance in the Voigt material in Figure 10.10(b), the retardation time (also called characteristic time) can be given as –

$$\tau = \eta D \tag{10.7}$$

The constants in Equations 10.4 and 10.6 can be obtained by fitting these expressions to the available experimental data. Note that, for viscoelastic solids like asphalt concrete, $\eta_0 \rightarrow \infty$; therefore, the second term in Equation 10.6 vanishes. The Boltzmann superposition integral representing stress-strain relation for a LVE material can be given as:

$$\sigma(t) = \int_0^t E(t-\tau) \frac{d\varepsilon(t)}{d\tau} \, d\tau \,. \tag{10.8}$$

Therefore, by using Equation 10.8, the integral relationship between the uniaxial $E(t)$ and $D(t)$ can be found as:

$$\int_0^t E(t-\tau) \frac{dD(\tau)}{d\tau} \, d\tau = 1 \qquad (t > 0) \,. \tag{10.9}$$

Using relationship between Carson transforms of $E(t)$ and $D(t)$ (also called *s*-multiplied Laplace transform) and complex function E^*, and finally, Equation 10.4, Park and

Schapery (1999) found the expressions for storage modulus $E'(\omega)$ and loss modulus $E''(\omega)$, which can be given respectively as:

$$E'(\omega) = E_e + \sum_{i=1}^{m} \frac{\omega^2 \rho_i^{\,2} E_i}{\omega^2 \rho_i^{\,2} + 1}, \text{ and} \tag{10.10}$$

$$E''(\omega) = \sum_{i=1}^{m} \frac{\omega \rho_i E_i}{\omega^2 \rho_i^{\,2} + 1}. \tag{10.11}$$

The complex or dynamic modulus $|E^*(\omega)|$ in circular frequency domain then can be found as:

$$\left|E^*(\omega)\right| = \sqrt{E'(\omega)^2 + E''(\omega)^2}\,. \tag{10.12}$$

and, the phase angle (ϕ) can be found as:

$$\phi(\omega) = \tan^{-1}\left(\frac{E''(\omega)}{E'(\omega)}\right). \tag{10.13}$$

In Equations 10.10, 10.11, 10.12, and 10.13, ω is the angular frequency of loading; ρ_i, E_i (i = 1, 2, …, m), E_e can be found by fitting tested $E(t)$ to the Prony series expression of $E(t)$ given by Equation 10.4. The relationship, $\omega = 2\pi f$ can be used to transform the angular frequency domain to ordinary frequency (f) domain. Figure 10.11(a) presents tested $E(t)$ fitted by Equation 10.4 in case of AC sample 1. The Prony series coefficients are also included in the figure. Figure 10.11(b) shows the $|E^*|$-function of AC sample 1 by using Equations 10.10, 10.11, and 10.12 and the relationship $\omega = 2\pi f$.

10.6.1.2 Creep Compliance from Relaxation Modulus

To determine $D(t)$, the unknown retardation strengths, D_j ($j = 1, 2, \ldots, n$) and D_g in Equation 10.6 can be found by using the Prony series coefficients of known $E(t)$ and thus solving the system of equations given as:

$$\left[\mathbf{A}\right]\left\{\mathbf{D}\right\} = \left\{\mathbf{B}\right\} \tag{10.14}$$

or, $A_{kj} D_j = B_k$ (summed on j; and $k = 1, 2, \ldots, p$), where,

$$A_{kj} = \begin{cases} E_e(1 - e^{-(t_k/\tau_j)}) + \sum_{i=1}^{m} \dfrac{\rho_i E_i}{\rho_i - \tau_j}\left(e^{-(t_k/\rho_i)} - e^{-(t_k/\tau_j)}\right) & \text{when} \quad \rho_i \neq \tau_j \\ \text{or} & \text{, and} \\ E_e(1 - e^{-(t_k/\tau_j)}) + \sum_{i=1}^{m} \dfrac{t_k E_i}{\tau_j} e^{-(t_k/\rho_i)} & \text{when} \quad \rho_i = \tau_j \end{cases}$$

(10.15)

$$B_k = 1 - \left(E_e + \sum_{i=1}^{m} E_i\, e^{-(t_k/\rho_i)}\right) \Big/ \left(E_e + \sum_{i=1}^{m} E_i\right) \tag{10.16}$$

The symbol, t_k denotes a discrete time. For the system of linear algebraic equation as in Equation 10.14, collocation method is effected when $p = n$ and the least squares method may be used when $p > n$. Equations 10.15 and 10.16 are found from substituting Equations 10.4 and 10.6 in Equation 10.9. Detail of this derivation and selection of sampling points t_k in Equation 10.14 are given in Park and Schapery (1999).

The retardation times, τ_j corresponding to a set of pre-selected relaxation times, ρ_i can be determined by a graphical root-finding method which uses the relationship between Carson transformed $E(t)$ and $D(t)$ given as:

$$\tilde{\tilde{E}}(s)\,\tilde{\tilde{D}}(s) = 1, \tag{10.17}$$

where,

$$\tilde{\tilde{E}}(s) \equiv s\int_0^\infty E(t)\, e^{-st} dt\,, \text{ and} \tag{10.18}$$

$$\tilde{\tilde{D}}(s) \equiv s\int_0^\infty D(t)\, e^{-st} dt\,. \tag{10.19}$$

The $\tilde{\tilde{E}}(s)$ and $\tilde{\tilde{D}}(s)$ in Equations 10.18 and 10.19 are referred as operational modulus and operational compliance, respectively. When $E(t)$ and $D(t)$ are represented by the Equations 10.4 and 10.6, respectively, the operational modulus and compliance can be found as:

$$\tilde{\tilde{E}}(s) = E_e + \sum_{i=1}^{m} \frac{s\rho_i\, E_i}{s\rho_i + 1}, \text{ and} \tag{10.20}$$

$$\tilde{\tilde{D}}(s) = D_g + \frac{1}{\eta_0\, s} + \sum_{j=1}^{n} \frac{D_j}{s\tau_j + 1}\,. \tag{10.21}$$

From Equation 10.20:

$$\lim_{s \to -(1/\rho_i)} \tilde{\tilde{E}}(s) = \pm\infty \qquad (i = 1, 2, ..., m) \tag{10.22}$$

Similarly, from Equation 10.21:

$$\lim_{s \to -(1/\tau_j)} \tilde{\tilde{D}}(s) = \pm\infty \qquad (j = 1, 2, ..., n) \tag{10.23}$$

From Equations 10.17 and 10.23, one can obtain:

$$\lim_{s \to -(1/\tau_j)} \tilde{E}(s) = 0 \qquad (j = 1, 2, ..., n) \tag{10.24}$$

Equation 10.24 indicates that for given ρ_i and E_i, the τ_j can be determined by taking the negative reciprocal of the solutions of expression $\tilde{E}(s) = 0$ where $s < 0$. Graphical representation of the source function can be used to expedite the solution. Also, the relaxation and retardation times for viscoelastic solids are interlaced with each other as:

$$\rho_1 < \tau_1 < \rho_2 \quad ... \quad \rho_{N-1} < \tau_{N-1} < \rho_N < \tau_N \tag{10.25}$$

A typical graphical solution, recommended by Park and Schapery (1999), of the expression $\tilde{E}(s) = 0$ is presented in the Figure 10.12(a). This graphical solution was obtained while converting complex modulus $E^*(\omega)$ test data to $D(t)$ for AC sample 1. Figure 10.12(a) shows $|\tilde{E}(s)|$ versus -1/s plot in logarithmic scale. The absolute value of $\tilde{E}(s)$ is used as because some of the negative numbers cannot be plotted in logarithmic scale. A total of 10,000 equidistant points in log-scale are plotted for the value of *-1/s* in between 1.0×10^{-8} to 1.0×10^{8}. The abscissa corresponding to each maximum gives the known ρ_i, and the abscissa corresponding to each minimum gives the unknown τ_j. The glassy compliance, D_g can be calculated from the following expression:

$$D_g = \frac{1}{E_e + \sum_{i=1}^{m} E_i} \tag{10.26}$$

Figure 10.12(b) shows the $D(t)$-function obtained from $E(t)$-function in case of AC sample 1.

10.6.2 Case 2: Creep Compliance as Source LVE Function

10.6.2.1 Relaxation Modulus from Creep Compliance

To evaluate $E(t)$ from $D(t)$ one need to fit the tested $D(t)$ data to Prony series representation of $D(t)$ given in Equation 10.6. This fitting operation will ultimately evaluate the values of D_j, τ_j, and D_g. The retardation time τ_j is generally pre-selected with a log decade interval. Figure 10.13 shows the $D(t)$ of AC sample 1 fitted by the Prony series expression in Equation 10.6. The coefficients are also incorporated in the figure.

The unknown relaxation strengths, E_i (i = 1, 2, …, m) and equilibrium modulus E_e in Equation 10.4 then can be determined by using the Prony series coefficients of known $D(t)$ and thus solving a system of equations given as:

$$[\mathbf{C}]\{\mathbf{E}\} = \{\mathbf{F}\} \tag{10.27}$$

or, $C_{ki}E_i = F_k$ (summed on i; and k = 1, 2, …, p), where,

$$C_{ki} = \begin{cases} D_g e^{-(t_k/\rho_i)}) + \sum_{j=1}^{n} \dfrac{\rho_i D_j}{\rho_i - \tau_j}\left(e^{-(t_k/\rho_i)} - e^{-(t_k/\tau_j)}\right) & when \rho_i \neq \tau_j \\ \qquad\qquad or \qquad\qquad & \text{, and} \\ D_g e^{-(t_k/\rho_i)}) + \sum_{j=1}^{n} \dfrac{t_k D_j}{\tau_j} e^{-(t_k/\rho_i)} & when \rho_i = \tau_j \end{cases} \tag{10.28}$$

$$F_k = 1 - \left(D_g + \sum_{j=1}^{n} D_j \left(1 - e^{-(t_k/\tau_j)}\right)\right) \Big/ D_g + \sum_{j=1}^{n} D_j \,. \tag{10.29}$$

Equations 10.28 and 10.29 also found from substituting Equations 10.4 and 10.6 in Equation 10.9. The ρ_i corresponding to a set of pre-selected τ_j can be determined by root-

finding method using the relationship between Carson transformed $E(t)$ and $D(t)$. From Equations 10.17 and 10.22, one can obtain:

$$\lim_{s \to -(1/\rho_i)} \tilde{D}(s) = 0 \qquad (i = 1, 2, ..., m). \tag{30}$$

This also indicates, for given τ_j and D_j, the ρ_i can be determined by taking the negative reciprocal of the solutions of expression $\tilde{D}(s) = 0$ where $s < 0$. Graphical root finding method can be used to evaluate the unknown ρ_i. Figure 14(a) shows $|\tilde{D}(s)|$ versus -1/s plot in logarithmic scale in case of AC sample 1. The abscissa corresponding to each maximum gives the unknown ρ_i, and the abscissa corresponding to each minimum gives the known retardation time, τ_j. The E_e can be determined from the expression given as:

$$E_e = \frac{1}{D_g + \sum_{j=1}^{n} D_j}. \tag{10.31}$$

After evaluating all the ρ_i, E_i and E_e, Equation 10.4 can be used to determine $E(t)$. Figure 10.14(b) shows the converted $E(t)$ found from tested $D(t)$ by the method described. The calculated Prony series coefficients are also included in the figure.

10.6.2.2 Complex Modulus from Creep Compliance

The storage modulus, $E'(\omega)$ and loss modulus $E'(\omega)$ can be determined by substituting Prony coefficients already determined in earlier section in the Equations 10.10 and 10.11, and finally the $E^*(\omega)$ and $\phi(\omega)$ can be found by Equations 10.12 and 10.13, respectively. Also, the angular frequency domain can be transformed into ordinary frequency domain

by using the relationship $\omega = 2\pi f$. Figure 10.16 shows the converted |*E**|-function from *D*(*t*) function.

10.6.3 Case 3: Complex Modulus as Source LVE Function

10.6.3.1 Relaxation Modulus from Complex Modulus

Equation 10.10 can be used to fit storage modulus, $E'(\omega)$ data transformed in angular frequency space which can be found from |*E**|-test. This fitting operation will evaluate the Prony coefficients ρ_i, E_i, and E_e. Figure 10.16(a) shows the Prony series fit for $E'(\omega)$ in case of AC sample 1. The evaluated Prony series coefficients are also included in this figure. After that, to determine *E*(*t*) Equation 10.4 can be used which is shown in Figure 10.16(b) for AC sample 1.

10.6.3.2 Creep Compliance from Complex Modulus

For *D*(*t*), Equations 10.14, 10.15, and 10.16 can be used to determine D_j. The same root finding method described in earlier sections can be employed to find the corresponding τ_j for pre-selected ρ_i. Figure 10.17(a) shows the graphical method of finding τ_j. The glassy compliance D_g can be found from Equation 10.26. Figure 10.17(b) shows the *D*(*t*) function found by this process for the AC sample 1.

10.7 Development of Computer Programs

A set of MATLAB® computer programs were written to implement the numerical interconversion method developed in the earlier section. These are presented in Appendix I of this document.

10.8 Comparison of Laboratory Tested Material Functions

Figures 10.18(a) and 10.18(b) presents the $|E^*|$ mastercurves for the two AC samples in log-log scale and in normal scale up to 1000 seconds reduced frequency. Higher $|E^*|$-values in case of AC sample 1 can be observed in these figures at the mid and lower loading-frequency regions, which also corresponds to the normal to high-temperature |E*|-values. This is due to the use of higher grade binder in AC sample 1. However, at higher-frequency region, AC sample 2 shows higher $|E^*|$-values. Figure 10.18(c) presents the ϕ versus f_r plots for the AC samples. Higher ϕ-values can be observed at mid and high-frequency region in case of AC sample 1.

Figures 10.19(a) and 10.19(b) show the $D(t)$ mastercurves for the two AC samples in log-log scale and in normal scale up to f_r = 1000 sec. In general, higher $D(t)$-values can be observed in case of AC sample 1 with intermediate grade binder when compared to $D(t)$-values of AC sample 2 with higher graded binder. Figure 10.19(c) and 10.19(d) shows the tested $E(t)$ mastercurves of the AC samples in log-log scale and semi-scale up to f_r = 1000. In general, lower E(t)-values can be observed in case of AC sample 1 when compared to $E(t)$ of AC sample 2 which has higher grade binder.

10.9 Comparison of Tested and Converted Material Functions

10.9.1 Dynamic Modulus

Figures 10.20 shows the $|E^*|$-functions obtained from laboratory test, and converted from $D(t)$ and $E(t)$-functions for both of the AC samples. To observed the overall differences in these functions log-log scale is used. To observed the differences in these functions at the intermediate loading-frequency region, normal scale up to f_r = 1000 Hz is considered. In

general, it can be observed from these figures that $|E^*|$-function converted from $D(t)$ matches the tested data better than the $|E^*|$ converted from $E(t)$. However, $|E^*|$-function for both of the AC samples converted from $E(t)$ gives lower estimates of $|E^*|$-values for almost the entire loading-frequency domain considered.

10.9.2 Phase Angle

Figures 10.21(a) and 10.21(b) show the ϕ-functions obtained from laboratory test, and converted from $E(t)$ and $D(t)$ functions for AC sample 1 and AC sample 2, respectively. In general, for both of the AC samples, ϕ-functions converted from $D(t)$ matching better with the tested data. However, ϕ-function converted from $E(t)$ shows smaller peak ϕ compared to the peak ϕ determined from other two sources.

10.9.3 Creep Compliance

Figures 10.22 shows the $D(t)$-functions obtained from laboratory test, and converted from $E(t)$ and $|E^*|$-functions for both of the AC samples. Also, to observed the overall differences in these functions log-log scale is used. Again, to observed the differences in these functions at the intermediate loading-time region, normal scale up to t_r = 1000 seconds is considered. Overall, considering these functions in log-log scale, converted $D(t)$-functions from $|E^*|$ are matching the actual test data better than the converted $D(t)$-functions from $E(t)$. However, at intermediate time region, converted $D(t)$ from $E(t)$ is found to be better matching the actual test data in case of AC sample 1.

10.9.4 Relaxation Modulus

Figure 10.23 presents the $E(t)$-functions obtained from laboratory test, and converted from $D(t)$ and $|E^*|$-functions for both of the AC samples, in log-log scale and in normal scale up

to t_r = 1000 seconds. The converted $E(t)$ from $D(t)$ can be found to be matching fairly to the tested $E(t)$-functions. However, in general, converted $E(t)$-functions from $|E^*|$-functions show higher estimates.

10.9.5 Statistical Analysis

To check if the LVE material functions found from various sources are significantly different or not, statistical package called single factor analysis of variance (ANOVA) was in this study. ANOVA is a collection of statistical models generally used to analyze the differences among data-group means and variation among and between groups. In its simplest form, ANOVA is used to conduct a statistical test of whether or not the means of several data-groups are equal, and therefore generalizes the *t*-test to more than two data-groups.

Table 10.3 and Table 10.4 present the data summary and the results of ANOVA analysis of the LVE functions from various sources for AC sample 1 and AC sample 2, respectively. The statistical α-value in all the ANOVA analyses is considered to be 0.05. For $|E^*|$ and ϕ-functions, the data points between $1x10^{-6}$ Hz and $1x10^{6}$ Hz loading-frequencies, and for $D(t)$ and $E(t)$-functions, data points between $1x10^{-6}$ sec and $1x10^{6}$ sec loading-times were considered in the ANOVA analyses. These ranges of loading frequency or loading time, approximately corresponds to the tested and converted data-ranges evaluated for the LVE functions. In brief, Tables 10.3 and 10.4 present the statistical *p*-values and the *f*-statistics for the data-groups. For AC sample 1, the statistical *p*-values for $|E^*|$, $D(t)$, and $E(t)$ functions found from various sources found greater than the "Type I Error" assumption of α = 0.05 with *F*-values to be less than the $F_{critical}$-values. This indicates that the null hypothesis, which considers that, related LVE functions from

different sources are from a common population, is to be true, and therefore, these is no significant difference in data from different sources. However, in case of ϕ-functions, the p-value and F-values are found to be $p = 0.03$ which is less than $\alpha = 0.05$, and $F = 3.59$ which is greater than $F_{critical} = 3.09$, indicating significant difference in the three groups of ϕ-data. For AC sample 2, the statistical p-values for $|E^*|$, ϕ, and $D(t)$ functions found from various sources found greater than the "Type I Error" assumption of $\alpha = 0.05$ with F-values to be less than the $F_{critical}$-values. Therefore, there are no significant differences of these LVE functions from various sources. However, in case of $E(t)$-functions, the p-value and F-values are found to be $p = 0.04$ which is less than $\alpha = 0.05$, and $F = 3.17$ which is greater than $F_{critical} = 3.05$, indicating significant difference in the three groups of $E(t)$-data.

10.9.6 Discussion on the Tested and Converted Material Functions

The ANOVA analyses indicate there are significant differences in the ϕ-data for AC sample 1 and $E(t)$-data for AC sample 2 found from laboratory tests and converted from other LVE material functions. However, observing p and F-values of these LVE functions found from different sources, one can recognize that, these values are not varying too much from the limiting values, and, considering specimen to specimen variation of the test results, the statistically significant differences can be justified as minimal, especially, when someone considering modeling materials like asphalt concrete.

The comparison of various tested and converted LVE material functions for the AC samples are presented in earlier paragraphs. By observing these comparisons, one can easily recognize that laboratory tested relaxation modulus $E(t)$ and LVE material functions converted from this $E(t)$ deviating much from the other LVE material functions tested or

converted from complex modulus E^* or creep compliance $D(t)$. The exact reasons about this deviation caused by $E(t)$ or its target function are yet to be investigated. The possible reason may be due to different control mechanisms of the tests. $E(t)$ tests are done in a strain controlled mechanism while the laboratory test for E^* or $D(t)$ are stress controlled. The device used in this study for testing uses a load cell for stress-controlled tests. On the other hand, in a strain controlled test, e.g. relaxation modulus, the strain in the material specimen is controlled by the LVDTs attached to it. The average strain from the three LVDTs is accounted as the feedback strain from the system for a given input strain. In case of material like AC, mostly showing time dependent deformation under load, the system tries back and forth to adjust the strain level constant over time in a strain-controlled test, such as, in relaxation test. Figure 10.24 shows the input strain and the feedback strain from the system in a strain controlled, relaxation test. As the asphalt specimen continues to relax the system try back and forth to reach the feedback strain to be equal to the input strain. Therefore, although the given input strain level is 50 με, the actual strain level in the material seems to be moving between approximately 47 με to 53 με. This phenomenon may cause a little erroneous E(t)-function, and thus can explain the deviation in target functions converted from $E(t)$-function.

10.10 Validation by Finite Element Modelling

As a second attempt, finite element method (FEM) of modeling activity in cased of AC was undertaken in this study to validate the numerical method of interconversion of LVE material functions documented. The commercial FEM software ABAQUS® 6.14 was used in this study to develop the FEM model. However, before going to any details of the validation process, a brief summary of the processes and calculation involved in FEM

modeling for linear viscoelastic material with ABAQUS® is presented in the following sections.

10.10.1 Constituents of ABAQUS Linear Viscoelastic FEM Model

10.10.1.1 Shear Behavior Under Small Strain

If a time varying shear strain, $\gamma(t)$, is applied to a LVE material, the shear strain response can be defined as –

$$\tau(t) = \int_0^t G_R(t-s)\,\dot{\gamma}(s)\,ds \tag{10.32}$$

where, $G_R(t)$ is the time-dependent "shear relaxation modulus" that characterizes the response of the material. Now, consider a relaxation test (in shear mode) in which a sudden strain (γ) is applied to a specimen at $t = 0$, as in a step function and held constant for a long time. Thus, from Equation 10.32, one can obtain –

$$\tau(t) = \int_0^t G_R(t-s)\,\dot{\gamma}(s)\,ds = G_R(t)\,\gamma \qquad (\text{since } \dot{\gamma} = 0 \text{ for } t > 0), \tag{10.33}$$

where γ is the constant strain. At $t = \infty$, $G_R(t) \rightarrow G_\infty$, a constant, called "long-term modulus". The $G_R(t)$ often written in dimensionless form, given as:

$$g_R(t) = \frac{G_R(t)}{G_0}, \tag{10.34}$$

where $G_0 = G_R(0)$, i.e. the shear relaxation modulus at $t = 0$, which is also called the instantaneous shear modulus. Thus, with the help of Equation 10.34, the Equation 10.32 can be also written as:

$$\tau(t) = G_0 \int_0^t g_R(t-s)\,\dot{\gamma}(s)\,ds \tag{10.35}$$

The dimensionless relation function has the limiting values of $g_R(0) = 1$, and $g_R(\infty) = G_\infty / G_0$.

10.10.1.2 Volumetric Behavior

The volumetric behavior can be written in a form that is similar to the shear behavior, and can be given as:

$$p(t) = -K_0 \int_0^t k_R(t-s)\,\dot{\varepsilon}^{vol}(s)\,ds, \tag{10.36}$$

where p is the hydrostatic pressure, K_0 is the instantaneous elastic bulk modulus, $k_R(t)$ is the dimensionless bulk relaxation modulus, and ε^{vol} is the volume strain.

10.10.1.3 Numerical Implementation in ABAQUS

ABAQUS assumes that the viscoelastic material is defined by a Prony series expansion of the dimensionless relaxation modulus, given as:

$$g_R(t) = 1 - \sum_{i=1}^{N} \bar{g}_i^P \left(1 - e^{-t/\tau_i^G}\right), \tag{10.37}$$

where N, $\bar{g}_i^P$, and τ_i^G are material constants, and $i = 1, 2, \ldots, N$. For linear isotropic case, substitution in small-strain expression for the shear stress yields:

$$\tau(t) = G_0 \left(\gamma - \sum_{i=1}^{N} \gamma_i\right), \tag{10.38}$$

where

$$\gamma_i = \frac{\bar{g}_i^P}{\tau_i^G} \int_0^t e^{-s/\tau_i^G} \; \gamma(t-s)\, ds \,. \tag{10.39}$$

The γ_i are interpreted as state variables that control the stress relaxation. The summation of all the γ_i is the "creep" strain, the difference between the total mechanical strain and the instantaneous elastic strain (the stress divided by the instantaneous elastic modulus), i.e.,

$$\gamma^{cr} = \sum_{i=1}^{N} \gamma_i \,. \tag{10.40}$$

In case of volumetric response, a similar Prony series expansion is used. This can be given as:

$$p(t) = -K_0 \left(\varepsilon^{vol} - \sum_{i=1}^{N} \varepsilon_i^{vol} \right), \tag{10.41}$$

where,

$$\varepsilon_i^{vol} = \frac{\bar{k}_i^P}{\tau_i^K} \int_0^t e^{-s/\tau_i^K} \; \varepsilon^{vol}(t-s)\, ds \tag{10.42}$$

ABAQUS assumes that, $\tau_i^G = \tau_i^K = \tau_i$.

10.10.1.4 Rate-Independent Part of the Material Response

The elastic modulus must be specified in ABAQUS to define the rate-independent part of the material behavior. The rate-independent elasticity can be defined in terms of either instantaneous elastic modulus or long-term elastic modulus, whichever is convenient. The

effective relation moduli are obtained by multiplying the instantaneous elastic moduli with the dimensionless relaxation functions. Thus, for linear isotropic case:

$$G_R(t) = G_0\left[1 - \sum_{k=1}^{N} \bar{g}_k^P\left(1 - e^{-t/\tau_k}\right)\right], \text{ and} \tag{10.43}$$

$$K_R(t) = K_0\left[1 - \sum_{k=1}^{N} \bar{k}_k^P\left(1 - e^{-t/\tau_k}\right)\right], \tag{10.44}$$

where, G_0 and K_0 are the instantaneous shear and bulk moduli determined from the values of instantaneous elastic moduli E_0 and Poisson's ratio ν_0, given as:

$$G_0 = \frac{E_0}{2\left(1+\nu_0\right)}, \text{ and} \tag{10.45}$$

$$K_0 = \frac{E_0}{3\left(1-2\nu_0\right)}. \tag{10.46}$$

If the long-term elastic moduli are defined, the instantaneous moduli are determined from:

$$G_\infty = G_0\left(1 - \sum_{k=1}^{N} \bar{g}_k^P\right), \text{ and} \tag{10.47}$$

$$K_\infty = K_0\left(1 - \sum_{k=1}^{N} \bar{k}_k^P\right). \tag{10.48}$$

10.10.2 Development of the Dynamic Linear Viscoelastic Finite Element Model

10.10.2.1 Model Geometry, Boundary Condition, and Mesh Generation

A FEM model with three-dimensional geometry was chosen in this study to model the behavior of linear viscoelastic asphalt concrete. The model has the same dimensions as the AC test-specimens used for E^*, $E(t)$, and $D(t)$ testing in the laboratory. Figure 10.25 presents a schematic of the FEM geometry considered in this study. This geometry of the FEM model is chosen so that the model represents exactly the laboratory test-specimen, and therefore, the test data obtained in the laboratory can be used directly to validate the finite element analysis (FEA) model. As boundary condition, the base of the AC FEM model was kept at a fixed position with 17 restraints as shown in Figure 10.25. Sixteen of these restraints, having 2 degrees of freedoms (roller support) were used toward the circumference of the base. The remaining restraint with no degree of freedom (pinned support) was used at the center of the base. The restraints with 2 degrees of freedoms (roller support) were used to ensure that no constraints or stress generated in the horizontal (x-y) plane. The 8-noded brick element (C3D8) is used for the mesh generation of the FEM model. To avoid complexity, constant mesh sizes were used for the FEM model. Figure 10.26 shows the mesh elements of the FEM model. The dimensions of the larges mesh element are 0.2 inch in length, 0.2 inch in width, and 0.25 inch in depth.

10.10.2.2 Assigning Material Properties

Viscoelasticity of the AC material is assigned to the FEM according to the Generalized Maxwell Model. When a LVE material is represented by the generalized Maxwell model, consisting of a spring and m-Maxwell elements connected in parallel, the $E(t)$ can be given

by Equation 10.4. However, in ABAQUS the relaxation strengths are assigned as dimensionless number, as a fraction of instantaneous relaxation modulus, E_0, which can be defined as:

$$E_0 = E_e + \sum_{i=1}^{m} E_i \tag{10.48}$$

Now, when the source function is $E(t)$, using Equation 10.4 and 10.48, one can derive:

$$E(t) = E_0 - \sum_{i=1}^{m} E_i + \sum_{i=1}^{m} E_i e^{-(t/\rho_i)}$$

or,
$$E(t) = E_0 - \sum_{i=1}^{m} E_i \left(1 - e^{-(t/\rho_i)}\right)$$

or,
$$E(t) = E_0 \left[1 - \sum_{i=1}^{m} \frac{E_i}{E_0} \left(1 - e^{-(t/\rho_i)}\right)\right] \tag{10.49}$$

Taking the dimensionless relaxation strengths,

$$e_i = \frac{E_i}{E_0} = \frac{E_i}{E_e + \sum_{i=1}^{m} E_i}, \tag{10.50}$$

the Equation 10.49 can be rewritten as:

$$E(t) = E_0 \left[1 - \sum_{i=1}^{m} e_i \left(1 - e^{-(t/\rho_i)}\right)\right]. \tag{10.51}$$

For a three dimensional, isotropic case ABAQUS uses Equations 10.43 and 10.44 for estimating shear and bulk relaxation moduli, respectively. However, considering a

simple case, as loading to in uniaxial direction, the dimensional relaxation function in Equation 10.43 and 10.44 can be replaced by Equation 10.51. The instantaneous shear and bulk moduli can be found from Equation 10.45 and 10.46. In this case, the Poisson's ratio of asphalt concrete is considered to be 0.35, which can be found in most of the literature. Long-time relaxation modulus (*Ee*), and relaxation strengths (E_i) summarized in Table 10.1 and Table 10.2 were used to calculate the dimensionless relaxation strengths (e_i) and the instantaneous modulus (E_0).

10.10.2.3 Load Application

For the validation of the FEM model, the sinusoidal stresses on the AC geometry were applied by periodic load defining method in ABAQUS. The definition uses Fourier series for the implementation of the perioding load. This can be given as:

$$a = A_0 + \sum_{n=1}^{N}\left[A_n \cos n\omega\left(t - t_0\right) + B_n \sin\, n\omega\left(t - t_0\right)\right] \qquad \text{for } t \geq t_0, \text{ and} \tag{10.52}$$

$$a = A_0 \qquad \text{for } t < t_0, \tag{10.53}$$

where, t_0, N, ω, A_0, A_n, and B_n, and, $n = 1, 2, \ldots, N$ are constants, and can be defined by the user to simulate sinusoidal loading on the model. For the present study, the values of these constants were set as: A_0 = -1 psi, N = 1, A_n = 0, B_n = 1, and t_0 = 0.01 second. The circular frequency, ω was obtained by the following relation:

$$\omega = 2\pi\ f \tag{10.54}$$

where, f is the ordinary frequency of the sinusoidal loading, i.e., 25, 10, 5, 1, 0.5, and 0.1 Hz for this study. To estimate the $E(t)$ and $D(t)$ from the FEM model, unit strain or unit

stress, can be applied as a step function to the FEM model, respectively. Generally, in ABAQUS, a pure step function cannot be assigned directly. Therefore, ramp functions with very small time to reach the constant stress or strain were used to simulate the step-loadings. For simulating creep and relaxation tests, a 1000 seconds of loading time is considered.

10.10.2.4 Dynamic FEM Analysis

For simulating load-displacement behaviors in cyclic, static-strain, or static-stress loading modes, the FEM model generated in this study should be considered as a dynamic system as the stress or strains varies as a function of time. Typically, a dynamic system is idealized by a mass, damper, and a spring subjected to loading. The general equation of a dynamic system can be written as:

$$[M]\{\ddot{u}\}+[C]\{\dot{u}\}+[k]\{u\}=\{F(t)\} \tag{10.55}$$

where $[M]=$mass of the system, $[C]=$damping coefficient, $[K]=$stiffness of the system, and $\{u\},\{\dot{u}\},\{\ddot{u}\}=$displacement, velocity, and acceleration respectively. There are two algorithms to solve the above differential equation. These are implicit and explicit algorithms. The implicit algorithm is used in the dynamic FEM due to its unconditional stability. As AC is considered to be an isotropic, viscoelastic material for which Generalized Maxwell Material model is used, there is no need to assign any additional damping to this layer (Wang and Al-Qadi 2013).

10.10.3 FEM Simulation Results for AC Sample 1

10.10.3.1 Dynamic Modulus

Figures 10.27, 10.28, and 10.29 show the E^*-test FEM simulations at various loading frequencies (25, 10, 5, 1, 0.5, 0.1 Hz) with dimensionless relaxation strengths (e_i) found from E^*, $E(t)$, and $D(t)$ test data, either by direct test or interconversion. The simulated $|E^*|$ for each of the cases are calculated by the expression given in Equation 2.9. Figure 10.30(a) shows the FEM-simulated $|E^*|$ and the laboratory tested and converted $|E^*|$ from various source functions at various loading frequencies. The two plots, i.e., the $|E^*|$ from $|E^*|$-test data, and the $|E^*|$ from FEM simulation when $|E^*|$-test data is used to find e_i and E_0, can be considered as the validation of the FEM model developed in this study. These two plots are close enough to claim the validity of the FEM model. The figure also shows the converted $|E^*|$ from $E(t)$ and $D(t)$ source functions and $|E^*|$ from FEM simulations when e_i and E_0 of respective source functions were used. In both of these cases, the simulated $|E^*|$ plots are found to be in close proximity of the converted $|E^*|$ plots found from laboratory tested $E(t)$ and $D(t)$-source functions. This indicates that a close convergence can be attended by using the developed numerical interconversion method.

10.10.3.2 Phase Angle

Figure 10.30(b) shows the FEM-simulated ϕ and the laboratory tested and converted ϕ from various LVE source functions at various loading frequencies. The two plots, i.e., the ϕ from ϕ-test data, and the ϕ from FEM simulation when $|E^*|$-test data is used to find the e_i and E_0 can be considered as the validation of the FEM model, as the two plots are close enough to claim the validity of the FEM model. The figure also shows the ϕ found by interconversion

of $E(t)$ and $D(t)$-functions and ϕ from FEM simulations when e_i and E_0 of respective source functions were used. In both of these cases, the simulated ϕ plots are found to be in close proximity of the ϕ plots found by converting laboratory tested $E(t)$ and $D(t)$-source functions. This also indicates that a close convergence can be attended by the developed numerical interconversion method.

10.10.3.3 Creep Compliance

Figure 10.31(a) shows the FEM-simulated $D(t)$-data when e_i and E_0 from various LVE source functions were used. The figure also incorporates the $D(t)$-data found from either by direct test or converted from E^* and $E(t)$-test data. All the FEM-simulated $D(t)$ can be seen in close proximity of the $D(t)$-data found from either by direct test or converted from E^* and $E(t)$-test data. This indicates the numerical interconversion method of LVE material functions can produce sufficiently accurate representation of the AC material behavior.

10.10.3.4 Relaxation Modulus

Similarly, Figure 10.31(b) shows the FEM-simulated $E(t)$-data when e_i and E_0 from various LVE source functions were used. The figure also incorporates the $E(t)$-data found from either by direct test or converted from E^* and $D(t)$-test data. All the FEM-simulated $E(t)$ can be found in close proximity of the $E(t)$-data found from either by direct test or converted from E^* and $D(t)$-test data, indicating sufficient accuracy of the interconversion method developed in this study.

10.10.4FEM Simulation Results for AC Sample 2

10.10.4.1 Dynamic Modulus

Figures 10.32, 10.33, and 10.34 show the FEM simulations of E^*-test at various loading frequencies with used dimensionless relaxation strengths (e_i) found from E^*, $E(t)$, and $D(t)$ test data, either by direct test or from interconversion. Figure 10.35(a) shows the FEM-simulated $|E^*|$ and the laboratory tested and converted $|E^*|$ from various source functions at various loading frequencies. The two plots, i.e., the $|E^*|$ from $|E^*|$-test data, and the $|E^*|$ from FEM simulation when $|E^*|$-test data is used to find e_i and E_0, are close enough to claim the validity of the FEM model developed for AC sample 2. The figure also shows the converted $|E^*|$ from $E(t)$ and $D(t)$ source functions and $|E^*|$ from FEM simulations when e_i and E_0 of respective source functions were used. In both of these cases, the simulated $|E^*|$ plots are in close proximity of the converted $|E^*|$ plots found from laboratory tested $E(t)$ and $D(t)$-source functions. Therefore, it can be said that close convergence can be attainable by using the numerical interconversion method documented herein.

10.10.4.2 Phase Angle

Figure 10.35(b) shows the ϕ found from FEM-simulation and the laboratory tested and converted ϕ from various LVE source functions. The ϕ from ϕ-test data, and the ϕ from FEM simulations when $|E^*|$-test data is used to find the e_i and E_0 are close enough to claim the validity of the FEM model. The figure also shows the ϕ found by interconversion of $E(t)$ and $D(t)$-functions and ϕ from FEM simulations when e_i and E_0 of respective source functions were used. In both of these cases, the simulated ϕ plots are found to be in close proximity of the ϕ plots found by converting laboratory tested $E(t)$ and $D(t)$-source

functions, indicating that a close convergence can be attended by the developed numerical interconversion method.

10.10.4.3 Creep Compliance

Figure 10.36(a) shows the $D(t)$-data derived from FEM simulation when e_i and E_0 from various LVE source functions were used. The figure also incorporates the $D(t)$-data found from either by direct test or converted from E^* and $E(t)$-test data. All the FEM-simulated $D(t)$ can be seen in close proximity of the $D(t)$-data found from either by direct test or converted from E^* and $E(t)$-test data. This indicates the numerical interconversion method of LVE material functions can produce sufficiently accurate representation of the AC material behavior.

10.10.4.4 Relaxation Modulus

Figure 10.36(b) shows the FEM-simulated $E(t)$-data when e_i and E_0 from various LVE source functions were used. The figure also incorporates the $E(t)$-data found from either by direct test or converted from E^* and $D(t)$-test data. All the FEM-simulated $E(t)$ can be found in close proximity of the $E(t)$-data found from either by direct test or converted from E^* and $D(t)$-test data, indicating sufficient accuracy of the interconversion method developed in this study.

10.10.5 General Discussion on FEA Results

The FEA analysis is conducted for two AC samples to justify the accuracy of the interconversion method developed in this study. The analysis showed significant accuracy of the method of interconversion. This also confirms that the deviations in tested and

converted LVE functions shown in Figures 10.19, 10.20, 10.21, and 10.22 are due to the sample to sample variation or the limitations associated with the laboratory testing, rather than the numerical interconversion method itself.

10.11 Conclusions

In this study, an exact numerical approach to interconvert one material function to another in case of asphalt concrete is also presented. Based on the results in this study, it can be concluded that the numerical method reviewed in this study proved to be applicable in case of asphalt concrete to interconvert one material function to another. Although, the converted and tested relaxation modulus seen to be not matched properly, with a certain tread off in degree of accuracy, the method can be well used for application in asphalt industry.

Table 10.1 Summary of Prony Series Coefficients for AC Sample 1

Dynamic Modulus from Creep Compliance				*Dynamic Modulus from Relaxation Modulus*	
τ_j	D_j	ρ_i	E_i	ρ_i	E_i
1.0000E-05	9.8712E-05	7.2092E-06	1.1019E+03	1.0000E-06	7.9004E+02
1.0000E-04	1.5127E-04	7.0272E-05	7.8668E+02	1.0000E-05	7.3305E+02
1.0000E-03	2.6894E-04	6.5295E-04	6.5819E+02	1.0000E-04	6.4151E+02
1.0000E-02	4.1041E-04	6.3413E-03	4.6257E+02	1.0000E-03	4.2815E+02
1.0000E-01	1.5823E-03	4.2920E-02	4.1938E+02	1.0000E-02	2.4306E+02
1.0000E+00	2.3990E-03	5.3158E-01	1.4822E+02	1.0000E-01	1.2124E+02
1.0000E+01	6.8314E-03	4.4225E+00	8.9530E+01	1.0000E+00	7.1319E+01
1.0000E+02	9.8586E-03	5.7039E+01	3.0587E+01	1.0000E+01	3.9271E+01
1.0000E+03	6.7599E-03	7.7462E+02	9.6092E+00	1.0000E+02	1.7026E+01
1.0000E+04	3.6994E-03	8.8796E+03	3.7935E+00	1.0000E+03	1.0813E+01
1.0000E+05	3.1340E-03	9.1137E+04	2.6489E+00	1.0000E+04	6.0969E+00
				1.0000E+05	2.3009E+00
				1.0000E+06	1.5925E+00
D_q =	2.6804E-04	E_e =	2.8199E+01	E_e =	1.9324E+01

Creep Compliance from Relaxation Modulus				*Creep Compliance from Dynamic Modulus*			
ρ_i	E_i	τ_j	D_j	ρ_i	E_i	τ_j	D_j
1.0000E-06	7.9004E+02	1.3238E-06	9.7825E-05	1.0000E-06	6.2666E+02	1.1722E-06	4.0765E-05
1.0000E-05	7.3305E+02	1.4412E-05	1.7847E-04	1.0000E-05	7.2114E+02	1.2529E-05	6.9546E-05
1.0000E-04	6.4151E+02	1.6460E-04	3.7001E-04	1.0000E-04	8.5040E+02	1.4257E-04	1.4331E-04
1.0000E-03	4.2815E+02	1.7854E-03	7.4043E-04	1.0000E-03	7.7584E+02	1.6403E-03	3.0345E-04
1.0000E-02	2.4306E+02	1.8392E-02	1.4334E-03	1.0000E-02	5.5550E+02	1.8872E-02	6.7929E-04
1.0000E-01	1.2124E+02	1.7343E-01	2.3287E-03	1.0000E-01	3.0838E+02	2.0395E-01	1.5072E-03
1.0000E+00	7.1319E+01	1.7411E+00	4.0801E-03	1.0000E+00	1.4461E+02	2.0102E+00	3.0659E-03
1.0000E+01	3.9271E+01	1.7097E+01	6.9494E-03	1.0000E+01	6.3694E+01	1.8135E+01	5.1407E-03
1.0000E+02	1.7026E+01	1.4435E+02	7.5890E-03	1.0000E+02	2.8748E+01	1.5654E+02	6.6909E-03
1.0000E+03	1.0813E+01	1.3763E+03	9.3020E-03	1.0000E+03	1.3908E+01	1.3763E+03	7.2398E-03
1.0000E+04	6.0969E+00	1.2694E+04	9.3535E-03				
1.0000E+05	2.3009E+00	1.1120E+05	4.9505E-03				
1.0000E+06	1.5925E+00	1.0839E+06	4.0557E-03				
E_e =	1.9324E+01	D_q =	3.2002E-04	E_e =	3.9804E+01	D_q =	2.4221E-04

Relaxation Modulus from Creep Compliance				*Relaxation Modulus from Dynamic Modulus*	
τ_j	D_j	ρ_i	E_i	ρ_i	E_i
1.0000E-05	9.8712E-05	7.2092E-06	1.1019E+03	1.0000E-06	6.2666E+02
1.0000E-04	1.5127E-04	7.0272E-05	7.8668E+02	1.0000E-05	7.2114E+02
1.0000E-03	2.6894E-04	6.5295E-04	6.5819E+02	1.0000E-04	8.5040E+02
1.0000E-02	4.1041E-04	6.3413E-03	4.6257E+02	1.0000E-03	7.7584E+02
1.0000E-01	1.5823E-03	4.2920E-02	4.1938E+02	1.0000E-02	5.5550E+02
1.0000E+00	2.3990E-03	5.3158E-01	1.4822E+02	1.0000E-01	3.0838E+02
1.0000E+01	6.8314E-03	4.4225E+00	8.9530E+01	1.0000E+00	1.4461E+02
1.0000E+02	9.8586E-03	5.7039E+01	3.0587E+01	1.0000E+01	6.3694E+01
1.0000E+03	6.7599E-03	7.7462E+02	9.6092E+00	1.0000E+02	2.8748E+01
1.0000E+04	3.6994E-03	8.8796E+03	3.7935E+00	1.0000E+03	1.3908E+01
1.0000E+05	3.1340E-03	9.1137E+04	2.6489E+00		
D_g =	2.6804E-04	E_e =	2.8199E+01	E_e =	3.9804E+01

Table 10.2 Summary of Prony Series Coefficients for AC Sample 2

Dynamic Modulus from Creep Compliance				Dynamic Modulus from Relaxation Modulus	
τj	Dj	ρi	Ei	ρi	Ei
1.0000E-05	1.2005E-04	6.3369E-06	1.7265E+03	1.0000E-06	4.3588E+02
1.0000E-04	1.3680E-04	7.1316E-05	8.0558E+02	1.0000E-05	4.1122E+02
1.0000E-03	1.8096E-04	7.2391E-04	5.6665E+02	1.0000E-04	4.8591E+02
1.0000E-02	2.2585E-04	7.2943E-03	4.2279E+02	1.0000E-03	4.6163E+02
1.0000E-01	8.5535E-04	4.9736E-02	5.3711E+02	1.0000E-02	3.2734E+02
1.0000E+00	1.4190E-03	5.4147E-01	2.3909E+02	1.0000E-01	1.8393E+02
1.0000E+01	3.8692E-03	4.5885E+00	1.4528E+02	1.0000E+00	1.1245E+02
1.0000E+02	5.3745E-03	5.8100E+01	5.2197E+01	1.0000E+01	6.0691E+01
1.0000E+03	5.9196E-03	6.8090E+02	2.4217E+01	1.0000E+02	2.8519E+01
1.0000E+04	1.0882E-02	6.3971E+03	1.8143E+01	1.0000E+03	1.8632E+01
1.0000E+05	3.3695E-03	9.0135E+04	3.2169E+00	1.0000E+04	1.4115E+01
				1.0000E+05	6.9743E+00
				1.0000E+06	3.8915E+00
Dg	2.1882E-04	Ee	3.0701E+01	Ee	2.0444E+01

Creep Compliance from Relaxation Modulus				Creep Compliance from Dynamic Modulus			
ρi	Ei	τj	Dj	ρi	Ei	τj	Dj
1.0000E-06	4.3588E+02	1.1984E-06	7.4907E-05	1.0000E-06	2.7435E+02	1.0902E-06	2.7779E-05
1.0000E-05	4.1122E+02	1.2346E-05	1.0609E-04	1.0000E-05	4.1396E+02	1.1604E-05	5.2958E-05
1.0000E-04	4.8591E+02	1.3792E-04	2.0872E-04	1.0000E-04	5.6041E+02	1.2765E-04	1.0425E-04
1.0000E-03	4.6163E+02	1.5751E-03	4.3045E-04	1.0000E-03	6.3591E+02	1.4555E-03	2.1654E-04
1.0000E-02	3.2734E+02	1.7148E-02	8.4645E-04	1.0000E-02	5.6271E+02	1.6948E-02	4.7188E-04
1.0000E-01	1.8393E+02	1.6901E-01	1.4194E-03	1.0000E-01	3.7483E+02	1.9095E-01	1.0389E-03
1.0000E+00	1.1245E+02	1.7347E+00	2.5537E-03	1.0000E+00	1.9559E+02	1.9608E+00	2.1416E-03
1.0000E+01	6.0691E+01	1.6723E+01	4.1605E-03	1.0000E+01	8.9595E+01	1.8186E+01	3.7104E-03
1.0000E+02	2.8519E+01	1.4595E+02	4.8370E-03	1.0000E+02	4.0335E+01	1.5791E+02	4.9132E-03
1.0000E+03	1.8632E+01	1.4123E+03	6.2355E-03	1.0000E+03	1.9154E+01	1.3754E+03	5.2787E-03
1.0000E+04	1.4115E+01	1.4548E+04	9.8181E-03				
1.0000E+05	6.9743E+00	1.2981E+05	9.5017E-03				
1.0000E+06	3.8915E+00	1.1973E+06	8.3321E-03				
Ee	2.0444E+01	Dg	3.8886E-04	Ee	5.4744E+01	Dg	3.1041E-04

Relaxation Modulus from Creep Compliance				Relaxation Modulus from Dynamic Modulus	
τj	Dj	ρi	Ei	ρi	Ei
1.0000E-05	1.2005E-04	6.3369E-06	1.7265E+03	1.0000E-06	2.7435E+02
1.0000E-04	1.3680E-04	7.1316E-05	8.0558E+02	1.0000E-05	4.1396E+02
1.0000E-03	1.8096E-04	7.2391E-04	5.6665E+02	1.0000E-04	5.6041E+02
1.0000E-02	2.2585E-04	7.2943E-03	4.2279E+02	1.0000E-03	6.3591E+02
1.0000E-01	8.5535E-04	4.9736E-02	5.3711E+02	1.0000E-02	5.6271E+02
1.0000E+00	1.4190E-03	5.4147E-01	2.3909E+02	1.0000E-01	3.7483E+02
1.0000E+01	3.8692E-03	4.5885E+00	1.4528E+02	1.0000E+00	1.9559E+02
1.0000E+02	5.3745E-03	5.8100E+01	5.2197E+01	1.0000E+01	8.9595E+01
1.0000E+03	5.9196E-03	6.8090E+02	2.4217E+01	1.0000E+02	4.0335E+01
1.0000E+04	1.0882E-02	6.3971E+03	1.8143E+01	1.0000E+03	1.9154E+01
1.0000E+05	3.3695E-03	9.0135E+04	3.2169E+00		
Dg	2.1882E-04	Ee	3.0701E+01	Ee	5.4744E+01

Table 10.3 ANOVA Analysis Results for AC Sample 1

Data Summary for |E*|-functions

Groups	*Count*	*Sum*	*Average*	*Variance*
|E*| from |E*|-test	32	41095.70484	1284.240776	2302207.874
|E*| from D(t)-test	32	37987.44561	1187.107675	1976399.801
|E*| from E(t)-test	32	26085.84868	815.1827711	1117193.233

	Source of Variation	*SS*	*df*	*MS*	*F*	*P-value*	*F crit*
ANOVA	Between Groups	3922969.448	2	1961484.724	1.090561767	0.340285664	3.094337433
	Within Groups	167269828.1	93	1798600.302			
	Total	171192797.6	95				

Data Summary for ϕ-functions

Groups	*Count*	*Sum*	*Average*	*Variance*
ϕ from |E*|-test	32	619.8842177	19.3713818	43.42665861
ϕ from D(t)-test	32	466.8178246	14.58805702	98.35282129
ϕ from E(t)-test	32	479.1813152	14.9744161	47.22244857

	Source of Variation	*SS*	*df*	*MS*	*F*	*P-value*	*F crit*
ANOVA	Between Groups	451.8696185	2	225.9348093	3.586230221	0.031597975	3.094337433
	Within Groups	5859.059783	93	63.00064282			
	Total	6310.929401	95				

Data Summary for D(t)-functions

Groups	*Count*	*Sum*	*Average*	*Variance*
D(t) from D(t)-test	100	1.24608048	0.012460805	0.00017012
D(t) from E(t)-test	32	0.53678103	0.016774407	0.000331197
D(t) from |E*|-test	34	0.337597327	0.009929333	0.000107435

	Source of Variation	*SS*	*df*	*MS*	*F*	*P-value*	*F crit*
ANOVA	Between Groups	0.000797046	2	0.000398523	2.119088247	0.123439099	3.051470854
	Within Groups	0.03065433	163	0.000188063			
	Total	0.031451376	165				

Data Summary for E(t)-functions

Groups	*Count*	*Sum*	*Average*	*Variance*
E(t) from E(t)-test	98	48927.27907	499.2579497	492300.3919
E(t) from D(t)-test	38	30641.4266	806.3533315	1226435.891
E(t) from |E*|-test	34	29420.60289	865.3118497	1344671.439

	Source of Variation	*SS*	*df*	*MS*	*F*	*P-value*	*F crit*
ANOVA	Between Groups	4718619.994	2	2359309.997	2.865376213	0.059766569	3.050119738
	Within Groups	137505423.5	167	823385.7692			
	Total	142224043.4	169				

Table 10.4 ANOVA Analysis Results for AC Sample 2

Data Summary for |E*|-functions

Groups	*Count*	*Sum*	*Average*	*Variance*
|E*| from |E*|-test	32	37341.99281	1166.937275	1504875.553
|E*| from D(t)-test	39	54993.75973	1410.096403	2622735.488
|E*| from E(t)-test	39	31360.2889	804.1099717	787039.5812

	Source of Variation	*SS*	*df*	*MS*	*F*	*P-value*	*F crit*
ANOVA	Between Groups	7242017.461	2	3621008.73	2.198628017	0.115943582	3.081192934
	Within Groups	176222594.8	107	1646940.138			
	Total	183464612.2	109				

Data Summary for ϕ-functions

Groups	*Count*	*Sum*	*Average*	*Variance*
ϕ from |E*|-test	32	553.3568007	17.29240002	52.51924752
ϕ from D(t)-test	39	595.7191333	15.27484957	62.77050454
ϕ from E(t)-test	39	553.3672222	14.18890313	32.36040871

	Source of Variation	*SS*	*df*	*MS*	*F*	*P-value*	*F crit*
ANOVA	Between Groups	171.76394	2	85.88197	1.752669405	0.178249234	3.081192934
	Within Groups	5243.071377	107	49.00066707			
	Total	5414.835317	109				

Data Summary for D(t)-functions

Groups	*Count*	*Sum*	*Average*	*Variance*
D(t) from D(t)-test	100	0.954336139	0.009543361	0.000117731
D(t) from E(t)-test	38	0.453591882	0.011936628	0.000197175
D(t) from |E*|-test	38	0.275959843	0.007262101	5.55248E-05

	Source of Variation	*SS*	*df*	*MS*	*F*	*P-value*	*F crit*
ANOVA	Between Groups	0.000415308	2	0.000207654	1.710244755	0.183864316	3.048211568
	Within Groups	0.021005281	173	0.000121418			
	Total	0.021420589	175				

Data Summary for E(t)-functions

Groups	*Count*	*Sum*	*Average*	*Variance*
E(t) from E(t)-test	91	50856.9855	558.8679725	468727.0206
E(t) from D(t)-test	38	36957.67707	972.5704492	1597976.954
E(t) from |E*|-test	38	32066.84417	843.8643202	1010596.9

	Source of Variation	*SS*	*df*	*MS*	*F*	*P-value*	*F crit*
ANOVA	Between Groups	5369011.352	2	2684505.676	3.174120214	0.044412792	3.051126821
	Within Groups	138702664.4	164	845747.9539			
	Total	144071675.8	166				

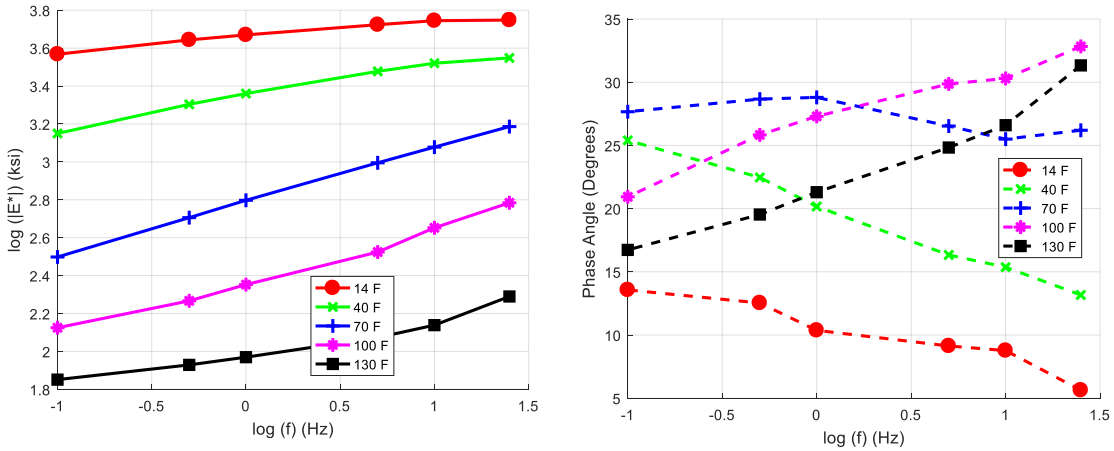

(a) (b)

Figure 10.1 (a) Average log-|E*| versus log-(f) plot, and (b) average ϕ versus log-(f) plot for AC sample 1.

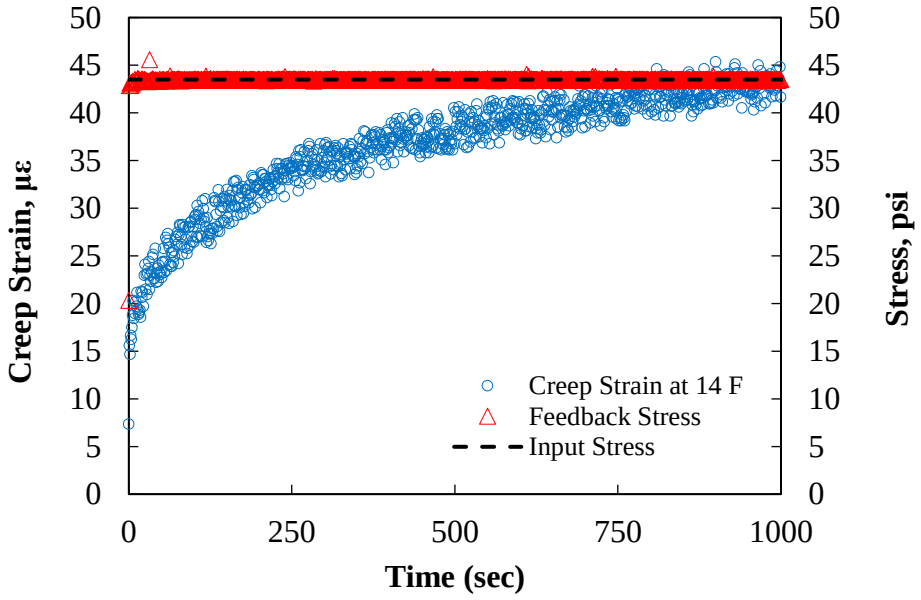

Figure 10.2 Typical uniaxial creep compliance test at 14 °F test temperature.

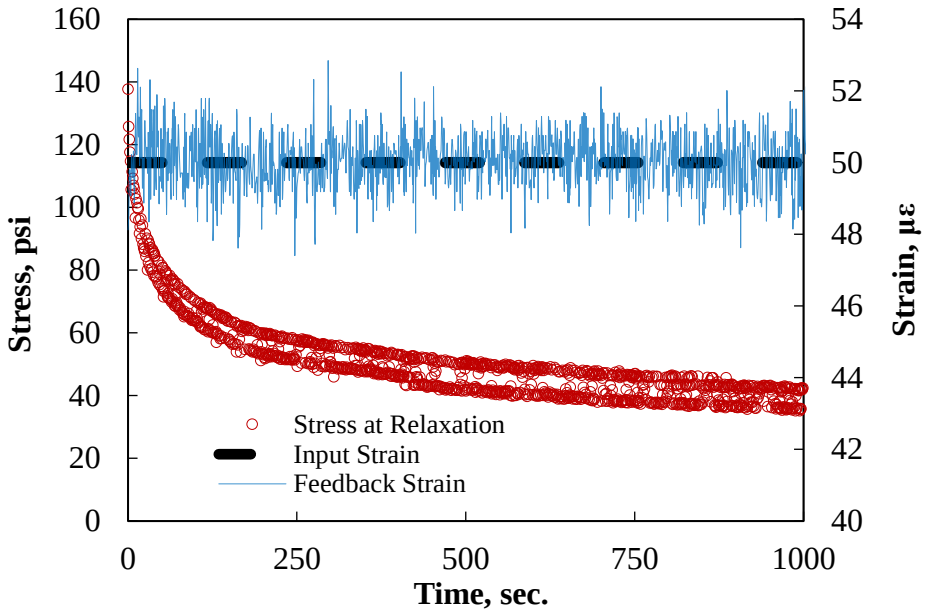

Figure 10.3 Typical uniaxial relaxation modulus test at 14 °F test temperature.

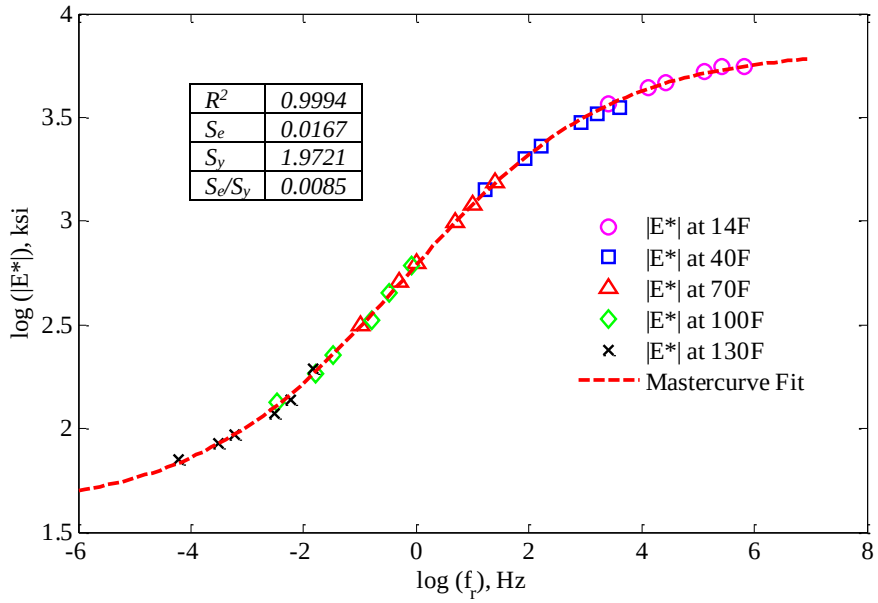

(a)

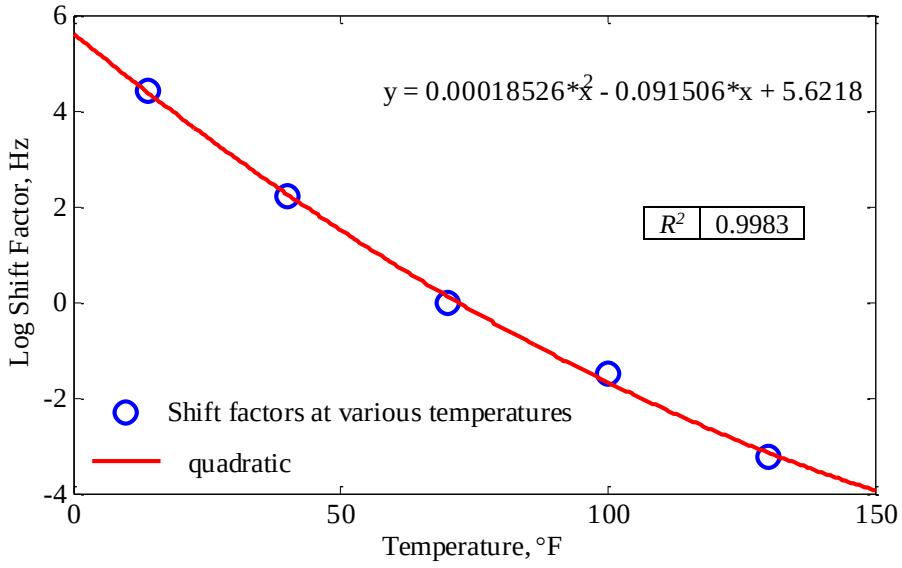

(b)

Figure 10.4 (a) Development and fitting of |E*|-mastercurve, and (b) fitted a_T-function.

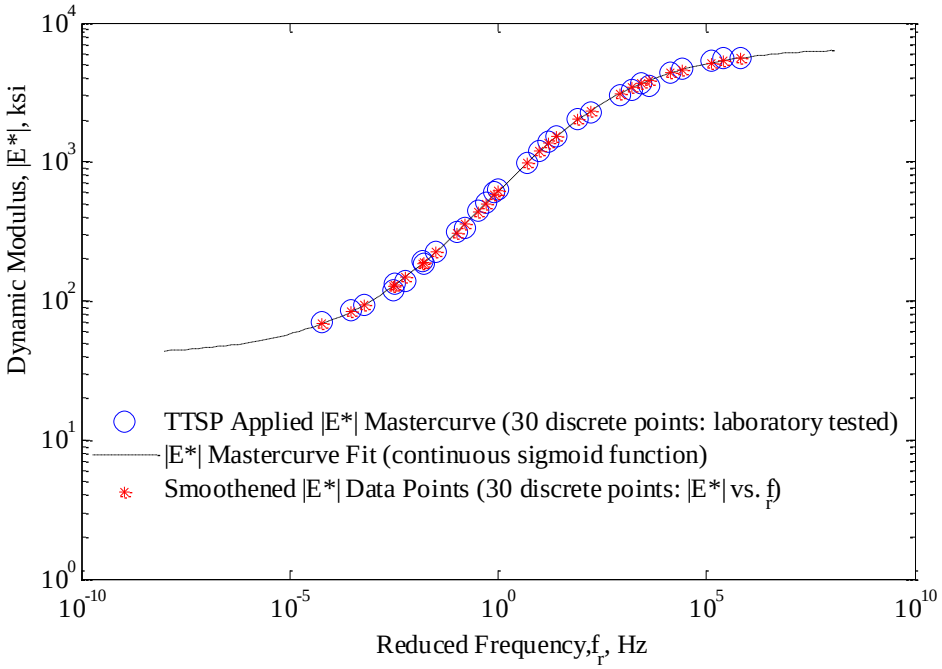

Figure 10.5 Tested and fitted |E*|-mastercurves and the 30-smoothened |E*|-data points.

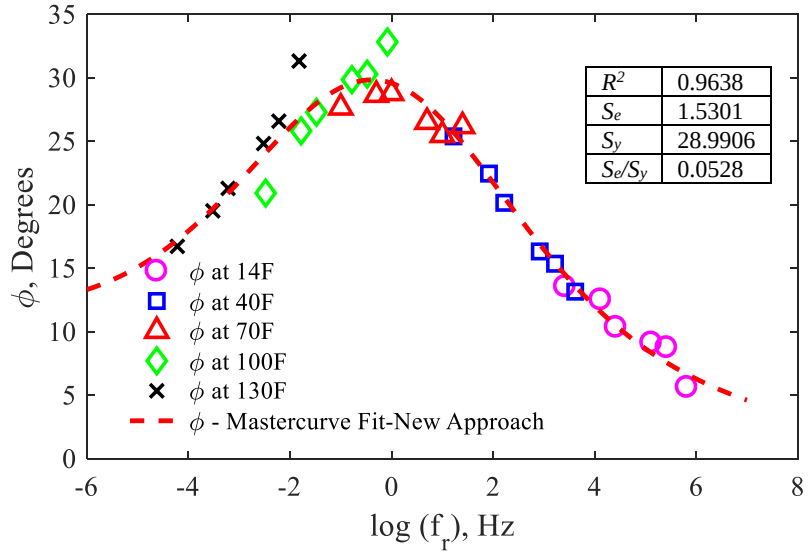

(a)

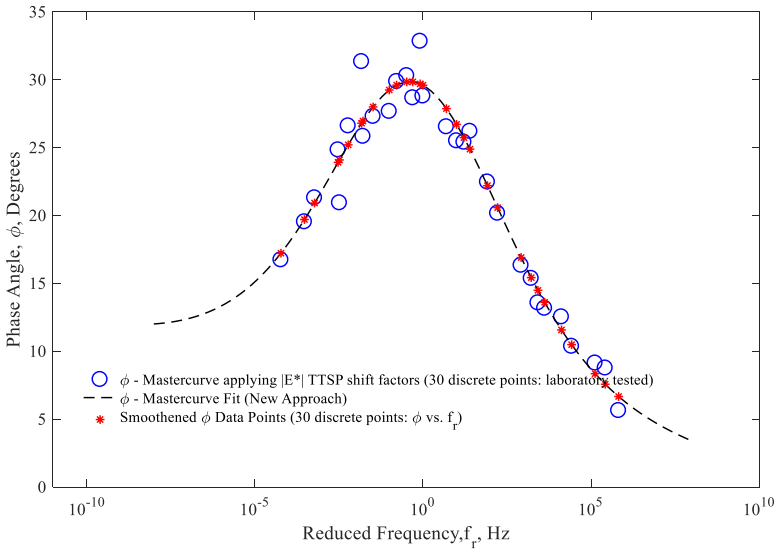

(b)

Figure 10.6 (a) Fitting of ϕ-mastercurve, and (b) tested and fitted ϕ-mastercurves and the 30-smoothened ϕ-data points.

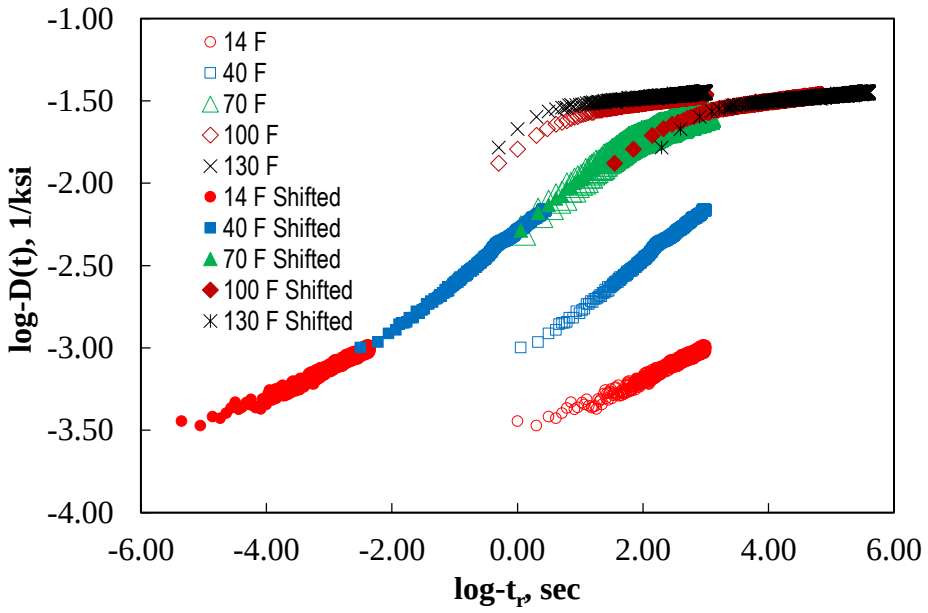

(a)

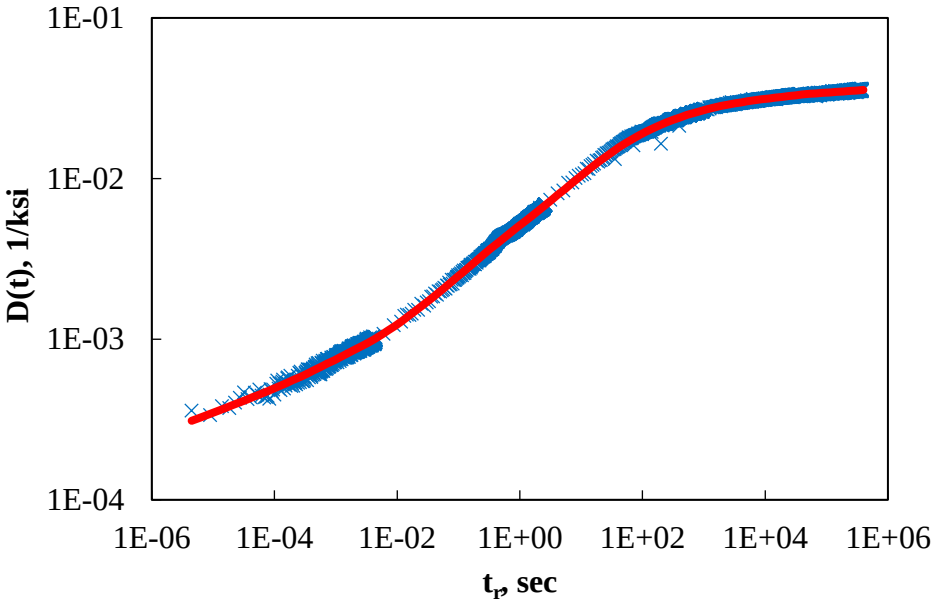

(b)

Figure 10.7 (a) Development of *D*(*t*)-function, and (b) unsmooth and smoothened D(t)-function.

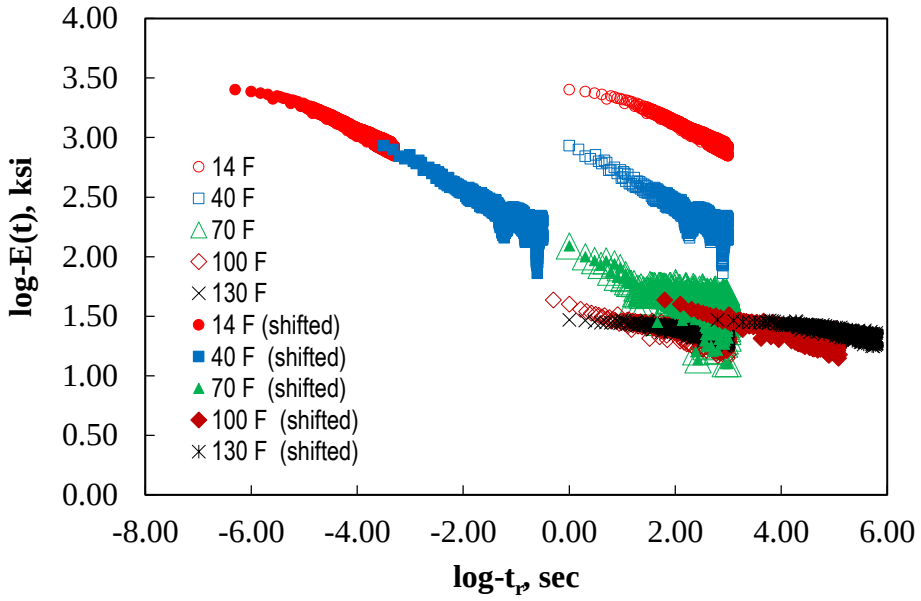

(a)

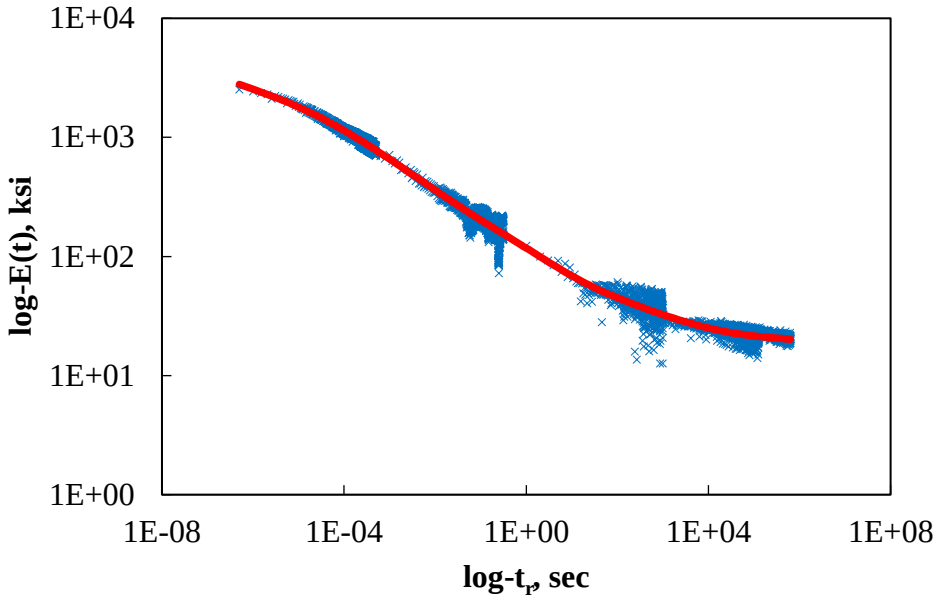

(b)

Figure 10.8 (a) Development of *E*(*t*)-function, and (b) unsmooth and smoothened E(t)-function.

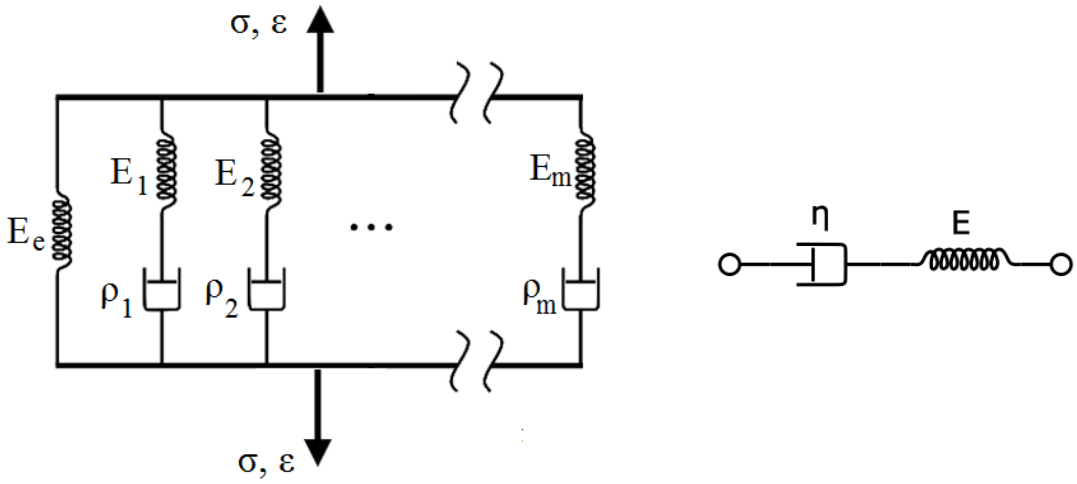

(a) (b)

Figure 10.9 (a) Generalized Maxwell or Maxwell-Wiechert model, and (b) Maxwell material.

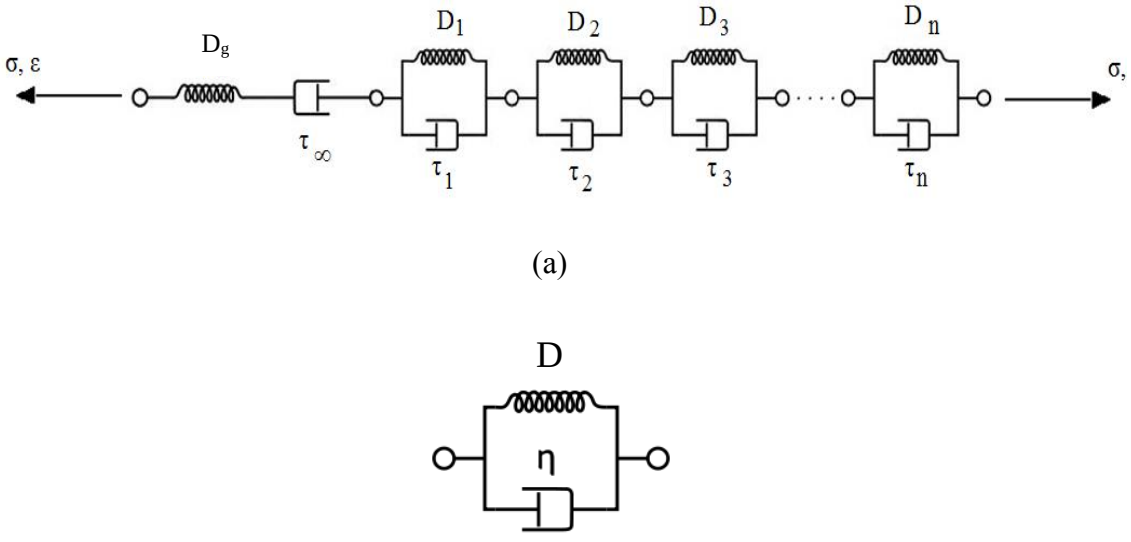

(a)

(b)

Figure 10.10 (a) Generalized Voigt model, and (b) Voigt material.

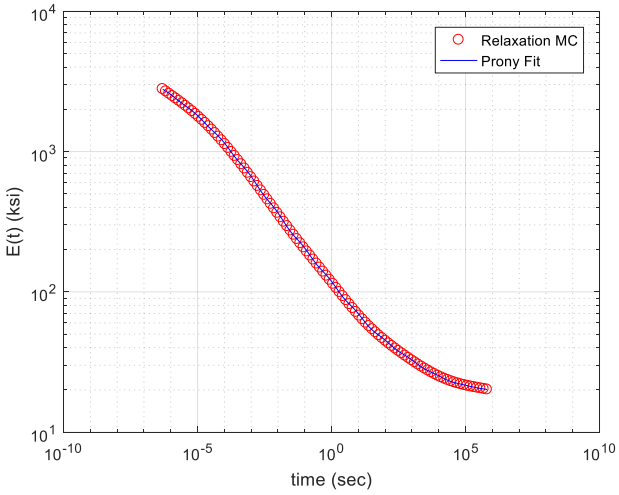

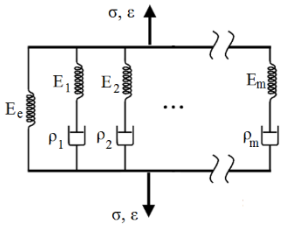

ρ_i	E_i
1.000E-06	7.900E+02
1.000E-05	7.330E+02
1.000E-04	6.415E+02
1.000E-03	4.282E+02
1.000E-02	2.431E+02
1.000E-01	1.212E+02
1.000E+00	7.132E+01
1.000E+01	3.927E+01
1.000E+02	1.703E+01
1.000E+03	1.081E+01
1.000E+04	6.096E+00
1.000E+05	2.303E+00
1.000E+06	1.587E+00
E_e = 1.933E+01	

(a)

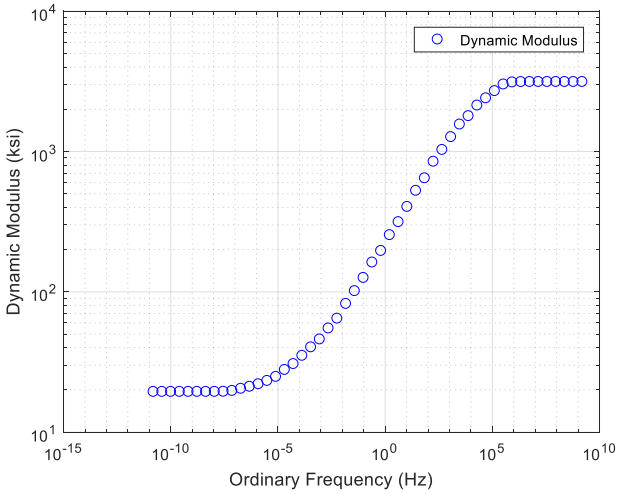

(b)

Figure 10.11 (a) Prony series fitting of $E(t)$, and (b) converted $|E^*|$ from $E(t)$ for AC sample 1.

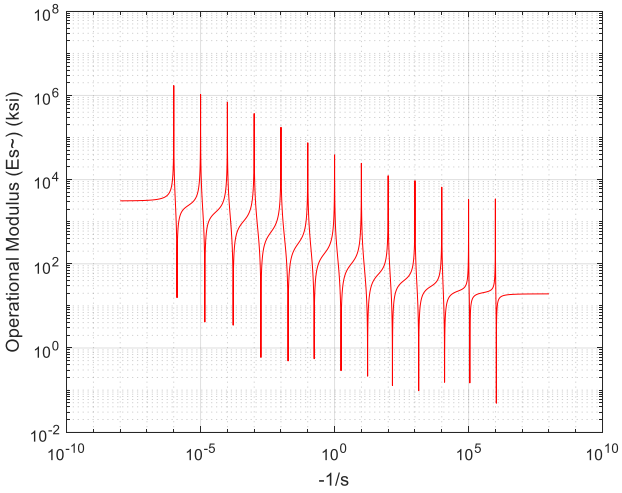

(a)

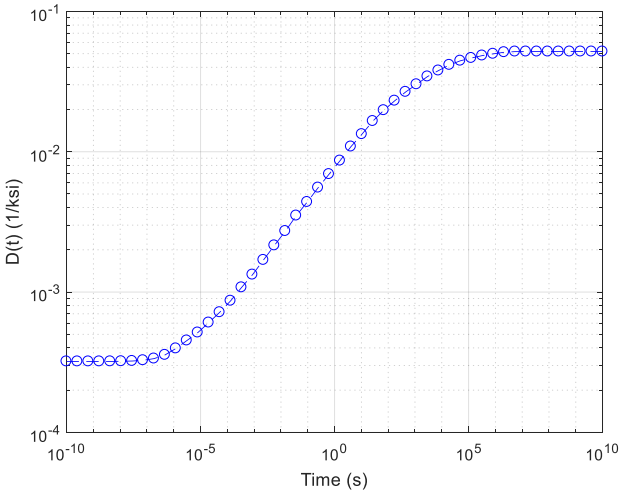

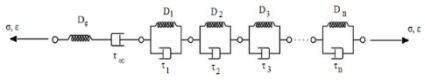

τ_i	D_i
1.324E-06	9.783E-05
1.441E-05	1.785E-04
1.646E-04	3.700E-04
1.785E-03	7.404E-04
1.839E-02	1.433E-03
1.734E-01	2.329E-03
1.741E+00	4.080E-03
1.710E+01	6.949E-03
1.443E+02	7.589E-03
1.376E+03	9.302E-03
1.269E+04	9.352E-03
1.112E+05	4.957E-03
1.084E+06	4.040E-03
D_g = 3.200E-04	

(b)

Figure 10.12 $\tilde{E}(s)$ versus -1/s plot, a root finding by graphical method, and (b) converted $D(t)$ from $E(t)$.

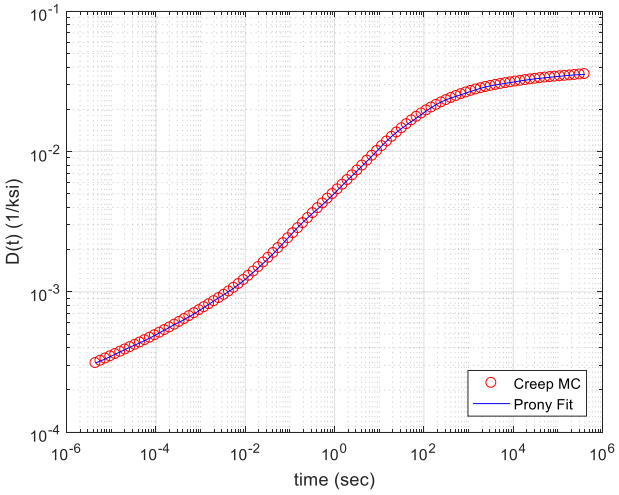

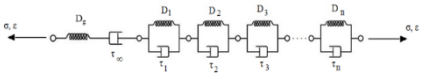

τ_i	D_i
1.000E-05	9.871E-05
1.000E-04	1.513E-04
1.000E-03	2.689E-04
1.000E-02	4.104E-04
1.000E-01	1.582E-03
1.000E+00	2.399E-03
1.000E+01	6.831E-03
1.000E+02	9.859E-03
1.000E+03	6.760E-03
1.000E+04	3.699E-03
1.000E+05	3.134E-03

D_g = 2.680E-04

Figure 10.13 Prony series fitting of $D(t)$ for AC sample 1.

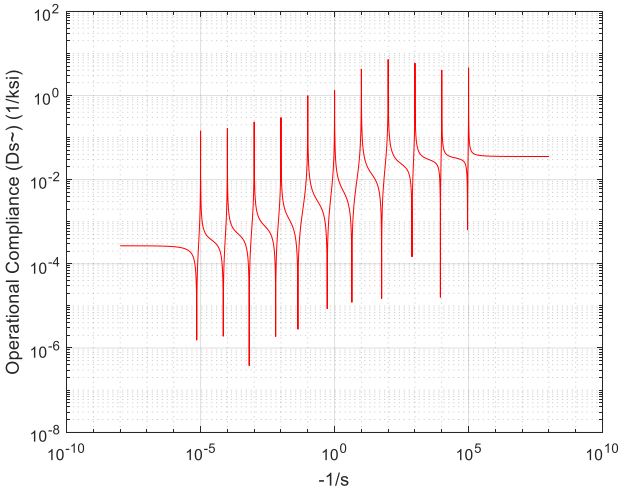

(a)

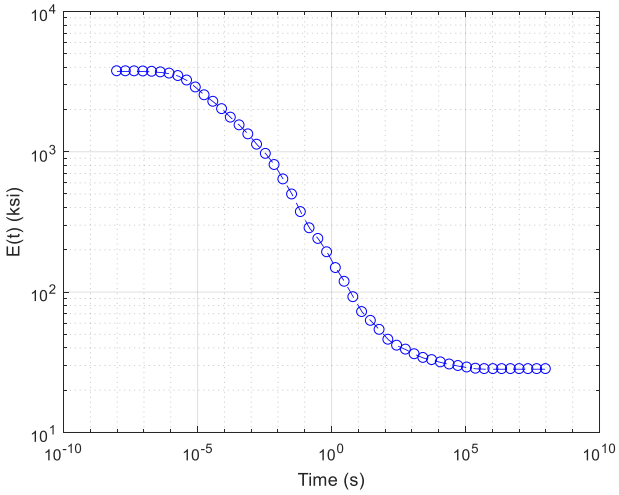

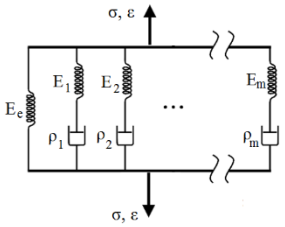

ρ_i	E_i
7.183E-06	1.104E+03
7.027E-05	7.865E+02
6.530E-04	6.578E+02
6.341E-03	4.625E+02
4.292E-02	4.196E+02
5.316E-01	1.483E+02
4.422E+00	8.954E+01
5.704E+01	3.059E+01
7.746E+02	9.609E+00
8.880E+03	3.793E+00
9.114E+04	2.649E+00

E_e = 2.820E+01

(b)

Figure 10.14 $\tilde{D}(s)$ versus -1/s plot, a root finding by graphical method, and (b) Converted $E(t)$ from $D(t)$.

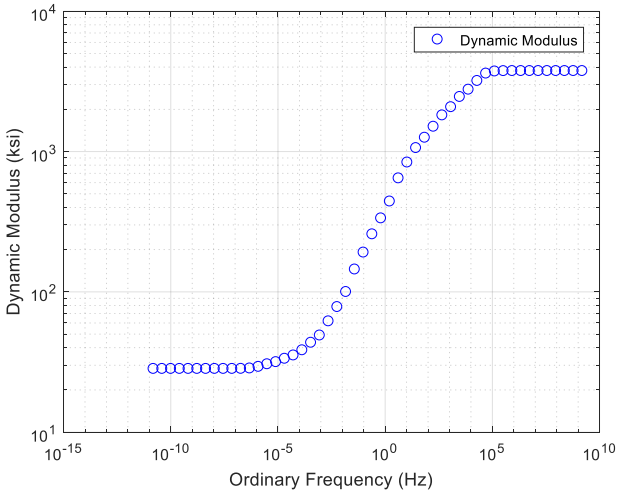

Figure 10.15 Converted |*E**| from *D*(*t*) for AC sample 1.

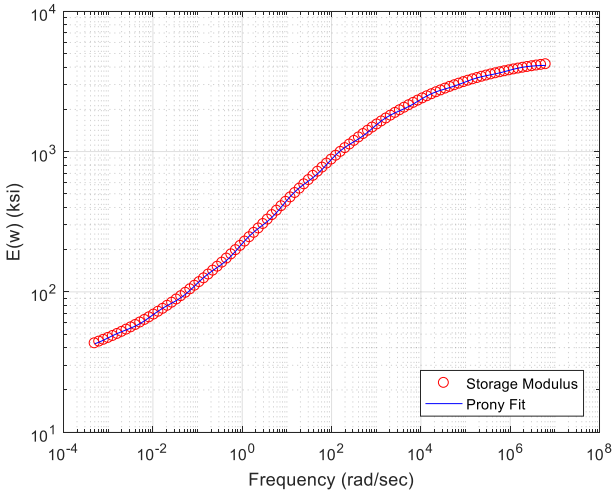

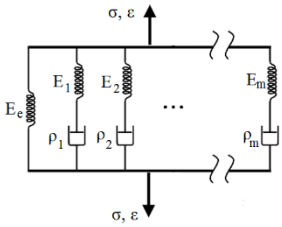

ρ_i	E_i
1.000E-06	6.267E+02
1.000E-05	7.211E+02
1.000E-04	8.504E+02
1.000E-03	7.758E+02
1.000E-02	5.555E+02
1.000E-01	3.084E+02
1.000E+00	1.446E+02
1.000E+01	6.369E+01
1.000E+02	2.875E+01
1.000E+03	1.391E+01

E_e = 3.980E+01

(a)

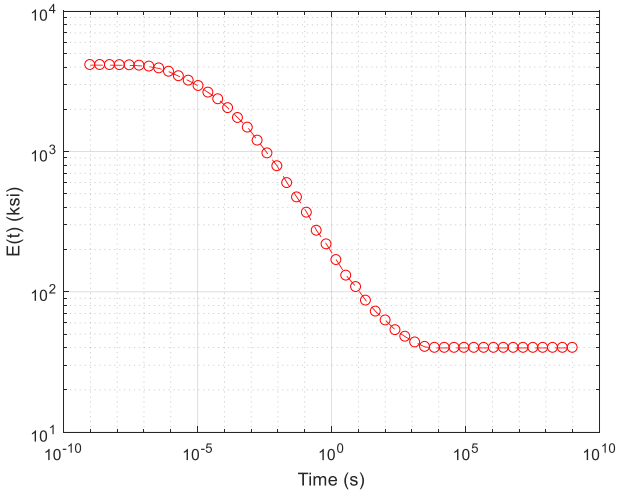

(b)

Figure 10.16 (a) Prony series fitting of $E'(\omega)$, and (b) converted $E(t)$ from E^* for AC sample 1.

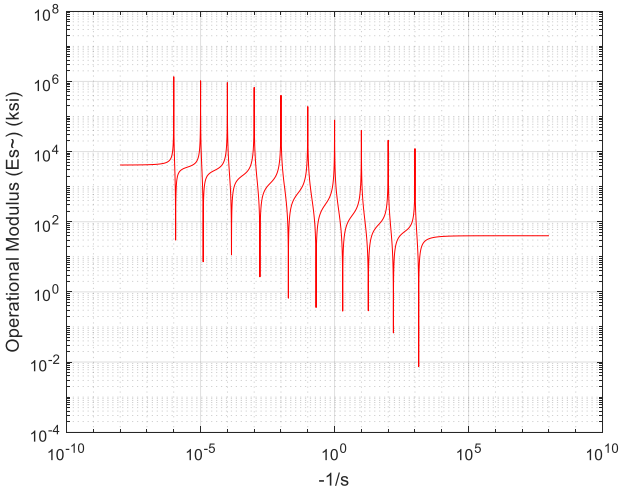

(a)

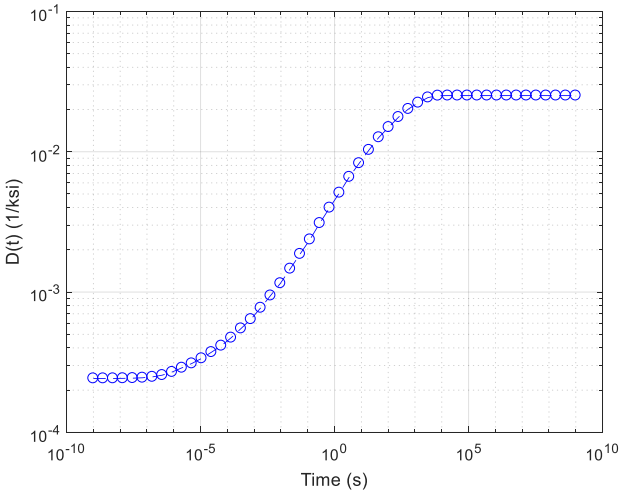

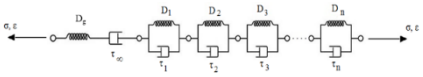

τ_i	D_i
1.174E-06	4.080E-05
1.252E-05	6.944E-05
1.423E-04	1.434E-04
1.642E-03	3.037E-04
1.888E-02	6.793E-04
2.041E-01	1.507E-03
2.008E+00	3.063E-03
1.811E+01	5.142E-03
1.566E+02	6.695E-03
1.377E+03	7.237E-03

D_g = 2.422E-04

(b)

Figure 10.17 (a) $\tilde{\tilde{E}}(s)$ versus -1/s plot, a root finding by graphical method, (b) converted $D(t)$ from E^* for AC sample 1.

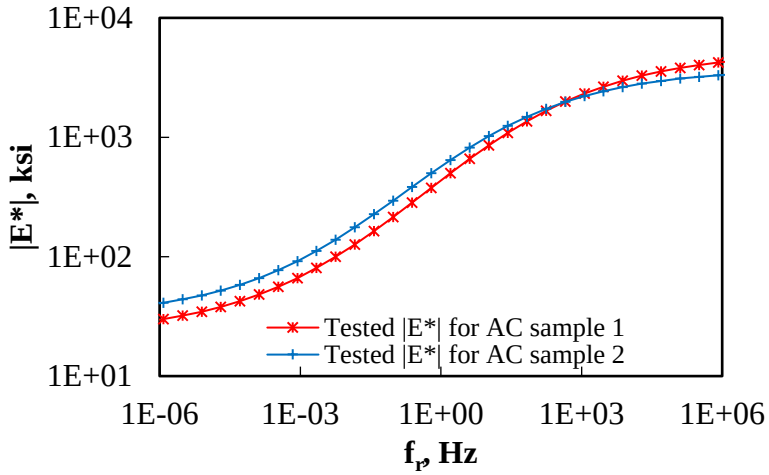

(a)

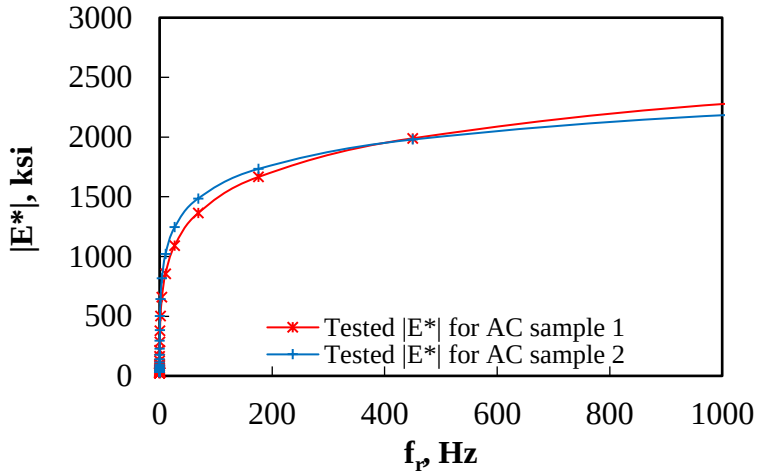

(b)

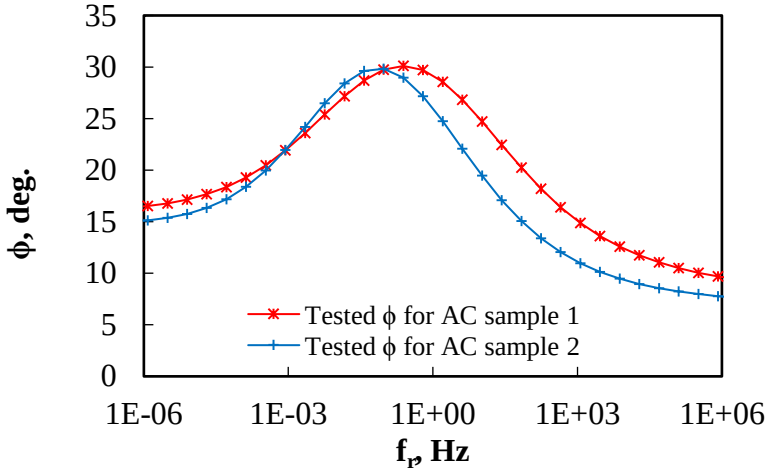

(c)

Figure 10.18 (a) Tested |E*|-functions in log-log scale, (b) tested-|E*|-functions in normal scale up to f_r = 1000 sec., and (c) tested ϕ-functions in semi-log space for AC samples.

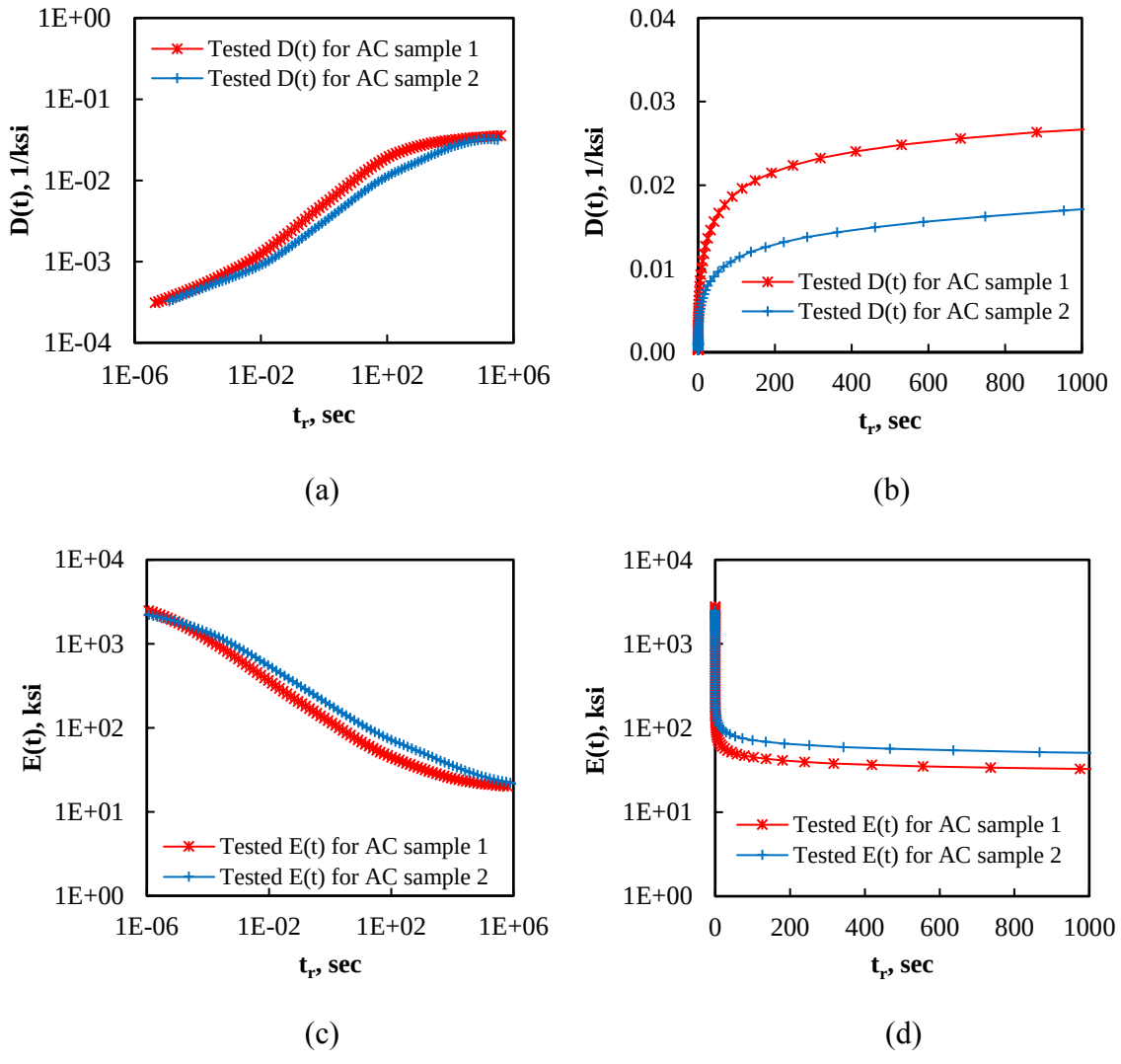

Figure 10.19 (a) Tested D(t)-functions in log-log scale, (b) tested D(t)-functions in normal scale up to t_r = 1000 sec., (c) tested E(t)-functions in log-log scale, and (d) tested E(t)-functions in normal scale up to t_r = 1000 seconds.

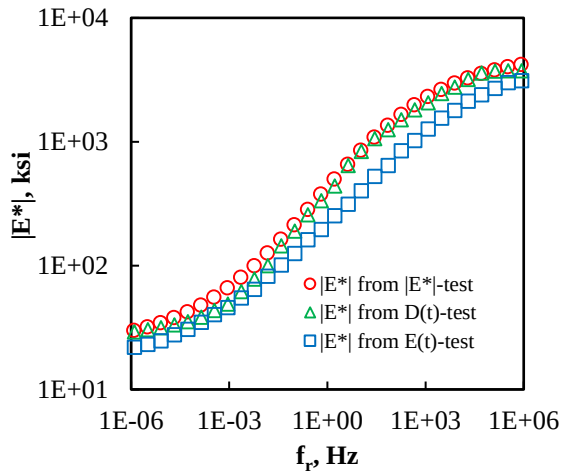

(a) |E*| in log-log scale for AC sample 1

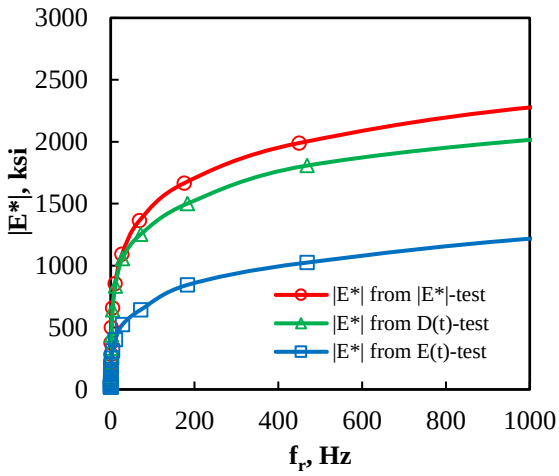

(b) |E*| in normal scale for AC sample 1

(up to f_r = 1000 Hz)

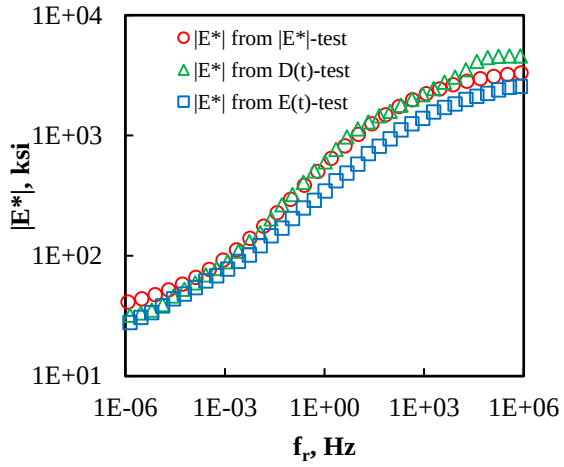

(c) |E*| in log-log scale for AC sample 2

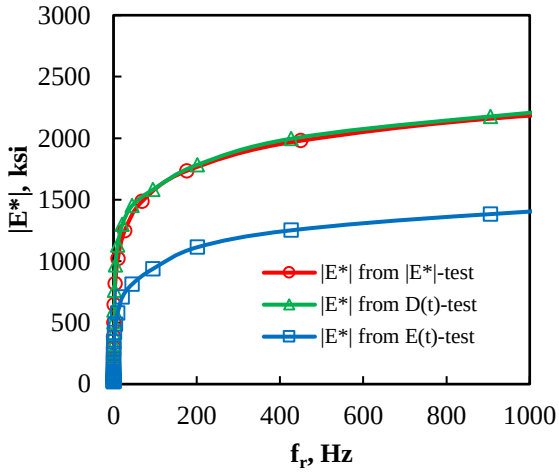

(d) |E*| in normal scale for AC sample 1

(up to f_r = 1000 Hz)

Figure 10.20 Tested and converted |E*|-functions.

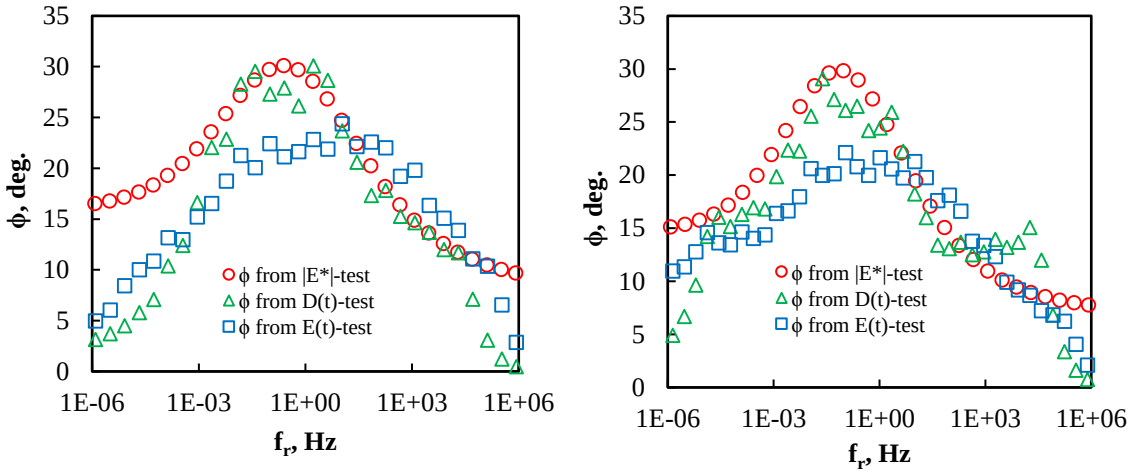

(a) ϕ in semi-log scale for AC sample 1

(b) ϕ in semi-log scale for AC sample 1

Figure 10.21 Tested and converted ϕ-functions.

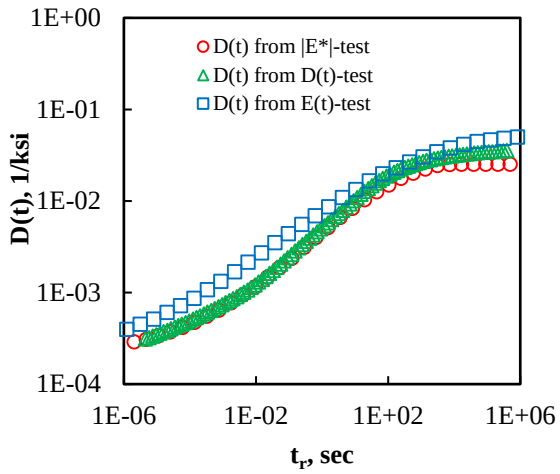

(a) D(t) in log-log scale for AC sample 1

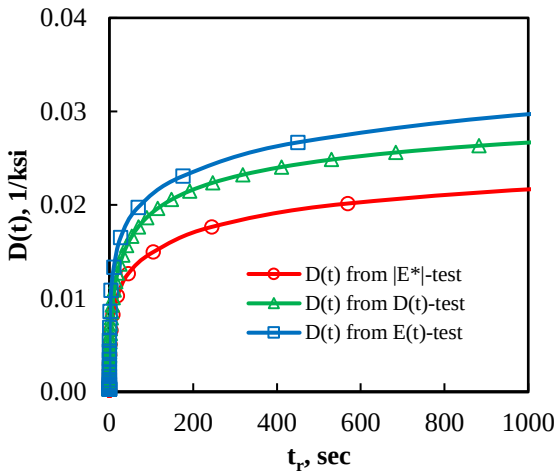

(b) D(t) in normal scale for AC sample 1

(up to t_r = 1000 sec.)

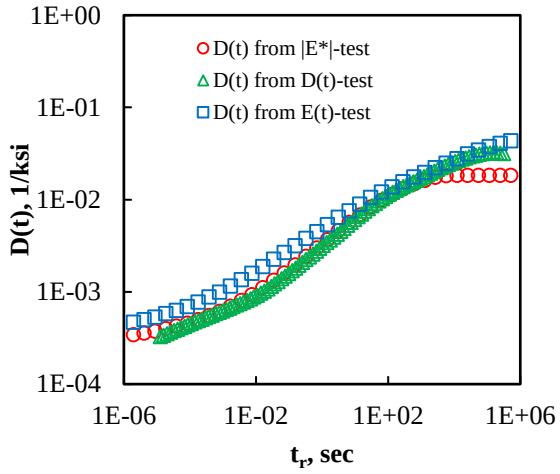

(c) D(t) in log-log scale for AC sample 2

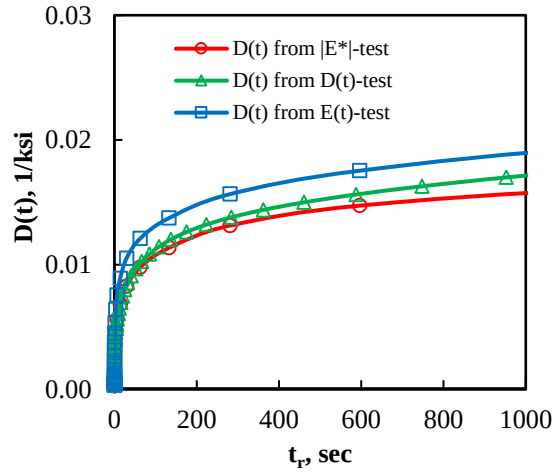

(d) D(t) in normal scale for AC sample 2

(up to t_r = 1000 sec.)

Figure 10.22 Tested and converted D(t)-functions.

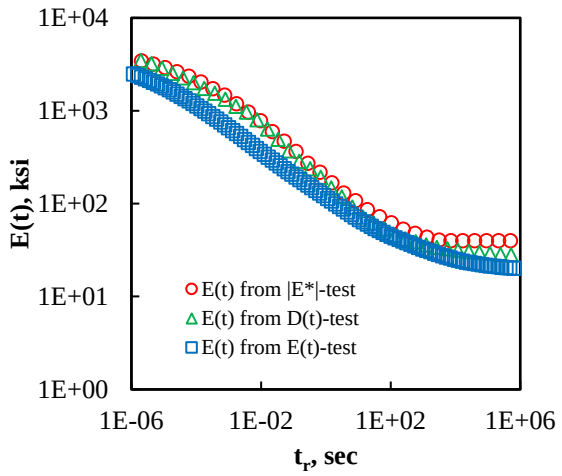

(a) E(t) in log-log scale for AC sample 1

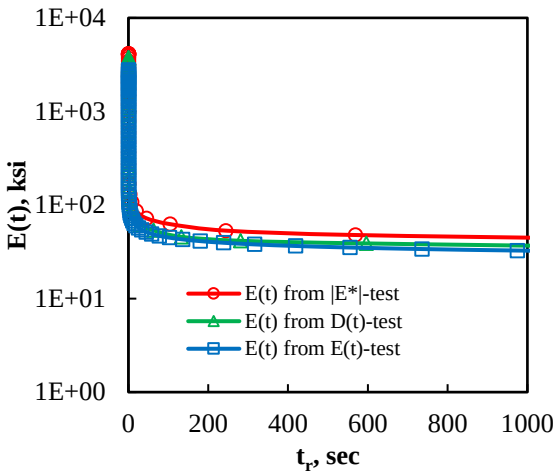

(b) E(t) in log-normal scale for AC sample 1

(up to t_r = 1000 sec.)

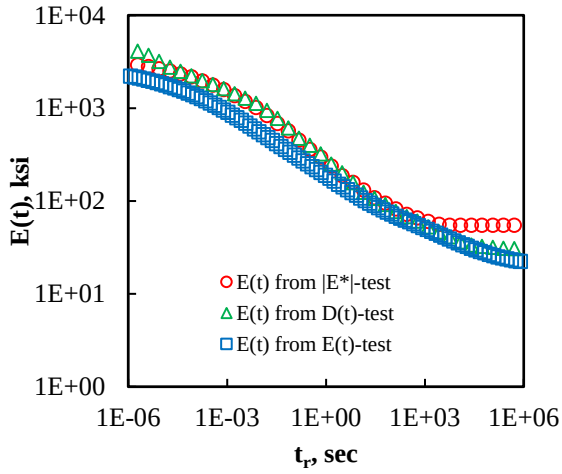

(c) E(t) in log-log scale for AC sample 2

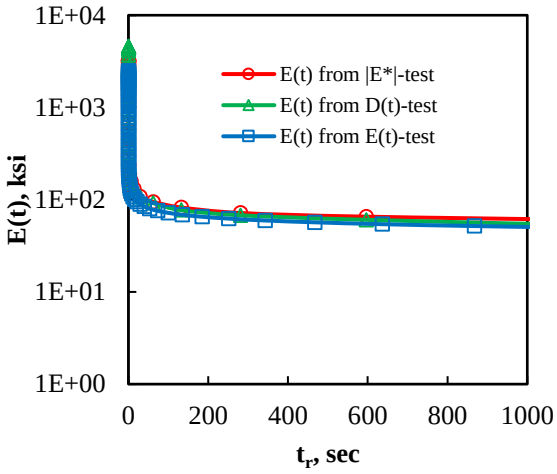

(d) E(t) in log-normal scale for AC sample 2

(up to t_r = 1000 sec.)

Figure 10.23 Tested and converted E(t)-functions.

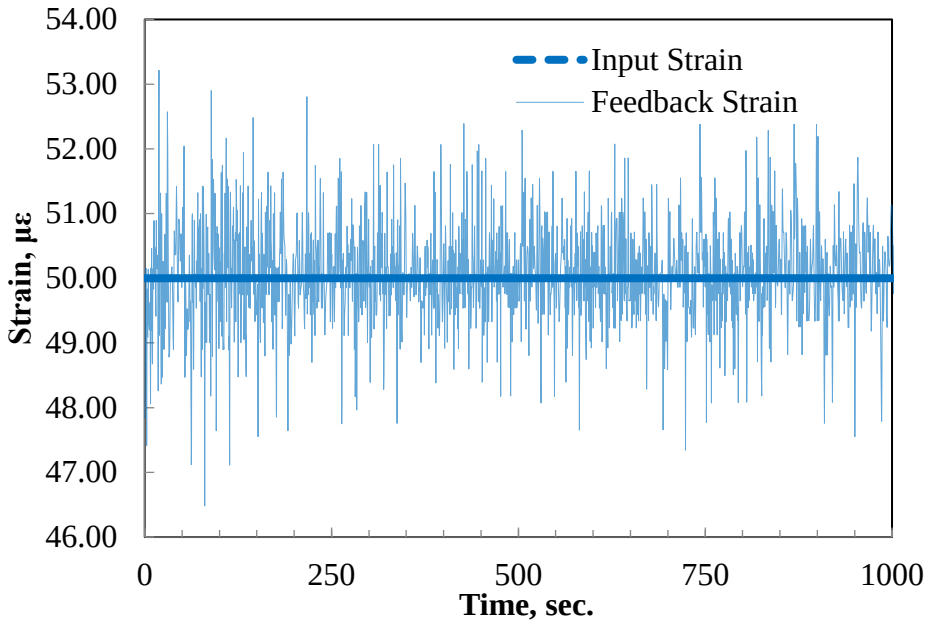

Figure 10.24 Input and feedback strains in a strain controlled test.

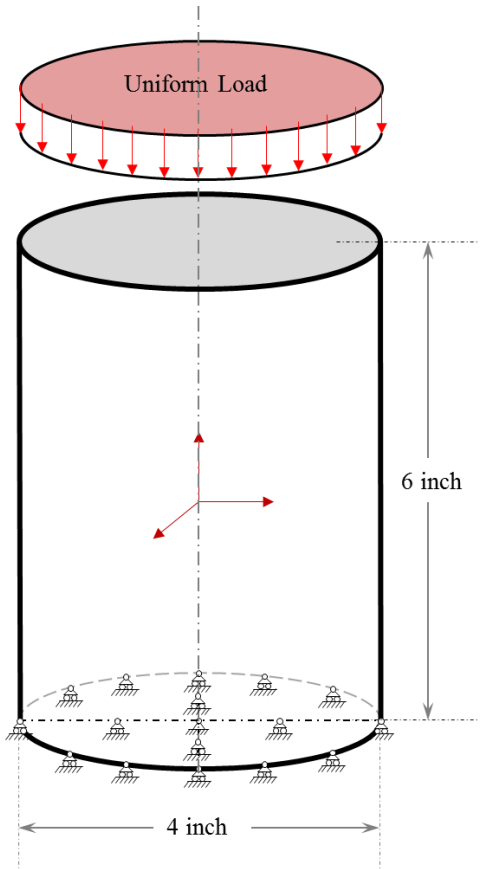

Figure 10.25 Asphalt Concrete FEM Model Geometry.

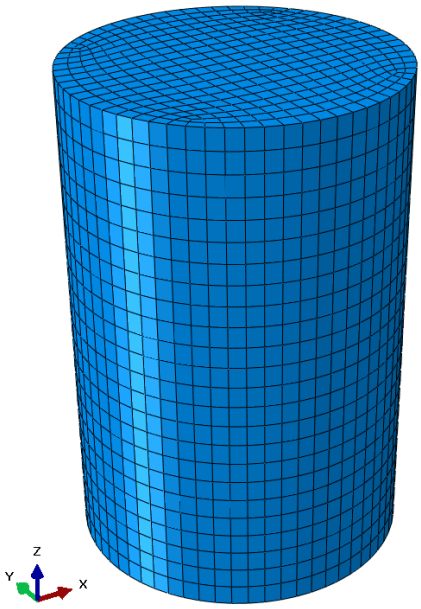

Figure 10.26 Asphalt Concrete FEM Model Mesh Generation.

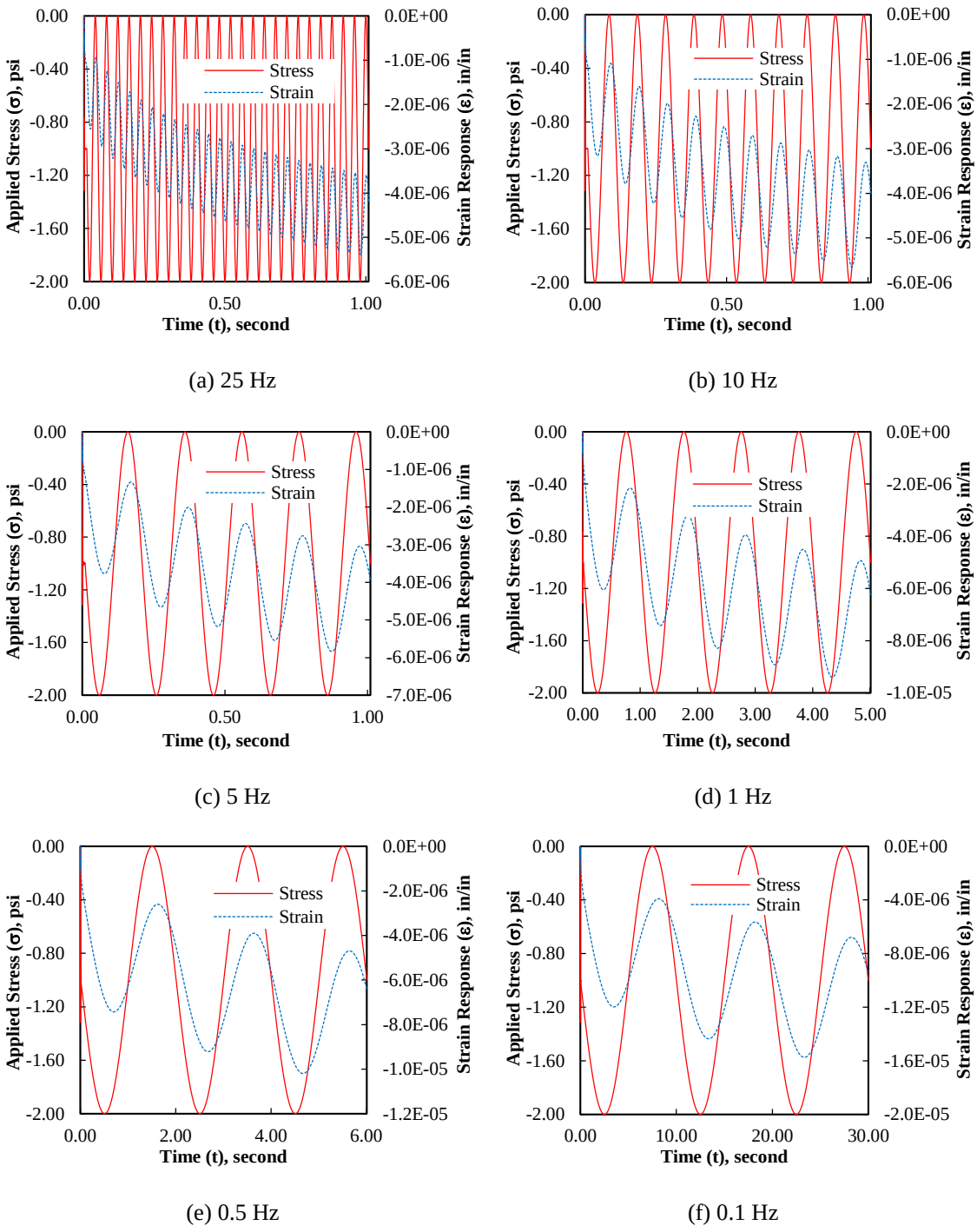

Figure 10.27 FEM simulation results for E*-testing at various loading frequencies for the AC sample 1. E*-test data was used to find e_i.

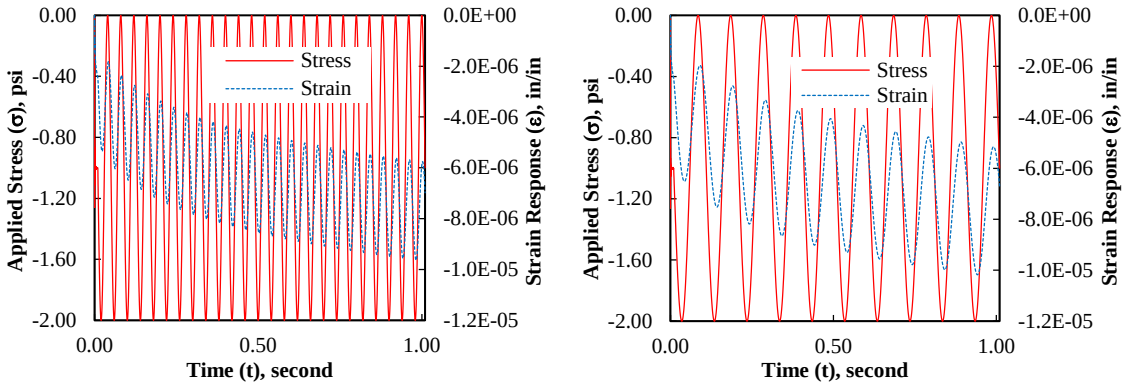

(a) 25 Hz

(b) 10 Hz

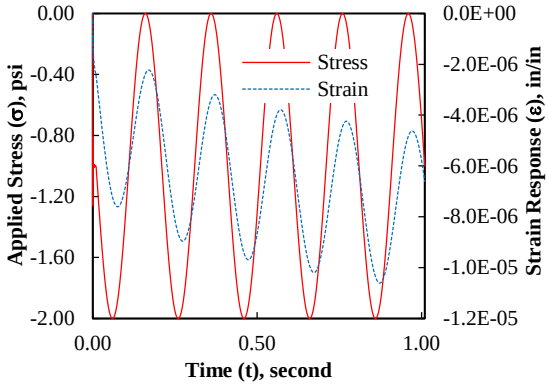

(c) 5 Hz

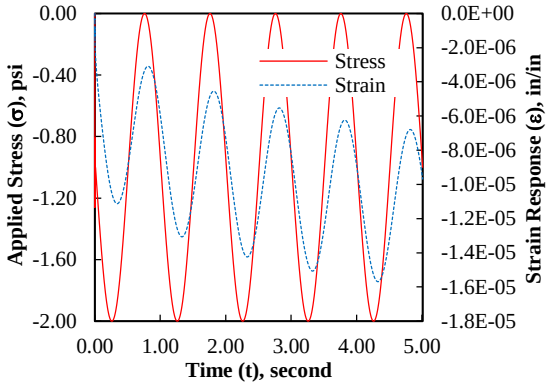

(d) 1 Hz

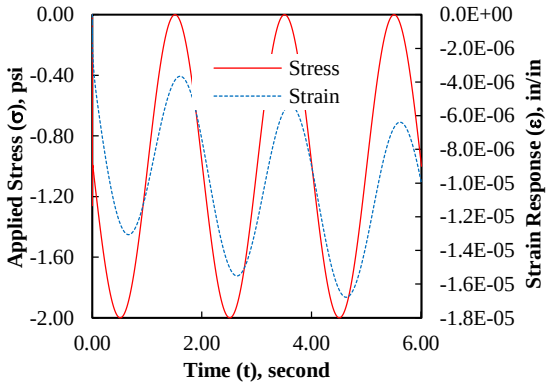

(e) 0.5 Hz

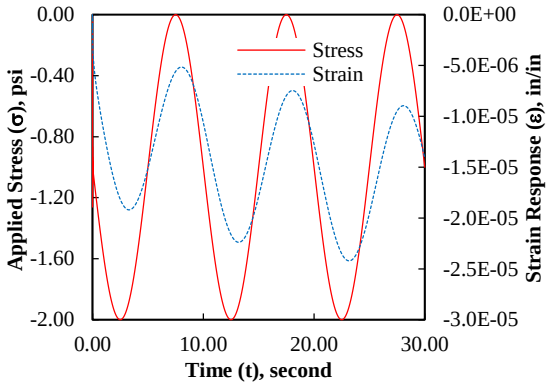

(f) 0.1 Hz

Figure 10.28 FEM simulation results for E*-testing at various loading frequencies for the AC sample 1. E(t)-test data was used to find e_i.

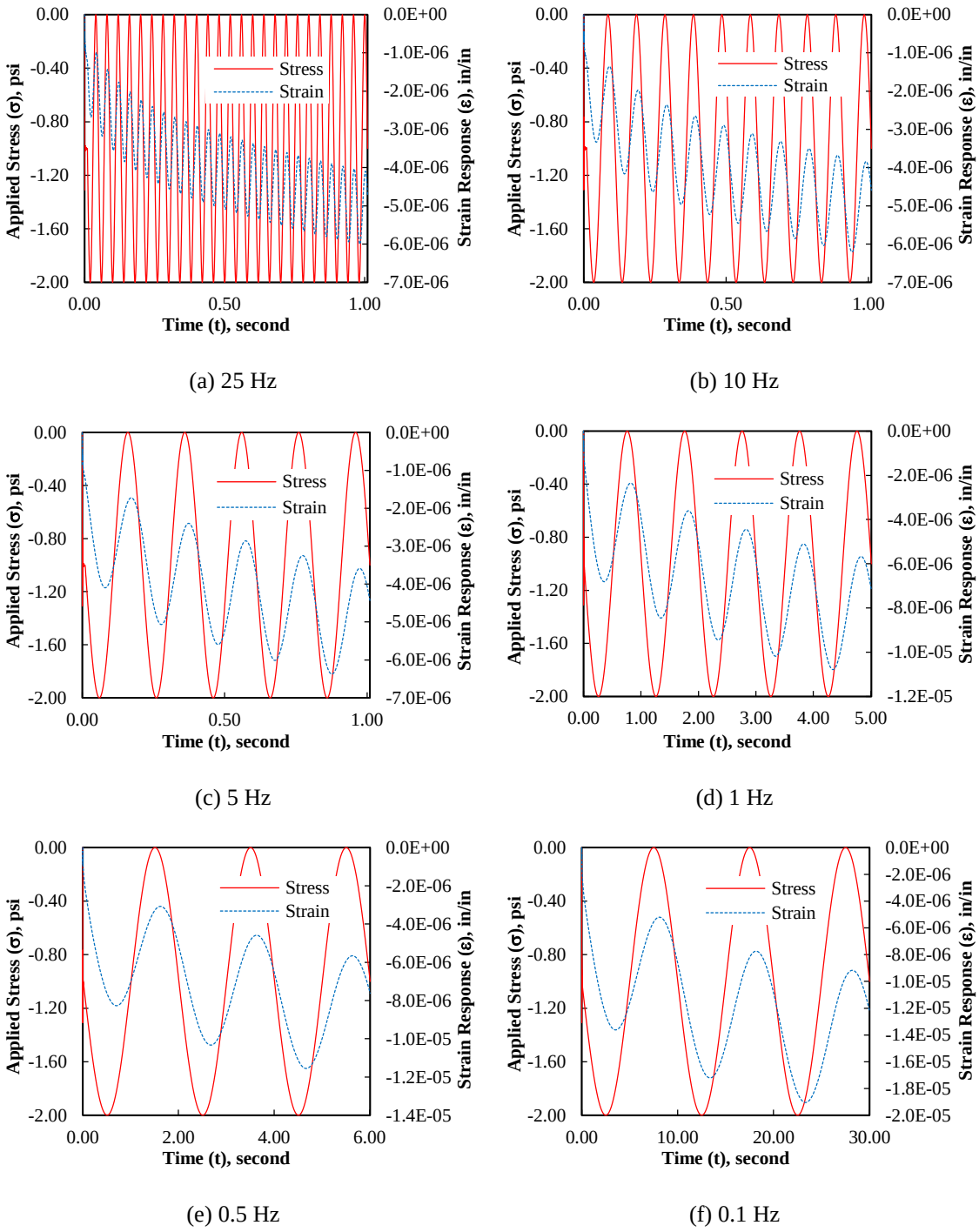

Figure 10.29 FEM simulation results for E*-testing at various loading frequencies for the AC sample 1. D(t)-test data was used to find e_i.

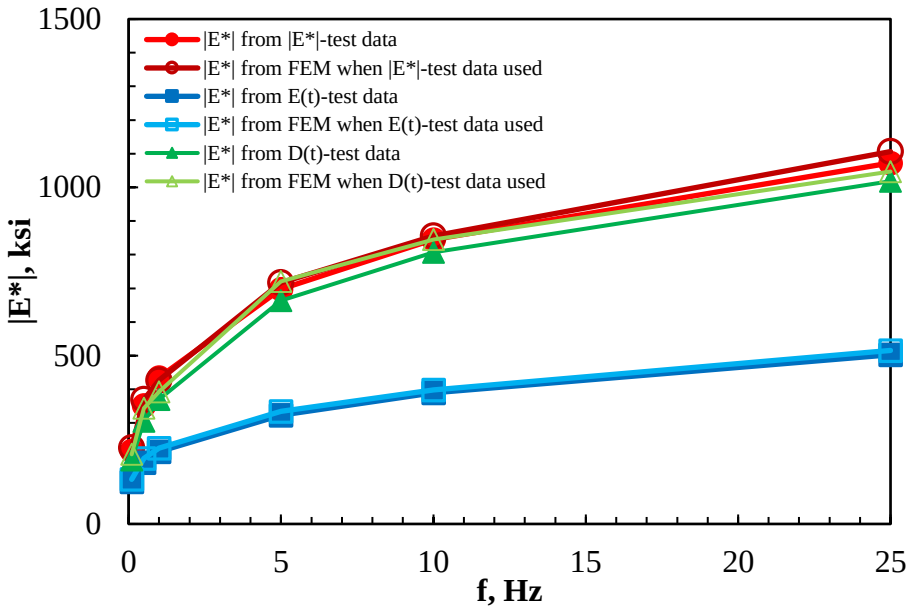

(a) Dynamic Modulus

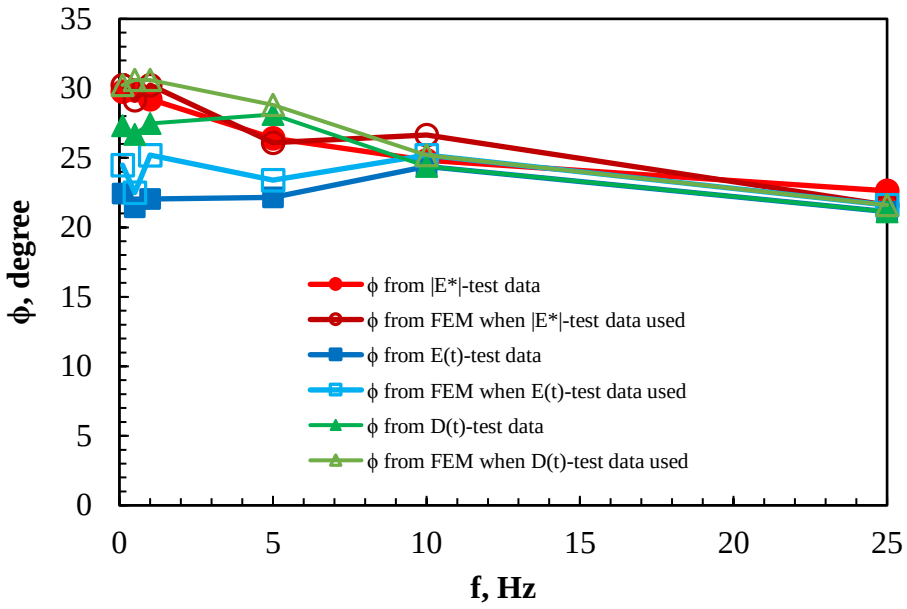

(b) Phase Angle

Figure 10.30 Laboratory tested and FEM simulated |E*| and ϕ at various loading frequencies for AC sample 1.

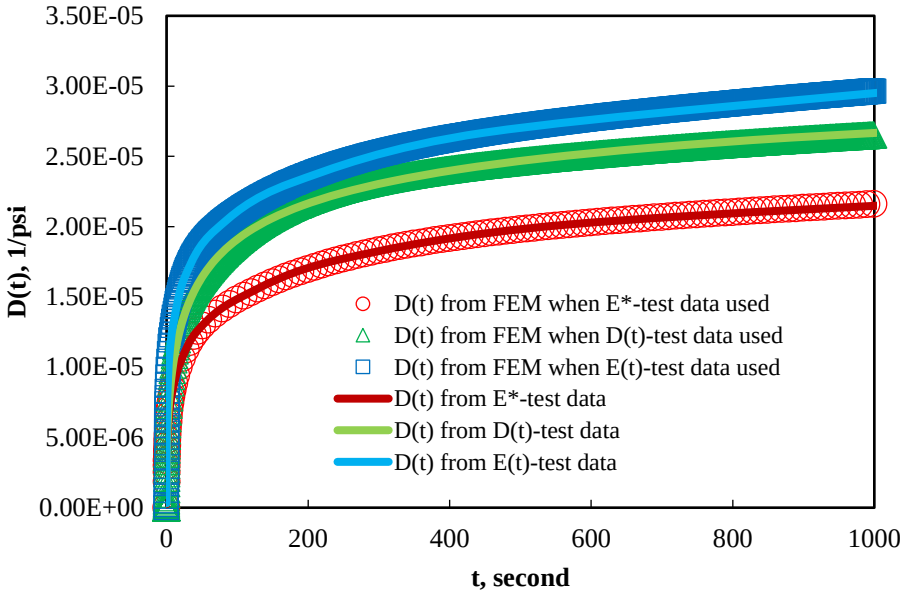

(a) Creep Compliance

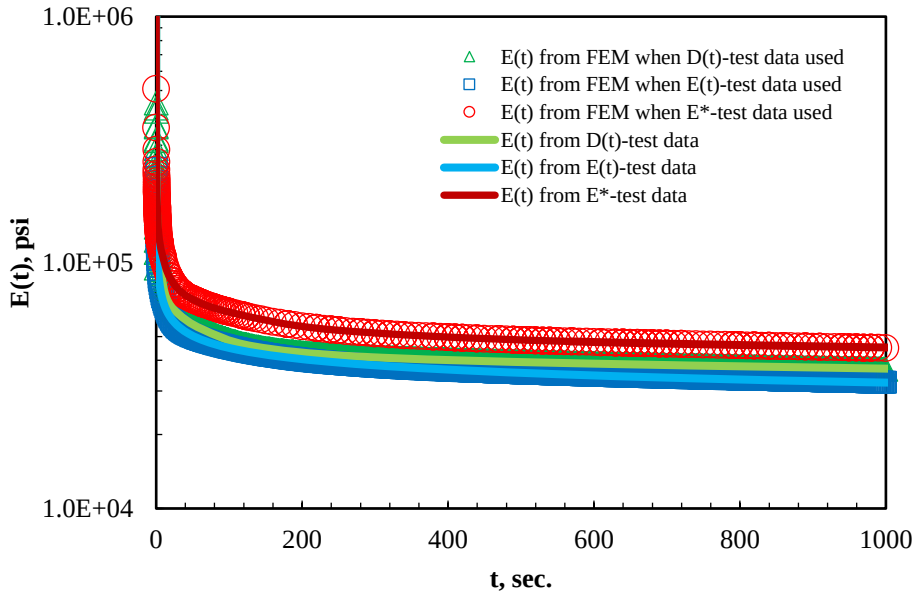

(b) Relaxation Modulus

Figure 10.31 Laboratory tested and FEM simulated D(t) and E(t) up to 1000 seconds loading time for AC sample 1.

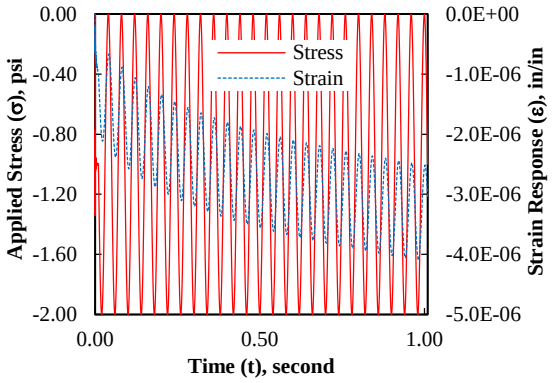

(a) 25 Hz

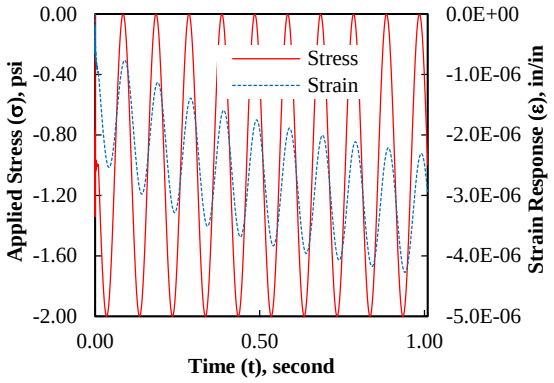

(b) 10 Hz

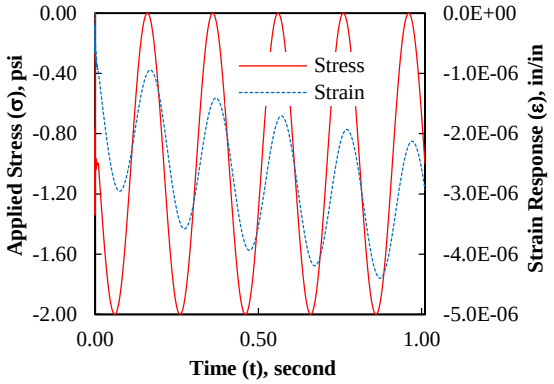

(c) 5 Hz

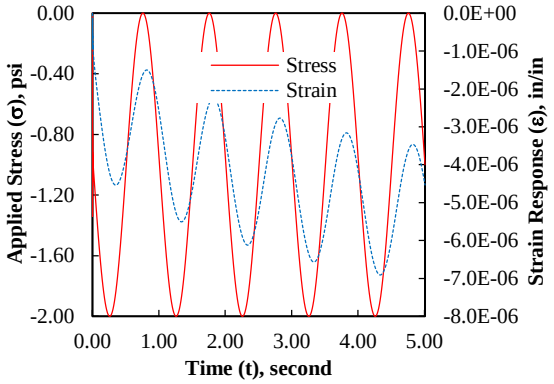

(d) 1 Hz

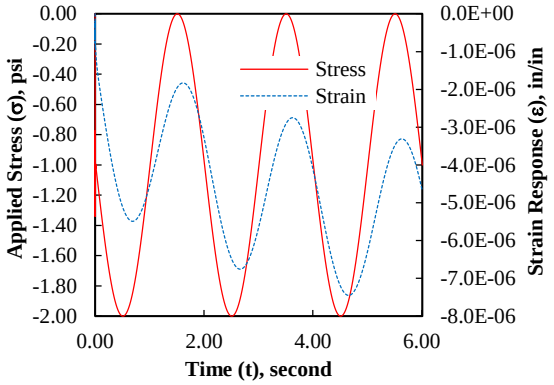

(e) 0.5 Hz

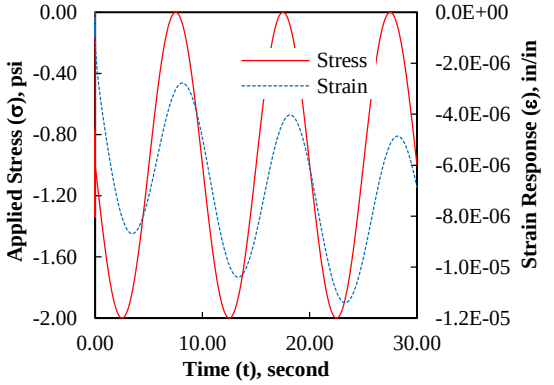

(f) 0.1 Hz

Figure 10.32 FEM simulation results for E*-testing at various loading frequencies for the AC sample 2. E*-test data was used to find e_i.

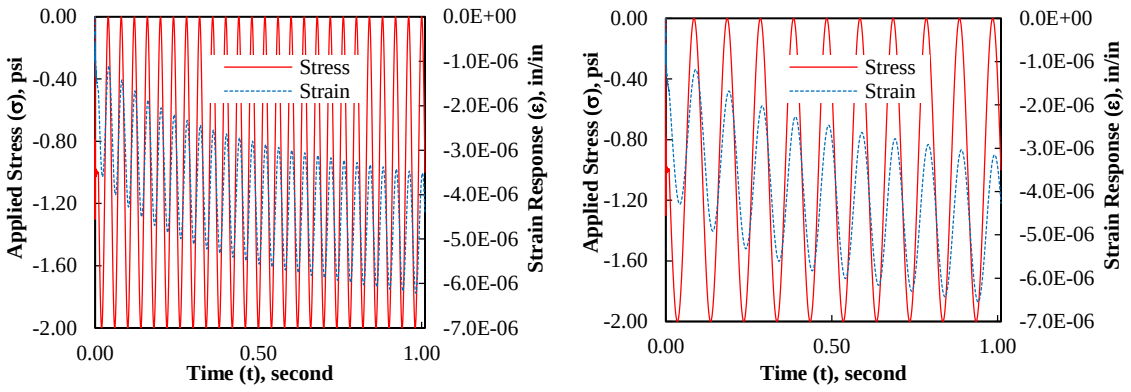

(a) 25 Hz

(b) 10 Hz

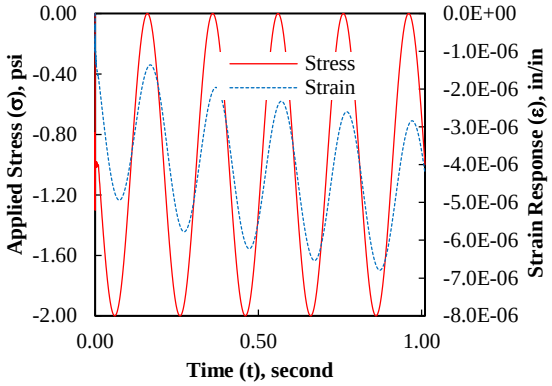

(c) 5 Hz

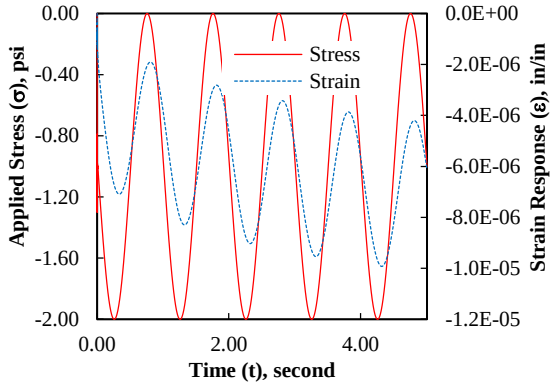

(d) 1 Hz

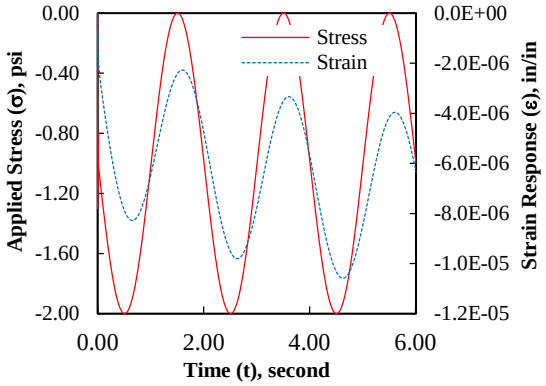

(e) 0.5 Hz

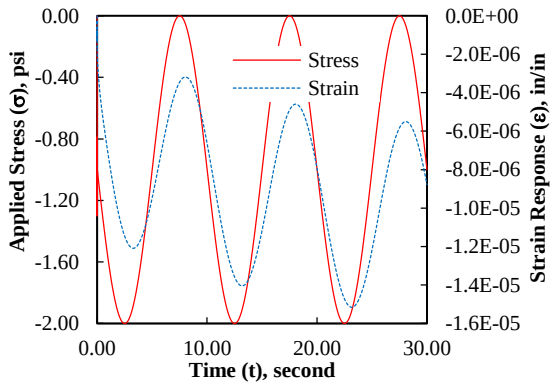

(f) 0.1 Hz

Figure 10.33 FEM simulation results for E*-testing at various loading frequencies for the AC sample 2. E(t)-test data was used to find e_i.

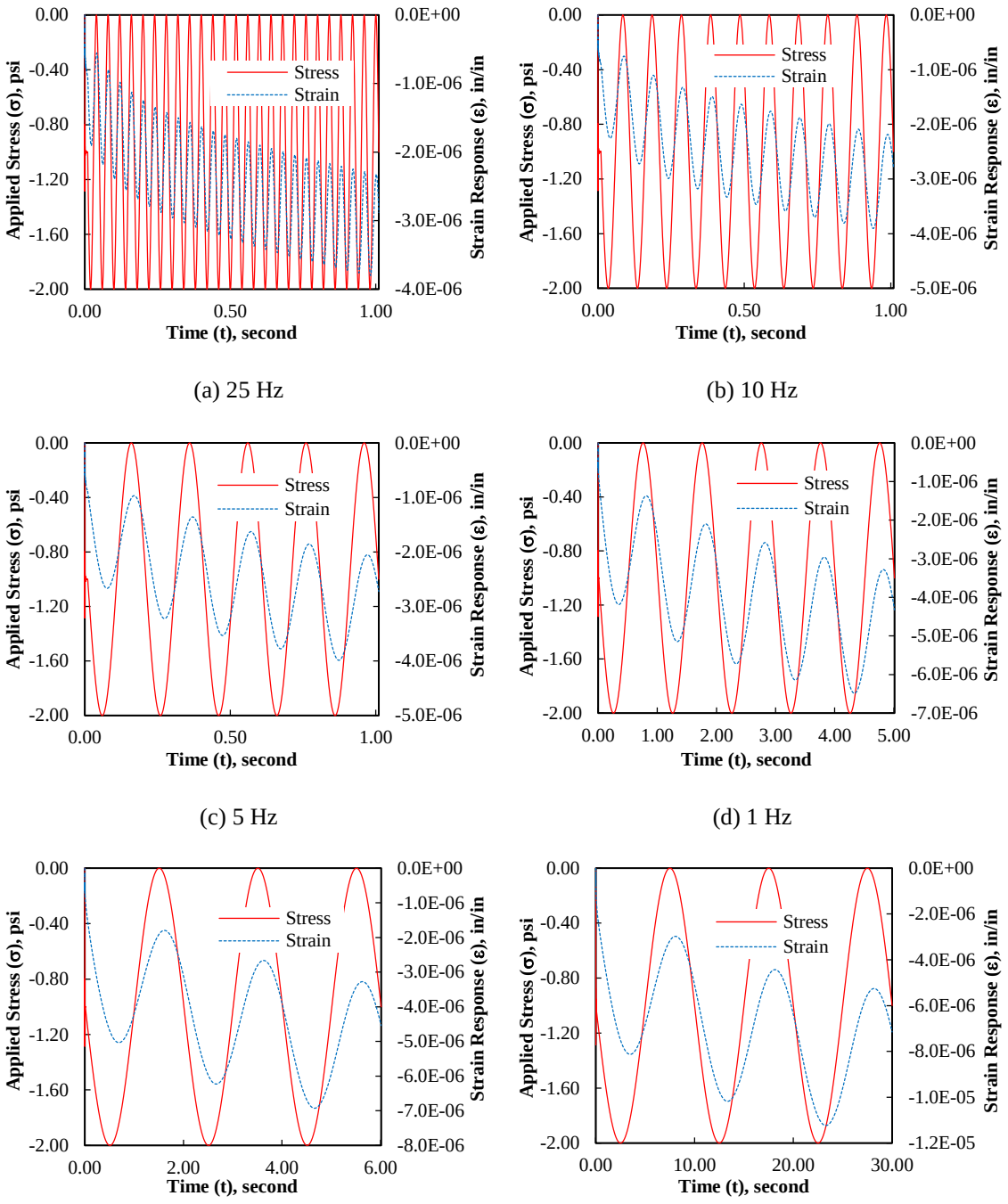

Figure 10.34 FEM simulation results for E*-testing at various loading frequencies for the AC sample 2. D(t)-test data was used to find e_i.

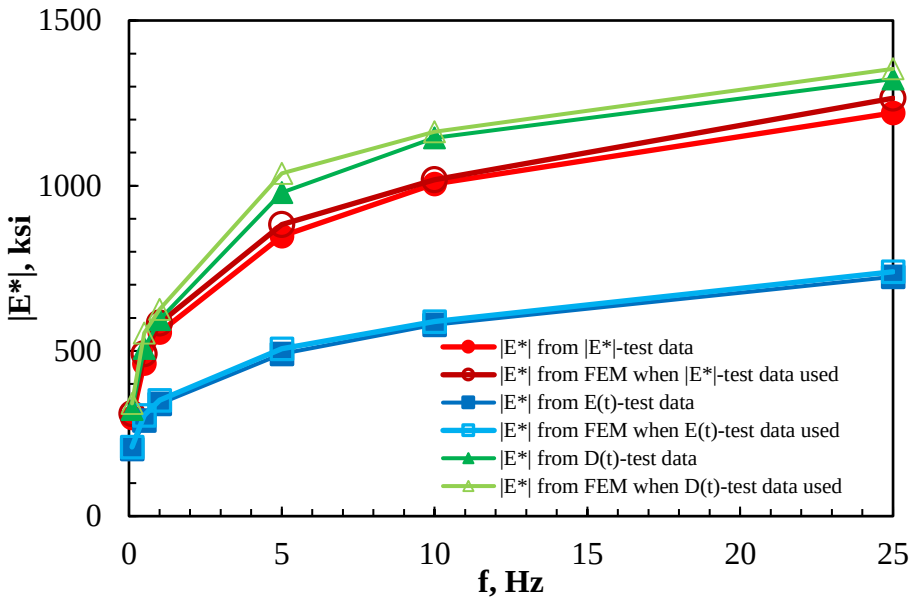

(a) Dynamic Modulus

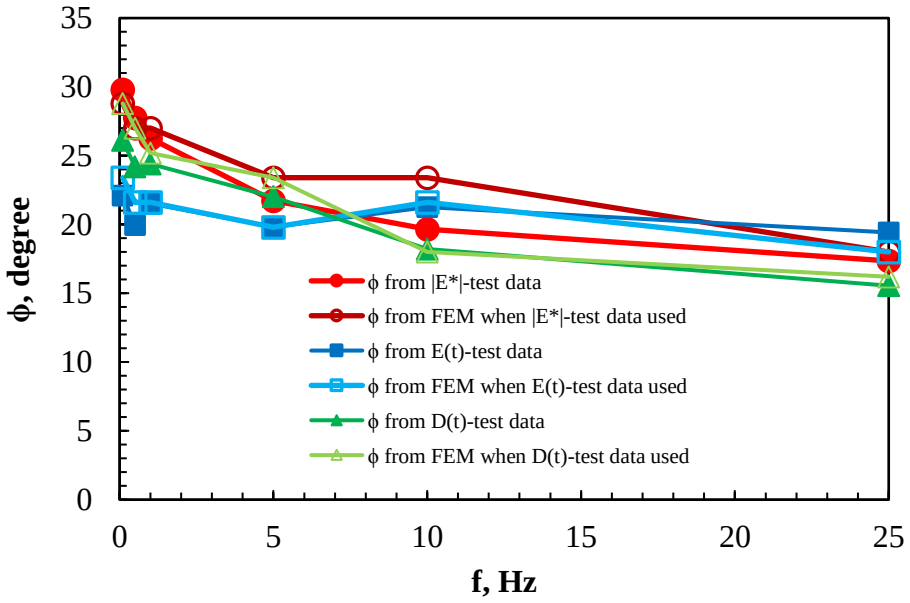

(b) Phase Angle

Figure 10.35 Laboratory tested and FEM simulated |E*| and ϕ at various loading frequencies for AC sample 2.

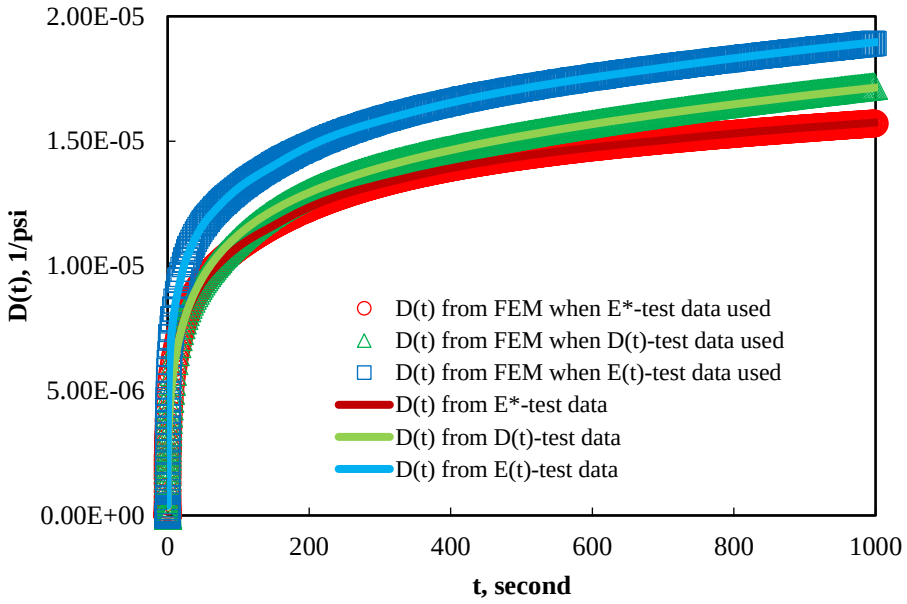

(a) Creep Compliance

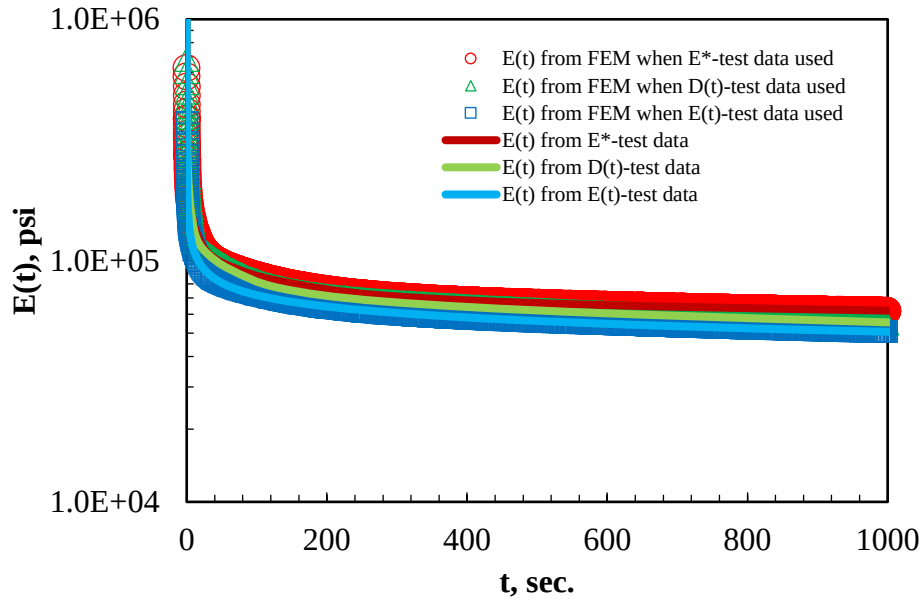

(b) Relaxation Modulus

Figure 10.36 Laboratory tested and FEM simulated D(t) and E(t) up to 1000 seconds loading time for AC sample 2.

Chapter 11

Conclusions and Recommendations

11.1 General

The recently developed mechanistic-empirical design method of asphalt pavements uses the nationally calibrated, binder viscosity-based dynamic modulus predictive model for the design and analysis of asphalt pavements. In this study, this nationally-calibrated model is assessed for asphalt-aggregate mixtures typically used in New Mexico. The assessment of this model indicated significant underprediction and bias of the model in its current form for predicting complex modulus of the Superpave asphalt-aggregate mixtures of New Mexico. As the primary aim of this study is to investigate the predictability issue of complex modulus of New Mexico mixes, thus, as a first attempt, the nationally-calibrated viscosity-based Witczak's complex modulus model is calibrated for the local Superpave mixtures of New Mexico. A total of 54 asphalt-aggregate mixtures with different aggregate gradations, compositions, and binder grades were collected either from the manufacturing plants or from the pavement construction sites and hence used in this study. The loose asphalt-aggregate mixtures were then compacted, cored and sawed to cylindrical specimens and tested for dynamic modulus and phase angle in the laboratory. Independence assurance testing is performed to assess the precision and accuracy of the test results. The time-temperature superposition principle was applied to develop mastercurves of complex modulus and phase angle functions of the asphalt concrete samples. The evaluated complex modulus mastercurve parameters were then used to

calibrate the viscosity-based Witczak model for predicting dynamic or complex modulus of local asphalt concrete materials.

Though the calibrated Witczak model showed a good correlation, as a second attempt, a new set of regression-based models for predicting dynamic modulus and phase angle functions of local asphalt-aggregate mixtures was also developed and validated in this study. Different material attributes such as mix volumetrics, aggregate gradations, and asphalt binder characteristics are the main factors affecting the viscoelastic material functions, such as, complex modulus of asphalt concrete. The current study had an aim to justify the effect of these mixture variables on the complex modulus of asphalt concrete and thus develop or modify predictive models to estimate the complex modulus of asphalt concrete more accurately. With the aim at hand, the effect of aggregate gradation on the complex modulus function of asphalt concrete was determined in this study. To characterize various aggregate gradations, the two well-known gradation parameters of the aggregate blend, namely, the fineness modulus and the uniformity coefficient, were considered. This study evaluated the effect of these aggregate parameters to the complex modulus and phase angle functions of asphalt concrete, and hence, used that to develop these new predictive models. Statistical evaluation showed that fairly accurate estimations of dynamic modulus and phase angle of the local mixes can be possible by using these new predictive models.

Characterizing stiffness property of asphalt concrete by the dynamic shear modulus of an asphalt binders is considered to be more accurate and more acceptable in recent years. The recent mechanistic-empirical method of pavement design and analysis has a binder shear modulus based dynamic modulus model. Several researchers claimed that this binder

shear modulus based model is more biased and inaccurate when compared to the tested data or the predicted data from viscosity based model. Besides the viscosity-based model discussed earlier, new regression-based predictive models based on binder shear modulus were developed based on laboratory testing of ten AC mixtures and four asphalt binders used in the mixtures to predict complex modulus and phase angle of asphalt concrete. The new binder shear modulus based model also gradation parameters and mixture volumetrics. The cylindrical asphalt concrete specimens were prepared and tested for complex modulus and phase angle, and the asphalt binders used in these mixtures were tested for complex shear modulus and phase angle using dynamic shear rheometer. For the asphalt concrete specimens, complex modulus and phase angle functions were generated by applying time-temperature superposition principle. Also, for the asphalt-binders, the dynamic shear modulus and phase angle functions were also generated by applying time-temperature superposition principle. Effect studies of different material attributes on model parameters were conducted and relationship among AC complex modulus and phase angle with mixture attributes were evaluated. Non-linear optimization technique was used to correlate the model parameters to the material attributes to develop the final form of the model. Statistical evaluation showed good accuracy of the predictions made by these models.

Apart from the regression-based modeling and to improve the accuracy of the characterization problem, an advanced dynamic modulus and phase angle predictive model is also developed in this study based on the artificial neural network methodology. A database containing 1,620 dynamic moduli with phase angles was used to develop this artificial neural network based model. A neural architecture with two twelve-node hidden layers was found to be remarkably suitable for predicting the dynamic modulus and phase

angle of asphalt concrete. Statistical evaluation showed an excellent prediction ability of this model.

Lastly, viscoelastic time-domain material functions, such as, relaxation modulus and creep compliance, or frequency domain function, such as, complex modulus can be used to characterize the linear viscoelastic behavior of asphalt concrete in modeling and analysis of pavement structure. Among these, the complex modulus has been adopted in the recent pavement Mechanistic-Empirical (M-E) design software AASHTOWare-ME. However, for advanced analysis of pavement, such as, use of finite element method requires that the complex modulus function to be converted into relaxation modulus or creep compliance functions. There are a number of exact or approximate methods available in the literature to convert one linear viscoelastic material function to another. All these methods (i.e. exact or approximate methods) are applicable for any linear viscoelastic material up to a certain level of accuracy. However, the applicability and accuracy of these interconversion methods for asphalt concrete material were not studied very much in the past and thus question arises if these methods are even applicable in case of asphalt concrete, and if so, what is the precision level of the interconversion method being used. Therefore, to investigate these facts, this study undertaken an effort to validate a numerical interconversion technique by conducting representative laboratory tests. The method was previously used in asphalt industry with adopting a simplification of considering time constants to be identical in Generalized Maxwell and Generalized Voigt model. However, in the present context, the assumption is regarded as over-simplification and therefore, an exact approach to estimate the time constants in these two micro-mechanical models are proposed. For validation purpose, cylindrical asphalt concrete specimens were tested for

complex modulus, relaxation modulus, and creep compliance at different test temperatures and loading rates. The time-temperature superposition principle was applied to develop broadband linear viscoelastic material functions. The numerical interconversion technique was used to convert one material function to another, and hence, were compared to the laboratory tested material functions in case of aged and unaged asphalt concrete samples. The comparison showed good agreement with the laboratory test data. Toward the end, a statistical evaluation was conducted to determine if the interconverted material functions are similar to the laboratory tested material functions.

11.2 Conclusions

Based on this study, the following conclusions can be made:

- The fineness modulus of the aggregate blend has an effect on the minimum $|E^*|$, the maximum $|E^*|$, and the overall shape of the $|E^*|$-function. Therefore, a change in fineness modulus, can cause changes in overall $|E^*|$-function of an asphalt concrete material. On the other hand, the uniformity coefficient has none or very trivial effect on the shape of the $|E^*|$-mastercurve but it affects the magnitude of the $|E^*|$.

- The nationally-calibrated Witczak's $|E^*|$ model was assessed in this study. The assessment indicated significant underprediction and bias in case of representative Superpave asphalt-aggregate mixtures of New Mexico. Therefore, this study modified the model based on test data of 54 asphalt concrete samples. Statistical analysis showed that this locally calibrated model gives a fairly good estimation of dynamic modulus of asphalt concrete typically used in New Mexico.

- New predictive models for dynamic modulus and phase angle of asphalt concrete based on binder viscosity are developed in this study based on observed data of 54 asphalt concrete mixtures typically used in New Mexico. The developed models use two fundamental aggregate gradation parameters: the fineness modulus and the uniformity coefficient, mix volumetric parameters (air void content and effective binder volume), binder viscosity, and loading frequency as direct input. The developed models possess fairly good statistics, considering "goodness of fit" between predicted and observed data.

- New predictive models for dynamic modulus and phase angle of asphalt concrete based on binder shear modulus are also developed in this study based on observed data of 10 asphalt concrete mixtures, and four asphalt binders typically used in New Mexico. In this case, also, the developed models use two fundamental aggregate gradation parameters: the fineness modulus and the uniformity coefficient, mix volumetric parameters (air void content and effective binder volume), and binder rheological properties (dynamic shear modulus and binder phase angle) as direct input. The developed $|E^*(\omega)|$ and $\phi(\omega)$ models possesses fairly good statistics, considering goodness of fit of the data.

- An artificial neural network model is also developed in this study for predicting dynamic modulus and phase angle of Superpave asphalt concrete based on the laboratory tested data of 54 asphalt concrete mixtures. Considering goodness-of-fit statistics, the model can be considered as an excellent option for predicting dynamic modulus and phase angle of asphalt concrete. As such, the artificial neural network methodology is proven to be a promising modeling technique, especially for data sets having the kind of nonlinear relationships frequently encountered in characterization problem.

- The numerical method reviewed and amended in this study proved to be applicable in case of asphalt concrete to interconvert one material function to another. Specifically, the converted and tested $|E^*|$, ϕ, and $D(t)$ matched very good, however, the converted and tested relaxation modulus did not match very well. Indeed, the procedure outlined can be well used for application in asphalt industry.

11.3 Recommendations

The following research recommendation are made:

- The new viscosity based models developed in this study has shown promising results in predicting dynamic modulus and phase angle of New Mexico mixtures. It is recommended to validate the accuracy of this model with further dynamic modulus test results in the future.

- The artificial neural network based model developed in this study proved to be an excellent option for predicting dynamic modulus and phase angle of asphalt concretes of New Mexico. However, due to limitation of $|G_b^*|$ test data, the tradition binder viscosity was considered as binder variable. Therefore, it is recommended to incorporate $|G_b^*|$ in the model instead of viscosity of the binder.

- The numerical interconversion method presented in this study was validated using two asphalt concrete samples of only one asphalt-aggregate mixture. To make the method more acceptable, it is recommended to use more mixtures for validating the method.

References

AASHTO (2008). *Mechanistic Empirical Pavement Design Guide. A manual of practice*. American Association of State Highway and Transportation Officials, Washington, D.C.

AASHTO R 30-02 (2002). "Standard Practice for Mixture Conditioning of Hot-Mix Asphalt (HMA)." Standard by American Association of State and Highway Transportation Officials (AASHTO).

AASHTO T 2-91 (2006). "Standard Method of Test for Sampling of Aggregates (ASTM D 75-03)." Standard by American Association of State Highway Transportation Officials (AASHTO).

AASHTO T 342-11 (2015), "Standard Method of Test for Determining Dynamic Modulus of Hot-Mix Asphalt Concrete Mixtures." Standard by American Association of State Highway Transportation Officials (AASHTO).

AASHTO M 323-13 (2013), "Standard Specification for Superpave Volumetric Mix Design." Standard by American Association of State Highway Transportation Officials (AASHTO).

AASHTO MP 2 (2011). "Standard Specification for Superpave Volumetric Mix Design." Standard by American Association of State Highway Transportation Officials (AASHTO).

AASHTO T 168-03 (2011). "Standard Method of Test for Sampling Bituminous Paving Mixtures (ASTM D 979-01(2006)e1)." Standard by American Association of State Highway Transportation Officials (AASHTO).

AASHTO T 27-14 (2014), "Standard Method of Test for Sieve Analysis of Fine and Coarse Aggregates (ASTM Designation C 136-06)." Standard by American Association of State Highway Transportation Officials (AASHTO).

AASHTO T 308-16 (2016), "Standard Method of Test for Determining the Asphalt Binder Content of Hot Mix Asphalt (HMA) by the Ignition Method." Standard by American Association of State Highway Transportation Officials (AASHTO).

AASHTO T 315-12 (2012). "Standard Method of Test for Determining the Rheological Properties of Asphalt Binder Using a Dynamic Shear Rheometer (DSR)." Standard by American Association of State Highway Transportation Officials (AASHTO)..

AASHTO T 209-12 (2012). "Standard Method of Test for Theoretical Maximum Specific Gravity (Gmm) and Density of Hot-Mix Asphalt (HMA)." Standard by American Association of State Highway Transportation Officials (AASHTO).

AASHTO T 312-15 (2015), "Standard Method of Test for Preparing and Determining the Density of Asphalt Mixture Specimens by Means of the Superpave Gyratory Compactor." Standard by American Association of State Highway Transportation Officials (AASHTO).

AASHTO T 166-16 (2016). "Standard Method of Test for Bulk Specific Gravity (Gmb) of Compacted Hot Mix Asphalt (HMA) Using Saturated Surface-Dry Specimens." Standard by American Association of State Highway Transportation Officials (AASHTO).

AASHTO T 240-13 (2013). "Standard Method of Test for Effect of Heat and Air on a Moving Film of Asphalt (Rolling Thin-Film Oven Test) (ASTM Designation: D

2872-04).” Standard by American Association of State Highway Transportation Officials (AASHTO).

AASHTO TP 62-07 (2007). “Standard Method of Test for Determining Dynamic Modulus of Hot-Mix Asphalt Concrete Mixtures.” Standard by American Association of State Highway Transportation Officials (AASHTO).

AASHTO TP 7-94 (1994). “Standard test method for determining the permanent deformation and fatigue cracking characteristics of hot-mix asphalt (HMA) using the simple shear test (SST) device.” Standard by American Association of State Highway Transportation Officials (AASHTO).

Ahmed, M., Rahman, A. S. M. A., Islam, M. R., and Tarefder, R. A. (2015). “Combined effect of asphalt concrete cross-anisotropy and temperature variation on pavement stress-strain under dynamic loading.” *Construction and Building Materials*, Vol. 93, pp. 685-694.

Al-Khateeb, G., Shenoy, A., Gibson, N., and Harman, T. (2006). “A new simplistic model for dynamic modulus predictions of asphalt paving mixtures.” *Journal of the Association of Asphalt Paving Technologists*, Vol. 75.

Al-Khateeb, G., Qi, X., Shenoy, A., Stuart, K. and Mitchell, T. (2005). “Assessment of aging at FHWA's pavement testing facility.” *Transportation Research Record: Journal of the Transportation Research Board*, No. 1940, pp.146-155.

Andersen, T.J. and Wilamowski, B.M. (1995). “A modified regression algorithm for fast one-layer neural network training.” In *World Congress of Neural Networks*, Vol. 1, pp. 687-690.

Andrei, D., Witczak, M. W., and Mirza, M. W. (1999). *Development of a revised predictive model for the dynamic (complex) modulus of asphalt mixtures*. NCHRP 1-37, Interim Report, University of Maryland, College Park, Md.

ARA, Inc., ERES Consultants Division (2004). "Guide for mechanistic-empirical design of new & rehabilitated pavement structures." *NCHRP Project 1-37A*, (Final Report) <http://onlinepubs.trb.org/onlinepubs/archive/mepdg/guide.htm> (July 19, 2013).

ASTM (1998). *Viscosity-Temperature Chart for Asphalts*, ASTM D 2493, *Annual Book of ASTM Standards*, Vol. 0.403, pp. 230-234.

ASTM D2493/D2493M-16 (2016). "Standard practice for Viscosity-Temperature Chart for Asphalt Binders." ASTM International, West Conshohocken, PA, 2016, https://doi.org/10.1520/D2493_D2493M-16.

ASTM D3497-79 (2003). "Standard Test Method for Dynamic Modulus of Asphalt Mixtures (Withdrawn 2009)." ASTM International, West Conshohocken, PA, 1979, www.astm.org.

Bari, J. and Witczak, M. (2006). "Development of a new revised version of the Witczak E* predictive model for hot mix asphalt mixtures (with discussion)." *Journal of the Association of Asphalt Paving Technologists*, 75, pp. 381–423.

Bari, J. (2005). *Development of a New Revised Version of the Witczak E* Predictive Model for Hot Mix Asphalt Mixtures*. Ph.D. Dissertation, Arizona State University, Tempe, AZ.

Baumgaertel, M. and Winter, H.H. (1989). "Determination of discrete relaxation and retardation time spectra from dynamic mechanical data." *Rheologica Acta*, 28(6), pp.511-519.

Birgisson, B., Sholar, G., and Roque, R. (2005). "Evaluation of a predicted dynamic modulus for Florida mixtures." *In Transportation Research Record: Journal of the Transportation Research Board*, Vol. 1929(1), pp. 200-207.

Birgisson, B., Sholar, G., and Roque, R. (2005). "Evaluation of Predicted Dynamic Modulus for Florida Mixtures." *84th Annual Meeting of the Transportation Research Board*, Paper No. 05-1309, Washington D.C.

Bonaquist, R. and Christensen, D. W. (2005). "Practical Procedure for Developing Dynamic Modulus Master Curves for Pavement Structural Design." *Transportation Research Record: Journal of the Transportation Research Board*, No. 1929, pp. 208–217.

Bonaquist, R. F., Christensen, D. W., and Stumps, W. (2003). *Simple performance tester for Superpave mix design: First-article development and evaluation*. NCHRP Rep. 513, National Cooperative Highway Research Program, Washington, DC.

Booij, H.C. and Thoone, G.P.J.M. (1982). "Generalization of Kramers-Kronig transforms and some approximations of relations between viscoelastic quantities." Rheologica Acta, 21(1), pp.15-24.

Bose N. K., and Liang, P. (1996). *Neural networks, fundamentals*. McGraw-Hill, New York.

Brown, E. R., Kandhal, P. S., Roberts, F. L., Kim, Y. R., Lee, D. Y., and Kennedy, T. W. (2009). *Hot Mix Asphalt Materials, Mixture Design, and Construction*. Third Edition, NAPA Research and Education Foundation, Lanham, MD.

Buttlar, W., Bauer, J. and Sherman, D. (2002). "Dynamic modulus of asphalt concrete with a hollow cylinder tensile tester." *Transportation Research Record: Journal of the Transportation Research Board*, No. 1789, pp. 183-190.

Chen, J.S. and Huang, L.S. (2000). "Developing an aging model to evaluate engineering properties of asphalt paving binders." *Materials and Structures*, 33(9), pp.559-565.

Christensen, R. M. (1982). *Theory of Viscoelasticity: An Introduction*. Second Ed., Academic Press Inc., NY, USA.

Ceylan, H., Schwartz, C. W., Kim, S., & Gopalakrishnan, K. (2009). "Accuracy of predictive models for dynamic modulus of hot-mix asphalt." *Journal of Materials in Civil Engineering*, 21(6), 286-293.

Christiansen, D. (2006). "Published Discussion to 'Bari and Witczak'." *Journal of the Association of Asphalt Paving Technologists*, Vol. 75, pp. 422–423.

Ceylan, H., Gopalakrishnan, K., & Kim, S. (2009). "Looking to the future: the next-generation hot mix asphalt dynamic modulus prediction models." *International Journal of Pavement Engineering*, 10(5), 341-352.

Ceylan, C., and Kim, S., Gopalakrishnan, K. (2007). "Hot Mix Asphalt Dynamic Modulus Prediction Models Using Neural Networks Approach." *Civil, Construction and Environmental Engineering Conference Presentation and Proceedings*, Paper No. 29.

Clyne, T. R., Li, X., Marasteanu, M. O., & Skok, E. L. (2003). *Dynamic and resilient modulus of Mn/DOT asphalt mixtures* (No. MN/RC-2003-09).

Ceylan, H., Gopalakrishnan, K., & Kim, S. (2008). "Advanced approaches to hot-mix asphalt dynamic modulus prediction." *Canadian Journal of Civil Engineering*, 35(7), 699-707.

Christensen Jr, D.W., Pellinen, T. and Bonaquist, R.F. (2003). "Hirsch model for estimating the modulus of asphalt concrete." *Journal of the Association of Asphalt Paving Technologists*, 72, pp. 97–121.

Dongré, R., Myers, L., D'Angelo, J., Paugh, C., and Gudimettla, J. (2005). "Field Evaluation of Witczak and Hirsch Models for Predicting Dynamic Modulus of Hot-Mix Asphalt (With Discussion)." *Journal of the Association of Asphalt Paving Technologists*, 74, pp. 381-442.

Daniel, J., Kim, Y. and Lee, H.J. (1998). "Effects of aging on viscoelastic properties of asphalt-aggregate mixtures." Transportation Research Record: Journal of the Transportation Research Board, No. 1630, pp.21-27.

El-Badawy, S., Bayomy, F., and Awed, A. (2012). "Performance of MEPDG dynamic modulus predictive models for asphalt concrete mixtures: local calibration for Idaho." *Journal of Materials in Civil Engineering*, 24(11), 1412-1421.

Far, M., Underwood, B., Ranjithan, S., Kim, Y., and Jackson, N. (2009). "Application of artificial neural networks for estimating dynamic modulus of asphalt concrete." *Transportation Research Record: Journal of the Transportation Research Board*, No. 2127, pp. 173-186.

Ferry, J. D. (1980). *Viscoelastic properties of polymers*. 3rd ed., Wiley, New York.

Garcia, G., and Thompson, M., (2007). "HMA dynamic modulus - Temperature relations." Research Report FHWA-ICT-07-006, Illinois Center for Transportation,

Department of Civil and Environmental Engineering, University of Illinois, 205 North Mathews – MC-250 Urbana, IL 61801.

GCTS (2013). "Servo-Hydraulic Asphalt Testing System (ATM-025)," http://www.gcts.com/?s=prod_ver&p=products&ID=46 (August 2013).

GCTS (2013). *Advanced Testing Systems for Highway Materials*, Published by GCTS, USA, 2013.

Gibson, N. (2002). *Time-temperature Superposition for Asphalt Concrete At large Compressive Strains*. Ph.D. Dissertation. University of Maryland, College Park, MD.

Hagan, M.T. and Menhaj, M.B. (1994). "Training feedforward networks with the Marquardt algorithm." *IEEE transactions on Neural Networks*, 5(6), pp.989-993.

Hagan, M. T., Demuth, H. B., Beale, M. H., and De Jesús, O. (1996). *Neural network design*, Volume 20, PWS publishing company, Boston.

Haykin, S. (1994). *Neural Network*. Prentice-Hall, Englewood Cliffs, NJ.

Hossain, Z. and Zaman, M. (2012). "Behavior of selected warm mix asphalt additive modified binders and prediction of dynamic modulus of the mixes." *Journal of Testing and Evaluation*, 41(1), pp.159-170.

Hopkins, I.L. and Hamming, R.W. (1957). "On creep and relaxation." *Journal of Applied Physics*, 28(8), pp.906-909.

Hecht-Nielsen, R. (1988). "Theory of the backpropagation neural network." *Neural Networks*, 1(Supplement-1), pp.445-448.

Jeong, M.G., Loulizi, A. and Flintsch, G.W. (2007). "Laboratory Validation of Viscoelastic Interconversion for Hot Mix Asphalt." *In Analysis of Asphalt Pavement Materials and Systems: Engineering Methods*, GSP 176, pp. 87-101.

Kim, Y. R. (2009). *Modeling of Asphalt Concrete*. 1st ed., ASCE Press, Reston, VA.

Kim, Y.R., King, M., and Momen, M. (2005). "Typical Dynamic Moduli Values of Hot Mix Asphalt in North Carolina and Their Prediction." *84th Annual Meeting of the Transportation Research Board*, Paper No. 05-2568, Washington D.C.

Kim, Y.R. and Lee, Y.C. (1995). "Interrelationships among stiffnesses of asphalt-aggregate mixtures (with discussion)." *Journal of the Association of Asphalt Paving Technologists*, 64.

King, M., Momen, M., and Kim, Y. R. (2005). "Typical Dynamic Modulus Values of Hot-Mix Asphalt in North Carolina and their Prediction." *84th Annual Meeting of the Transportation Research Board*, Washington, D.C.

Knoff, W.F. and Hopkins, I.L. (1972). "An improved numerical interconversion for creep compliance and relaxation modulus." *Journal of applied polymer science*, 16(11), pp.2963-2972.

Lakes R. S., (2009). *Viscoelastic materials*. Cambridge University Press, Avenue of Americas, NY, USA.

Leaderman, H. (1958). "Viscoelasticity phenomena in amorphous high polymeric systems." *Rheology 2*, pp. 1-61.

Lee, K., Kim, H., Kim, N. and Kim, Y. (2006). "Dynamic modulus of asphalt mixtures for development of Korean pavement design guide." *Journal of Testing and Evaluation*, 35(2), pp.143-150.

Levenberg, K. (1944). “A method for the solution of certain problems in least squares.” *Quarterly of Applied Mathematics*, 5, 164–168, 1944.

Li, R. (2000). “Time-temperature superposition method for glass transition temperature of plastic materials.” *Materials Science and Engineering: A*, 278(1), pp.36-45.

Marquardt, D. (1963). “An algorithm for least-squares estimation of nonlinear parameters.” *SIAM Journal on Applied Mathematics*, 11(2), 431–441, June 1963.

Mead, D.W. (1994). “Numerical interconversion of linear viscoelastic material functions.” *Journal of Rheology*, 38(6), pp.1769-1795.

Menard, K. P. (1999). *Dynamic Mechanical Analysis: A Practical Introduction*. CRC Press.

MEPDG (2008). *Mechanistic Empirical Pavement Design Guide. A manual of practice*. American Association of State Highway and Transportation Officials (AASHTO), Washington, D.C.

Meyers, M. A., and Chawla, K. K. (1999). *Mechanical Behavior of Materials*. Prentice Hall, Inc., New Jersey, pp. 98–103.

Mohammad, L.N., Wu, Z., Myers, L., Cooper, S. and Abadie, C. (2005). “A practical look at the simple performance tests: Louisiana's experience (with discussion).” *Journal of the Association of Asphalt Paving Technologists*, 74, pp. 557-600.

Mun, S., Chehab, G.R. and Kim, Y.R. (2007). “Determination of time-domain viscoelastic functions using optimized interconversion techniques.” *Road materials and pavement design*, 8(2), pp.351-365.

NCHRP. (2004). *Guide for Mechanistic-Empirical Design of new-rehabilitated pavement structures*. Report 1-37A, National Cooperative Highway Research Program (NCHRP), Washington, D.C.

NCHRP (2007). *Research Result Digest 324: Simulating the Effects of Hot Mix Asphalt Aging for Performance Testing and Pavement Structural Design*. National Cooperative Highway Research Program (NCHRP).

Obulareddy, S. (2006). *Fundamental Characterization of Louisiana HMA Mixtures for the 2002 Mechanistic-Empirical Design Guide*. MS Thesis, Louisiana State University, Baton Rouge, LA.

Osborne, M.R. (1992). "Fisher's method of scoring." International Statistical Review, 86, pp. 271–286.

Park, S.W. and Schapery, R.A. (1999). "Methods of interconversion between linear viscoelastic material functions. Part I—A numerical method based on Prony series." *International Journal of Solids and Structures*, 36(11), pp.1653-1675.

Park, S.W. and Kim, Y.R. (1999). "Interconversion between relaxation modulus and creep compliance for viscoelastic solids." *Journal of materials in Civil Engineering*, 11(1), pp.76-82.

Park, S.W. and Kim, Y.R. (1999). "Interconversion between relaxation modulus and creep compliance for viscoelastic solids." *Journal of materials in Civil Engineering*, 11(1), pp.76-82.

Park, S.W. and Kim, Y.R. (2001). "Fitting Prony-series viscoelastic models with power-law presmoothing." *Journal of Materials in Civil Engineering*, 13(1), pp.26-32.

Pellinen, T. K. (2001). *Investigation of the Use of Dynamic Modulus as an Indicator of Hot-Mix Asphalt Performance*. Ph.D. dissertation, Arizona State University, Tempe.

Raad, L., Saboundjian, S. and Minassian, G. (2001). "Field aging effects on fatigue of asphalt concrete and asphalt-rubber concrete." *Transportation Research Record: Journal of the Transportation Research Board*, No. 1767, pp.126-134.

Rahman, A. S. M. A., Mannan, U. A. and Tarefder, R. A. (2016). "Predicting dynamic modulus of asphalt concrete from binder rheological properties." *Journal of Testing and Evaluation*, 45(1), pp. 28-39.

Rahman, A.S.M.A., Islam, M.R. and Tarefder, R.A. (2016). "Modifying the viscosity based Witczak model and developing phase angle predictive model for New Mexico's Superpave mixes." *95th Annual Meeting of the Transportation Research Board*, Paper No. 16-3180, Washington D.C.

Rowe, G. and Sharrock, M. (2011). "Alternate shift factor relationship for describing temperature dependency of viscoelastic behavior of asphalt materials." *Transportation Research Record: Journal of the Transportation Research Board*, (2207), pp.125-135.

Rumelhart, D. E., Hinton, G. E., and Williams, R. J. (1986). "Learning representations by back-propagating errors." *Nature*, 323, 533–536, 1986.

Ramkumar, D.H.S., Caruthers, J.M., Mavridis, H. and Shroff, R. (1997). "Computation of the linear viscoelastic relaxation spectrum from experimental data." *Journal of applied polymer science*, 64(11), pp.2177-2189.

Said, S. (2005). "Aging effect on mechanical characteristics of bituminous mixtures." *Transportation Research Record: Journal of the Transportation Research Board,* No. 1901, pp.1-9.

Schapery, R.A. and Park, S.W. (1999). "Methods of interconversion between linear viscoelastic material functions. Part II—an approximate analytical method." *International Journal of Solids and Structures,* 36(11), pp.1677-1699.

Schapery, R. A. (1962). "Approximate methods of transform inversion for viscoelastic stress analysis." *Proc. 4th U.S. Nat. Cong. Appl. Mech.*, pp. 1075-1085.

Schapery, R. A. (1974). "Viscoelastic behavior and analysis of composite materials." *Composite Materials,* ed. G. P. Sendeckyj, Chap. 4, Vol. 2. pp. 85-168, Academic Press, New York.

SHRP-A-379. (1994). *The Superpave mix design system manual of specifications, test methods, and practices: M-003*. Strategic Highway Research Program, National Research Council, Washington, DC.

Shu, X. and Huang, B. (2008). "Dynamic modulus prediction of HMA mixtures based on the viscoelastic micromechanical model." *Journal of Materials in Civil Engineering,* 20(8), pp.530-538.

Schwartz, C. W. (2005). "Evaluation of the Witczak dynamic modulus prediction model." *84th Annual Meeting of the Transportation Research Board*, Paper No. 05-2112, Washington D.C.

Schwartz, C., Gibson, N. and Schapery, R. (2002). "Time-temperature superposition for asphalt concrete at large compressive strains." *Transportation Research Record: Journal of the Transportation Research Board*, No. 1789, pp. 101-112.

Singh, D., Zaman, M. and Commuri, S. (2011). "Evaluation of predictive models for estimating dynamic modulus of hot-mix asphalt in Oklahoma." *Transportation Research Record: Journal of the Transportation Research Board,* No. 2210, pp. 57-72.

Singh, D., Zaman, M. and Commuri, S. (2011). "Effect of long term oven aging on dynamic modulus of hot mix asphalt." In *Geo-Frontiers 2011: Advances in Geotechnical Engineering,* pp. 4773-4781.

Singh, D., Zaman, M. and Commuri, S. (2012). "A laboratory investigation into the effect of long-term oven aging on RAP mixes using dynamic modulus test." *International Journal of Pavement Research and Technology,* 5(3), pp.142-152.

Soleymani, H., Zhai, H. and Bahia, H. (2004). "Role of modified binders in rheology and damage resistance behavior of asphalt mixtures." *Transportation Research Record: Journal of the Transportation Research Board,* No. 1875, pp. 70-79.

Sotil, A., Kaloush, K. and Witczak, M. (2004). "Reduced confined dynamic modulus testing protocol for asphalt mixtures." *Transportation Research Record: Journal of the Transportation Research Board,* No. 1891, pp.153-162.

Sotil, A. (2003). *Material Characterization of Asphalt Rubber Mixtures Using the Dynamic Modulus Test*. Master's thesis, Arizona State University, Tempe.

Staverman, A. J., Schwarzl, F. (1955). *Physik der Hochpolymeren*. ed. H. A. Stuart, pp. 1-121. Band Iv. Springer-Verlag, Berlin.

Tarbox, S. and Daniel, J. (2012). "Effects of Long-Term Oven Aging on Reclaimed Asphalt Pavement Mixtures." *Transportation Research Record: Journal of the Transportation Research Board,* No. 2294, pp.1-15.

Tarefder, R. A., and Rahman, A. S. M. A. (2016). *Enhanced Statewide and Independent Assurance Testing for Dynamic Modulus of NMDOT Superpave Mixes for the Implementation of Mechanistic Empirical Pavement Design Guide, Final Report*. Report No. NM12SP-02, 2016, New Mexico Department of Transportation, Albuquerque, NM.

Tarefder, R. and Faisal, H. (2013). "Nanoindentation characterization of asphalt concrete aging." *Journal of Nanomechanics and Micromechanics*, 4(1), p.A4013003.

Tashman, L. and Elangovan, M. A. (2004). "Dynamic Modulus Test – Laboratory Evaluation and Future Implementation in the State of Washington", Final research report, Washington State University (WSU), Transportation Research Center (TRAC), Pullman, WA 99164-2910.

Tran, N.H., and Hall, K.D. (2005). "Evaluating the Predictive Equation in Determining Dynamic Moduli of Typical Asphalt Mixtures Used in Arkansas." *Journal of the Association of Asphalt Paving Technologists*, Volume 74, pp. 1-17.

Varma, S., Kutay, M. and Levenberg, E. (2013). "Viscoelastic genetic algorithm for inverse analysis of asphalt layer properties from falling weight deflections." *Transportation Research Record: Journal of the Transportation Research Board*, No. 2369, pp.38-46.

Van Gurp, M. and Palmen, J. (1998). "Time-temperature superposition for polymeric blends." *Rheol. Bull*, 67(1), pp.5-8.

Witczak M. W. and Sotil A. (2004). "A Recommended Methodology for Developing Dynamic Modulus E* Master Curves from Nonlinear Optimization". Arizona State University, Tempe.

Witczak, M. (2005). *Simple performance tests: Summary of recommended methods and database*. NCHRP Rep. 547, Transportation Research Board of the National Academies, National Research Council, Washington, D.C.

Wilamowski, B.M. and Torvik, L. (1993). "Modification of gradient computation in the back-propagation algorithm." *ANNIE'93-Artificial Neural Networks in Engineering*, pp.175-180.

Wilamowski, B. M., and Torvik, L. (1993). "Modification of gradient computation in the back-propagation algorithm." In *Artificial Neural Networks in Engineering (ANNIE'93)*, St. Louis, MO, November 14–17, 1993.

Wilamowski, B. M. (1996). "Neural networks and fuzzy systems." Chaps. 124.1 to 124.8 in *The Electronic Handbook*, CRC Press, Boca Raton, FL, pp. 1893–1914.

Wilamowski, B.M. and Jaeger, R.C. (1996). "Implementation of RBF type networks by MLP networks." In *IEEE International Conference on Neural Networks*, Vol. 3, pp. 1670-1675.

Wilamowski, B.M., Chen, Y. and Malinowski, A. (1999). "Efficient algorithm for training neural networks with one hidden layer." In *1999 International Joint Conference on Neural Networks (IJCNN'99)*, Vol. 3, pp. 1725-1728.

Wilamowski, B. M. (2002). "Neural networks and fuzzy systems." Chap. 32 in *Mechatronics Handbook*, ed. R. R. Bishop, CRC Press, Boca Raton, FL, pp. 33-1–32-26.

Wilamowski, B.M., Hunter, D. and Malinowski, A. (2003). "Solving parity-N problems with feedforward neural networks." In *Proceedings of the IJCNN'03 International Joint Conference on Neural Networks*, Vol. 4, pp. 2546-2551.

Wilamowski, B.M. (2009). "Neural network architectures and learning algorithms." *IEEE Industrial Electronics Magazine*, 3(4), pp. 56–63.

Wilamowski, B.M. and Yu, H. (2010). "Improved computation for Levenberg–Marquardt training." *IEEE transactions on neural networks*, 21(6), pp.930-937.

Wang, H. and Al-Qadi, I.L. (2012). "Importance of nonlinear anisotropic modeling of granular base for predicting maximum viscoelastic pavement responses under moving vehicular loading." *Journal of engineering mechanics*, 139(1), pp.29-38.

Weldegiorgis, M.T. (2014). *On Dynamic Modulus of Asphalt Concrete for Moisture Damage*. Doctoral Dissertation. Department of Civil Engineering, University of New Mexico, Albuquerque, NM.

Witczak, M. W., Bonaquist, R., Von Quintus, H., and Kaloush, K. (2000). "Specimen Geometry and Aggregate Size Effects in Uniaxial Compression and Constant Height Shear Test." *Journal of the Association of Asphalt Paving Technologists*, Vol. 69, pp.733–793.

Weldegiorgis, M.T. and Tarefder, R.A. (2013). "Dynamic Modulus Testing and Mechanical Modeling for New Mexico Asphalt Mixtures." In *ICSDEC 2012: Developing the Frontier of Sustainable Design, Engineering, and Construction*, pp. 481-488.

Weldegiorgis, M. T., Faisal, H. M., and Tarefder, R. A. (2013). "Use of BBR Test Data to Enhance the Accuracy of |G*|-Based Witczak Model Predictions." *International Journal of Pavement Conference*, Paper No: 122-2, 2013, São Paulo, Brazil, pp. 1.

Werbos, P. J. (1988). "Back-propagation: Past and future." *Proceedings of International Conference on Neural Networks*, vol. 1, pp. 343–354, San Diego, CA, 1988.

Woo, W., Chowdhury, A. and Glover, C. (2008). "Field aging of unmodified asphalt binder in three Texas long-term performance pavements." *Transportation Research Record: Journal of the Transportation Research Board*, (2051), pp.15-22.

Yang, X. and You, Z. (2015). "New predictive equations for dynamic modulus and phase angle using a nonlinear least-squares regression model." *Journal of Materials in Civil Engineering*, 27(3), p.04014131.

Yu, H. and Wilamowski, B. M. (2011). "Levenberg-Marquardt Training." *The Industrial Electronics Handbook*, Vol. 5−Intelligent Systems, 2nd ed. (CRC Press, Boca Raton, 2011).

Yu, H. and Wilamowski, B.M. (2009). "C++ implementation of neural networks trainer." In *13th International Conference on Intelligent Engineering Systems* (INES-09), pp. 257-262.

Zeng, M. and Huang, S. (2006). "Characterizing the Asphalt-Aggregate Mixtures Using Rheological Properties of Asphalt Binders." *Journal of Testing and Evaluation*, Vol. 34, No. 6, Paper ID JTE100507, pp. 1-12.

Appendix A

Table A-1 Summary of Collected Samples from NMDOT District 1

#	Mix Type	SP Gradation	Spec. Binder PG	Used Binder PG	% RAP	Project No.	Project Location	County	Agg. Source	Agg. Source Location	Agg. Type	WMA Additive	SML Mix Design No.	Asphalt Source
1	WMA	SP-IV	76-22	70-22	35	1100630	I-25	Socorro	Abo Arroyo Pit	Bernardo, NM	Sand & Gravel	Foaming	2012-WMA-D1-14-131	NuStar
2	WMA	SP–III	76-22	64-28	35	1C00003	I-25	Sierra	T or C Pit	T or C, NM	Sand & Gravel	Water	2012-WMA-D1-12-102	NuStar
3	WMA	SP–IV	76-22	70-28	35	1100641	I-25	Socorro	Sagen Pit	Socorro, NM	Volcanic	Foaming	2014-WMA-D1-08-18R	Holly Frontier
4	WMA	SP–III	76-22	58-28	35	1100900	I-25	Sierra	T or C Pit	T or C, NM	Sand & Gravel	Foaming	2014-WMA-D1-16-116	Western
5	WMA	SP-IV	76-22	58-28	35	1101010	NM 180	Grant	Oliver Pit	Deming, Luna, NM	Sand & Gravel	Foaming	2015-WMA-D1-05-05	Western
6	WMA	SP-III	76-22	64-22	35	1101020	I-25	Dona Ana	Vado Pit	Dona Ana, NM	Monzonite	Foaming	2015-WMA-D1-04-14	Western
7	WMA	SP-IV	70-22	70-22	0	1100680	Hudson Bridge, NM 90	Grant	Mimbres Pit	Silver City, NM	Sand & Gravel	Evotherm	2015-WMA-D1-03-03	Holly Frontier
8	WMA	SP-III	76-22	64-22	35	1100620	I-10	Dona Ana	Vado Pit	Vado, NM	Monzonite	Foaming	2016-WMA-D1-01-05	Western Refining

Table A-2 Summary of Collected Samples from NMDOT District 2

#	Mix Type	SP Gradation	Spec. Binder PG	Used Binder PG	% RAP	Project No.	Project Location	County	Agg. Source	Agg. Source Location	Agg. Type	WMA Additive	SML Mix Design No.	Asphalt Source
1	WMA	SP-III	76-22	64-22	33	2100880	US 380	Chaves	Ford Pit	Chaves, NM	Limestone	Foaming	2013-WMA-D2-08-28	Western
2	WMA	SP-III	70-22	64-22	35	2101060	US 70/380	Chaves	Ford Pit	Roswell, Chaves, NM	Limestone	Foaming	2013-WMA-D2-09-29	Western
3	HMA	SP-III	70-22	58-28	35	2100380	US 82 / NM 209	Lea	Cox Pit	Lea, NM	River Deposits	N/A	2012-D2-05-25R	Holly Frontier
4	HMA	SP-III	70-22	64-22	35	G3A92	US 54	Otero	3 Rivers Pit	Otero, NM	River Deposits	N/A	2014-HMA-D2-01-21	Holly Frontier
5	WMA	SP-III	70-22	64-28	25	CN-2100250/ 2100251	US 54	Lincoln	3 Rivers Pit	Lincoln, Otero, NM	River Deposits	Foaming	2014-WMA-D2-02-22	Holly Frontier
6	WMA	SP-III	76-22	70-28	27	2100910	NM 529	Lea	Cox Pit	Lea, NM	Sand & Gravel	Foaming	2015-WMA-D2-04-24	Holly Frontier
7	WMA	SP-IV	76-22	70-28	27	2100910	NM 529	Lea	Cox Pit	Lea, NM	Sand & Gravel	Foaming	2015-WMA-D2-05-25	Holly Frontier
8	WMA	SP-IV	76-22	70-22	25	2101280	NM 176	Lea	Thunder Run Pit	Carlsbad	Limestone	Foaming	2015-WMA-D2-08-28	Holly Frontier
9	WMA	SP-IV	70-22	64-22	25	2100900	US 54	Otero	Three Rivers	Alamogordo	Sand & Gravel	Foaming	2016-WMA-D2-02-04	Western Refining

Table A-3 Summary of Collected Samples from NMDOT District 3

#	Mix Type	SP Gradation	Spec. Binder PG	Used Binder PG	% RAP	Project No.	Project Location	County	Agg. Source	Agg. Source Location	Agg. Type	WMA Additive	SML Mix Design No.	Asphalt Source
1	HMA	SP-III	76-22	70-22	35	A300850	I-40	Bernalillo	South Valley Pit	Los Lunas, NM	Basalt	N/A	2012-D3-01-31	Holly Frontier
2	HMA	SP-IV	70-22	64-22	25	Various	Various	Various	Bar J Pit	Sandoval, NM	Alluvial Lime-stone	N/A	2013-HMA-CMD-44-144	Western
3	HMA	SP-IV	70-22	64-22	25	Comm. Mix	Various	Bernalillo	Bar J Pit	Sandoval, NM	Alluvial Lime-stone	N/A	2014-HMA-CMD-57-127	Western
4	HMA	SP-III	70-22	64-22	25	Comm. Mix	Various	Bernalillo	Bar J Pit	Bernalillo	Alluvial Lime-stone	N/A	2014-HMA-CMD-30-100	Holly Frontier
5	HMA	SP-III	70-22	64-22	35	A300411	NM 333	Bernalillo	Davis Pit	Torrance, NM	Quartzite	N/A	2014-SMA-D3-05-35	Western
6	WMA	SP-III	76-22	70-28	25	A300380	NM 528	Sandoval	Placitas/Baca	Sandoval, NM	Sand & Gravel	Foaming	2014-WMA-D3-04-34R	Holly Frontier
7	WMA	SP-III	76-22	70-22	15	A301010 / A301610	I-25	Bernalillo	Los Lunas Pit	Los Lunas, NM	Basalt	Foaming	2015-WMA-D3-01-31	Western Refining
8	WMA	SP-IV	76-22	70-22	15	A301010 / A301610	I-25	Bernalillo	Los Lunas Pit	Los Lunas, NM	Basalt	Foaming	2015-WMA-D3-02-32	Western Refining
9	HMA	SP-III	76-22	70-22	35	3100460	I-25 Bus Loop	Valencia	Los Lunas Pit	Los Lunas, NM	Basalt	N/A	2015-HMA-D3-08-38	Western Refining
10	HMA	SP-III	70-22	70-22	15	3100340	Belen Main St.	Valencia	Los Lunas Pit	Los Lunas, NM	Basalt	N/A	2015-HMA-D3-10-140	Western Refining
11	HMA	SP-III	70-22	70-22	15	Various	Various	Bernalillo	Beca Pit	Sandoval, NM	Sand & Gravel	N/A	2016-HMA-CMD-02-03	Holly Frontier

Table A-4 Summary of Collected Samples from NMDOT District 4

#	Mix Type	SP Gradation	Spec. Binder PG	Used Binder PG	% RAP	Project No.	Project Location	County	Agg. Source	Agg. Source Location	Agg. Type	WMA Additive	SML Mix Design No.	Asphalt Source
1	HMA	SP – III	64-28	64-28	0	4100650	US 64	Colfax	Tinaja Pit	Raton, NM	Basalt	N/A	2013-HMA-D4-02-42	Nustar
2	WMA	SP – III	70-22	70-22	0	4C00001	I-40	Quay	Moon Pit	Guadalupe, NM	Sand & Gravel	Other	2012-WMA-D4-03-43 TS	Nustar
3	WMA	SP – III	76-22	76-22	0	4100670	I-40	Quay	Paula Pit	Quay, NM	Sand & Gravel	Foaming	2013-WMA-D4-01-41	Holly Frontier
4	HMA	SP – III	70-22	70-22	0	4C00002	I-40	Guadalupe	Moon Pit	Guadalupe, NM	Alluvial Lime-stone	N/A	2012-D4-05-45	Holly Frontier
5	HMA	SP – III	76-22	70-28	20	4100600	I-40	Guadalupe	Moon Pit	Guadalupe, NM	Sand & Gravel	N/A	2014-HMA-D4-04-44 TS-1	Holly Frontier
6	WMA	SP – III	76-22	70-28	20	4100600	I-40	Guadalupe	Moon Pit	Guadalupe, NM	Sand & Gravel	Foaming	2014-WMA-D4-05-45 TS-2	Holly Frontier
7	WMA	SP – III	76-22	70-28	20	4100600	I-40	Guadalupe	Moon Pit	Guadalupe, NM	Sand & Gravel	Evotherm	2014-WMA-D4-07-47 TS-3	Holly Frontier
8	WMA	SP – III	76-22	70-28	20	4100600	I-40	Guadalupe	Moon Pit	Guadalupe, NM	Sand & Gravel	Cecabase RT	2014-WMA-D4-08-48 TS-4	Holly Frontier
9	WMA	SP – III	76-22	70-28+	20	4100600	I-40	Guadalupe	Moon Pit	Guadalupe, NM	Sand & Gravel	Cecabase RT	2014-WMA-D4-09-49 TS-5	Holly Frontier
10	WMA	SP – III	64-28	64-28	0	4100590	I-25	San Miguel	Moon Pit	Guadalupe, NM	Sand & Gravel	Foaming	2015-WMA-D4-04-44	Holly Frontier
11	WMA	SP - III	64-28	64-28	0	4100800	I-25	San Miguel	Moon Pit	Guadalupe, NM	Sand & Gravel	Foaming	2016-WMA-D4-03-43	Holly Frontier

Table A-5 Summary of Collected Samples from NMDOT District 5

#	Mix Type	SP Gradation	Spec. Binder PG	Used Binder PG	% RAP	Project No.	Project Location	County	Agg. Source	Agg. Source Location	Agg. Type	WMA Additive	SML Mix Design No.	Asphalt Source
1	HMA	SP – III	58-28	58-28	30	Comm. Mix	Various	Various	Lumberton Pit	Chama, NM	Sand & Gravel	N/A	2011-CMD-45-70R	Nustar
2	HMA	SP – IV	70-22	64-22	25	Various	Various	Various	Bar J pit	Sandoval, NM	Alluvial Lime-stone	N/A	2013-HMA-CMD-44-144	Western
3	HMA	SP – IV	70-22	64-22	25	Comm. Mix	Various	Bernalillo	Bar J Pit	Sandoval, NM	Alluvial Lime-stone	N/A	2014-HMA-CMD-57-127	Western
4	HMA	SP – III	70-22	64-22	25	Comm. Mix	Various	Bernalillo	Bar J Pit	Sandoval, NM	Alluvial Lime-stone	N/A	2014-HMA-CMD-30-100	Holly Frontier
5	HMA	SP – III	64-28	58-28	35	5100411	I-40 & US 285	Moriarty, NM	Davis Pit	Torrance, NM	Quartzite	N/A	2014-HMA-D5-10-60	Western

Table A-6 Summary of Collected Samples from NMDOT District 6

#	Mix Type	SP Gradation	Spec. Binder PG	Used Binder PG	% RAP	Project No.	Project Location	County	Agg. Source	Agg. Source Location	Agg. Type	WMA Additive	SML Mix Design No.	Asphalt Source
1	WMA	SP – III	76-28	76-28	0%	5100451	US 60	Catron, NM	Weldon Ranch Pit	Catron, NM	Dacite	Evotherm	2013-WMA-D6-10-10	Holly Frontier
2	HMA	SP – III	70-22	70-22	0%	6C00002	I-40	Cibola, NM	Tinaja Pit	Cibola, NM	Lime-stone	N/A	2012-D6-02-62	Holly Frontier
3	HMA	SP – III	76-28	76-28	15%	6100713	I-40	Cibola, NM	Rinconada Pit	Cibola, NM	Basalt	N/A	2013-HMA-D6-04-64	Nustar
4	HMA	SP – IV	70-22	70-22	0%	Comm. Mix	Various	Various	Page Pit	McKinley, NM	Sand & Gravel	N/A	2013-HMA-CMD-62-162	Western
5	HMA	SP – III	70-22	70-22	15%	6100650	I – 40	McKinley	Tinaja Pit	Cibola, NM	Limestone	N/A	2015-HMA-D6-07-67	Holly Frontier
6	HMA	SP – III	70-22	70-22	0%	6100783	US 491	McKinley	Page Pit	McKinley, NM	Crushed Granite	N/A	2015-HMA-D6-09-69	Western Refining
7	HMA	SP – III	70-22	70-22	15%	6100783	US 491	McKinley	Page Pit	McKinley, NM	Crushed Granite	N/A	2015-HMA-D6-05-65	Western Refining
8	HMA	SP – III	64-28	70-22	0%	6100721	NM 12	Catron	I-25 Pit	Socorro, NM	Rhyolite	N/A	2015-HMA-CMD-03-63	Holly Frontier
9	HMA	SP – III	76-28	76-28	15%	6101100R	I-40	Cibola	Baca Pit / Placitas	Sandoval, NM	Sand & Gravel	N/A	2015-HMA-D6-08-68	Holly Frontier
10	HMA	SP – III	70-22	58-28	35%	F100110	US 64	San Juan	Horn Canyon	San Juan, NM	Sand & Gravel	N/A	2016-HMA-D5-01-07	Western Refining

Table A-7 Summary of Tested AC Mixtures and Specimens

Serial No.	NMDOT District ID	Superpave Gradation Type	Binder PG grade (Spec./Used)	AC Mix Type	RAP Fraction (%)	No. of Tested Specimen	Spec. ID	Max. Specific Gravity (G_{mm})	Bulk Specific Gravity (G_{mb})	Air Void %	Asphalt Content (%)	Project Info.
1	D-1	SP – IV	76-22/70-22	WMA	35.0	3	1	2.489	2.341	6.0	4.7	Project # 1100630 Mix Design # 2012-WMA-D1-14-131 Contractor: MSCI
							2		2.339	6.0		
							3		2.342	5.9		
2	D-4	SP – III	70-22/70-22	HMA	0.0	5	1	2.478	2.352	5.1	4.2	Project # 4C00002 Mix Design # 2012-D4-05-45 Contractor: FSG
							2		2.344	5.4		
							3		2.347	5.3		
							4		2.334	5.8		
							5		2.352	5.1		
3	D-6	SP – III	70-22/70-22	HMA	0.0	3	1	2.488	2.348	5.6	4.4	Project # 6C00002 Mix Design # 2012-D6-02-62 Contractor: FSG
							2		2.341	5.9		
							3		2.339	6.0		
4	D-3	SP - III	76-22/70-22	HMA	35.0	3	1	2.573	2.444	5.0	4.4	Project # A300850 Mix Design # 2012-D3-01-31 Contractor: MSCI
							2		2.444	5.0		
							3		2.439	5.2		
5	D-2	SP - III	70-22/58-28	HMA	35.0	3	1	2.471	2.323	6.0	4.5	Project # 2100380 Mix Design # 2012-D2-05-25R Contractor: FSG
							2		2.330	5.7		
							3		2.323	6.0		
6	D-3	SP-IV	70-22/64-22	HMA	25.0	3	2	2.424	2.279	6.0	5.0	Project # Various Mix Design #2013-HMA-CMD-44-144 Contractor: FSG
							3		2.279	6.0		
							4		2.298	5.2		
7	D-5	SP-IV	70-22/64-22	HMA	25.0	3	2	2.424	2.279	6.0	5.0	Project # Various Mix Design #2013-HMA-CMD-44-144 Contractor: FSG
							3		2.279	6.0		
							4		2.298	5.2		
8	D-5	SP - III	58-28/58-28	HMA	30.0	3	4	2.510	2.362	5.9	4.1	Project # CMD Mix Design # 2011-CMD-45-70R Contractor: JHCC
							5		2.359	6.0		
							7		2.364	5.8		

Serial No.	NMDOT District ID	Superpave Gradation Type	Binder PG grade (Spec./Used)	AC Mix Type	RAP Fraction (%)	No. of Tested Specimen	Spec. ID	Max. Specific Gravity (G_{mm})	Bulk Specific Gravity (G_{mb})	Air Void %	Asphalt Content (%)	Project Info.
9	D-1	SP – III	76-22/64-28	WMA	35.0	3	4	2.348	2.217	5.6	5.7	Project # 1C00003 Mix Design # 2012-WMA-D1-12-102 Contractor: JHCC
							5		2.228	5.1		
							6		2.214	5.7		
10	D-6	SP - III	76-28/76-28	WMA	0.0	3	2	2.407	2.272	5.6	5.8	Project # 5100451 Mix Design # 2013-WMA-D6-10-10 Contractor: RSG
							3		2.287	5.0		
							5		2.287	5.0		
11	D-6	SP - III	76-28/76-28	HMA	15.0	3	3	2.492	2.342	6.0	4.9	Project # 6100713 Mix Design # 2013-HMA-D6-04-64 Contractor: FSG
							4		2.345	5.9		
							5		2.342	6.0		
12	D-4	SP - III	64-28/64-28	HMA	0.0	3	1	2.564	2.410	6.0	5.6	Project # 4100650 Mix Design # 2013-HMA-D4-02-42 Contractor: NMC
							2		2.410	6.0		
							6		2.410	6.0		
13	D-4	SP – III	70-22/70-22	WMA	0.0	3	1	2.459	2.317	5.8	4.5	Project # 4C00001 Mix Design #2012-WMA-D4-03-43 TS Contractor: FSG
							2		2.310	6.0		
							3		2.312	6.0		
14	D-4	SP - III	76-22/76-22	WMA	0.0	3	1	2.478	2.337	5.7	4.2	Project # 4100670 Mix Design # 2013-WMA-D4-01-41 Contractor: FSG
							2		2.347	5.3		
							3		2.346	5.3		
15	D-6	SP - IV	70-22/70-22	HMA	0.0	3	1	2.417	2.271	6.0	5.0	Project # CMD Mix Design #2013-HMA-CMD-62-162 Contractor: VHCC
							2		2.285	5.5		
							3		2.296	5.0		
16	D-2	SP – III	76-22/64-22	WMA	33	3	1	2.457	2.334	5.0	4.9	Project # 2100880 Mix Design # 2013-WMA-D2-08-28 Contractor: MSCI
							2		2.334	5.0		
							3		2.313	5.8		
17	D-2	SP – III	70-22/64-22	WMA	35	3	1	2.464	2.316	6.0	4.8	Project # 2101060 Mix Design # 2013-WMA-D2-09-29 Contractor: MSCI
							2		2.318	5.9		
							3		2.315	6.0		

Serial No.	NMDOT District ID	Superpave Gradation Type	Binder PG grade (Spec./Used)	AC Mix Type	RAP Fraction (%)	No. of Tested Specimen	Spec. ID	Max. Specific Gravity (G_{mm})	Bulk Specific Gravity (G_{mb})	Air Void %	Asphalt Content (%)	Project Info.
18	D-2	SP – III	70-22/64-22	HMA	35	3	1	2.458	2.310	6.0	5.2	Project # G3A92 Mix Design # 2014-HMA-D2-01-21 Contractor: FNF
							2		2.318	5.7		
							3		2.309	6.0		
19	D-2	SP – III	70-22/64-28	WMA	25	3	1	2.452	2.329	5.0	4.7	Project # CN-2100250/ 2100251 Mix Design # 2014-WMA-D2-02-22 Contractor: FNF
							2		2.330	5.0		
							3		2.330	5.0		
20	D-3	SP – III	76-22/70-28	WMA	25	3	4	2.435	2.305	5.3	5.0	Project # A300380 Mix Design # 2014-WMA-D3-04-34R Contractor: AUI
							5		2.306	5.3		
							7		2.299	5.6		
21	D-1	SP – III	76-22/58-28	WMA	35	3	3	2.358	2.229	5.5	5.8	Project # 1100900 Mix Design # 2014-WMA-D1-16-116 Contractor: MSCI
							4		2.235	5.2		
							5		2.218	5.9		
22	D-4	SP – III	76-22/70-28	HMA	20	3	1	2.473	2.337	5.5	4.6	Project # 4100600 Mix Design #2014-HMA-D4-04-44-TS-1 Contractor: FSG
							2		2.345	5.2		
							3		2.339	5.4		
23	D-4	SP – III	76-22/70-28	WMA	20	3	4	2.474	2.351	5.0	4.6	Project # 4100600 Mix Design #2014-WMA-D4-05-45-TS2 Contractor: FSG
							5		2.325	6.0		
							6		2.350	5.0		
							8		2.326	6.0		
24	D-4	SP – III	76-22/70-28	WMA	20	3	1	2.479	2.352	5.1	4.6	Project # 4100600 Mix Design #2014-WMA-D4-07-47-TS3 Contractor: FSG
							2		2.356	5.0		
							3		2.346	5.3		
25	D-4	SP – III	76-22/70-28	WMA	20	3	1	2.470	2.322	6.0	4.6	Project # 4100600 Mix Design #2014-WMA-D4-08-48-TS4 Contractor: FSG
							2		2.327	5.8		
							3		2.321	6.0		

Serial No.	NMDOT District ID	Superpave Gradation Type	Binder PG grade (Spec./Used)	AC Mix Type	RAP Fraction (%)	No. of Tested Specimen	Spec. ID	Max. Specific Gravity (G_{mm})	Bulk Specific Gravity (G_{mb})	Air Void %	Asphalt Content (%)	Project Info.
26	D-4	SP – III	76-22/70-28+	WMA	20	3	4	2.475	2.331	5.8	4.6	Project # 4100600 Mix Design #2014-WMA-D4-09-49-TS5 Contractor: FSG
							5		2.341	5.4		
							6		2.352	5.0		
27	D-5	SP – III	64-28/58-28	HMA	35	3	1	2.522	2.372	6.0	4.7	Project # 5100411 Mix Design #2014-HMA-D5-10-60 Contractor: MSCI
							2		2.371	6.0		
							4		2.370	6.0		
28	D-3	SP – III	70-22/64-22	HMA	35	3	7	2.518	2.367	6.0	5.1	Project # A300411 Mix Design #2014-SMA-D3-05-35 Contractor: MSCI
							12		2.367	6.0		
							13		2.369	5.9		
29	D-3	SP - IV	76-22/70-22	WMA	15	3	2	2.580	2.425	6.0	5.2	Project # A301010/A301610 Mix Design #2015-WMA-D3-02-32 Contractor: MSCI
							6		2.436	5.6		
							10		2.451	5.0		
30	D-1	SP – IV	76-22/70-28	WMA	35	3	1	2.255	2.135	5.3	6.0	Project # 1100641 Mix Design #2014-WMA-D1-08-18 Contractor: FSG
							5		2.124	5.8		
							9		2.135	5.3		
31	D-3	SP – IV	70-22/64-22	HMA	25	3	2	2.425	2.292	5.5	5.1	Project # CMD Mix Design #2014-HMA-CMD-57-127 Contractor: FSG
							3		2.296	5.3		
							7		2.301	5.1		
32	D-3	SP – III	70-22/64-22	HMA	25	3	1	2.459	2.319	5.7	4.7	Project # CMD Mix Design #2014-HMA-CMD-30-100 Contractor: FSG
							2		2.311	6.0		
							4		2.331	5.2		
33	D-5	SP – III	70-22/64-22	HMA	25	3	1	2.459	2.336	5.0	4.7	Project # CMD Mix Design #2014-HMA-CMD-30-100 Contractor: FSG
							3		2.311	6.0		
							4		2.311	6.0		

Serial No.	NMDOT District ID	Superpave Gradation Type	Binder PG grade (Spec./Used)	AC Mix Type	RAP Fraction (%)	No. of Tested Specimen	Spec. ID	Max. Specific Gravity (G_{mm})	Bulk Specific Gravity (G_{mb})	Air Void %	Asphalt Content (%)	Project Info.
34	D-5	SP – IV	70-22/64-22	HMA	25	3	1	2.425	2.296	5.3	4.6	Project # CMD Mix Design #2014-HMA-CMD-57-127 Contractor: FSG
							2		2.280	6.0		
							3		2.299	5.2		
35	D-1	SP – IV	76-22/58-28	WMA	35	3	1	2.382	2.256	5.3	5.2	Project # 1101010 Mix Design #2015-WMA-D1-05-05 Contractor: MSCI
							3		2.251	5.5		
							5		2.239	6.0		
36	D-4	SP – III	64-28/64-28	WMA	0	3	1	2.476	2.335	5.7	4.5	Project # 4100590 Mix Design #2015-WMA-D4-04-44 Contractor: FSG
							2		2.347	5.2		
							3		2.337	5.6		
37	D-6	SP – III	70-22/70-22	HMA	15	3	1	2.518	2.377	5.6	4.4	Project # 6100650 Mix Design #2015-HMA-D6-07-67 Contractor: FNF
							2		2.380	5.5		
							3		2.390	5.1		
38	D-3	SP – III	76-22/70-22	WMA	15	3	3	2.597	2.441	6.0	4.9	Project # A301010/A301610 Mix Design #2015-WMA-D3-01-31R Contractor: MSCI
							4		2.444	5.9		
							5		2.446	5.8		
39	D-6	SP – III	70-22/70-22	HMA	15	3	1	2.441	2.312	5.3	4.8	Project # 6100783 Mix Design #2015-HMA-D6-05-65 Contractor: FSG
							2		2.302	5.7		
							7		2.309	5.4		
40	D-6	SP – III	70-22/70-22	HMA	0	3	2	2.435	2.308	5.2	4.7	Project # 6100783 Mix Design #2015-HMA-D6-09-69 Contractor: FSG
							3		2.306	5.3		
							4		2.304	5.4		
41	D-1	SP – III	76-22/64-22	WMA	35	3	1	2.385	2.263	5.1	5.0	Project # 1101020 Mix Design #2015-WMA-D1-04-14 Contractor: MC
							2		2.266	5.0		
							6		2.266	5.0		

Serial No.	NMDOT District ID	Superpave Gradation Type	Binder PG grade (Spec./Used)	AC Mix Type	RAP Fraction (%)	No. of Tested Specimen	Spec. ID	Max. Specific Gravity (G_{mm})	Bulk Specific Gravity (G_{mb})	Air Void %	Asphalt Content (%)	Project Info.
42	D-1	SP – IV	70-22/70-22	WMA	0	3	1	2.371	2.252	5.0	5.2	Project # 1100560 Mix Design #2015-WMA-D1-03-03 Contractor: IHC
							2		2.245	5.3		
							5		2.236	5.7		
43	D-2	SP – IV	76-22/70-28	WMA	27	3	1	2.478	2.347	5.3	4.7	Project # 2100910 Mix Design #2015-WMA-D2-05-25 Contractor: FSG
							2		2.349	5.2		
							4		2.337	5.7		
44	D-2	SP – III	76-22/70-28	WMA	27	3	2	2.503	2.353	6.0	4.3	Project # 2100910 Mix Design #2015-WMA-D2-04-24 Contractor: FSG
							3		2.375	5.1		
							4		2.368	5.4		
45	D-2	SP - IV	76-22/70-22	WMA	25	3	1	2.521	2.370	6.0	5.6	Project # 2101280 Mix Design #2015-WMA-D2-08-28 Contractor: JHCC
							3		2.382	5.5		
							4		2.395	5.0		
46	D-2	SP - IV	70-22/64-22	WMA	25	3	1	2.449	2.327	5.0	5.2	Project # 2100900 Mix Design #2016-WMA-D2-02-04 Contractor: MSCI
							3		2.327	5.0		
							5		2.302	6.0		
47	D-3	SP – III	70-22/70-22	HMA	15	3	1	2.580	2.436	5.6	5.2	Project # 3100340 Mix Design #2015-HMA-D3-10-140 Contractor: MSCI
							2		2.429	5.9		
							3		2.424	6.0		
48	D-6	SP – III	76-28/76-28	HMA	15	3	1	2.448	2.313	5.5	5.0	Project # 6101100R Mix Design #2015-HMA-D6-08-68 Contractor: AUI
							2		2.316	5.4		
							3		2.316	5.4		
49	D-3	SP – III	76-22/70-22	HMA	35	3	1	2.571	2.422	5.8	4.8	Project # 3100460 Mix Design #2015-HMA-D3-08-38 Contractor: MSCI
							2		2.422	5.8		
							3		2.419	5.9		
50	D-6	SP – III	64-28/70-22	HMA	0	3	1	2.310	2.174	5.9	6.0	Project # 6100721 Mix Design #2015-HMA-CMD-03-63 Contractor: AUI
							2		2.178	5.7		
							3		2.183	5.5		

Serial No.	NMDOT District ID	Superpave Gradation Type	Binder PG grade (Spec./Used)	AC Mix Type	RAP Fraction (%)	No. of Tested Specimen	Spec. ID	Max. Specific Gravity (G_{mm})	Bulk Specific Gravity (G_{mb})	Air Void %	Asphalt Content (%)	Project Info.
51	D-1	SP – III	76-22/64-22	WMA	35	3	1	2.390	2.254	5.7	4.8	Project # 1100620 Mix Design #2016-WMA-D1-01-05 Contractor: MSCI
							2		2.254	5.7		
							3		2.256	5.6		
52	D-4	SP – III	64-28/64-28	WMA	0	3	1	2.473	2.325	6.0	4.5	Project # 4100800 Mix Design #2016-WMA-D4-03-43 Contractor: FSG
							2		2.325	6.0		
							3		2.325	6.0		
53	D-3	SP – III	70-22/70-22	HMA	15	3	1	2.444	2.307	5.6	5.1	Project # Various Mix Design #2016-HMA-CMD-02-03 Contractor: VMC
							2		2.307	5.6		
							3		2.297	6.0		
54	D-5	SP – III	70-22/58-28	HMA	35	3	1	2.507	2.362	5.8	4.4	Project # F100110 Mix Design #2016-HMA-D5-01-07 Contractor: MSCI
							2		2.364	5.7		
							3		2.367	5.6		

Appendix B

Table B-1 Overall Dynamic Modulus test results at various test temperatures for Mix 1 Specimen 1

Temperature (°C)	Frequency (Hz)	Stress Amplitude (P-P) (KPa)	SE (%)	Dynamic Modulus (MPa)	Phase Angle (deg.)	UC (deg.)	Strain (P-P) Recoverable (microstrain)	Accumulated Strain (microstrain)	SE (%)	UC (%)
-10	25	2933	7.8	55460.12	8.4	9.8	52.894	59.915	20.6	10.2
-10	10	2969	5.5	54389.65	8.9	4.3	54.588	9.534	6.8	20.5
-10	5	2866	5	51986.14	9.1	4.3	55.124	9.124	7.7	20.8
-10	1	2557	1.7	46733.47	9	5.3	54.715	6.236	8.2	22.5
-10	0.5	2399	1	44816.23	14.3	3	53.537	6.359	6.9	22.8
-10	0.1	2180	0.6	41243.43	10.4	4.5	52.845	14.163	14.2	23.8
4.4	25	1206	6.3	19731.16	21.5	4.9	61.144	249.757	8.7	5.4
4.4	10	1029	6.5	16840.4	20.1	3.2	61.13	188.538	7.5	3.1
4.4	5	881	5.7	14638.4	21.4	3.5	60.164	193.464	7.5	3
4.4	1	604	3	10545.8	24	2.4	57.27	181.312	7.1	1
4.4	0.5	518	2	8861.35	29	3.6	58.428	191.843	4.6	4.6
4.4	0.1	356	1.1	5797.713	30.5	1.7	61.351	267.691	7.1	11.7
21.1	25	1206	6.3	19731.16	21.5	4.9	61.144	249.757	8.7	5.4
21.1	10	1029	6.5	16840.4	20.1	3.2	61.13	188.538	7.5	3.1
21.1	5	881	5.7	14638.4	21.4	3.5	60.164	193.464	7.5	3
21.1	1	604	3	10545.8	24	2.4	57.27	181.312	7.1	1
21.1	0.5	518	2	8861.35	29	3.6	58.428	191.843	4.6	4.6
21.1	0.1	356	1.1	5797.713	30.5	1.7	61.351	267.691	7.1	11.7
37.8	25	460	8.5	7028.716	27	5	65.411	391.761	9.3	23
37.8	10	382	8.9	5618.785	30.6	3.8	67.995	469.587	8.6	10.3
37.8	5	322	8.8	4486.981	31.7	3.8	71.865	500.965	8.9	8.2
37.8	1	231	4.6	2592.145	34.1	4.5	89.029	495.524	6.6	1.1
37.8	0.5	194	3.1	2133.756	34.4	3.6	91.05	505.025	7.8	6.3
37.8	0.1	132	1.7	1327.894	33.6	4.7	99.056	570.807	6.9	21.4
54.4	25	117	10.6	1787.454	36.4	5.4	65.235	105.078	9.4	16.8
54.4	10	96	9.8	1304.009	32.9	0.7	73.577	156.689	7.5	4.9
54.4	5	76	9	1036.774	32.7	0.6	73.254	161.977	6.7	8.8
54.4	1	53	6.6	612.751	30.6	0.5	86.82	158.227	5.8	6
54.4	0.5	49	5.6	515.219	28.6	1.1	95.175	163.486	6.6	6.3
54.4	0.1	38	3	378.361	24.5	3.3	101.735	201.908	7.9	7.2

Table B-2 Overall Dynamic Modulus test results at various test temperatures for Mix 1 Specimen 2

Temperature (°C)	Frequency (Hz)	Stress Amplitude (P-P) (KPa)	SE (%)	Dynamic Modulus (MPa)	Phase Angle (deg.)	UC (deg.)	Strain (P-P) Recoverable (microstrain)	Accumulated Strain (microstrain)	SE (%)	UC (%)
-10	25	2668	6.2	56596.65	11.3	7	47.136	55.607	12.5	32.4
-10	10	2744	5.4	54271.61	6.8	3.5	50.554	20.92	10.6	32.9
-10	5	2643	4.9	53228.31	7.4	3.3	49.646	22.89	8.1	34.2
-10	1	2370	1.5	49906.32	8.9	3.5	47.494	22.67	9.6	35.5
-10	0.5	2224	0.8	46710.15	7	3.5	47.609	26.196	10	37.2
-10	0.1	2023	0.5	43725.33	8.8	6	46.276	38.515	13.6	38.3
4.4	25	2318	5.3	45407.97	12.7	4.4	51.038	83.14	6.5	8.2
4.4	10	2324	4.5	40495.61	10	1.5	57.382	20.53	5.7	17.2
4.4	5	2183	4.2	38142.73	10.9	1.6	57.227	18.472	6.3	17.5
4.4	1	1800	1.1	32798.17	12.9	2.5	54.879	18.309	6.5	17.2
4.4	0.5	1601	0.7	30560.52	15.9	3.4	52.4	23.31	6.8	17
4.4	0.1	1350	0.5	24745.73	16.2	2.8	54.574	56.914	7.6	17.4
21.1	25	1202	7	21406.01	17.7	4.5	56.173	223.762	7.5	10.7
21.1	10	1033	7.7	18471.76	15.8	1.4	55.937	161.839	7.6	14.2
21.1	5	882	6.9	16762.04	15.9	1	52.635	156.147	10.9	12.1
21.1	1	570	3.6	11837.97	22.9	2.1	48.183	130.645	8.2	7
21.1	0.5	481	2.6	10441.89	21.4	1.4	46.102	130.952	6.6	3
21.1	0.1	314	1.6	6723.828	24.2	1.8	46.761	163.893	7.5	4
37.8	25	458	8.3	7866.765	29.4	8.4	58.235	428.722	7.6	21
37.8	10	383	9	6034.284	30.7	5.3	63.493	581.792	7.6	15
37.8	5	322	8.9	4909.446	32	5	65.681	656.505	7.2	11.7
37.8	1	239	4.8	2817.841	34.1	4	84.994	679.134	7.3	6.9
37.8	0.5	204	3.5	2305.023	34.3	4.7	88.68	714.432	5.9	3.2
37.8	0.1	139	1.6	1471.852	33.8	4.5	94.241	802.71	7.3	16.9
54.4	25	115	10.2	1690.981	36.2	5.5	68.151	184.083	9.4	0.4
54.4	10	96	9.3	1296.947	33.6	1.7	73.684	289.539	7.5	10.3
54.4	5	76	8.5	1029.943	33.4	1.6	74.176	325.412	6.4	11.3
54.4	1	53	6.4	647.182	31.5	4.1	81.852	337.162	6.3	19.2
54.4	0.5	48	4.9	558.993	30.1	5.8	85.942	357.772	6.8	23.8
54.4	0.1	38	2.7	459.116	25.1	8	83.507	405.692	8.1	44.8

Table B-3 Overall Dynamic Modulus test results at various test temperature for Mix 1 Specimen 3

Temperature (°C)	Frequency (Hz)	Stress Amplitude (P-P) (KPa)	SE (%)	Dynamic Modulus (MPa)	Phase Angle (deg.)	UC (deg.)	Strain (P-P) Recoverable (microstrain)	Accumulated Strain (microstrain)	SE (%)	UC (%)
-10	25	2453	5	52925.26	5.1	0.4	46.341	37.393	12.4	41.9
-10	10	2534	5	56206.16	4.9	1.1	45.078	-3.501	8.7	13.8
-10	5	2482	4.4	55051.96	5	0.9	45.089	-4.406	6.7	11.3
-10	1	2189	1.1	51348.1	8.2	1.7	42.63	-7.041	9.1	13.5
-10	0.5	2060	0.6	51659.95	8.6	1.8	39.867	-4.879	10.9	13.4
-10	0.1	1874	0.5	44655.75	8.3	2.5	41.96	6.589	11.3	16.4
4.4	25	2115	5.6	42456.45	9.5	3.1	49.808	79.259	9.6	6
4.4	10	2178	4.9	40323.79	8.7	2	54.007	34.497	8.6	9.1
4.4	5	2142	4.4	38570.93	9	2.8	55.539	42.568	9.1	11.4
4.4	1	1888	1.2	32919.88	9.4	1.8	57.36	39.827	8.2	9.2
4.4	0.5	1779	0.7	31843.95	14.7	5.3	55.852	49.634	12.9	8.2
4.4	0.1	1620	0.4	25239.06	12.9	1.8	64.196	87.742	8.1	3.4
21.1	25	1437	5.4	23527.66	16.8	3.8	61.097	311.908	6.8	36.5
21.1	10	1463	4.9	20506.78	15.9	2.2	71.344	337.534	5.4	33.5
21.1	5	1451	4.1	18164.44	17.1	2.1	79.876	429.139	4.4	35.2
21.1	1	1209	1.3	13481.78	20.7	2.1	89.64	473.717	3.8	38
21.1	0.5	1100	0.7	11412.19	22.7	1.9	96.377	542.863	2.4	37.4
21.1	0.1	1000	0.4	8032.104	25.9	1.1	124.502	849.174	3.2	37
37.8	25	509	6.4	9757.597	26.7	5.9	52.208	350.694	5.5	15.4
37.8	10	462	6.5	7788.303	26.5	4	59.324	452.333	4.1	14.4
37.8	5	418	6.1	6511.437	27.3	4.3	64.221	512.844	5.6	18.3
37.8	1	350	3.1	4054.201	28.8	4.9	86.42	531.15	5.9	26.7
37.8	0.5	279	1.5	3042.864	29.7	4.8	91.571	541.888	6	29.4
37.8	0.1	218	0.7	1916.126	28	4.5	113.824	632.675	7.7	33.6
54.4	25	184	8.2	3647.667	34	6.5	50.323	359.176	6.5	31.1
54.4	10	167	7.9	2699.599	31.1	2.5	62.007	561.633	5.6	30.9
54.4	5	132	7.6	2107.297	30.9	2.4	62.408	603.789	5.3	35.2
54.4	1	103	5.1	1244.888	29.2	1.9	82.632	618.592	7.2	41.6
54.4	0.5	89	3.6	1024.59	26.6	1.7	86.65	638.933	8.4	42.6
54.4	0.1	79	1.6	779.192	22.7	1.5	101.271	705.36	10.6	38.9

Table B-4 Overall Dynamic Modulus test results at various test temperatures for Mix 2 Specimen 1

Temperature (°C)	Frequency (Hz)	Stress Amplitude (P-P) (KPa)	SE (%)	Dynamic Modulus (MPa)	Phase Angle (deg.)	UC (deg.)	Strain (P-P) Recoverable (microstrain)	Accumulated Strain (microstrain)	SE (%)	UC (%)
-10	25	2673	6	48593.45	8.5	15.8	55.012	60.054	12.5	15.8
-10	10	2765	5.3	49362.83	6.9	2.9	56.011	1.693	7.8	25.5
-10	5	2660	5.1	47430.57	7.5	2	56.082	-1.824	8.1	23.8
-10	1	2371	1.5	42701.75	8.3	2.6	55.519	-1.146	7.6	23.5
-10	0.5	2228	0.8	42569.65	10.8	1.5	52.333	-2.391	7.3	25.9
-10	0.1	2026	0.5	37583.27	10.7	3.2	53.894	14.69	7.5	22.7
4.4	25	2449	5.8	38006.47	14.2	1	64.442	281.828	8.5	40.7
4.4	10	2536	5.2	32035.7	12.4	2.8	79.147	261.199	6.2	38.5
4.4	5	2452	4.9	28853.22	13.2	1.5	84.978	315.1	5.5	40.8
4.4	1	2191	1.4	23026.68	16.1	1.7	95.133	356.289	8.7	41.6
4.4	0.5	2057	0.8	19987.06	20.7	1.2	102.899	422.524	3.8	39.6
4.4	0.1	1929	0.5	14309.9	24.7	2.8	134.794	720.359	4.4	39.1
21.1	25	1141	6.2	21293.29	22.3	4.9	53.578	606.395	9	14.1
21.1	10	1156	6	16928.09	21.8	2.1	68.278	752.274	9	4.5
21.1	5	1128	5	14162.92	23.4	2.6	79.668	923.653	6	4.3
21.1	1	989	1.9	9021.536	27.5	5.6	109.628	1042.746	6.8	9.7
21.1	0.5	908	1.2	7234.181	28.4	10.2	125.567	1165.011	6.2	15.6
21.1	0.1	784	0.5	4278.122	27.4	12.1	183.149	1515.618	7	26.9
37.8	25	143	10.1	2728.513	41.5	4.7	52.299	32.968	7.8	3.4
37.8	10	141	9.3	1982.441	36.3	3.4	70.921	52.849	6.8	0.4
37.8	5	131	9.1	1492.899	34.6	3.5	87.623	77.282	6.9	2.7
37.8	1	115	6.6	863.627	28.1	2.9	133.572	101.25	7.3	9.3
37.8	0.5	104	4.8	693.828	24.9	2.2	149.729	124.989	8	10.2
37.8	0.1	89	2.1	511.384	16.6	0.3	174.194	181.6	10.3	13
54.4	25	82	10.7	1094.836	36.6	1	74.989	22.511	8.6	14.8
54.4	10	79	9.6	856.377	29	3.4	92.634	46.734	8.4	21.2
54.4	5	70	9.3	796.925	25	4.6	87.58	53.802	6.1	34
54.4	1	55	8.1	698.137	15.2	3.6	79.393	51.97	6.5	44.9
54.4	0.5	48	6.4	692.074	10.8	4.5	69.364	50.355	9.2	42.6
54.4	0.1	43	2.9	736.152	5.9	4.3	57.818	43.749	10.6	20.6

Table B-5 Overall Dynamic Modulus test results at various test temperatures for Mix 2 Specimen 2

Temperature (°C)	Frequency (Hz)	Stress Amplitude (P-P) (KPa)	SE (%)	Dynamic Modulus (MPa)	Phase Angle (deg.)	UC (deg.)	Strain (P-P) Recoverable (microstrain)	Accumulated Strain (microstrain)	SE (%)	UC (%)
-10	25	2035	5.2	33262.04	6.5	6	61.195	54.915	7.9	26.2
-10	10	2094	5.1	31745.42	7.8	2.1	65.975	3.248	7	13.4
-10	5	2023	4.3	31102.61	7.6	2.6	65.04	1.223	6.7	14.4
-10	1	1816	1.1	27916.35	9.6	2.4	65.067	-1.372	5	13
-10	0.5	1711	0.6	26538.15	7.8	4.3	64.468	1.302	4.9	12.3
-10	0.1	1622	0.4	23942.75	11.2	2.7	67.751	23.626	6.1	12.4
4.4	25	1834	6	29382.98	14.6	0.8	62.41	218.726	7.3	11.7
4.4	10	1884	5.8	28876.17	11	0.5	65.234	192.264	7.1	0.2
4.4	5	1830	4.9	26650.53	12	0.2	68.674	231.098	5.7	0.5
4.4	1	1639	1.5	21882.37	14.1	0.3	74.905	262.043	7.6	2.4
4.4	0.5	1542	0.8	19326.83	18.2	1.4	79.785	308.736	3.4	4.9
4.4	0.1	1447	0.4	14746.8	22.4	1.9	98.125	537.669	3.2	5.5
21.1	25	1017	6.1	18394.86	27.9	4.2	55.288	539.363	6.2	8.4
21.1	10	1030	5.8	14081.16	26.4	4.6	73.121	623.839	5.9	6.6
21.1	5	1003	4.8	11578.65	28.1	4.3	86.659	806.815	5.9	3.9
21.1	1	857	1.9	7108.418	32.6	3	120.585	944.592	4.9	0.5
21.1	0.5	776	1.2	5555.256	34.4	2.3	139.675	1109.755	4.7	0.2
21.1	0.1	699	0.6	3172.767	34.7	0.2	220.432	1710.604	5.9	0.7
37.8	25	296	9.4	5773.582	34.3	4.9	51.313	283.81	6.4	11.1
37.8	10	290	9.7	3048.823	38.9	2.4	95.198	458.129	6.1	2.5
37.8	5	274	8.3	2179.851	37.3	2.4	125.743	607.998	6.3	3.2
37.8	1	241	5.3	1263.883	32.3	3.2	190.319	722.633	8.4	17.7
37.8	0.5	220	3.8	1023.313	29.1	3.4	215.051	824.525	9.4	24.3
37.8	0.1	184	1.5	667.072	21.9	3.6	275.233	1027.083	12.2	30.9
54.4	25	132	10.8	2087.882	32.1	4.3	63.359	366.961	9.2	20.7
54.4	10	130	10	1207.322	29.6	6.5	107.481	653.116	6.4	19.3
54.4	5	113	9.8	950.481	26	6	118.889	761.864	6.1	25.9
54.4	1	91	8.7	841.755	21	3.7	108.016	820.479	7	6.3
54.4	0.5	80	7.1	756.809	18.8	2.4	105.064	847.955	7.6	12.4
54.4	0.1	71	3	613.127	14.6	2.1	115.796	894.718	10.7	12.9

Table B-6 Overall Dynamic Modulus test results at various test temperatures for Mix 2 Specimen 3

Temperature (°C)	Frequency (Hz)	Stress Amplitude (P-P) (KPa)	SE (%)	Dynamic Modulus (MPa)	Phase Angle (deg.)	UC (deg.)	Strain (P-P) Recoverable (microstrain)	Accumulated Strain (microstrain)	SE (%)	UC (%)
-10	25	2672	6.2	60865.94	23.8	0.6	43.905	84.354	29.2	31
-10	10	2764	5.5	59451.84	4.7	0.9	46.492	43.519	8.7	16.7
-10	5	2655	5.1	56701.92	5.3	1.2	46.825	43.331	8.3	17.3
-10	1	2372	1.5	51452.82	4.3	0.7	46.105	43.438	9.4	20
-10	0.5	2230	0.8	48845.56	8.3	1.3	45.651	45.298	7.2	22.2
-10	0.1	2027	0.5	45657.43	8	1.6	44.391	59.534	8	25.4
4.4	25	2134	5.9	48238.7	11.8	3.3	44.238	124.015	18.1	14.8
4.4	10	2190	5.1	41044.97	11.7	2.4	53.351	89.89	8.9	16.1
4.4	5	2124	4.5	37952.51	11.4	1.8	55.97	111.208	7.6	12.1
4.4	1	1908	1.3	30606.9	14.3	0.9	62.35	128.811	9.6	9.6
4.4	0.5	1795	0.7	27136.77	15.9	0.9	66.161	160.375	9.6	4.3
4.4	0.1	1687	0.4	19957.51	21.1	0.8	84.512	332.611	4.9	1.5
21.1	25	922	6.8	15581.74	21	0.4	59.186	374.3	6.2	4.3
21.1	10	928	6.9	12674.39	22.1	2.1	73.19	440.778	6.6	6.3
21.1	5	903	5.7	10797.07	23.7	2.1	83.671	546.052	5.4	4.5
21.1	1	818	2.2	7127.091	28.1	2.1	114.751	649.284	4	4.5
21.1	0.5	770	1.4	5791.931	28.7	1.5	132.909	787.326	4.2	4.3
21.1	0.1	721	0.5	3525.148	29.5	1.3	204.621	1267.218	5.1	1.6
37.8	25	429	9.1	10040.95	31.4	5.7	42.749	275.216	7.4	23
37.8	10	420	9.7	7859.311	27.8	0.7	53.489	464.024	6.6	24.4
37.8	5	368	9.2	6078.831	28.3	0.1	60.487	577.762	6.8	22.4
37.8	1	299	5.3	3526.512	26.8	0.4	84.82	646.371	8.1	20.1
37.8	0.5	262	3.2	2740.392	25.3	0.8	95.779	715.203	8.5	19.9
37.8	0.1	230	1.2	1803.911	20.6	1.5	127.503	887.336	11.3	22.7
54.4	25	113	9.9	2595.634	36.8	0.5	43.637	131.215	6.9	30.4
54.4	10	110	9.2	1883.18	30.6	1	58.445	346.1	4.7	26.2
54.4	5	97	9.1	1497.973	27.5	1.4	64.524	478.474	5.6	27.1
54.4	1	78	7.9	953.248	21.6	2.8	81.495	522.893	7.9	33.2
54.4	0.5	67	6.3	782.62	20.3	2.8	86.228	571.167	8.3	36.4
54.4	0.1	60	3	598.176	15.3	2	100.047	653.4	12.8	42.5

Table B-7 Overall Dynamic Modulus test results at various test temperatures for Mix 2 Specimen 4

Temperature (°C)	Frequency (Hz)	Stress Amplitude (P-P) (KPa)	SE (%)	Dynamic Modulus (MPa)	Phase Angle (deg.)	UC (deg.)	Strain (P-P) Recoverable (microstrain)	Accumulated Strain (microstrain)	SE (%)	UC (%)
-10	25	2451	5.6	47774.51	8.7	11.2	51.31	64.935	10.6	16.6
-10	10	2489	4.7	46895.26	6.2	3.2	53.08	17.915	6.3	1.3
-10	5	2335	4.7	46093.38	6	2.7	50.652	16.346	6.6	1
-10	1	1997	1.3	41227.5	9.5	4	48.43	17.156	8.3	0.2
-10	0.5	1838	0.7	39054.78	5.3	4.2	47.068	19.181	6.2	1
-10	0.1	1743	0.4	35845.2	10.1	3.9	48.637	33.335	8.1	0.8
4.4	25	1572	6.7	33249.8	11.6	11	47.288	138.448	16.1	29.7
4.4	10	1593	6.1	28443.78	11.7	2.1	56	97.213	8.9	20.2
4.4	5	1511	5.2	26129.15	12.6	2.5	57.824	109.971	7.3	21.7
4.4	1	1348	1.7	20863.92	15.8	2.5	64.614	121.77	4.5	23.5
4.4	0.5	1282	0.9	18174.76	18.1	2.8	70.555	147.217	5.1	25.4
4.4	0.1	1188	0.4	13536.09	21.5	2.7	87.761	290.921	3.5	30
21.1	25	819	7.4	16471.15	21.4	0.5	49.705	385.921	24.6	27.4
21.1	10	810	6.3	12672.33	22.3	0.6	63.937	562.141	6.8	10.4
21.1	5	770	5.5	10496.28	25	2.5	73.376	730.124	5.2	12.8
21.1	1	645	2.4	6364.68	29.9	3.8	101.409	842.183	4.1	20.8
21.1	0.5	561	1.6	4982.615	31.2	4	112.516	947.11	3.3	24.8
21.1	0.1	520	0.8	2870.04	30.7	3.6	181.12	1351.659	5.2	32
37.8	25	228	8.1	4162.861	35.9	2.9	54.728	284.89	6	9.3
37.8	10	222	7.5	2568.023	32.8	5.5	86.331	492.159	4.8	17.5
37.8	5	192	7.3	1953.952	30.8	5	98.268	613.462	4.9	24.5
37.8	1	158	5.4	1218.172	25.4	4.6	129.508	698.813	7.8	29
37.8	0.5	138	4.2	1028.786	23	4.5	133.867	757.448	9.6	30.1
37.8	0.1	121	1.8	782.897	17.4	3.4	154.283	853.177	12.9	33.7
54.4	25	61	9.7	994.498	37.1	8.9	61.571	146.784	6.3	19.2
54.4	10	59	8.5	800.841	28.5	8.4	73.561	268.984	4.4	25.1
54.4	5	52	8.6	648.575	25.6	7.6	79.566	334.163	4.7	31.4
54.4	1	41	7.4	452.565	20.8	6.3	91.694	347.068	5.5	40.1
54.4	0.5	36	5.9	403.258	19.5	6.2	90.15	352.887	7.1	42.1
54.4	0.1	31	2.8	331.386	17	6.2	94.687	369.095	9	45.9

Table B-8 Overall Dynamic Modulus test results at various test temperatures for Mix 2 Specimen 5

Temperature (°C)	Frequency (Hz)	Stress Amplitude (P-P) (KPa)	SE (%)	Dynamic Modulus (MPa)	Phase Angle (deg.)	UC (deg.)	Strain (P-P) Recoverable (microstrain)	Accumulated Strain (microstrain)	SE (%)	UC (%)
-10	25	2665	5.7	51286.47	4.9	12.8	51.971	130.948	17.3	45
-10	10	2703	4.9	58543.05	7.2	2.2	46.178	86.273	12.7	34
-10	5	2536	4.6	57388.84	6.8	1.1	44.197	84.799	12.9	36.1
-10	1	2261	1.3	51628.09	5.7	1.1	43.789	83.219	13	37.7
-10	0.5	2149	0.7	52144.82	5.6	4.6	41.207	85.088	18.3	34.3
-10	0.1	1992	0.5	44936.6	13	4.9	44.33	102.148	21.2	37.6
4.4	25	2135	5.1	35992.76	13	7.6	59.321	259.955	7.5	25.5
4.4	10	2157	4.1	34119.09	13.8	4.7	63.223	236.963	6.1	29.9
4.4	5	2039	4.1	31476.91	14.3	4.6	64.767	274.575	6	29.9
4.4	1	1820	1.1	24647.33	18.4	4	73.849	308.035	7.5	31.6
4.4	0.5	1735	0.6	22958.58	20.2	3.9	75.568	362.115	5.3	35.6
4.4	0.1	1609	0.4	16140.55	23.6	4	99.68	605.823	7	35.8
21.1	25	1082	6.1	17681.27	24.8	7.6	61.216	538.526	6.3	24
21.1	10	1084	5.8	14723.49	24.9	5.4	73.628	640.674	5.7	31.6
21.1	5	1031	5.2	12249.16	26.4	5	84.166	808.947	4.8	32.9
21.1	1	857	2.1	7572.243	30.4	3.7	113.152	923.8	5.7	37.8
21.1	0.5	744	1.4	5967.639	31.7	3.4	124.636	1043.165	4.3	37.3
21.1	0.1	690	0.5	3653.523	30.7	2.6	188.799	1530.43	5.4	40.9
37.8	25	205	8.8	3829.816	41.3	3.6	53.505	232.566	7.8	7.5
37.8	10	199	8.3	2522.286	39.3	2.8	78.819	367.605	6.2	6.4
37.8	5	174	8.1	1913.679	38.8	2.6	90.819	468.837	6.3	3.9
37.8	1	143	5.6	1077.288	34.6	1.7	132.864	549.252	7	0.8
37.8	0.5	125	4	914.616	33	0.5	136.451	610.395	7.7	8
37.8	0.1	109	1.6	760.284	26.8	0.2	143.41	711.185	8.9	27
54.4	25	76	9.6	1159.274	42.2	1.3	65.3	100.901	8.2	4.2
54.4	10	72	8.7	868.291	35.2	1.4	82.93	223.117	6.2	2
54.4	5	63	8.7	723.639	32.1	0.9	87.652	262.779	6.7	11
54.4	1	50	7.8	605.224	25.7	2.3	82.796	264.816	6.6	18.5
54.4	0.5	44	6	573.482	22.6	3.7	77.477	265.565	6.9	22.1
54.4	0.1	38	2.7	499.409	17.9	6.8	76.404	258.683	8.9	26.4

Table B-9 Overall Dynamic Modulus test results at various test temperatures for Mix 3 Specimen 1

Temperature (°C)	Frequency (Hz)	Stress Amplitude (P-P) (KPa)	SE (%)	Dynamic Modulus (MPa)	Phase Angle (deg.)	UC (deg.)	Strain (P-P) Recoverable (microstrain)	Accumulated Strain (microstrain)	SE (%)	UC (%)
-10	25	2553	5.4	41933.46	8.1	3.5	60.892	55.695	6.1	28.3
-10	10	2630	5.1	46048.15	4.9	0.4	57.105	1.144	7.6	30.1
-10	5	2524	4.8	44723.03	5.1	0.1	56.427	-1.428	5.5	25.3
-10	1	2255	1.2	41156.29	7.1	0.6	54.78	-4.263	4.2	23.8
-10	0.5	2121	0.7	39908.99	7.8	0.5	53.153	-4.327	4.3	24.1
-10	0.1	1931	0.5	35508.56	8.4	0.3	54.375	10.074	3.8	24.8
4.4	25	1390	6.6	22707.13	14.9	1.7	61.205	165.103	9.2	12.6
4.4	10	1416	6.7	21324.17	13	0.5	66.408	121.629	7.9	21.5
4.4	5	1379	5.6	19489	14.4	0.9	70.77	136.684	6.7	20.2
4.4	1	1243	1.9	15376.92	17.8	2.2	80.836	151.015	6.3	17.1
4.4	0.5	1168	1.2	13698.68	21.1	3.9	85.24	178.368	4.9	15.8
4.4	0.1	1059	0.5	10444.45	24	3.8	101.39	327.335	4.3	14.1
21.1	25	658	8.1	12610.45	23.7	1.6	52.147	330.369	9	17.6
21.1	10	558	9.6	11004.81	23.2	0.3	50.728	402.135	10.3	13.7
21.1	5	475	9.4	9504.007	25.2	0.9	49.992	427.221	11	14.3
21.1	1	308	5.5	5910.236	32.8	3.4	52.184	402.794	9.5	20.8
21.1	0.5	261	3.3	4909.359	33	2.2	53.138	411.235	8.2	18.5
21.1	0.1	171	1.4	2889.792	35.7	2.8	59.256	461.085	8	19.9
37.8	25	287	9.9	5563.766	34.1	0.6	51.508	534.587	9	6.3
37.8	10	242	10.8	4091.462	34.6	0.6	59.107	760.723	8.5	2.1
37.8	5	177	10.1	3290.94	35.8	0.6	53.913	802.608	8.1	0.9
37.8	1	107	6.1	1698.372	39.2	1.5	62.865	795.261	6.9	6.3
37.8	0.5	83	4.7	1372.188	38.4	0.4	60.364	806.211	8.3	9.4
37.8	0.1	51	2.2	876.082	35	0.8	57.829	835.703	8.2	24
54.4	25	253	11.9	4501.747	37.1	7.6	56.24	535.651	9.8	16.7
54.4	10	201	10.9	3501.911	29.1	4.9	57.34	719.076	7.5	10.8
54.4	5	149	10.9	2607.238	28.4	3.7	56.967	752.094	7.9	17.1
54.4	1	86	9.8	1475.65	24.5	4.5	58.371	717.583	7.2	27.8
54.4	0.5	68	8.7	1190.097	22.8	3.6	57.103	690.971	8.5	30.1
54.4	0.1	42	4.6	758.327	19.3	3.8	55.745	671.044	8.8	36.3

Table B-10 Overall Dynamic Modulus test results at various test temperatures for Mix 3 Specimen 2

Temperature (°C)	Frequency (Hz)	Stress Amplitude (P-P) (KPa)	SE (%)	Dynamic Modulus (MPa)	Phase Angle (deg.)	UC (deg.)	Strain (P-P) Recoverable (microstrain)	Accumulated Strain (microstrain)	SE (%)	UC (%)
-10	25	2360	5.6	41660.29	21.5	20.3	56.642	20.613	23.8	31.8
-10	10	2418	4.2	46287.19	6.7	2.3	52.249	7.444	6.8	23.4
-10	5	2388	4.5	45390.7	6.2	2.1	52.603	6.575	7.4	24.6
-10	1	2101	1.2	41907.66	7.4	2.2	50.145	3.918	8.8	24.5
-10	0.5	1977	0.6	40966.38	9.9	2.8	48.255	4.883	8.6	25
-10	0.1	1800	0.4	36459.14	9.7	2.5	49.364	13.841	7.5	25
4.4	25	1980	5.5	29823.28	17	3.8	66.378	237.303	11.1	29.4
4.4	10	2030	4.9	26732.68	11.1	1.5	75.926	207.328	7.3	27
4.4	5	2002	4.1	24696.53	12.2	2.2	81.065	247.365	7.5	29.1
4.4	1	1768	1	20701.65	14.2	1.5	85.422	268.882	6.2	29.1
4.4	0.5	1666	0.6	18707.41	17.5	2	89.059	309.462	5.3	31.4
4.4	0.1	1518	0.4	14470.4	20.8	1.7	104.918	491.488	4.1	29.9
21.1	25	1022	6.1	16840.79	19.5	0.4	60.691	565.408	8.3	37.1
21.1	10	990	5.9	14134.33	19.6	4	70.055	784.804	7.5	34.7
21.1	5	948	4.9	12369.27	20.7	4	76.609	975.03	6.2	37.5
21.1	1	807	1.9	8603.379	24.6	4.5	93.78	1082.234	4.3	40.6
21.1	0.5	742	1.2	7540.28	25.3	4.4	98.387	1194.692	3.9	42.3
21.1	0.1	701	0.6	4999.675	27.5	2.6	140.303	1467.008	4.4	44.9
37.8	25	405	8.5	7679.346	30.1	3.9	52.685	508.571	6.9	22.4
37.8	10	385	8.9	5734.169	29.7	6.3	67.112	879.007	7.4	28
37.8	5	366	8.2	4774.977	29.3	5	76.634	1134.548	6.9	29.2
37.8	1	320	4.2	3126.042	28.7	4.4	102.493	1261.008	9.5	28.6
37.8	0.5	284	2.5	2681.108	27.3	4.6	106.1	1386.249	9.2	25.6
37.8	0.1	271	0.8	1943.953	24.8	4.2	139.625	1663.87	11.2	25.4
54.4	25	184	9.4	3761.164	33.6	7.2	49.001	314.934	7.2	1.9
54.4	10	157	8.5	2899.22	27.7	7.4	53.991	435.114	6.2	4.2
54.4	5	126	8.5	2398.704	25.1	6.4	52.518	463.818	6.7	8.2
54.4	1	111	6.1	1785.968	19.8	6.4	62.091	468.271	9.4	2
54.4	0.5	93	4.9	1494.703	18.3	5.8	62.412	474.147	9.9	2.1
54.4	0.1	78	2.4	1269.857	14.3	5.3	61.183	498.768	11.5	4.7

Table B-11 Overall Dynamic Modulus test results at various test temperatures for Mix 3 Specimen 3

Temperature (°C)	Frequency (Hz)	Stress Amplitude (P-P) (KPa)	SE (%)	Dynamic Modulus (MPa)	Phase Angle (deg.)	UC (deg.)	Strain (P-P) Recoverable (microstrain)	Accumulated Strain (microstrain)	SE (%)	UC (%)
-10	25	2244	5.2	63439.03	5.6	7.4	35.366	37.235	11.4	42.1
-10	10	2803	4.8	57251.18	7.2	2.8	48.954	11.871	8.3	27.1
-10	5	2671	5	57385.34	6.8	2.9	46.539	8.293	6.7	26.3
-10	1	2282	1.4	52184.61	8.5	2.8	43.727	9.338	11.3	27.2
-10	0.5	2126	0.7	52262.6	10.6	3.9	40.676	9.969	9.3	27.5
-10	0.1	1945	0.5	47745.63	7.7	2.7	40.727	17.829	10.9	28.4
4.4	25	2089	5.2	41226.72	13.8	0.4	50.668	202.776	7.7	42.8
4.4	10	2152	4.7	38301.59	13.2	5.9	56.193	178.298	7.4	34.8
4.4	5	2121	4.4	34718.77	14.1	6.4	61.101	209.843	5.3	35.9
4.4	1	1867	1.2	25117.87	23.9	1.8	74.348	229.163	5.4	23
4.4	0.5	1756	0.6	23264.15	26.5	1.4	75.467	265.807	4.9	20.2
4.4	0.1	1601	0.4	16457.9	29.2	2.4	97.252	431.777	8.3	12.5
21.1	25	1108	5.6	14468.1	22.6	1.7	76.572	444.08	7.2	15.5
21.1	10	1034	5.5	12323.46	23.8	1.3	83.869	399.183	6.7	17.5
21.1	5	887	4.5	10764.96	25.1	0.7	82.37	428.294	6.1	16
21.1	1	777	1.7	7355.78	28.5	0.2	105.607	458.538	7.1	13.3
21.1	0.5	652	1.2	6088.746	32	0.4	107.141	491.093	5.2	9.7
21.1	0.1	580	0.7	4027.1	31.5	2.7	144.054	683.14	6.8	8.5
37.8	25	509	6.6	6419.858	37.8	1.5	79.334	677.904	6.9	34.3
37.8	10	470	7.2	4894.244	36.1	5.3	95.948	1015.54	6.3	35.6
37.8	5	400	6.9	3979.566	36	6.4	100.586	1182.313	7.8	36.3
37.8	1	358	3.9	2567.518	33.4	5.7	139.447	1285.876	11.3	37.7
37.8	0.5	298	2.7	2158.417	32.1	6.9	137.88	1360.335	12	36.4
37.8	0.1	267	1.1	1750.657	28.3	7.1	152.559	1554.802	16.3	30.1
54.4	25	184	9.4	3761.164	33.6	7.2	49.001	314.934	7.2	1.9
54.4	10	157	8.5	2899.22	27.7	7.4	53.991	435.114	6.2	4.2
54.4	5	126	8.5	2398.704	25.1	6.4	52.518	463.818	6.7	8.2
54.4	1	111	6.1	1785.968	19.8	6.4	62.091	468.271	9.4	2
54.4	0.5	93	4.9	1494.703	18.3	5.8	62.412	474.147	9.9	2.1
54.4	0.1	78	2.4	1269.857	14.3	5.3	61.183	498.768	11.5	4.7

Table B-12 Overall Dynamic Modulus test results at various test temperatures for Mix 4 Specimen 1

Temperature (°C)	Frequency (Hz)	Stress Amplitude (P-P) (KPa)	SE (%)	Dynamic Modulus (MPa)	Phase Angle (deg.)	UC (deg.)	Strain (P-P) Recoverable (microstrain)	Accumulated Strain (microstrain)	SE (%)	UC (%)
-10	25	2292	5.6	41103.27	7.3	4.7	55.767	76.018	7.9	5.8
-10	10	2363	4.7	41455.44	7.8	0.1	57.008	20.727	8.1	25.8
-10	5	2289	4.7	39323.35	6.5	1.1	58.202	17.029	8.9	25
-10	1	2044	1.4	34660.72	8.7	0.4	58.985	18.57	15.1	24.8
-10	0.5	1920	0.8	34014.3	5.8	3.1	56.449	25.074	7.9	27.1
-10	0.1	1749	0.5	28865.92	8.5	2.5	60.589	46.584	8.6	27.1
4.4	25	1023	6	18929.43	17.3	7.9	54.054	41.862	7.3	9
4.4	10	1035	6	17527.36	13.9	3.2	59.078	20.252	6.9	10.9
4.4	5	1007	4.8	16102.91	14.2	3.4	62.536	25.514	5.5	10.2
4.4	1	907	1.8	13137.68	15.6	3.7	69.02	24.662	5.4	9.3
4.4	0.5	854	1.2	12182.08	16.3	3.6	70.069	32.774	6.6	10
4.4	0.1	774	0.6	9534.64	18.4	3.3	81.208	92.623	4.8	7
21.1	25	772	6.3	13282.98	19.6	3.6	58.124	192.826	10.2	1.7
21.1	10	652	6.6	11759.66	19.1	2.5	55.454	192.39	8	2.8
21.1	5	555	6.4	10033	19.1	2.6	55.283	187.875	7.3	4.7
21.1	1	384	3.6	7067.281	24.1	4.4	54.405	168.622	7.5	12.5
21.1	0.5	330	2.5	6168.229	22.6	3.5	53.484	175.835	7.3	15
21.1	0.1	225	1.4	3965.26	24.4	3.3	56.721	212.518	5.8	26.1
37.8	25	376	9.1	5674.834	31.9	3.8	66.274	480.231	8.4	28.5
37.8	10	308	9.5	3875.534	30.1	5.2	79.447	676.649	7.5	25.1
37.8	5	266	7.6	3002.556	30.2	4.6	88.623	766.459	7.4	25.2
37.8	1	195	5.4	2521.885	28.5	0.7	77.377	796.971	5.8	22.3
37.8	0.5	169	3.9	2064.906	27.9	0.1	81.761	816.218	5.4	26.2
37.8	0.1	118	1.8	1356.83	25.3	1.5	86.733	839.632	5	33.5
54.4	25	117	8.5	2048.971	27.7	1.5	57.217	137.876	8.5	20.5
54.4	10	104	8.2	1537.008	25.6	2.2	67.655	189.169	4.9	29.5
54.4	5	83	8.2	1251.865	24.8	2.4	66.32	190.083	5.3	28.3
54.4	1	57	6.3	836.202	23.6	2.2	67.891	185	6.7	27.2
54.4	0.5	51	4.6	756.652	21.6	2	67.67	181.45	7	23.5
54.4	0.1	42	2	607.353	18	2.1	68.709	188.66	9.1	15.6

Table B-13 Overall Dynamic Modulus test results at various test temperatures for Mix 4 Specimen 2

Temperature (°C)	Frequency (Hz)	Stress Amplitude (P-P) (KPa)	SE (%)	Dynamic Modulus (MPa)	Phase Angle (deg.)	UC (deg.)	Strain (P-P) Recoverable (microstrain)	Accumulated Strain (microstrain)	SE (%)	UC (%)
-10	25	2503	5.3	45013.7	4.7	9.4	55.606	73.751	8.4	15.8
-10	10	2580	5	42255.66	9.1	0.9	61.065	19.834	8.7	37.8
-10	5	2532	4.5	40176.29	8.9	0.6	63.017	21.261	7	36.2
-10	1	2227	1.2	35917.47	9.9	0.7	61.999	21.154	7.1	34.9
-10	0.5	2092	0.7	34332.25	9.5	1.1	60.928	24.328	4.6	33.6
-10	0.1	1904	0.5	29741.43	11.2	0.7	64.008	42.862	3.9	30.1
4.4	25	1932	5.3	36151.97	19	11.1	53.436	100.328	11.4	13.1
4.4	10	1982	5	31497.9	11.6	1.1	62.925	46.513	7	8.5
4.4	5	1925	4.2	28679.67	11.8	0.7	67.114	53.518	6.8	13.6
4.4	1	1728	1.1	23489.29	15.4	2	73.551	56.794	8.6	12.7
4.4	0.5	1625	0.6	22386.37	14.1	0.8	72.584	65.878	4.4	10.7
4.4	0.1	1477	0.4	16505.44	17.3	1.3	89.503	134.398	4.9	13.1
21.1	25	963	5.6	16813.74	20.1	3.3	57.282	220.044	7	7.1
21.1	10	821	5.6	14347.67	18.8	1.6	57.249	209.443	5.7	1.5
21.1	5	701	5.1	12437.03	19.8	1.6	56.397	221.811	7.3	1.7
21.1	1	484	2.8	9277.273	23.3	1.9	52.139	214.597	8.4	0.4
21.1	0.5	416	2	7915.122	21.8	1.2	52.601	223.168	4.7	1.4
21.1	0.1	282	0.7	5393.019	24.6	1.8	52.348	270.449	8.5	4.9
37.8	25	385	8.8	7080.848	25.8	5.3	54.437	812.072	8.3	5.8
37.8	10	318	9.4	6060.599	26.3	6.9	52.418	1119.5	8.5	0.4
37.8	5	274	7.3	5451.957	26.1	6	50.175	1268.666	7.4	14.5
37.8	1	201	4.6	3832.178	25.6	2.6	52.345	1292.403	7.5	18.7
37.8	0.5	174	3.2	3278.247	24.7	2.3	53.192	1314.58	8.3	17.1
37.8	0.1	118	1.3	2141.108	23.9	2.1	55.3	1348.111	8.9	8.8
54.4	25	181	9.3	3148.377	29.1	4	57.483	320.21	9.2	12.2
54.4	10	160	9.4	2660.132	24.9	0.3	60.311	464.07	6.1	25.2
54.4	5	130	9.3	2151.969	24.1	0.4	60.202	481.067	6.5	22.9
54.4	1	94	7	1360.474	22.2	0.8	68.93	471.66	6.9	21.5
54.4	0.5	85	5.1	1164.576	21.5	1.3	72.975	471.106	7.1	21.6
54.4	0.1	68	2	885.28	17.6	0.6	77.082	487.622	8.6	20.1

Table B-14 Overall Dynamic Modulus test results at various test temperatures for Mix 4 Specimen 3

Temperature (°C)	Frequency (Hz)	Stress Amplitude (P-P) (KPa)	SE (%)	Dynamic Modulus (MPa)	Phase Angle (deg.)	UC (deg.)	Strain (P-P) Recoverable (microstrain)	Accumulated Strain (microstrain)	SE (%)	UC (%)
-10	25	2402	5.6	45287.28	9.1	5.7	53.036	90.089	10.7	7
-10	10	2478	4.8	42962.26	8.7	2.8	57.671	53.282	9.1	19.8
-10	5	2399	4.6	40478.53	8.8	2	59.27	52.63	8.9	22.1
-10	1	2146	1.3	35607.81	10.5	0.8	60.281	54.302	9.5	23.3
-10	0.5	2017	0.7	34321.87	4.9	3.4	58.758	57.872	14.3	23
-10	0.1	1834	0.5	29767.25	11.4	1.4	61.608	79.319	10.1	26.3
4.4	25	1526	5.6	25638.24	19.5	0.1	59.505	127.278	9.7	4.7
4.4	10	1566	5.5	22181.63	16.7	3.5	70.587	64.307	8.3	4.7
4.4	5	1523	4.6	20028.82	16.6	2.8	76.026	69.184	6.6	1.7
4.4	1	1365	1.4	16143.68	17.1	3.1	84.58	68.836	7.1	1
4.4	0.5	1284	0.9	14246.23	17.6	2	90.1	78.006	4.9	2.8
4.4	0.1	1165	0.5	11422.13	20.6	0.5	101.971	146.487	5.2	0.6
21.1	25	912	6.8	15055.17	14.9	40.6	60.603	267.786	29.8	14.4
21.1	10	804	6.9	15274.2	20.4	4.5	52.66	238.63	8.4	30.3
21.1	5	687	6.2	13293.49	22.1	5.4	51.67	238.994	8.7	26.3
21.1	1	475	3.6	9812.369	24.4	4.3	48.392	212.203	6.9	28.4
21.1	0.5	408	2.5	8421.691	30.1	8.3	48.453	210.219	8.4	28.3
21.1	0.1	281	0.9	5927.294	27.9	6.8	47.348	229.664	8.4	40.2
37.8	25	438	8.7	6613.062	25.7	3.7	66.304	160.183	11.5	15.7
37.8	10	365	9.4	5362.113	24.4	4.6	68.129	177.098	11	12.8
37.8	5	301	8.4	4618.976	25.9	4.6	65.155	174.802	7.4	15.3
37.8	1	217	4.3	2826.813	26.9	6.6	76.793	169.063	5.6	16.8
37.8	0.5	188	2.8	2319.891	27.8	6.9	81.063	183.868	4.6	13.2
37.8	0.1	124	1.9	1480.574	26.7	7.5	83.962	239.341	4.8	6.4
54.4	25	123	9.9	1646.063	37	7.8	74.649	68.373	8.2	7.6
54.4	10	104	10.1	1360.321	31.7	6.2	76.691	89.02	7.6	12.6
54.4	5	84	10	1221.683	31.1	6.2	69.077	83.112	9.7	3.6
54.4	1	58	7.4	995.168	24.3	0	58.584	72.493	9	15.4
54.4	0.5	53	5.5	882.618	21.8	0.9	60.602	64.951	6.6	9.3
54.4	0.1	47	2.4	752.994	18.2	1.5	62.667	65.928	9.5	8.4

Table B-15 Overall Dynamic Modulus test results at various test temperatures for Mix 5 Specimen 1

Temperature (°C)	Frequency (Hz)	Stress Amplitude (P-P) (KPa)	SE (%)	Dynamic Modulus (MPa)	Phase Angle (deg.)	UC (deg.)	Strain (P-P) Recoverable (microstrain)	Accumulated Strain (microstrain)	SE (%)	UC (%)
-10	25	1891	5.5	33324.45	18.8	4.8	56.759	66.772	9.4	5.2
-10	10	1949	5.5	32099.31	7.6	2.6	60.706	27.713	7.4	6.4
-10	5	1888	4.7	31355.96	7.5	3	60.207	27.383	6	6.3
-10	1	1691	1.2	28510.49	8.7	3.3	59.32	30.41	7.4	8.7
-10	0.5	1590	0.7	28322.69	7.2	1.8	56.137	31.197	5.4	7
-10	0.1	1448	0.4	25136.67	10.7	3.2	57.611	50.679	5.5	7.4
4.4	25	1526	5.7	25370.24	17.6	0.6	60.154	103.207	14	31.6
4.4	10	1563	5.6	23183.93	11.3	3	67.399	58.833	8.3	29.6
4.4	5	1511	4.5	21458.73	11.9	3.4	70.431	65.522	8.5	30.7
4.4	1	1361	1.3	18184.55	14.3	3	74.86	72.71	6.9	33.3
4.4	0.5	1281	0.8	16652.63	14.1	2.8	76.943	88.824	5.7	33.8
4.4	0.1	1165	0.4	13428.32	18.6	2.8	86.73	176.845	5.9	32.2
21.1	25	762	6	14191.35	23.1	0.6	53.714	253.697	8.7	1.2
21.1	10	641	5.9	12089.39	20.3	5	53.062	334.503	6.8	13.9
21.1	5	546	5.4	10435.32	21.3	4.5	52.338	379.267	5.7	11.9
21.1	1	381	2.9	7467.116	23.2	2.6	50.998	389.459	7.2	8.5
21.1	0.5	327	2.2	6265.002	27	4.5	52.269	412.833	4.5	6.7
21.1	0.1	222	1	4024.445	28.1	4.1	55.115	482.716	5.2	5.5
37.8	25	303	7.3	6178.737	32.5	6.9	49.105	514.897	7.4	19.6
37.8	10	248	7.4	4162.4	27.9	3.1	59.5	747.873	3.8	4.2
37.8	5	214	4.5	3281.14	28.7	3	65.19	885.939	4.9	5.7
37.8	1	155	2.2	2072.474	27.2	1.7	74.993	939.588	4	8.1
37.8	0.5	136	1.4	1714.432	25.4	0.8	79.281	985.163	3.8	6.6
37.8	0.1	95	0.7	1201.35	20.8	1.2	79.18	1045.921	4.3	2.8
54.4	25	130	5.4	2070.318	29.8	2.6	62.676	424.448	4.5	26.9
54.4	10	115	4.3	1215.736	25.8	0.2	94.312	642.785	3.7	15.6
54.4	5	91	3.6	999.358	23	0.9	90.621	698.545	4.6	18.3
54.4	1	69	2	771.319	19.2	1.7	89.036	709.932	4	17
54.4	0.5	60	1.6	717.102	17.4	1.9	83.696	721.325	4.1	15.5
54.4	0.1	52	1.5	611.995	15.4	2.5	85.653	756.714	4.2	14.8

Table B-16 Overall Dynamic Modulus test results at various test temperatures for Mix 5 Specimen 2

Temperature (°C)	Frequency (Hz)	Stress Amplitude (P-P) (KPa)	SE (%)	Dynamic Modulus (MPa)	Phase Angle (deg.)	UC (deg.)	Strain (P-P) Recoverable (microstrain)	Accumulated Strain (microstrain)	SE (%)	UC (%)
-10	10	1945	4.8	34619.25	5.8	1.5	56.172	12.823	5.9	12.2
-10	10	1943	4.9	33731.72	6.3	1.2	57.588	19.038	9	7.8
-10	5	1877	4	33161.43	7	0.7	56.613	20.783	8.1	10.5
-10	1	1687	1	31307.68	7.2	2.8	53.877	18.064	7.2	13.8
-10	0.5	1589	0.6	30400.42	8.2	3.3	52.254	12.802	8.3	13.4
-10	0.1	1445	0.5	27195.52	8.5	1.1	53.149	22.54	6.7	14.5
4.4	10	1561	5.3	25495.65	9.1	1.1	61.225	51.208	6.8	22.9
4.4	10	1563	5.2	25199.81	9.4	1.4	62.021	65.255	8	21.4
4.4	5	1517	4.2	23755.33	9.6	1	63.857	73.034	7.2	18.8
4.4	1	1362	1.1	20255.93	12.6	1.2	67.248	84.638	11.8	21.4
4.4	0.5	1281	0.6	19294.67	10.4	1.1	66.405	95.97	6.4	20.1
4.4	0.1	1166	0.4	15204.55	14.9	1.2	76.656	159.855	7.3	20.6
21.1	10	881	4.9	18522.96	16.7	2.2	47.568	179.102	5	2.4
21.1	10	879	4.8	18251.04	16.8	2.3	48.165	261.624	4.5	5.8
21.1	5	752	4	16220.49	17.9	2.5	46.385	286.226	4.5	7.7
21.1	1	530	1.8	11762.27	20.8	2.7	45.073	291.376	3.9	9.8
21.1	0.5	458	1.3	9894.903	21.5	2.4	46.327	298.583	3.2	13.6
21.1	0.1	328	0.9	6754.332	23.7	3	48.509	348.732	5.9	18.2
37.8	25	426	6.8	6854.71	28	1.1	62.161	383.647	6	3.3
37.8	10	357	7.5	5030.56	28.7	0.7	70.941	557.567	4.4	18
37.8	5	299	7.4	4084.626	29	0.1	73.143	655.328	4.5	20.4
37.8	1	218	2.3	2440.416	28.1	0.4	89.509	703.41	4.4	24.6
37.8	0.5	190	1.4	2055.285	27	0.8	92.36	751.031	5	25.8
37.8	0.1	134	0.7	1494.358	23.9	1.5	89.681	820.527	5.7	32
54.4	25	130	5.7	2104.693	32.7	0.8	61.551	117.086	5.1	34.7
54.4	10	114	4.9	1648.261	27.5	1.4	68.877	223.291	2.8	28.9
54.4	5	90	3.8	1400.177	25.3	0.6	64.336	259.368	3.3	30.2
54.4	1	68	2	1112.519	20.9	0.2	61.209	268.255	4.5	30.8
54.4	0.5	60	1.6	1055.592	19.4	0.3	57.155	277.144	5.2	30.2
54.4	0.1	53	1.1	1004.78	16.5	2.1	52.584	297.865	5.8	36

Table B-17 Overall Dynamic Modulus test results at various test temperatures for Mix 5 Specimen 3

Temperature (°C)	Frequency (Hz)	Stress Amplitude (P-P) (KPa)	SE (%)	Dynamic Modulus (MPa)	Phase Angle (deg.)	UC (deg.)	Strain (P-P) Recoverable (microstrain)	Accumulated Strain (microstrain)	SE (%)	UC (%)
-10	10	1976	5.4	30351.77	7.5	0.8	65.106	16.873	8.2	4.2
-10	10	1952	5.2	30017.88	7.3	0.8	65.034	19.107	7.7	4.4
-10	5	1889	4.3	29172.29	7	0.5	64.737	19.387	7	3.8
-10	1	1692	1.2	27307.31	6	1.2	61.962	18.357	7.8	3.7
-10	0.5	1591	0.6	24986.46	7.4	0.6	63.671	20.219	5.4	7
-10	0.1	1450	0.4	23291.83	9.5	0.7	62.255	28.698	6.6	6.4
4.4	10	1475	5.3	20806.69	10.9	1.3	70.873	61.786	7	5.2
4.4	10	1492	5.1	20751.43	10.6	1.3	71.915	80.778	7.1	4.7
4.4	5	1469	4.3	19512.41	11	0.8	75.303	91.725	5.4	3.8
4.4	1	1309	1.2	16223.07	14	0.2	80.699	100.774	8.2	4.5
4.4	0.5	1221	0.7	15318.58	12.7	1.6	79.722	117.948	3.7	3.2
4.4	0.1	1101	0.4	12059.57	16.9	0.8	91.283	202.293	3.7	3.8
21.1	25	716	6.3	11656.85	12.7	0.9	61.422	180.378	18.8	2.9
21.1	10	605	5.9	11919.92	20.3	0.4	50.773	232.899	10.9	0.9
21.1	5	512	5.3	10452.23	20.8	0.2	48.963	258.693	8	2.2
21.1	1	356	2.9	7376.433	23.5	0.5	48.312	258.435	7	3.6
21.1	0.5	306	2.1	6251.143	23.9	1.2	48.89	275.197	6.4	5
21.1	0.1	211	0.8	4081.869	27.2	1.1	51.721	323.234	7.3	5.3
37.8	25	472	6.1	7247.547	27.4	3.3	65.159	678.428	6.8	3.2
37.8	10	395	6.4	5626.907	26.4	1.5	70.261	1012.517	5.5	6
37.8	5	332	6.1	4534.992	27.1	3.4	73.166	1193.217	4.9	13.3
37.8	1	233	3.7	2839.93	24.9	4.8	81.955	1252.848	6	24.8
37.8	0.5	209	1.9	2361.258	22.9	4.1	88.395	1308.804	5.5	29.4
37.8	0.1	145	1.7	1828.09	17.5	4.7	79.207	1363.806	7.1	34.3
54.4	25	159	6.2	2798.549	25.9	3.8	56.728	465.952	5.1	8.8
54.4	10	140	5.7	2508.733	20.2	2.2	55.834	773.056	5.4	1.5
54.4	5	112	5.7	2301.089	16.8	1.1	48.833	857.738	6.9	1.4
54.4	1	84	3.4	2016.346	12	0.4	41.511	877.985	7.2	1.5
54.4	0.5	72	3.3	1941.631	10.4	0.3	36.926	895.516	8.2	1.9
54.4	0.1	63	2.9	1746.869	11	0.3	35.839	938.126	10.4	0.2

Table B-18 Overall Dynamic Modulus test results at various test temperatures for Mix 6 Specimen 2

Temperature (°C)	Frequency (Hz)	Stress Amplitude (P-P) (KPa)	SE (%)	Dynamic Modulus (MPa)	Phase Angle (deg.)	UC (deg.)	Strain (P-P) Recoverable (microstrain)	Accumulated Strain (microstrain)	SE (%)	UC (%)
-10	25	1544	5.6	30505.73	17.7	1.9	50.607	50.32	14.1	26.4
-10	10	1796	4.9	32166.74	7.4	1.5	55.839	16.781	5.9	36.3
-10	5	1748	4.3	30857.17	7	1.2	56.643	12.695	5.9	36.8
-10	1	1566	1.4	27343.02	7.2	1.1	57.264	13.345	3.3	37.1
-10	0.5	1473	0.8	26264.64	7	0.5	56.067	18.443	4.3	36.6
-10	0.1	1338	0.4	22876.71	9.6	1.3	58.472	33.187	3.1	36.6
4.4	25	1344	6.2	20143.2	19.3	1.7	66.7	108.208	12.6	39.2
4.4	10	1320	5.6	20178.77	11.7	0.8	65.404	58.518	7.9	46.2
4.4	5	1251	5	18513.45	11.5	1.2	67.549	59.99	8.8	46.1
4.4	1	1032	2.1	15232.91	14.4	1.3	67.735	58.949	7.8	45.1
4.4	0.5	917	1.4	14228.64	14.6	0.4	64.418	63.174	5.8	44.6
4.4	0.1	771	0.5	10953.74	16.9	0.5	70.43	109.121	6.4	46
21.1	25	722	7.2	10648.39	24.2	2.1	67.779	332.165	10.5	35
21.1	10	605	7.3	9491.854	19.4	1.5	63.7	363.269	6.6	39.5
21.1	5	515	7.3	8262.834	20.2	1.7	62.276	375.985	6	40
21.1	1	334	4.9	5736.474	22.5	1.9	58.279	354.187	9.3	41.9
21.1	0.5	283	2.8	4602.978	24.3	2.6	61.588	356.993	4.2	43.3
21.1	0.1	186	1	3317.369	24.8	3.3	56.1	403.019	4.3	43
37.8	25	315	9.9	4173.948	28.1	5.3	75.389	538.953	9.2	27.3
37.8	10	261	8.4	3205.373	26.7	4.7	81.522	765.809	8.4	29.1
37.8	5	223	8.2	2776.227	27	4.9	80.153	864.353	9.1	30.3
37.8	1	164	6.1	1772.109	28.3	5.5	92.508	885.378	7.9	31.1
37.8	0.5	139	4.2	1557.049	27.5	6.4	89.47	910.478	8.9	30.6
37.8	0.1	95	2.1	1159.107	25.5	5	81.907	964.704	8	26.7
54.4	25	98	8.6	1523.76	28.9	4.2	64.36	323.522	7.1	42.7
54.4	10	79	7.4	1199.15	24.8	3.7	65.861	490.272	5.4	47.9
54.4	5	62	7.1	1044.302	23.9	4	59.657	554.186	5.2	46.2
54.4	1	44	5.7	783.499	22	4.1	56.02	574.349	5.6	38.3
54.4	0.5	39	4.9	737.06	20.8	4.4	53.114	588.02	7.5	36
54.4	0.1	32	2.7	618.201	16.3	3	51.401	618.469	9.2	29.7

Table B-19 Overall Dynamic Modulus test results at various test temperatures for Mix 6 Specimen 3

Temperature (°C)	Frequency (Hz)	Stress Amplitude (P-P) (KPa)	SE (%)	Dynamic Modulus (MPa)	Phase Angle (deg.)	UC (deg.)	Strain (P-P) Recoverable (microstrain)	Accumulated Strain (microstrain)	SE (%)	UC (%)
-10	25	1818	5.4	40765.55	19	7.6	44.586	42.598	15	34.6
-10	10	2117	4.5	38810.26	8.5	1.7	54.548	9.825	7.4	22.7
-10	5	2059	4.3	37303.06	8.4	2.1	55.203	13.321	8.1	21.2
-10	1	1842	1.4	32555.23	9.1	2.7	56.57	14.62	5.5	20.5
-10	0.5	1732	0.8	30783.93	10.6	2.6	56.252	7.722	5.8	20.1
-10	0.1	1574	0.4	26501.73	12	3.2	59.399	34.273	6.1	17.6
4.4	25	1516	5.5	28185.1	16	16.8	53.79	115.765	10.2	30.1
4.4	10	1487	4.9	24623.31	13.1	2.4	60.391	60.942	7.3	19.9
4.4	5	1410	4.5	22686.65	13.2	2.6	62.172	66.084	6.9	18.3
4.4	1	1164	1.9	18615.75	13.9	3.5	62.546	66.938	10.7	15.7
4.4	0.5	1035	1.2	16234.93	17.2	3.1	63.766	70.537	5.5	15
4.4	0.1	872	0.5	13348.3	18.1	2.6	65.345	115.452	4.5	10.2
21.1	25	773	6.5	12898.04	21.8	1.4	59.955	271.944	7.5	22
21.1	10	647	7	10720.49	19.6	1	60.386	308.659	7.9	24.4
21.1	5	547	7	9436.271	20.4	0.5	58.008	324.633	6.3	23.7
21.1	1	357	4.9	6572.449	22.4	0.9	54.253	309.09	5.3	20.6
21.1	0.5	301	3.5	5526.583	23.3	1.5	54.443	312.679	4.8	19.4
21.1	0.1	198	1.3	3892.895	23.9	2.5	50.884	343.593	5	14.1
37.8	25	342	10.2	5595.372	24.6	2.8	61.209	637.311	10.2	13.9
37.8	10	282	10.2	4453.293	24	2.3	63.431	896.936	7.5	13.2
37.8	5	240	8.7	3716.738	23.5	2.3	64.475	1028.309	6.6	14
37.8	1	175	6.2	2570.902	23.9	1.7	68.108	1059.316	6.3	16.4
37.8	0.5	149	4.5	2247.268	22.8	1.5	66.429	1083.824	5.8	18.6
37.8	0.1	102	2.1	1607.736	19.9	0.3	63.526	1121.66	5.9	23
54.4	25	126	8.8	1988.632	26	6.5	63.403	332.83	7.5	14.7
54.4	10	101	8.2	1601.656	23.7	1.3	63.334	516.81	6.9	15.4
54.4	5	80	7.5	1368.718	22.2	1.3	58.555	571.946	6.2	17.8
54.4	1	57	7.2	982.561	19.8	1.8	58.046	579.588	8.8	20.7
54.4	0.5	51	5.9	891.327	17.8	1.2	57.698	586.757	6.8	22.2
54.4	0.1	41	4	727.647	13.5	1.1	56.119	610.691	10	22.6

Table B-20 Overall Dynamic Modulus test results at various test temperatures for Mix 6 Specimen 4

Temperature (°C)	Frequency (Hz)	Stress Amplitude (P-P) (KPa)	SE (%)	Dynamic Modulus (MPa)	Phase Angle (deg.)	UC (deg.)	Strain (P-P) Recoverable (microstrain)	Accumulated Strain (microstrain)	SE (%)	UC (%)
-10	25	1998	5	43840.27	3.8	7.8	45.582	64.662	7.7	29.6
-10	10	2326	4.3	38004.7	9.1	2.3	61.216	19.008	5.6	29.9
-10	5	2260	4.3	35841.58	9.4	2.4	63.047	16.849	5.8	30.2
-10	1	2023	1.3	32022.29	9.9	3	63.17	15.414	3.5	31.4
-10	0.5	1903	0.7	30047.13	9.9	2.8	63.338	17.153	3.3	31.5
-10	0.1	1730	0.5	26335.9	11	2.7	65.703	35.397	3.4	31.7
4.4	25	1666	4.9	28349.64	10.1	6.1	58.768	135.62	8	27.4
4.4	10	1642	4.4	24500.15	13.4	2.9	67.012	73.695	5.4	31.8
4.4	5	1552	4.2	22347.31	13.9	2.9	69.448	78.411	4.7	32.2
4.4	1	1278	1.5	18333.27	14.8	3.1	69.733	77.18	5.4	33
4.4	0.5	1137	0.9	16392.13	17.3	3.7	69.355	83.013	4.3	32.6
4.4	0.1	959	0.5	13156.36	18.6	3.6	72.912	130.838	3.7	33.7
21.1	25	774	6.5	12734.51	20.6	1.5	60.815	245.638	9.6	29.5
21.1	10	646	6.7	10788.39	20.8	2.7	59.858	246.68	6.9	31.5
21.1	5	547	6.8	9320.953	21.9	3.2	58.692	246.681	6.5	32
21.1	1	356	4.5	6547.43	25.7	3.9	54.394	223.068	8.1	35.6
21.1	0.5	297	3.4	5535.278	24.5	3.5	53.624	223.435	4.8	37
21.1	0.1	195	1.6	3805.385	25.6	2	51.293	255.27	4.4	41.7
37.8	25	307	9.3	4746.642	27.9	2.4	64.653	318.795	7.4	29.6
37.8	10	254	8.1	3548.337	27.2	4.2	71.506	424.831	6.9	31.9
37.8	5	214	7.1	2938.456	27.4	4	72.893	465.693	6.2	34.3
37.8	1	156	4.9	1834.02	27.7	4.3	85.308	470.899	5.7	39.3
37.8	0.5	134	3.6	1536.453	27.1	4.3	87.296	477.731	6	41.3
37.8	0.1	91	2.2	1043.451	25.4	4.1	87.156	529.034	6.1	46.9
54.4	25	126	7.9	1770.888	31.3	4.2	71.244	309.857	6.2	22.4
54.4	10	104	7.4	1098.341	28.6	4.5	94.517	454.234	9	48.1
54.4	5	82	7.2	1104.618	27.4	4.5	74.003	511.489	5.6	22.7
54.4	1	58	6.1	774.359	25	4.9	74.719	521.731	6.6	22.3
54.4	0.5	51	4.8	698.839	23.2	4.1	72.264	531.008	6.7	20.7
54.4	0.1	41	3.4	560.769	19	4	73.03	576.714	8	24.1

Table B-21 Overall Dynamic Modulus test results at various test temperatures for Mix 7 Specimen 2

Temperature (°C)	Frequency (Hz)	Stress Amplitude (P-P) (KPa)	SE (%)	Dynamic Modulus (MPa)	Phase Angle (deg.)	UC (deg.)	Strain (P-P) Recoverable (microstrain)	Accumulated Strain (microstrain)	SE (%)	UC (%)
-10	25	1544	5.6	30505.73	17.7	1.9	50.607	50.32	14.1	26.4
-10	10	1796	4.9	32166.74	7.4	1.5	55.839	16.781	5.9	36.3
-10	5	1748	4.3	30857.17	7	1.2	56.643	12.695	5.9	36.8
-10	1	1566	1.4	27343.02	7.2	1.1	57.264	13.345	3.3	37.1
-10	0.5	1473	0.8	26264.64	7	0.5	56.067	18.443	4.3	36.6
-10	0.1	1338	0.4	22876.71	9.6	1.3	58.472	33.187	3.1	36.6
4.4	25	1344	6.2	20143.2	19.3	1.7	66.7	108.208	12.6	39.2
4.4	10	1320	5.6	20178.77	11.7	0.8	65.404	58.518	7.9	46.2
4.4	5	1251	5	18513.45	11.5	1.2	67.549	59.99	8.8	46.1
4.4	1	1032	2.1	15232.91	14.4	1.3	67.735	58.949	7.8	45.1
4.4	0.5	917	1.4	14228.64	14.6	0.4	64.418	63.174	5.8	44.6
4.4	0.1	771	0.5	10953.74	16.9	0.5	70.43	109.121	6.4	46
21.1	25	722	7.2	10648.39	24.2	2.1	67.779	332.165	10.5	35
21.1	10	605	7.3	9491.854	19.4	1.5	63.7	363.269	6.6	39.5
21.1	5	515	7.3	8262.834	20.2	1.7	62.276	375.985	6	40
21.1	1	334	4.9	5736.474	22.5	1.9	58.279	354.187	9.3	41.9
21.1	0.5	283	2.8	4602.978	24.3	2.6	61.588	356.993	4.2	43.3
21.1	0.1	186	1	3317.369	24.8	3.3	56.1	403.019	4.3	43
37.8	25	315	9.9	4173.948	28.1	5.3	75.389	538.953	9.2	27.3
37.8	10	261	8.4	3205.373	26.7	4.7	81.522	765.809	8.4	29.1
37.8	5	223	8.2	2776.227	27	4.9	80.153	864.353	9.1	30.3
37.8	1	164	6.1	1772.109	28.3	5.5	92.508	885.378	7.9	31.1
37.8	0.5	139	4.2	1557.049	27.5	6.4	89.47	910.478	8.9	30.6
37.8	0.1	95	2.1	1159.107	25.5	5	81.907	964.704	8	26.7
54.4	25	98	8.6	1523.76	28.9	4.2	64.36	323.522	7.1	42.7
54.4	10	79	7.4	1199.15	24.8	3.7	65.861	490.272	5.4	47.9
54.4	5	62	7.1	1044.302	23.9	4	59.657	554.186	5.2	46.2
54.4	1	44	5.7	783.499	22	4.1	56.02	574.349	5.6	38.3
54.4	0.5	39	4.9	737.06	20.8	4.4	53.114	588.02	7.5	36
54.4	0.1	32	2.7	618.201	16.3	3	51.401	618.469	9.2	29.7

Table B-22 Overall Dynamic Modulus test results at various test temperatures for Mix 7 Specimen 3

Temperature (°C)	Frequency (Hz)	Stress Amplitude (P-P) (KPa)	SE (%)	Dynamic Modulus (MPa)	Phase Angle (deg.)	UC (deg.)	Strain (P-P) Recoverable (microstrain)	Accumulated Strain (microstrain)	SE (%)	UC (%)
-10	25	1818	5.4	40765.55	19	7.6	44.586	42.598	15	34.6
-10	10	2117	4.5	38810.26	8.5	1.7	54.548	9.825	7.4	22.7
-10	5	2059	4.3	37303.06	8.4	2.1	55.203	13.321	8.1	21.2
-10	1	1842	1.4	32555.23	9.1	2.7	56.57	14.62	5.5	20.5
-10	0.5	1732	0.8	30783.93	10.6	2.6	56.252	7.722	5.8	20.1
-10	0.1	1574	0.4	26501.73	12	3.2	59.399	34.273	6.1	17.6
4.4	25	1516	5.5	28185.1	16	16.8	53.79	115.765	10.2	30.1
4.4	10	1487	4.9	24623.31	13.1	2.4	60.391	60.942	7.3	19.9
4.4	5	1410	4.5	22686.65	13.2	2.6	62.172	66.084	6.9	18.3
4.4	1	1164	1.9	18615.75	13.9	3.5	62.546	66.938	10.7	15.7
4.4	0.5	1035	1.2	16234.93	17.2	3.1	63.766	70.537	5.5	15
4.4	0.1	872	0.5	13348.3	18.1	2.6	65.345	115.452	4.5	10.2
21.1	25	773	6.5	12898.04	21.8	1.4	59.955	271.944	7.5	22
21.1	10	647	7	10720.49	19.6	1	60.386	308.659	7.9	24.4
21.1	5	547	7	9436.271	20.4	0.5	58.008	324.633	6.3	23.7
21.1	1	357	4.9	6572.449	22.4	0.9	54.253	309.09	5.3	20.6
21.1	0.5	301	3.5	5526.583	23.3	1.5	54.443	312.679	4.8	19.4
21.1	0.1	198	1.3	3892.895	23.9	2.5	50.884	343.593	5	14.1
37.8	25	342	10.2	5595.372	24.6	2.8	61.209	637.311	10.2	13.9
37.8	10	282	10.2	4453.293	24	2.3	63.431	896.936	7.5	13.2
37.8	5	240	8.7	3716.738	23.5	2.3	64.475	1028.309	6.6	14
37.8	1	175	6.2	2570.902	23.9	1.7	68.108	1059.316	6.3	16.4
37.8	0.5	149	4.5	2247.268	22.8	1.5	66.429	1083.824	5.8	18.6
37.8	0.1	102	2.1	1607.736	19.9	0.3	63.526	1121.66	5.9	23
54.4	25	126	8.8	1988.632	26	6.5	63.403	332.83	7.5	14.7
54.4	10	101	8.2	1601.656	23.7	1.3	63.334	516.81	6.9	15.4
54.4	5	80	7.5	1368.718	22.2	1.3	58.555	571.946	6.2	17.8
54.4	1	57	7.2	982.561	19.8	1.8	58.046	579.588	8.8	20.7
54.4	0.5	51	5.9	891.327	17.8	1.2	57.698	586.757	6.8	22.2
54.4	0.1	41	4	727.647	13.5	1.1	56.119	610.691	10	22.6

Table B-23 Overall Dynamic Modulus test results at various test temperatures for Mix 7 Specimen 4

Temperature (°C)	Frequency (Hz)	Stress Amplitude (P-P) (KPa)	SE (%)	Dynamic Modulus (MPa)	Phase Angle (deg.)	UC (deg.)	Strain (P-P) Recoverable (microstrain)	Accumulated Strain (microstrain)	SE (%)	UC (%)
-10	25	1998	5	43840.27	3.8	7.8	45.582	64.662	7.7	29.6
-10	10	2326	4.3	38004.7	9.1	2.3	61.216	19.008	5.6	29.9
-10	5	2260	4.3	35841.58	9.4	2.4	63.047	16.849	5.8	30.2
-10	1	2023	1.3	32022.29	9.9	3	63.17	15.414	3.5	31.4
-10	0.5	1903	0.7	30047.13	9.9	2.8	63.338	17.153	3.3	31.5
-10	0.1	1730	0.5	26335.9	11	2.7	65.703	35.397	3.4	31.7
4.4	25	1666	4.9	28349.64	10.1	6.1	58.768	135.62	8	27.4
4.4	10	1642	4.4	24500.15	13.4	2.9	67.012	73.695	5.4	31.8
4.4	5	1552	4.2	22347.31	13.9	2.9	69.448	78.411	4.7	32.2
4.4	1	1278	1.5	18333.27	14.8	3.1	69.733	77.18	5.4	33
4.4	0.5	1137	0.9	16392.13	17.3	3.7	69.355	83.013	4.3	32.6
4.4	0.1	959	0.5	13156.36	18.6	3.6	72.912	130.838	3.7	33.7
21.1	25	774	6.5	12734.51	20.6	1.5	60.815	245.638	9.6	29.5
21.1	10	646	6.7	10788.39	20.8	2.7	59.858	246.68	6.9	31.5
21.1	5	547	6.8	9320.953	21.9	3.2	58.692	246.681	6.5	32
21.1	1	356	4.5	6547.43	25.7	3.9	54.394	223.068	8.1	35.6
21.1	0.5	297	3.4	5535.278	24.5	3.5	53.624	223.435	4.8	37
21.1	0.1	195	1.6	3805.385	25.6	2	51.293	255.27	4.4	41.7
37.8	25	307	9.3	4746.642	27.9	2.4	64.653	318.795	7.4	29.6
37.8	10	254	8.1	3548.337	27.2	4.2	71.506	424.831	6.9	31.9
37.8	5	214	7.1	2938.456	27.4	4	72.893	465.693	6.2	34.3
37.8	1	156	4.9	1834.02	27.7	4.3	85.308	470.899	5.7	39.3
37.8	0.5	134	3.6	1536.453	27.1	4.3	87.296	477.731	6	41.3
37.8	0.1	91	2.2	1043.451	25.4	4.1	87.156	529.034	6.1	46.9
54.4	25	126	7.9	1770.888	31.3	4.2	71.244	309.857	6.2	22.4
54.4	10	104	7.4	1098.341	28.6	4.5	94.517	454.234	9	48.1
54.4	5	82	7.2	1104.618	27.4	4.5	74.003	511.489	5.6	22.7
54.4	1	58	6.1	774.359	25	4.9	74.719	521.731	6.6	22.3
54.4	0.5	51	4.8	698.839	23.2	4.1	72.264	531.008	6.7	20.7
54.4	0.1	41	3.4	560.769	19	4	73.03	576.714	8	24.1

Table B-24 Overall Dynamic Modulus test results at various test temperatures for Mix 8 Specimen 4

Temperature (°C)	Frequency (Hz)	Stress Amplitude (P-P) (KPa)	SE (%)	Dynamic Modulus (MPa)	Phase Angle (deg.)	UC (deg.)	Strain (P-P) Recoverable (microstrain)	Accumulated Strain (microstrain)	SE (%)	UC (%)
-10	25	3164	8.7	65134.95	8.2	1.2	48.57	21.701	10	13.7
-10	10	3162	8.6	64615.02	7.8	0.8	48.934	23.058	9.8	11.5
-10	5	3053	7.4	61903.32	8	1.1	49.318	21.791	7.2	8.9
-10	1	2690	2.4	55073.28	10.1	1.8	48.836	20.851	6.1	8.9
-10	0.5	2515	1.3	53175.09	8.3	0.9	47.288	23.874	3.7	10.5
-10	0.1	2284	0.7	47354.61	11.1	0.2	48.237	46.115	4.9	14.1
4.4	25	2112	4.6	32072.48	14.3	2.3	65.86	111.668	5	14
4.4	10	2121	4.4	32181.91	14.4	1.8	65.915	150.389	4.1	16.3
4.4	5	2058	4.1	29209.03	16.1	3	70.473	175.895	4.3	13.1
4.4	1	1847	1	22953.12	19.3	3.3	80.463	196.26	7.8	6.4
4.4	0.5	1738	0.5	21061.1	19.2	4.8	82.541	231.761	4.8	2.4
4.4	0.1	1581	0.4	15612.25	23.1	3.8	101.269	390.763	5.6	1.1
21.1	25	1035	6.1	19210.23	20.1	1.6	53.877	362.916	8	4.7
21.1	10	996	6.1	15981.07	20.4	2.1	62.303	387.901	7	5.3
21.1	5	836	6	13858.27	21.7	1.9	60.34	412.073	7.5	6.3
21.1	1	730	2.8	9757.153	24.9	1.5	74.768	445.607	5	6.8
21.1	0.5	603	2	8137.639	26.7	2.5	74.042	461.443	5.5	8.5
21.1	0.1	449	0.9	5522.133	25.7	1.9	81.301	518.135	5.9	11.7
37.8	25	415	8.6	7241.364	28.4	1.4	57.378	561.468	7.3	11.3
37.8	10	388	9	5537.97	27.5	0.7	70.139	904.915	5.5	7.9
37.8	5	319	9	4626.216	26.3	1.5	68.97	1069.072	5.6	2.6
37.8	1	280	5.1	3061.791	23.9	2.7	91.456	1190.593	6.1	9.9
37.8	0.5	237	3.7	2487.62	22.9	2	95.284	1255.337	7.3	12.1
37.8	0.1	177	1.8	1666.826	18.8	1.1	106.309	1343.257	10.5	14.7
54.4	25	105	10	1957.756	33.7	7.4	53.732	122.316	7.5	18.9
54.4	10	97	8.8	1330.382	30.4	4.2	72.653	210.827	4.9	28
54.4	5	80	8.5	1154.682	27.3	3.3	69.058	252.928	3.9	17.7
54.4	1	70	7.9	878.467	21.5	3.8	80.214	272.678	5.7	12
54.4	0.5	58	6.2	766.806	18.7	4.6	76.162	276.914	7.8	13
54.4	0.1	44	3.2	614.118	14.2	5.5	70.872	290.395	9.1	18.2

Table B-25 Overall Dynamic Modulus test results at various test temperatures for Mix 8 Specimen 5

Temperature (°C)	Frequency (Hz)	Stress Amplitude (P-P) (KPa)	SE (%)	Dynamic Modulus (MPa)	Phase Angle (deg.)	UC (deg.)	Strain (P-P) Recoverable (microstrain)	Accumulated Strain (microstrain)	SE (%)	UC (%)
-10	25	2051	5.6	46131.54	11.5	13	44.451	53.326	24.3	18.1
-10	10	2739	5.1	45427.18	6.3	1.9	60.284	32.077	9.2	28.5
-10	5	2660	5	44036.02	5.9	1.3	60.408	35.004	9.6	27.9
-10	1	2368	1.6	39748.21	7.1	1.5	59.584	36.663	8.3	27.4
-10	0.5	2221	0.9	38589.09	9	2.4	57.567	39.74	8.1	26.2
-10	0.1	2017	0.6	34331.17	8.1	1.3	58.755	58.905	10	25.5
4.4	25	1732	5.3	31603.48	15.5	10.4	54.81	159.12	12.1	36.2
4.4	10	1689	5.3	27752.04	13.2	3.9	60.852	106.391	7.3	31.7
4.4	5	1650	4.9	25391.57	13.6	4.3	64.999	116.793	7.1	33.5
4.4	1	1478	1.8	20162.69	16.1	4.5	73.293	125.134	6.4	35.8
4.4	0.5	1387	1	18283.82	16.6	5	75.835	146.184	5.9	35.3
4.4	0.1	1259	0.5	14151.61	20.6	4.5	88.992	258.484	5.8	38.2
21.1	25	693	7.5	14705.91	24.6	7.8	47.124	407.987	12.5	3.8
21.1	10	656	8.1	11356.5	23.4	1.5	57.745	584.687	7.9	8.2
21.1	5	545	8.2	9749.506	24.8	2	55.877	661.236	7.4	6.7
21.1	1	482	4.4	6656.742	29.5	1.8	72.396	728.196	6.4	7.7
21.1	0.5	386	3.2	5575.477	31.3	2.3	69.286	775.099	5.9	9.2
21.1	0.1	313	1.5	4090.979	29.1	4.6	76.509	944.506	5.2	26.7
37.8	25	238	8.8	4067.406	31.7	1.2	58.569	507.895	8.3	22
37.8	10	182	7.9	2915.669	32.9	2.2	62.434	707.264	5.9	32.8
37.8	5	172	7.6	2277.373	32.5	2.8	75.487	903.792	5.5	35.5
37.8	1	145	5.5	1335.484	31.2	3.1	108.517	1027.907	6.5	39.8
37.8	0.5	128	4	1068.655	30	3.4	119.694	1134.858	7.5	40.8
37.8	0.1	94	1.8	697.841	25.1	3.3	134.147	1296.527	10.2	47.6
54.4	25	57	8.9	983.736	37.4	5.8	58.19	143.144	10.4	25.9
54.4	10	44	7.2	684.382	33.5	5	64.431	211.326	10	35.7
54.4	5	41	6.8	550.243	29.8	6.3	75.141	271.043	9.1	37.8
54.4	1	35	6.3	397.499	23.5	7.4	87.082	294.035	11.8	43.3
54.4	0.5	30	5.1	355.347	21.9	6.3	83.258	314.057	12.2	40.9
54.4	0.1	21	4.1	276.284	19	5.4	74.744	339.276	11	32.3

Table B-26 Overall Dynamic Modulus test results at various test temperatures for Mix 8 Specimen 7

Temperature (°C)	Frequency (Hz)	Stress Amplitude (P-P) (KPa)	SE (%)	Dynamic Modulus (MPa)	Phase Angle (deg.)	UC (deg.)	Strain (P-P) Recoverable (microstrain)	Accumulated Strain (microstrain)	SE (%)	UC (%)
-10	25	2051	4.9	52201.33	15.2	8.8	39.294	27.919	15.2	7.7
-10	10	2850	5.5	50379.58	6.5	1.3	56.578	-3.317	6.7	26
-10	5	2771	5.1	48098.03	6.5	1.3	57.603	-6.174	6.3	25.5
-10	1	2466	1.7	44160.37	8.4	1.6	55.834	-6.1	6.9	25
-10	0.5	2312	1	43673.28	8.6	1.4	52.949	-1.368	4.9	23.4
-10	0.1	2102	0.6	37064.04	10	1.9	56.707	23.988	6.3	23.5
4.4	25	2152	4.8	35356.52	13.9	7.7	60.879	226.864	11.4	5.8
4.4	10	2107	4.4	33025.22	11.8	2	63.813	176.716	6.1	15.7
4.4	5	2052	4.1	30205.67	13	2.1	67.935	198.686	5.3	15.8
4.4	1	1842	1.2	24372.05	16	3.2	75.572	215.905	4	15.9
4.4	0.5	1732	0.7	22002.48	18.4	3.3	78.716	252.826	4.8	15.9
4.4	0.1	1574	0.4	16198.11	22.2	5.2	97.165	430.308	3.8	19.4
21.1	25	982	6.3	16114.86	24.9	6.6	60.922	605.719	7.2	17.5
21.1	10	938	6.2	14028.25	21.4	3.8	66.894	743.937	5.8	26.5
21.1	5	780	6.1	12096.54	22.9	3.8	64.491	828.843	5.6	24.4
21.1	1	688	2.9	7899.575	27.5	4.1	87.13	914.011	3.7	27.2
21.1	0.5	551	2.1	6628.894	29.5	4.8	83.092	981.01	3.6	25.8
21.1	0.1	449	0.8	4184.771	30.3	6.9	107.38	1249.805	4.1	28.5
37.8	25	267	8.3	4741.729	35.8	3.9	56.39	341.459	7.4	20.8
37.8	10	213	7.6	3428.916	36.3	4.6	62.049	428.108	5.8	28.6
37.8	5	202	7.1	2618.546	36.3	3.8	77.004	520.331	5.6	30.7
37.8	1	169	4.9	1465.581	35	2	115.299	572.759	7.8	34.9
37.8	0.5	148	3.5	1163.261	33.4	0.9	127.454	629.375	9.2	39
37.8	0.1	108	1.6	788.923	26.4	3.1	136.733	757.628	9.7	56.5
54.4	25	80	9.2	1268.335	28.7	16.3	63.069	310.873	9.2	47.3
54.4	10	64	7.3	926.567	32.9	5.2	68.971	419.14	5.6	21.2
54.4	5	60	7.5	759.25	29.5	5.4	78.762	510.955	5	20
54.4	1	49	6.8	533.959	24.4	5.6	91.988	537.758	5.9	22.1
54.4	0.5	43	5.4	474.044	23.1	5.5	91.643	558.741	6.9	24.4
54.4	0.1	31	3.1	387.107	20.4	4.8	79.836	582.218	8.4	32.7

Table B-27 Overall Dynamic Modulus test results at various test temperatures for Mix 9 Specimen 4

Temperature (°C)	Frequency (Hz)	Stress Amplitude (P-P) (KPa)	SE (%)	Dynamic Modulus (MPa)	Phase Angle (deg.)	UC (deg.)	Strain (P-P) Recoverable (microstrain)	Accumulated Strain (microstrain)	SE (%)	UC (%)
-10	25	2259	5.1	51464.09	6.3	7.2	43.887	65.847	16.4	28.7
-10	10	2543	4.5	45714.24	6.3	1.3	55.627	37.827	6.2	6
-10	5	2473	4.4	44201.25	6.9	1.9	55.941	36.588	6	5.3
-10	1	2215	1.4	40150.22	7.7	1.5	55.18	33.748	4.2	5.5
-10	0.5	2079	0.8	39218.15	7.7	1.6	53.014	34.055	7.3	6.6
-10	0.1	1889	0.5	35298.37	8.7	2.3	53.527	50.979	6.3	7.2
4.4	25	1869	5.6	34766.2	9.2	5.3	53.771	161.927	10.5	17.6
4.4	10	1873	5	29627.62	11.3	2.3	63.207	107.79	6	9
4.4	5	1822	4.6	27039.39	12.5	2.3	67.376	114.89	5.9	7.3
4.4	1	1568	1.6	22836.44	14.4	2.1	68.683	118.244	3.2	8.9
4.4	0.5	1460	0.9	20265.26	15.2	2.1	72.066	132.843	3.3	8
4.4	0.1	1324	0.5	16300.12	18.6	2.6	81.232	216.928	3.2	11.3
21.1	25	852	7	18066.68	10.3	7.3	47.174	348.152	10.1	25.6
21.1	10	840	7	14112.01	19.7	2.6	59.492	447.535	7.1	17.4
21.1	5	811	6.4	12036.38	21	2.5	67.399	535.493	7.3	17.4
21.1	1	659	3.4	8322.609	25	3.8	79.163	570.696	4.9	25.1
21.1	0.5	600	2.2	7138.057	28	4.3	84.055	631.094	3.8	26.9
21.1	0.1	447	1.1	4840.052	29.4	4.5	92.363	800.879	4.5	28.4
37.8	25	349	10	6604.424	24.6	1.3	52.834	232.334	9.1	37.4
37.8	10	319	10	5322.194	25.4	2.1	59.914	297.724	7.5	33.4
37.8	5	272	7.6	4256.99	26.7	2.6	63.783	307.357	6.7	30.2
37.8	1	219	5	2527.008	29.8	4.6	86.81	294.629	6.2	27.6
37.8	0.5	183	3.5	2066.541	29.6	4.6	88.638	295.667	5.6	26.3
37.8	0.1	148	1.3	1331.015	27.3	4.3	110.926	378.151	6.1	27.5
54.4	25	154	8.5	2522.434	32.3	3.7	61.232	339.501	6.6	23.4
54.4	10	142	8.3	1927.121	28.4	1.3	73.678	507.6	6.5	22.9
54.4	5	110	7.8	1571.024	28.1	1.1	70.104	558.556	6.6	22.2
54.4	1	83	6	876.615	26.2	1.9	94.961	566.567	8.8	41
54.4	0.5	69	4.7	902.544	24.6	2.4	76.067	575.477	6.9	11.8
54.4	0.1	53	2.4	681.811	20.4	1.7	77.7	610.437	7.5	16.9

Table B-28 Overall Dynamic Modulus test results at various test temperatures for Mix 9 Specimen 5

Temperature (°C)	Frequency (Hz)	Stress Amplitude (P-P) (KPa)	SE (%)	Dynamic Modulus (MPa)	Phase Angle (deg.)	UC (deg.)	Strain (P-P) Recoverable (microstrain)	Accumulated Strain (microstrain)	SE (%)	UC (%)
-10	25	2715	4.7	51076.61	13.2	9.2	53.163	-10.841	13.4	24.6
-10	10	2811	5.1	51260.49	5.1	0.6	54.829	6.633	5.6	11.3
-10	5	2723	4.8	50078.25	4.2	0.5	54.371	3.288	7	11.6
-10	1	2331	1.5	46612.07	5.6	0.6	50.013	0.908	7.6	11.9
-10	0.5	2164	0.9	43079.74	3.8	1.5	50.235	3.53	6.6	11.5
-10	0.1	1966	0.5	39979.79	7.3	0.5	49.17	9.8	7.9	12.4
4.4	25	2250	4.9	38535.46	12.7	3.3	58.379	123.07	7.9	30
4.4	10	2257	3.7	35320.13	9.1	0.3	63.894	61.818	7.6	16.1
4.4	5	2201	4.1	33860.54	9.4	0.1	65.006	65.534	5.9	17.4
4.4	1	1896	1.3	28799.44	9.8	0.9	65.847	67.379	9.5	17.8
4.4	0.5	1764	0.7	26028.3	10.8	0.9	67.763	75.959	6.6	16.6
4.4	0.1	1601	0.4	21556.27	14.4	0.9	74.271	141.334	5.9	17.9
21.1	25	1132	5.9	21112.42	18.3	2.9	53.626	317.287	8.8	11.2
21.1	10	1126	6	17967.56	15.9	0.5	62.696	374.112	6.8	8.6
21.1	5	1098	5.5	15759.47	17.1	0.9	69.688	458.795	5.8	7.7
21.1	1	884	2.7	11625.83	20.9	2.1	76.031	486.549	5.3	9.1
21.1	0.5	752	1.8	10061.71	22.1	1.8	74.749	518.047	3.5	7.4
21.1	0.1	575	0.8	7523.367	24.3	2.3	76.485	640.254	3.6	9.1
37.8	25	513	8.1	9716.865	22.4	3	52.822	557.115	8.5	9.3
37.8	10	480	8.6	7700.762	22.9	2.4	62.341	816.064	7.2	11.8
37.8	5	406	8.5	6071.81	25.4	5.8	66.836	900.029	7.1	24.9
37.8	1	271	4.5	3579.814	27.5	5.9	75.595	890.817	6.3	34.6
37.8	0.5	198	3.3	2840.768	28.6	6.1	69.832	889.917	5.8	39.2
37.8	0.1	168	1.2	2242.877	27.4	5.6	75.113	982.796	5.2	19.6
54.4	25	204	9.5	4057.345	30.8	7.5	50.23	279.218	9	6
54.4	10	186	8.7	3153.6	28.1	4.5	59.101	397.869	6.8	4.6
54.4	5	146	8.3	2541.365	27.7	4.1	57.456	406.384	6.8	7.1
54.4	1	98	6.3	1567.682	25.7	1.4	62.525	399.334	7.9	15.5
54.4	0.5	91	4.6	1352.123	23.7	2.4	67.316	406.747	5.8	12.3
54.4	0.1	71	1.9	925.877	20.4	1.9	76.889	445.498	7	13.1

Table B-29 Overall Dynamic Modulus test results at various test temperatures for Mix 9 Specimen 6

Temperature (°C)	Frequency (Hz)	Stress Amplitude (P-P) (KPa)	SE (%)	Dynamic Modulus (MPa)	Phase Angle (deg.)	UC (deg.)	Strain (P-P) Recoverable (microstrain)	Accumulated Strain (microstrain)	SE (%)	UC (%)
-10	25	2569	4.7	44116.31	9.4	2.9	58.221	100.154	12.7	24.3
-10	10	2655	4.5	42173.48	7.6	2.6	62.963	52.298	5.7	36
-10	5	2572	4.3	41067.23	8.1	3.4	62.617	55.99	4.4	36
-10	1	2210	1.3	37439.24	9	3.5	59.022	54.29	3.7	35.7
-10	0.5	2056	0.7	35643.31	9.1	3.8	57.678	56.048	8.2	35.1
-10	0.1	1868	0.5	32845.89	9	3	56.862	70.104	8.2	35.5
4.4	25	1959	5	31287.14	11.7	1.1	62.622	120.306	7.2	5
4.4	10	1963	4.3	28839.77	9.9	2.1	68.053	53.782	5.8	13.5
4.4	5	1908	4	26935.26	10.4	2.2	70.829	55.788	5.6	13
4.4	1	1648	1.3	22695.05	12.5	1.9	72.625	56.096	6	11.2
4.4	0.5	1535	0.7	20983.19	10.8	3	73.137	62.78	3	10.7
4.4	0.1	1393	0.4	17069.14	15.4	1.7	81.617	127.79	4	9.3
21.1	25	1023	6.1	16593.37	17.3	2.5	61.621	303.56	7.9	15.5
21.1	10	1014	6.4	14061.09	18.6	3.3	72.107	337.002	6.6	13.8
21.1	5	982	5.6	12382.94	19.3	3.3	79.309	407.561	5.4	12.4
21.1	1	753	2.6	8860.794	22.4	3.5	84.934	425.005	3.9	10.7
21.1	0.5	677	1.8	7601.381	23.6	3.5	89.052	457.702	3.5	10.5
21.1	0.1	518	0.8	5446.924	25.9	2.9	95.127	587.218	4	10.4
37.8	25	482	8.3	9252.508	22.7	5	52.134	460.747	8.7	19
37.8	10	452	9	7278.157	26.3	4.8	62.112	680.323	7.1	12.3
37.8	5	382	8.7	6172.353	25.9	4	61.821	768.808	6.1	15.1
37.8	1	254	4.6	3765.736	27.1	4.3	67.478	768.124	4.7	12.9
37.8	0.5	187	3.3	3009.419	27.3	3.9	62.017	768.228	4.4	12.7
37.8	0.1	158	1.2	2023.902	25.3	3.7	78.286	838.111	4.4	13.2
54.4	25	186	8.9	3406.995	27.1	5	54.508	359.869	8.2	13
54.4	10	167	8	2630.132	27.3	4.6	63.664	541.928	5.6	7.4
54.4	5	131	7.3	2096.747	26.7	4.7	62.616	574.8	5	10.9
54.4	1	89	5.5	1283.116	25.3	4.2	69.2	580.368	5.6	11.6
54.4	0.5	83	4.2	1106.484	24	3.2	74.575	594.462	5.8	11.3
54.4	0.1	64	1.9	805.138	19.9	2.4	80	631.519	7.5	8.2

Table B-30 Overall Dynamic Modulus test results at various test temperatures for Mix 10 Specimen 2

Temperature (°C)	Frequency (Hz)	Stress Amplitude (P-P) (KPa)	SE (%)	Dynamic Modulus (MPa)	Phase Angle (deg.)	UC (deg.)	Strain (P-P) Recoverable (microstrain)	Accumulated Strain (microstrain)	SE (%)	UC (%)
-10	25	2099	4.9	40525.1	1.1	15.9	51.803	92.095	8.5	25.2
-10	10	2142	4.6	38239.61	8.5	2.8	56.008	37.391	5.8	15.1
-10	5	2078	4.3	36099.48	9	2.7	57.55	37.239	5.9	15.8
-10	1	1867	1.3	31737.14	10.5	2.6	58.819	39.805	4.2	15.9
-10	0.5	1754	0.8	29217.06	11.9	2.9	60.02	43.798	3.7	16.7
-10	0.1	1596	0.4	24868.52	13.6	2.3	64.179	73.771	4.1	17.8
4.4	25	1324	5.7	24604.66	12.5	1.4	53.809	257.106	7.6	23.2
4.4	10	1279	5.4	22569.3	14.9	2.4	56.665	235.004	6.4	25.3
4.4	5	1203	4.8	20448.77	15.9	2.2	58.843	267.52	6.5	25.9
4.4	1	1062	2	15251.34	20.8	2.2	69.66	294.107	4.7	24.7
4.4	0.5	952	1.3	13137.89	22.4	2.4	72.473	330.789	4.4	26.1
4.4	0.1	901	0.5	9258.444	26.3	2.9	97.266	555.915	5.5	23.8
21.1	25	540	8.1	9593.804	28	3.4	56.317	535.263	8.3	29.4
21.1	10	507	8.1	7533.726	28.8	4.3	67.288	780.724	7.5	24.1
21.1	5	478	7.8	6058.171	29.3	4.1	78.907	940.646	6.8	22.1
21.1	1	404	4.6	3719.065	31.1	3.7	108.652	1040.341	5.8	20.5
21.1	0.5	340	3.3	2974.895	31.1	3.9	114.411	1109.645	6.1	19.7
21.1	0.1	237	1.4	1823.163	28.9	4.5	129.762	1247.671	5.8	18.3
37.8	25	205	7.9	3583.057	36.5	5.7	57.262	466.586	7	21.2
37.8	10	186	7.7	2612.281	32.5	3.4	71.312	779.219	5.8	16
37.8	5	148	7	2147.056	31.1	3.1	69.13	886.863	5.3	18.2
37.8	1	109	5.2	1400.727	27.2	4.1	77.487	912.937	5.2	18.7
37.8	0.5	83	4.1	1190.589	24.8	4	69.764	923.636	5.2	21.8
37.8	0.1	67	2.2	920.862	19.6	2.7	73.196	960.083	7.2	22.3
54.4	25	72	8.3	960.079	33.2	6	75.4	51.777	6.6	21.3
54.4	10	61	7.1	754.261	27.7	4.8	80.494	84.006	4.1	32.4
54.4	5	50	7.1	652.99	26.6	4.1	76.859	92.669	4.5	32.3
54.4	1	35	6.3	538.915	23.6	4.4	65.872	86.872	5.9	22.8
54.4	0.5	27	5.4	528.55	21.3	4.2	51.137	81.22	5.3	15.7
54.4	0.1	22	3.6	455.129	17.7	3.2	47.851	90.93	5.7	14.8

Table B-31 Overall Dynamic Modulus test results at various test temperatures for Mix 10 Specimen 3

Temperature (°C)	Frequency (Hz)	Stress Amplitude (P-P) (KPa)	SE (%)	Dynamic Modulus (MPa)	Phase Angle (deg.)	UC (deg.)	Strain (P-P) Recoverable (microstrain)	Accumulated Strain (microstrain)	SE (%)	UC (%)
-10	25	2102	4.6	39745.51	8.1	1	52.885	95.46	6.6	22.9
-10	10	2139	4.3	39791.53	7.6	0.7	53.743	53.398	5.4	27.7
-10	5	2080	4.2	37716.19	8.3	0.7	55.143	58.916	5.1	27.7
-10	1	1866	1.4	33690.09	9.3	0.9	55.401	60.35	5.1	28.1
-10	0.5	1753	0.7	31960.58	10.8	0.8	54.847	67.059	5.3	28.3
-10	0.1	1597	0.4	25861.46	12.9	0.9	61.739	107.702	4.3	29.7
4.4	25	1321	5.3	24740.69	13.4	2.2	53.413	205.772	6.9	16.9
4.4	10	1277	4.6	21879.14	17.2	3.7	58.354	173.213	5.2	19.2
4.4	5	1204	4.6	19637.24	18.5	4	61.305	194.774	4.6	20.6
4.4	1	1062	1.8	15006.93	21.4	4.6	70.761	211.384	6.7	19.6
4.4	0.5	952	1.2	13075.55	26.2	3.3	72.79	240.169	4.3	23
4.4	0.1	900	0.5	9154.618	25.4	2.5	98.322	420.364	3.7	36
21.1	25	541	7.7	9261.728	23.9	2.1	58.437	354.565	7.7	32.3
21.1	10	515	8.1	7235.983	24.4	1.6	71.145	486.136	7.4	33.3
21.1	5	483	7.5	6051.111	25.4	1.8	79.811	580.522	6.2	34.8
21.1	1	403	4.4	3758.55	27.6	1.9	107.169	637.523	4.4	37
21.1	0.5	340	3.2	3004.449	27.7	2.2	113.206	677.768	4.4	38.2
21.1	0.1	239	1.1	1767.672	26.1	2.5	135.112	786.203	4.8	42.4
37.8	25	208	8.7	4104.072	30.3	2.5	50.64	372.57	8.5	23
37.8	10	189	7.7	2981.668	28.6	3.4	63.286	555.318	5.7	31.2
37.8	5	151	7.3	2364.448	28	3.2	63.802	613.652	4.9	32.1
37.8	1	109	5.5	1425.473	26.4	3.4	76.34	618.067	5	37.9
37.8	0.5	84	4.4	1143.491	25.5	3.9	73.246	616.646	4.8	40
37.8	0.1	68	2	809.133	21.1	3.5	84.419	646.304	7.1	43.3
54.4	25	73	9.9	1315.544	31.3	3.3	55.704	140.054	8.7	35.3
54.4	10	61	7.7	1032.219	26	2.9	59.578	176.211	4.7	36.8
54.4	5	50	7.1	888.584	23.5	2.8	56.453	196.307	4.2	35.4
54.4	1	35	6.1	642.906	19.4	2.9	54.794	193.076	4.3	38.3
54.4	0.5	27	4.9	560.777	18.1	3.4	47.94	193.661	5.1	40.8
54.4	0.1	22	2.7	458.92	15.5	3.5	48.624	204.325	8.4	41.8

Table B-32 Overall Dynamic Modulus test results at various test temperatures for Mix 10 Specimen 5

Temperature (°C)	Frequency (Hz)	Stress Amplitude (P-P) (KPa)	SE (%)	Dynamic Modulus (MPa)	Phase Angle (deg.)	UC (deg.)	Strain (P-P) Recoverable (microstrain)	Accumulated Strain (microstrain)	SE (%)	UC (%)
-10	25	2622	4.9	35468.3	7.7	7.2	73.928	129.842	15	40.7
-10	10	2347	4.1	36843.17	10.2	4.3	63.709	53.858	6.3	24.6
-10	5	2278	3.7	35605.55	10.1	4.4	63.966	58.519	4.5	19.7
-10	1	2049	1.1	31231.3	11.3	4.2	65.597	59.113	5.7	19.3
-10	0.5	1927	0.7	29780.51	14.9	2.5	64.721	66.564	7.3	19.1
-10	0.1	1756	0.5	25728.48	14.2	3.2	68.265	106.024	5.1	19
4.4	25	1548	4.9	23733.32	13.6	1.7	65.221	248.132	6.8	23.8
4.4	10	1507	4.9	24085.73	14	4.4	62.582	229.688	5.6	2.6
4.4	5	1421	4.3	21992.21	14.6	4.9	64.592	263.131	5.4	4.4
4.4	1	1250	1.6	17153.89	18.3	4.9	72.886	287.598	3.8	6.6
4.4	0.5	1123	1	15378.09	18.8	5.6	73.054	322.459	3.9	6.8
4.4	0.1	1063	0.4	10781.23	24.5	4.5	98.603	549.61	4.2	11.2
21.1	25	673	7	12884.84	26.7	9.2	52.223	344.057	11.1	7.7
21.1	10	632	7.1	9966.283	23.3	6.1	63.438	464.965	7.8	6.9
21.1	5	588	6.6	8330.133	24.9	6	70.593	563.22	7	9.5
21.1	1	515	3.6	5486.283	27.7	6.2	93.831	632.786	4.5	17.3
21.1	0.5	420	2.7	4522.887	27.2	7	92.969	662.569	5.3	18.8
21.1	0.1	322	1.3	2921.681	28	5.6	110.157	795.711	5.4	20.7
37.8	25	286	8.8	4889.541	31.7	3	58.433	685.151	9.3	4.4
37.8	10	263	7.8	3688.706	29.8	4.9	71.33	1019.638	5.9	6.9
37.8	5	210	6.6	2401.873	30.5	4.8	87.624	1103.357	6.5	33.2
37.8	1	152	4.3	1829.223	28.3	4.6	83.246	1132.808	5	6.6
37.8	0.5	117	3.2	1488.454	27.2	4.3	78.867	1131.702	5.2	3.6
37.8	0.1	96	1.5	1027.748	22.1	3.5	93.465	1168.589	6.7	6.8
54.4	25	93	7.2	1754.808	29.5	5.1	52.738	184.439	6.6	21.7
54.4	10	77	6.4	1058.841	26.1	3.9	73.105	229.008	5.2	39.9
54.4	5	63	6	905.943	24.4	4.9	69.903	247.006	4.5	38.1
54.4	1	45	5.1	746.7	20.9	3.8	60.745	247.336	5.5	22.3
54.4	0.5	35	3.7	666.762	19.2	3.6	52.932	244.159	5	18.2
54.4	0.1	29	2	554.082	17	3.4	52.331	247.78	6.9	17.3

Table B-33 Overall Dynamic Modulus test results at various test temperatures for Mix 11 Specimen 3

Temperature (°C)	Frequency (Hz)	Stress Amplitude (P-P) (KPa)	SE (%)	Dynamic Modulus (MPa)	Phase Angle (deg.)	UC (deg.)	Strain (P-P) Recoverable (microstrain)	Accumulated Strain (microstrain)	SE (%)	UC (%)
-10	25	2058	5	41201.01	2.8	4.2	49.941	51.768	10.7	29.2
-10	10	2073	4	36359.94	7.4	2.1	57.016	5.895	5.7	11.1
-10	5	2018	3.9	35627.73	7.4	2.4	56.653	7.328	5.1	12.4
-10	1	1818	1.2	32426.11	9.8	2.7	56.073	8.517	7.3	12.2
-10	0.5	1712	0.7	29491.27	8.2	2.9	58.035	11.49	5.1	12.5
-10	0.1	1560	0.4	27663.08	9.7	3	56.378	28.136	7.3	13.2
4.4	25	1545	5.3	27273.02	7.4	2.3	56.636	149.916	12.5	19.4
4.4	10	1493	5.5	22506.64	10.9	1.3	66.333	94.892	7.1	1.7
4.4	5	1406	4.8	20971.85	11.4	1.4	67.062	102.508	6.3	2.3
4.4	1	1240	1.7	17367.08	12.9	2.3	71.426	107.562	10	4.4
4.4	0.5	1115	1	15339.74	16.2	1.7	72.711	123.137	4.3	3.2
4.4	0.1	1056	0.5	12118.35	18.9	2.6	87.157	212.113	3.6	3.7
21.1	25	724	6.4	12746.07	16.2	2	56.836	300.195	8.6	6.2
21.1	10	647	6.3	11024.84	20.5	3.8	58.674	356.535	7.2	5.9
21.1	5	566	6.5	9359.623	21.8	3.6	60.518	388.935	6.6	5.4
21.1	1	477	3.3	6326.627	27.1	3.6	75.471	408.075	5.8	1.1
21.1	0.5	347	2.7	5241.061	26.3	3.7	66.193	413.264	5.2	7.7
21.1	0.1	306	1.5	3350.849	28.3	3.9	91.467	536.15	4.9	3.9
37.8	25	303	9.2	4923.236	29.2	4.7	61.528	389.656	10	12.8
37.8	10	280	7.1	3377.191	30.1	3.9	83	591.843	5.7	3
37.8	5	212	7.1	2747.117	30.2	4.4	77.288	646.337	5.8	6.1
37.8	1	189	4.6	1637.644	29.5	4	115.39	692.086	6	12.1
37.8	0.5	149	3.4	1284.36	28.4	3.4	115.738	707.817	6	18
37.8	0.1	113	1.5	840.469	24.3	2.9	134.767	789.345	7	24.3
54.4	25	103	8.4	1660.933	31.9	4.4	61.817	184.156	8	14.8
54.4	10	90	7.3	1299.912	27.9	4.3	69.135	314.266	5.1	4.5
54.4	5	74	6.8	1071.726	25.7	5.2	69.357	357.376	4.3	2.8
54.4	1	53	5.6	738.99	23.2	4.2	72.301	358.577	4.3	8.6
54.4	0.5	43	4.3	643.438	21.6	3.3	67.146	357.931	5.7	9.3
54.4	0.1	37	3.1	525.785	17.3	2.3	69.921	375.227	8.1	10.8

Table B-34 Overall Dynamic Modulus test results at various test temperatures for Mix 11 Specimen 4

Temperature (°C)	Frequency (Hz)	Stress Amplitude (P-P) (KPa)	SE (%)	Dynamic Modulus (MPa)	Phase Angle (deg.)	UC (deg.)	Strain (P-P) Recoverable (microstrain)	Accumulated Strain (microstrain)	SE (%)	UC (%)
-10	25	2053	4.8	42479.79	3.8	3.8	48.325	65.251	8	23.7
-10	10	2091	4.7	38837.52	6	0.5	53.838	24.131	8.2	15.7
-10	5	2036	4.5	38150.36	6.3	0.1	53.36	23.288	8.3	16.9
-10	1	1823	1.4	34464.33	5.6	0.9	52.894	22.836	8.1	17.4
-10	0.5	1713	0.7	31786.76	7.6	0.4	53.899	24.51	7.7	16.7
-10	0.1	1562	0.4	29027.26	9.4	0.7	53.797	39.082	6.6	18.7
4.4	25	1552	5.5	26849.34	8.8	2.9	57.818	160.148	9.3	15.7
4.4	10	1509	5.4	23270.89	11.6	0	64.834	105.448	8.1	11
4.4	5	1422	5.2	21622.15	11.8	0.2	65.76	115.873	7.2	12.2
4.4	1	1246	1.9	17395.94	14.9	0.8	71.611	123.423	6.7	11.3
4.4	0.5	1117	1.1	16565.75	16.6	0.8	67.425	140.085	3.7	14.2
4.4	0.1	1057	0.5	11936.98	19.7	1.2	88.585	255.182	4.5	11.9
21.1	25	627	7.3	10507.11	19.4	1.2	59.661	257.455	9.7	24.1
21.1	10	574	7.3	8810.332	20.6	0.8	65.166	326.968	6.6	25.5
21.1	5	519	7	7533.774	21.9	1.2	68.929	367.127	6.1	24.7
21.1	1	454	3.8	5103.199	25.6	1.4	89.052	390.964	4.8	25.3
21.1	0.5	297	3.3	4032.981	27.8	1.6	73.637	384.813	4.4	30.5
21.1	0.1	270	1.1	2659.731	28.1	2	101.391	511.821	4.2	29.9
37.8	25	303	8.5	4692.704	29.6	3.2	64.596	328.799	9.4	27.7
37.8	10	281	6.8	3436.891	29.2	3.4	81.821	468.911	6.6	24.1
37.8	5	212	6.8	2758.789	30.6	3.3	76.91	486.67	6	26
37.8	1	188	4.8	1724.475	30.2	2.3	109.028	502.32	5.3	26.1
37.8	0.5	149	3.8	1370.113	30.2	2.5	108.862	508.951	5.7	28.4
37.8	0.1	114	1.7	906.99	26.4	2.8	125.58	585.7	7.6	31.2
54.4	25	104	7.9	1410.161	34.6	3.7	74.018	188.486	7.2	23.3
54.4	10	91	6.8	1121.481	30.8	2.3	81.58	276.445	4.3	25.9
54.4	5	75	6.7	925.921	29.5	2.7	80.637	285.056	4.1	25.5
54.4	1	53	5.7	661.853	27.6	3.1	80.136	300.79	4.9	27.6
54.4	0.5	44	4.6	567.976	27	3.7	76.759	311.953	6.6	24.2
54.4	0.1	38	2.4	475.571	23.4	4.4	78.983	344.142	8.7	23

Table B-35 Overall Dynamic Modulus test results at various test temperatures for Mix 11 Specimen 5

Temperature (°C)	Frequency (Hz)	Stress Amplitude (P-P) (KPa)	SE (%)	Dynamic Modulus (MPa)	Phase Angle (deg.)	UC (deg.)	Strain (P-P) Recoverable (microstrain)	Accumulated Strain (microstrain)	SE (%)	UC (%)
-10	25	2061	5	46716.07	1.5	15.5	44.111	56.262	10.7	37.7
-10	10	2094	4.6	42681.54	7.9	2.2	49.063	19.498	7.4	10.6
-10	5	2036	4.4	41102.59	7.8	2.5	49.545	16.976	7.9	11.2
-10	1	1823	1.4	36517.81	10.9	0.8	49.925	17.247	8.6	8.9
-10	0.5	1712	0.7	34837.6	6.7	3.4	49.155	19.202	8	8.3
-10	0.1	1562	0.5	31647.03	11.2	1.4	49.347	33.9	8.2	10.9
4.4	25	1554	5.3	27486.2	8.2	2.4	56.527	148.623	8.3	16.1
4.4	10	1509	5.3	23739.11	11.7	1.4	63.582	97.219	7.5	8.5
4.4	5	1424	5.1	22136.75	11.9	1.6	64.333	106.524	6.8	8.1
4.4	1	1245	1.9	17897.18	14.6	1.7	69.538	113.909	5.8	7.1
4.4	0.5	1115	1.2	16050.03	14.2	1.9	69.478	126.463	3.8	7.4
4.4	0.1	1059	0.6	12146.51	19.8	0.8	87.208	230.937	4.4	11.5
21.1	25	623	7	12949.89	18.8	0.6	48.098	255.498	7.8	10.2
21.1	10	572	7.2	10671.78	19.8	1.4	53.623	340.1	8.4	10.1
21.1	5	517	7	9192.873	21.3	1.2	56.267	388.469	6.8	13.5
21.1	1	455	3.7	6370.723	25.4	1.2	71.436	420.696	6.7	16.5
21.1	0.5	295	3	4989.948	28.4	1	59.206	413.548	6.5	16.8
21.1	0.1	269	0.9	3225.581	27.5	2.2	83.356	540.895	4.5	21.8
37.8	25	302	8.4	4429.518	28.4	2.8	68.153	398.765	7.4	26
37.8	10	281	7.1	3248.135	28.3	4.2	86.375	612.375	5.9	29.5
37.8	5	211	7	2579.926	28.2	4.4	81.765	653.198	5.7	32.1
37.8	1	189	5	1623.553	27.2	4.6	116.247	690.096	5.5	37
37.8	0.5	148	3.6	1284.874	26.9	4.6	115.218	703.317	5.8	39.3
37.8	0.1	113	1.7	854.622	23.6	4.1	131.945	788.075	7.1	44.5
54.4	25	103	9.2	1855.987	28.4	5.9	55.677	145.934	9.2	15
54.4	10	90	7.5	1288.234	27.8	5.4	69.903	201.074	5.3	20.7
54.4	5	76	6.8	1034.961	26.3	5	72.983	212.219	4.9	25.4
54.4	1	54	5.9	680.428	23.8	4.3	78.736	216.656	6.1	28.7
54.4	0.5	43	4.8	593.526	22.2	4.5	72.306	222.691	5.5	29.8
54.4	0.1	37	2.7	459.895	18.4	3.5	80.791	257.069	7.5	30.6

Table B-36 Overall Dynamic Modulus test results at various test temperatures for Mix 12 Specimen 1

Temperature (°C)	Frequency (Hz)	Stress Amplitude (P-P) (KPa)	SE (%)	Dynamic Modulus (MPa)	Phase Angle (deg.)	UC (deg.)	Strain (P-P) Recoverable (microstrain)	Accumulated Strain (microstrain)	SE (%)	UC (%)
-10	25	2103	4.9	41143.5	11.4	10.5	51.107	74.345	6.9	3.3
-10	10	2131	4.4	42141.26	6	0.7	50.558	27.96	6.1	9.2
-10	5	2079	4.3	40435.13	6.9	1.7	51.42	30.819	5.7	9.1
-10	1	1867	1.4	37074.35	8.3	3.3	50.372	28.81	8.3	8.4
-10	0.5	1755	0.8	35904.31	8.2	2.9	48.892	25.762	6.7	10
-10	0.1	1595	0.5	30385.26	10	2.4	52.498	45.714	7.7	7.1
4.4	25	1329	5.8	29808.92	16.6	13.1	44.578	103.406	9.8	9.1
4.4	10	1288	5.8	27813.45	11.8	3.1	46.318	76.213	7.7	4.1
4.4	5	1212	5.5	25699.81	12.9	3.3	47.175	81.886	7.2	2.7
4.4	1	1065	2.3	21142.48	15.1	4.2	50.362	85.815	6.9	7.2
4.4	0.5	953	1.5	19340.09	12.1	5.4	49.285	94.409	9.8	7
4.4	0.1	902	0.6	14439.6	19.6	3.6	62.458	173.366	5.7	10.4
21.1	25	703	7.6	12169.27	21.3	7.1	57.794	241.371	10.8	10.5
21.1	10	667	8.4	10207.47	17.8	1.9	65.393	290.388	8.1	6.9
21.1	5	628	7.9	8963.812	18.6	1.8	70.081	330.883	8.5	10.3
21.1	1	527	4.4	6362.728	22.5	1.9	82.858	343.406	7.2	13.2
21.1	0.5	442	3.1	5286.229	24	2.5	83.585	351.795	6.5	13.6
21.1	0.1	308	1.6	3617.636	23.8	3.4	85.169	399.165	6.2	12.7
37.8	25	285	10.2	5105.947	26.8	2.5	55.83	418.504	10.5	14
37.8	10	261	9.5	3946.33	24.6	3.1	66.052	685.666	7.9	25.1
37.8	5	207	8.3	3278.927	24.8	3.1	63.187	782.051	7.6	28.4
37.8	1	152	5.1	2026.723	26.2	3.5	75.111	790.685	6.4	32.1
37.8	0.5	117	3.7	1642.512	25.6	4.1	71.15	795.261	5.2	32.7
37.8	0.1	95	2.3	1113.645	22.7	3.8	85.201	862.115	5.8	37.2
54.4	25	115	8.8	1849.901	29.6	3.5	62.309	486.091	8.9	30.8
54.4	10	97	7.5	1406.925	26	4.1	69.124	688.242	6	36.7
54.4	5	80	7.4	1166	25	4.2	68.865	761.937	9.1	40.2
54.4	1	58	5.8	901.625	22.7	3	63.789	796.903	5.8	24.7
54.4	0.5	44	4.3	832.141	21.1	2.6	53.195	803.972	4.9	19.9
54.4	0.1	35	3.5	665.996	16.6	1.5	53.167	826.018	6.8	18

Table B-37 Overall Dynamic Modulus test results at various test temperatures for Mix 12 Specimen 2

Temperature (°C)	Frequency (Hz)	Stress Amplitude (P-P) (KPa)	SE (%)	Dynamic Modulus (MPa)	Phase Angle (deg.)	UC (deg.)	Strain (P-P) Recoverable (microstrain)	Accumulated Strain (microstrain)	SE (%)	UC (%)
-10	25	2057	4.9	40139.77	5.5	5.8	51.246	71.43	18.3	57.1
-10	10	2094	4.7	32029.69	8.2	1.5	65.373	10.128	6.6	22.5
-10	5	2034	4.4	30596.04	8.1	1.6	66.485	9.448	6	22.3
-10	1	1821	1.4	26927.62	10.2	2	67.634	10.859	3.9	21.7
-10	0.5	1713	0.8	25186.05	9.3	2.1	68.001	13.884	5	21.7
-10	0.1	1562	0.4	21572.29	10.9	2.2	72.393	40.639	8.3	22.8
4.4	25	1544	5.4	19326.52	10.6	2.9	79.868	280.274	8.8	20.8
4.4	10	1487	5.3	16447.72	13.3	1	90.404	209.214	6.1	13.1
4.4	5	1403	4.8	14986.28	14.1	0.8	93.649	236.439	6.4	13.8
4.4	1	1240	1.6	11595.33	17.5	1.2	106.909	257.138	4.2	12.8
4.4	0.5	1115	1	10296.46	18.2	0.5	108.278	292.998	3.6	12.1
4.4	0.1	1055	0.5	7315.297	21.9	0.5	144.209	510.641	2.7	14.1
21.1	25	622	6.9	7935.746	22.5	0.7	78.327	564.077	6.5	8.2
21.1	10	555	6.9	6413.608	22.8	0.8	86.488	796.019	5.3	7.6
21.1	5	470	6.5	5357.676	23.7	0.8	87.808	908.55	4.6	5.9
21.1	1	377	3.7	3477.923	26.7	1.2	108.392	973.026	4.4	6
21.1	0.5	295	2.7	2810.066	27.6	1.2	104.92	1030.939	5.1	6
21.1	0.1	249	0.8	1764.557	27.1	2.5	140.88	1259.326	4.9	5.4
37.8	25	179	7.6	2949.063	29.9	2.8	60.792	372.986	8.6	13.9
37.8	10	160	7.1	2257.674	29.1	1.7	70.821	584.428	6.9	9.3
37.8	5	121	6.5	1775.911	27.9	2	67.971	655.714	4.9	11.9
37.8	1	108	4.7	1147.821	26	2.5	93.882	720.653	6.5	8.1
37.8	0.5	85	3.5	963.658	24.2	2.6	88.298	754.158	7	10.7
37.8	0.1	65	2.5	709.436	19.6	2.7	91.298	814.876	8.2	11.7
54.4	25	61	8.4	909.002	28.9	6.1	66.657	162.004	9.7	33.8
54.4	10	51	7.2	737.384	23.6	1.3	68.692	229.44	5.4	29.5
54.4	5	39	6.6	616.142	21.5	1.2	63.544	237.612	7.1	33
54.4	1	28	6.5	453.924	16.2	1.7	61.76	235.395	12.6	34.2
54.4	0.5	23	5.2	391.008	16.5	0.9	57.954	231.684	6.4	35
54.4	0.1	18	5	324.504	12.2	2.1	54.783	235.222	6.5	34

Table B-38 Overall Dynamic Modulus test results at various test temperatures for Mix 12 Specimen 6

Temperature (°C)	Frequency (Hz)	Stress Amplitude (P-P) (KPa)	SE (%)	Dynamic Modulus (MPa)	Phase Angle (deg.)	UC (deg.)	Strain (P-P) Recoverable (microstrain)	Accumulated Strain (microstrain)	SE (%)	UC (%)
-10	25	2056	5	27415.13	10.9	6	74.978	120.584	7	8.1
-10	10	2086	4.4	26125.52	8.9	0.8	79.832	49.598	5.6	13.1
-10	5	2034	4.3	24861.95	9.2	0.9	81.82	44.64	5.1	13.4
-10	1	1825	1.4	22106.85	9.5	1.1	82.536	44.909	4.5	13.6
-10	0.5	1715	0.7	20005.11	11.3	0.8	85.727	50.072	2.5	14.9
-10	0.1	1561	0.4	17065.33	13	0.8	91.49	94.523	3	16.4
4.4	25	1246	6	16883.35	16.5	6.7	73.807	252.647	8.9	15.1
4.4	10	1204	5.8	14991.56	14.8	1.4	80.304	207.445	6.4	17.5
4.4	5	1136	5.5	13510.61	16	1.2	84.052	229.903	5.8	17.6
4.4	1	995	2.2	10358.66	19.5	1.1	96.038	248.409	5.4	17
4.4	0.5	890	1.4	9369.185	20.7	1.7	95.039	281.151	3.6	17.3
4.4	0.1	844	0.6	6533.087	23.8	1.9	129.222	490.159	3.2	19.6
21.1	25	500	7.5	8684.843	22.7	4.2	57.561	450.827	6.7	17
21.1	10	445	7.5	6702.557	24.2	2.7	66.387	641.038	6.2	20.6
21.1	5	374	7.6	5470.571	25.8	2.3	68.432	721.356	6.4	21.4
21.1	1	298	4.1	3381.052	29.7	2	88.006	758.686	5.7	23.5
21.1	0.5	238	2.3	2657.649	29.6	2.7	89.481	797.107	4.5	25.9
21.1	0.1	198	1	1633.286	30.5	2	121.001	1003.798	5	30.5
37.8	25	180	8	2901.148	30.2	8.8	62.191	337.139	7.1	33.2
37.8	10	163	6.1	2112.072	29.3	5.7	77.066	540.234	4.5	32.8
37.8	5	123	5.7	1660.015	28.6	5.8	73.967	575.063	4.3	36.2
37.8	1	109	4.7	1064.437	26.4	4.6	102.031	623.396	5.4	41.7
37.8	0.5	86	3.4	866.85	25.3	4.1	99.506	645.865	6.4	42.2
37.8	0.1	67	1.5	622.127	21.5	3.1	106.908	707.346	8.5	42.1
54.4	25	61	6.7	1121.864	30.3	2.2	54.524	145.273	5.8	13.8
54.4	10	49	5.7	768.566	29	7.5	64.183	158.943	3.5	13.5
54.4	5	39	5.5	636.112	27.3	7.3	61.322	155.108	4.9	15.8
54.4	1	28	5.2	519.976	21	3.9	54.766	157.28	5.6	19.5
54.4	0.5	23	4.5	487.196	19.1	2.7	47.355	154.272	5.1	18.5
54.4	0.1	18	3.1	409.363	14.2	1.4	44.155	158.174	7	12.9

Table B-39 Overall Dynamic Modulus test results at various test temperatures for Mix 13 Specimen 1

Temperature (°C)	Frequency (Hz)	Stress Amplitude (P-P) (KPa)	SE (%)	Dynamic Modulus (MPa)	Phase Angle (deg.)	UC (deg.)	Strain (P-P) Recoverable (microstrain)	Accumulated Strain (microstrain)	SE (%)	UC (%)
-10	25	2268	5	41576.08	2.6	5	54.544	64.217	10.3	33
-10	10	2312	4.2	43391	5.3	0.2	53.275	21.702	6.4	36.3
-10	5	2258	4.5	42255.52	5.5	0.4	53.428	21.783	5.5	36.7
-10	1	2020	1.4	40176.78	6.3	0.3	50.284	23.501	5.8	37.2
-10	0.5	1895	0.8	39533.12	6.3	0.1	47.928	24.226	4.8	37.6
-10	0.1	1726	0.5	34692.06	6.7	0.5	49.741	33.594	5.5	37.5
4.4	25	1615	5.9	48908.5	6.6	1.3	33.025	69.496	13.3	7.1
4.4	10	1567	5.4	38937.06	8.7	1.2	40.246	30.752	6.6	28.1
4.4	5	1471	5.1	36868.52	9	1	39.902	31.637	8.5	28.5
4.4	1	1296	1.8	31350.19	11.7	1.5	41.337	31.664	6.5	26.4
4.4	0.5	1164	1.1	28813.17	9.2	1.3	40.406	35.876	5.8	25.4
4.4	0.1	1100	0.5	23373.31	14.6	2.4	47.079	80.508	8.2	23.6
21.1	25	1041	6.4	19139.94	17.2	3.1	54.366	364.719	10.4	27.1
21.1	10	945	6.2	13751.81	19.2	1.4	68.75	378.326	6.4	22.6
21.1	5	800	6.1	12112.84	20.3	1.3	66.019	415.44	5.8	24
21.1	1	634	2.9	8794.374	23.2	1.5	72.062	431.17	10.9	29.3
21.1	0.5	502	2	7238.853	26.1	1.3	69.365	454.16	4.9	27.9
21.1	0.1	415	1.1	4844.417	28.9	2.1	85.734	617.37	4.6	25
37.8	25	408	8.3	6848.172	25.2	2.1	59.576	389.457	7.9	26.1
37.8	10	359	9	5069.208	27.8	1	70.751	600.784	6.6	24.1
37.8	5	280	7.9	4050.573	28.6	1.1	69.076	686.454	7.3	26.3
37.8	1	223	4.1	2297.448	30.4	1.2	97.233	721.737	5.9	24.7
37.8	0.5	171	2.7	1811.102	30.7	1.2	94.612	750.598	5.5	26.6
37.8	0.1	141	1.7	1121.096	29	1.6	125.551	926.87	6.3	25.8
54.4	25	134	7.8	2037.501	32.2	1.2	65.865	420.485	8	40.1
54.4	10	102	6.4	1448.737	32.7	0.7	70.271	612.54	4.4	33.8
54.4	5	85	5.9	1128.171	31.7	0.7	75.405	707.342	3.8	33.6
54.4	1	64	4.8	684.606	29	1.2	93.392	740.272	4.2	34.9
54.4	0.5	48	3.8	559.303	27.7	1.3	86.016	761.865	5.3	37.9
54.4	0.1	43	3	409.78	22.6	2.1	103.777	855.151	7.7	43.1

Table B-40 Overall Dynamic Modulus test results at various test temperatures for Mix 13 Specimen 2

Temperature (°C)	Frequency (Hz)	Stress Amplitude (P-P) (KPa)	SE (%)	Dynamic Modulus (MPa)	Phase Angle (deg.)	UC (deg.)	Strain (P-P) Recoverable (microstrain)	Accumulated Strain (microstrain)	SE (%)	UC (%)
-10	25	2615	4.7	43497	8.8	12.9	60.119	111.093	20.1	24.8
-10	10	2682	4.7	50103.04	5.9	0.5	53.524	54.449	6.7	22.3
-10	5	2609	4.8	47631.16	6	0.7	54.774	53.3	6.2	21.8
-10	1	2330	1.6	43046.34	6.3	0.6	54.118	53.402	7.4	21.8
-10	0.5	2183	0.9	41539.63	9.9	1.4	52.549	56.112	4.9	23.1
-10	0.1	1988	0.6	37434.95	9	0.7	53.116	68.127	4.8	25.4
4.4	25	1899	5.3	40656.36	6.7	4.3	46.708	174.856	12.9	53.1
4.4	10	1845	4.6	29909.13	11.2	0.8	61.695	115.816	7.6	19.1
4.4	5	1731	4	26705.24	11.9	0.8	64.808	130.893	6.3	20.9
4.4	1	1529	1.4	21269.41	17.5	2	71.88	141.064	9	20.5
4.4	0.5	1375	0.8	20047.47	18.5	2	68.607	162.826	3.6	22.6
4.4	0.1	1303	0.4	14016.21	22.9	3	92.957	304.723	4.3	22.8
21.1	25	934	6.4	15536.73	13	7.8	60.125	564.758	19.1	49.6
21.1	10	853	6.2	11973.19	20.5	2.6	71.242	693.518	6.2	34.1
21.1	5	719	6	10486.74	22	2.8	68.528	787.562	5.5	35.8
21.1	1	572	3.3	7129.146	25.7	3.5	80.195	833.745	4.2	39.5
21.1	0.5	452	2.5	5970.626	29.5	3.8	75.778	877.603	4.3	41.9
21.1	0.1	374	1.2	3867.644	29.9	3.1	96.796	1100.378	4.9	43.9
37.8	25	346	8.3	6339.406	28.3	3.3	54.589	488.475	7.5	32.5
37.8	10	301	8.1	4622.637	28.9	3.4	65.073	771.436	5.5	35.5
37.8	5	250	6.8	3532.99	29.1	3.4	70.788	901.504	5.7	36.4
37.8	1	191	5	2069.342	28.9	4	92.266	938.628	5.4	39.5
37.8	0.5	158	3.9	1619.522	28.7	4.1	97.456	965.448	5.3	41.7
37.8	0.1	121	1.9	1053.422	25.1	4.2	114.477	1063.465	6.7	44.2
54.4	25	133	8.9	1857.111	30.2	6.8	71.848	427.409	7.4	41.4
54.4	10	101	7.8	1304.988	29.6	3.9	77.766	598.663	4.7	46.7
54.4	5	85	7.7	1047.298	28.1	4.3	81.07	667.274	5.5	49.9
54.4	1	63	6.1	670.269	24.4	4.5	94.247	682.742	5.4	55.1
54.4	0.5	48	5.1	556.319	22.9	5.3	86.379	688.518	6.4	56.9
54.4	0.1	42	3.3	423.373	18.9	5	99.525	736.055	8.9	60.9

Table B-41 Overall Dynamic Modulus test results at various test temperatures for Mix 13 Specimen 3

Temperature (°C)	Frequency (Hz)	Stress Amplitude (P-P) (KPa)	SE (%)	Dynamic Modulus (MPa)	Phase Angle (deg.)	UC (deg.)	Strain (P-P) Recoverable (microstrain)	Accumulated Strain (microstrain)	SE (%)	UC (%)
-10	25	1715	5.6	34640.16	12.5	11.3	49.504	68.46	9.7	31.5
-10	10	1757	5.4	33020.89	6.6	0.4	53.196	31.521	7.5	22.4
-10	5	1714	5.1	31993.66	6.6	0.1	53.561	32.996	7.7	23.5
-10	1	1538	2	28579.66	6	0.5	53.809	32.491	5	22.4
-10	0.5	1442	1.1	28299.84	7.8	0.6	50.951	33.883	9	22.5
-10	0.1	1313	0.5	25035.73	7.2	1.4	52.46	49.752	14.6	21
4.4	25	1300	5.9	26643.89	13.2	10.8	48.804	131.835	11.3	14.9
4.4	10	1259	6	23441.25	11.1	1	53.712	99.099	6.5	15.2
4.4	5	1184	5.8	21553.56	12.3	0.7	54.934	106.229	7.3	14.8
4.4	1	1041	2.6	17809.01	13.4	1.2	58.448	112.318	7.3	13.5
4.4	0.5	933	1.7	16087.93	17.2	0.9	57.97	124.723	4.6	12.9
4.4	0.1	885	0.7	12741.8	18.9	1.8	69.439	225.932	4.8	9.8
21.1	25	864	6.8	15283.12	21.6	7.4	56.562	591.551	8.4	9.7
21.1	10	786	6.6	12583.89	20.2	3	62.438	789.136	6.7	5.8
21.1	5	665	6.5	11006.2	21.6	2.9	60.405	906.633	6.8	6.5
21.1	1	526	3.6	7535.815	26.8	2.9	69.822	962.855	5.9	8.1
21.1	0.5	416	2.9	6393.541	25.5	4.9	65.088	1008.698	6.6	8.4
21.1	0.1	346	1.2	4142.357	28	3.7	83.614	1187.43	5.8	9.1
37.8	25	346	9.1	5638.37	28.3	4.9	61.426	410.997	7	15
37.8	10	298	8.5	4297.051	26.6	5.8	69.456	641.351	4.9	18.3
37.8	5	247	7.3	3329.054	26.7	6.1	74.209	753.861	5.1	22.4
37.8	1	191	5.2	2054.453	26.7	6.9	92.891	776.739	6.9	33.1
37.8	0.5	156	4.3	1625.76	26.4	7.4	96.06	799.755	7.7	38.5
37.8	0.1	119	2.4	1016.143	23.4	8.4	116.831	913.58	10.3	52
54.4	25	115	9.8	1881.347	34	10.8	60.867	387.819	8.5	34.8
54.4	10	85	9	1471.912	30.4	9.8	57.549	498.243	6.7	24.4
54.4	5	71	8.3	1217.296	29.2	10.8	58.516	548.063	5.6	23
54.4	1	53	7.4	751.85	26.5	12.9	71.015	560.983	8.3	40.5
54.4	0.5	41	6.4	605.758	25.6	14.3	67.696	558.931	9.1	49.5
54.4	0.1	35	4.9	451.093	20.5	12.6	77.384	600.953	11.2	63.1

Table B-42 Overall Dynamic Modulus test results at various test temperatures for Mix 14 Specimen 1

Temperature (°C)	Frequency (Hz)	Stress Amplitude (P-P) (KPa)	SE (%)	Dynamic Modulus (MPa)	Phase Angle (deg.)	UC (deg.)	Strain (P-P) Recoverable (microstrain)	Accumulated Strain (microstrain)	SE (%)	UC (%)
-10	25	2280	5	47857.91	5.3	11.2	47.637	77.764	22.2	44.3
-10	10	2319	4.5	52804.62	6	2.4	43.917	43.455	6.5	15.6
-10	5	2255	4.3	52182.55	6.4	2.3	43.223	42.301	6.2	14.9
-10	1	2018	1.4	47889.18	7.6	1.9	42.143	43.864	8.3	14.6
-10	0.5	1894	0.8	47178.09	9.2	2.1	40.139	44.947	10.6	16.3
-10	0.1	1729	0.5	41679.08	7.6	2.9	41.472	55.287	9.1	16.7
4.4	25	1909	5.6	50556.94	3.2	9.4	37.756	88.985	27.9	59.8
4.4	10	1858	5	39863.77	10.1	1	46.607	45.385	8.9	23.9
4.4	5	1744	4.7	36916.69	10.1	1	47.239	45.573	7.6	23.8
4.4	1	1533	1.7	30246.56	14.9	1.3	50.672	47.337	18.7	25.4
4.4	0.5	1375	1	30558.82	12	1.7	45.002	52.266	6.3	29.9
4.4	0.1	1303	0.5	22114.97	16.6	1.1	58.911	103.979	8.6	27.1
21.1	25	1291	5.7	19885.61	14.5	6	64.902	563.679	7.2	19.8
21.1	10	1184	5.5	17157.78	18.5	2.7	68.983	622.792	5.6	28.4
21.1	5	1009	5.4	15210.96	19.5	2.4	66.335	677.05	5.5	27.5
21.1	1	790	2.7	11032	23.9	2	71.617	693.159	6.2	26.4
21.1	0.5	625	2.1	9693.759	25	1.8	64.498	709.734	4.5	22.9
21.1	0.1	521	0.9	6787.682	26.6	1.8	76.784	834.802	5.2	21.7
37.8	25	563	6.8	9047.188	25.5	3.7	62.265	570.4	8.2	35.6
37.8	10	503	6.8	7108.25	24.7	4.7	70.773	796.937	6.7	37.2
37.8	5	408	7.1	5994.677	25.8	4.5	68.04	867.544	7.6	39.8
37.8	1	306	5.1	3731.871	27.1	5.1	81.934	886.909	7.4	45
37.8	0.5	254	3	2994.179	28.2	5	84.759	913.55	6.3	45.8
37.8	0.1	196	1.3	2408.03	24.3	2.8	81.422	999.761	7.7	26.2
54.4	25	177	9	3107.343	31.5	4.6	56.979	344.332	9.8	62.7
54.4	10	133	7.8	2367.122	27.9	4.8	56.216	416.476	7.7	60.6
54.4	5	111	7.7	1947.148	27.3	4.7	57.114	453.3	8.5	59.4
54.4	1	84	6.6	1228.597	27	4.4	68.057	468.321	8	64.6
54.4	0.5	63	4.8	1001.852	24.4	5.8	63.351	483.27	7.8	61.1
54.4	0.1	57	2.5	747.624	22.1	4.3	76.781	533.615	9.7	62.8

Table B-43 Overall Dynamic Modulus test results at various test temperatures for Mix 14 Specimen 2

Temperature (°C)	Frequency (Hz)	Stress Amplitude (P-P) (KPa)	SE (%)	Dynamic Modulus (MPa)	Phase Angle (deg.)	UC (deg.)	Strain (P-P) Recoverable (microstrain)	Accumulated Strain (microstrain)	SE (%)	UC (%)
-10	25	2281	4.9	56231.53	6.6	16.8	40.562	65.959	13.7	56.7
-10	10	2326	4.4	50045.31	6.2	0.7	46.473	29.21	6.9	30.9
-10	5	2263	4.5	48574.15	6	0.5	46.584	30.332	7.1	30.7
-10	1	2023	1.5	44057.53	5.8	1.5	45.917	33.225	7.2	31.7
-10	0.5	1897	0.8	43591.11	4.2	2.3	43.509	35.839	8.6	32.9
-10	0.1	1730	0.5	38020.71	8.9	0.6	45.493	50.974	7.8	33.4
4.4	25	1626	5.4	39953.28	2.6	23	40.69	79.354	14.3	37.8
4.4	10	1578	5.1	36476.82	9.3	1.1	43.262	47.435	8.7	29.5
4.4	5	1482	4.7	33861.98	10.2	0.5	43.773	45.762	8.3	29
4.4	1	1303	1.7	28502.57	13.6	0.5	45.699	45.419	13.8	30.2
4.4	0.5	1170	1	27822.55	13.1	1.5	42.039	47.641	6.5	32.6
4.4	0.1	1108	0.5	20897.22	15.7	1.7	53.007	95.49	6.3	33.4
21.1	25	1291	5.8	16977.31	15.4	5.6	76.033	445.718	7.1	35
21.1	10	1188	5.6	14498.82	19	1.3	81.916	415.831	6.7	34.7
21.1	5	1009	5.4	12832.77	20.3	1.4	78.65	431.699	5.8	35
21.1	1	790	2.6	9104.49	24.2	1.4	86.753	432.237	5.2	36.3
21.1	0.5	626	1.9	8252.42	25.1	1	75.813	437.838	5.3	38.8
21.1	0.1	522	1	5386.069	27.3	2.8	96.912	544.445	4.8	34.8
37.8	25	450	7.2	7682.78	28.1	3	58.613	396.491	7.8	41.1
37.8	10	401	7.8	5873.28	26.1	1	68.283	529.608	7.2	39.3
37.8	5	320	7.6	4826.917	26.9	1	66.326	576.746	7.1	38.9
37.8	1	247	4.3	2932.336	28.5	0.8	84.203	593.652	7	40.6
37.8	0.5	203	3.3	2415.271	28.5	1	84.021	612.213	7.4	41.8
37.8	0.1	157	1.5	1697.349	25.8	2.2	92.612	694.434	7.1	43.6
54.4	25	178	8.6	3115.589	28	5.3	57.028	446.761	9.8	46.5
54.4	10	134	7.7	2508.188	27.2	3.4	53.465	542.674	5.9	49.1
54.4	5	113	7.5	2047.405	26.3	2.9	55.167	574.424	6.4	52.1
54.4	1	84	6.3	1314.844	25	3.1	63.782	572.162	5.9	55
54.4	0.5	64	5	1080.146	23.4	4.5	58.984	583.813	6.5	55
54.4	0.1	58	2.7	822.611	19.7	3.5	70.048	627.048	7.8	57.3

Table B-44 Overall Dynamic Modulus test results at various test temperatures for Mix 14 Specimen 3

Temperature (°C)	Frequency (Hz)	Stress Amplitude (P-P) (KPa)	SE (%)	Dynamic Modulus (MPa)	Phase Angle (deg.)	UC (deg.)	Strain (P-P) Recoverable (microstrain)	Accumulated Strain (microstrain)	SE (%)	UC (%)
-10	25	2275	4.9	65625.27	16.4	10.4	34.672	-21.061	26.7	44.4
-10	10	2320	4.5	60890.79	6	1.2	38.105	4.316	7.1	14.5
-10	5	2253	4.3	59427.64	5	1.7	37.915	5.99	7.8	15.5
-10	1	2018	1.3	53069.64	4.1	2	38.019	3.892	13	15.3
-10	0.5	1893	0.7	51328.14	10.8	2.6	36.888	4.761	8.6	16.3
-10	0.1	1729	0.5	46710.28	7.6	1.7	37.021	12.979	9.1	18.5
4.4	25	2105	5.1	40587.47	13.7	7.2	51.87	17.084	18.9	29.4
4.4	10	2050	4.7	39781.86	9.9	1.5	51.534	25.65	6.4	23.6
4.4	5	1926	4.3	37629.47	10	2	51.183	28.597	7.7	24.9
4.4	1	1693	1.6	32344.71	10	2.7	52.353	27.871	13	27.3
4.4	0.5	1520	0.9	28592.58	16.6	2.3	53.151	33.203	5.1	26.3
4.4	0.1	1441	0.5	23246.31	15.8	2.3	61.973	80.968	6.1	28.4
21.1	25	1294	6.3	22161.47	15.8	7	58.369	306.305	15.7	38.5
21.1	10	1179	5.6	19152.42	17.5	1.3	61.559	303.289	7.2	33.6
21.1	5	1002	5.3	16956.13	18.8	1.5	59.074	326.997	8.1	34.1
21.1	1	790	2.8	12740.91	21.8	1.7	62.039	331.323	8.7	39.1
21.1	0.5	625	2.2	10857.75	21.6	3.5	57.602	341.357	6.3	42
21.1	0.1	521	0.9	7751.817	25.1	2.4	67.256	430.984	6	42.1
37.8	25	449	8.2	8534.216	12.9	11.1	52.628	413.224	23.4	57.1
37.8	10	399	8.6	7497.141	26.5	3	53.243	582.722	7.4	41.3
37.8	5	318	8.6	6440.616	27.3	3.3	49.393	639.947	9.8	45.3
37.8	1	246	5.3	3836.221	29.7	4.3	64.015	656.101	7.9	51.1
37.8	0.5	202	4.1	3148.057	27.2	1.9	64.321	672.387	8.3	55
37.8	0.1	156	1.5	2231.624	26.8	2.6	70.051	742.227	9.1	55.4
54.4	25	175	7.7	3161.995	26.5	7.1	55.485	407.573	10.8	53
54.4	10	132	7.1	2635.11	28.8	3.4	50.168	525.979	6.3	55.9
54.4	5	111	7.3	2142.699	28	3.1	51.628	572.271	5.7	55.7
54.4	1	83	6.2	1425.374	26	2.4	58.525	594.594	6.4	56.7
54.4	0.5	64	4.6	1171.758	25	2.5	54.447	609.818	5.5	58.5
54.4	0.1	58	1.9	892.608	21.1	2.2	64.982	653.577	8.8	55.2

Table B-45 Overall Dynamic Modulus test results at various test temperatures for Mix 15 Specimen 1

Temperature (°C)	Frequency (Hz)	Stress Amplitude (P-P) (KPa)	SE (%)	Dynamic Modulus (MPa)	Phase Angle (deg.)	UC (deg.)	Strain (P-P) Recoverable (microstrain)	Accumulated Strain (microstrain)	SE (%)	UC (%)
-10	25	2265	4.9	28501.47	7.5	5	79.453	191.638	6.5	6.7
-10	10	2313	4.6	28299.95	11.2	1.9	81.746	105.987	5.3	11.3
-10	5	2255	4.3	26307.93	11.1	2.2	85.731	114.505	4.9	12
-10	1	2021	1.4	22297.34	12.4	2.2	90.647	115.175	5	13.5
-10	0.5	1897	0.8	20726.15	14.8	1.9	91.543	122.396	4.4	14.6
-10	0.1	1729	0.5	17071.37	14.7	1.9	101.288	175.358	3.6	16.4
4.4	25	1264	5.8	17269.07	13.6	4	73.194	186.814	6.3	8.7
4.4	10	1222	5.7	15234.95	16.1	2.2	80.213	112.246	6.6	17.1
4.4	5	1149	5.2	13495.77	16.8	3	85.144	115.871	6.2	18.5
4.4	1	1016	2.3	10445.72	18.6	3.2	97.22	118.947	4.1	20.9
4.4	0.5	912	1.6	9256.073	18.7	3.5	98.567	130.473	4.2	22.1
4.4	0.1	861	0.7	7203.917	21.5	2.7	119.486	236.408	3.3	23.9
21.1	25	507	8	7653.918	20.7	7.6	66.226	160.385	8.5	25.5
21.1	10	454	7.9	6363.451	20.8	3.7	71.406	189.863	8	24.1
21.1	5	380	7.9	5545.272	21.3	3.5	68.509	187.555	6.8	25.5
21.1	1	304	5.2	3829.546	23.4	3.6	79.328	178.825	8.5	27.7
21.1	0.5	241	3.4	3212.709	22.6	4.8	75.012	175.879	6.2	28.6
21.1	0.1	199	1.7	2525.999	22.7	5	78.836	229.556	6.5	29.8
37.8	25	222	7.5	3094.28	23.2	6.2	71.635	289.72	6.9	20.7
37.8	10	197	6.6	2632.393	22.5	3.6	74.72	395.23	4.7	23.4
37.8	5	158	6.9	2274.216	22.2	3.8	69.556	401.037	4.9	22.9
37.8	1	121	5.2	1607.918	23.2	4.7	75.374	393.956	4.7	23.7
37.8	0.5	100	3.8	1409.638	23.2	4.2	71.099	397.5	4.4	21.7
37.8	0.1	77	1.6	1144.341	21.5	3.7	67.361	438.193	5	18.3
54.4	25	108	9.4	1697.177	21.4	5.4	63.603	312.72	9.4	26.9
54.4	10	82	7.4	1488.521	19.3	1.9	55.422	391.992	4.7	26.3
54.4	5	69	6.8	1355.047	18.1	1.3	50.759	411.704	4.5	24.5
54.4	1	52	6.3	1057.24	17.9	1	48.859	414.366	5.9	22.6
54.4	0.5	38	5.4	932.347	16.6	1.5	40.454	415.279	5.1	22.4
54.4	0.1	34	5.1	800.206	15.9	1.4	42.32	438.382	7	20.5

Table B-46 Overall Dynamic Modulus test results at various test temperatures for Mix 15 Specimen 2

Temperature (°C)	Frequency (Hz)	Stress Amplitude (P-P) (KPa)	SE (%)	Dynamic Modulus (MPa)	Phase Angle (deg.)	UC (deg.)	Strain (P-P) Recoverable (microstrain)	Accumulated Strain (microstrain)	SE (%)	UC (%)
-10	25	2270	5.3	37849.2	11.1	2.7	59.963	156.385	12.9	43.7
-10	10	2310	4.4	30093.85	11.6	2.1	76.762	24.885	5.9	16.8
-10	5	2258	4.5	28047.31	11.8	2.4	80.494	32.534	5.6	16.7
-10	1	2023	1.5	23649.84	12.5	2.9	85.539	36.577	5.1	21.2
-10	0.5	1897	0.9	21964.5	13.9	2.8	86.388	45.856	5.8	23.6
-10	0.1	1726	0.5	17781.22	14.8	2.7	97.057	97.901	4.7	26.1
4.4	25	1275	6	17280.66	11	12.4	73.755	191.537	10.9	23.1
4.4	10	1226	6.2	15785.28	16.5	3	77.68	128.193	6.2	16.9
4.4	5	1151	5.7	13956.78	17.3	2.9	82.443	134.946	6.1	17
4.4	1	1017	2.6	10780.38	18.7	2.9	94.364	140.247	4.3	20.7
4.4	0.5	912	1.8	9759.484	19.7	2.6	93.411	150.73	3.3	22.7
4.4	0.1	861	0.7	7667.418	19.9	2.1	112.34	241.509	3.4	23.4
21.1	25	507	7.9	7698.279	21.4	4.7	65.866	186.926	7.7	23.7
21.1	10	455	8.3	6810.985	20.5	3.2	66.812	232.372	6.8	20
21.1	5	380	8.7	6038.188	20.5	3.4	62.993	239.439	9.5	22.5
21.1	1	304	6	4072.074	22.3	2.7	74.715	233.995	7.1	27.1
21.1	0.5	243	3.8	3494.804	23	3.1	69.402	233.878	5.1	36.4
21.1	0.1	200	1.7	2655.032	21.9	3.4	75.481	281.215	5.4	39.4
37.8	25	223	8.3	2752.333	23.2	4.7	81.025	375.9	7.8	18
37.8	10	196	7.7	2424.614	22.8	1.1	80.871	507.573	5.4	22.8
37.8	5	158	7.9	2095.196	22.7	1.3	75.324	525.64	5.6	22.9
37.8	1	122	6.7	1429.156	23.9	1.7	85.016	525.152	6	23.2
37.8	0.5	100	5.1	1248.016	23.2	1.7	79.869	534.622	5.8	24.8
37.8	0.1	75	3	1028.465	21.8	1.7	73.068	583.722	5.2	27.4
54.4	25	109	9.5	1455.66	20	6.5	75.123	370.054	7.8	24.8
54.4	10	82	7.7	1312.607	19.7	2.5	62.167	451.943	6.4	36.2
54.4	5	70	7.8	1177.465	19.4	2.2	59.099	477.8	6.1	35.6
54.4	1	51	6.5	912.099	19.4	2.6	56.017	486.63	6.5	37.3
54.4	0.5	38	5.9	829.492	20	3.2	46.14	491.075	7	34.6
54.4	0.1	34	4.8	707.262	19.2	2.7	47.681	521.463	10.4	30

Table B-47 Overall Dynamic Modulus test results at various test temperatures for Mix 15 Specimen 3

Temperature (°C)	Frequency (Hz)	Stress Amplitude (P-P) (KPa)	SE (%)	Dynamic Modulus (MPa)	Phase Angle (deg.)	UC (deg.)	Strain (P-P) Recoverable (microstrain)	Accumulated Strain (microstrain)	SE (%)	UC (%)
-10	25	2264	5	33289.13	12	5.4	68.022	195.693	6.6	6.6
-10	10	2308	4.4	32118.32	12.4	2.4	71.873	134.68	5.6	13.6
-10	5	2254	4.4	29603.43	12.8	2.4	76.152	145.045	5.2	14.4
-10	1	2023	1.4	24358.65	14	3	83.039	149.523	3.6	16.1
-10	0.5	1896	0.8	22470.63	14.4	2.8	84.382	160.337	5.7	16.9
-10	0.1	1727	0.5	18293.31	16.6	2.7	94.382	215.534	4	19
4.4	25	1266	5.8	18297.33	17.8	3.1	69.215	217.955	6.4	14.8
4.4	10	1222	6.1	16361.54	17.9	2.6	74.664	170.68	6.1	17.6
4.4	5	1146	5.4	14522.12	18.5	2.6	78.929	186.236	5.2	17.4
4.4	1	1015	2.4	11114.71	20.7	2.6	91.343	194.318	3.7	19.1
4.4	0.5	912	1.6	9941.867	22.7	2.7	91.746	210.073	3.1	19.5
4.4	0.1	861	0.6	7523.771	22.9	1.9	114.394	326.072	3.4	20.5
21.1	25	505	8	6796.222	26.3	4.4	74.233	268.958	8.7	10.1
21.1	10	452	8.3	5607.734	25.9	1.4	80.692	339.659	6.8	9.1
21.1	5	379	8.2	4948.584	26.5	1.9	76.606	351.813	6.6	11.2
21.1	1	302	5.3	3372.683	28.4	2.1	89.526	344.928	7.5	10.2
21.1	0.5	240	3.4	2806.027	29.5	2.6	85.535	346.109	5.4	11.2
21.1	0.1	200	1.5	2239.327	28.6	2	89.183	421.751	6.2	13.6
37.8	25	222	8.7	2289.098	23.9	5.4	97.112	429.897	8.2	8.4
37.8	10	196	7.5	1965.073	22.9	1.9	99.82	584.224	5.6	12.1
37.8	5	157	7.3	1691.695	22.9	2	92.955	611.595	5.1	13.3
37.8	1	122	6	1174.391	24	2	103.748	614.019	5.4	12.4
37.8	0.5	98	4.2	1020.521	24	1.8	96.161	628.576	5.5	12.8
37.8	0.1	76	2.6	828.437	22.6	0.7	91.528	692.82	6.3	17.1
54.4	25	108	9.6	1186.803	20.9	14.4	91.4	298.962	7.2	20.6
54.4	10	81	7.5	1063.915	20.9	1.1	76.004	360.713	3.9	24.5
54.4	5	69	7.2	942.097	20.5	0.9	73.018	387.389	3.9	25.8
54.4	1	51	6.6	736.434	20.1	1.2	69.875	404.093	5.1	28.7
54.4	0.5	40	5.2	634.257	18.9	1.6	62.331	415.714	5	32.3
54.4	0.1	34	3.6	549.804	17.4	1.5	62.029	448.913	6.2	34.6

Table B-48 Overall Dynamic Modulus test results at various test temperatures for Mix 16 Specimen 1

Temperature (°C)	Frequency (Hz)	Stress Amplitude (P-P) (KPa)	SE (%)	Dynamic Modulus (MPa)	Phase Angle (deg.)	UC (deg.)	Strain (P-P) Recoverable (microstrain)	Accumulated Strain (microstrain)	SE (%)	UC (%)
-10	25	2284	5.4	62342.77	8.1	5.1	36.644	46.233	16	22.3
-10	10	2329	5.2	56646.85	6.8	1.7	41.106	15.867	8.7	6.6
-10	5	2271	4.9	54493.52	6.3	1.7	41.676	14.073	8.6	8
-10	1	2031	1.8	50848.38	6	1.7	39.951	13.663	8.4	4.9
-10	0.5	1900	1	46982.8	6	2.5	40.449	14.574	12.2	3.7
-10	0.1	1731	0.5	44308.52	9.1	1.9	39.073	21.275	14.4	3
4.4	25	1775	5.6	38382.81	13.4	4	46.254	57.877	10.3	16.5
4.4	10	1725	5.8	37835.29	11	3	45.582	17.542	10.9	12.2
4.4	5	1623	5.2	36943.51	10.4	3	43.921	16.872	8.2	13.7
4.4	1	1428	2.1	30872.23	11.9	2.9	46.266	15.969	7.3	13.2
4.4	0.5	1281	1.3	28390.55	10.3	4	45.107	17.721	6.4	12.5
4.4	0.1	1212	0.7	24493.71	13.8	3.8	49.466	38.905	7.2	16.3
21.1	25	1304	6.2	20360.42	18.1	1.1	64.061	245.957	8.9	13.7
21.1	10	1200	6.5	18480	17.3	2.6	64.958	200.294	8	18.4
21.1	5	1020	6	16394.13	17.6	2.4	62.239	210.666	7.6	21.7
21.1	1	804	3.3	12572.27	20	1.9	63.981	209.003	7.1	23.7
21.1	0.5	637	2.6	11021.49	21.9	2.5	57.784	213.778	5.9	25.7
21.1	0.1	529	1	8419.009	22.6	2.7	62.839	268.921	5.3	28.5
37.8	25	589	8.1	10122.31	21.8	3.4	58.191	444.19	10.1	23.1
37.8	10	529	8.8	8339.733	22.1	2.9	63.454	604.607	6.8	29.1
37.8	5	425	8.5	7235.206	21.2	2.8	58.689	657.397	6.7	32.3
37.8	1	323	6.5	4860.407	25.2	1.8	66.389	672.376	9.6	35.1
37.8	0.5	266	4.5	4113.189	22	4.2	64.603	691.047	6.6	39.1
37.8	0.1	205	1.8	2933.517	23.5	2.1	69.895	760.714	6.6	49.6
54.4	25	214	9.3	3864.823	18.9	10.8	55.285	349.019	10.8	46
54.4	10	165	9.5	3392.31	23	3.6	48.69	446.72	10.4	62.6
54.4	5	139	8.8	2906.487	24	2.1	47.827	476.712	8.7	66.4
54.4	1	103	6	1855.934	23.7	3.8	55.691	480.42	12	76.3
54.4	0.5	77	4.5	1452.414	25.4	3.5	53.133	486.467	7.9	76.2
54.4	0.1	71	2.7	1077.453	22.9	4.1	65.623	538.196	9	77.5

Table B-49 Overall Dynamic Modulus test results at various test temperatures for Mix 16 Specimen 2

Temperature (°C)	Frequency (Hz)	Stress Amplitude (P-P) (KPa)	SE (%)	Dynamic Modulus (MPa)	Phase Angle (deg.)	UC (deg.)	Strain (P-P) Recoverable (microstrain)	Accumulated Strain (microstrain)	SE (%)	UC (%)
-10	25	2282	5.6	57304.09	14.2	7.9	39.818	25.442	32.3	26.8
-10	10	2314	4.9	53862.29	6.5	2.3	42.956	5.408	7.4	28.5
-10	5	2248	4.5	52396.14	6.2	2.4	42.899	6.651	6.8	29.6
-10	1	2019	1.6	47185.61	8	2.1	42.778	4.286	8.8	28.6
-10	0.5	1893	0.9	44905.67	5.2	3.4	42.163	4.763	9.5	26.9
-10	0.1	1727	0.5	41430.11	6.9	1.7	41.695	9.356	9.9	29.6
4.4	25	1751	6	46478.93	1.7	22.8	37.666	23.843	31	58.7
4.4	10	1717	5.9	36112.5	8.8	0.9	47.555	12.419	7.5	23.1
4.4	5	1613	5.3	34358.68	8.2	1.3	46.936	12.394	8.2	24.1
4.4	1	1422	2.1	29332.85	9.5	1.6	48.463	11.069	7.4	25.2
4.4	0.5	1278	1.3	28847.23	10.5	1.5	44.286	13.154	6.9	29.9
4.4	0.1	1208	0.6	22891.58	13.6	1.1	52.762	39.998	9.3	27.1
21.1	25	1302	6.6	22719.41	11.5	17	57.328	323.93	16	47.5
21.1	10	1191	6.6	17912.91	16	2.2	66.473	281.68	7	24
21.1	5	1009	5.9	16045.91	16.6	2.6	62.897	289.476	6.4	26.2
21.1	1	799	3	11787.67	18.7	4	67.749	287.415	5.7	30.4
21.1	0.5	633	2.2	10278.85	19.9	3.4	61.553	288.359	3.9	31.7
21.1	0.1	525	1	7767.575	23.1	2.3	67.637	346.934	7	35.5
37.8	25	585	7.7	9876.513	12.7	12.6	59.21	483.298	13.1	37.2
37.8	10	520	8.1	8096.854	21.4	2.5	64.268	668.013	7.7	23.1
37.8	5	421	8.2	7053.337	22.1	2.5	59.638	714.243	7.3	27.8
37.8	1	320	5.2	4695.865	23.9	3.4	68.106	716.813	7.5	32.6
37.8	0.5	263	3.2	3870.72	24.9	2.6	68.039	723.408	8.1	35
37.8	0.1	200	1.6	2720.325	22.8	3.1	73.598	775.39	8.4	40.2
54.4	25	214	9.3	4475.969	19.5	12.3	47.783	412.723	9.6	38.4
54.4	10	164	7.6	3620.36	22.6	0.9	45.377	517.553	5.8	28.3
54.4	5	138	8.2	3057.176	22.2	0.8	45.291	555.237	5.4	27.5
54.4	1	105	6	2064.929	23.4	0.9	50.836	561.967	10	30.2
54.4	0.5	78	4.1	1689.916	24.3	2.3	46.073	566.863	7.4	27.1
54.4	0.1	70	3.2	1316.528	19.2	0.9	53.28	604.773	10.1	25.6

Table B-50 Overall Dynamic Modulus test results at various test temperatures for Mix 16 Specimen 3

Temperature (°C)	Frequency (Hz)	Stress Amplitude (P-P) (KPa)	SE (%)	Dynamic Modulus (MPa)	Phase Angle (deg.)	UC (deg.)	Strain (P-P) Recoverable (microstrain)	Accumulated Strain (microstrain)	SE (%)	UC (%)
-10	25	2285	5.7	58786.97	24.5	11.8	38.868	-169.699	73.6	47.9
-10	10	2318	4.4	54245	7.2	1	42.733	6.09	13.8	21.2
-10	5	2268	4.8	52667.63	7.7	0.5	43.061	4.261	10	20.7
-10	1	2029	1.7	50994	7.3	1.8	39.78	5.01	8.6	22.6
-10	0.5	1900	1	49786.98	5.5	2.6	38.165	5.047	15.7	25
-10	0.1	1728	0.5	42368.51	7.6	2.9	40.788	15.79	10.8	22.6
4.4	25	1786	6.4	42546.7	4.8	27.2	41.977	80.554	27.6	60.6
4.4	10	1722	5.3	34298.84	11.4	2	50.199	28.054	7.2	19.4
4.4	5	1619	5.1	32163.25	10.6	2.8	50.349	28.389	9.2	21.8
4.4	1	1425	2	26708.15	12.8	2.9	53.347	29.278	6.3	25.4
4.4	0.5	1279	1.2	23777.78	11.6	3.9	53.797	33.712	5.1	25.5
4.4	0.1	1208	0.6	19811.47	16.2	2.5	60.974	74.377	6.7	30.5
21.1	25	1315	6.3	17628.36	20.3	12.8	74.578	580.407	12.5	34.4
21.1	10	1197	6.2	12684.25	22	5.5	94.347	559.058	6.3	18.7
21.1	5	1018	6	11053.64	23	5.2	92.082	589.843	6.7	20.3
21.1	1	802	2.9	7748.002	26.2	5.2	103.554	591.496	4.9	25.1
21.1	0.5	634	2.2	6749.01	25.8	6.6	93.934	599.015	5.6	26.8
21.1	0.1	526	1	5020.957	27.4	5.7	104.752	711.274	6.2	27.4
37.8	25	589	7.6	6407.768	20.3	10.4	91.859	753.83	7.8	37
37.8	10	527	8	5469.541	25.1	5.6	96.27	1001.964	5.8	32.4
37.8	5	423	7.9	4597.413	25.7	5.9	91.901	1081.008	6	32.5
37.8	1	322	5.1	2949.828	27.2	6.5	109.25	1101.442	6.7	32.1
37.8	0.5	263	3.1	2406.109	27.1	6.4	109.346	1124.658	6.2	33
37.8	0.1	201	1.5	1748.423	25.3	6.5	115.206	1203.138	6.9	37.2
54.4	25	214	9.4	2947.01	27.2	14.5	72.725	400.19	11.2	46.1
54.4	10	164	9	2463.566	24.7	3.3	66.543	490.903	5.9	47
54.4	5	138	8.7	2135.927	23.9	2.7	64.682	523.34	9.2	50.6
54.4	1	104	5.9	1448.264	22.6	3.9	72.048	532.817	9	53.4
54.4	0.5	77	4.4	1196.105	23.5	2.9	64.624	538.922	6.2	52.8
54.4	0.1	70	2.9	962.248	19.8	2.7	72.68	581.589	8.3	48.3

Table B-51 Overall Dynamic Modulus test results at various test temperatures for Mix 17 Specimen 1

Temperature (°C)	Frequency (Hz)	Stress Amplitude (P-P) (KPa)	SE (%)	Dynamic Modulus (MPa)	Phase Angle (deg.)	UC (deg.)	Strain (P-P) Recoverable (microstrain)	Accumulated Strain (microstrain)	SE (%)	UC (%)
-10	25	2256	5.9	58550.22	38.8	32	38.533	-69.942	55.8	38.9
-10	10	2310	4.4	66406.73	4.7	1.1	34.79	0.46	10.2	33.4
-10	5	2255	4.4	66731.07	3.9	1.1	33.799	-0.871	9.6	32.9
-10	1	2024	1.5	66874.88	4.3	1.4	30.263	0.919	14.1	38.2
-10	0.5	1895	0.8	67030.19	4.8	1.4	28.278	0.895	14.7	40.7
-10	0.1	1727	0.5	59593.38	7	3.3	28.973	3.033	19.3	35.7
4.4	25	1781	5.7	61792.88	26.2	17.8	28.819	46.212	41.1	79.9
4.4	10	1723	5	47149.26	7.8	3.1	36.552	16.161	6.8	36.2
4.4	5	1620	4.7	44173.01	8.7	2.8	36.67	14.911	7	36.1
4.4	1	1424	1.9	39497.95	10.7	2.4	36.065	14.304	8.8	41
4.4	0.5	1279	1.1	37864.69	14.9	1.7	33.774	15.899	6.9	43
4.4	0.1	1210	0.5	32045.63	11.7	2.9	37.77	31.137	9.3	44.7
21.1	25	1824	5.3	25980.13	8.8	10.4	70.197	324.78	7.3	12
21.1	10	1675	4.9	22607.78	14.9	3.2	74.085	265.562	6.2	17.3
21.1	5	1425	4.7	20578.1	15.7	3.1	69.23	268.024	6	17
21.1	1	1119	2	15989.99	19.3	3.9	69.955	265.315	5.5	19.2
21.1	0.5	888	1.4	14104.73	19.2	5.2	62.949	277.65	4	19.5
21.1	0.1	739	0.7	10806.83	24.9	2.8	68.359	366.127	5.6	17
37.8	25	988	6.3	11232.14	24.6	2.9	87.946	767.844	7.2	25.3
37.8	10	893	6	9787.58	23.9	1	91.233	943.386	5.3	39.9
37.8	5	724	5.7	8284.546	24.6	1.7	87.45	1069.269	4.6	42.4
37.8	1	548	3.1	5318.96	28.7	1.6	103.05	1123.353	3.8	44.3
37.8	0.5	452	2.4	4277.931	29.9	1.8	105.582	1182.828	4.1	45.3
37.8	0.1	347	1	2562.33	29.6	1.6	135.371	1395.034	5.6	46.4
54.4	25	215	8.4	5599.277	33.5	1.4	38.381	577.007	9	36.3
54.4	10	164	7	3983.638	31.9	1.4	41.279	761.14	4.5	38.8
54.4	5	139	6.8	3076.234	31.4	2	45.224	853.781	5.9	38.7
54.4	1	104	4.8	1766.858	30.1	3.1	58.914	887.793	5.3	39.3
54.4	0.5	76	3.8	1399.567	28.5	3.4	53.979	904.202	4.9	35.6
54.4	0.1	70	2.9	976.025	22.9	4	71.894	998.285	8.4	35.1

Table B-52 Overall Dynamic Modulus test results at various test temperatures for Mix 17 Specimen 2

Temperature (°C)	Frequency (Hz)	Stress Amplitude (P-P) (KPa)	SE (%)	Dynamic Modulus (MPa)	Phase Angle (deg.)	UC (deg.)	Strain (P-P) Recoverable (microstrain)	Accumulated Strain (microstrain)	SE (%)	UC (%)
-10	25	2282	5.5	60693.05	10.9	14.6	37.604	17.629	39.8	51.9
-10	10	2313	4.5	52782.9	3.4	0.1	43.829	-6.255	6.4	19.5
-10	5	2256	4.3	52065.28	3.7	0.3	43.329	2.515	6.6	19.2
-10	1	2017	1.3	49098.8	5.8	1.6	41.078	1.063	6.2	19.7
-10	0.5	1892	0.8	49302.85	7.4	2	38.377	0.863	9.2	21.6
-10	0.1	1729	0.6	44331.21	4.2	0.8	39.005	8.794	10.4	19.8
4.4	25	1779	5.6	57426.63	15.8	17.3	30.971	49.009	23.8	57.1
4.4	10	1724	5.3	41197.97	6.6	0.4	41.848	14.144	10.4	10.3
4.4	5	1625	5	41078.39	7.2	0.4	39.55	14.219	8.9	11.5
4.4	1	1427	2.1	35871.47	8.3	1.7	39.775	13.777	11.2	12
4.4	0.5	1279	1.3	32453.27	8.6	0.9	39.41	15.591	11.5	12
4.4	0.1	1210	0.5	29615.32	10	0.6	40.862	34.629	11	13.1
21.1	25	1816	5.3	25435.43	1.7	10.4	71.395	437.083	9.6	49
21.1	10	1669	5.1	19279.5	14.2	1.5	86.553	390.063	5.9	34.2
21.1	5	1417	4.6	17358.41	15.4	1.3	81.608	418.283	7.1	33.5
21.1	1	1116	2	13585.55	19	1.4	82.17	427.833	5.7	36.9
21.1	0.5	887	1.4	12031.73	18.6	2.8	73.711	443.803	3.6	36
21.1	0.1	738	0.6	8796.901	24.1	1.7	83.876	577.421	4.3	35.6
37.8	25	582	7.3	9973.874	15.5	14.2	58.391	368.222	9.9	47.8
37.8	10	524	7.1	8697.585	23.9	2.4	60.235	491.508	6.4	37.1
37.8	5	423	7.2	7256.487	25.6	2.4	58.336	537.451	6.6	37.8
37.8	1	321	5.1	4341.847	29	3.2	73.823	552.697	5.5	42.9
37.8	0.5	265	3	3322.305	30	3.6	79.726	580.281	5.1	44.6
37.8	0.1	204	1.3	1982.011	29	4.7	103.132	715.838	6.8	47.6
54.4	25	218	9.1	3952.812	22.2	26	55.17	511.263	10.1	52.2
54.4	10	168	8	3032.674	32.1	4.7	55.45	675.46	6.9	46.2
54.4	5	141	8	2296.293	32	4.9	61.396	755.337	7.7	48.1
54.4	1	105	6.7	1225.621	31.3	5.4	85.845	802.632	11.2	50.2
54.4	0.5	79	5.3	909.845	31.1	5.4	87.234	829.732	6.1	57.1
54.4	0.1	73	2.4	623.905	25.1	4.9	117.72	957.869	11.5	55.5

Table B-53 Overall Dynamic Modulus test results at various test temperatures for Mix 17 Specimen 3

Temperature (°C)	Frequency (Hz)	Stress Amplitude (P-P) (KPa)	SE (%)	Dynamic Modulus (MPa)	Phase Angle (deg.)	UC (deg.)	Strain (P-P) Recoverable (microstrain)	Accumulated Strain (microstrain)	SE (%)	UC (%)
-10	25	2273	4.9	58070.86	19.9	16.1	39.139	40.768	17	6.2
-10	10	2308	4.4	65785.08	3.9	0.3	35.086	13.735	7.9	9.4
-10	5	2249	4.5	64610.82	2.2	0.4	34.808	14.642	9.6	9.1
-10	1	2019	1.3	61701.02	1.2	0.8	32.726	13.067	7.8	9.6
-10	0.5	1895	0.8	58023.17	5.4	0.6	32.668	15.987	8.2	10.7
-10	0.1	1727	0.4	56492.7	4.5	1.1	30.578	18.025	11.5	11
4.4	25	1767	5.4	50369.63	24.1	20	35.076	42.746	23.2	11.4
4.4	10	1717	5	54043.19	6.1	0.4	31.762	16.299	10.3	7.7
4.4	5	1614	4.9	51321.77	6.4	1	31.451	16.063	9.9	8.8
4.4	1	1423	1.7	45207.13	6.3	1.2	31.481	15.342	11.8	9.8
4.4	0.5	1277	1.1	41648.24	5.3	1.5	30.671	15.476	10.6	9.8
4.4	0.1	1207	0.5	38754.67	8.9	2.1	31.15	25.365	11.8	11
21.1	25	1818	5.2	29803.82	8.1	4.7	61.008	281.333	6.9	7.5
21.1	10	1667	5	30903.82	12.4	0.6	53.933	257.407	6.4	7.7
21.1	5	1419	4.9	27888.18	13.8	0.6	50.895	275.479	6.9	10.3
21.1	1	1118	2	22373.57	18.6	1.2	49.962	280.358	9	10.7
21.1	0.5	887	1.5	20433.48	15.8	0.3	43.405	287.92	6	11.2
21.1	0.1	739	0.7	14982.74	22.4	0.9	49.312	358.053	7.1	14.3
37.8	25	582	7.4	18769.12	18.9	4	30.995	378.418	10	26.5
37.8	10	518	7	15580.43	20	0.5	33.231	564.651	6.6	28.2
37.8	5	418	7.2	13254.87	20.8	0.7	31.557	650.575	6.9	29
37.8	1	319	4.8	8991.238	25.4	0.7	35.478	688.887	8.2	30.3
37.8	0.5	261	2.7	6940.923	27.4	0.7	37.607	728.944	4.8	32.7
37.8	0.1	202	1.3	4276.668	29.1	0.9	47.182	842.432	3.7	35.1
54.4	25	211	7.6	6487.339	31.6	0.3	32.561	525.993	8.9	44.7
54.4	10	162	7.4	4567.424	30.4	1	35.499	746.886	7.1	49.7
54.4	5	138	6.9	3549.342	30.1	1.4	38.78	867.285	6.5	48.8
54.4	1	105	4.9	2038.968	29.6	1.9	51.561	933.13	5.6	49.8
54.4	0.5	79	3.1	1699.877	28.5	3.2	46.4	973.959	4.5	46.5
54.4	0.1	72	1.6	1230.265	25.2	3.8	58.132	1096.049	5.2	30.5

Table B-54 Overall Dynamic Modulus test results at various test temperatures for Mix 18 Specimen 1

Temperature (°C)	Frequency (Hz)	Stress Amplitude (P-P) (KPa)	SE (%)	Dynamic Modulus (MPa)	Phase Angle (deg.)	UC (deg.)	Strain (P-P) Recoverable (microstrain)	Accumulated Strain (microstrain)	SE (%)	UC (%)
-10	25	2036	6.1	29232.64	22.2	18.3	69.634	99.176	27.8	37.3
-10	10	2083	5.3	28398.76	6.2	1.6	73.337	41.359	12.8	48.6
-10	5	2025	4.7	27386.22	6	1.6	73.927	42.064	9.7	47
-10	1	1820	1.6	24419.96	8.3	0.8	74.515	45.827	13.1	43.6
-10	0.5	1708	0.9	24061.7	5	1.8	70.992	48.656	9.3	44.2
-10	0.1	1556	0.5	22048.05	9	0.3	70.563	67.842	9.3	45.6
4.4	25	1406	5.9	25239.58	3.6	8.9	55.718	84.771	16.6	21.2
4.4	10	1350	5.8	21575.43	9.3	1	62.593	45.118	8.3	27.5
4.4	5	1268	5	20628.86	9.6	0.9	61.487	46.714	6.7	27.8
4.4	1	1124	2	17995.49	9.9	1.5	62.463	43.378	9.7	28.2
4.4	0.5	1010	1.3	16044.23	12.5	0.6	62.948	51.477	3.8	26
4.4	0.1	956	0.5	13725.64	14.5	0.7	69.677	101.597	4.6	29
21.1	25	789	6.8	13738.11	7.8	6.6	57.443	271.7	12.3	42.5
21.1	10	712	6.5	12614.23	15.9	1.6	56.458	356.977	7.8	34.2
21.1	5	600	6	11625.8	16.6	1.8	51.63	396.713	7.7	38.2
21.1	1	479	3.3	8418.121	19.4	1.8	56.873	412.609	7	38.6
21.1	0.5	379	2.6	7350.393	23.2	1.4	51.606	426.868	6	41.8
21.1	0.1	316	1.2	5127.608	25.6	1.5	61.717	543.519	7.8	41.8
37.8	25	356	8.3	5529.083	23.6	3	64.454	495.406	8.3	25.2
37.8	10	310	8.2	4416.507	26.3	3.6	70.093	733.479	5.9	29.2
37.8	5	256	6.2	3495.281	27.4	3.6	73.163	833.963	6.2	30.7
37.8	1	193	4.2	2144.187	29	3.9	89.972	866.712	5	36.6
37.8	0.5	162	3.1	1736.92	29.6	3.6	93.07	903.107	5.6	36.7
37.8	0.1	124	1.8	1130.8	27.5	3	109.512	1029.353	7.1	36.7
54.4	25	139	8.2	2572.633	30.5	5.1	54.045	483.316	8.1	29
54.4	10	106	7.3	1854.346	32.5	4.1	57.181	629.832	7.4	38.2
54.4	5	91	6.6	1499.371	31.8	4	60.463	725.307	7.9	38.2
54.4	1	68	5	921.711	30.4	3.9	73.628	774.616	9.9	35.8
54.4	0.5	50	3.6	718.535	29.4	6	70.151	802.385	9.2	36.4
54.4	0.1	46	2.1	606.536	23.4	3.5	76.465	879.295	13.8	30.9

Table B-55 Overall Dynamic Modulus test results at various test temperatures for Mix 18 Specimen 2

Temperature (°C)	Frequency (Hz)	Stress Amplitude (P-P) (KPa)	SE (%)	Dynamic Modulus (MPa)	Phase Angle (deg.)	UC (deg.)	Strain (P-P) Recoverable (microstrain)	Accumulated Strain (microstrain)	SE (%)	UC (%)
-10	25	2042	4.8	50261.88	2.5	7.1	40.625	75.62	9	15.7
-10	10	2077	4.5	49458.26	5.8	1.1	42	42.706	6.4	9.7
-10	5	2023	4.4	47807.76	5.7	1	42.325	43.7	6.5	8.8
-10	1	1817	1.3	42125.11	7.2	1.3	43.131	46.461	10.1	9.8
-10	0.5	1707	0.8	42803.32	3.2	1.9	39.875	48.883	7.4	10.5
-10	0.1	1556	0.5	38336.47	8.3	0.9	40.575	61.871	8.2	11.4
4.4	25	1406	5.3	37427.72	0.6	8.3	37.554	62.731	8.6	10.1
4.4	10	1350	5.4	37574.24	8.4	1.3	35.923	34.789	7.3	9.4
4.4	5	1268	4.9	35215.56	9.2	1.3	36.005	35.173	6.9	9.5
4.4	1	1122	1.9	30908.04	10.9	1	36.301	35.235	6.6	10.5
4.4	0.5	1007	1.3	28916.04	14.8	1.8	34.836	37.877	8.2	11.5
4.4	0.1	954	0.5	22922.83	15.1	1.1	41.604	72.336	6.4	11.3
21.1	25	1022	6	18001.2	16.3	7.9	56.754	467.723	8.3	23.2
21.1	10	929	5.9	15009.74	20.7	5.1	61.918	534.993	7.8	26.8
21.1	5	784	5.3	13474.04	21.5	5.5	58.161	594.491	7.1	27.9
21.1	1	623	2.8	9431.195	26.5	4.6	66.038	623.22	5.6	28.5
21.1	0.5	493	2	8400.214	27.4	5.5	58.647	649.576	6.6	26.1
21.1	0.1	411	1	6089.21	30.2	5.7	67.485	803.348	6.1	20.1
37.8	25	359	7.7	8574.387	33.6	5.9	41.816	719.488	9.2	35
37.8	10	314	7.4	6950.602	27.1	2.4	45.107	1026.773	6.8	36.5
37.8	5	258	5.6	5424.323	28.2	2.1	47.652	1173.25	7.1	35.9
37.8	1	194	4.1	3156.388	33.9	5.6	61.321	1236.496	6	26.5
37.8	0.5	163	3.1	2509.56	34.3	5.5	64.958	1293.27	6.2	26.6
37.8	0.1	126	1.3	1597.778	30.8	4.1	78.593	1424.722	6.5	25.2
54.4	25	139	7.8	2607.368	34.3	3.2	53.187	648.171	8.5	37.5
54.4	10	106	7.4	1862.58	30.9	2.9	56.794	859.353	6.9	32.7
54.4	5	91	6.4	1484.216	28.6	3.3	61.188	968.429	4.7	33.3
54.4	1	68	5	952.894	25.6	3.6	71.361	993.253	5	34.5
54.4	0.5	50	3.3	780.793	24.3	3.4	63.651	1003.63	5.6	35.9
54.4	0.1	45	2.4	586.226	20.2	3.2	77.493	1064.799	7.5	32.9

Table B-56 Overall Dynamic Modulus test results at various test temperatures for Mix 18 Specimen 3

Temperature (°C)	Frequency (Hz)	Stress Amplitude (P-P) (KPa)	SE (%)	Dynamic Modulus (MPa)	Phase Angle (deg.)	UC (deg.)	Strain (P-P) Recoverable (microstrain)	Accumulated Strain (microstrain)	SE (%)	UC (%)
-10	25	2045	5.4	45669.42	6.3	11.4	44.771	73.184	32.7	44.4
-10	10	2080	4.8	49658.09	5.8	1.7	41.894	38.837	6.5	18
-10	5	2025	4.6	48219.5	5	2.4	42.001	38.952	7.4	19.1
-10	1	1821	1.6	43973.9	6.8	2.4	41.41	40.427	10.1	22
-10	0.5	1707	1	44104.45	8.8	2.2	38.693	41.023	10.4	24.9
-10	0.1	1554	0.5	39036.74	5.7	3.1	39.815	49.409	14.4	26.5
4.4	25	1405	6.4	36040.72	7.9	12.2	38.974	64.492	43.6	52.8
4.4	10	1349	5.7	36423.68	8.1	1.7	37.039	35.163	11.7	23.9
4.4	5	1268	5.2	34158.29	8	2.4	37.128	35.937	10.1	25.8
4.4	1	1124	2.2	28718.31	11.4	1.6	39.13	37.411	13.4	27.7
4.4	0.5	1010	1.4	25983.87	10.1	2.7	38.877	43.053	9.1	29.8
4.4	0.1	955	0.5	22108.8	14.6	2.3	43.212	80.518	8.9	32.6
21.1	25	1030	6.9	21160.37	15.4	11.7	48.689	363.408	27.8	41.3
21.1	10	935	6.3	18548.5	17.1	1.7	50.433	383.301	6.9	21.8
21.1	5	792	6.1	16442.06	18.1	2.1	48.143	407.474	6.4	24.7
21.1	1	625	3.4	11593.34	21.4	2.5	53.88	414.433	7.3	28.4
21.1	0.5	496	2.5	9913.376	22.6	2.6	50.01	425.845	5.1	32.5
21.1	0.1	412	1.1	6753.272	27.1	2.2	61.024	521.792	5.9	35.3
37.8	25	360	9.5	10369.92	12.3	17.4	34.704	456.537	13.5	41.2
37.8	10	316	9.2	8203.706	24.6	1.4	38.46	639.936	6.9	28.1
37.8	5	260	7.6	5967.746	27.6	3.5	43.51	725.362	7	33.9
37.8	1	195	5.7	3620.502	29.7	4.9	53.764	747.373	7.7	29.7
37.8	0.5	165	4.6	2966.184	29.4	6.3	55.505	768.205	6.8	27.8
37.8	0.1	126	2	2126.801	24.4	4.1	59.356	827.496	8.2	10.6
54.4	25	140	10.3	3153.821	37.9	4.7	44.303	452.486	12.3	45.6
54.4	10	109	9.6	2345.264	32.6	7.9	46.656	564.137	7.8	35.2
54.4	5	92	8.8	1913.894	31.1	8.6	48.067	621.709	7	31.7
54.4	1	68	7.4	1160.662	29.1	9.1	58.796	638.1	9.2	29.3
54.4	0.5	51	5.8	967.964	27.4	10.3	52.759	643.32	7.5	30.7
54.4	0.1	46	2.7	695.321	23.7	9.7	66.285	695.825	8.1	32.9

Table B-57 Overall Dynamic Modulus test results at various test temperatures for Mix 19 Specimen 1

Temperature (°C)	Frequency (Hz)	Stress Amplitude (P-P) (KPa)	SE (%)	Dynamic Modulus (MPa)	Phase Angle (deg.)	UC (deg.)	Strain (P-P) Recoverable (microstrain)	Accumulated Strain (microstrain)	SE (%)	UC (%)
-10	25	2037	5	53006.39	5.1	9	38.426	88.262	17.8	29.3
-10	10	2068	4.3	44462.52	7.1	1.9	46.507	49.729	6.5	8.6
-10	5	2012	4.1	43105.32	6.8	1.8	46.681	49.033	7.2	9.2
-10	1	1811	1.3	39871.25	6.7	2.5	45.431	50.109	8.2	10.3
-10	0.5	1702	0.8	36507.99	9.1	2.1	46.612	50.684	8.4	11.8
-10	0.1	1553	0.5	34339.49	9.3	1.8	45.227	59.37	7.8	10.8
4.4	25	1396	5.6	32232.96	1.8	19.6	43.306	89.768	15.6	19.7
4.4	10	1345	4.8	30305.13	11	2.6	44.37	56.548	9.7	23.9
4.4	5	1260	4.2	27605.97	11.5	2.5	45.65	60.7	9	24.9
4.4	1	1119	1.7	22971.17	15.1	2.8	48.719	62.984	11.9	27.5
4.4	0.5	1006	1.1	22087.53	15.8	3.5	45.534	69.094	11.3	28.1
4.4	0.1	950	0.6	16920.17	19.2	1.8	56.14	132.13	5.2	25.2
21.1	25	1016	5.4	14175.32	24.1	3.5	71.683	709.312	7.9	15.2
21.1	10	922	4.7	12479.03	24.6	3	73.92	863.462	6	17.2
21.1	5	783	4.5	11575.53	26	4.3	67.66	981.611	6.6	14.8
21.1	1	620	2.4	8448.248	30.9	4.3	73.358	1051.227	6	14.4
21.1	0.5	491	1.8	7600.584	29.4	4.1	64.651	1108.638	5.5	16.3
21.1	0.1	408	1	4362.874	33.8	4.4	93.569	1295.351	5.3	18.9
37.8	25	356	7.5	7558.957	31.3	0.9	47.075	347.604	7.2	23.9
37.8	10	309	7.3	5247.326	32.6	5.9	58.877	551.511	6.9	23.6
37.8	5	255	5.4	4030.422	33	6.3	63.204	649.558	6.6	23.3
37.8	1	193	4	2526.307	30.8	4.2	76.415	678.147	6.1	21.9
37.8	0.5	161	2.8	2110.264	29.2	3.3	76.434	694.84	5.8	19.7
37.8	0.1	124	1.4	1506.109	23.6	2.5	82.271	738.964	6.3	15.3
54.4	25	139	7.9	2278.64	34.7	8.9	61.173	345.559	9.8	65.6
54.4	10	105	6.4	1677.021	32.2	6.6	62.775	436.608	5.9	56.2
54.4	5	89	6.2	1444.633	30.5	6.8	61.841	491.157	6.2	48.9
54.4	1	67	4.9	1162.65	23.7	2.5	58.038	498.573	6.2	24.5
54.4	0.5	50	3.8	985.391	21.8	1.3	50.943	490.362	6.6	17.9
54.4	0.1	46	2.2	737.583	18.1	3.4	62.385	507.779	7.2	22.5

Table B-58 Overall Dynamic Modulus test results at various test temperatures for Mix 19 Specimen 2

Temperature (°C)	Frequency (Hz)	Stress Amplitude (P-P) (KPa)	SE (%)	Dynamic Modulus (MPa)	Phase Angle (deg.)	UC (deg.)	Strain (P-P) Recoverable (microstrain)	Accumulated Strain (microstrain)	SE (%)	UC (%)
-10	25	2034	4.8	33406.71	0.3	7.9	60.892	70.467	8	30.5
-10	10	2070	4.4	35986.89	6.2	0.9	57.508	24.333	6.5	28.4
-10	5	2012	3.9	34836.96	5.8	0.9	57.76	22.012	5.2	28.2
-10	1	1813	1.2	31228.55	6.5	0.8	58.058	22.589	5.4	28.6
-10	0.5	1704	0.7	31020.34	4.5	1.9	54.917	23.72	8.1	30.5
-10	0.1	1556	0.4	27644.98	8.1	0.7	56.282	39.06	5.3	30.8
4.4	25	1396	5.2	25218.43	7.1	3.6	55.351	100.942	6.2	26
4.4	10	1344	4.6	25871.53	10	0.7	51.962	59.226	5.8	26.4
4.4	5	1261	3.8	23990.78	10.8	0.4	52.543	61.52	5.1	26.1
4.4	1	1119	1.4	20249.24	12.7	0.3	55.255	64.573	4.8	27.5
4.4	0.5	1008	0.9	18685.68	11.3	1.6	53.946	71.62	4.7	28.2
4.4	0.1	955	0.5	14705.42	16.4	0.4	64.935	131.859	5.3	26.9
21.1	25	1021	5.7	13800.11	18.7	1.7	73.963	597.769	6.5	24.9
21.1	10	929	4.9	11864.18	20.1	1.3	78.305	707.674	4.9	24.1
21.1	5	787	4.6	10437.89	21.7	1.8	75.41	796.249	4.1	24.4
21.1	1	622	2.4	7332.655	25.3	2.2	84.793	843.237	3.4	24.9
21.1	0.5	494	1.9	6269.282	28.6	3	78.752	886.862	3.3	25.7
21.1	0.1	411	1	4042.431	29.4	2.4	101.755	1089.03	4.2	25.6
37.8	25	358	8.2	6207.433	29.7	1.8	57.647	487.853	7.7	32.7
37.8	10	314	8.2	4668.168	29.9	1.4	67.228	763.15	6.7	31.1
37.8	5	259	6.8	3575.944	30.2	1.1	72.363	914.924	7.2	32.1
37.8	1	194	4.6	1970.679	34.3	5.9	98.417	989.437	7.6	26.3
37.8	0.5	163	3.4	1564.185	33.1	6	104.132	1053.944	7.6	29
37.8	0.1	126	1.4	1072.243	24.5	2.4	117.11	1189.083	7.4	47.5
54.4	25	138	8.8	1501.439	38.7	4.8	92.022	568.324	7.5	4.5
54.4	10	105	7.5	1054.469	34.5	3.9	99.54	742.965	4.6	15.8
54.4	5	89	6.8	725.314	32.1	3.4	123.24	849.707	8.1	30.5
54.4	1	67	5.7	472.187	26.9	3.3	142.775	888.88	8	36.8
54.4	0.5	49	4.4	427.565	23	7.3	115.716	907.154	5.7	41.7
54.4	0.1	46	2.3	290.608	18	6.8	158.55	997.341	8.5	51.3

Table B-59 Overall Dynamic Modulus test results at 14 °F (-10 °C) test temperature for Mix 19 Specimen 3

Temperature (°C)	Frequency (Hz)	Stress Amplitude (P-P) (KPa)	SE (%)	Dynamic Modulus (MPa)	Phase Angle (deg.)	UC (deg.)	Strain (P-P) Recoverable (microstrain)	Accumulated Strain (microstrain)	SE (%)	UC (%)
-10	25	2046	5	42285.58	13.9	11.8	48.389	81.016	11.9	46
-10	10	2073	4.3	48152.68	5.2	0.4	43.052	50.281	6.9	32.6
-10	5	2017	4	46604.51	5.4	0.8	43.289	48.405	7.9	32.5
-10	1	1814	1.2	43576.17	6.7	1.7	41.62	48.394	10.4	31.9
-10	0.5	1704	0.6	40008.01	4.8	0.5	42.583	49.76	12	32.5
-10	0.1	1553	0.5	36975.64	9.3	2.2	41.997	62.737	16.5	31.2
4.4	25	1402	5.4	32490.29	18.7	9.9	43.164	82.039	13	30.6
4.4	10	1356	4.8	34129.82	10.6	2.7	39.733	54.459	5.2	21.3
4.4	5	1273	4.4	33016.5	9.8	2.9	38.556	58.486	10.6	20.9
4.4	1	1123	1.6	26545.83	13.6	3.5	42.304	59.334	7.6	20.3
4.4	0.5	1007	1	25530.49	18	3.7	39.461	66.461	8.4	18
4.4	0.1	955	0.5	18930.79	18.1	2.5	50.473	125.339	8	19.3
21.1	25	1021	5.5	17896.93	20.4	2.7	57.049	624.82	7.4	21
21.1	10	938	5.2	15928.43	20.2	2.6	58.888	732.753	5.6	15.3
21.1	5	794	5.1	13763.16	21.8	2.5	57.678	800.03	5.3	14.8
21.1	1	623	2.7	9133.639	26.8	2.1	68.226	825.366	4.1	13.3
21.1	0.5	494	2.1	7391.265	28.8	2.7	66.836	846.086	5	13.2
21.1	0.1	412	1.1	4749.562	29.4	3.2	86.65	1000.661	4.7	10.6
37.8	25	293	8.8	5901.723	35.1	3.7	49.634	345.379	8.2	29
37.8	10	257	7.1	4217.732	33.5	8.2	60.944	465.453	5.5	20.4
37.8	5	203	7.2	3242.392	33.7	8.8	62.489	501.403	6	21.3
37.8	1	148	5.5	1723.676	33.6	9	85.968	508.146	5.7	21.5
37.8	0.5	134	4.3	1354.588	32	9.3	98.9	537.089	5.8	24.1
37.8	0.1	108	1.7	857.414	27.3	8.8	126.481	658.138	7.4	29.4
54.4	25	140	8.8	1712.2	34.5	4.1	82.018	490.099	7.4	71.2
54.4	10	104	7.7	1263.235	29.2	4.3	82.369	625.966	5.6	65.1
54.4	5	89	7.2	1008.152	26.9	4.2	87.795	697.806	4.2	66.2
54.4	1	68	6.1	650.398	22.5	3.9	103.996	714.983	5.9	70.1
54.4	0.5	50	5	525.238	21.5	3.6	94.589	731.405	5.3	70.6
54.4	0.1	45	2.6	405.641	17.2	3.5	112.001	808.483	8.3	72.4

Table B-60 Overall Dynamic Modulus test results at various test temperatures for Mix 20 Specimen 4

Temperature (°C)	Frequency (Hz)	Stress Amplitude (P-P) (KPa)	SE (%)	Dynamic Modulus (MPa)	Phase Angle (deg.)	UC (deg.)	Strain (P-P) Recoverable (microstrain)	Accumulated Strain (microstrain)	SE (%)	UC (%)
-10	25	2049	5.5	55353.09	16.8	13.8	37.021	51.338	26.6	27.7
-10	10	2082	4.8	52555.25	8.2	0.6	39.613	14.95	9.5	22.8
-10	5	2026	4.6	50398.99	6.8	1.4	40.197	16.933	10.5	22.5
-10	1	1821	1.7	45970.81	5.5	3	39.603	18.412	15.2	20.5
-10	0.5	1706	0.9	40108.64	13.8	0.8	42.533	20.636	13.1	18.6
-10	0.1	1557	0.5	37412.81	8	2.4	41.618	32.76	22.7	18
4.4	25	1903	5.5	38410.44	15.9	10.7	49.554	165.793	22.4	39.5
4.4	10	1849	5.1	31724.6	12.7	2	58.296	103.285	7.1	23.2
4.4	5	1738	4.7	28896.6	14.4	2	60.161	113.193	7.1	22.7
4.4	1	1533	1.8	22852.19	14.8	2.9	67.069	117.726	9.3	20.8
4.4	0.5	1376	1.1	19587.88	17.8	2.8	70.245	133.696	5.2	19.1
4.4	0.1	1304	0.5	14751.36	21.2	2.3	88.365	248.269	5.1	21.4
21.1	25	937	7.1	15233.62	21.7	3.2	61.491	563.64	12.3	27.1
21.1	10	852	6.7	12476.67	22.6	2.4	68.283	699.983	6.7	26.9
21.1	5	720	6.5	10564.79	23.9	2.6	68.185	791.717	6.3	27.5
21.1	1	571	3.9	6780.083	27.9	2.2	84.228	837.842	5.7	28.3
21.1	0.5	452	3	5564.758	28.8	3	81.179	883.356	6.1	29.6
21.1	0.1	377	1.2	3425.816	31	1.2	109.984	1131.728	4.8	31.6
37.8	25	244	10.5	4305.194	31.9	0.8	56.699	708.37	11	20.6
37.8	10	216	9.6	3046.783	31.1	1.4	70.733	1063.323	8.1	22.8
37.8	5	174	9.9	2335.329	31.3	1.5	74.489	1216.663	7.9	23.5
37.8	1	132	8.5	1367.496	30.6	2	96.698	1298.511	7.4	25.7
37.8	0.5	110	6.9	1084.503	29.5	2.1	101.708	1368.555	7	26.7
37.8	0.1	85	3	686.59	25.3	2	123.987	1523.052	6.8	27.7
54.4	25	89	13.7	1249.945	35.2	3	71.092	420.616	12.1	27.5
54.4	10	68	10.7	895.211	31.7	2	75.501	602.771	8.6	29.7
54.4	5	55	10.6	711.469	29.4	2.7	77.554	678.594	7.7	31
54.4	1	41	9.3	455.16	24.8	3.8	89.591	718.748	6.8	32.6
54.4	0.5	31	7.6	385.732	23.2	4.1	80.291	729.406	5.8	33.8
54.4	0.1	28	3.8	296.964	19	4.9	95.525	772.329	6.9	36.5

Table B-61 Overall Dynamic Modulus test results at various test temperatures for Mix 20 Specimen 5

Temperature (°C)	Frequency (Hz)	Stress Amplitude (P-P) (KPa)	SE (%)	Dynamic Modulus (MPa)	Phase Angle (deg.)	UC (deg.)	Strain (P-P) Recoverable (microstrain)	Accumulated Strain (microstrain)	SE (%)	UC (%)
-10	25	2047	5.4	45189.55	3	6.5	45.291	64.19	15.1	12.5
-10	10	2080	5.1	50555.19	7.6	0.3	41.143	32.942	13.7	16.5
-10	5	2031	4.7	48139.07	7.3	0.5	42.199	29.77	12.8	16
-10	1	1815	1.6	41152.72	7.1	0.8	44.102	30.713	11.2	17.3
-10	0.5	1702	0.9	41923.9	11	1.1	40.604	32.843	12.2	19.7
-10	0.1	1558	0.5	35544.93	10.6	1.3	43.83	48.392	13.9	20.3
4.4	25	1909	5.5	45848.7	5.5	5.1	41.638	155.716	12.3	3.9
4.4	10	1852	5.5	40794.01	12.8	0.4	45.402	115.04	8.2	9.2
4.4	5	1743	5.1	37445.12	12.9	0.8	46.535	127.426	7.7	10.3
4.4	1	1535	2	29199.18	17.8	0.9	52.561	137.433	10.7	11.3
4.4	0.5	1377	1.2	26352.81	16.1	1.5	52.263	156.182	6.6	13.1
4.4	0.1	1303	0.5	18092.89	22.6	0.8	72.021	282.949	5.3	11.6
21.1	25	937	7.4	19526.62	18.9	1.4	47.996	503.743	9.8	4.1
21.1	10	851	7.3	14860.15	22.9	0.9	57.263	615.227	8.3	4
21.1	5	720	7	12319.32	24.6	1	58.474	697.416	7.9	4.4
21.1	1	570	4	7941.227	28.4	0.9	71.836	740.949	5.7	4.7
21.1	0.5	452	3	6649.569	31.2	1.2	67.936	782.322	4.6	4.6
21.1	0.1	376	1.1	3793.219	32.1	0.9	99.122	980.292	5.1	3.6
37.8	25	244	11.2	4013.143	33.2	1.7	60.833	278.791	10.6	24
37.8	10	213	10.2	2831.758	32.1	1.8	75.147	404.858	9	22
37.8	5	172	10	2207.188	31.9	2	78.007	471.542	8.6	22.6
37.8	1	132	7.9	1307.18	30.1	1.6	100.985	512.012	7.3	22.6
37.8	0.5	110	6.2	1059.424	28.7	1.4	103.866	542.653	6.7	24.2
37.8	0.1	85	2.8	718.365	24	1.5	118.097	634.602	7.1	23.8
54.4	25	99	11.6	1497.806	28.7	12.7	65.777	318.107	10	56.1
54.4	10	74	10.2	1120.276	29.2	2.9	65.75	441.774	7.6	50
54.4	5	61	9.4	933.061	26.1	2.1	65.845	505.507	6.4	53.8
54.4	1	46	8.5	648.497	21.1	1.5	70.925	512.857	5.7	59.4
54.4	0.5	35	7	536.488	19.3	2.1	65.482	514.627	6.9	60.9
54.4	0.1	32	3.8	430.05	15.7	0.9	74.009	537.768	7.6	62.1

Table B-62 Overall Dynamic Modulus test results at 14 °F (-10 °C) test temperature for Mix 20 Specimen 7

Temperature (°C)	Frequency (Hz)	Stress Amplitude (P-P) (KPa)	SE (%)	Dynamic Modulus (MPa)	Phase Angle (deg.)	UC (deg.)	Strain (P-P) Recoverable (microstrain)	Accumulated Strain (microstrain)	SE (%)	UC (%)
-10	25	2050	5.5	39229.79	12	7.3	52.247	59.921	12.9	26.7
-10	10	2083	5.4	40048.09	7.1	0.6	52.013	19.036	9.5	20.3
-10	5	2034	4.9	38176.7	6.9	0.7	53.268	18.047	8.1	20.5
-10	1	1820	1.7	34521.07	6.1	0.7	52.707	19.154	9.5	20.4
-10	0.5	1705	0.9	31505.24	8.4	0.9	54.103	22.234	8.9	21.3
-10	0.1	1557	0.5	28261.36	10.3	1.1	55.107	43.84	5.9	20.1
4.4	25	1897	5.2	26396.29	10.9	3.9	71.865	243.196	11.1	20.4
4.4	10	1853	5.1	23230.07	13	0.1	79.749	164.588	7.2	13.5
4.4	5	1742	4.9	21213	13.6	0.2	82.096	183.497	6.2	12.9
4.4	1	1534	1.9	16672.97	16.1	0.2	92	197.128	4.2	12.7
4.4	0.5	1376	1.1	15091.27	17.7	0.4	91.211	224.591	3.4	11.9
4.4	0.1	1303	0.5	10624.95	22	1.4	122.652	410.822	3.1	12.5
21.1	25	656	7.6	12005.89	20.7	4.3	54.604	361.475	9.7	15.5
21.1	10	591	7.6	9857.425	21.9	1.2	59.989	418.725	7.9	17.8
21.1	5	499	7.6	8618.443	23.5	1	57.894	439.602	8.8	20.5
21.1	1	398	4.7	5246.146	29.5	2.1	75.861	446.285	6.1	14.6
21.1	0.5	316	3.7	4204.969	31.4	2	75.06	459.375	6.6	16.3
21.1	0.1	263	1.1	2518.126	31	1	104.536	614.228	5.7	18.6
37.8	25	246	10	4097.029	32.4	2.1	60.15	435.957	10.6	28.1
37.8	10	217	8.7	2873.723	32	2	75.401	677.739	8	25.3
37.8	5	175	9.1	2278.004	32.1	2.4	76.661	778.893	8.1	27.8
37.8	1	132	7.5	1322.039	31.7	2.2	99.872	821.135	7.5	28
37.8	0.5	110	6.1	1041.402	30.7	2.1	105.376	856.625	7.4	27.9
37.8	0.1	85	2.7	661.191	26.3	2.1	128.196	962.28	7.7	28.7
54.4	25	89	11.8	1139.484	34.5	7.7	77.689	244.635	9.8	33.8
54.4	10	67	9.4	826.174	31.5	3.4	81.007	332.935	6.5	28.2
54.4	5	56	9.1	654.203	28.8	3.6	85.342	362.031	6.1	31.9
54.4	1	41	8.1	416.741	23.4	3.9	98.066	385.843	5.8	37.8
54.4	0.5	31	6.7	346.42	21.2	4.4	89.561	389.921	5.2	41.6
54.4	0.1	28	3.7	265.446	15.9	4.2	106.686	427.054	6.9	48.1

Table B-63 Overall Dynamic Modulus test results at various test temperatures for Mix 21 Specimen 3

Temperature (°C)	Frequency (Hz)	Stress Amplitude (P-P) (KPa)	SE (%)	Dynamic Modulus (MPa)	Phase Angle (deg.)	UC (deg.)	Strain (P-P) Recoverable (microstrain)	Accumulated Strain (microstrain)	SE (%)	UC (%)
-10	25	2054	5.5	53076.34	5.6	6.8	38.708	40.331	23.8	29.8
-10	10	2083	4.9	54032.17	6.2	0.7	38.542	11.834	7.7	20
-10	5	2031	4.8	53724.2	5.9	0.7	37.798	13.513	8.4	19.9
-10	1	1820	1.6	47955.02	6.6	0.4	37.946	10.659	8.1	19.2
-10	0.5	1706	0.8	45792.42	4.8	1.3	37.263	11.524	8.3	18.5
-10	0.1	1556	0.4	42080.37	8.2	1.1	36.988	21.388	11	17.6
4.4	25	1907	5.3	38425.38	11.5	5.7	49.634	117.409	17	22.4
4.4	10	1854	5.6	34867.25	10.2	0.7	53.177	65.845	7.9	17.2
4.4	5	1747	4.9	32138.16	11	0.9	54.354	68.959	7.2	17.5
4.4	1	1535	1.8	26521.15	13.4	1.3	57.871	72.007	6	16.3
4.4	0.5	1376	1	23694.49	13.2	2.2	58.087	80.744	5.5	16
4.4	0.1	1303	0.5	19222.23	18.1	2.3	67.798	155.719	6.3	15.1
21.1	25	1030	6.6	19775.41	16.3	3	52.106	380.072	8.5	27.5
21.1	10	939	6.4	17159.6	18.6	0.5	54.693	429.639	6.6	23.5
21.1	5	795	6.2	14928.61	19.9	0.6	53.283	476.688	6.5	23.3
21.1	1	627	3.4	10391.54	24.9	0.7	60.378	496.726	5.2	24.5
21.1	0.5	496	2.6	8740.551	25.7	0.8	56.758	519.305	6.1	26.4
21.1	0.1	415	1	5619.502	28.9	0.2	73.812	674.378	4.6	28.1
37.8	25	337	10.2	7868.764	27.1	2.8	42.864	545.342	9.3	30.4
37.8	10	294	9.1	5912.976	27.3	1.2	49.663	800.698	7	26.5
37.8	5	244	8.2	4589.306	28.3	1.4	53.143	922.24	7	29.2
37.8	1	187	6.2	2559.232	31.6	2.4	72.928	981.313	6.7	26.1
37.8	0.5	154	4.9	2019.86	30.8	2.9	76.107	1029.956	6.5	27
37.8	0.1	119	2.1	1251.654	26.9	3.3	95.063	1155.263	7	35.3
54.4	25	90	11.3	1941.394	35.4	4.6	46.21	198.85	11.8	25.4
54.4	10	68	9.6	1384.512	33.2	4.7	49.089	322.194	10.3	20.1
54.4	5	56	9	1135.182	30.4	3.7	48.95	361.264	8.9	24.3
54.4	1	44	10	753.366	26.6	2.6	57.921	382.031	14.3	28.7
54.4	0.5	31	6.5	592.666	25.3	2.8	51.763	382.633	8.7	29.5
54.4	0.1	29	2.7	487.355	19.2	2.1	58.504	417.385	9.9	35.1

Table B-64 Overall Dynamic Modulus test results at various test temperatures for Mix 21 Specimen 4

Temperature (°C)	Frequency (Hz)	Stress Amplitude (P-P) (KPa)	SE (%)	Dynamic Modulus (MPa)	Phase Angle (deg.)	UC (deg.)	Strain (P-P) Recoverable (microstrain)	Accumulated Strain (microstrain)	SE (%)	UC (%)
-10	25	2055	5.5	35062.88	3	8	58.595	65.088	14.1	21.9
-10	10	2087	5.1	44895.22	7.7	2	46.485	31.321	8.2	19.9
-10	5	2032	4.8	43679.69	5.5	1.8	46.529	32.593	7.6	20
-10	1	1820	1.7	40282.89	4.2	1.4	45.173	30.21	16.4	20
-10	0.5	1705	0.9	37730.93	8.9	2	45.191	31.414	10.3	19.1
-10	0.1	1557	0.5	35067.67	7.7	1.9	44.411	39.76	9.4	19.4
4.4	25	1904	5.4	26991.43	9.4	5	70.548	112.886	10.2	19
4.4	10	1850	5	28896.06	10.2	2.4	64.03	48.347	7.6	5.1
4.4	5	1736	4.6	27384.84	10.1	2.4	63.384	50.509	6.5	3.5
4.4	1	1529	1.7	23511.41	11.9	2.4	65.044	48.738	5.7	1.6
4.4	0.5	1374	1	22064.66	11.7	2.5	62.261	53.943	5.8	1.4
4.4	0.1	1304	0.5	17446.11	15.6	2.6	74.759	106.688	5.1	2.5
21.1	25	1028	6.3	16134.94	13.9	4.2	63.695	303.273	13.8	8.4
21.1	10	939	6	14189.57	16.8	2.4	66.155	322.733	7	11.2
21.1	5	794	5.6	12941.88	17.5	2.8	61.378	351.656	9.6	12.5
21.1	1	626	3	9172.371	21.9	2.7	68.293	362.244	7.2	12.5
21.1	0.5	496	2.2	8479.057	24.1	3.3	58.45	376.881	6.7	14.7
21.1	0.1	414	0.9	5633.039	26.1	3.6	73.548	504.786	4.7	17.3
37.8	25	340	9	7141.55	23.9	3.8	47.581	561.101	9.3	11
37.8	10	294	7.9	6217.609	27.2	5.7	47.273	873.555	7.4	18.3
37.8	5	245	7.2	5146.355	26	4.1	47.632	1014.95	7.7	20.4
37.8	1	186	5.5	3208.431	29.6	5.1	57.946	1083.12	6.2	23.2
37.8	0.5	155	4.2	2618.315	29.8	4.3	59.159	1141.712	5.2	24.9
37.8	0.1	119	1.8	1660.01	28.9	3.8	71.629	1275.556	4.3	27.1
54.4	25	89	10.4	2833.886	29.5	2.2	31.25	354.376	10.6	14.2
54.4	10	67	8.6	2069.768	27.3	2.1	32.415	496.319	13.1	19.9
54.4	5	56	8.5	1667.286	28.1	1.2	33.346	560.774	9.7	21.2
54.4	1	42	6.9	1027.65	25.5	0.3	40.47	588.829	12.5	16.8
54.4	0.5	31	5.6	892.765	22.1	0.8	35.083	597.8	10	19.9
54.4	0.1	28	3.3	662.931	19.2	1.2	42.592	631.441	8.8	13.5

Table B-65 Overall Dynamic Modulus test results at various test temperatures for Mix 21 Specimen 5

Temperature (°C)	Frequency (Hz)	Stress Amplitude (P-P) (KPa)	SE (%)	Dynamic Modulus (MPa)	Phase Angle (deg.)	UC (deg.)	Strain (P-P) Recoverable (microstrain)	Accumulated Strain (microstrain)	SE (%)	UC (%)
-10	25	2052	5.5	41265.75	7.6	3.4	49.723	59.315	8.5	7.6
-10	10	2084	5.3	44147.3	6	1.8	47.196	26.797	7.5	10
-10	5	2039	4.9	43220.82	5.9	1.6	47.167	27.438	7.7	9.8
-10	1	1823	1.9	42584.06	6.6	1.3	42.81	24.367	10	9.9
-10	0.5	1707	1	37513.21	7.5	0.9	45.508	25.279	11.5	12
-10	0.1	1556	0.5	36235.24	6.8	1.2	42.941	29.425	9.3	11.8
4.4	25	1900	5.3	31789.98	8.5	4.3	59.777	77.137	9.3	8
4.4	10	1849	5.1	33639.7	8.8	1.4	54.968	28.773	6.5	6.3
4.4	5	1743	4.6	32157.86	8.4	1.5	54.215	26.794	6.1	7.2
4.4	1	1532	1.7	28210.72	8.9	1.3	54.316	26.5	9	7.4
4.4	0.5	1375	1	25081.77	7.4	2.4	54.821	28.909	6.9	7.1
4.4	0.1	1304	0.4	22532.73	13.2	1.4	57.85	51.903	10.2	8.3
21.1	25	1030	6.7	23056.47	17.7	0.4	44.679	146.395	10.6	15.7
21.1	10	940	6.2	19136.93	14.3	1.5	49.136	139.547	7.1	12.7
21.1	5	799	6.1	17432.38	14.9	1.4	45.844	144.785	7.4	12.3
21.1	1	627	3.3	14320.03	16.1	2.6	43.784	145.017	13.3	12.1
21.1	0.5	498	2.4	12406.68	21.6	1.1	40.104	149.327	7.8	11.6
21.1	0.1	415	1	9090.637	22	2.3	45.607	204.327	6.9	12.4
37.8	25	604	8	12122.32	20.7	4.9	49.849	575.106	12.2	34.8
37.8	10	540	7.6	8864.02	21.2	2.6	60.883	833	7	27.3
37.8	5	439	7.7	7761.092	22.5	2.8	56.527	940.339	6.6	27.6
37.8	1	329	5.4	5223.147	26.5	3	63.002	980.188	6	29.4
37.8	0.5	271	3.2	4226.876	27.3	2.9	64.096	1030.925	5.1	30.9
37.8	0.1	209	1.2	2808.631	28.4	3.1	74.334	1190.505	4.9	36
54.4	25	249	9.8	5707.835	27.6	3.3	43.555	632.516	10.7	18.1
54.4	10	234	8.8	3665.811	29.3	4.5	63.89	1060.86	7	22.4
54.4	5	200	8.7	2898.655	30	4.4	69.028	1281.435	6.7	24.7
54.4	1	158	6.7	2040.24	28.6	3.7	77.397	1384.93	6.6	11.5
54.4	0.5	119	5.4	1633.965	28.1	4.2	72.664	1430.616	6.3	9
54.4	0.1	99	2.5	1096.415	24.7	3.9	90.398	1576.154	7.5	10.4

Table B-66 Overall Dynamic Modulus test results at various test temperatures for Mix 22 Specimen 1

Temperature (°C)	Frequency (Hz)	Stress Amplitude (P-P) (KPa)	SE (%)	Dynamic Modulus (MPa)	Phase Angle (deg.)	UC (deg.)	Strain (P-P) Recoverable (microstrain)	Accumulated Strain (microstrain)	SE (%)	UC (%)
-10	25	2054	5.5	40196.8	14.6	3.9	51.086	68.077	15.7	7.8
-10	10	2080	5.3	46936.82	8.9	3.8	44.311	35.516	9.4	5.4
-10	5	2031	4.7	45751.45	9.2	3.6	44.381	33.196	10.1	5.8
-10	1	1819	1.6	40536.63	9.6	4.7	44.876	32.77	11.7	3.6
-10	0.5	1704	0.8	38517.38	13.2	3.1	44.251	34.105	9.7	5.1
-10	0.1	1557	0.5	34512.55	13.4	3.6	45.113	46.876	12	10.3
4.4	25	1909	5.4	27204.43	14.8	4.5	70.184	247.112	10.3	12.1
4.4	10	1856	5.6	25648.45	12.2	1	72.366	185.777	7.4	9
4.4	5	1751	5	23933.63	11.7	1.6	73.169	205.529	11.4	11
4.4	1	1537	1.9	19053.94	15	1.6	80.691	219.556	10.4	14.3
4.4	0.5	1377	1	16700.45	19.8	0.3	82.45	246.41	4	15.6
4.4	0.1	1303	0.5	12514.81	21.3	0.8	104.136	413.079	5	19.6
21.1	25	1037	6.5	12219.42	21.8	2	84.855	943.727	6.8	11.1
21.1	10	944	6.7	11115.93	23.7	2.4	84.891	1102.197	5.9	19.7
21.1	5	801	6.5	9584.32	24.7	0.8	83.537	1227.443	6.2	23.8
21.1	1	628	3.6	6309.327	28.7	0.4	99.541	1287.572	5.6	28.6
21.1	0.5	497	2.7	5164.816	29.2	1.4	96.168	1342.341	5.2	32.1
21.1	0.1	415	1.3	3308.318	29.1	2	125.498	1583.031	5.1	35.5
37.8	25	292	9.6	4922.743	34	0.4	59.271	385.494	10	5.7
37.8	10	265	8.2	3690.187	31.9	2.1	71.882	600.388	6.3	11.8
37.8	5	215	8.2	2927.545	31.5	2.6	73.349	700.613	6.3	14.5
37.8	1	163	6.8	1738.826	30.5	2.7	93.59	745.734	7.5	22.1
37.8	0.5	135	5.6	1425.448	28.6	3.3	94.456	775.065	7.6	28
37.8	0.1	104	2.9	981.237	22.9	2.8	105.924	838.363	9.9	38.1
54.4	25	76	12.4	1489.665	32.3	9.9	50.744	131.678	9	31.1
54.4	10	70	10.1	1194.746	26.2	7.1	58.318	205.688	9.2	38.2
54.4	5	58	9.8	980.985	23.3	6.5	59.615	230.134	6.5	42.2
54.4	1	46	8.8	711.221	18.3	6.2	64.621	253.26	8.7	49.6
54.4	0.5	33	6.8	622.49	17.4	4.8	53.655	261.064	10.1	47.7
54.4	0.1	29	3.7	507.414	14.8	5.6	56.337	274.747	8.7	52.1

Table B-67 Overall Dynamic Modulus test results at various test temperatures for Mix 22 Specimen 2

Temperature (°C)	Frequency (Hz)	Stress Amplitude (P-P) (KPa)	SE (%)	Dynamic Modulus (MPa)	Phase Angle (deg.)	UC (deg.)	Strain (P-P) Recoverable (microstrain)	Accumulated Strain (microstrain)	SE (%)	UC (%)
-10	25	2050	5.8	54003.51	2.9	17.5	37.958	71.631	25.1	41.6
-10	10	2089	5.7	48196.72	8.1	1.5	43.336	35.626	14.8	41
-10	5	2039	5.2	48551.2	7.8	1.7	41.992	36.647	10.3	41.6
-10	1	1823	1.9	43968.92	6.4	3.7	41.468	38.052	11.4	43.2
-10	0.5	1706	1	39707	11.3	0.5	42.971	38.978	12.3	39.8
-10	0.1	1558	0.5	36613.35	9.6	2.5	42.544	50.502	13.1	43.4
4.4	25	1906	5.5	30278.75	10.5	2.6	62.937	210.383	14.7	16.2
4.4	10	1863	5.5	30191.92	15.3	2.2	61.712	155.609	7.4	15.1
4.4	5	1752	5.2	27232.2	16.4	2.7	64.333	171.897	6.8	15.7
4.4	1	1536	2.1	21639.17	20	3	70.988	184.548	8.1	17.2
4.4	0.5	1376	1.2	20190.78	20.8	2.8	68.165	206.379	5.3	19.1
4.4	0.1	1305	0.6	14065.41	23.2	1.1	92.762	335.995	4.6	13.3
21.1	25	1031	6.5	17394.55	20.6	3.6	59.252	569.273	7.1	29.8
21.1	10	939	6.3	14986.08	20.7	1.7	62.665	877.54	5.6	35.5
21.1	5	795	5.9	13324.99	20.9	1.8	59.638	1122.049	4.9	35.2
21.1	1	628	3.4	10179.64	22.6	4.1	61.659	1295.166	4.2	30
21.1	0.5	497	2.7	9378.187	23	5.1	53.029	1420.172	4.8	23.4
21.1	0.1	415	1.1	7365.588	24.5	3	56.41	1617.601	5.2	10.6
37.8	25	249	9.1	4285.625	29.7	7.4	58.053	588.526	9.8	33.9
37.8	10	220	8.1	3817.172	28.6	1.7	57.604	856.913	16	41.8
37.8	5	179	7.7	3069.609	29.5	3.5	58.165	957.156	8.9	41.9
37.8	1	134	6.3	1833.957	30	4.2	73.039	997.937	8.4	38.3
37.8	0.5	112	5.2	1480.911	29	4.4	75.752	1034.291	9.3	40
37.8	0.1	86	2.5	937.759	26.3	5.1	91.269	1126.167	9.4	44.2
54.4	25	75	9.4	1861.003	30.9	6.3	40.273	199.391	11	27.7
54.4	10	70	8.5	1413.29	29	6.2	49.304	360.699	7.3	26.4
54.4	5	60	7.9	1171.907	27	5.8	50.999	427.117	7.2	31.1
54.4	1	47	7.2	784.77	24.5	5.7	59.63	442.424	12.4	40.5
54.4	0.5	34	5.8	652.978	23	5.8	52.413	449.358	10.1	45
54.4	0.1	28	3.8	486.54	19.3	4.8	58.217	487.434	9.7	51

Table B-68 Overall Dynamic Modulus test results at various test temperatures for Mix 22 Specimen 3

Temperature (°C)	Frequency (Hz)	Stress Amplitude (P-P) (KPa)	SE (%)	Dynamic Modulus (MPa)	Phase Angle (deg.)	UC (deg.)	Strain (P-P) Recoverable (microstrain)	Accumulated Strain (microstrain)	SE (%)	UC (%)
-10	25	2056	5.5	57751.04	22.9	6.9	35.594	79.373	28.1	17.1
-10	10	2095	5.1	63223.1	6.8	0.7	33.129	52.97	10	21.6
-10	5	2042	4.9	65276.22	3.9	1.3	31.29	54.334	16.7	23.9
-10	1	1822	1.8	55316.53	9.2	1.5	32.935	54.138	8.7	22.4
-10	0.5	1707	1	51564.79	6.5	0.9	33.098	55.274	15.3	23.2
-10	0.1	1557	0.5	47027.13	7.5	0.7	33.109	65.3	19	24.8
4.4	25	1911	5.6	44861.02	5.9	31.8	42.6	181.804	31.7	46.4
4.4	10	1859	5.7	36835.64	12.4	0.2	50.468	145.728	9.3	25.5
4.4	5	1747	5.2	33764.23	12.5	0.6	51.73	161.39	10	26.8
4.4	1	1535	1.8	26353.27	15.8	0.6	58.255	172.351	7.6	26.1
4.4	0.5	1377	1.1	22758.54	14.9	1.3	60.492	192.206	7.3	25.7
4.4	0.1	1303	0.5	17174.3	21.4	1.8	75.873	321.514	7.6	24.8
21.1	25	723	6.9	13978.16	21.2	5.7	51.706	330.249	8	30.8
21.1	10	657	7.2	11166.85	23.4	4.3	58.879	342.47	7.4	29.9
21.1	5	556	7.2	9359.777	24.8	4.3	59.404	347.219	7	33.1
21.1	1	441	4.4	5846.142	28.6	2.9	75.376	346.282	6.5	39.5
21.1	0.5	350	3.6	4551.014	30.2	2.4	76.809	352.928	6.3	43.9
21.1	0.1	285	1.2	2712.9	30.1	1.7	104.994	484.012	5.9	45.1
37.8	25	295	9.1	4383.383	33.2	0.5	67.259	709.245	9.6	42
37.8	10	268	8.4	3066.019	30.8	1.5	87.356	1007.039	7.7	45.8
37.8	5	217	8.3	2329.947	30.4	1.7	92.961	1136.774	7	46.7
37.8	1	162	7.1	1364.213	29	1.2	118.864	1192.982	7.3	52.4
37.8	0.5	135	5.8	1074.904	27.8	1.4	125.161	1243.576	7.6	56.5
37.8	0.1	104	3.2	682.074	23.4	1.6	152.074	1385.481	8.5	63.5
54.4	25	75	10.5	1259.615	31.7	5.3	59.777	302.713	10.3	32.2
54.4	10	69	9.7	902.419	28.1	5.6	76.964	451.088	7.8	45.3
54.4	5	59	9	737.708	25.8	5.4	80.297	516.609	6.4	48.3
54.4	1	46	8.4	503.205	22	5.3	92.045	532.446	7.5	58.8
54.4	0.5	34	6.5	445.079	19.8	5.7	76.568	557.651	6.4	66.8
54.4	0.1	29	4.4	355.741	15.4	5	80.457	594.312	7.5	77.8

Table B-69 Overall Dynamic Modulus test results at various test temperatures for Mix 23 Specimen 4

Temperature (°C)	Frequency (Hz)	Stress Amplitude (P-P) (KPa)	SE (%)	Dynamic Modulus (MPa)	Phase Angle (deg.)	UC (deg.)	Strain (P-P) Recoverable (microstrain)	Accumulated Strain (microstrain)	SE (%)	UC (%)
-10	25	2060	5.1	52058.99	12.9	20.2	39.577	104.26	24.9	24.9
-10	10	2095	5	43971.08	7.1	1.6	47.645	64.208	7	12
-10	5	2041	4.7	41917.07	7.3	1.9	48.693	65.663	6	11.6
-10	1	1822	1.7	36461.27	7.8	2	49.958	69.14	9.2	11.3
-10	0.5	1706	0.9	36622.32	6	3	46.578	72.808	7.9	13.7
-10	0.1	1557	0.5	31331.45	11.4	1.1	49.701	98.528	9.5	13.9
4.4	25	1913	5.3	35101.01	2.4	14.1	54.507	248.925	19.1	31.6
4.4	10	1862	5.3	27412.08	12	1.5	67.936	194.57	5.6	17
4.4	5	1750	4.8	25069.95	12.6	1.5	69.798	212.861	5.4	16.9
4.4	1	1536	1.8	19922.26	16.3	1.3	77.089	227.275	4.6	19.3
4.4	0.5	1377	1	17753.01	19.1	1	77.59	253.336	4.6	20.3
4.4	0.1	1303	0.5	13253.7	21.9	0.8	98.309	433.573	4.5	21.9
21.1	25	729	7.9	12769.71	12.4	11.6	57.114	545.735	13.4	24.3
21.1	10	658	8	12621.81	21.6	1.1	52.101	720.424	10.1	35.6
21.1	5	556	8	10343.7	22.4	1.7	53.728	815.458	9	33.9
21.1	1	440	5.4	6856.431	28.4	0.9	64.147	860.345	6.5	40.6
21.1	0.5	349	4.3	5579.131	27.7	1.8	62.505	897.49	7.8	44.6
21.1	0.1	285	1.4	3400.371	28.4	1.8	83.812	1103.766	10.8	46.5
37.8	25	208	11	4175.177	32	1	49.78	158.144	9.6	23.1
37.8	10	194	9.2	3143.199	30	0.9	61.64	195.138	6.7	26.6
37.8	5	161	9.3	2443.25	29.3	1.3	66.013	200.289	6.8	30.5
37.8	1	119	8.1	1388.904	27.7	2.2	85.461	197.246	7.1	39.8
37.8	0.5	99	6.5	1095.21	26.1	2.8	90.601	200.838	7.5	45.5
37.8	0.1	85	3.3	741.312	21.2	2.6	114.022	266.98	8.2	51.1
54.4	25	77	11.7	1283.705	32.8	1.7	60.171	168.266	10.9	52.6
54.4	10	71	9.4	1027.131	26.9	2	68.943	287.334	5.8	48
54.4	5	60	9.2	838.936	24.1	2.4	71.282	317.422	5.2	49.4
54.4	1	46	8.4	576.028	20.2	2.7	80.622	337.855	5.6	55.6
54.4	0.5	35	6.4	480.764	19.2	2.6	71.863	344.435	6.2	59.8
54.4	0.1	29	3.4	390.596	15	2.6	73.132	374.186	8.1	61

Table B-70 Overall Dynamic Modulus test results at various test temperatures for Mix 23 Specimen 5

Temperature (°C)	Frequency (Hz)	Stress Amplitude (P-P) (KPa)	SE (%)	Dynamic Modulus (MPa)	Phase Angle (deg.)	UC (deg.)	Strain (P-P) Recoverable (microstrain)	Accumulated Strain (microstrain)	SE (%)	UC (%)
-10	25	2055	5.4	37900.17	19.5	8.3	54.208	104.144	10.6	44.5
-10	10	2094	5.2	36111.71	7.9	2.1	57.98	60.216	7.2	41.1
-10	5	2045	4.9	34864.68	7.6	2.4	58.665	58.56	6.6	41.5
-10	1	1825	1.8	30496.24	8.7	2	59.833	58.228	5.7	39.8
-10	0.5	1708	0.9	29783.43	10.7	2.3	57.351	60.838	9.2	41.8
-10	0.1	1558	0.5	26097.87	12.2	1.3	59.694	81.381	12.5	42
4.4	25	1911	5.3	25801.43	11.9	1.3	74.07	276.443	7.4	44.7
4.4	10	1861	5.2	24073.18	12.3	1.7	77.321	220.73	5.8	46.7
4.4	5	1752	4.8	22037.62	13.3	1.4	79.497	244.342	5.9	45.7
4.4	1	1537	1.9	18062.86	14.9	1.9	85.067	260.966	5.7	48.6
4.4	0.5	1377	1.1	15982.93	16.3	1.9	86.134	289.572	4.4	47.3
4.4	0.1	1305	0.6	11897.03	21.3	1.2	109.731	480.587	4.6	47.5
21.1	25	719	7.7	16370.5	23.5	6.7	43.914	657.241	10.3	15.4
21.1	10	651	7.8	13335.22	17.4	3.8	48.814	930.433	8.3	21.7
21.1	5	554	8.1	11646.26	19.4	3.8	47.574	1050.148	8.6	21
21.1	1	439	5.2	8333.769	23.9	2.5	52.691	1096.72	8.2	25.3
21.1	0.5	348	4.2	6806.116	24.4	2.5	51.104	1129.044	7.9	26.4
21.1	0.1	278	1.5	4400.087	29.5	1.6	63.078	1301.781	7.7	26.5
37.8	25	374	10.8	7634.122	32.9	3.6	48.958	554.426	9.4	27
37.8	10	323	11.2	5858.79	30.8	3.9	55.057	879.198	9	25.1
37.8	5	268	9.9	4402.409	31.6	3.7	60.926	1046.731	9.1	25.5
37.8	1	204	7.5	2565.696	31.4	3.3	79.669	1102.215	8.9	27.4
37.8	0.5	169	5.9	1964.751	31.1	3.4	86.154	1140.765	8.1	28.1
37.8	0.1	129	2.6	1186.3	28.5	3.7	108.834	1238.226	10.1	30.5
54.4	25	74	12.5	1889.102	42.1	2.4	38.988	131.398	18.8	56.2
54.4	10	69	10.1	1368.58	36.3	4.6	50.151	213.329	9	44.3
54.4	5	59	9.5	1099.745	33.9	5.5	53.634	269.581	10.9	40.6
54.4	1	45	8.8	731.293	29.9	5.8	62.044	279.933	9.7	39
54.4	0.5	34	7.2	537.584	28.6	6	63.414	388.286	11.4	43.4
54.4	0.1	28	4.1	501.947	23.5	6.7	56.628	559.297	10	40.5

Table B-71 Overall Dynamic Modulus test results at various test temperatures for Mix 23 Specimen 6

Temperature (°C)	Frequency (Hz)	Stress Amplitude (P-P) (KPa)	SE (%)	Dynamic Modulus (MPa)	Phase Angle (deg.)	UC (deg.)	Strain (P-P) Recoverable (microstrain)	Accumulated Strain (microstrain)	SE (%)	UC (%)
-10	25	2038	5.3	37554.11	5.7	5	54.269	68.012	17.4	30.2
-10	10	2092	5.1	38911.06	7.5	1.5	53.759	24.468	7.6	17.5
-10	5	2038	5	37134.09	8.2	1.4	54.895	24.476	7.7	17.7
-10	1	1822	1.7	34981.57	9.3	1.7	52.076	25.51	11.6	16.9
-10	0.5	1707	0.9	34148.18	10.6	1.7	49.98	27.25	10.5	16.2
-10	0.1	1557	0.5	29326.9	9	1.7	53.075	41.78	9.5	15.3
4.4	25	1909	5.4	27115.38	10	5	70.415	208.913	14.2	18.4
4.4	10	1863	5.4	27034.82	12.9	3.8	68.906	148.259	6	6.1
4.4	5	1753	5.1	25314.73	13.6	3.7	69.255	159.636	5.7	5.9
4.4	1	1536	1.9	20157.36	17.2	3.8	76.191	168.396	7.4	7.4
4.4	0.5	1377	1.1	19327.89	18.3	3.6	71.22	188.13	4.2	5.7
4.4	0.1	1305	0.6	13907.95	22.1	3	93.804	329.116	5.5	7.7
21.1	25	724	8.1	14871.48	18.4	17.9	48.699	479.164	15.6	39.1
21.1	10	651	8.1	14172.33	20.3	1.6	45.907	624.328	9.1	28.4
21.1	5	550	8.2	12427.91	21.6	2.1	44.271	694.839	9.2	29.6
21.1	1	439	4.8	8168.225	26.9	1.1	53.714	725.375	7.6	30.6
21.1	0.5	347	3.7	6737.607	27.4	2.6	51.509	749.996	10.4	36.2
21.1	0.1	279	1.4	4172.189	29.9	2.3	66.971	907.417	8.2	37.3
37.8	25	245	9.9	6375.878	26.1	5.7	38.414	652.133	10.5	37.8
37.8	10	215	9.5	5025.377	28	1.4	42.701	944.027	8.1	31.1
37.8	5	174	9.6	3894.349	28.2	1.5	44.665	1064.669	10.6	33.4
37.8	1	136	6.9	2372.56	29.1	2.2	57.189	1115.85	9.2	36.1
37.8	0.5	110	5.1	1923.7	26.6	2.3	57.405	1147.745	7.5	37.9
37.8	0.1	85	2.5	1310.507	23.2	2.7	64.567	1224.331	7.2	37.6
54.4	25	73	12.9	1892.874	29.9	7	38.755	277.507	15.3	64.1
54.4	10	70	10.3	1549.487	26.5	2.8	45.196	488.742	8.9	40
54.4	5	60	9.9	1305.581	24.5	2	46.151	574.121	7.9	37.2
54.4	1	45	8.5	915.012	20.3	1.7	49.553	591.112	8.4	36
54.4	0.5	34	7.4	791.761	18.4	1.5	43.043	595.843	8.9	36.6
54.4	0.1	27	4.5	637.053	15.6	1.6	41.973	617.74	9	33

Table B-72 Overall Dynamic Modulus test results at various test temperatures for Mix 23 Specimen 8

Temperature (°C)	Frequency (Hz)	Stress Amplitude (P-P) (KPa)	SE (%)	Dynamic Modulus (MPa)	Phase Angle (deg.)	UC (deg.)	Strain (P-P) Recoverable (microstrain)	Accumulated Strain (microstrain)	SE (%)	UC (%)
-10	25	2054	5.6	35816.65	9.3	2.9	57.35	151.596	8.6	28.2
-10	10	2091	5.4	33484.47	7.1	0.9	62.452	106.675	6.1	25.7
-10	5	2037	5	32229.48	7.2	1.1	63.211	108.86	6.8	25.9
-10	1	1820	1.7	29130.94	11.1	0.8	62.472	110.918	8.5	27.7
-10	0.5	1705	0.9	26806.05	7	2.1	63.615	117.326	5.5	28.5
-10	0.1	1558	0.5	24363.17	11.1	1.4	63.948	150.655	7.3	29.8
4.4	25	1912	5.5	21116.33	17	3.9	90.531	343.868	7.4	16.6
4.4	10	1861	5.5	21143.07	14.5	4.4	88.038	254.344	8.6	18.5
4.4	5	1752	5.1	19561.34	14.6	3.8	89.584	267.998	5.8	16.9
4.4	1	1537	1.9	15899.3	15.7	3.3	96.663	277.246	9.6	13.5
4.4	0.5	1377	1	13941.05	17.7	3.7	98.76	298.658	5.6	12.1
4.4	0.1	1305	0.6	11275.31	20.7	3.8	115.711	440.016	4.9	9
21.1	25	727	7.7	11876.76	18.6	10.2	61.18	443.822	10.9	9.4
21.1	10	658	7.7	10545.4	19.8	3.3	62.362	523.439	7.7	3.1
21.1	5	558	8.1	9219.746	20.5	3	60.531	552.966	7.4	2.8
21.1	1	440	5.2	6421.434	21.9	3.7	68.543	561.772	8.4	4.4
21.1	0.5	348	4.1	5243.84	23.2	4	66.425	574.253	8.1	6
21.1	0.1	284	1.3	3527.821	26.6	3.7	80.509	704.783	7.5	7.9
37.8	25	208	10.5	7085.931	27.5	4.1	29.412	303.305	10.4	15.8
37.8	10	195	9.4	5634.779	23.8	3.5	34.694	501.522	7.8	18.9
37.8	5	163	9.5	4637.363	24.2	2.9	35.048	594.086	9.3	18.1
37.8	1	119	7.5	2856.458	25.5	2.3	41.705	619.592	8	14.6
37.8	0.5	99	5.8	2354.79	24.6	2	41.994	638.037	7.5	10.9
37.8	0.1	84	2.4	1585.009	23.3	1.1	52.925	707.13	6.4	9.1
54.4	25	75	10.6	2869.426	31.7	4.7	26.239	373.713	17.2	29.2
54.4	10	72	9.7	2166.887	27.2	2.6	33.206	585.36	8.4	13.4
54.4	5	61	8.8	1741.947	25	1.2	34.738	666.304	6.4	9.2
54.4	1	47	8.2	1139.736	23.7	2	41.082	680.654	7.2	7
54.4	0.5	34	6	931.976	22.6	2.4	36.812	687.456	6.4	7.7
54.4	0.1	29	3.5	679.16	18.7	2	42.867	721.376	8.1	10.9

Table B-73 Overall Dynamic Modulus test results at various test temperatures for Mix 24 Specimen 1

Temperature (°C)	Frequency (Hz)	Stress Amplitude (P-P) (KPa)	SE (%)	Dynamic Modulus (MPa)	Phase Angle (deg.)	UC (deg.)	Strain (P-P) Recoverable (microstrain)	Accumulated Strain (microstrain)	SE (%)	UC (%)
-10	25	2050	5.4	49439	0.6	11.7	41.474	94.188	11	12.9
-10	10	2083	5.3	54299.15	5.2	0.3	38.363	64.181	7.4	16.8
-10	5	2028	4.8	52654.02	5.3	0.3	38.514	67.537	9	16
-10	1	1816	1.6	46420.01	7.9	0.7	39.122	66.436	11.4	16.4
-10	0.5	1705	0.9	43970.91	4.2	0.9	38.771	68.535	15.1	16.8
-10	0.1	1556	0.5	40653.1	7.8	1.2	38.27	85.396	12.6	19.2
4.4	25	1907	5.4	42986.38	4.4	11.6	44.372	143.088	8.7	5.5
4.4	10	1861	5	39118.81	8.7	1.1	47.585	103.538	6.3	11
4.4	5	1752	5	36554.07	10.3	1.2	47.919	113.878	7.1	14.2
4.4	1	1535	1.8	29610.11	14.5	2.9	51.85	120.926	16.2	14.3
4.4	0.5	1376	1	29397.41	16.2	3.5	46.797	135.437	11.6	16.9
4.4	0.1	1303	0.5	20461.98	20.7	5.8	63.684	254.939	7.1	19.4
21.1	25	720	7.6	17597.75	20.8	12.7	40.929	423.963	15.3	12.2
21.1	10	652	7.5	19460.91	19.1	1.9	33.488	556.298	16.1	27.8
21.1	5	552	7.6	16418.04	19.7	1.2	33.629	615.775	10.7	26.7
21.1	1	439	4.8	10927.51	24.5	1.9	40.191	641.56	12.6	24.9
21.1	0.5	348	3.8	9156.973	21.8	1	38.045	658.772	12	27.7
21.1	0.1	279	1.4	5704.47	29.8	2.7	48.967	780.615	13.1	25.3
37.8	25	209	11.4	7464.388	34.7	6.7	27.969	410.95	16.1	30
37.8	10	197	10	5402.426	31.6	3.7	36.486	603.111	12.9	30.1
37.8	5	162	10.6	4164.301	29.5	5.2	38.907	673.993	9.1	29.5
37.8	1	119	8.7	2521.394	29.7	5.5	47.237	693.729	9.1	32.9
37.8	0.5	99	6.5	2001.398	28.9	5.1	49.569	704.541	7.8	36
37.8	0.1	84	3	1356.61	23.7	6	62.08	750.368	7.8	39.2
54.4	25	75	12	1764.062	34.1	5.4	42.722	177.12	10.8	52.9
54.4	10	70	10.5	1398.706	27	3.6	49.797	289.042	8.5	41.4
54.4	5	59	10.1	1148.336	25.2	3.1	50.955	329.517	8	43.6
54.4	1	46	8.7	779.091	19.3	4.9	58.85	339.731	7.4	50
54.4	0.5	34	6.7	643.84	19.8	4.1	52.817	346.946	5.9	51.3
54.4	0.1	28	3.6	507.833	15.3	5.2	56.11	369.545	7.8	58.8

Table B-74 Overall Dynamic Modulus test results at various test temperatures for Mix 24 Specimen 2

Temperature (°C)	Frequency (Hz)	Stress Amplitude (P-P) (KPa)	SE (%)	Dynamic Modulus (MPa)	Phase Angle (deg.)	UC (deg.)	Strain (P-P) Recoverable (microstrain)	Accumulated Strain (microstrain)	SE (%)	UC (%)
-10	25	2059	5.5	56132.62	3.3	16.2	36.672	48.119	13.1	8.3
-10	10	2092	5.2	53920.18	4.6	0.5	38.799	16.341	7.4	11.3
-10	5	2036	4.9	51367.51	5.8	0.9	39.639	18.19	9.6	10.5
-10	1	1817	1.7	46855.2	5.6	0.4	38.788	17.96	13.7	12
-10	0.5	1704	0.9	45468.67	14.5	4.1	37.48	19.068	20.2	12.3
-10	0.1	1557	0.5	41047.64	4.2	0.6	37.942	26.112	22.7	13.8
4.4	25	1893	5.3	39916.93	10.8	10.7	47.425	124.756	7.9	35.5
4.4	10	1851	5	39122.25	9	1	47.317	63.008	6.8	19.2
4.4	5	1740	4.7	37080.76	10.5	1	46.919	62.552	6.6	20.4
4.4	1	1531	1.6	30028.09	14	4.5	50.998	62.13	11.5	23.6
4.4	0.5	1376	1	29040.99	18.9	5.4	47.385	71.429	9.3	26.6
4.4	0.1	1303	0.4	20007.16	21.3	6.2	65.125	176.115	7	29.3
21.1	25	719	7.3	19825.95	12.9	17.9	36.246	262.549	14	12.8
21.1	10	649	7.8	18387.18	16.9	1.9	35.272	320.497	18	16.6
21.1	5	547	7.6	16990.13	20.4	1.8	32.2	341.237	17.9	19.2
21.1	1	439	4.6	11032.66	22.9	2.2	39.785	343.657	14.3	20
21.1	0.5	348	3.7	8817.711	21.7	0.7	39.431	346.161	9.6	21.3
21.1	0.1	282	1.2	5594.716	28.1	1.6	50.382	425.364	12	21.6
37.8	25	206	10.7	7117.933	32.2	6.7	28.947	180.187	12.5	20.8
37.8	10	194	10.1	5303.646	30.1	4.1	36.566	287.002	8.6	24.8
37.8	5	160	10.2	4226.577	29.6	5.3	37.941	325.45	8.1	24.7
37.8	1	119	8	2614.88	28.9	5.9	45.393	331.201	9.2	24.6
37.8	0.5	99	6	2076.557	28.1	5.3	47.636	334.964	7.7	26.7
37.8	0.1	83	2.5	1307.966	22	5.3	63.599	360.76	7.8	40.8
54.4	25	75	12.5	1746.978	32.6	5.4	42.759	75.751	12.9	49.5
54.4	10	68	10.8	1392.548	27.6	2.7	49.11	142.954	7.5	40.6
54.4	5	59	10	1125.38	24.8	3.7	52.025	175.244	6.3	40.6
54.4	1	46	8.1	765.028	20.7	4.3	59.781	183.225	7.2	50.1
54.4	0.5	34	6.5	638.968	19.3	4.4	53.466	183.562	7.7	52.7
54.4	0.1	28	3	484.56	15.3	5	58.401	205.965	7.8	58.5

Table B-75 Overall Dynamic Modulus test results at various test temperatures for Mix 24 Specimen 3

Temperature (°C)	Frequency (Hz)	Stress Amplitude (P-P) (KPa)	SE (%)	Dynamic Modulus (MPa)	Phase Angle (deg.)	UC (deg.)	Strain (P-P) Recoverable (microstrain)	Accumulated Strain (microstrain)	SE (%)	UC (%)
-10	25	2056	5.3	59622.18	0.8	12.9	34.49	40.767	13.5	22
-10	10	2078	4.5	53487.4	4.8	0.5	38.852	11.414	7	8.6
-10	5	2019	4.3	52226.32	5.4	0.3	38.665	7.805	7.5	8.8
-10	1	1814	1.4	46691.88	10.4	1.5	38.851	7.241	14.4	9
-10	0.5	1704	0.8	44432.82	122.2	205.3	38.352	7.948	18.1	8.7
-10	0.1	1555	0.5	40559.71	8.8	1.3	38.347	17.839	18.1	10.2
4.4	25	1903	5.3	43125.54	7.3	18.5	44.13	128.463	12.3	38.6
4.4	10	1854	4.9	39823.37	10.1	0.8	46.559	62.432	9.1	24.9
4.4	5	1749	5	38089.05	10.5	0.8	45.924	59.198	7.8	25.5
4.4	1	1535	1.8	29405.06	17.3	5.2	52.204	57.394	17.1	30.5
4.4	0.5	1378	1.1	29082.27	17.3	6.6	47.373	65.647	6.2	34.1
4.4	0.1	1303	0.5	19515.93	22	6.4	66.783	166.095	7.2	36
21.1	25	719	7.4	20547.58	11.3	20.8	34.997	204.554	17.1	13.2
21.1	10	648	7.5	18649.08	18.8	1.5	34.765	230.151	11	13.3
21.1	5	549	7.7	16741.64	19.2	0.8	32.764	235.135	11.7	15.3
21.1	1	440	4.7	10946.44	25	1.5	40.196	229.485	9.8	17.9
21.1	0.5	342	3.9	9059.764	24.9	1	37.749	226.52	14.5	21.3
21.1	0.1	277	1.6	5496.956	27.4	0.9	50.438	291.256	9.4	18.8
37.8	25	206	10.8	6902.033	29.8	4.7	29.776	147.43	12.6	30.1
37.8	10	191	9.8	5164.835	29.4	4	36.964	221.98	9.2	29.2
37.8	5	161	9.7	3994.326	29	4.4	40.221	245.534	8.5	30
37.8	1	119	7.4	2445.173	28.6	5.1	48.559	245.961	8	32.8
37.8	0.5	98	5.7	1916.956	27.5	5	51.024	245.54	6.8	34.1
37.8	0.1	81	3.3	1232.75	22.1	4.1	65.787	267.123	8.9	45.5
54.4	25	74	12.9	1740.926	33.2	5.6	42.36	56.49	12.5	48.4
54.4	10	68	10.7	1370.035	27.2	3.4	49.961	111.815	7.1	39.5
54.4	5	59	10	1109.642	24.8	3.6	53.17	137.12	6.9	41.4
54.4	1	46	8.1	742.078	21.2	3.8	61.545	142.875	8.8	50.3
54.4	0.5	35	6.5	621.722	19.5	4.5	55.646	142.546	7.5	53.2
54.4	0.1	28	3.2	475.626	16	4.3	58.445	163.116	9.3	59.4

Table B-76 Overall Dynamic Modulus test results at various test temperatures for Mix 25 Specimen 1

Temperature (°C)	Frequency (Hz)	Stress Amplitude (P-P) (KPa)	SE (%)	Dynamic Modulus (MPa)	Phase Angle (deg.)	UC (deg.)	Strain (P-P) Recoverable (microstrain)	Accumulated Strain (microstrain)	SE (%)	UC (%)
-10	25	2041	5.3	52921.12	13.1	3.4	38.564	81.104	22.9	12.2
-10	10	2082	5	42527.4	5.9	0.8	48.967	39.86	7.1	17
-10	5	2026	4.8	40938.53	6.1	0.8	49.488	37.841	6.7	17.3
-10	1	1817	1.4	35668.88	8.4	1.6	50.948	39.551	6.5	18.8
-10	0.5	1707	0.8	35142.63	4.2	0.4	48.58	42.876	13.7	18.7
-10	0.1	1557	0.5	30568.01	9.9	1.6	50.939	65.808	8.4	20.8
4.4	25	1900	5.2	30602.96	13.3	7.7	62.075	425.054	14.4	26.5
4.4	10	1844	4.5	26218.45	15.1	5.7	70.317	385.481	7.2	20.6
4.4	5	1738	4.3	23254.5	16.7	6.7	74.72	430.647	7.2	23.3
4.4	1	1531	1.6	17328	19.2	7.2	88.333	459.026	6.7	29.2
4.4	0.5	1375	1	14897.56	19.2	6.9	92.284	503.551	5.3	30.9
4.4	0.1	1300	0.5	10476.72	24.2	3.2	124.09	784.202	4.9	38.3
21.1	25	719	7.5	11391.79	22.7	0.2	63.111	777.186	9.3	42.3
21.1	10	653	7.7	10051.81	23.3	4.9	65.005	999.269	7.4	33.5
21.1	5	553	7.9	8175.757	24.7	4.2	67.592	1104.833	8.1	36.3
21.1	1	439	5	5308.735	29	3.3	82.646	1152.784	5.6	39.7
21.1	0.5	348	3.9	4315.786	27.9	3.6	80.731	1189.019	6.3	41.2
21.1	0.1	281	1.6	2600.747	26.9	2.6	107.993	1363.547	5.2	43.5
37.8	25	209	10.4	4003.831	36.8	3.8	52.089	718.649	10.9	43.3
37.8	10	195	9.6	2958.796	35.1	3.7	65.904	1056.853	8.1	32.9
37.8	5	162	9.7	2341.441	34	3.1	69.225	1215.387	8.2	31.1
37.8	1	119	7.6	1697.114	28.1	2.6	70.159	1281.518	6.5	19.6
37.8	0.5	99	6.4	1437.673	26	2.9	68.839	1310.26	6.1	13.8
37.8	0.1	84	2.7	1086.881	20	2.3	76.918	1367.123	8	4.4
54.4	25	75	12.4	1544.789	34.1	2.9	48.839	361.186	13	24.6
54.4	10	69	10.4	1024.068	26.5	3.4	67.784	588.129	8.1	46.5
54.4	5	59	10.2	934.986	24	2.8	63.065	663.24	7.9	35.3
54.4	1	47	9.4	733.401	19.5	2.7	63.536	669.602	6.6	34.5
54.4	0.5	34	7.4	690.984	17.1	2.6	49.623	666.946	6.8	27.4
54.4	0.1	29	4.2	316.218	16.2	3.4	90.209	630.361	14.5	83.7

Table B-77 Overall Dynamic Modulus test results at various test temperatures for Mix 25 Specimen 2

Temperature (°C)	Frequency (Hz)	Stress Amplitude (P-P) (KPa)	SE (%)	Dynamic Modulus (MPa)	Phase Angle (deg.)	UC (deg.)	Strain (P-P) Recoverable (microstrain)	Accumulated Strain (microstrain)	SE (%)	UC (%)
-10	25	2043	5.2	44332.2	7.6	10.8	46.08	64.837	20.2	26.2
-10	10	2077	4.7	42598.48	6	0.6	48.756	22.057	6.5	15.9
-10	5	2023	4.3	40787.73	6	0.8	49.597	20.174	6.2	16.7
-10	1	1816	1.4	36234.99	5.9	1.1	50.118	17.818	6.2	18.3
-10	0.5	1707	0.8	35996.05	5.7	1.5	47.417	20.191	9.3	18.6
-10	0.1	1557	0.5	30252.82	11.2	1.4	51.476	40.028	12.5	20.4
4.4	25	1907	5.2	29003.3	15.9	4.3	65.746	280.248	13.9	22.5
4.4	10	1864	5.3	25839.14	14.9	6.5	72.152	180.637	6	19.5
4.4	5	1748	4.9	23364.28	15.8	6.4	74.813	183.305	5.2	20.7
4.4	1	1536	1.8	17712.12	18.9	7.5	86.715	187.468	7	26.7
4.4	0.5	1376	1.1	15078.83	20.6	7.3	91.284	208.92	5.2	28.6
4.4	0.1	1300	0.5	10733.58	24.1	4.8	121.103	425.345	4.8	36
21.1	25	727	7.9	8830.374	23.6	12.9	82.315	715.842	13.1	50.5
21.1	10	656	8	7402.066	25.2	3.7	88.591	906.345	7.5	41.9
21.1	5	558	8	6162.156	26.5	3.5	90.526	1006.851	7.1	43.2
21.1	1	442	5.4	3862.825	28.5	2.9	114.308	1050.529	5.8	43.6
21.1	0.5	350	4.2	3068.42	29.4	2.8	114.122	1092.88	5.3	43.9
21.1	0.1	284	1.4	1900.691	28.2	2.1	149.347	1290.324	5.6	44.2
37.8	25	206	10.9	4253.025	35.5	4.1	48.436	357.721	11.8	31.8
37.8	10	195	10.1	2650.058	32.9	2.7	73.481	557.31	10.5	42.3
37.8	5	161	10	2316.815	32.7	2.4	69.631	656.495	8.1	37.6
37.8	1	117	8	1684.848	26.5	2.6	69.666	682.078	7.3	19.9
37.8	0.5	98	6.5	1415.843	24.5	2.8	69.45	694.893	6.2	15.3
37.8	0.1	82	3.1	1085.177	18.3	2	75.145	734.978	7.9	6
54.4	25	73	11.7	812.266	33.7	3.7	90.272	228.76	9.4	48.8
54.4	10	68	10.8	586.729	27.4	4.5	116.252	352.964	5.5	52.5
54.4	5	58	10.4	473.241	24.6	4.3	123.394	408.236	5.8	54.2
54.4	1	45	9.2	336.839	20.7	4.8	134.909	424.475	5.1	57.4
54.4	0.5	34	7.3	277.711	19.7	5.3	121.968	435.65	5.3	59.4
54.4	0.1	28	4.4	233.63	16.3	5.6	121.966	474.43	9.1	63.8

Table B-78 Overall Dynamic Modulus test results at various test temperatures for Mix 25 Specimen 3

Temperature (°C)	Frequency (Hz)	Stress Amplitude (P-P) (KPa)	SE (%)	Dynamic Modulus (MPa)	Phase Angle (deg.)	UC (deg.)	Strain (P-P) Recoverable (microstrain)	Accumulated Strain (microstrain)	SE (%)	UC (%)
-10	25	2048	5.3	55379.92	10.3	8.7	36.975	59.503	19.6	17.4
-10	10	2083	4.7	42868.78	6	0.7	48.584	16.159	6	16.4
-10	5	2028	4.4	42014.79	4.8	0.8	48.276	12.388	12.7	16.5
-10	1	1817	1.4	36054.28	7.9	1	50.407	10.954	7.4	18
-10	0.5	1707	0.8	34942.81	8.6	1.3	48.855	12.47	8.3	18.4
-10	0.1	1558	0.5	30505.49	11.1	1.3	51.059	32.215	12.5	19.6
4.4	25	1898	5.1	31119.57	13.8	3.7	60.978	269.212	15.1	26.4
4.4	10	1856	5.3	26854.06	13.1	4	69.131	152.794	7	16.9
4.4	5	1744	4.8	24137.99	14.9	5.8	72.232	151.302	6.1	18
4.4	1	1532	1.7	17767.87	18	8	86.22	149.437	9.9	25.1
4.4	0.5	1375	1	14806.3	20.9	7.6	92.886	162.177	5.5	27.8
4.4	0.1	1298	0.5	10704.14	23.8	5.4	121.236	357.136	5.2	35.7
21.1	25	723	7.7	9394.374	23.8	3.3	76.989	521.917	8.9	45.8
21.1	10	653	7.9	7425.524	25.2	3.6	87.983	613.417	7.3	44.1
21.1	5	553	8	6166.775	26.4	3.4	89.677	660.555	6.7	45.3
21.1	1	441	5.2	3824.937	29.4	3.2	115.279	681.527	6.2	45.8
21.1	0.5	349	3.9	3131.849	30.1	3.4	111.407	704.329	6.5	46.2
21.1	0.1	284	1.2	1901.809	27.9	3	149.287	864.437	5.8	46.1
37.8	25	207	11.1	3879.708	33.7	2.9	53.362	298.245	11.8	45.8
37.8	10	191	9.6	2498.968	31.2	0.6	76.482	432.273	6.7	56.7
37.8	5	159	9.9	1999.942	30	0.3	79.372	491.798	7.3	57.8
37.8	1	119	8.2	1453.655	26	2.5	81.589	535.292	7.4	38.6
37.8	0.5	98	6.5	1326.056	23.8	2.8	73.898	552.295	6.7	22.3
37.8	0.1	82	3.2	861.202	18.1	2.2	95.575	558.907	9.5	37.3
54.4	25	75	12.4	713.66	33.8	2.8	104.766	162.214	8.9	53.3
54.4	10	69	11	574.78	27.2	3.7	119.584	307.09	5.5	52.5
54.4	5	58	10.5	468.525	24.7	3.6	124.811	378.764	5	53.4
54.4	1	46	9.3	326.729	20.6	3.9	140.883	388.998	5.6	56.7
54.4	0.5	35	7.5	263.551	19.4	4.8	131.963	398.799	6.1	59.4
54.4	0.1	28	4.3	213.306	15.4	4.7	132.91	450.156	9.1	63.1

Table B-79 Overall Dynamic Modulus test results at 14 °F (-10 °C) test temperature for Mix 26 Specimen 4

Temperature (°C)	Frequency (Hz)	Stress Amplitude (P-P) (KPa)	SE (%)	Dynamic Modulus (MPa)	Phase Angle (deg.)	UC (deg.)	Strain (P-P) Recoverable (microstrain)	Accumulated Strain (microstrain)	SE (%)	UC (%)
-10	25	2052	5.5	37498.1	8	3.5	54.71	82.626	26.1	63.6
-10	10	2091	5.1	32224.05	5.5	1	64.895	28.285	7.5	41.2
-10	5	2045	4.9	31096.65	5.3	0.9	65.774	31.216	7.3	42.3
-10	1	1827	1.9	27535.99	7.9	1.2	66.348	35.906	12.4	41.6
-10	0.5	1709	1	27107.38	3	3.2	63.063	38.577	6.8	44.1
-10	0.1	1560	0.5	24157.22	8.3	0.8	64.583	57.43	9.8	45.6
4.4	25	1911	5.7	32163.9	11.3	3.2	59.418	231.678	12.5	36.4
4.4	10	1861	5.4	24838.42	9.8	2.7	74.922	186.774	5.9	23
4.4	5	1754	5.2	23247.56	10	2.7	75.444	210.426	6.8	21.9
4.4	1	1538	2	19780.6	12.1	2.3	77.766	222.681	6.2	18.1
4.4	0.5	1378	1.2	18562.45	17.5	2.2	74.249	243.079	6	17.8
4.4	0.1	1305	0.6	14089.53	18.7	0.6	92.618	413.362	4.7	17.8
21.1	25	575	8.1	18581.63	2.2	23.8	30.948	447.763	13.2	26.2
21.1	10	545	7.8	13073.85	19.5	3.8	41.707	592.541	8.1	22.3
21.1	5	448	8.9	11336.86	21.5	3.6	39.476	624.867	8.1	18.5
21.1	1	334	7.1	7560.013	26.7	3.5	44.165	626.86	9.7	15.9
21.1	0.5	277	4.4	6149.051	30.8	2.9	45.023	644.262	8.6	15
21.1	0.1	235	1.7	3859.663	29.9	3.6	61	765.365	6.5	16
37.8	25	210	9.8	5588.563	20.9	13.4	37.526	626.16	15.3	22.8
37.8	10	198	8.6	4611.443	28.6	3.6	42.876	894.722	6.8	20.1
37.8	5	163	9	3683.734	29.6	3.5	44.267	1010.934	7.5	19
37.8	1	120	7.8	2026.093	29.6	4.6	59.391	1066.688	7.7	16.9
37.8	0.5	100	6.4	1659.757	29.5	4.6	60.368	1102.193	9.4	20.2
37.8	0.1	85	2.6	1106.671	24.2	5	76.4	1182.771	7.8	25
54.4	25	75	10.2	1681.074	17.6	26.3	44.741	270.068	13	4.6
54.4	10	72	9.6	1482.511	27.8	6.2	48.389	394.405	7	24.2
54.4	5	60	9.3	1183.721	24.8	6.2	50.807	435.409	7.4	20.1
54.4	1	47	8.8	842.914	21.9	6.7	55.657	447.771	6	18.1
54.4	0.5	35	7.1	683.292	20.4	6.6	51.255	454.126	5.6	16.4
54.4	0.1	29	4.1	550.316	16.6	6.4	52.536	473.67	7.8	19.6

Table B-80 Overall Dynamic Modulus test results at various test temperatures for Mix 26 Specimen 5

Temperature (°C)	Frequency (Hz)	Stress Amplitude (P-P) (KPa)	SE (%)	Dynamic Modulus (MPa)	Phase Angle (deg.)	UC (deg.)	Strain (P-P) Recoverable (microstrain)	Accumulated Strain (microstrain)	SE (%)	UC (%)
-10	25	2050	5.5	30600.42	4.3	20.7	66.98	75.149	22.3	52.2
-10	10	2085	4.9	32168.95	5	1.1	64.806	18.676	8.7	42.4
-10	5	2034	4.8	31389.78	4.6	1.5	64.794	19.784	9.5	44.3
-10	1	1822	1.7	28096.83	8.1	1.6	64.863	20.811	8.2	44.3
-10	0.5	1710	0.9	27550.39	11.4	3.8	62.051	21.482	12.6	47.2
-10	0.1	1557	0.5	23835.06	7.5	1.5	65.343	35.832	9.2	47
4.4	25	1896	5.5	25212.26	5.7	12.4	75.2	167.493	9.1	46.2
4.4	10	1864	5.3	24173.1	10.7	2.9	77.095	77.262	5.4	25.8
4.4	5	1758	5.2	22416.64	10.9	2.9	78.423	79.72	6.3	25
4.4	1	1540	2	18870.73	12.6	3	81.591	75.831	5.7	24.5
4.4	0.5	1379	1.2	17121.82	18.3	3	80.559	87.489	6.3	24.5
4.4	0.1	1305	0.6	13341.04	19	1.4	97.839	225.845	4.8	25.3
21.1	25	578	8.3	16691.5	5.2	24.3	34.64	209.066	14	21.1
21.1	10	543	8	12933.11	19.6	3.7	42.02	262.005	11.8	24.2
21.1	5	445	8.9	10999.57	21.4	3.2	40.445	261.845	9.6	21.3
21.1	1	335	6.5	7342.603	27.2	3.2	45.616	249.88	7.9	17.8
21.1	0.5	277	3.9	5924.575	31	2.9	46.707	252.421	9.8	17.8
21.1	0.1	235	1.4	3762.152	28.9	4.1	62.467	329.068	8.4	17.8
37.8	25	210	9.4	5798.78	17	16.2	36.128	222.592	15.9	18.8
37.8	10	197	8.7	4629.82	29	3.6	42.52	333.349	6.9	22.2
37.8	5	164	8.9	3652.524	28.9	3.9	44.984	376.399	6.9	22
37.8	1	121	7.5	2095.756	27.9	5.4	57.588	385.557	8.5	20.5
37.8	0.5	100	6	1615.874	27.9	5.1	61.868	391.223	6.1	21.7
37.8	0.1	85	2.8	1111.555	23.9	4.9	76.46	442.717	8	26.9
54.4	25	76	11	1711.402	21.7	17.9	44.361	95.583	12.4	7.3
54.4	10	72	9.9	1452.683	27.4	5.6	49.395	169.584	6.5	24.4
54.4	5	61	9.4	1206.887	25.7	5.9	50.317	197.313	6.1	21.4
54.4	1	47	8.4	803.267	22.3	6.2	58.636	201.868	5.4	16.6
54.4	0.5	35	6.7	679.073	19.4	7.1	51.355	202.096	6	18.6
54.4	0.1	28	3.1	539.512	16.9	6.1	52.488	219.518	7.3	21.1

Table B-81 Overall Dynamic Modulus test results at various test temperatures for Mix 26 Specimen 6

Temperature (°C)	Frequency (Hz)	Stress Amplitude (P-P) (KPa)	SE (%)	Dynamic Modulus (MPa)	Phase Angle (deg.)	UC (deg.)	Strain (P-P) Recoverable (microstrain)	Accumulated Strain (microstrain)	SE (%)	UC (%)
-10	25	2042	5.3	28587.89	3.1	20	71.424	66.648	10.6	26
-10	10	2081	4.5	31834.56	5.4	0.9	65.373	11.121	7.2	39.6
-10	5	2035	4.8	31081.19	5.8	1	65.487	5.964	7.3	40.8
-10	1	1824	1.6	27553.9	7.9	1	66.189	8.351	10.1	40.4
-10	0.5	1710	0.9	26605.65	3.2	3.1	64.26	9.404	7.3	42.1
-10	0.1	1557	0.4	23987.63	7.6	1.5	64.927	23.182	9.1	45.1
4.4	25	1907	5.4	22526.3	5.1	13.7	84.646	173.963	8.2	18.9
4.4	10	1855	4.7	23604.33	10.6	3	78.575	74.792	5.4	29.9
4.4	5	1746	4.7	22170.45	10.7	3.3	78.748	67.562	5.7	28.5
4.4	1	1536	1.8	18352.15	12.7	3.4	83.687	62.45	7.1	29.3
4.4	0.5	1379	1.1	16089.28	13.1	3.5	85.689	66.959	4	28.3
4.4	0.1	1304	0.5	12903.12	18.5	2	101.073	196.086	4.7	30.4
21.1	25	575	8.2	15536.07	9.7	23.7	37.008	189.61	11.2	30.7
21.1	10	545	8.1	12254.83	19.7	3.6	44.469	225.176	10.6	21.6
21.1	5	445	9	11026.54	20.6	3.4	40.373	214.739	13	21.5
21.1	1	335	6.4	7407.602	23.1	4.8	45.177	200.679	17.2	21.8
21.1	0.5	276	3.8	5512.561	25.9	4.3	50.134	200.226	8.5	17.6
21.1	0.1	235	1.4	3704.768	28.4	4.1	63.388	262.847	7.4	20
37.8	25	210	10.1	5897.961	16.6	17.1	35.59	187.897	16.2	17.3
37.8	10	197	8.8	4674.969	28.9	3.6	42.206	262.849	7.6	23.7
37.8	5	164	8.9	3673.354	28.7	4.1	44.579	289.825	7.3	22.5
37.8	1	121	7.4	2135.375	29.2	4.8	56.66	289.883	8.4	24.1
37.8	0.5	100	5.9	1616.057	29.8	4.3	62.044	291.878	8.2	23
37.8	0.1	84	2.5	1102.436	23.1	5.3	76.53	336.655	7.9	28.2
54.4	25	77	10.7	1715.573	20.8	18.9	44.939	85.255	11.8	5.2
54.4	10	70	9.7	1447.99	27.5	4.9	48.228	146.068	6.2	26.1
54.4	5	61	9.4	1156.758	25.1	5.7	52.633	171.278	7.2	21.1
54.4	1	47	8.2	813.061	21.5	6.2	58.258	174.144	5	20
54.4	0.5	35	6.4	657.866	20.4	6.2	52.981	173.568	4.9	18.2
54.4	0.1	29	3.3	521.26	16.3	5.8	54.884	186.929	7.7	22.1

Table B-82 Overall Dynamic Modulus test results at various test temperatures for Mix 27 Specimen 1

Temperature (°C)	Frequency (Hz)	Stress Amplitude (P-P) (KPa)	SE (%)	Dynamic Modulus (MPa)	Phase Angle (deg.)	UC (deg.)	Strain (P-P) Recoverable (microstrain)	Accumulated Strain (microstrain)	SE (%)	UC (%)
-10	25	2057	5.4	54029.36	11.6	9.2	38.077	109.19	35	30.1
-10	10	2094	5.1	46864.28	5.9	0.5	44.677	76.465	10.4	11.4
-10	5	2040	4.9	47001.72	5.2	0.1	43.406	77.372	8.4	11.6
-10	1	1817	1.6	42142.69	4.1	0.6	43.125	79.896	7.9	12.5
-10	0.5	1703	0.8	38906.23	8.8	0.9	43.773	81.777	7.8	13.1
-10	0.1	1558	0.5	36225.88	7.8	1.3	43.018	94.264	10.6	13.3
4.4	25	1913	5.3	28482.21	17.1	11.2	67.162	186.477	12.5	34.7
4.4	10	1867	5.3	25632.67	11.4	1.4	72.842	116.868	6.4	40.9
4.4	5	1754	4.9	23892.75	12	1.1	73.43	125.522	6	41.3
4.4	1	1535	1.7	19213.88	15.5	1.2	79.878	134.425	7.1	41.2
4.4	0.5	1375	0.9	18125.19	16.2	1.2	75.883	150.712	4.4	41.9
4.4	0.1	1304	0.5	13433.58	19.6	0.2	97.07	289.169	4.4	42
21.1	25	725	7.9	16889.97	21.5	12.9	42.899	529.778	20.6	23
21.1	10	654	7.8	13228.93	21.2	1.9	49.43	733.759	8.4	9.7
21.1	5	554	7.8	11521.28	22.5	1.7	48.043	826.939	9	9.8
21.1	1	439	4.9	7759.105	27.6	1.6	56.54	870.26	8.1	12.7
21.1	0.5	349	3.8	6262.964	30.1	3.1	55.756	901.511	9.7	15.5
21.1	0.1	284	1.1	3877.665	30.8	1.8	73.249	1085.501	7	16.3
37.8	25	211	9.7	6799.548	21.2	3.7	30.964	447.741	17.7	6.5
37.8	10	195	8.4	4565.658	28.5	2.3	42.711	689.657	8.1	11.5
37.8	5	162	8.5	3650.683	28.8	2.5	44.287	804.429	7.2	12.9
37.8	1	119	7	2145.581	27.9	3.8	55.393	853.791	7.1	16.8
37.8	0.5	99	5.6	1723.772	27.6	4.5	57.642	889.956	6.1	17.9
37.8	0.1	84	2.6	1116.934	23.6	5.2	75.554	980.514	6.5	25.8
54.4	25	76	10.6	2106.836	28.3	6.6	36.239	285.75	10.9	39
54.4	10	72	9.2	1456.248	29.5	5.2	49.299	475.97	6.7	20.4
54.4	5	60	8.6	1153.6	26.8	5.6	52.282	551.027	7.6	22.1
54.4	1	47	7.5	822.618	21.8	6	57.087	579.915	6.8	28.6
54.4	0.5	35	5.8	670.752	20.9	6.1	51.655	591.052	6.4	30.9
54.4	0.1	29	3.3	514.516	17.9	4.6	56.404	619.318	7.6	37.9

Table B-83 Overall Dynamic Modulus test results at various test temperatures for Mix 27 Specimen 2

Temperature (°C)	Frequency (Hz)	Stress Amplitude (P-P) (KPa)	SE (%)	Dynamic Modulus (MPa)	Phase Angle (deg.)	UC (deg.)	Strain (P-P) Recoverable (microstrain)	Accumulated Strain (microstrain)	SE (%)	UC (%)
-10	25	2059	5.4	38390.61	11	11.6	53.632	84.712	15.5	14.1
-10	10	2096	5.2	48958.38	6.9	2.2	42.805	51.465	8.3	5.7
-10	5	2035	4.7	47921.1	6.9	2.3	42.471	51.783	7.9	6.4
-10	1	1819	1.5	41476.7	11.8	5.7	43.853	51.029	9.1	8.6
-10	0.5	1705	0.8	38193.9	7.7	4.8	44.636	52.43	7.1	8.3
-10	0.1	1559	0.5	34504.8	12.2	5.1	45.196	68.153	8	11.8
4.4	25	1917	5.5	25069.8	17.5	9	76.458	243.062	10.9	20.3
4.4	10	1865	5.2	26251.23	16.1	4.3	71.058	177.993	6.3	17.7
4.4	5	1755	4.9	24016.21	16.6	3.9	73.058	196.613	6.4	18.3
4.4	1	1537	1.8	19111.71	18.5	4.2	80.407	209.732	7.7	21.5
4.4	0.5	1377	1	16846.29	21.1	4.2	81.763	232.755	5.4	21.8
4.4	0.1	1305	0.5	12449.43	23.1	2.9	104.843	398.391	6.2	25.5
21.1	25	736	7.6	11730.21	23.2	5.9	62.773	544.198	9.9	25.2
21.1	10	659	7.5	12619.77	24	4	52.223	718.871	8.3	30.7
21.1	5	558	7.6	11023.29	25.4	3.8	50.627	808.712	7	32.5
21.1	1	441	5.2	7378.49	30.8	4.8	59.71	850.228	7.5	31.4
21.1	0.5	349	4.2	6320.28	29.7	3.6	55.241	885.758	8	32
21.1	0.1	285	1.4	3767.282	32.9	4.1	75.784	1084.562	4.9	32.7
37.8	25	207	10.2	6216.173	31.8	10.4	33.346	611.569	18.1	50.4
37.8	10	195	8.8	4859.35	31.2	6.6	40.073	990.159	8.1	39
37.8	5	161	9.2	3893.845	31.5	6.8	41.296	1158.406	7.8	37.5
37.8	1	118	8	2307.899	31.8	6.5	51.274	1232.118	7.9	38.5
37.8	0.5	99	6.2	1864.38	30.2	6.1	53.112	1295.448	7	37.9
37.8	0.1	84	2.7	1219.854	27.8	5.5	68.938	1435.231	7.1	39.9
54.4	25	77	10.5	2670.349	33.2	8.4	28.679	333.771	13.8	42.7
54.4	10	70	9.1	1922.715	29.5	2.6	36.375	630.137	12.2	27.8
54.4	5	59	9.1	1517.687	29.1	3.3	39	744.318	7.3	29.2
54.4	1	47	8	1098.701	24.6	3	42.658	798.853	6	21.3
54.4	0.5	35	6.5	932.973	22.5	2.6	37.284	808.32	7.7	17.3
54.4	0.1	29	3.2	725.502	16.2	1.2	39.491	828.373	8.4	12.2

Table B-84 Overall Dynamic Modulus test results at various test temperatures for Mix 27 Specimen 4

Temperature (°C)	Frequency (Hz)	Stress Amplitude (P-P) (KPa)	SE (%)	Dynamic Modulus (MPa)	Phase Angle (deg.)	UC (deg.)	Strain (P-P) Recoverable (microstrain)	Accumulated Strain (microstrain)	SE (%)	UC (%)
-10	25	2058	5.4	48761.22	9.8	3.8	42.214	63.694	21.5	29.1
-10	10	2091	5.1	42341.8	8	4.2	49.385	22.751	7.6	27.7
-10	5	2036	4.8	40501.97	8.5	4.5	50.266	24.072	6.9	27.9
-10	1	1821	1.7	35264.04	9	4.6	51.653	22.931	7.4	29.7
-10	0.5	1708	0.9	35413.29	8	5.2	48.239	24.395	7.1	29.5
-10	0.1	1557	0.5	29646.37	12.5	4.2	52.518	40.977	13.3	30.9
4.4	25	1913	5.6	33062.45	14	2.5	57.856	235.704	15.2	40.1
4.4	10	1865	5.3	26953.64	13.2	3.1	69.19	168.865	6.9	34.3
4.4	5	1759	5.1	24950.62	13.8	3.3	70.491	181.272	6.2	35.8
4.4	1	1540	1.9	19787.74	16.2	3	77.812	192.135	4.4	37.2
4.4	0.5	1380	1.2	18607.43	17.6	2.8	74.164	214.562	4.1	38.2
4.4	0.1	1305	0.5	13304.81	20.9	1.4	98.1	376.834	4.4	39.7
21.1	25	580	7.6	15933.94	14.2	21.3	36.393	355.564	13.5	49.9
21.1	10	549	8	11933.8	22.5	3.8	46.018	501.604	9.2	43
21.1	5	447	8.8	10197.63	23.7	3.5	43.839	552.464	10.4	42
21.1	1	334	6.8	6572.966	26.6	3.9	50.887	562.44	7.3	45.4
21.1	0.5	277	4.2	5129.051	29.2	3.2	54.081	585.411	5.2	44.8
21.1	0.1	236	1.6	3246.882	30.5	2	72.76	735.403	4.6	45.3
37.8	25	209	8.5	5012.096	31.3	7.7	41.671	609.523	9.5	51.6
37.8	10	196	7.7	3690.532	30	2.6	53.096	964.833	6.4	43.3
37.8	5	165	7.8	2931.037	30.2	2.7	56.262	1140.387	6.1	43.8
37.8	1	121	6	1719.113	30.2	2	70.115	1218.14	6.3	43.7
37.8	0.5	100	4.7	1362.496	29.3	1.9	73.355	1274.598	5.7	43.8
37.8	0.1	85	2.4	900.191	25.3	1.6	94.383	1388.895	6.4	43.4
54.4	25	75	9.4	1663.473	35.1	9	44.861	264.407	9.3	32.6
54.4	10	71	8.8	1345.031	29.9	4.5	52.915	448.186	6.7	36.9
54.4	5	60	8	1138.39	27.3	3.6	52.653	541.279	5.8	33
54.4	1	46	6.8	830.995	22.9	2.4	55.791	574.754	5	26.4
54.4	0.5	34	5.7	751.339	19.7	1.4	45.833	590.691	6.7	18.8
54.4	0.1	29	4	692.043	15	0.1	41.686	619.497	7.8	20.1

Table B-85 Overall Dynamic Modulus test results at various test temperatures for Mix 28 Specimen 7

Temperature (°C)	Frequency (Hz)	Stress Amplitude (P-P) (KPa)	SE (%)	Dynamic Modulus (MPa)	Phase Angle (deg.)	UC (deg.)	Strain (P-P) Recoverable (microstrain)	Accumulated Strain (microstrain)	SE (%)	UC (%)
-10	25	2203	4.9	36168.69	20.8	16.2	60.922	87.955	11.1	33
-10	10	2247	4.8	37481.53	10.5	3.6	59.937	32.557	7.6	12.6
-10	5	2186	4.4	35965.55	10.9	3.7	60.771	31.879	5.8	11.4
-10	1	1961	1.3	31898.83	13.1	5.1	61.463	32.894	8.6	8.9
-10	0.5	1842	0.7	31140.01	12.3	4.7	59.153	33.809	6.1	9.3
-10	0.1	1680	0.4	26533.75	11.7	4.1	63.313	48.792	8.4	8.8
4.4	25	1759	5.4	22882.17	16.9	8.1	76.887	174.14	8.1	20.9
4.4	10	1712	5.2	22555.88	13.9	3.4	75.905	98.44	6.7	21.2
4.4	5	1610	4.4	21331.48	14.6	3.3	75.488	102.338	6.5	17.6
4.4	1	1420	1.5	17233.54	16.3	3.1	82.412	106.967	5.7	20
4.4	0.5	1276	0.9	16049.73	18.9	3.7	79.528	119.346	4.1	20.5
4.4	0.1	1208	0.5	11801.69	19.6	2.1	102.372	230.353	4	24.8
21.1	25	674	6.9	10826.36	26.4	10.9	62.286	378.73	9.3	14.3
21.1	10	642	6.8	9534.139	22.7	3.8	67.331	568.894	6.9	17.5
21.1	5	528	7	8240.882	24.1	4.2	64.129	645.385	6.7	18.8
21.1	1	393	5.1	5618.454	27.9	4.5	69.99	666.397	11.1	20.9
21.1	0.5	324	3.9	5196.052	27.5	4.5	62.392	698.955	9.3	18.2
21.1	0.1	276	1.4	3161.551	29.1	4.4	87.194	892.327	6.3	23.6
37.8	25	212	9.6	4520.164	31.2	8.6	46.801	394.26	9.9	25.4
37.8	10	198	8.6	3478.659	30.4	7.8	56.784	668.227	8	28.6
37.8	5	164	8.6	2810.519	30.3	7	58.423	801.992	9.9	30.8
37.8	1	120	6.9	1718.537	31.5	6.4	69.79	856.376	7.2	37.5
37.8	0.5	101	5.3	1396.025	31.6	7.1	72.022	900.827	8	38.7
37.8	0.1	85	2.4	950.617	28.9	7.4	89.066	1033.703	10.8	40.4
54.4	25	85	10.3	1430.742	34.6	5	59.307	368.683	9.5	36.1
54.4	10	74	9.1	1099.544	31.2	5.7	67.377	626.878	6.6	38.2
54.4	5	61	8.7	976.024	29.3	5.2	62.22	729.042	6.8	35.7
54.4	1	47	7.6	751.427	25.9	4.8	63.167	757.915	8.7	35
54.4	0.5	38	6.3	666.989	24.7	5.4	57.134	777.354	9.2	34.7
54.4	0.1	33	4.6	588.6	21.2	4.1	56.826	829.483	12.4	28.5

Table B-86 Overall Dynamic Modulus test results at various test temperatures for Mix 28 Specimen 12

Temperature (°C)	Frequency (Hz)	Stress Amplitude (P-P) (KPa)	SE (%)	Dynamic Modulus (MPa)	Phase Angle (deg.)	UC (deg.)	Strain (P-P) Recoverable (microstrain)	Accumulated Strain (microstrain)	SE (%)	UC (%)
-10	25	2202	5	80692.81	9.6	17.3	27.293	85.901	25.5	27.2
-10	10	2253	4.8	55527.96	6.8	0.5	40.578	53.054	10.2	14
-10	5	2196	4.6	53103.4	6	0.7	41.358	55.721	9.4	14
-10	1	1963	1.5	48748.78	1.6	1.7	40.275	56.032	17.9	14.2
-10	0.5	1842	0.9	43172.39	12.5	1.4	42.66	57.555	13.6	15.6
-10	0.1	1679	0.5	41713.68	5.8	2.1	40.258	64.189	20.4	13.7
4.4	25	1762	5.5	46603.97	10.1	14.2	37.814	88.411	14.1	8.5
4.4	10	1717	5.1	35265.07	10.1	0.7	48.687	43.603	8.3	14.4
4.4	5	1619	5	32220.7	11.8	0.2	50.246	46.346	8.4	15.6
4.4	1	1422	1.8	27877.59	11.1	0.8	50.999	46.362	6.1	15.9
4.4	0.5	1277	1.1	24929.65	12.3	0.7	51.23	50.949	8.7	16.6
4.4	0.1	1207	0.5	19946.62	17.9	2	60.503	114.484	9.2	15.9
21.1	25	671	6.8	16287.98	15.8	2	41.223	193.256	9	21.7
21.1	10	636	7	15675.83	19.6	4.5	40.558	282.247	8.6	20.1
21.1	5	523	6.7	14628.79	21.1	4.6	35.772	312.953	10.9	18
21.1	1	392	4.6	11190.79	22.9	5.1	35.047	313.191	12.8	19.7
21.1	0.5	323	3.4	8988.685	28.1	4.9	35.96	321.922	8	20.1
21.1	0.1	275	1	6673.406	26.4	2.5	41.255	390.124	8.9	17.2
37.8	25	208	9.2	7026.604	22.4	2.7	29.661	299.962	14.1	34.2
37.8	10	195	8.4	5107.172	25.5	1.9	38.089	527.369	9.2	42.5
37.8	5	160	8.4	4248.592	25.4	2.2	37.768	623.482	8.7	42.2
37.8	1	118	6.3	2783.746	27.7	2.4	42.317	649.681	8.8	43.9
37.8	0.5	98	5	2290.221	26.6	2.7	42.668	671.111	7.8	43.5
37.8	0.1	82	2.9	1592.425	25.2	2.9	51.269	743.579	6.4	46.8
54.4	25	83	10.3	2533.93	25.4	6.8	32.786	361.886	11.7	32.5
54.4	10	73	9.2	1858.231	28.7	4.8	39.108	589.09	9.5	2.9
54.4	5	61	9.4	1550.522	26.9	4.7	39.157	676.248	11.5	3.2
54.4	1	47	7.5	1107.053	22.2	4.6	42.36	702.297	7.7	5.1
54.4	0.5	37	6.2	928.404	24.1	4.7	39.801	719.105	6.7	4.6
54.4	0.1	33	4.7	753.11	19.6	3.8	43.229	759.898	9.9	6.2

Table B-87 Overall Dynamic Modulus test results at various test temperatures for Mix 28 Specimen 13

Temperature (°C)	Frequency (Hz)	Stress Amplitude (P-P) (KPa)	SE (%)	Dynamic Modulus (MPa)	Phase Angle (deg.)	UC (deg.)	Strain (P-P) Recoverable (microstrain)	Accumulated Strain (microstrain)	SE (%)	UC (%)
-10	25	2216	5.1	45158.31	15.6	6.2	49.062	83.33	21.8	36.8
-10	10	2255	4.9	41357.25	11.6	4.5	54.514	30.46	8.1	33.1
-10	5	2187	4.3	40188.23	11.9	4.5	54.431	27.722	6.5	32.5
-10	1	1960	1.3	36087.09	14	2	54.309	28.69	8.2	31.2
-10	0.5	1843	0.8	36364.25	12.9	4	50.672	31.109	13.2	34.3
-10	0.1	1680	0.4	30576.82	16.4	1.3	54.95	50.622	11.9	32.3
4.4	25	1766	5.4	27869.56	13.9	3.1	63.358	155.185	16.2	19.3
4.4	10	1723	5.4	24044.16	18.4	0.1	71.652	74.184	8.7	19.4
4.4	5	1618	4.8	22095.8	19.2	0.3	73.228	78.328	6.7	20.1
4.4	1	1423	1.7	17542.02	21.4	1	81.123	78.228	6.4	21
4.4	0.5	1276	1	15824.24	19.5	1.6	80.606	88.92	5.5	19.7
4.4	0.1	1209	0.4	12368.88	23.7	1.2	97.783	172.797	6.3	23.1
21.1	25	675	7	11056.69	23.6	1.1	61.042	313.893	10.6	23.8
21.1	10	641	6.6	8964.564	24.7	1.1	71.538	418.928	7.7	21.5
21.1	5	529	7	7922.716	25.7	1.4	66.747	459.498	7.6	22.7
21.1	1	393	5.1	5636.72	28.5	1.3	69.678	460.504	13.4	23.8
21.1	0.5	324	3.8	4687.382	30.5	1.3	69.151	482.103	6.9	22.7
21.1	0.1	276	1.1	3202.865	31.9	2	86.022	627.713	6.6	24.7
37.8	25	210	8.2	5329.045	28.1	5.2	39.324	433.977	9.4	47.5
37.8	10	197	7.9	4090.852	28	3.6	48.205	689.085	8.6	47.8
37.8	5	164	7.9	3393.356	27.2	2.4	48.364	791.596	8.1	50.5
37.8	1	121	5.6	2193.252	27.6	1.2	55.303	818.847	6.3	56.5
37.8	0.5	101	4.4	1783.965	28.1	1.3	56.419	844.676	6.4	58
37.8	0.1	84	1.8	1153.558	28.5	1.8	73.018	952.996	6	57.1
54.4	25	86	9.8	1811.424	29.9	1.6	47.327	437.532	8.2	31.8
54.4	10	75	9	1385.982	26.8	1.8	53.907	717.954	6.5	48.1
54.4	5	61	8.5	1147.816	25.9	2.2	53.027	825.709	6.4	49.9
54.4	1	47	6.6	766.666	24.7	1.4	61.035	861.95	6.2	54.2
54.4	0.5	38	5.1	643.856	21.9	2.2	59.674	880.351	6.8	54.9
54.4	0.1	33	3.6	491.881	19.6	1.3	67.67	954.451	6.3	60.5

Table B-88 Overall Dynamic Modulus test results at various test temperatures for Mix 29 Specimen 2

Temperature (°C)	Frequency (Hz)	Stress Amplitude (P-P) (KPa)	SE (%)	Dynamic Modulus (MPa)	Phase Angle (deg.)	UC (deg.)	Strain (P-P) Recoverable (microstrain)	Accumulated Strain (microstrain)	SE (%)	UC (%)
-10	25	2224	5.4	40307.86	8.4	5.8	55.178	87.496	15.4	32.1
-10	10	2271	5.2	36536.07	7.1	1.3	62.144	35.239	6.8	32.4
-10	5	2208	5	35811.09	6.6	1.6	61.666	35.656	8.9	32.9
-10	1	1968	1.7	31246.55	8.3	1.6	62.996	37.818	5.2	33.1
-10	0.5	1843	0.9	30047.8	10	2	61.319	40.608	4	33.9
-10	0.1	1681	0.5	26308.58	9	1.9	63.905	63.4	8.3	34.2
4.4	25	1774	5.7	25412.58	10.2	3.7	69.797	270.939	8.4	28.9
4.4	10	1729	6.3	23016.26	12.5	1.4	75.137	217.851	6.9	35.4
4.4	5	1625	5.4	21148.14	13.1	1.6	76.85	241.202	6	35.8
4.4	1	1427	2.1	16746.84	16	1.4	85.213	257.929	4.5	37.1
4.4	0.5	1279	1.2	15067.46	19.2	1.1	84.856	287.383	3.3	37.6
4.4	0.1	1209	0.5	11167.12	21.6	1.5	108.243	475.357	3.2	39.3
21.1	25	678	7	12739.37	21.1	3.5	53.189	573.542	10.1	29.2
21.1	10	641	6.9	10275.87	23.7	1.8	62.411	757.881	6.8	33.4
21.1	5	529	7.3	8860.583	24.9	2.3	59.751	821.856	6.7	36.5
21.1	1	393	5.6	5677.128	29	1.8	69.188	842.594	6.3	39.8
21.1	0.5	325	4.4	4644.188	28.6	2.3	69.911	877.421	7	40.6
21.1	0.1	276	1.5	2697.848	31	2.2	102.366	1081.471	5.3	39.5
37.8	25	212	9.9	3690.832	37.1	4.4	57.357	298.769	11.1	30
37.8	10	176	9.3	2485.356	34.8	3.7	70.977	418.166	7.8	29.5
37.8	5	143	9.2	1923.726	34.5	4.2	74.126	476.473	8.2	30.2
37.8	1	100	8.1	1092.436	33.2	5.1	91.479	492.411	7.3	28.5
37.8	0.5	79	6	848.588	32	4.6	93.618	500.07	6.5	29.7
37.8	0.1	59	3.2	480.215	25.7	3.5	123.627	503.909	7.9	37.4
54.4	25	64	11.1	850.375	38.4	2	75.041	193.659	8.7	41
54.4	10	53	9	620.922	32	2.8	85.32	286.001	6.4	40.1
54.4	5	40	8	500.092	29.1	3.3	79.266	305.044	5.1	41.9
54.4	1	29	7.3	333.444	23.3	4.5	86.135	302.031	6.1	53.2
54.4	0.5	24	5.9	282.503	21.4	4.7	83.847	310.134	6	61.6
54.4	0.1	18	3.5	234.984	14.7	4.1	78.279	336.651	8.1	74.7

Table B-89 Overall Dynamic Modulus test results at various test temperatures for Mix 29 Specimen 6

Temperature (°C)	Frequency (Hz)	Stress Amplitude (P-P) (KPa)	SE (%)	Dynamic Modulus (MPa)	Phase Angle (deg.)	UC (deg.)	Strain (P-P) Recoverable (microstrain)	Accumulated Strain (microstrain)	SE (%)	UC (%)
-10	25	2214	5	42870	1.8	3.6	51.635	109.014	9.6	35.2
-10	10	2270	5.1	49443.67	6.9	0.8	45.903	69.889	6.8	8.1
-10	5	2205	4.8	48791.25	6.5	0.8	45.198	71.73	7.2	7
-10	1	1968	1.6	42457.72	9.6	1.5	46.357	72.851	6.9	6.1
-10	0.5	1843	0.8	40378.34	7.3	0.2	45.632	75.104	9.2	5.4
-10	0.1	1682	0.5	36116.1	8.8	0.5	46.565	91.263	9.3	3.7
4.4	25	1763	5.6	34382.04	9.4	1	51.285	185.761	9.9	10.1
4.4	10	1714	4.9	32574.36	11.6	1.8	52.604	153.553	6.1	3.5
4.4	5	1615	4.5	29876.38	12.4	1.8	54.058	172.48	5.8	4.1
4.4	1	1422	1.6	24755.48	13.7	2.2	57.454	186.424	11.8	6.6
4.4	0.5	1277	1	21366.83	18.6	2.9	59.765	209.243	4.1	9.5
4.4	0.1	1207	0.5	16569.79	20.2	2.5	72.87	357.473	5.5	13
21.1	25	674	7.1	19683.14	17.2	5.8	34.223	410.213	10.8	29
21.1	10	639	7.3	16134.8	18.6	2.6	39.626	668.706	8.2	24.5
21.1	5	526	7.4	14171.11	19.4	2.7	37.135	775.519	8.5	25.8
21.1	1	394	5	10183.84	23.9	3.2	38.688	808.258	8.5	33.1
21.1	0.5	324	3.7	8598.164	27.3	2.1	37.729	845.688	9.1	34.5
21.1	0.1	275	1.1	5280.984	31.2	0.6	52.03	1054.116	7.1	34.6
37.8	25	212	9	7987.296	29.1	0.9	26.596	607.487	11.4	35.9
37.8	10	177	9	5642.224	27.5	1.8	31.313	890.574	9.9	33.5
37.8	5	142	9.3	4618.945	27.9	2.4	30.851	1016.302	15.2	36.1
37.8	1	100	7.9	2618.045	29.5	0.5	38.369	1033.307	9.9	35.8
37.8	0.5	80	6	2023.556	30.7	1.7	39.62	1049.548	12.7	34.7
37.8	0.1	59	2.9	1283.537	24.6	0.2	46.174	1091.03	9.4	35.6
54.4	25	105	9.6	1442.564	34.8	3.2	72.589	802.674	8.2	75.4
54.4	10	80	8.9	998.456	29.3	1.6	80.394	1025.359	6.2	80.3
54.4	5	70	9	804.105	27.3	1.6	87.045	1163.75	5.5	80.4
54.4	1	49	7.2	508.105	22.1	1.5	96.047	1182.022	5.7	82.9
54.4	0.5	39	5.8	422.676	19.9	2.1	92.19	1187.618	5.7	86.4
54.4	0.1	34	3	329.303	16.3	2	102.829	1227.073	8.8	88.9

Table B-90 Overall Dynamic Modulus test results at various test temperatures for Mix 29 Specimen 10

Temperature (°C)	Frequency (Hz)	Stress Amplitude (P-P) (KPa)	SE (%)	Dynamic Modulus (MPa)	Phase Angle (deg.)	UC (deg.)	Strain (P-P) Recoverable (microstrain)	Accumulated Strain (microstrain)	SE (%)	UC (%)
-10	25	2199	5	50588.61	4.1	2.5	43.474	87.459	9.9	1.8
-10	10	2254	4.6	54107.96	5.9	1	41.657	58.668	7.8	7.6
-10	5	2189	4.2	52075.5	6.6	1	42.04	57.687	6.2	7.5
-10	1	1960	1.3	48759.98	8.4	0.7	40.201	57.935	14.1	5.5
-10	0.5	1842	0.7	48651.9	5	1.8	37.852	59.256	13.6	4.2
-10	0.1	1681	0.5	41025.32	8.2	0.9	40.98	69.651	10.2	3.9
4.4	25	1769	5.4	37026.4	8	0.4	47.769	99.781	7.7	3.6
4.4	10	1717	4.9	36347.93	10	1.6	47.249	62.997	7.8	0.5
4.4	5	1612	4.5	34154.3	11.4	1.5	47.212	68.84	6.4	1.1
4.4	1	1421	1.5	28169.3	12.3	1.8	50.435	70.236	7.2	3.3
4.4	0.5	1276	0.9	27130.15	13.2	2	47.051	76.531	5.2	4.7
4.4	0.1	1208	0.5	20452.23	16.3	1.3	59.047	133.351	4.8	4.5
21.1	25	995	6	19333.04	16.7	1	51.457	459.275	10.6	10.5
21.1	10	965	5.9	17094.14	17.9	1.7	56.463	637.533	6.9	12.7
21.1	5	797	5.9	15088.41	19.1	1.7	52.808	723.614	7	15.7
21.1	1	591	3.4	10952.42	23.5	1.6	53.997	746.337	8	19.4
21.1	0.5	487	2.5	9416.386	20.9	3	51.697	775.047	6.5	21.3
21.1	0.1	412	1.1	6342.68	25.9	1.3	64.915	942.094	7.1	24.5
37.8	25	330	9.1	7472.012	28.4	1.8	44.22	417.332	9.2	20.8
37.8	10	281	8.1	5646.242	27.7	2.1	49.808	617.615	6.9	24.9
37.8	5	229	8.2	4647.167	26.4	0.7	49.223	706.108	6.6	28.9
37.8	1	161	5.5	2864.062	27	1.4	56.228	717.415	8.1	32.4
37.8	0.5	128	3.9	2240.769	26.5	1	57.051	723.685	6.1	33.7
37.8	0.1	95	1.5	1447.5	23.1	1.1	65.891	762.718	6.1	34.2
54.4	25	107	9.5	2163.447	34.2	3.6	49.622	333.765	9	32.4
54.4	10	83	8.4	1621.204	30.6	8.1	51.105	455.536	6.4	25.8
54.4	5	71	7.8	1310.155	28.7	7.2	54.338	521.746	5.7	23
54.4	1	49	5.9	928.722	22.6	4.8	53.187	525.244	5.2	27.3
54.4	0.5	39	4.7	814.582	20.7	2.3	48.011	527.249	6.2	31.3
54.4	0.1	34	2.5	633.681	15.6	2.7	53.116	544.565	6.8	26.7

Table B-91 Overall Dynamic Modulus test results at various test temperatures for Mix 30 Specimen 1

Temperature (°C)	Frequency (Hz)	Stress Amplitude (P-P) (KPa)	SE (%)	Dynamic Modulus (MPa)	Phase Angle (deg.)	UC (deg.)	Strain (P-P) Recoverable (microstrain)	Accumulated Strain (microstrain)	SE (%)	UC (%)
-10	25	2058	5	47374.33	12.4	11.8	43.447	101.44	12.2	11.7
-10	10	2089	4.8	47247.24	6	0.7	44.213	71.14	8.1	13.9
-10	5	2033	4.5	45163.1	6.4	0.5	45.02	72.133	8.7	13.1
-10	1	1816	1.4	41938.6	6.3	0.8	43.292	71.348	13.8	15.8
-10	0.5	1704	0.7	37771.35	4.5	1.3	45.102	72.515	9.8	15.1
-10	0.1	1559	0.5	35362.07	8.3	1	44.081	83.899	9.7	17.7
4.4	25	1917	5.3	29498.77	9.9	3.4	64.981	143.579	10.4	20.3
4.4	10	1865	5.2	29377.06	8.8	0.1	63.479	80.805	7.7	17.4
4.4	5	1752	5	27235.65	9.8	0.5	64.335	83.651	7.9	18
4.4	1	1535	1.7	23808.03	10.5	1.5	64.465	85.921	7.1	20.6
4.4	0.5	1375	0.9	21693.05	10.2	2	63.405	91.336	6.5	21.6
4.4	0.1	1303	0.5	18085.77	15.4	1.8	72.065	147.362	7.1	20.4
21.1	25	575	7.8	15253.65	23.8	13.5	37.699	48.01	13.1	22.3
21.1	10	542	7.7	15198.03	17.4	6.7	35.689	58.25	9.6	20.6
21.1	5	442	8.2	13582.94	17.3	7.5	32.574	52.829	10.7	20.7
21.1	1	332	5.7	10228	18.9	7.5	32.507	46.418	17.1	18.6
21.1	0.5	275	3.6	8832.061	16.4	10	31.154	47.013	11.7	16.2
21.1	0.1	234	1.5	7302.016	22.5	6.6	32.057	75.234	13	16.3
37.8	25	207	9.8	6762.313	19	4.6	30.637	96.485	14.5	39.3
37.8	10	194	9.2	6563.408	22.2	3.5	29.625	164.951	16.2	49.7
37.8	5	161	9.6	5715.615	19.2	6	28.224	177.788	13.5	49.9
37.8	1	119	7.4	3961.49	23.1	6	30.055	179.4	16.5	50.9
37.8	0.5	99	5.6	3405.176	25.7	6.2	29.204	188.315	12.3	50.4
37.8	0.1	84	2.2	2588.203	27.3	7.2	32.323	242.897	10.9	45.2
54.4	25	166	10.2	3855.848	24.1	3.3	42.951	536.557	11.6	58.1
54.4	10	155	9.6	3073.292	23.6	3.7	50.553	897.899	8.9	54.7
54.4	5	133	9.6	2561.227	23.8	4.9	52.117	1046.508	11	55.4
54.4	1	105	7.7	1780.557	25.3	5.9	59.206	1100.725	7	56
54.4	0.5	78	5.6	1490.015	26.7	6.5	52.237	1129.195	7.6	50.1
54.4	0.1	65	2.7	1105.249	27	6.7	58.508	1231.63	7.8	48.8

Table B-92 Overall Dynamic Modulus test results at various test temperatures for Mix 30 Specimen 5

Temperature (°C)	Frequency (Hz)	Stress Amplitude (P-P) (KPa)	SE (%)	Dynamic Modulus (MPa)	Phase Angle (deg.)	UC (deg.)	Strain (P-P) Recoverable (microstrain)	Accumulated Strain (microstrain)	SE (%)	UC (%)
-10	25	1853	5.6	35907.55	8.6	10.7	51.598	168.994	27.1	34.1
-10	10	1880	5.2	34055.06	8.6	3.2	55.201	124.539	8.7	14.3
-10	5	1833	4.8	32331.91	8.5	3	56.685	123.142	8.8	16
-10	1	1636	1.7	27420.65	9.9	4.5	59.671	123.748	7.1	19.6
-10	0.5	1536	1	26329.29	10.6	5	58.326	125.854	8.5	22.9
-10	0.1	1403	0.5	22742.43	12.3	3.4	61.707	150.351	10.3	25.8
4.4	25	1120	6.1	20143.44	9.4	19.7	55.619	113.95	17.3	34.3
4.4	10	1072	6.1	20756.42	12.2	1.9	51.66	85.278	7.8	24.3
4.4	5	1013	5.8	18757.54	14	2.7	54.007	88.649	8.5	25.5
4.4	1	892	2.8	15425.51	15.4	4.5	57.854	91.609	5.6	30
4.4	0.5	800	1.9	13882.67	17	4.8	57.598	100.218	5.4	33.2
4.4	0.1	757	0.7	10476.42	19.7	4.3	72.28	172.366	5.1	37.3
21.1	25	471	8.4	10758.77	19.8	8.5	43.776	142.456	15	26.7
21.1	10	439	8.6	11619.81	16	0.2	37.796	206.347	9.5	17.8
21.1	5	357	9	10724.48	16.2	0.8	33.311	221.519	10.2	20.5
21.1	1	273	5	7574.844	19.7	0.5	36.019	221.294	7.5	20.2
21.1	0.5	225	3.4	6617.865	18.3	1.4	34.017	224.366	7.5	20.8
21.1	0.1	191	1.4	4864.645	22.4	0.8	39.299	271.481	8.8	18.8
37.8	25	180	9.2	5548.969	23.8	10.4	32.423	458.92	13.9	26.2
37.8	10	167	8.5	4385.521	25.2	6.5	38.051	744.217	11.7	16.9
37.8	5	139	8.4	3950.322	21.7	3	35.207	860.351	8.1	2.3
37.8	1	104	6.4	2850.206	22	3.3	36.652	886.252	15.3	3.4
37.8	0.5	87	4.6	2359.908	22.3	1.7	36.691	907.182	7.9	0.9
37.8	0.1	72	2	1732.839	24.2	1	41.688	981.878	5.8	1.2
54.4	25	84	9.6	2116.298	27.8	6.9	39.824	103.687	8.4	41.9
54.4	10	71	8.7	1670.901	25.7	7.2	42.357	161.514	6.6	38.5
54.4	5	60	8.4	1477.163	25.6	7.8	40.712	180.846	7.1	35.7
54.4	1	49	6.5	1235.854	24.2	1.8	39.801	188.391	6.6	8.1
54.4	0.5	39	4.7	1029.207	20.6	1.6	37.464	187.764	8.3	4.6
54.4	0.1	29	2.7	771.526	18.5	1	36.953	196.661	9.5	6.6

Table B-93 Overall Dynamic Modulus test results at various test temperatures for Mix 30 Specimen 9

Temperature (°C)	Frequency (Hz)	Stress Amplitude (P-P) (KPa)	SE (%)	Dynamic Modulus (MPa)	Phase Angle (deg.)	UC (deg.)	Strain (P-P) Recoverable (microstrain)	Accumulated Strain (microstrain)	SE (%)	UC (%)
-10	25	1845	5.4	34585.95	14.9	5.8	53.335	129.917	33	22.6
-10	10	1870	4.9	38823.82	9	3.2	48.155	92.423	8.2	20.8
-10	5	1824	4.8	37096.4	9.5	3.2	49.158	97.757	8.5	22.3
-10	1	1635	1.7	35805.68	7.8	2.9	45.656	96.71	12	29.9
-10	0.5	1536	0.9	30721.88	10.7	2.8	49.998	99.496	11.7	25.3
-10	0.1	1400	0.5	27209.23	11.9	3.4	51.454	116.886	12	23.3
4.4	25	1114	6	20760.21	14.4	7.2	53.665	83.059	21.8	35.1
4.4	10	1069	6.4	22898.33	12.9	3.7	46.681	57.1	8	22.2
4.4	5	1006	5.6	21668.9	13.6	3.3	46.407	59.822	8.3	25.7
4.4	1	890	2.5	18267.27	15.6	2.5	48.731	60.856	10.4	27.7
4.4	0.5	799	1.6	17155.28	19.4	5.1	46.566	67.172	6.6	29.3
4.4	0.1	755	0.6	13053.06	19.2	3.1	57.817	112.706	7.1	26.9
21.1	25	469	7.9	11760.42	12.3	7.8	39.919	129.807	15.8	24.1
21.1	10	441	8.1	10182.61	20.7	4.2	43.271	180.815	13.2	30.9
21.1	5	356	8.7	8860.715	22.1	4.3	40.222	192.713	17.1	26.2
21.1	1	273	4.6	7023.654	26.1	5	38.87	190.722	11.3	26.8
21.1	0.5	226	3.1	6231.303	24.7	4.1	36.271	197.522	12.6	23.5
21.1	0.1	191	1.1	4386.783	26.1	3.2	43.647	255.105	7.9	17.8
37.8	25	181	9.4	6781.607	22.2	10.4	26.741	305.723	21.4	37.4
37.8	10	170	7.8	4721.551	27.6	5.4	35.922	513.201	8.4	25.7
37.8	5	142	7.5	4200.113	26.8	4.8	33.813	603.981	9.3	18.6
37.8	1	104	5.8	3095.458	28	5.1	33.462	641.115	6.6	8.2
37.8	0.5	87	4.1	2733.314	28.2	5.7	31.779	675.703	7.2	4.2
37.8	0.1	73	1.8	1895.716	28.7	5.7	38.439	767.77	6.7	2.7
54.4	25	106	10.2	2771.896	26.7	10.9	38.335	80.505	14.8	41.5
54.4	10	92	8.7	2151.614	26.1	4.1	42.791	149.391	7.7	35.8
54.4	5	77	8.2	1848.478	24.5	3.7	41.431	172.436	6.8	28.8
54.4	1	59	7	1357.818	23.2	3	43.482	179.887	6.6	25.3
54.4	0.5	49	6.2	1170.178	22.6	2.2	42.26	185.393	8.6	24.5
54.4	0.1	43	3.5	852	19.6	2.3	50.305	218.576	7.9	24.5

Table B-94 Overall Dynamic Modulus test results at various test temperatures for Mix 31 Specimen 2

Temperature (°C)	Frequency (Hz)	Stress Amplitude (P-P) (KPa)	SE (%)	Dynamic Modulus (MPa)	Phase Angle (deg.)	UC (deg.)	Strain (P-P) Recoverable (microstrain)	Accumulated Strain (microstrain)	SE (%)	UC (%)
-10	25	2281	5.1	53927.77	3.9	1.7	42.304	91.756	22	29.9
-10	10	2327	4.6	42448	7.2	2.3	54.825	47.131	7.1	9.9
-10	5	2267	4.5	40020.47	7.1	2.6	56.643	49.355	5.8	11.1
-10	1	2027	1.8	36428.66	5.9	3.5	55.64	48.459	10.8	11.5
-10	0.5	1897	0.9	33588.18	10.7	2.4	56.47	51.117	9.1	12.5
-10	0.1	1730	0.5	30695.55	8.9	3.1	56.348	63.773	6.5	13.4
4.4	25	2108	5.2	30183.81	10.1	1.5	69.841	207.213	12.2	25.4
4.4	10	2052	4.5	23387.63	11.2	2.5	87.724	121.757	7.2	11.1
4.4	5	1930	4.3	21376.64	12	2.7	90.297	127.687	7.2	10.3
4.4	1	1696	1.6	17705.62	14.7	2.5	95.766	132.566	7	13.7
4.4	0.5	1521	0.9	16835.3	14.2	3.5	90.359	144.637	5.3	17.1
4.4	0.1	1441	0.5	12616.9	18.3	3.2	114.173	265.864	4.5	18.5
21.1	25	785	7.5	14883.11	18.5	3.8	52.713	241.059	14.1	49.1
21.1	10	712	6.9	11367.65	17.6	3.3	62.626	304.242	6.5	27.2
21.1	5	604	7	10081.14	18.3	3.2	59.945	323.271	6	29.7
21.1	1	476	4.8	7378.697	21.1	3.2	64.552	325.483	7.2	33.7
21.1	0.5	377	3.9	6324.609	21.9	3.4	59.595	331.453	5.2	35.3
21.1	0.1	313	1.6	4696.798	24.3	2.7	66.685	409.92	6.3	39.3
37.8	25	282	9.8	5213.125	20.1	7.6	54.137	417.505	10.9	55.7
37.8	10	250	7.7	4402.667	21.9	2	56.876	627.905	6.3	54.7
37.8	5	202	7.7	3724.441	22.6	1.8	54.344	688.157	6.6	56.9
37.8	1	154	6.6	2433.506	25	2.1	63.158	694.74	6.3	62.5
37.8	0.5	126	5.3	2013.737	25.9	2.2	62.621	707.251	6.9	62.8
37.8	0.1	97	2.1	1390.966	26.4	2.2	70.059	783.546	6.5	62.7
54.4	25	183	9.6	2713.622	22	7.6	67.404	446.041	11.7	16.7
54.4	10	136	7.1	2113.659	27.6	6.2	64.379	605.678	6.6	9.9
54.4	5	116	7.6	1686.702	27.2	6.1	68.765	663.075	5.9	15
54.4	1	85	5.4	1043.782	27.8	6.7	81.842	663.724	5.5	23
54.4	0.5	66	4.5	834.842	27.3	6.9	78.874	666.005	5.5	26.3
54.4	0.1	58	3.5	598.328	23.3	5.6	97.257	751.255	7.7	37.3

Table B-95 Overall Dynamic Modulus test results at various test temperatures for Mix 31 Specimen 3

Temperature (°C)	Frequency (Hz)	Stress Amplitude (P-P) (KPa)	SE (%)	Dynamic Modulus (MPa)	Phase Angle (deg.)	UC (deg.)	Strain (P-P) Recoverable (microstrain)	Accumulated Strain (microstrain)	SE (%)	UC (%)
-10	25	2262	4.8	37488.82	14	10.1	60.344	112.67	10.8	38.1
-10	10	2315	4.4	33496.86	8	2	69.119	55.602	5.7	27.7
-10	5	2255	4.5	32171.89	8.2	2.3	70.093	52.521	5.6	28.7
-10	1	2020	1.4	29560.18	9.3	2.9	68.348	52.847	4	29.4
-10	0.5	1896	0.8	28769.7	8.7	2.5	65.905	53.808	4.4	29.1
-10	0.1	1728	0.5	25118.65	9.5	2.3	68.783	68.331	4.5	30.5
4.4	25	1761	5.4	22277.7	7	9.1	79.061	184.26	8.2	45
4.4	10	1710	5	20387.57	12.6	2.8	83.875	97.402	5.9	41.6
4.4	5	1606	4.4	19096.68	12.9	3	84.079	99.975	5.1	41.5
4.4	1	1421	1.7	15966.27	14.8	3.4	88.969	102.919	6.3	41.7
4.4	0.5	1275	1	14776.01	14	3.6	86.315	112.619	2.4	41.1
4.4	0.1	1206	0.5	11766.5	18.4	3.4	102.529	206.058	4	43.1
21.1	25	785	6.3	12436.57	17.1	5.6	63.117	262.489	7.1	29.8
21.1	10	706	6	11168.48	18.8	3.2	63.201	311.879	5.7	35.2
21.1	5	597	5.5	10059.11	19.5	3	59.315	330.812	5.3	33.3
21.1	1	477	3	7120.481	22.2	3.9	66.952	332.594	4.8	33
21.1	0.5	378	2.4	6387.788	23.6	3.2	59.156	338.175	4.8	28.5
21.1	0.1	315	1	4582.039	24.6	1.1	68.836	426.702	6.5	24.4
37.8	25	355	7.8	6700.764	22.6	1.8	53.021	307.215	7.5	26
37.8	10	308	7.3	5388.697	21.4	2.2	57.139	423.527	4.2	23.2
37.8	5	255	5.2	4366.978	22.3	2.4	58.405	457.574	4.2	21.3
37.8	1	192	3.4	2847.282	23.2	3.2	67.564	456.904	4.2	22
37.8	0.5	162	2.4	2334.442	23.4	3.6	69.396	465.322	4.2	23.8
37.8	0.1	125	1.1	1564.781	22.8	3.6	79.811	533.411	4.8	30
54.4	25	139	7.4	2459.066	27	3	56.41	130.213	6.5	22.8
54.4	10	105	6.4	1789.865	25.4	3.6	58.696	162.279	5.3	29.1
54.4	5	89	6.1	1478.409	25.2	3.2	60.3	184.358	4.1	32.3
54.4	1	68	4.5	938.439	24.5	2.9	72.327	192.087	3.9	39.2
54.4	0.5	50	3.6	770.194	23.1	3.2	64.444	196.417	5.4	41.5
54.4	0.1	45	2.6	559.552	20	2.6	80.091	249.047	6.7	44.8

Table B-96 Overall Dynamic Modulus test results at various test temperatures for Mix 31 Specimen 7

Temperature (°C)	Frequency (Hz)	Stress Amplitude (P-P) (KPa)	SE (%)	Dynamic Modulus (MPa)	Phase Angle (deg.)	UC (deg.)	Strain (P-P) Recoverable (microstrain)	Accumulated Strain (microstrain)	SE (%)	UC (%)
-10	25	2264	5.2	53110.52	22.1	6.8	42.634	109.208	39.8	21.7
-10	10	2309	4.7	63516.92	7.5	1.3	36.351	81.981	8.9	17.9
-10	5	2245	4.4	60937.32	7.2	1.5	36.847	86.534	9.9	18.7
-10	1	2016	1.4	54757.24	10.2	1.4	36.825	87.576	11.7	19.7
-10	0.5	1895	0.8	53665.31	13.9	2.3	35.31	90.239	16.4	21.9
-10	0.1	1727	0.5	45418.2	11.5	1.2	38.022	105.792	13.4	21.9
4.4	25	1765	5.6	43804.35	12.2	2.5	40.294	108.924	44.6	42.1
4.4	10	1707	5.3	40298.07	11.7	1.1	42.351	63.57	7.7	17.7
4.4	5	1600	4.7	37286.04	12.8	1.3	42.924	65.326	6.6	17.9
4.4	1	1418	1.6	31438.96	13.8	1.3	45.092	65.512	7.5	20.6
4.4	0.5	1276	1	28098.71	19.2	3.5	45.423	69.753	9.4	20.9
4.4	0.1	1208	0.5	21992.86	18.3	1.3	54.913	114.956	6.4	21.6
21.1	25	785	7	21985.2	3.7	14.3	35.72	167.768	23.7	34.1
21.1	10	709	6.8	17498.99	19.5	3.4	40.497	200.271	8	9.7
21.1	5	599	6.4	15409.45	20.9	3.7	38.868	212.559	8	9.4
21.1	1	478	3.5	11182.98	25.2	4.3	42.732	215.499	5.5	8.4
21.1	0.5	378	2.7	9929.429	25.6	4.2	38.094	220.336	7.7	3.9
21.1	0.1	315	1.1	6914.117	26.3	3.8	45.602	281.11	7.7	2.9
37.8	25	356	9.6	7201.051	24.6	4.1	49.416	711.307	10.4	14.6
37.8	10	309	8.7	5826.477	26.8	1.9	53.101	1075.572	7.2	24.9
37.8	5	257	6.8	4598.852	26.7	2	55.803	1243.089	6.5	24.9
37.8	1	192	4.4	2968.811	28.4	2.7	64.676	1309.829	5.7	23.2
37.8	0.5	160	2.9	2490.084	28.6	3.1	64.391	1363.953	5.6	19.5
37.8	0.1	122	2.1	1672.934	26.6	3	72.823	1477.639	6.7	15.8
54.4	25	139	8.2	3539.957	28.3	3.8	39.338	522.279	8.4	54
54.4	10	107	6.9	2734.668	28.3	1.1	39.016	741.423	5.3	37.2
54.4	5	91	6.6	2194.432	26.7	0.7	41.69	836.937	5.1	34.9
54.4	1	67	5.1	1466.156	25.1	2.5	45.542	856.34	5.6	27.8
54.4	0.5	49	5.1	1175.721	23.5	2	41.332	860.275	8.6	22.5
54.4	0.1	44	4.5	889.323	19.2	2.4	49.484	901.414	7.7	20.8

Table B-97 Overall Dynamic Modulus test results at various test temperatures for Mix 32 Specimen 1

Temperature (°C)	Frequency (Hz)	Stress Amplitude (P-P) (KPa)	SE (%)	Dynamic Modulus (MPa)	Phase Angle (deg.)	UC (deg.)	Strain (P-P) Recoverable (microstrain)	Accumulated Strain (microstrain)	SE (%)	UC (%)
-10	25	2103	4.9	41143.5	11.4	10.5	51.107	74.345	6.9	3.3
-10	10	2131	4.4	42141.26	6	0.7	50.558	27.96	6.1	9.2
-10	5	2079	4.3	40435.13	6.9	1.7	51.42	30.819	5.7	9.1
-10	1	1867	1.4	37074.35	8.3	3.3	50.372	28.81	8.3	8.4
-10	0.5	1755	0.8	35904.31	8.2	2.9	48.892	25.762	6.7	10
-10	0.1	1595	0.5	30385.26	10	2.4	52.498	45.714	7.7	7.1
4.4	25	1329	5.8	29808.92	16.6	13.1	44.578	103.406	9.8	9.1
4.4	10	1288	5.8	27813.45	11.8	3.1	46.318	76.213	7.7	4.1
4.4	5	1212	5.5	25699.81	12.9	3.3	47.175	81.886	7.2	2.7
4.4	1	1065	2.3	21142.48	15.1	4.2	50.362	85.815	6.9	7.2
4.4	0.5	953	1.5	19340.09	12.1	5.4	49.285	94.409	9.8	7
4.4	0.1	902	0.6	14439.6	19.6	3.6	62.458	173.366	5.7	10.4
21.1	25	703	7.6	12169.27	21.3	7.1	57.794	241.371	10.8	10.5
21.1	10	667	8.4	10207.47	17.8	1.9	65.393	290.388	8.1	6.9
21.1	5	628	7.9	8963.812	18.6	1.8	70.081	330.883	8.5	10.3
21.1	1	527	4.4	6362.728	22.5	1.9	82.858	343.406	7.2	13.2
21.1	0.5	442	3.1	5286.229	24	2.5	83.585	351.795	6.5	13.6
21.1	0.1	308	1.6	3617.636	23.8	3.4	85.169	399.165	6.2	12.7
37.8	25	285	10.2	5105.947	26.8	2.5	55.83	418.504	10.5	14
37.8	10	261	9.5	3946.33	24.6	3.1	66.052	685.666	7.9	25.1
37.8	5	207	8.3	3278.927	24.8	3.1	63.187	782.051	7.6	28.4
37.8	1	152	5.1	2026.723	26.2	3.5	75.111	790.685	6.4	32.1
37.8	0.5	117	3.7	1642.512	25.6	4.1	71.15	795.261	5.2	32.7
37.8	0.1	95	2.3	1113.645	22.7	3.8	85.201	862.115	5.8	37.2
54.4	25	115	8.8	1849.901	29.6	3.5	62.309	486.091	8.9	30.8
54.4	10	97	7.5	1406.925	26	4.1	69.124	688.242	6	36.7
54.4	5	80	7.4	1166	25	4.2	68.865	761.937	9.1	40.2
54.4	1	58	5.8	901.625	22.7	3	63.789	796.903	5.8	24.7
54.4	0.5	44	4.3	832.141	21.1	2.6	53.195	803.972	4.9	19.9
54.4	0.1	35	3.5	665.996	16.6	1.5	53.167	826.018	6.8	18

Table B-98 Overall Dynamic Modulus test results at various test temperatures for Mix 32 Specimen 2

Temperature (°C)	Frequency (Hz)	Stress Amplitude (P-P) (KPa)	SE (%)	Dynamic Modulus (MPa)	Phase Angle (deg.)	UC (deg.)	Strain (P-P) Recoverable (microstrain)	Accumulated Strain (microstrain)	SE (%)	UC (%)
-10	25	2044	4.8	42947.76	3	6.9	47.594	88.094	8.3	9.5
-10	10	2084	4.3	39790.13	7.7	3	52.368	42.905	4.9	12
-10	5	2026	3.9	38221.47	7.9	3	52.997	45.615	4.7	12.2
-10	1	1823	1.2	34116.72	8.3	3.4	53.435	43.858	5	12.6
-10	0.5	1714	0.7	32819.51	9.1	3.7	52.225	45.971	5.5	12.8
-10	0.1	1561	0.4	28840.71	11	2.9	54.129	68.344	4.7	11.8
4.4	25	1642	5	29630.49	8.4	4.9	55.401	162.381	7.6	15.9
4.4	10	1595	5	26946.25	11.9	3.6	59.191	115.99	5.8	14.5
4.4	5	1504	4.5	24953.6	12.1	3.6	60.262	127.329	5.4	14.8
4.4	1	1323	1.7	20480.81	13.7	3.9	64.605	130.931	8.2	16
4.4	0.5	1187	1.1	18715.45	17.9	2.3	63.408	142.845	3.9	16.8
4.4	0.1	1121	0.5	13789.53	19.8	2.3	81.292	263.97	5	15.9
21.1	25	884	6.2	13291.48	19.3	2.4	66.526	656.472	7.4	39.6
21.1	10	847	6.9	11158.6	20.2	2.9	75.934	954.426	6.6	35.5
21.1	5	799	5.9	9716.854	21.5	2.9	82.208	1177.588	4.8	34.8
21.1	1	662	3.1	6820.216	25.6	2.7	97.072	1309.013	4.4	36.2
21.1	0.5	558	2.3	5756.268	28	2.4	96.971	1414.674	4	34.2
21.1	0.1	390	1.2	3927.36	27.4	3.2	99.418	1596.313	4.4	33.8
37.8	25	303	9.4	6618.52	24.8	0.4	45.845	285.541	9.5	14.6
37.8	10	277	8.4	5128.066	24.7	0.8	53.923	475.64	6.7	13.9
37.8	5	221	8	4307.702	24.4	0.2	51.341	522.569	6.9	10.1
37.8	1	171	5.2	2781.653	24.9	0.7	61.296	534.14	5.9	8.8
37.8	0.5	132	3.6	2264.353	24.3	0.2	58.229	536.098	5.7	8.5
37.8	0.1	109	1.6	1554.066	22	0.4	70.105	586.527	6.8	7.2
54.4	25	116	8.7	2248.057	32.4	3.1	51.72	341.936	21	14.3
54.4	10	96	7.7	1890.545	25	0.3	51.038	520.998	4.2	7.4
54.4	5	80	7.2	1557.363	23.4	0.5	51.387	569.987	4.2	7.2
54.4	1	57	6.6	1110.018	21	0.8	51.151	573.441	6.2	7
54.4	0.5	43	5.2	932.318	20	1.1	46.242	577.043	7.1	5.4
54.4	0.1	35	5.2	740.07	16.8	1.1	47.012	599.532	8.6	6.7

Table B-99 Overall Dynamic Modulus test results at various test temperatures for Mix 32 Specimen 4

Temperature (°C)	Frequency (Hz)	Stress Amplitude (P-P) (KPa)	SE (%)	Dynamic Modulus (MPa)	Phase Angle (deg.)	UC (deg.)	Strain (P-P) Recoverable (microstrain)	Accumulated Strain (microstrain)	SE (%)	UC (%)
-10	25	2057	5.3	41400.13	10.2	1.8	49.693	26.786	17.4	10.6
-10	10	2084	4.6	42300.32	7	1	49.273	7.53	6.4	18.3
-10	5	2031	4.3	41167.91	6.6	1.2	49.327	5.646	8	18.4
-10	1	1822	1.4	36552.44	6.6	1.5	49.85	3.491	6.1	15.4
-10	0.5	1712	0.8	36100.26	4.3	1.9	47.429	4.266	10.7	15.3
-10	0.1	1559	0.5	31421.99	10.4	1.7	49.617	17.2	11	13.1
4.4	25	1555	5.8	30119.17	13	1.4	51.644	110.836	16.8	16.3
4.4	10	1503	5.6	29176.61	10.9	1.1	51.51	61.965	8.4	9.4
4.4	5	1415	4.9	26917.75	11.2	1.3	52.577	63.756	7.8	8.9
4.4	1	1243	1.8	22624.41	14.1	1.8	54.958	65.986	9.5	6.4
4.4	0.5	1116	1.1	20610.11	11.8	2	54.148	71.569	5.2	5.1
4.4	0.1	1055	0.5	16218.54	16.3	1.7	65.078	123.798	5.9	9.1
21.1	25	858	6.2	13671.29	14.5	5.5	62.778	301.794	7.9	13.2
21.1	10	824	6.2	11615.55	18.6	2.5	70.946	405.471	7.2	14
21.1	5	774	5.7	9934.635	18.7	1.8	77.924	490.674	6.4	14.4
21.1	1	646	2.8	7221.042	20.7	1.5	89.4	534.561	5.4	13.9
21.1	0.5	545	2.1	6118.873	22.4	2	88.99	574.366	4.3	14.9
21.1	0.1	380	1.1	4337.275	24.5	2.6	87.531	696.288	6.5	16.2
37.8	25	372	8.8	5942.965	23.3	1.4	62.572	597.268	9.2	22.4
37.8	10	325	9.5	4572.678	23.2	1.6	70.988	891.031	7.2	27.3
37.8	5	264	7.6	3675.927	24	1.6	71.828	1023.783	6.3	27.9
37.8	1	205	4.9	2413.462	25.5	1.5	84.884	1080.813	7.5	28.8
37.8	0.5	158	3.3	1956.665	25.7	1.4	80.643	1121.326	7.1	31.3
37.8	0.1	129	1.9	1470.242	24.1	2.6	87.607	1243.535	9.7	21.7
54.4	25	125	9.6	2643.125	28.2	1.7	47.188	224.139	8.9	13.5
54.4	10	104	8.2	2331.951	24.8	0.8	44.544	310.867	8.2	26.4
54.4	5	87	8.1	1916.612	23.9	0.6	45.499	331.869	9.6	26.4
54.4	1	63	6.7	1079.047	23.3	2.2	58.137	333.302	8.5	25.6
54.4	0.5	47	5.1	810.262	22.2	3	58.407	334.913	5.9	34.5
54.4	0.1	38	3.4	600.793	19.8	2.1	63.925	367.023	9.2	36.4

Table B-100 Overall Dynamic Modulus test results at various test temperatures for Mix 33 Specimen 1

Temperature (°C)	Frequency (Hz)	Stress Amplitude (P-P) (KPa)	SE (%)	Dynamic Modulus (MPa)	Phase Angle (deg.)	UC (deg.)	Strain (P-P) Recoverable (microstrain)	Accumulated Strain (microstrain)	SE (%)	UC (%)
-10	25	2221	5.4	49395.1	9.6	7.3	44.967	53.366	24.7	24.6
-10	10	2276	5.1	52674.28	6.6	1	43.213	18.861	8.3	39.2
-10	5	2211	5	50751.4	6.8	0.6	43.573	17.674	8.1	38.9
-10	1	1969	1.7	46384.54	8	1.2	42.439	19.572	7.8	38.7
-10	0.5	1843	0.9	45142.54	8.4	2.2	40.822	21.053	13.3	39.6
-10	0.1	1683	0.5	39509.75	7.2	1.6	42.596	33.488	11.4	37.4
4.4	25	1766	5.8	36183.87	11.9	6.8	48.817	132.485	33.6	43.8
4.4	10	1729	5.1	34454.36	10.7	0.3	50.178	94.974	6.5	41.9
4.4	5	1624	4.8	31912.32	11	0.1	50.88	102.809	8.4	41.8
4.4	1	1423	1.7	26127.06	13	1.1	54.465	108.376	10.6	42.2
4.4	0.5	1277	1	24542.48	16.6	1.8	52.025	118.508	6.2	43.8
4.4	0.1	1209	0.5	18609.82	17.4	1.2	64.982	200.974	7.3	42
21.1	25	874	6.8	16005.27	19.5	12.8	54.577	455.853	17.7	64.7
21.1	10	840	6.8	12467.96	21.7	2.9	67.38	573.95	8.1	35.6
21.1	5	692	6.6	10478.2	22.4	3.2	66.047	613.149	7	36.6
21.1	1	512	3.9	6963.125	27.4	1.5	73.482	613.781	8.1	42.5
21.1	0.5	422	2.7	5839.772	26.4	2.8	72.216	627.561	6.5	46.1
21.1	0.1	359	1.1	3954.57	28.2	1.1	90.901	749.897	8.6	46.3
37.8	25	287	9	5631.035	23.3	7.4	50.998	415.844	7.8	16.7
37.8	10	242	7.4	4302.072	26	0.5	56.269	521.819	5.6	9.3
37.8	5	197	7.6	3373.655	25.4	1.2	58.493	536.711	4.9	13.6
37.8	1	135	6.4	1988.134	25.6	1.9	68.038	532.419	6	22.7
37.8	0.5	108	5	1539.813	25.7	2	69.926	537.307	5.8	29.9
37.8	0.1	83	3.1	997.089	22	2.3	83.351	586.336	6.8	41.2
54.4	25	105	10.3	1419.22	29.8	4.3	74.285	308.167	8.5	50.2
54.4	10	88	8.3	1078.707	25	1.9	81.599	439.404	5.5	42
54.4	5	60	7.5	846.234	23.6	2.2	71.098	454.549	6.4	50.6
54.4	1	49	7.2	590.263	18.9	3.1	83.452	475.216	4.7	56.7
54.4	0.5	43	6.2	515.591	17.9	2.8	84.328	484.936	5.1	59.5
54.4	0.1	37	3.5	406.585	14	2.5	90.524	520.739	8.2	66.4

Table B-101 Overall Dynamic Modulus test results at various test temperatures for Mix 33 Specimen 3

Temperature (°C)	Frequency (Hz)	Stress Amplitude (P-P) (KPa)	SE (%)	Dynamic Modulus (MPa)	Phase Angle (deg.)	UC (deg.)	Strain (P-P) Recoverable (microstrain)	Accumulated Strain (microstrain)	SE (%)	UC (%)
-10	25	2204	4.8	58756.69	10.6	2	37.518	92.9	11.2	0.5
-10	10	2254	4.4	55440.07	6.7	0.5	40.661	59.728	7.8	14.1
-10	5	2188	4.1	52651.69	6.8	0.8	41.561	62.954	7.7	13.5
-10	1	1959	1.2	48096.84	3.7	1.4	40.732	60.639	12.7	14
-10	0.5	1843	0.7	42647.88	8.7	0.9	43.207	62.005	9.5	14.8
-10	0.1	1681	0.4	39866.88	8.8	2	42.16	72.92	10.1	16.1
4.4	25	1766	5	37621.16	12.9	1.2	46.935	150.184	11.4	9.2
4.4	10	1727	4.7	33632.25	11.7	1	51.359	98.18	6.2	15.3
4.4	5	1621	4.3	30783.18	11.9	1.1	52.655	106.077	6	15.6
4.4	1	1423	1.3	24783.22	14.5	5.3	57.414	108.907	16.9	16.7
4.4	0.5	1277	0.8	21081.36	20.4	2.5	60.598	119.722	5	16
4.4	0.1	1209	0.4	16249.57	21.6	4.7	74.389	224.301	5.8	17.5
21.1	25	870	5.7	13438.75	23	3.9	64.755	530.075	6.4	22
21.1	10	831	5.2	11188.7	22.9	4.6	74.251	677.79	6.5	22.4
21.1	5	686	5.2	9449.059	23.8	4.5	72.576	732.2	5.7	21.7
21.1	1	510	2.8	6465.538	28.5	5.2	78.851	745.76	7.8	22.2
21.1	0.5	422	2.1	5750.45	27.1	5.1	73.394	766.572	6.2	28.6
21.1	0.1	358	0.8	3899.051	27.9	5	91.919	914.193	6.6	29.2
37.8	25	281	7.9	5281.384	25.9	0.8	53.296	697.852	9.6	32
37.8	10	239	6.8	3985.996	24.8	1.7	60.079	928.247	7.9	35.2
37.8	5	195	6.7	3295.478	25	2.1	59.188	1025.332	5.8	39.1
37.8	1	136	5.1	2032.862	24.7	2.9	67.133	1036.708	8.9	43.4
37.8	0.5	108	4.1	1597.445	25.4	2.8	67.359	1046.719	6.6	45.4
37.8	0.1	82	1.8	1066.48	21.8	3.5	77.077	1097.303	7.3	51.7
54.4	25	103	9.4	1499.387	29.4	0.8	68.965	510.785	7.5	38.4
54.4	10	86	8.9	1147.607	25	3.3	75.346	719.603	4.9	43.5
54.4	5	61	8.3	911.337	23.7	3.7	66.846	752.67	5	46.2
54.4	1	49	6.9	636.825	20	3.9	77.207	768.258	6.5	51.2
54.4	0.5	44	5.7	569.547	17.4	4.5	76.434	781.562	6.6	55.4
54.4	0.1	37	2.6	456.128	14.5	3.3	80.443	816.385	8.9	59.4

Table B-102 Overall Dynamic Modulus test results at various test temperatures for Mix 33 Specimen 4

Temperature (°C)	Frequency (Hz)	Stress Amplitude (P-P) (KPa)	SE (%)	Dynamic Modulus (MPa)	Phase Angle (deg.)	UC (deg.)	Strain (P-P) Recoverable (microstrain)	Accumulated Strain (microstrain)	SE (%)	UC (%)
-10	25	2217	4.7	51790.57	19.5	11.3	42.802	56.997	12	15
-10	10	2262	4.6	54869.45	8.1	3.5	41.228	21.593	8.9	19.2
-10	5	2199	4.5	54070.12	7.5	3.6	40.673	22.414	9.6	18
-10	1	1963	1.3	49287.51	10.8	3.5	39.822	24.357	9.7	20.2
-10	0.5	1843	0.7	44959.35	6.3	6.1	40.99	25.552	11.6	18
-10	0.1	1682	0.4	41345.67	10.4	4.2	40.67	37.245	9.9	21.2
4.4	25	1773	4.7	33849.09	22	10.2	52.383	128.565	10	29.2
4.4	10	1734	4.7	32883.63	13.1	4.3	52.726	75.881	6.3	30.6
4.4	5	1632	4.7	30265.3	14.1	4.2	53.925	82.153	6.4	31
4.4	1	1425	1.5	24116.21	15.4	5	59.108	87.875	6.1	34.9
4.4	0.5	1277	0.7	21274.66	15	6	60.011	97.763	5	32.6
4.4	0.1	1210	0.4	16459.85	19.4	4.4	73.535	169.582	6	41.3
21.1	25	876	6.2	14743.07	26.4	10.6	59.387	326.475	10	53.6
21.1	10	837	5.9	12347.25	19.5	1.7	67.789	378.991	5.6	50.1
21.1	5	690	5.8	10617.08	20.3	1.4	64.972	397.93	6.8	50.3
21.1	1	510	3.2	7570.749	21.5	3.1	67.407	391.363	10.8	56.2
21.1	0.5	421	2.3	6092.329	25.9	1.4	69.175	400.244	4.9	52.4
21.1	0.1	359	1.3	4335.598	25	1.6	82.844	492.911	7.1	55.6
37.8	25	285	8.2	7598.427	26.7	3	37.556	271.971	8.9	4.8
37.8	10	241	6.9	5745.897	25	2.2	41.937	352.32	6.7	1.2
37.8	5	196	7	4611.565	25.8	2.2	42.594	373.098	6.1	4.1
37.8	1	137	5.7	2794.418	26.6	3.7	49.186	365.567	6	11.8
37.8	0.5	109	4.6	2197.365	27	4.6	49.405	367.644	5.8	17
37.8	0.1	82	2.5	1411.602	24.3	5.3	58.415	396.805	6.3	26.4
54.4	25	106	9.6	1896.454	28.5	3.7	55.704	311.811	8	29.2
54.4	10	88	8.4	1378.239	25.8	4.2	63.951	487.333	5.3	36.3
54.4	5	60	8.3	1080.716	23	4.8	55.957	513.075	13.6	41.4
54.4	1	49	7.5	765.463	19.6	5.1	64.459	523.759	5.1	55.1
54.4	0.5	44	6.4	654.057	18.5	4.6	66.669	534.166	6.3	57.6
54.4	0.1	37	3.7	511.663	14.5	3.5	72.892	564.436	8.6	65.8

Table B-103 Overall Dynamic Modulus test results at various test temperatures for Mix 34 Specimen 1

Temperature (°C)	Frequency (Hz)	Stress Amplitude (P-P) (KPa)	SE (%)	Dynamic Modulus (MPa)	Phase Angle (deg.)	UC (deg.)	Strain (P-P) Recoverable (microstrain)	Accumulated Strain (microstrain)	SE (%)	UC (%)
-10	25	2223	4.9	47398.33	2.4	12	46.891	114.209	17.6	61
-10	10	2269	4.6	39682.32	8.9	5.1	57.179	62.317	7.6	52.7
-10	5	2209	4.7	37108.58	10	4.7	59.516	62.296	8.6	51
-10	1	1965	1.5	34437.98	10.6	5.4	57.054	64.098	7.9	54.9
-10	0.5	1842	0.7	31252.96	9.6	6.1	58.934	65.649	5.8	52.7
-10	0.1	1682	0.5	29026.33	10.1	6.4	57.952	80.056	9.5	56.6
4.4	25	1774	5	27107.8	9.8	8.5	65.433	158.456	7.6	59
4.4	10	1730	4.6	22927.97	12.7	4.4	75.471	84.316	6	58.9
4.4	5	1627	4.6	21499.24	12.4	4.6	75.673	87.594	6.7	60.8
4.4	1	1424	1.5	17267.98	14.3	4.8	82.441	89.866	4.7	63.5
4.4	0.5	1277	0.8	16270.73	16.2	4.6	78.468	97.932	4.6	66.5
4.4	0.1	1210	0.5	12618.4	17	4.5	95.852	174.625	5.5	68.7
21.1	25	875	5.8	11854.4	21.1	3.9	73.807	334.2	7.6	40.5
21.1	10	837	5.6	10195.73	18.5	1.9	82.114	415.283	6.7	42.2
21.1	5	692	5.5	8950.808	19.6	1.8	77.352	444.173	8	41.7
21.1	1	510	3.2	6483.594	23.1	2	78.638	443.836	6	42
21.1	0.5	423	2.6	5668.123	22.6	1.9	74.595	457.571	6.4	42.9
21.1	0.1	360	1	4054.111	24.8	1.1	88.897	577.756	7	42.2
37.8	25	287	8.2	5201.612	27.7	2.9	55.164	599.239	8.7	34.7
37.8	10	240	6.7	4097.95	26.7	2.8	58.621	826.942	6.8	31.5
37.8	5	196	6.9	3363.986	25.9	2.2	58.382	909.45	5.5	31.8
37.8	1	137	6	2120.073	28.1	2.3	64.766	926.146	5.7	31
37.8	0.5	109	4.8	1749.965	28.2	2.9	62.443	949.987	5.5	31.2
37.8	0.1	82	2.1	1216.372	27.6	4.3	67.804	1018.132	6.4	30.3
54.4	25	107	9.5	1897.28	30	0.2	56.294	405.227	9.1	30
54.4	10	88	8.4	1412.784	28.3	2.4	62.573	599.316	8.5	27.2
54.4	5	61	7.9	1187.087	28	3.8	51.758	632.587	7.7	27.5
54.4	1	49	6.9	798.205	25.9	5	61.964	657.921	7.5	30.9
54.4	0.5	44	6.1	680.779	25	6.2	64.921	669.744	7.4	36.6
54.4	0.1	37	3.2	530.66	21.7	6	70.436	721.475	8.5	46

Table B-104 Overall Dynamic Modulus test results at various test temperatures for Mix 34 Specimen 2

Temperature (°C)	Frequency (Hz)	Stress Amplitude (P-P) (KPa)	SE (%)	Dynamic Modulus (MPa)	Phase Angle (deg.)	UC (deg.)	Strain (P-P) Recoverable (microstrain)	Accumulated Strain (microstrain)	SE (%)	UC (%)
-10	25	2220	4.7	49705.39	10.8	10.1	44.654	99.691	16.1	24.1
-10	10	2272	4.9	48827.36	6.5	0.7	46.534	62.007	7.3	12.2
-10	5	2210	4.8	47358.32	6.2	0.7	46.668	59.384	7.5	12.5
-10	1	1964	1.5	40800.96	8.1	2.9	48.147	60.153	7.1	12.9
-10	0.5	1841	0.8	41389.57	3.7	3.7	44.472	61.977	17	15.9
-10	0.1	1683	0.6	34989.25	10.8	3.6	48.092	79.956	9.8	16.4
4.4	25	1776	5.1	30162.7	19.1	7.2	58.89	168.963	13.8	11.5
4.4	10	1736	4.9	27926.24	14.1	5.6	62.163	106.951	7.1	14
4.4	5	1634	4.7	25425.86	14.5	4.9	64.253	115.215	7	15.5
4.4	1	1426	1.6	20713.75	16	5	68.826	121.337	13.6	20.1
4.4	0.5	1278	0.8	17859.2	21	5.7	71.534	133.152	6.9	23.8
4.4	0.1	1209	0.4	13193.06	19.7	3.3	91.656	232.858	5.6	30.8
21.1	25	878	5.8	14273.65	21.9	2.7	61.511	531.614	12.3	49.7
21.1	10	840	5.5	10336.99	21.2	3.4	81.286	722.266	5.6	35.6
21.1	5	695	5.7	8906.166	22.1	3.5	78.011	785.321	5.7	35.1
21.1	1	511	3.1	6135.553	25.2	3.6	83.259	788.138	7.2	34.8
21.1	0.5	422	2.1	5391.483	25.8	4.1	78.276	805.075	4.8	34.4
21.1	0.1	359	1	3632.459	27.9	3.4	98.843	951.842	5.5	34.3
37.8	25	286	8	4629.319	35.8	2.3	61.826	794.984	9.8	9.3
37.8	10	243	6.2	3752.929	34.2	4.8	64.671	1147.848	5.4	17.9
37.8	5	199	6.4	3408.903	30	4.3	58.3	1300.302	5.5	16.4
37.8	1	137	5.3	2386.144	25.8	2.7	57.515	1352.265	5.6	5.8
37.8	0.5	109	4.4	1949.514	24.9	2.5	56.037	1378.532	5.6	6.2
37.8	0.1	83	2.1	1347.676	21.9	1.4	61.318	1411.63	5.9	5.9
54.4	25	106	9.4	1698.433	32.4	5.1	62.673	547.065	10.5	28.2
54.4	10	89	7.6	1343.726	28.2	5.2	66.048	780.654	5.5	22.7
54.4	5	61	7.5	1240.111	22.7	0.4	49.485	798.037	6.7	4
54.4	1	49	6.8	945.424	18.8	1.3	51.737	813.418	6.8	4.8
54.4	0.5	44	5.7	812.006	17.6	1.1	54.74	825.822	6.1	6.5
54.4	0.1	37	2.9	664.97	13.8	1.6	55.987	845.99	7.5	8.1

Table B-105 Overall Dynamic Modulus test results at various test temperatures for Mix 34 Specimen 3

Temperature (°C)	Frequency (Hz)	Stress Amplitude (P-P) (KPa)	SE (%)	Dynamic Modulus (MPa)	Phase Angle (deg.)	UC (deg.)	Strain (P-P) Recoverable (microstrain)	Accumulated Strain (microstrain)	SE (%)	UC (%)
-10	25	2226	5.3	52201.26	7.2	3.5	42.648	132.012	27.6	33.9
-10	10	2274	5	55078.17	6.1	0.7	41.288	100.075	8.9	20.4
-10	5	2214	4.8	52901.42	6.2	1	41.852	101.921	7.5	20.1
-10	1	1973	1.8	49518.16	6.2	0.5	39.852	99.894	13.7	23.1
-10	0.5	1847	0.9	43505.15	6.2	1.2	42.444	101.121	9.2	19
-10	0.1	1681	0.5	40634.68	6.8	0.7	41.365	110.656	10	22
4.4	25	1778	5.8	35820.09	12.2	3.3	49.63	145.534	27.4	45.7
4.4	10	1731	5.2	34300.24	10.8	0.3	50.478	118.642	8.2	35
4.4	5	1631	4.9	31552.59	11.6	0.3	51.686	129.398	7.1	35.6
4.4	1	1427	1.8	26447.03	12.6	1	53.97	135.821	5.4	37.8
4.4	0.5	1279	1	24295.46	16.8	1.3	52.629	146.133	5.9	39.3
4.4	0.1	1210	0.5	18690.95	16.2	2.9	64.717	238.021	8.1	38.6
21.1	25	880	6.9	11550.76	25.5	4.5	76.164	636.661	12.5	38.2
21.1	10	841	6.4	10226.18	27	2	82.278	804.599	6.1	26.7
21.1	5	695	6.6	9046.527	25.3	2.7	76.816	888.565	5.8	32
21.1	1	513	4.2	6127.206	29.1	4	83.716	913.222	7.9	35.9
21.1	0.5	422	3.3	5073.172	31	3.1	83.217	942.323	5.9	34.3
21.1	0.1	360	1.7	3565.706	30.7	3.1	100.958	1077.659	6.6	35.1
37.8	25	287	9.3	6029.443	23.8	13.9	47.673	599.336	17.3	45.4
37.8	10	241	7.6	4616.427	26.7	4.7	52.121	758.461	7.1	34.2
37.8	5	197	7.3	3830.312	27	4.9	51.37	803.427	5.9	33.6
37.8	1	136	5.8	2365.434	27.8	5.8	57.495	798.59	6.7	37.4
37.8	0.5	108	4.8	1848.169	28.4	5.8	58.358	803.377	6.8	41.2
37.8	0.1	83	2.3	1244.292	26	6.3	66.318	854.434	7.2	42.8
54.4	25	107	9.1	1735.488	28.9	9.1	61.427	544.732	8.9	60.5
54.4	10	88	8	1268.753	27.6	3.3	69.588	729.775	5.4	55.1
54.4	5	61	7.4	976.474	26.7	3	62.817	737.556	5.6	60.3
54.4	1	49	7.2	638.589	23.8	3.5	76.521	752.481	5.9	64.4
54.4	0.5	44	6.1	556.704	22	3.9	79.212	777.677	5.5	67.6
54.4	0.1	37	3.8	413.848	18.1	3.7	90.236	824.99	8.8	70.2

Table B-106 Overall Dynamic Modulus test results at various test temperatures for Mix 35 Specimen 1

Temperature (°C)	Frequency (Hz)	Stress Amplitude (P-P) (KPa)	SE (%)	Dynamic Modulus (MPa)	Phase Angle (deg.)	UC (deg.)	Strain (P-P) Recoverable (microstrain)	Accumulated Strain (microstrain)	SE (%)	UC (%)
-10	25	2220	4.9	46942.73	9.8	6.1	47.298	82.18	10.9	19
-10	10	2269	4.7	46196.19	8.2	6.1	49.118	41.728	7.7	20.8
-10	5	2208	4.7	45218.5	7.9	6.3	48.839	43.726	6.8	21.7
-10	1	1966	1.6	42165.77	8.2	6.5	46.627	41.34	9.9	22.1
-10	0.5	1841	0.8	40533.26	9.8	6.4	45.422	41.682	10.5	22.4
-10	0.1	1683	0.5	35151.4	9.6	5.6	47.881	52.336	8.6	20.6
4.4	25	1774	5.2	36161.5	12.9	5.7	49.069	104.464	7.8	15.3
4.4	10	1731	4.7	33912.05	11	5.5	51.036	56.735	6.2	16.8
4.4	5	1630	4.6	31932.2	10.8	5.2	51.036	58.227	8.2	16.4
4.4	1	1427	1.6	27052.48	14.4	5.3	52.734	59.214	9.8	16.1
4.4	0.5	1277	0.9	25156.99	9.5	4.9	50.777	64.802	6.9	16.3
4.4	0.1	1210	0.5	20034.05	16.6	3.9	60.387	121.529	7.2	14.6
21.1	25	875	6.1	21348.68	17.8	5.9	40.977	278.262	11.3	10.4
21.1	10	836	5.9	18358.69	17.8	4.5	45.56	352.855	8.2	12.9
21.1	5	689	5.8	15974.06	19.1	4.5	43.147	382.091	8	12.7
21.1	1	512	3.3	11347.04	22.1	4.9	45.105	386.369	9.2	13.1
21.1	0.5	422	2.4	9384.401	24.7	4.9	44.965	403.021	10.6	13
21.1	0.1	357	1.4	6300.103	26.7	4.1	56.679	500.84	8.1	16.3
37.8	25	285	8.6	6368.875	32	3.4	44.798	641.052	8.3	32.7
37.8	10	243	7.7	4815.958	30.1	2.8	50.44	871.181	7.4	37.2
37.8	5	197	7.9	3880.275	31.7	2.8	50.889	967.598	8.1	35.8
37.8	1	137	6.8	2348.163	33.3	3.4	58.166	1005.09	8.6	31.7
37.8	0.5	109	5.5	1846.503	34	4.5	58.958	1045.382	6.8	30.1
37.8	0.1	83	2.4	1216.354	30.6	4.8	67.972	1123.674	6.4	37.2
54.4	25	107	9.6	2748.02	33.6	0.4	38.968	402.368	11.1	31.3
54.4	10	89	8.7	1950.928	30.8	3.2	45.608	551.377	7.6	40.3
54.4	5	60	8	1546.655	29.4	4.3	39.017	565.384	9	42
54.4	1	49	7.2	963.59	27	4.6	51.131	594.263	9	45.7
54.4	0.5	44	6	810.016	23.6	5.5	54.13	612.275	7.3	44.7
54.4	0.1	37	3.7	603.604	19.9	5.3	61.07	652.609	7.5	46.4

Table B-107 Overall Dynamic Modulus test results at various test temperatures for Mix 35 Specimen 3

Temperature (°C)	Frequency (Hz)	Stress Amplitude (P-P) (KPa)	SE (%)	Dynamic Modulus (MPa)	Phase Angle (deg.)	UC (deg.)	Strain (P-P) Recoverable (microstrain)	Accumulated Strain (microstrain)	SE (%)	UC (%)
-10	25	2226	5.1	54163.44	4.2	0.8	41.104	88.796	16.1	30.2
-10	10	2268	4.5	53078.82	4.7	0.4	42.737	59.762	8.8	16.6
-10	5	2204	4.6	51553.63	4.9	0.5	42.745	60.878	8	14.6
-10	1	1961	1.4	49319.51	6.3	0.8	39.769	58.728	9.2	17.2
-10	0.5	1842	0.8	44889.82	4.3	1.6	41.025	59.593	9	14.6
-10	0.1	1683	0.5	42304.01	5.5	1.1	39.788	67.18	9.1	18
4.4	25	1777	5.4	40913.35	7.9	1.3	43.434	95.867	11.9	26.8
4.4	10	1732	4.8	38132.48	8.3	1.2	45.425	53.36	6.7	19.5
4.4	5	1635	4.8	36285	8.2	1.5	45.05	54.867	6.4	19.1
4.4	1	1427	1.7	30804.84	13	2	46.338	58.01	16.1	22.4
4.4	0.5	1279	1	29687.4	10.2	4.1	43.084	64.126	8.1	26.1
4.4	0.1	1210	0.5	22953.78	15.9	5.8	52.715	116.228	6.8	30.2
21.1	25	873	6.3	22973.3	18.2	5.4	37.999	228.05	12.7	47.2
21.1	10	833	5.9	18548.54	18.4	5.9	44.936	286.154	10	47.4
21.1	5	690	5.9	16810.81	19.4	6.5	41.026	307.138	9.9	45.7
21.1	1	513	3.5	11818.2	24.3	6.9	43.408	307.825	11	49.7
21.1	0.5	421	2.5	10128.02	24.4	8.5	41.614	316.665	12.6	52
21.1	0.1	356	1.4	6977.684	28.9	3.8	51.053	398.881	16.4	55.6
37.8	25	285	8.1	7653.288	32	3.9	37.211	276.001	8.6	9.8
37.8	10	242	7.3	5858.897	30.8	2.5	41.365	426.926	6.7	19.9
37.8	5	197	7.1	4728.875	31.1	2.9	41.735	488.192	6.4	23.7
37.8	1	137	5.6	2825.785	32.3	3.6	48.569	498.588	6.7	29.4
37.8	0.5	109	4.6	2190.098	32	4.7	49.831	506.859	6.4	33.7
37.8	0.1	83	2.1	1360.975	29	4.4	60.905	557.43	6.9	38.9
54.4	25	106	9.9	2103.593	36.6	3	50.214	287.698	9.5	12.2
54.4	10	89	8	1479.24	34.3	3	59.944	438.389	6.4	12.3
54.4	5	61	7.7	1150.108	34.6	4	52.876	463.385	6.3	13.3
54.4	1	50	7	705.325	31.7	5.1	70.823	500.375	6.7	10.8
54.4	0.5	44	5.1	609.476	28.9	4.7	72.902	526.645	7.8	12.1
54.4	0.1	37	3.4	443.742	24.7	4.8	82.622	588.927	9.9	12.2

Table B-108 Overall Dynamic Modulus test results at 14 °F (-10 °C) test temperature for Mix 35 Specimen 5

Temperature (°C)	Frequency (Hz)	Stress Amplitude (P-P) (KPa)	SE (%)	Dynamic Modulus (MPa)	Phase Angle (deg.)	UC (deg.)	Strain (P-P) Recoverable (microstrain)	Accumulated Strain (microstrain)	SE (%)	UC (%)
-10	25	2217	4.8	41976.73	6	1.5	52.824	114.315	7.5	24.4
-10	10	2262	4.4	39530.7	7.2	1.2	57.219	69.308	8.2	17.9
-10	5	2200	4.4	38815.7	7	2	56.685	69.386	7.7	18.9
-10	1	1964	1.3	35873.3	6.8	2.6	54.742	71.968	7.6	19.9
-10	0.5	1844	0.7	32511.58	8.8	1.8	56.721	75.144	7.7	17.9
-10	0.1	1682	0.5	30207.81	9.5	1.9	55.668	97.265	7.6	21.2
4.4	25	1769	4.8	26581.42	11.7	3.7	66.548	177.479	8	27.7
4.4	10	1732	4.7	24581.47	12.6	3.5	70.46	113.645	7.7	24
4.4	5	1632	4.6	22983.26	12.8	3.7	71.016	120.507	6.4	23.1
4.4	1	1428	1.6	18824.84	14.9	3.7	75.851	127.596	6.2	24.6
4.4	0.5	1279	0.9	16795.18	16.4	3.9	76.14	142.778	5.9	23.3
4.4	0.1	1211	0.5	13281.07	20.7	3.8	91.179	256.124	4.5	23.3
21.1	25	875	5.9	13913.93	20.6	4.4	62.916	602.615	7.4	21.1
21.1	10	838	5.8	13146.84	20.9	4.1	63.741	866.411	5.4	16.6
21.1	5	696	5.9	12052.43	19.8	0.3	57.768	1007.582	5.4	23.7
21.1	1	514	3.4	8431.223	24.1	0.3	60.953	1065.962	4.9	27.1
21.1	0.5	424	2.6	6967.296	26.8	0.8	60.841	1121.733	7.3	28
21.1	0.1	359	1.4	4740.607	27.9	0.2	75.818	1333.369	7	35.7
37.8	25	285	8	6638.913	27	0.5	42.965	777.213	9.4	34.1
37.8	10	242	7.1	5061.389	26.7	1.6	47.742	1068.119	6.4	38.8
37.8	5	198	6.6	3999.659	27.8	1.6	49.489	1190.407	6	41.5
37.8	1	137	5.5	2298.321	29.1	1.9	59.525	1207.461	6.7	48.5
37.8	0.5	108	4.6	1753.257	29.3	2.5	61.783	1222.449	6.5	52.1
37.8	0.1	82	2.3	1098.193	25.5	2.9	74.645	1297.661	6.4	58
54.4	25	105	9.6	2032.462	32.4	1.8	51.879	160.278	10.7	44
54.4	10	89	7.5	1464.135	29.7	2.5	60.635	295.608	5.1	50.1
54.4	5	61	7.4	1108.213	28.8	2.6	55.222	291.625	5.4	50.6
54.4	1	49	6.7	701.379	23.9	2.9	70.54	305.162	5.3	54.5
54.4	0.5	44	5.7	595.352	21.7	2.9	74.044	314.185	5.3	57
54.4	0.1	37	3.4	435.17	16.6	3.1	85.369	350.258	8.3	61

Table B-109 Overall Dynamic Modulus test results at various test temperatures for Mix 36 Specimen 1

Temperature (°C)	Frequency (Hz)	Stress Amplitude (P-P) (KPa)	SE (%)	Dynamic Modulus (MPa)	Phase Angle (deg.)	UC (deg.)	Strain (P-P) Recoverable (microstrain)	Accumulated Strain (microstrain)	SE (%)	UC (%)
-10	25	2220	6.1	33222.43	17	4.8	66.812	44.105	26.4	55.2
-10	10	2277	5.5	36241.28	12.4	4.6	62.831	-15.203	9.3	36.2
-10	5	2216	5.4	34830.35	12.4	4.9	63.611	-14.125	8.5	33.9
-10	1	1974	2	30908.26	15.2	5	63.854	-12.143	8.7	37.6
-10	0.5	1845	1.1	30356.2	14.2	5.8	60.792	-9.831	7.5	40.8
-10	0.1	1681	0.6	26142.22	13.2	6.5	64.3	8.997	10.7	40.3
4.4	25	1756	7.2	25738.15	10.1	19.7	68.23	156.751	31.7	68.8
4.4	10	1726	5.4	26498.2	13.8	3.9	65.155	67.294	7.8	33
4.4	5	1628	5.2	24625.37	14.7	4	66.124	63.031	6.4	33.7
4.4	1	1429	2	18482.41	20.8	5.3	77.328	59.795	10.1	44.5
4.4	0.5	1281	1.2	17533.98	18.5	6.9	73.033	64.386	6.9	52.8
4.4	0.1	1210	0.5	12918.9	21.8	6.6	93.627	140.83	7.1	53
21.1	25	869	7.3	12602.24	19.6	14.5	68.93	287.13	19.7	29.7
21.1	10	831	7.1	11709.32	21.1	5.1	70.951	334.03	8.2	24.1
21.1	5	690	7.2	10508.67	21.7	5.4	65.617	344.816	8.6	23.6
21.1	1	513	4.1	7268.673	25.3	7.9	70.516	333.307	9	32.8
21.1	0.5	421	2.9	6332.771	26.8	7.8	66.428	341.694	6	33.7
21.1	0.1	356	1.4	4727.458	29.4	6.1	75.381	449.625	7.5	33.8
37.8	25	281	8.6	5081.56	24.7	3.3	55.262	249.895	9.3	37.9
37.8	10	235	7.6	4021.988	23.8	3.6	58.47	331.578	7.6	37.8
37.8	5	193	7.6	3382.691	24.5	3.4	57.014	344.708	6.8	36.5
37.8	1	135	5.8	2182.551	26	3.5	61.674	327.688	6.3	36.4
37.8	0.5	107	4.7	1816.369	27.5	3.4	58.731	326.9	5.5	35.3
37.8	0.1	80	2.9	1298.745	27.2	4.1	61.872	380.242	6.1	33.5
54.4	25	105	10.4	2121.973	26.6	5.1	49.553	257.384	12	33.8
54.4	10	88	8.4	1667.895	24.4	4.4	52.487	397.291	9.2	32.4
54.4	5	61	8.1	1448.68	25.5	4.8	41.977	419.988	12.2	38.5
54.4	1	49	6.7	971.586	25	6.2	50.429	434.302	11.5	39.7
54.4	0.5	44	5.6	858.241	25.6	4.7	50.814	453.033	9.7	39.7
54.4	0.1	36	4.1	629.043	23.8	5.1	56.461	512.867	11.1	44.7

Table B-110 Overall Dynamic Modulus test results at various test temperatures for Mix 36 Specimen 2

Temperature (°C)	Frequency (Hz)	Stress Amplitude (P-P) (KPa)	SE (%)	Dynamic Modulus (MPa)	Phase Angle (deg.)	UC (deg.)	Strain (P-P) Recoverable (microstrain)	Accumulated Strain (microstrain)	SE (%)	UC (%)
-10	25	2221	5.4	41074.57	14.7	13.1	54.068	46.825	17.7	8.8
-10	10	2271	5	51453.47	9.1	4.6	44.142	2.313	9.3	38.8
-10	5	2210	4.8	48696.13	8.9	4.9	45.386	2.92	10.7	39.6
-10	1	1970	1.7	44376.56	9.2	5.1	44.396	0.93	9	41.4
-10	0.5	1844	0.8	40513.35	10.8	4.7	45.521	2.332	11.1	40
-10	0.1	1682	0.5	36028.07	12	4.4	46.695	16.688	9.4	40.2
4.4	25	1776	6.5	26208.42	18.6	12.3	67.778	137.25	19.9	20.6
4.4	10	1742	6.3	27362.81	14.1	3.1	63.653	71.155	10.4	50.4
4.4	5	1632	5.6	25917.62	12.7	3.3	62.986	75.818	11.8	53.5
4.4	1	1428	2.1	20625.44	15.6	2.8	69.215	77.958	12.6	52.9
4.4	0.5	1279	1.2	19536.88	13.6	4.8	65.479	84.597	9.8	54
4.4	0.1	1211	0.5	14618.81	20.4	2.9	82.816	157.114	13.6	54.2
21.1	25	872	6.3	14289.73	12.3	11	61.022	321.34	18.4	44.9
21.1	10	837	6.7	12482.37	20	4	67.067	402.22	9.2	53.4
21.1	5	689	6.4	10967.2	20.6	4.1	62.84	419.592	7.5	51.4
21.1	1	512	3.8	8184.936	23.5	4	62.5	405.802	14.2	50.1
21.1	0.5	422	2.9	6832.314	27.9	6.1	61.787	410.341	10.8	45.5
21.1	0.1	360	1.1	5116.994	27.1	5.2	70.322	492.196	8.2	48.7
37.8	25	281	9	4245.766	14.5	28.7	66.264	335.999	21.4	56.9
37.8	10	240	7.4	3912.633	28.1	3.5	61.229	487.84	7.5	36.7
37.8	5	195	7.2	3636.778	27.9	1.7	53.513	533.966	6.1	36.3
37.8	1	136	6.3	2407.582	27.2	4.1	56.562	525.526	6.1	47.1
37.8	0.5	107	5.6	1983.248	27.5	4.6	54.114	528.588	7.1	52.6
37.8	0.1	82	2.4	1332.782	27.3	4.5	61.717	587.173	5.1	56.5
54.4	25	106	9.7	1759.514	27.1	4.9	60.348	345.97	11	75.7
54.4	10	88	8	1324.149	26.4	1.4	66.127	499.58	6.6	66.9
54.4	5	60	7.6	1059.894	26.3	2.1	57.078	518.991	7.3	65.5
54.4	1	49	6.8	717.416	27.6	0.9	68.291	532.871	7.3	64.6
54.4	0.5	44	5.4	601.44	27	1.1	73.947	549.275	7.1	64.5
54.4	0.1	37	2.2	428.322	23.8	1.1	87.18	606.003	7.7	63.4

Table B-111 Overall Dynamic Modulus test results at various test temperatures for Mix 36 Specimen 3

Temperature (°C)	Frequency (Hz)	Stress Amplitude (P-P) (KPa)	SE (%)	Dynamic Modulus (MPa)	Phase Angle (deg.)	UC (deg.)	Strain (P-P) Recoverable (microstrain)	Accumulated Strain (microstrain)	SE (%)	UC (%)
-10	25	2206	4.9	36282.52	6.4	2.3	60.797	128.144	17.4	22.1
-10	10	2257	4.5	34924.52	6.9	0.7	64.638	78.637	6.8	23.1
-10	5	2191	4.3	33559.95	6.9	0.5	65.273	77.369	5.7	23.6
-10	1	1961	1.2	29454.78	6.1	0.7	66.579	77.507	6.8	23.7
-10	0.5	1843	0.7	27648.4	8.3	0.9	66.656	80.105	5.9	23.7
-10	0.1	1681	0.4	24561.32	10.3	0.6	68.441	101.603	13.4	24.3
4.4	25	1765	5.4	23873.06	11.1	2.1	73.933	189.252	14.5	21.6
4.4	10	1719	5.1	21500.93	11.6	0.9	79.93	111.83	6.5	17.8
4.4	5	1614	4.5	19788.64	12.6	1.1	81.554	119.457	7.1	18.1
4.4	1	1423	1.5	16263.43	14	0.6	87.479	122.965	5.7	18.7
4.4	0.5	1278	0.9	14737.58	13.7	0.7	86.695	132.037	7.2	18.9
4.4	0.1	1209	0.4	11508.88	17.6	0.4	105.085	242.768	4.2	18.2
21.1	25	876	6.6	12226.27	17.1	1.5	71.62	374.67	9.1	16.4
21.1	10	829	6.3	10175.04	17.6	0.5	81.431	460.02	6.2	10.1
21.1	5	686	6.3	8916.507	18.5	0.5	76.931	473.387	7.4	10.9
21.1	1	511	3.8	6539.803	21.9	0.8	78.203	467.341	5.2	13.3
21.1	0.5	422	2.8	5799.351	20.6	0.1	72.727	473.002	7.3	15.5
21.1	0.1	359	1.2	4310.703	21.1	0.5	83.283	555.795	8.4	15
37.8	25	282	9.3	5930.401	20.7	1.4	47.606	444.986	8.9	3.6
37.8	10	237	8.3	4947.66	21	1.4	47.896	585.242	7.3	8.6
37.8	5	194	8.1	4199.342	20.5	1.4	46.115	623.27	6.9	10.2
37.8	1	136	5.3	2793.155	22.8	1.2	48.753	619.672	6.9	10.6
37.8	0.5	108	4	2311.737	23.7	1.3	46.691	625.086	6.2	12.5
37.8	0.1	82	1.7	1696.16	22.9	1.3	48.481	675.044	5.3	14.3
54.4	25	104	9.8	2965.788	21.2	5.8	35.214	461.32	11.7	34.8
54.4	10	88	8.5	2437.485	21.5	0.8	35.92	665.76	7.2	26.3
54.4	5	62	7.5	2041.599	20.6	1.1	30.534	690.177	7.4	27.6
54.4	1	50	5.8	1490.532	20.5	1.1	33.514	703.763	8.6	25.1
54.4	0.5	44	4.5	1295.651	20.6	1.5	34.312	719.947	7.9	25.3
54.4	0.1	37	2.3	946.955	19.5	1.4	38.905	766.033	7.3	19.8

Table B-112 Overall Dynamic Modulus test results at various test temperatures for Mix 37 Specimen 1

Temperature (°C)	Frequency (Hz)	Stress Amplitude (P-P) (KPa)	SE (%)	Dynamic Modulus (MPa)	Phase Angle (deg.)	UC (deg.)	Strain (P-P) Recoverable (microstrain)	Accumulated Strain (microstrain)	SE (%)	UC (%)
-10	25	1853	5.6	35907.55	8.6	10.7	51.598	168.994	27.1	34.1
-10	10	1880	5.2	34055.06	8.6	3.2	55.201	124.539	8.7	14.3
-10	5	1833	4.8	32331.91	8.5	3	56.685	123.142	8.8	16
-10	1	1636	1.7	27420.65	9.9	4.5	59.671	123.748	7.1	19.6
-10	0.5	1536	1	26329.29	10.6	5	58.326	125.854	8.5	22.9
-10	0.1	1403	0.5	22742.43	12.3	3.4	61.707	150.351	10.3	25.8
4.4	25	1120	6.1	20143.44	9.4	19.7	55.619	113.95	17.3	34.3
4.4	10	1072	6.1	20756.42	12.2	1.9	51.66	85.278	7.8	24.3
4.4	5	1013	5.8	18757.54	14	2.7	54.007	88.649	8.5	25.5
4.4	1	892	2.8	15425.51	15.4	4.5	57.854	91.609	5.6	30
4.4	0.5	800	1.9	13882.67	17	4.8	57.598	100.218	5.4	33.2
4.4	0.1	757	0.7	10476.42	19.7	4.3	72.28	172.366	5.1	37.3
21.1	25	471	8.4	10758.77	19.8	8.5	43.776	142.456	15	26.7
21.1	10	439	8.6	11619.81	16	0.2	37.796	206.347	9.5	17.8
21.1	5	357	9	10724.48	16.2	0.8	33.311	221.519	10.2	20.5
21.1	1	273	5	7574.844	19.7	0.5	36.019	221.294	7.5	20.2
21.1	0.5	225	3.4	6617.865	18.3	1.4	34.017	224.366	7.5	20.8
21.1	0.1	191	1.4	4864.645	22.4	0.8	39.299	271.481	8.8	18.8
37.8	25	180	9.2	5548.969	23.8	10.4	32.423	458.92	13.9	26.2
37.8	10	167	8.5	4385.521	25.2	6.5	38.051	744.217	11.7	16.9
37.8	5	139	8.4	3950.322	21.7	3	35.207	860.351	8.1	2.3
37.8	1	104	6.4	2850.206	22	3.3	36.652	886.252	15.3	3.4
37.8	0.5	87	4.6	2359.908	22.3	1.7	36.691	907.182	7.9	0.9
37.8	0.1	72	2	1732.839	24.2	1	41.688	981.878	5.8	1.2
54.4	25	84	9.6	2116.298	27.8	6.9	39.824	103.687	8.4	41.9
54.4	10	71	8.7	1670.901	25.7	7.2	42.357	161.514	6.6	38.5
54.4	5	60	8.4	1477.163	25.6	7.8	40.712	180.846	7.1	35.7
54.4	1	49	6.5	1235.854	24.2	1.8	39.801	188.391	6.6	8.1
54.4	0.5	39	4.7	1029.207	20.6	1.6	37.464	187.764	8.3	4.6
54.4	0.1	29	2.7	771.526	18.5	1	36.953	196.661	9.5	6.6

Table B-113 Overall Dynamic Modulus test results at various test temperatures for Mix 37 Specimen 2

Temperature (°C)	Frequency (Hz)	Stress Amplitude (P-P) (KPa)	SE (%)	Dynamic Modulus (MPa)	Phase Angle (deg.)	UC (deg.)	Strain (P-P) Recoverable (microstrain)	Accumulated Strain (microstrain)	SE (%)	UC (%)
-10	25	1845	5.4	34585.95	14.9	5.8	53.335	129.917	33	22.6
-10	10	1870	4.9	38823.82	9	3.2	48.155	92.423	8.2	20.8
-10	5	1824	4.8	37096.4	9.5	3.2	49.158	97.757	8.5	22.3
-10	1	1635	1.7	35805.68	7.8	2.9	45.656	96.71	12	29.9
-10	0.5	1536	0.9	30721.88	10.7	2.8	49.998	99.496	11.7	25.3
-10	0.1	1400	0.5	27209.23	11.9	3.4	51.454	116.886	12	23.3
4.4	25	1114	6	20760.21	14.4	7.2	53.665	83.059	21.8	35.1
4.4	10	1069	6.4	22898.33	12.9	3.7	46.681	57.1	8	22.2
4.4	5	1006	5.6	21668.9	13.6	3.3	46.407	59.822	8.3	25.7
4.4	1	890	2.5	18267.27	15.6	2.5	48.731	60.856	10.4	27.7
4.4	0.5	799	1.6	17155.28	19.4	5.1	46.566	67.172	6.6	29.3
4.4	0.1	755	0.6	13053.06	19.2	3.1	57.817	112.706	7.1	26.9
21.1	25	469	7.9	11760.42	12.3	7.8	39.919	129.807	15.8	24.1
21.1	10	441	8.1	10182.61	20.7	4.2	43.271	180.815	13.2	30.9
21.1	5	356	8.7	8860.715	22.1	4.3	40.222	192.713	17.1	26.2
21.1	1	273	4.6	7023.654	26.1	5	38.87	190.722	11.3	26.8
21.1	0.5	226	3.1	6231.303	24.7	4.1	36.271	197.522	12.6	23.5
21.1	0.1	191	1.1	4386.783	26.1	3.2	43.647	255.105	7.9	17.8
37.8	25	181	9.4	6781.607	22.2	10.4	26.741	305.723	21.4	37.4
37.8	10	170	7.8	4721.551	27.6	5.4	35.922	513.201	8.4	25.7
37.8	5	142	7.5	4200.113	26.8	4.8	33.813	603.981	9.3	18.6
37.8	1	104	5.8	3095.458	28	5.1	33.462	641.115	6.6	8.2
37.8	0.5	87	4.1	2733.314	28.2	5.7	31.779	675.703	7.2	4.2
37.8	0.1	73	1.8	1895.716	28.7	5.7	38.439	767.77	6.7	2.7
54.4	25	106	10.2	2771.896	26.7	10.9	38.335	80.505	14.8	41.5
54.4	10	92	8.7	2151.614	26.1	4.1	42.791	149.391	7.7	35.8
54.4	5	77	8.2	1848.478	24.5	3.7	41.431	172.436	6.8	28.8
54.4	1	59	7	1357.818	23.2	3	43.482	179.887	6.6	25.3
54.4	0.5	49	6.2	1170.178	22.6	2.2	42.26	185.393	8.6	24.5
54.4	0.1	43	3.5	852	19.6	2.3	50.305	218.576	7.9	24.5

Table B-114 Overall Dynamic Modulus test results at various test temperatures for Mix 37 Specimen 3

Temperature (°C)	Frequency (Hz)	Stress Amplitude (P-P) (KPa)	SE (%)	Dynamic Modulus (MPa)	Phase Angle (deg.)	UC (deg.)	Strain (P-P) Recoverable (microstrain)	Accumulated Strain (microstrain)	SE (%)	UC (%)
-10	25	2195	4.5	42612.09	3.4	1.4	51.509	86.119	10.5	29.4
-10	10	2250	4.3	40702.51	6.1	0.5	55.273	42.062	6.8	30.3
-10	5	2190	4.1	38779.48	5.2	0.3	56.474	44.063	7.5	30.2
-10	1	1961	1.2	35104.67	6.7	0.6	55.849	40.677	12.5	29.8
-10	0.5	1842	0.7	33815.87	9.4	1.5	54.482	41.558	7.6	29.4
-10	0.1	1681	0.4	30132.13	7.3	0.2	55.785	52.151	7	28.8
4.4	25	1761	5.3	29904.15	7.3	1.5	58.9	114.853	7.7	25.3
4.4	10	1711	4.7	26675.17	9.9	0.3	64.157	53.704	6.2	26.5
4.4	5	1607	4	24805.81	9.8	0.2	64.799	53.841	5.4	26.6
4.4	1	1420	1.4	21272.34	11.1	0.6	66.775	54.778	5.4	26.4
4.4	0.5	1278	0.9	18904.19	12.9	0.8	67.585	59.08	4.1	25.6
4.4	0.1	1209	0.4	15737.31	13.9	0.6	76.824	102.061	5	24.9
21.1	25	864	6.1	17023.25	14.1	1.8	50.78	137.348	8.4	19
21.1	10	825	5.8	14137.11	15.3	0.5	58.348	144.279	7.2	18.9
21.1	5	684	5.5	12493.49	16	0.6	54.72	143.908	5.6	19.8
21.1	1	511	3.2	9270.313	18.7	0.7	55.122	137.259	5.2	19.4
21.1	0.5	422	2.6	8239.109	19.2	0.8	51.21	139.488	4.8	19
21.1	0.1	359	1.1	6215.696	20.7	1.2	57.802	186.564	5.1	17.5
37.8	25	282	8.5	8154.142	18.9	1.7	34.537	269.193	11.7	9.7
37.8	10	238	7.1	6452.869	20.3	0.6	36.886	364.516	8	14.2
37.8	5	194	7	5509.199	20.6	0.8	35.218	384.982	6.8	13.5
37.8	1	137	5.4	3749.426	21	0.7	36.511	380.735	8.9	11.6
37.8	0.5	108	4.5	3135.115	22.3	0.6	34.566	383.89	7.1	10.8
37.8	0.1	83	2.1	2234.83	23.2	0.1	37.015	415.832	7.3	8.6
54.4	25	106	9.8	3746.791	21.8	1.8	28.167	346.499	11.7	22.1
54.4	10	87	8.8	2945.505	21.1	1	29.58	486.344	9.8	18.5
54.4	5	62	8	2492.631	21	1.3	24.749	498.076	8.4	18.8
54.4	1	51	6.9	1656.091	21.5	1.3	30.877	504.409	10.5	19.1
54.4	0.5	44	5	1509.78	18.6	1.7	29.277	513.368	7.8	19.5
54.4	0.1	37	3	1115.23	19.3	0.9	32.911	542.844	8.9	18.9

Table B-115 Overall Dynamic Modulus test results at various test temperatures for Mix 38 Specimen 3

Temperature (°C)	Frequency (Hz)	Stress Amplitude (P-P) (KPa)	SE (%)	Dynamic Modulus (MPa)	Phase Angle (deg.)	UC (deg.)	Strain (P-P) Recoverable (microstrain)	Accumulated Strain (microstrain)	SE (%)	UC (%)
-10	25	2221	4.8	49056.21	2.5	4.9	45.267	118.699	17.7	22.1
-10	10	2270	4.6	49296.31	6.5	1	46.056	81.586	8.2	23.4
-10	5	2209	4.7	46929.31	5.7	0.9	47.07	81.608	8.6	23.1
-10	1	1969	1.7	43193.04	8.7	2.6	45.593	84.307	11	22.8
-10	0.5	1844	0.8	38921.42	5.3	1.6	47.377	86.887	8.4	21.3
-10	0.1	1682	0.5	36281.59	9.5	1.2	46.369	109.389	8.4	20.2
4.4	25	1766	4.8	34965.63	10.5	2.8	50.507	170.606	11.2	21.5
4.4	10	1729	4.5	32470.39	10.9	1	53.237	121	7.3	22.9
4.4	5	1624	4.4	30132.19	12.7	1.7	53.891	136.492	6.6	23.4
4.4	1	1425	1.5	24076.99	14.8	3.8	59.186	149.516	7.2	26.3
4.4	0.5	1279	0.9	21716.55	15.3	2	58.876	168.277	8.5	21.9
4.4	0.1	1209	0.4	16445.68	21.6	3.9	73.535	301.626	5.7	26.3
21.1	25	874	6	18133.94	16.8	1.6	48.222	584.711	7.6	3.2
21.1	10	838	5.9	14920.13	19.2	1.8	56.137	833.892	6.5	6
21.1	5	695	6.1	12961.47	20.5	2.4	53.637	931.279	5.5	7.2
21.1	1	513	3.8	8856.172	23.8	2.8	57.911	941.178	4.7	10.3
21.1	0.5	424	3	7426.571	25.2	3.2	57.08	975.115	4	10.7
21.1	0.1	359	1.7	4633.75	28.4	2.4	77.522	1157.023	5.1	13.6
37.8	25	210	7.9	5083.638	31.5	6.6	41.29	213.719	9.2	30.9
37.8	10	177	7.3	3603.554	33	4.8	49.061	303.212	6.6	31.7
37.8	5	123	7.3	2900.25	33	5.2	42.523	302.978	6.2	28.6
37.8	1	101	5.8	1759.575	30.5	4.2	57.129	309.985	5.4	23.1
37.8	0.5	80	4.6	1515.489	27.4	0.4	52.665	313.245	5.3	12.7
37.8	0.1	65	2.5	979.521	22.5	1.3	65.912	340.373	6	11.5
54.4	25	63	7.8	1034.58	34.6	8.2	60.884	25.606	7.4	65.8
54.4	10	52	6.9	736.726	29.5	3.5	70.211	38.065	4.3	57.7
54.4	5	35	5.9	577.425	26.9	3.8	60.679	21.358	5	58.3
54.4	1	29	6.3	433.599	20.7	3.9	67.054	12.167	4.5	52.7
54.4	0.5	23	5.5	381.261	19.5	4	61.597	-0.234	6.6	48.7
54.4	0.1	19	3.5	284.282	15.9	6	65.968	-19.453	6.2	59.2

Table B-116 Overall Dynamic Modulus test results at various test temperatures for Mix 38 Specimen 4

Temperature (°C)	Frequency (Hz)	Stress Amplitude (P-P) (KPa)	SE (%)	Dynamic Modulus (MPa)	Phase Angle (deg.)	UC (deg.)	Strain (P-P) Recoverable (microstrain)	Accumulated Strain (microstrain)	SE (%)	UC (%)
-10	25	2223	4.9	37312.05	2.7	6.7	59.587	135.123	14.5	23
-10	10	2268	4.8	38675.47	8.6	4.3	58.655	86.572	8	11.9
-10	5	2210	4.6	36384.7	9.1	3.5	60.728	87.451	8.2	10.6
-10	1	1968	1.6	33528.13	8.4	5.1	58.706	89.212	10.2	11.6
-10	0.5	1844	0.8	30304.16	8.8	3.4	60.853	93.458	8.7	9.6
-10	0.1	1682	0.5	27303.81	12.3	2.6	61.602	128	7.7	12.4
4.4	25	1779	5.4	26386.22	10.8	11.1	67.408	250.389	13.8	21
4.4	10	1734	5.1	24898.08	12.2	2.4	69.628	211.045	7.1	8
4.4	5	1634	4.9	23324.42	12.5	1.9	70.063	236.778	6	8
4.4	1	1429	1.8	19322.39	14.2	1.6	73.981	251.312	13.8	8.9
4.4	0.5	1279	1	16567.65	17.7	1.9	77.202	278.484	4.2	7.5
4.4	0.1	1211	0.5	12879.15	20.3	0.9	94.043	450.815	4.6	8.3
21.1	25	743	7.4	14283.55	17	6.8	52.041	537.973	12.5	29
21.1	10	703	7.2	12012.5	20.6	2.6	58.539	862.794	7.5	18.8
21.1	5	580	7	10456.49	21.8	2.6	55.461	1020.84	6.7	20.9
21.1	1	430	5.1	6988.223	25.3	1.7	61.474	1081.583	6.3	21.9
21.1	0.5	355	3.7	5730.012	27.3	1.9	61.97	1147.648	4.4	22.1
21.1	0.1	301	1.6	3478.71	30.6	1.5	86.629	1427.256	4.7	22
37.8	25	209	8.4	3184.749	33	4.8	65.615	450.425	10.3	55.4
37.8	10	176	8	2115.495	34	3.1	83.372	678.9	6	53.7
37.8	5	123	7.8	1632.505	35.2	3	75.527	710.475	7.5	55.4
37.8	1	100	6.6	1161.463	32.3	3.6	85.709	767.922	5.6	35.1
37.8	0.5	79	5.3	920.652	30.2	4	86.166	792.417	5.3	34.8
37.8	0.1	64	2.8	597.618	24.7	4.3	107.421	873.406	6.6	36.7
54.4	25	63	10.1	839.538	36	14	74.684	288.938	11	68.3
54.4	10	50	7.8	606.058	36	4	83.281	451.28	6.1	40.1
54.4	5	35	7	465.628	35	4.9	74.108	448.566	5.1	38.4
54.4	1	29	7.2	327.021	27.7	5	88.577	485.239	5.8	38.4
54.4	0.5	24	6.1	290.491	26.3	5.3	81.752	491.434	6.7	36.6
54.4	0.1	19	4.7	224.259	22.7	5.1	84.321	505.589	13.8	35.6

Table B-117 Overall Dynamic Modulus test results at various test temperatures for Mix 38 Specimen 5

Temperature (°C)	Frequency (Hz)	Stress Amplitude (P-P) (KPa)	SE (%)	Dynamic Modulus (MPa)	Phase Angle (deg.)	UC (deg.)	Strain (P-P) Recoverable (microstrain)	Accumulated Strain (microstrain)	SE (%)	UC (%)
-10	25	2224	5.1	49305.26	1.3	7.1	45.112	79.849	14.3	4.9
-10	10	2272	4.9	46951.73	5.3	0.3	48.383	42.212	7.4	11.6
-10	5	2214	5	45924.84	4.4	0.9	48.2	40.626	8.9	11.5
-10	1	1970	1.7	40694.23	5.7	0.3	48.409	42.397	8.6	11.3
-10	0.5	1844	0.8	39540.63	7.5	0.2	46.646	44.631	7.4	10.2
-10	0.1	1682	0.5	35055.64	7.5	0.7	47.993	55.584	7.8	8.2
4.4	25	1777	5.5	33710.54	9.5	2.1	52.699	136.84	13.5	7.8
4.4	10	1727	5.4	30508.97	10.3	1	56.622	91.989	10	13.4
4.4	5	1627	5	29324.68	10.1	1.4	55.492	98.463	6.5	10.2
4.4	1	1425	1.9	23247.76	13.6	1.1	61.29	107.256	5.6	9.7
4.4	0.5	1278	1	21205.16	13.1	1.2	60.255	120.01	5.2	8.7
4.4	0.1	1210	0.5	16633.24	19.1	1.2	72.745	238.116	7.1	6.8
21.1	25	739	6.6	16521.64	17.8	2.2	44.745	799.911	10.6	16.8
21.1	10	705	6.9	13761.69	19.8	1.1	51.221	1186.076	7.2	7.4
21.1	5	579	6.8	12452.41	20.4	1.6	46.468	1358.426	10.6	9.6
21.1	1	429	5	8239.191	24.7	1.8	52.063	1419.205	5.7	9.5
21.1	0.5	355	3.7	6864.504	27.2	1.7	51.723	1475.719	4.5	11.1
21.1	0.1	302	1.6	4336.393	30	1.6	69.731	1744.276	4.3	13.8
37.8	25	205	8.4	6331.45	27.7	2.6	32.381	869.716	8.3	22.7
37.8	10	176	7.4	4614.134	28.8	1.5	38.144	1273.71	6.9	14.4
37.8	5	124	7.7	3629.881	28.7	0.8	34.162	1353.526	8.4	15.6
37.8	1	100	6.7	2183.496	28.4	0.5	45.773	1415.827	6	13.6
37.8	0.5	80	5.1	1726.496	27.3	0.5	46.429	1443.045	6.6	13.4
37.8	0.1	65	2.9	1085.526	24.6	0.4	59.709	1522.882	7.8	10.9
54.4	25	63	9.9	1755.578	30.3	6.6	35.741	408.308	11.1	23.2
54.4	10	50	7	1265.569	27.4	1.3	39.826	591.537	5	13.1
54.4	5	35	6.9	961.316	25.6	1.1	36.692	582.275	5.2	11.7
54.4	1	29	6.7	693.459	18.8	0.8	42.168	602.307	4.4	10.7
54.4	0.5	24	5.6	614.71	17	0.3	38.367	602.307	6.8	11.2
54.4	0.1	19	4.5	506.254	12.1	0.6	37.246	609.417	6.2	10.5

Table B-118 Overall Dynamic Modulus test results at various test temperatures for Mix 39 Specimen 1

Temperature (°C)	Frequency (Hz)	Stress Amplitude (P-P) (KPa)	SE (%)	Dynamic Modulus (MPa)	Phase Angle (deg.)	UC (deg.)	Strain (P-P) Recoverable (microstrain)	Accumulated Strain (microstrain)	SE (%)	UC (%)
-10	25	2218	5	35323.71	7.4	5.6	62.8	125.924	7.1	33.6
-10	10	2267	5	34362.68	8.7	5.1	65.974	73.134	6.9	24.3
-10	5	2211	4.9	33143.56	8.8	4.9	66.716	78.228	6.2	24.7
-10	1	1970	1.8	28982.23	9.2	5.6	67.987	82.917	6.1	25.4
-10	0.5	1842	0.9	28849.3	9.6	5.7	63.855	89.947	7.5	29
-10	0.1	1683	0.6	24615.45	11.4	5	68.371	123.388	8.1	28.3
4.4	25	1771	5.3	25987.36	12.4	3.9	68.151	282.488	8.3	26.3
4.4	10	1726	5.1	23741.71	13.6	4.6	72.682	249.634	6.2	16.6
4.4	5	1624	4.6	21698.9	15	4.6	74.863	280.897	5.9	15.3
4.4	1	1426	1.7	17539.15	16	5.7	81.32	297.786	6.9	20.6
4.4	0.5	1278	1	15658.39	21.6	2.6	81.588	326.475	5.7	19.4
4.4	0.1	1209	0.5	11832.39	22.2	3.9	102.203	520.264	4.6	21.7
21.1	25	741	6.8	11597.81	24.5	6.5	63.91	681.67	7.9	17.1
21.1	10	708	7	8552.239	24.9	5.5	82.774	917.517	7	28.1
21.1	5	583	7	7294.842	26.6	5.5	79.867	1015.587	6.8	28.3
21.1	1	431	4.7	4795.822	29.4	5.7	89.782	1052.3	5.6	30.6
21.1	0.5	355	3.5	3977.906	30.6	5.8	89.241	1099.061	5.5	29.1
21.1	0.1	301	1.3	2557.511	30.2	5.5	117.862	1318.187	6.3	28.8
37.8	25	212	8.4	3567.238	28.9	3.7	59.292	497.941	7.9	42
37.8	10	178	8.2	2661.809	29.2	3.2	66.99	681.183	7.1	45.5
37.8	5	124	7.9	2069.493	30.2	3.2	59.879	737.936	6.7	47.6
37.8	1	101	6.7	1232.633	29.1	3.4	81.795	779.718	6.3	49.3
37.8	0.5	80	5.4	986.576	27.5	4.4	81.042	807.905	6.6	51.6
37.8	0.1	65	2.5	666.518	23.2	4.6	97.201	903.555	8.4	56.1
54.4	25	63	9.4	953.729	31.3	3.7	65.909	204.545	8	57.7
54.4	10	52	8.2	739.77	26.7	3.9	70.376	302.139	6	55.3
54.4	5	35	6.9	583.969	25.9	4.9	60.142	309.504	5.7	60.9
54.4	1	29	6.7	426.036	21.8	4.7	68.811	323.001	5.7	66.8
54.4	0.5	24	5.9	390.495	18.7	6.5	61.66	340.147	7.2	70.5
54.4	0.1	19	5.1	330.796	15.8	6.4	57.584	356.922	9.9	75.8

Table B-119 Overall Dynamic Modulus test results at various test temperatures for Mix 39 Specimen 2

Temperature (°C)	Frequency (Hz)	Stress Amplitude (P-P) (KPa)	SE (%)	Dynamic Modulus (MPa)	Phase Angle (deg.)	UC (deg.)	Strain (P-P) Recoverable (microstrain)	Accumulated Strain (microstrain)	SE (%)	UC (%)
-10	25	2216	4.9	49582.17	4.1	1.2	44.699	93.142	14	14.9
-10	10	2269	5.1	47343.62	6	0.2	47.932	58.161	8.1	9.1
-10	5	2212	4.9	46331.54	6.4	0.5	47.741	61.674	7.2	9.4
-10	1	1974	1.7	44435.62	6.1	0.4	44.43	59.419	8.6	10.3
-10	0.5	1848	0.9	39635.33	6.6	0.2	46.62	60.042	10.9	7.9
-10	0.1	1683	0.5	36086.42	9.1	0.1	46.641	69.378	10.7	8.3
4.4	25	1771	5.2	34907.35	7.8	0.3	50.731	152.273	8.2	8.6
4.4	10	1726	5.3	31077.64	10.7	0.6	55.552	116.782	7.1	5
4.4	5	1630	4.8	28860.26	11	1.4	56.478	130.716	6.5	5.7
4.4	1	1427	1.7	23997.59	12.2	1.1	59.461	138.336	13.9	7.1
4.4	0.5	1278	1	20540.94	18	0.4	62.229	154.92	9.6	7.4
4.4	0.1	1211	0.5	16587.34	19.5	1.2	73.004	285.101	5.7	10.2
21.1	25	743	6.7	17132.52	16.2	2.1	43.342	680.919	10.2	18.2
21.1	10	706	7.2	14119.34	19.6	1.4	50.018	994.182	7.3	17.9
21.1	5	582	6.9	12336.46	20.9	1.1	47.149	1130.907	7	18.2
21.1	1	430	4.9	8651.09	26.6	0.9	49.663	1194.456	5.8	21.4
21.1	0.5	355	3.8	6982.8	29.5	0	50.89	1258.754	8.4	20.8
21.1	0.1	302	1.6	4410.874	31.1	4.3	68.495	1474.694	6.1	28
37.8	25	210	9.3	4933.61	29.4	9	42.521	804.145	11.8	46.9
37.8	10	177	9.3	3550.739	31.8	6.6	49.789	1135.855	8.5	53.9
37.8	5	123	9.3	3133.839	31.3	7.4	39.388	1215.613	7.8	43.5
37.8	1	100	8	2143.184	28.8	4.6	46.506	1265.101	6.9	32.7
37.8	0.5	80	5.8	1856.349	25.7	2.1	43.089	1288.509	5.7	28.3
37.8	0.1	64	2.9	1292.543	22.1	1.1	49.89	1337.453	6.8	27.4
54.4	25	63	10.2	1599.141	34.1	6.8	39.547	322.834	12.1	52.2
54.4	10	52	8.4	1266.845	28.3	5.8	40.832	455.774	9.4	44.4
54.4	5	35	7.1	1212.097	23.6	1.5	28.887	453.605	10	24.3
54.4	1	29	6.4	910.692	19.4	1.8	32.074	463.669	8.7	24.8
54.4	0.5	24	5.3	805.747	13.7	3.6	29.214	466.613	11.1	23.5
54.4	0.1	19	3.3	696.176	11.1	3.2	26.895	473.612	11.8	28.2

Table B-120 Overall Dynamic Modulus test results at various test temperatures for Mix 39 Specimen 7

Temperature (°C)	Frequency (Hz)	Stress Amplitude (P-P) (KPa)	SE (%)	Dynamic Modulus (MPa)	Phase Angle (deg.)	UC (deg.)	Strain (P-P) Recoverable (microstrain)	Accumulated Strain (microstrain)	SE (%)	UC (%)
-10	25	2222	5.3	42925.22	6.6	8.3	51.759	137.223	19	26.4
-10	10	2267	4.9	41815.81	6.4	0.7	54.207	95.624	6.9	19.9
-10	5	2206	4.7	39582.7	6.8	0.8	55.725	94.416	8.7	18.4
-10	1	1968	1.6	37901.87	6.4	0.7	51.924	96.197	6.3	21.8
-10	0.5	1844	0.9	34174.44	6.5	0.9	53.97	98.473	10.9	18.4
-10	0.1	1682	0.5	31302.85	8.4	1.4	53.737	118.383	7	20.3
4.4	25	1769	5.3	28936.57	9.9	3.3	61.146	246.763	12.3	22.2
4.4	10	1727	5.3	27110.97	11.4	1.8	63.707	222.969	7.2	15.5
4.4	5	1632	4.9	25092.63	12.2	1.9	65.026	250.873	6.4	17.6
4.4	1	1429	1.9	20483.3	14.7	3.1	69.784	271.966	5.4	20.5
4.4	0.5	1280	1.1	18444.89	13.8	4	69.398	302.682	5.7	20.7
4.4	0.1	1210	0.5	14019.69	20.3	3.4	86.274	495.322	5	25
21.1	25	737	6.8	15160.49	21.5	2.1	48.587	449.025	10	30.8
21.1	10	702	6.6	12311.85	20.6	2.6	57.049	618.807	6.6	33.2
21.1	5	578	6.6	10624.75	21.4	2.3	54.42	696.692	6.1	34.1
21.1	1	430	5	6972.861	28.4	4.1	61.673	732.452	6.6	36.9
21.1	0.5	355	4	5691.701	29.8	3.7	62.355	763.972	8.2	36.3
21.1	0.1	302	1.8	3738.8	28.2	3.9	80.727	927.483	6.3	41.1
37.8	25	209	9.9	4203.168	29.2	4.7	49.826	339.979	10.1	38.8
37.8	10	175	9.2	3182.326	28.4	5	54.975	473.851	7.7	46.6
37.8	5	123	9.4	2511.917	28.9	6.1	49.022	483.422	7.8	46
37.8	1	100	7.6	1525.022	27.9	6.5	65.711	492.21	7.3	50.8
37.8	0.5	80	5.6	1233.295	27.4	7	64.556	498.242	6.5	52.5
37.8	0.1	65	2.8	818.642	23.3	7.3	78.855	544.727	7.1	59.9
54.4	25	64	11	1461.633	31	18.4	43.759	95.245	15.3	57.9
54.4	10	52	8.7	1124.197	30.5	9	45.822	155.424	10	47.8
54.4	5	35	7.2	930.91	29.5	10.4	37.208	162.22	9.7	47.7
54.4	1	29	6.9	610.648	23.1	10.2	48.021	173.817	8.3	58.9
54.4	0.5	24	6	521.289	22.9	9.4	46.1	180.89	13	62.2
54.4	0.1	19	4.2	418.235	16.8	9.2	44.542	197.656	10.4	66

Table B-121 Overall Dynamic Modulus test results at various test temperatures for Mix 40 Specimen 2

Temperature (°C)	Frequency (Hz)	Stress Amplitude (P-P) (KPa)	SE (%)	Dynamic Modulus (MPa)	Phase Angle (deg.)	UC (deg.)	Strain (P-P) Recoverable (microstrain)	Accumulated Strain (microstrain)	SE (%)	UC (%)
-10	25	2222	5	39339.66	8.7	1.3	56.484	116.191	11.6	13
-10	10	2268	5.1	41010.57	9.3	3.5	55.293	69.612	7.7	14.3
-10	5	2208	4.7	39858.77	9.6	3.8	55.396	73.002	6.4	11.7
-10	1	1966	1.5	36479.56	10.1	4.8	53.881	72.856	7.2	10.1
-10	0.5	1843	0.8	36047.84	12.3	4.6	51.138	77.263	8.7	7.4
-10	0.1	1683	0.6	29580.68	13.7	4.8	56.897	105.63	11.1	8.5
4.4	25	1774	5.4	28527.02	12.8	3.3	62.204	211.683	11.5	7.1
4.4	10	1734	5.6	25863.13	14	3.6	67.05	155.951	7.1	12.7
4.4	5	1637	5.1	23719.2	15	3.8	69.001	174.516	5.9	13
4.4	1	1429	2	19233.65	17.9	4.4	74.321	190.822	7.6	13.1
4.4	0.5	1279	1.2	16809.63	20.6	4.5	76.098	215.212	4.9	12.8
4.4	0.1	1211	0.5	12416.72	22.6	3.4	97.504	387.663	5.5	16.9
21.1	25	740	6.3	13928.85	23.4	5.3	53.128	601.686	9.2	5.2
21.1	10	708	6.7	11077.32	23.1	3.9	63.911	887.913	7.3	11
21.1	5	581	6.2	9535.617	24.5	4.9	60.979	997.421	6.2	11.3
21.1	1	430	4.2	6445.746	28	5.2	66.786	1028.066	5.7	9.8
21.1	0.5	355	3.2	5429.752	28.9	5.4	65.35	1066.409	4.4	9
21.1	0.1	301	1.4	3447.842	29.9	4.2	87.344	1271.039	4.3	12.1
37.8	25	214	9	4199.957	31.7	4	50.973	695.838	9.4	16.2
37.8	10	178	8.5	3314.865	29.6	1.7	53.844	978.683	7.8	13.7
37.8	5	125	8.7	2654.339	29.1	2.2	47.169	1052.918	8.6	14.3
37.8	1	101	7.7	1656.686	27.9	2.8	60.666	1097.448	6.5	17.9
37.8	0.5	79	5.7	1392.036	27.1	4.4	57.019	1131.142	6.2	16.8
37.8	0.1	65	3	1009.379	23.2	4.5	63.938	1188.404	6.5	12
54.4	25	62	9.1	1892.369	30.5	1.9	32.872	202.135	9.7	5.3
54.4	10	52	7.9	1420.324	27.2	2	36.533	290.232	6	14.3
54.4	5	35	6.7	1169.069	25.8	1.8	29.924	304.207	9.6	10.7
54.4	1	29	6.6	830.571	18	1.4	34.967	312.069	7.6	6
54.4	0.5	23	5.6	695.293	17.8	0.6	33.45	312.101	5.9	6
54.4	0.1	19	4.4	584.329	13	0.6	32.495	322.013	10.3	6.6

Table B-122 Overall Dynamic Modulus test results at various test temperatures for Mix 40 Specimen 3

Temperature (°C)	Frequency (Hz)	Stress Amplitude (P-P) (KPa)	SE (%)	Dynamic Modulus (MPa)	Phase Angle (deg.)	UC (deg.)	Strain (P-P) Recoverable (microstrain)	Accumulated Strain (microstrain)	SE (%)	UC (%)
-10	25	2214	6.1	43394.5	14.5	9.1	51.019	73.479	27.6	11.6
-10	10	2280	5.5	46237.97	6.2	0.6	49.312	34.705	7.8	11.4
-10	5	2221	5.3	45408.97	5.5	0.6	48.908	32.437	7.6	11.9
-10	1	1978	2.1	40355.92	7.7	0.6	49.019	35.119	11.7	11.4
-10	0.5	1849	1.1	39852.88	10	0.6	46.393	37.43	10	9.9
-10	0.1	1682	0.5	35259.11	8.8	1.2	47.713	51.617	9	9.3
4.4	25	1754	7.2	20966.82	20.9	10.2	83.679	355.19	25.5	27.7
4.4	10	1734	6.5	21198.35	14.2	2.7	81.791	288.87	9.3	25
4.4	5	1637	5.7	19707.92	14.8	2.6	83.077	300.491	7.4	26.4
4.4	1	1434	2.3	15835.5	17.4	2.6	90.576	308.104	6.2	26.4
4.4	0.5	1282	1.5	14808.84	18.2	2.6	86.58	324.842	5.3	29
4.4	0.1	1211	0.5	10894.99	21.7	2.3	111.198	458.743	4.1	27.6
21.1	25	746	7.4	10974.56	21.2	9.2	67.943	476.804	17.7	20.6
21.1	10	711	7.9	9105.431	22.4	1.5	78.089	658.541	8.4	20
21.1	5	583	7.9	7923.54	23.2	2.1	73.548	723.354	8.5	21.1
21.1	1	431	5.5	5332.932	26.9	1.6	80.745	742.363	7	21.5
21.1	0.5	356	4	4428.138	28.4	1.3	80.382	776.479	6	22.3
21.1	0.1	301	1.8	2840.353	29	1.1	106.128	954.377	5.6	24.6
37.8	25	210	9	4284.79	26.3	9.3	49.072	525.618	10.1	27.7
37.8	10	177	8.4	3025.012	29.7	3.6	58.544	720.817	7.3	24.4
37.8	5	124	8	2373.297	30.1	3.9	52.133	764.316	7.3	30
37.8	1	100	6.9	1431.434	29	4.1	69.943	795.204	6.6	40.8
37.8	0.5	80	5.3	1148.567	27.2	5.1	69.728	831.67	7.5	48.6
37.8	0.1	64	2.9	765.864	23.3	5.2	84.094	924.638	8.6	58.5
54.4	25	63	9.4	1467.802	35.2	4.5	43.195	206.97	8.7	47.3
54.4	10	51	7.8	1112.094	29.2	4.6	45.684	281.005	5.5	43.7
54.4	5	35	6.7	871.555	27.5	4.7	40.731	292.986	5.6	48.4
54.4	1	29	6.1	580.992	22.5	5	49.906	299.042	6.1	54.8
54.4	0.5	24	4.9	500.726	20.1	5.6	47.196	300.908	7.5	60.2
54.4	0.1	18	6.7	377.87	16.8	4.1	48.503	312.187	9	66.3

Table B-123 Overall Dynamic Modulus test results at various test temperatures for Mix 40 Specimen 4

Temperature (°C)	Frequency (Hz)	Stress Amplitude (P-P) (KPa)	SE (%)	Dynamic Modulus (MPa)	Phase Angle (deg.)	UC (deg.)	Strain (P-P) Recoverable (microstrain)	Accumulated Strain (microstrain)	SE (%)	UC (%)
-10	25	2214	5.9	44299.03	22.6	8.7	49.984	111.43	28.7	59.8
-10	10	2278	5.2	49076.04	7.2	1.4	46.424	73.858	11.7	54.6
-10	5	2217	5.1	46378.36	7.8	2.3	47.797	70.552	8.8	52.2
-10	1	1973	1.9	41147.29	13.8	5.4	47.956	69.818	15.2	49.6
-10	0.5	1845	1	41656.86	8.6	3.7	44.298	71.247	13.9	55.6
-10	0.1	1683	0.5	34515.41	12.5	4.1	48.748	92.824	11.7	49.7
4.4	25	1772	6.2	15495.51	4.1	32.7	114.377	198.036	24.6	76.1
4.4	10	1734	5.7	29982.04	13.8	3.9	57.838	153.374	9.6	55.5
4.4	5	1631	5.3	27582.33	14.1	3.8	59.141	169.737	7.1	54.8
4.4	1	1429	2.1	22098.69	16.9	3.1	64.654	182.512	9	53.1
4.4	0.5	1280	1.3	19294.38	18.3	3.7	66.316	200.098	5.8	50.1
4.4	0.1	1211	0.6	15176.96	20.5	3.5	79.764	334.489	10.3	53
21.1	25	735	7.2	6441.782	13.2	23.8	114.13	479.368	18.9	66.2
21.1	10	701	7.4	13105.59	22.5	4.2	53.474	686.663	10.3	60.9
21.1	5	577	7.2	11101.61	23.6	4.3	52.015	752.883	7.4	57.9
21.1	1	429	4.9	7418.045	26.8	5	57.813	768.651	6.4	54.8
21.1	0.5	355	3.7	6230.103	28	5.2	56.934	791.522	6	53.6
21.1	0.1	302	1.6	4001.532	29.6	4.3	75.385	930.805	5.7	50.2
37.8	25	211	9.1	5284.999	22.2	14.4	39.901	578.82	16.8	36.3
37.8	10	175	8.1	4879.846	27.6	2.1	35.942	798.822	8.7	61.9
37.8	5	122	8	3898.444	27.7	2.7	31.286	840.394	11.3	57.8
37.8	1	99	7.1	2480.951	26.7	2.6	40.1	876.713	8	53.1
37.8	0.5	79	5.3	2044.484	25.2	3.1	38.787	891.037	7.2	48.3
37.8	0.1	64	2.4	1416.722	20.7	1.2	45.293	914.182	7.8	45.2
54.4	25	64	9.9	2114.11	30.8	5.2	30.313	231.386	9.5	29.7
54.4	10	51	8.5	1591.57	25.6	2.1	32.284	312.071	6.7	28.8
54.4	5	36	7.3	1299.04	23.2	2.8	27.338	307.655	6.5	23.9
54.4	1	29	6.6	948.169	18.6	2.9	30.86	303.767	8	17.7
54.4	0.5	24	5.4	877.044	15.9	3	26.887	296.238	7.3	13.9
54.4	0.1	19	4.2	732.519	9.8	2.5	25.615	287.27	11.9	10.5

Table B-124 Overall Dynamic Modulus test results at various test temperatures for Mix 41 Specimen 1

Temperature (°C)	Frequency (Hz)	Stress Amplitude (P-P) (KPa)	SE (%)	Dynamic Modulus (MPa)	Phase Angle (deg.)	UC (deg.)	Strain (P-P) Recoverable (microstrain)	Accumulated Strain (microstrain)	SE (%)	UC (%)
-10	25	2208	5	53131.01	1.8	10	41.559	76.803	20.7	25.5
-10	10	2253	4.6	54105.22	4.4	3.6	41.65	48.061	8.2	27.6
-10	5	2189	4.3	52892.62	5	3.6	41.384	58.331	7.5	27.1
-10	1	1959	1.3	52291.1	2.5	5.6	37.472	64.4	16.5	26.7
-10	0.5	1844	0.8	46043.07	5.9	4.5	40.045	71.28	7.2	27.1
-10	0.1	1680	0.5	46515.86	124.9	203.8	36.107	76.244	8.6	25.7
4.4	25	1771	5.8	41895.79	1.6	9.8	42.273	43.401	22	27.4
4.4	10	1723	4.7	41188.4	6.8	1.8	41.834	6.172	8.2	31.7
4.4	5	1624	4.6	40483.73	6.7	1.7	40.106	3.325	7.4	31.3
4.4	1	1424	1.6	36980.13	6.5	1.8	38.518	2.833	7	31.2
4.4	0.5	1278	0.9	35399.2	12.9	2.5	36.089	3.997	9.4	30.8
4.4	0.1	1210	0.4	30767.06	8.9	1.6	39.33	16.936	8.5	29.7
21.1	25	1450	5.5	27049.51	11.4	2.2	53.615	270.243	12.2	22
21.1	10	1401	5	23423.37	14	0.7	59.814	267.524	6.6	32.4
21.1	5	1164	4.8	21604.73	14.8	1.2	53.89	273.241	6.7	31.8
21.1	1	858	2.1	17107.56	17.9	1	50.151	263.844	7	31.1
21.1	0.5	709	1.4	15782.38	17.2	0.8	44.947	267.441	5.7	30.1
21.1	0.1	605	0.7	11650.99	22.4	0.4	51.901	321.559	7	28.1
37.8	25	668	6.8	12434.91	22.4	7.3	53.729	597.279	9.7	10.7
37.8	10	574	6.6	9847.43	25.4	5.9	58.263	799.267	8.5	3
37.8	5	399	7.1	9741.283	23.2	1.6	40.919	812.431	7.7	23.5
37.8	1	322	4.7	6476.423	26.3	2.5	49.743	820.087	5.8	22.5
37.8	0.5	257	2.7	5112.449	27.6	3	50.208	828.531	6.3	22.2
37.8	0.1	209	1.2	3333.239	28.6	3.9	62.591	902.876	5.5	19.4
54.4	25	308	9	6098.085	26	2.7	50.579	639.592	8.9	23.7
54.4	10	260	7.3	3211.209	27.7	3.4	80.907	869.808	6.8	33.9
54.4	5	181	7.5	3184.362	29.7	4.5	56.785	912.526	6.9	24.1
54.4	1	150	6	2079.174	29	3.9	72.259	943.259	5.6	34.7
54.4	0.5	125	4.9	1654.732	28.8	4.1	75.717	966.933	6	35.1
54.4	0.1	100	2.6	905.602	23.7	4.2	110.152	1024.883	9	32.3

Table B-125 Overall Dynamic Modulus test results at various test temperatures for Mix 41 Specimen 2

Temperature (°C)	Frequency (Hz)	Stress Amplitude (P-P) (KPa)	SE (%)	Dynamic Modulus (MPa)	Phase Angle (deg.)	UC (deg.)	Strain (P-P) Recoverable (microstrain)	Accumulated Strain (microstrain)	SE (%)	UC (%)
-10	25	2222	4.9	38000.76	11.1	8.5	58.477	98.063	7.2	19
-10	10	2266	4.6	45070.17	6	1.7	50.267	59.319	11.1	18.3
-10	5	2204	4.6	42568.02	5.1	2	51.772	61.019	7.6	17.1
-10	1	1966	1.5	40118.94	8.9	1	49	60.944	7.9	18.8
-10	0.5	1843	0.7	40405.55	10.6	1.2	45.622	61.783	9.1	21.8
-10	0.1	1682	0.5	36120.67	6.8	1.6	46.566	70.997	9.9	20.3
4.4	25	1773	5.3	29399.17	16.7	7	60.316	73.052	7.8	3.7
4.4	10	1737	5.1	31471.4	10.9	3.2	55.184	27.214	7.9	10.1
4.4	5	1633	5	30369.51	10.7	3.5	53.782	26.921	8	10.6
4.4	1	1427	1.7	26883.95	11.4	3.6	53.062	25.325	7.3	10.4
4.4	0.5	1277	0.9	26876.21	14.8	3.9	47.507	26.539	6.5	11.4
4.4	0.1	1211	0.5	22014.08	14.2	3.4	55	46.133	7.2	11.6
21.1	25	1459	5.6	20444.43	16.7	4.4	71.388	342.185	7	4.6
21.1	10	1411	5.4	19406.45	17.2	4.3	72.722	339.479	5.8	4.6
21.1	5	1169	5	18235.65	16.6	2	64.099	357.901	5.6	11.9
21.1	1	858	2.3	14425.55	18.3	0.8	59.487	359.55	4.9	17.7
21.1	0.5	709	1.6	13177.5	20.3	0.3	53.772	367.647	5.1	21.1
21.1	0.1	606	0.7	9601.45	24.3	3.4	63.089	441.111	5.2	16.2
37.8	25	669	6.7	12009.04	19.2	1.3	55.737	675.967	7.2	18
37.8	10	573	6.9	10286.83	20.3	0.5	55.675	884.596	7.9	23.6
37.8	5	398	7.7	8719.042	21.2	1	45.674	902.999	7.9	26.4
37.8	1	323	5	5680.811	24.5	1.3	56.866	917.091	5.9	29.5
37.8	0.5	257	3.2	4482.657	25.6	1.8	57.322	929.245	4.9	32.4
37.8	0.1	208	1.5	2845.993	27.4	0.3	73.127	1026.012	5.6	36.5
54.4	25	231	8.6	3862.661	28.3	1.9	59.813	387.828	6.9	35.5
54.4	10	190	8	2881.555	28	1.5	66.096	525.242	6	44.2
54.4	5	179	8.1	2296.424	27.3	1.5	77.917	613.712	5.5	46.2
54.4	1	127	6.8	1389.72	26.3	1.5	91.727	629.046	5.5	52
54.4	0.5	91	5.3	1054.684	25.8	2.2	86.37	630.819	6.2	55.5
54.4	0.1	73	2.6	712.662	21.2	1.9	101.945	674.478	7.3	58.5

Table B-126 Overall Dynamic Modulus test results at various test temperatures for Mix 41 Specimen 6

Temperature (°C)	Frequency (Hz)	Stress Amplitude (P-P) (KPa)	SE (%)	Dynamic Modulus (MPa)	Phase Angle (deg.)	UC (deg.)	Strain (P-P) Recoverable (microstrain)	Accumulated Strain (microstrain)	SE (%)	UC (%)
-10	25	2225	5.1	53008.19	1.1	6.8	41.971	57.995	17.4	31.2
-10	10	2268	5.1	53095.97	4.2	0.2	42.713	30.796	7.9	10.2
-10	5	2215	4.9	51842.25	4.1	0.3	42.728	29.961	7.1	9.7
-10	1	1970	1.7	47316.61	8.1	2.6	41.645	30.836	14.7	8.1
-10	0.5	1843	0.9	47040.09	0.5	2.4	39.184	32.662	9.8	10.5
-10	0.1	1682	0.5	44189.31	6.7	1.4	38.061	41.993	13.5	11.6
4.4	25	1773	5.5	46692.82	3.8	10.8	37.963	48.156	22.2	32.4
4.4	10	1729	5	42365.8	6.7	0.2	40.823	16.446	8.6	11.4
4.4	5	1629	4.7	41499.29	6.5	0.2	39.243	16.741	8.5	13.3
4.4	1	1424	1.7	36978.17	9.7	0.6	38.516	16.581	13.9	15
4.4	0.5	1277	1	36209.8	5.5	1.5	35.271	18.393	13.2	18
4.4	0.1	1210	0.5	30150.36	9	0.4	40.148	33.17	11.6	15.2
21.1	25	1459	5.7	28127.84	8.7	3.9	51.861	304.369	16.9	16.4
21.1	10	1405	5.3	23511.97	13.1	0.1	59.736	336.32	7.1	0.4
21.1	5	1167	5.1	21435.93	14	0.3	54.454	362.873	6.9	1.7
21.1	1	858	2.3	16646.88	16.4	0.6	51.559	362.021	6.5	4.1
21.1	0.5	709	1.6	14732.74	16.8	0.4	48.119	369.73	5.4	4.3
21.1	0.1	606	0.7	10772.9	22.4	1.6	56.268	441.045	5.5	3.5
37.8	25	668	7.2	8950.818	24.8	3.7	74.625	506.569	8.4	38.8
37.8	10	570	7.1	6749.787	27.3	3.8	84.449	621.512	6	39.5
37.8	5	397	7.6	5653.066	28.8	3.8	70.143	624.216	6	40
37.8	1	322	5	3442.344	31.4	3.7	93.505	636.329	5.8	41.8
37.8	0.5	257	2.9	2646.714	31.8	4.1	96.997	646.542	5.4	43.1
37.8	0.1	208	1.2	1613.273	30.2	3.5	128.805	754.154	5.6	44.8
54.4	25	231	8.3	2968.155	33.1	4.7	77.763	641.458	8	44.7
54.4	10	191	7.4	2182.712	32.4	4.2	87.611	890.298	5.4	45.5
54.4	5	179	7.6	1754.989	30.8	4	101.727	1052.127	5	48.7
54.4	1	127	7	1094.844	27.6	3.7	116.301	1096.319	5.6	59.8
54.4	0.5	91	5.5	863.345	25.8	4.4	105.355	1119.18	6.1	62.5
54.4	0.1	73	3.2	602.375	21.7	4.2	120.835	1194.214	7.9	63.8

Table B-127 Overall Dynamic Modulus test results at various test temperatures for Mix 42 Specimen 1

Temperature (°C)	Frequency (Hz)	Stress Amplitude (P-P) (KPa)	SE (%)	Dynamic Modulus (MPa)	Phase Angle (deg.)	UC (deg.)	Strain (P-P) Recoverable (microstrain)	Accumulated Strain (microstrain)	SE (%)	UC (%)
-10	25	2223	4.6	50288.77	0.3	6.5	44.212	104.209	22.2	6.3
-10	10	2269	4.8	52789.41	5.5	0	42.976	72.286	8.9	17.2
-10	5	2210	4.8	50557.27	5.7	0.7	43.715	76.137	8.2	16.8
-10	1	1966	1.6	47584.83	6.4	0.5	41.323	74.955	12.1	17.2
-10	0.5	1843	0.7	46515.18	7.4	0.9	39.613	76.439	13.7	17.4
-10	0.1	1682	0.5	39024.22	9.4	0.6	43.094	92.613	10.4	16.5
4.4	25	1777	5.1	37477.18	9.9	3.5	47.418	134.422	19.5	18.8
4.4	10	1725	5	34684.57	10.4	0.8	49.741	97.296	8.8	12.1
4.4	5	1627	4.7	32473.12	10.3	0.9	50.11	104.045	7	12.2
4.4	1	1422	1.4	26248.25	14	0.9	54.191	109.13	5.4	11
4.4	0.5	1276	0.8	23372.63	15.2	1.1	54.595	120.889	5.2	9.6
4.4	0.1	1210	0.5	17924.77	20.3	3	67.502	229.68	5.6	7.6
21.1	25	618	6.9	14296.22	22	7.2	43.244	222.962	13.4	45.1
21.1	10	587	6.4	11599.5	21.5	2.8	50.578	258.419	10.8	34.6
21.1	5	495	6.2	9805.235	22.7	2.8	50.492	261.931	7.3	34.8
21.1	1	358	4.2	6427.648	26.5	3.9	55.652	246.221	6.4	40
21.1	0.5	290	2.7	5109.889	27.6	4	56.74	252.502	4.4	43.3
21.1	0.1	254	1.1	3202.754	28.3	4.7	79.279	350.33	3.8	46.7
37.8	25	222	8.3	4212.068	30.5	6.5	52.811	189.793	9.2	41.6
37.8	10	187	7.4	3163.481	30.1	4.7	59.152	255.868	6.4	42
37.8	5	130	7.4	2485.749	28.7	3.2	52.485	252.163	6.4	46.2
37.8	1	106	6.2	1506.878	27.6	2	70.333	253.659	6.3	49.9
37.8	0.5	85	4.7	1228.33	26.3	1.9	68.852	261.586	5.6	52.7
37.8	0.1	67	2.3	824.837	22.1	1.3	80.847	301.062	5.4	56.4
54.4	25	115	8.7	1406.988	30.9	5.1	81.964	483.427	6.5	34.5
54.4	10	93	8	1090.353	27.6	3.8	85.643	650.336	5.7	39.9
54.4	5	87	7.9	938.345	24.4	2.4	92.398	776.084	4.6	43.2
54.4	1	62	7.4	690.344	19.6	0.9	89.76	789.072	4.7	48.4
54.4	0.5	44	5.9	575.376	19.2	1.3	76.489	797.807	5	48
54.4	0.1	35	3.3	460.953	15.1	1.9	75.743	824.816	7.9	45.3

Table B-128 Overall Dynamic Modulus test results at various test temperatures for Mix 42 Specimen 2

Temperature (°C)	Frequency (Hz)	Stress Amplitude (P-P) (KPa)	SE (%)	Dynamic Modulus (MPa)	Phase Angle (deg.)	UC (deg.)	Strain (P-P) Recoverable (microstrain)	Accumulated Strain (microstrain)	SE (%)	UC (%)
-10	25	2224	4.8	43263.11	6	3.9	51.418	103.438	15.7	13.3
-10	10	2268	4.9	40495.14	9.3	3	56.012	59.285	7.2	18.7
-10	5	2207	4.6	38399	9.3	3.1	57.466	62.28	7.3	19.9
-10	1	1965	1.5	35542.47	9.7	4.6	55.283	62.777	8.1	19.9
-10	0.5	1841	0.8	31321.72	10.8	5	58.779	67.062	8.8	17.7
-10	0.1	1685	0.5	27354.53	15.9	4.2	61.591	95.618	12	19.7
4.4	25	1772	5.1	27334.94	14.9	3.4	64.821	269.931	12.8	22.6
4.4	10	1734	5	22744	16	3.6	76.242	208.026	7.7	23.8
4.4	5	1632	4.8	20574.36	17	3.5	79.314	224.805	6.5	26.9
4.4	1	1426	1.6	16005.05	19.2	3.8	89.111	238.322	5.4	29.2
4.4	0.5	1278	0.8	13720.41	18.9	5.1	93.151	265.869	4.5	29.1
4.4	0.1	1211	0.5	9654.797	23.2	1.6	125.389	450.757	4	35.1
21.1	25	625	7	10873.02	23.1	3.8	57.444	578.293	13.2	42.2
21.1	10	590	6.6	8424.807	25.3	3.1	70.084	809.58	6.7	35.8
21.1	5	498	6.6	6882.977	26.2	2.2	72.423	913.252	6.7	36.5
21.1	1	358	4.6	4287.366	29.4	1.8	83.614	948.179	6.4	39.5
21.1	0.5	291	3	3310.699	31	0.7	87.833	1003.065	5	39.8
21.1	0.1	255	1.1	1988.957	30.1	0.3	127.985	1249.942	3.9	40.7
37.8	25	224	7.6	2753.741	32.7	4.1	81.32	789.934	8.6	42.4
37.8	10	189	7.2	1915.326	32.5	2.5	98.49	1107.834	5.8	40.2
37.8	5	132	7.2	1463.499	32.1	3.6	89.944	1191.3	5.7	41.9
37.8	1	107	6.9	890.263	28.6	3.1	119.89	1247.068	5.7	45
37.8	0.5	85	5.5	717.904	27.1	3.4	118.349	1287.944	6	46.6
37.8	0.1	67	3.1	507.69	22.1	3.6	131.013	1386.853	7.4	49.9
54.4	25	59	8.5	821.004	34.3	6.3	71.449	142.356	7.7	57
54.4	10	46	7.4	622.674	28	4.7	74.013	210.782	5.4	58
54.4	5	44	7.2	540.827	24.8	5.2	80.509	271.49	5.3	57.2
54.4	1	31	7.2	381.353	19.7	5.1	81.391	275.285	5.2	60.5
54.4	0.5	22	5.5	334.929	18	3.7	65.242	283.189	4.8	62.4
54.4	0.1	17	3.8	280.642	13.4	3.6	60.574	303.944	7	66.2

Table B-129 Overall Dynamic Modulus test results at various test temperatures for Mix 42 Specimen 5

Temperature (°C)	Frequency (Hz)	Stress Amplitude (P-P) (KPa)	SE (%)	Dynamic Modulus (MPa)	Phase Angle (deg.)	UC (deg.)	Strain (P-P) Recoverable (microstrain)	Accumulated Strain (microstrain)	SE (%)	UC (%)
-10	25	2221	5	35305.16	9	7.2	62.91	70.4	8.1	27
-10	10	2263	4.8	38210.55	9.3	4.8	59.221	21.428	11.6	27
-10	5	2197	4.5	38211.2	9.8	4.5	57.484	20.019	9.5	29.6
-10	1	1963	1.4	34005.86	7.8	5.1	57.722	21.931	7.2	27.4
-10	0.5	1842	0.7	32072.09	12.3	5.9	57.435	22.905	9.6	25.9
-10	0.1	1682	0.4	29022.63	12.2	4.8	57.944	37.328	8.8	26.4
4.4	25	1776	5.2	25710.35	13.5	9.2	69.074	175.955	8.4	25
4.4	10	1734	5.4	23993.08	12.9	3.2	72.253	112.062	8.4	26.5
4.4	5	1627	4.8	22018.99	12.8	3.1	73.908	118.178	7.2	27
4.4	1	1427	1.7	17874.16	13.5	3	79.815	126.527	8.1	27.6
4.4	0.5	1278	0.9	15802.01	14	2.6	80.904	140.707	8.6	26.4
4.4	0.1	1211	0.5	12265.96	19	1.4	98.706	248.079	4.8	29.8
21.1	25	625	6.8	11615.98	18.8	0.7	53.827	329.301	9.6	29.4
21.1	10	593	7	10013.74	20.6	0.1	59.171	447.153	6.5	33.7
21.1	5	497	6.9	8813.724	20.8	1.6	56.433	495.52	9.1	37.2
21.1	1	358	4.8	5945.796	24.1	1.7	60.284	498.533	8.4	39.3
21.1	0.5	291	2.9	4666.894	27.9	0.3	62.305	518.813	8.5	38.8
21.1	0.1	255	1.2	3133.193	26.3	1.9	81.375	650.64	5.2	41.8
37.8	25	224	8.2	3974.28	26.2	2.3	56.361	507.944	8.2	39.8
37.8	10	188	7.9	3080.441	27.2	2.8	60.993	711.488	6.1	44.4
37.8	5	131	7.9	2437.363	27.7	3	53.652	757.7	6.5	45.7
37.8	1	106	6.6	1480.7	27.7	3.2	71.826	781.533	6.3	48.9
37.8	0.5	86	4.9	1203.417	27.1	3.5	71.318	810.195	6	49.7
37.8	0.1	67	2.4	807.222	25.3	2.7	82.684	891.145	6.8	51
54.4	25	59	8.9	1374.606	30.6	3	42.715	274.66	9.7	47.3
54.4	10	47	7.3	1085.767	28.5	6.4	43.486	379.358	10.2	50.5
54.4	5	44	7.4	1025.814	28.7	5	43.232	443.042	9.4	46.6
54.4	1	32	6.4	959.882	21.4	5.3	32.824	454.23	13.9	33.6
54.4	0.5	22	5.1	857.913	20.9	2.7	25.808	458.042	11.2	23.3
54.4	0.1	17	4.2	693.249	15.8	1.4	24.648	466.554	10.1	23.1

Table B-130 Overall Dynamic Modulus test results at various test temperatures for Mix 43 Specimen 1

Temperature (°C)	Frequency (Hz)	Stress Amplitude (P-P) (KPa)	SE (%)	Dynamic Modulus (MPa)	Phase Angle (deg.)	UC (deg.)	Strain (P-P) Recoverable (microstrain)	Accumulated Strain (microstrain)	SE (%)	UC (%)
-10	25	2220	4.9	47831.91	4.7	3.6	46.413	114.202	14.1	9.6
-10	10	2264	4.8	47798.21	5	0.3	47.366	84.511	8.8	6.1
-10	5	2203	4.6	46423.18	5.3	0.5	47.445	83.256	7.5	6.9
-10	1	1966	1.5	41511.07	8.7	0.9	47.361	84.346	11.6	7.3
-10	0.5	1843	0.7	39358.15	1.3	2.3	46.823	83.428	11.5	7.7
-10	0.1	1681	0.4	36139.29	8	0.8	46.514	94.986	9.9	6.9
4.4	25	1776	5.1	34980.15	8.9	2.5	50.759	172.034	11.2	5.9
4.4	10	1731	5	31503.08	10.6	0.5	54.933	127.237	6.4	9.7
4.4	5	1630	4.7	29824.4	10.8	0.6	54.651	139.192	7	8.5
4.4	1	1424	1.5	24269.98	15.4	1.5	58.661	143.604	7.3	9.7
4.4	0.5	1276	0.7	22165.87	14.1	1.4	57.55	159.508	6.5	9.9
4.4	0.1	1210	0.5	16470.91	19.4	1.9	73.448	281.887	5.1	11.4
21.1	25	623	7	17092.93	15.1	2.6	36.457	322.136	11.8	8.6
21.1	10	590	6.4	13805.45	19.7	1.2	42.712	403.504	6.1	15.4
21.1	5	497	6.6	11879.89	21.4	1.2	41.795	425.21	6.7	15.8
21.1	1	359	4.1	7816.75	26.4	3.7	45.881	414.411	6.4	14
21.1	0.5	290	2.7	6435.84	26.9	4.3	45.133	420.047	6.9	15.1
21.1	0.1	254	1	4096.04	27	3.1	62.101	500.184	6.5	19
37.8	25	222	7.9	5587.291	28.5	6.8	39.712	446.717	9	11.7
37.8	10	189	8	4222.683	26.6	2.2	44.672	571.601	8.1	20.6
37.8	5	131	8.3	3295.311	25.8	2.5	39.66	580.083	8.6	19.1
37.8	1	106	7.2	1999.582	28.8	6.8	53.057	583.533	7.4	13.8
37.8	0.5	85	5.3	1699.884	25.2	4.5	50.261	593.655	7.5	16.7
37.8	0.1	66	2.6	1218.003	18.6	1.7	54.587	619.24	8.9	16
54.4	25	57	9.2	1692.008	32.8	6.5	33.427	90.177	11.5	9.5
54.4	10	46	7.2	1358.756	28.6	6.7	34.165	108.843	6.4	11.5
54.4	5	43	7	1123.569	25.9	7.1	38.214	116.355	7.1	8.9
54.4	1	31	6	843.457	19.1	2.8	36.414	120.969	6.4	14.5
54.4	0.5	22	4.9	720.444	18.8	2.3	30.746	121.77	9.2	12
54.4	0.1	17	3.6	557.722	13	1.9	30.767	127.015	10.8	10.6

Table B-131 Overall Dynamic Modulus test results at various test temperatures for Mix 43 Specimen 2

Temperature (°C)	Frequency (Hz)	Stress Amplitude (P-P) (KPa)	SE (%)	Dynamic Modulus (MPa)	Phase Angle (deg.)	UC (deg.)	Strain (P-P) Recoverable (microstrain)	Accumulated Strain (microstrain)	SE (%)	UC (%)
-10	25	2224	4.9	48173.14	5.2	12.4	46.168	83.343	20	15.1
-10	10	2266	4.8	45796.95	6.2	1.3	49.483	41.913	8.2	24.5
-10	5	2205	4.6	43549.7	5.5	1.3	50.64	40.206	7.5	24.8
-10	1	1966	1.4	40173.41	6	2.7	48.934	42.127	9.1	23.7
-10	0.5	1843	0.7	35940.66	8.6	3.8	51.273	45.089	9.4	22.8
-10	0.1	1682	0.5	32193.56	12.3	6.5	52.26	61.121	10.8	21.7
4.4	25	1775	5	30497.19	11.4	15.4	58.202	247.856	14.4	7.2
4.4	10	1728	4.7	28051.84	14.7	6.2	61.606	193.841	7.2	15.4
4.4	5	1628	4.8	24956.43	16.1	7	65.222	211.115	5.9	14.5
4.4	1	1426	1.6	18963.81	19	7.6	75.174	224.24	9.2	16.7
4.4	0.5	1278	0.9	16357.27	20.8	7.3	78.113	251.323	7.5	17.7
4.4	0.1	1210	0.5	11669.22	24.9	6.3	103.719	441.853	4.7	23.8
21.1	25	624	7.2	14096.19	20.9	5.3	44.248	442.686	13.4	7.3
21.1	10	592	6.9	10702.73	26.7	8	55.296	577.491	6	11.4
21.1	5	498	6.8	8695.815	27.9	8.4	57.253	640.53	6	15.6
21.1	1	358	5	5267.449	30.8	8.5	68.021	649.811	6.2	24.2
21.1	0.5	291	3.3	3986.086	31.7	8.2	73.008	660.995	6.1	26
21.1	0.1	254	1.3	2388.957	29	5.9	106.474	769.898	6.6	34
37.8	25	221	7.4	3380.281	33.2	7	65.376	645.076	7.5	28.8
37.8	10	186	7.2	2318.16	32.1	6.4	80.34	849.791	5.4	35.4
37.8	5	131	7.2	1869.482	31.7	7.5	69.962	881.555	5.4	29.8
37.8	1	106	7	1111.568	27.8	6.3	95.189	899.654	5.6	34.4
37.8	0.5	84	5.6	940.573	26.2	6.5	89.827	931.878	6.3	32.4
37.8	0.1	66	3.3	682.281	22	7	97.341	988.67	7.6	29.7
54.4	25	57	8.9	1309.487	26.3	4.7	43.672	292.424	10	41.2
54.4	10	47	7.1	1018.822	23.9	1	46.178	368.081	5	25.1
54.4	5	43	7	844.949	21.4	0.9	51.123	386.341	4.7	24.2
54.4	1	31	6.9	645.165	16.5	0.5	47.984	410.589	10.7	24.7
54.4	0.5	21	5.5	527.126	15	0.6	40.649	412.92	7.8	23.7
54.4	0.1	17	5	448.046	11.4	0.7	37.853	422.613	8.2	23.2

Table B-132 Overall Dynamic Modulus test results at various test temperatures for Mix 43 Specimen 4

Temperature (°C)	Frequency (Hz)	Stress Amplitude (P-P) (KPa)	SE (%)	Dynamic Modulus (MPa)	Phase Angle (deg.)	UC (deg.)	Strain (P-P) Recoverable (microstrain)	Accumulated Strain (microstrain)	SE (%)	UC (%)
-10	25	2217	5	43704.89	12.2	2.2	50.734	76.938	25	26
-10	10	2264	4.8	45509.56	7.2	3.9	49.737	39.154	7.5	38.6
-10	5	2199	4.5	43853.32	6.7	4.7	50.136	38.312	8.8	40
-10	1	1961	1.4	39111.38	9.9	3.8	50.13	37.343	8.9	38.4
-10	0.5	1841	0.7	37242.6	4.1	5.9	49.44	40.46	11.5	37
-10	0.1	1682	0.5	34069.54	10.7	4.1	49.372	51.706	10.7	36.9
4.4	25	1771	5.3	34886.26	19.2	8	50.751	125.776	18.6	38.4
4.4	10	1732	5	28789.24	12.8	3.5	60.174	66.174	10	38.1
4.4	5	1631	4.9	27228.53	13.4	3.4	59.901	69.864	8.1	38.2
4.4	1	1427	1.7	21904.55	15.5	4.1	65.164	73.868	10	38.6
4.4	0.5	1278	0.9	21187.04	17.1	4.3	60.335	81.69	7.3	38.3
4.4	0.1	1210	0.4	15630.83	19.2	3.5	77.383	156.681	6.7	39.1
21.1	25	622	7.3	17167.31	12.1	13.6	36.224	220.117	24.9	16.4
21.1	10	593	7.6	15201.47	21	3.1	38.987	293.893	10.2	16.8
21.1	5	500	7.5	13121.95	20.9	2.5	38.095	316.625	8.8	16.5
21.1	1	359	5.3	9121.587	25.4	2	39.327	313.319	8.7	14.6
21.1	0.5	291	3.6	7663.101	24.5	1.9	38.003	320.8	7.6	15.8
21.1	0.1	255	1.2	5023.206	26.7	3.2	50.688	386.269	6.1	16.4
37.8	25	221	8.3	5326.051	21.2	19.1	41.468	503.853	13.1	50.1
37.8	10	188	7.9	4392.32	29.6	4.9	42.715	666.989	8.9	39.3
37.8	5	130	7.3	4170.263	25.4	0.6	31.158	679.945	9.6	19.1
37.8	1	107	6.3	2607.381	26.1	3	40.892	689.542	7.4	27.2
37.8	0.5	84	4.8	2207.263	24.7	2	38.233	690.021	7.5	23.2
37.8	0.1	67	2.3	1526.237	21.3	2.1	43.615	712.263	7.3	24.2
54.4	25	58	8.8	2582.344	29.1	3.5	22.426	92.298	16.8	49
54.4	10	46	6.9	1812.164	25	2.5	25.522	131.061	11.7	25.8
54.4	5	44	6.5	1555.333	23.8	2.1	28.036	163.347	10.4	29.4
54.4	1	31	6.3	1006.087	19	2.2	30.995	166.662	7.9	26.6
54.4	0.5	22	5.4	835.868	21.3	1.5	26.183	167.149	8.5	27.6
54.4	0.1	17	4.2	638.437	15.9	1.8	26.732	177.253	15.8	30.5

Table B-133 Overall Dynamic Modulus test results at various test temperatures for Mix 44 Specimen 2

Temperature (°C)	Frequency (Hz)	Stress Amplitude (P-P) (KPa)	SE (%)	Dynamic Modulus (MPa)	Phase Angle (deg.)	UC (deg.)	Strain (P-P) Recoverable (microstrain)	Accumulated Strain (microstrain)	SE (%)	UC (%)
-10	25	2224	5.4	50234	5.5	22.2	44.269	69.624	30.9	19.4
-10	10	2268	4.9	55503.6	6.9	2.2	40.868	22.683	8.4	27.2
-10	5	2209	4.8	52932.03	7	3.4	41.741	20.118	7.9	24.3
-10	1	1972	1.7	46671.84	10.5	5.4	42.246	21.939	9.2	21.3
-10	0.5	1847	0.9	45724.62	12	6.1	40.385	23.155	8.6	21.3
-10	0.1	1682	0.5	39805.52	10	5.1	42.255	42.375	15.2	19.2
4.4	25	1780	5.6	30300.89	10.9	10.9	58.753	204.98	24.8	13.4
4.4	10	1733	5.4	29736.48	16.3	5.6	58.28	141.551	7.2	5.6
4.4	5	1632	5	27726.71	17.1	5.4	58.863	152.238	6.2	4.1
4.4	1	1430	1.9	21282.98	19.2	6.3	67.174	164.754	6.4	11.2
4.4	0.5	1281	1.1	18957.49	19.1	6.3	67.556	185.421	6	12.9
4.4	0.1	1211	0.5	13585.66	23.3	4.4	89.164	323.183	7.1	21.3
21.1	25	623	7.8	11179.15	24.1	7.4	55.761	504.934	12	11.7
21.1	10	589	7.6	11001.31	23.1	3.8	53.525	745.567	8.4	24.9
21.1	5	497	7.6	9290.451	24.5	3.6	53.497	869.309	8.4	27.1
21.1	1	358	4.7	6131.396	28	3.6	58.426	912.25	7.9	29.3
21.1	0.5	288	3.1	5038.689	30.8	3.4	57.081	965.349	5.6	33.6
21.1	0.1	252	1	3078.018	30.8	3.2	82.032	1163.604	4.5	38
37.8	25	221	7.8	4524.321	30.2	3.7	48.915	521.099	9.7	18.6
37.8	10	187	7.2	3432.672	30.7	4.2	54.529	737.644	8.4	30.2
37.8	5	131	7.4	2717.276	29	4.5	48.118	768.939	9.4	38
37.8	1	107	5.8	1623.231	27.8	4.6	65.907	795.284	7.8	46.2
37.8	0.5	85	4.3	1327.223	26.1	4.4	63.871	807.54	7.1	48.8
37.8	0.1	66	2.3	889.841	21.4	4.8	73.88	850.613	9.1	55.3
54.4	25	60	9.2	1340.943	29.2	4.1	44.41	206.371	10	48.4
54.4	10	46	6.7	958.085	27.8	3.2	48.515	285.691	5.6	60.7
54.4	5	45	6.6	777.975	24.8	3	57.339	343.169	7.6	64
54.4	1	31	6.1	538.454	20.6	2.9	57.418	340.602	5	66.5
54.4	0.5	22	5	455.853	19.8	2.6	48.141	343.576	7.7	63.8
54.4	0.1	17	3.4	374.934	15.2	2.3	44.272	357.369	9.3	65.4

Table B-134 Overall Dynamic Modulus test results at various test temperatures for Mix 44 Specimen 3

Temperature (°C)	Frequency (Hz)	Stress Amplitude (P-P) (KPa)	SE (%)	Dynamic Modulus (MPa)	Phase Angle (deg.)	UC (deg.)	Strain (P-P) Recoverable (microstrain)	Accumulated Strain (microstrain)	SE (%)	UC (%)
-10	25	2217	4.8	52348.97	4.4	6.6	42.358	86.086	14.8	33.1
-10	10	2262	4.6	53031.44	5.9	0.2	42.649	54.222	7.8	13.6
-10	5	2197	4.6	51688.01	5.9	0.2	42.511	57.399	8	14.3
-10	1	1966	1.4	46469.55	6.8	0.4	42.306	56.823	13.3	15.4
-10	0.5	1845	0.7	45552.81	10.7	1.7	40.492	60.383	8.2	17.5
-10	0.1	1682	0.4	39102.81	10.4	1.2	43.011	76.588	15.5	17.5
4.4	25	1776	5.3	36719.84	7.5	3.4	48.379	154.136	14.8	26.1
4.4	10	1732	5.1	35736.87	10.5	1	48.477	112.643	9.4	15.5
4.4	5	1630	4.8	32721.5	11.1	1.2	49.806	122.789	8.2	14.9
4.4	1	1426	1.6	26578.51	13.7	1.4	53.65	132.83	9	16.2
4.4	0.5	1277	0.9	23289.91	13.2	2.2	54.813	145.731	7.7	16.4
4.4	0.1	1211	0.5	18387.92	18	2.3	65.881	252.373	12.2	17.8
21.1	25	621	6.9	18081.56	11.7	5.1	34.334	304.848	14.3	23.2
21.1	10	592	6.6	15810.19	19.8	0.6	37.428	433.686	7.4	20.3
21.1	5	498	6.6	14205.65	21.3	1.2	35.08	491.966	10.4	22.1
21.1	1	359	4.3	9033.858	25.9	0.5	39.735	503.062	12.8	22.6
21.1	0.5	291	2.7	7657.378	28.5	1.5	38.024	527.414	12.2	26.8
21.1	0.1	254	1	4874.749	29.2	1.1	52.103	661.545	7	21.4
37.8	25	223	7.9	5502.288	28.4	3.3	40.556	604.353	10.9	47.5
37.8	10	188	7.1	4064.787	29.2	1.2	46.177	862.552	7.2	60.3
37.8	5	131	7.4	3184.998	30	2.1	41.08	916.173	7.5	62.8
37.8	1	107	6	1944.317	29.8	2.2	55.007	960.76	7.5	64.3
37.8	0.5	85	4.6	1551.306	28.6	2.8	54.957	988.11	6.3	63.8
37.8	0.1	66	2.4	1005.516	24.6	2.3	65.951	1053.131	5.7	68.6
54.4	25	59	10.1	1380.483	32.7	3	42.513	320.589	11	64.6
54.4	10	47	6.3	1071.426	26	1.8	43.641	453.62	7.1	77
54.4	5	43	6.6	870.542	23.9	1.7	49.635	520.407	6.1	78.1
54.4	1	32	5.8	611.345	19.9	0.7	51.899	554.677	7.1	77
54.4	0.5	22	5.5	553.154	16.4	1.8	39.15	558.439	8.8	80
54.4	0.1	17	4.2	435.165	15.1	0.3	39.026	570.325	10.3	75.5

Table B-135 Overall Dynamic Modulus test results at various test temperatures for Mix 44 Specimen 4

Temperature (°C)	Frequency (Hz)	Stress Amplitude (P-P) (KPa)	SE (%)	Dynamic Modulus (MPa)	Phase Angle (deg.)	UC (deg.)	Strain (P-P) Recoverable (microstrain)	Accumulated Strain (microstrain)	SE (%)	UC (%)
-10	25	2226	5.1	47421.73	3.2	6.3	46.934	90.562	12.5	18.8
-10	10	2272	5.1	48107.86	6.6	1.7	47.223	52.119	7.1	7.1
-10	5	2211	4.9	46566.55	6.6	1.5	47.478	48.173	7.9	5.5
-10	1	1968	1.6	41106.69	8.7	2.2	47.866	48.791	10.3	7.3
-10	0.5	1841	0.9	41501.76	3.8	2.3	44.371	52.079	10.9	6.4
-10	0.1	1686	0.6	36381.21	9.5	1.6	46.346	66.275	10.2	7.5
4.4	25	1784	5.4	33910.87	7.5	2.6	52.594	175.63	11.1	13.6
4.4	10	1734	5.4	31507.25	10.9	1.1	55.05	120.793	7.7	12.9
4.4	5	1633	5	28417.55	12.4	1.2	57.48	126.668	7.7	13.4
4.4	1	1426	1.8	22975.46	17.4	2.9	62.078	134.437	8.5	10.2
4.4	0.5	1277	1	20942.37	15.1	3.5	60.967	149.983	6.5	10.3
4.4	0.1	1212	0.6	14912.14	24	4.8	81.253	256.447	6.4	6.7
21.1	25	624	7	16112.98	21.4	4.9	38.725	346.795	13.9	9.7
21.1	10	592	6.6	12949.7	22.1	5.4	45.726	509.93	10.2	22.1
21.1	5	500	6.6	11078.57	25.6	4.5	45.125	601.735	9.8	11.1
21.1	1	359	4.7	7841.265	31.1	5.8	45.795	642.944	11.5	2.1
21.1	0.5	291	3.2	6262.557	32	4.2	46.387	688.172	9.7	4.5
21.1	0.1	255	1.1	3884.885	33	4.9	65.677	833.917	7.2	11.6
37.8	25	224	7.9	5364.354	27.9	4.7	41.736	713.768	9.9	18.9
37.8	10	187	7.5	3978.245	30.9	2.6	47.092	1043.872	9.6	25.3
37.8	5	131	7.7	3254.252	31	3.4	40.37	1135.386	9.4	30
37.8	1	107	6.5	2057.418	30.7	3.2	51.775	1191.679	6.3	28.1
37.8	0.5	85	5.5	1778.914	29.4	3.2	47.715	1227.899	6.5	22.7
37.8	0.1	66	2.8	1365.214	24.7	1.1	48.225	1285.244	6.5	13.8
54.4	25	59	8.2	1972.505	36.6	3.7	29.664	281.556	9.7	35.5
54.4	10	46	6.8	1749.063	29.7	5.7	26.339	407.166	7.8	31.1
54.4	5	44	6.6	1442.956	28.2	6.1	30.231	498.215	8.8	33.6
54.4	1	32	6.1	1132.281	21.8	2.3	27.829	508.067	7.2	23.1
54.4	0.5	22	5	979.931	17.4	1.7	22.649	509.49	9.3	21
54.4	0.1	17	4.8	805.41	12.9	2	21.413	515.876	14.6	25.6

Table B-136 Overall Dynamic Modulus test results at various test temperatures for Mix 45 Specimen 1

Temperature (°C)	Frequency (Hz)	Stress Amplitude (P-P) (KPa)	SE (%)	Dynamic Modulus (MPa)	Phase Angle (deg.)	UC (deg.)	Strain (P-P) Recoverable (microstrain)	Accumulated Strain (microstrain)	SE (%)	UC (%)
-10	25	2226	5	53894.37	2.7	6	41.304	59.918	15.7	14.6
-10	10	2268	4.9	54456.68	7.1	1.3	41.645	27.611	7.5	18
-10	5	2196	4.5	54150.98	5.6	2	40.557	27.309	12.5	16
-10	1	1959	1.3	50797.57	9.2	2.6	38.568	27.423	11.6	12.1
-10	0.5	1840	0.7	46915	9.4	2.2	39.225	27.906	9.7	12.6
-10	0.1	1685	0.5	43943.6	8.9	2.8	38.334	36.31	11.8	9.2
4.4	25	1775	5.4	37520.7	7.2	4.1	47.299	97.43	19.3	24.8
4.4	10	1725	5.2	37314.24	11.9	2.3	46.22	62.344	8.7	14.8
4.4	5	1628	4.7	35367.4	12	3.1	46.043	64.09	9.7	14.6
4.4	1	1424	1.6	29395.68	13.9	3	48.459	65.507	10.9	18.6
4.4	0.5	1277	0.9	28732.74	14.6	3.7	44.454	70.503	11.1	24.1
4.4	0.1	1210	0.5	22618.54	16.8	3.5	53.487	116.757	8.8	23.3
21.1	25	626	7.2	22287.98	13.1	11.7	28.071	187.884	17.7	32.4
21.1	10	594	7.2	18627	18.5	4	31.884	291.482	9.4	28.3
21.1	5	501	6.9	16441.66	18.4	4.2	30.482	346.076	10.7	34.1
21.1	1	359	4.7	11591.85	24.8	3.4	30.975	362.01	15.1	35
21.1	0.5	291	3.1	10675.33	25.5	5.7	27.239	390.281	12.1	40.8
21.1	0.1	254	1.1	6449.72	29.6	3	39.44	499.316	8.8	39.2
37.8	25	420	8.1	9215.497	25.2	4.7	45.544	537.739	9.4	26.7
37.8	10	374	8	6813.179	27.7	3.8	54.942	876.456	6.2	28
37.8	5	262	6.4	5371.045	29.1	4.1	48.845	991.537	5.9	27.5
37.8	1	201	4.4	3465.504	30.3	3.6	58.074	1059.674	5.5	32.1
37.8	0.5	171	3.5	2810.427	29.8	3.3	60.97	1120.114	5.5	31.3
37.8	0.1	135	1.6	1787.446	26.8	2.2	75.326	1254.057	5.8	31
54.4	25	105	8.3	2187.497	37.4	6.2	48.011	438.535	8.4	49.8
54.4	10	94	7.6	1503.612	32.2	2.9	62.808	746.531	7.4	34.5
54.4	5	88	7.3	1152.693	29.3	2.5	76.32	912.544	7	35.7
54.4	1	64	6.7	866.248	25.2	2.9	73.945	1001.648	5.9	58.5
54.4	0.5	45	5.3	714.527	22.8	4.3	62.779	1016.088	6.6	64.9
54.4	0.1	35	3.8	534.609	18.7	5.2	65.977	1041.741	9.2	70.1

Table B-137 Overall Dynamic Modulus test results at various test temperatures for Mix 45 Specimen 3

Temperature (°C)	Frequency (Hz)	Stress Amplitude (P-P) (KPa)	SE (%)	Dynamic Modulus (MPa)	Phase Angle (deg.)	UC (deg.)	Strain (P-P) Recoverable (microstrain)	Accumulated Strain (microstrain)	SE (%)	UC (%)
-10	25	2219	4.7	62880.68	3.4	12.7	35.294	59.549	18.2	39.5
-10	10	2265	4.6	66427.09	7.2	4.6	34.092	32.333	7.1	24.9
-10	5	2200	4.5	64837.62	9.1	3.6	33.926	30.3	12	22.1
-10	1	1964	1.4	62679.17	6.8	6	31.328	32.797	11	26.5
-10	0.5	1843	0.7	56281.72	6.9	6.2	32.744	30.872	12.5	20.8
-10	0.1	1681	0.5	55293.13	8.6	5.8	30.409	35.917	14.1	26.3
4.4	25	1776	5.1	45358.1	3.4	9.8	39.15	68.727	20	53
4.4	10	1730	4.7	44464.05	9.9	1.7	38.899	31.654	10.2	38.7
4.4	5	1628	4.7	42477.12	10.5	1.6	38.319	32.53	9.9	40.6
4.4	1	1425	1.5	36697.38	11.9	2.3	38.838	32.36	17.7	43
4.4	0.5	1277	0.8	32210.8	17.4	2.6	39.653	37.86	10.5	40.3
4.4	0.1	1210	0.4	26095.21	18	3.1	46.368	74.75	10.7	39.1
21.1	25	926	5.9	22289.56	12	7	41.527	348.198	13	37
21.1	10	886	5.4	17913.72	18.7	2.3	49.463	466.399	8.5	26.2
21.1	5	749	5.2	15820.83	19.9	3.1	47.321	541.322	7.1	26.7
21.1	1	539	2.5	11100.75	24.2	4.2	48.545	569.278	5.4	26.7
21.1	0.5	447	1.9	9423.854	26.6	4.8	47.435	605.182	5.3	26.4
21.1	0.1	381	1	6338.318	30	3.8	60.058	761.583	5.4	28.6
37.8	25	416	7.3	7503.531	32.2	3.5	55.407	625.372	8.3	25.9
37.8	10	375	7.4	5136.104	32.9	1.5	72.961	993.262	5.7	24.9
37.8	5	263	5.9	4106.794	32.5	3.4	63.961	1124.874	5.6	29.7
37.8	1	201	4.1	2604.974	31.5	4.8	77.186	1194.729	5.5	35.3
37.8	0.5	171	3.1	2182.699	30.2	4.9	78.335	1248.07	6	39
37.8	0.1	134	1.6	1514.179	24.6	3.7	88.354	1350.811	7.3	48.5
54.4	25	105	9.1	3707.609	33.2	3.1	28.224	455.04	11.2	5
54.4	10	93	8	2733.813	28.5	2.4	34.059	710.051	5.6	6.5
54.4	5	88	7.9	2212.112	27	2.1	39.82	870.889	4.5	8.2
54.4	1	63	6.4	1462.271	22.4	1.2	42.927	883.792	6.9	6
54.4	0.5	45	4.9	1215.446	20.6	1	37.173	892.219	6	7.8
54.4	0.1	35	3.4	931.476	17.3	0.5	38.088	908.053	8.3	6

Table B-138 Overall Dynamic Modulus test results at various test temperatures for Mix 45 Specimen 4

Temperature (°C)	Frequency (Hz)	Stress Amplitude (P-P) (KPa)	SE (%)	Dynamic Modulus (MPa)	Phase Angle (deg.)	UC (deg.)	Strain (P-P) Recoverable (microstrain)	Accumulated Strain (microstrain)	SE (%)	UC (%)
-10	25	2205	4.8	72556.98	7.1	14.4	30.392	33.294	15.4	16.8
-10	10	2274	4.8	76607.79	4.8	4.4	29.69	6.937	11.2	14.5
-10	5	2209	4.7	73960.71	7.4	3.8	29.868	14.623	15.1	14.3
-10	1	1966	1.5	67933.61	11.1	4.7	28.943	19.059	12.8	10.4
-10	0.5	1843	0.7	68346.79	7.5	5.6	26.973	18.439	18.2	8.5
-10	0.1	1683	0.5	62382.58	6.9	4	26.973	21.756	19.4	7.9
4.4	25	1776	4.9	58244.97	7.6	10.6	30.498	54.943	11.5	4.4
4.4	10	1734	5.1	55869.2	9.8	4.2	31.032	27.421	8.8	10.5
4.4	5	1631	4.9	53455.12	9.4	4.4	30.514	26.471	10.6	10.1
4.4	1	1426	1.6	43198.53	11.4	4.6	33.017	28.31	11.1	9.3
4.4	0.5	1278	0.8	45263.05	11.9	5.5	28.235	32.254	18.7	5.1
4.4	0.1	1210	0.5	35726.31	14.6	5.1	33.869	55.452	10.7	5.3
21.1	25	927	5.8	35176.31	8.3	6.8	26.36	164.84	12.3	24.3
21.1	10	891	5.8	25535.45	17.1	2.7	34.898	198.841	7.8	43.6
21.1	5	754	5.8	23017.56	18.9	2.4	32.779	214.575	10.2	40.4
21.1	1	541	3	16764.44	20.4	3.2	32.241	213.295	11.1	34.8
21.1	0.5	448	2.4	15894.11	24.9	3	28.159	220.881	8.4	33.8
21.1	0.1	382	1.1	10386.78	27	3.5	36.824	288.47	8.6	36
37.8	25	423	8	12685.87	26.5	1.4	33.347	533.046	10.7	40.9
37.8	10	377	8.6	8794.428	26.2	1.9	42.839	800.337	7.4	52
37.8	5	264	7.2	6851.672	27.1	2.5	38.517	873.728	8.8	48.1
37.8	1	202	5.6	4110.643	29.8	2.6	49.038	903.462	7.7	48.6
37.8	0.5	171	4	3287.36	30.5	2.6	52.021	939.491	6.1	47.9
37.8	0.1	135	1.8	1979.76	27.7	3.6	67.985	1043.332	6.6	50.7
54.4	25	104	10	4690.694	36.7	2.5	22.241	153.773	16.5	37
54.4	10	93	7.9	3092.538	31.3	5.5	30.213	263.42	13	26.3
54.4	5	88	7.8	2484.732	30.6	6.4	35.571	343.859	12	29.4
54.4	1	66	8.8	1517.937	29.7	7.3	43.684	381.07	11.4	28.4
54.4	0.5	45	4.9	1198.625	26.2	6.9	37.746	393.813	13.3	26.2
54.4	0.1	36	3.2	897.393	22.4	7.8	39.636	428.608	10.9	28.9

Table B-139 Overall Dynamic Modulus test results at various test temperatures for Mix 46 Specimen 1

Temperature (°C)	Frequency (Hz)	Stress Amplitude (P-P) (KPa)	SE (%)	Dynamic Modulus (MPa)	Phase Angle (deg.)	UC (deg.)	Strain (P-P) Recoverable (microstrain)	Accumulated Strain (microstrain)	SE (%)	UC (%)
-10	25	2224	4.8	55017.77	8	1.5	40.419	93.049	12.5	9.2
-10	10	2275	4.9	56764.79	5.5	0.3	40.075	59.436	14.3	17.7
-10	5	2211	4.8	52949.92	5.8	0.9	41.753	59.556	9.6	16.3
-10	1	1971	1.6	50534.7	8.4	1.5	39.005	57.917	7.7	19.6
-10	0.5	1846	0.8	47860.43	11.3	2.6	38.578	59.958	14.9	19.5
-10	0.1	1683	0.5	43115.99	6.7	1.1	39.03	69.648	12.2	21.8
4.4	25	1778	5	36421.67	9.8	4.8	48.808	119.828	8.1	21.3
4.4	10	1740	5	37511.96	10	0.9	46.388	72.262	6.6	13.6
4.4	5	1633	4.7	35239.07	10.5	1.4	46.339	75.304	7.7	15
4.4	1	1427	1.5	28427.05	13.4	5.2	50.203	74.214	6	23.3
4.4	0.5	1278	0.8	25127.61	15.8	4.5	50.857	80.796	13	23.5
4.4	0.1	1212	0.5	20162.58	18	6.3	60.113	142.46	12.2	31
21.1	25	930	6	15535.3	18.9	3.6	59.888	489.175	8.7	35.5
21.1	10	894	6	13903.96	22.1	4.4	64.294	602.827	9.4	39.3
21.1	5	756	5.9	11672.23	22.8	2.9	64.754	667.976	10.2	36.6
21.1	1	542	3.1	8327.264	28.4	3.6	65.063	676.275	7.8	45
21.1	0.5	448	2.3	7146.084	28.2	3.4	62.701	702.901	7.7	48.9
21.1	0.1	382	1.2	4606.304	31.3	4.2	82.949	867.855	8.5	45.7
37.8	25	334	9	5289.069	30	3.7	63.099	829.995	9.7	28.8
37.8	10	294	7.9	3978.961	29.2	2.9	73.842	1177.442	7	34.6
37.8	5	227	7.4	3036.992	29.8	3.6	74.83	1281.388	6.9	38.1
37.8	1	172	5.3	1822.562	30.1	4.5	94.113	1339.913	6.7	44.8
37.8	0.5	150	3.9	1471.009	29.6	5.1	102.117	1395.079	6.2	47.6
37.8	0.1	130	2	932.531	26.8	5	139.382	1571.901	6.9	52.6
54.4	25	105	8.6	1523.279	34	3.9	68.995	226.463	8.1	47.1
54.4	10	94	8.1	1094.451	30	4.8	86.205	365.105	6.6	47.9
54.4	5	82	7.6	869.262	27.4	4.7	93.928	457.552	6.5	49.8
54.4	1	59	6.4	569.298	23.4	4.3	104.056	483.998	5.1	54.5
54.4	0.5	49	5.2	495.442	22.2	3.6	99.733	505.741	5.5	48.7
54.4	0.1	39	3.3	412.9	17.1	2.5	95.162	542.485	7.6	37.9

Table B-140 Overall Dynamic Modulus test results at various test temperatures for Mix 46 Specimen 3

Temperature (°C)	Frequency (Hz)	Stress Amplitude (P-P) (KPa)	SE (%)	Dynamic Modulus (MPa)	Phase Angle (deg.)	UC (deg.)	Strain (P-P) Recoverable (microstrain)	Accumulated Strain (microstrain)	SE (%)	UC (%)
-10	25	2222	4.9	46145.43	5.2	3.2	48.146	93.448	8.5	15.4
-10	10	2274	4.8	48755.2	4.9	0.4	46.646	59.656	5.9	8.3
-10	5	2214	5.1	48280.88	3.8	0.3	45.855	62.173	9	7.9
-10	1	1971	1.7	45242.9	4.4	0.7	43.557	61.141	14.4	6.1
-10	0.5	1843	0.8	39834.75	6.9	0.5	46.264	62.966	14.3	7.9
-10	0.1	1680	0.5	38444.55	5.2	1	43.698	70.95	14	5.4
4.4	25	1777	5.1	36294.15	6.4	1.1	48.972	91.169	8.7	13.8
4.4	10	1730	4.8	35126.88	8.8	0.8	49.245	47.186	6.7	8.6
4.4	5	1623	4.7	33779.2	8.5	1	48.054	51.009	10	7.3
4.4	1	1423	1.5	27554.12	12.3	1.1	51.661	51.575	10.5	7.4
4.4	0.5	1277	0.8	26617.11	12	1.4	47.961	56.748	11.6	5.4
4.4	0.1	1210	0.4	20738.48	14.8	2.2	58.362	121.625	7	10.1
21.1	25	926	5.9	18301.03	19	5.5	50.6	562.4	9.8	27.9
21.1	10	888	5.6	16531.59	20	4.1	53.707	770.49	6.1	32.4
21.1	5	751	5.7	15105.95	19.7	0.9	49.707	873.332	7.4	27
21.1	1	540	3	10343.56	24.9	1.9	52.203	898.049	6.4	26
21.1	0.5	447	2.4	8996.485	24.3	1.6	49.706	926.75	6.8	24.6
21.1	0.1	382	1.1	5743.269	26.9	4	66.512	1070.522	9	29.3
37.8	25	335	8	7937.961	25.4	1.3	42.15	442.927	9	26.7
37.8	10	291	6.8	5731.974	25.4	0.9	50.702	689.47	7.4	27.2
37.8	5	226	6.7	4623.841	26.5	0.9	48.886	754.386	6	26.8
37.8	1	171	4.9	2880.005	26.8	0.7	59.202	768.01	5.8	23.4
37.8	0.5	150	3.9	2331.044	26.6	0.6	64.397	783.429	5.5	21.6
37.8	0.1	129	1.6	1536.797	24.9	0.7	84.234	876.923	6.7	18.5
54.4	25	106	9.1	2647.967	34.1	6.1	39.867	293.793	9.9	25.5
54.4	10	93	6.8	2018.421	29.9	3.5	45.937	449.278	4.5	17.7
54.4	5	82	6.6	1620.454	27.8	3.4	50.609	543.663	4.6	16.6
54.4	1	60	5.8	1054.106	22.8	2.4	56.857	547.838	5.1	13.9
54.4	0.5	50	4.5	888.905	21	1.9	56.024	549.01	5.7	13.2
54.4	0.1	39	2.2	649.351	17.7	1.3	59.492	566.264	7.5	12.7

Table B-141 Overall Dynamic Modulus test results at various test temperatures for Mix 46 Specimen 5

Temperature (°C)	Frequency (Hz)	Stress Amplitude (P-P) (KPa)	SE (%)	Dynamic Modulus (MPa)	Phase Angle (deg.)	UC (deg.)	Strain (P-P) Recoverable (microstrain)	Accumulated Strain (microstrain)	SE (%)	UC (%)
-10	25	2222	4.6	51850.23	3.2	4.2	42.845	86.092	17	19
-10	10	2268	4.7	51427.17	5.2	0.6	44.108	51.62	7.9	23.5
-10	5	2206	4.7	48457.18	6.2	0.7	45.517	55.083	12.3	22.8
-10	1	1964	1.5	46353.63	7.5	2.3	42.366	55.267	15.6	23.6
-10	0.5	1840	0.7	40372.76	8.4	1.4	45.587	57.266	14.6	20.7
-10	0.1	1684	0.5	38851.48	6.2	1.5	43.333	69.409	16.7	22.9
4.4	25	1773	5.1	38623.34	7.1	3.6	45.9	104.938	14.3	24.4
4.4	10	1729	4.6	36006.37	9.5	0.4	48.006	58.268	7.4	23
4.4	5	1622	4.4	33347.27	9.9	0.5	48.635	60.552	6.3	21.9
4.4	1	1421	1.4	28414.83	11.8	1.1	50.021	64.387	7.9	21.4
4.4	0.5	1277	0.8	24783.4	16.6	2	51.525	71.517	9.6	20.2
4.4	0.1	1210	0.5	20113.15	16.8	1.2	60.139	135.185	6.6	20.5
21.1	25	926	5.7	19858.48	14.2	3	46.647	512.604	12.2	22.6
21.1	10	886	5.5	16168.81	19.5	1.5	54.796	721.434	5.7	13.1
21.1	5	749	5.3	13997.21	20.1	1.6	53.533	827.672	6.7	12.8
21.1	1	540	3.1	9894.32	23.6	1.6	54.53	848.992	5	13.5
21.1	0.5	447	2.3	8125.313	25.3	1.3	55.07	878.64	6.6	13
21.1	0.1	382	1.1	5328.832	28	1.9	71.712	1039.414	4.8	11.2
37.8	25	251	8.6	5525.262	31	7.2	45.517	372.218	14	52.6
37.8	10	208	7.9	3823.857	32.5	3.9	54.426	534.904	8.4	49.8
37.8	5	164	7.9	2882.801	30.3	2.4	56.896	591.588	8	58.1
37.8	1	120	6	1667.85	28.9	1.5	71.952	612.259	6.5	64.3
37.8	0.5	100	4.4	1316.04	27.9	1.7	76.11	636.01	6	68
37.8	0.1	80	2	855.99	22.8	1.6	93.17	710.448	6.6	70.5
54.4	25	105	8.5	1455.286	31.7	3.6	71.951	573.856	8.3	66.6
54.4	10	92	7.6	1066.496	27.8	2.1	85.933	906.812	4.7	59.6
54.4	5	80	7.6	867.965	25.5	1.5	92.698	1051.913	4.4	61.1
54.4	1	59	6.6	585.195	20.8	1.4	101.409	1100.07	5.8	66.3
54.4	0.5	49	5.3	495.039	18.8	1.7	98.811	1121.736	5.7	66.4
54.4	0.1	39	2.8	381.994	15.7	1	102.663	1159.701	8.8	68.2

Table B-142 Overall Dynamic Modulus test results at various test temperatures for Mix 47 Specimen 1

Temperature (°C)	Frequency (Hz)	Stress Amplitude (P-P) (KPa)	SE (%)	Dynamic Modulus (MPa)	Phase Angle (deg.)	UC (deg.)	Strain (P-P) Recoverable (microstrain)	Accumulated Strain (microstrain)	SE (%)	UC (%)
-10	25	2219	4.9	42672.84	3.6	2.9	52.011	109.148	13.9	19.6
-10	10	2272	4.7	41280.91	6	0.6	55.032	69.052	6.2	25.6
-10	5	2208	4.7	39905.44	5.7	0.9	55.324	73.327	8.8	25.8
-10	1	1966	1.6	36806.82	7.8	0.5	53.427	70.785	9.4	24.5
-10	0.5	1842	0.8	34397.28	6.3	0.7	53.536	70.282	5.6	23.4
-10	0.1	1683	0.6	31616.25	7.6	0.9	53.222	80.55	7.6	22.1
4.4	25	1780	5.2	29214.75	6.4	2.2	60.935	179.479	13.9	25.8
4.4	10	1730	4.8	26343.48	10.1	0.9	65.668	133.355	7.4	23.7
4.4	5	1626	4.7	24711.7	11.1	1.5	65.786	146.634	5.9	22.7
4.4	1	1426	1.6	20819.95	13.9	1.5	68.494	155.405	6.1	20.8
4.4	0.5	1279	0.9	20020.42	11.2	0.9	63.892	171.185	8.5	20.5
4.4	0.1	1210	0.4	15058.99	18.1	0.7	80.33	297.973	4.5	18.2
21.1	25	741	6.4	15129.38	14.5	2.2	49.007	355.762	8.7	15.2
21.1	10	710	6.2	12874.57	18.9	0.9	55.116	547.494	5.9	10.1
21.1	5	600	6.1	11804.78	19.2	1.2	50.788	644.506	8.1	12.2
21.1	1	434	4	8343.828	22.3	2.4	51.988	664.013	10.3	15.5
21.1	0.5	359	3	6752.387	25.9	2.1	53.155	689.491	5.2	13.5
21.1	0.1	306	1.3	4412.411	27.3	1.3	69.388	857.819	5.6	16
37.8	25	251	8	5366.564	27.5	1.5	46.792	438.933	8.3	13.9
37.8	10	209	7.4	3907.295	28.3	0.7	53.364	670.144	5.7	11.6
37.8	5	165	7.1	3078.735	28.2	1	53.521	761.358	6.1	12.1
37.8	1	120	5.7	1907.794	25.7	0.5	62.704	782.939	5.5	11.9
37.8	0.5	100	4.3	1536.727	24.4	0.4	65.028	801.267	5.5	11.3
37.8	0.1	79	2.4	1062.799	19.9	0.8	74.551	847.05	7	10.3
54.4	25	106	9	1383.488	32.1	1.5	76.441	369.332	7.7	47.7
54.4	10	94	7.6	987.63	28.4	1.9	94.722	653.938	4.1	61.1
54.4	5	81	7.8	799.187	25.7	2	100.782	799.212	3.9	62.3
54.4	1	59	7.3	533.584	21.1	2.5	110.057	825.599	5	63.9
54.4	0.5	49	6.1	448.943	19.8	2.7	108.526	844.373	5.8	62.6
54.4	0.1	39	4.5	345.227	15.8	2.9	113.199	877.253	8.5	62.7

Table B-143 Overall Dynamic Modulus test results at various test temperatures for Mix 47 Specimen 2

Temperature (°C)	Frequency (Hz)	Stress Amplitude (P-P) (KPa)	SE (%)	Dynamic Modulus (MPa)	Phase Angle (deg.)	UC (deg.)	Strain (P-P) Recoverable (microstrain)	Accumulated Strain (microstrain)	SE (%)	UC (%)
-10	25	2222	4.7	54969.43	1.6	6.5	40.416	82.646	22.5	30.4
-10	10	2266	4.7	52674.65	5.6	0.3	43.022	53.446	8.5	18.2
-10	5	2204	4.5	50700.07	6.1	0.1	43.48	52.657	9.1	18.3
-10	1	1965	1.4	45038.27	7.1	0.2	43.632	49.457	11.8	17.7
-10	0.5	1843	0.7	44909.8	6.6	0.7	41.039	51.364	14.2	20.6
-10	0.1	1683	0.5	39011.89	7.6	1	43.134	65.855	11.3	20.5
4.4	25	1772	5.2	31225.82	5.4	7.4	56.763	143.922	11.3	31.3
4.4	10	1734	5	28317.13	11.8	2.9	61.224	91	7.5	20.5
4.4	5	1631	4.8	26310.39	12.5	3	61.995	99.187	7.1	20.3
4.4	1	1426	1.6	21755.09	14.8	2.9	65.538	106.26	6.8	23.6
4.4	0.5	1277	0.8	19551.1	13.4	2.9	65.3	121.005	5.8	23.6
4.4	0.1	1212	0.5	14842.66	19.1	1.7	81.639	226.507	6.6	24.7
21.1	25	744	6.5	12535.72	20.2	2.1	59.375	364.057	9	19.1
21.1	10	709	6	10515.33	22.7	2.6	67.404	498.725	5.8	24.4
21.1	5	597	5.9	9220.092	22.7	2.6	64.712	566.112	6.2	28.4
21.1	1	431	3.6	6067.334	27.4	3.1	71.048	571.325	6.3	29.6
21.1	0.5	357	2.8	5158.115	27	3.6	69.2	592.867	6.9	30.7
21.1	0.1	305	1.3	3134.296	28.9	2.3	97.323	770.222	5.8	32.8
37.8	25	211	8.3	4602.528	29	6	45.799	369.202	9.4	23.2
37.8	10	186	7.7	3120.617	31.5	4.9	59.755	529.124	7	28.8
37.8	5	134	7.5	2452.639	31.5	5.2	54.44	558.538	7.1	24.7
37.8	1	100	5.7	1431.158	29.8	4.7	70.131	577.481	6.7	27
37.8	0.5	80	4.2	1196.516	27.9	3.5	66.692	596.819	6.8	18.6
37.8	0.1	64	2.3	826.32	22.4	2.2	77.93	641.405	6.2	9.5
54.4	25	64	7.5	1400.842	32.5	3.1	45.725	42.262	7.9	13.7
54.4	10	51	6.6	1002.585	29.4	1.1	51.001	88.664	4.8	6.7
54.4	5	40	6.1	807.581	26.1	1.2	49.731	94.141	4	9.6
54.4	1	29	5.7	559.869	19.2	1.7	51.74	99.81	4.6	14.3
54.4	0.5	24	5.1	485.909	16.2	1.7	49.1	100.038	7.3	11.8
54.4	0.1	19	4.1	394.813	12.6	1.4	47.288	109.427	6.2	12.6

Table B-144 Overall Dynamic Modulus test results at various test temperatures for Mix 47 Specimen 3

Temperature (°C)	Frequency (Hz)	Stress Amplitude (P-P) (KPa)	SE (%)	Dynamic Modulus (MPa)	Phase Angle (deg.)	UC (deg.)	Strain (P-P) Recoverable (microstrain)	Accumulated Strain (microstrain)	SE (%)	UC (%)
-10	25	2217	4.9	51201.95	7.6	9.8	43.307	111.211	25.1	41
-10	10	2261	4.6	45274.25	5.6	0.8	49.94	72.953	6.8	21.8
-10	5	2200	4.5	43966.84	5	0.4	50.047	70.197	8.1	21.4
-10	1	1962	1.4	40446.34	8.3	2.1	48.519	70.614	8.7	21.8
-10	0.5	1840	0.7	38100.57	4.2	0.8	48.299	72.147	6.6	21.5
-10	0.1	1684	0.5	34395.65	9	1	48.951	90.946	10	22.4
4.4	25	1771	4.9	32754.5	7.5	3.9	54.069	153.634	13.5	29.3
4.4	10	1735	5.1	29636.8	9.9	0.4	58.548	109.209	7.1	17.1
4.4	5	1634	5	27785.16	10	0.3	58.81	118.077	6.6	17.4
4.4	1	1427	1.7	23369.58	10.6	0.7	61.052	121.859	8.2	17.6
4.4	0.5	1277	0.9	20671.05	10.6	1.8	61.779	133.461	4.5	16.1
4.4	0.1	1212	0.5	16511.71	17.8	0.7	73.388	254.994	5.2	17.4
21.1	25	743	6.2	17178.05	12.6	4.1	43.251	560.561	11.9	25.7
21.1	10	713	6	13757.24	18.1	0.2	51.792	862.691	11.1	14.7
21.1	5	599	6.1	12197.26	20.1	0.1	49.104	1008.093	8.5	14
21.1	1	431	4.1	8694.699	23.6	0.6	49.54	1047.527	6.4	16.1
21.1	0.5	358	3.4	7271.801	24.7	1	49.206	1093.53	4.9	16.3
21.1	0.1	305	1.6	4608.041	28.4	1	66.25	1316.324	4.6	16.2
37.8	25	212	8.5	5438.903	25.3	4.6	39.025	852.464	11.7	11.4
37.8	10	188	7.6	4002.984	29.5	0.3	46.916	1292.616	8.1	9.5
37.8	5	135	7.5	3049.91	28.6	1.2	44.146	1399.617	8.8	9
37.8	1	100	6.5	1855.832	27.1	0.4	53.931	1437.071	6.7	10.3
37.8	0.5	80	4.8	1477.53	26.3	0.7	54.178	1461.145	8	10.5
37.8	0.1	65	2.4	991.134	21.6	0.3	65.165	1514.836	7.1	12.1
54.4	25	64	8.6	1634.192	31.9	1.1	39.156	342.482	9.6	9.5
54.4	10	51	6.9	1172.32	27.2	1.3	43.89	492.093	5.4	7.6
54.4	5	40	6.4	942.372	25.1	1.5	42.438	514.662	6.2	7.6
54.4	1	29	6.5	637.916	20	1.4	45.203	517.05	6.7	5.2
54.4	0.5	24	5.2	564.527	16	1.2	42.229	517.895	5.8	1.5
54.4	0.1	19	4.3	462.367	12.2	0.3	40.5	522.257	6.4	0.8

Table B-145 Overall Dynamic Modulus test results at various test temperatures for Mix 48 Specimen 1

Temperature (°C)	Frequency (Hz)	Stress Amplitude (P-P) (KPa)	SE (%)	Dynamic Modulus (MPa)	Phase Angle (deg.)	UC (deg.)	Strain (P-P) Recoverable (microstrain)	Accumulated Strain (microstrain)	SE (%)	UC (%)
-10	25	2222	4.8	44758.535	1.6	5	49.643	107.761	9.9	33.2
-10	10	2262	4.7	43404.902	5.3	0.4	52.124	67.462	6.4	26.5
-10	5	2199	4.4	42283.012	5.1	0.3	52.001	66.539	5.6	26.8
-10	1	1958	1.3	39550.633	4.7	0.5	49.512	68.008	4.3	28.2
-10	0.5	1839	0.7	37937.711	7.8	2	48.48	68.187	6.6	27.7
-10	0.1	1685	0.5	33745.887	6.6	0.2	49.938	79.055	7.1	26.5
4.4	25	1776	5.1	32620.344	5.3	3.4	54.432	148.921	7.9	28.2
4.4	10	1741	5.1	29556.154	9.6	0.4	58.896	101.746	6.3	23.9
4.4	5	1633	4.8	27396.143	10.1	0.4	59.616	108.209	6.8	22.7
4.4	1	1426	1.6	22784.67	13.2	1.6	62.599	112.195	7.6	21.9
4.4	0.5	1280	0.9	21644.236	12.7	1.4	59.121	120.903	4.8	24.6
4.4	0.1	1212	0.5	16537.506	17.8	1	73.263	231.093	4.3	21.6
21.1	25	745	6.4	16618.844	12.4	3.9	44.85	391.874	8.4	19.7
21.1	10	712	6.5	14051.213	18.5	0.6	50.681	521.304	5.9	15.9
21.1	5	600	6.2	12266.451	19.7	0.7	48.901	563.363	5.5	16.3
21.1	1	431	3.9	8450.877	22.8	0.8	51.012	558.876	4.2	15.2
21.1	0.5	358	3	7016.405	24.4	0.8	50.957	567.192	4	15.2
21.1	0.1	305	1.3	4500.621	26	0.6	67.87	653.983	4.3	15.5
37.8	25	209	8.7	5397.117	26.9	0.5	38.771	402.92	9.3	12.4
37.8	10	186	7.8	4013.175	28.2	0.3	46.413	538.174	6.5	11.3
37.8	5	133	8.3	3146.493	28.5	0.2	42.127	547.852	7.3	11.1
37.8	1	99	6	1845.458	27	0.5	53.713	552.428	6.1	10.6
37.8	0.5	79	4.4	1484.881	25.6	0.5	52.953	559.517	5.4	10.2
37.8	0.1	64	2.2	977.44	21	0.8	65.565	587.677	7	9
54.4	25	64	8.6	991.603	38.9	3.7	64.214	81.055	7.6	72.2
54.4	10	51	7.3	612.943	33.1	5.5	83.544	36.641	6.7	62.5
54.4	5	41	6.6	513.407	29.8	4.9	79.178	-1.916	5.4	72
54.4	1	28	5.5	344.114	22.8	5.1	82.638	19.698	7.8	86.7
54.4	0.5	23	4.8	286.024	21	5.1	81.988	-1.606	6.2	86.6
54.4	0.1	19	4.1	225.039	15.7	4.4	83.051	-0.001	10.5	85.9

Table B-146 Overall Dynamic Modulus test results at various test temperatures for Mix 48 Specimen 2

Temperature (°C)	Frequency (Hz)	Stress Amplitude (P-P) (KPa)	SE (%)	Dynamic Modulus (MPa)	Phase Angle (deg.)	UC (deg.)	Strain (P-P) Recoverable (microstrain)	Accumulated Strain (microstrain)	SE (%)	UC (%)
-10	25	2222	4.7	45249.629	1.7	4.6	49.099	61.545	9.4	34.3
-10	10	2265	4.4	43684.941	5.3	0.5	51.84	19.034	6.4	27.8
-10	5	2199	4.5	42301.371	5	0.7	51.987	19.543	5.9	27.4
-10	1	1963	1.4	39283.074	6.2	0.7	49.977	18.668	6	28.3
-10	0.5	1844	0.7	37467.242	8.9	2.8	49.206	20.024	7.5	27.5
-10	0.1	1681	0.5	33898.207	6.4	0.4	49.599	28.919	7.4	27.5
4.4	25	1767	5	32100.883	5.4	3.6	55.059	131.081	7.3	28.5
4.4	10	1728	4.7	29108.689	9.8	0.4	59.368	59.901	6.2	23.7
4.4	5	1623	4.5	27230.141	10.3	0.5	59.619	56.209	5.2	23
4.4	1	1424	1.5	22679.549	11.5	0.6	62.805	55.335	4.4	21.9
4.4	0.5	1278	0.8	20472.393	12.7	0.7	62.425	59.584	3.5	20.7
4.4	0.1	1209	0.4	16494.563	17.3	0.6	73.322	146.382	3.6	21.7
21.1	25	739	6.1	16562.43	12.8	3.6	44.643	259.919	8	20.5
21.1	10	708	6.2	13680.506	18.4	0.7	51.728	318.883	5.9	15.6
21.1	5	597	6.1	11948.972	19.8	0.7	49.987	325.086	5.1	15.5
21.1	1	432	3.6	8150.684	23.1	0.5	52.957	311.436	4.8	15.1
21.1	0.5	357	2.8	6721.455	24.5	0.9	53.109	311.177	3.8	14.7
21.1	0.1	304	1.4	4295.614	24.9	0.6	70.824	375.287	4.7	14.2
37.8	25	207	8.6	5345.256	28.4	1.9	38.751	270.847	9.3	13.7
37.8	10	186	7.8	3880.171	28.1	0.3	47.865	366.172	6.9	12
37.8	5	133	8.2	3027.336	28.5	0.1	44.021	365.441	6.5	12.7
37.8	1	100	6	1797.144	26.8	0.1	55.415	364.459	5.5	11
37.8	0.5	79	4.4	1434.098	25.8	0.4	55.086	367.809	5.1	10.3
37.8	0.1	65	5.2	971.654	19.1	0.6	66.627	394.144	11	9.3
54.4	25	64	8.7	783.795	39.9	2	81.698	135.51	8.8	57.4
54.4	10	52	6.7	548.475	33.5	5.2	94.526	182.905	5.7	55.9
54.4	5	40	6	416.514	31.2	5.7	96.184	173.659	5	59.7
54.4	1	29	5.9	269.665	26.6	7.1	108.261	164.155	5.6	67.2
54.4	0.5	24	5	241.514	24.8	6	98.297	158.742	5.5	74.2
54.4	0.1	19	3.5	198.76	18.6	3.7	94.522	168.854	6.9	85.8

Table B-147 Overall Dynamic Modulus test results at various test temperatures for Mix 48 Specimen 3

Temperature (°C)	Frequency (Hz)	Stress Amplitude (P-P) (KPa)	SE (%)	Dynamic Modulus (MPa)	Phase Angle (deg.)	UC (deg.)	Strain (P-P) Recoverable (microstrain)	Accumulated Strain (microstrain)	SE (%)	UC (%)
-10	25	2210	4.6	45837.445	2.1	4.3	48.21	54.569	10.2	35.2
-10	10	2254	4.1	43187.379	5.2	0.4	52.184	12.924	6.9	26.3
-10	5	2190	4.1	42539.082	4.8	0.5	51.484	10.957	6.1	27.8
-10	1	1960	1.2	38565.203	4.2	1	50.813	9.632	7.9	26.2
-10	0.5	1842	0.7	36848.996	7.1	1.2	50	10.04	5.3	25.6
-10	0.1	1681	0.4	33651.598	7.7	1.3	49.942	22.421	9	26.6
4.4	25	1771	5.2	32126.201	5.6	3	55.129	129.275	7.1	28.7
4.4	10	1725	4.6	29103.594	9.5	0.2	59.274	60.096	5.9	23.8
4.4	5	1621	4.5	27057.27	10.5	0.7	59.925	57.31	5.2	22.4
4.4	1	1423	1.3	22692.057	11.5	0.6	62.69	52.681	4	22.5
4.4	0.5	1278	0.7	20482.59	12.3	0.5	62.373	56.151	3.8	20.8
4.4	0.1	1210	0.4	16457.811	17.3	0.5	73.51	134.785	3.5	21.8
21.1	25	735	6.5	16163.371	13.4	2.8	45.483	244.508	8.8	18.2
21.1	10	707	6.1	13581.941	18.8	0.5	52.048	273.06	6	16
21.1	5	596	5.9	11648.528	19.8	0.6	51.136	267.229	5	14.8
21.1	1	431	3.5	7917.835	23.5	0.9	54.403	248.906	4.2	13.8
21.1	0.5	357	2.5	6542.796	24.9	1.1	54.565	245.969	4.1	13.6
21.1	0.1	304	1.4	4174.147	25	0.7	72.946	305.25	4.5	13.8
37.8	25	209	8.7	5220.563	29.4	3.4	40.075	243.604	9.6	11.6
37.8	10	188	7.8	3854.317	28.4	0.2	48.743	307.175	6.7	12.1
37.8	5	133	8	2978.282	28.4	0.5	44.645	305.01	6.4	11.9
37.8	1	100	6.1	1773.647	26.5	0.6	56.163	304.366	5.7	10.6
37.8	0.5	80	4.4	1413.735	25.7	0.2	56.837	308.04	5.8	10.3
37.8	0.1	64	2.1	938.498	20.6	0.5	68.224	334.779	5.9	9.9
54.4	25	64	7.9	765.316	38.9	2.7	84.05	99.873	7.3	55
54.4	10	51	6.5	508.324	32.4	4.2	100.196	126.877	4.4	54.2
54.4	5	41	6.3	386.754	29.9	4.5	107.027	120.825	4.1	56.2
54.4	1	30	6.5	235.175	24.6	5.2	126.004	111.809	5.5	60.3
54.4	0.5	24	5.8	196.691	23.4	4.6	121.436	106.537	6.3	60.4
54.4	0.1	19	4.6	142.891	19.3	4.2	134.17	130.447	7	61.3

Table B-148 Overall Dynamic Modulus test results at various test temperatures for Mix 49 Specimen 1

Temperature (°C)	Frequency (Hz)	Stress Amplitude (P-P) (KPa)	SE (%)	Dynamic Modulus (MPa)	Phase Angle (deg.)	UC (deg.)	Strain (P-P) Recoverable (microstrain)	Accumulated Strain (microstrain)	SE (%)	UC (%)
-10	25	2199	4.5	59268.828	1.5	8.2	37.099	79.299	9.5	26.2
-10	10	2249	4.5	66867.227	5.2	0.7	33.641	55.266	9.8	31.6
-10	5	2183	4.2	64309.609	5.4	0.7	33.951	57.04	8.5	30.9
-10	1	1957	1.1	57424.352	4.1	0.9	34.079	53.628	9.6	27.9
-10	0.5	1842	0.6	57118.059	5.3	0.7	32.257	55.687	18.5	29.8
-10	0.1	1682	0.5	51289.594	5.6	1.8	32.788	60.879	19.8	28.6
4.4	25	1763	4.7	42970.027	5.8	11.1	41.033	94.189	10.5	17.8
4.4	10	1722	4.6	39193.961	10.9	5.5	43.944	48.364	8.3	11.9
4.4	5	1614	4	36786.582	11	5.8	43.87	51.669	9.3	13
4.4	1	1420	1.1	30099.152	15.1	4.5	47.189	55.383	11.7	15.1
4.4	0.5	1276	0.7	30855.979	17.8	5.3	41.367	59.517	8.3	20.3
4.4	0.1	1209	0.4	23003.293	16.8	4.9	52.573	100.41	9.1	18.8
21.1	25	739	6.2	19729.689	15.3	18.5	37.454	247.838	14.3	41.5
21.1	10	702	5.5	16672.102	22.8	5.4	42.078	338.002	8	34.1
21.1	5	593	5.5	15446.716	24.3	6.7	38.384	376.914	7.7	32.6
21.1	1	431	3.2	10899.782	27.9	5.8	39.545	380.78	7.7	38.2
21.1	0.5	356	2.4	9264.681	29.7	6.4	38.449	396.118	9.1	38.7
21.1	0.1	304	1.1	6509.719	33.1	7.3	46.716	502.726	8.2	42.2
37.8	25	293	8.6	7246.711	23.1	20	40.478	626.458	14.9	43.5
37.8	10	257	6.5	4401.795	30.3	4	58.421	930.212	7.3	51.1
37.8	5	185	6.6	3463.669	31.2	4.2	53.308	1019.363	8	54.8
37.8	1	141	4.6	2032.198	33.2	3.4	69.477	1066.259	7.9	55.4
37.8	0.5	111	3.3	1609.809	33.4	3.9	69.008	1095.545	7.4	55
37.8	0.1	90	1.6	869.802	29.5	2.2	103.42	1190.021	6.4	63.3
54.4	25	88	9.7	1569.916	37.8	5.8	56.195	302.637	12.9	37.4
54.4	10	72	7.9	1143.065	33.9	2.5	62.811	411.056	12.5	48.4
54.4	5	58	7.3	888.599	31.8	3.6	64.891	442.52	7.5	46.7
54.4	1	42	6	605.589	27.5	2.4	68.713	454.082	8.2	49.9
54.4	0.5	34	4.9	508.596	26	2.3	67.354	461.773	7.9	54.2
54.4	0.1	26	3.3	383.561	19.2	2.6	68.415	496.467	6.1	57.7

Table B-149 Overall Dynamic Modulus test results at various test temperatures for Mix 49 Specimen 2

Temperature (°C)	Frequency (Hz)	Stress Amplitude (P-P) (KPa)	SE (%)	Dynamic Modulus (MPa)	Phase Angle (deg.)	UC (deg.)	Strain (P-P) Recoverable (microstrain)	Accumulated Strain (microstrain)	SE (%)	UC (%)
-10	25	2204	4.6	61869.379	1.9	7	35.618	37.049	8.8	30.4
-10	10	2256	4.3	65978.945	5.7	1	34.193	8.568	9	31.8
-10	5	2186	4.1	64013.309	5	0.6	34.145	10.353	8.1	30.5
-10	1	1959	1.2	59871.203	5.7	1.3	32.726	8.59	18.3	30.8
-10	0.5	1842	0.6	58298.656	7.6	3	31.601	9.521	23.9	31.1
-10	0.1	1682	0.4	51499.41	6.3	3.2	32.662	18.092	17.4	28.8
4.4	25	1761	4.8	44430.473	10.1	14.9	39.632	78.711	8.6	14.5
4.4	10	1722	4.3	43789.766	11.5	5	39.314	30.044	8.8	19.8
4.4	5	1614	4.1	40203.184	12.8	7.1	40.14	24.945	8.9	16
4.4	1	1421	1.2	31862.559	14.7	6.5	44.585	20.867	10.8	11.7
4.4	0.5	1277	0.7	27797.701	10	7.5	45.947	22.712	13.9	10.5
4.4	0.1	1209	0.4	23779.713	19.3	6.2	50.85	61.429	14.1	12.5
21.1	25	742	6.2	22754.637	15.7	14.6	32.591	170.743	14.2	42.3
21.1	10	705	5.5	19838.955	19.8	4.6	35.52	215.351	9.1	37.4
21.1	5	593	5.2	17810.523	20.8	5	33.306	226.953	10	37.6
21.1	1	432	3.2	12434.931	22.4	7.6	34.749	216.529	13.2	45.1
21.1	0.5	357	2.4	10636.575	25	6.5	33.599	221.13	13.7	48.3
21.1	0.1	305	1.3	6929.585	28.2	4.7	44.063	289.502	8.9	52
37.8	25	293	7.6	5661.07	23.8	16.7	51.684	393.037	10.5	47.1
37.8	10	261	6.7	4149.214	30.3	4.6	62.799	563.312	7.8	49.1
37.8	5	187	6.9	3470.639	32.1	4.4	53.801	617.185	7.9	49.8
37.8	1	141	4.9	2339.261	32.3	3.5	60.248	641.75	7	50.6
37.8	0.5	111	3.4	1863.697	31.2	4.1	59.812	650.806	8.7	53.1
37.8	0.1	90	1.6	1018.139	28.7	2.6	88.114	700.209	7.6	53.8
54.4	25	89	9.4	1506.75	38.6	4.4	58.918	166.071	9.3	38.1
54.4	10	72	7.6	1128.726	33.7	4.3	64.069	239.355	6.1	45.7
54.4	5	58	6.9	913.073	31.8	4	63.069	257.217	8.2	44.6
54.4	1	41	5.4	642.357	26.3	3.3	64.146	259.914	7.2	57.6
54.4	0.5	34	4.6	527.276	24.2	2.5	64.625	262.55	5.5	61.1
54.4	0.1	27	2.8	386.183	18.3	2	69.159	283.972	6.2	63.3

Table B-150 Overall Dynamic Modulus test results at various test temperatures for Mix 49 Specimen 3

Temperature (°C)	Frequency (Hz)	Stress Amplitude (P-P) (KPa)	SE (%)	Dynamic Modulus (MPa)	Phase Angle (deg.)	UC (deg.)	Strain (P-P) Recoverable (microstrain)	Accumulated Strain (microstrain)	SE (%)	UC (%)
-10	25	2202	4.6	62246.945	4.9	6.5	35.369	37.25	8.4	30.9
-10	10	2252	4.2	66054.891	4.4	0.4	34.096	7.346	8.6	31.1
-10	5	2180	4	63640.715	5.7	1.5	34.258	6.54	9	30.4
-10	1	1956	1.1	58358.715	6.5	1.8	33.525	10.362	13.9	29.6
-10	0.5	1843	0.6	58887.453	11.3	4.9	31.289	11.278	16	32
-10	0.1	1681	0.4	52322.367	8	3.6	32.13	15.424	14.2	30.2
4.4	25	1759	4.9	48002.215	7.6	10.3	36.645	79.454	9.5	29.7
4.4	10	1718	4.2	42467.563	10	2.9	40.459	30.58	12.7	21.5
4.4	5	1607	3.9	42339.539	10	3.9	37.947	25.592	10.8	24
4.4	1	1418	1.1	33505.137	13.5	7.3	42.331	21.362	11.6	14.1
4.4	0.5	1277	0.6	28271.611	12.9	6.7	45.161	22.619	10.6	8.8
4.4	0.1	1209	0.4	24929.584	19.4	7.3	48.516	56.829	15.1	12.1
21.1	25	737	5.9	22580.033	14.7	14.5	32.645	163.583	11.5	38.9
21.1	10	704	5.4	19464.398	19.8	4.7	36.173	201.28	7.1	35.8
21.1	5	592	5.2	18054.865	20.7	5.2	32.799	206.576	18.1	40.7
21.1	1	432	3.1	12396.519	23.6	6.8	34.872	185.844	13.1	42.7
21.1	0.5	358	2.4	10523.365	27.1	5.4	33.983	184.296	10.2	46.1
21.1	0.1	305	1.2	6701.295	28.2	5.1	45.542	241.042	7.7	51.5
37.8	25	293	7.6	5789.235	26.3	14.5	50.596	338.499	10.9	42.1
37.8	10	261	6.6	4337.854	31.4	6.8	60.138	444.402	10.7	48.8
37.8	5	187	7.2	3387.555	32.3	5.8	55.096	456.734	9.1	49.4
37.8	1	141	4.9	2082.284	33.2	4	67.834	458.194	6.9	48.5
37.8	0.5	112	3.4	1664.144	32.8	3.7	67.067	455.752	6.1	50.5
37.8	0.1	90	1.5	844.409	28.7	3.1	106.791	481.313	5.9	57
54.4	25	89	9.2	1554.747	39	5.7	57.252	133.184	9.5	35.8
54.4	10	72	7.6	1213.12	34.4	5	59.7	194.383	6.1	42.9
54.4	5	57	6.9	1002.499	32	3.7	57.301	203.5	6.6	49
54.4	1	41	5.7	645.725	25.8	2.8	64.051	201.698	5.8	61.4
54.4	0.5	34	4.2	529.38	23.5	2.7	64.71	200.523	6.7	62.8
54.4	0.1	26	2.9	379.996	18.4	1.6	69.1	216.726	8.1	64.2

Table B-151 Overall Dynamic Modulus test results at various test temperatures for Mix 50 Specimen 1

Temperature (°C)	Frequency (Hz)	Stress Amplitude (P-P) (KPa)	SE (%)	Dynamic Modulus (MPa)	Phase Angle (deg.)	UC (deg.)	Strain (P-P) Recoverable (microstrain)	Accumulated Strain (microstrain)	SE (%)	UC (%)
-10	25	2199	4.4	36963.832	12.8	5.7	59.499	105.517	12	19
-10	10	2255	4.5	36669.418	13.2	2.4	61.499	52.213	7.7	19.7
-10	5	2181	4.1	35278.945	13.2	2.5	61.819	55.901	6.8	19
-10	1	1956	1	31672.824	12.5	2.2	61.754	53.389	8.2	19.8
-10	0.5	1841	0.6	30981.768	16.8	2.3	59.411	52.993	10	19.1
-10	0.1	1681	0.4	27572.209	16.1	1.7	60.964	65.072	8.1	19.5
4.4	25	1765	4.7	28689.402	15	5.3	61.507	157.908	8.7	22.7
4.4	10	1728	4.6	26632.436	14.6	2.9	64.87	83.039	6.1	28.6
4.4	5	1619	4.2	25394.764	15.2	2.4	63.748	82.799	5.5	29.4
4.4	1	1420	1.1	20749.355	18.9	3.3	68.415	83.618	4.9	27
4.4	0.5	1276	0.7	19609.416	20.5	3.6	65.054	94.023	5.9	27.5
4.4	0.1	1209	0.4	14490.772	24.2	4	83.405	174.723	9.7	23
21.1	25	735	5.6	18394.852	18.7	4.6	39.972	331.302	9.6	24.4
21.1	10	701	4.9	15547.084	19.5	3.4	45.087	450.648	6.7	31.5
21.1	5	589	4.8	13679.857	20.7	3.8	43.051	494.84	5.9	32
21.1	1	430	3.1	9672.432	25	3.4	44.41	497.439	10	34.5
21.1	0.5	356	2.5	7994.593	24.5	3.6	44.583	509.632	11.3	34.1
21.1	0.1	303	1.3	5342.714	27.2	3.6	56.8	601.685	8.6	34.4
37.8	25	294	7.5	6453.83	29.6	5.8	45.602	573.414	8.7	33.1
37.8	10	261	6	4738.243	28.7	4.9	55.187	768.872	9	34.8
37.8	5	187	6.8	3757.222	29.7	5.4	49.68	795.674	10	39.1
37.8	1	141	5.2	2221.709	29.3	4.6	63.455	806.392	7.9	43.4
37.8	0.5	111	3.8	1733.676	29.9	3.7	64.032	811.498	7.5	45.5
37.8	0.1	88	2.3	1117.892	26.1	3.7	78.524	865.291	8.2	48.4
54.4	25	88	9.2	2100.526	35.5	7.5	41.9	168.834	9.4	55.9
54.4	10	71	8.2	1607.209	33.4	5.4	44.425	212.008	8.7	44.1
54.4	5	57	7.1	1240.064	31.1	6.3	46.365	226.626	7.1	43.8
54.4	1	41	5.8	774.686	28.2	7.3	53.229	223.957	6.4	45.4
54.4	0.5	34	4.4	672.571	26.4	7.6	50.133	218.018	7.7	43
54.4	0.1	26	3.4	534.02	21.8	9.1	49.392	228.592	10	36.3

Table B-152 Overall Dynamic Modulus test results at various test temperatures for Mix 50 Specimen 2

Temperature (°C)	Frequency (Hz)	Stress Amplitude (P-P) (KPa)	SE (%)	Dynamic Modulus (MPa)	Phase Angle (deg.)	UC (deg.)	Strain (P-P) Recoverable (microstrain)	Accumulated Strain (microstrain)	SE (%)	UC (%)
-10	25	2202	4.7	39142.211	12.4	4.8	56.258	72.053	9.2	13.4
-10	10	2255	4.3	39244.512	11.7	4	57.473	19.69	6.8	13.4
-10	5	2186	4.2	38313.422	11.8	3.6	57.051	14.846	6.5	14.9
-10	1	1958	1.1	33669.266	13.7	2.9	58.149	13.279	10	12.9
-10	0.5	1842	0.6	32307.434	15	2.6	57.006	17.742	10	12.9
-10	0.1	1681	0.4	28891.336	17.3	2.9	58.191	28.494	12.4	12.8
4.4	25	1763	4.8	31353.945	11.1	1.7	56.232	142.163	11.8	32.1
4.4	10	1723	4.4	28492.252	12.5	1.2	60.484	63.857	6.9	33.1
4.4	5	1615	4.2	26882.83	12.9	0.6	60.07	56.918	6	32.5
4.4	1	1418	1.2	22202.979	15.8	1.1	63.843	56.102	10.4	31.8
4.4	0.5	1276	0.7	19450.102	18.4	1.2	65.584	64.48	5.4	29.6
4.4	0.1	1206	0.4	15733.013	21.7	2.8	76.684	128.146	8.2	28.2
21.1	25	737	6	18192.402	17.2	3.1	40.502	224.318	7.7	32.6
21.1	10	702	5.1	14822.555	19.5	3.8	47.38	281.837	7.2	29.7
21.1	5	594	4.9	13151.347	20.8	3.7	45.133	292.379	6.1	31.1
21.1	1	430	3.1	9038.337	22.6	4.3	47.593	284.47	8.3	34.3
21.1	0.5	357	2.5	7510.179	22.9	4.1	47.487	286.854	8.1	34.2
21.1	0.1	303	1.4	5014.957	25.5	3.5	60.41	347.06	8.7	35.6
37.8	25	306	7.4	6237.687	29	4.5	48.999	337.789	7.8	37.5
37.8	10	258	6.2	4577.651	28.6	4.4	56.411	424.706	7.8	37.7
37.8	5	187	7	3567.943	28.6	5	52.282	421.575	6.6	41.3
37.8	1	140	5.4	2098.787	29.2	4.1	66.739	416.01	5.7	47.2
37.8	0.5	99	4.1	1574.089	30.7	3.8	62.585	409.818	6.4	51.9
37.8	0.1	77	2.5	1010.047	26.1	3.6	76.362	452.828	7.1	53.7
54.4	25	89	8.9	2081.854	35.8	7	42.608	78.74	8.4	48.7
54.4	10	73	7.9	1564.887	32.5	5.3	46.519	112.65	7.6	39.1
54.4	5	57	7.2	1222.985	31.7	6.3	46.501	125.777	8.4	41.5
54.4	1	41	5.4	767.605	27.4	7.6	53.58	130.144	6.4	42.4
54.4	0.5	34	4.5	644.183	27.4	7.7	52.587	132.378	7.2	40.8
54.4	0.1	26	2.9	506.032	22.7	8.7	52.205	152.911	10.9	35.2

Table B-153 Overall Dynamic Modulus test results at various test temperatures for Mix 50 Specimen 3

Temperature (°C)	Frequency (Hz)	Stress Amplitude (P-P) (KPa)	SE (%)	Dynamic Modulus (MPa)	Phase Angle (deg.)	UC (deg.)	Strain (P-P) Recoverable (microstrain)	Accumulated Strain (microstrain)	SE (%)	UC (%)
-10	25	2201	4.5	41168.664	10.5	5	53.464	63.576	9.9	14.7
-10	10	2254	4.2	41058.727	10.9	3.5	54.886	12.358	6.3	19
-10	5	2180	4	40027.836	11.2	3.2	54.472	10.886	5.3	20.9
-10	1	1957	1	35076.566	16.5	5	55.788	10.304	15.2	17.9
-10	0.5	1842	0.6	35236.164	9.3	1.4	52.267	8.189	8.8	20.7
-10	0.1	1681	0.4	31098.664	15.4	2.9	54.042	23.971	10	19.8
4.4	25	1746	4.3	32222.674	10.5	1.4	54.198	123.693	8.3	34.4
4.4	10	1719	4.3	29215.295	12.3	1.5	58.845	51.959	6.4	33.1
4.4	5	1608	3.9	27242.371	12.9	1.5	59.041	49.98	5.6	32.4
4.4	1	1417	1.2	22773.158	15.2	1.3	62.243	42.706	10.7	32.1
4.4	0.5	1276	0.7	20227.348	18.1	1.9	63.073	40.923	7.5	30.3
4.4	0.1	1208	0.4	16817.189	19.9	1.8	71.837	99.447	10.9	28.7
21.1	25	738	5.4	17896.82	18.1	2.8	41.244	194.923	7.3	33
21.1	10	704	5.2	14553.065	19.4	3.5	48.361	226.364	6.7	31.1
21.1	5	591	4.8	12637.744	20.9	3.3	46.726	225.451	6.1	31.4
21.1	1	430	3.1	9074.369	23.1	3	47.394	213.632	8.8	33.3
21.1	0.5	357	2.4	7239.29	27.7	3.6	49.265	212.42	6.2	34.4
21.1	0.1	302	1.6	4869.301	25.2	3.4	61.977	264.684	8.1	35.9
37.8	25	309	7.7	5519.176	28	3.7	55.94	478.681	7.9	45.9
37.8	10	263	6.4	4124.486	28.2	3.6	63.866	606.151	5.8	43.3
37.8	5	188	6.9	3204.578	28.5	3.5	58.758	607.137	6.2	49.5
37.8	1	141	5.4	1887.771	28.4	2.7	74.868	597.077	6.4	55
37.8	0.5	100	4	1401.397	29.4	2.8	71.187	590.731	6.7	62.8
37.8	0.1	79	1.8	906.845	23.7	3.2	86.7	633.466	9.8	67.2
54.4	25	88	8.9	2047.32	34.7	8	43.227	73.78	12.4	48
54.4	10	73	7.9	1519.924	32.8	5.5	47.734	103.527	7.4	40.1
54.4	5	58	7.2	1169.619	31.4	6	49.165	111.445	7	42.6
54.4	1	41	5.4	729.007	27.6	6.8	56.679	113.515	7.6	43.7
54.4	0.5	34	4.3	631.725	25.3	7.9	53.619	112.649	6.7	43.1
54.4	0.1	26	2.8	498.849	21.5	9.2	53.007	131.182	9.2	37.6

Table B-154 Overall Dynamic Modulus test results at various test temperatures for Mix 51 Specimen 1

Temperature (°C)	Frequency (Hz)	Stress Amplitude (P-P) (KPa)	SE (%)	Dynamic Modulus (MPa)	Phase Angle (deg.)	UC (deg.)	Strain (P-P) Recoverable (microstrain)	Accumulated Strain (microstrain)	SE (%)	UC (%)
-10	25	2214	4.6	46987.141	3.6	3.2	47.12	94.865	12.8	32.1
-10	10	2249	3.9	47091.098	5.5	0.2	47.756	59.642	5.7	13.9
-10	5	2185	4	45410.141	6.2	0.5	48.115	62.549	6.5	14.2
-10	1	1959	1.1	42114.555	4.3	0.8	46.527	60.349	8.6	15.6
-10	0.5	1843	0.7	37849.113	9.1	1.6	48.693	61.419	8.7	12.2
-10	0.1	1679	0.5	34904.926	9.3	1.3	48.093	75.417	12.7	14.6
4.4	25	1764	4.9	34127.691	6.1	3.3	51.675	147.453	9.3	29.3
4.4	10	1726	5.1	30870.547	10.1	0.5	55.913	97.37	6.8	19.4
4.4	5	1617	4.4	28706.137	11.3	0.7	56.314	107.821	6.3	19.4
4.4	1	1421	1.2	23656.746	15.2	1.7	60.083	116.488	11	19.2
4.4	0.5	1276	0.7	22431.139	12.8	0.7	56.902	128.089	5.4	21.4
4.4	0.1	1209	0.4	16796.389	17.5	1	71.958	231.225	6	18.2
21.1	25	739	5.7	16582.65	17.5	2.9	44.554	513	8.2	18.5
21.1	10	701	5.8	13583.73	20.2	1.2	51.57	723.306	6.9	13.5
21.1	5	593	5.3	11654.026	21.3	0.5	50.911	813.826	7.7	15.3
21.1	1	431	3.2	8157.852	24.9	0.5	52.81	829.427	7.5	21
21.1	0.5	357	2.5	6581.637	25.1	0.5	54.231	851.409	6.4	20.6
21.1	0.1	304	1.2	4144.207	27.1	1.6	73.404	984.241	4.9	22.4
37.8	25	251	7.7	5344.35	28.9	5	46.931	219.406	9.2	17.6
37.8	10	225	6.9	3830.446	28.8	2.4	58.765	379.476	5.7	14.9
37.8	5	153	7.5	3035.339	28.4	0.6	50.331	381.195	6.9	18.3
37.8	1	120	5.5	1822.606	26.8	0.8	65.799	385.257	6.5	19.5
37.8	0.5	89	3.7	1424.934	26.1	1	62.587	384.743	6.2	21.3
37.8	0.1	64	1.9	907.627	21.1	1.7	70.457	409.427	7.2	22.3
54.4	25	88	9.4	1577.864	31.9	2.4	55.897	318.307	8.3	13.9
54.4	10	71	7.6	1151.777	27.6	2.3	61.428	426.556	5.5	13.5
54.4	5	56	7.2	908.288	25	2.4	62.099	441.352	5.2	14.8
54.4	1	41	6.3	616.148	18.1	2.9	66.963	436.686	5.2	19.3
54.4	0.5	34	5.2	530.68	16.5	2.2	64.03	432.177	6.2	19.8
54.4	0.1	26	3.2	434.841	11.7	2.3	60.848	440.864	7.5	25

Table B-155 Overall Dynamic Modulus test results at various test temperatures for Mix 51 Specimen 2

Temperature (°C)	Frequency (Hz)	Stress Amplitude (P-P) (KPa)	SE (%)	Dynamic Modulus (MPa)	Phase Angle (deg.)	UC (deg.)	Strain (P-P) Recoverable (microstrain)	Accumulated Strain (microstrain)	SE (%)	UC (%)
-10	25	2203	4.7	47147.574	1.3	6.1	46.728	63.284	13.9	30
-10	10	2261	4.5	47395.504	5.5	0.3	47.707	21.083	6.3	15
-10	5	2191	4.3	44668.082	6.6	0.7	49.057	23.315	7.7	14.3
-10	1	1962	1.2	42690.441	5.1	0.1	45.968	24.985	7.3	16.9
-10	0.5	1844	0.6	38294.035	8.9	1.4	48.157	26.464	7.9	14.2
-10	0.1	1681	0.4	35413.625	6.6	0.6	47.469	38.301	10.8	16
4.4	25	1760	4.8	33995.977	6.8	1.9	51.773	116.114	8.4	26.8
4.4	10	1721	4.4	30874.361	9.9	0.3	55.743	52.25	6.3	18.5
4.4	5	1613	4	28534.348	11	0.8	56.515	48.633	7.6	18.6
4.4	1	1420	1.2	23261.063	14.9	1	61.047	47.753	9.7	19
4.4	0.5	1277	0.7	22559.234	13.2	1.1	56.599	53.675	7.4	22.4
4.4	0.1	1209	0.4	16560.498	18.4	1.4	72.998	146.961	6.5	18
21.1	25	736	5.8	17028.986	15.9	0.2	43.212	260.712	8.3	20.9
21.1	10	702	5.4	13496.584	19.7	0.8	52.01	339.254	5.6	13.2
21.1	5	592	5	11507.478	21	0.4	51.411	367.08	5.9	14.7
21.1	1	431	3.1	7645.675	23.6	0.8	56.32	358.733	7.5	16.6
21.1	0.5	357	2.4	6385.18	26.5	1.1	55.975	360.12	8.5	20.5
21.1	0.1	304	1.1	4033.825	25.9	1.4	75.466	434.123	5.7	22.2
37.8	25	250	7.3	5368.382	28.6	3.1	46.524	329.895	9.1	17
37.8	10	226	6.9	3623.07	30.5	5.1	62.509	471.818	5.6	16.8
37.8	5	153	7.4	3006.916	28.2	0.7	50.88	468.83	6.2	16.6
37.8	1	120	5.2	1816.217	26.4	0.7	66.068	469.286	5.6	19
37.8	0.5	89	3.5	1404.529	26	1.1	63.421	466.278	5.5	20.7
37.8	0.1	64	1.6	891.483	21.3	1.3	71.817	488.22	6.7	21.7
54.4	25	87	8.4	1531.933	32.5	1.6	57.08	273.842	7.9	14.1
54.4	10	71	7.5	1119.256	27.7	2.7	63.772	377.659	7.1	12.8
54.4	5	56	6.9	890.344	24.9	2.1	63.161	392.122	4.1	15.9
54.4	1	41	6.6	599.349	19.2	2.3	69.117	386.053	4.4	19.6
54.4	0.5	34	5.2	517.489	16	3.1	65.56	379.981	5.8	22
54.4	0.1	27	3	418.04	12.2	2.6	64.155	385.368	8	27

Table B-156 Overall Dynamic Modulus test results at various test temperatures for Mix 51 Specimen 3

Temperature (°C)	Frequency (Hz)	Stress Amplitude (P-P) (KPa)	SE (%)	Dynamic Modulus (MPa)	Phase Angle (deg.)	UC (deg.)	Strain (P-P) Recoverable (microstrain)	Accumulated Strain (microstrain)	SE (%)	UC (%)
-10	25	2200	4.6	47066.398	1	5.9	46.739	55.759	12.7	29.8
-10	10	2255	4.3	47581.949	5.9	0.1	47.385	17.403	8.2	18.3
-10	5	2185	4.2	46955.809	4.5	0.3	46.539	19.488	8	18.8
-10	1	1959	1.1	40964.996	3.9	0.8	47.823	17.256	6.5	17.3
-10	0.5	1843	0.6	39374.668	9	1.2	46.797	18.293	8.1	17.9
-10	0.1	1681	0.4	35238.613	8.1	0.3	47.71	26.394	7.8	18.3
4.4	25	1760	4.8	33604.984	6.7	2.3	52.371	124.624	7.9	26.1
4.4	10	1725	4.5	30628.422	10.5	0.5	56.31	55.295	5.9	18.2
4.4	5	1618	4.2	28634.518	10.9	0.3	56.518	53.391	6.8	18.3
4.4	1	1421	1.2	23682.588	11.8	1.3	60.003	51.622	12.1	20
4.4	0.5	1278	0.7	20338.467	16.4	1.2	62.815	58.004	6.6	16.9
4.4	0.1	1209	0.4	16423.951	18.3	1	73.616	144.817	6.7	18.8
21.1	25	736	6	17112.25	17.3	1	43.024	260.235	8.5	20.6
21.1	10	701	5.3	13362.747	19.7	0.6	52.459	312.849	5.3	13
21.1	5	591	5	11486.502	20.4	0.5	51.415	325.016	6	14.4
21.1	1	431	3.1	7598.02	23.7	0.9	56.741	310.939	6.5	17.1
21.1	0.5	357	2.4	6243.247	26	0.9	57.21	310.352	6.3	18.9
21.1	0.1	304	1.2	3953.098	25.2	1.5	76.9	371.249	4.9	21.7
37.8	25	247	7.2	5132.799	30.2	5.7	48.086	275.691	7.7	16
37.8	10	226	6.9	3467.301	30.5	5.3	65.261	402.993	5.8	20.7
37.8	5	153	7.3	2978.314	28.3	0.8	51.447	396.402	6.2	16.3
37.8	1	120	5.2	1809.643	26.3	1	66.118	394.023	6.1	19.4
37.8	0.5	89	3.6	1390.329	26.2	1.2	63.954	388.82	5.6	20
37.8	0.1	64	1.6	878.79	21	1.3	72.436	409.214	7.4	21.2
54.4	25	88	8.7	1263.436	33.8	1.3	69.365	236.988	8.1	19.6
54.4	10	71	7.5	929.302	28.4	3.7	76.436	327.451	5.3	22.6
54.4	5	57	7.3	829.531	25.3	2.3	68.23	350.158	5.1	11.6
54.4	1	41	6.6	586.314	18.7	2.8	70.39	348.291	4.6	18.5
54.4	0.5	34	5.4	508.601	16.4	3.1	66.303	341.427	5.2	22.4
54.4	0.1	27	3.1	413.254	12.4	2.6	64.588	346.588	7.1	28.2

Table B-157 Overall Dynamic Modulus test results at various test temperatures for Mix 52 Specimen 1

Temperature (°C)	Frequency (Hz)	Stress Amplitude (P-P) (KPa)	SE (%)	Dynamic Modulus (MPa)	Phase Angle (deg.)	UC (deg.)	Strain (P-P) Recoverable (microstrain)	Accumulated Strain (microstrain)	SE (%)	UC (%)
-10	25	2203	4.6	65500.68	3.9	7.5	33.638	74.535	9.9	17.7
-10	10	2257	4.6	67027.078	8.1	3.8	33.678	48.633	9.2	18.9
-10	5	2198	4.5	64285.785	9.1	4.4	34.193	51.111	10.7	18.1
-10	1	1963	1.2	58630.18	10.8	5.4	33.473	51.483	18	19.8
-10	0.5	1844	0.7	52558.688	16.7	7.7	35.088	53.775	22.7	17.9
-10	0.1	1681	0.5	46298.426	11.2	5.5	36.308	67.008	18.2	18.5
4.4	25	1760	4.8	46141.109	9.7	8.5	38.138	191.751	12.8	17.1
4.4	10	1729	4.9	38604.891	15.5	5.6	44.798	157.877	8.3	13.2
4.4	5	1617	4.5	35375.766	15.7	5.6	45.72	176.517	7.9	9.1
4.4	1	1421	1.3	26681.061	20.5	5.5	53.271	189.646	7.7	12.4
4.4	0.5	1277	0.7	23269.762	20.4	4.5	54.895	216.224	8	11.7
4.4	0.1	1210	0.4	15254.341	26.1	3.2	79.292	388.438	6.6	19
21.1	25	623	6.4	12168.522	29.3	5.4	51.212	436.868	8.2	26.2
21.1	10	573	6.3	8879.911	30.2	5.1	64.579	573.7	6.5	28.1
21.1	5	507	6	7064.308	31.5	4.9	71.797	673.815	5.4	28.6
21.1	1	404	3.4	4018.471	33.7	4.4	100.634	727.817	5.1	29.4
21.1	0.5	351	2.5	3221.047	33.7	4.3	108.993	793.648	5.4	28.7
21.1	0.1	296	1.3	1831.872	30.1	3.3	161.804	1058.811	6.2	30.1
37.8	25	168	8.8	2735.025	39.7	4.2	61.32	271.825	8.3	31.8
37.8	10	123	8.5	1870.281	36.1	5.6	65.568	352.475	7.1	36
37.8	5	102	8.4	1423.405	33.8	5	71.63	405.203	6.5	37.9
37.8	1	79	5.8	873.339	28.3	4.5	90.715	435.532	5.9	40.5
37.8	0.5	64	4.3	750.677	25.8	4.5	85.896	459.061	6.2	45.3
37.8	0.1	54	2.2	609.117	18.4	2.5	88.596	500.735	8.2	55.7
54.4	25	63	8.6	964.675	31.2	1.4	64.971	227.46	7.2	56
54.4	10	51	8.2	720.727	24.7	1.7	70.77	298.229	4.5	62.5
54.4	5	41	7.4	602.674	22	1.6	67.238	310.845	4.2	60.9
54.4	1	30	6.9	472.748	17.4	2	62.553	313.116	6.9	57.6
54.4	0.5	23	5.3	433.151	16.4	2.7	53.702	313.906	7.7	53.8
54.4	0.1	19	4.4	406.423	12.8	3.7	45.88	323.607	7.7	44.1

Table B-158 Overall Dynamic Modulus test results at various test temperatures for Mix 52 Specimen 2

Temperature (°C)	Frequency (Hz)	Stress Amplitude (P-P) (KPa)	SE (%)	Dynamic Modulus (MPa)	Phase Angle (deg.)	UC (deg.)	Strain (P-P) Recoverable (microstrain)	Accumulated Strain (microstrain)	SE (%)	UC (%)
-10	25	2206	4.6	64526.23	3.7	8.5	34.188	42.73	11.5	18
-10	10	2256	4.3	66715.922	7.5	3	33.82	5.728	9	17.3
-10	5	2189	4.1	66154.789	7.6	3.3	33.086	3.932	13.3	18.7
-10	1	1960	1.1	54519.848	11.9	5.1	35.953	2.545	9.7	14.4
-10	0.5	1843	0.6	54410.344	11.2	4.8	33.875	4.402	14	17.4
-10	0.1	1681	0.4	46562.691	12.8	5.2	36.099	18.116	11.4	17
4.4	25	1765	4.9	41227.113	12.4	8.6	42.82	180.852	12.4	11.2
4.4	10	1729	4.9	35858.66	15.9	5.6	48.23	119.207	7.8	8.4
4.4	5	1621	4.5	32253.646	16.9	5.5	50.264	129.817	8.9	9
4.4	1	1422	1.3	24169.936	21	5	58.844	139.144	6.9	12.4
4.4	0.5	1278	0.7	21103.168	20.1	4.7	60.564	159.378	5.3	12.5
4.4	0.1	1209	0.4	14441.879	25.6	3.2	83.728	330.25	5.8	18.5
21.1	25	623	6.4	11366.603	29.4	5.1	54.815	399.421	7.6	26.6
21.1	10	552	6.4	8379.534	30.5	5	65.896	449.246	6	28.8
21.1	5	443	6.6	6747.492	31.9	4.8	65.682	458.34	5.9	28.5
21.1	1	323	4	3768.494	33.2	4.2	85.755	448.44	5.2	29.3
21.1	0.5	261	2.5	2811.287	33.1	3.7	92.692	451.891	4	29.6
21.1	0.1	200	1	1620.573	30.7	4.6	123.313	535.341	5.3	29.9
37.8	25	168	8.7	2639.661	39	4	63.833	239.504	7.9	32.3
37.8	10	124	8.1	1813.137	35.5	5.3	68.424	285.731	6.9	36.3
37.8	5	103	7.9	1432.403	33.6	4.8	71.604	328.046	6.4	41.8
37.8	1	80	5.7	951.311	26.4	2.8	84.197	357.954	5.6	54.5
37.8	0.5	64	4.1	777.933	24.2	2.6	82.707	368.083	6.3	57.4
37.8	0.1	54	2.2	595.64	17.6	1.9	90.128	394.199	7.1	59.9
54.4	25	62	8.1	875.748	31.7	0.9	71.022	187.315	6.9	58.4
54.4	10	51	7.4	673.486	24.5	1.2	75.68	260.648	4.3	62.7
54.4	5	41	7.1	568.364	22.2	1.3	71.431	273.175	3.7	61.6
54.4	1	29	6.4	436.454	17.1	0.9	65.419	273.232	4.6	60.4
54.4	0.5	23	5	404.07	14.6	1.7	57.625	270.063	6.6	57.5
54.4	0.1	18	3.4	353.703	12.7	2.4	51.931	274.701	8.7	52.4

Table B-159 Overall Dynamic Modulus test results at various test temperatures for Mix 52 Specimen 3

Temperature (°C)	Frequency (Hz)	Stress Amplitude (P-P) (KPa)	SE (%)	Dynamic Modulus (MPa)	Phase Angle (deg.)	UC (deg.)	Strain (P-P) Recoverable (microstrain)	Accumulated Strain (microstrain)	SE (%)	UC (%)
-10	25	2211	4.7	65553.586	2.4	10.5	33.729	45.144	13.6	20.4
-10	10	2260	4.4	66531.125	7.3	2.5	33.966	9.834	11.5	17.8
-10	5	2193	4.4	64508.449	8.2	3.8	34.001	9.738	9.6	18.1
-10	1	1962	1.2	59843.234	10.5	5.3	32.79	7.66	8.9	19.5
-10	0.5	1844	0.7	54052.512	16.2	6.7	34.12	8.601	19	16.7
-10	0.1	1681	0.4	46384.059	11.8	4.4	36.248	31.796	14.2	16.4
4.4	25	1763	4.9	40224.441	13.2	9.5	43.82	170.011	12.1	12.9
4.4	10	1724	4.7	34179.988	16.1	5.5	50.442	94.142	6	6.5
4.4	5	1617	4.2	30292.402	17.6	5.6	53.377	93.092	6.6	8.6
4.4	1	1422	1.3	23364.652	20.7	5.4	60.856	93.231	8.9	12.2
4.4	0.5	1278	0.8	19531.242	23.1	4.4	65.445	109.414	5.3	12.4
4.4	0.1	1209	0.4	13762.024	26.6	2.9	87.87	291.078	5.2	16
21.1	25	623	6.6	11167.323	29.3	5.2	55.755	446.912	7.7	26.6
21.1	10	553	6.4	8296.722	30.4	4.9	66.619	498.334	5.8	28.5
21.1	5	443	6.5	6649.336	32	4.9	66.681	504.059	5.9	28.5
21.1	1	323	3.9	3766.281	33.4	4.3	85.842	492.109	7.1	28.8
21.1	0.5	261	2.4	2735.371	34.6	4.7	95.493	493.743	4.7	30
21.1	0.1	199	1	1594.386	30.3	4.5	125.115	571.59	5.3	30.7
37.8	25	168	8.7	2574.337	38.7	4.1	65.148	228.244	7.7	34.3
37.8	10	123	9	1738.21	35.4	3.9	70.908	248.9	6.5	36.7
37.8	5	102	8.5	1305.26	33.1	3.7	77.994	266.911	6.4	37.7
37.8	1	80	5.9	835.791	26.1	2.2	95.317	290.17	6.1	44.3
37.8	0.5	64	4.5	753.057	23.8	2.8	85.173	307.331	5.4	57.4
37.8	0.1	54	2.4	572.073	17.8	1.8	94.404	331.282	7.1	61.3
54.4	25	63	8.3	834.736	33	1.4	75.94	189.592	7.1	58.2
54.4	10	51	7.6	639.674	25.4	2	80.339	254.855	4.2	59.8
54.4	5	40	7	518.659	22.9	2.5	77.53	262.595	5.9	57.8
54.4	1	30	6.8	421.406	16.9	1.4	70.061	259.888	4.7	60.4
54.4	0.5	24	5.7	376.38	15.7	1.1	64.152	251.17	5.1	58.5
54.4	0.1	19	3.7	177.361	14.1	1.8	105.091	190.839	8.8	76.9

Table B-160 Overall Dynamic Modulus test results at various test temperatures for Mix 53 Specimen 1

Temperature (°C)	Frequency (Hz)	Stress Amplitude (P-P) (KPa)	SE (%)	Dynamic Modulus (MPa)	Phase Angle (deg.)	UC (deg.)	Strain (P-P) Recoverable (microstrain)	Accumulated Strain (microstrain)	SE (%)	UC (%)
-10	25	2203	4.6	70474.203	8.6	2.4	31.263	73.21	19.2	29.5
-10	10	2264	4.6	74678.742	4.9	0.5	30.315	52.854	9.3	16.7
-10	5	2188	4.3	72972.742	4.8	0.8	29.985	54.512	7.9	14.5
-10	1	1958	1.1	67263.375	3.8	0.5	29.106	53.277	6.7	14.9
-10	0.5	1841	0.6	66585.164	3.9	1.7	27.656	52.557	13.2	13.8
-10	0.1	1681	0.5	57515.91	7.7	1	29.23	60.688	9.2	14
4.4	25	1767	4.9	49255.473	13.7	5.9	35.881	105.537	10.6	31.9
4.4	10	1726	4.7	50039.828	11.4	2.8	34.491	75.303	7.3	20.8
4.4	5	1615	4.4	46334.512	11.9	3.2	34.849	84.127	7	19.7
4.4	1	1421	1.3	37383.836	15.6	4.8	38.005	87.2	6.9	24.3
4.4	0.5	1276	0.8	35491.375	18.8	5.2	35.96	97.203	7.7	24.1
4.4	0.1	1209	0.4	25554.568	21.3	5.7	47.306	165.907	6.7	26.5
21.1	25	626	6.7	24178.332	20.8	8.8	25.907	353.968	12.1	35.9
21.1	10	553	6.5	22016.563	21.1	4.3	25.117	519.42	11.9	22.5
21.1	5	442	6.5	19169.07	22.6	4.3	23.056	594.997	10.7	24.5
21.1	1	322	4.1	13196.77	23.8	2.5	24.387	622.391	12.8	19.5
21.1	0.5	260	2.4	10440.302	25.4	1.6	24.86	649.828	7.6	17.8
21.1	0.1	198	1.2	6813.163	27.8	2.9	29.096	703.945	7	16.2
37.8	25	328	7.6	7326.497	34.6	3.3	44.827	841.948	6.6	20
37.8	10	247	7	5251.527	33.5	4.1	47.084	1066.134	7	16.2
37.8	5	204	6.7	4060.51	33	3.2	50.249	1185.357	5.9	16.4
37.8	1	160	4.4	2329.323	31.2	2.2	68.614	1247.91	5.3	17
37.8	0.5	129	3.6	1874.205	28.4	1.2	69.042	1276.958	6.4	12.2
37.8	0.1	109	1.7	1231.808	22.7	0.5	88.591	1336.782	6.5	6.2
54.4	25	66	8.8	1345.868	38.9	3.8	48.669	108.483	8.1	59.8
54.4	10	51	6.3	998.639	33.1	4.1	51.085	124.65	5.8	52
54.4	5	39	5.5	807.982	30.6	4.2	48.626	120.04	5.8	49
54.4	1	29	5	586.543	23.7	4	49.72	131.119	5.5	36.5
54.4	0.5	23	4.1	546.801	21.1	3.5	42.749	131.731	5.5	23.6
54.4	0.1	19	3.3	513.228	11.9	0.9	36.532	139.704	5.9	6.5

Table B-161 Overall Dynamic Modulus test results at various test temperatures for Mix 53 Specimen 2

Temperature (°C)	Frequency (Hz)	Stress Amplitude (P-P) (KPa)	SE (%)	Dynamic Modulus (MPa)	Phase Angle (deg.)	UC (deg.)	Strain (P-P) Recoverable (microstrain)	Accumulated Strain (microstrain)	SE (%)	UC (%)
-10	25	2193	4.3	70067.195	9.1	2.4	31.301	38.133	13.4	27.2
-10	10	2259	4.3	74536.359	5.2	0.5	30.306	13.16	10.3	15.8
-10	5	2183	4.1	73180.445	4.8	0.4	29.835	9.322	11	14.9
-10	1	1955	1.1	68402.383	7.5	0.5	28.587	10.334	10	14.3
-10	0.5	1842	0.6	66871.922	6.2	1.1	27.541	10.084	12.5	13.2
-10	0.1	1680	0.4	58319.496	6.1	1.5	28.813	18.267	13.1	13.4
4.4	25	1764	4.7	48411.086	13.6	6.3	36.436	87.641	8.1	28
4.4	10	1721	4.5	48640.172	11.6	3.5	35.378	44.066	6.6	18.5
4.4	5	1614	4	43651.445	13.5	3.7	36.981	44.482	10	20
4.4	1	1419	1.1	36360.289	15.4	5.3	39.02	44.675	6.4	24.5
4.4	0.5	1276	0.7	32469.646	12.6	6.6	39.309	49.291	12.5	24.9
4.4	0.1	1209	0.4	24878.738	21	5.8	48.591	112.042	7.1	27
21.1	25	1237	4.9	19282.584	23.6	4.9	64.138	879.471	6.3	49.7
21.1	10	1112	4.9	16968.535	23.1	5.6	65.561	1066.038	6.3	43.1
21.1	5	896	4.5	15849.984	24.9	6.5	56.521	1197.583	6.3	35.6
21.1	1	646	2.1	10574.156	29.9	6.5	61.102	1244.826	4.5	33.7
21.1	0.5	420	1.8	9625.451	30.3	4.7	43.677	1263.321	5.8	23.4
21.1	0.1	399	1	5751.667	31.6	4.3	69.304	1394.677	5.3	27
37.8	25	328	7.7	7117.835	34.9	2.9	46.111	484.773	6.6	13.9
37.8	10	248	7.1	5067.077	33.3	2.5	48.905	590.933	6	12.6
37.8	5	204	6.8	3936.791	32.8	1.8	51.777	647.405	5.5	14.3
37.8	1	159	4.6	2307.914	29.9	0.9	69.044	672.285	5	11.5
37.8	0.5	129	3.5	1849.717	27.6	1.2	69.734	683.7	4.9	7.5
37.8	0.1	109	1.7	1223.257	21.4	1.5	89.5	729.025	6.8	2.7
54.4	25	64	7.8	1284.812	40.1	3.3	49.518	52.506	7.6	54.5
54.4	10	51	6.2	906.831	34	3.5	56.295	59.954	6.6	49.6
54.4	5	40	5.4	760.281	29.9	3.5	52.573	60.219	5.9	55
54.4	1	29	4.9	523.835	23.3	3.5	55.325	59.799	5.5	48.9
54.4	0.5	26	4.6	475.298	20.4	3.7	55.399	57.833	5.6	44.4
54.4	0.1	23	3.4	435.082	16	4.1	53.762	62.532	7.1	28.1

Table B-162 Overall Dynamic Modulus test results at various test temperatures for Mix 53 Specimen 3

Temperature (°C)	Frequency (Hz)	Stress Amplitude (P-P) (KPa)	SE (%)	Dynamic Modulus (MPa)	Phase Angle (deg.)	UC (deg.)	Strain (P-P) Recoverable (microstrain)	Accumulated Strain (microstrain)	SE (%)	UC (%)
-10	25	2206	4.8	69528	8.8	3	31.726	30.637	13.4	26.1
-10	10	2262	4.3	73658.695	6	0.5	30.705	4.021	12	12.7
-10	5	2193	4.3	72942.758	5.5	0.7	30.061	3.626	9.6	13
-10	1	1958	1.1	65172.641	7.9	1.1	30.039	5.741	9.4	14
-10	0.5	1841	0.6	65446.414	7	0.9	28.129	8.255	12.2	12.5
-10	0.1	1681	0.5	58083.117	5.9	0.9	28.936	12.535	13.3	11.4
4.4	25	1762	4.9	48736.172	13.3	7.4	36.164	94.012	10.7	28.8
4.4	10	1723	4.6	47710.789	11.7	3.5	36.114	51.096	9.8	18.3
4.4	5	1617	4.2	44187.559	12.2	3.9	36.587	51.77	10.1	17.8
4.4	1	1420	1.2	36427.305	13.6	6.1	38.992	51.093	12.2	26.5
4.4	0.5	1276	0.7	32904.348	20.9	5.6	38.79	58.374	9.7	26.9
4.4	0.1	1208	0.4	24063.908	21.5	5.6	50.206	123.937	7.2	27.4
21.1	25	1239	5.4	22879.355	22.6	4.3	54.141	692.766	7.4	22.6
21.1	10	1113	4.9	19052.063	23.1	4.5	58.421	773.881	4.7	22.9
21.1	5	900	4.6	16310.753	24.6	4.2	55.152	855.38	5	22
21.1	1	647	2.1	10770.306	28.5	4.6	60.101	881.644	3.9	23.3
21.1	0.5	420	1.8	9061.895	28.8	2.3	46.364	882.021	4.2	18.9
21.1	0.1	400	0.8	5555.708	29.3	2.6	71.954	966.493	4.7	20.3
37.8	25	329	7.7	6971.804	35.5	3.4	47.204	416.625	6.4	15
37.8	10	248	7.2	4905.189	34.4	2.8	50.53	489.783	5.3	13.3
37.8	5	205	7	3788.812	33.7	2.5	53.993	523.862	5.4	13.8
37.8	1	160	4.6	2240.066	30	1.5	71.334	538.42	5.2	13.1
37.8	0.5	130	3.5	1781.525	27.9	0.4	72.838	543.619	5.7	9.1
37.8	0.1	109	1.7	1205.38	20.9	1.5	90.167	582.764	7.1	4.1
54.4	25	63	7.9	1091.043	39.4	3.2	58.018	49.665	9.1	42.2
54.4	10	52	6.3	745.982	33.9	3.9	69.165	38.272	5.1	42
54.4	5	40	5.3	577.751	31.3	3.6	69.064	21.863	4.5	42.8
54.4	1	29	4.9	366.804	24.8	3.4	80.119	8.777	5	44.6
54.4	0.5	27	4.5	326.629	21.9	3.6	81.714	2.226	5.5	46.8
54.4	0.1	23	2.9	280.721	16.1	3.6	83.152	5.272	6.9	52.8

Table B-163 Overall Dynamic Modulus test results at various test temperatures for Mix 54 Specimen 1

Temperature (°C)	Frequency (Hz)	Stress Amplitude (P-P) (KPa)	SE (%)	Dynamic Modulus (MPa)	Phase Angle (deg.)	UC (deg.)	Strain (P-P) Recoverable (microstrain)	Accumulated Strain (microstrain)	SE (%)	UC (%)
-10	25	2208	4.8	62557.195	7.4	4.3	35.298	70.128	18.5	17.5
-10	10	2258	4.6	66128.141	6.1	1	34.153	46.949	8.5	11.4
-10	5	2189	4.2	63581.648	5	0.3	34.43	48.375	9.2	12.3
-10	1	1960	1.1	55698.52	8.7	1.7	35.182	47.039	10.7	10.4
-10	0.5	1843	0.6	54762.797	5.3	0.9	33.655	50.227	11.9	11.6
-10	0.1	1681	0.4	49385.094	6.6	0.6	34.041	60.361	12.3	11.8
4.4	25	1765	4.9	45540.027	13.4	7.8	38.749	78.154	13.2	18.1
4.4	10	1727	4.8	44681.66	10.1	1.1	38.645	39.928	7.4	5.6
4.4	5	1621	4.2	42918.188	10.7	1.3	37.761	43.134	6.9	7.5
4.4	1	1421	1.2	35292.297	15.8	2.7	40.271	46.202	22.2	6
4.4	0.5	1277	0.7	33952.816	12.2	1.3	37.604	50.753	10.5	6.8
4.4	0.1	1209	0.4	25565.324	16.9	2.3	47.277	94.7	7.1	2.1
21.1	25	1240	5.2	21213.982	22.2	3	58.451	915.046	8.9	23.3
21.1	10	1114	5.2	17878.99	20.1	1.5	62.325	1113.602	5.3	17.1
21.1	5	901	4.8	15390.791	21.9	1.8	58.547	1230.944	5	16.1
21.1	1	649	2.3	10098.719	25.5	1.1	64.225	1255.17	5.2	21.4
21.1	0.5	421	1.9	8057.699	27.1	1.5	52.281	1245.171	4.4	25.1
21.1	0.1	400	0.8	5277.906	28.7	1.6	75.76	1405.103	6	28.5
37.8	25	326	8.4	7282.484	37	5.2	44.76	903.168	9.2	34.2
37.8	10	246	6.8	5085.52	32.6	1.8	48.363	1159.9	6.5	32.7
37.8	5	203	6.5	3988.155	32.6	1.9	50.825	1307.802	7.1	32.4
37.8	1	159	4.1	2290.834	30.5	2.4	69.523	1393.19	5.5	31.1
37.8	0.5	129	3.2	1810.494	28.5	1.8	71.146	1434.525	5.1	32.9
37.8	0.1	108	1.4	1197.231	22.9	2.1	90.432	1515.155	6.2	30.4
54.4	25	64	8.8	1597.192	41.1	10.7	40.31	101.398	10.4	28.6
54.4	10	51	6.4	1215.752	34	8.8	41.586	134.049	12.2	24.6
54.4	5	40	5.8	975.206	31.6	7.7	40.985	146.651	7.9	21.9
54.4	1	30	5.6	681.299	24.5	7.2	43.786	145.057	7.2	9.5
54.4	0.5	27	4.6	622.189	21.1	6.5	43.026	141.935	8	6.7
54.4	0.1	24	2.9	515.36	14	5	45.891	146.253	10.3	9.9

Table B-164 Overall Dynamic Modulus test results at various test temperatures for Mix 54 Specimen 2

Temperature (°C)	Frequency (Hz)	Stress Amplitude (P-P) (KPa)	SE (%)	Dynamic Modulus (MPa)	Phase Angle (deg.)	UC (deg.)	Strain (P-P) Recoverable (microstrain)	Accumulated Strain (microstrain)	SE (%)	UC (%)
-10	25	2208	4.6	64281.066	8	18.7	34.345	31.747	21.7	10.9
-10	10	2266	4.8	69096.844	3.8	0.5	32.8	8.216	9.7	10.3
-10	5	2197	4.5	66426.664	4.5	0.5	33.079	15.4	9.5	10.7
-10	1	1963	1.2	58835.094	6.6	1.1	33.357	12.538	8.5	8.6
-10	0.5	1844	0.7	58470.555	10.9	2.7	31.539	14.535	18.4	10.5
-10	0.1	1681	0.5	51959.824	7.3	0.6	32.361	22.051	9.3	10
4.4	25	1766	4.8	44352.461	13.6	0.8	39.808	68.581	8.7	17.5
4.4	10	1728	4.4	44069.801	9.5	0.9	39.212	22.542	7.3	13.6
4.4	5	1619	4.1	41557.43	10.5	1.1	38.963	18.937	6.8	15.4
4.4	1	1422	1.2	33780.117	13.1	1.2	42.102	19.16	7.1	14.7
4.4	0.5	1277	0.7	34290.859	12.5	1.3	37.244	20.803	17.7	17
4.4	0.1	1209	0.4	25528.098	14.4	5.7	47.352	74.068	29.9	8.7
21.1	25	1237	5.4	20323.686	20.6	1.1	60.883	681.423	7.4	10.5
21.1	10	1114	4.7	17101.744	21	1.6	65.136	660.925	5	9.5
21.1	5	901	4.6	14322.49	23.6	2.7	62.934	683.755	4.4	11.6
21.1	1	648	2.1	8647.645	29.9	5.2	74.987	669.507	5.9	18.5
21.1	0.5	421	1.9	6981.766	32	5.7	60.329	642.285	5.2	16
21.1	0.1	400	0.7	4590.715	31.9	4.4	87.042	786.043	6.2	12.6
37.8	25	326	7.9	6935.381	36.7	5.2	47.028	492.088	9.3	10.5
37.8	10	246	7.1	4830.855	34.7	4.1	50.946	601.377	8.9	13.6
37.8	5	204	6.7	3632.425	33.9	4.5	56.146	667.343	5.5	9.9
37.8	1	159	4.4	2037.715	32.3	5.8	78.193	706.784	4.8	6.1
37.8	0.5	129	3.3	1615.783	30.8	6.1	79.85	723.516	5.7	9.5
37.8	0.1	109	1.4	1143.305	22.7	3.4	95.549	771.13	6.9	17.8
54.4	25	64	8.1	1554.68	39.8	4.7	40.87	90.339	9.2	34
54.4	10	51	6.7	1139.87	33.6	6.4	44.906	117.959	7.2	30.2
54.4	5	40	6	936.905	30.7	7.4	43.126	122.664	7.2	22.8
54.4	1	29	5.4	663.962	23.3	5.8	44.423	121.072	6.5	10.2
54.4	0.5	27	4.6	618.376	18.9	5	42.871	117.217	6.5	8.3
54.4	0.1	24	2.9	511.701	12.5	4.8	46.456	118.989	7.1	10.7

Table B-165 Overall Dynamic Modulus test results at various test temperatures for Mix 54 Specimen 3

Temperature (°C)	Frequency (Hz)	Stress Amplitude (P-P) (KPa)	SE (%)	Dynamic Modulus (MPa)	Phase Angle (deg.)	UC (deg.)	Strain (P-P) Recoverable (microstrain)	Accumulated Strain (microstrain)	SE (%)	UC (%)
-10	25	2208	4.8	65349.723	8.4	4.1	33.794	32.454	15.6	21.2
-10	10	2260	4.4	67071.031	5.2	0.1	33.694	5.729	9.3	17.5
-10	5	2188	4.1	65396.73	5.4	0.8	33.45	2.663	8.6	17.4
-10	1	1958	1.1	60707.047	3.8	0.9	32.261	5.27	9	18
-10	0.5	1843	0.6	59543.211	6	0.4	30.947	7.275	12.3	19.3
-10	0.1	1681	0.4	53034.426	8.5	1.3	31.696	10.676	12.4	18.3
4.4	25	1765	4.7	45511.668	10.7	0.3	38.782	80.658	11	26.8
4.4	10	1727	4.3	43525.059	11.1	1.7	39.676	33.71	7.1	17.4
4.4	5	1619	4	40918.496	11.1	1.3	39.571	32.702	6.7	19.1
4.4	1	1422	1.1	34094.238	10.5	0.4	41.694	29.516	19.1	18.7
4.4	0.5	1278	0.6	29206.088	16.7	3	43.743	31.905	8.6	17
4.4	0.1	1209	0.4	24008.885	17.9	2	50.355	80.786	6.3	16
21.1	25	1238	5.3	17045.326	23.7	3.6	72.606	685.799	6.9	41.1
21.1	10	1115	4.6	14215.612	23.4	4.5	78.414	610.125	5.6	32.9
21.1	5	899	4.4	11740.501	24.7	4.1	76.544	612.957	5.8	36.7
21.1	1	647	2	7333.441	29	3.1	88.277	584.437	3.6	43.5
21.1	0.5	420	1.8	5841.904	30.4	3.7	71.977	545.299	4.1	43.6
21.1	0.1	400	0.9	3562.662	30.9	3.7	112.248	690.617	4.7	42.3
37.8	25	328	8.1	6324.347	36.8	5.3	51.825	421.208	7.4	10.5
37.8	10	247	7	4393.283	34.6	5.4	56.156	482.955	5.6	7.1
37.8	5	204	6.7	3413.279	34.6	5.8	59.765	520.902	5.5	5.4
37.8	1	160	4.6	1911.53	32.6	6.8	83.629	541.313	5.4	6.9
37.8	0.5	129	3.7	1515.074	31.1	7.3	85.068	548.147	5.3	3.8
37.8	0.1	109	1.7	1086.932	23.5	5.7	99.929	581.299	7	6.3
54.4	25	64	8.4	1499.594	39.3	5.3	42.419	84.167	9.4	35.4
54.4	10	51	6.7	1075.812	33.3	6.7	47.631	103.58	6.4	32.1
54.4	5	40	6	875.975	30.3	7.2	45.731	104.581	7.1	30
54.4	1	29	5.5	621.422	23.1	6.6	47.065	101.603	5.3	17.3
54.4	0.5	27	5.2	572.426	19.6	6.4	46.543	98.218	5.8	14
54.4	0.1	23	2.6	500.926	12.8	4.6	46.419	97.672	7.1	10.9

Appendix C

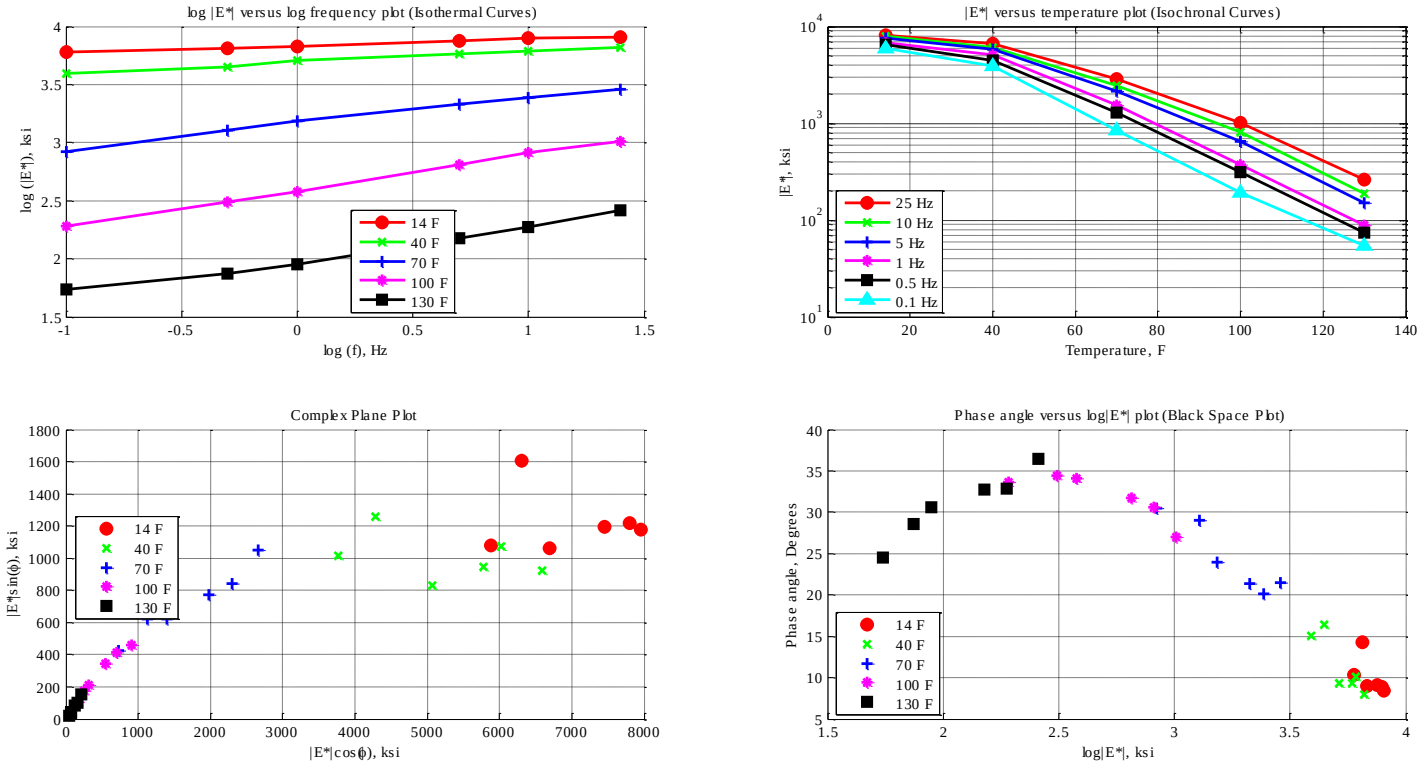

Figure C-1 Isothermal curves or |E*| versus frequency plot (top-left), isochronal curves or |E*| versus temperature plot (top-right), complex plane plot (bottom-left), and black space plot (bottom-right) for Mix 1 Specimen 1 in English unit system.

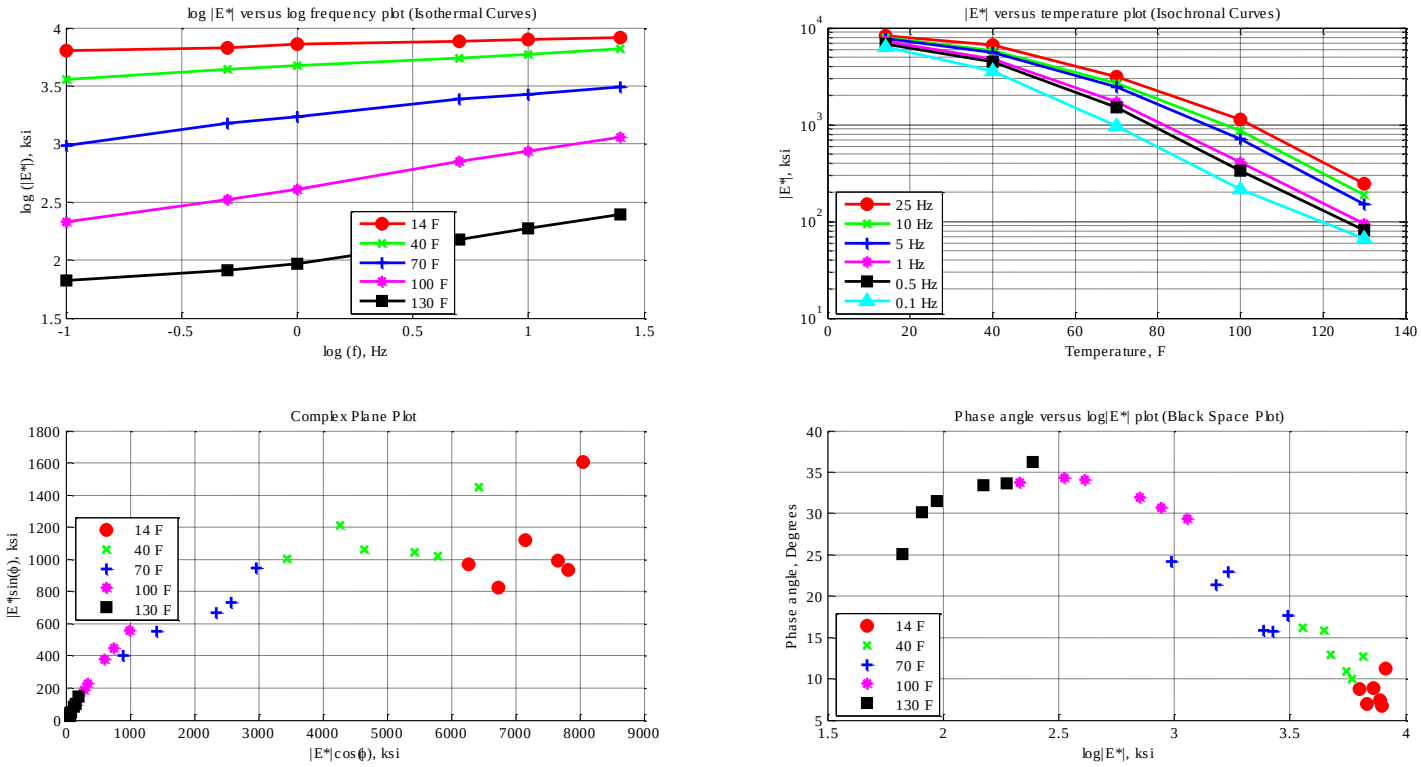

Figure C-2 Isothermal curves or |E*| versus frequency plot (top-left), isochronal curves or |E*| versus temperature plot (top-right), complex plane plot (bottom-left), and black space plot (bottom-right) for Mix 1 Specimen 2 in English unit system.

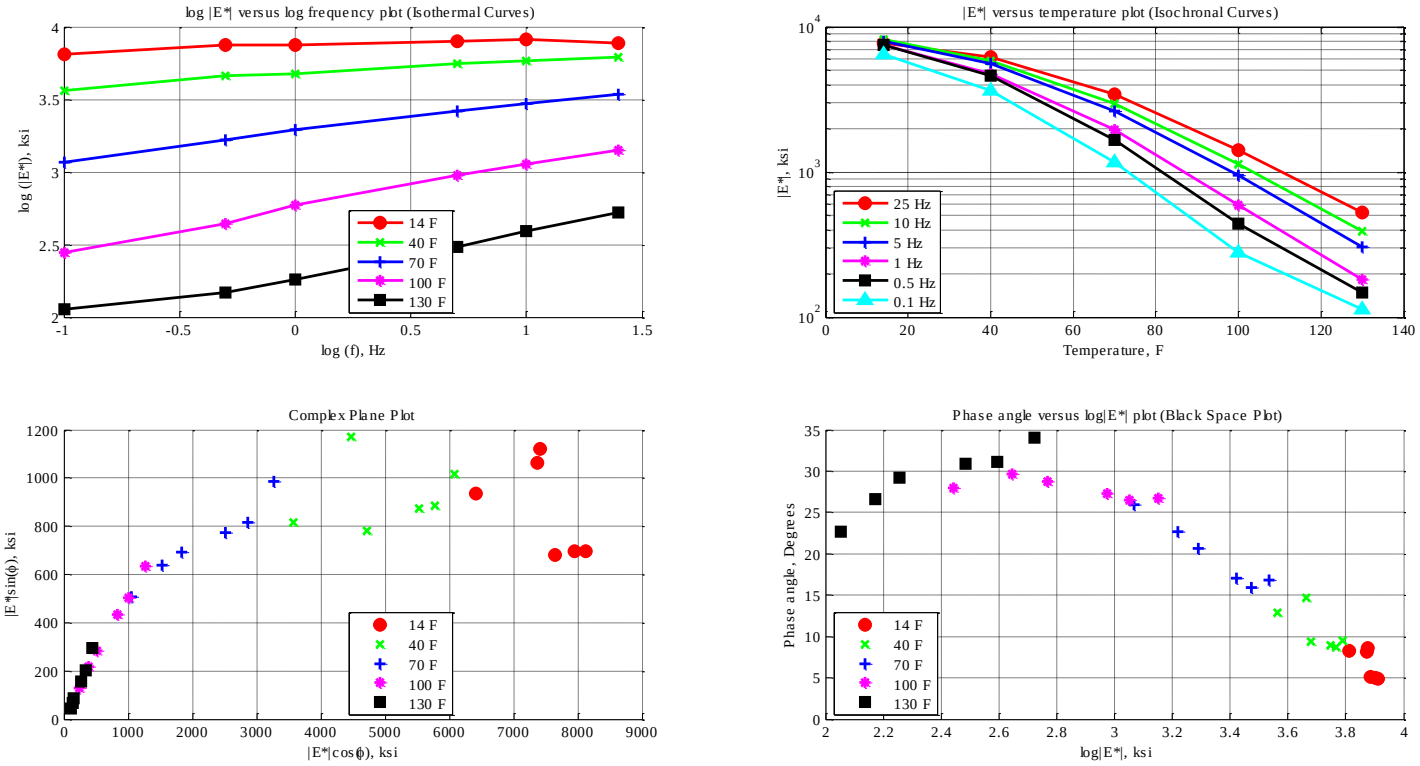

Figure C-3 Isothermal curves or |E*| versus frequency plot (top-left), isochronal curves or |E*| versus temperature plot (top-right), complex plane plot (bottom-left), and black space plot (bottom-right) for Mix 1 Specimen 3 in English unit system.

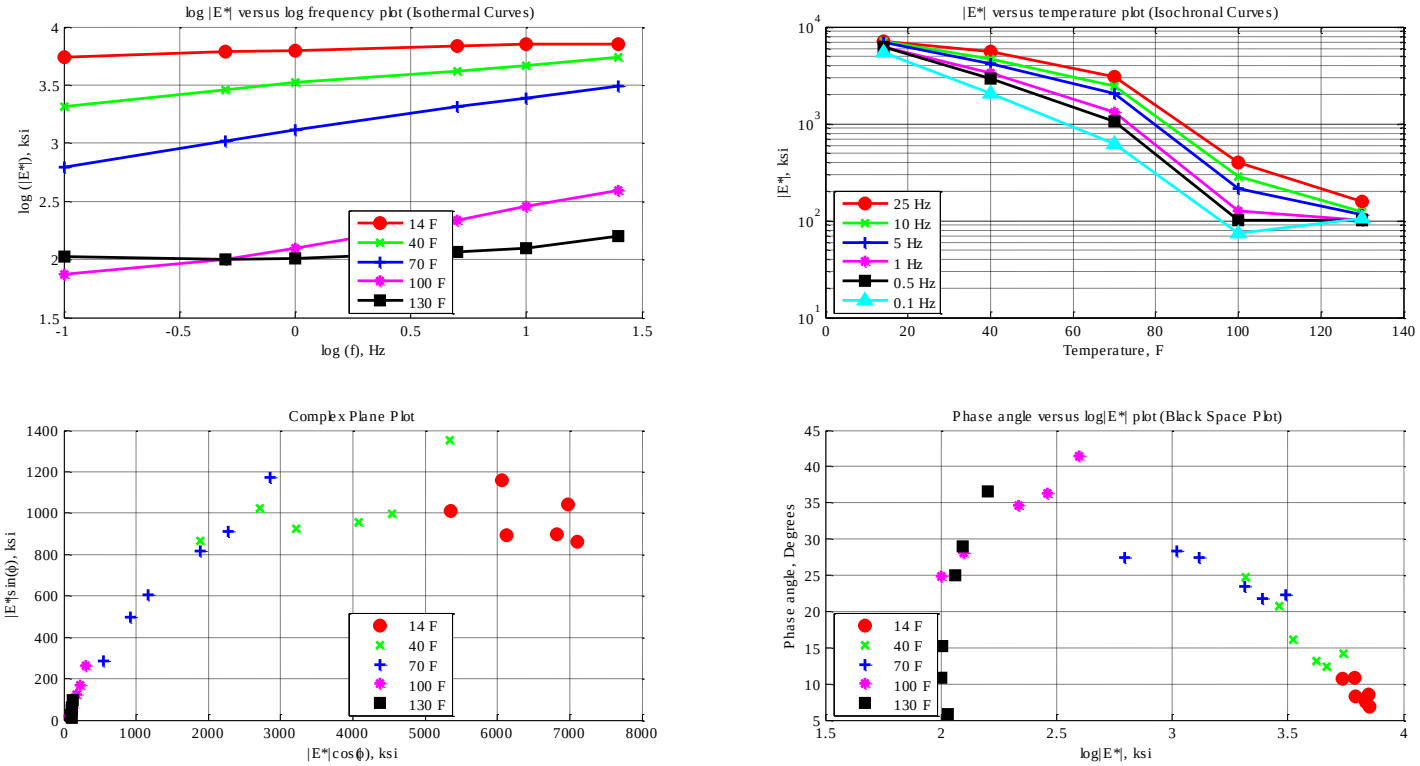

Figure C-4 Isothermal curves or |E*| versus frequency plot (top-left), isochronal curves or |E*| versus temperature plot (top-right), complex plane plot (bottom-left), and black space plot (bottom-right) for Mix 2 Specimen 1 in English unit system.

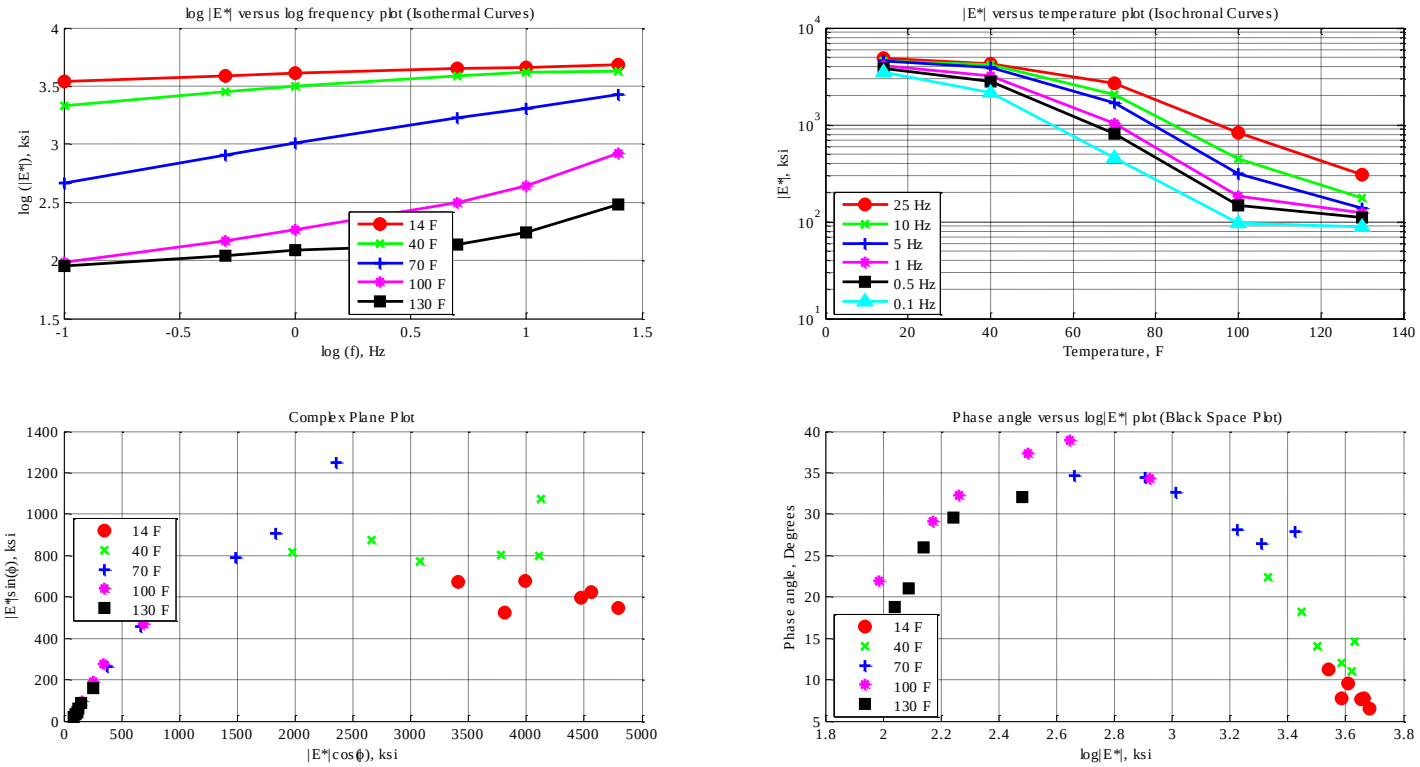

Figure C-5 Isothermal curves or |E*| versus frequency plot (top-left), isochronal curves or |E*| versus temperature plot (top-right), complex plane plot (bottom-left), and black space plot (bottom-right) for Mix 2 Specimen 2 in English unit system.

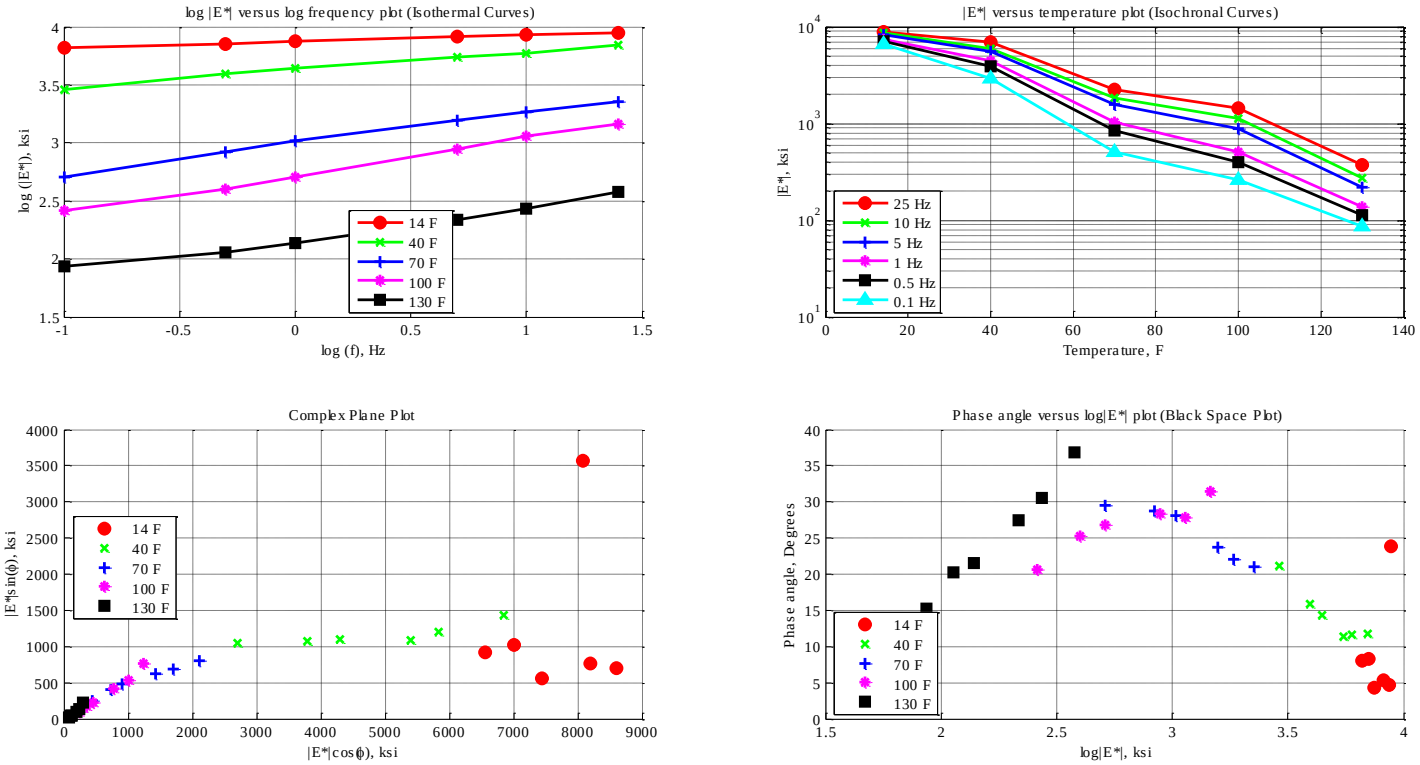

Figure C-6 Isothermal curves or |E*| versus frequency plot (top-left), isochronal curves or |E*| versus temperature plot (top-right), complex plane plot (bottom-left), and black space plot (bottom-right) for Mix 2 Specimen 3 in English unit system.

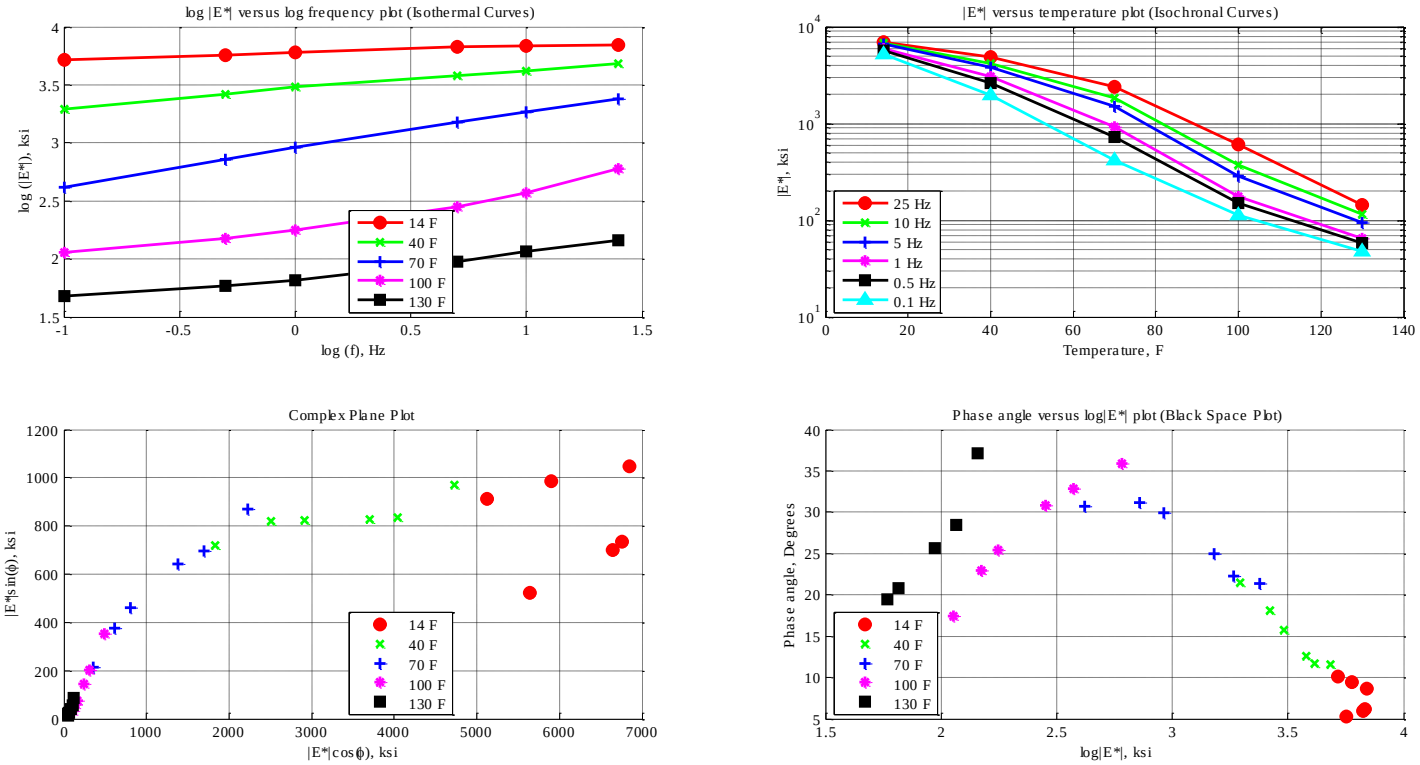

Figure C-7 Isothermal curves or |E*| versus frequency plot (top-left), isochronal curves or |E*| versus temperature plot (top-right), complex plane plot (bottom-left), and black space plot (bottom-right) for Mix 2 Specimen 4 in English unit system.

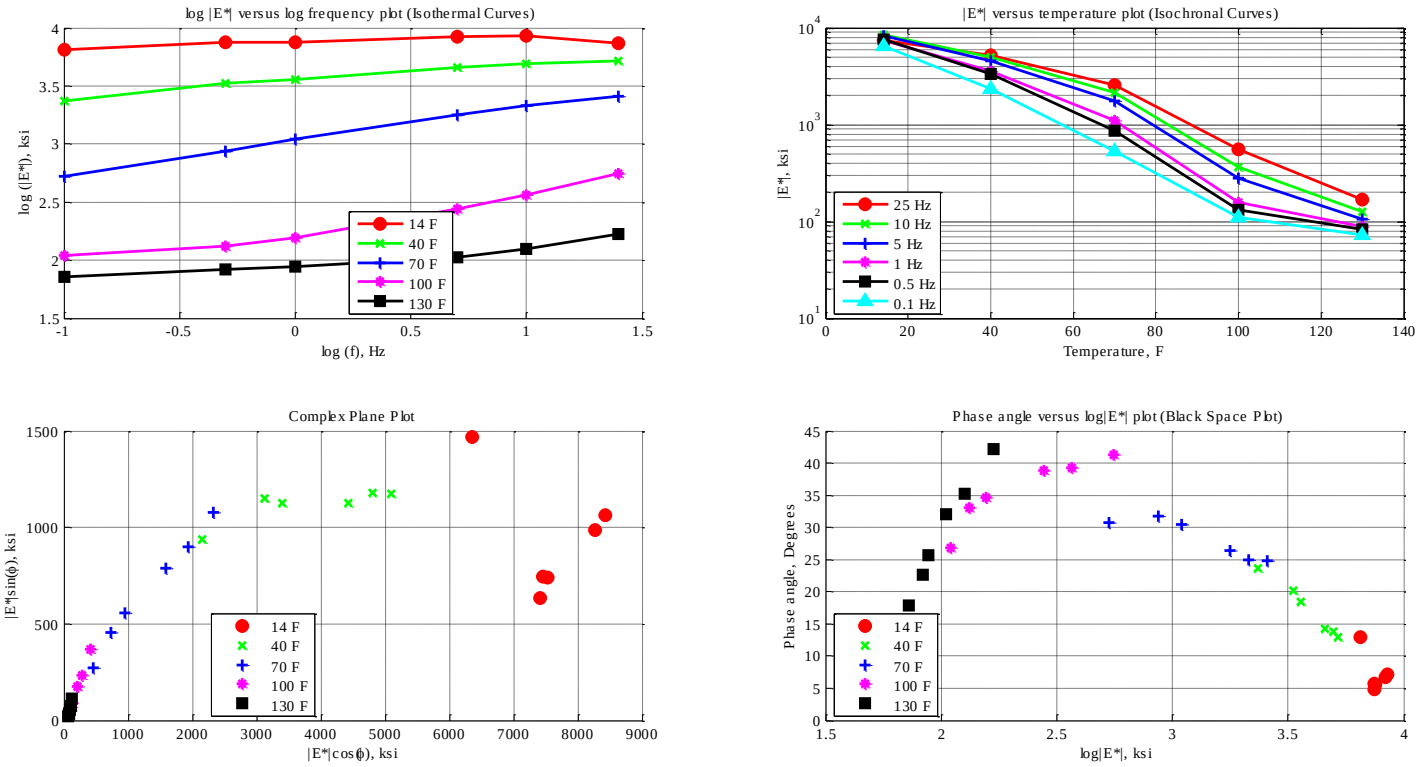

Figure C-8 Isothermal curves or |E*| versus frequency plot (top-left), isochronal curves or |E*| versus temperature plot (top-right), complex plane plot (bottom-left), and black space plot (bottom-right) for Mix 2 Specimen 5 in English unit system.

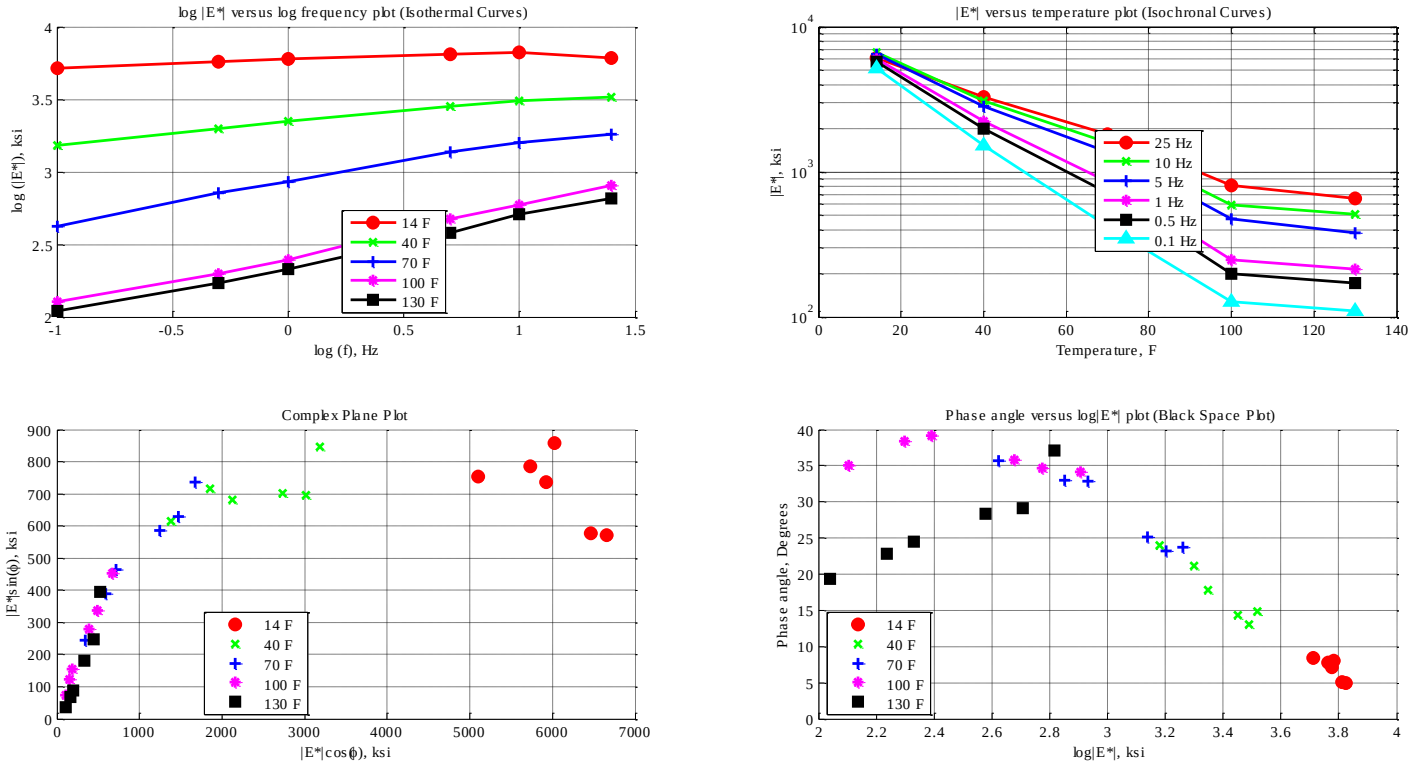

Figure C-9 Isothermal curves or |E*| versus frequency plot (top-left), isochronal curves or |E*| versus temperature plot (top-right), complex plane plot (bottom-left), and black space plot (bottom-right) for Mix 3 Specimen 1 in English unit system.

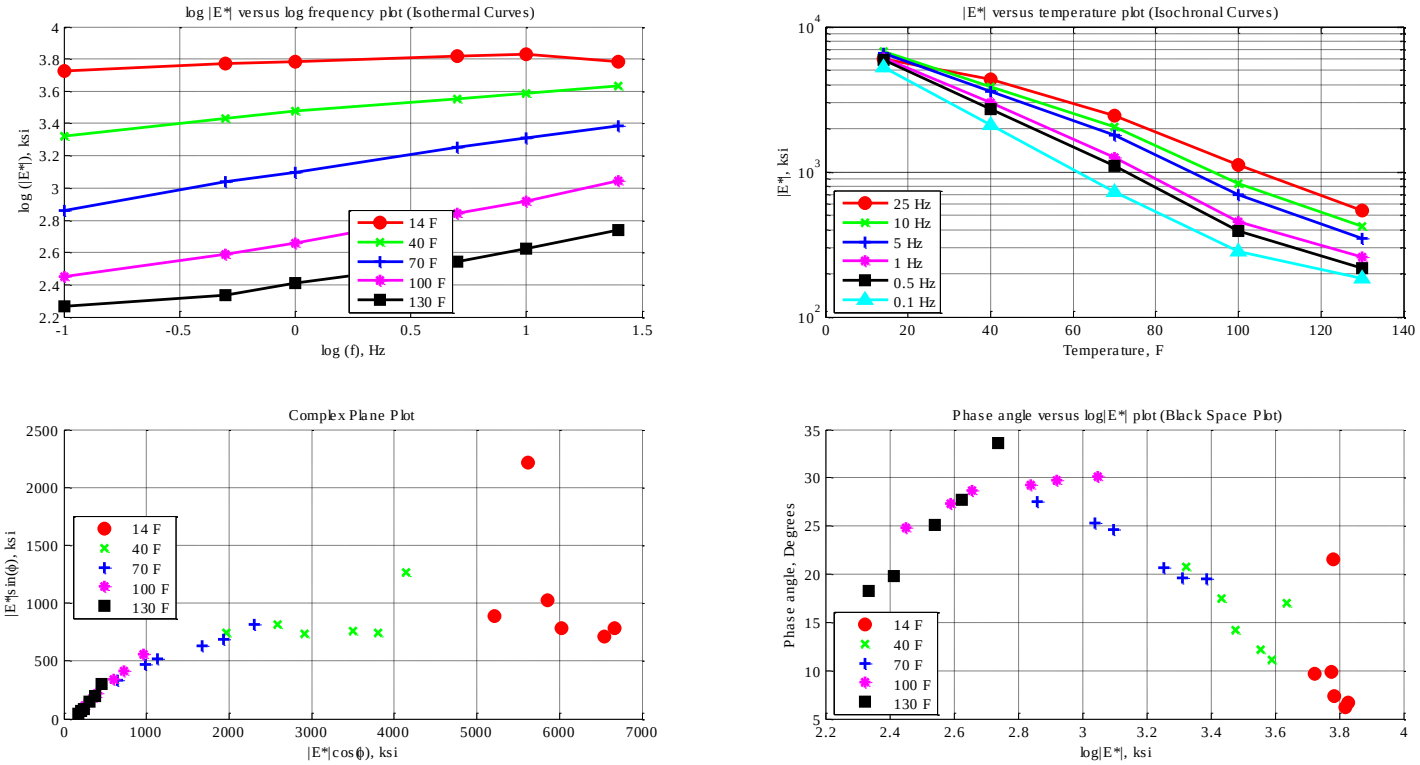

Figure C-10 Isothermal curves or |E*| versus frequency plot (top-left), isochronal curves or |E*| versus temperature plot (top-right), complex plane plot (bottom-left), and black space plot (bottom-right) for Mix 3 Specimen 2 in English unit system.

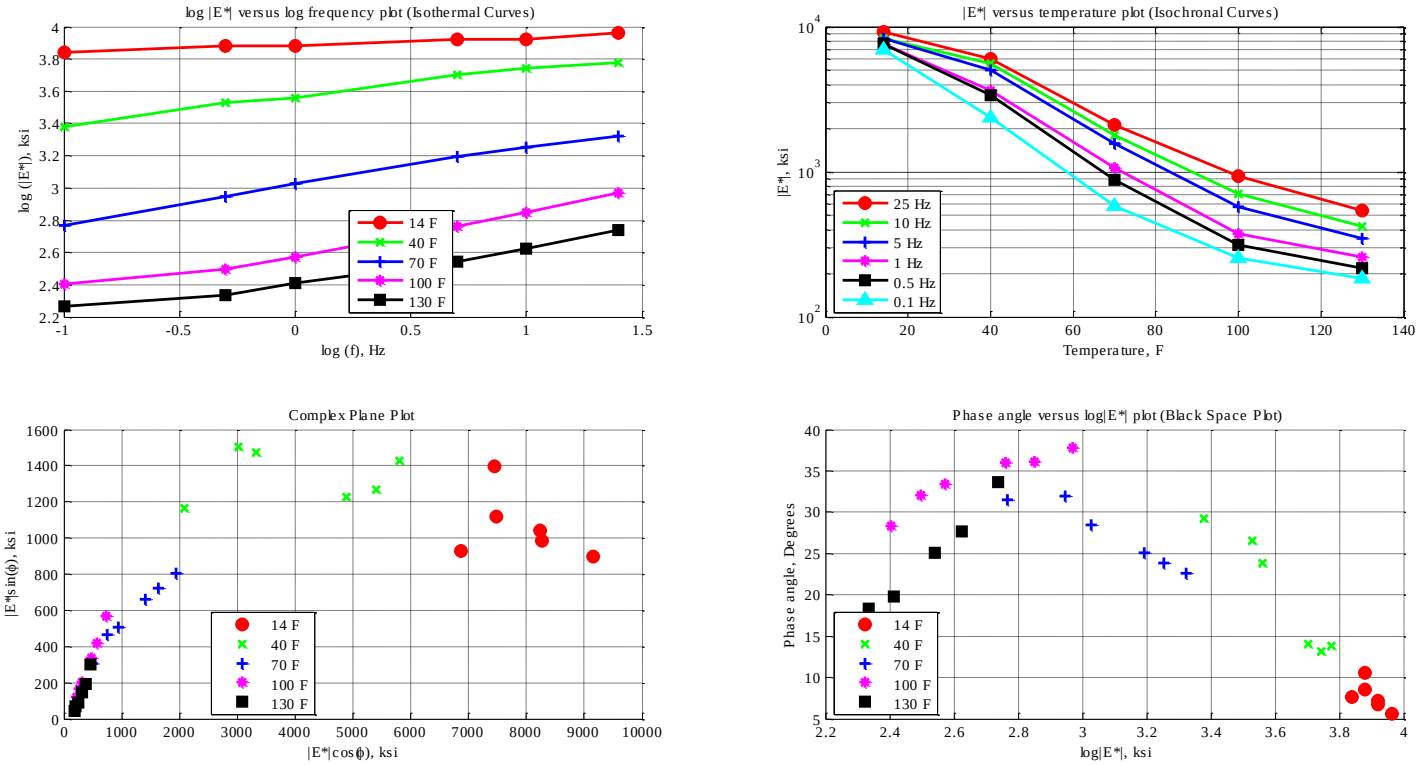

Figure C-11 Isothermal curves or |E*| versus frequency plot (top-left), isochronal curves or |E*| versus temperature plot (top-right), complex plane plot (bottom-left), and black space plot (bottom-right) for Mix 3 Specimen 3 in English unit system.

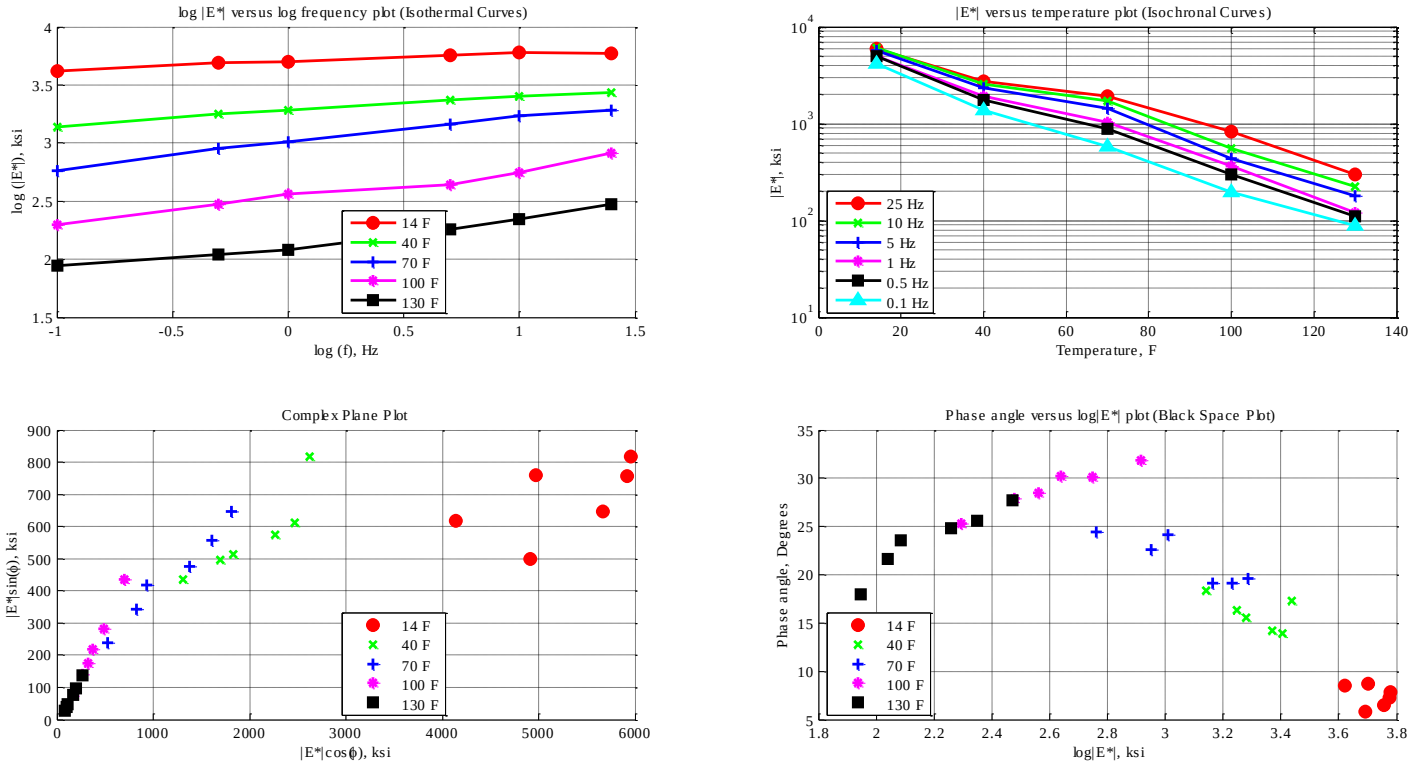

Figure C-12 Isothermal curves or |E*| versus frequency plot (top-left), isochronal curves or |E*| versus temperature plot (top-right), complex plane plot (bottom-left), and black space plot (bottom-right) for Mix 4 Specimen 1 in English unit system.

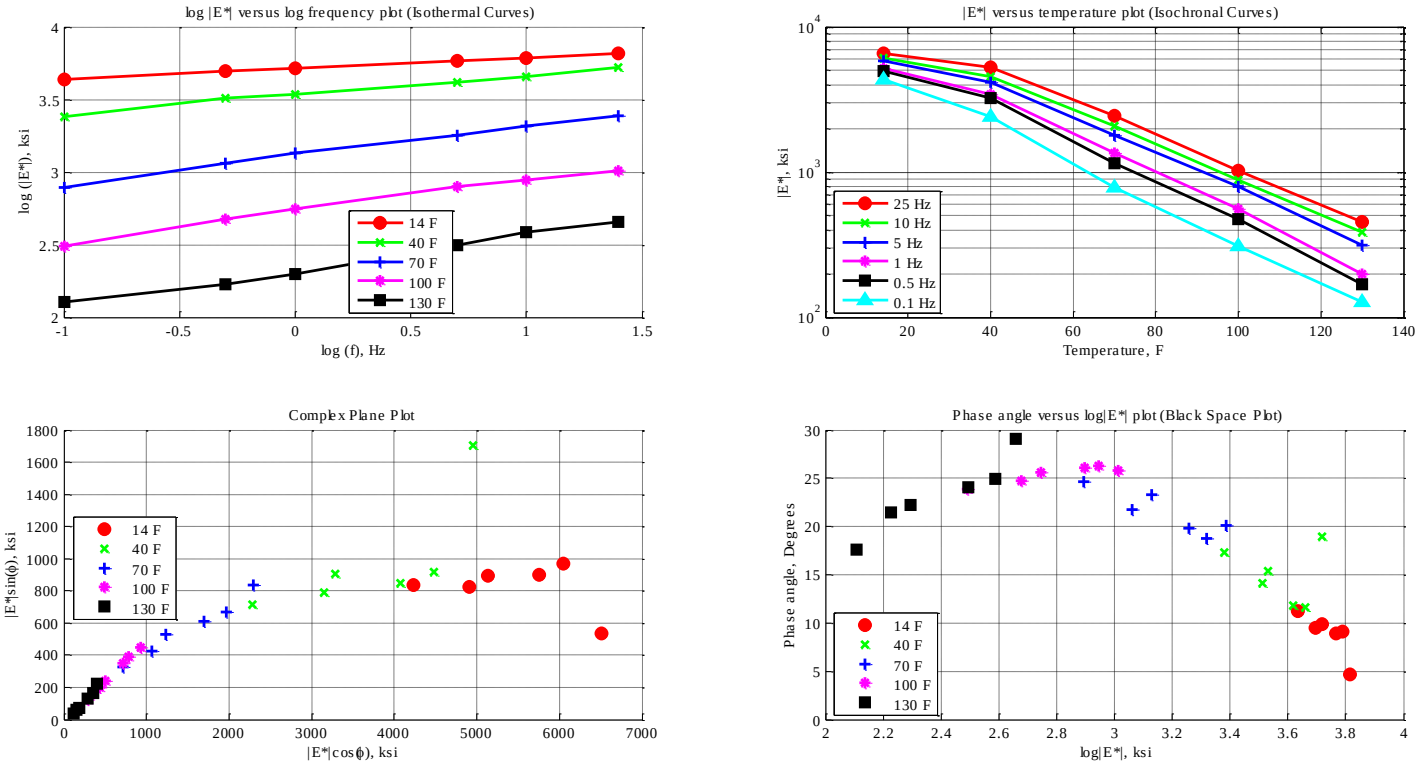

Figure C-13 Isothermal curves or |E*| versus frequency plot (top-left), isochronal curves or |E*| versus temperature plot (top-right), complex plane plot (bottom-left), and black space plot (bottom-right) for Mix 4 Specimen 2 in English unit system.

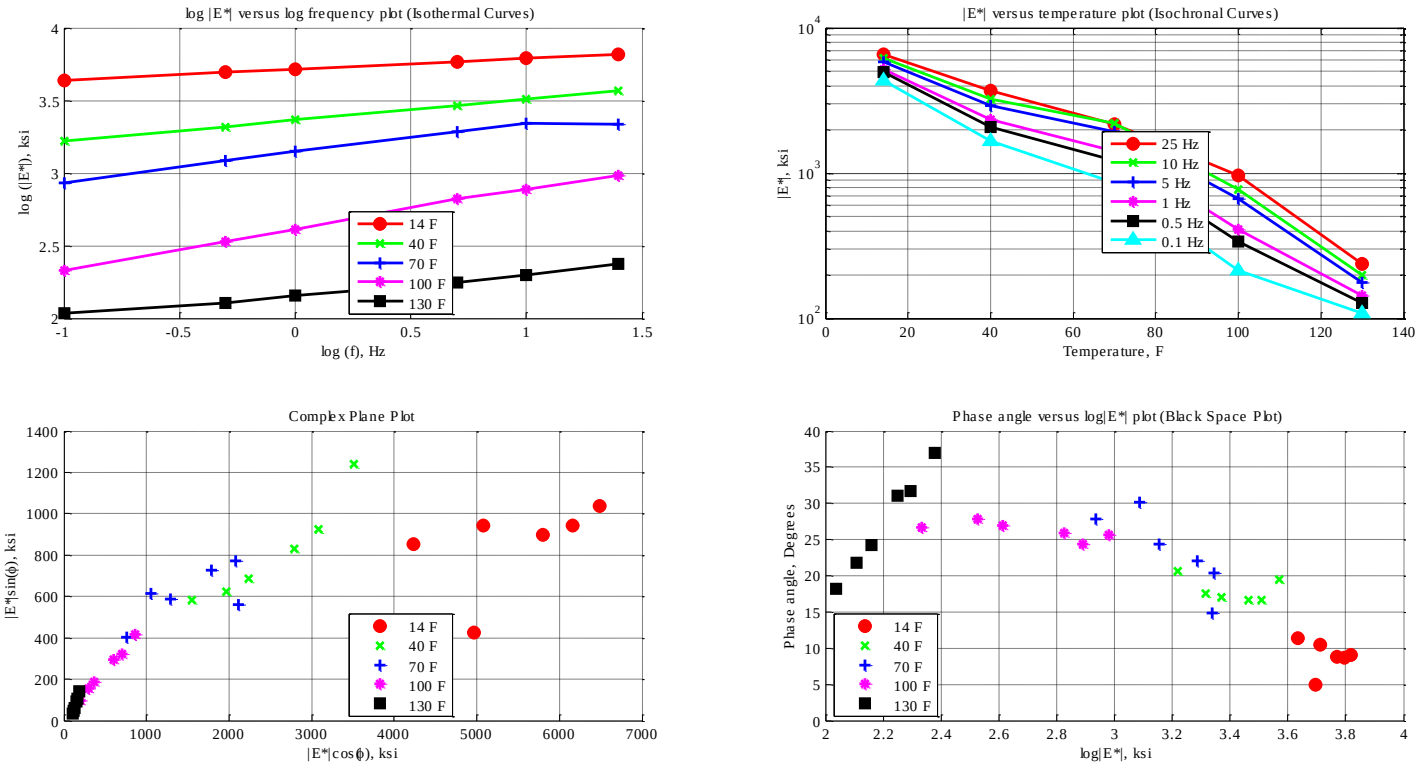

Figure C-14 Isothermal curves or |E*| versus frequency plot (top-left), isochronal curves or |E*| versus temperature plot (top-right), complex plane plot (bottom-left), and black space plot (bottom-right) for Mix 4 Specimen 3 in English unit system.

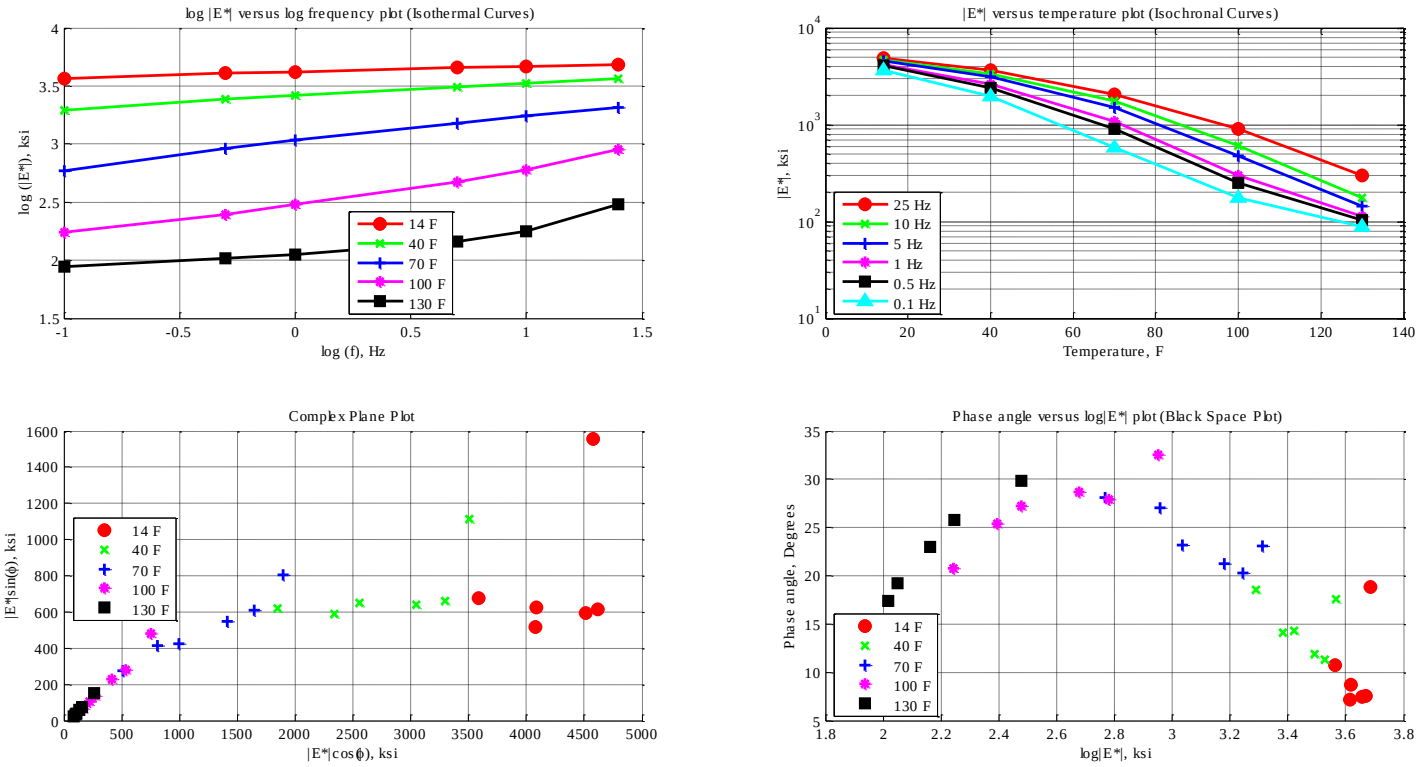

Figure C-15 Isothermal curves or |E*| versus frequency plot (top-left), isochronal curves or |E*| versus temperature plot (top-right), complex plane plot (bottom-left), and black space plot (bottom-right) for Mix 5 Specimen 1 in English unit system.

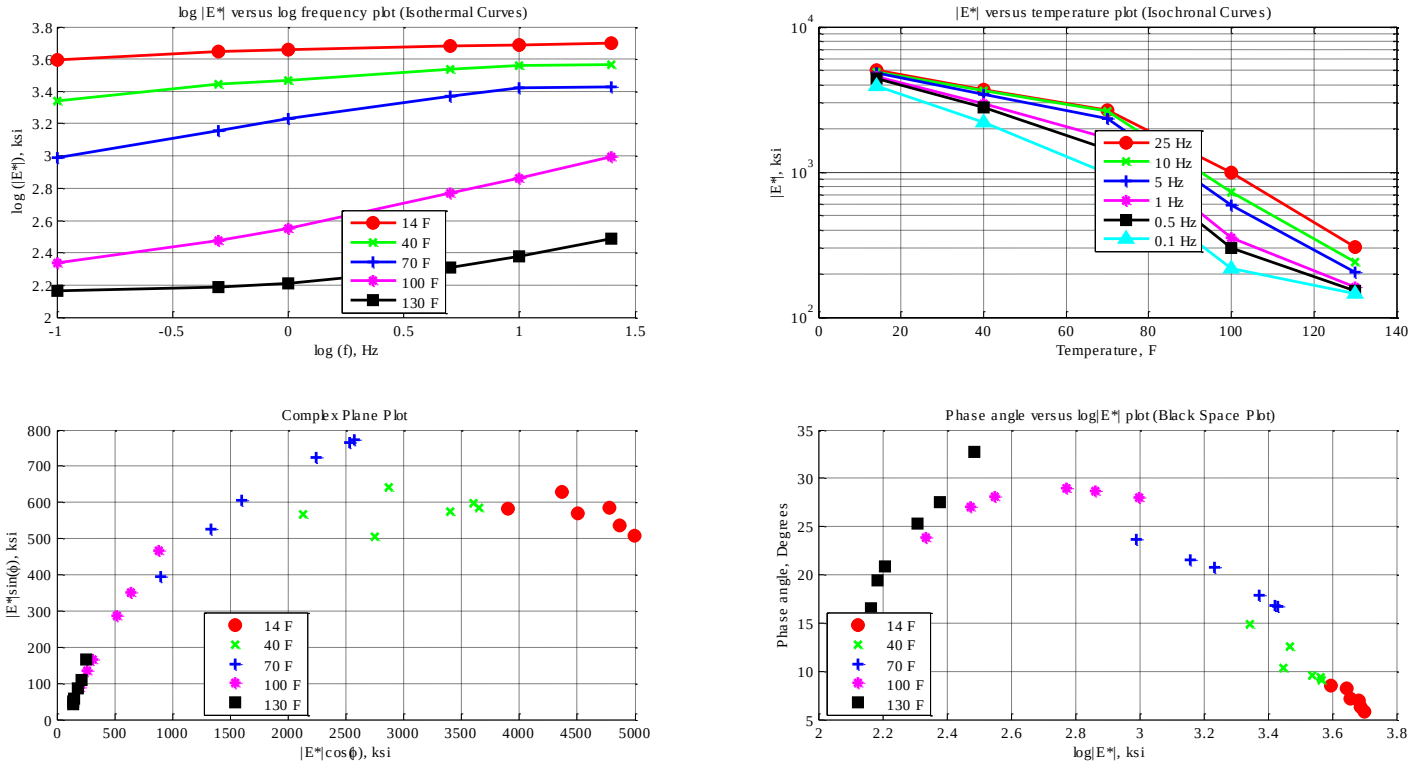

Figure C-16 Isothermal curves or |E*| versus frequency plot (top-left), isochronal curves or |E*| versus temperature plot (top-right), complex plane plot (bottom-left), and black space plot (bottom-right) for Mix 5 Specimen 2 in English unit system.

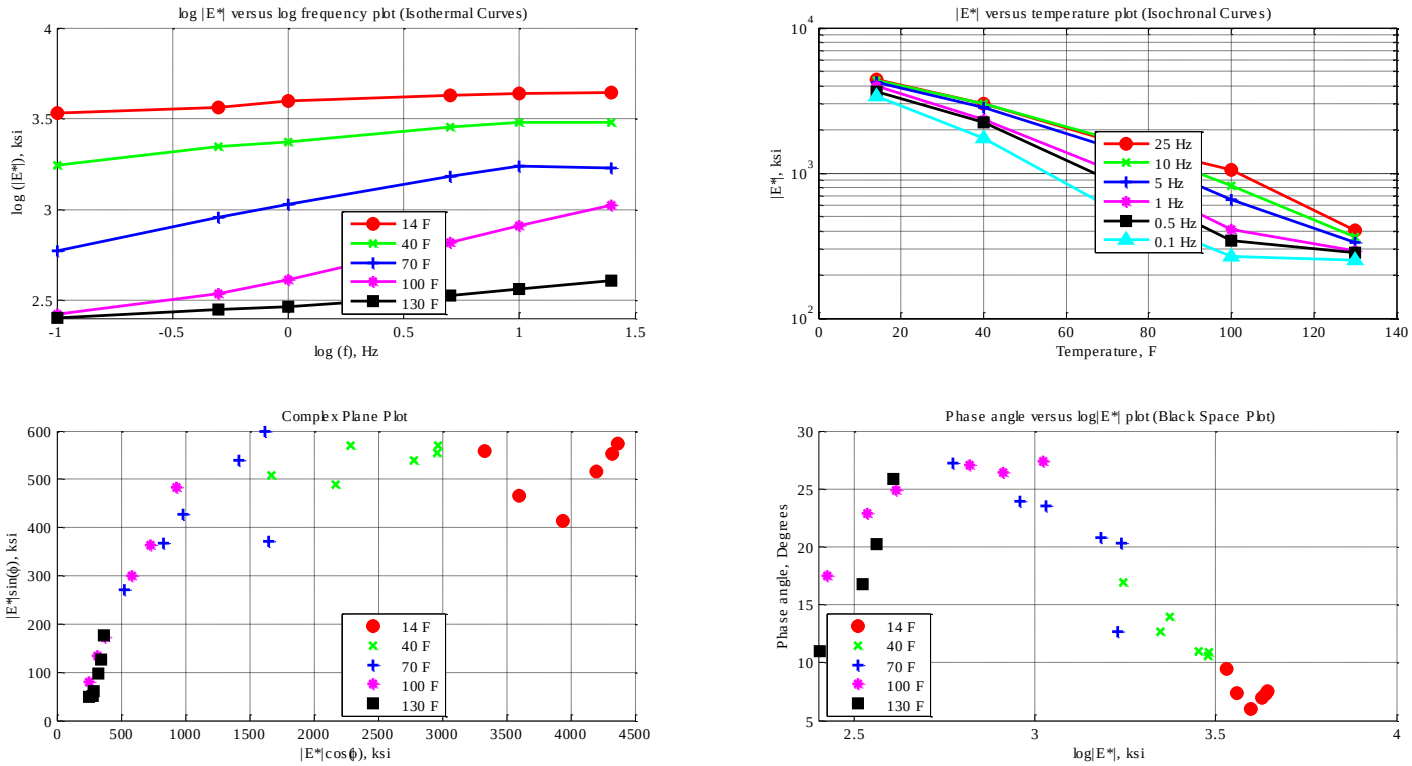

Figure C-17 Isothermal curves or |E*| versus frequency plot (top-left), isochronal curves or |E*| versus temperature plot (top-right), complex plane plot (bottom-left), and black space plot (bottom-right) for Mix 5 Specimen 3 in English unit system.

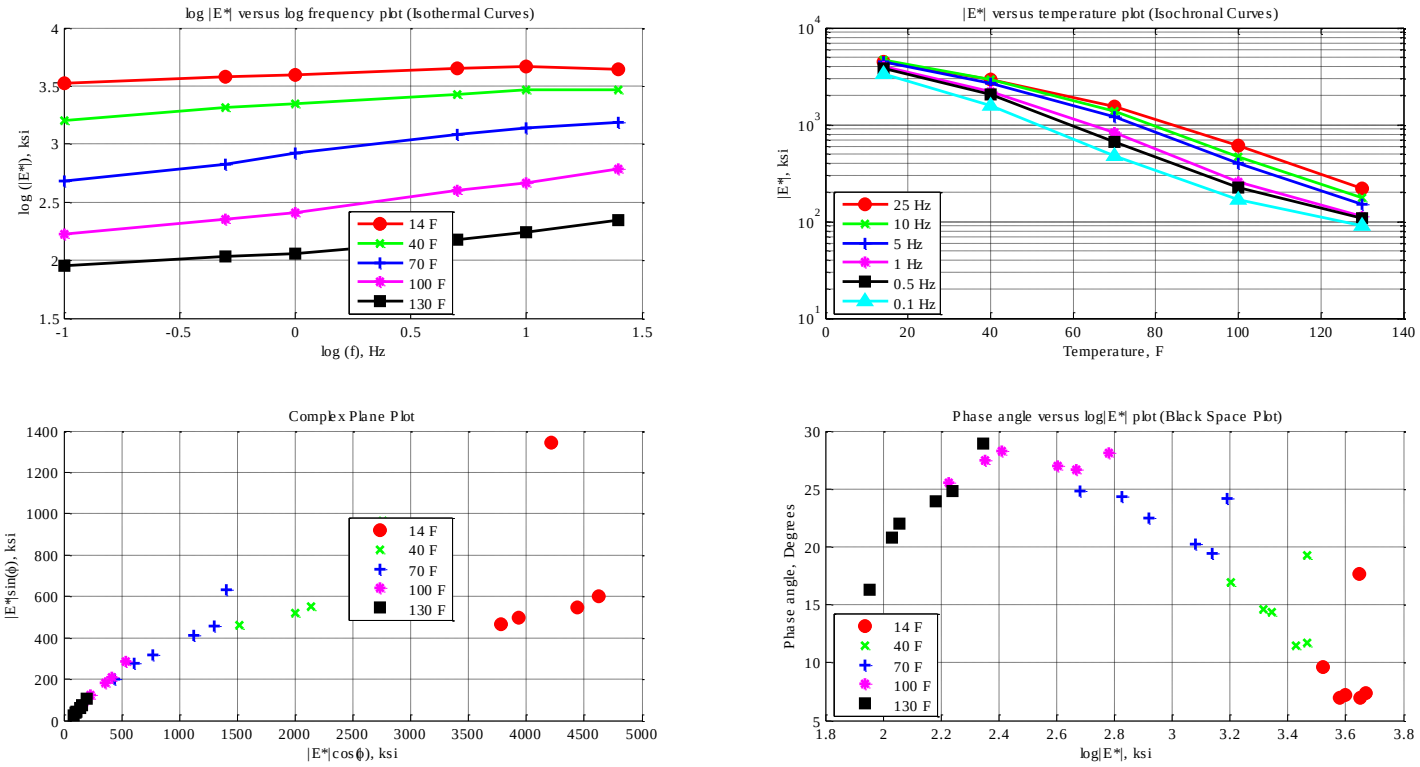

Figure C-18 Isothermal curves or |E*| versus frequency plot (top-left), isochronal curves or |E*| versus temperature plot (top-right), complex plane plot (bottom-left), and black space plot (bottom-right) for Mix 6 Specimen 2 in English unit system.

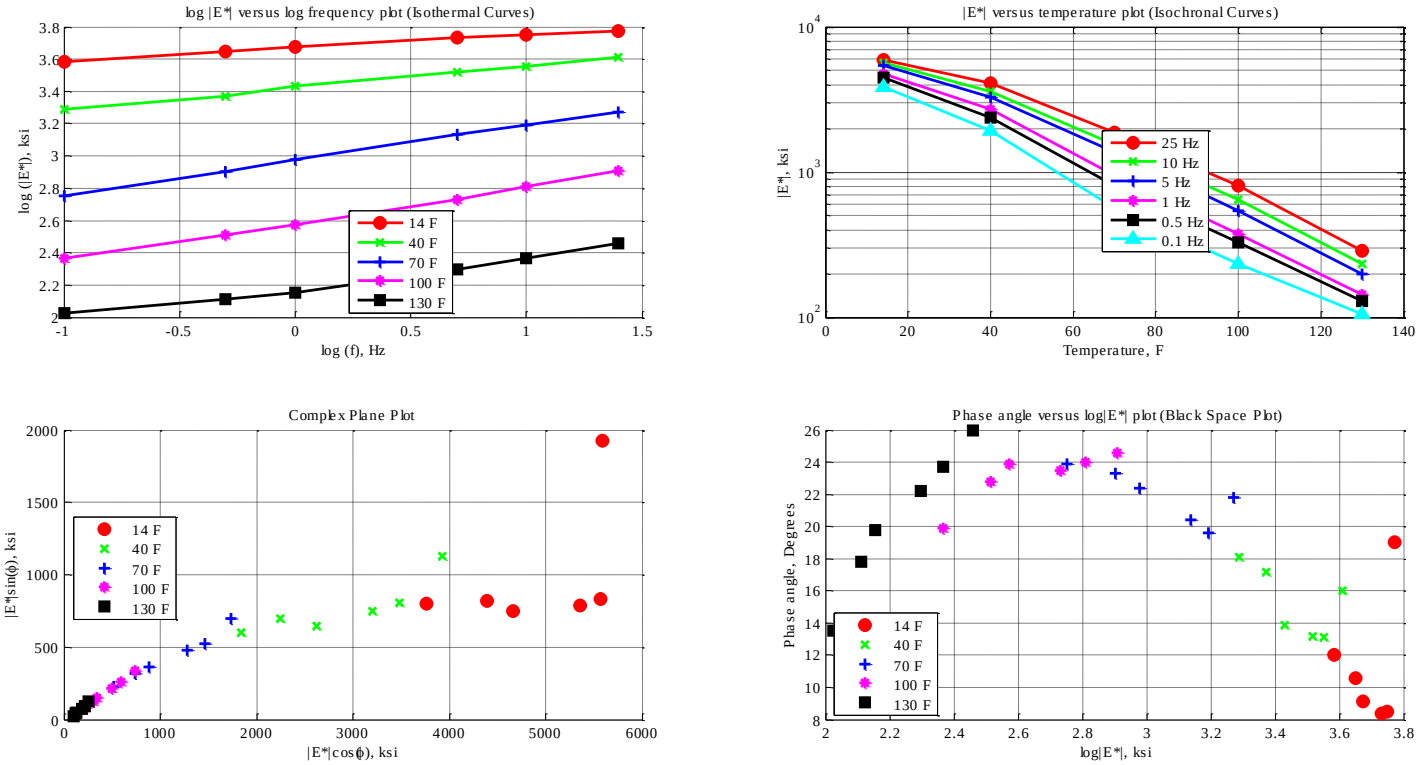

Figure C-19 Isothermal curves or |E*| versus frequency plot (top-left), isochronal curves or |E*| versus temperature plot (top-right), complex plane plot (bottom-left), and black space plot (bottom-right) for Mix 6 Specimen 3 in English unit system.

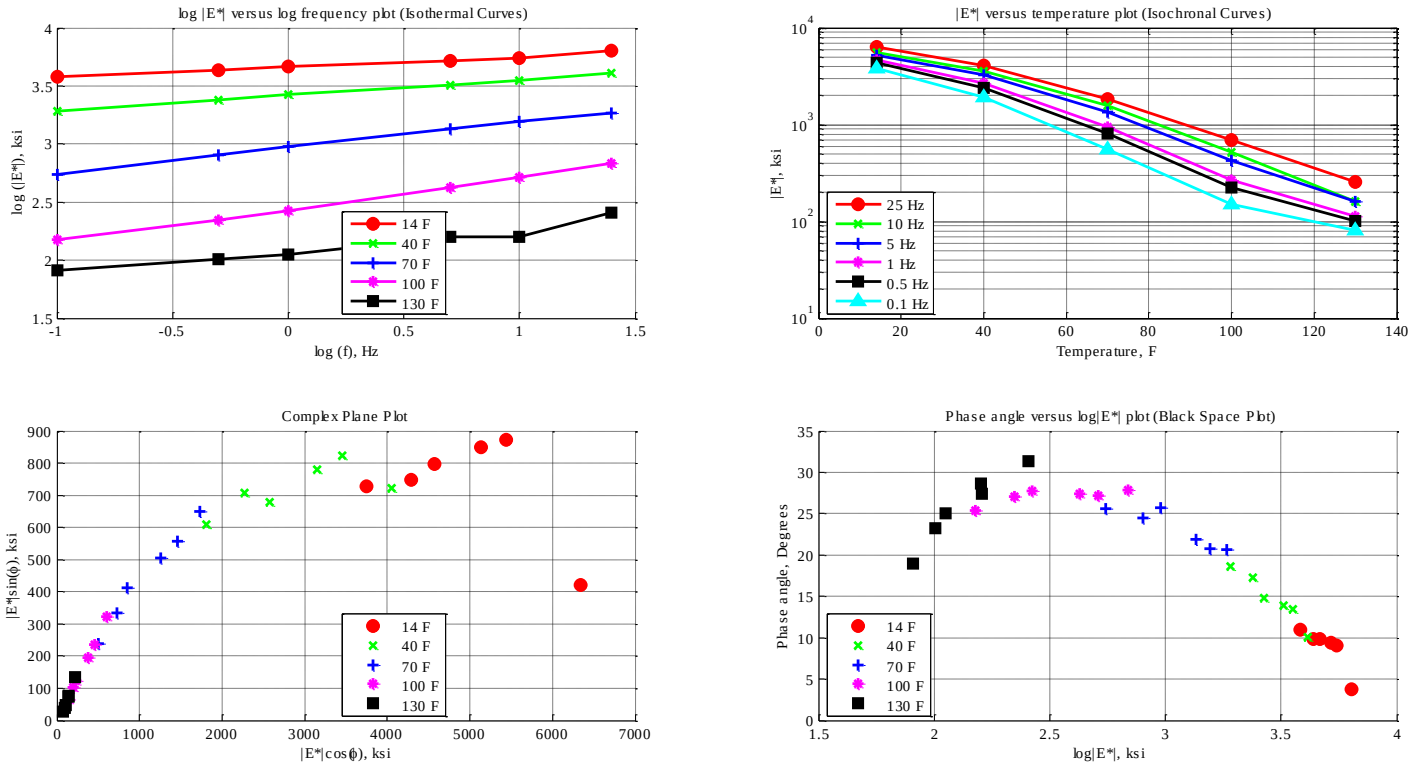

Figure C-20 Isothermal curves or |E*| versus frequency plot (top-left), isochronal curves or |E*| versus temperature plot (top-right), complex plane plot (bottom-left), and black space plot (bottom-right) for Mix 6 Specimen 4 in English unit system.

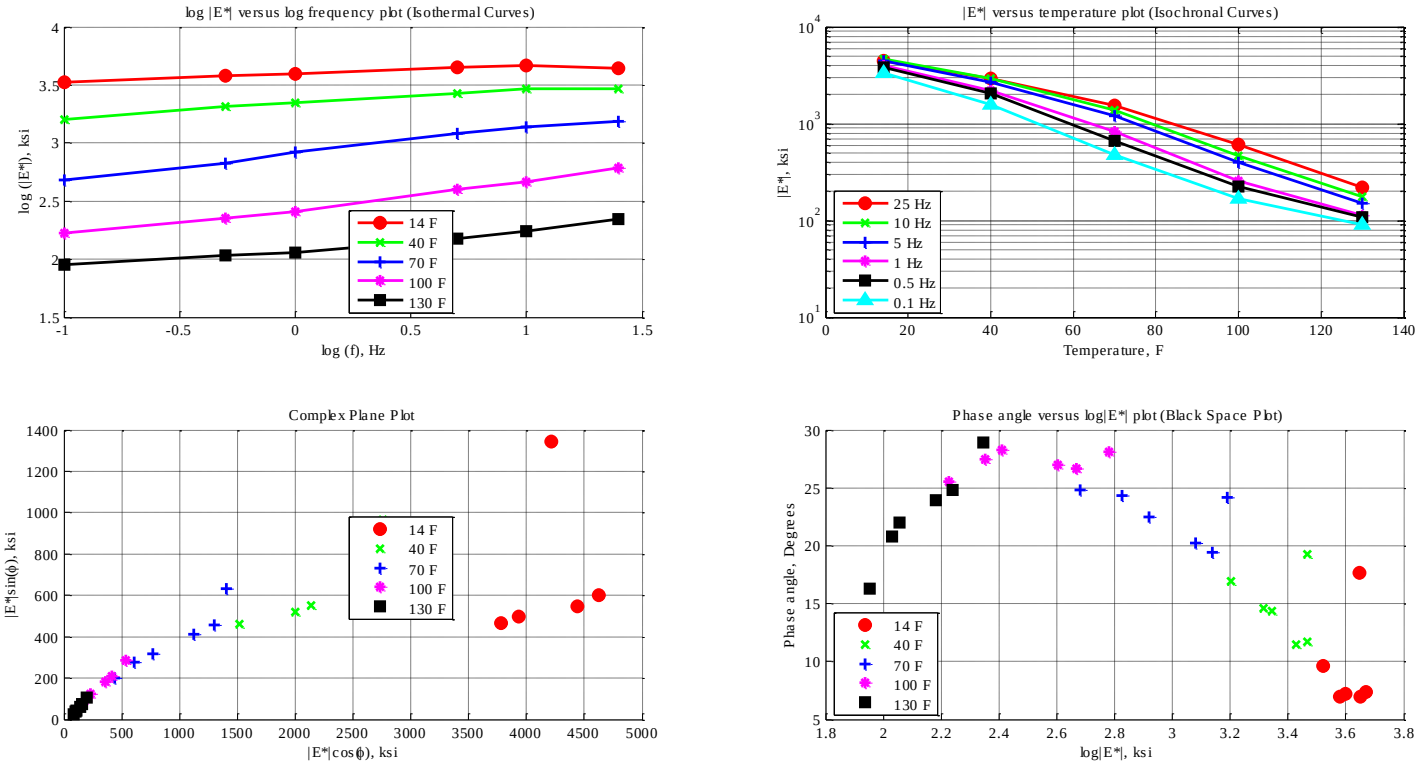

Figure C-21 Isothermal curves or |E*| versus frequency plot (top-left), isochronal curves or |E*| versus temperature plot (top-right), complex plane plot (bottom-left), and black space plot (bottom-right) for Mix 7 Specimen 2 in English unit system.

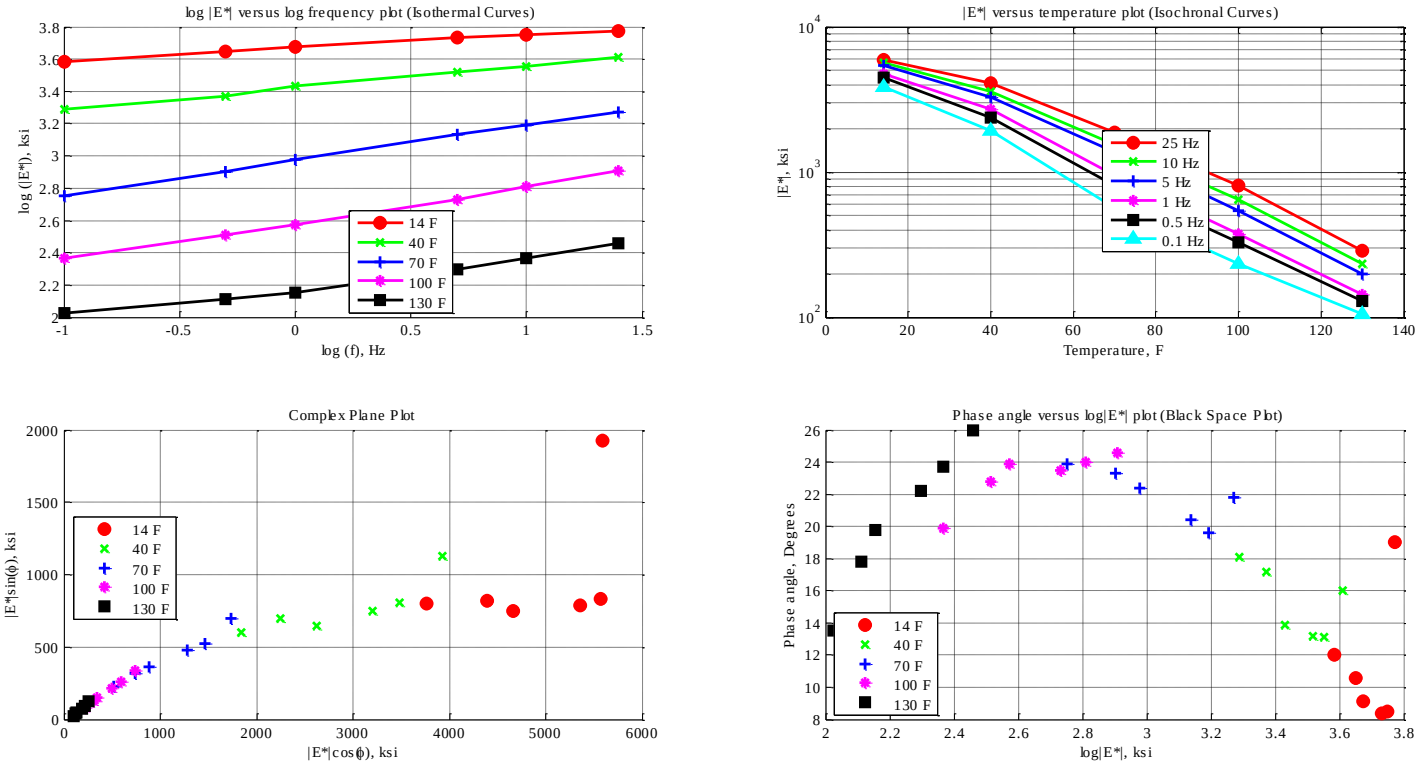

Figure C-22 Isothermal curves or |E*| versus frequency plot (top-left), isochronal curves or |E*| versus temperature plot (top-right), complex plane plot (bottom-left), and black space plot (bottom-right) for Mix 7 Specimen 3 in English unit system.

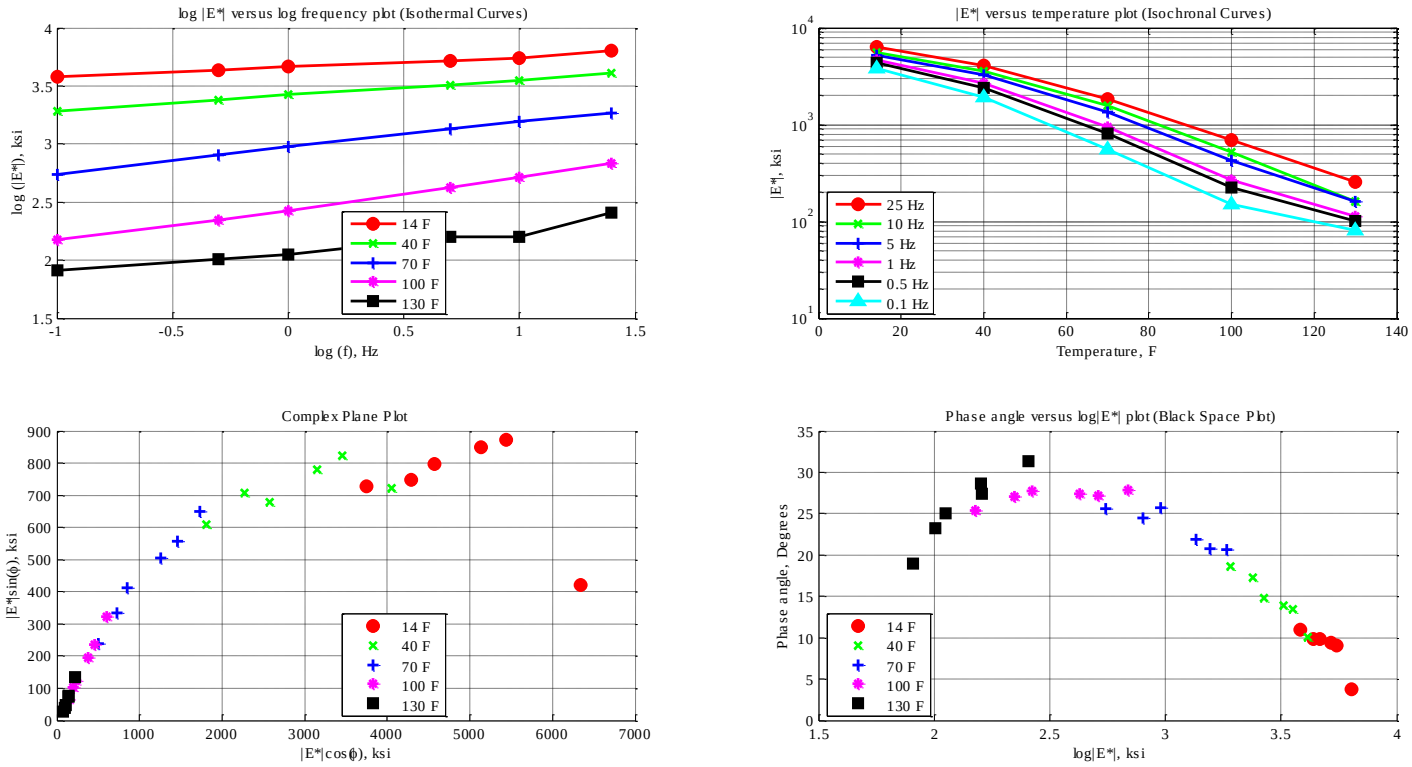

Figure C-23 Isothermal curves or |E*| versus frequency plot (top-left), isochronal curves or |E*| versus temperature plot (top-right), complex plane plot (bottom-left), and black space plot (bottom-right) for Mix 7 Specimen 4 in English unit system.

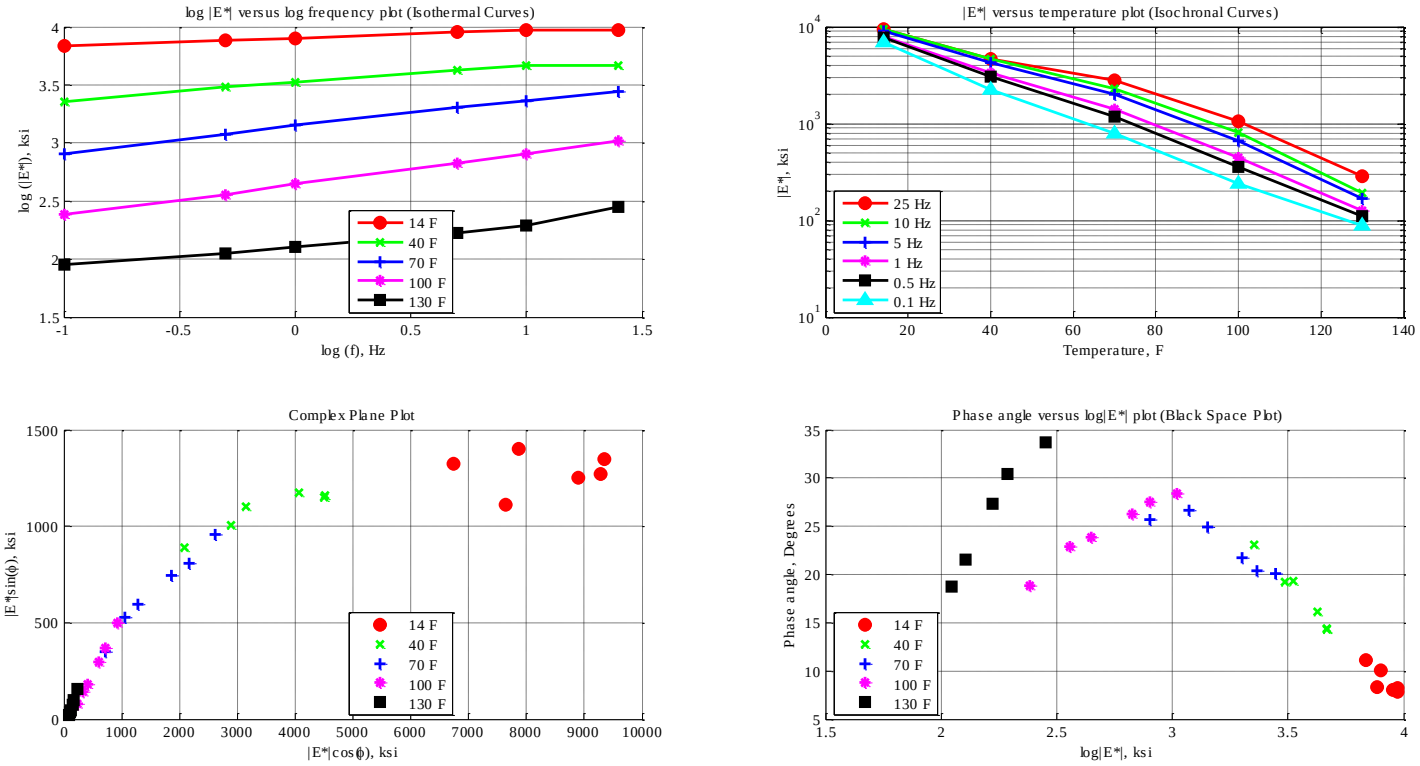

Figure C-24 Isothermal curves or |E*| versus frequency plot (top-left), isochronal curves or |E*| versus temperature plot (top-right), complex plane plot (bottom-left), and black space plot (bottom-right) for Mix 8 Specimen 4 in English unit system.

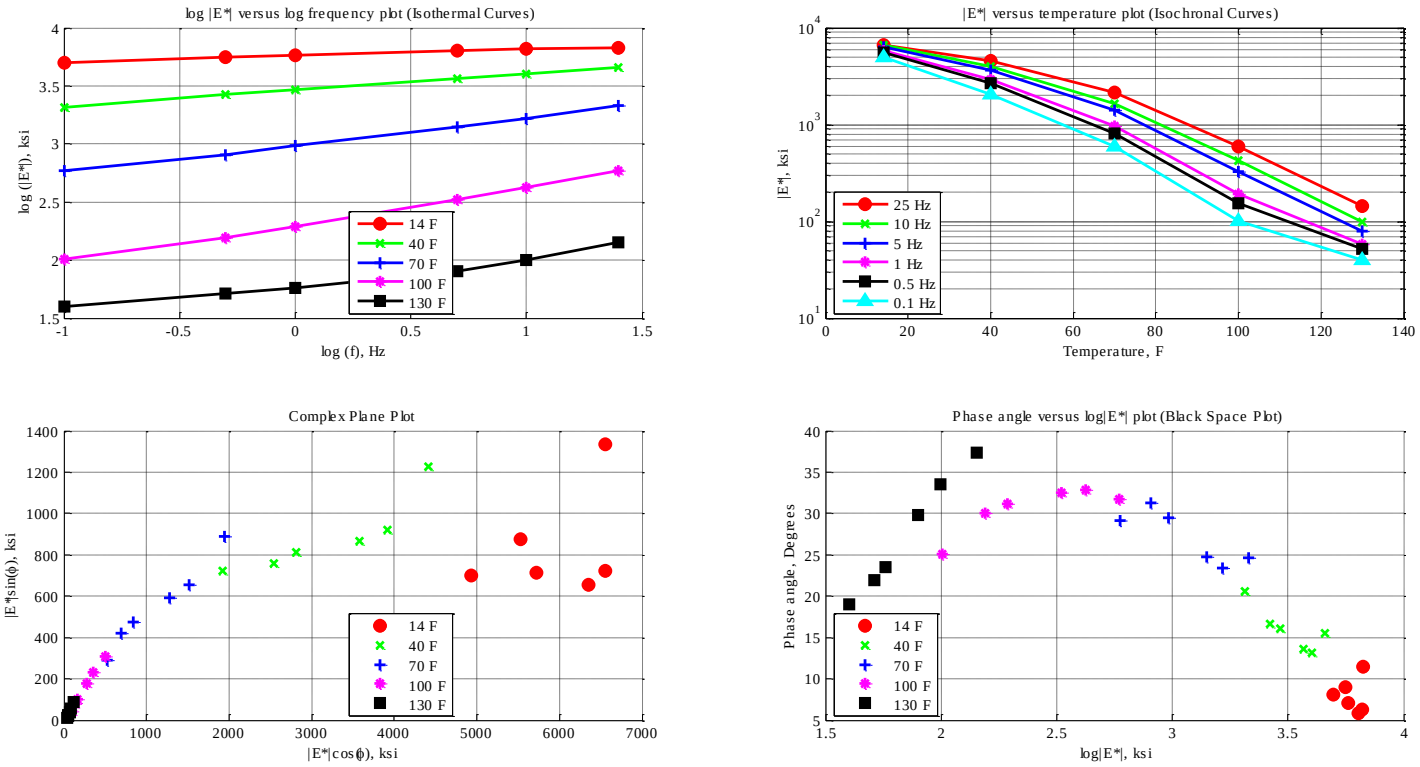

Figure C-25 Isothermal curves or |E*| versus frequency plot (top-left), isochronal curves or |E*| versus temperature plot (top-right), complex plane plot (bottom-left), and black space plot (bottom-right) for Mix 8 Specimen 5 in English unit system.

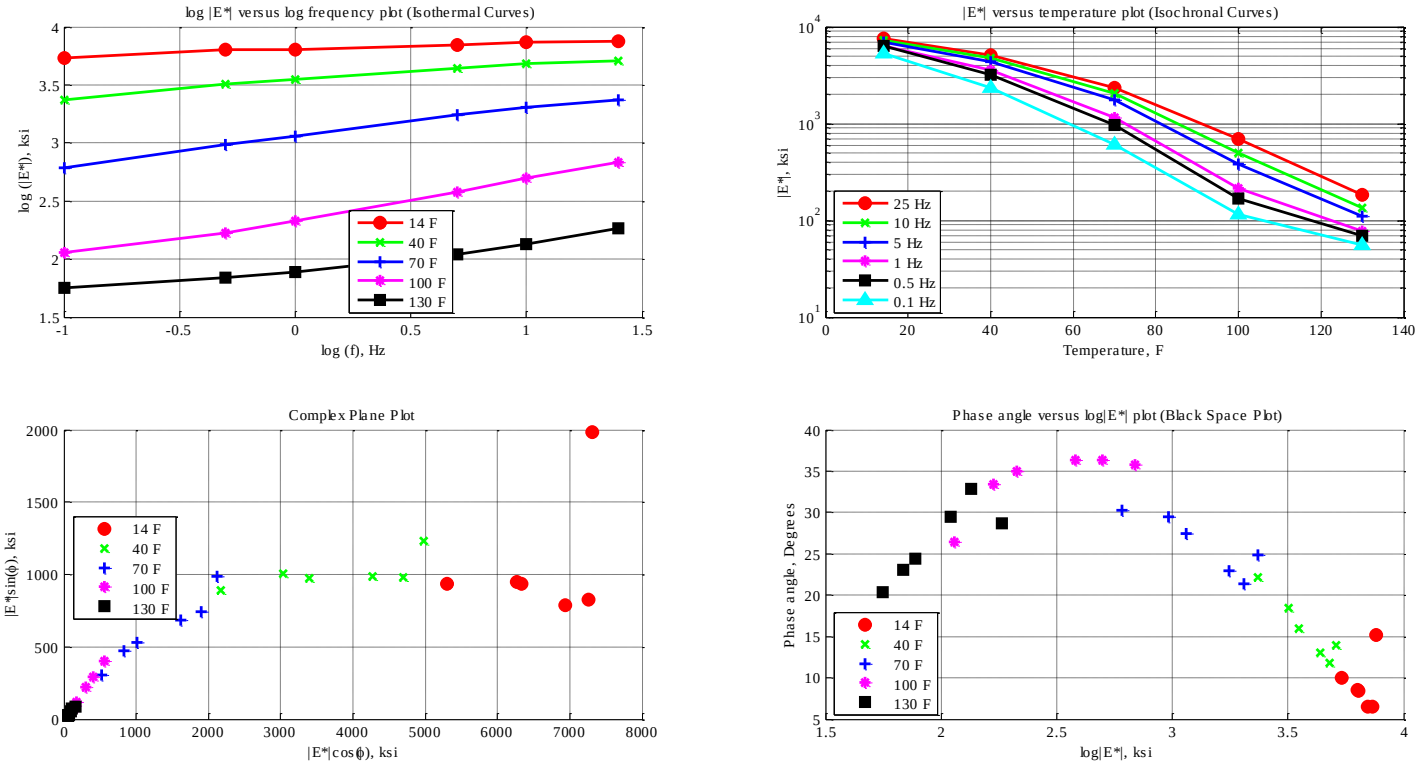

Figure C-26 Isothermal curves or |E*| versus frequency plot (top-left), isochronal curves or |E*| versus temperature plot (top-right), complex plane plot (bottom-left), and black space plot (bottom-right) for Mix 8 Specimen 7 in English unit system.

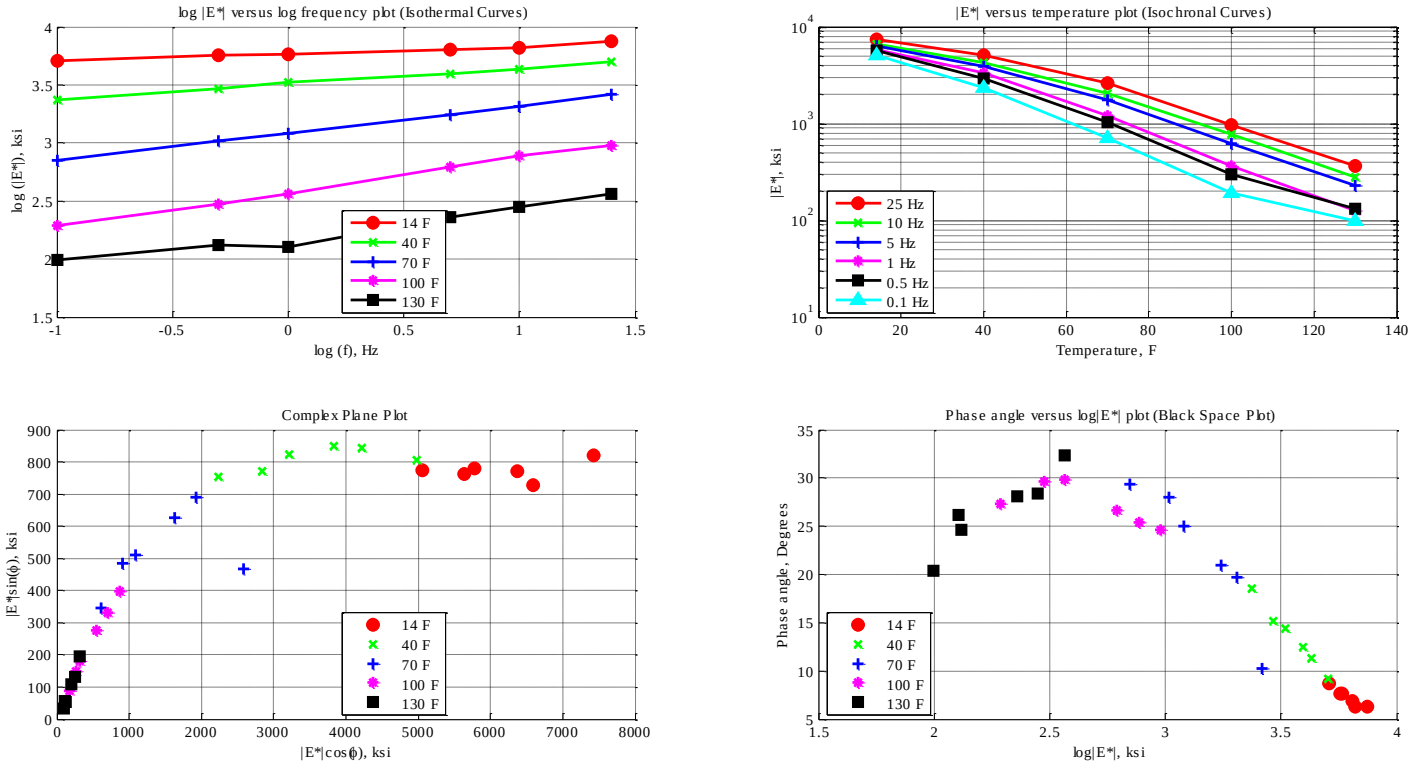

Figure C-27 Isothermal curves or |E*| versus frequency plot (top-left), isochronal curves or |E*| versus temperature plot (top-right), complex plane plot (bottom-left), and black space plot (bottom-right) for Mix 9 Specimen 4 in English unit system.

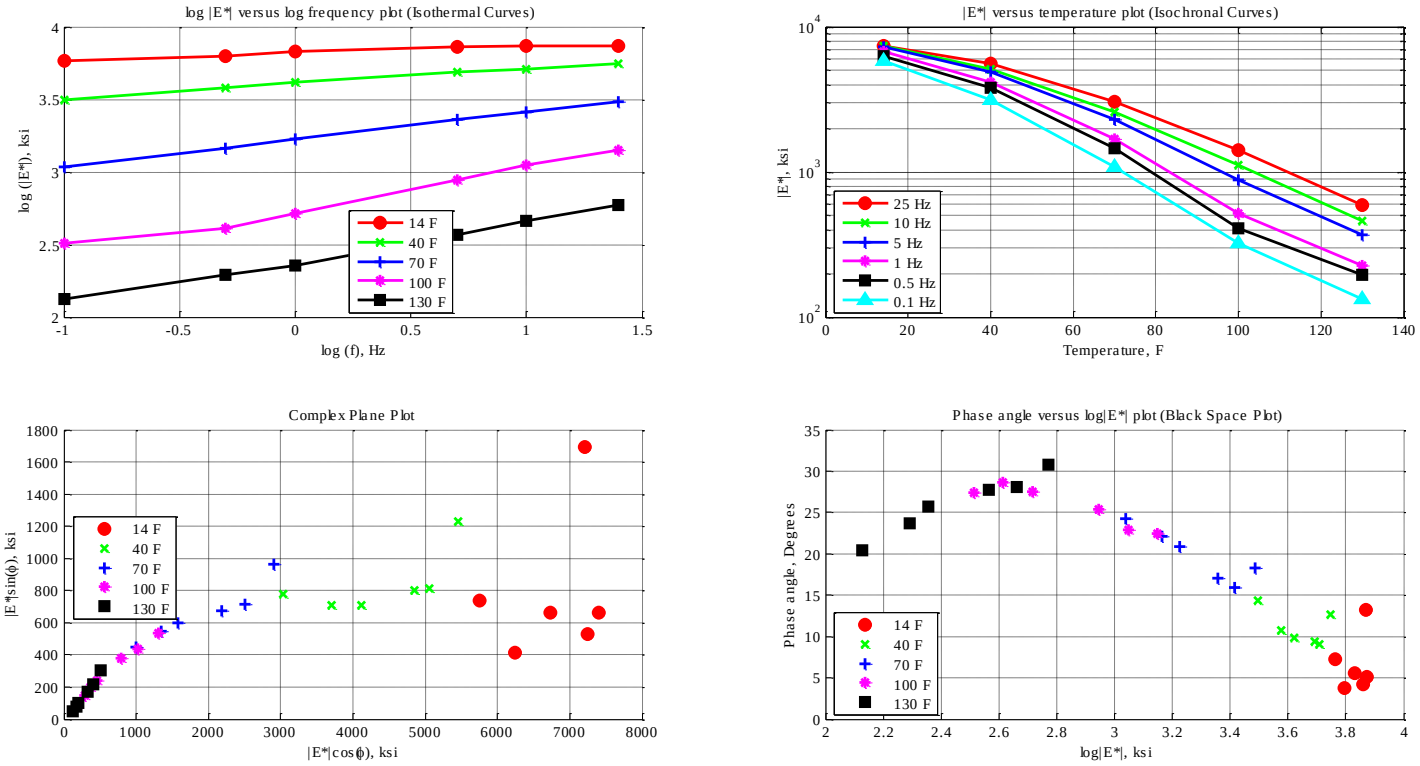

Figure C-28 Isothermal curves or |E*| versus frequency plot (top-left), isochronal curves or |E*| versus temperature plot (top-right), complex plane plot (bottom-left), and black space plot (bottom-right) for Mix 9 Specimen 5 in English unit system.

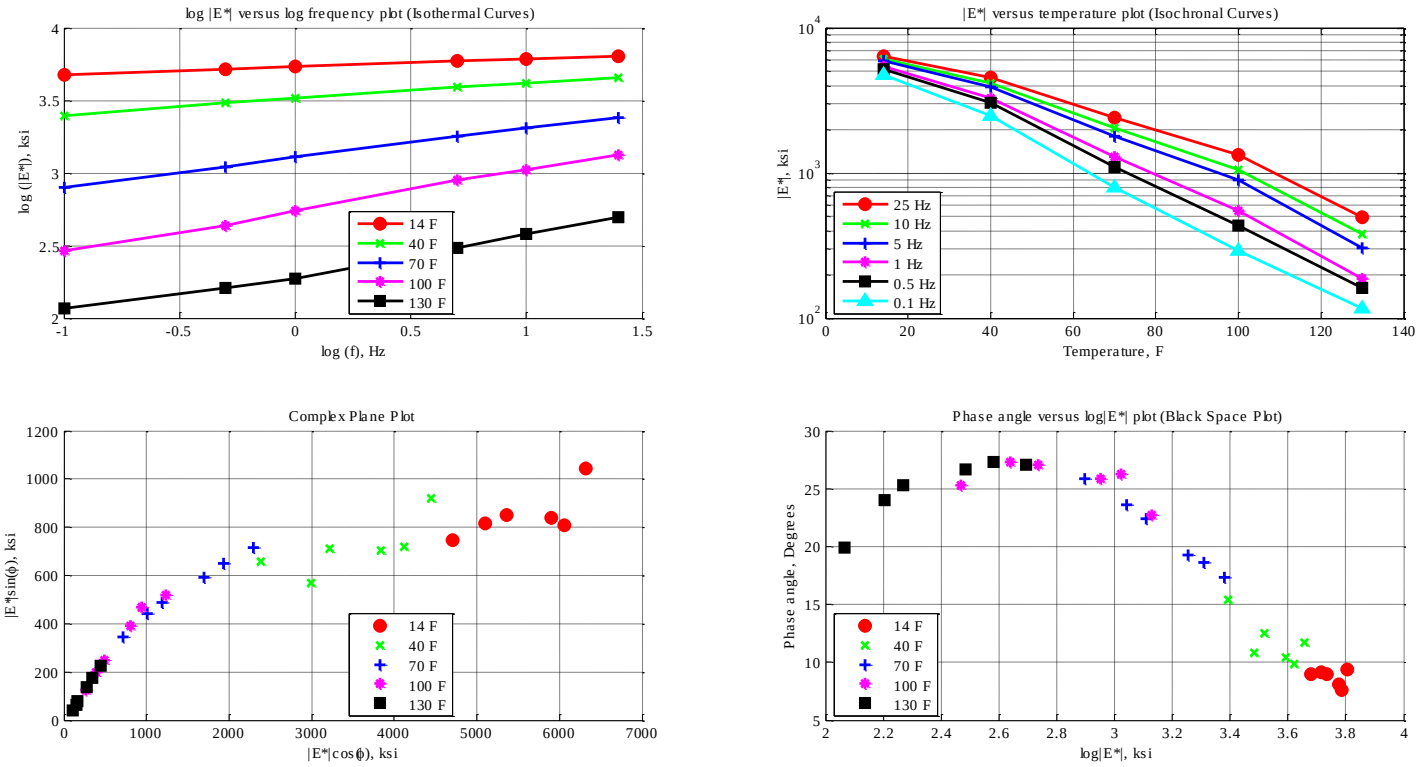

Figure C-29 Isothermal curves or |E*| versus frequency plot (top-left), isochronal curves or |E*| versus temperature plot (top-right), complex plane plot (bottom-left), and black space plot (bottom-right) for Mix 9 Specimen 6 in English unit system.

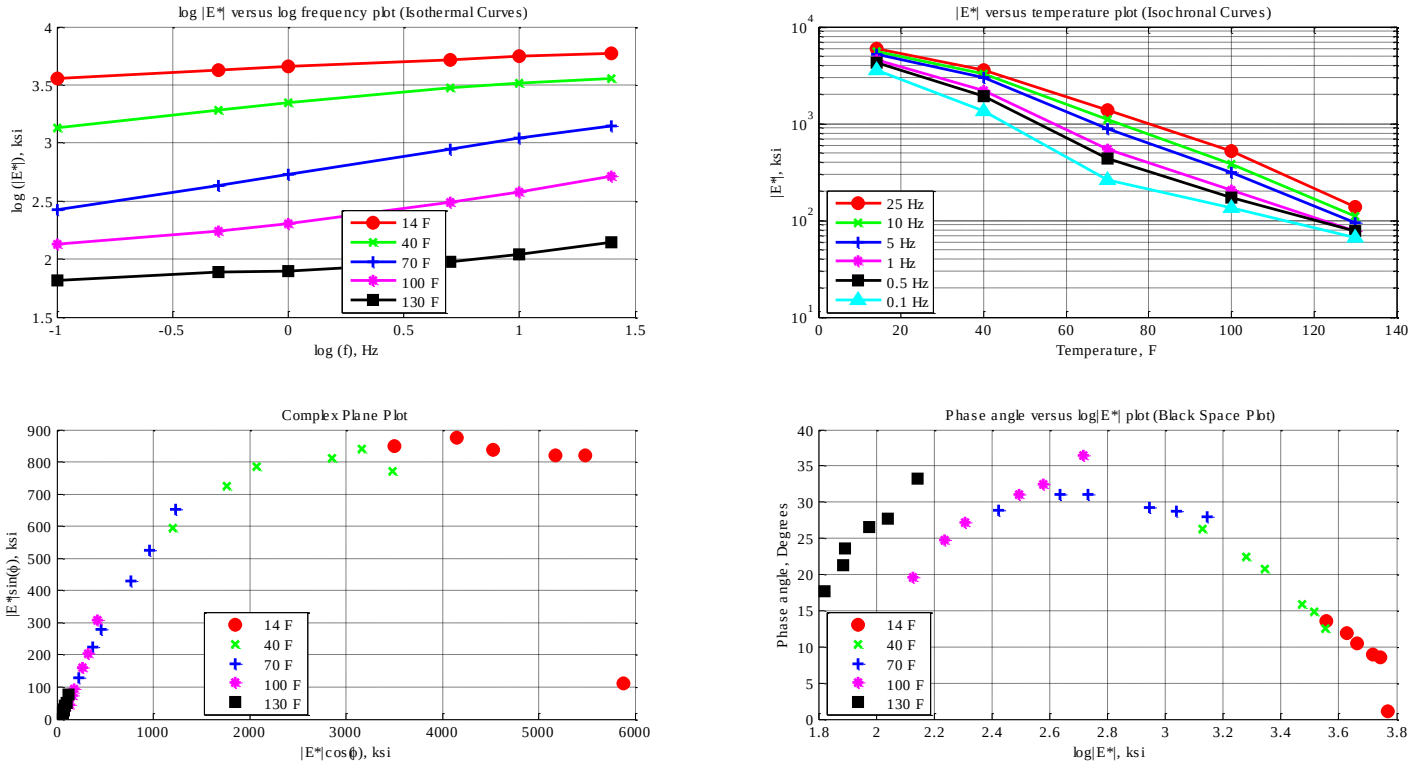

Figure C-30 Isothermal curves or |E*| versus frequency plot (top-left), isochronal curves or |E*| versus temperature plot (top-right), complex plane plot (bottom-left), and black space plot (bottom-right) for Mix 10 Specimen 2 in English unit system.

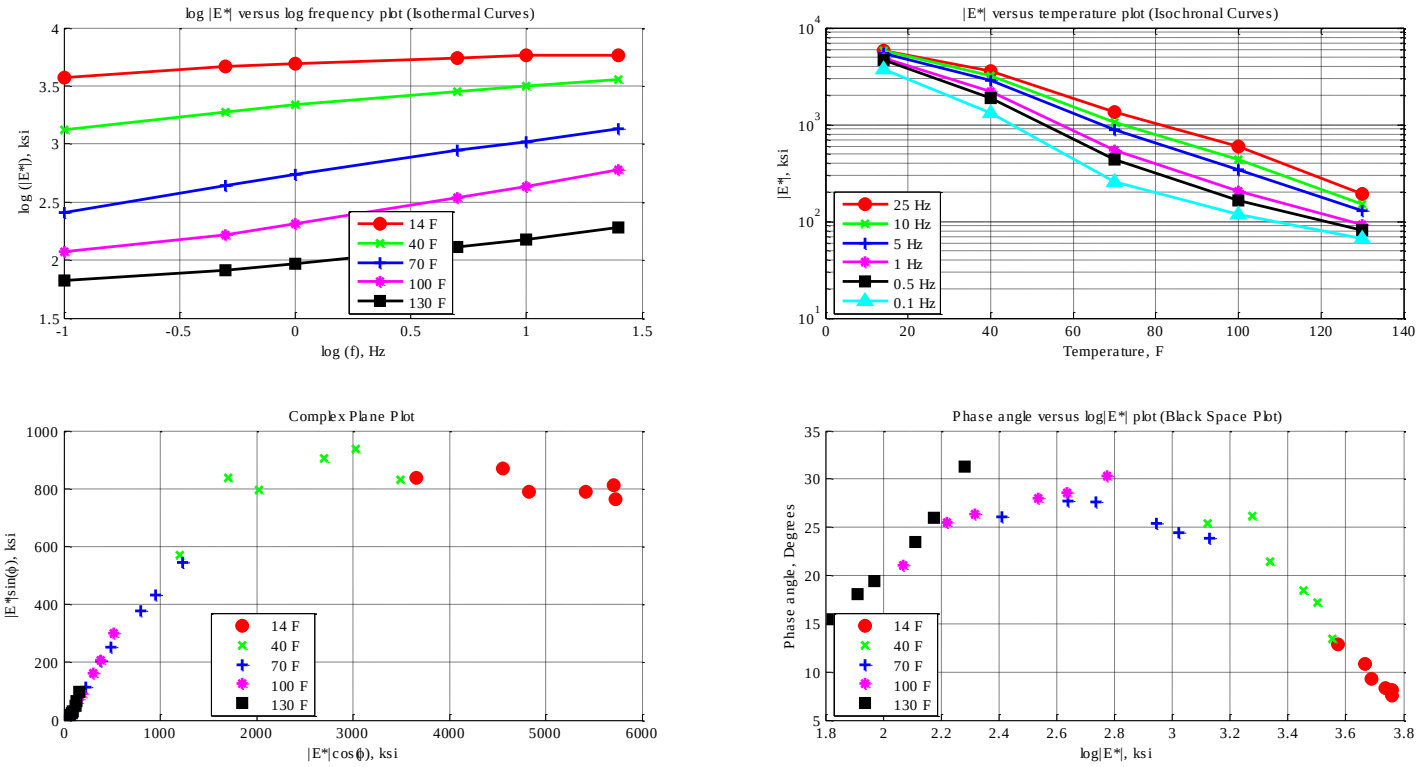

Figure C-31 Isothermal curves or |E*| versus frequency plot (top-left), isochronal curves or |E*| versus temperature plot (top-right), complex plane plot (bottom-left), and black space plot (bottom-right) for Mix 10 Specimen 3 in English unit system.

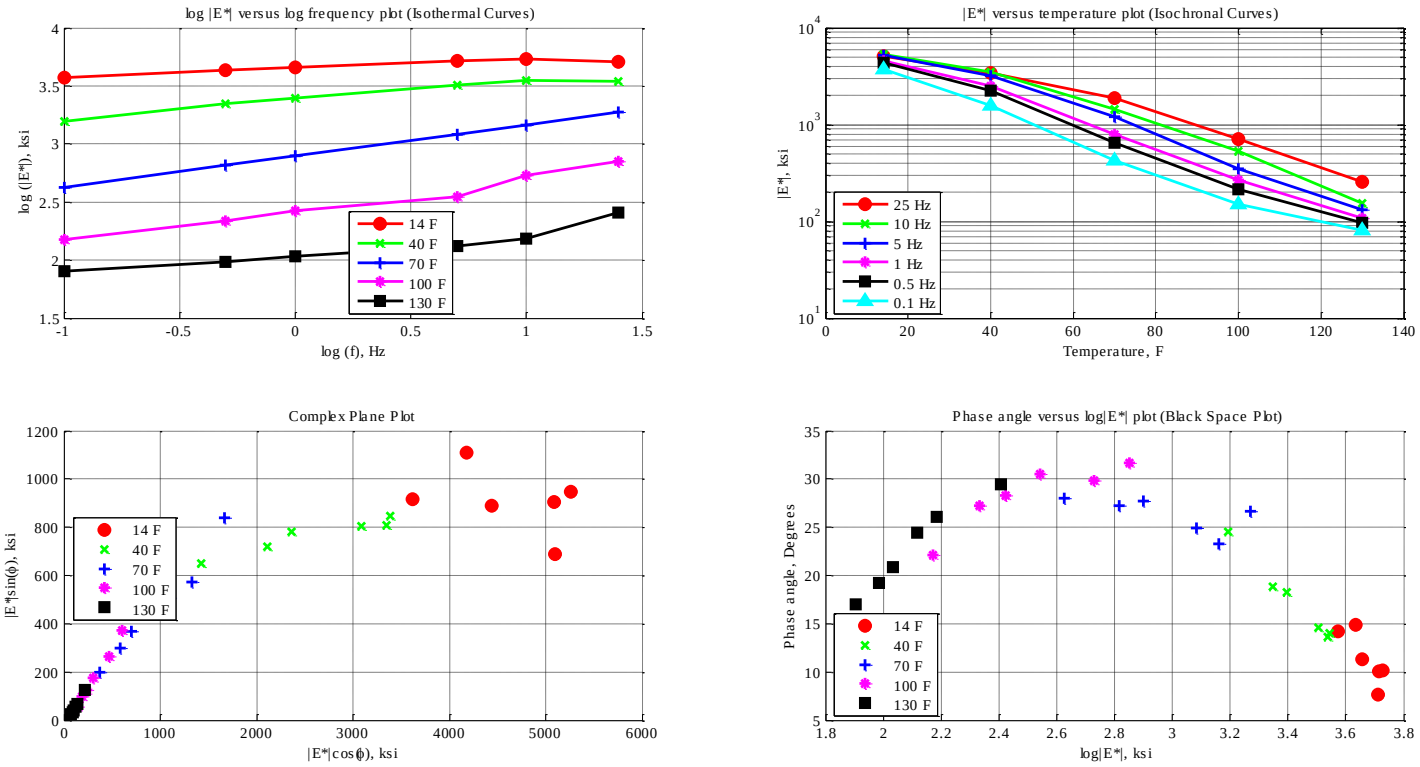

Figure C-32 Isothermal curves or |E*| versus frequency plot (top-left), isochronal curves or |E*| versus temperature plot (top-right), complex plane plot (bottom-left), and black space plot (bottom-right) for Mix 10 Specimen 5 in English unit system.

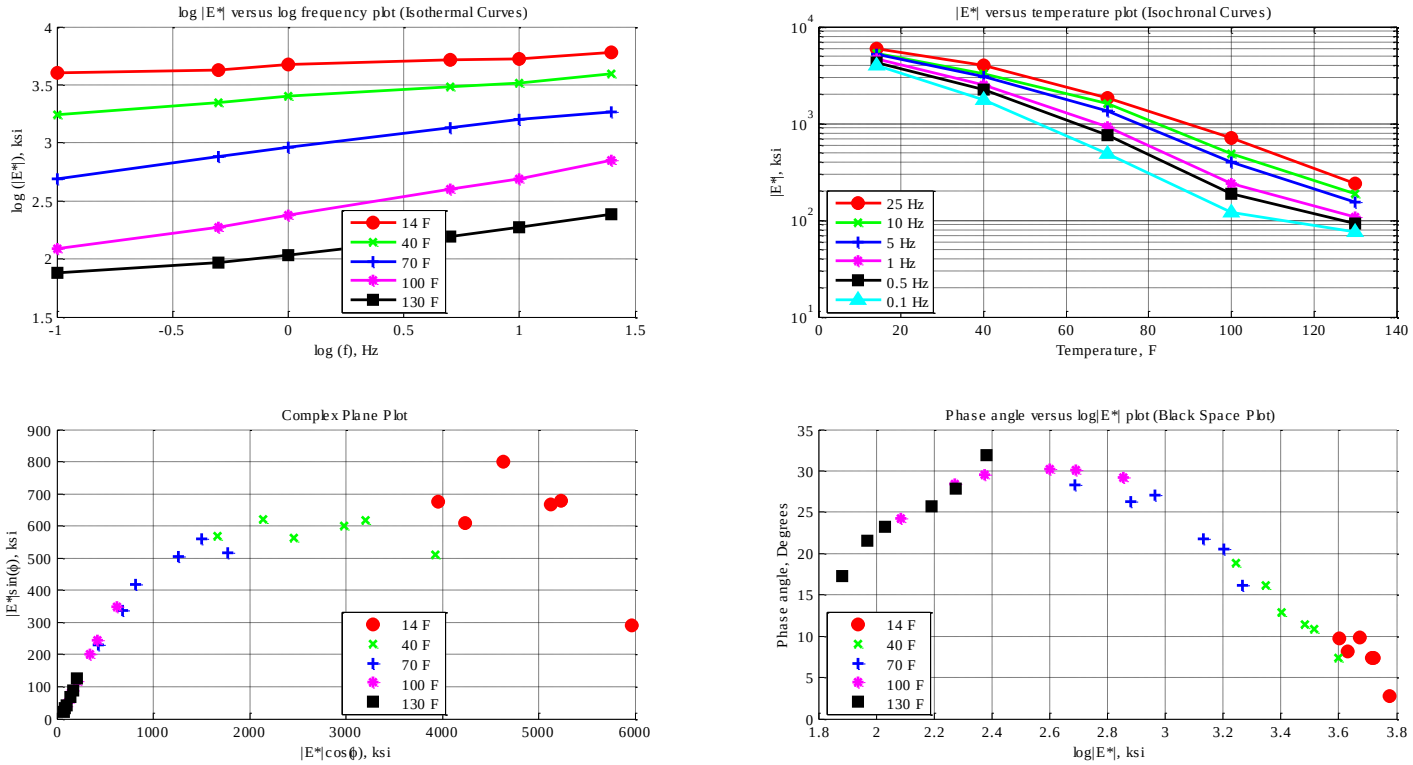

Figure C-33 Isothermal curves or |E*| versus frequency plot (top-left), isochronal curves or |E*| versus temperature plot (top-right), complex plane plot (bottom-left), and black space plot (bottom-right) for Mix 11 Specimen 3 in English unit system.

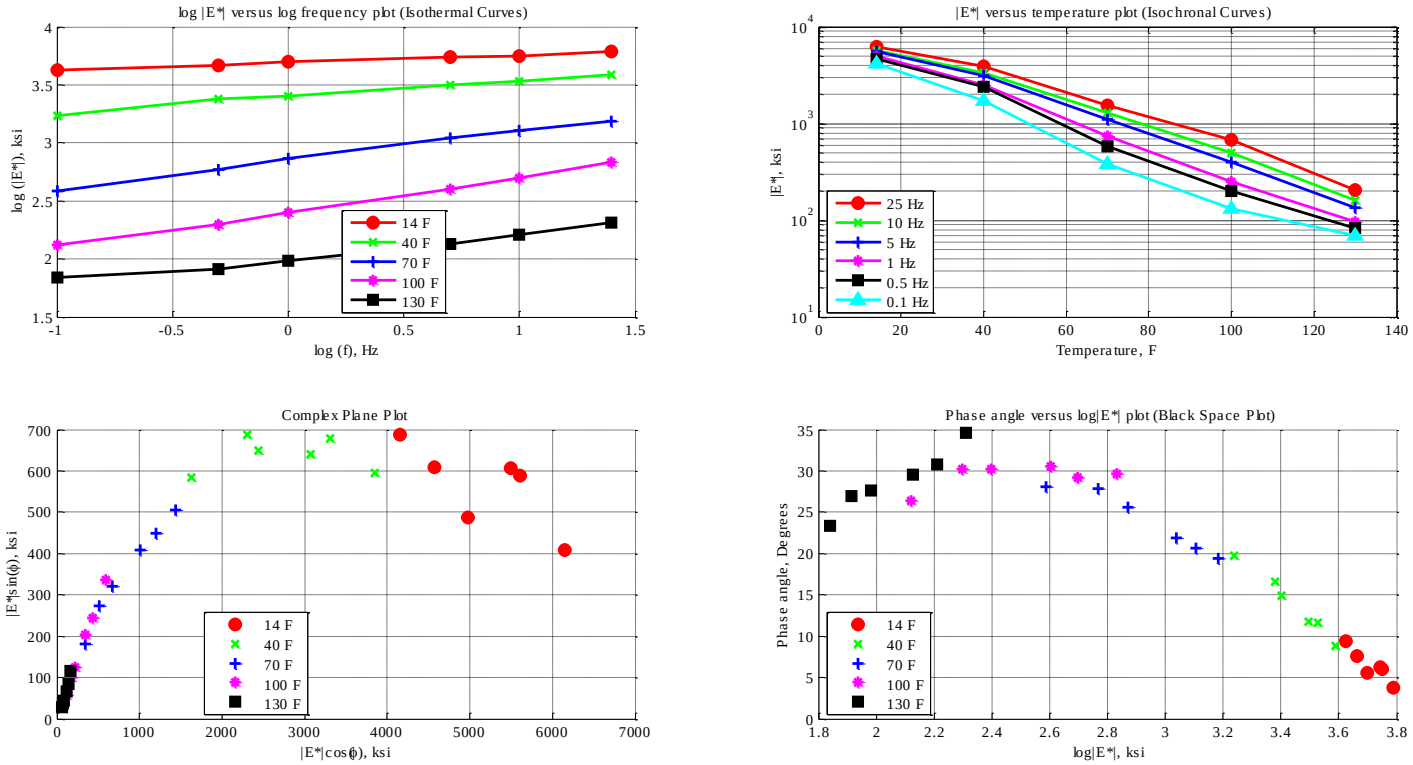

Figure C-34 Isothermal curves or |E*| versus frequency plot (top-left), isochronal curves or |E*| versus temperature plot (top-right), complex plane plot (bottom-left), and black space plot (bottom-right) for Mix 11 Specimen 4 in English unit system.

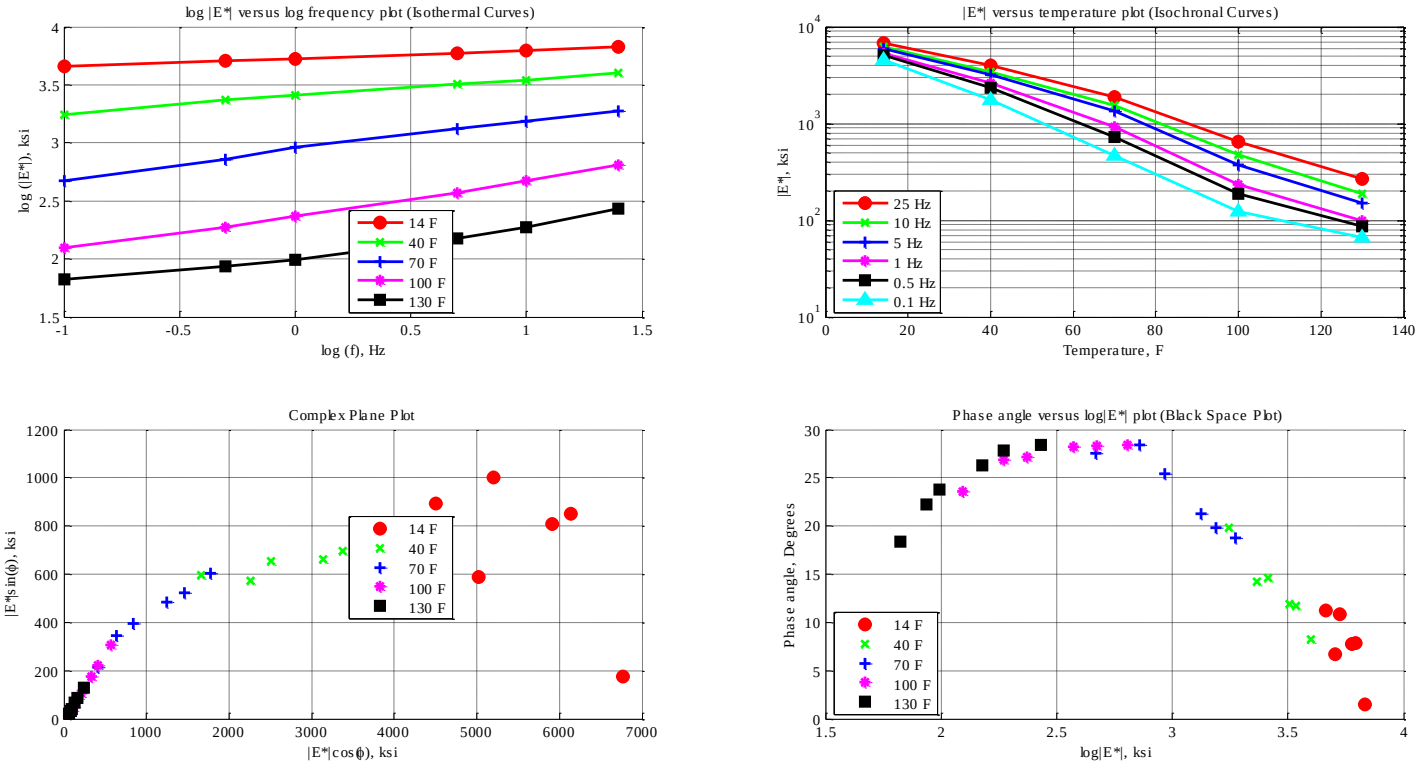

Figure C-35 Isothermal curves or |E*| versus frequency plot (top-left), isochronal curves or |E*| versus temperature plot (top-right), complex plane plot (bottom-left), and black space plot (bottom-right) for Mix 11 Specimen 5 in English unit system.

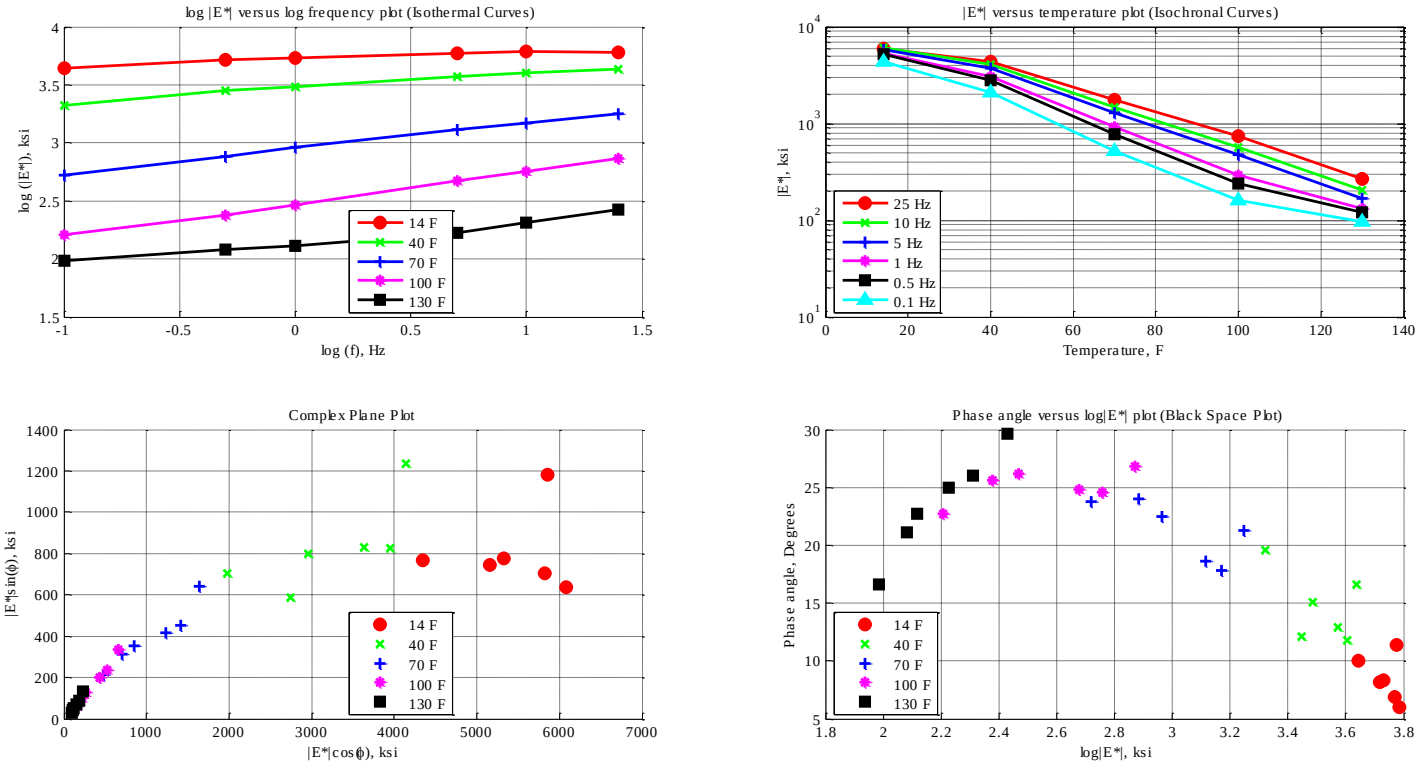

Figure C-36 Isothermal curves or |E*| versus frequency plot (top-left), isochronal curves or |E*| versus temperature plot (top-right), complex plane plot (bottom-left), and black space plot (bottom-right) for Mix 12 Specimen 1 in English unit system.

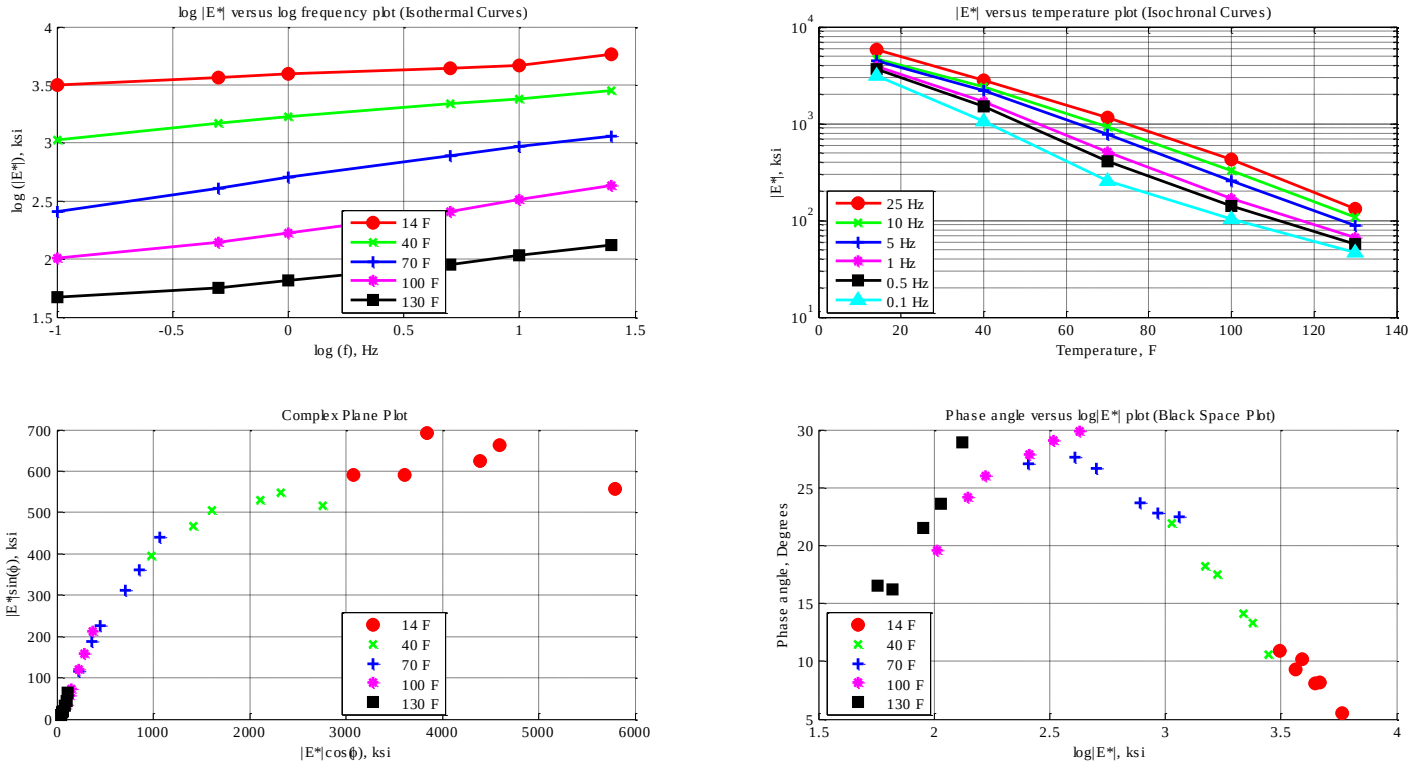

Figure C-37 Isothermal curves or |E*| versus frequency plot (top-left), isochronal curves or |E*| versus temperature plot (top-right), complex plane plot (bottom-left), and black space plot (bottom-right) for Mix 12 Specimen 2 in English unit system.

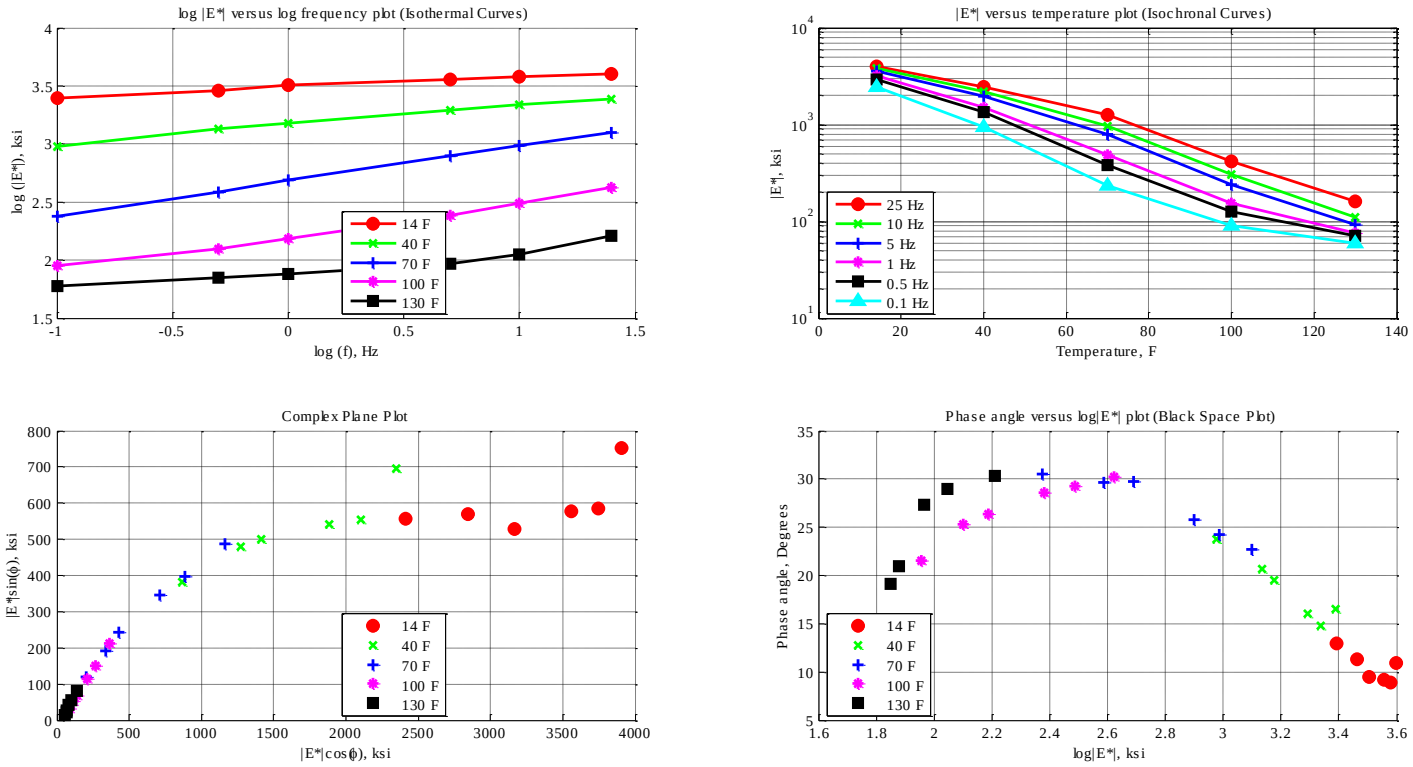

Figure C-38 Isothermal curves or |E*| versus frequency plot (top-left), isochronal curves or |E*| versus temperature plot (top-right), complex plane plot (bottom-left), and black space plot (bottom-right) for Mix 12 Specimen 6 in English unit system.

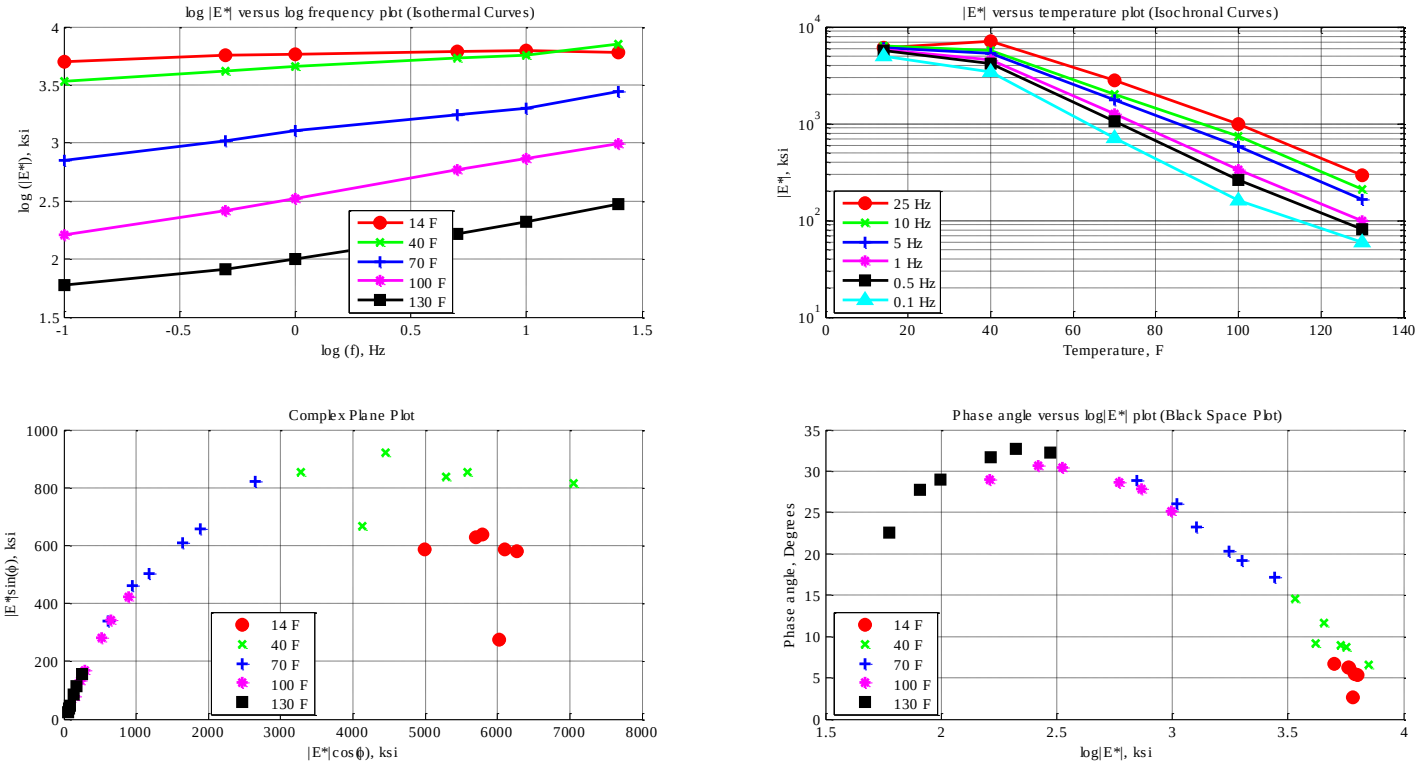

Figure C-39 Isothermal curves or |E*| versus frequency plot (top-left), isochronal curves or |E*| versus temperature plot (top-right), complex plane plot (bottom-left), and black space plot (bottom-right) for Mix 13 Specimen 1 in English unit system.

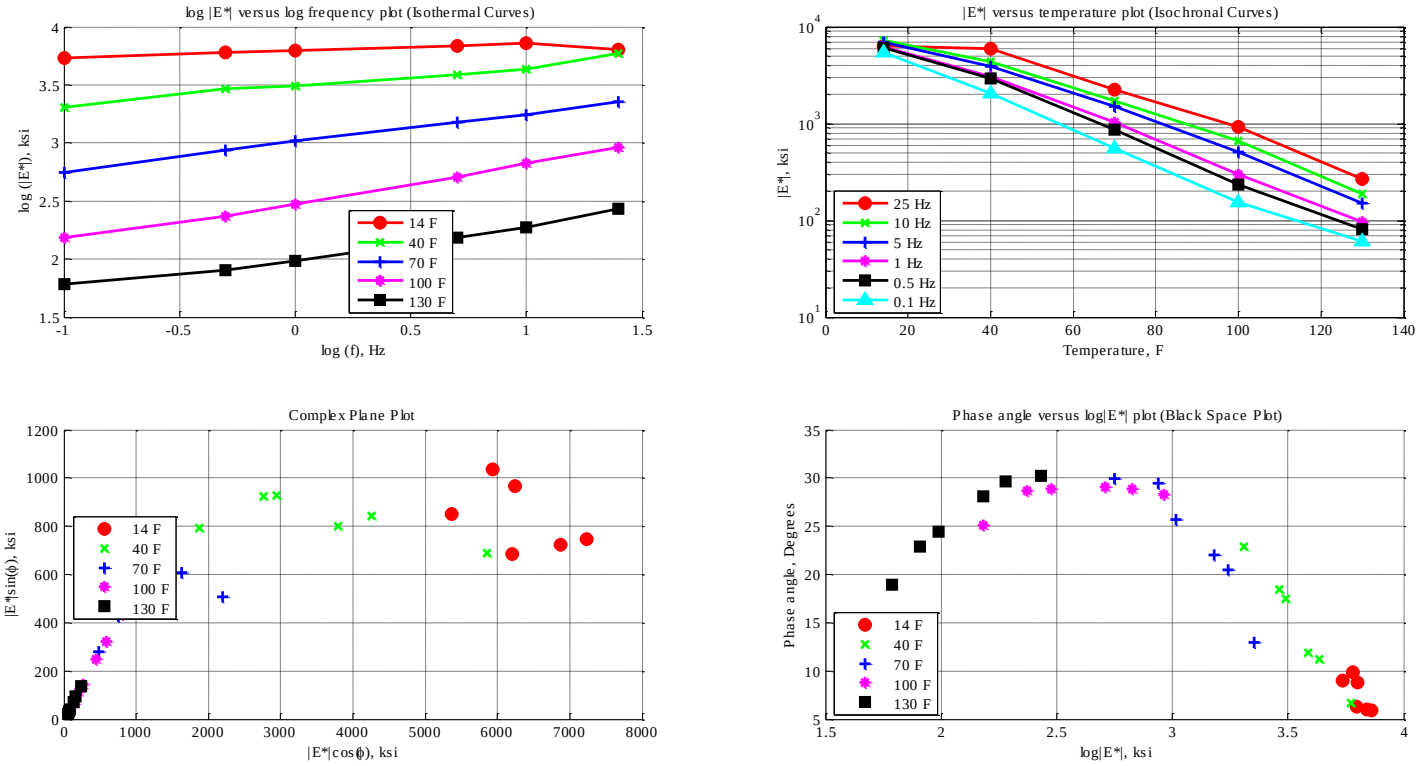

Figure C-40 Isothermal curves or |E*| versus frequency plot (top-left), isochronal curves or |E*| versus temperature plot (top-right), complex plane plot (bottom-left), and black space plot (bottom-right) for Mix 13 Specimen 2 in English unit system.

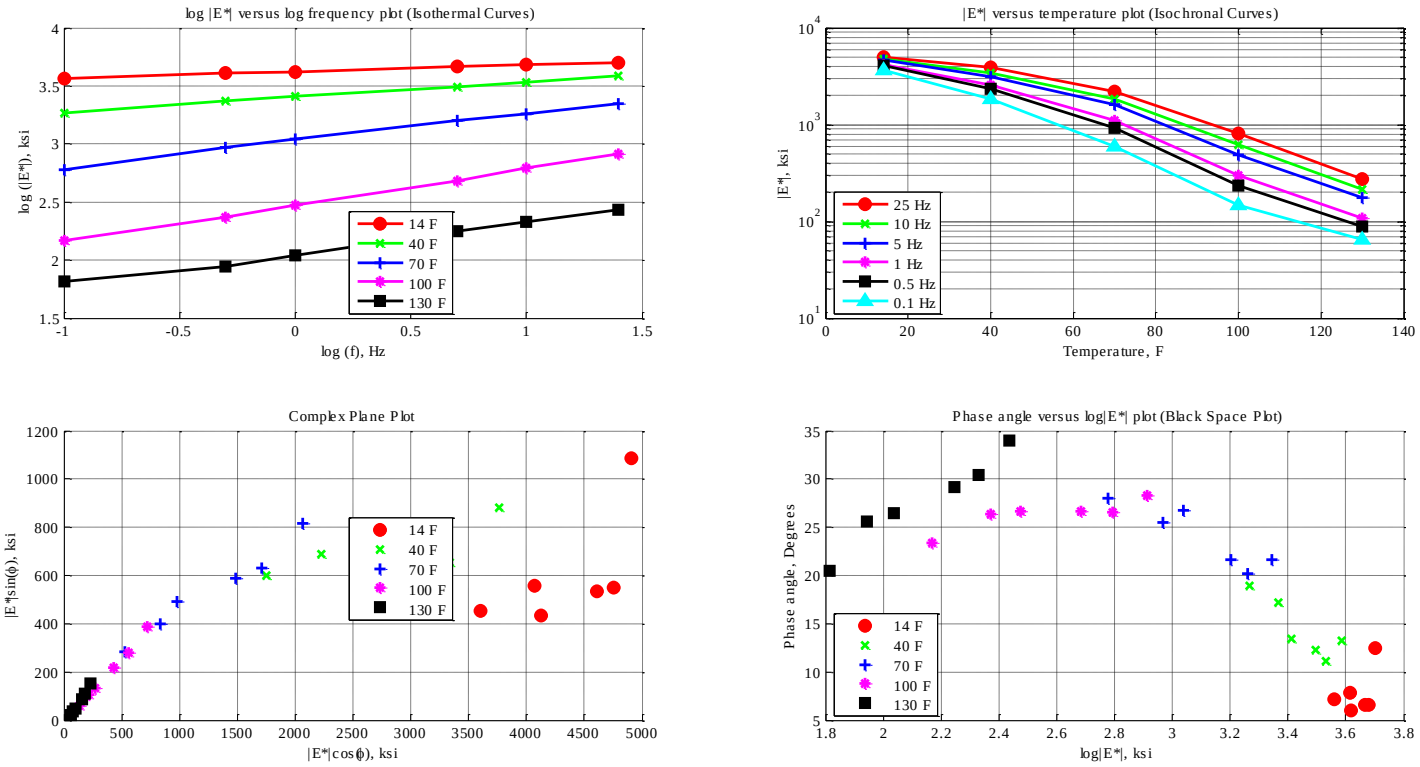

Figure C-41 Isothermal curves or |E*| versus frequency plot (top-left), isochronal curves or |E*| versus temperature plot (top-right), complex plane plot (bottom-left), and black space plot (bottom-right) for Mix 13 Specimen 3 in English unit system.

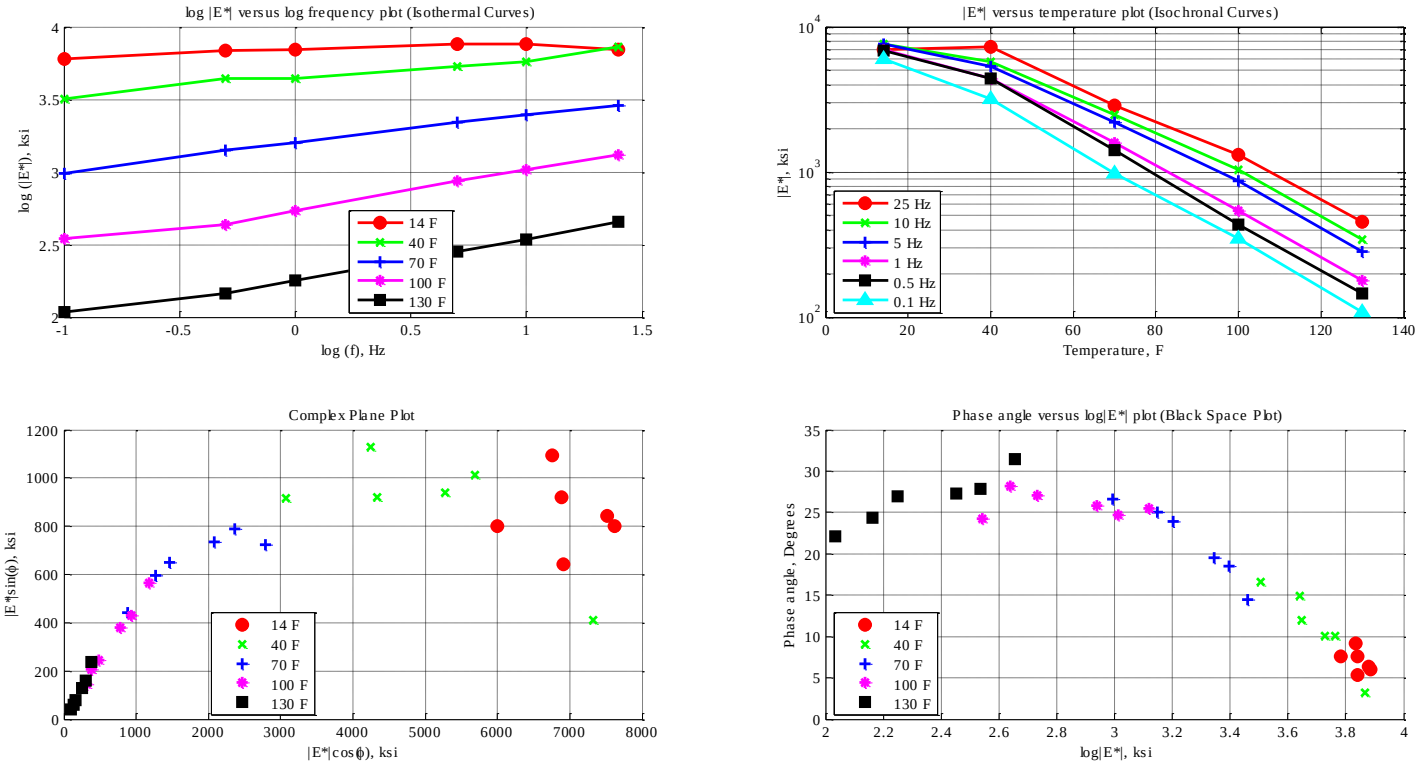

Figure C-42 Isothermal curves or |E*| versus frequency plot (top-left), isochronal curves or |E*| versus temperature plot (top-right), complex plane plot (bottom-left), and black space plot (bottom-right) for Mix 14 Specimen 1 in English unit system.

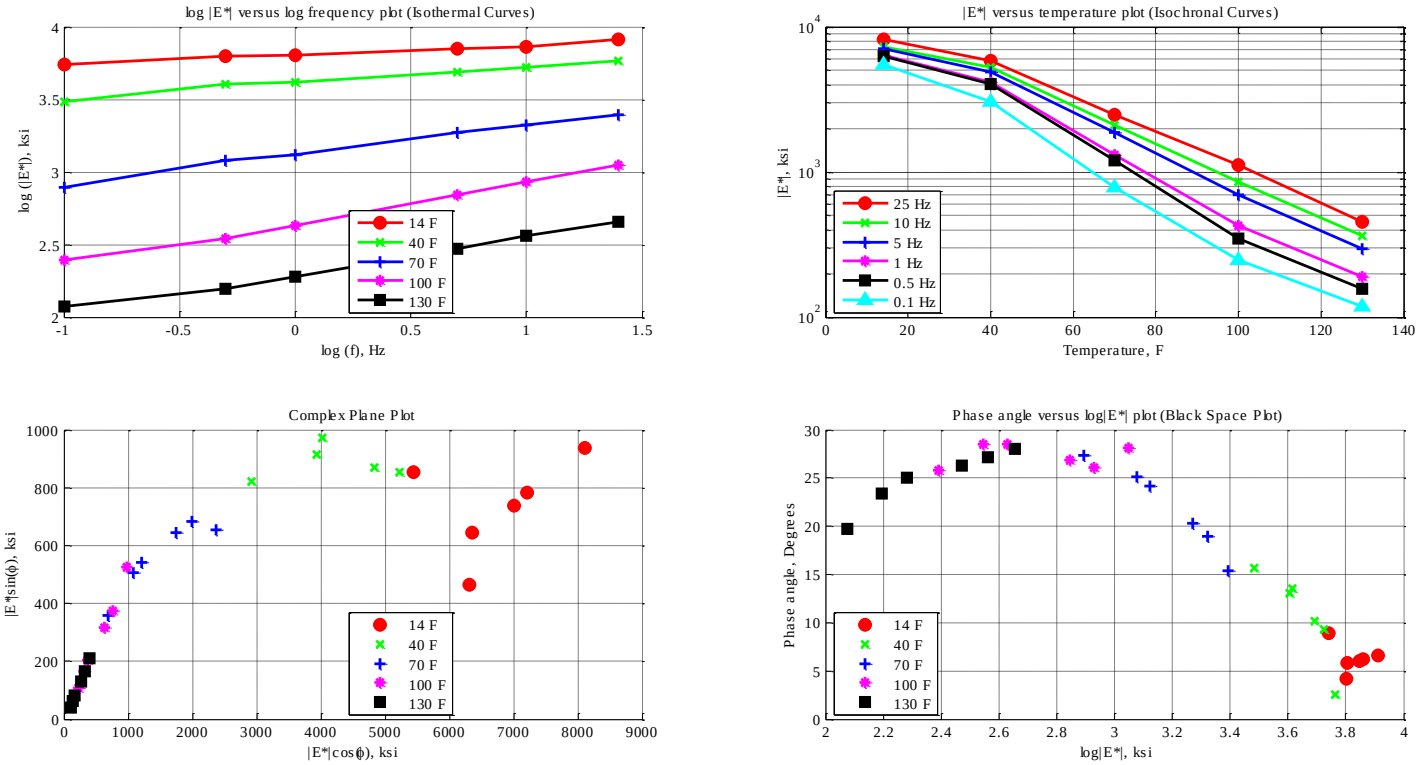

Figure C-43 Isothermal curves or |E*| versus frequency plot (top-left), isochronal curves or |E*| versus temperature plot (top-right), complex plane plot (bottom-left), and black space plot (bottom-right) for Mix 14 Specimen 2 in English unit system.

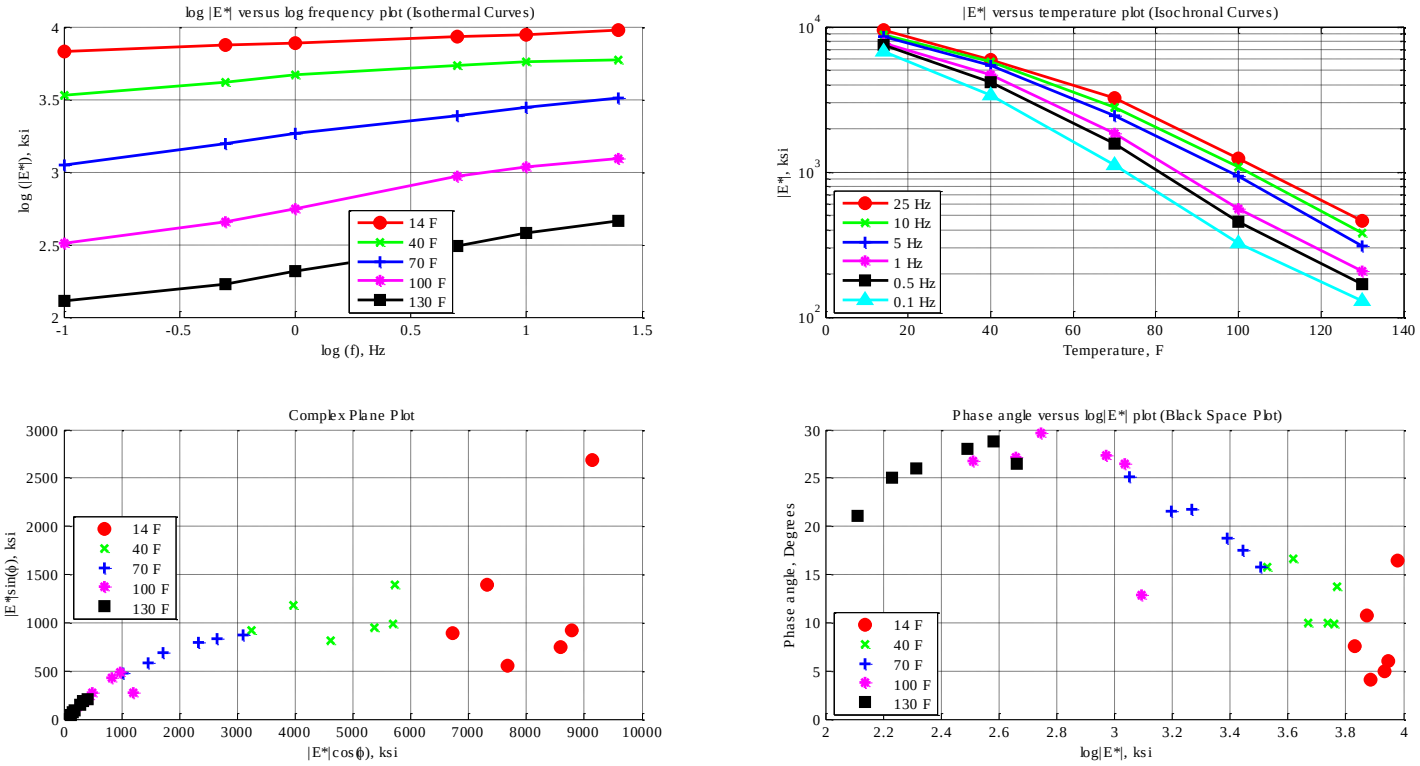

Figure C-44 Isothermal curves or |E*| versus frequency plot (top-left), isochronal curves or |E*| versus temperature plot (top-right), complex plane plot (bottom-left), and black space plot (bottom-right) for Mix 14 Specimen 3 in English unit system.

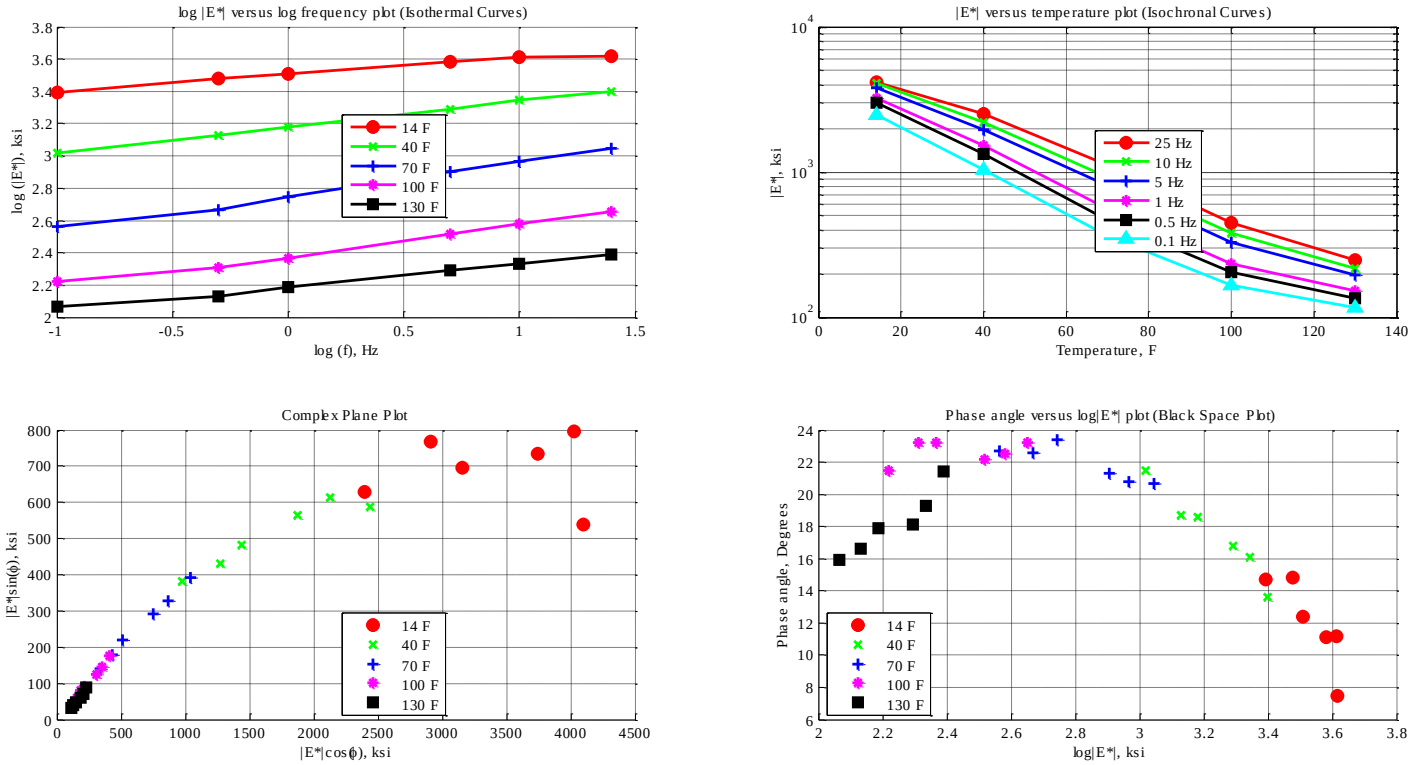

Figure C-45 Isothermal curves or |E*| versus frequency plot (top-left), isochronal curves or |E*| versus temperature plot (top-right), complex plane plot (bottom-left), and black space plot (bottom-right) for Mix 15 Specimen 1 in English unit system.

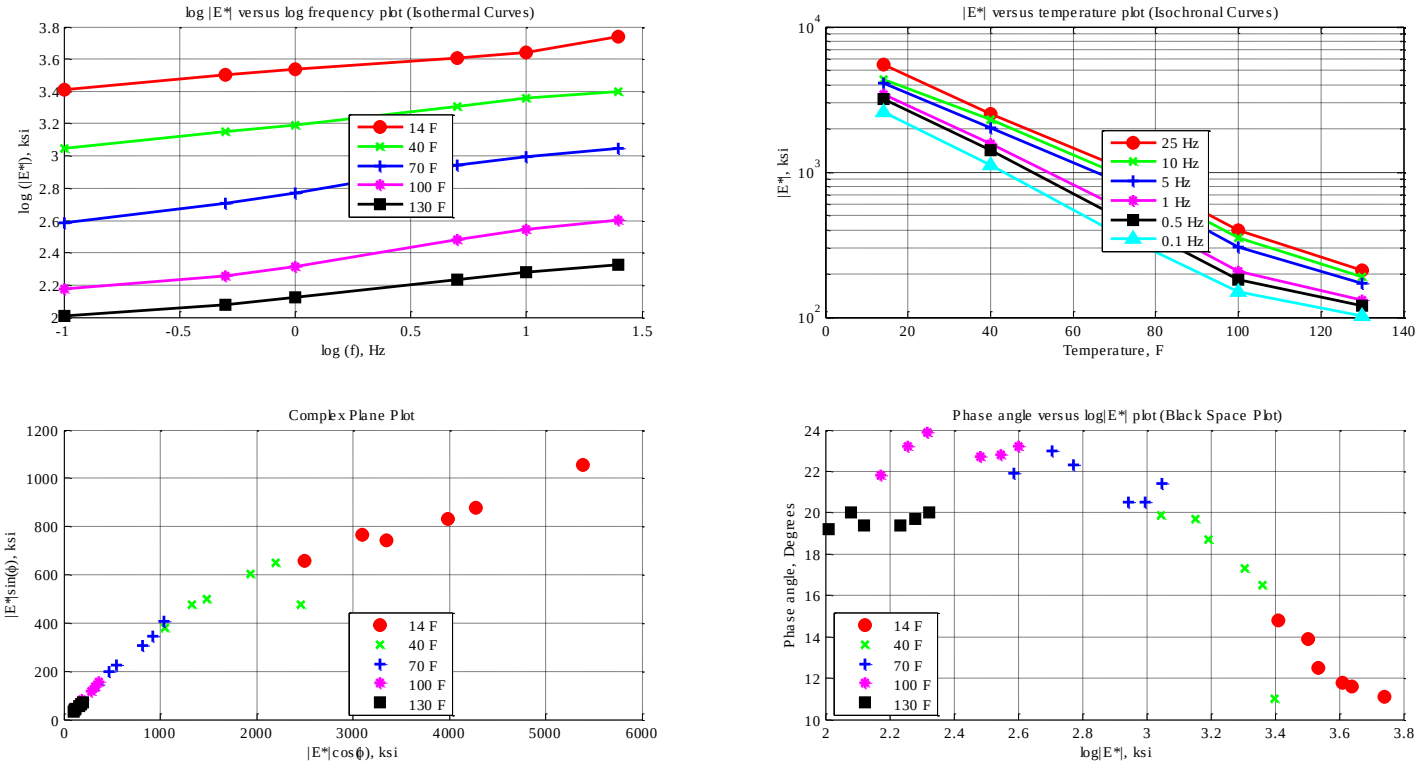

Figure C-46 Isothermal curves or |E*| versus frequency plot (top-left), isochronal curves or |E*| versus temperature plot (top-right), complex plane plot (bottom-left), and black space plot (bottom-right) for Mix 15 Specimen 2 in English unit system.

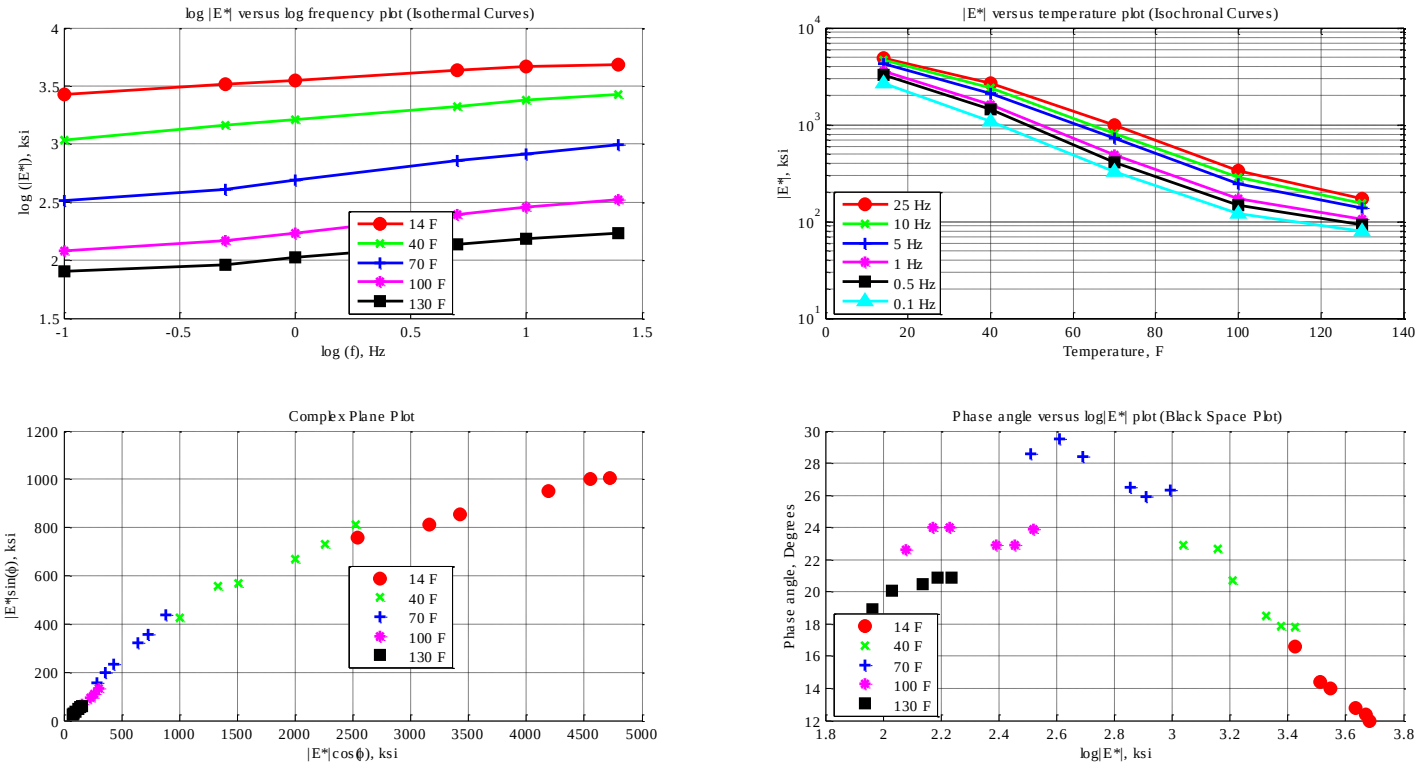

Figure C-47 Isothermal curves or |E*| versus frequency plot (top-left), isochronal curves or |E*| versus temperature plot (top-right), complex plane plot (bottom-left), and black space plot (bottom-right) for Mix 15 Specimen 3 in English unit system.

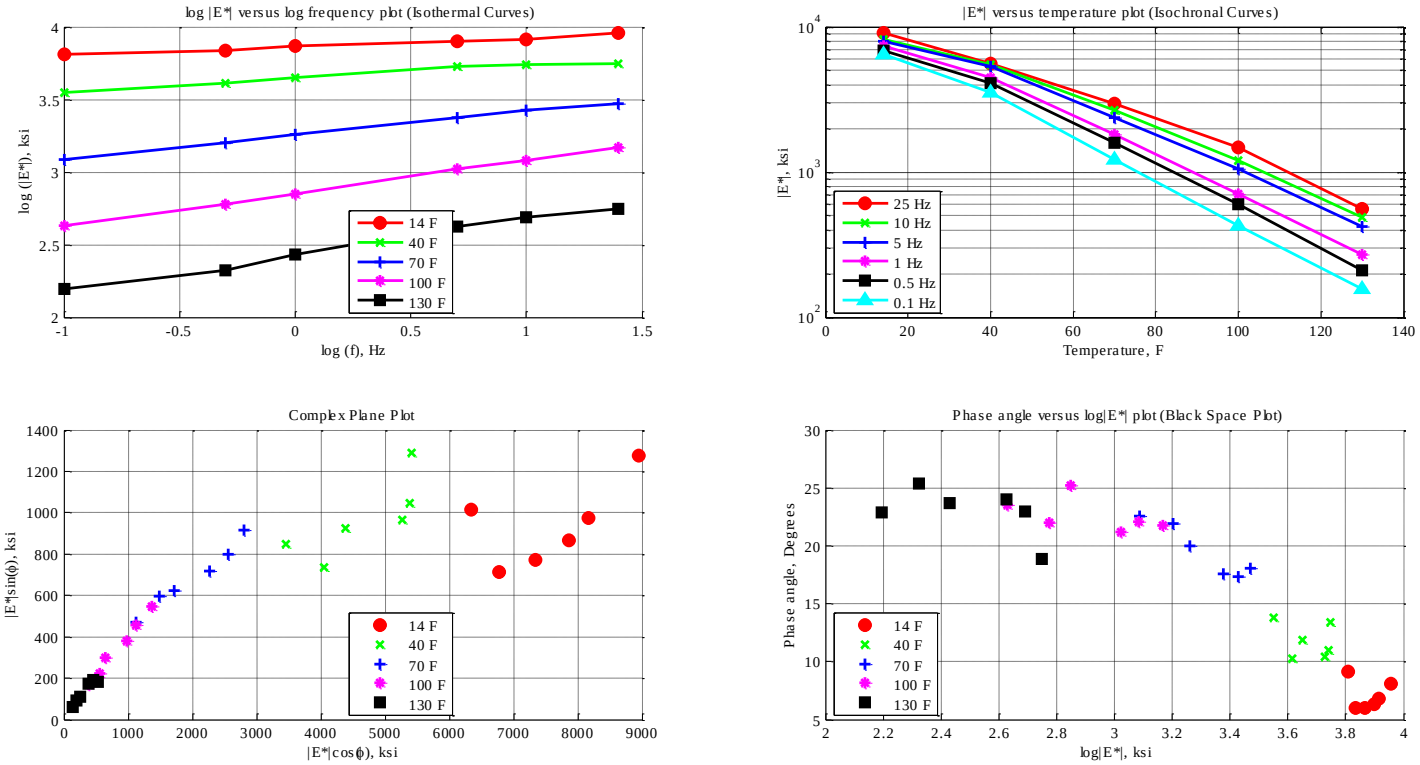

Figure C-48 Isothermal curves or |E*| versus frequency plot (top-left), isochronal curves or |E*| versus temperature plot (top-right), complex plane plot (bottom-left), and black space plot (bottom-right) for Mix 16 Specimen 1 in English unit system.

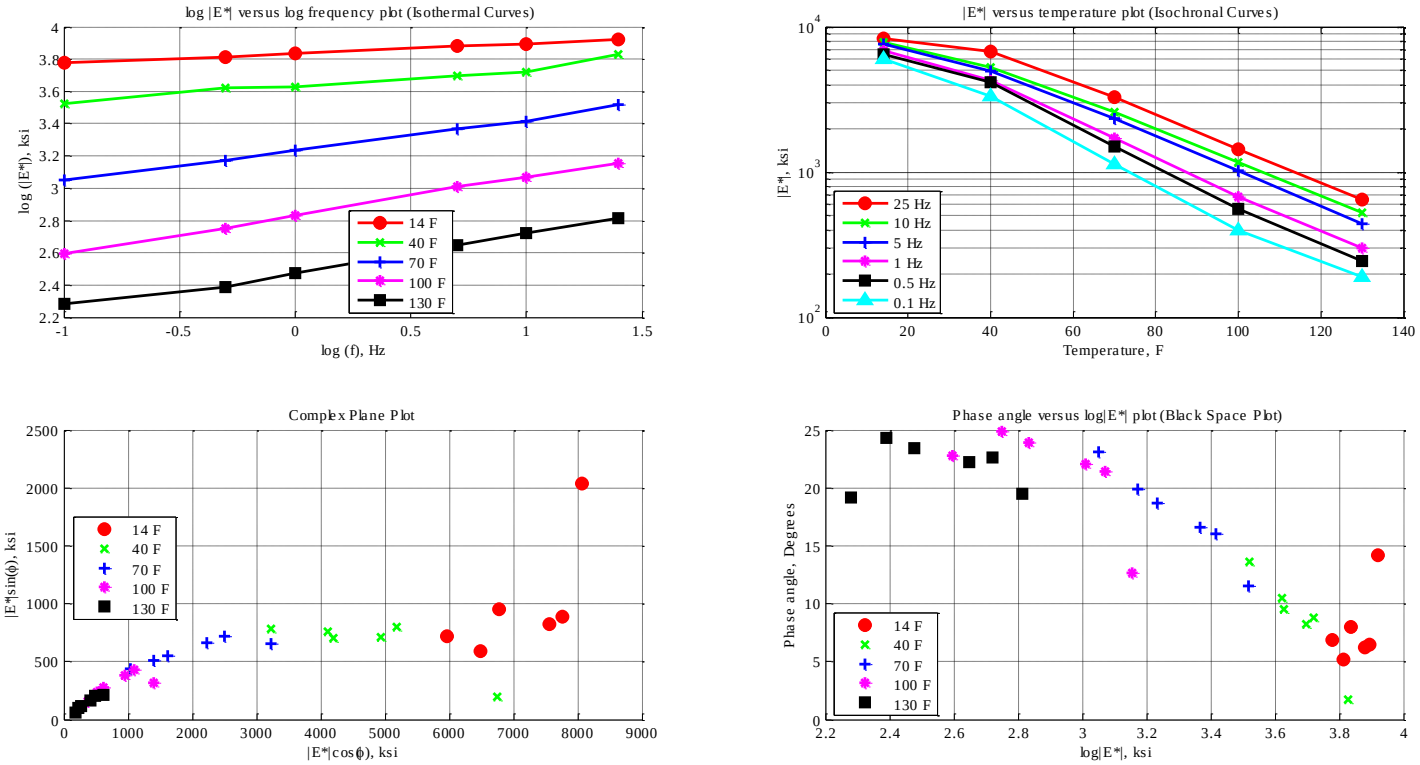

Figure C-49 Isothermal curves or |E*| versus frequency plot (top-left), isochronal curves or |E*| versus temperature plot (top-right), complex plane plot (bottom-left), and black space plot (bottom-right) for Mix 16 Specimen 2 in English unit system.

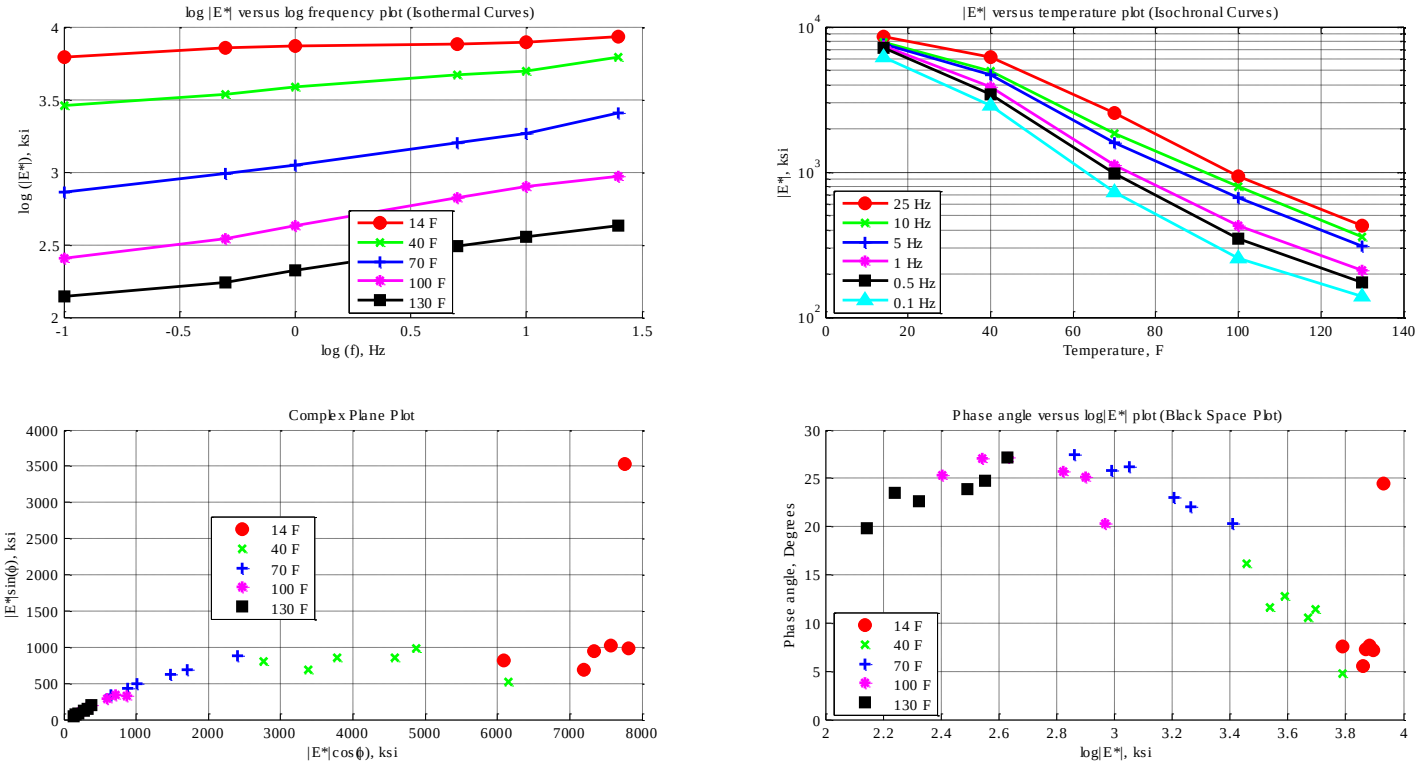

Figure C-50 Isothermal curves or |E*| versus frequency plot (top-left), isochronal curves or |E*| versus temperature plot (top-right), complex plane plot (bottom-left), and black space plot (bottom-right) for Mix 16 Specimen 3 in English unit system.

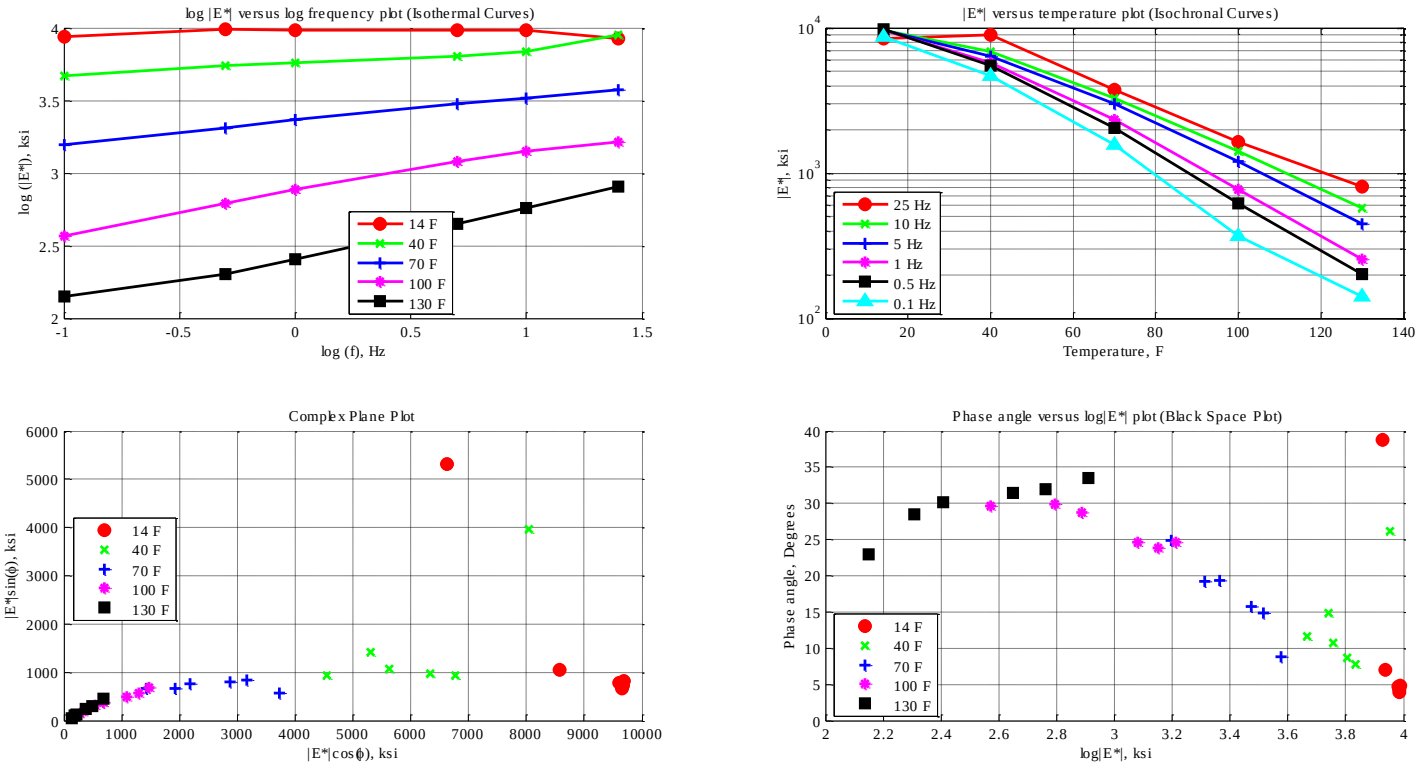

Figure C-51 Isothermal curves or |E*| versus frequency plot (top-left), isochronal curves or |E*| versus temperature plot (top-right), complex plane plot (bottom-left), and black space plot (bottom-right) for Mix 17 Specimen 1 in English unit system.

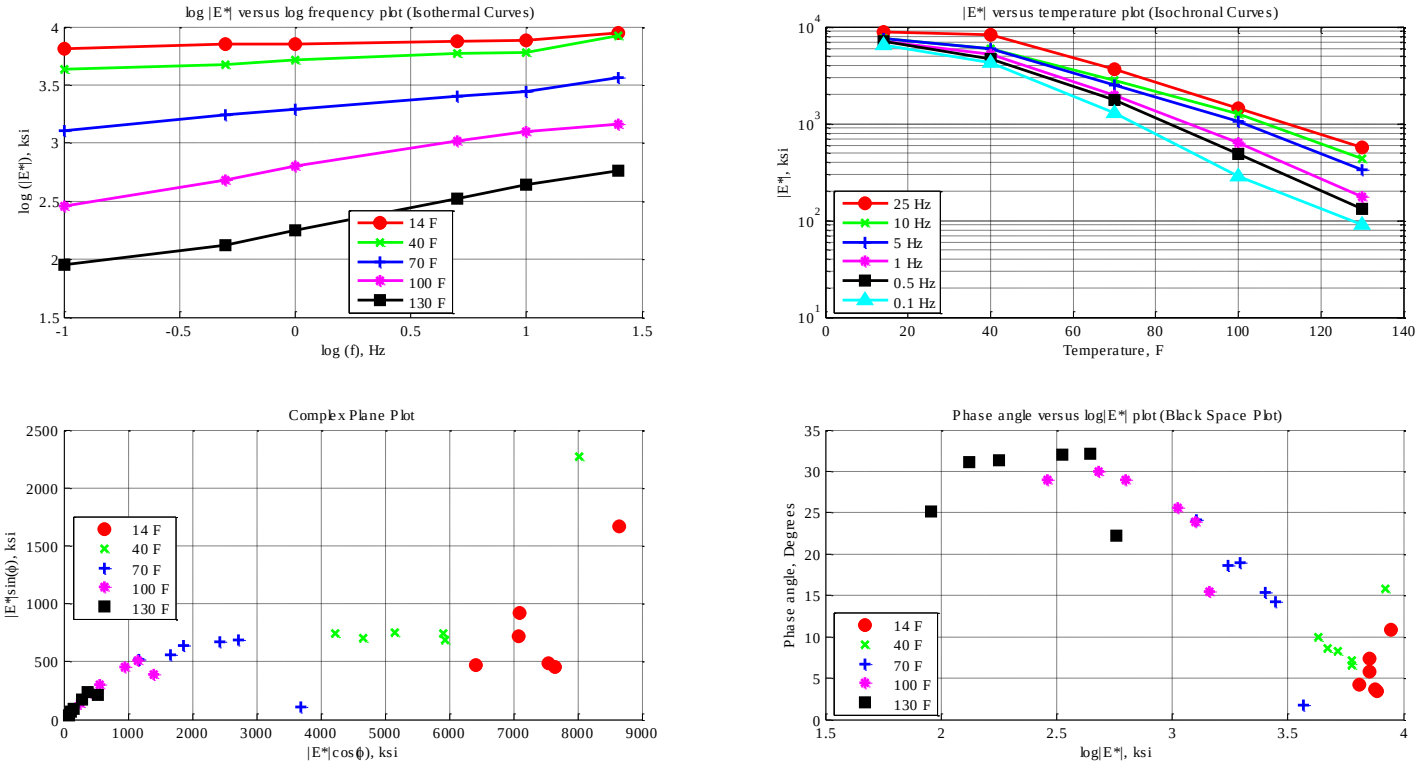

Figure C-52 Isothermal curves or |E*| versus frequency plot (top-left), isochronal curves or |E*| versus temperature plot (top-right), complex plane plot (bottom-left), and black space plot (bottom-right) for Mix 17 Specimen in English unit system.

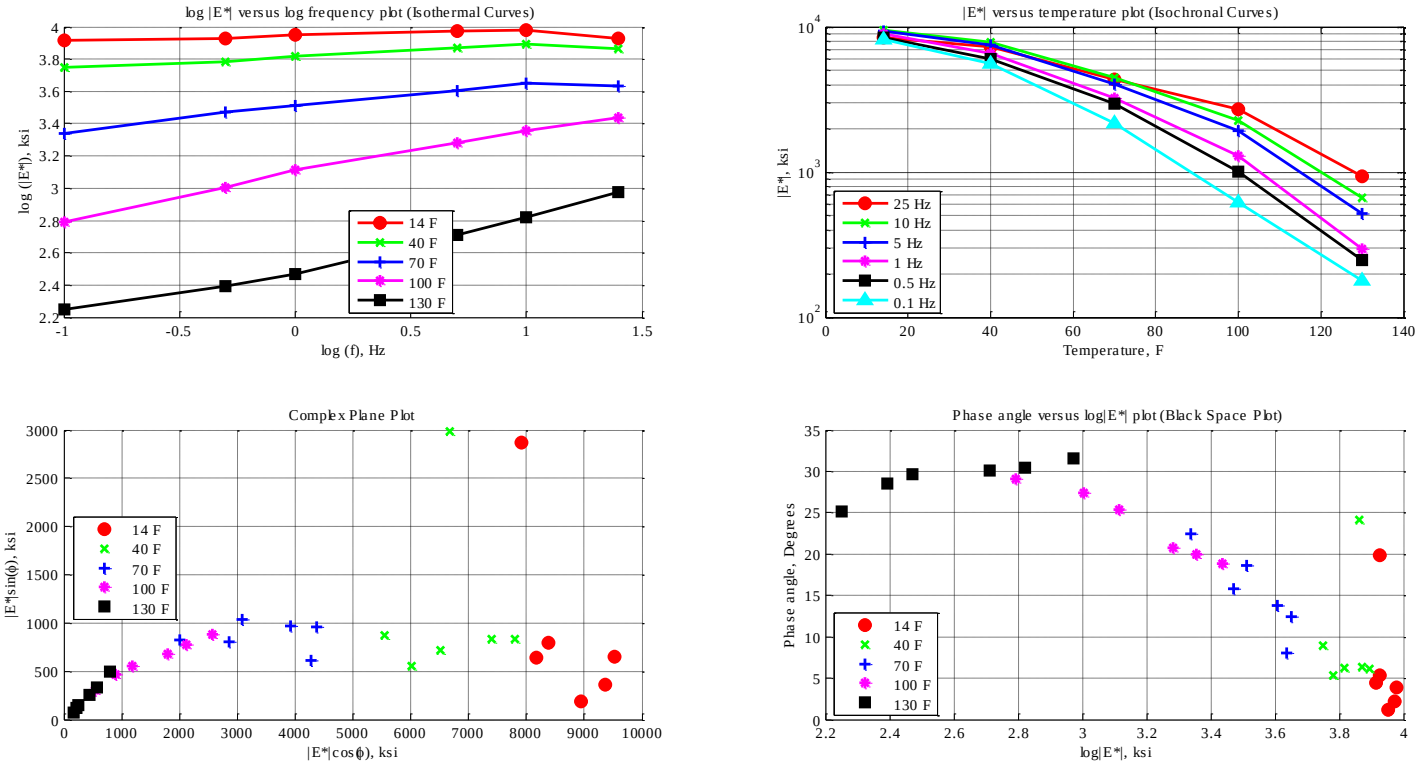

Figure C-53 Isothermal curves or |E*| versus frequency plot (top-left), isochronal curves or |E*| versus temperature plot (top-right), complex plane plot (bottom-left), and black space plot (bottom-right) for Mix 17 Specimen 3 in English unit system.

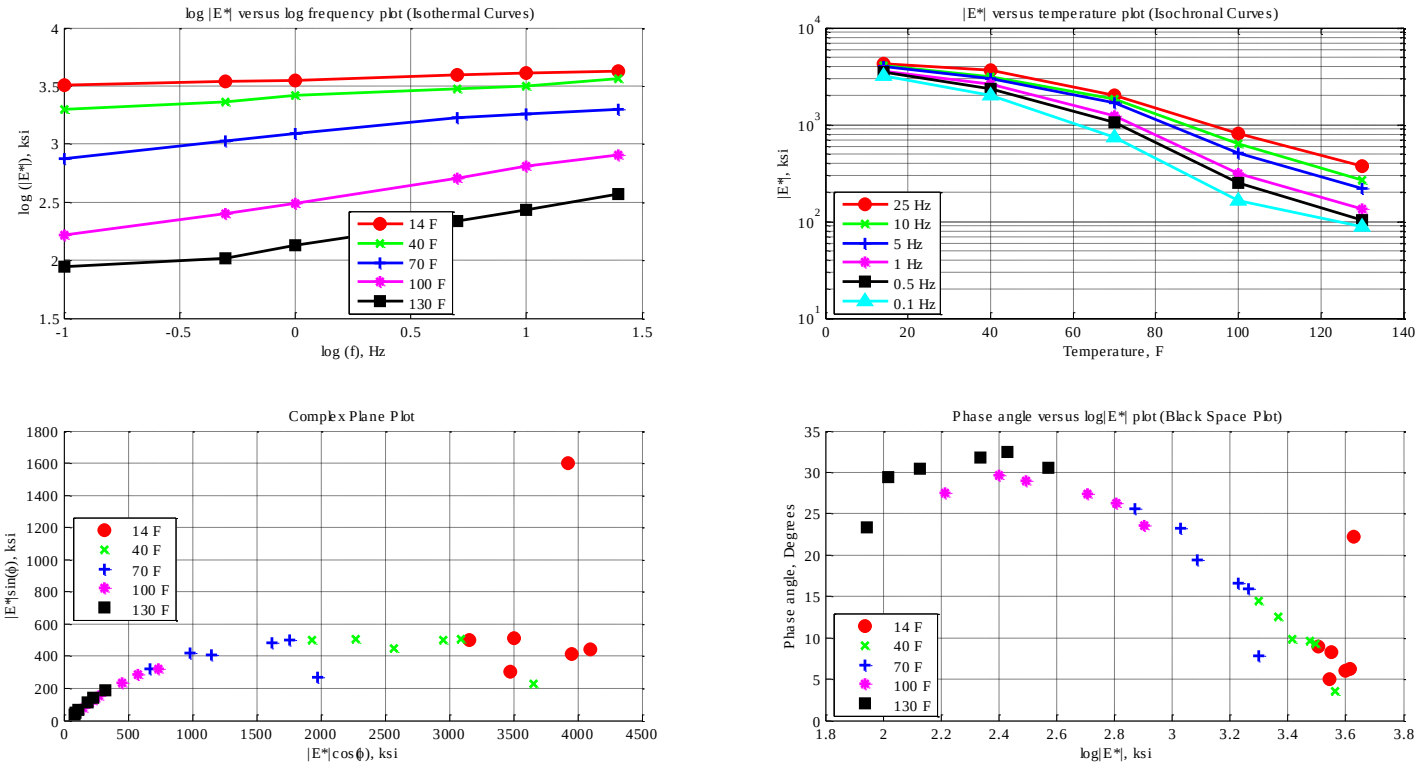

Figure C-54 Isothermal curves or |E*| versus frequency plot (top-left), isochronal curves or |E*| versus temperature plot (top-right), complex plane plot (bottom-left), and black space plot (bottom-right) for Mix 18 Specimen 1 in English unit system.

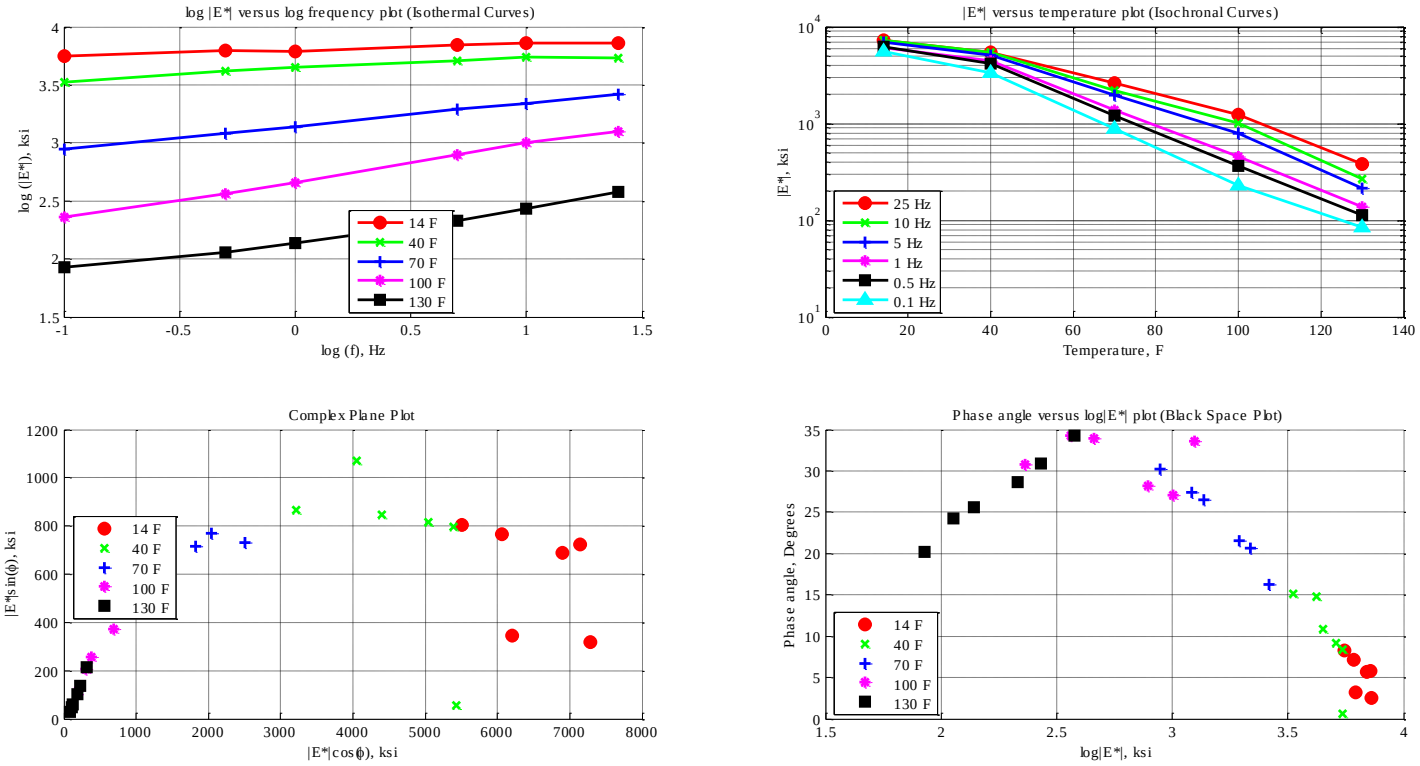

Figure C-55 Isothermal curves or |E*| versus frequency plot (top-left), isochronal curves or |E*| versus temperature plot (top-right), complex plane plot (bottom-left), and black space plot (bottom-right) for Mix 18 Specimen 2 in English unit system.

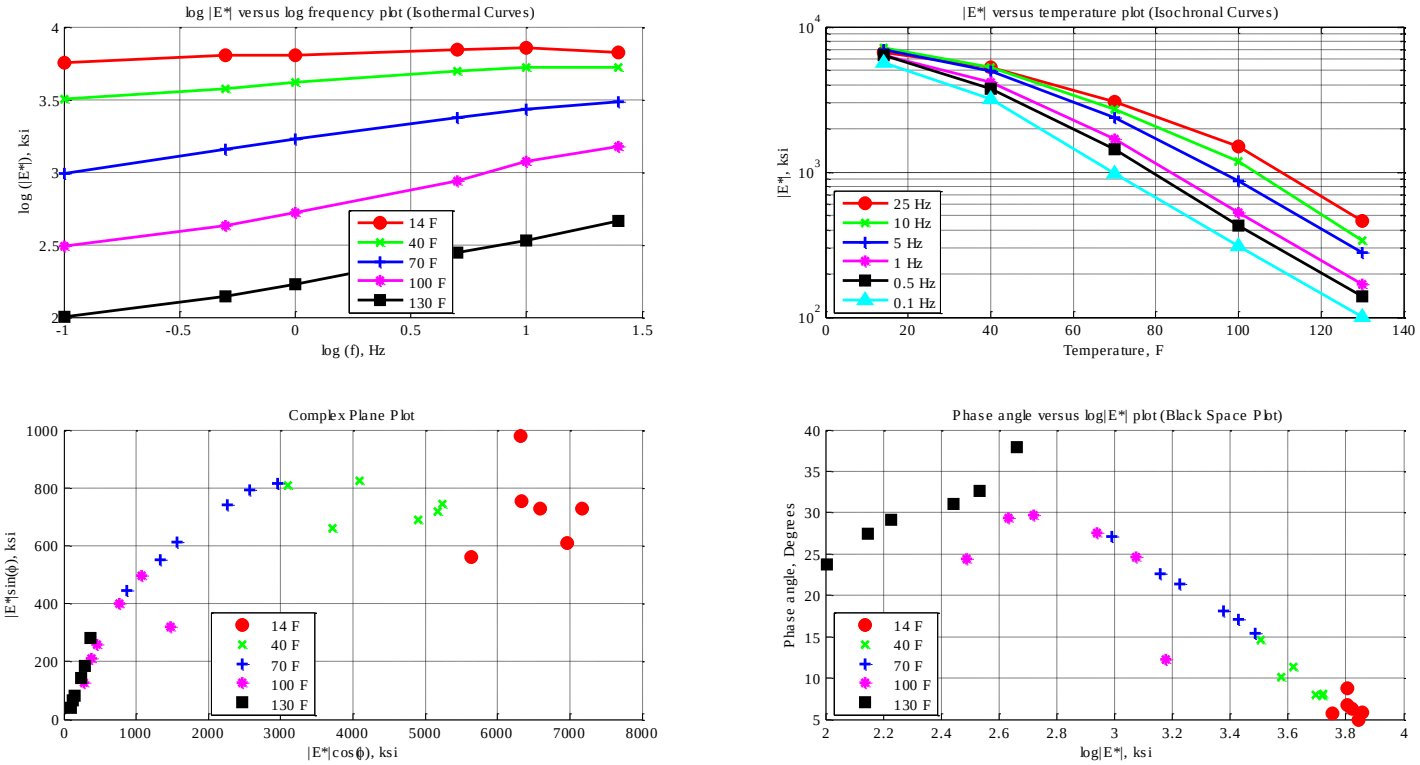

Figure C-56 Isothermal curves or |E*| versus frequency plot (top-left), isochronal curves or |E*| versus temperature plot (top-right), complex plane plot (bottom-left), and black space plot (bottom-right) for Mix 18 Specimen 3 in English unit system.

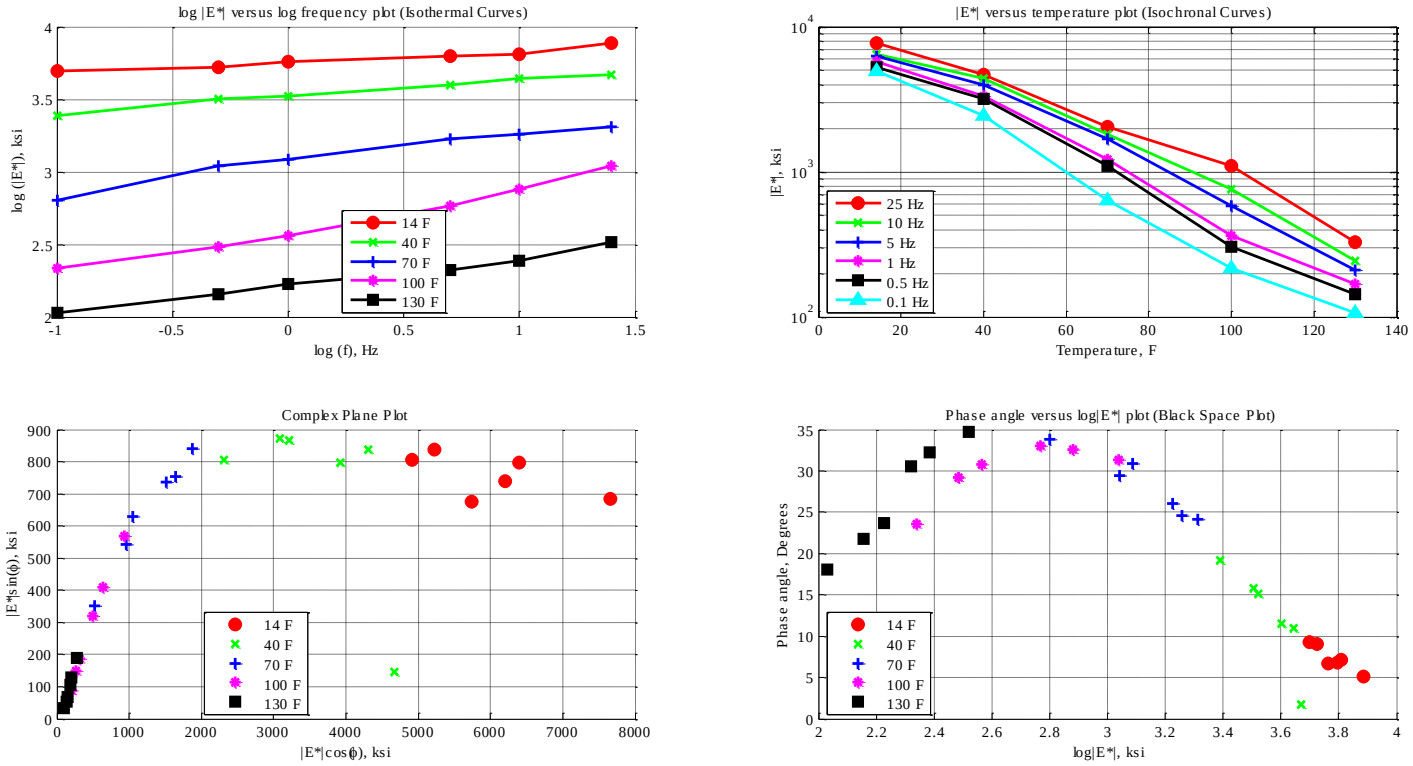

Figure C-57 Isothermal curves or |E*| versus frequency plot (top-left), isochronal curves or |E*| versus temperature plot (top-right), complex plane plot (bottom-left), and black space plot (bottom-right) for Mix 19 Specimen 1 in English unit system.

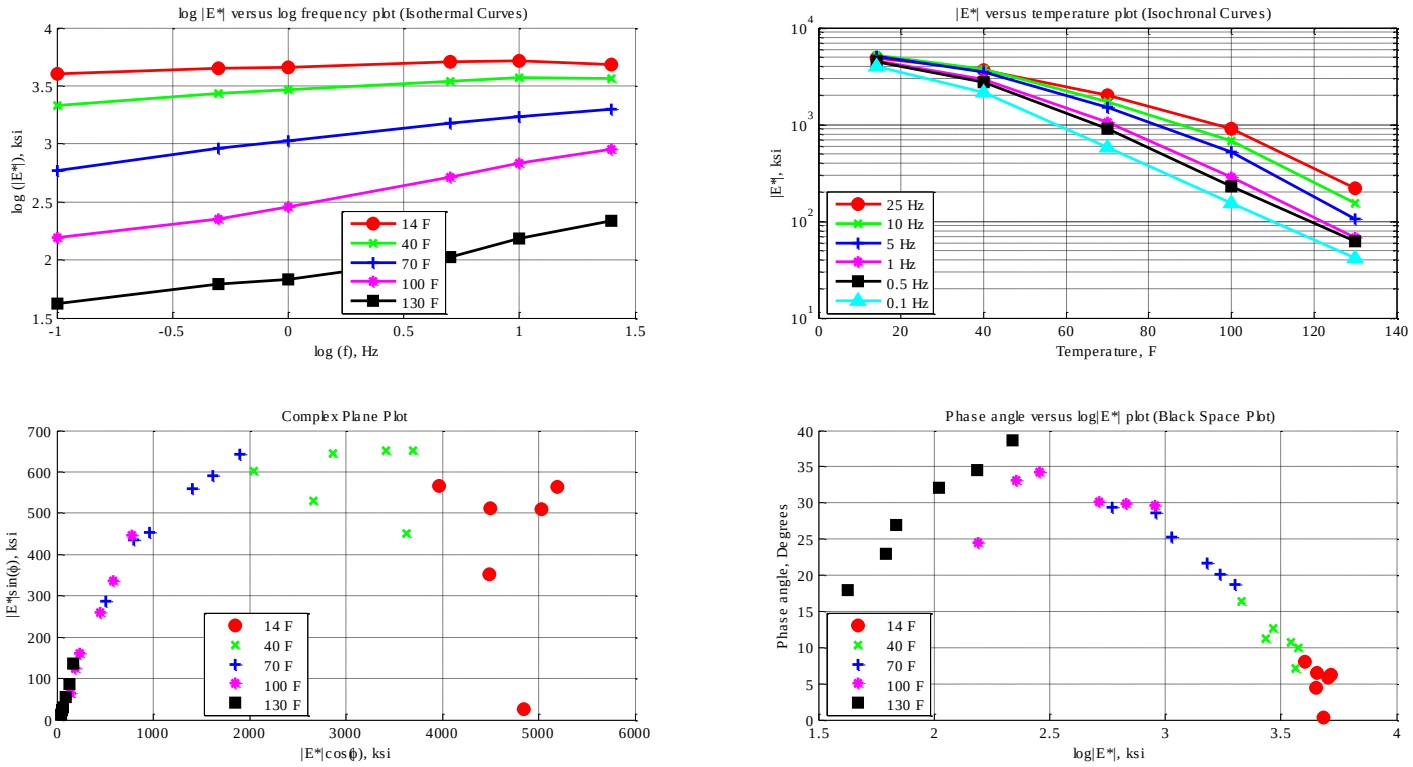

Figure C-58 Isothermal curves or |E*| versus frequency plot (top-left), isochronal curves or |E*| versus temperature plot (top-right), complex plane plot (bottom-left), and black space plot (bottom-right) for Mix 19 Specimen 2 in English unit system.

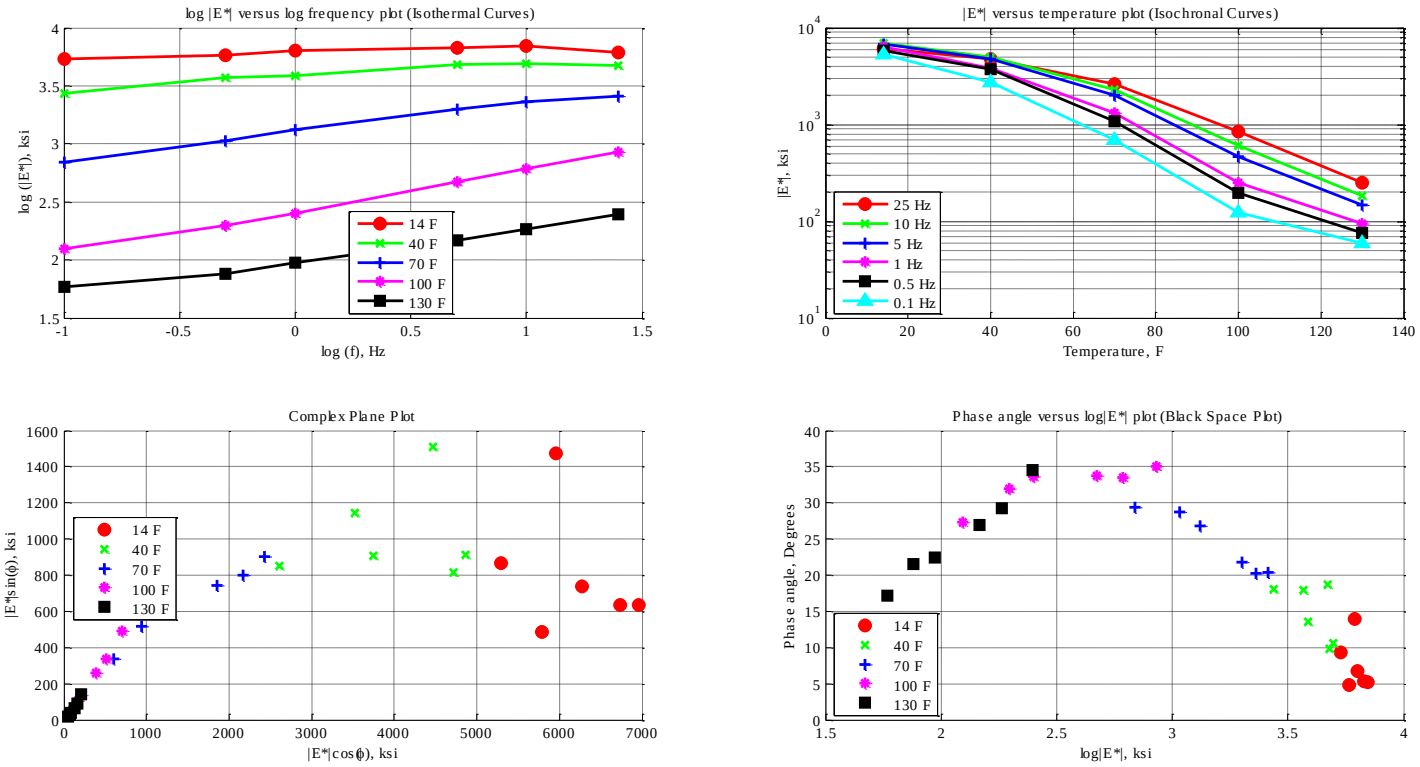

Figure C-59 Isothermal curves or |E*| versus frequency plot (top-left), isochronal curves or |E*| versus temperature plot (top-right), complex plane plot (bottom-left), and black space plot (bottom-right) for Mix 19 Specimen 3 in English unit system.

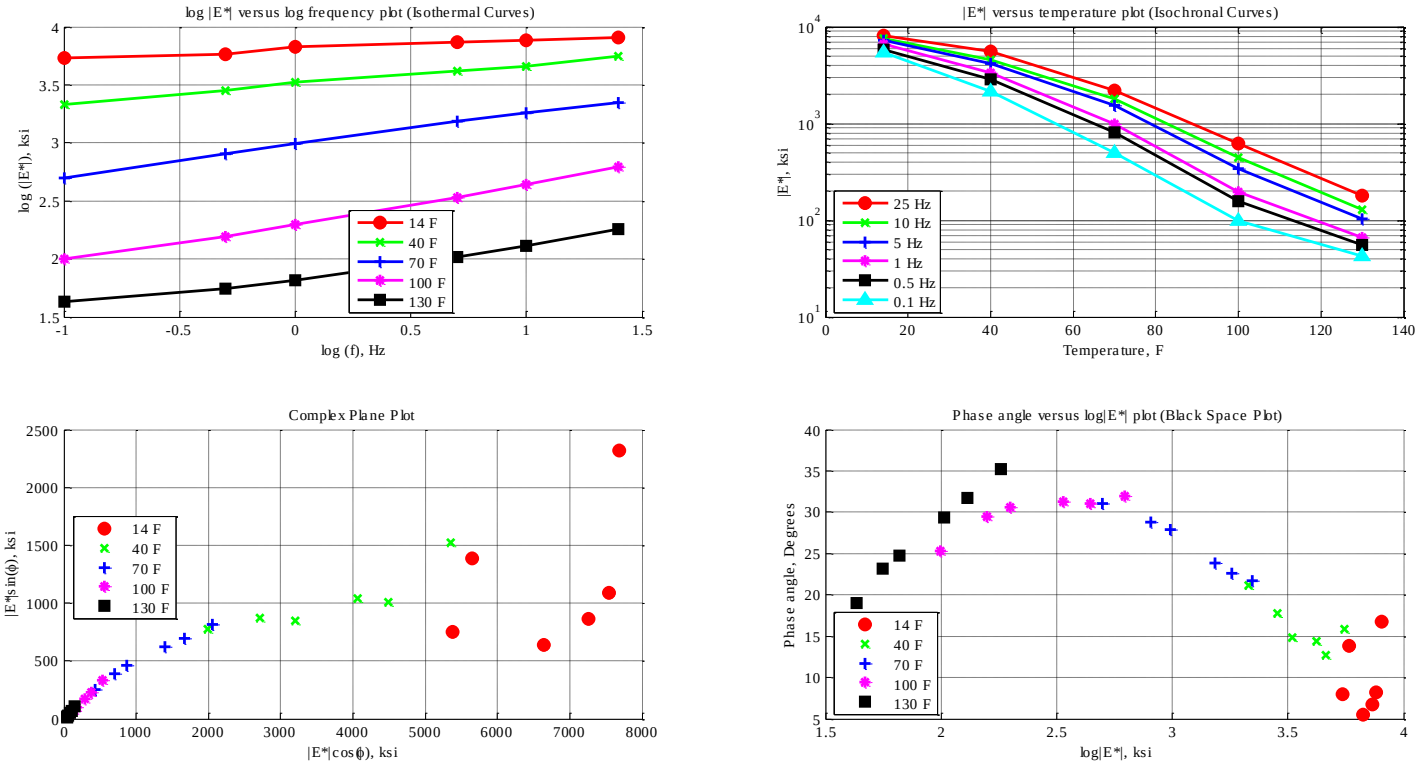

Figure C-60 Isothermal curves or |E*| versus frequency plot (top-left), isochronal curves or |E*| versus temperature plot (top-right), complex plane plot (bottom-left), and black space plot (bottom-right) for Mix 20 Specimen 4 in English unit system.

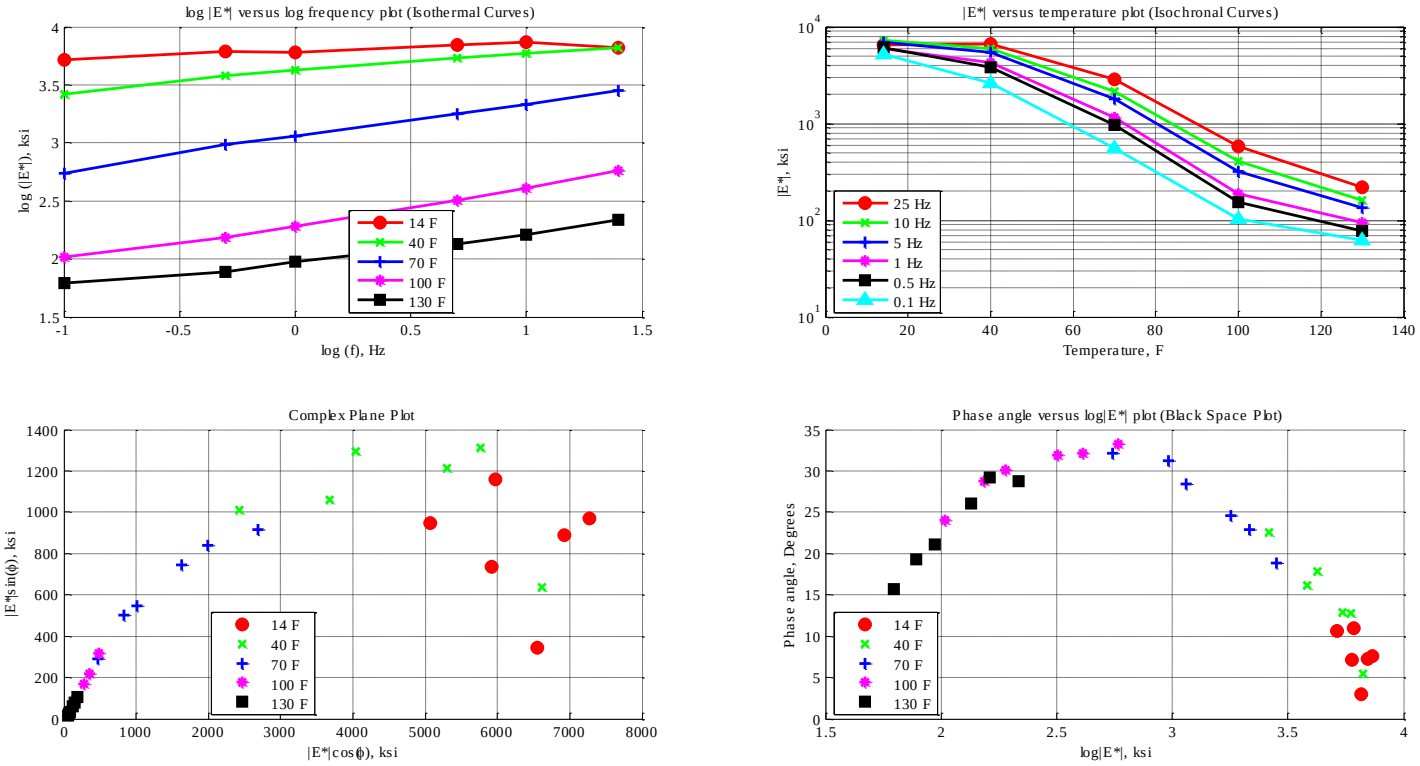

Figure C-61 Isothermal curves or |E*| versus frequency plot (top-left), isochronal curves or |E*| versus temperature plot (top-right), complex plane plot (bottom-left), and black space plot (bottom-right) for Mix 20 Specimen 5 in English unit system.

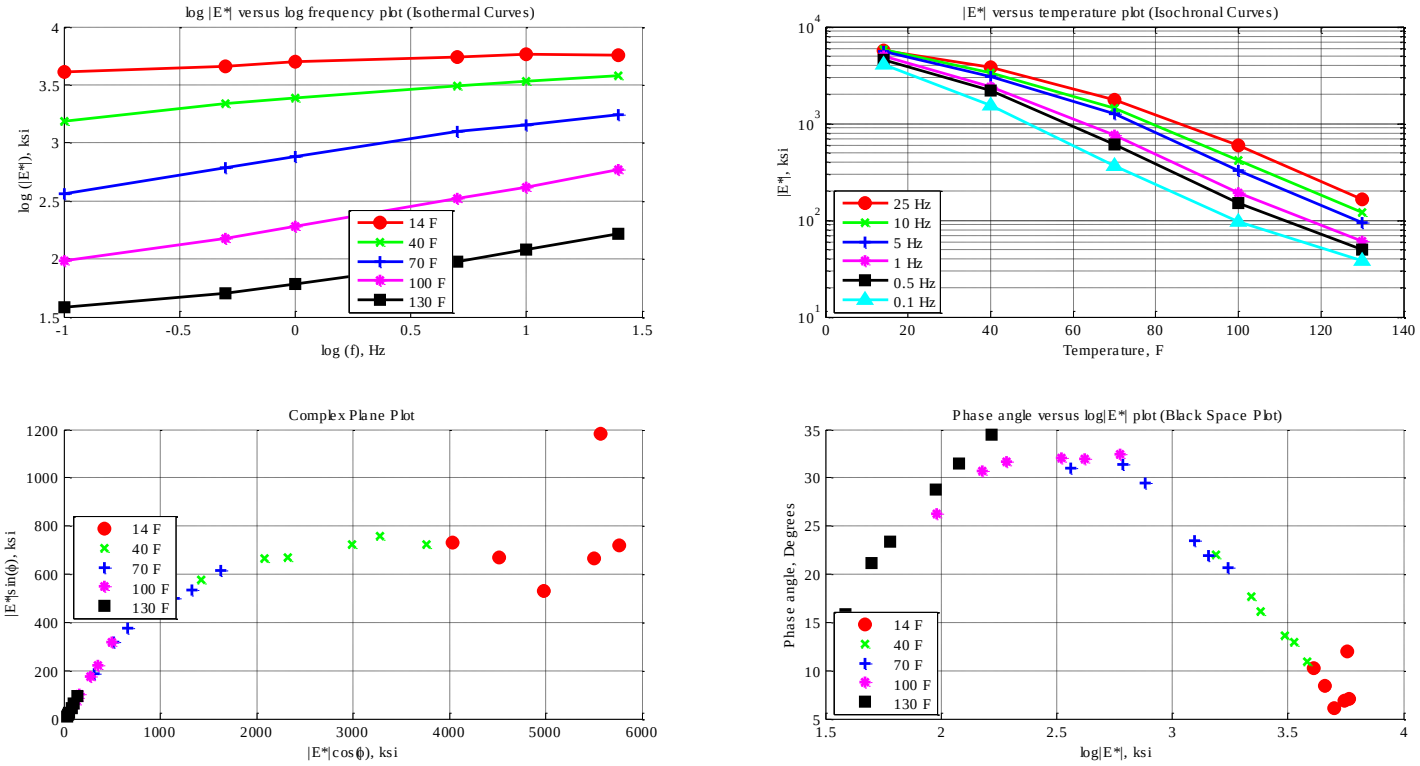

Figure C-62 Isothermal curves or |E*| versus frequency plot (top-left), isochronal curves or |E*| versus temperature plot (top-right), complex plane plot (bottom-left), and black space plot (bottom-right) for Mix 20 Specimen 7 in English unit system.

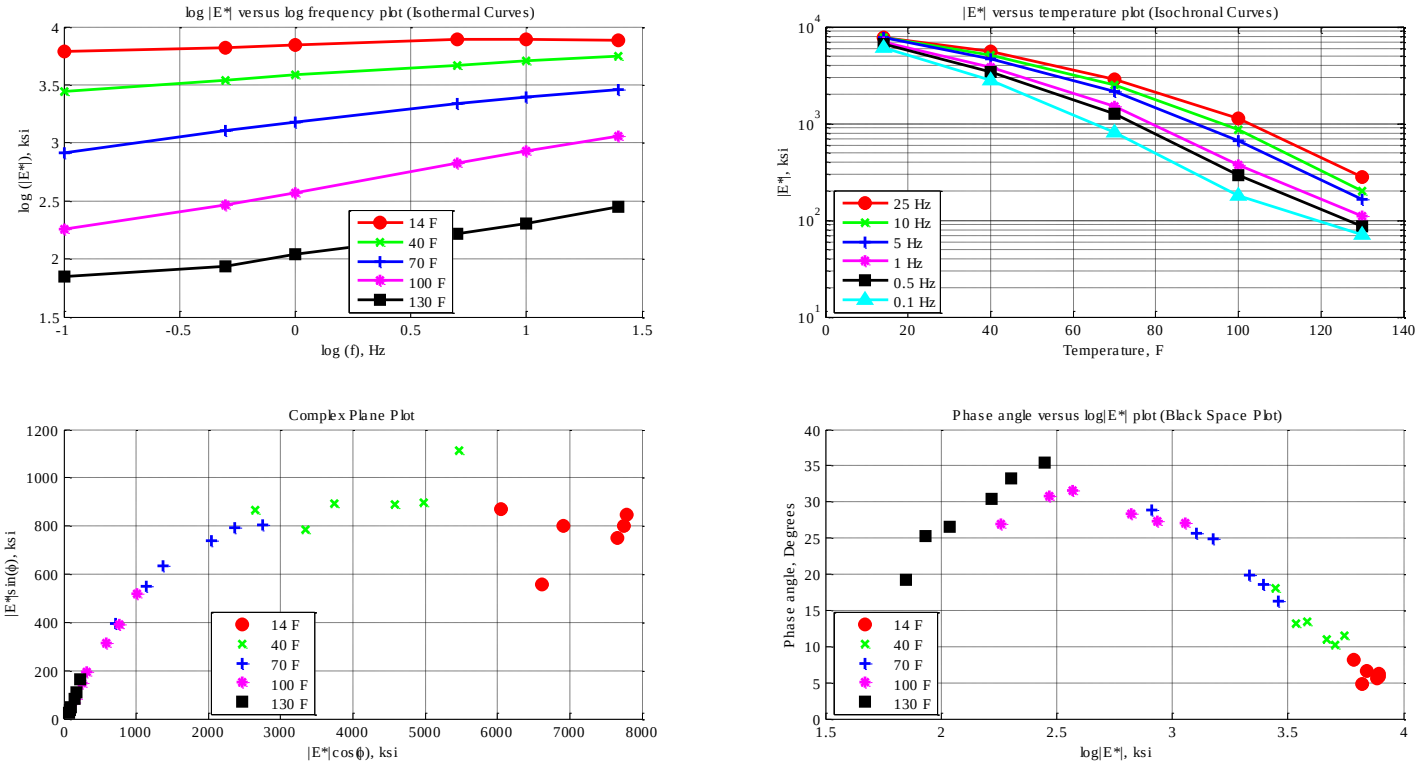

Figure C-63 Isothermal curves or |E*| versus frequency plot (top-left), isochronal curves or |E*| versus temperature plot (top-right), complex plane plot (bottom-left), and black space plot (bottom-right) for Mix 21 Specimen 3 in English unit system.

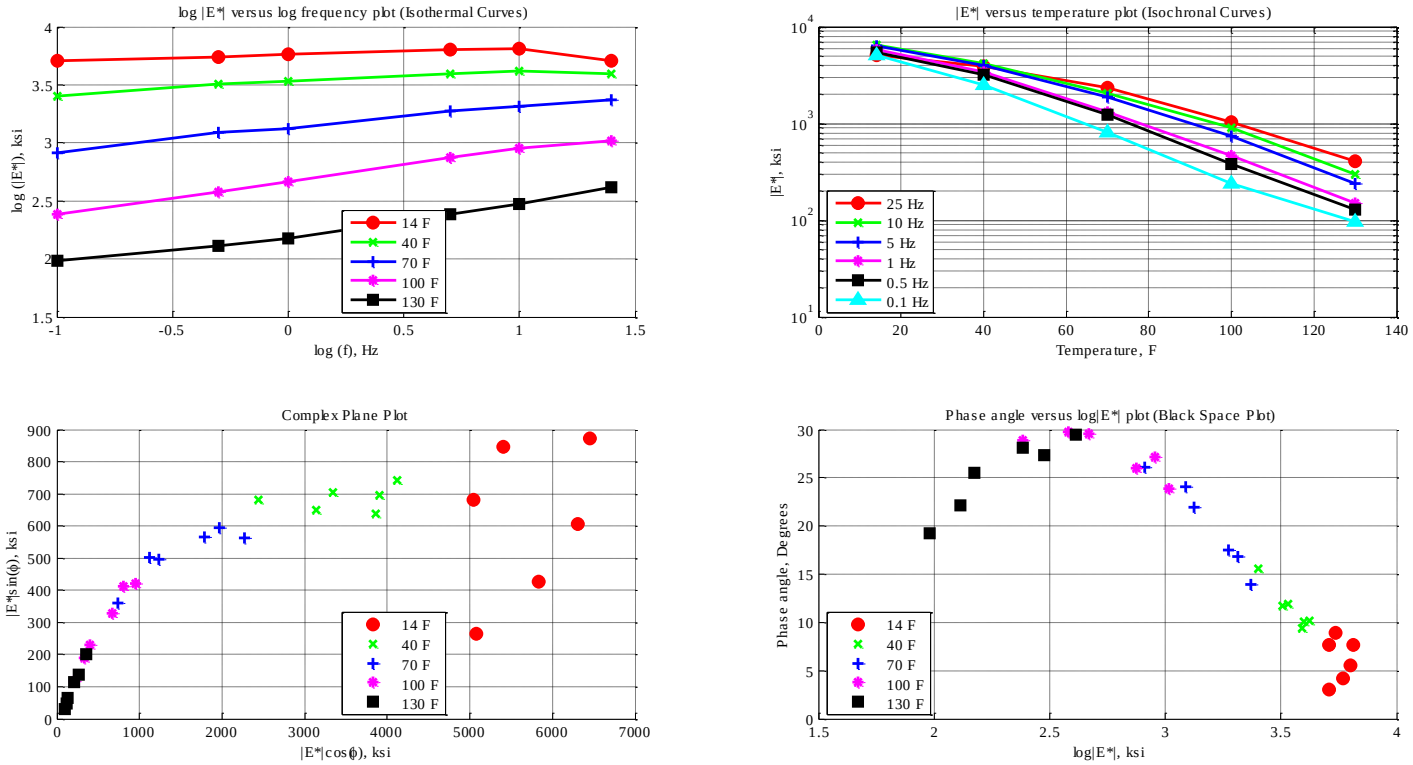

Figure C-64 Isothermal curves or |E*| versus frequency plot (top-left), isochronal curves or |E*| versus temperature plot (top-right), complex plane plot (bottom-left), and black space plot (bottom-right) for Mix 21 Specimen 4 in English unit system.

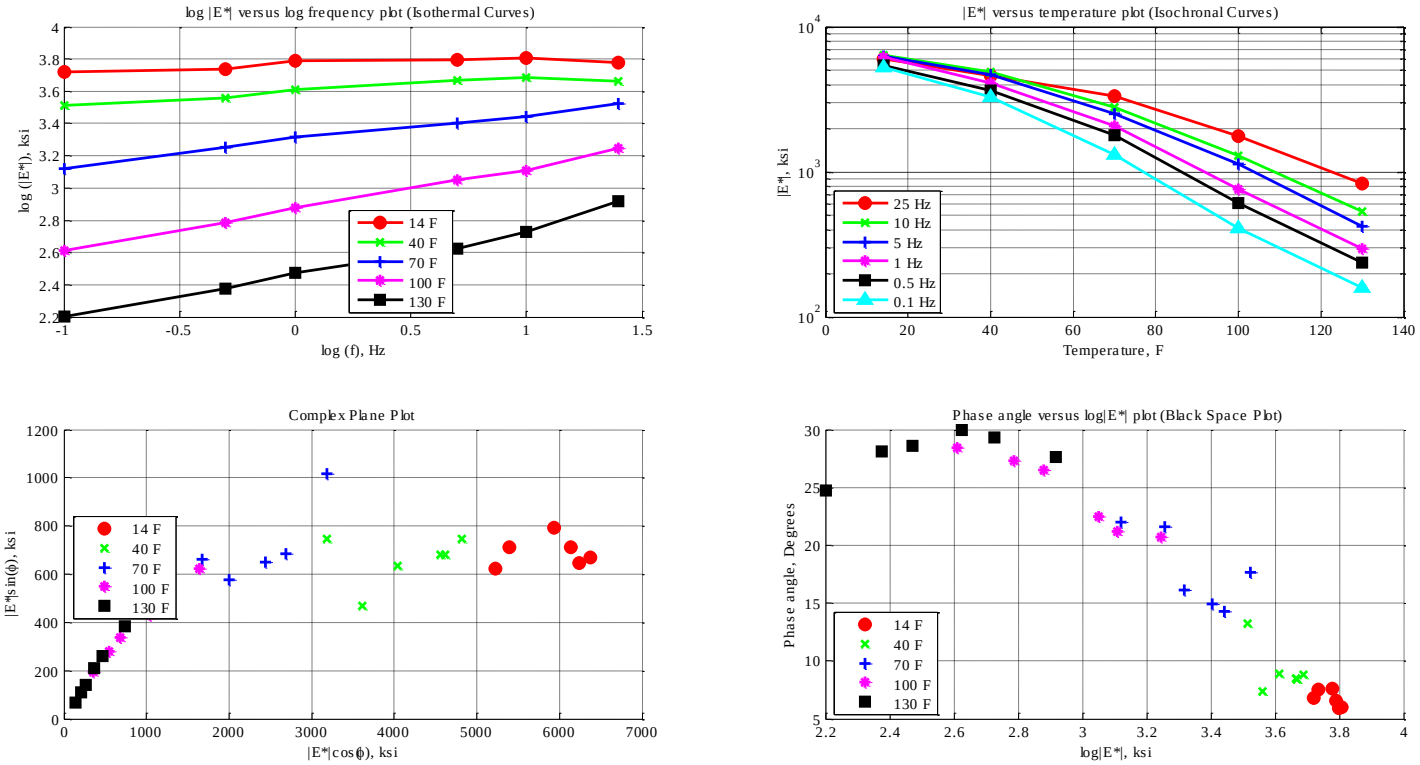

Figure C-65 Isothermal curves or |E*| versus frequency plot (top-left), isochronal curves or |E*| versus temperature plot (top-right), complex plane plot (bottom-left), and black space plot (bottom-right) for Mix 21 Specimen 5 in English unit system.

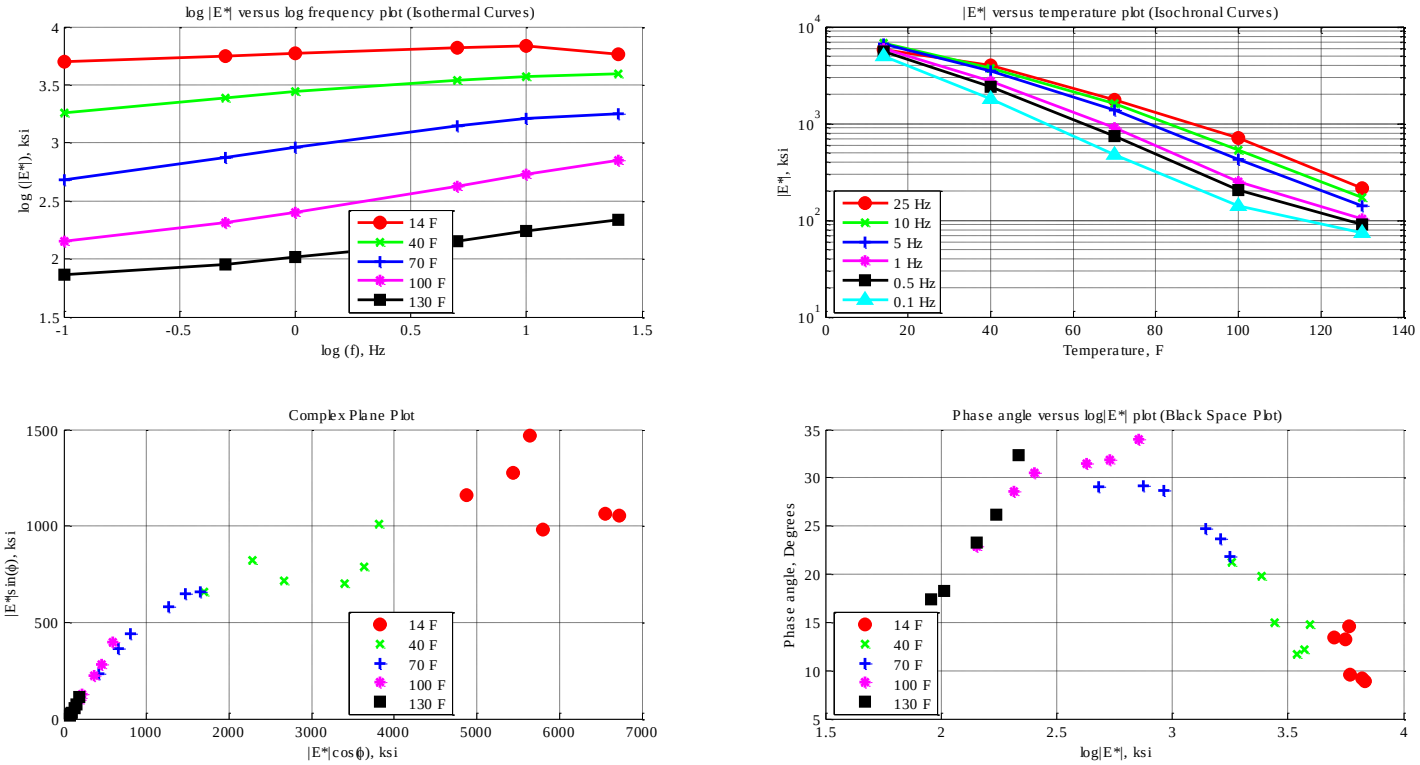

Figure C-66 Isothermal curves or |E*| versus frequency plot (top-left), isochronal curves or |E*| versus temperature plot (top-right), complex plane plot (bottom-left), and black space plot (bottom-right) for Mix 22 Specimen 1 in English unit system.

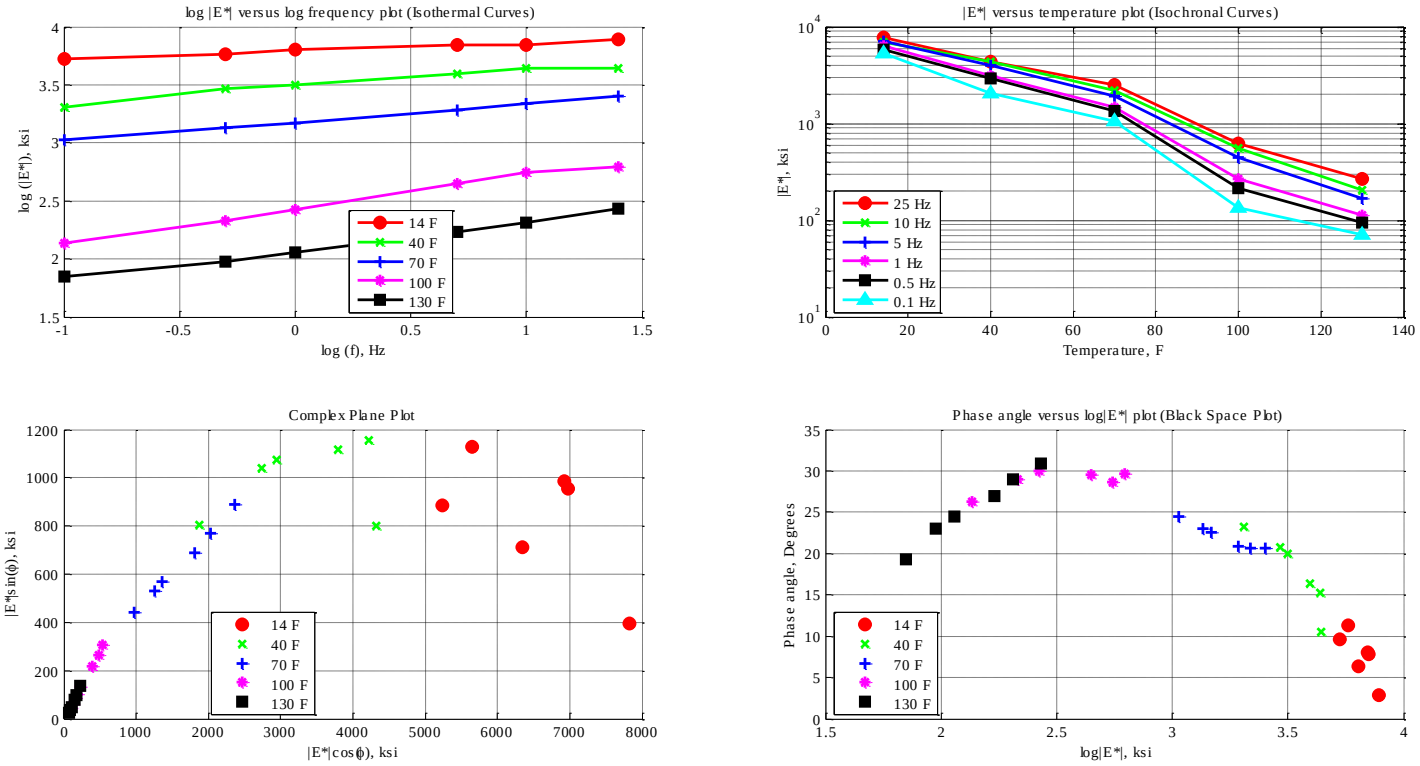

Figure C-67 Isothermal curves or |E*| versus frequency plot (top-left), isochronal curves or |E*| versus temperature plot (top-right), complex plane plot (bottom-left), and black space plot (bottom-right) for Mix 22 Specimen 2 in English unit system.

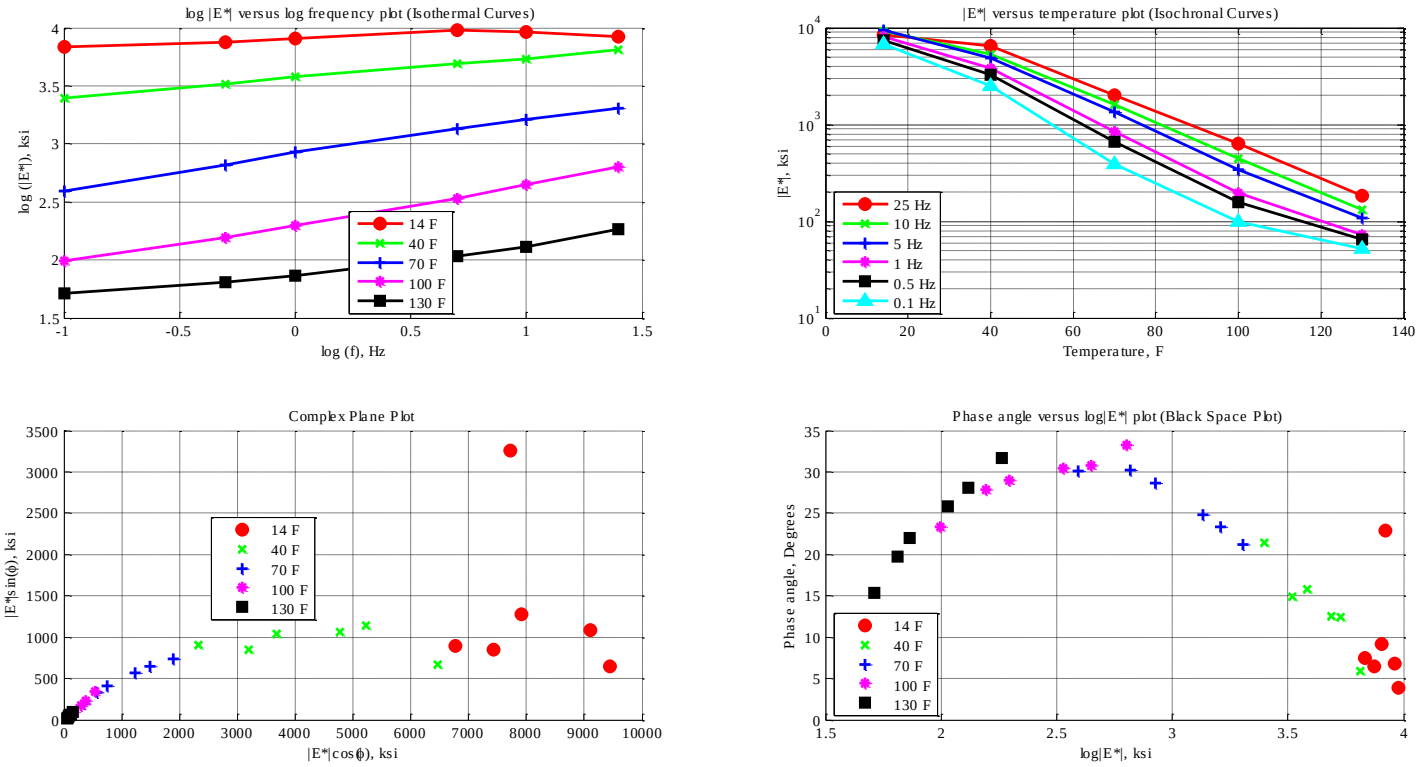

Figure C-68 Isothermal curves or |E*| versus frequency plot (top-left), isochronal curves or |E*| versus temperature plot (top-right), complex plane plot (bottom-left), and black space plot (bottom-right) for Mix 22 Specimen 3 in English unit system.

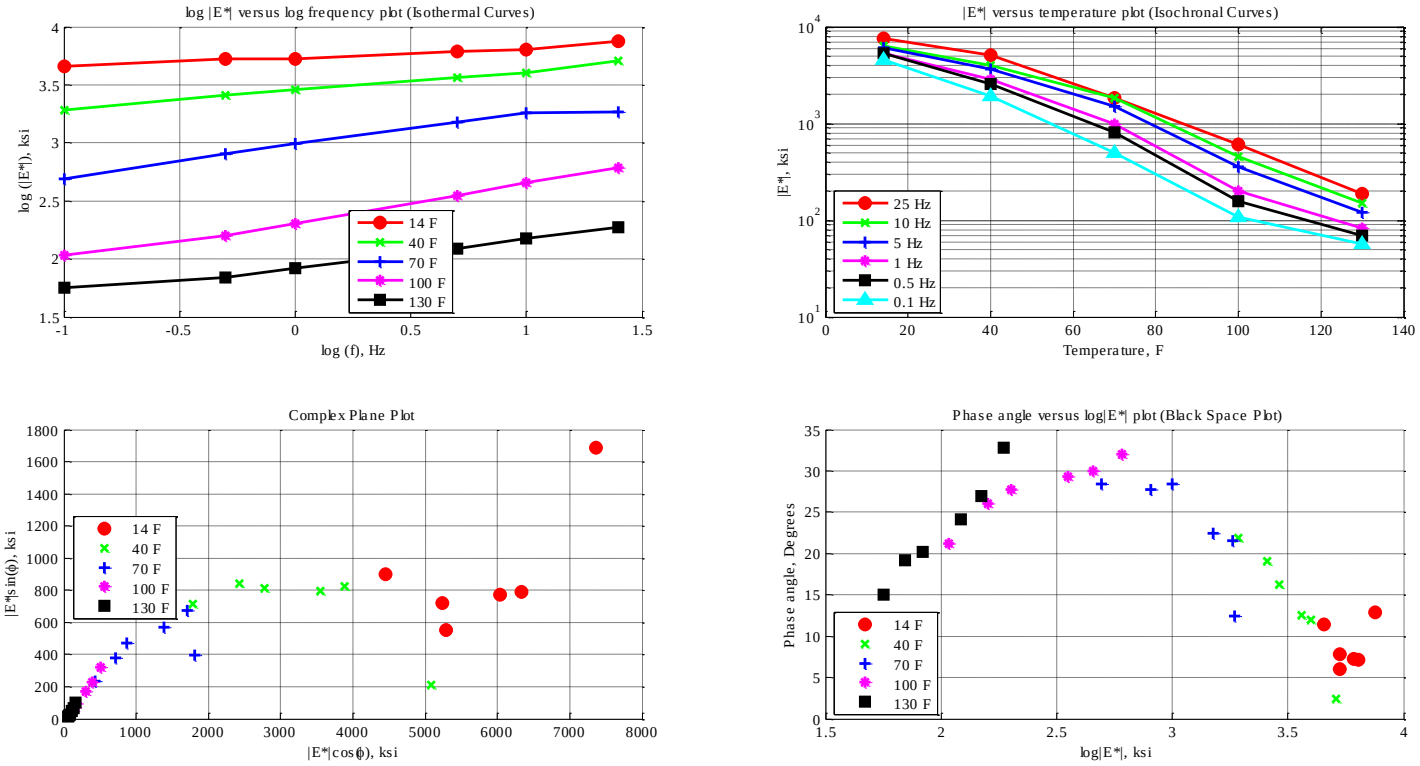

Figure C-69 Isothermal curves or |E*| versus frequency plot (top-left), isochronal curves or |E*| versus temperature plot (top-right), complex plane plot (bottom-left), and black space plot (bottom-right) for Mix 23 Specimen 4 in English unit system.

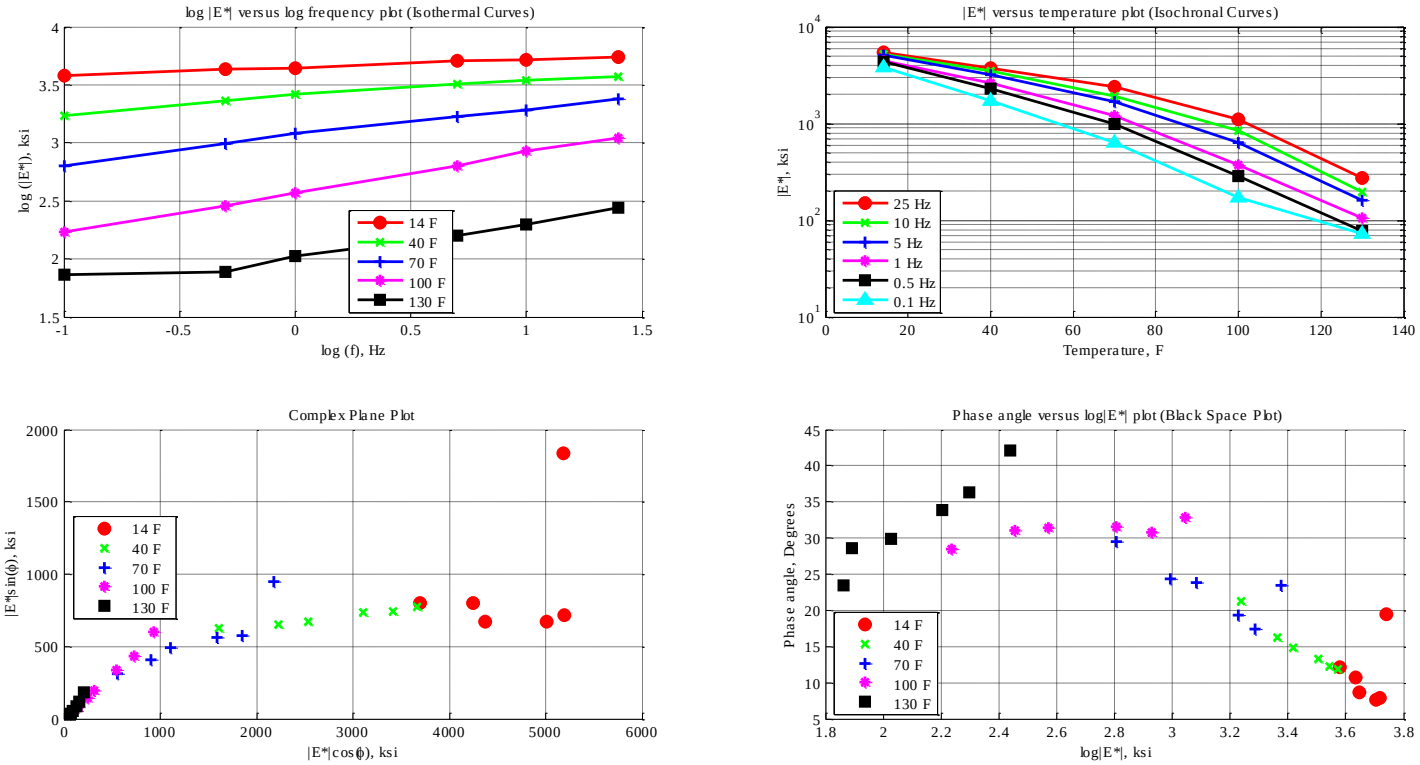

Figure C-70 Isothermal curves or |E*| versus frequency plot (top-left), isochronal curves or |E*| versus temperature plot (top-right), complex plane plot (bottom-left), and black space plot (bottom-right) for Mix 23 Specimen 5 in English unit system.

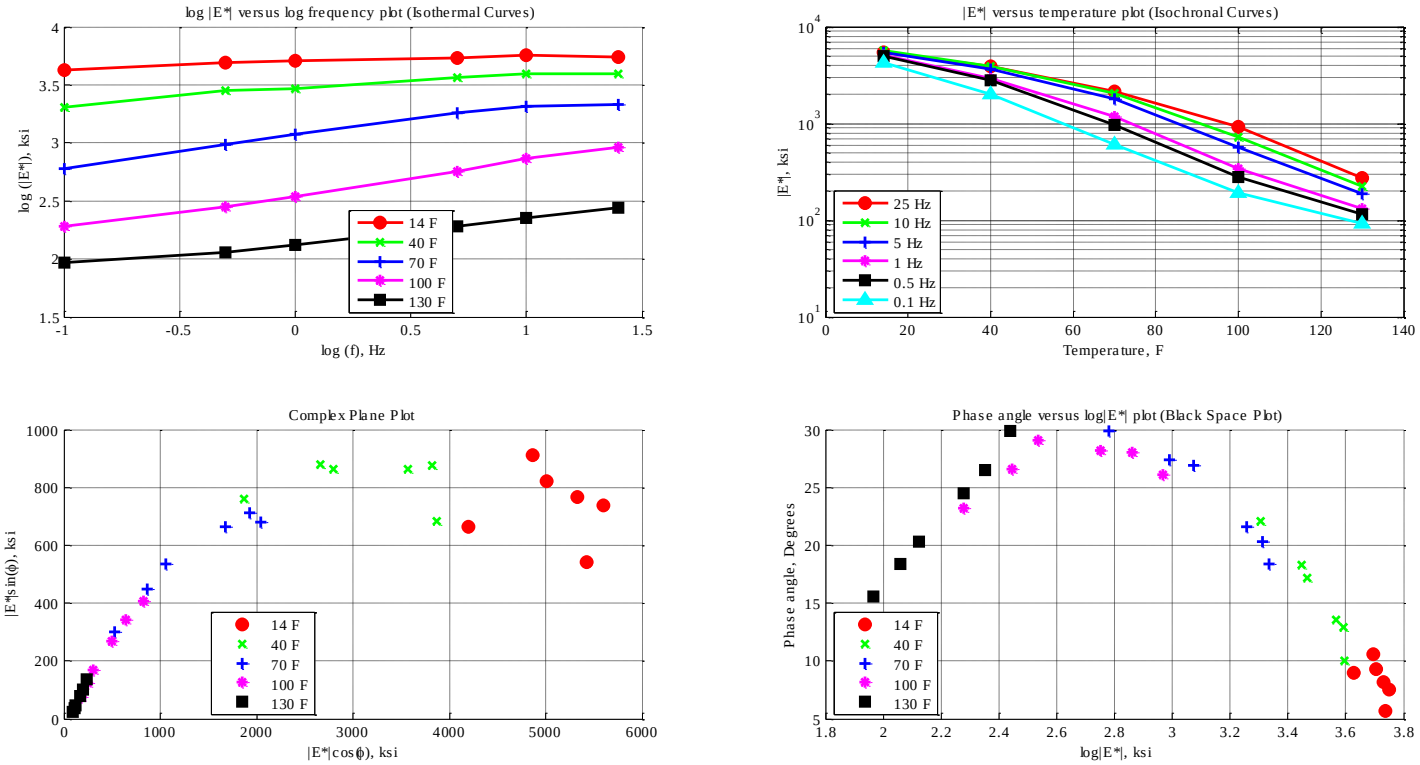

Figure C-71 Isothermal curves or |E*| versus frequency plot (top-left), isochronal curves or |E*| versus temperature plot (top-right), complex plane plot (bottom-left), and black space plot (bottom-right) for Mix 23 Specimen 6 in English unit system.

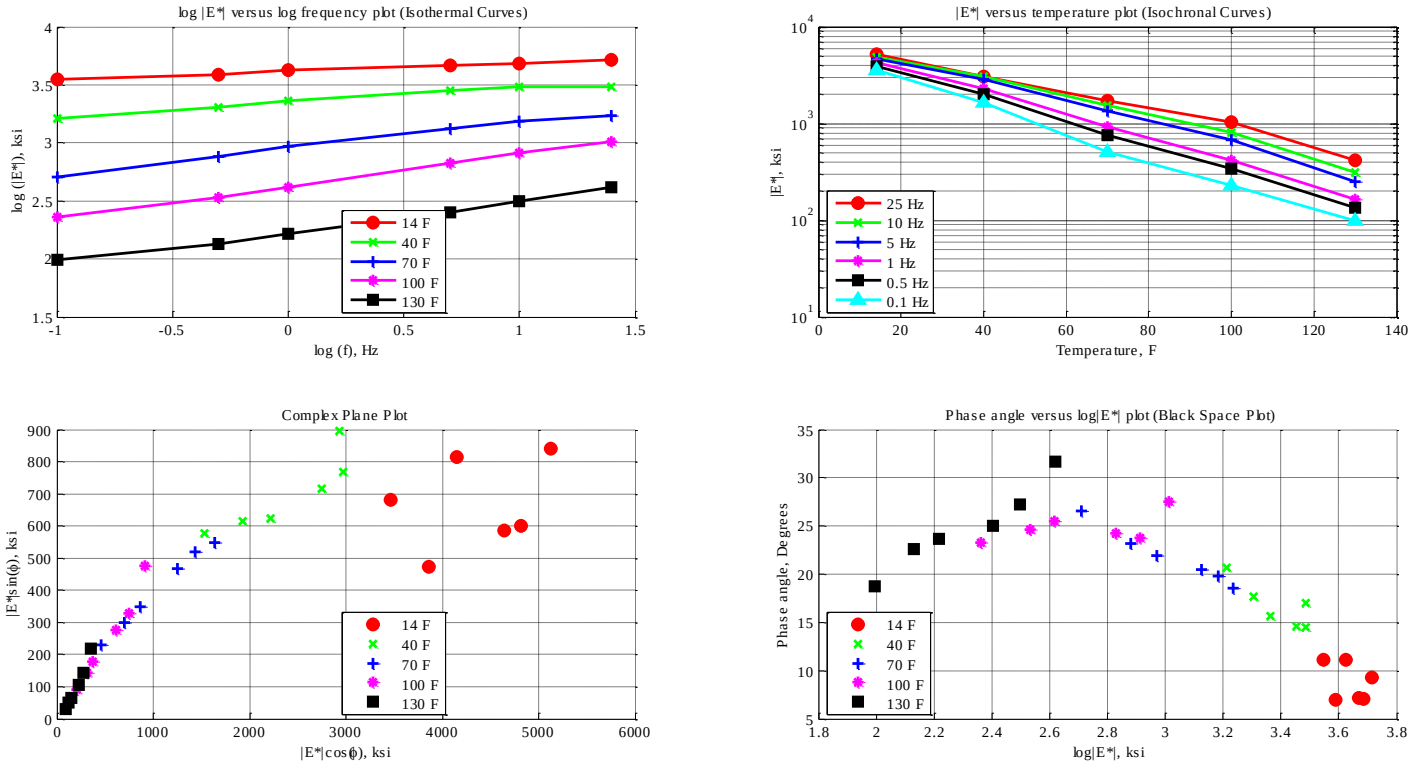

Figure C-72 Isothermal curves or |E*| versus frequency plot (top-left), isochronal curves or |E*| versus temperature plot (top-right), complex plane plot (bottom-left), and black space plot (bottom-right) for Mix 23 Specimen 8 in English unit system.

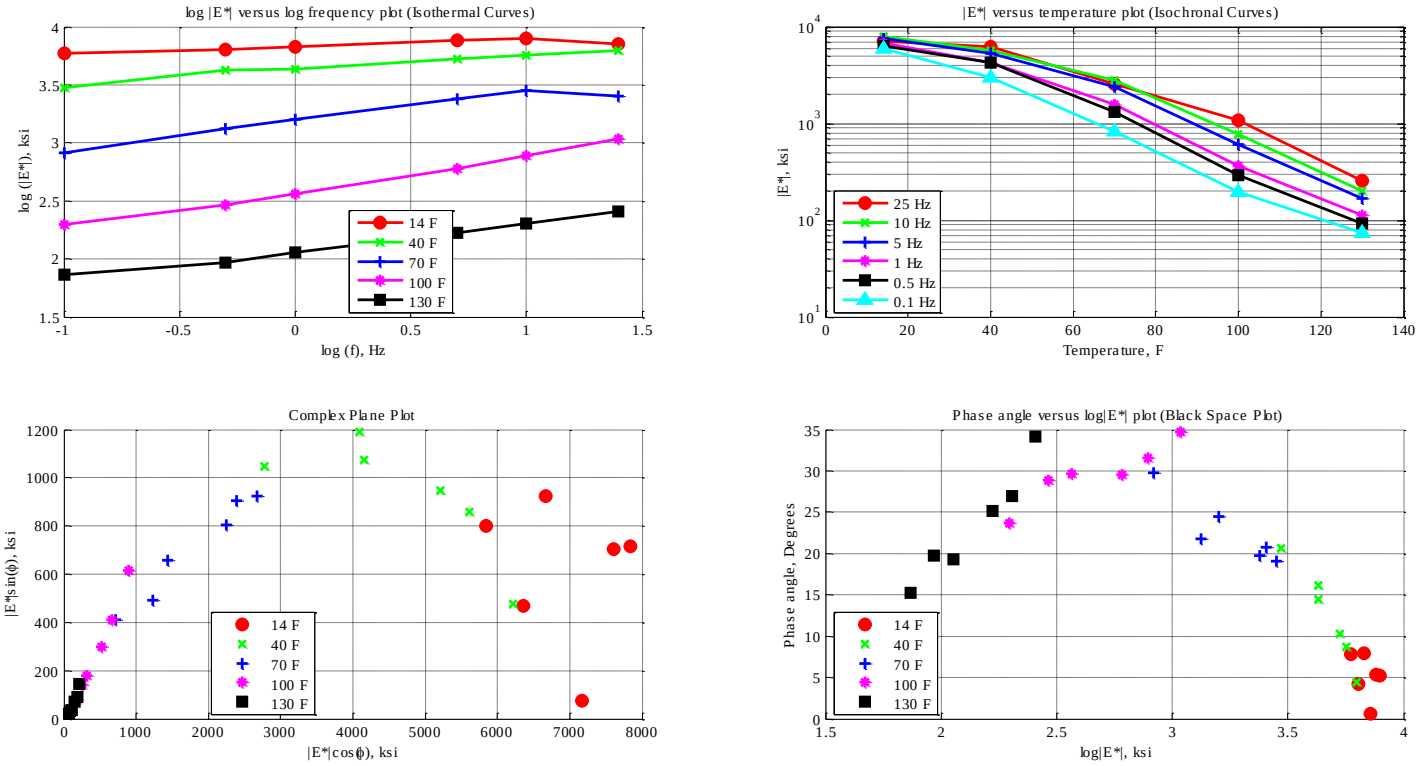

Figure C-73 Isothermal curves or |E*| versus frequency plot (top-left), isochronal curves or |E*| versus temperature plot (top-right), complex plane plot (bottom-left), and black space plot (bottom-right) for Mix 24 Specimen 1 in English unit system.

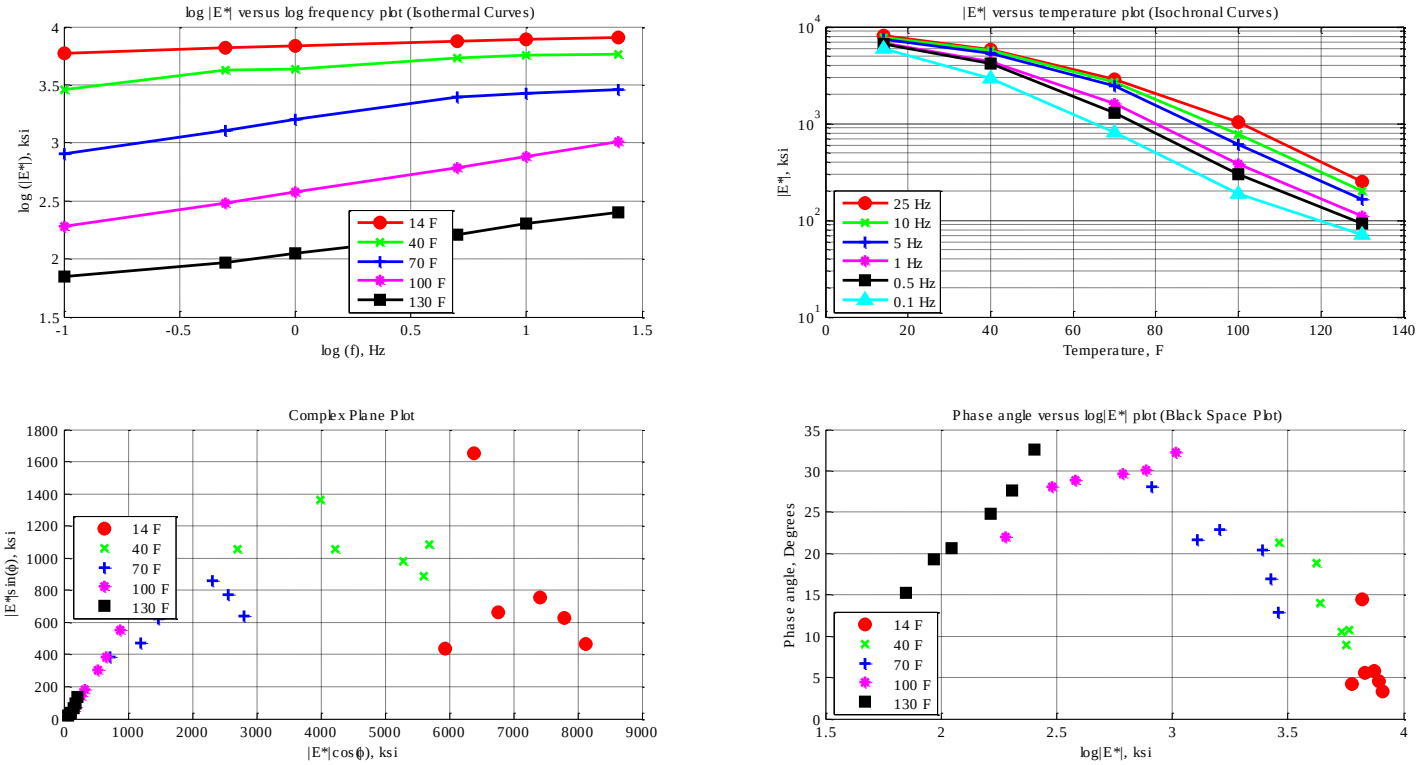

Figure C-74 Isothermal curves or |E*| versus frequency plot (top-left), isochronal curves or |E*| versus temperature plot (top-right), complex plane plot (bottom-left), and black space plot (bottom-right) for Mix 24 Specimen 2 in English unit system.

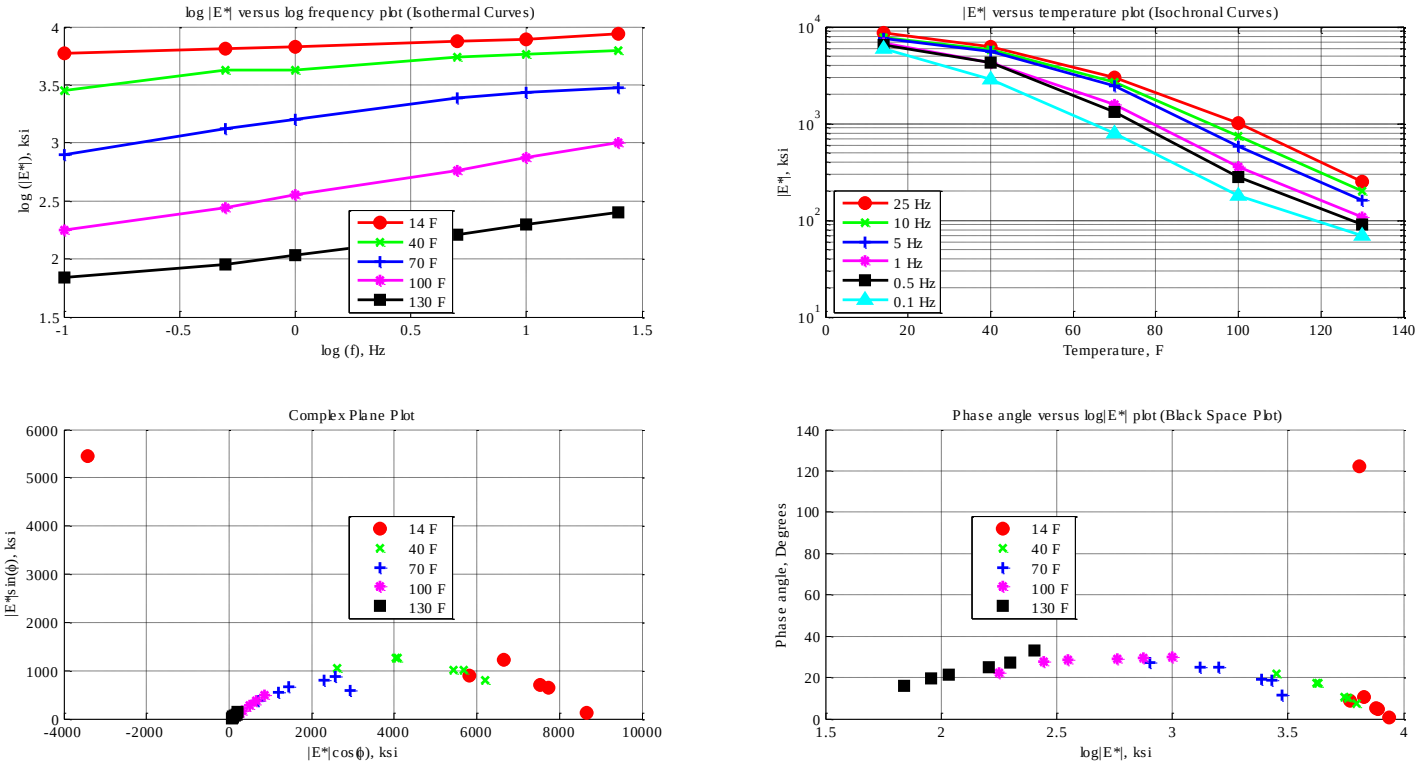

Figure C-75 Isothermal curves or |E*| versus frequency plot (top-left), isochronal curves or |E*| versus temperature plot (top-right), complex plane plot (bottom-left), and black space plot (bottom-right) for Mix 24 Specimen 3 in English unit system.

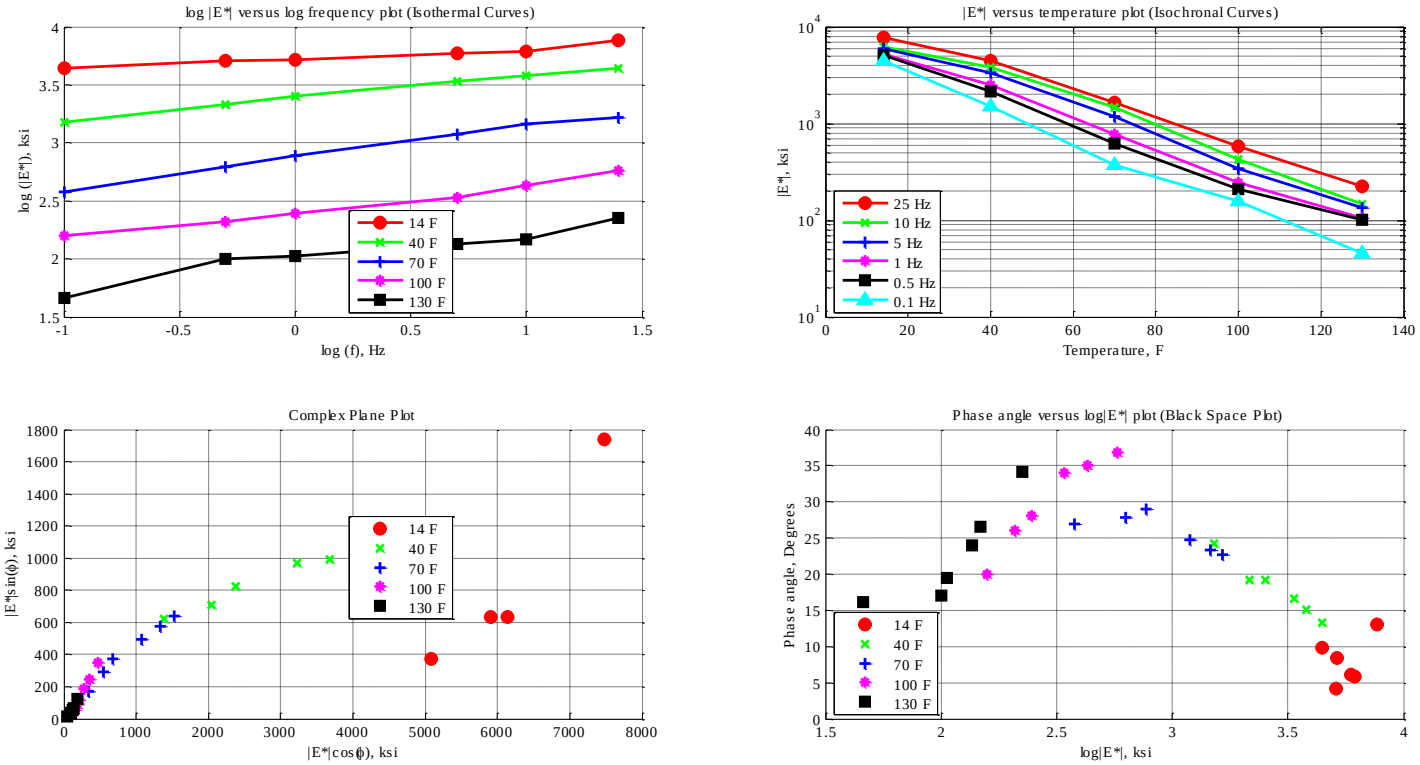

Figure C-76 Isothermal curves or |E*| versus frequency plot (top-left), isochronal curves or |E*| versus temperature plot (top-right), complex plane plot (bottom-left), and black space plot (bottom-right) for Mix 25 Specimen 1 in English unit system.

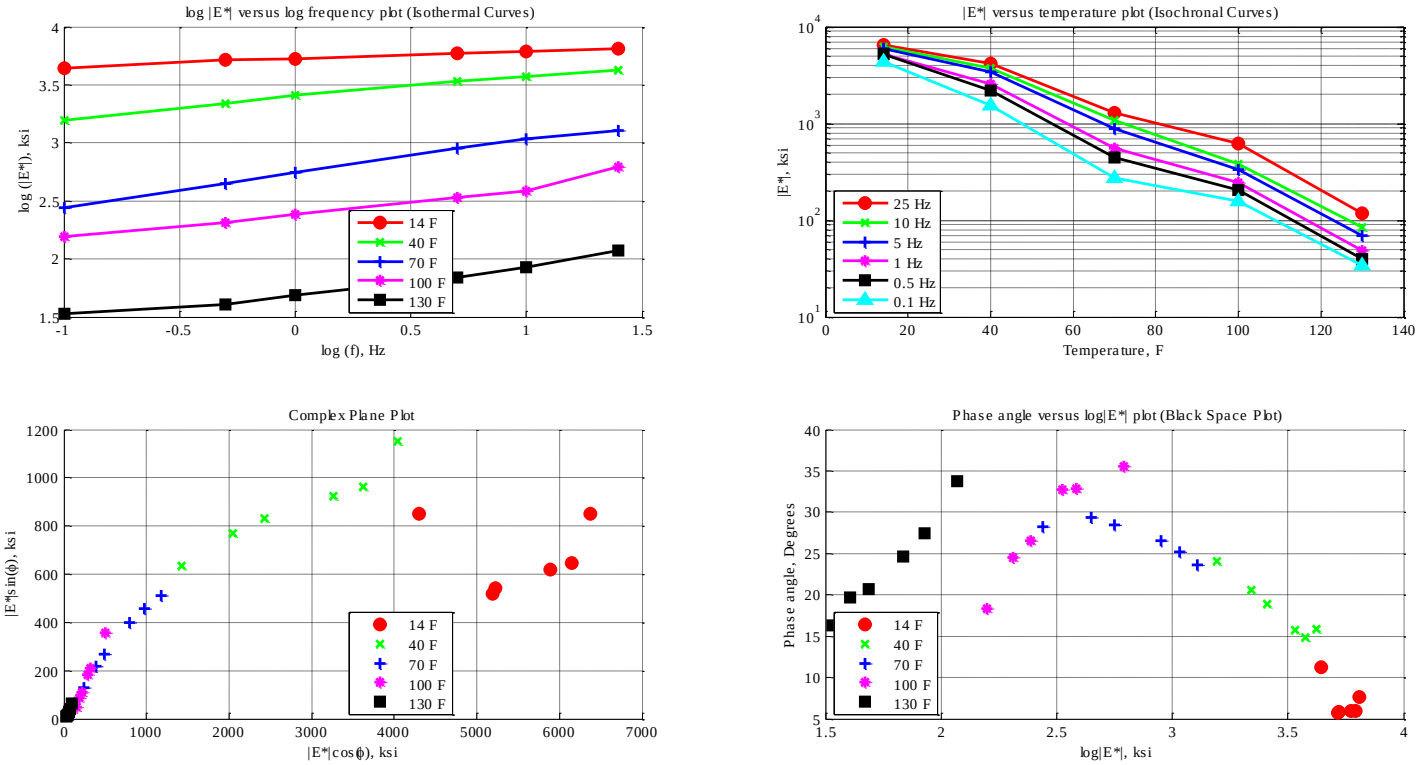

Figure C-77 Isothermal curves or |E*| versus frequency plot (top-left), isochronal curves or |E*| versus temperature plot (top-right), complex plane plot (bottom-left), and black space plot (bottom-right) for Mix 25 Specimen 2 in English unit system.

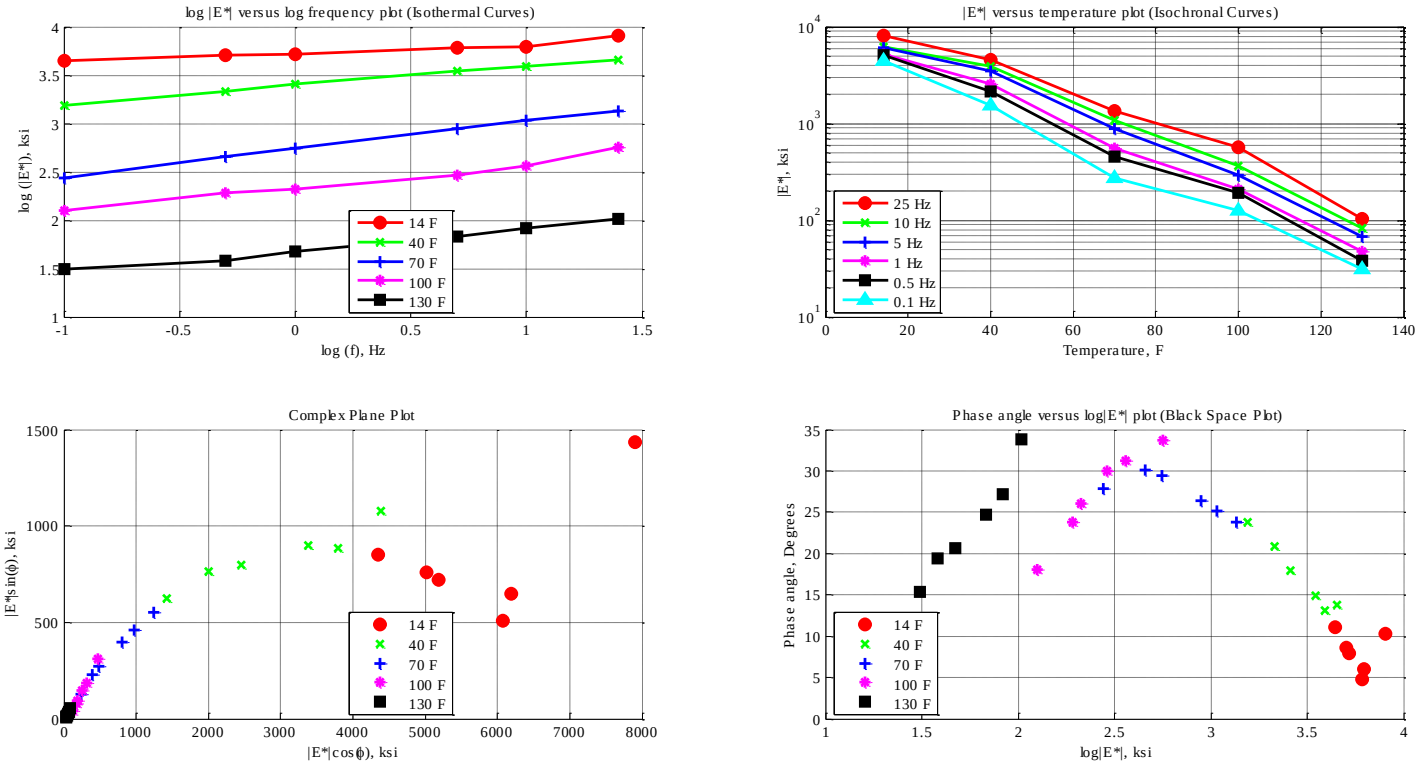

Figure C-78 Isothermal curves or |E*| versus frequency plot (top-left), isochronal curves or |E*| versus temperature plot (top-right), complex plane plot (bottom-left), and black space plot (bottom-right) for Mix 25 Specimen 3 in English unit system.

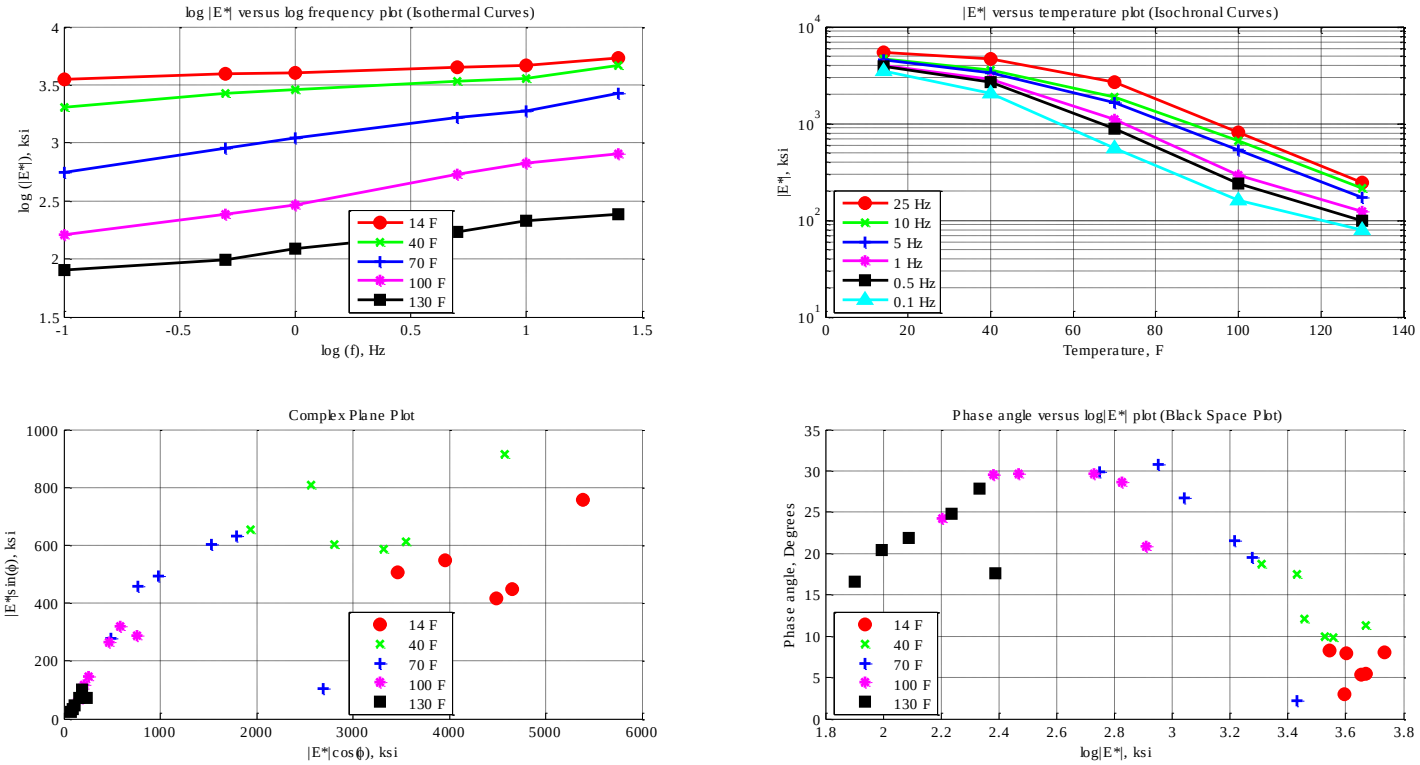

Figure C-79 Isothermal curves or |E*| versus frequency plot (top-left), isochronal curves or |E*| versus temperature plot (top-right), complex plane plot (bottom-left), and black space plot (bottom-right) for Mix 26 Specimen 4 in English unit system.

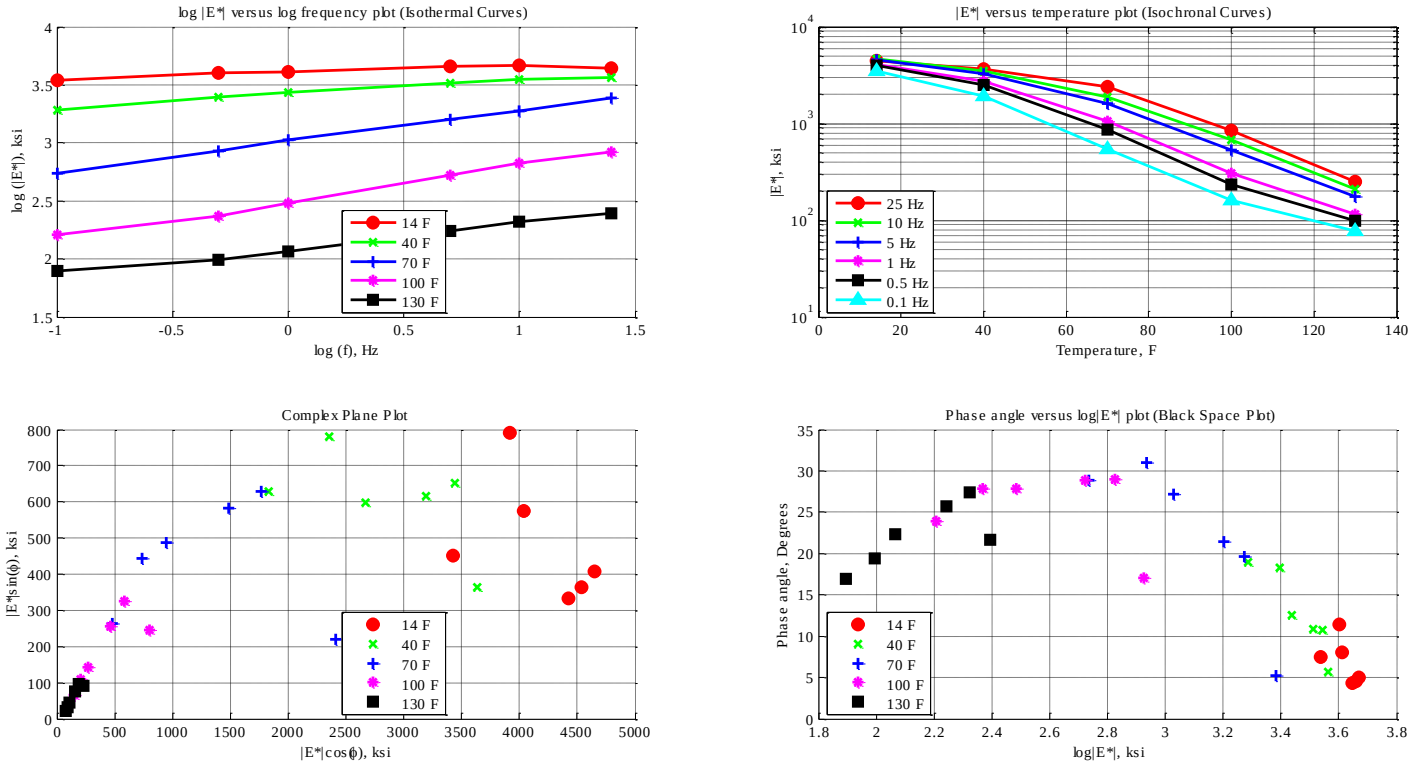

Figure C-80 Isothermal curves or |E*| versus frequency plot (top-left), isochronal curves or |E*| versus temperature plot (top-right), complex plane plot (bottom-left), and black space plot (bottom-right) for Mix 26 Specimen 5 in English unit system.

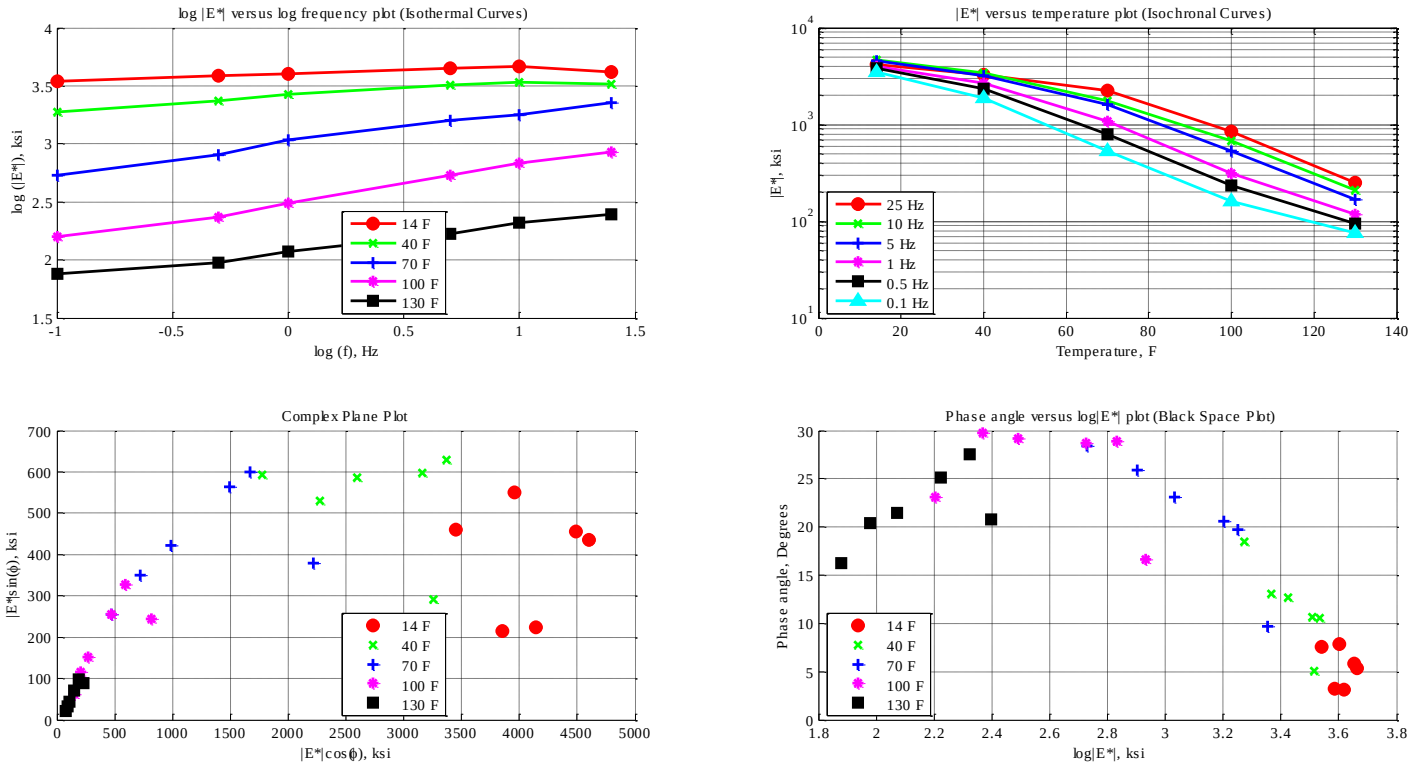

Figure C-81 Isothermal curves or |E*| versus frequency plot (top-left), isochronal curves or |E*| versus temperature plot (top-right), complex plane plot (bottom-left), and black space plot (bottom-right) for Mix 26 Specimen 6 in English unit system.

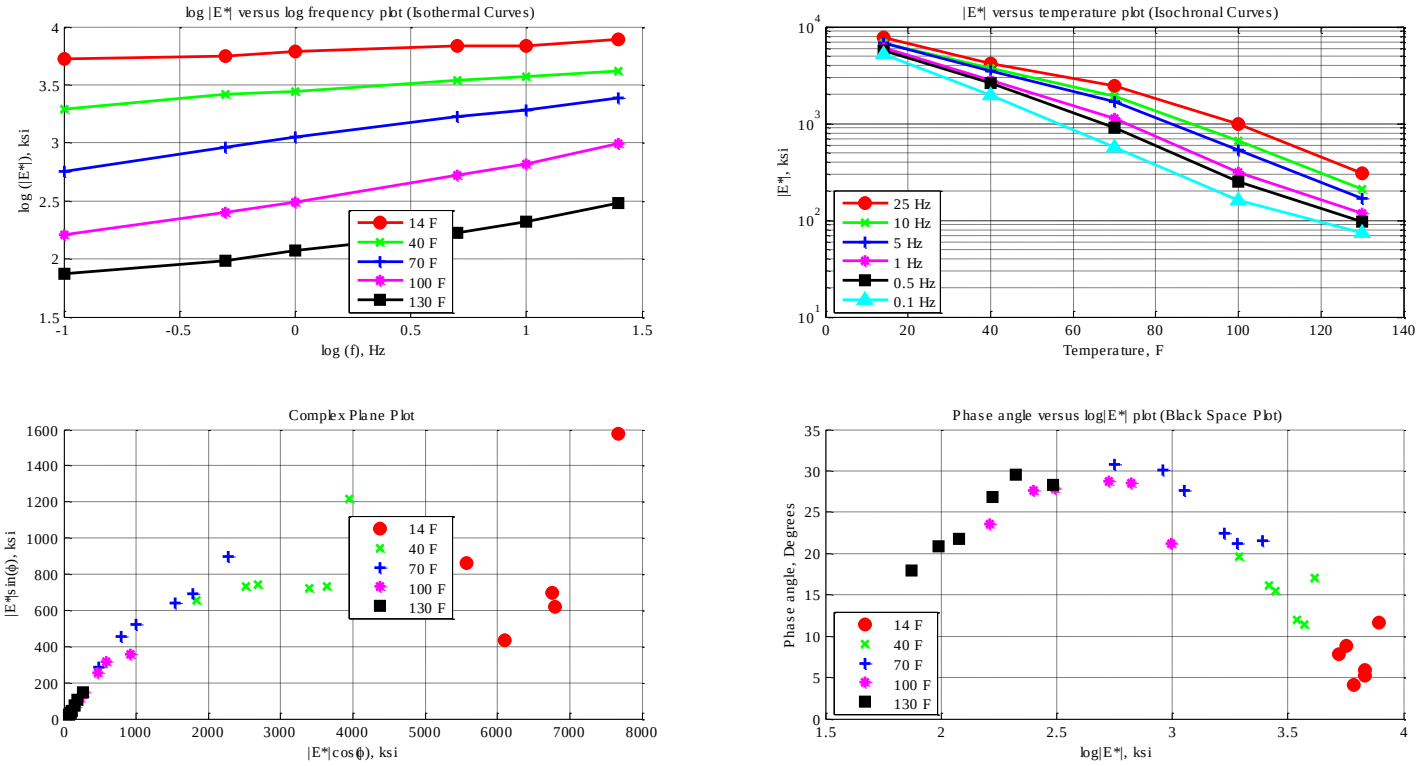

Figure C-82 Isothermal curves or |E*| versus frequency plot (top-left), isochronal curves or |E*| versus temperature plot (top-right), complex plane plot (bottom-left), and black space plot (bottom-right) for Mix 27 Specimen 1 in English unit system.

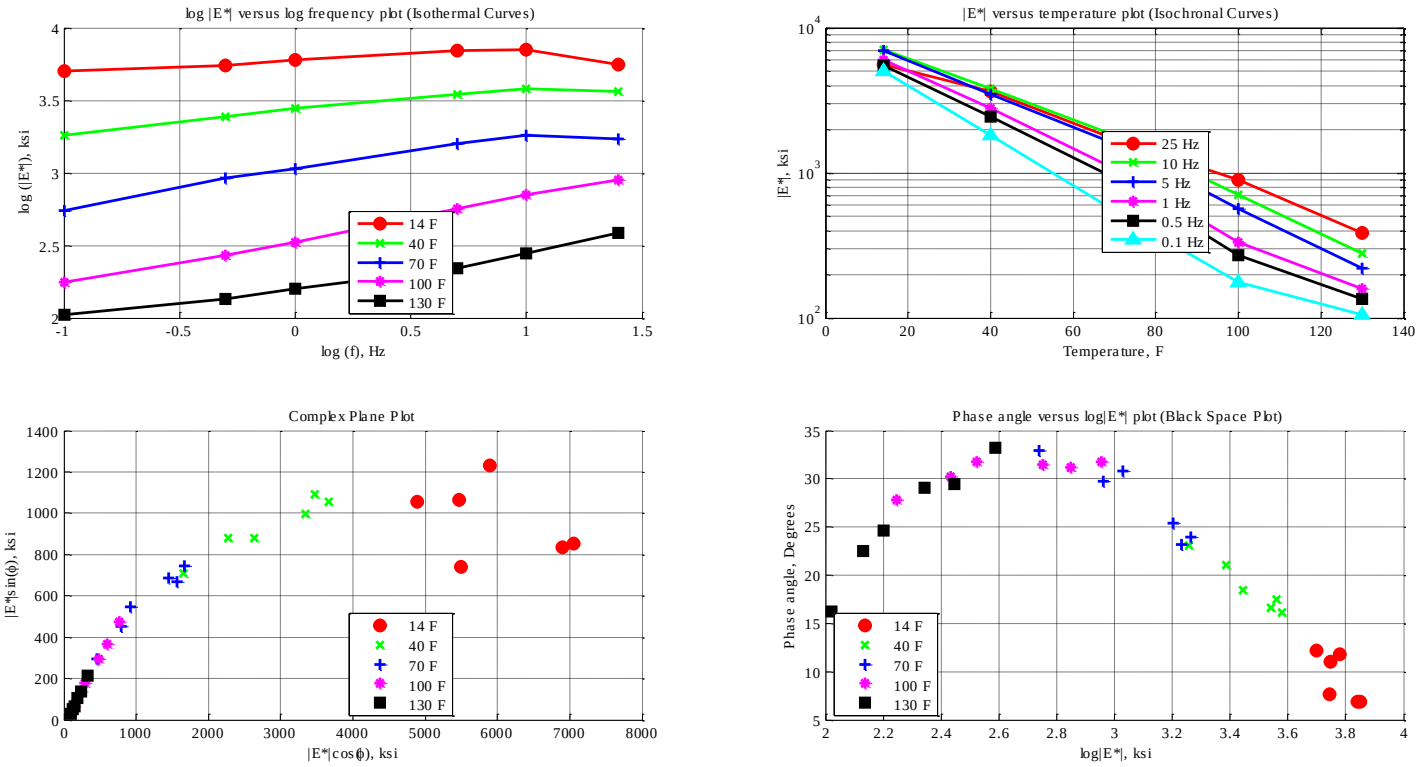

Figure C-83 Isothermal curves or |E*| versus frequency plot (top-left), isochronal curves or |E*| versus temperature plot (top-right), complex plane plot (bottom-left), and black space plot (bottom-right) for Mix 27 Specimen 2 in English unit system.

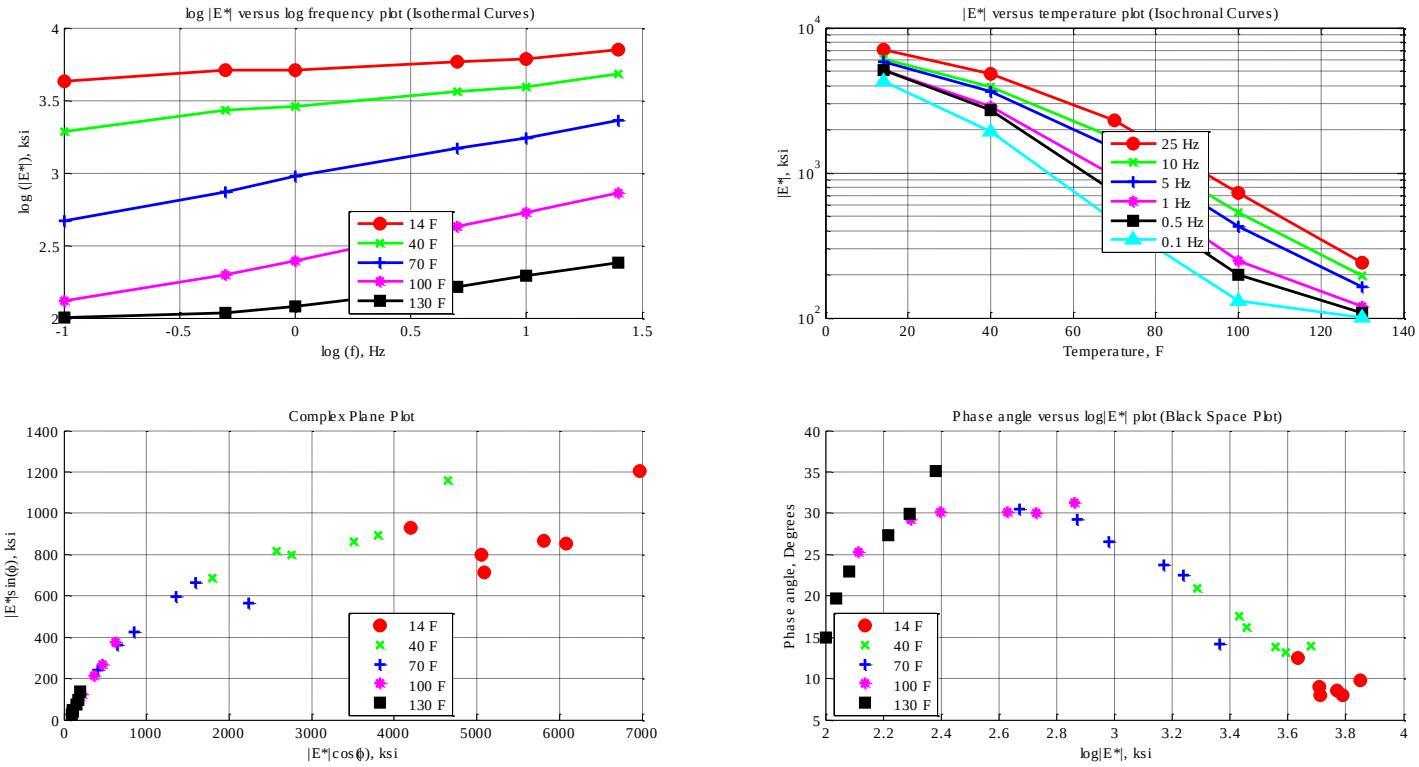

Figure C-84 Isothermal curves or |E*| versus frequency plot (top-left), isochronal curves or |E*| versus temperature plot (top-right), complex plane plot (bottom-left), and black space plot (bottom-right) for Mix 27 Specimen 4 in English unit system.

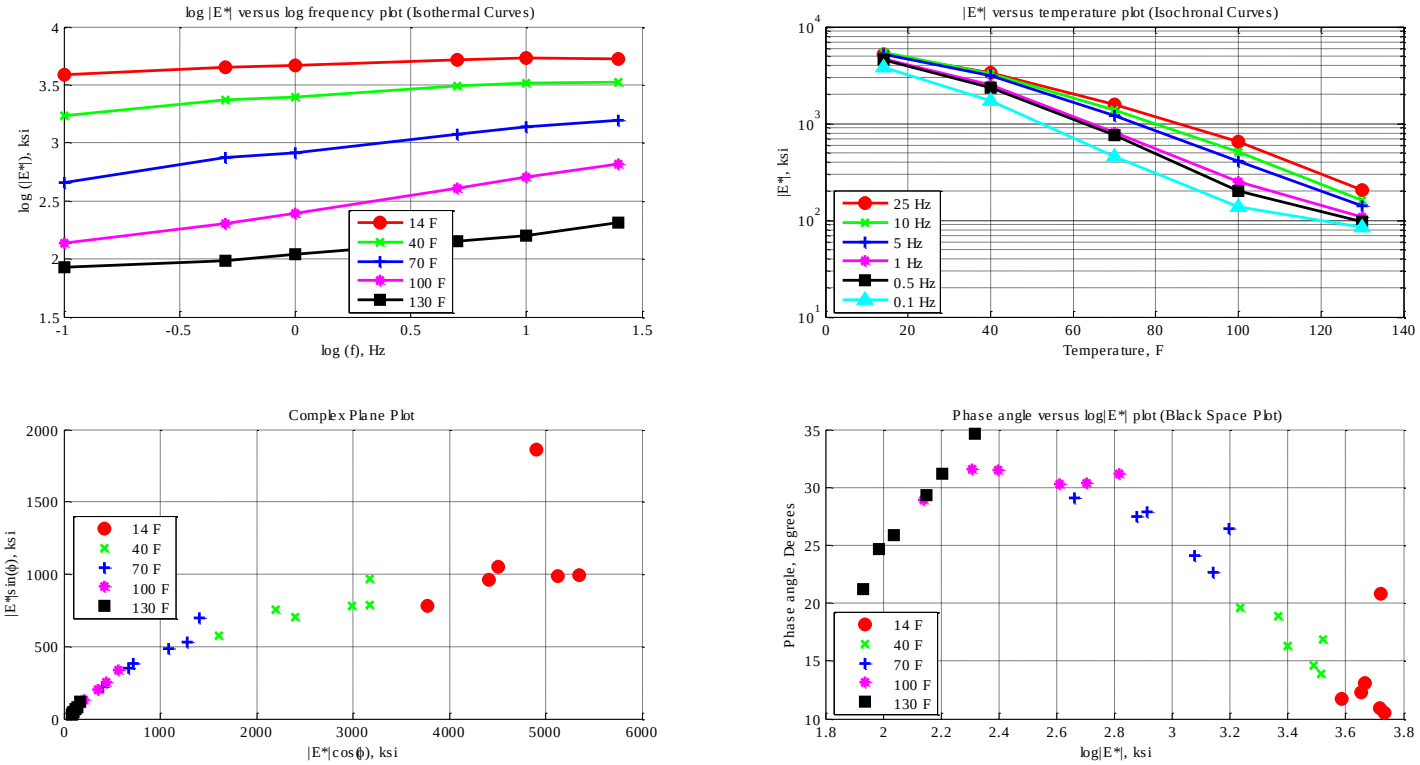

Figure C-85 Isothermal curves or |E*| versus frequency plot (top-left), isochronal curves or |E*| versus temperature plot (top-right), complex plane plot (bottom-left), and black space plot (bottom-right) for Mix 28 Specimen 7 in English unit system.

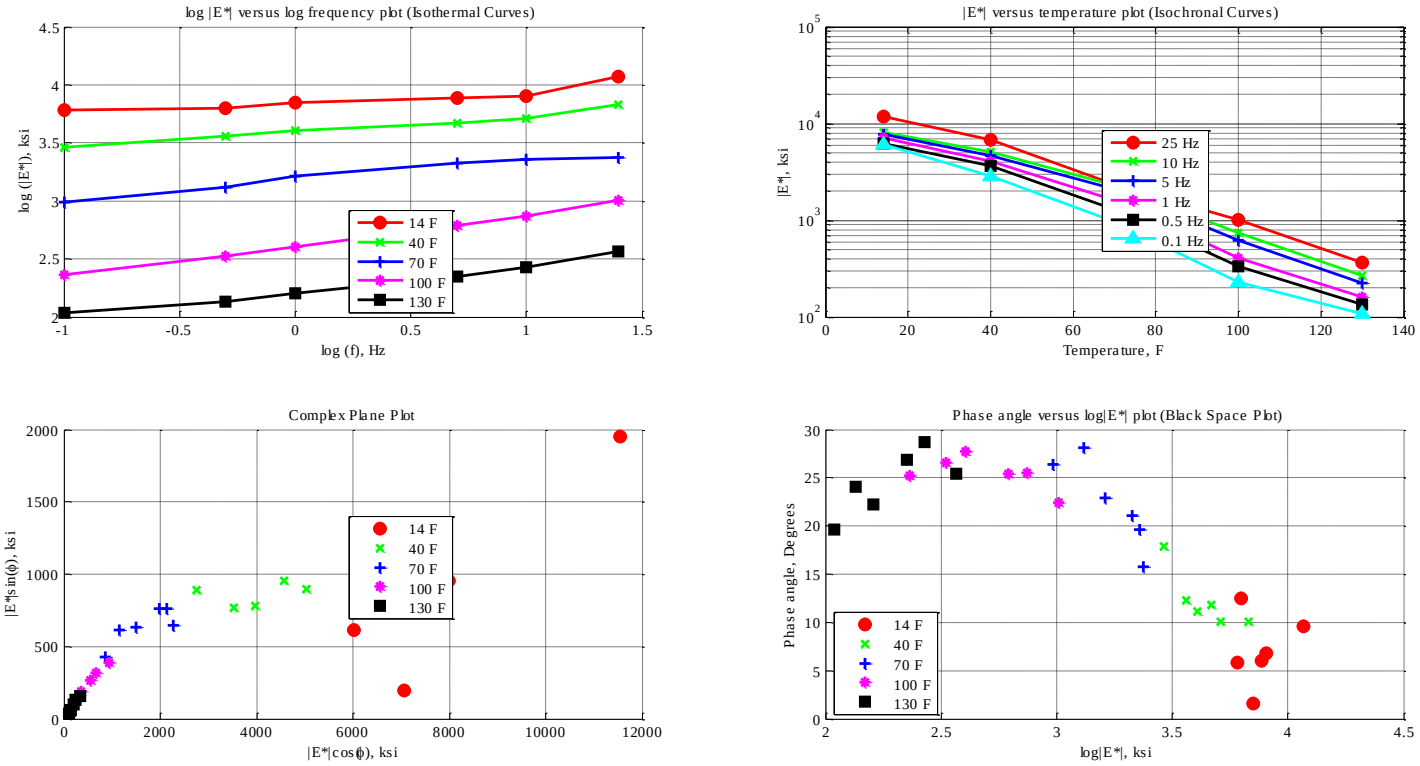

Figure C-86 Isothermal curves or |E*| versus frequency plot (top-left), isochronal curves or |E*| versus temperature plot (top-right), complex plane plot (bottom-left), and black space plot (bottom-right) for Mix 28 Specimen 12 in English unit system.

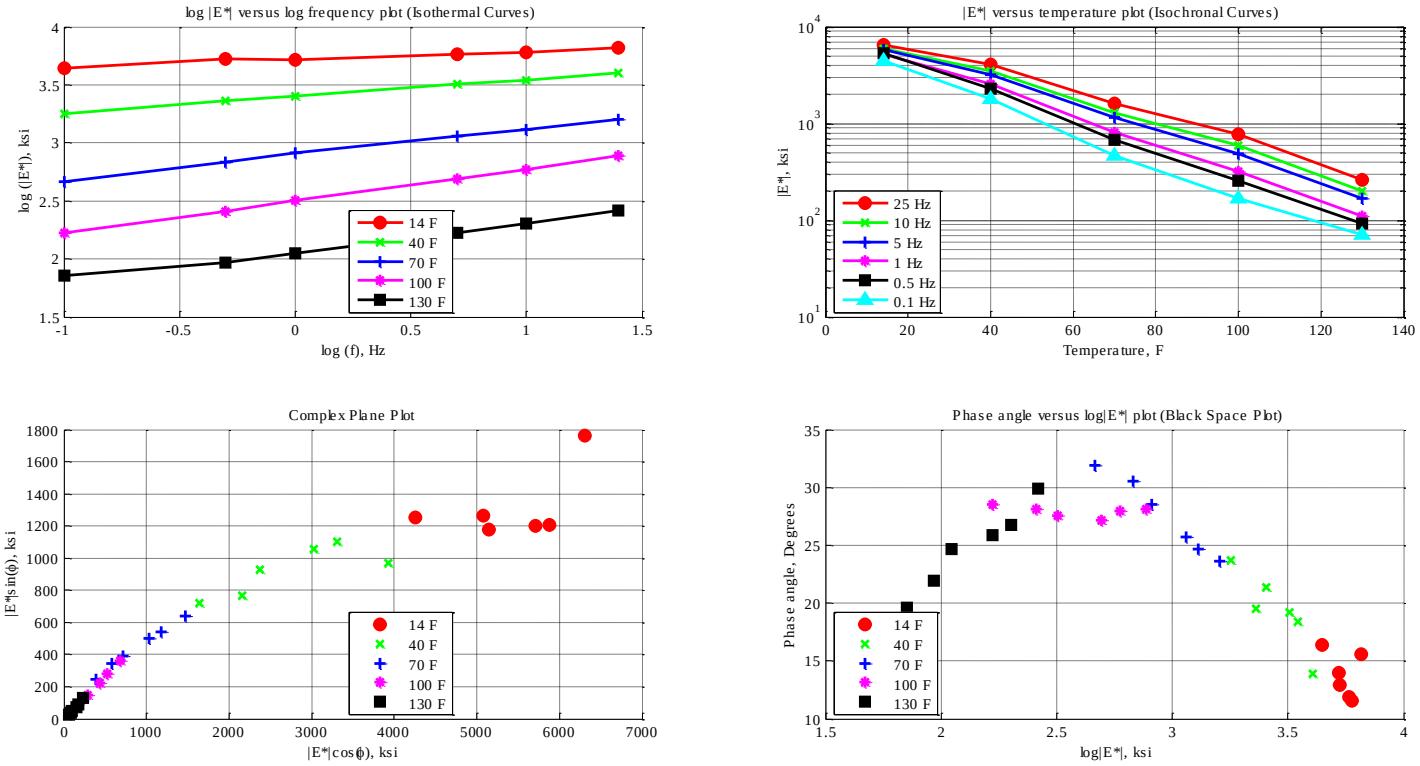

Figure C-87 Isothermal curves or |E*| versus frequency plot (top-left), isochronal curves or |E*| versus temperature plot (top-right), complex plane plot (bottom-left), and black space plot (bottom-right) for Mix 28 Specimen 13 in English unit system.

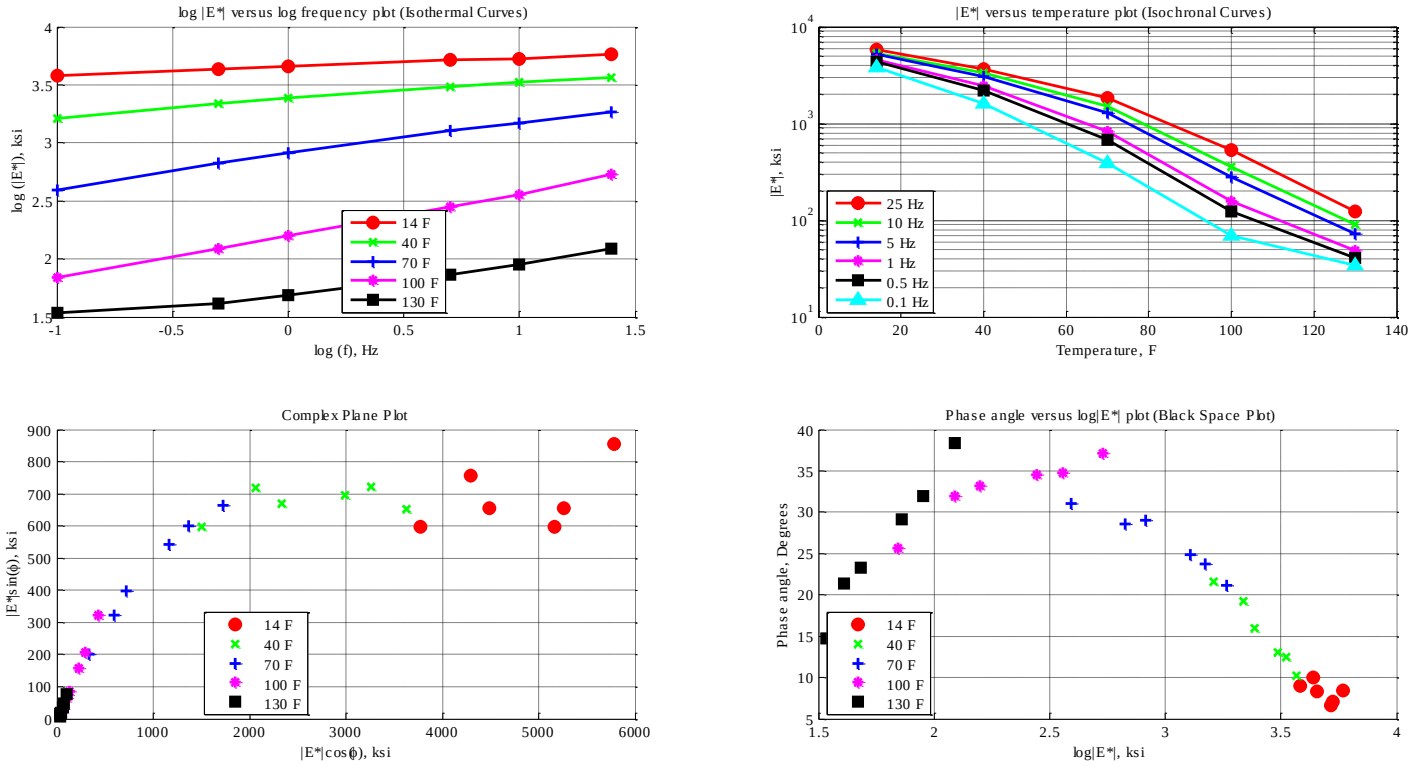

Figure C-88 Isothermal curves or |E*| versus frequency plot (top-left), isochronal curves or |E*| versus temperature plot (top-right), complex plane plot (bottom-left), and black space plot (bottom-right) for Mix 29 Specimen 2 in English unit system.

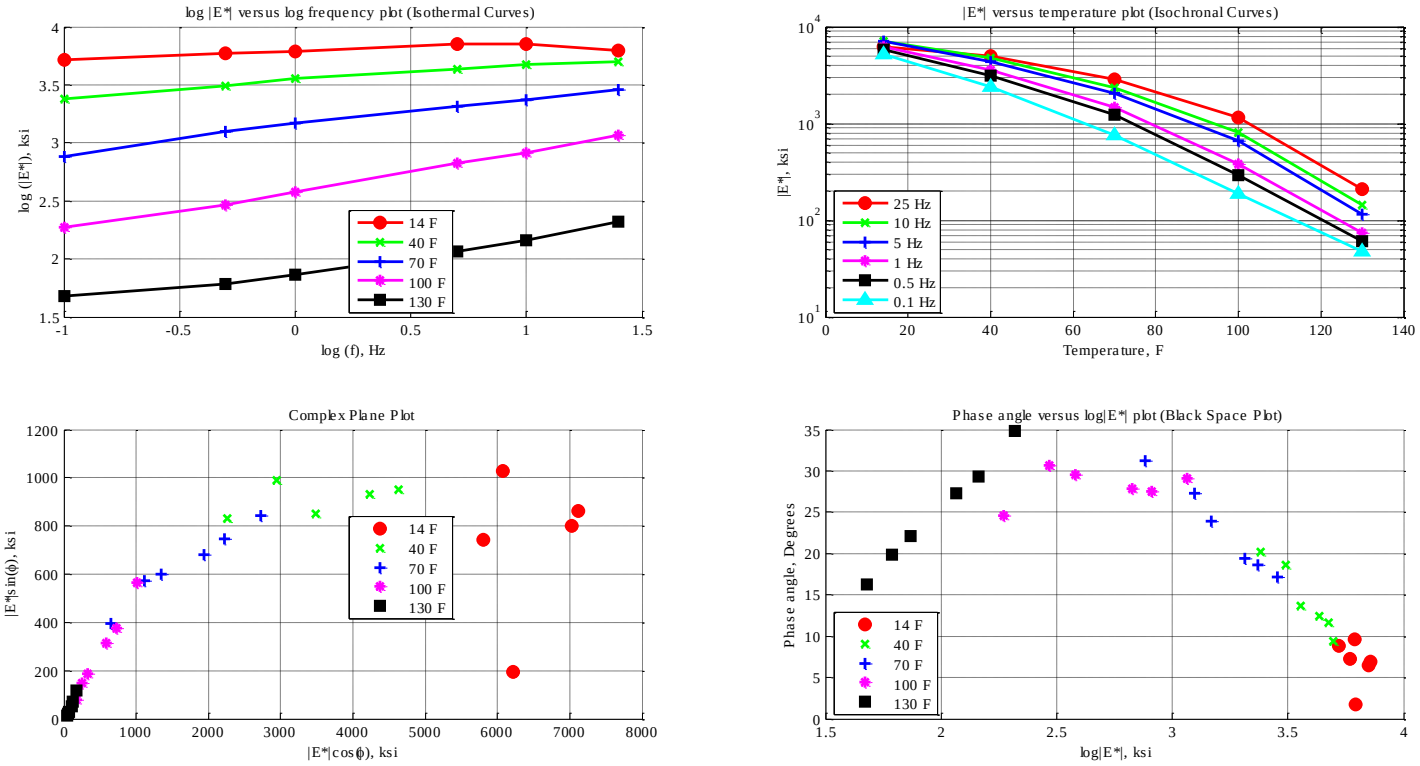

Figure C-89 Isothermal curves or |E*| versus frequency plot (top-left), isochronal curves or |E*| versus temperature plot (top-right), complex plane plot (bottom-left), and black space plot (bottom-right) for Mix 29 Specimen 6 in English unit system.

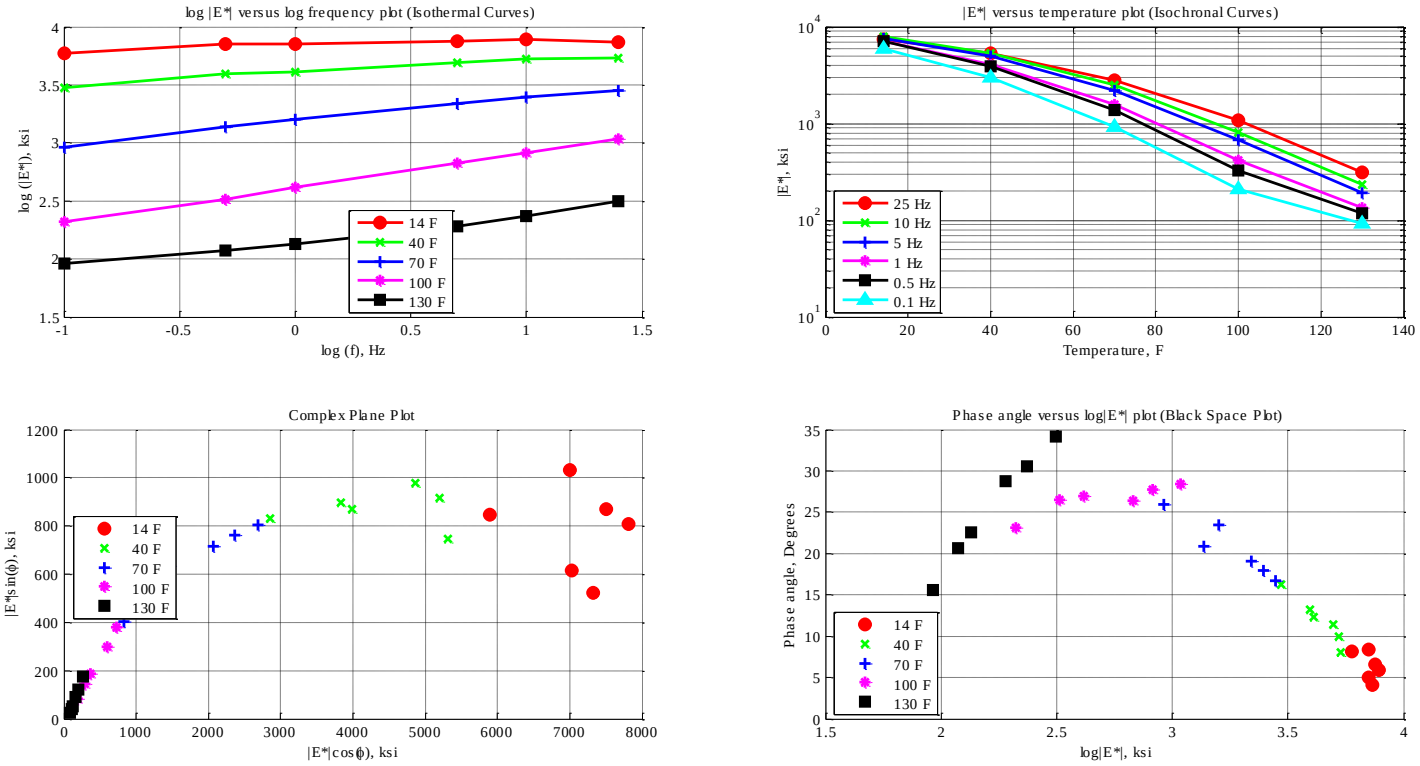

Figure C-90 Isothermal curves or |E*| versus frequency plot (top-left), isochronal curves or |E*| versus temperature plot (top-right), complex plane plot (bottom-left), and black space plot (bottom-right) for Mix 29 Specimen 10 in English unit system.

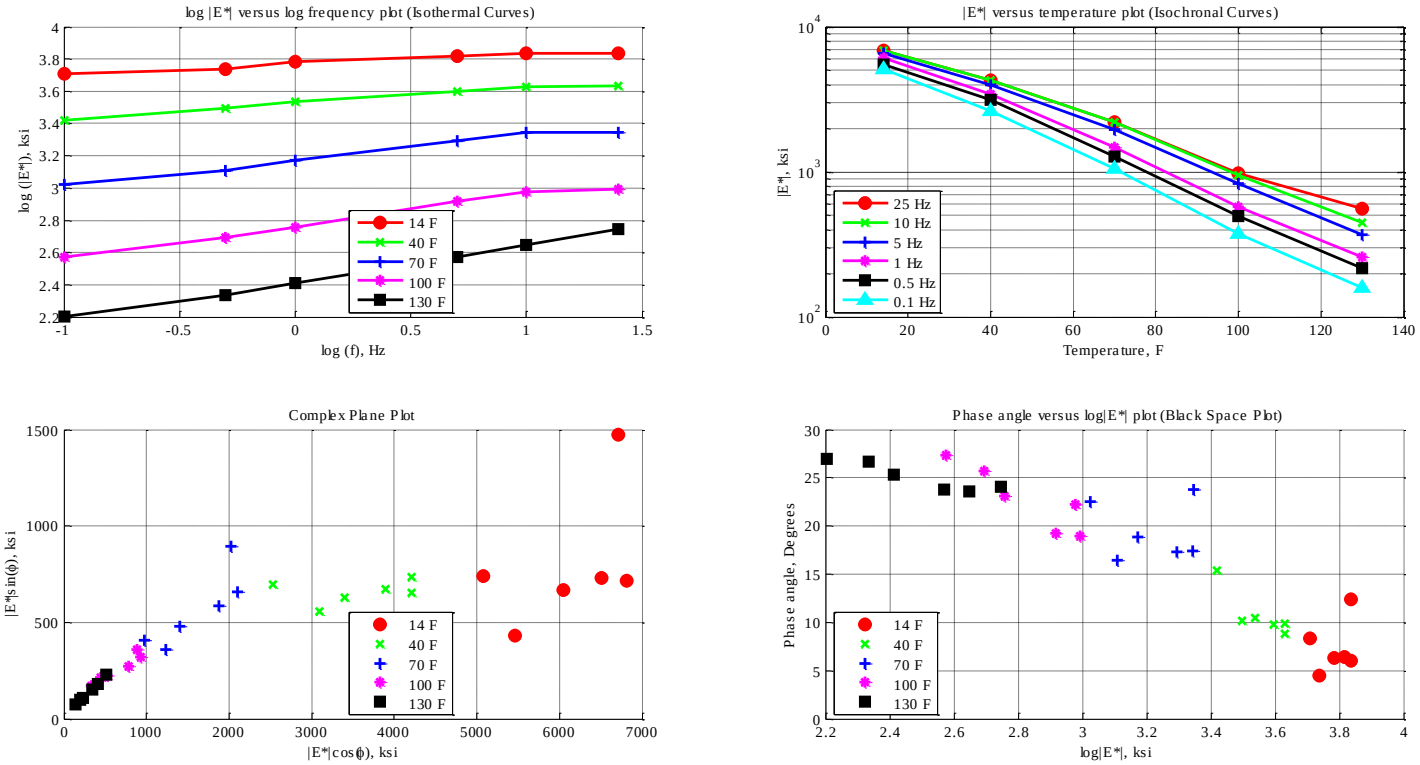

Figure C-91 Isothermal curves or |E*| versus frequency plot (top-left), isochronal curves or |E*| versus temperature plot (top-right), complex plane plot (bottom-left), and black space plot (bottom-right) for Mix 30 Specimen 1 in English unit system.

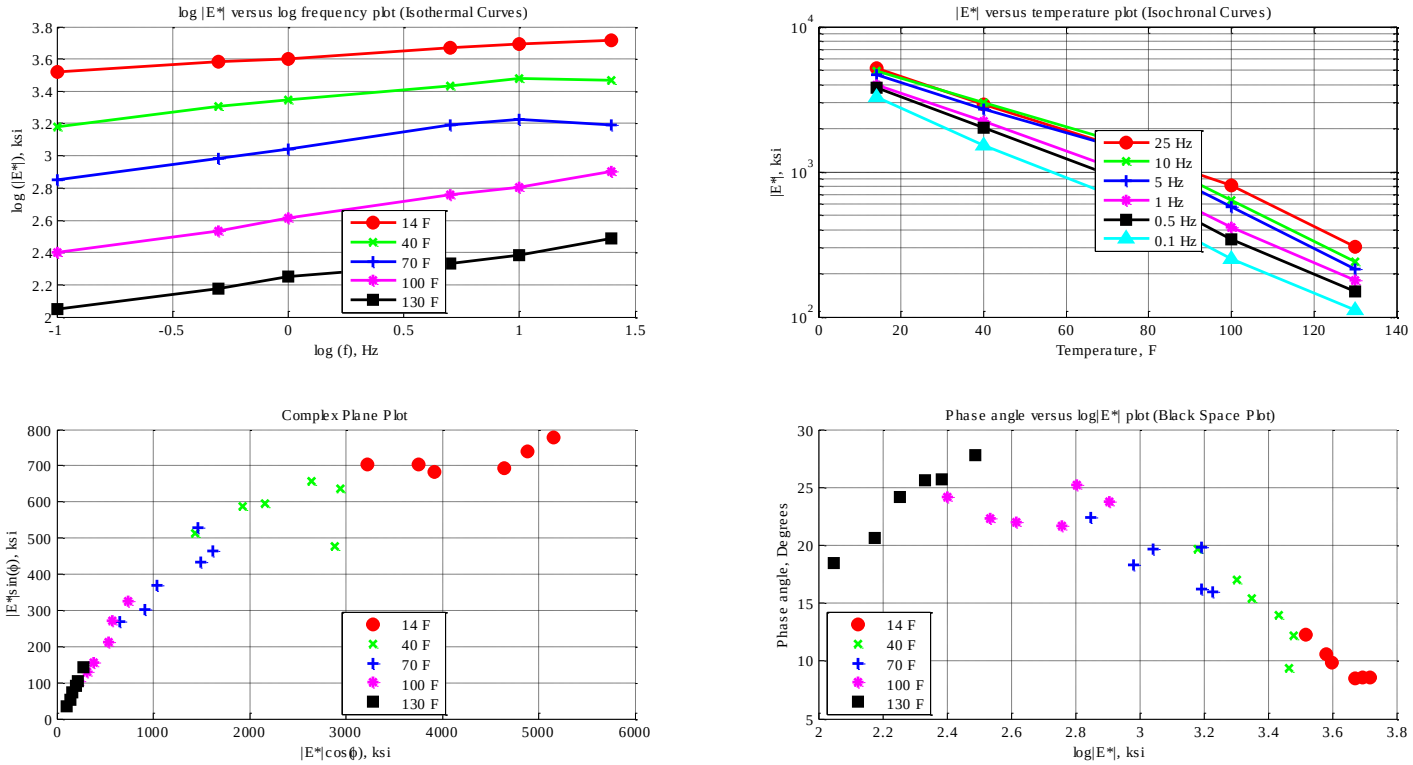

Figure C-92 Isothermal curves or |E*| versus frequency plot (top-left), isochronal curves or |E*| versus temperature plot (top-right), complex plane plot (bottom-left), and black space plot (bottom-right) for Mix 30 Specimen 5 in English unit system.

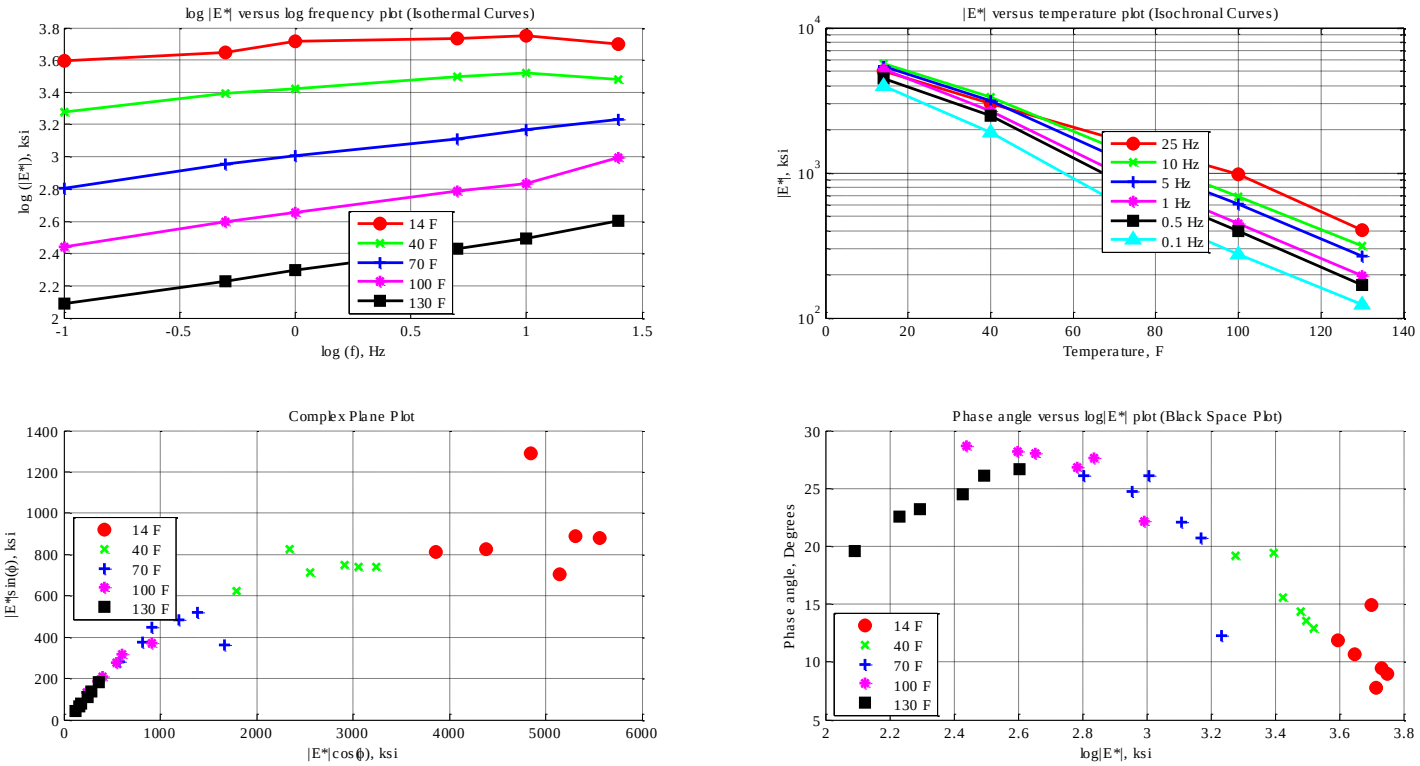

Figure C-93 Isothermal curves or |E*| versus frequency plot (top-left), isochronal curves or |E*| versus temperature plot (top-right), complex plane plot (bottom-left), and black space plot (bottom-right) for Mix 30 Specimen 9 in English unit system.

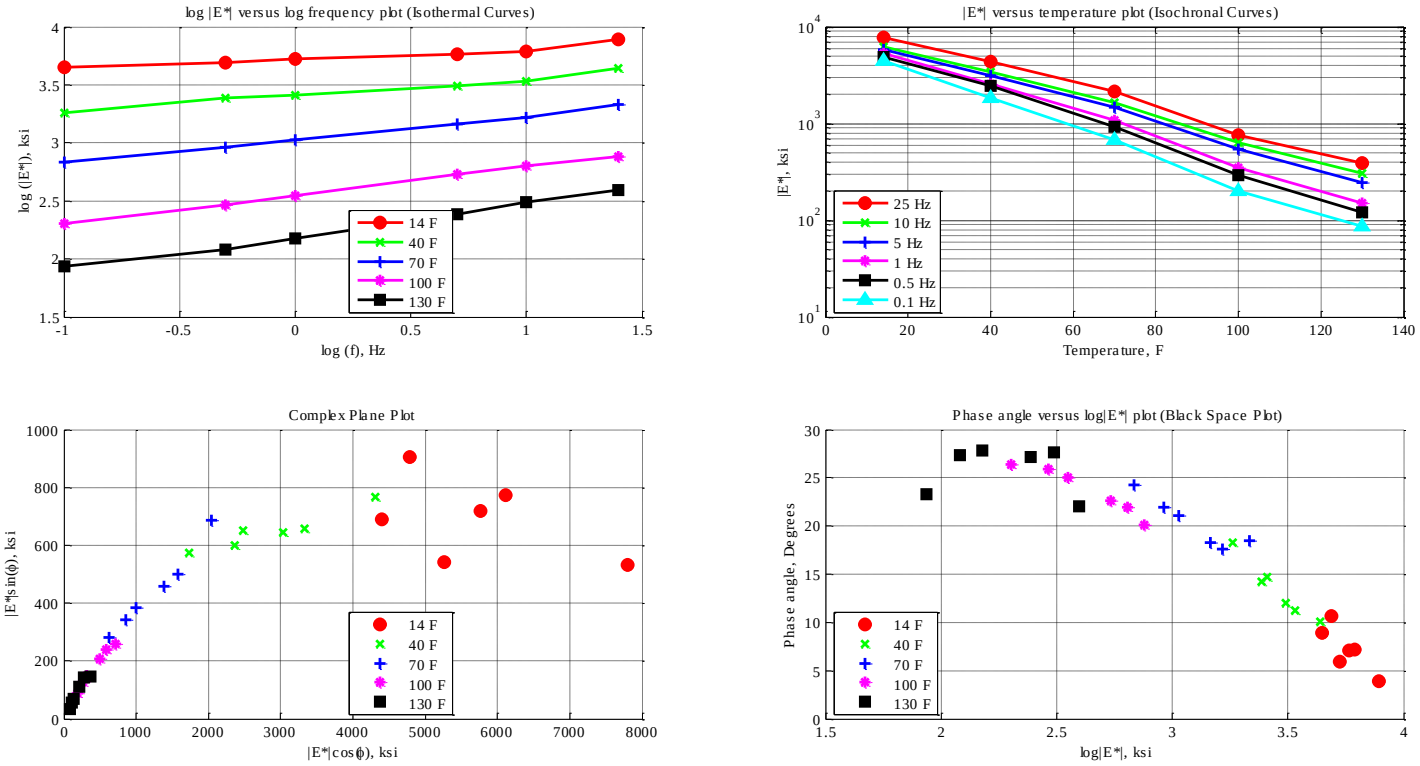

Figure C-94 Isothermal curves or |E*| versus frequency plot (top-left), isochronal curves or |E*| versus temperature plot (top-right), complex plane plot (bottom-left), and black space plot (bottom-right) for Mix 31 Specimen 2 in English unit system.

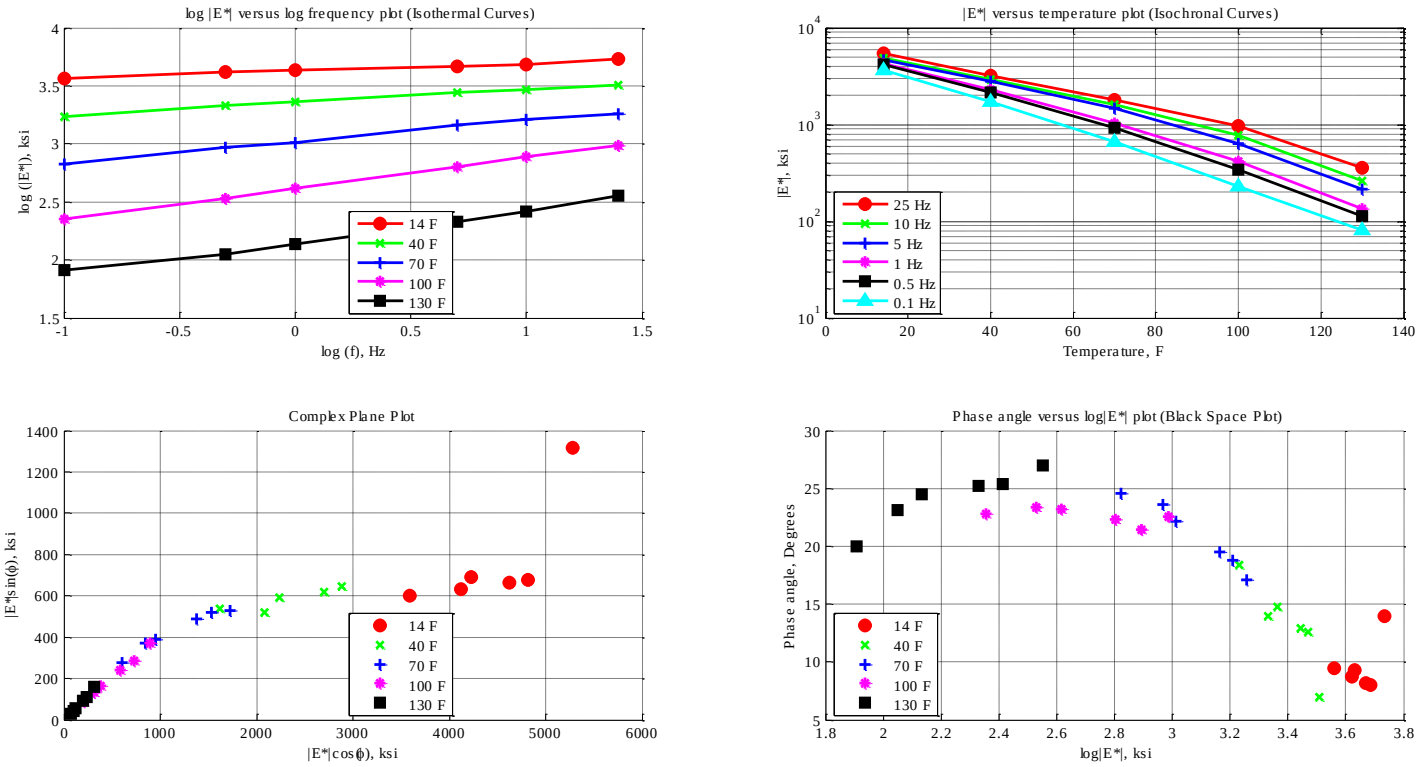

Figure C-95 Isothermal curves or |E*| versus frequency plot (top-left), isochronal curves or |E*| versus temperature plot (top-right), complex plane plot (bottom-left), and black space plot (bottom-right) for Mix 31 Specimen 3 in English unit system.

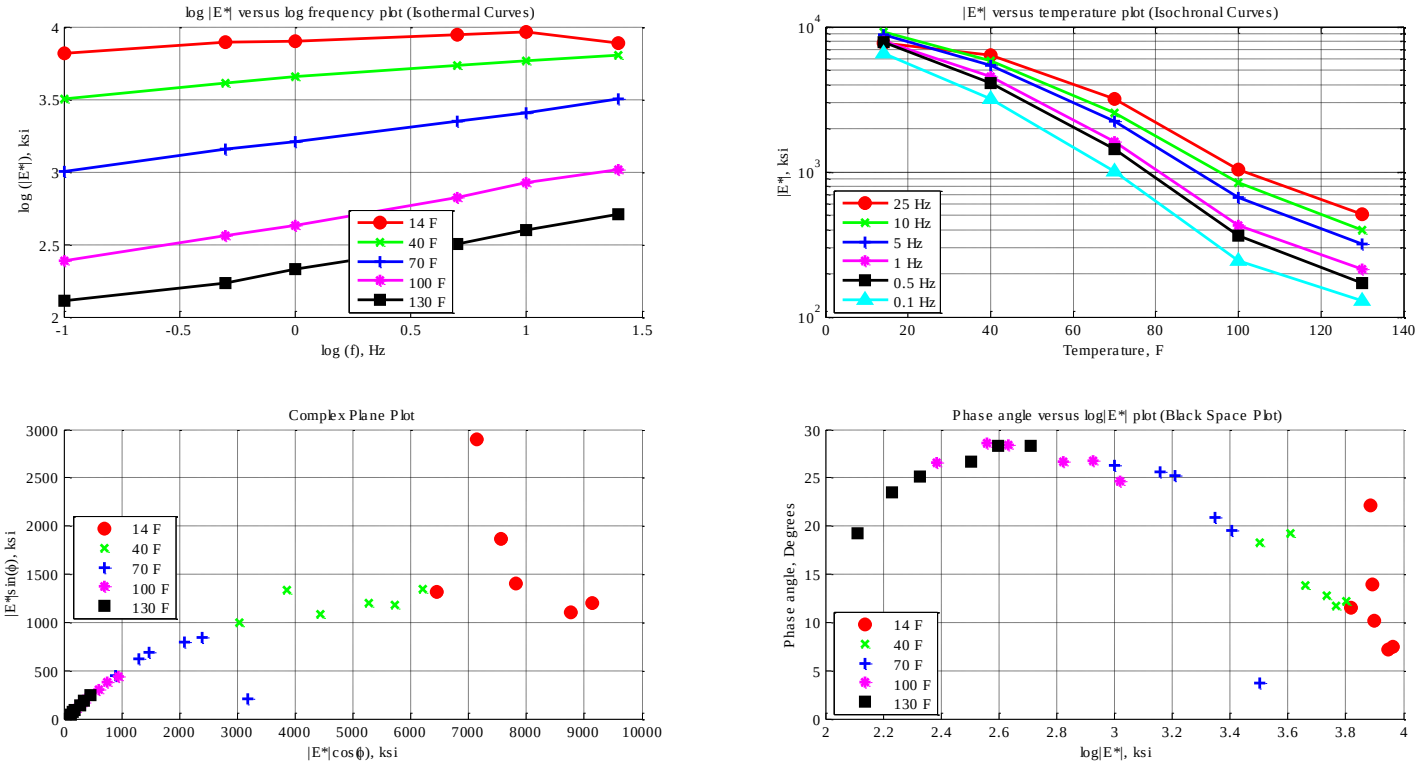

Figure C-96 Isothermal curves or |E*| versus frequency plot (top-left), isochronal curves or |E*| versus temperature plot (top-right), complex plane plot (bottom-left), and black space plot (bottom-right) for Mix 31 Specimen 7 in English unit system.

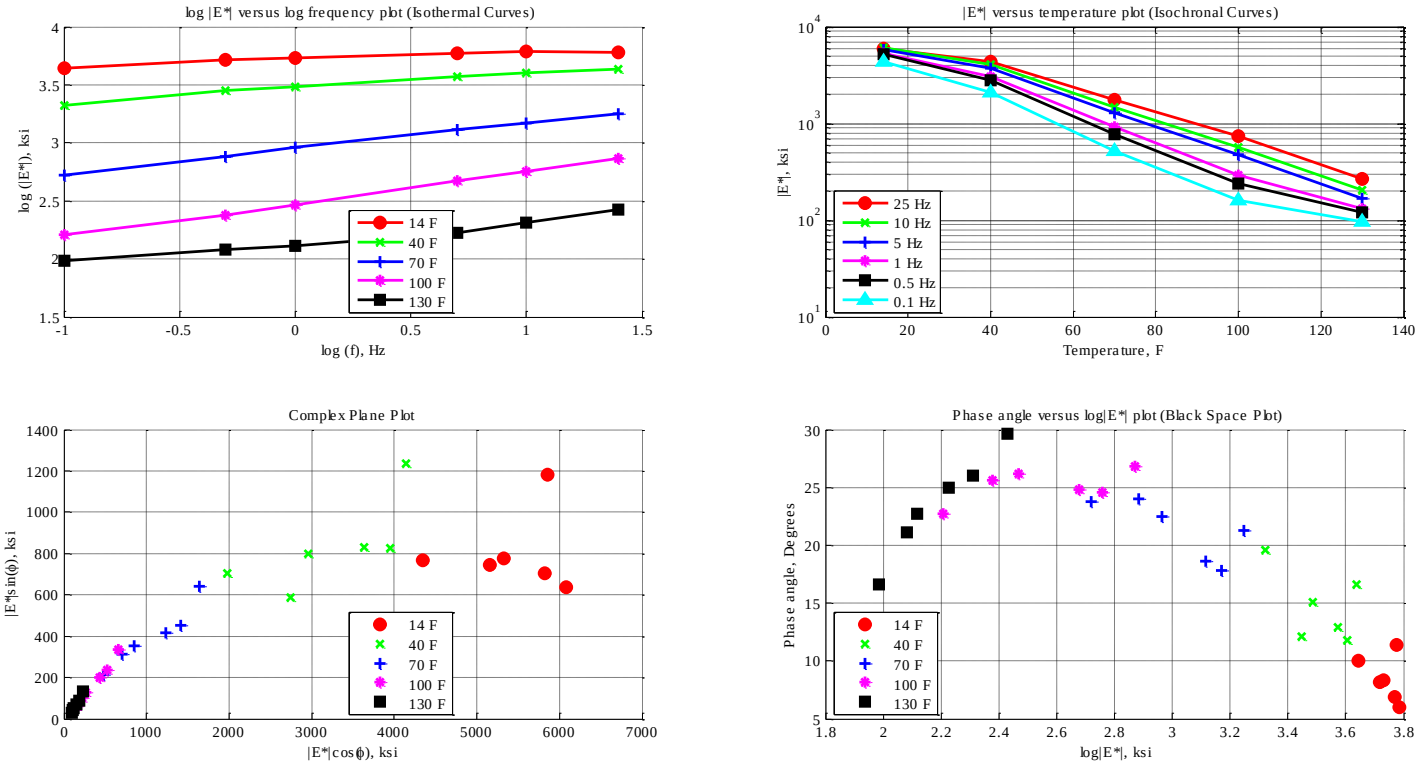

Figure C-97 Isothermal curves or |E*| versus frequency plot (top-left), isochronal curves or |E*| versus temperature plot (top-right), complex plane plot (bottom-left), and black space plot (bottom-right) for Mix 32 Specimen 1 in English unit system.

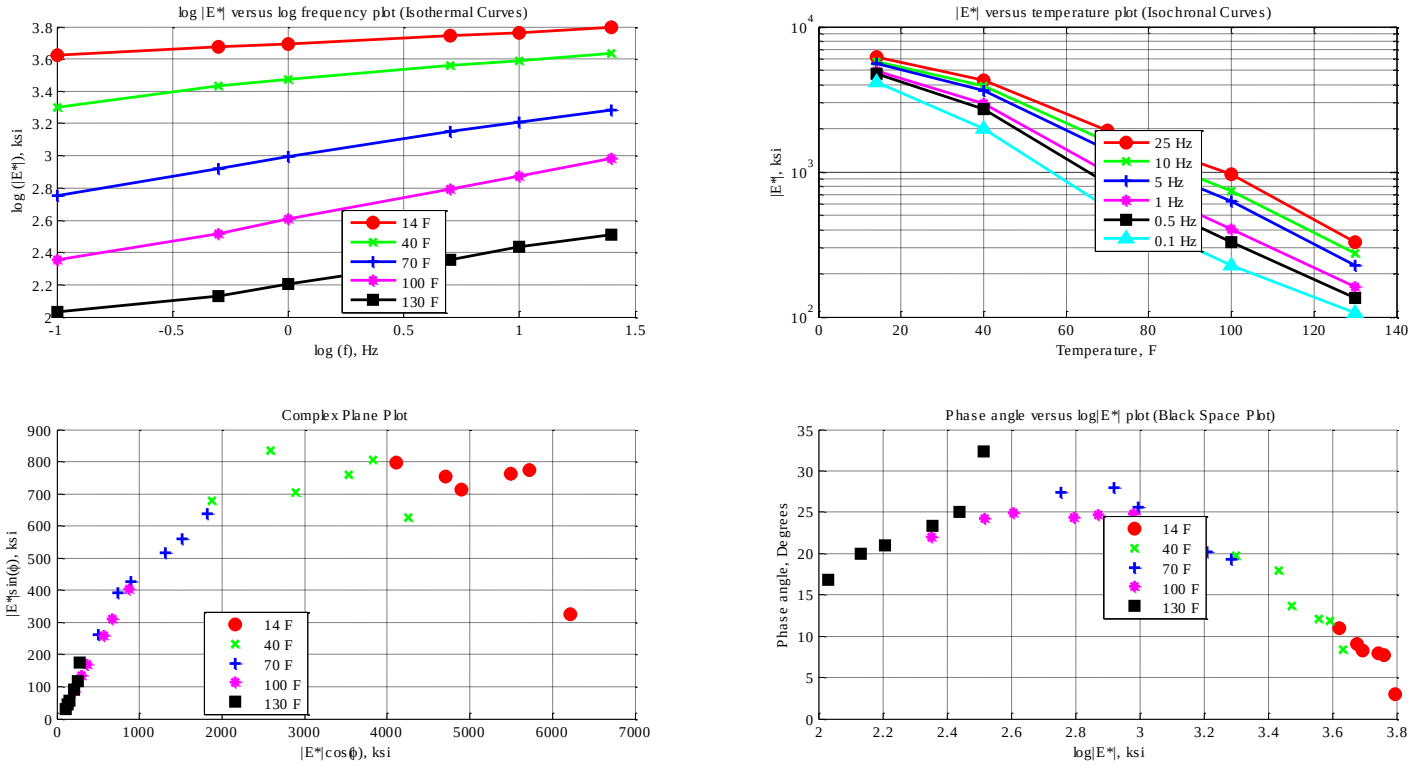

Figure C-98 Isothermal curves or |E*| versus frequency plot (top-left), isochronal curves or |E*| versus temperature plot (top-right), complex plane plot (bottom-left), and black space plot (bottom-right) for Mix 32 Specimen 2 in English unit system.

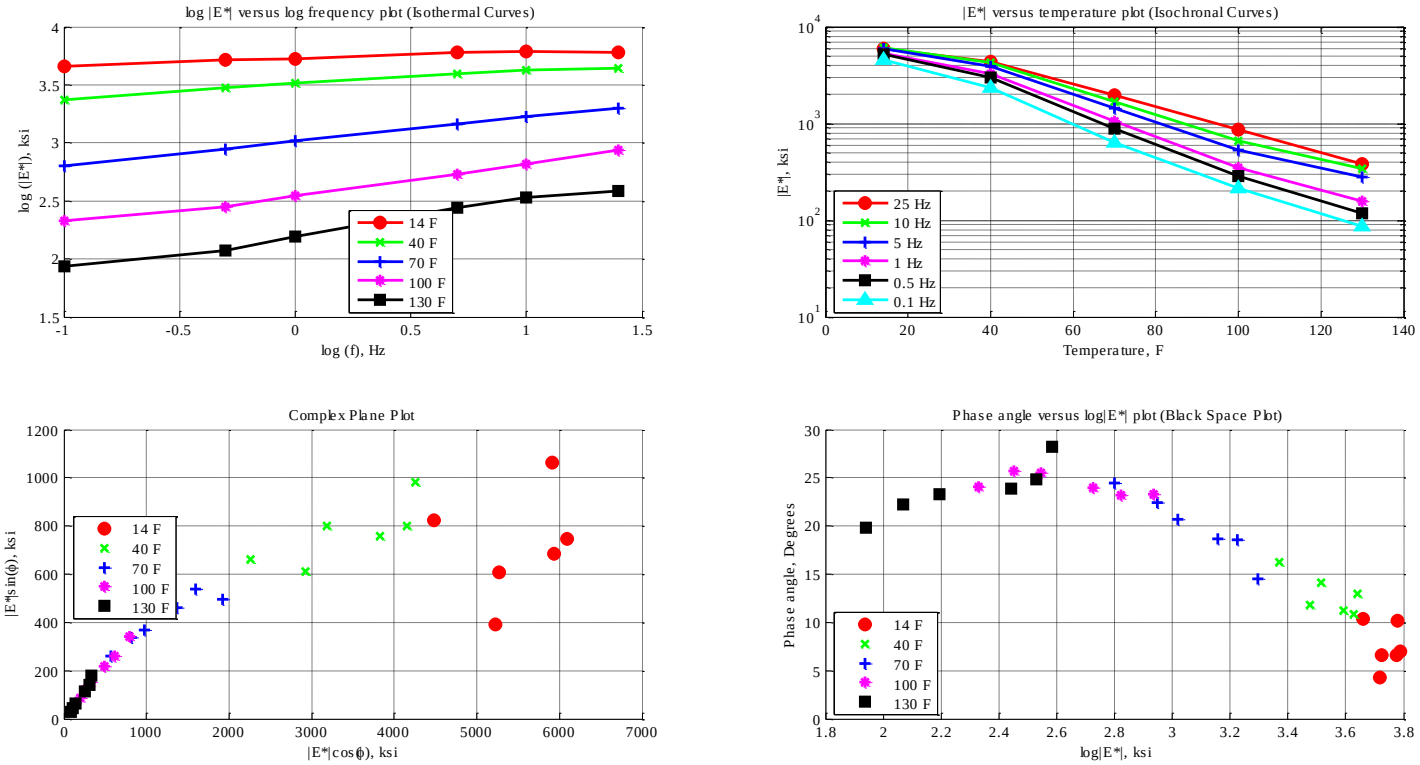

Figure C-99 Isothermal curves or |E*| versus frequency plot (top-left), isochronal curves or |E*| versus temperature plot (top-right), complex plane plot (bottom-left), and black space plot (bottom-right) for Mix 32 Specimen 4 in English unit system.

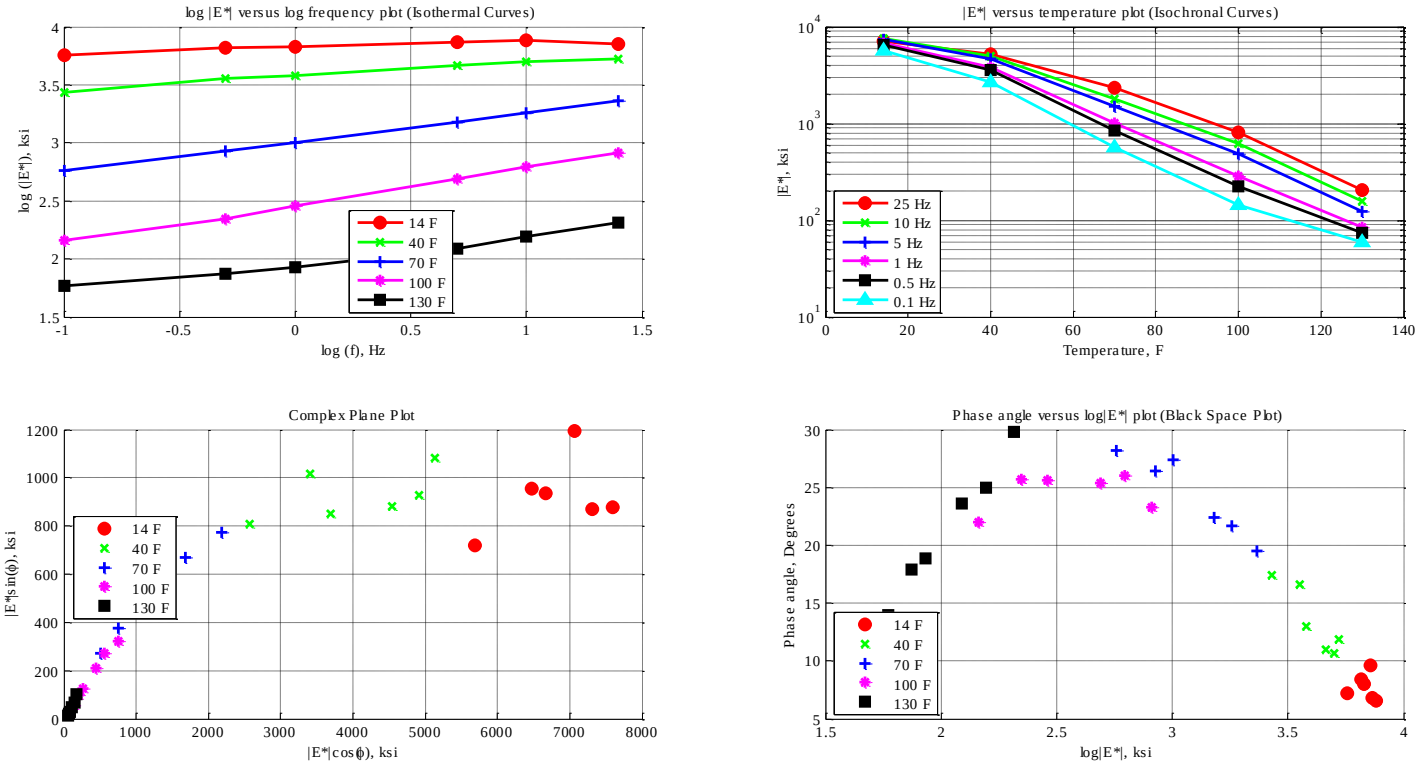

Figure C-100 Isothermal curves or |E*| versus frequency plot (top-left), isochronal curves or |E*| versus temperature plot (top-right), complex plane plot (bottom-left), and black space plot (bottom-right) for Mix 33 Specimen 1 in English unit system.

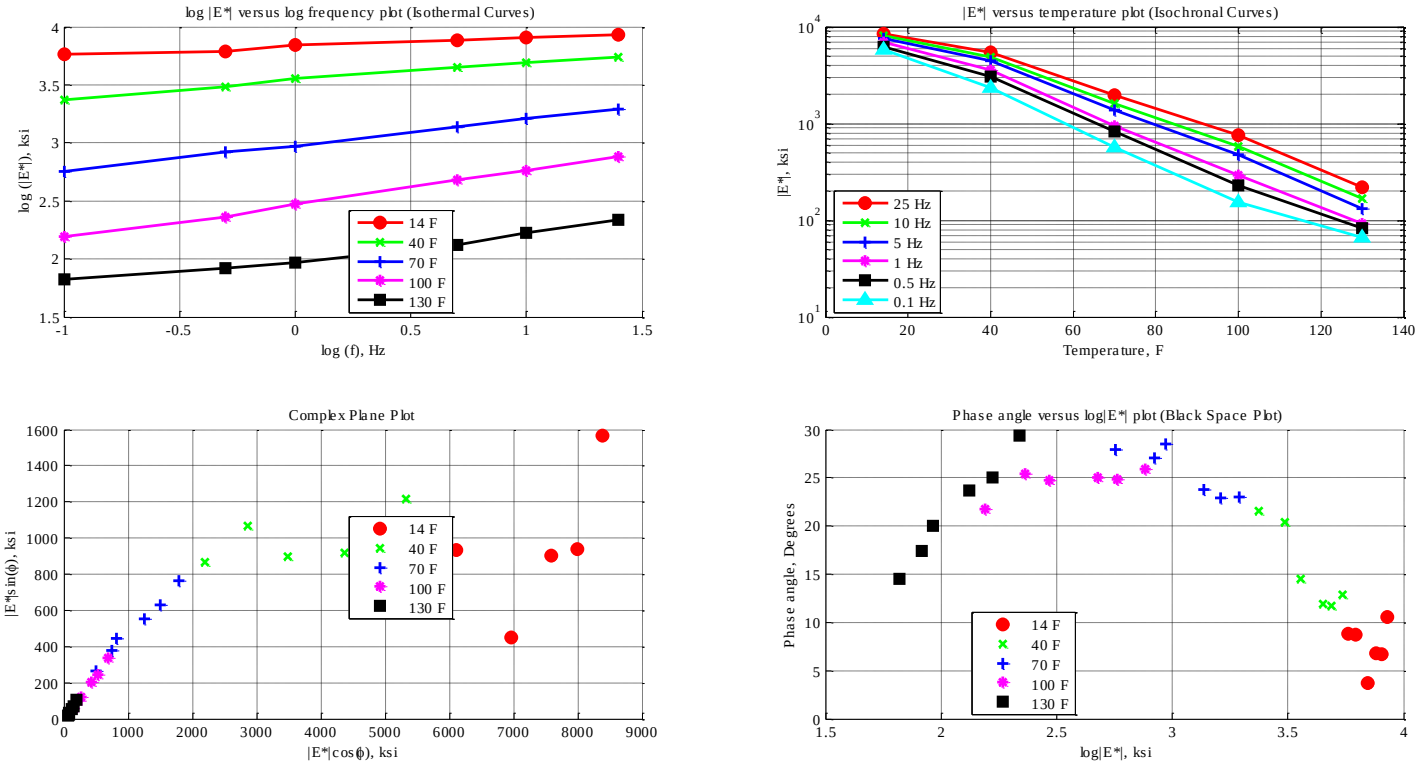

Figure C-101 Isothermal curves or |E*| versus frequency plot (top-left), isochronal curves or |E*| versus temperature plot (top-right), complex plane plot (bottom-left), and black space plot (bottom-right) for Mix 33 Specimen 3 in English unit system.

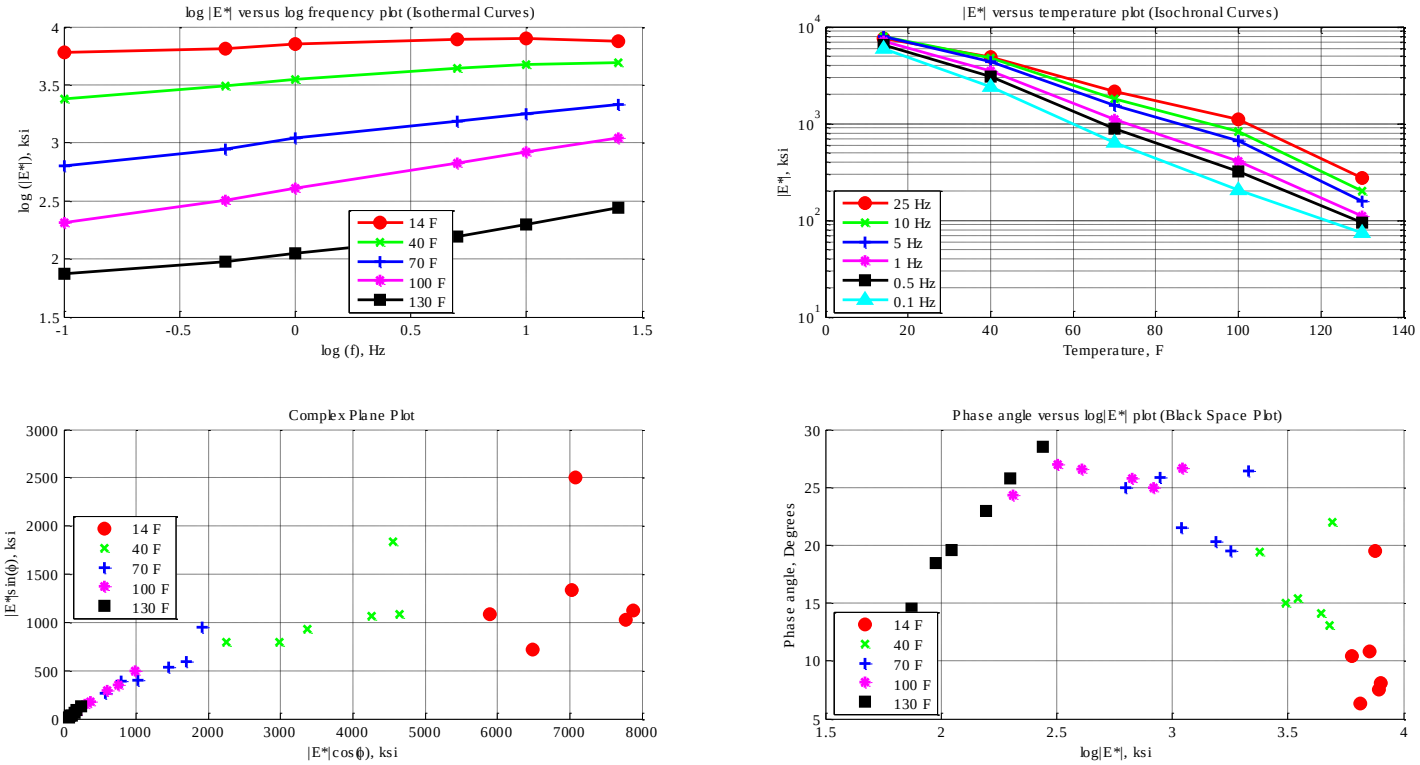

Figure C-102 Isothermal curves or |E*| versus frequency plot (top-left), isochronal curves or |E*| versus temperature plot (top-right), complex plane plot (bottom-left), and black space plot (bottom-right) for Mix 33 Specimen 4 in English unit system.

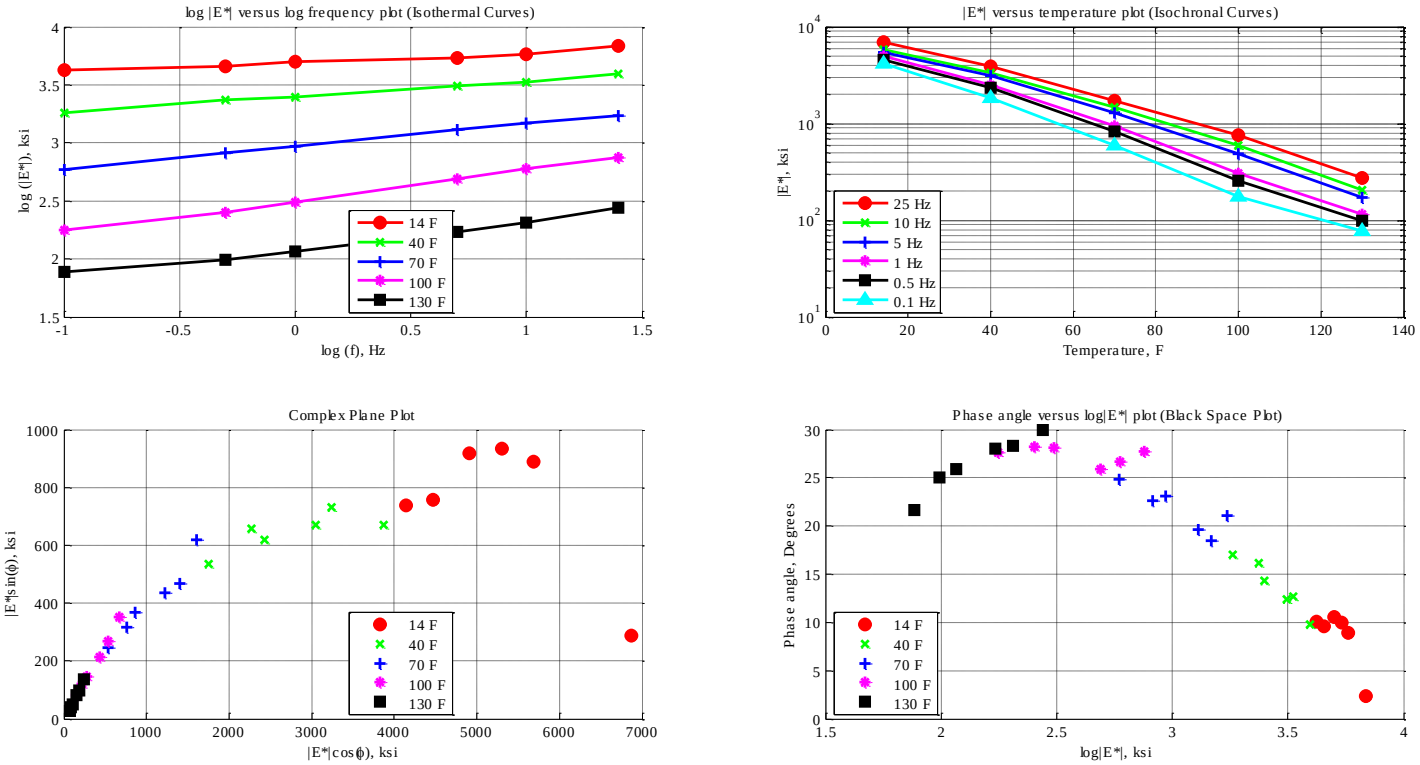

Figure C-103 Isothermal curves or |E*| versus frequency plot (top-left), isochronal curves or |E*| versus temperature plot (top-right), complex plane plot (bottom-left), and black space plot (bottom-right) for Mix 34 Specimen 1 in English unit system.

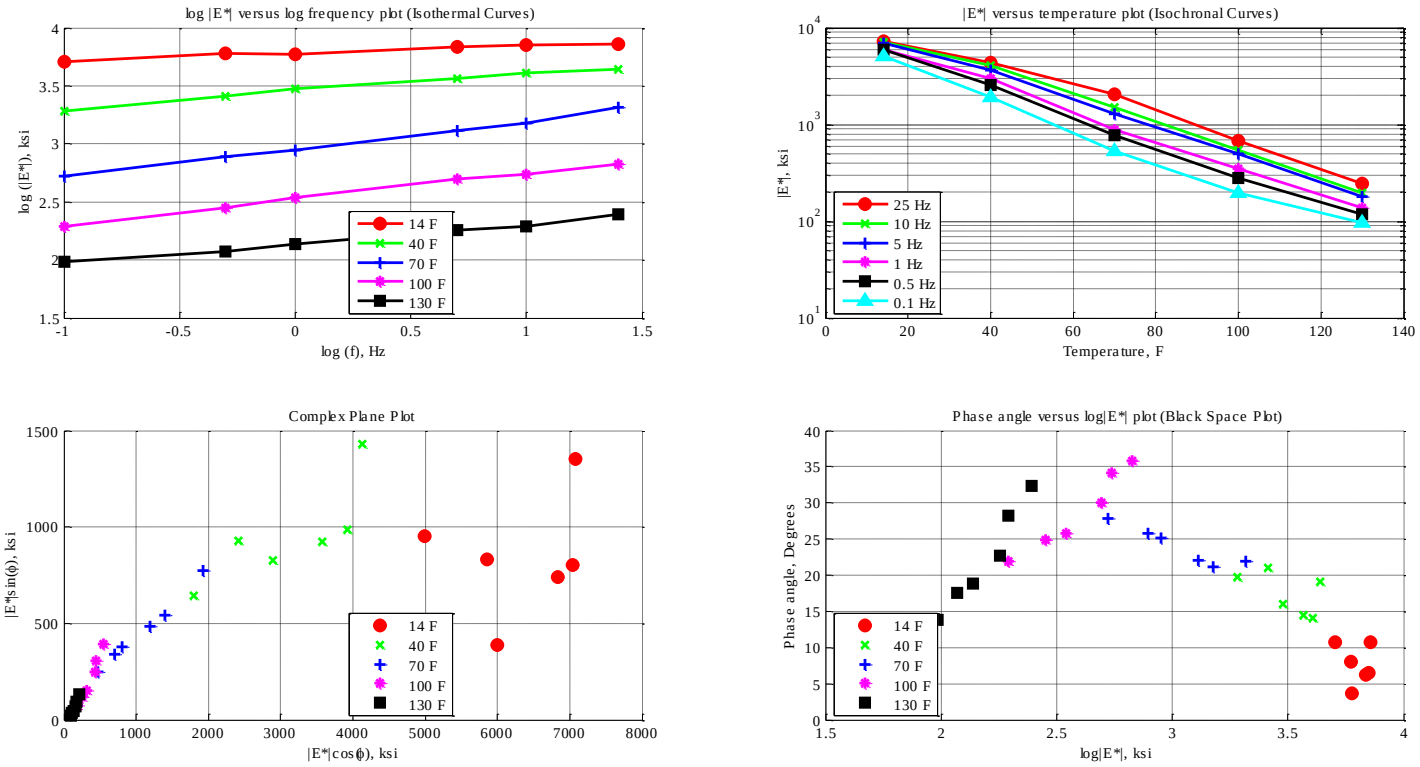

Figure C-104 Isothermal curves or |E*| versus frequency plot (top-left), isochronal curves or |E*| versus temperature plot (top-right), complex plane plot (bottom-left), and black space plot (bottom-right) for Mix 34 Specimen 2 in English unit system.

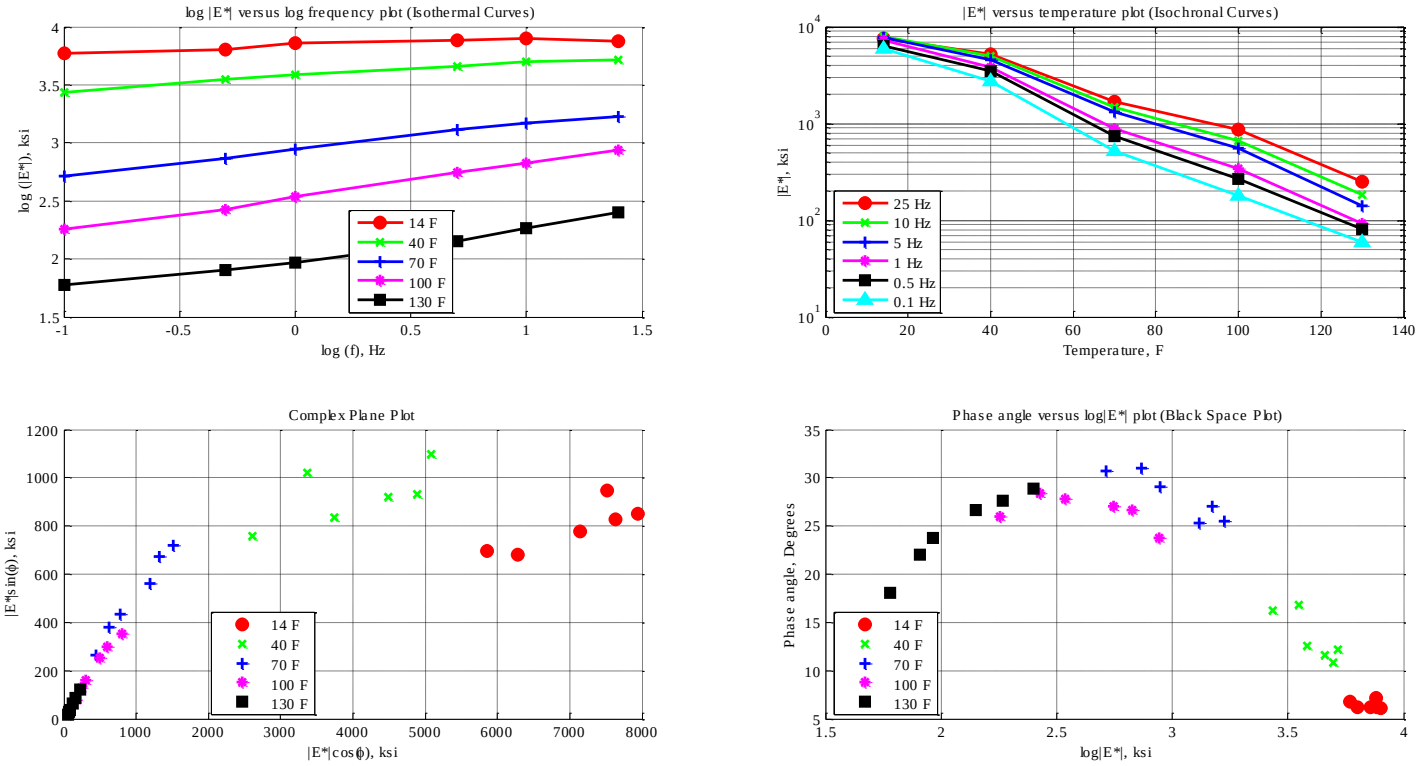

Figure C-105 Isothermal curves or |E*| versus frequency plot (top-left), isochronal curves or |E*| versus temperature plot (top-right), complex plane plot (bottom-left), and black space plot (bottom-right) for Mix 34 Specimen 3 in English unit system.

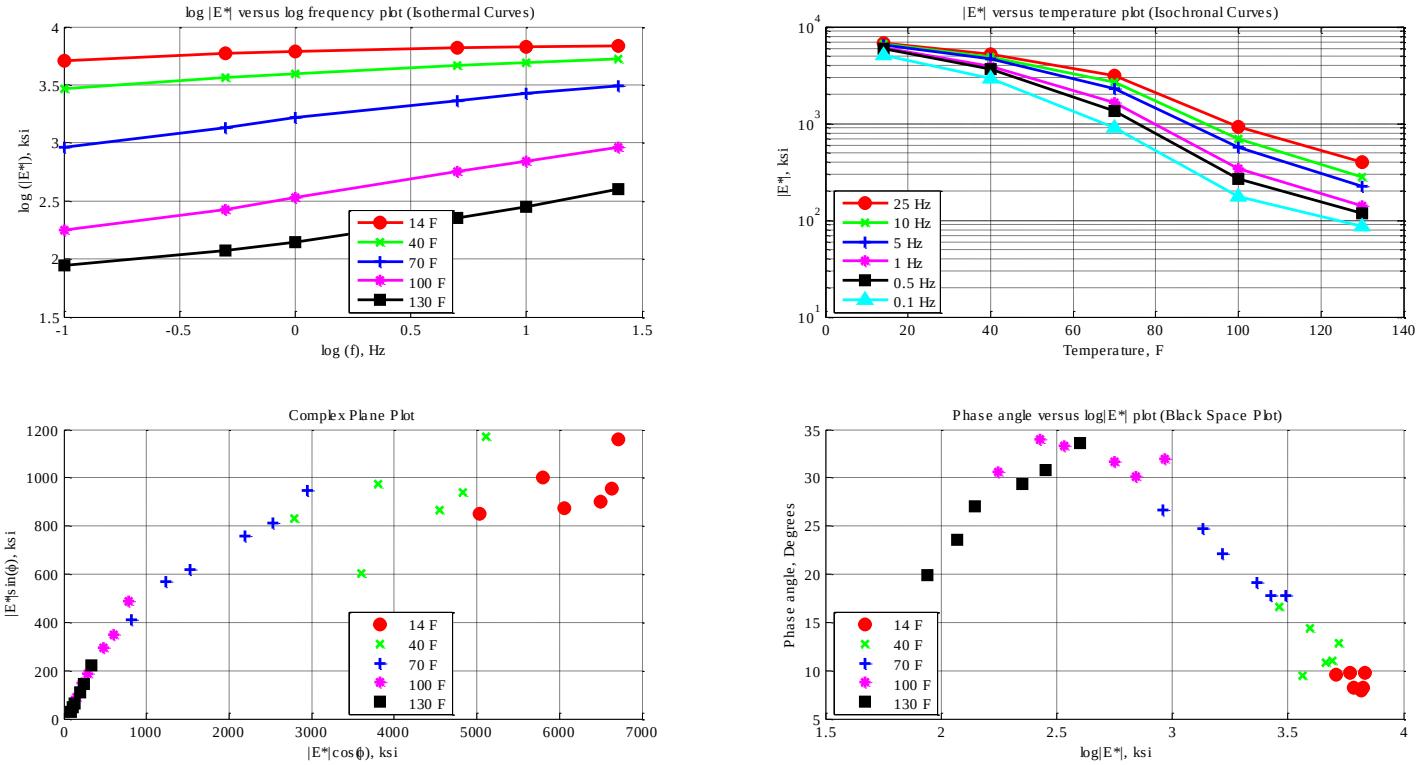

Figure C-106 Isothermal curves or |E*| versus frequency plot (top-left), isochronal curves or |E*| versus temperature plot (top-right), complex plane plot (bottom-left), and black space plot (bottom-right) for Mix 35 Specimen 1 in English unit system.

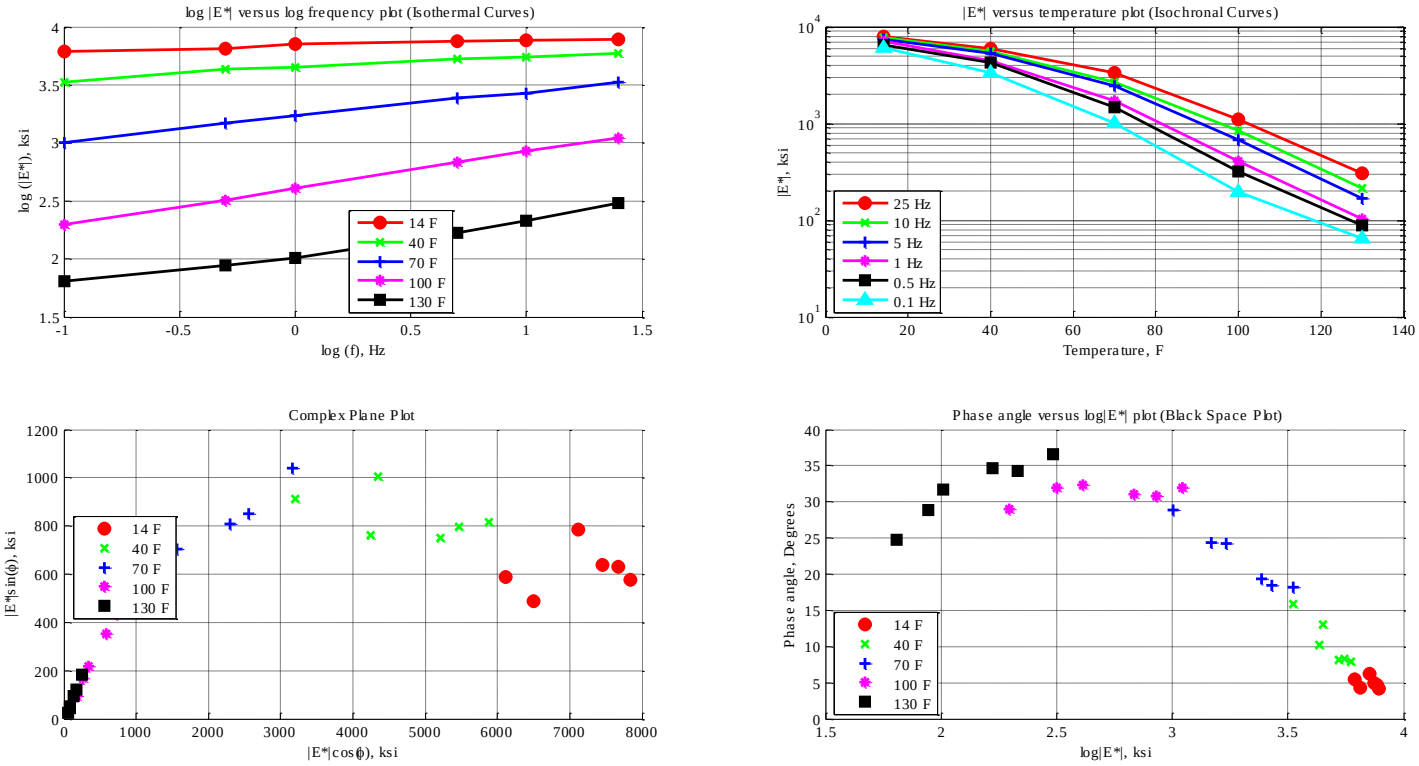

Figure C-107 Isothermal curves or |E*| versus frequency plot (top-left), isochronal curves or |E*| versus temperature plot (top-right), complex plane plot (bottom-left), and black space plot (bottom-right) for Mix 35 Specimen 3 in English unit system.

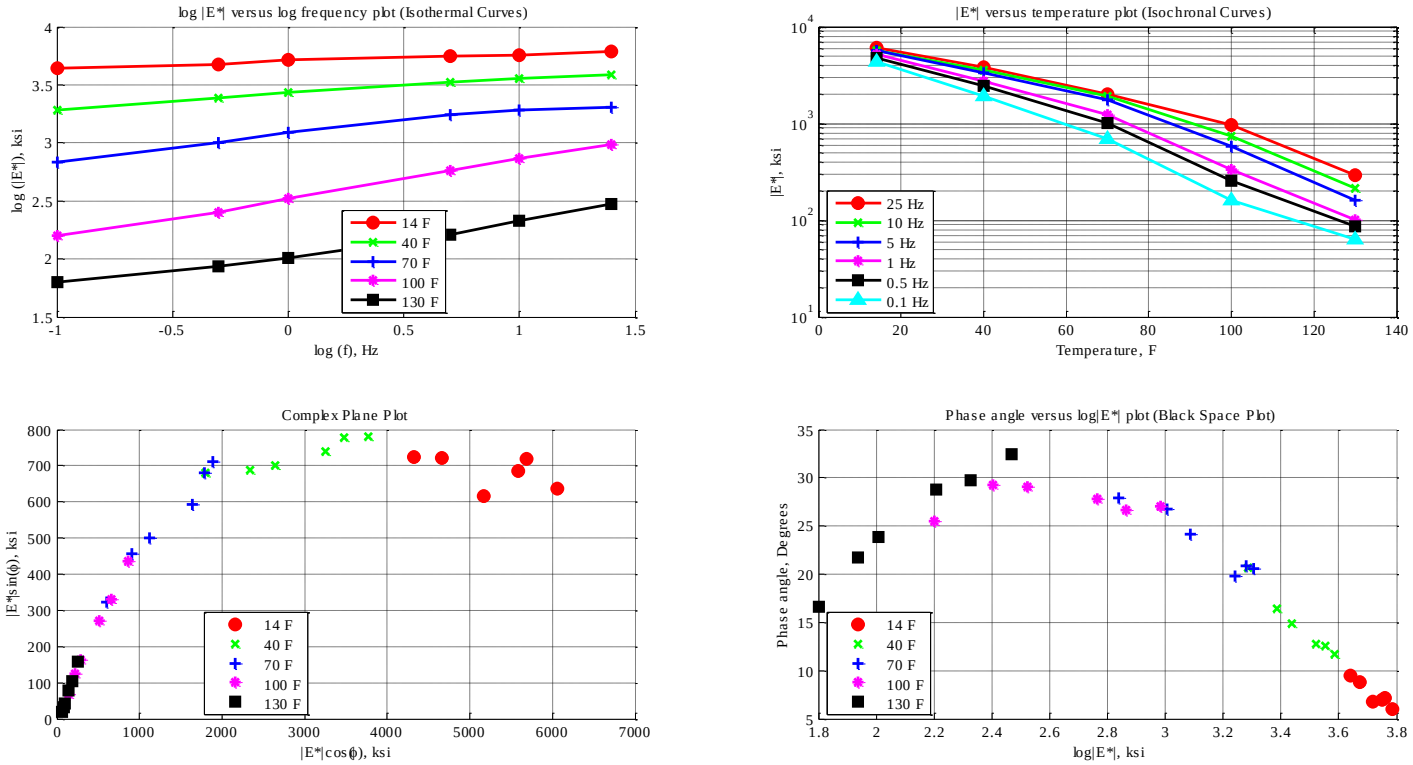

Figure C-108 Isothermal curves or |E*| versus frequency plot (top-left), isochronal curves or |E*| versus temperature plot (top-right), complex plane plot (bottom-left), and black space plot (bottom-right) for Mix 35 Specimen 5 in English unit system.

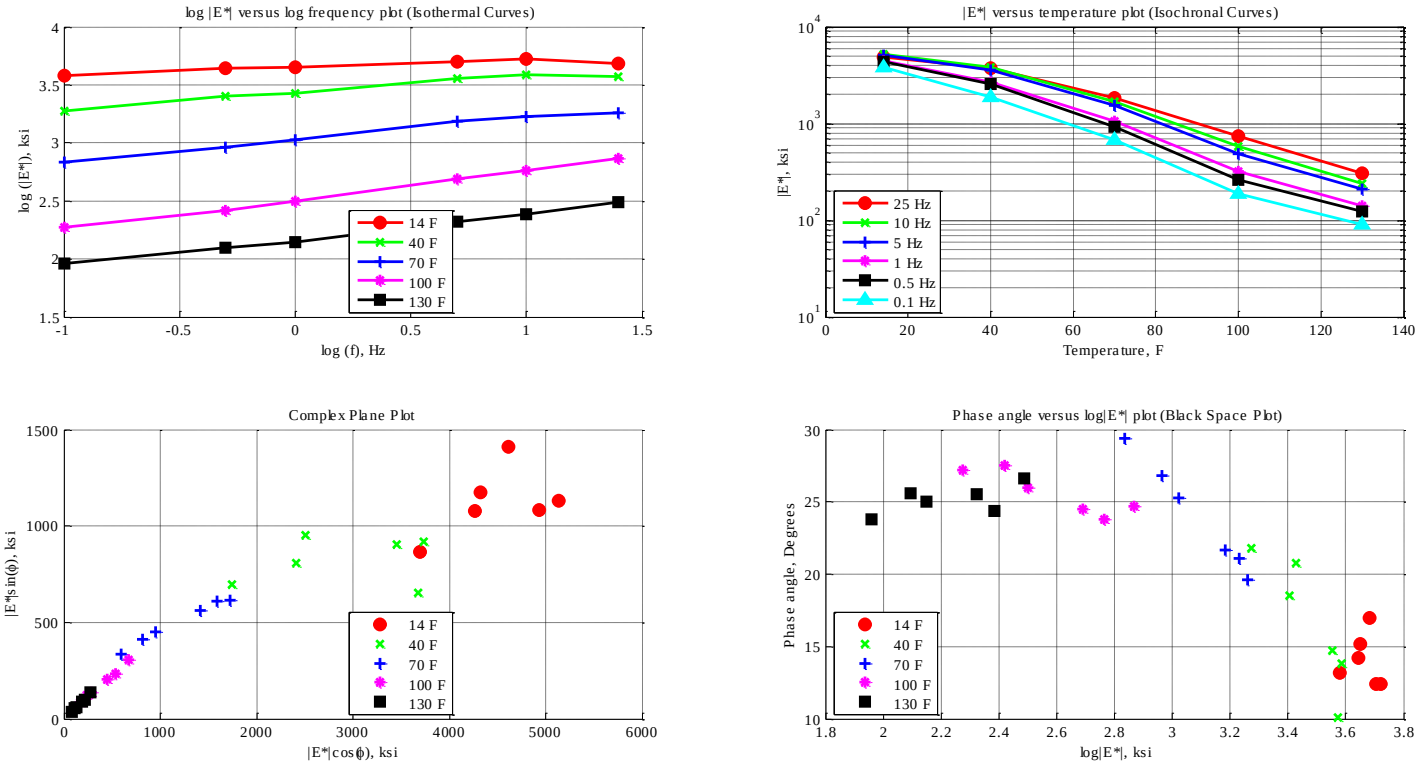

Figure C-109 Isothermal curves or |E*| versus frequency plot (top-left), isochronal curves or |E*| versus temperature plot (top-right), complex plane plot (bottom-left), and black space plot (bottom-right) for Mix 36 Specimen 1 in English unit system.

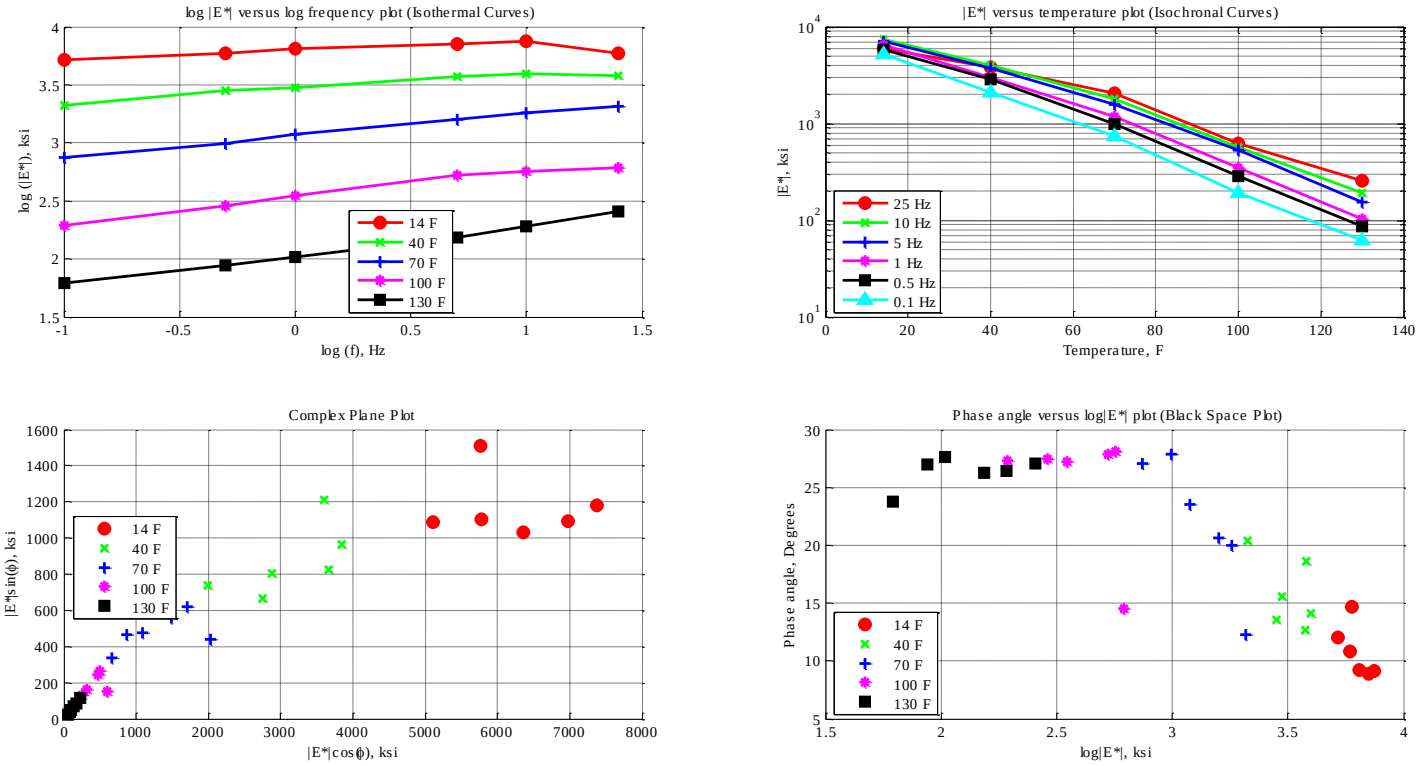

Figure C-110 Isothermal curves or |E*| versus frequency plot (top-left), isochronal curves or |E*| versus temperature plot (top-right), complex plane plot (bottom-left), and black space plot (bottom-right) for Mix 36 Specimen 2 in English unit system.

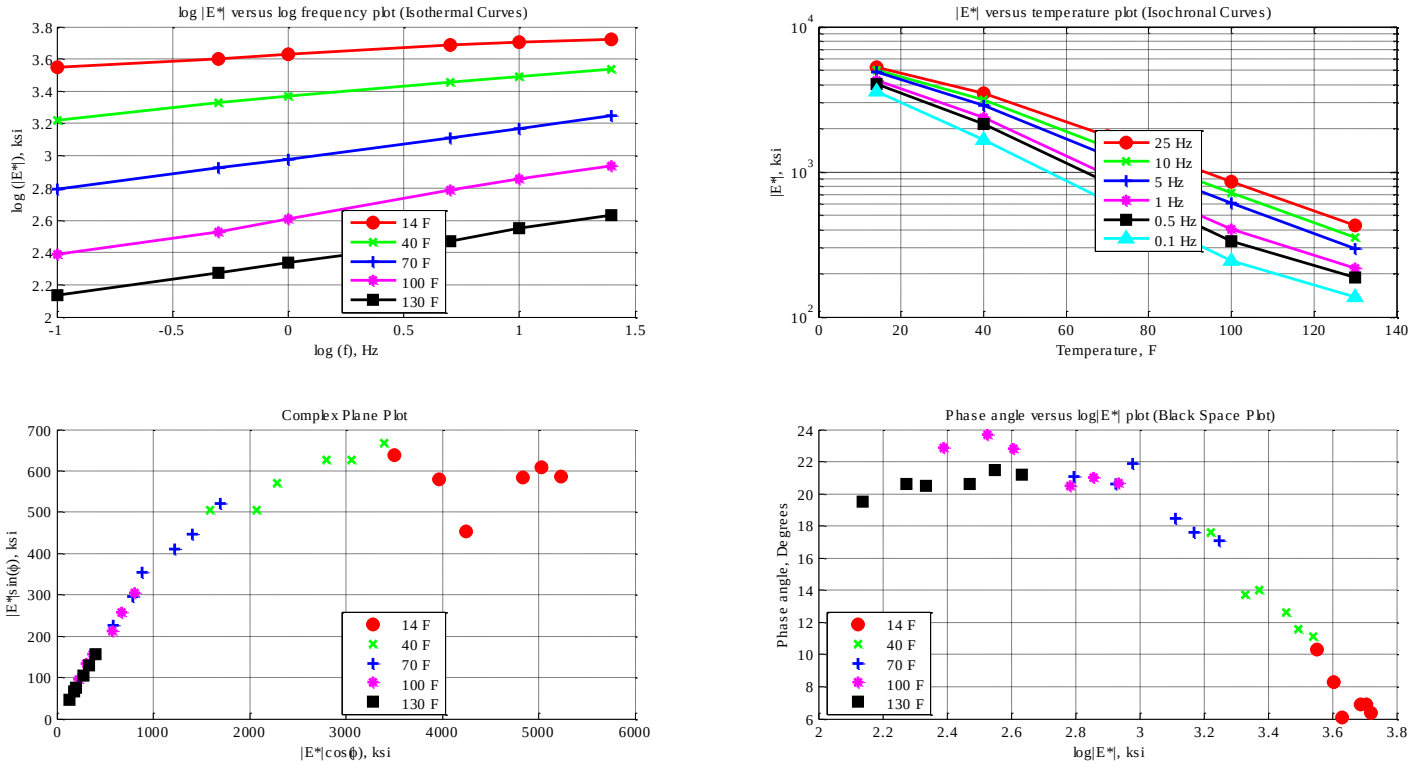

Figure C-111 Isothermal curves or |E*| versus frequency plot (top-left), isochronal curves or |E*| versus temperature plot (top-right), complex plane plot (bottom-left), and black space plot (bottom-right) for Mix 36 Specimen 3 in English unit system.

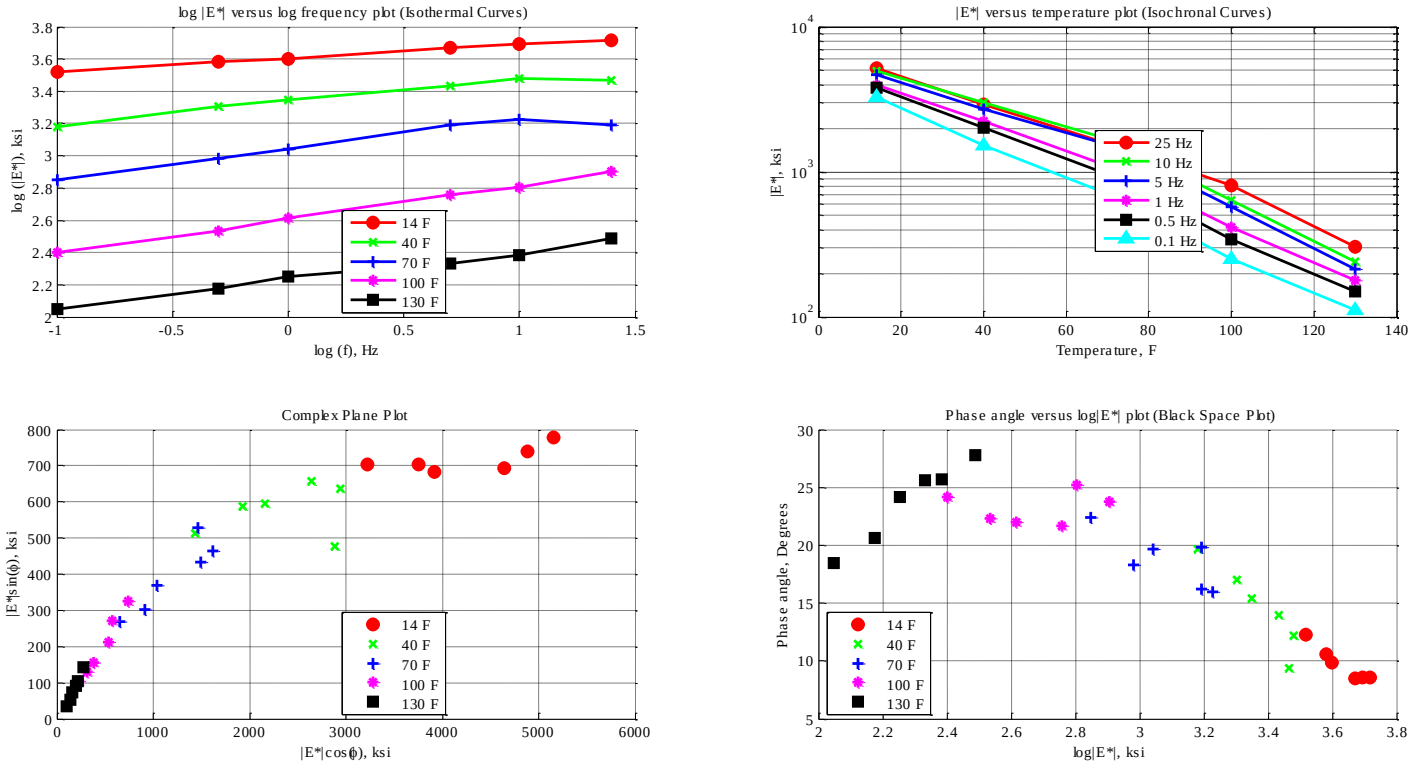

Figure C-112 Isothermal curves or |E*| versus frequency plot (top-left), isochronal curves or |E*| versus temperature plot (top-right), complex plane plot (bottom-left), and black space plot (bottom-right) for Mix 37 Specimen 1 in English unit system.

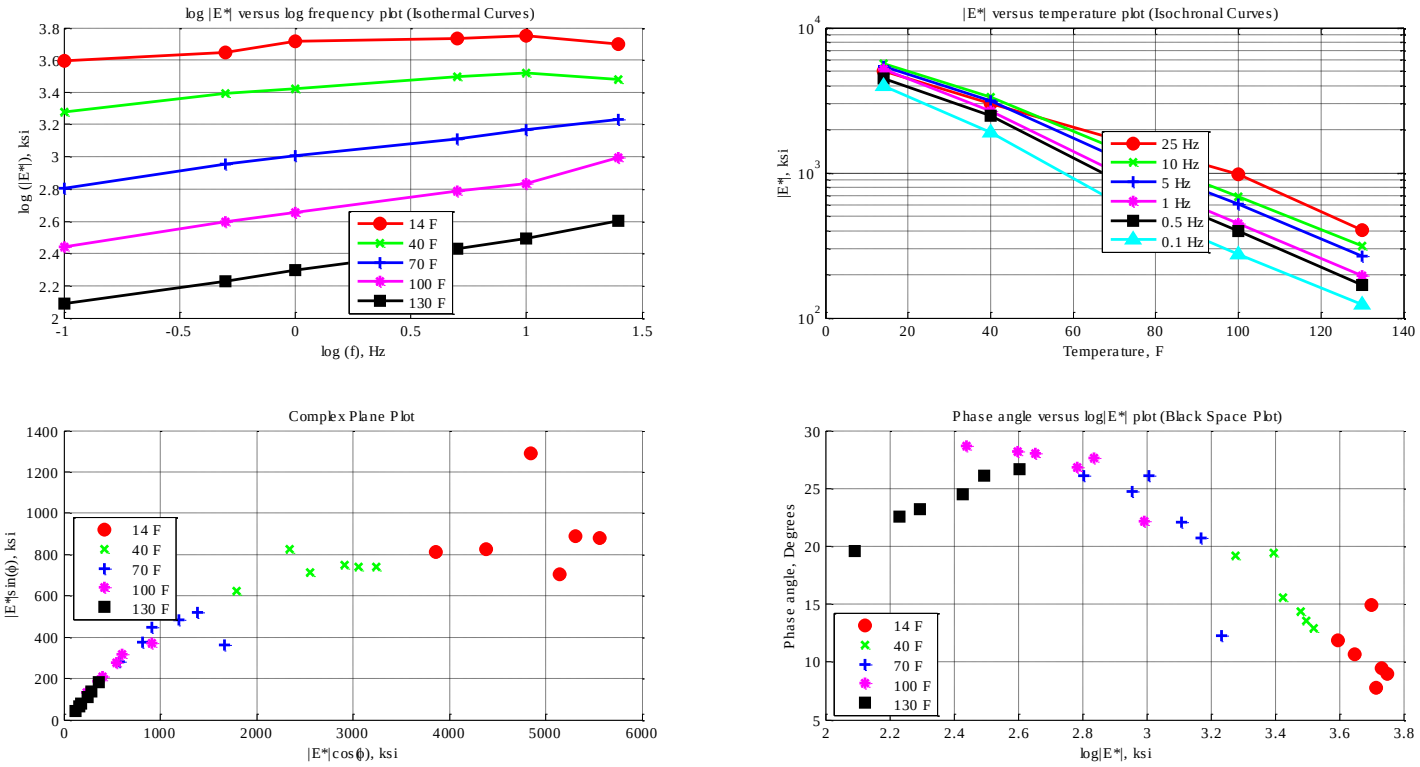

Figure C-113 Isothermal curves or |E*| versus frequency plot (top-left), isochronal curves or |E*| versus temperature plot (top-right), complex plane plot (bottom-left), and black space plot (bottom-right) for Mix 37 Specimen 2 in English unit system.

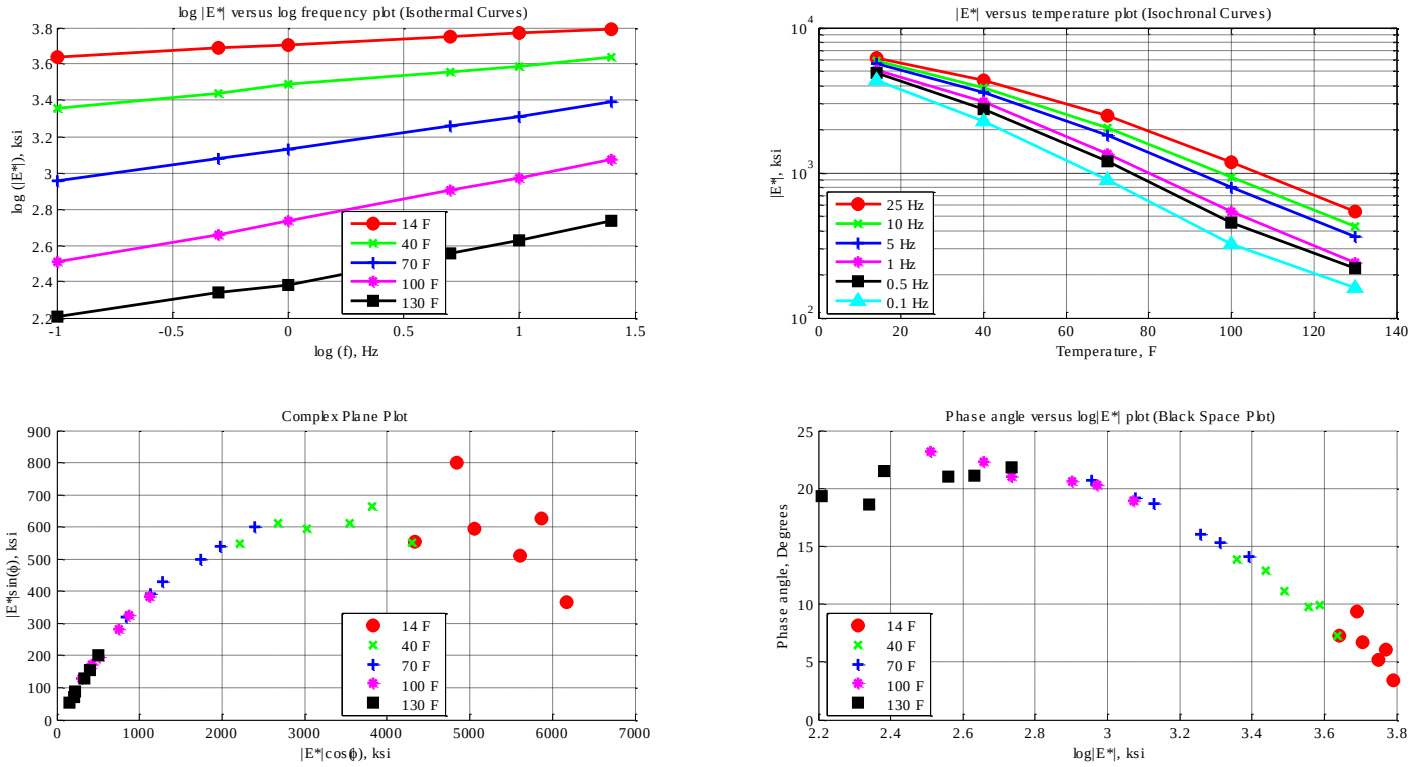

Figure C-114 Isothermal curves or |E*| versus frequency plot (top-left), isochronal curves or |E*| versus temperature plot (top-right), complex plane plot (bottom-left), and black space plot (bottom-right) for Mix 37 Specimen 3 in English unit system.

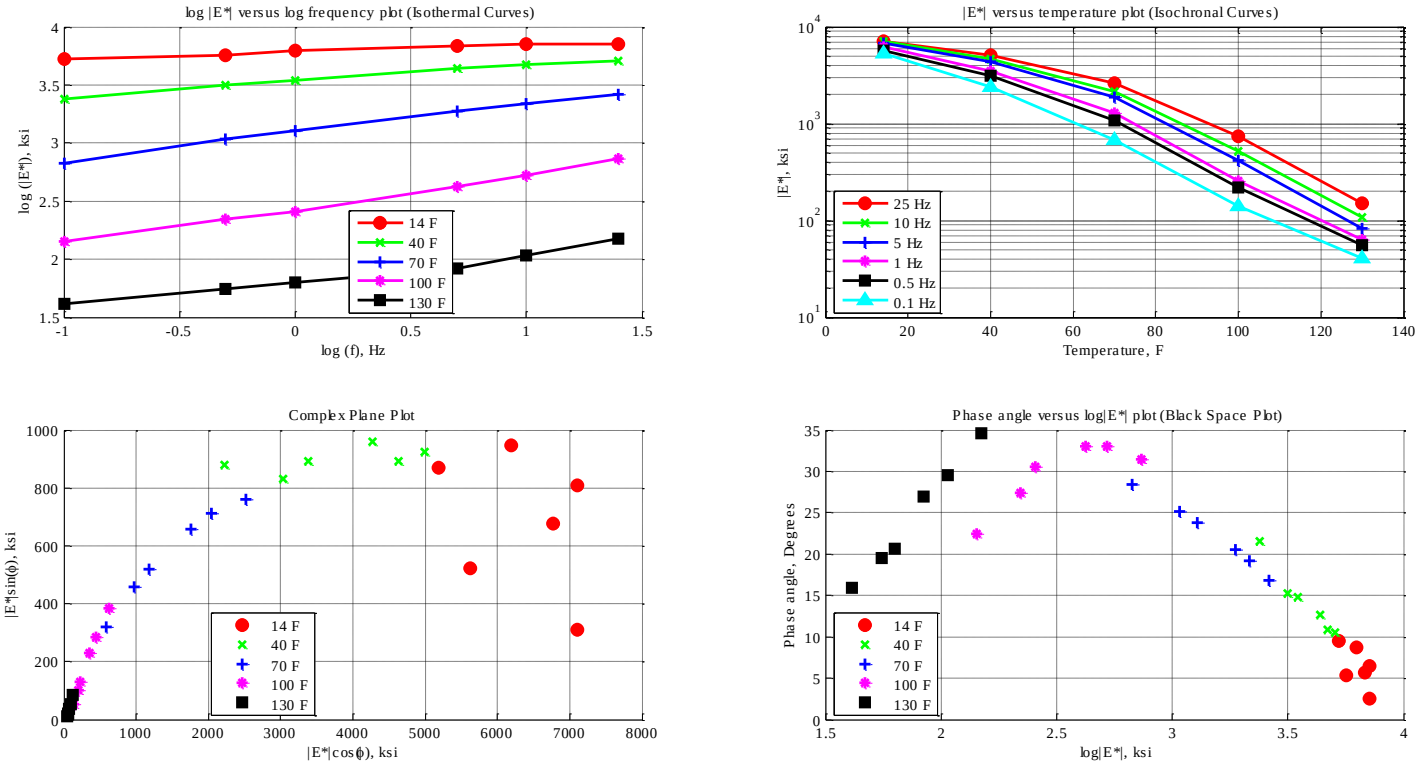

Figure C-115 Isothermal curves or |E*| versus frequency plot (top-left), isochronal curves or |E*| versus temperature plot (top-right), complex plane plot (bottom-left), and black space plot (bottom-right) for Mix 38 Specimen 3 in English unit system.

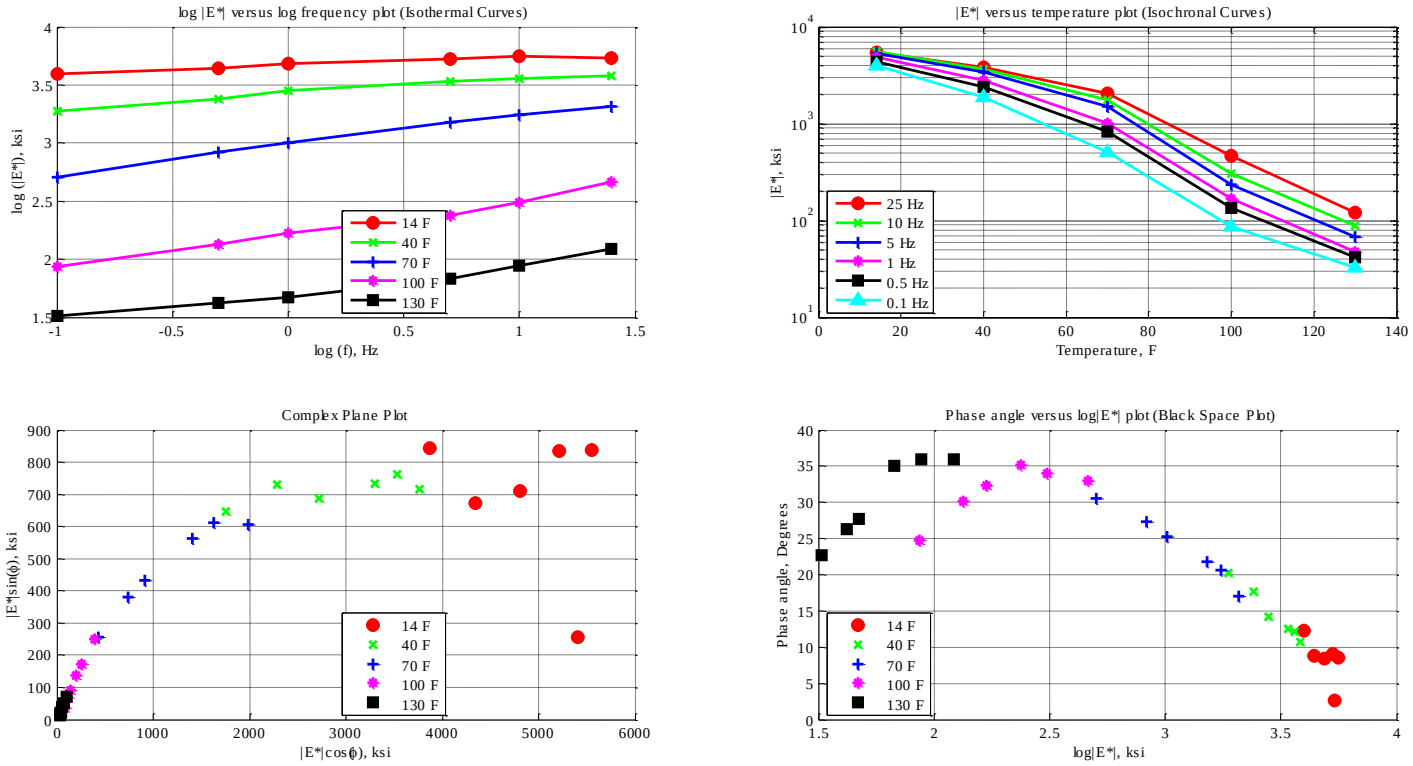

Figure C-116 Isothermal curves or |E*| versus frequency plot (top-left), isochronal curves or |E*| versus temperature plot (top-right), complex plane plot (bottom-left), and black space plot (bottom-right) for Mix 38 Specimen 4 in English unit system.

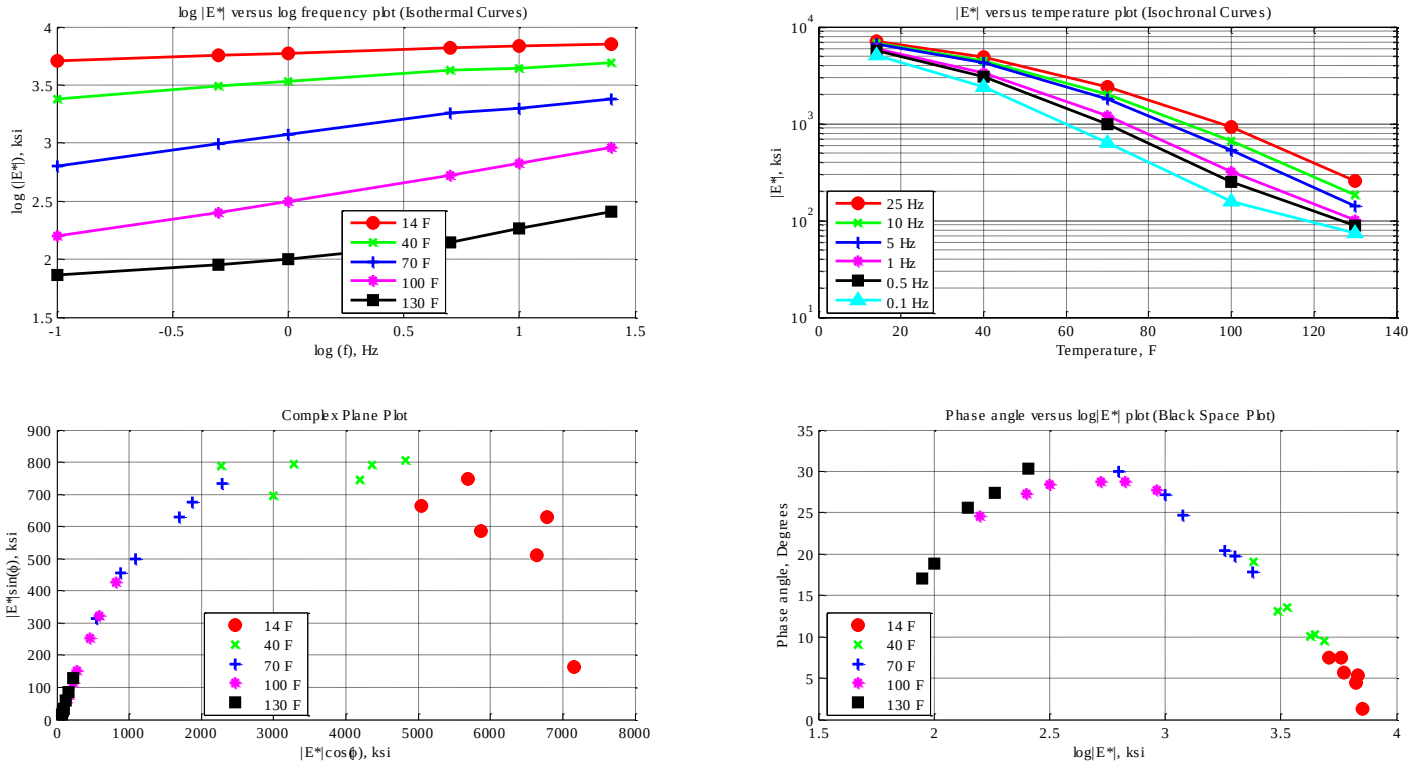

Figure C-117 Isothermal curves or |E*| versus frequency plot (top-left), isochronal curves or |E*| versus temperature plot (top-right), complex plane plot (bottom-left), and black space plot (bottom-right) for Mix 38 Specimen 5 in English unit system.

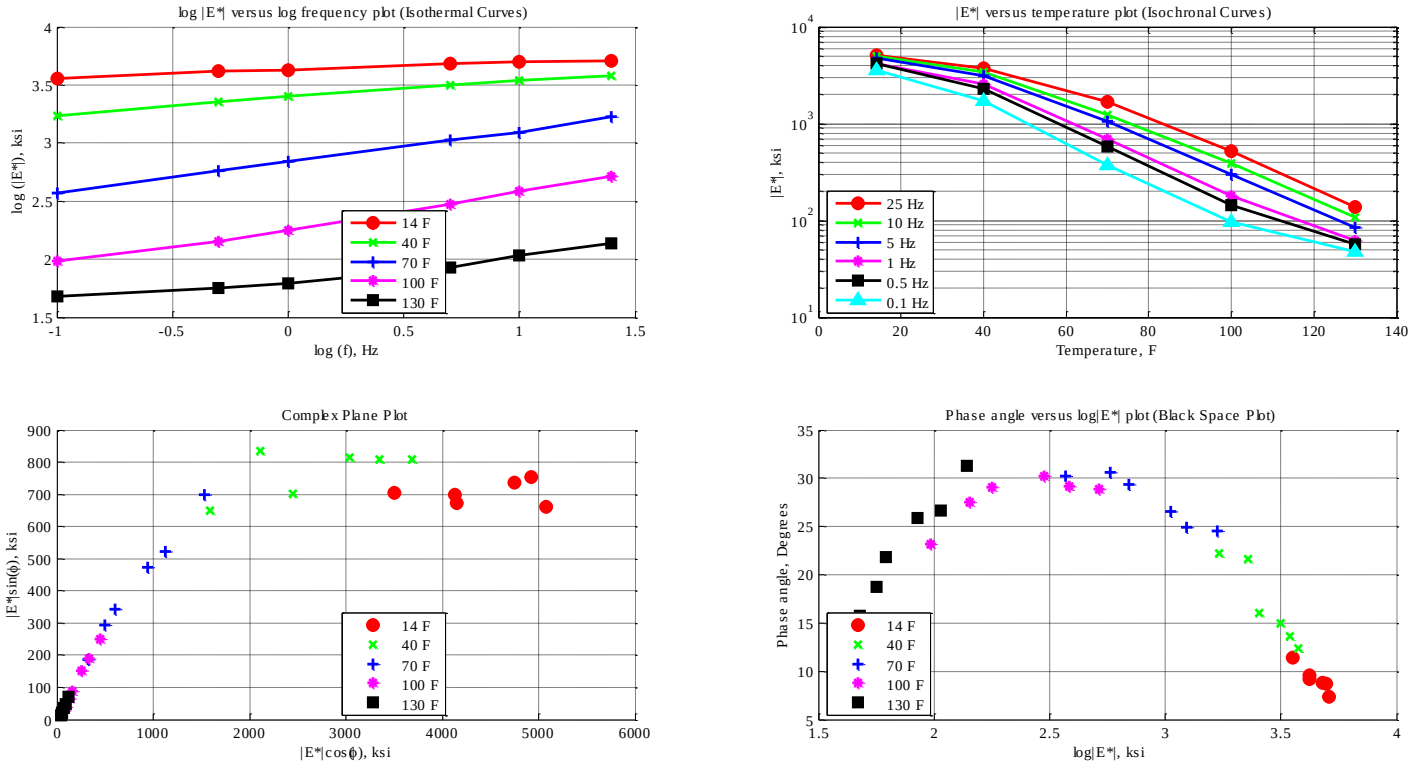

Figure C-118 Isothermal curves or |E*| versus frequency plot (top-left), isochronal curves or |E*| versus temperature plot (top-right), complex plane plot (bottom-left), and black space plot (bottom-right) for Mix 39 Specimen 1 in English unit system.

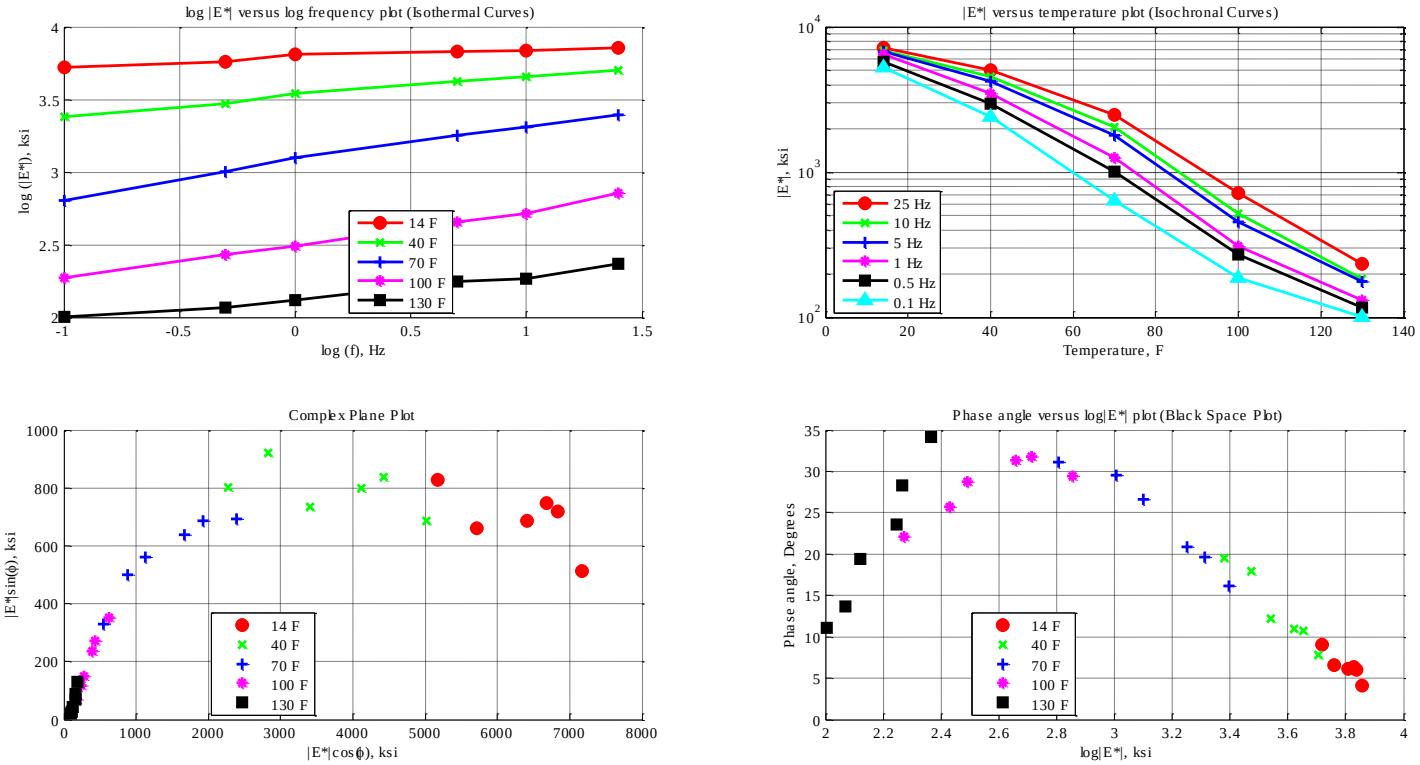

Figure C-119 Isothermal curves or |E*| versus frequency plot (top-left), isochronal curves or |E*| versus temperature plot (top-right), complex plane plot (bottom-left), and black space plot (bottom-right) for Mix 39 Specimen 2 in English unit system.

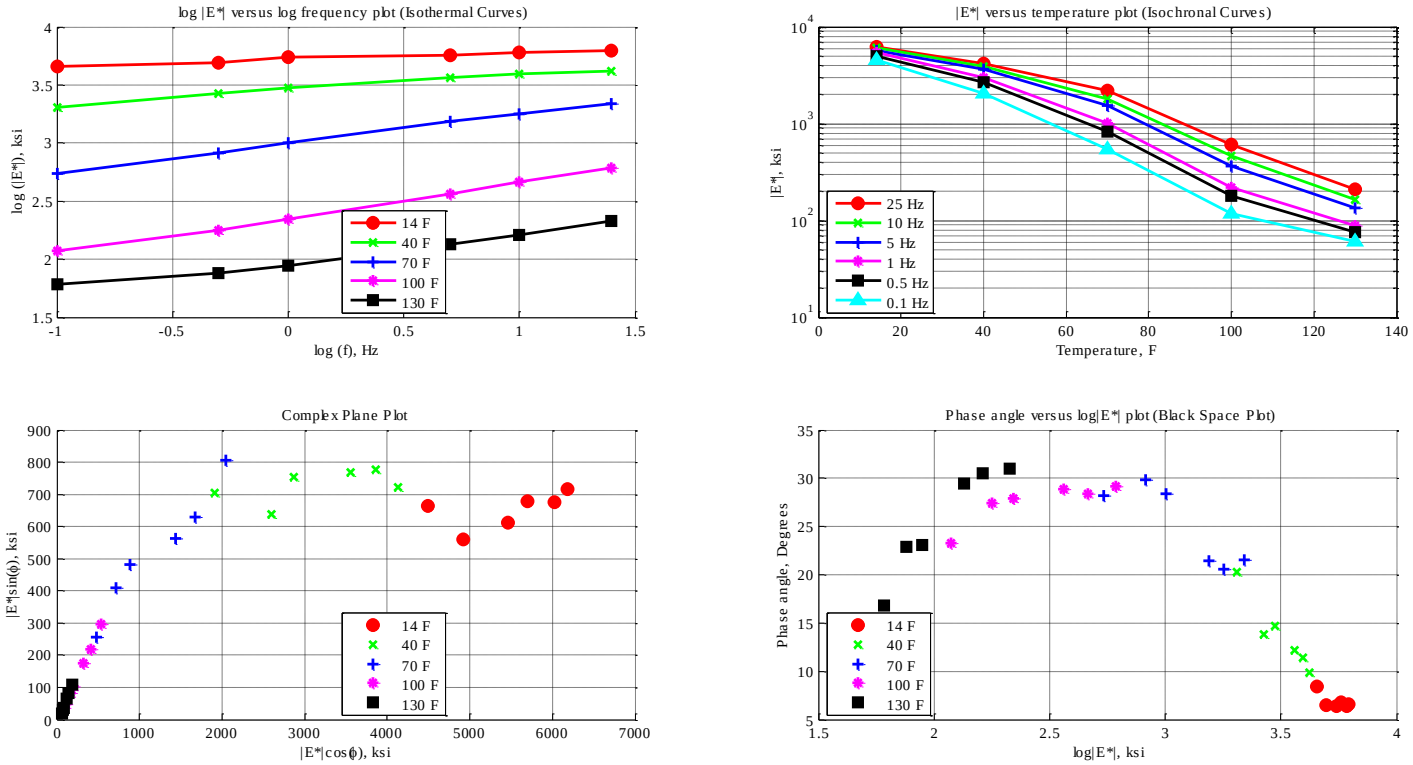

Figure C-120 Isothermal curves or |E*| versus frequency plot (top-left), isochronal curves or |E*| versus temperature plot (top-right), complex plane plot (bottom-left), and black space plot (bottom-right) for Mix 39 Specimen 7 in English unit system.

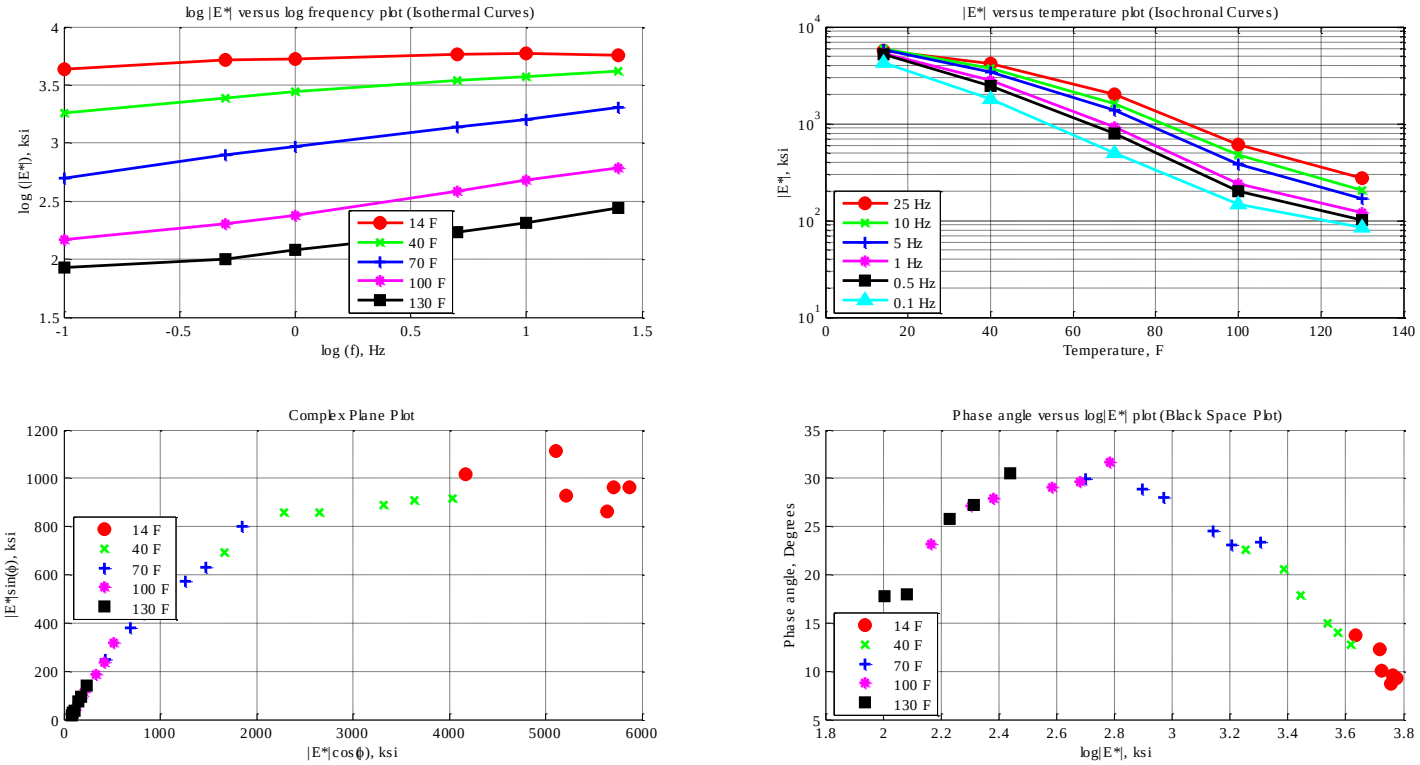

Figure C-121 Isothermal curves or |E*| versus frequency plot (top-left), isochronal curves or |E*| versus temperature plot (top-right), complex plane plot (bottom-left), and black space plot (bottom-right) for Mix 40 Specimen 2 in English unit system.

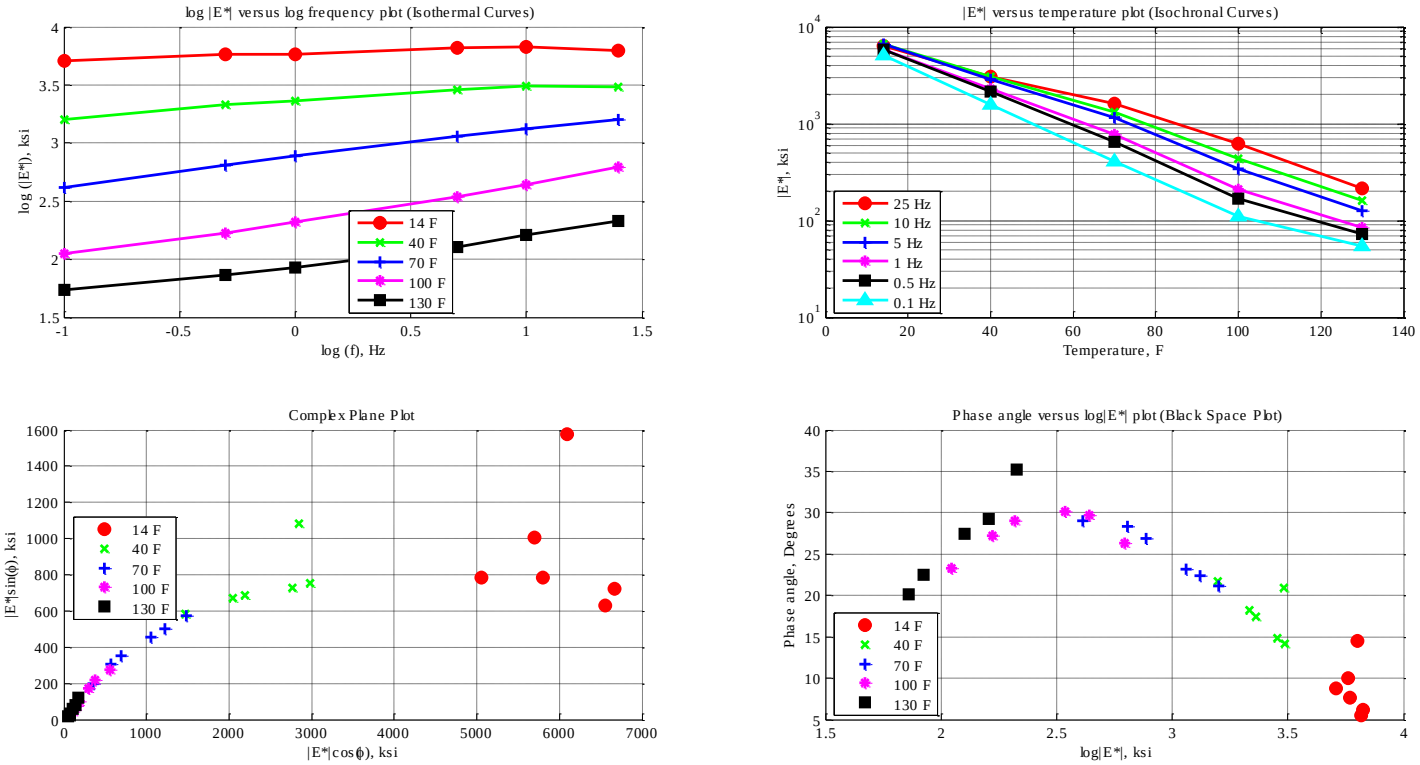

Figure C-122 Isothermal curves or |E*| versus frequency plot (top-left), isochronal curves or |E*| versus temperature plot (top-right), complex plane plot (bottom-left), and black space plot (bottom-right) for Mix 40 Specimen 3 in English unit system.

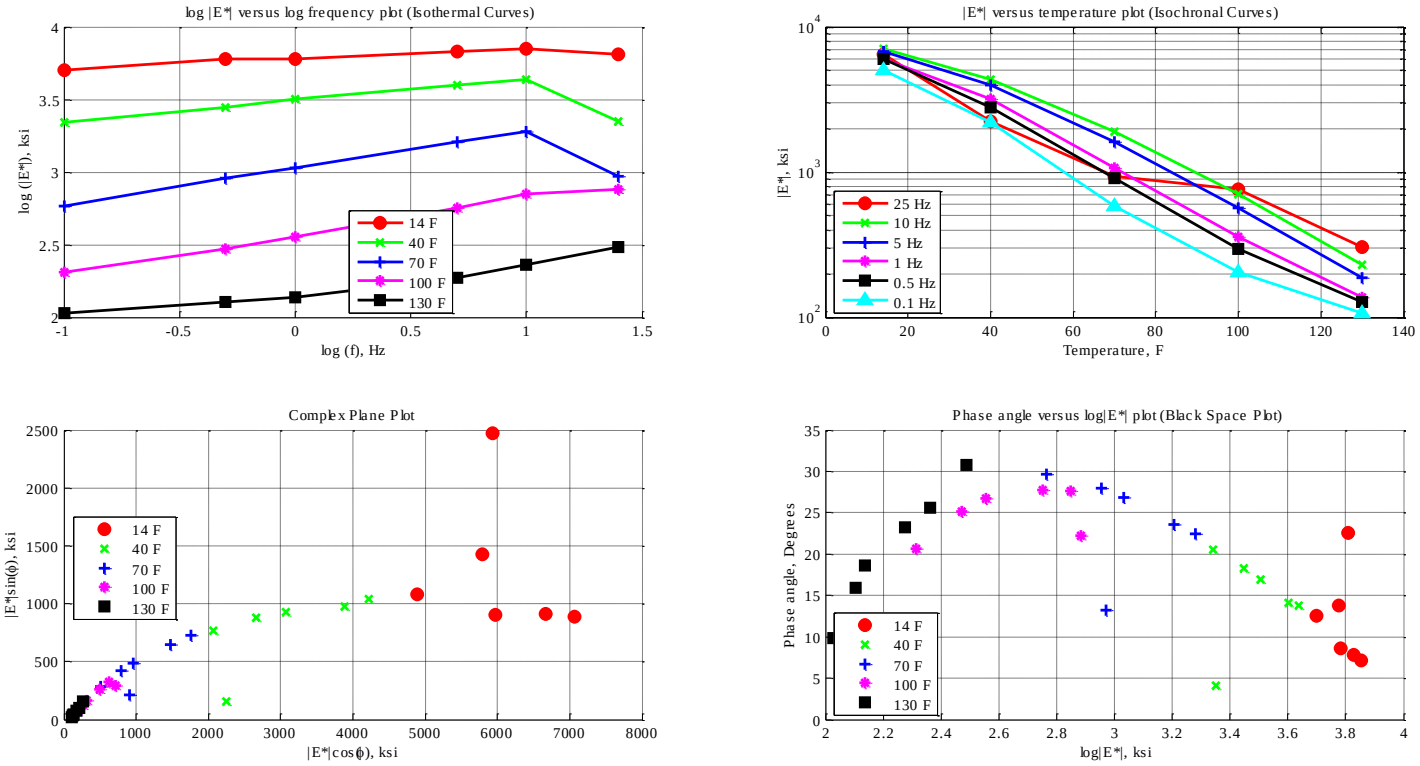

Figure C-123 Isothermal curves or |E*| versus frequency plot (top-left), isochronal curves or |E*| versus temperature plot (top-right), complex plane plot (bottom-left), and black space plot (bottom-right) for Mix 40 Specimen 4 in English unit system.

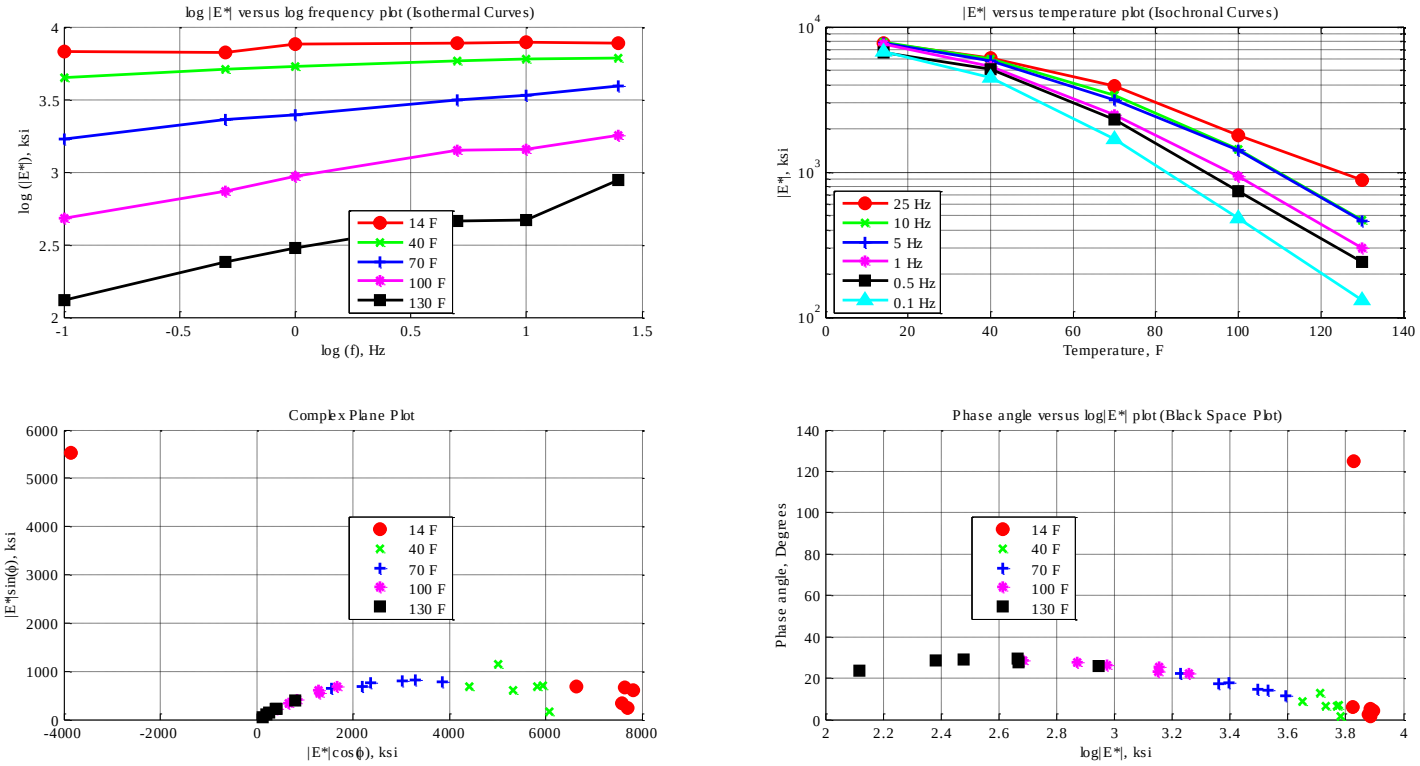

Figure C-124 Isothermal curves or |E*| versus frequency plot (top-left), isochronal curves or |E*| versus temperature plot (top-right), complex plane plot (bottom-left), and black space plot (bottom-right) for Mix 41 Specimen 1 in English unit system.

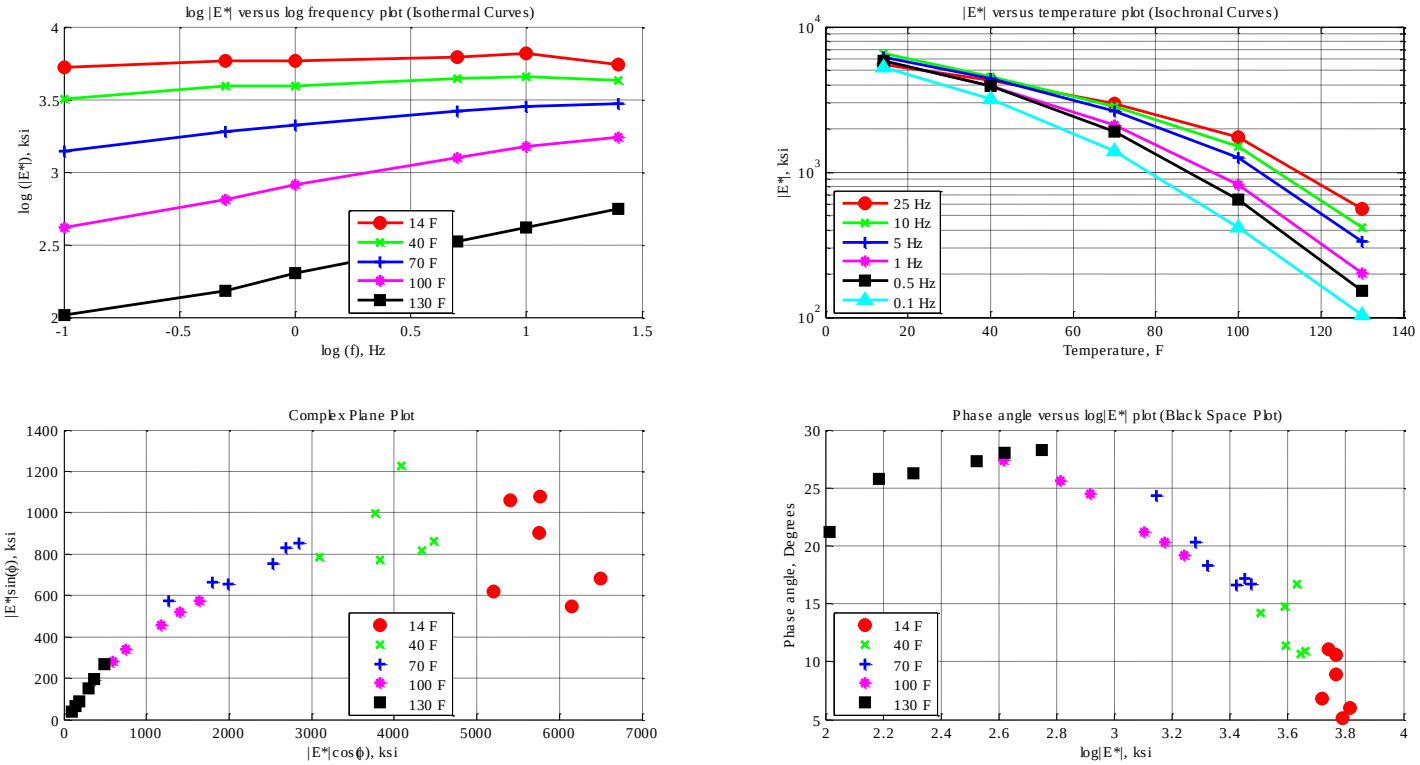

Figure C-125 Isothermal curves or |E*| versus frequency plot (top-left), isochronal curves or |E*| versus temperature plot (top-right), complex plane plot (bottom-left), and black space plot (bottom-right) for Mix 41 Specimen 2 in English unit system.

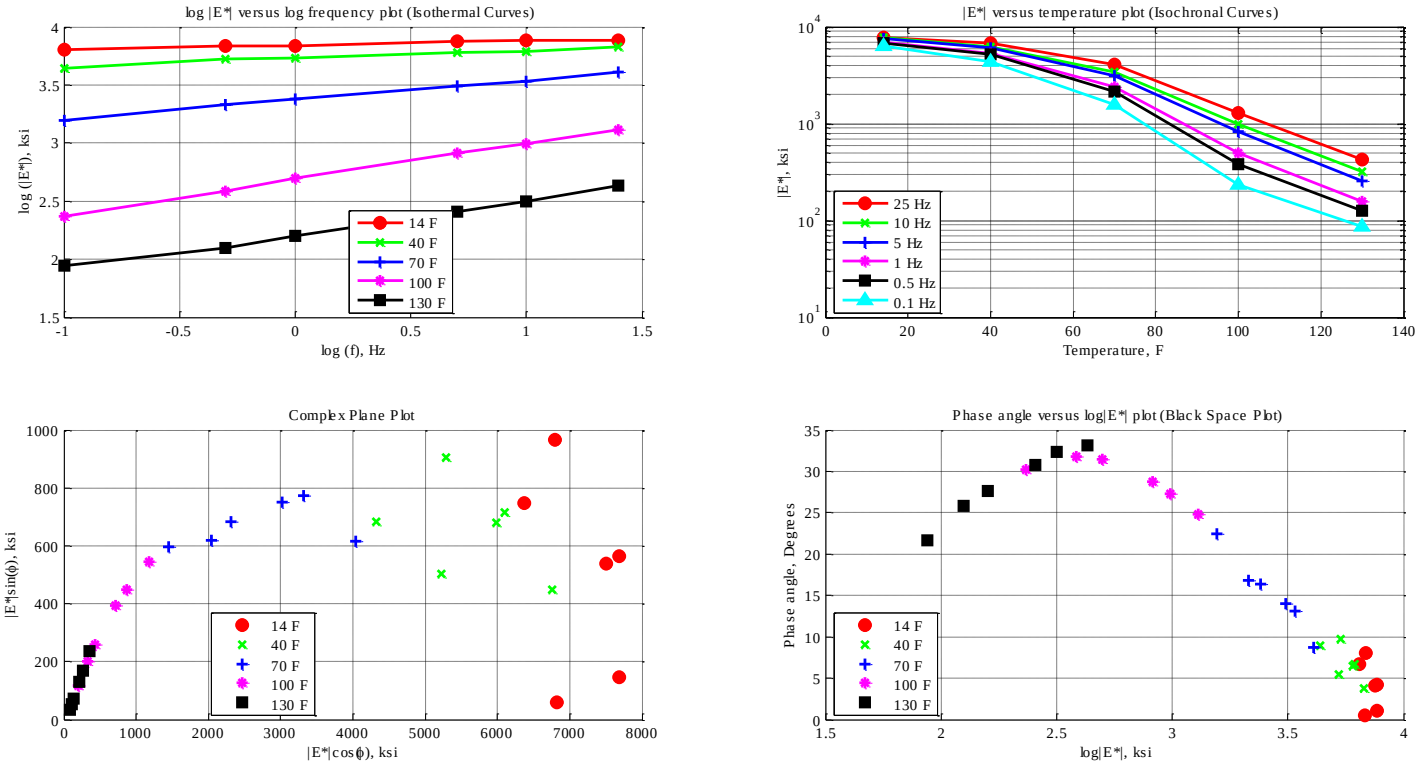

Figure C-126 Isothermal curves or |E*| versus frequency plot (top-left), isochronal curves or |E*| versus temperature plot (top-right), complex plane plot (bottom-left), and black space plot (bottom-right) for Mix 41 Specimen 6 in English unit system.

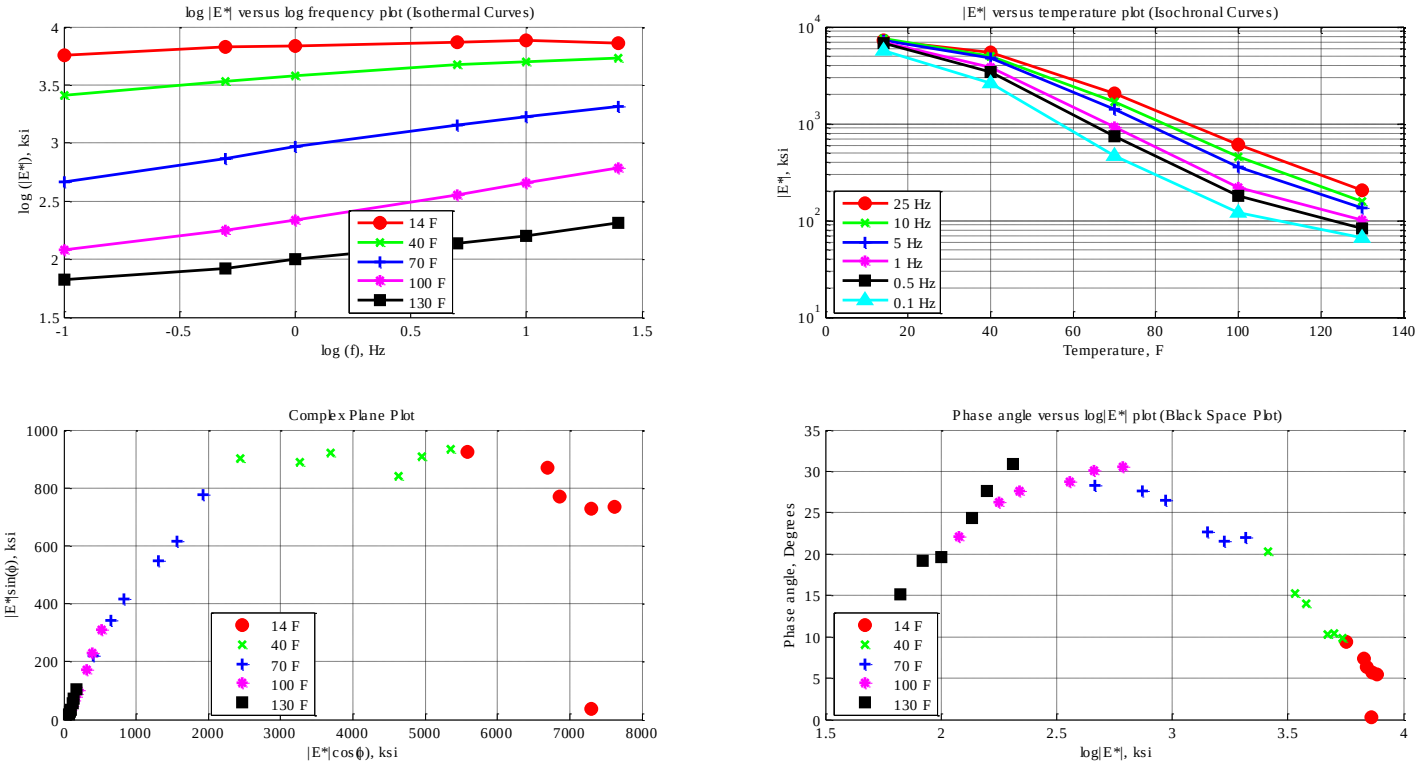

Figure C-127 Isothermal curves or |E*| versus frequency plot (top-left), isochronal curves or |E*| versus temperature plot (top-right), complex plane plot (bottom-left), and black space plot (bottom-right) for Mix 42 Specimen 1 in English unit system.

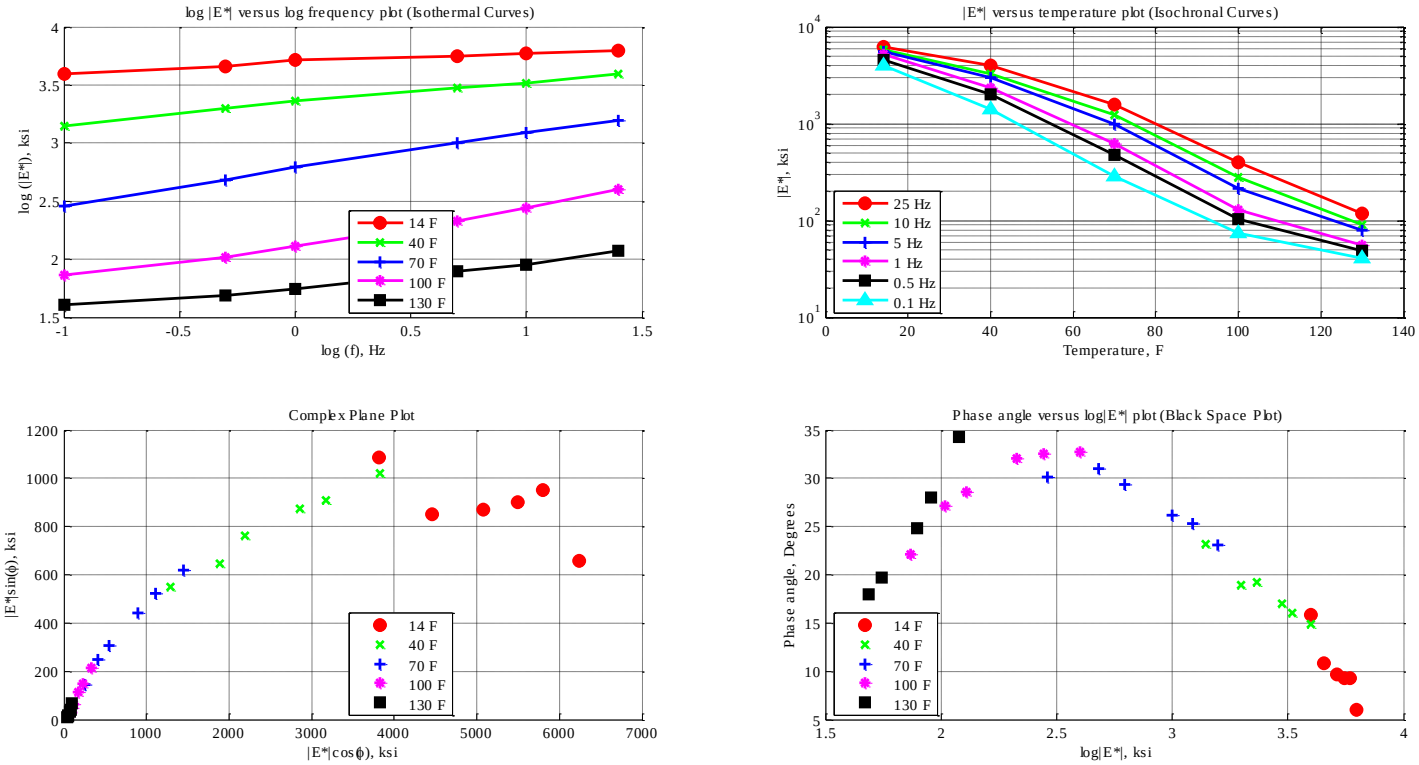

Figure C-128 Isothermal curves or |E*| versus frequency plot (top-left), isochronal curves or |E*| versus temperature plot (top-right), complex plane plot (bottom-left), and black space plot (bottom-right) for Mix 42 Specimen 2 in English unit system.

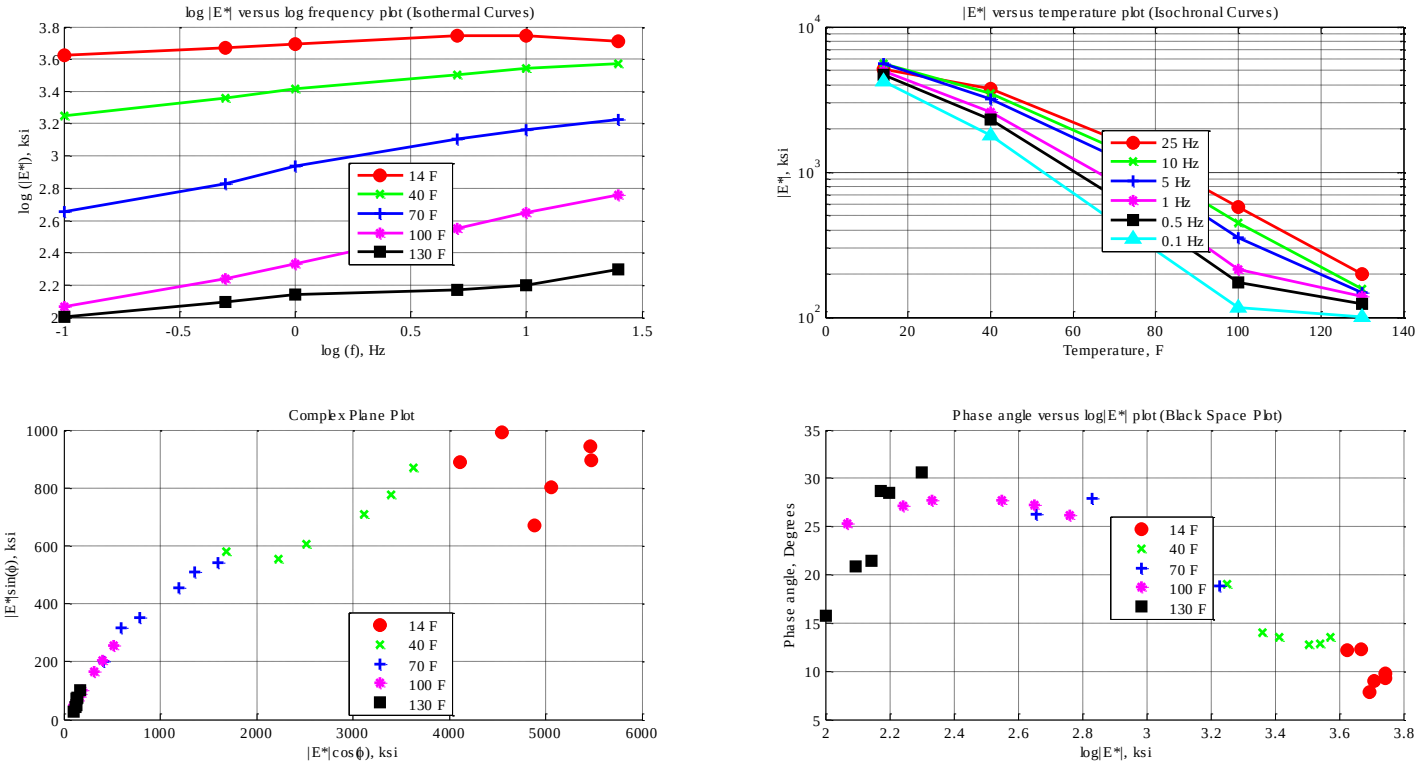

Figure C-129 Isothermal curves or |E*| versus frequency plot (top-left), isochronal curves or |E*| versus temperature plot (top-right), complex plane plot (bottom-left), and black space plot (bottom-right) for Mix 42 Specimen 5 in English unit system.

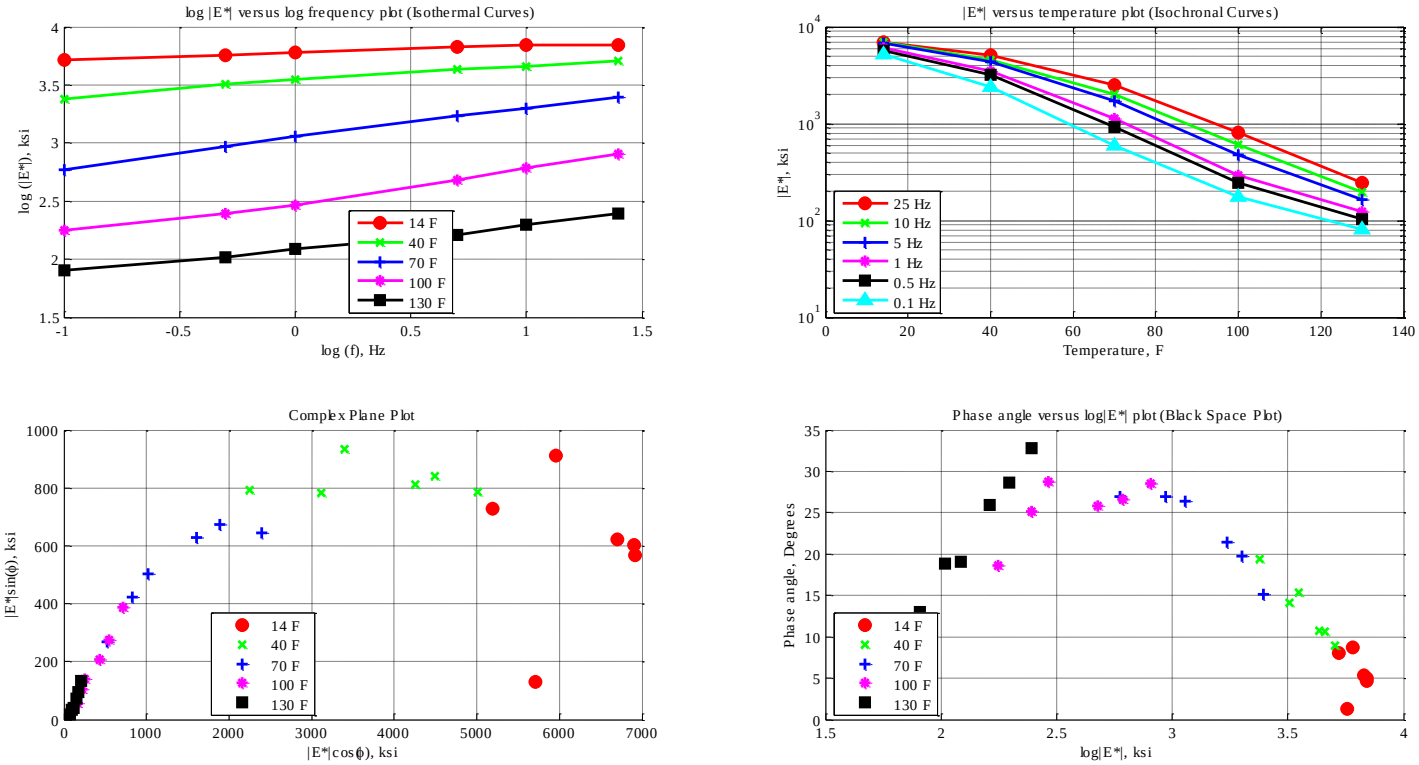

Figure C-130 Isothermal curves or |E*| versus frequency plot (top-left), isochronal curves or |E*| versus temperature plot (top-right), complex plane plot (bottom-left), and black space plot (bottom-right) for Mix 43 Specimen 1 in English unit system.

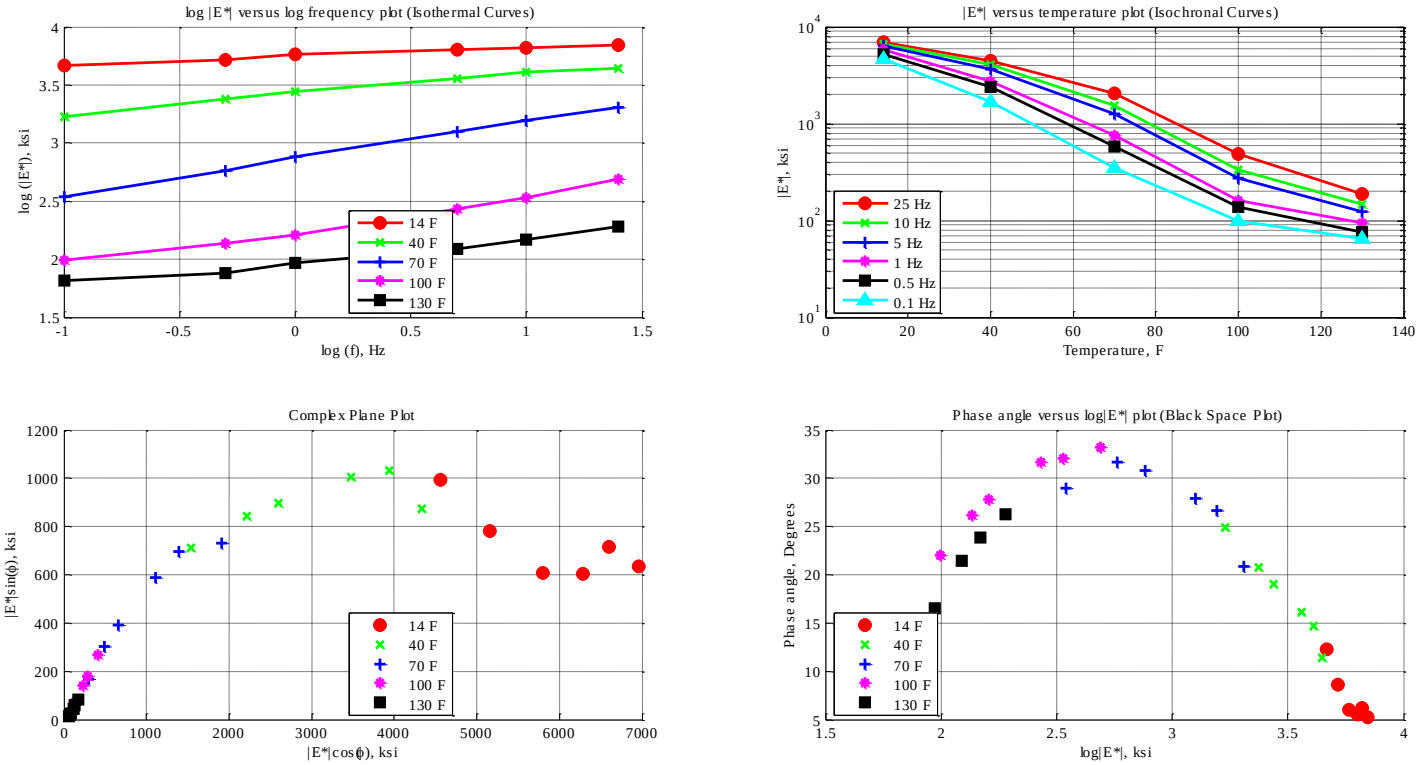

Figure C-131 Isothermal curves or |E*| versus frequency plot (top-left), isochronal curves or |E*| versus temperature plot (top-right), complex plane plot (bottom-left), and black space plot (bottom-right) for Mix 43 Specimen 2 in English unit system.

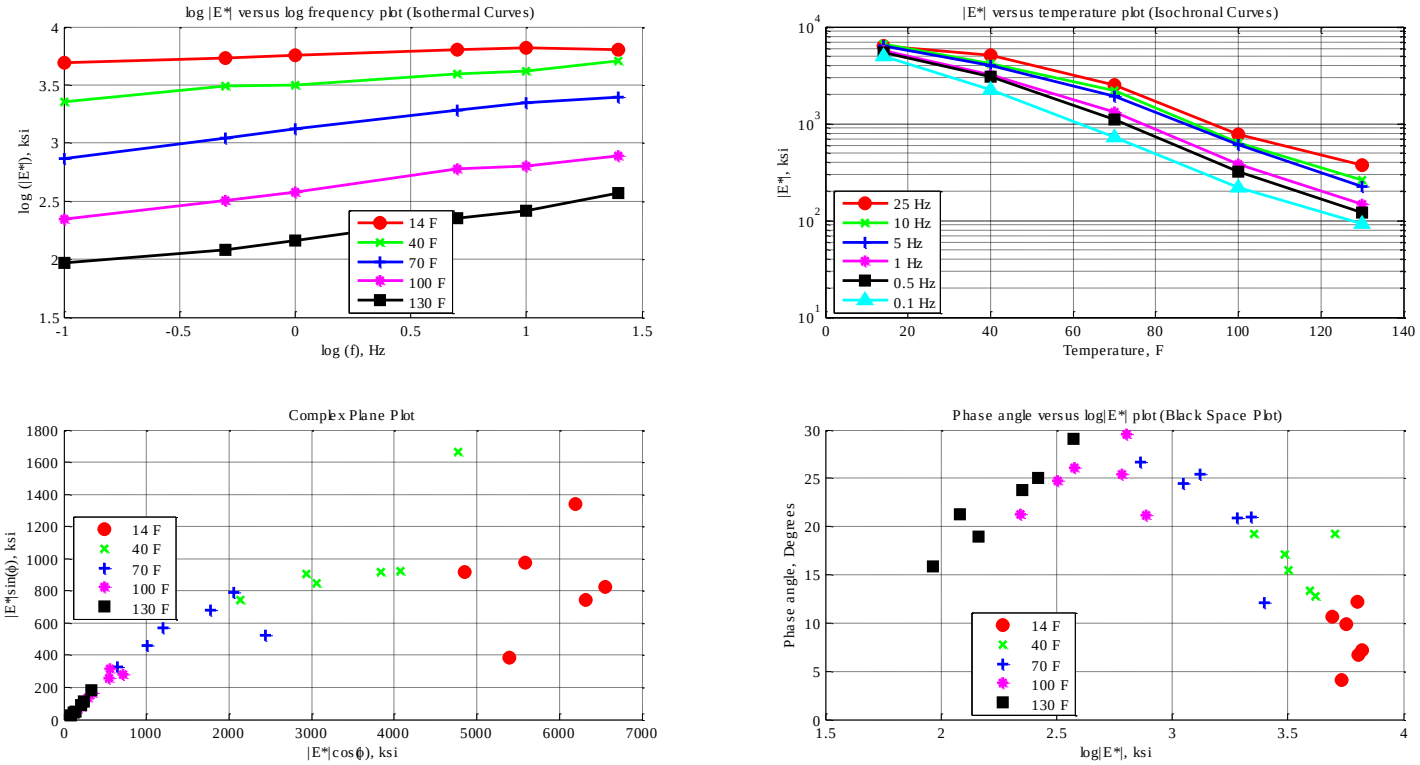

Figure C-132 Isothermal curves or |E*| versus frequency plot (top-left), isochronal curves or |E*| versus temperature plot (top-right), complex plane plot (bottom-left), and black space plot (bottom-right) for Mix 43 Specimen 4 in English unit system.

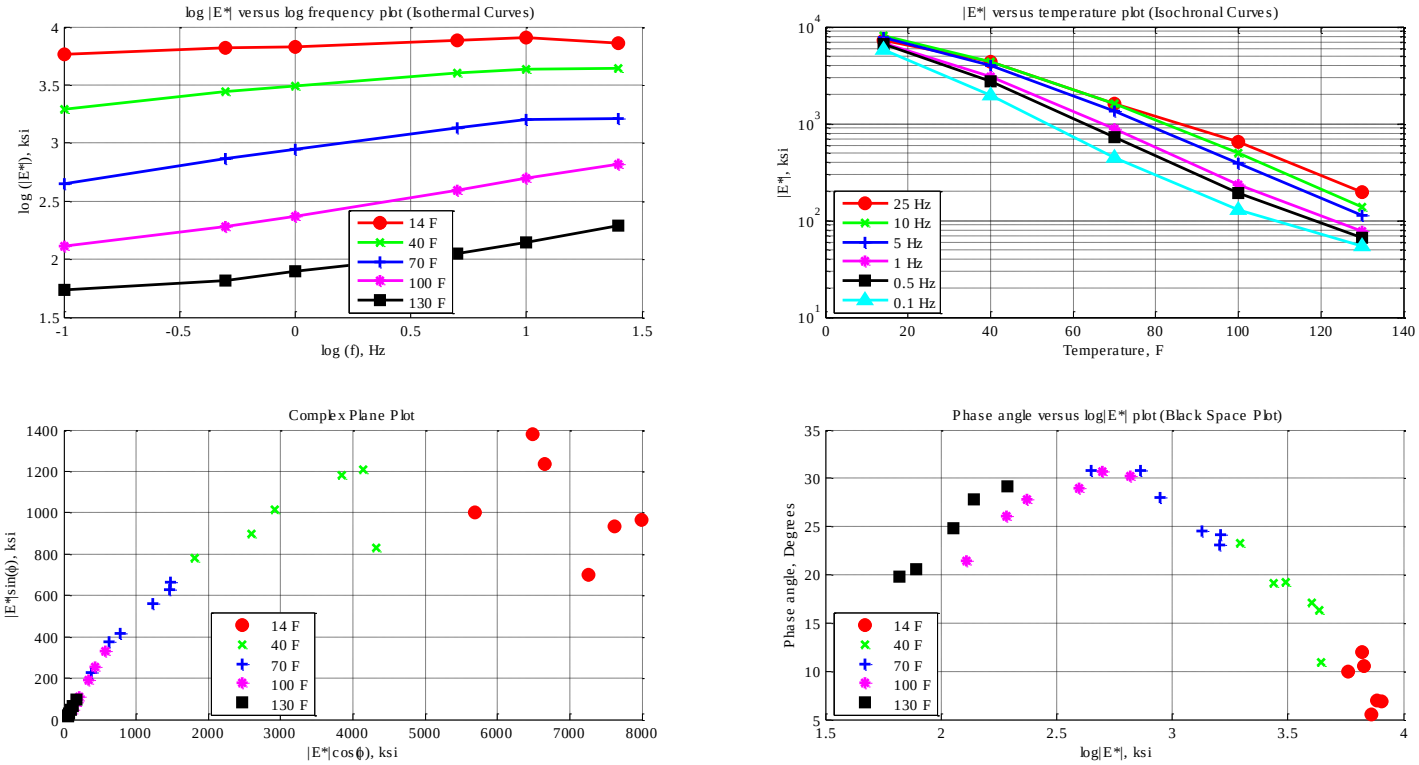

Figure C-133 Isothermal curves or |E*| versus frequency plot (top-left), isochronal curves or |E*| versus temperature plot (top-right), complex plane plot (bottom-left), and black space plot (bottom-right) for Mix 44 Specimen 2 in English unit system.

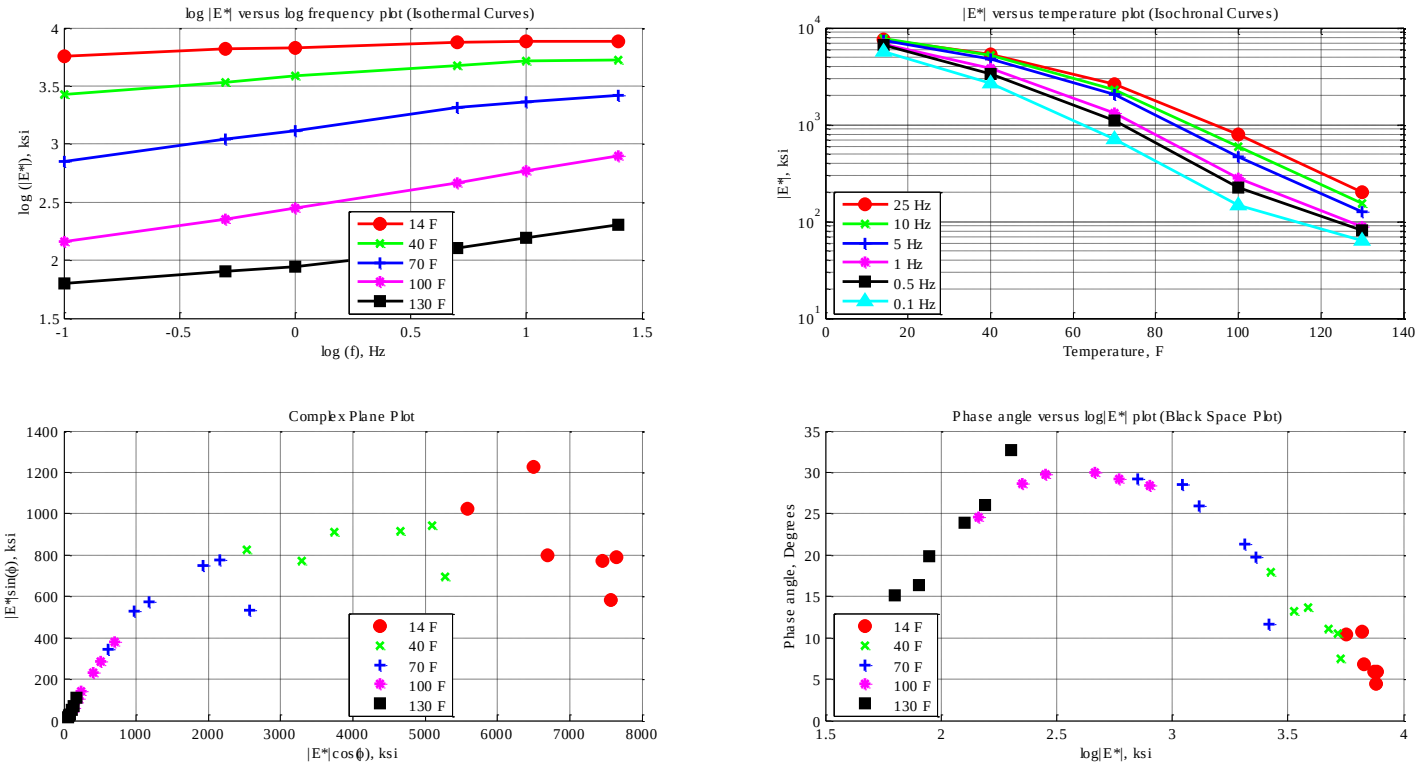

Figure C-134 Isothermal curves or |E*| versus frequency plot (top-left), isochronal curves or |E*| versus temperature plot (top-right), complex plane plot (bottom-left), and black space plot (bottom-right) for Mix 44 Specimen 3 in English unit system.

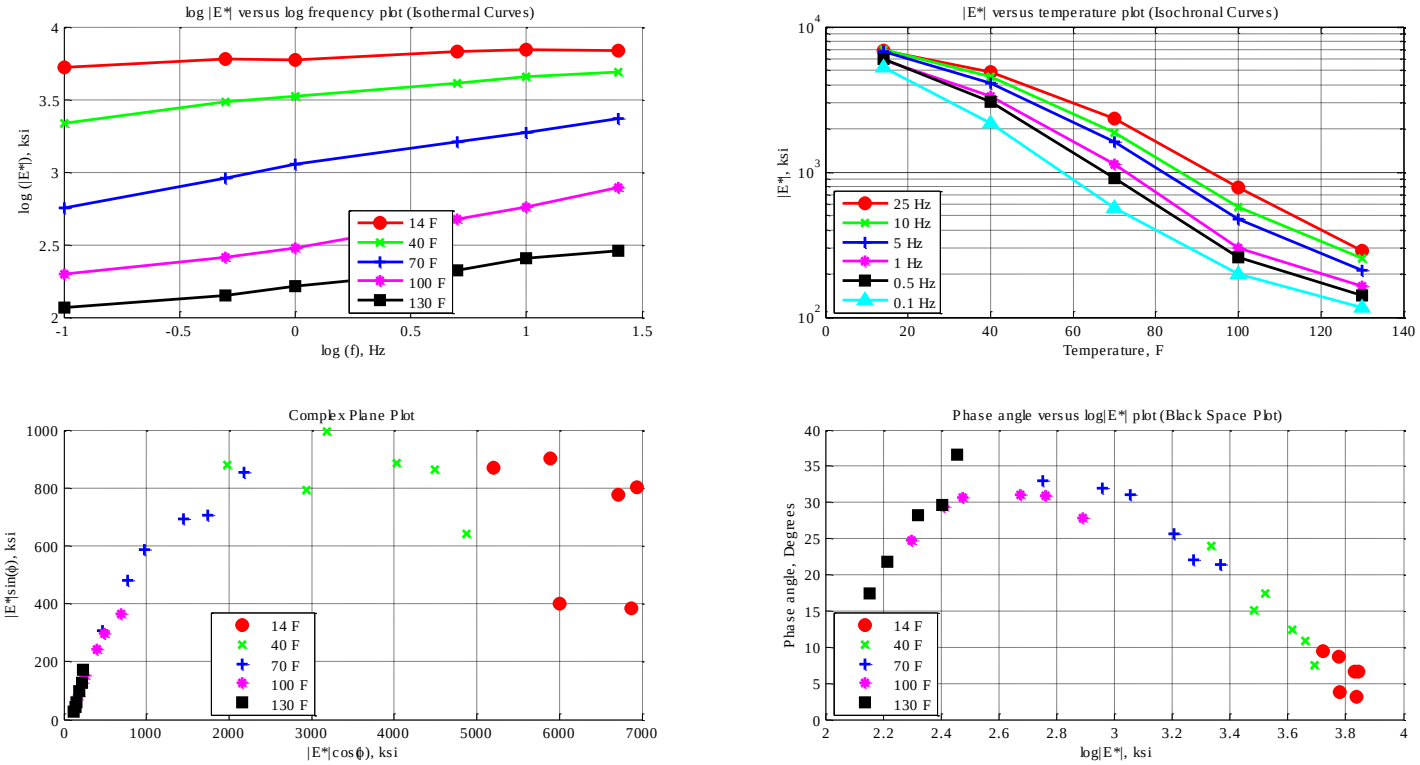

Figure C-135 Isothermal curves or |E*| versus frequency plot (top-left), isochronal curves or |E*| versus temperature plot (top-right), complex plane plot (bottom-left), and black space plot (bottom-right) for Mix 44 Specimen 4 in English unit system.

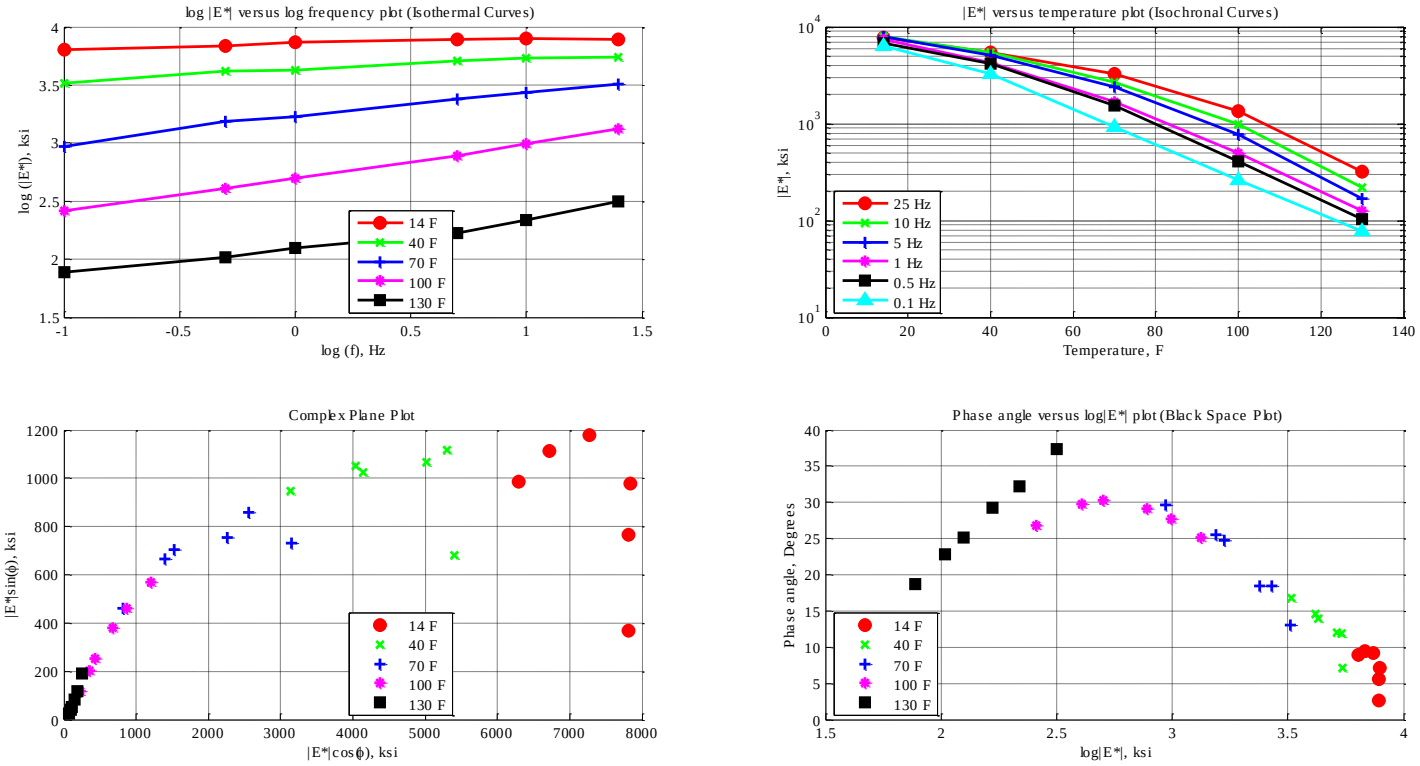

Figure C-136 Isothermal curves or |E*| versus frequency plot (top-left), isochronal curves or |E*| versus temperature plot (top-right), complex plane plot (bottom-left), and black space plot (bottom-right) for Mix 45 Specimen 1 in English unit system.

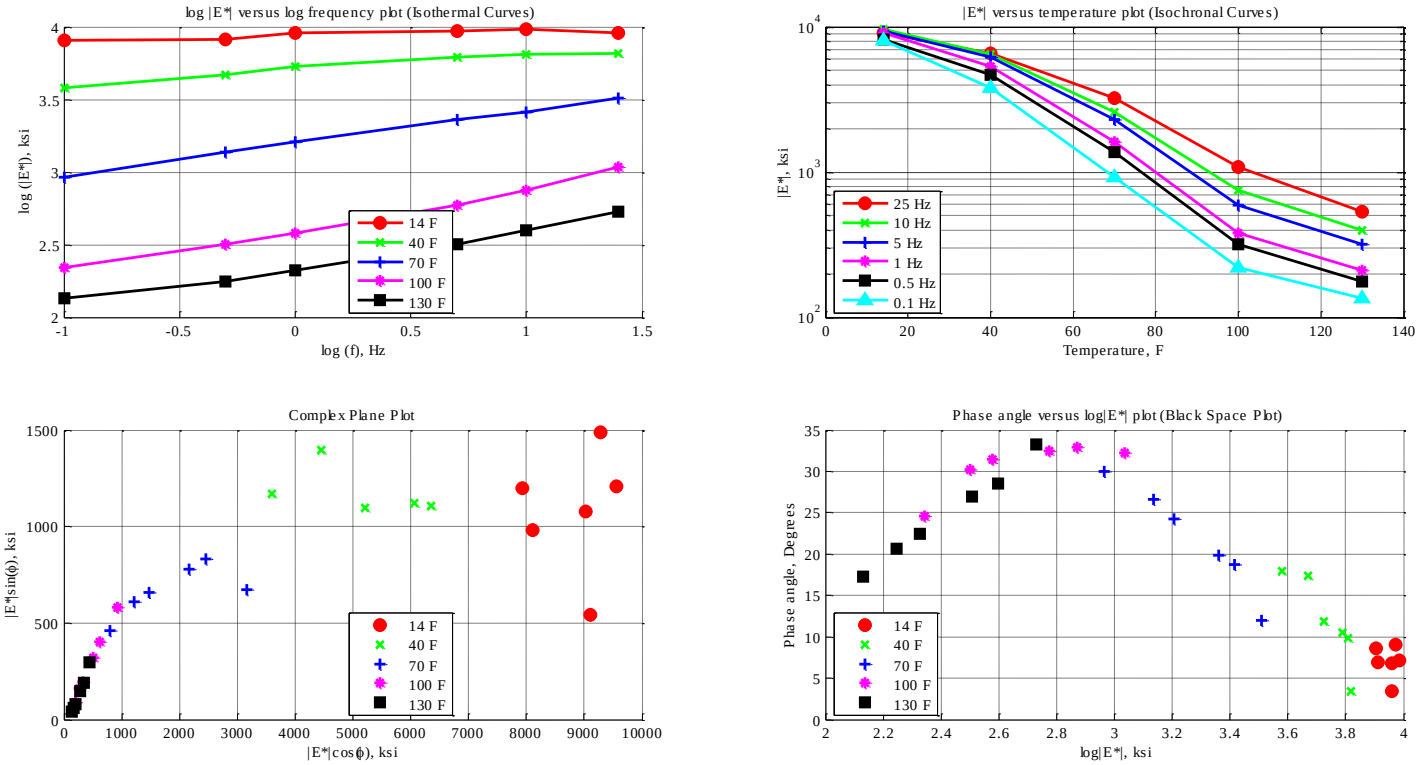

Figure C-137 Isothermal curves or |E*| versus frequency plot (top-left), isochronal curves or |E*| versus temperature plot (top-right), complex plane plot (bottom-left), and black space plot (bottom-right) for Mix 45 Specimen 3 in English unit system.

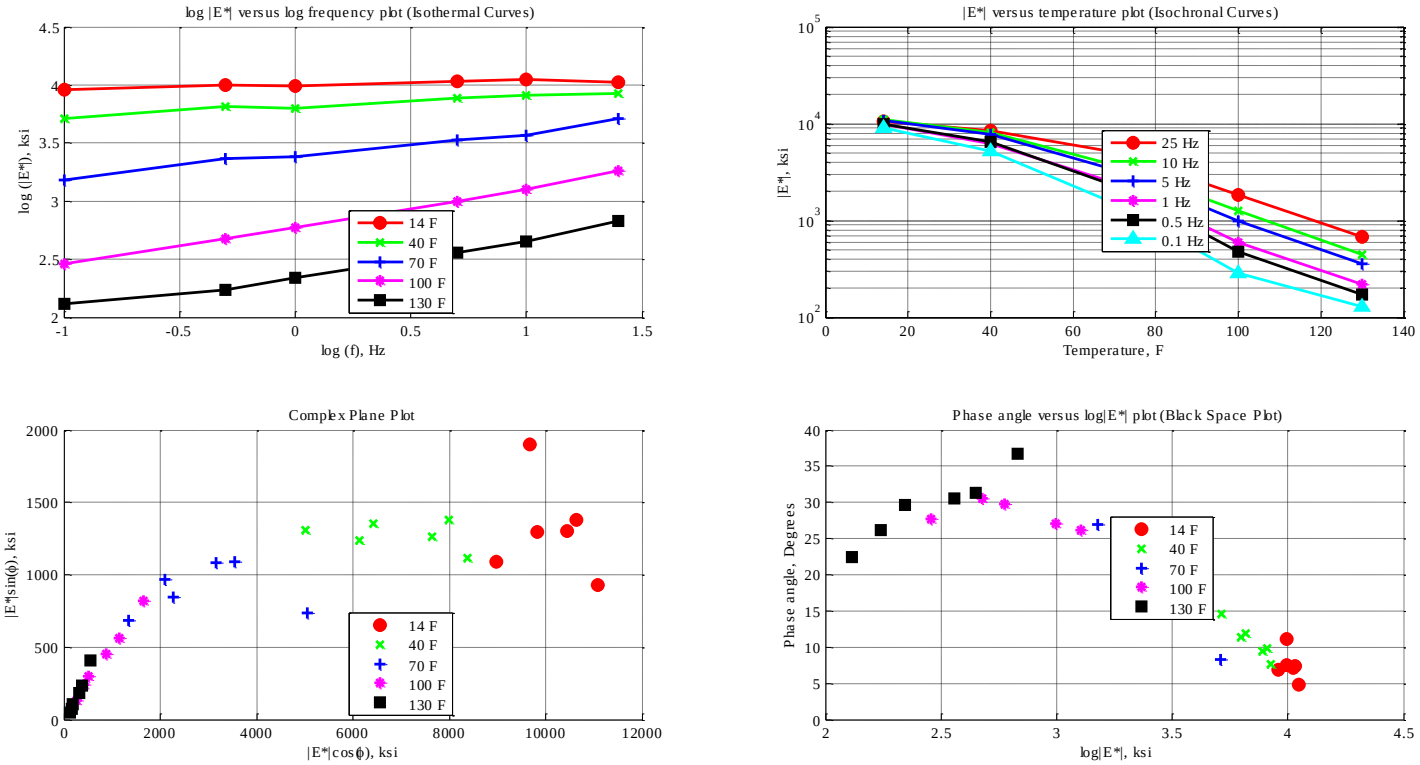

Figure C-138 Isothermal curves or |E*| versus frequency plot (top-left), isochronal curves or |E*| versus temperature plot (top-right), complex plane plot (bottom-left), and black space plot (bottom-right) for Mix 45 Specimen 4 in English unit system.

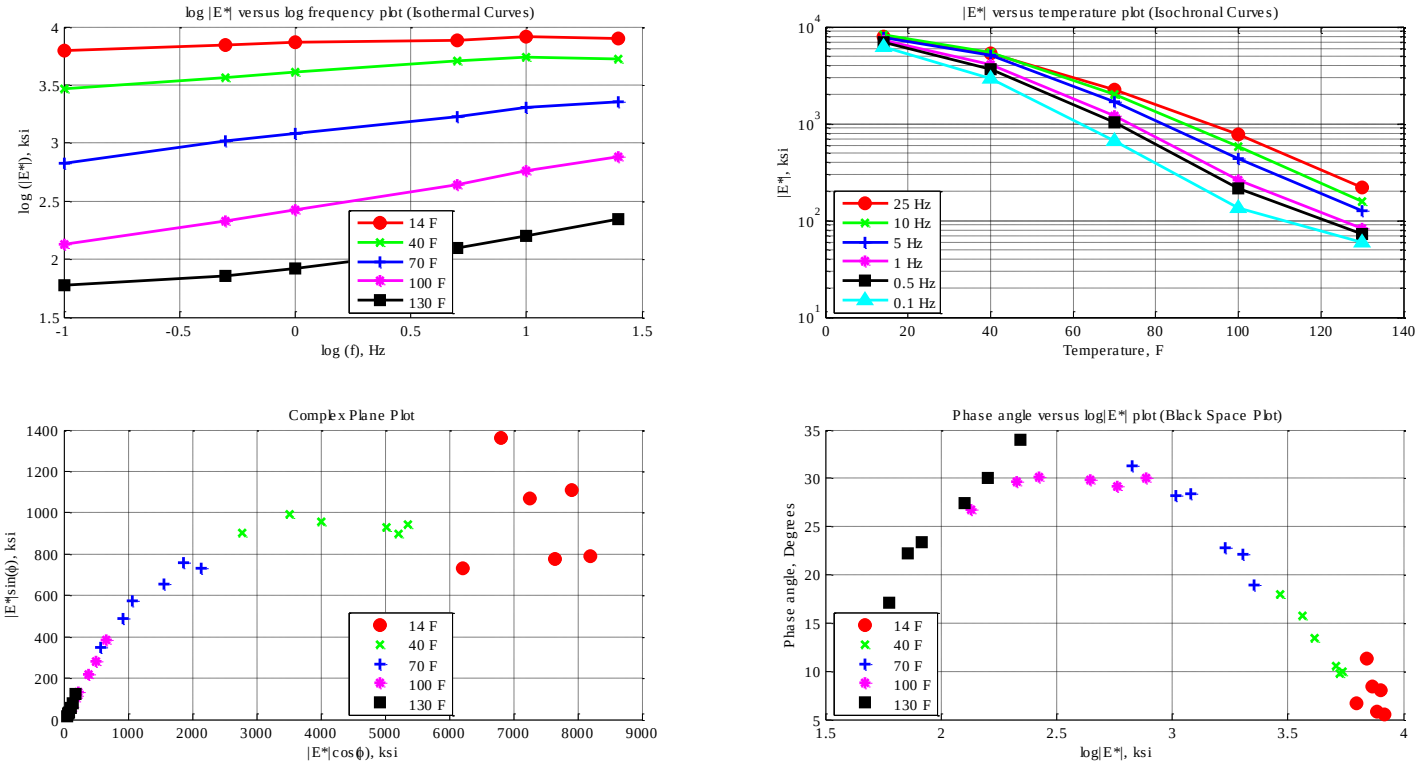

Figure C-139 Isothermal curves or |E*| versus frequency plot (top-left), isochronal curves or |E*| versus temperature plot (top-right), complex plane plot (bottom-left), and black space plot (bottom-right) for Mix 46 Specimen 1 in English unit system.

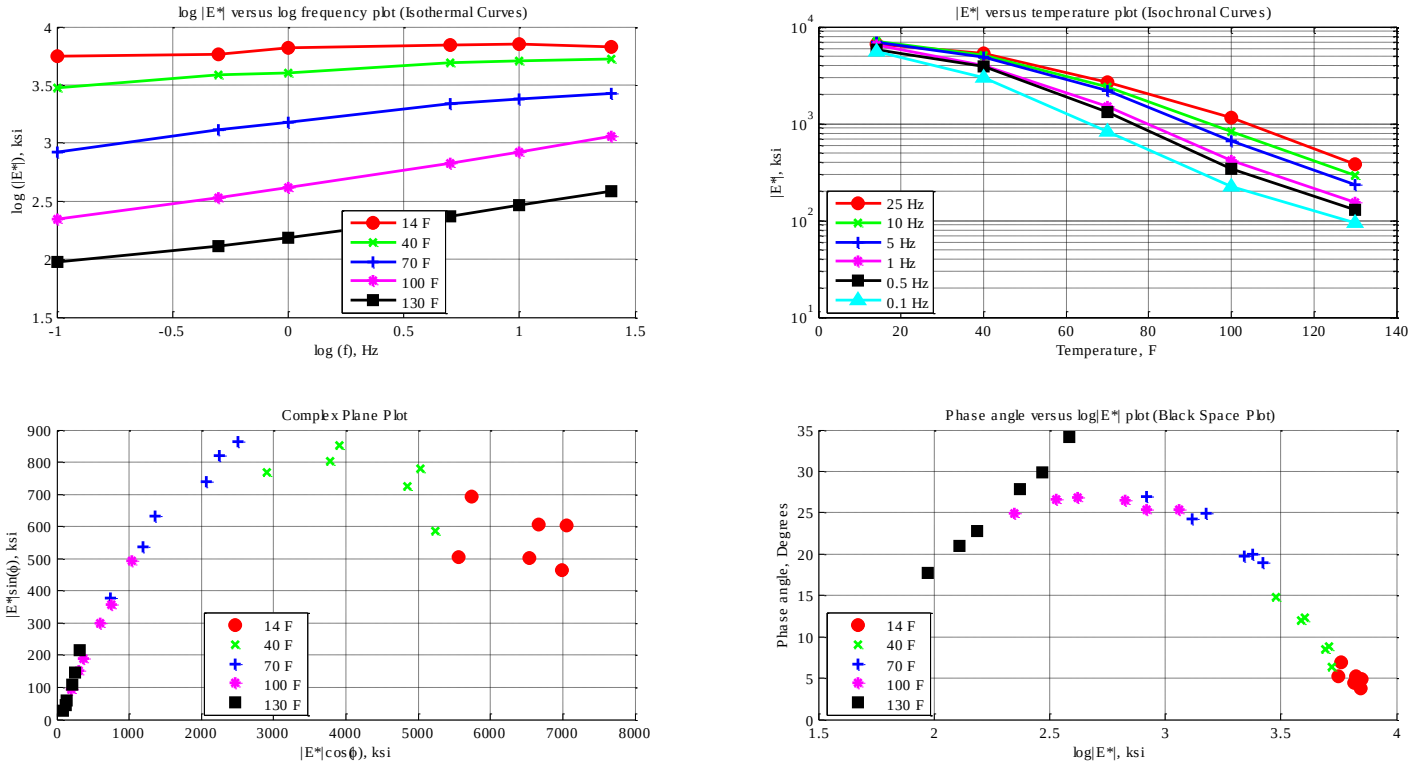

Figure C-140 Isothermal curves or |E*| versus frequency plot (top-left), isochronal curves or |E*| versus temperature plot (top-right), complex plane plot (bottom-left), and black space plot (bottom-right) for Mix 46 Specimen 3 in English unit system.

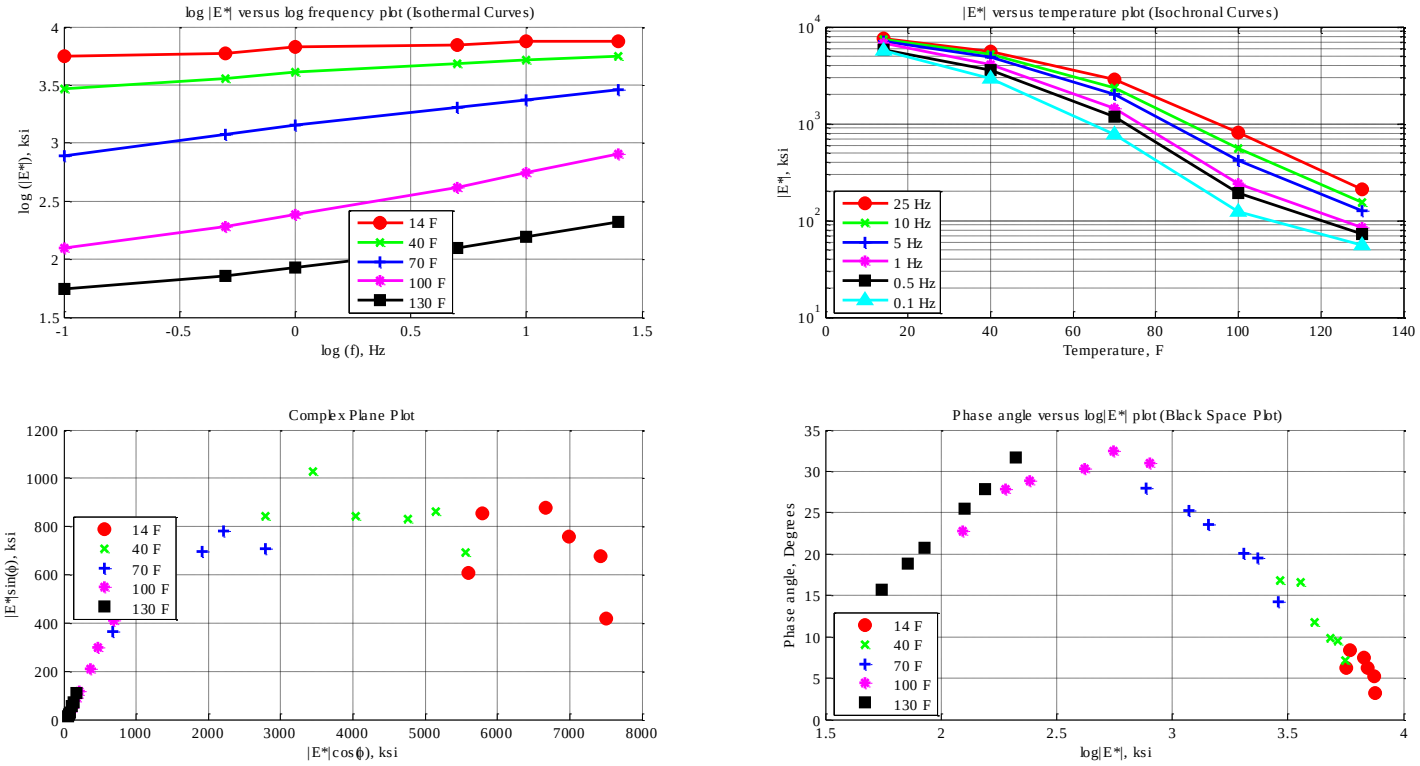

Figure C-141 Isothermal curves or |E*| versus frequency plot (top-left), isochronal curves or |E*| versus temperature plot (top-right), complex plane plot (bottom-left), and black space plot (bottom-right) for Mix 46 Specimen 5 in English unit system.

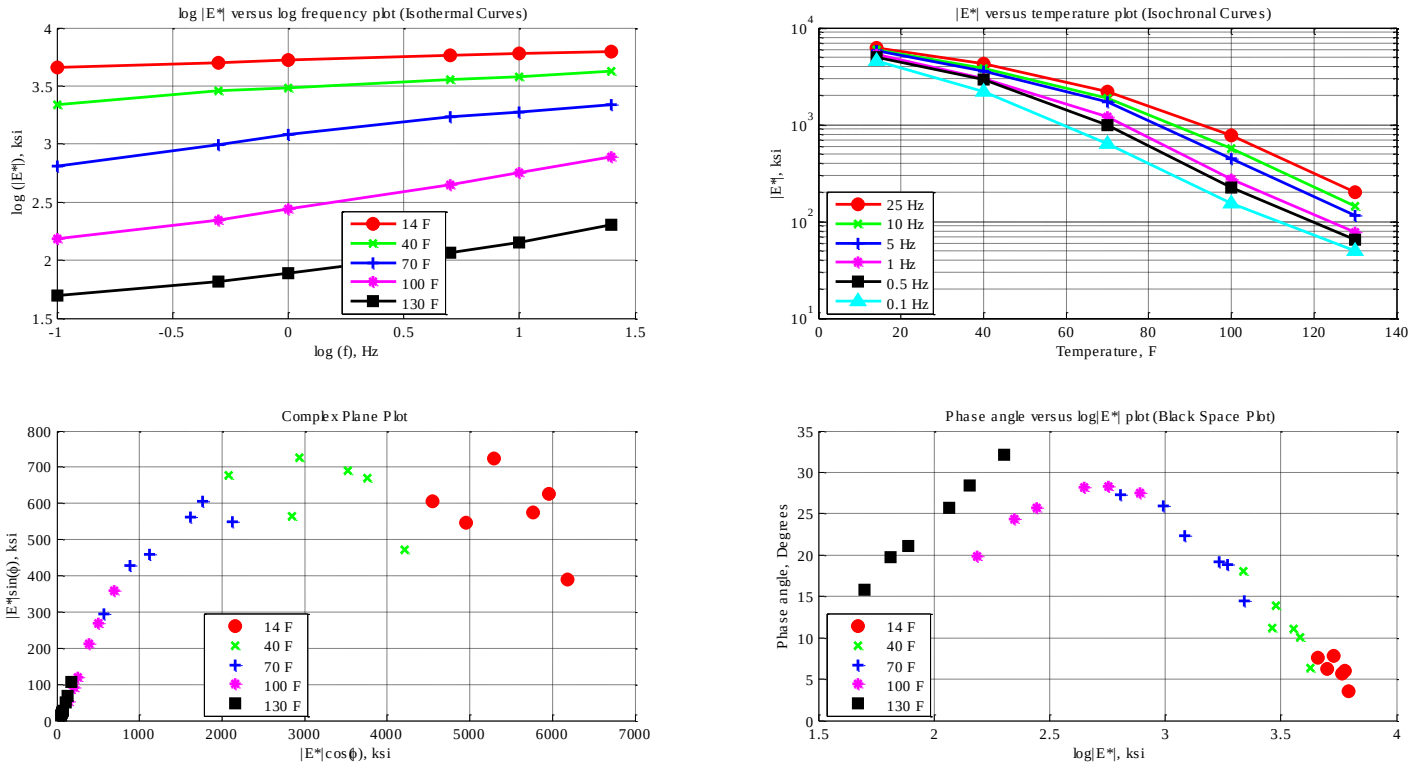

Figure C-142 Isothermal curves or |E*| versus frequency plot (top-left), isochronal curves or |E*| versus temperature plot (top-right), complex plane plot (bottom-left), and black space plot (bottom-right) for Mix 47 Specimen 1 in English unit system.

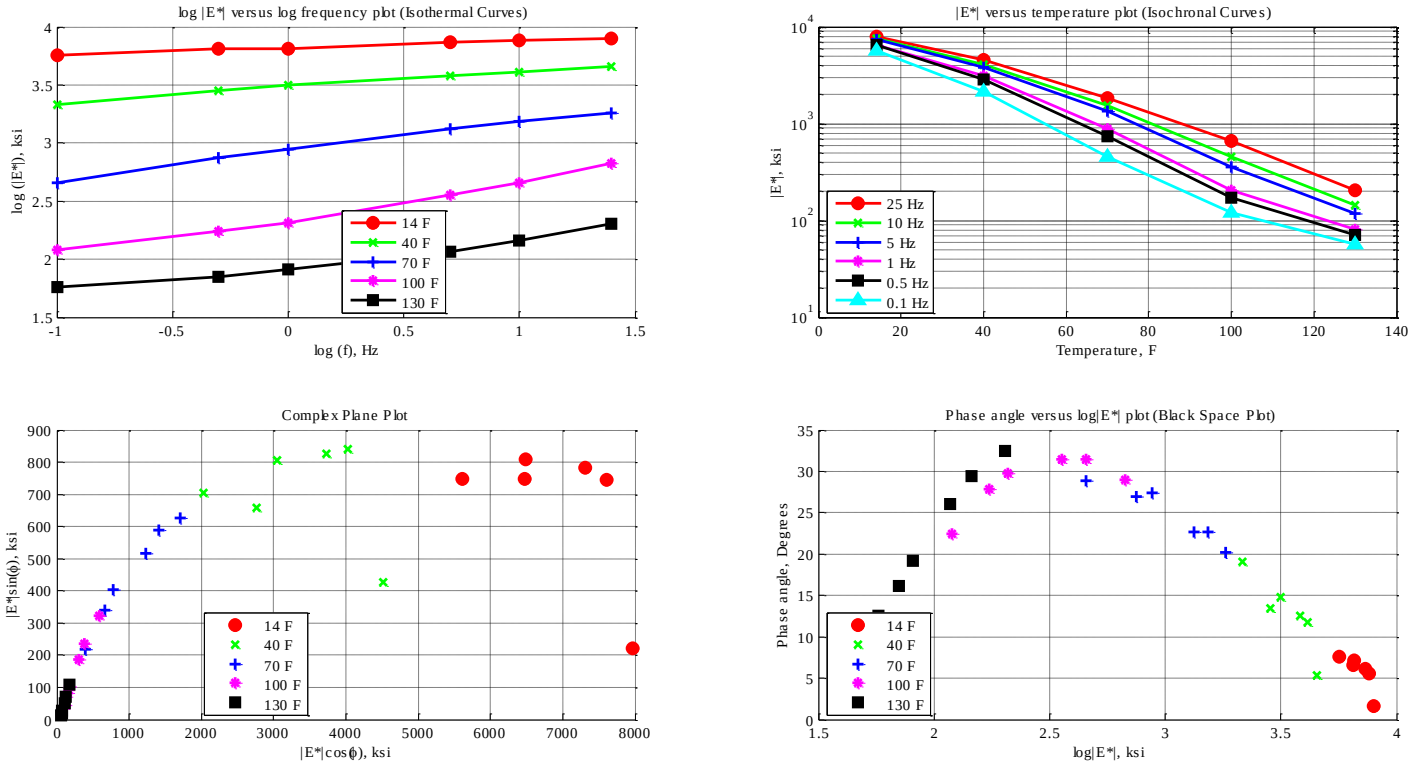

Figure C-143 Isothermal curves or |E*| versus frequency plot (top-left), isochronal curves or |E*| versus temperature plot (top-right), complex plane plot (bottom-left), and black space plot (bottom-right) for Mix 47 Specimen 2 in English unit system.

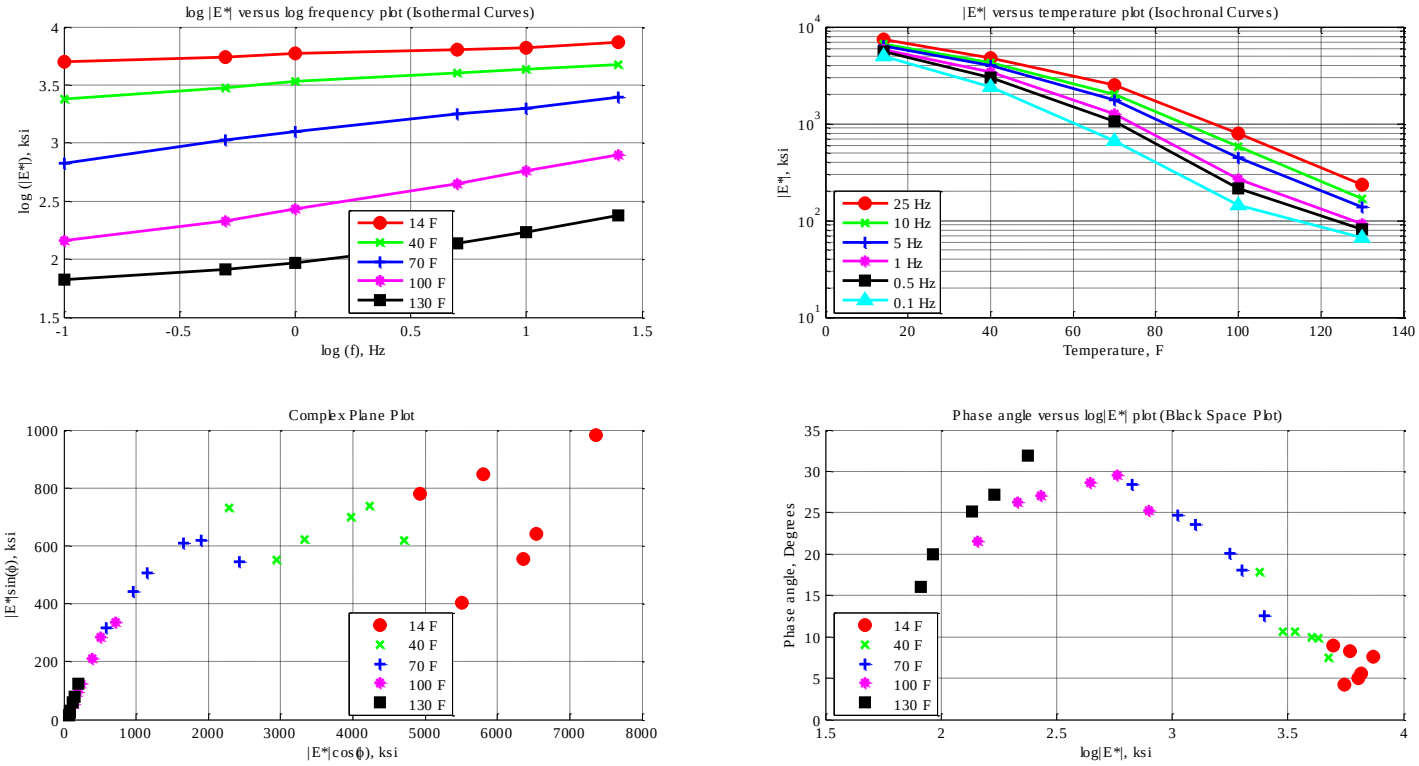

Figure C-144 Isothermal curves or |E*| versus frequency plot (top-left), isochronal curves or |E*| versus temperature plot (top-right), complex plane plot (bottom-left), and black space plot (bottom-right) for Mix 47 Specimen 3 in English unit system.

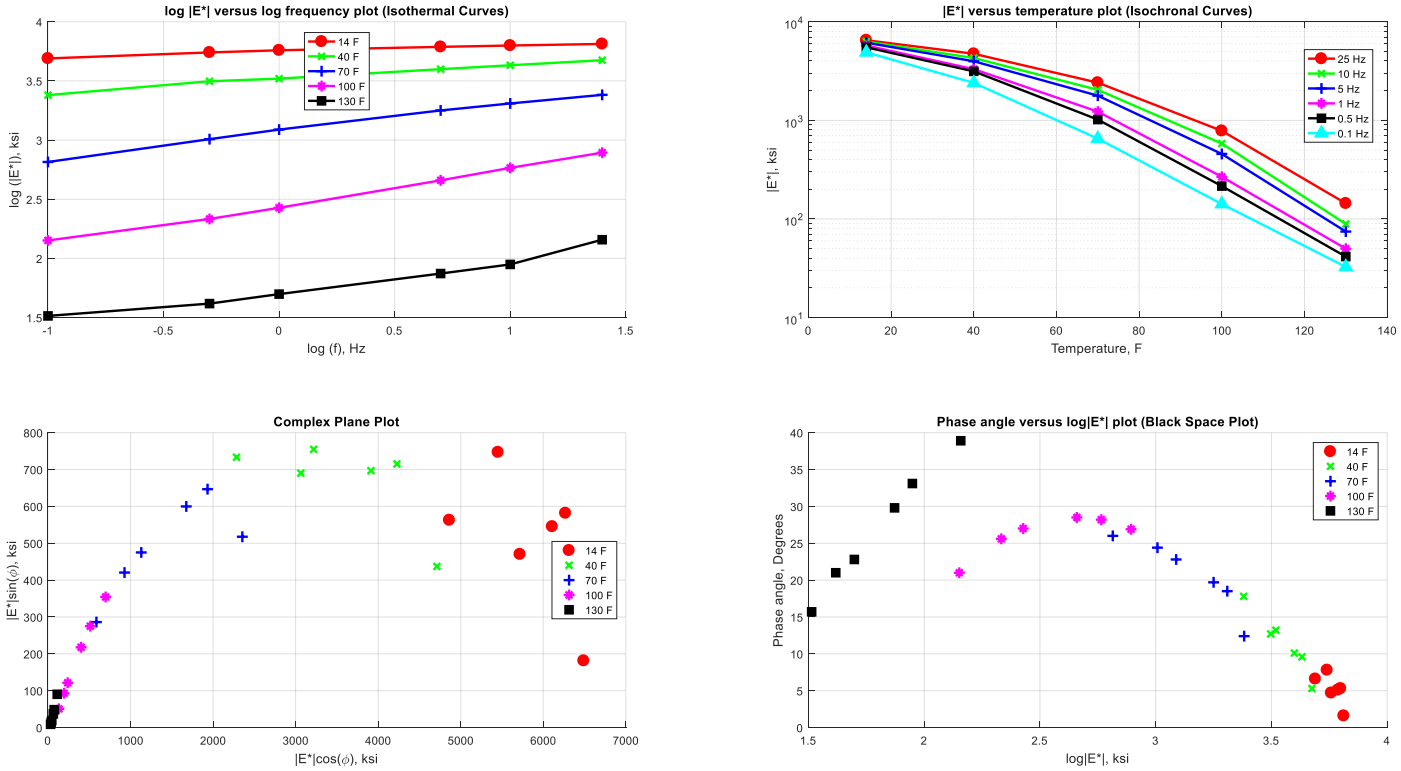

Figure C-145 Isothermal curves or |E*| versus frequency plot (top-left), isochronal curves or |E*| versus temperature plot (top-right), complex plane plot (bottom-left), and black space plot (bottom-right) for Mix 48 Specimen 1 in English unit system.

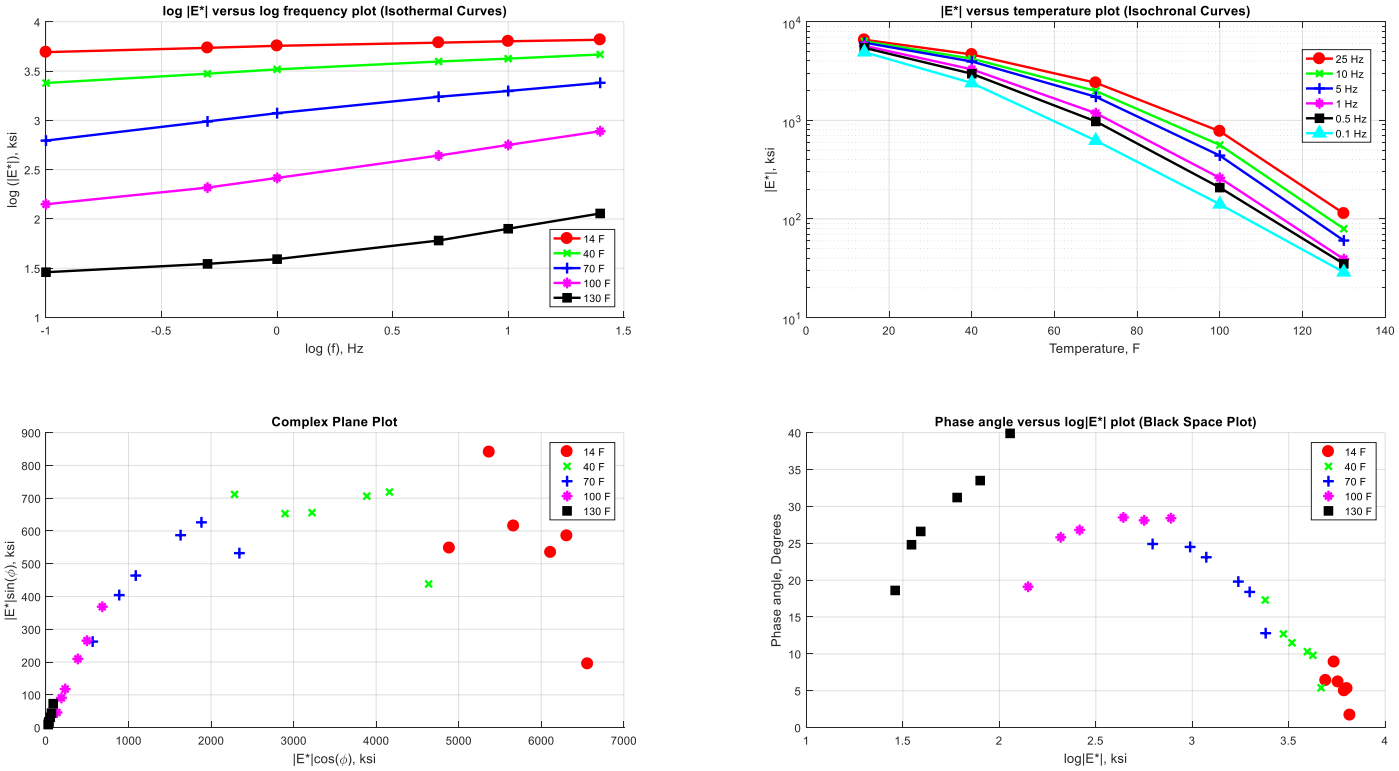

Figure C-146 Isothermal curves or |E*| versus frequency plot (top-left), isochronal curves or |E*| versus temperature plot (top-right), complex plane plot (bottom-left), and black space plot (bottom-right) for Mix 48 Specimen 2 in English unit system.

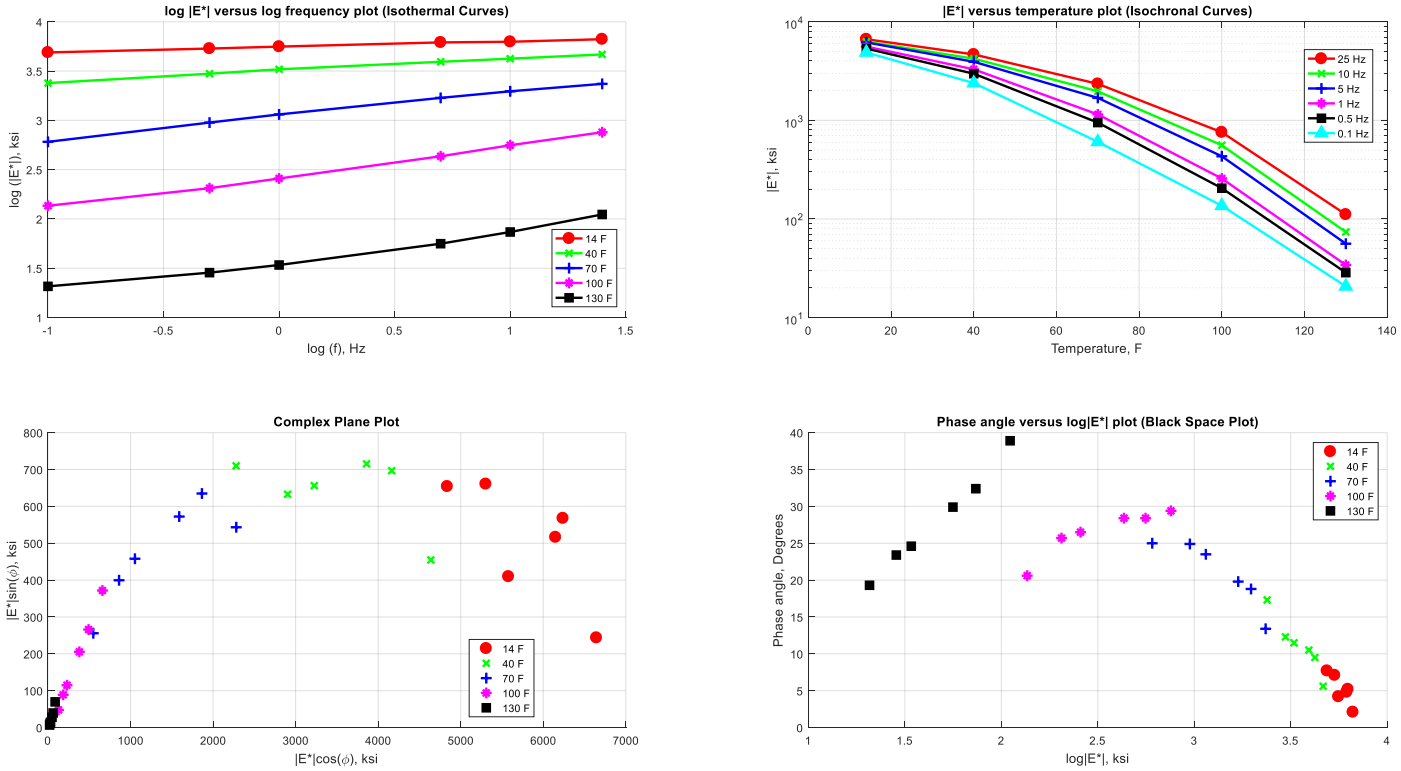

Figure C-147 Isothermal curves or |E*| versus frequency plot (top-left), isochronal curves or |E*| versus temperature plot (top-right), complex plane plot (bottom-left), and black space plot (bottom-right) for Mix 48 Specimen 3 in English unit system.

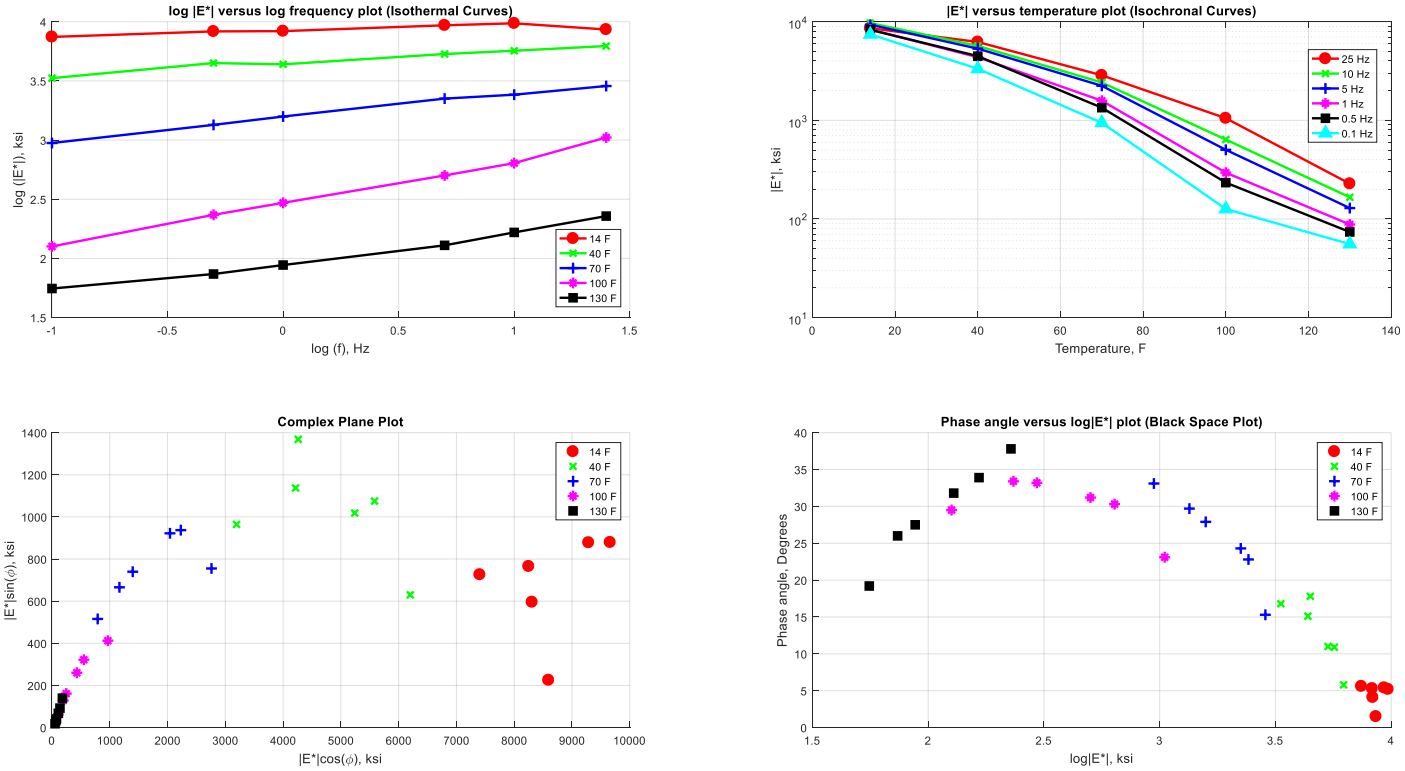

Figure C-148 Isothermal curves or |E*| versus frequency plot (top-left), isochronal curves or |E*| versus temperature plot (top-right), complex plane plot (bottom-left), and black space plot (bottom-right) for Mix 49 Specimen 1 in English unit system.

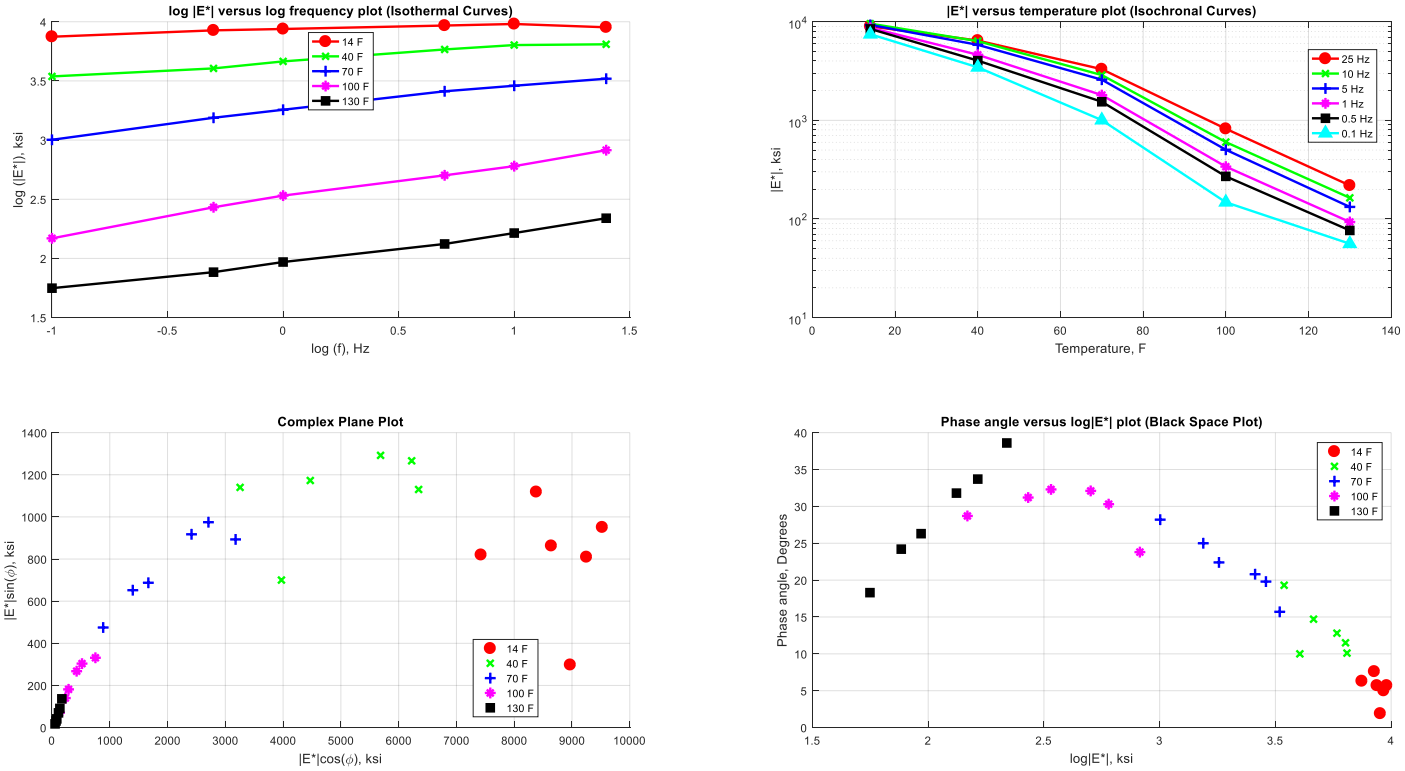

Figure C-149 Isothermal curves or |E*| versus frequency plot (top-left), isochronal curves or |E*| versus temperature plot (top-right), complex plane plot (bottom-left), and black space plot (bottom-right) for Mix 49 Specimen 2 in English unit system.

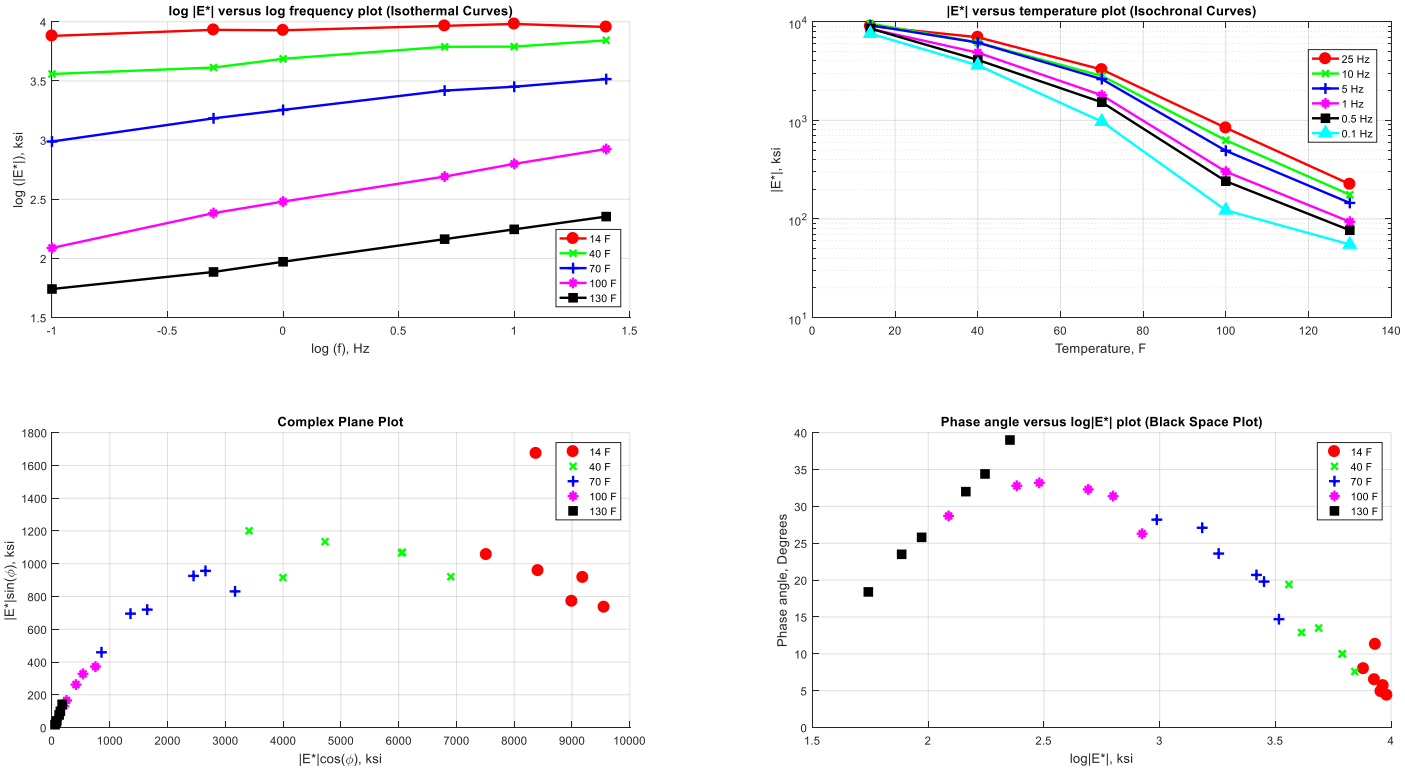

Figure C-150 Isothermal curves or |E*| versus frequency plot (top-left), isochronal curves or |E*| versus temperature plot (top-right), complex plane plot (bottom-left), and black space plot (bottom-right) for Mix 49 Specimen 3 in English unit system.

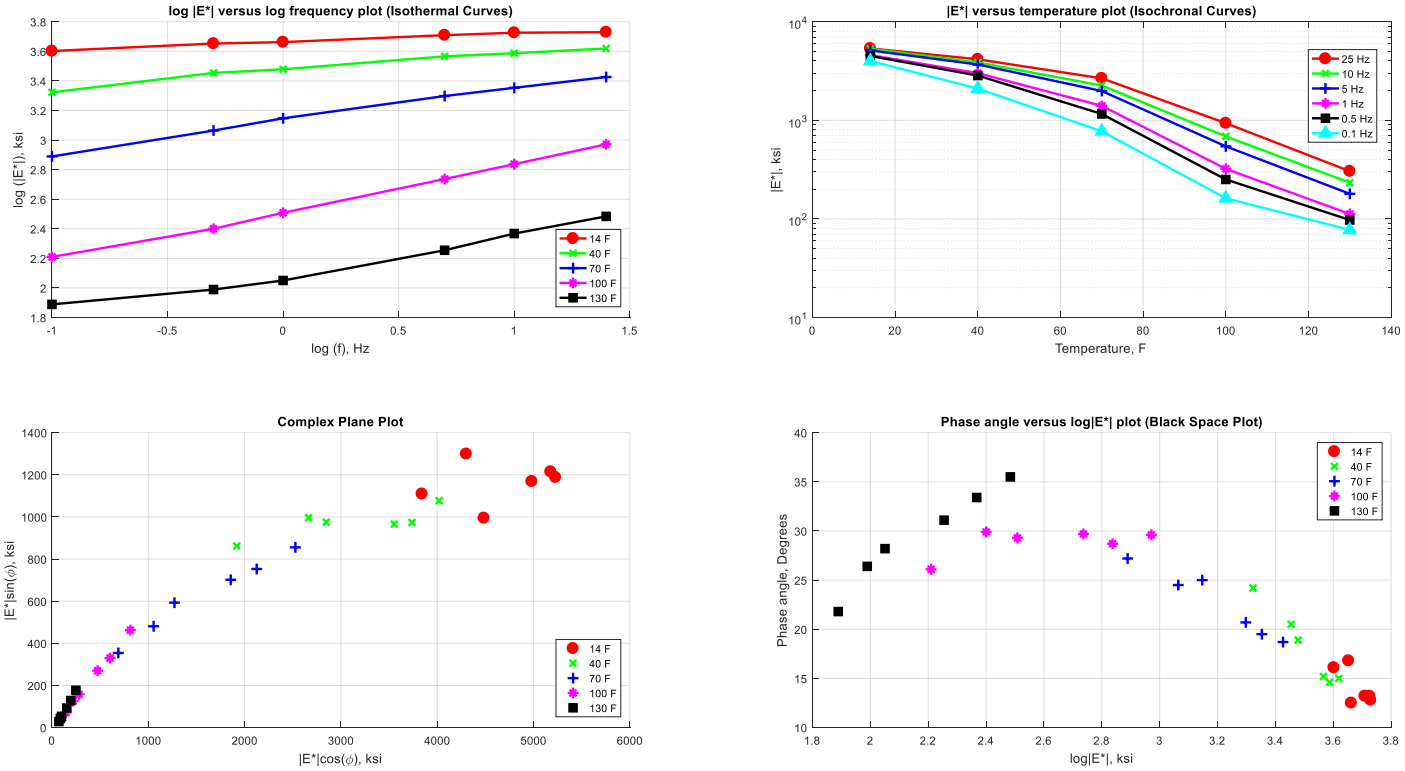

Figure C-151 Isothermal curves or |E*| versus frequency plot (top-left), isochronal curves or |E*| versus temperature plot (top-right), complex plane plot (bottom-left), and black space plot (bottom-right) for Mix 50 Specimen 1 in English unit system.

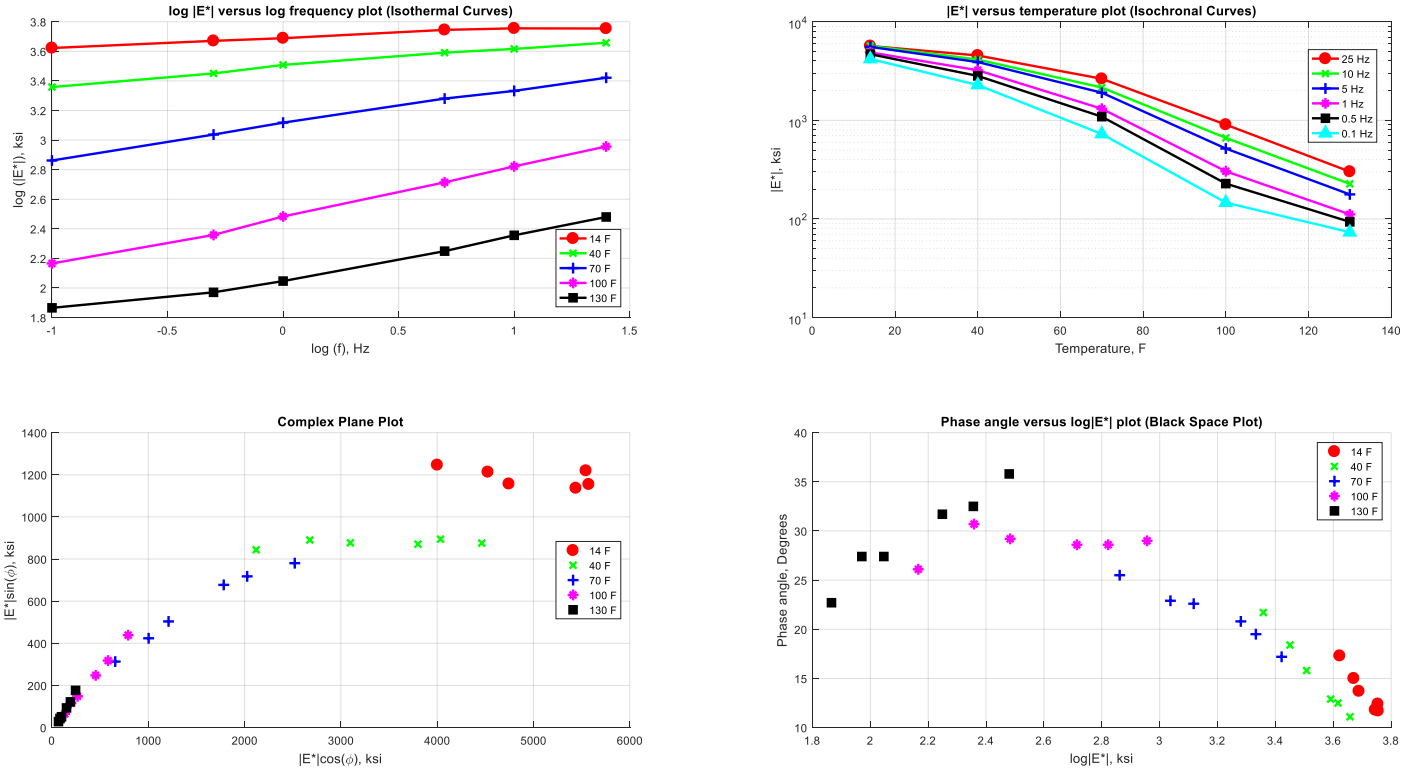

Figure C-152 Isothermal curves or |E*| versus frequency plot (top-left), isochronal curves or |E*| versus temperature plot (top-right), complex plane plot (bottom-left), and black space plot (bottom-right) for Mix 50 Specimen 2 in English unit system.

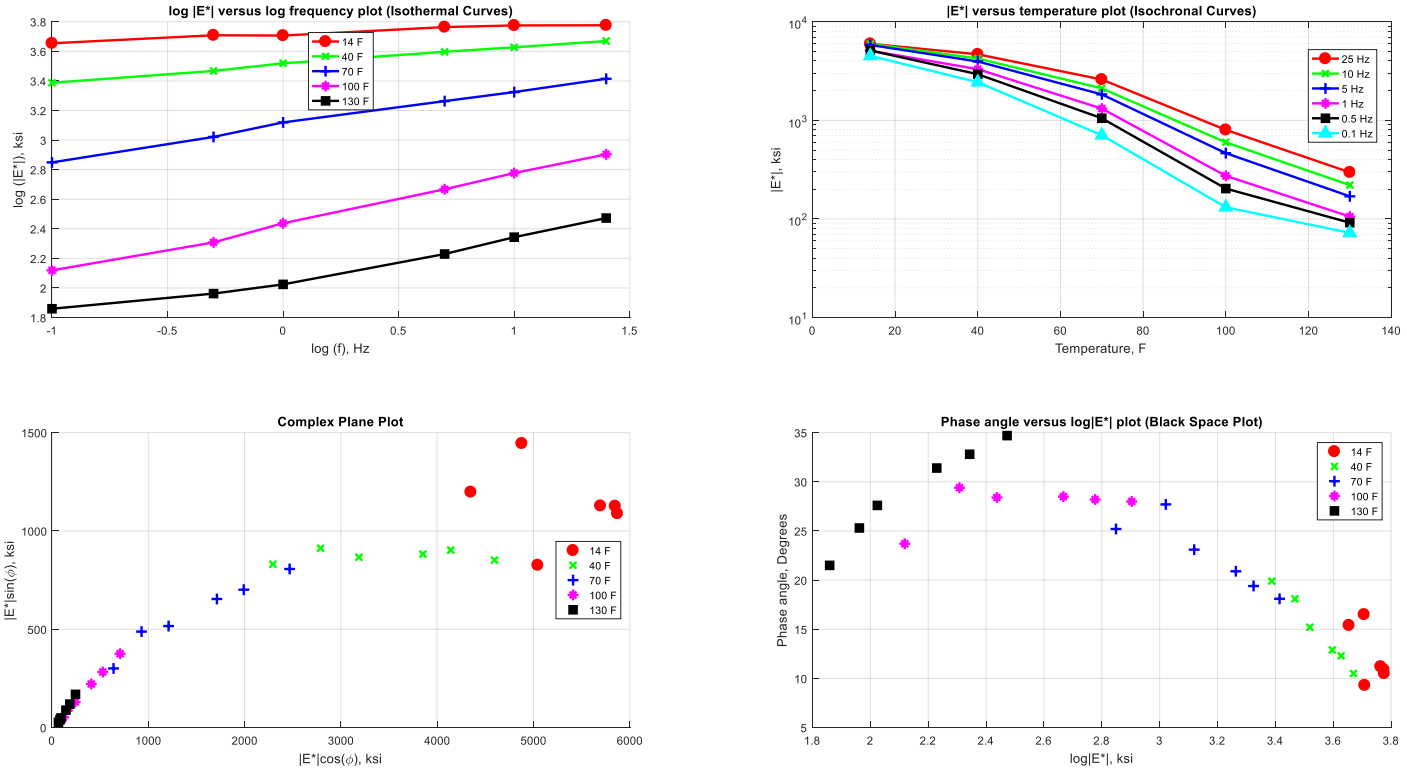

Figure C-153 Isothermal curves or |E*| versus frequency plot (top-left), isochronal curves or |E*| versus temperature plot (top-right), complex plane plot (bottom-left), and black space plot (bottom-right) for Mix 50 Specimen 3 in English unit system.

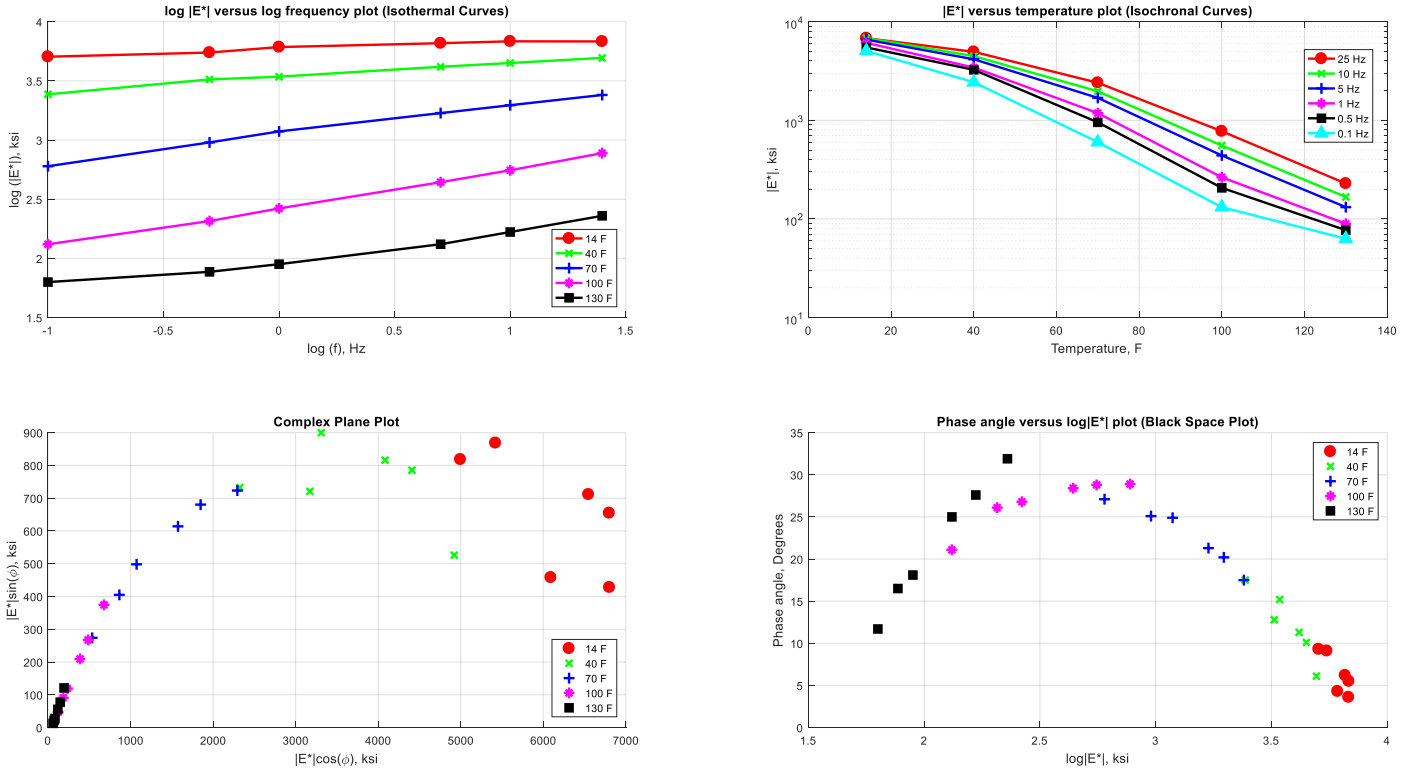

Figure C-154 Isothermal curves or |E*| versus frequency plot (top-left), isochronal curves or |E*| versus temperature plot (top-right), complex plane plot (bottom-left), and black space plot (bottom-right) for Mix 51 Specimen 1 in English unit system.

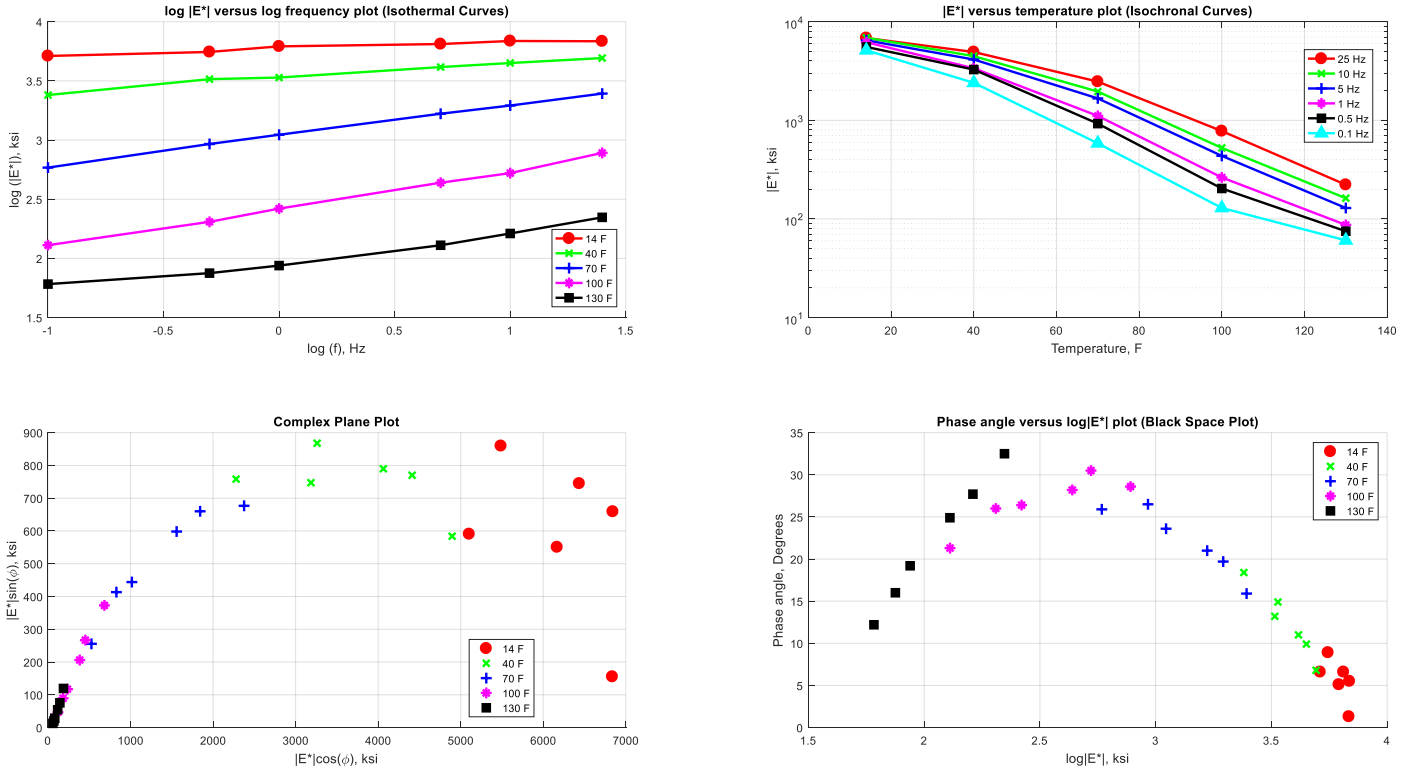

Figure C-155 Isothermal curves or |E*| versus frequency plot (top-left), isochronal curves or |E*| versus temperature plot (top-right), complex plane plot (bottom-left), and black space plot (bottom-right) for Mix 51 Specimen 2 in English unit system.

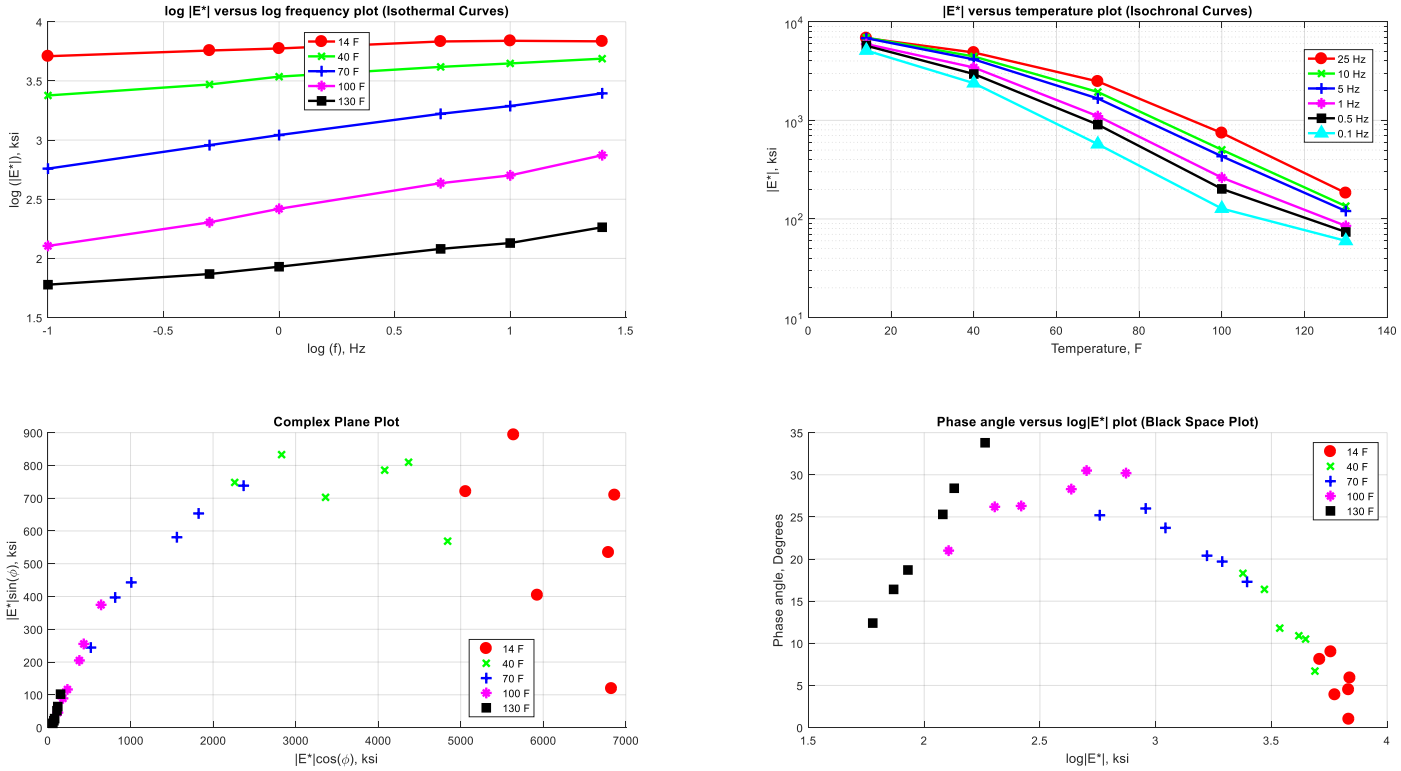

Figure C-156 Isothermal curves or |E*| versus frequency plot (top-left), isochronal curves or |E*| versus temperature plot (top-right), complex plane plot (bottom-left), and black space plot (bottom-right) for Mix 51 Specimen 3 in English unit system.

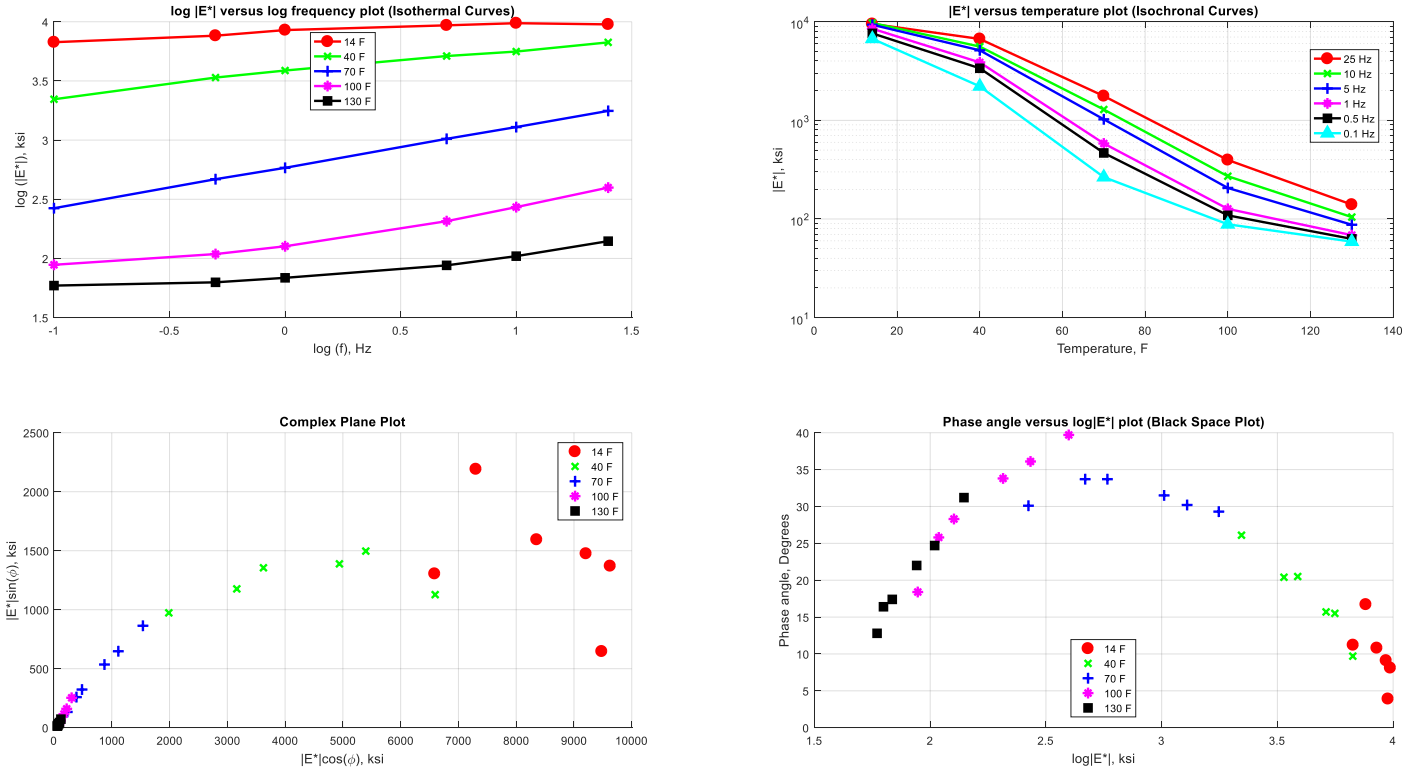

Figure C-157 Isothermal curves or |E*| versus frequency plot (top-left), isochronal curves or |E*| versus temperature plot (top-right), complex plane plot (bottom-left), and black space plot (bottom-right) for Mix 52 Specimen 1 in English unit system.

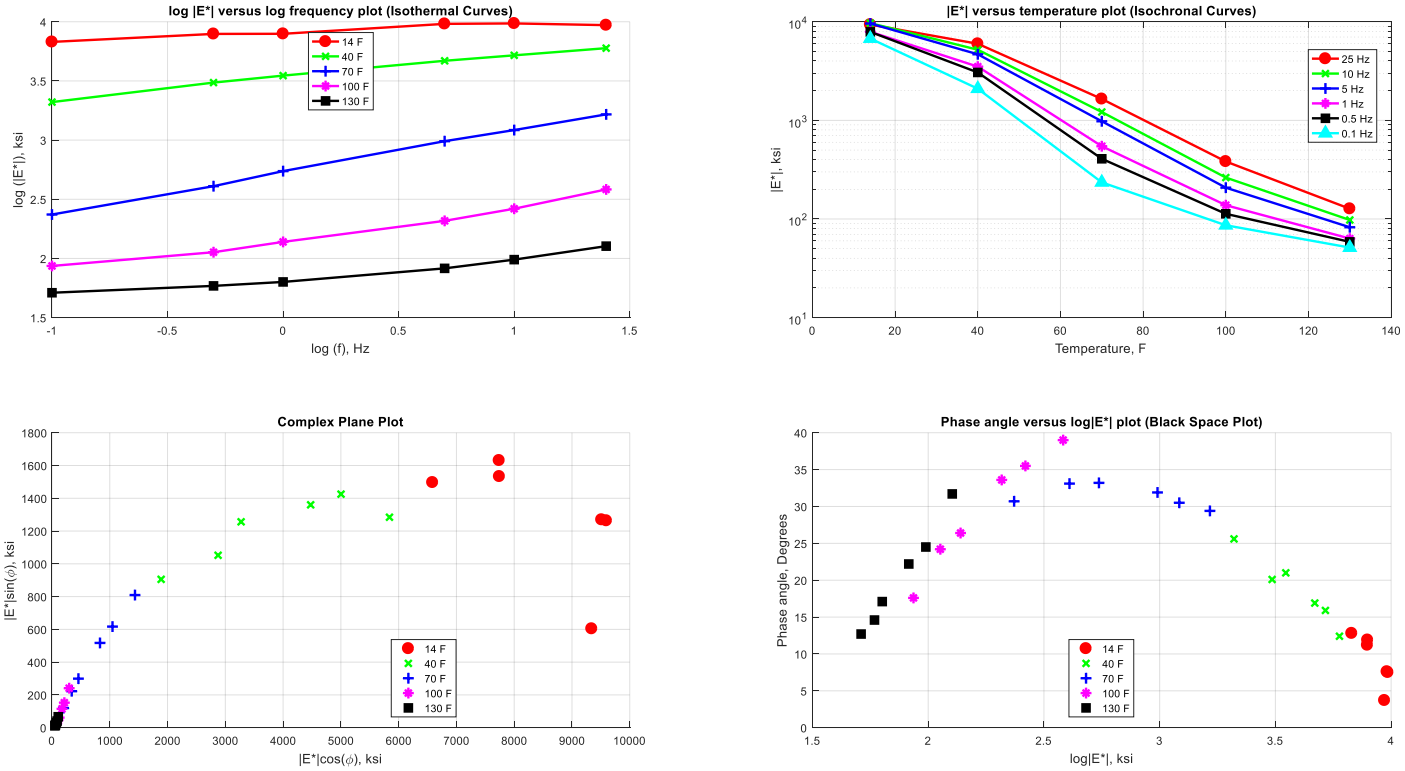

Figure C-158 Isothermal curves or |E*| versus frequency plot (top-left), isochronal curves or |E*| versus temperature plot (top-right), complex plane plot (bottom-left), and black space plot (bottom-right) for Mix 52 Specimen 2 in English unit system.

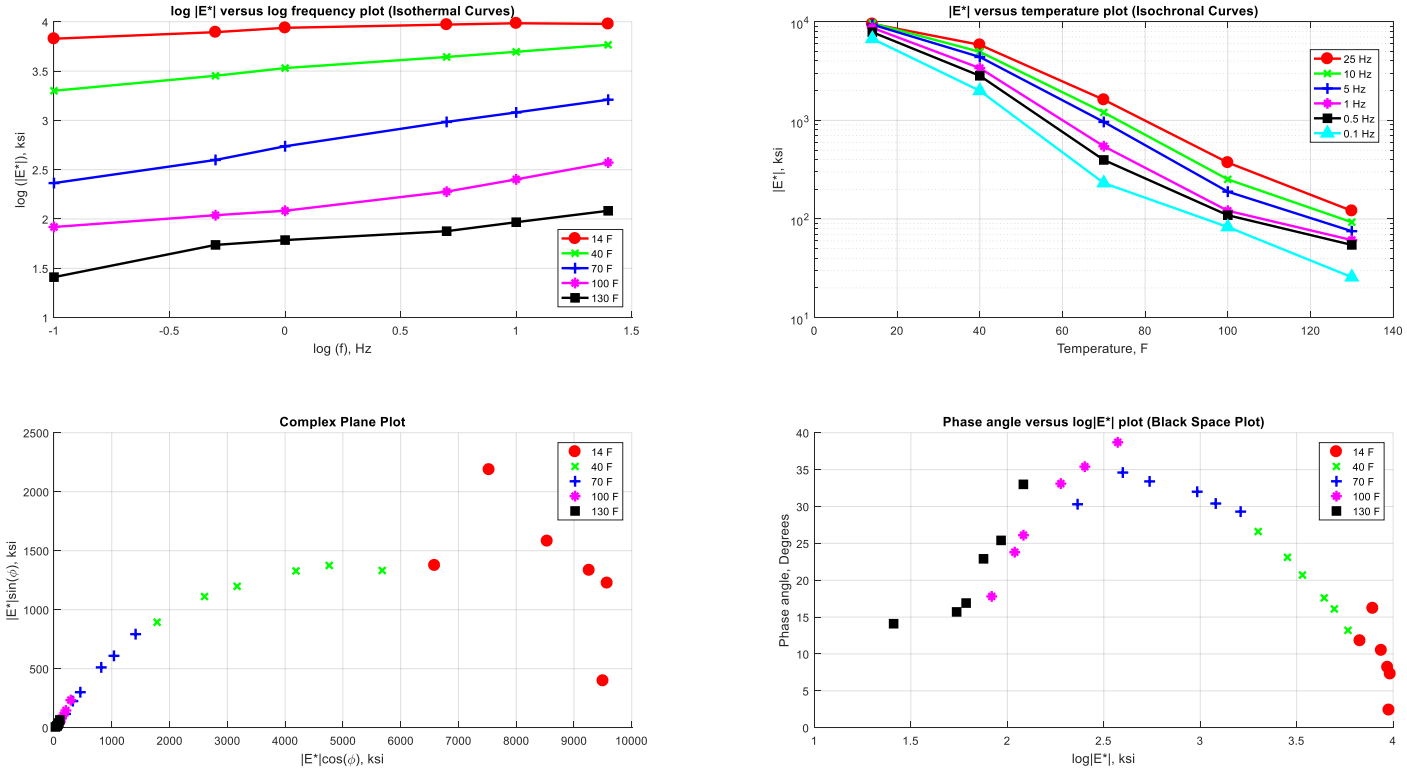

Figure C-159 Isothermal curves or |E*| versus frequency plot (top-left), isochronal curves or |E*| versus temperature plot (top-right), complex plane plot (bottom-left), and black space plot (bottom-right) for Mix 52 Specimen 3 in English unit system.

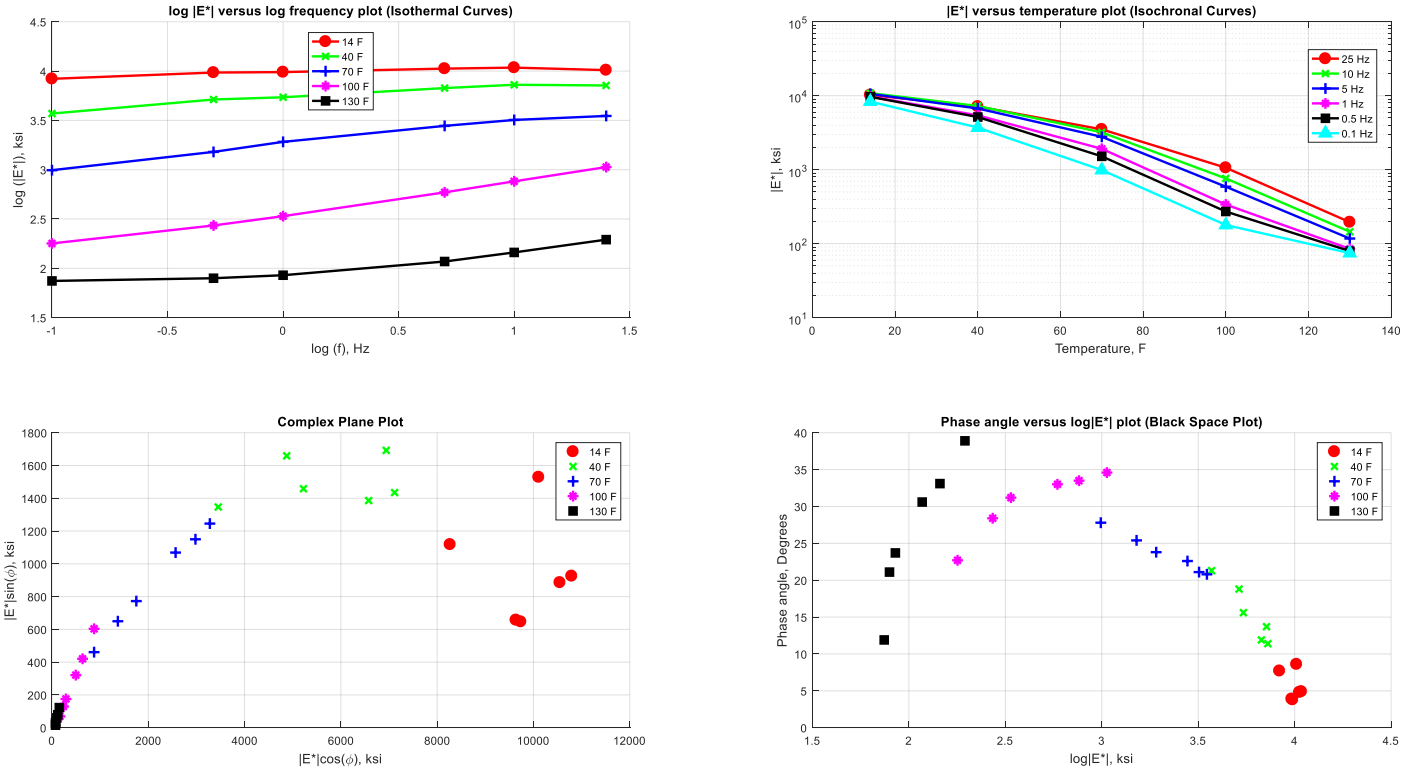

Figure C-160 Isothermal curves or |E*| versus frequency plot (top-left), isochronal curves or |E*| versus temperature plot (top-right), complex plane plot (bottom-left), and black space plot (bottom-right) for Mix 53 Specimen 1 in English unit system.

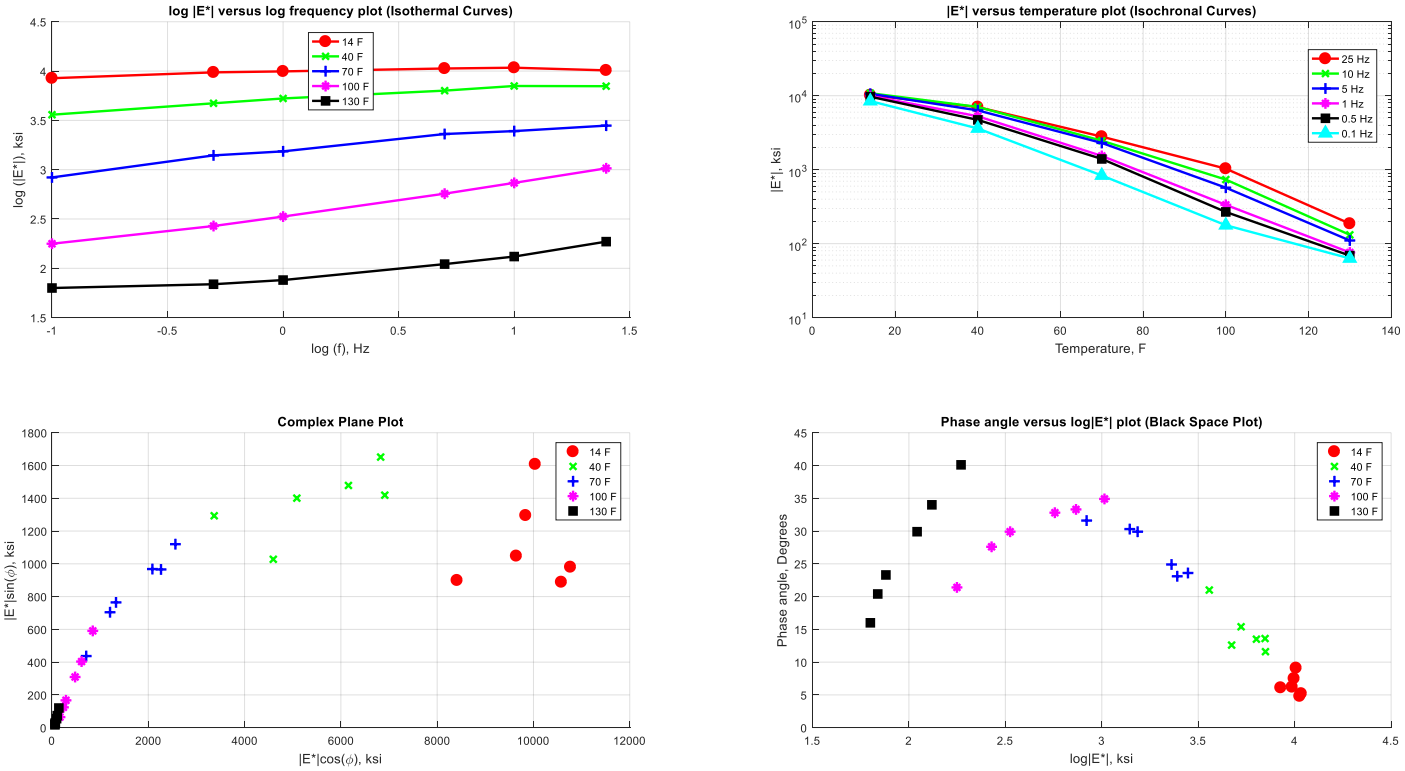

Figure C-161 Isothermal curves or |E*| versus frequency plot (top-left), isochronal curves or |E*| versus temperature plot (top-right), complex plane plot (bottom-left), and black space plot (bottom-right) for Mix 53 Specimen 2 in English unit system.

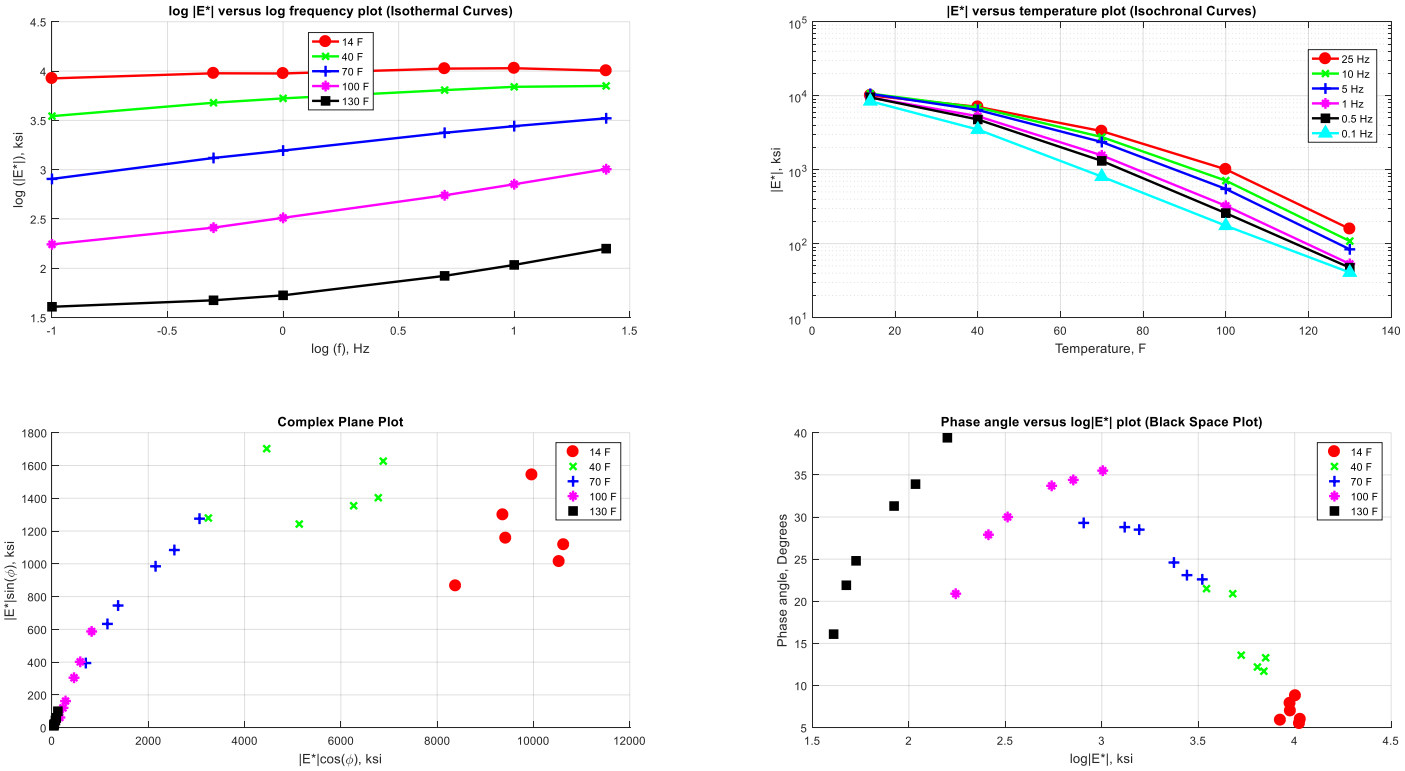

Figure C-162 Isothermal curves or |E*| versus frequency plot (top-left), isochronal curves or |E*| versus temperature plot (top-right), complex plane plot (bottom-left), and black space plot (bottom-right) for Mix 53 Specimen 3 in English unit system.

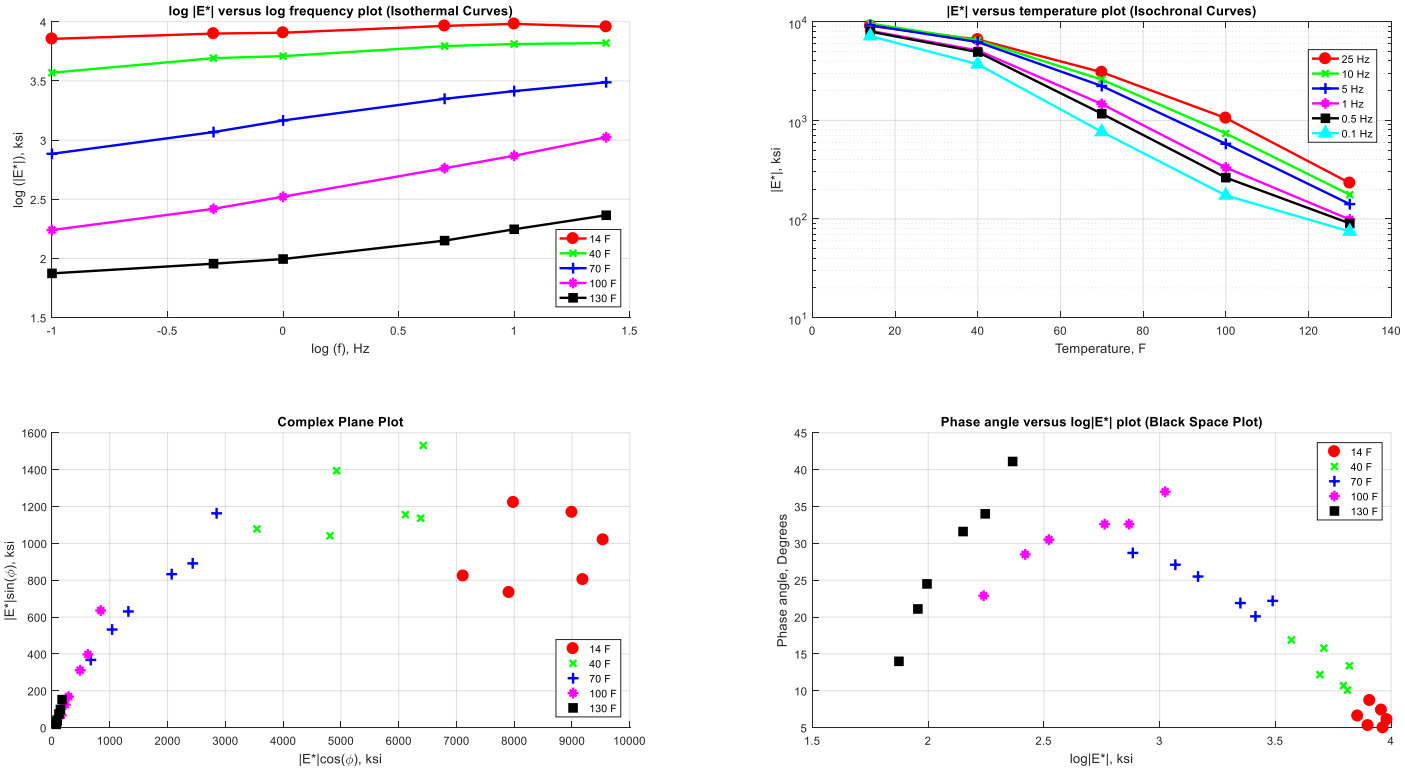

Figure C-163 Isothermal curves or |E*| versus frequency plot (top-left), isochronal curves or |E*| versus temperature plot (top-right), complex plane plot (bottom-left), and black space plot (bottom-right) for Mix 54 Specimen 1 in English unit system.

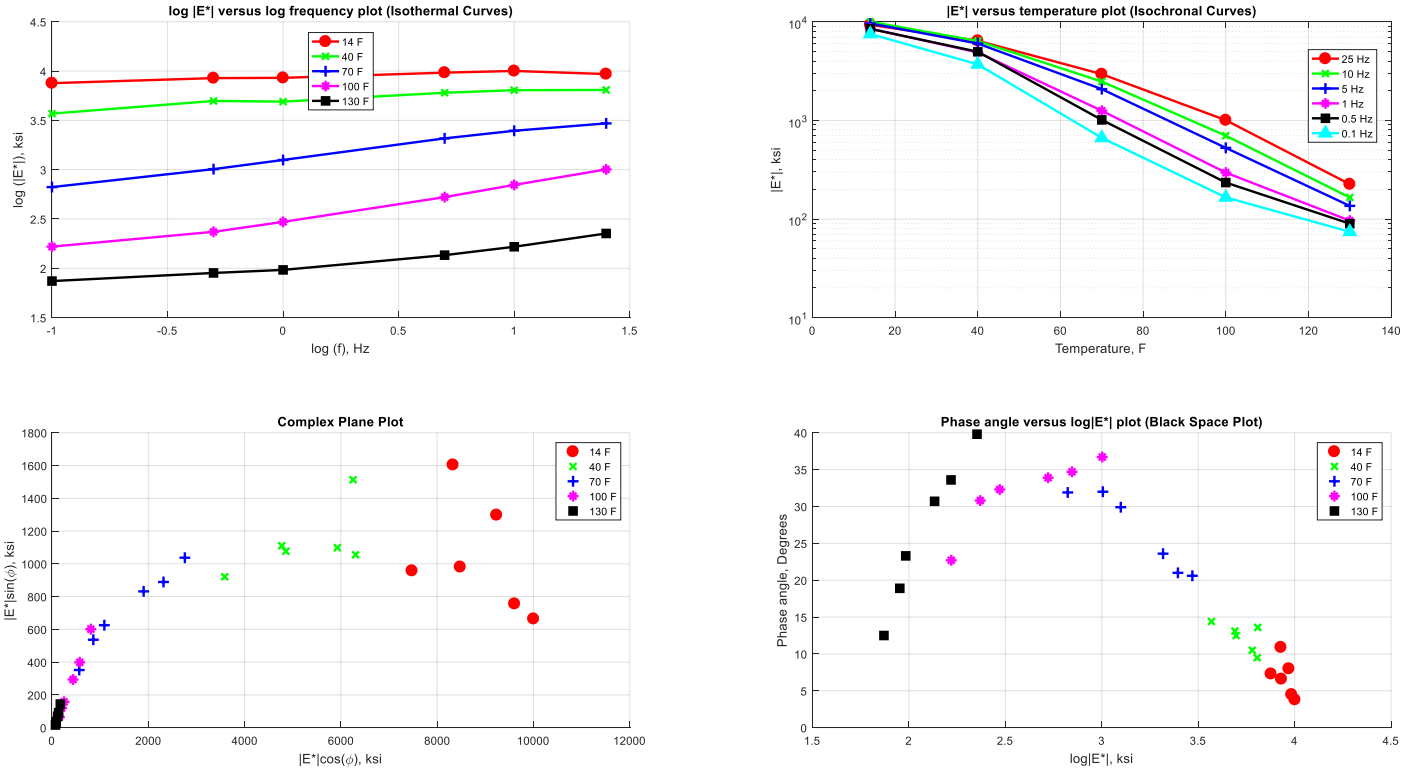

Figure C-164 Isothermal curves or |E*| versus frequency plot (top-left), isochronal curves or |E*| versus temperature plot (top-right), complex plane plot (bottom-left), and black space plot (bottom-right) for Mix 54 Specimen 2 in English unit system.

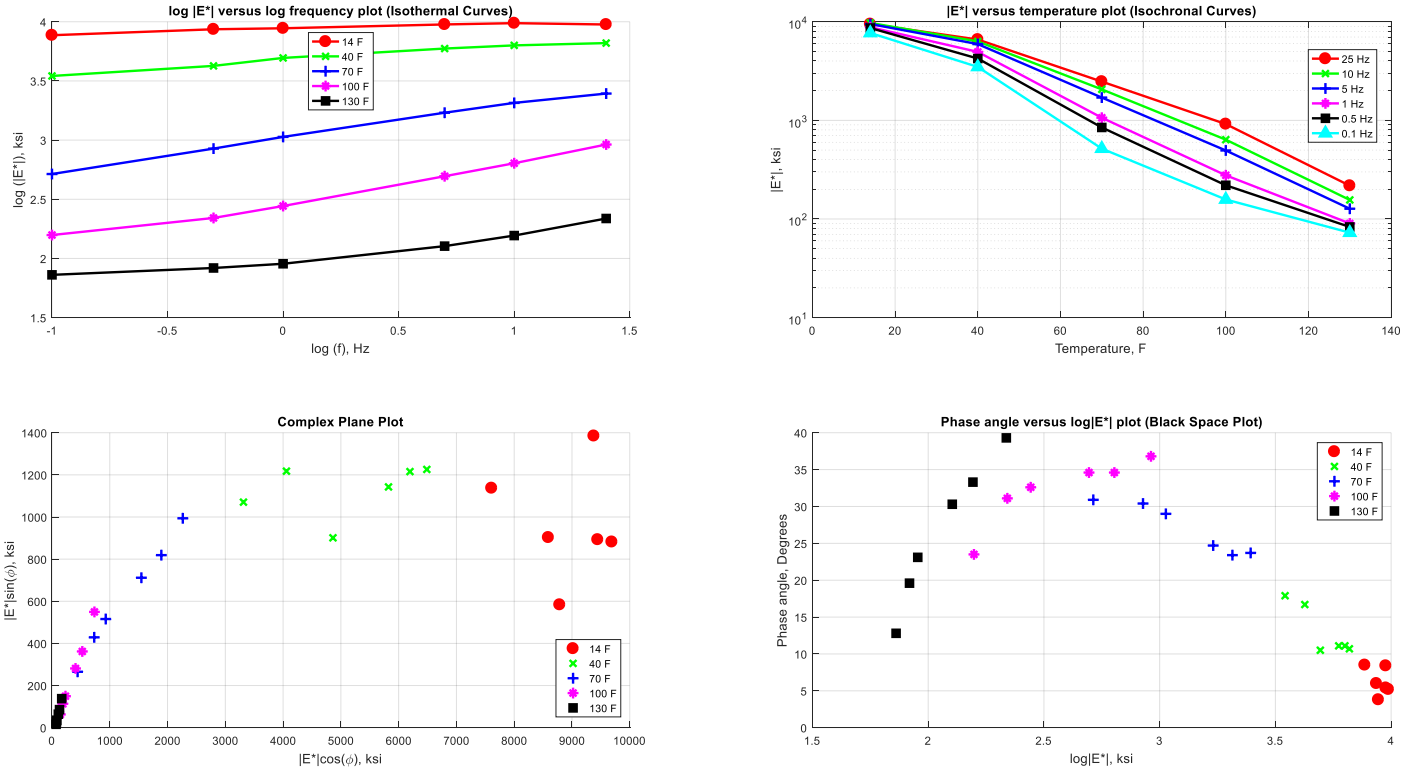

Figure C-165 Isothermal curves or |E*| versus frequency plot (top-left), isochronal curves or |E*| versus temperature plot (top-right), complex plane plot (bottom-left), and black space plot (bottom-right) for Mix 54 Specimen 3 in English unit system.

Appendix D

Table D-1 Dynamic Modulus Summary Sheet for the Mix 1

Conditions		Specimen 1		Specimen 2		Specimen 3		Modulus		Phase Angle (Degrees)	
Temperature, °F	Frequency, Hz	Modulus, ksi	Phage Angle, degree	Modulus, ksi	Phage Angle, degree	Modulus, ksi	Phage Angle, degree	Avg. Modulus, ksi	CV, %	Avg. P. Angle, degree	Standard Dev, degree
14.000000	25.000000	8045.181059	8.400000	8210.049623	11.300000	7677.468755	5.100000	7977.566479	3.417740	8.266667	3.102150
14.000000	10.000000	7889.896192	8.900000	7872.772584	6.800000	8153.403313	4.900000	7972.024030	1.973304	6.866667	2.000833
14.000000	5.000000	7541.236971	9.100000	7721.428918	7.400000	7985.972946	5.000000	7749.546278	2.886585	7.166667	2.059935
14.000000	1.000000	6779.272024	9.000000	7239.534179	8.900000	7448.682044	8.200000	7155.829416	4.785819	8.700000	0.435890
14.000000	0.500000	6501.153197	14.300000	6775.889603	7.000000	7493.918757	8.600000	6923.653852	7.403786	9.966667	3.837100
14.000000	0.100000	5982.872876	10.400000	6342.904268	8.800000	6477.873573	8.300000	6267.883572	4.082490	9.166667	1.096966
40.000000	25.000000	6648.102630	8.000000	6586.991152	12.700000	6158.837558	9.500000	6464.643780	4.123860	10.066667	2.400694
40.000000	10.000000	6116.783080	10.100000	5874.392701	10.000000	5849.468649	8.700000	5946.881477	2.483081	9.600000	0.781025
40.000000	5.000000	5854.072642	9.300000	5533.077848	10.900000	5595.193449	9.000000	5660.781313	3.007571	9.733333	1.021437
40.000000	1.000000	5142.553166	9.300000	4757.783547	12.900000	4775.438083	9.400000	4891.924932	4.440580	10.533333	2.050203
40.000000	0.500000	4462.460747	16.400000	4433.183951	15.900000	4619.361030	14.700000	4505.001909	2.222283	15.666667	0.873689
40.000000	0.100000	3909.224869	15.100000	3589.676058	16.200000	3661.240012	12.900000	3720.046980	4.507869	14.733333	1.680278
70.000000	25.000000	2862.251208	21.500000	3105.208201	17.700000	3412.980841	16.800000	3126.813417	8.826870	18.666667	2.494661
70.000000	10.000000	2442.910158	20.100000	2679.558965	15.800000	2974.763829	15.900000	2699.077651	9.872392	17.266667	2.454248
70.000000	5.000000	2123.482039	21.400000	2431.542339	15.900000	2634.978804	17.100000	2396.667727	10.745151	18.133333	2.891943
70.000000	1.000000	1529.798976	24.000000	1717.245642	22.900000	1955.700040	20.700000	1734.248219	12.308446	22.533333	1.680278
70.000000	0.500000	1285.449239	29.000000	1514.726406	21.400000	1655.480802	22.700000	1485.218816	12.575401	24.366667	4.064890
70.000000	0.100000	841.030516	30.500000	975.375037	24.200000	1165.156773	25.900000	993.854109	16.385841	26.866667	3.259346
100.000000	25.000000	1019.602841	27.000000	1141.172291	29.400000	1415.461034	26.700000	1192.078722	17.010580	27.700000	1.479865
100.000000	10.000000	815.074780	30.600000	875.348087	30.700000	1129.790400	26.500000	940.071089	17.769162	29.266667	2.396525
100.000000	5.000000	650.892506	31.700000	712.176319	32.000000	944.565076	27.300000	769.211300	20.140290	30.333333	2.631223
100.000000	1.000000	376.022933	34.100000	408.762950	34.100000	588.112374	28.800000	457.632752	24.949758	32.333333	3.059956
100.000000	0.500000	309.527897	34.400000	334.372309	34.300000	441.405340	29.700000	361.768515	19.370759	32.800000	2.685144
100.000000	0.100000	192.627572	33.600000	213.510473	33.800000	277.957953	28.000000	228.031999	19.506055	31.800000	3.292416
130.000000	25.000000	259.292476	36.400000	245.297865	36.200000	529.139552	34.000000	344.576631	46.430679	35.533333	1.331666
130.000000	10.000000	189.162755	32.900000	188.138324	33.600000	391.610475	31.100000	256.303851	45.719209	32.533333	1.289703
130.000000	5.000000	150.396988	32.700000	149.406066	33.400000	305.689689	30.900000	201.830914	44.564879	32.333333	1.289703
130.000000	1.000000	88.887168	30.600000	93.881814	31.500000	180.586517	29.200000	121.118500	42.570976	30.433333	1.159023
130.000000	0.500000	74.738936	28.600000	81.088900	30.100000	148.629547	26.600000	101.485794	40.351414	28.433333	1.755942
130.000000	0.100000	54.885978	24.500000	66.600497	25.100000	113.031509	22.700000	78.172661	39.338071	24.100000	1.249000

Table D-2 Dynamic Modulus Summary Sheet for the Mix 2

Conditions		Specimen 1		Specimen 2		Specimen 3		Modulus		Phase Angle (Degrees)	
Temperature, °F	Frequency, Hz	Modulus, ksi	Phage Angle, degree	Modulus, ksi	Phage Angle, degree	Modulus, ksi	Phage Angle, degree	Avg. Modulus, ksi	CV, %	Avg. P. Angle, degree	Standard Dev, degree
14.000000	25.000000	8829.363193	23.800000	6930.288284	8.700000	7439.740829	4.900000	7733.130769	12.710820	12.466667	9.997166
14.000000	10.000000	8624.230221	4.700000	6802.741535	6.200000	8492.399053	7.200000	7973.123603	12.739319	6.033333	1.258306
14.000000	5.000000	8225.319769	5.300000	6686.419574	6.000000	8324.965784	6.800000	7745.568376	11.859710	6.033333	0.750555
14.000000	1.000000	7463.872695	4.300000	5980.562611	9.500000	7489.297792	5.700000	6977.911033	12.379387	6.500000	2.690725
14.000000	0.500000	7085.656417	8.300000	5665.382646	5.300000	7564.255918	5.600000	6771.764994	14.583876	6.400000	1.652271
14.000000	0.100000	6623.179159	8.000000	5199.792782	10.100000	6518.614075	13.000000	6113.862005	12.975952	10.366667	2.510644
40.000000	25.000000	6997.624392	11.800000	4823.297961	11.600000	5221.198634	13.000000	5680.706996	20.379624	12.133333	0.757188
40.000000	10.000000	5954.084215	11.700000	4126.124872	11.700000	4949.399162	13.800000	5009.869416	18.273505	12.400000	1.212436
40.000000	5.000000	5505.484792	11.400000	3790.359093	12.600000	4566.118029	14.300000	4620.653971	18.587465	12.766667	1.457166
40.000000	1.000000	4439.911512	14.300000	3026.571871	15.800000	3575.401767	18.400000	3680.628383	19.358688	16.166667	2.074448
40.000000	0.500000	3936.527075	15.900000	2636.475414	18.100000	3330.427536	20.200000	3301.143342	19.705911	18.066667	2.150194
40.000000	0.100000	2895.085516	21.100000	1963.577947	21.500000	2341.387760	23.600000	2400.017074	19.521245	22.066667	1.342882
70.000000	25.000000	2260.325986	21.000000	2389.344829	21.400000	2564.888540	24.800000	2404.853118	6.356829	22.400000	2.088061
70.000000	10.000000	1838.577625	22.100000	1838.279521	22.300000	2135.825404	24.900000	1937.560850	8.861771	23.100000	1.562050
70.000000	5.000000	1566.249981	23.700000	1522.615918	25.000000	1776.892569	26.400000	1621.919489	8.383420	25.033333	1.350309
70.000000	1.000000	1033.873360	28.100000	923.276144	29.900000	1098.448205	30.400000	1018.532570	8.697602	29.466667	1.209683
70.000000	0.500000	840.191765	28.700000	722.790394	31.200000	865.680400	31.700000	809.554186	9.414164	30.533333	1.607275
70.000000	0.100000	511.366644	29.500000	416.335066	30.700000	529.989038	30.700000	485.896916	12.545390	30.300000	0.692820
100.000000	25.000000	1456.565498	31.400000	603.874861	35.900000	555.562534	41.300000	872.000964	58.121923	36.200000	4.956813
100.000000	10.000000	1140.090995	27.800000	372.523736	32.800000	365.889015	39.300000	626.167915	71.080423	33.300000	5.766281
100.000000	5.000000	881.810185	28.300000	283.445086	30.800000	277.602985	38.800000	480.952752	72.182768	32.633333	5.484828
100.000000	1.000000	511.564509	26.800000	176.711028	25.400000	156.274048	34.600000	281.516528	70.862368	28.933333	4.957150
100.000000	0.500000	397.528008	25.300000	149.238229	23.000000	132.676448	33.000000	226.480895	65.507700	27.100000	5.237366
100.000000	0.100000	261.679769	20.600000	113.568966	17.400000	110.288668	26.800000	161.845801	53.430060	21.600000	4.779121
130.000000	25.000000	376.529056	36.800000	144.264327	37.100000	168.167139	42.200000	229.653507	55.630848	38.700000	3.034798
130.000000	10.000000	273.178725	30.600000	116.171966	28.500000	125.956429	35.200000	171.769040	51.208017	31.433333	3.426855
130.000000	5.000000	217.299650	27.500000	94.083886	25.600000	104.972854	32.100000	138.785463	49.149892	28.400000	3.342155
130.000000	1.000000	138.280501	21.600000	65.650193	20.800000	87.795283	25.700000	97.241992	38.281064	22.700000	2.628688
130.000000	0.500000	113.528783	20.300000	58.497598	19.500000	83.190710	22.600000	85.072364	32.400421	20.800000	1.609348
130.000000	0.100000	86.772883	15.300000	48.071669	17.000000	72.445499	17.900000	69.096684	28.317900	16.733333	1.320353

Table D-3 Dynamic Modulus Summary Sheet for the Mix 3

Conditions		Specimen 1		Specimen 2		Specimen 3		Modulus		Phase Angle (Degrees)	
Temperature, °F	Frequency, Hz	Modulus, ksi	Phage Angle, degree	Modulus, ksi	Phage Angle, degree	Modulus, ksi	Phage Angle, degree	Avg. Modulus, ksi	CV, %	Avg. P. Angle, degree	Standard Dev, degree
14.000000	25.000000	6082.971051	8.100000	6043.343468	21.500000	9202.621380	5.600000	7109.645300	25.496050	11.733333	8.550049
14.000000	10.000000	6679.857238	4.900000	6714.533404	6.700000	8304.996486	7.200000	7233.129043	12.835750	6.266667	1.209683
14.000000	5.000000	6487.632360	5.100000	6584.486503	6.200000	8324.458646	6.800000	7132.192503	14.492988	6.033333	0.862168
14.000000	1.000000	5970.233148	7.100000	6079.228294	7.400000	7570.027228	8.500000	6539.829557	13.667639	7.666667	0.737111
14.000000	0.500000	5789.296596	7.800000	5942.684336	9.900000	7581.341664	10.600000	6437.774199	15.429613	9.433333	1.457166
14.000000	0.100000	5150.958375	8.400000	5288.852719	9.700000	6926.097864	7.700000	5788.636319	17.058949	8.600000	1.014889
40.000000	25.000000	3293.951725	14.900000	4326.237667	17.000000	5980.449317	13.800000	4533.546236	29.892575	15.233333	1.625833
40.000000	10.000000	3093.335999	13.000000	3877.907770	11.100000	5556.122906	13.200000	4175.788892	30.129049	12.433333	1.159023
40.000000	5.000000	2827.121722	14.400000	3582.538695	12.200000	5036.390219	14.100000	3815.350212	29.430684	13.566667	1.193035
40.000000	1.000000	2230.614293	17.800000	3003.031716	14.200000	3643.659312	23.900000	2959.101774	23.910839	18.633333	4.903400
40.000000	0.500000	1987.163798	21.100000	2713.742643	17.500000	3374.754272	26.500000	2691.886904	25.783155	21.700000	4.529901
40.000000	0.100000	1515.097476	24.000000	2099.112126	20.800000	2387.422752	29.200000	2000.544118	22.215825	24.666667	4.239497
70.000000	25.000000	1829.302476	23.700000	2442.966878	19.500000	2098.777467	22.600000	2123.682274	14.483773	21.933333	2.177919
70.000000	10.000000	1596.384966	23.200000	2050.360114	19.600000	1787.671581	23.800000	1811.472220	12.582114	22.200000	2.271563
70.000000	5.000000	1378.674645	25.200000	1794.316602	20.700000	1561.592025	25.100000	1578.194424	13.199753	23.666667	2.569695
70.000000	1.000000	857.353379	32.800000	1248.027331	24.600000	1067.047549	28.500000	1057.476086	18.488623	28.633333	4.101626
70.000000	0.500000	712.163698	33.000000	1093.811573	25.300000	883.248479	32.000000	896.407917	21.325553	30.100000	4.186884
70.000000	0.100000	419.200339	35.700000	725.265160	27.500000	584.181037	31.500000	576.215512	26.585159	31.566667	4.100406
100.000000	25.000000	807.093588	34.100000	1113.984830	30.100000	931.280401	37.800000	950.786273	16.236316	34.000000	3.850974
100.000000	10.000000	593.517547	34.600000	831.812667	29.700000	709.971079	36.100000	711.767098	16.741110	33.466667	3.347138
100.000000	5.000000	477.391855	35.800000	692.669915	29.300000	577.285638	36.000000	582.449136	18.496358	33.700000	3.811824
100.000000	1.000000	246.370022	39.200000	453.471346	28.700000	372.450480	33.400000	357.430616	29.198518	33.766667	5.259594
100.000000	0.500000	199.052968	38.400000	388.928125	27.300000	313.105282	32.100000	300.362125	31.820541	32.600000	5.566866
100.000000	0.100000	127.086611	35.000000	281.994606	24.800000	253.954613	28.300000	221.011943	37.346904	29.366667	5.182985
130.000000	25.000000	653.034499	37.100000	545.603706	33.600000	545.603706	33.600000	581.413970	10.667992	34.766667	2.020726
130.000000	10.000000	507.995828	29.100000	420.567988	27.700000	420.567988	27.700000	449.710601	11.224215	28.166667	0.808290
130.000000	5.000000	378.212361	28.400000	347.961905	25.100000	347.961905	25.100000	358.045390	4.877904	26.200000	1.905256
130.000000	1.000000	214.061421	24.500000	259.076913	19.800000	259.076913	19.800000	244.071749	10.648388	21.366667	2.713546
130.000000	0.500000	172.638400	22.800000	216.825296	18.300000	216.825296	18.300000	202.096331	12.623345	19.800000	2.598076
130.000000	0.100000	110.004781	19.300000	184.208582	14.300000	184.208582	14.300000	159.473982	26.864310	15.966667	2.886751

Table D-4 Dynamic Modulus Summary Sheet for the Mix 4

Conditions		Specimen 1		Specimen 2		Specimen 3		Modulus		Phase Angle (Degrees)	
Temperature, °F	Frequency, Hz	Modulus, ksi	Phage Angle, degree	Modulus, ksi	Phage Angle, degree	Modulus, ksi	Phage Angle, degree	Avg. Modulus, ksi	CV, %	Avg. P. Angle, degree	Standard Dev, degree
14.000000	25.000000	5962.541937	7.300000	6529.797375	4.700000	6569.483854	9.100000	6353.941055	5.343800	7.033333	2.212088
14.000000	10.000000	6013.627858	7.800000	6129.710611	9.100000	6232.210876	8.700000	6125.183115	1.785446	8.533333	0.665833
14.000000	5.000000	5704.342216	6.500000	5828.071936	8.900000	5871.914744	8.800000	5801.442965	1.497938	8.066667	1.357694
14.000000	1.000000	5027.969198	8.700000	5210.275866	9.900000	5165.356404	10.500000	5134.533823	1.849853	9.700000	0.916515
14.000000	0.500000	4934.198212	5.800000	4980.320677	9.500000	4978.814493	4.900000	4964.444461	0.527850	6.733333	2.437895
14.000000	0.100000	4187.361684	8.500000	4314.365320	11.200000	4318.111122	11.400000	4273.279375	1.741765	10.366667	1.619671
40.000000	25.000000	2745.949411	17.300000	5244.293593	19.000000	3719.145900	19.500000	3903.129635	32.263669	18.600000	1.153256
40.000000	10.000000	2542.562412	13.900000	4569.162310	11.600000	3217.721111	16.700000	3443.148611	29.970680	14.066667	2.554082
40.000000	5.000000	2335.928189	14.200000	4160.342931	11.800000	2905.429630	16.600000	3133.900250	29.784586	14.200000	2.400000
40.000000	1.000000	1905.783903	15.600000	3407.414360	15.400000	2341.842241	17.100000	2551.680168	30.273948	16.033333	0.929157
40.000000	0.500000	1767.162505	16.300000	3247.421200	14.100000	2066.593764	17.600000	2360.392490	33.157315	16.000000	1.769181
40.000000	0.100000	1383.118343	18.400000	2394.319456	17.300000	1656.922723	20.600000	1811.453507	28.872515	18.766667	1.680278
70.000000	25.000000	1926.861333	19.600000	2439.042793	20.100000	2183.940156	14.900000	2183.281427	11.729654	18.200000	2.868798
70.000000	10.000000	1705.885655	19.100000	2081.308610	18.800000	2215.713477	20.400000	2000.969247	13.205518	19.433333	0.850490
70.000000	5.000000	1455.411961	19.100000	1804.145889	19.800000	1928.386230	22.100000	1729.314693	14.179370	20.333333	1.569501
70.000000	1.000000	1025.197174	24.100000	1345.784053	23.300000	1423.406395	24.400000	1264.795874	16.690206	23.933333	0.568624
70.000000	0.500000	894.778479	22.600000	1148.187076	21.800000	1221.671222	30.100000	1088.212259	15.759847	24.833333	4.578573
70.000000	0.100000	575.210374	24.400000	782.324608	24.600000	859.827855	27.900000	739.120946	19.908129	25.633333	1.965536
100.000000	25.000000	823.205386	31.900000	1027.165237	25.800000	959.307048	25.700000	936.559224	11.090095	27.800000	3.551056
100.000000	10.000000	562.194500	30.100000	879.165406	26.300000	777.841308	24.400000	739.733738	21.884236	26.933333	2.902298
100.000000	5.000000	435.558163	30.200000	790.874300	26.100000	670.040026	25.900000	632.157496	28.578614	27.400000	2.426932
100.000000	1.000000	365.830844	28.500000	555.905172	25.600000	410.064451	26.900000	443.933489	22.404376	27.000000	1.452584
100.000000	0.500000	299.540346	27.900000	475.550578	24.700000	336.529098	27.800000	370.540007	25.045426	26.800000	1.819341
100.000000	0.100000	196.825099	25.300000	310.594396	23.900000	214.775708	26.700000	240.731734	25.407925	25.300000	1.400000
130.000000	25.000000	297.228776	27.700000	456.711316	29.100000	238.781950	37.000000	330.907347	34.088288	31.266667	5.014313
130.000000	10.000000	222.962163	25.600000	385.885295	24.900000	197.331512	31.700000	268.726323	38.056848	27.400000	3.740321
130.000000	5.000000	181.598618	24.800000	312.169919	24.100000	177.220343	31.100000	223.662960	34.283965	26.666667	3.855299
130.000000	1.000000	121.301520	23.600000	197.353707	22.200000	144.361519	24.300000	154.338915	25.266116	23.366667	1.069268
130.000000	0.500000	109.761801	21.600000	168.936261	21.500000	128.034739	21.800000	135.577600	22.348645	21.633333	0.152753
130.000000	0.100000	88.104121	18.000000	128.420895	17.600000	109.231163	18.200000	108.585393	18.571691	17.933333	0.305505

Table D-5 Dynamic Modulus Summary Sheet for the Mix 5

Conditions		Specimen 1		Specimen 2		Specimen 3		Modulus		Phase Angle (Degrees)	
Temperature, °F	Frequency, Hz	Modulus, ksi	Phage Angle, degree	Modulus, ksi	Phage Angle, degree	Modulus, ksi	Phage Angle, degree	Avg. Modulus, ksi	CV, %	Avg. P. Angle, degree	Standard Dev, degree
14.000000	25.000000	4834.127164	18.800000	5021.954183	5.800000	4402.902162	7.500000	4752.994503	6.677911	10.700000	7.066116
14.000000	10.000000	4656.404760	7.600000	4893.206172	6.300000	4354.466821	7.300000	4634.692584	5.826172	7.066667	0.680686
14.000000	5.000000	4548.573160	7.500000	4810.478066	7.000000	4231.803455	7.000000	4530.284894	6.396297	7.166667	0.288675
14.000000	1.000000	4135.801844	8.700000	4541.569109	7.200000	3961.266027	6.000000	4212.878993	7.067156	7.300000	1.352775
14.000000	0.500000	4108.558533	7.200000	4409.960031	8.200000	3624.597234	7.400000	4047.705266	9.788311	7.600000	0.529150
14.000000	0.100000	3646.386631	10.700000	3945.049059	8.500000	3378.769891	9.500000	3656.735194	7.746839	9.566667	1.101514
40.000000	25.000000	3680.269451	17.600000	3698.461154	9.100000	3018.269367	10.900000	3465.666657	11.182962	12.533333	4.479211
40.000000	10.000000	3363.117651	11.300000	3655.546020	9.400000	3010.254085	10.600000	3342.972585	9.665568	10.433333	0.960902
40.000000	5.000000	3112.856764	11.900000	3446.007212	9.600000	2830.517925	11.000000	3129.793967	9.843907	10.833333	1.159023
40.000000	1.000000	2637.895140	14.300000	2938.374766	12.600000	2353.357734	14.000000	2643.209213	11.067785	13.633333	0.907377
40.000000	0.500000	2415.671345	14.100000	2798.932314	10.400000	2222.151494	12.700000	2478.918384	11.841691	12.400000	1.868154
40.000000	0.100000	1947.944421	18.600000	2205.609586	14.900000	1749.391483	16.900000	1967.648497	11.625370	16.800000	1.852026
70.000000	25.000000	2058.632736	23.100000	2686.985727	16.700000	1690.971929	12.700000	2145.530131	23.474890	17.500000	5.245951
70.000000	10.000000	1753.716375	20.300000	2647.541213	16.800000	1729.132495	20.300000	2043.463361	25.608052	19.133333	2.020726
70.000000	5.000000	1513.772765	21.300000	2352.984343	17.900000	1516.225626	20.800000	1794.327578	26.963444	20.000000	1.835756
70.000000	1.000000	1083.198224	23.200000	1706.263978	20.800000	1070.043524	23.500000	1286.501909	28.261452	22.500000	1.479865
70.000000	0.500000	908.816608	27.000000	1435.378981	21.500000	906.806188	23.900000	1083.667259	28.107608	24.133333	2.757414
70.000000	0.100000	583.795896	28.100000	979.800022	23.700000	592.125963	27.200000	718.573960	31.488303	26.333333	2.324507
100.000000	25.000000	896.302795	32.500000	994.361102	28.000000	1051.347004	27.400000	980.670300	7.996935	29.300000	2.787472
100.000000	10.000000	603.807988	27.900000	729.745414	28.700000	816.252977	26.400000	716.602126	14.907938	27.666667	1.167619
100.000000	5.000000	475.970243	28.700000	592.525900	29.000000	657.857100	27.100000	575.451081	16.011400	28.266667	1.021437
100.000000	1.000000	300.638179	27.200000	354.012751	28.100000	411.967235	24.900000	355.539388	15.660776	26.733333	1.650253
100.000000	0.500000	248.699725	25.400000	298.144700	27.000000	342.529897	22.900000	296.458107	15.832867	25.100000	2.066398
100.000000	0.100000	174.270788	20.800000	216.775249	23.900000	265.187234	17.500000	218.744424	20.796050	20.733333	3.200521
130.000000	25.000000	300.325424	29.800000	305.311946	32.700000	405.964405	25.900000	337.200592	17.675942	29.466667	3.412233
130.000000	10.000000	176.357656	25.800000	239.100797	27.500000	363.922983	20.200000	259.793812	36.752038	24.500000	3.819686
130.000000	5.000000	144.969331	23.000000	203.113121	25.300000	333.801633	16.800000	227.294695	42.548621	21.700000	4.396590
130.000000	1.000000	111.889432	19.200000	161.384744	20.900000	292.496113	12.000000	188.590096	49.486302	17.366667	4.724757
130.000000	0.500000	104.024581	17.400000	153.126773	19.400000	281.657771	10.400000	179.603042	51.072954	15.733333	4.725816
130.000000	0.100000	88.777501	15.400000	145.755860	16.500000	253.405116	11.000000	162.646159	51.401999	14.300000	2.910326

Table D-6 Dynamic Modulus Summary Sheet for the Mix 6

Conditions		Specimen 1		Specimen 2		Specimen 3		Modulus		Phase Angle (Degrees)	
Temperature, °F	Frequency, Hz	Modulus, ksi	Phage Angle, degree	Modulus, ksi	Phage Angle, degree	Modulus, ksi	Phage Angle, degree	Avg. Modulus, ksi	CV, %	Avg. P. Angle, degree	Standard Dev, degree
14.000000	25.000000	4425.235833	17.700000	5913.551152	19.000000	6359.577457	3.800000	5566.121481	18.197444	13.500000	8.425556
14.000000	10.000000	4666.186757	7.400000	5629.912118	8.500000	5513.054586	9.100000	5269.717820	9.980210	8.333333	0.862168
14.000000	5.000000	4476.216730	7.000000	5411.274122	8.400000	5199.267511	9.400000	5028.919454	9.748653	8.266667	1.205543
14.000000	1.000000	3966.445192	7.200000	4722.542362	9.100000	4645.231469	9.900000	4444.739674	9.359715	8.733333	1.386843
14.000000	0.500000	3810.012590	7.000000	4465.592935	10.600000	4358.711059	9.900000	4211.438861	8.351751	9.166667	1.908752
14.000000	0.100000	3318.551707	9.600000	3844.406755	12.000000	3820.350467	11.000000	3661.102976	8.109628	10.866667	1.205543
40.000000	25.000000	2922.022309	19.300000	4088.599679	16.000000	4112.468112	10.100000	3707.696700	18.354215	15.133333	4.660830
40.000000	10.000000	2927.182181	11.700000	3571.918527	13.100000	3554.052344	13.400000	3351.051017	10.957454	12.733333	0.907377
40.000000	5.000000	2685.607054	11.500000	3290.980556	13.200000	3241.756221	13.900000	3072.781277	10.941384	12.866667	1.234234
40.000000	1.000000	2209.723848	14.400000	2700.447089	13.900000	2659.469700	14.800000	2523.213546	10.790290	14.366667	0.450925
40.000000	0.500000	2064.041100	14.600000	2355.079480	17.200000	2377.882864	17.300000	2265.667815	7.723361	16.366667	1.530795
40.000000	0.100000	1588.975901	16.900000	1936.337538	18.100000	1908.494104	18.600000	1811.269181	10.656304	17.866667	0.873689
70.000000	25.000000	1544.681804	24.200000	1871.021860	21.800000	1847.299650	20.600000	1754.334438	10.371541	22.200000	1.833030
70.000000	10.000000	1376.911701	19.400000	1555.140517	19.600000	1564.989968	20.800000	1499.014062	7.061866	19.933333	0.757188
70.000000	5.000000	1198.627035	20.200000	1368.848694	20.400000	1352.120381	21.900000	1306.532037	7.180998	20.833333	0.929157
70.000000	1.000000	832.147036	22.500000	953.415627	22.400000	949.786309	25.700000	911.782991	7.566562	23.533333	1.877054
70.000000	0.500000	667.719317	24.300000	801.699731	23.300000	802.961049	24.500000	757.460032	10.260647	24.033333	0.642910
70.000000	0.100000	481.225711	24.800000	564.712929	23.900000	552.018513	25.600000	532.652384	8.445812	24.766667	0.850490
100.000000	25.000000	605.483169	28.100000	811.678433	24.600000	688.559570	27.900000	701.907057	14.780250	26.866667	1.965536
100.000000	10.000000	464.979296	26.700000	646.005642	24.000000	514.730498	27.200000	541.905145	17.258116	25.966667	1.721434
100.000000	5.000000	402.726321	27.000000	539.159161	23.500000	426.259659	27.400000	456.048380	15.992057	25.966667	2.145538
100.000000	1.000000	257.066493	28.300000	372.941371	23.900000	266.047455	27.700000	298.685106	21.582730	26.633333	2.386071
100.000000	0.500000	225.869360	27.500000	325.994227	22.800000	222.881653	27.100000	258.248413	22.725642	25.800000	2.605763
100.000000	0.100000	168.142914	25.500000	233.222141	19.900000	151.365570	25.400000	184.243542	23.467993	23.600000	3.204684
130.000000	25.000000	221.040376	28.900000	288.475852	26.000000	256.889371	31.300000	255.468533	13.207178	28.733333	2.653928
130.000000	10.000000	173.951650	24.800000	232.340161	23.700000	159.328048	28.600000	188.539953	20.489226	25.700000	2.570992
130.000000	5.000000	151.489018	23.900000	198.549601	22.200000	160.238606	27.400000	170.092408	14.715493	24.500000	2.651415
130.000000	1.000000	113.656293	22.000000	142.532717	19.800000	112.330422	25.000000	122.839811	13.894060	22.266667	2.610236
130.000000	0.500000	106.919738	20.800000	129.298088	17.800000	101.375305	23.200000	112.531044	13.136772	20.600000	2.705550
130.000000	0.100000	89.677758	16.300000	105.554265	13.500000	81.346531	19.000000	92.192851	13.339741	16.266667	2.750152

Table D-7 Dynamic Modulus Summary Sheet for the Mix 7

Conditions		Specimen 1		Specimen 2		Specimen 3		Modulus		Phase Angle (Degrees)	
Temperature, °F	Frequency, Hz	Modulus, ksi	Phage Angle, degree	Modulus, ksi	Phage Angle, degree	Modulus, ksi	Phage Angle, degree	Avg. Modulus, ksi	CV, %	Avg. P. Angle, degree	Standard Dev, degree
14.000000	25.000000	4425.235833	17.700000	5913.551152	19.000000	6359.577457	3.800000	5566.121481	18.197444	13.500000	8.425556
14.000000	10.000000	4666.186757	7.400000	5629.912118	8.500000	5513.054586	9.100000	5269.717820	9.980210	8.333333	0.862168
14.000000	5.000000	4476.216730	7.000000	5411.274122	8.400000	5199.267511	9.400000	5028.919454	9.748653	8.266667	1.205543
14.000000	1.000000	3966.445192	7.200000	4722.542362	9.100000	4645.231469	9.900000	4444.739674	9.359715	8.733333	1.386843
14.000000	0.500000	3810.012590	7.000000	4465.592935	10.600000	4358.711059	9.900000	4211.438861	8.351751	9.166667	1.908752
14.000000	0.100000	3318.551707	9.600000	3844.406755	12.000000	3820.350467	11.000000	3661.102976	8.109628	10.866667	1.205543
40.000000	25.000000	2922.022309	19.300000	4088.599679	16.000000	4112.468112	10.100000	3707.696700	18.354215	15.133333	4.660830
40.000000	10.000000	2927.182181	11.700000	3571.918527	13.100000	3554.052344	13.400000	3351.051017	10.957454	12.733333	0.907377
40.000000	5.000000	2685.607054	11.500000	3290.980556	13.200000	3241.756221	13.900000	3072.781277	10.941384	12.866667	1.234234
40.000000	1.000000	2209.723848	14.400000	2700.447089	13.900000	2659.469700	14.800000	2523.213546	10.790290	14.366667	0.450925
40.000000	0.500000	2064.041100	14.600000	2355.079480	17.200000	2377.882864	17.300000	2265.667815	7.723361	16.366667	1.530795
40.000000	0.100000	1588.975901	16.900000	1936.337538	18.100000	1908.494104	18.600000	1811.269181	10.656304	17.866667	0.873689
70.000000	25.000000	1544.681804	24.200000	1871.021860	21.800000	1847.299650	20.600000	1754.334438	10.371541	22.200000	1.833030
70.000000	10.000000	1376.911701	19.400000	1555.140517	19.600000	1564.989968	20.800000	1499.014062	7.061866	19.933333	0.757188
70.000000	5.000000	1198.627035	20.200000	1368.848694	20.400000	1352.120381	21.900000	1306.532037	7.180998	20.833333	0.929157
70.000000	1.000000	832.147036	22.500000	953.415627	22.400000	949.786309	25.700000	911.782991	7.566562	23.533333	1.877054
70.000000	0.500000	667.719317	24.300000	801.699731	23.300000	802.961049	24.500000	757.460032	10.260647	24.033333	0.642910
70.000000	0.100000	481.225711	24.800000	564.712929	23.900000	552.018513	25.600000	532.652384	8.445812	24.766667	0.850490
100.000000	25.000000	605.483169	28.100000	811.678433	24.600000	688.559570	27.900000	701.907057	14.780250	26.866667	1.965536
100.000000	10.000000	464.979296	26.700000	646.005642	24.000000	514.730498	27.200000	541.905145	17.258116	25.966667	1.721434
100.000000	5.000000	402.726321	27.000000	539.159161	23.500000	426.259659	27.400000	456.048380	15.992057	25.966667	2.145538
100.000000	1.000000	257.066493	28.300000	372.941371	23.900000	266.047455	27.700000	298.685106	21.582730	26.633333	2.386071
100.000000	0.500000	225.869360	27.500000	325.994227	22.800000	222.881653	27.100000	258.248413	22.725642	25.800000	2.605763
100.000000	0.100000	168.142914	25.500000	233.222141	19.900000	151.365570	25.400000	184.243542	23.467993	23.600000	3.204684
130.000000	25.000000	221.040376	28.900000	288.475852	26.000000	256.889371	31.300000	255.468533	13.207178	28.733333	2.653928
130.000000	10.000000	173.951650	24.800000	232.340161	23.700000	159.328048	28.600000	188.539953	20.489226	25.700000	2.570992
130.000000	5.000000	151.489018	23.900000	198.549601	22.200000	160.238606	27.400000	170.092408	14.715493	24.500000	2.651415
130.000000	1.000000	113.656293	22.000000	142.532717	19.800000	112.330422	25.000000	122.839811	13.894060	22.266667	2.610236
130.000000	0.500000	106.919738	20.800000	129.298088	17.800000	101.375305	23.200000	112.531044	13.136772	20.600000	2.705550
130.000000	0.100000	89.677758	16.300000	105.554265	13.500000	81.346531	19.000000	92.192851	13.339741	16.266667	2.750152

Table D-8 Dynamic Modulus Summary Sheet for the Mix 8

Conditions		Specimen 1		Specimen 2		Specimen 3		Modulus		Phase Angle (Degrees)	
Temperature, °F	Frequency, Hz	Modulus, ksi	Phage Angle, degree	Modulus, ksi	Phage Angle, degree	Modulus, ksi	Phage Angle, degree	Avg. Modulus, ksi	CV, %	Avg. P. Angle, degree	Standard Dev, degree
14.000000	25.000000	9448.636579	8.200000	6691.955157	11.500000	7572.453107	15.200000	7904.348281	17.812868	11.633333	3.501904
14.000000	10.000000	9373.213819	7.800000	6589.779107	6.300000	7308.185569	6.500000	7757.059498	18.628050	6.866667	0.814453
14.000000	5.000000	8979.848524	8.000000	6387.973869	5.900000	6977.218746	6.500000	7448.347046	18.240936	6.800000	1.081665
14.000000	1.000000	7989.065677	10.100000	5765.972728	7.100000	6406.011516	8.400000	6720.349974	17.028815	8.533333	1.504438
14.000000	0.500000	7713.709419	8.300000	5597.827783	9.000000	6335.353042	8.600000	6548.963415	16.399434	8.633333	0.351188
14.000000	0.100000	6869.376701	11.100000	4980.163719	8.100000	5376.600132	10.000000	5742.046851	17.349480	9.733333	1.517674
40.000000	25.000000	4652.512734	14.300000	4584.479165	15.500000	5128.903223	13.900000	4788.631707	6.194685	14.566667	0.832666
40.000000	10.000000	4668.387354	14.400000	4025.778495	13.200000	4790.719543	11.800000	4494.961797	9.141406	13.133333	1.301281
40.000000	5.000000	4237.133920	16.100000	3683.363923	13.600000	4381.709116	13.000000	4100.735653	8.988926	14.233333	1.644182
40.000000	1.000000	3329.636220	19.300000	2924.849577	16.100000	3535.469698	16.000000	3263.318498	9.519912	17.133333	1.877054
40.000000	0.500000	3055.174417	19.200000	2652.296506	16.600000	3191.733462	18.400000	2966.401462	9.454597	18.066667	1.331666
40.000000	0.100000	2264.750972	23.100000	2052.867519	20.600000	2349.737410	22.200000	2222.451967	6.879263	21.966667	1.266228
70.000000	25.000000	2786.682805	20.100000	2133.275931	24.600000	2337.661685	24.900000	2419.206807	13.816467	23.200000	2.688866
70.000000	10.000000	2318.253199	20.400000	1647.402274	23.400000	2034.973049	21.400000	2000.209507	16.836928	21.733333	1.527525
70.000000	5.000000	2010.314026	21.700000	1414.287334	24.800000	1754.753282	22.900000	1726.451547	17.319893	23.133333	1.563117
70.000000	1.000000	1415.396627	24.900000	965.643377	29.500000	1145.931790	27.500000	1175.657265	19.252661	27.300000	2.306513
70.000000	0.500000	1180.465940	26.700000	808.792415	31.300000	961.603677	29.500000	983.620677	18.992319	29.166667	2.318045
70.000000	0.100000	801.054203	25.700000	593.447482	29.100000	607.053180	30.300000	667.184955	17.406506	28.366667	2.386071
100.000000	25.000000	1050.450083	28.400000	590.027924	31.700000	687.846878	35.800000	776.108295	31.254525	31.966667	3.707200
100.000000	10.000000	803.351557	27.500000	422.954121	32.900000	497.406994	36.300000	574.570891	35.086490	32.233333	4.437717
100.000000	5.000000	671.090278	26.300000	330.361332	32.500000	379.852727	36.300000	460.434779	39.984740	31.700000	5.047772
100.000000	1.000000	444.150938	23.900000	193.728596	31.200000	212.600787	35.000000	283.493440	49.190940	30.033333	5.641217
100.000000	0.500000	360.860279	22.900000	155.021724	30.000000	168.745503	33.400000	228.209169	50.429167	28.766667	5.357549
100.000000	0.100000	241.793882	18.800000	101.230533	25.100000	114.443112	26.400000	152.489176	50.903142	23.433333	4.064890
130.000000	25.000000	283.996903	33.700000	142.703165	37.400000	183.987796	28.700000	203.562621	35.690406	33.266667	4.366158
130.000000	10.000000	192.988487	30.400000	99.278137	33.500000	134.410089	32.900000	142.225571	33.286217	32.266667	1.644182
130.000000	5.000000	167.501013	27.300000	79.819604	29.800000	110.138674	29.500000	119.153097	37.372383	28.866667	1.365040
130.000000	1.000000	127.432585	21.500000	57.662183	23.500000	77.457407	24.400000	87.517392	41.085133	23.133333	1.484363
130.000000	0.500000	111.234765	18.700000	51.547510	21.900000	68.765989	23.100000	77.182755	39.802800	21.233333	2.274496
130.000000	0.100000	89.085468	14.200000	40.078437	19.000000	56.154694	20.400000	61.772866	40.441537	17.866667	3.251666

Table D-9 Dynamic Modulus Summary Sheet for the Mix 9

Conditions		Specimen 1		Specimen 2		Specimen 3		Modulus		Phase Angle (Degrees)	
Temperature, °F	Frequency, Hz	Modulus, ksi	Phage Angle, degree	Modulus, ksi	Phage Angle, degree	Modulus, ksi	Phage Angle, degree	Avg. Modulus, ksi	CV, %	Avg. P. Angle, degree	Standard Dev, degree
14.000000	25.000000	7465.506968	6.300000	7409.298021	13.200000	6399.619774	9.400000	7091.474921	8.458366	9.633333	3.455913
14.000000	10.000000	6631.419867	6.300000	7435.972541	5.100000	6117.788363	7.600000	6728.393590	9.874884	6.333333	1.250333
14.000000	5.000000	6411.942685	6.900000	7264.474188	4.200000	5957.313015	8.100000	6544.576629	10.139652	6.400000	1.997498
14.000000	1.000000	5824.288998	7.700000	6761.661587	5.600000	5431.028582	9.000000	6005.659722	11.382701	7.433333	1.715615
14.000000	0.500000	5689.081065	7.700000	6249.252814	3.800000	5170.506702	9.100000	5702.946860	9.460139	6.866667	2.746513
14.000000	0.100000	5120.467986	8.700000	5799.566583	7.300000	4764.705782	9.000000	5228.246784	10.056559	8.333333	0.907377
40.000000	25.000000	5043.269806	9.200000	5590.048228	12.700000	4538.589961	11.700000	5057.302665	10.398222	11.200000	1.802776
40.000000	10.000000	4297.855036	11.300000	5123.624255	9.100000	4183.567721	9.900000	4535.015671	11.310720	10.100000	1.113553
40.000000	5.000000	3922.400893	12.500000	4911.892538	9.400000	3907.295103	10.400000	4247.196178	13.554671	10.766667	1.582193
40.000000	1.000000	3312.710332	14.400000	4177.718077	9.800000	3292.199951	12.500000	3594.209453	14.062545	12.233333	2.311565
40.000000	0.500000	2939.728198	15.200000	3775.728528	10.800000	3043.872601	10.800000	3253.109776	14.004653	12.266667	2.540341
40.000000	0.100000	2364.535232	18.600000	3127.005721	14.400000	2476.091601	15.400000	2655.877518	15.505384	16.133333	2.193931
70.000000	25.000000	2620.797643	10.300000	3062.619893	18.300000	2407.075234	17.300000	2696.830923	12.396808	15.300000	4.358899
70.000000	10.000000	2047.122320	19.700000	2606.418327	15.900000	2039.735739	18.600000	2231.092129	14.569681	18.066667	1.955335
70.000000	5.000000	1746.026179	21.000000	2286.108083	17.100000	1796.299026	19.300000	1942.811096	15.357367	19.133333	1.955335
70.000000	1.000000	1207.298143	25.000000	1686.471366	20.900000	1285.368584	22.400000	1393.046031	18.455562	22.766667	2.074448
70.000000	0.500000	1035.464115	28.000000	1459.575979	22.100000	1102.675035	23.600000	1199.238376	19.007875	24.566667	3.066486
70.000000	0.100000	702.109854	29.400000	1091.358132	24.300000	790.144200	25.900000	861.204062	23.701901	26.533333	2.608320
100.000000	25.000000	958.053999	24.600000	1409.552350	22.400000	1342.191581	22.700000	1236.599310	19.696535	23.233333	1.193035
100.000000	10.000000	772.050560	25.400000	1117.091487	22.900000	1055.787366	26.300000	981.643138	18.752478	24.866667	1.761628
100.000000	5.000000	617.529446	26.700000	880.791701	25.400000	895.376716	25.900000	797.899288	19.598338	26.000000	0.655744
100.000000	1.000000	366.573999	29.800000	519.296629	27.500000	546.266932	27.100000	477.379187	20.298958	28.133333	1.457166
100.000000	0.500000	299.777523	29.600000	412.088797	28.600000	436.553726	27.300000	382.806682	19.053593	28.500000	1.153256
100.000000	0.100000	193.080312	27.300000	325.357257	27.400000	293.592205	25.300000	270.676591	25.510788	26.666667	1.184624
130.000000	25.000000	365.910484	32.300000	588.568451	30.800000	494.227079	27.100000	482.902005	23.143447	30.066667	2.676440
130.000000	10.000000	279.552915	28.400000	457.468977	28.100000	381.533421	27.300000	372.851771	23.943883	27.933333	0.568624
130.000000	5.000000	227.896608	28.100000	368.656661	27.700000	304.159280	26.700000	300.237516	23.468729	27.500000	0.721110
130.000000	1.000000	127.163929	26.200000	227.411809	25.700000	186.131965	25.300000	180.235901	27.954115	25.733333	0.450925
130.000000	0.500000	130.925254	24.600000	196.142290	23.700000	160.509292	24.000000	162.525612	20.092365	24.100000	0.458258
130.000000	0.100000	98.905182	20.400000	134.309996	20.400000	116.795300	19.900000	116.670159	15.173322	20.233333	0.288675

Table D-10 Dynamic Modulus Summary Sheet for the Mix 10

Conditions		Specimen 1		Specimen 2		Specimen 3		Modulus		Phase Angle (Degrees)	
Temperature, °F	Frequency, Hz	Modulus, ksi	Phage Angle, degree	Modulus, ksi	Phage Angle, degree	Modulus, ksi	Phage Angle, degree	Avg. Modulus, ksi	CV, %	Avg. P. Angle, degree	Standard Dev, degree
14.000000	25.000000	5878.671028	1.100000	5765.581784	8.100000	5145.119031	7.700000	5596.457281	7.056950	5.633333	3.931073
14.000000	10.000000	5547.132369	8.500000	5772.257414	7.600000	5344.560621	10.200000	5554.650135	3.851682	8.766667	1.320353
14.000000	5.000000	5236.679410	9.000000	5471.203486	8.300000	5165.028853	10.100000	5290.970583	3.026758	9.133333	0.907377
14.000000	1.000000	4603.868069	10.500000	4887.166786	9.300000	4530.489383	11.300000	4673.841413	4.029942	10.366667	1.006645
14.000000	0.500000	4238.299062	11.900000	4636.280970	10.800000	4320.034651	14.900000	4398.204894	4.779022	12.533333	2.122106
14.000000	0.100000	3607.488423	13.600000	3751.527178	12.900000	3732.236917	14.200000	3697.084173	2.114893	13.566667	0.650641
40.000000	25.000000	3569.212532	12.500000	3588.945088	13.400000	3442.813807	13.600000	3533.657142	2.243819	13.166667	0.585947
40.000000	10.000000	3273.958346	14.900000	3173.841168	17.200000	3493.934543	14.000000	3313.911352	4.941112	15.366667	1.650253
40.000000	5.000000	2966.348901	15.900000	2848.626652	18.500000	3190.244541	14.600000	3001.740031	5.781214	16.333333	1.985783
40.000000	1.000000	2212.397349	20.800000	2176.942343	21.400000	2488.385644	18.300000	2292.575112	7.437095	20.166667	1.644182
40.000000	0.500000	1905.814656	22.400000	1896.771027	26.200000	2230.783001	18.800000	2011.122895	9.461628	22.466667	3.700450
40.000000	0.100000	1343.052672	26.300000	1327.991417	25.400000	1563.951901	24.500000	1411.665330	9.357662	25.400000	0.900000
70.000000	25.000000	1391.700819	28.000000	1343.529057	23.900000	1869.106600	26.700000	1534.778825	18.930183	26.200000	2.095233
70.000000	10.000000	1092.860834	28.800000	1049.669502	24.400000	1445.733539	23.300000	1196.087958	18.165496	25.500000	2.910326
70.000000	5.000000	878.813194	29.300000	877.789053	25.400000	1208.389593	24.900000	988.330613	19.282753	26.533333	2.409011
70.000000	1.000000	539.496722	31.100000	545.224513	27.600000	795.853714	27.700000	626.858316	23.351740	28.800000	1.992486
70.000000	0.500000	431.545590	31.100000	435.832766	27.700000	656.101119	27.200000	507.826492	25.289639	28.666667	2.122106
70.000000	0.100000	264.472512	28.900000	256.422851	26.100000	423.826236	28.000000	314.907200	29.981049	27.666667	1.429452
100.000000	25.000000	519.767066	36.500000	595.346784	30.300000	709.288851	31.700000	608.134234	15.688279	32.833333	3.251666
100.000000	10.000000	378.943911	32.500000	432.528098	28.600000	535.092770	29.800000	448.854926	17.677080	30.300000	1.997498
100.000000	5.000000	311.457227	31.100000	342.992646	28.000000	348.421608	30.500000	334.290494	5.970745	29.866667	1.644182
100.000000	1.000000	203.192906	27.200000	206.782621	26.400000	265.351590	28.300000	225.109039	15.502380	27.300000	0.953939
100.000000	0.500000	172.709770	24.800000	165.877619	25.500000	215.918800	27.200000	184.835396	14.680578	25.833333	1.234234
100.000000	0.100000	133.582508	19.600000	117.374824	21.100000	149.087654	22.100000	133.348329	11.891946	20.933333	1.258306
130.000000	25.000000	139.271422	33.200000	190.836050	31.300000	254.556767	29.500000	194.888080	29.632078	31.333333	1.850225
130.000000	10.000000	109.414957	27.700000	149.736228	26.000000	153.598081	26.100000	137.583089	17.786066	26.600000	0.953939
130.000000	5.000000	94.724336	26.600000	128.900182	23.500000	131.418321	24.400000	118.347613	17.319373	24.833333	1.594783
130.000000	1.000000	78.176336	23.600000	93.261527	19.400000	108.318140	20.900000	93.252001	16.161481	21.300000	2.128380
130.000000	0.500000	76.672764	21.300000	81.347692	18.100000	96.722137	19.200000	84.914198	12.353322	19.533333	1.625833
130.000000	0.100000	66.022133	17.700000	66.572065	15.500000	80.376499	17.000000	70.990232	11.457062	16.733333	1.123981

Table D-11 Dynamic Modulus Summary Sheet for the Mix 11

Conditions		Specimen 1		Specimen 2		Specimen 3		Modulus		Phase Angle (Degrees)	
Temperature, °F	Frequency, Hz	Modulus, ksi	Phage Angle, degree	Modulus, ksi	Phage Angle, degree	Modulus, ksi	Phage Angle, degree	Avg. Modulus, ksi	CV, %	Avg. P. Angle, degree	Standard Dev, degree
14.000000	25.000000	5976.719616	2.800000	6162.222155	3.800000	6776.748082	1.500000	6305.229951	6.641279	2.700000	1.153256
14.000000	10.000000	5274.462523	7.400000	5633.866666	6.000000	6191.489667	7.900000	5699.939619	8.106582	7.100000	0.984886
14.000000	5.000000	5168.246194	7.400000	5534.184965	6.300000	5962.442859	7.800000	5554.958006	7.155871	7.166667	0.776745
14.000000	1.000000	4703.810882	9.800000	4999.480236	5.600000	5297.363824	10.900000	5000.218314	5.935284	8.766667	2.797022
14.000000	0.500000	4278.076349	8.200000	4611.065633	7.600000	5053.627701	6.700000	4647.589894	8.371298	7.500000	0.754983
14.000000	0.100000	4012.874754	9.700000	4210.765772	9.400000	4590.796200	11.200000	4271.478909	6.875965	10.100000	0.964365
40.000000	25.000000	3956.291545	7.400000	3894.831337	8.800000	3987.216251	8.200000	3946.113044	1.191704	8.133333	0.702377
40.000000	10.000000	3264.868732	10.900000	3375.732138	11.600000	3443.654154	11.700000	3361.418341	2.684822	11.400000	0.435890
40.000000	5.000000	3042.228463	11.400000	3136.561711	11.800000	3211.212014	11.900000	3130.000729	2.705514	11.700000	0.264575
40.000000	1.000000	2519.311365	12.900000	2523.497723	14.900000	2596.208976	14.600000	2546.339355	1.698087	14.133333	1.078579
40.000000	0.500000	2225.219855	16.200000	2403.068173	16.600000	2328.257286	14.200000	2318.848438	3.850907	15.666667	1.285820
40.000000	0.100000	1757.917674	18.900000	1731.607551	19.700000	1762.003068	19.800000	1750.509431	0.942381	19.466667	0.493288
70.000000	25.000000	1848.976427	16.200000	1524.186509	19.400000	1878.542623	18.800000	1750.568520	11.231159	18.133333	1.700980
70.000000	10.000000	1599.289987	20.500000	1278.048442	20.600000	1548.075105	19.800000	1475.137845	11.700239	20.300000	0.435890
70.000000	5.000000	1357.729946	21.800000	1092.867797	21.900000	1333.540781	21.300000	1261.379508	11.609174	21.666667	0.321455
70.000000	1.000000	917.756082	27.100000	740.282606	25.600000	924.152757	25.400000	860.730482	12.124578	26.033333	0.929157
70.000000	0.500000	760.281207	26.300000	585.034149	27.800000	723.854137	28.400000	689.723164	13.407514	27.500000	1.081665
70.000000	0.100000	486.082402	28.300000	385.827124	28.100000	467.910718	27.500000	446.606748	11.960212	27.966667	0.416333
100.000000	25.000000	714.176730	29.200000	680.735191	29.600000	642.556782	28.400000	679.156234	5.276558	29.066667	0.611010
100.000000	10.000000	489.903638	30.100000	498.563867	29.200000	471.182457	28.300000	486.549987	2.876452	29.200000	0.900000
100.000000	5.000000	398.503553	30.200000	400.196722	30.600000	374.250415	28.200000	390.983563	3.712698	29.666667	1.285820
100.000000	1.000000	237.560669	29.500000	250.156587	30.200000	235.516594	27.200000	241.077950	3.288762	28.966667	1.569501
100.000000	0.500000	186.312422	28.400000	198.751964	30.200000	186.386985	26.900000	190.483790	3.759136	28.500000	1.652271
100.000000	0.100000	121.920502	24.300000	131.570202	26.400000	123.973571	23.600000	125.821425	4.040104	24.766667	1.457166
130.000000	25.000000	240.939029	31.900000	204.561425	34.600000	269.234042	28.400000	238.244832	13.608009	31.633333	3.108590
130.000000	10.000000	188.568434	27.900000	162.684794	30.800000	186.874394	27.800000	179.375874	8.072264	28.833333	1.703917
130.000000	5.000000	155.467211	25.700000	134.316379	29.500000	150.133990	26.300000	146.639193	7.501394	27.166667	2.042874
130.000000	1.000000	107.199708	23.200000	96.010025	27.600000	98.704560	23.800000	100.638098	5.803020	24.866667	2.386071
130.000000	0.500000	93.338700	21.600000	82.391996	27.000000	86.098342	22.200000	87.276346	6.379296	23.600000	2.959730
130.000000	0.100000	76.271666	17.300000	68.987500	23.400000	66.713501	18.400000	70.657556	7.066675	19.700000	3.251154

Table D-12 Dynamic Modulus Summary Sheet for the Mix 12

Conditions		Specimen 1		Specimen 2		Specimen 3		Modulus		Phase Angle (Degrees)	
Temperature, °F	Frequency, Hz	Modulus, ksi	Phage Angle, degree	Modulus, ksi	Phage Angle, degree	Modulus, ksi	Phage Angle, degree	Avg. Modulus, ksi	CV, %	Avg. P. Angle, degree	Standard Dev, degree
14.000000	25.000000	5968.377944	11.400000	5822.773240	5.500000	3976.906081	10.900000	5256.019088	21.121196	9.266667	3.271595
14.000000	10.000000	6113.115175	6.000000	4646.306092	8.200000	3789.831936	8.900000	4849.751068	24.226544	7.700000	1.513275
14.000000	5.000000	5865.618743	6.900000	4438.336134	8.100000	3606.535217	9.200000	4636.830031	24.640700	8.066667	1.150362
14.000000	1.000000	5378.096161	8.300000	3906.186391	10.200000	3206.874646	9.500000	4163.719066	26.617642	9.333333	0.960902
14.000000	0.500000	5208.366844	8.200000	3653.549961	9.300000	2901.990344	11.300000	3921.302383	29.996927	9.600000	1.571623
14.000000	0.100000	4407.761174	10.000000	3129.329042	10.900000	2475.539348	13.000000	3337.543188	29.446647	11.300000	1.539480
40.000000	25.000000	4324.154715	16.600000	2803.551974	10.600000	2449.140881	16.500000	3192.282523	31.203970	14.566667	3.435598
40.000000	10.000000	4034.687071	11.800000	2385.947176	13.300000	2174.712443	14.800000	2865.115563	35.543779	13.300000	1.500000
40.000000	5.000000	3728.077831	12.900000	2173.946948	14.100000	1959.882336	16.000000	2620.635705	36.824154	14.333333	1.563117
40.000000	1.000000	3066.980180	15.100000	1682.046381	17.500000	1502.653293	19.500000	2083.893285	41.081286	17.366667	2.203028
40.000000	0.500000	2805.521632	12.100000	1493.629392	18.200000	1359.117034	20.700000	1886.089353	42.367404	17.000000	4.423799
40.000000	0.100000	2094.644347	19.600000	1061.174986	21.900000	947.705678	23.800000	1367.841670	46.202814	21.766667	2.103172
70.000000	25.000000	1765.304690	21.300000	1151.178845	22.500000	1259.844699	22.700000	1392.109411	23.542098	22.166667	0.757188
70.000000	10.000000	1480.720574	17.800000	930.373760	22.800000	972.289413	24.200000	1127.794582	27.164572	21.600000	3.364521
70.000000	5.000000	1300.312629	18.600000	777.197666	23.700000	793.574492	25.800000	957.028262	31.075961	22.700000	3.702702
70.000000	1.000000	922.992982	22.500000	504.516070	26.700000	490.463724	29.700000	639.324259	38.441335	26.300000	3.616628
70.000000	0.500000	766.833388	24.000000	407.635090	27.600000	385.525104	29.600000	519.997861	41.163920	27.066667	2.837840
70.000000	0.100000	524.783181	23.800000	255.970981	27.100000	236.928487	30.500000	339.227550	47.454197	27.133333	3.350124
100.000000	25.000000	740.681238	26.800000	427.798336	29.900000	420.847669	30.200000	529.775748	34.483000	28.966667	1.882374
100.000000	10.000000	572.464342	24.600000	327.503747	29.100000	306.382362	29.300000	402.116817	36.781053	27.666667	2.657693
100.000000	5.000000	475.649220	24.800000	257.618020	27.900000	240.805861	28.600000	324.691034	40.347156	27.100000	2.022375
100.000000	1.000000	294.001426	26.200000	166.505739	26.000000	154.409851	26.400000	204.972339	37.731087	26.200000	0.200000
100.000000	0.500000	238.266833	25.600000	139.790601	24.200000	125.747394	25.300000	167.934943	36.509729	25.033333	0.737111
100.000000	0.100000	161.548084	22.700000	102.912532	19.600000	90.247274	21.500000	118.235963	32.173124	21.266667	1.563117
130.000000	25.000000	268.351192	29.600000	131.862067	28.900000	162.740353	30.300000	187.651204	38.141653	29.600000	0.700000
130.000000	10.000000	204.092003	26.000000	106.966738	23.600000	111.490075	29.000000	140.849605	38.918249	26.200000	2.705550
130.000000	5.000000	169.142830	25.000000	89.379075	21.500000	92.275972	27.300000	116.932626	38.687712	24.600000	2.920616
130.000000	1.000000	130.791941	22.700000	65.847333	16.200000	75.428998	21.000000	90.689424	38.657958	19.966667	3.370954
130.000000	0.500000	120.712421	21.100000	56.720583	16.500000	70.673851	19.100000	82.702285	40.686834	18.900000	2.306513
130.000000	0.100000	96.611019	16.600000	47.073349	12.200000	59.383204	14.200000	67.689191	38.103859	14.333333	2.203028

Table D-13 Dynamic Modulus Summary Sheet for the Mix 13

Conditions		Specimen 1		Specimen 2		Specimen 3		Modulus		Phase Angle (Degrees)	
Temperature, °F	Frequency, Hz	Modulus, ksi	Phage Angle, degree	Modulus, ksi	Phage Angle, degree	Modulus, ksi	Phage Angle, degree	Avg. Modulus, ksi	CV, %	Avg. P. Angle, degree	Standard Dev, degree
14.000000	25.000000	6031.128193	2.600000	6309.782446	8.800000	5024.986279	12.500000	5788.632306	11.675537	7.966667	5.002333
14.000000	10.000000	6294.405826	5.300000	7268.069561	5.900000	4790.091133	6.600000	6117.522173	20.407332	5.933333	0.650641
14.000000	5.000000	6129.689722	5.500000	6909.492710	6.000000	4641.079346	6.600000	5893.420593	19.555970	6.033333	0.550757
14.000000	1.000000	5828.142147	6.300000	6244.407437	6.300000	4145.836394	6.000000	5406.128659	20.552837	6.200000	0.173205
14.000000	0.500000	5734.771243	6.300000	6025.840812	9.900000	4105.244436	7.800000	5288.618830	19.572488	8.000000	1.808314
14.000000	0.100000	5032.516036	6.700000	5430.406410	9.000000	3631.744462	7.200000	4698.222303	20.109321	7.633333	1.209683
40.000000	25.000000	7094.787374	6.600000	5897.712072	6.700000	3865.028109	13.200000	5619.175852	29.057572	8.833333	3.781975
40.000000	10.000000	5648.306183	8.700000	4338.691569	11.200000	3400.445414	11.100000	4462.481055	25.300536	10.333333	1.415392
40.000000	5.000000	5348.238245	9.000000	3873.928416	11.900000	3126.612022	12.300000	4116.259561	27.463382	11.066667	1.800926
40.000000	1.000000	4547.735569	11.700000	3085.393249	17.500000	2583.418238	13.400000	3405.515685	29.967160	14.200000	2.981610
40.000000	0.500000	4179.709349	9.200000	2908.135190	18.500000	2333.754283	17.200000	3140.532941	30.079803	14.966667	5.036202
40.000000	0.100000	3390.590306	14.600000	2033.226497	22.900000	1848.356721	18.900000	2424.057841	34.740508	18.800000	4.150904
70.000000	25.000000	2776.486220	17.200000	2253.795564	13.000000	2217.006419	21.600000	2415.762734	12.953954	17.266667	4.300388
70.000000	10.000000	1994.871692	19.200000	1736.859972	20.500000	1825.449907	20.200000	1852.393857	7.077284	19.966667	0.680686
70.000000	5.000000	1757.118525	20.300000	1521.232893	22.000000	1596.586603	21.600000	1624.979340	7.414168	21.300000	0.888819
70.000000	1.000000	1275.733535	23.200000	1034.171464	25.700000	1093.163870	26.800000	1134.356290	11.102257	25.233333	1.844813
70.000000	0.500000	1050.085831	26.100000	866.113701	29.500000	927.462792	25.500000	947.887441	9.882111	27.033333	2.157159
70.000000	0.100000	702.743052	28.900000	561.049957	29.900000	600.900501	28.000000	621.564503	11.756105	28.933333	0.950438
100.000000	25.000000	993.412684	25.200000	919.609836	28.300000	817.915828	28.300000	910.312783	9.679864	27.266667	1.789786
100.000000	10.000000	735.351788	27.800000	670.571100	28.900000	623.340793	26.600000	676.421227	8.313486	27.766667	1.150362
100.000000	5.000000	587.586088	28.600000	512.504224	29.100000	482.920766	26.700000	527.670359	10.225264	28.133333	1.266228
100.000000	1.000000	333.273461	30.400000	300.183843	28.900000	298.024008	26.700000	310.493771	6.363196	28.666667	1.861003
100.000000	0.500000	262.722913	30.700000	234.931847	28.700000	235.836747	26.400000	244.497169	6.458333	28.600000	2.151743
100.000000	0.100000	162.628945	29.000000	152.811988	25.100000	147.404204	23.400000	154.281712	5.002568	25.833333	2.871121
130.000000	25.000000	295.564909	32.200000	269.397092	30.200000	272.912826	34.000000	279.291609	5.085115	32.133333	1.900877
130.000000	10.000000	210.157355	32.700000	189.304771	29.600000	213.519177	30.400000	204.327101	6.420030	30.900000	1.609348
130.000000	5.000000	163.655262	31.700000	151.923625	28.100000	176.583954	29.200000	164.054280	7.518856	29.666667	1.844813
130.000000	1.000000	99.310631	29.000000	97.230871	24.400000	109.065211	26.500000	101.868904	6.202427	26.633333	2.302897
130.000000	0.500000	81.133870	27.700000	80.701003	22.900000	87.872746	25.600000	83.235873	4.831424	25.400000	2.406242
130.000000	0.100000	59.443695	22.600000	61.415529	18.900000	65.436661	20.500000	62.098628	4.918501	20.666667	1.855622

Table D-14 Dynamic Modulus Summary Sheet for the Mix 14

Conditions		Specimen 1		Specimen 2		Specimen 3		Modulus		Phase Angle (Degrees)	
Temperature, °F	Frequency, Hz	Modulus, ksi	Phage Angle, degree	Modulus, ksi	Phage Angle, degree	Modulus, ksi	Phage Angle, degree	Avg. Modulus, ksi	CV, %	Avg. P. Angle, degree	Standard Dev, degree
14.000000	25.000000	6942.386783	5.300000	8157.083692	6.600000	9519.762590	16.400000	8206.411022	15.712054	9.433333	6.068223
14.000000	10.000000	7659.967694	6.000000	7259.696265	6.200000	8832.967705	6.000000	7917.543888	10.327092	6.066667	0.115470
14.000000	5.000000	7569.728689	6.400000	7046.286030	6.000000	8620.719275	5.000000	7745.577998	10.351866	5.800000	0.721110
14.000000	1.000000	6946.922886	7.600000	6391.093292	5.800000	7698.412728	4.100000	7012.142969	9.356562	5.833333	1.750238
14.000000	0.500000	6843.769260	9.200000	6323.432969	4.200000	7445.786452	10.800000	6870.996227	8.174534	8.066667	3.442867
14.000000	0.100000	6046.070207	7.600000	5515.377907	8.900000	6775.908316	7.600000	6112.452143	10.353973	8.033333	0.750555
40.000000	25.000000	7333.914282	3.200000	5795.720687	2.600000	5887.718719	13.700000	6339.117896	13.609876	6.500000	6.242596
40.000000	10.000000	5782.736001	10.100000	5291.417859	9.300000	5770.854370	9.900000	5615.002743	4.991907	9.766667	0.416333
40.000000	5.000000	5355.226048	10.100000	4912.102153	10.200000	5458.622799	10.000000	5241.983667	5.538472	10.100000	0.100000
40.000000	1.000000	4387.640575	14.900000	4134.652369	13.600000	4692.002508	10.000000	4404.765151	6.335625	12.833333	2.538372
40.000000	0.500000	4432.938215	12.000000	4036.006849	13.100000	4147.709441	16.600000	4205.551502	4.867133	13.900000	2.402082
40.000000	0.100000	3208.052118	16.600000	3031.401726	15.700000	3372.166503	15.800000	3203.873449	5.319212	16.033333	0.493288
70.000000	25.000000	2884.655670	14.500000	2462.769644	15.400000	3214.796942	15.800000	2854.074085	13.207268	15.233333	0.665833
70.000000	10.000000	2488.949357	18.500000	2103.234656	19.000000	2778.296889	17.500000	2456.826967	13.785080	18.333333	0.763763
70.000000	5.000000	2206.539292	19.500000	1861.552617	20.300000	2459.697512	18.800000	2175.929807	13.798467	19.533333	0.750555
70.000000	1.000000	1600.329650	23.900000	1320.719726	24.200000	1848.228050	21.800000	1589.759142	16.600815	23.300000	1.307670
70.000000	0.500000	1406.200537	25.000000	1197.116354	25.100000	1575.052226	21.600000	1392.789706	13.593187	23.900000	1.992486
70.000000	0.100000	984.637855	26.600000	781.316424	27.300000	1124.497651	25.100000	963.483977	17.910604	26.333333	1.123981
100.000000	25.000000	1312.407356	25.500000	1114.482974	28.100000	1237.994376	12.900000	1221.628235	8.183505	22.166667	8.129781
100.000000	10.000000	1031.140238	24.700000	851.992451	26.100000	1087.553724	26.500000	990.228804	12.420792	25.766667	0.945163
100.000000	5.000000	869.602599	25.800000	700.204459	26.900000	934.291607	27.300000	834.699555	14.482299	26.666667	0.776745
100.000000	1.000000	541.354391	27.100000	425.371877	28.500000	556.491659	29.700000	507.739309	14.127859	28.433333	1.301281
100.000000	0.500000	434.342974	28.200000	350.365155	28.500000	456.664896	27.200000	413.791008	13.545687	27.966667	0.680686
100.000000	0.100000	349.314758	24.300000	246.221623	25.800000	323.724869	26.800000	306.420417	17.518686	25.633333	1.258306
130.000000	25.000000	450.758823	31.500000	451.955008	28.000000	458.686776	26.500000	453.800202	0.941814	28.666667	2.565801
130.000000	10.000000	343.380543	27.900000	363.843924	27.200000	382.255542	28.800000	363.160003	5.354808	27.966667	0.802081
130.000000	5.000000	282.458081	27.300000	297.001608	26.300000	310.825190	28.000000	296.761626	4.779957	27.200000	0.854400
130.000000	1.000000	178.223304	27.000000	190.734506	25.000000	206.768260	26.000000	191.908690	7.455971	26.000000	1.000000
130.000000	0.500000	145.331117	24.400000	156.688637	23.400000	169.978099	25.000000	157.332618	7.840780	24.266667	0.808290
130.000000	0.100000	108.452177	22.100000	119.329976	19.700000	129.483913	21.100000	119.088689	8.832026	20.966667	1.205543

Table D-15 Dynamic Modulus Summary Sheet for the Mix 15

Conditions		Specimen 1		Specimen 2		Specimen 3		Modulus		Phase Angle (Degrees)	
Temperature, °F	Frequency, Hz	Modulus, ksi	Phage Angle, degree	Modulus, ksi	Phage Angle, degree	Modulus, ksi	Phage Angle, degree	Avg. Modulus, ksi	CV, %	Avg. P. Angle, degree	Standard Dev, degree
14.000000	25.000000	4134.493525	7.500000	5490.498534	11.100000	4829.002977	12.000000	4817.998345	14.073676	10.200000	2.381176
14.000000	10.000000	4105.259958	11.200000	4365.488232	11.600000	4659.162542	12.400000	4376.636911	6.331792	11.733333	0.611010
14.000000	5.000000	3816.292779	11.100000	4068.611088	11.800000	4294.346700	12.800000	4059.750189	5.890759	11.900000	0.854400
14.000000	1.000000	3234.507014	12.400000	3430.703993	12.500000	3533.525426	14.000000	3399.578811	4.468779	12.966667	0.896289
14.000000	0.500000	3006.585746	14.800000	3186.224715	13.900000	3259.645033	14.400000	3150.818498	4.132005	14.366667	0.450925
14.000000	0.100000	2476.414220	14.700000	2579.387098	14.800000	2653.671843	16.600000	2569.824387	3.463851	15.366667	1.069268
40.000000	25.000000	2505.093213	13.600000	2506.775067	11.000000	2654.255720	17.800000	2555.374667	3.351275	14.133333	3.431229
40.000000	10.000000	2210.019630	16.100000	2289.851274	16.500000	2373.445258	17.900000	2291.105387	3.566839	16.833333	0.945163
40.000000	5.000000	1957.729609	16.800000	2024.604709	17.300000	2106.614756	18.500000	2029.649691	3.674066	17.533333	0.873689
40.000000	1.000000	1515.281415	18.600000	1563.828743	18.700000	1612.327186	20.700000	1563.812448	3.102859	19.333333	1.184624
40.000000	0.500000	1342.708729	18.700000	1415.734767	19.700000	1442.191694	22.700000	1400.211730	3.679879	20.366667	2.081666
40.000000	0.100000	1045.017929	21.500000	1112.254525	19.900000	1091.416737	22.900000	1082.896397	3.178380	21.433333	1.501111
70.000000	25.000000	1110.296181	20.700000	1116.731297	21.400000	985.876689	26.300000	1070.968056	6.887367	22.800000	3.051229
70.000000	10.000000	923.097863	20.800000	988.018246	20.500000	813.471695	25.900000	908.195935	9.714017	22.400000	3.034798
70.000000	5.000000	804.410803	21.300000	875.914411	20.500000	717.853774	26.500000	799.392996	9.901225	22.766667	3.257811
70.000000	1.000000	555.523367	23.400000	590.705076	22.300000	489.249696	28.400000	545.159380	9.449641	24.700000	3.251154
70.000000	0.500000	466.043474	22.600000	506.964869	23.000000	407.049182	29.500000	460.019175	10.919007	25.033333	3.873414
70.000000	0.100000	366.427631	22.700000	385.145476	21.900000	324.842286	28.600000	358.805131	8.602376	24.400000	3.659235
100.000000	25.000000	448.863872	23.200000	399.260198	23.200000	332.062189	23.900000	393.395420	14.901364	23.433333	0.404145
100.000000	10.000000	381.861407	22.500000	351.720474	22.800000	285.058325	22.900000	339.546735	14.588991	22.733333	0.208167
100.000000	5.000000	329.903370	22.200000	303.934288	22.700000	245.401440	22.900000	293.079699	14.768702	22.600000	0.360555
100.000000	1.000000	233.248542	23.200000	207.316887	23.900000	170.360049	24.000000	203.641826	15.519851	23.700000	0.435890
100.000000	0.500000	204.485557	23.200000	181.040272	23.200000	148.039288	24.000000	177.855039	15.944232	23.466667	0.461880
100.000000	0.100000	166.000922	21.500000	149.191664	21.800000	120.175110	22.600000	145.122565	15.974296	21.966667	0.568624
130.000000	25.000000	246.196672	21.400000	211.161622	20.000000	172.160564	20.900000	209.839619	17.649553	20.766667	0.709460
130.000000	10.000000	215.928520	19.300000	190.410002	19.700000	154.334128	20.900000	186.890883	16.559194	19.966667	0.832666
130.000000	5.000000	196.566453	18.100000	170.805971	19.400000	136.662909	20.500000	168.011778	17.885272	19.333333	1.201388
130.000000	1.000000	153.365836	17.900000	132.311326	19.400000	106.828928	20.100000	130.835363	17.811344	19.133333	1.123981
130.000000	0.500000	135.248550	16.600000	120.328151	20.000000	92.006881	18.900000	115.861194	18.957333	18.500000	1.734935
130.000000	0.100000	116.079852	15.900000	102.597166	19.200000	79.755921	17.400000	99.477646	18.458213	17.500000	1.652271

Table D-16 Dynamic Modulus Summary Sheet for the Mix 16

Conditions		Specimen 1		Specimen 2		Specimen 3		Modulus		Phase Angle (Degrees)	
Temperature, °F	Frequency, Hz	Modulus, ksi	Phage Angle, degree	Modulus, ksi	Phage Angle, degree	Modulus, ksi	Phage Angle, degree	Avg. Modulus, ksi	CV, %	Avg. P. Angle, degree	Standard Dev, degree
14.000000	25.000000	9043.595062	8.100000	8312.672321	14.200000	8527.782398	24.500000	8628.016594	4.353597	15.600000	8.289150
14.000000	10.000000	8217.331179	6.800000	7813.395617	6.500000	7868.913777	7.200000	7966.546858	2.748398	6.833333	0.351188
14.000000	5.000000	7904.964120	6.300000	7600.712580	6.200000	7640.095298	7.700000	7715.257333	2.144669	6.733333	0.838650
14.000000	1.000000	7376.191576	6.000000	6844.859985	8.000000	7397.314556	7.300000	7206.122039	4.344089	7.100000	1.014889
14.000000	0.500000	6815.440157	6.000000	6514.126713	5.200000	7222.221409	5.500000	6850.596093	5.187199	5.566667	0.404145
14.000000	0.100000	6427.503390	9.100000	6009.954151	6.900000	6146.080620	7.600000	6194.512720	3.437659	7.866667	1.123981
40.000000	25.000000	5567.904153	13.400000	6742.347390	1.700000	6171.928284	4.800000	6160.726609	9.532995	6.633333	6.061628
40.000000	10.000000	5488.479555	11.000000	5238.568123	8.800000	4975.474140	11.400000	5234.173939	4.901078	10.400000	1.400000
40.000000	5.000000	5359.116188	10.400000	4984.155258	8.200000	4665.680489	10.600000	5002.983978	6.937881	9.733333	1.331666
40.000000	1.000000	4478.402241	11.900000	4255.095989	9.500000	3874.349678	12.800000	4202.615969	7.267538	11.400000	1.705872
40.000000	0.500000	4118.403197	10.300000	4184.650757	10.500000	3449.263139	11.600000	3917.439031	10.384412	10.800000	0.700000
40.000000	0.100000	3553.118287	13.800000	3320.708641	13.600000	2873.900739	16.200000	3249.242556	10.624087	14.533333	1.446836
70.000000	25.000000	2953.532632	18.100000	3295.734107	11.500000	2557.213140	20.300000	2935.493293	12.590416	16.633333	4.579665
70.000000	10.000000	2680.753989	17.300000	2598.491389	16.000000	1840.008376	22.000000	2373.084585	19.530960	18.433333	3.156475
70.000000	5.000000	2378.172409	17.600000	2327.659629	16.600000	1603.468221	23.000000	2103.100086	20.609118	19.066667	3.442867
70.000000	1.000000	1823.764281	20.000000	1709.948710	18.700000	1123.944238	26.200000	1552.552410	24.187434	21.633333	4.007909
70.000000	0.500000	1598.804608	21.900000	1491.074697	19.900000	979.028000	25.800000	1356.302435	24.414879	22.533333	3.000556
70.000000	0.100000	1221.282165	22.600000	1126.783546	23.100000	728.352379	27.400000	1025.472697	25.511734	24.366667	2.638813
100.000000	25.000000	1468.367345	21.800000	1432.711282	12.700000	929.526596	20.300000	1276.868408	23.599509	18.266667	4.878866
100.000000	10.000000	1209.782193	22.100000	1174.549568	21.400000	793.425078	25.100000	1059.252280	21.797087	22.866667	1.965536
100.000000	5.000000	1049.556788	21.200000	1023.174423	22.100000	666.912044	25.700000	913.214418	23.402128	23.000000	2.381176
100.000000	1.000000	705.062601	25.200000	681.193733	23.900000	427.909309	27.200000	604.721881	25.398214	25.433333	1.662328
100.000000	0.500000	596.669319	22.000000	561.496169	24.900000	349.036093	27.100000	502.400527	26.667323	24.666667	2.557994
100.000000	0.100000	425.543195	23.500000	394.617039	22.800000	253.630543	25.300000	357.930259	25.602814	23.866667	1.289703
130.000000	25.000000	560.640736	18.900000	649.295078	19.500000	427.500523	27.200000	545.812112	20.453624	21.866667	4.628535
130.000000	10.000000	492.096837	23.000000	525.178331	22.600000	357.370947	24.700000	458.215372	19.398392	23.433333	1.115049
130.000000	5.000000	421.622157	24.000000	443.481474	22.200000	309.842827	23.900000	391.648819	18.303180	23.366667	1.011599
130.000000	1.000000	269.226353	23.700000	299.543683	23.400000	210.088740	22.600000	259.619592	17.523585	23.233333	0.568624
130.000000	0.500000	210.690749	25.400000	245.143374	24.300000	173.509935	23.500000	209.781353	17.077484	24.400000	0.953939
130.000000	0.100000	156.297984	22.900000	190.978792	19.200000	139.586063	19.800000	162.287613	16.153228	20.633333	1.985783

Table D-17 Dynamic Modulus Summary Sheet for the Mix 17

Conditions		Specimen 1		Specimen 2		Specimen 3		Modulus		Phase Angle (Degrees)	
Temperature, °F	Frequency, Hz	Modulus, ksi	Phage Angle, degree	Modulus, ksi	Phage Angle, degree	Modulus, ksi	Phage Angle, degree	Avg. Modulus, ksi	CV, %	Avg. P. Angle, degree	Standard Dev, degree
14.000000	25.000000	8493.438860	38.800000	8804.283344	10.900000	8423.902299	19.900000	8573.874834	2.362363	23.200000	14.239733
14.000000	10.000000	9633.124261	4.700000	7656.816647	3.400000	9542.945312	3.900000	8944.295407	12.476116	4.000000	0.655744
14.000000	5.000000	9680.173239	3.900000	7552.717214	3.700000	9372.603976	2.200000	8868.498143	12.965331	3.266667	0.929157
14.000000	1.000000	9701.035107	4.300000	7122.392325	5.800000	8950.501807	1.200000	8591.309746	15.437878	3.766667	2.345918
14.000000	0.500000	9723.564033	4.800000	7151.993045	7.400000	8416.984125	5.400000	8430.847068	15.251629	5.866667	1.361372
14.000000	0.100000	8644.761637	7.000000	6430.793987	4.200000	8194.970526	4.500000	7756.842050	15.086105	5.233333	1.537314
40.000000	25.000000	8963.827680	26.200000	8330.447549	15.800000	7306.742923	24.100000	8200.339384	10.196761	22.033333	5.499394
40.000000	10.000000	6839.587400	7.800000	5976.279352	6.600000	7839.638287	6.100000	6885.168346	13.543828	6.833333	0.873689
40.000000	5.000000	6407.845250	8.700000	5958.931912	7.200000	7444.861679	6.400000	6603.879614	11.540410	7.433333	1.167619
40.000000	1.000000	5729.670267	10.700000	5203.604153	8.300000	6557.856807	6.300000	5830.377076	11.709704	8.433333	2.203028
40.000000	0.500000	5492.745261	14.900000	4707.750924	8.600000	6041.596481	5.300000	5414.030889	12.382597	9.600000	4.877499
40.000000	0.100000	4648.618387	11.700000	4296.071493	10.000000	5621.847515	8.900000	4855.512465	14.142201	10.200000	1.410674
70.000000	25.000000	3768.741740	8.800000	3689.726653	1.700000	4323.415767	8.100000	3927.294720	8.792779	6.200000	3.912800
70.000000	10.000000	3279.540059	14.900000	2796.732297	14.200000	4482.983893	12.400000	3519.752083	24.672502	13.833333	1.289703
70.000000	5.000000	2985.110409	15.700000	2518.053964	15.400000	4045.528314	13.800000	3182.897562	24.591102	14.966667	1.021437
70.000000	1.000000	2319.547881	19.300000	1970.753027	19.000000	3245.564835	18.600000	2511.955248	26.227618	18.966667	0.351188
70.000000	0.500000	2046.066265	19.200000	1745.352219	18.600000	2964.131476	15.800000	2251.849987	28.195222	17.866667	1.814754
70.000000	0.100000	1567.664920	24.900000	1276.100108	24.100000	2173.433427	22.400000	1672.399485	27.370442	23.800000	1.276715
100.000000	25.000000	1629.361871	24.600000	1446.834708	15.500000	2722.695173	18.900000	1932.963917	35.695937	19.666667	4.598188
100.000000	10.000000	1419.810442	23.900000	1261.693085	23.900000	2260.135954	20.000000	1647.213160	32.579993	22.600000	2.251666
100.000000	5.000000	1201.776631	24.600000	1052.643862	25.600000	1922.783917	20.800000	1392.401470	33.419803	23.666667	2.532456
100.000000	1.000000	771.581428	28.700000	629.839011	29.000000	1304.291112	25.400000	901.903850	39.428953	27.700000	1.997498
100.000000	0.500000	620.567199	29.900000	481.941739	30.000000	1006.867372	27.400000	703.125437	38.688244	29.100000	1.473092
100.000000	0.100000	371.697896	29.600000	287.515393	29.000000	620.383985	29.100000	426.532425	40.577585	29.233333	0.321455
130.000000	25.000000	812.244901	33.500000	573.404637	22.200000	941.069361	31.600000	775.572966	24.053896	29.100000	6.050620
130.000000	10.000000	577.876332	31.900000	439.927154	32.100000	662.561766	30.400000	560.121751	20.062460	31.466667	0.929157
130.000000	5.000000	446.246075	31.400000	333.105914	32.000000	514.876285	30.100000	431.409425	21.276529	31.166667	0.971253
130.000000	1.000000	256.304770	30.100000	177.791599	31.300000	295.777716	29.600000	243.291362	24.686412	30.333333	0.873689
130.000000	0.500000	203.024633	28.500000	131.984355	31.100000	246.588341	28.500000	193.865776	29.839384	29.366667	1.501111
130.000000	0.100000	141.584588	22.900000	90.505195	25.100000	178.465269	25.200000	136.851684	32.276273	24.400000	1.300000

Table D-18 Dynamic Modulus Summary Sheet for the Mix 18

Conditions		Specimen 1		Specimen 2		Specimen 3		Modulus		Phase Angle (Degrees)	
Temperature, °F	Frequency, Hz	Modulus, ksi	Phage Angle, degree	Modulus, ksi	Phage Angle, degree	Modulus, ksi	Phage Angle, degree	Avg. Modulus, ksi	CV, %	Avg. P. Angle, degree	Standard Dev, degree
14.000000	25.000000	4240.558265	22.200000	7291.111862	2.500000	6624.918748	6.300000	6052.196292	26.501032	10.333333	10.450997
14.000000	10.000000	4119.594595	6.200000	7174.536622	5.800000	7203.525324	5.800000	6165.885514	28.742006	5.933333	0.230940
14.000000	5.000000	3972.711745	6.000000	6935.111030	5.700000	6994.838758	5.000000	5967.553844	28.953941	5.566667	0.513160
14.000000	1.000000	3542.419350	8.300000	6110.771981	7.200000	6378.962444	6.800000	5344.051258	29.303812	7.433333	0.776745
14.000000	0.500000	3490.449273	5.000000	6209.155518	3.200000	6397.900493	8.800000	5365.835095	30.319070	5.666667	2.858904
14.000000	0.100000	3198.344248	9.000000	5561.183119	8.300000	5662.765284	5.700000	4807.430884	29.005830	7.666667	1.738774
40.000000	25.000000	3661.315589	3.600000	5429.357608	0.600000	5228.155394	7.900000	4772.942864	20.279722	4.033333	3.669242
40.000000	10.000000	3129.784393	9.300000	5450.612015	8.400000	5283.708659	8.100000	4621.368356	28.009939	8.600000	0.624500
40.000000	5.000000	2992.473054	9.600000	5108.455074	9.200000	4955.086046	8.000000	4352.004725	27.111266	8.933333	0.832666
40.000000	1.000000	2610.470356	9.900000	4483.596492	10.900000	4165.948579	11.400000	3753.338476	26.707289	10.733333	0.763763
40.000000	0.500000	2327.415634	12.500000	4194.631490	14.800000	3769.284274	10.100000	3430.443799	28.528045	12.466667	2.350177
40.000000	0.100000	1991.074972	14.500000	3325.242133	15.100000	3207.156503	14.600000	2841.157869	25.994937	14.733333	0.321455
70.000000	25.000000	1992.884191	7.800000	2611.297938	16.300000	3069.575783	15.400000	2557.919304	21.123688	13.166667	4.669404
70.000000	10.000000	1829.850522	15.900000	2177.349968	20.700000	2690.691348	17.100000	2232.630613	19.397508	17.900000	2.497999
70.000000	5.000000	1686.466724	16.600000	1954.577837	21.500000	2385.124962	18.100000	2008.723174	17.546580	18.733333	2.510644
70.000000	1.000000	1221.153349	19.400000	1368.112357	26.500000	1681.757851	21.400000	1423.674519	16.525923	22.433333	3.661056
70.000000	0.500000	1066.266098	23.200000	1218.555716	27.400000	1438.058719	22.600000	1240.960178	15.061414	24.400000	2.615339
70.000000	0.100000	743.823436	25.600000	883.315788	30.200000	979.646256	27.100000	868.928493	13.645300	27.633333	2.345918
100.000000	25.000000	802.062387	23.600000	1243.821680	33.600000	1504.286116	12.300000	1183.390061	29.997791	23.166667	10.656610
100.000000	10.000000	640.669374	26.300000	1008.271432	27.100000	1190.049782	24.600000	946.330196	29.575193	26.000000	1.276715
100.000000	5.000000	507.034064	27.400000	786.865644	28.200000	865.695921	27.600000	719.865210	26.183293	27.733333	0.416333
100.000000	1.000000	311.041043	29.000000	457.873411	33.900000	525.198930	29.700000	431.371128	25.386745	30.866667	2.650157
100.000000	0.500000	251.961890	29.600000	364.042950	34.300000	430.281951	29.400000	348.762264	25.844757	31.100000	2.773085
100.000000	0.100000	164.036631	27.500000	231.777609	30.800000	308.518987	24.400000	234.777742	30.789923	27.566667	3.200521
130.000000	25.000000	373.192474	30.500000	378.231219	34.300000	457.501036	37.900000	402.974910	11.734768	34.233333	3.700450
130.000000	10.000000	268.995994	32.500000	270.190439	30.900000	340.209768	32.600000	293.132067	13.910064	32.000000	0.953939
130.000000	5.000000	217.502447	31.800000	215.304026	28.600000	277.634174	31.100000	236.813549	14.935287	30.500000	1.682260
130.000000	1.000000	133.705666	30.400000	138.229149	25.600000	168.368486	29.100000	146.767767	12.838652	28.366667	2.482606
130.000000	0.500000	104.232455	29.400000	113.263754	24.300000	140.415240	27.400000	119.303816	15.785267	27.033333	2.569695
130.000000	0.100000	87.985605	23.400000	85.039386	20.200000	100.864975	23.700000	91.296655	9.218662	22.433333	1.939931

Table D-19 Dynamic Modulus Summary Sheet for the Mix 19

Conditions		Specimen 1		Specimen 2		Specimen 3		Modulus		Phase Angle (Degrees)	
Temperature, °F	Frequency, Hz	Modulus, ksi	Phage Angle, degree	Modulus, ksi	Phage Angle, degree	Modulus, ksi	Phage Angle, degree	Avg. Modulus, ksi	CV, %	Avg. P. Angle, degree	Standard Dev, degree
14.000000	25.000000	7689.237527	5.100000	4846.059712	0.300000	6134.050009	13.900000	6223.115749	22.877285	6.433333	6.897342
14.000000	10.000000	6449.842573	7.100000	5220.346392	6.200000	6985.146845	5.200000	6218.445270	14.551377	6.166667	0.950438
14.000000	5.000000	6252.963221	6.800000	5053.535296	5.800000	6760.564624	5.400000	6022.354380	14.555249	6.000000	0.721110
14.000000	1.000000	5783.822228	6.700000	4530.090462	6.500000	6321.266171	6.700000	5545.059620	16.575983	6.633333	0.115470
14.000000	0.500000	5295.939166	9.100000	4499.886571	4.500000	5803.660680	4.800000	5199.828806	12.638480	6.133333	2.573584
14.000000	0.100000	4981.370639	9.300000	4010.249413	8.100000	5363.776900	9.300000	4785.132317	14.582166	8.900000	0.692820
40.000000	25.000000	4675.792648	1.800000	3658.247518	7.100000	4713.120991	18.700000	4349.053719	13.762690	9.200000	8.643495
40.000000	10.000000	4396.136013	11.000000	3752.987957	10.000000	4950.956263	10.600000	4366.693411	13.729533	10.533333	0.503322
40.000000	5.000000	4004.589801	11.500000	3480.162023	10.800000	4789.454163	9.800000	4091.401996	16.105701	10.700000	0.854400
40.000000	1.000000	3332.254452	15.100000	2937.404588	12.700000	3850.802849	13.600000	3373.487296	13.579213	13.800000	1.212436
40.000000	0.500000	3204.071024	15.800000	2710.590436	11.300000	3703.516290	18.000000	3206.059250	15.485238	15.033333	3.415162
40.000000	0.100000	2454.480920	19.200000	2133.204995	16.400000	2746.146841	18.100000	2444.610919	12.541468	17.900000	1.410674
70.000000	25.000000	2056.306224	24.100000	2001.877338	18.700000	2596.173000	20.400000	2218.118854	14.811362	21.066667	2.761038
70.000000	10.000000	1810.238368	24.600000	1721.046568	20.100000	2310.616966	20.200000	1947.300634	16.319302	21.633333	2.569695
70.000000	5.000000	1679.174434	26.000000	1514.145866	21.700000	1996.518151	21.800000	1729.946150	14.171617	23.166667	2.454248
70.000000	1.000000	1225.523646	30.900000	1063.692980	25.300000	1324.948151	26.800000	1204.721592	10.945598	27.666667	2.898850
70.000000	0.500000	1102.559420	29.400000	909.437476	28.600000	1072.195091	28.800000	1028.063996	10.101448	28.933333	0.416333
70.000000	0.100000	632.889239	33.800000	586.404989	29.400000	688.983152	29.400000	636.092460	8.074934	30.866667	2.540341
100.000000	25.000000	1096.520905	31.300000	900.465507	29.700000	856.118463	35.100000	951.034958	13.451744	32.033333	2.773686
100.000000	10.000000	761.190023	32.600000	677.175938	29.900000	611.834584	33.500000	683.400182	10.955808	32.000000	1.873499
100.000000	5.000000	584.662934	33.000000	518.735237	30.200000	470.349363	33.700000	524.582511	10.938349	32.300000	1.852026
100.000000	1.000000	366.472311	30.800000	285.871546	34.300000	250.040683	33.600000	300.794847	19.825182	32.900000	1.852026
100.000000	0.500000	306.120089	29.200000	226.904526	33.100000	196.499869	32.000000	243.174828	23.272275	31.433333	2.010804
100.000000	0.100000	218.479878	23.600000	155.542208	24.500000	124.378585	27.300000	166.133557	28.854118	25.133333	1.929594
130.000000	25.000000	330.545126	34.700000	217.802436	38.700000	248.375946	34.500000	265.574503	21.954609	35.966667	2.369247
130.000000	10.000000	243.272793	32.200000	152.963868	34.500000	183.247978	29.200000	193.161546	23.795318	31.966667	2.657693
130.000000	5.000000	209.562018	30.500000	105.215834	32.100000	146.245010	26.900000	153.674287	34.207616	29.833333	2.663331
130.000000	1.000000	168.656870	23.700000	68.496608	26.900000	94.348335	22.500000	110.500604	47.055881	24.366667	2.274496
130.000000	0.500000	142.943244	21.800000	62.023631	23.000000	76.192317	21.500000	93.719731	46.109251	22.100000	0.793725
130.000000	0.100000	106.995605	18.100000	42.156312	18.000000	58.843282	17.200000	69.331733	48.560842	17.766667	0.493288

Table D-20 Dynamic Modulus Summary Sheet for the Mix 20

Conditions		Specimen 1		Specimen 2		Specimen 3		Modulus		Phase Angle (Degrees)	
Temperature, °F	Frequency, Hz	Modulus, ksi	Phage Angle, degree	Modulus, ksi	Phage Angle, degree	Modulus, ksi	Phage Angle, degree	Avg. Modulus, ksi	CV, %	Avg. P. Angle, degree	Standard Dev, degree
14.000000	25.000000	8029.655459	16.800000	6555.306899	3.000000	5690.769157	12.000000	6758.577172	17.498039	10.600000	7.005712
14.000000	10.000000	7623.793903	8.200000	7333.659988	7.600000	5809.473913	7.100000	6922.309268	14.079125	7.633333	0.550757
14.000000	5.000000	7311.001811	6.800000	6983.171384	7.300000	5538.006490	6.900000	6610.726562	14.270032	7.000000	0.264575
14.000000	1.000000	6668.638107	5.500000	5969.715275	7.100000	5007.711951	6.100000	5882.021778	14.177581	6.233333	0.808290
14.000000	0.500000	5818.258171	13.800000	6081.583819	11.000000	4570.228229	8.400000	5490.023406	14.706200	11.066667	2.700617
14.000000	0.100000	5427.194146	8.000000	5156.234442	10.600000	4099.662288	10.300000	4894.363625	14.331578	9.633333	1.422439
40.000000	25.000000	5571.912664	15.900000	6650.924530	5.500000	3829.110934	10.900000	5350.649376	26.610968	10.766667	5.201282
40.000000	10.000000	4602.048840	12.700000	5917.679195	12.800000	3369.810543	13.000000	4629.846193	27.520607	12.833333	0.152753
40.000000	5.000000	4191.812491	14.400000	5431.881405	12.900000	3077.209405	13.600000	4233.634434	27.822265	13.633333	0.750555
40.000000	1.000000	3314.995066	14.800000	4235.704910	17.800000	2418.622205	16.100000	3323.107394	27.340931	16.233333	1.504438
40.000000	0.500000	2841.466514	17.800000	3822.802748	16.100000	2189.176476	17.700000	2951.148579	27.864326	17.200000	0.953939
40.000000	0.100000	2139.868440	21.200000	2624.598425	22.600000	1541.281250	22.000000	2101.916038	25.817153	21.933333	0.702377
70.000000	25.000000	2209.825827	21.700000	2832.579697	18.900000	1741.603660	20.700000	2261.336395	24.202902	20.433333	1.418920
70.000000	10.000000	1809.896020	22.600000	2155.649205	22.900000	1429.942330	21.900000	1798.495852	20.182850	22.466667	0.513160
70.000000	5.000000	1532.554437	23.900000	1787.071022	24.600000	1250.212552	23.500000	1523.279337	17.629688	24.000000	0.556776
70.000000	1.000000	983.535526	27.900000	1151.973932	28.400000	761.018850	29.500000	965.509436	20.310512	28.600000	0.818535
70.000000	0.500000	807.237490	28.800000	964.602844	31.200000	609.983152	31.400000	793.941162	22.379915	30.466667	1.446836
70.000000	0.100000	496.957300	31.000000	550.253683	32.100000	365.285555	31.000000	470.832179	20.221921	31.366667	0.635085
100.000000	25.000000	624.522037	31.900000	582.156400	33.200000	594.325110	32.400000	600.334516	3.633434	32.500000	0.655744
100.000000	10.000000	441.973840	31.100000	410.781784	32.100000	416.869331	32.000000	423.208318	3.906823	31.733333	0.550757
100.000000	5.000000	338.768572	31.300000	320.180123	31.900000	330.452866	32.100000	329.800520	2.823337	31.766667	0.416333
100.000000	1.000000	198.372335	30.600000	189.622748	30.100000	191.778231	31.700000	193.257771	2.358805	30.800000	0.818535
100.000000	0.500000	157.320674	29.500000	153.682653	28.700000	151.068337	30.700000	154.023888	2.038713	29.633333	1.006645
100.000000	0.100000	99.598435	25.300000	104.207795	24.000000	95.913994	26.300000	99.906741	4.159366	25.200000	1.153256
130.000000	25.000000	181.320098	35.200000	217.275424	28.700000	165.296353	34.500000	187.963958	14.161662	32.800000	3.567913
130.000000	10.000000	129.861511	31.700000	162.509994	29.200000	119.846834	31.500000	137.406113	16.236394	30.800000	1.389244
130.000000	5.000000	103.207444	29.400000	135.352125	26.100000	94.900297	28.800000	111.153289	19.220713	28.100000	1.757840
130.000000	1.000000	66.026630	24.800000	94.072571	21.100000	60.453475	23.400000	73.517559	24.508359	23.100000	1.868154
130.000000	0.500000	55.955233	23.200000	77.824270	19.300000	50.252538	21.200000	61.344014	23.725799	21.233333	1.950214
130.000000	0.100000	43.078329	19.000000	62.384111	15.700000	38.506250	15.900000	47.989563	26.409741	16.866667	1.850225

Table D-21 Dynamic Modulus Summary Sheet for the Mix 21

Conditions		Specimen 1		Specimen 2		Specimen 3		Modulus		Phase Angle (Degrees)	
Temperature, °F	Frequency, Hz	Modulus, ksi	Phage Angle, degree	Modulus, ksi	Phage Angle, degree	Modulus, ksi	Phage Angle, degree	Avg. Modulus, ksi	CV, %	Avg. P. Angle, degree	Standard Dev, degree
14.000000	25.000000	7699.385082	5.600000	5086.307517	3.000000	5986.111250	7.600000	6257.267950	21.214919	5.400000	2.306513
14.000000	10.000000	7838.039843	6.200000	6512.610375	7.700000	6404.116130	6.000000	6918.255449	11.540506	6.633333	0.929157
14.000000	5.000000	7793.364522	5.900000	6336.283472	5.500000	6269.718516	5.900000	6799.788837	12.663705	5.766667	0.230940
14.000000	1.000000	6956.473654	6.600000	5843.534724	4.200000	6177.348398	6.600000	6325.785592	9.028519	5.800000	1.385641
14.000000	0.500000	6642.760850	4.800000	5473.342142	8.900000	5441.758708	7.500000	5852.620567	11.694996	7.066667	2.084067
14.000000	0.100000	6104.282177	8.200000	5087.002222	7.700000	5256.373379	6.800000	5482.552593	9.941586	7.566667	0.709460
40.000000	25.000000	5574.080623	11.500000	3915.443262	9.400000	4611.533314	8.500000	4700.352400	17.719484	9.800000	1.539480
40.000000	10.000000	5057.929674	10.200000	4191.732851	10.200000	4879.856944	8.800000	4709.839823	9.712484	9.733333	0.808290
40.000000	5.000000	4662.041162	11.000000	3972.512865	10.100000	4664.898167	8.400000	4433.150731	8.998716	9.833333	1.320353
40.000000	1.000000	3847.223578	13.400000	3410.623576	11.900000	4092.316035	8.900000	3783.387730	9.126753	11.400000	2.291288
40.000000	0.500000	3437.181612	13.200000	3200.753300	11.700000	3638.423718	7.400000	3425.452877	6.395382	10.766667	3.010537
40.000000	0.100000	2788.423264	18.100000	2530.775797	15.600000	3268.653267	13.200000	2862.617443	13.082159	15.633333	2.450170
70.000000	25.000000	2868.670222	16.300000	2340.573379	13.900000	3344.627845	17.700000	2851.290482	17.614930	15.966667	1.921805
70.000000	10.000000	2489.213226	18.600000	2058.373364	16.800000	2776.050742	14.300000	2441.212444	14.797504	16.566667	2.159475
70.000000	5.000000	2165.580761	19.900000	1877.380818	17.500000	2528.783219	14.900000	2190.581599	14.901068	17.433333	2.500667
70.000000	1.000000	1507.422946	24.900000	1330.566710	21.900000	2077.298503	16.100000	1638.429386	23.816904	20.966667	4.473626
70.000000	0.500000	1267.925839	25.700000	1229.992875	24.100000	1799.743679	21.600000	1432.554131	22.237246	23.800000	2.066398
70.000000	0.100000	815.178790	28.900000	817.142500	26.100000	1318.710175	22.000000	983.677155	29.496341	25.666667	3.470351
100.000000	25.000000	1141.462271	27.100000	1035.970818	23.900000	1758.493137	20.700000	1311.975409	29.747235	23.900000	3.200000
100.000000	10.000000	857.750850	27.300000	901.941663	27.200000	1285.836556	21.200000	1015.176356	23.191804	25.233333	3.493327
100.000000	5.000000	665.736023	28.300000	746.542921	26.000000	1125.843106	22.500000	846.040683	29.036585	25.600000	2.920616
100.000000	1.000000	371.248492	31.600000	465.422897	29.600000	757.682558	26.500000	531.451316	37.915224	29.233333	2.569695
100.000000	0.500000	293.005862	30.800000	379.819218	29.800000	613.161035	27.300000	428.662038	38.625274	29.300000	1.802776
100.000000	0.100000	181.568010	26.900000	240.805136	28.900000	407.426925	28.400000	276.600024	42.337981	28.066667	1.040833
130.000000	25.000000	281.623391	35.400000	411.090477	29.500000	827.992592	27.600000	506.902153	56.324056	30.833333	4.067350
130.000000	10.000000	200.840718	33.200000	300.245640	27.300000	531.771565	29.300000	344.285974	49.320688	29.933333	3.000556
130.000000	5.000000	164.672295	30.400000	241.860610	28.100000	420.486028	30.000000	275.672978	47.598406	29.500000	1.228821
130.000000	1.000000	109.285126	26.600000	149.073438	25.500000	295.962235	28.600000	184.773600	53.214201	26.900000	1.571623
130.000000	0.500000	85.973589	25.300000	129.506688	22.100000	237.026984	28.100000	150.835754	51.547909	25.166667	3.002221
130.000000	0.100000	70.696916	19.200000	96.166402	19.200000	159.048658	24.700000	108.637325	41.861232	21.033333	3.175426

Table D-22 Dynamic Modulus Summary Sheet for the Mix 22

Conditions		Specimen 1		Specimen 2		Specimen 3		Modulus		Phase Angle (Degrees)	
Temperature, °F	Frequency, Hz	Modulus, ksi	Phage Angle, degree	Modulus, ksi	Phage Angle, degree	Modulus, ksi	Phage Angle, degree	Avg. Modulus, ksi	CV, %	Avg. P. Angle, degree	Standard Dev, degree
14.000000	25.000000	5831.046297	14.600000	7833.881773	2.900000	8377.507262	22.900000	7347.478444	18.252560	13.466667	10.048051
14.000000	10.000000	6808.771201	8.900000	6991.535251	8.100000	9171.298768	6.800000	7657.201740	17.165891	7.933333	1.059874
14.000000	5.000000	6636.817206	9.200000	7042.956992	7.800000	9469.129553	3.900000	7716.301250	19.847805	6.966667	2.746513
14.000000	1.000000	5880.343744	9.600000	6378.239453	6.400000	8024.351541	9.200000	6760.978246	16.596386	8.400000	1.743560
14.000000	0.500000	5587.425209	13.200000	5759.995139	11.300000	7480.114613	6.500000	6275.844987	16.674907	10.333333	3.453018
14.000000	0.100000	5006.475003	13.400000	5311.222366	9.600000	6821.870486	7.500000	5713.189285	17.016094	10.166667	2.990541
40.000000	25.000000	3946.341566	14.800000	4392.309991	10.500000	6507.649964	5.900000	4948.767174	27.649781	10.400000	4.450843
40.000000	10.000000	3720.627133	12.200000	4379.714218	15.300000	5343.468156	12.400000	4481.269836	18.212985	13.300000	1.734935
40.000000	5.000000	3471.871414	11.700000	3950.369515	16.400000	4897.922298	12.500000	4106.721076	17.672695	13.533333	2.514624
40.000000	1.000000	2764.011283	15.000000	3139.031544	20.000000	3822.870202	15.800000	3241.971010	16.560377	16.933333	2.685765
40.000000	0.500000	2422.608522	19.800000	2928.924381	20.800000	3301.409386	14.900000	2884.314096	15.292910	18.500000	3.157531
40.000000	0.100000	1815.428557	21.300000	2040.363135	23.200000	2491.345499	21.400000	2115.712397	16.268781	21.966667	1.069268
70.000000	25.000000	1772.579137	21.800000	2523.296666	20.600000	2027.705565	21.200000	2107.860456	18.109523	21.200000	0.600000
70.000000	10.000000	1612.503727	23.700000	2173.917936	20.700000	1619.891323	23.400000	1802.104329	17.869177	22.600000	1.652271
70.000000	5.000000	1390.325046	24.700000	1932.955117	20.900000	1357.752286	24.800000	1560.344150	20.707053	23.466667	2.223361
70.000000	1.000000	915.246502	28.700000	1476.683921	22.600000	848.055746	28.600000	1079.995390	31.961350	26.633333	3.493327
70.000000	0.500000	749.220920	29.200000	1360.422886	23.000000	660.181291	30.200000	923.275032	41.286706	27.466667	3.900427
70.000000	0.100000	479.912751	29.100000	1068.470322	24.500000	393.539950	30.100000	647.307674	56.740464	27.900000	2.986637
100.000000	25.000000	714.105214	34.000000	621.683309	29.700000	635.864325	33.200000	657.217616	7.573402	32.300000	2.286919
100.000000	10.000000	535.307608	31.900000	553.728364	28.600000	444.764262	30.800000	511.266745	11.407873	30.433333	1.680278
100.000000	5.000000	424.676882	31.500000	445.285036	29.500000	337.987846	30.400000	402.649921	14.141095	30.466667	1.001665
100.000000	1.000000	252.238379	30.500000	266.038316	30.000000	197.896095	29.000000	238.724263	15.090710	29.833333	0.763763
100.000000	0.500000	206.778995	28.600000	214.824594	29.000000	155.928220	27.800000	192.510603	16.589036	28.466667	0.611010
100.000000	0.100000	142.340654	22.900000	136.033628	26.300000	98.943333	23.400000	125.772538	18.643021	24.200000	1.835756
130.000000	25.000000	216.094471	32.300000	269.961675	30.900000	182.722852	31.700000	222.926333	19.745916	31.633333	0.702377
130.000000	10.000000	173.312795	26.200000	205.015326	29.000000	130.907121	28.100000	169.745081	21.905022	27.766667	1.429452
130.000000	5.000000	142.304098	23.300000	169.999713	27.000000	107.013738	25.800000	139.772516	22.586135	25.366667	1.887679
130.000000	1.000000	103.171469	18.300000	113.840668	24.500000	72.996156	22.000000	96.669431	21.914199	21.600000	3.119295
130.000000	0.500000	90.299931	17.400000	94.722596	23.000000	64.564255	19.800000	83.195594	19.575603	20.066667	2.809508
130.000000	0.100000	73.606724	14.800000	70.578690	19.300000	51.604665	15.400000	65.263360	18.272543	16.500000	2.443358

Table D-23 Dynamic Modulus Summary Sheet for the Mix 23

Conditions		Specimen 1		Specimen 2		Specimen 3		Modulus		Phase Angle (Degrees)	
Temperature, °F	Frequency, Hz	Modulus, ksi	Phage Angle, degree	Modulus, ksi	Phage Angle, degree	Modulus, ksi	Phage Angle, degree	Avg. Modulus, ksi	CV, %	Avg. P. Angle, degree	Standard Dev, degree
14.000000	25.000000	5497.892223	19.500000	5447.690892	5.700000	5195.651104	9.300000	5380.411406	3.010252	11.500000	7.158212
14.000000	10.000000	5238.453669	7.900000	5644.533398	7.500000	4857.340059	7.100000	5246.775709	7.502944	7.500000	0.400000
14.000000	5.000000	5057.556283	7.600000	5386.763063	8.200000	4675.287250	7.200000	5039.868865	7.065016	7.666667	0.503322
14.000000	1.000000	4423.859916	8.700000	5074.513214	9.300000	4225.805558	11.100000	4574.726229	9.705761	9.700000	1.249000
14.000000	0.500000	4320.457943	10.700000	4953.619610	10.600000	3888.551148	7.000000	4387.542900	12.209429	9.433333	2.107922
14.000000	0.100000	3785.821394	12.200000	4254.231562	9.000000	3534.181978	11.100000	3858.078311	9.471621	10.766667	1.625833
40.000000	25.000000	3742.819513	11.900000	3933.424189	10.000000	3063.187377	17.000000	3579.810360	12.778503	12.966667	3.619853
40.000000	10.000000	3492.114445	12.300000	3921.738102	12.900000	3067.066348	14.500000	3493.639632	12.231883	13.233333	1.137248
40.000000	5.000000	3196.831247	13.300000	3672.217614	13.600000	2837.616701	14.600000	3235.555187	12.938918	13.833333	0.680686
40.000000	1.000000	2620.242779	14.900000	2924.076104	17.200000	2306.390861	15.700000	2616.903248	11.802353	15.933333	1.167619
40.000000	0.500000	2318.523740	16.300000	2803.751144	18.300000	2022.323312	17.700000	2381.532732	16.565213	17.433333	1.026320
40.000000	0.100000	1725.812305	21.300000	2017.521454	22.100000	1635.624652	20.700000	1792.986137	11.133018	21.366667	0.702377
70.000000	25.000000	2374.745163	23.500000	2157.293923	18.400000	1722.872469	18.600000	2084.970518	15.918683	20.166667	2.888483
70.000000	10.000000	1934.440266	17.400000	2055.872778	20.300000	1529.741531	19.800000	1840.018192	14.971684	19.166667	1.550269
70.000000	5.000000	1689.434412	19.400000	1802.823065	21.600000	1337.439045	20.500000	1609.898841	15.073781	20.500000	1.100000
70.000000	1.000000	1208.917041	23.900000	1184.902821	26.900000	931.509019	21.900000	1108.442960	13.866208	24.233333	2.516611
70.000000	0.500000	987.311937	24.400000	977.373853	27.400000	760.684335	23.200000	908.456708	14.097652	25.000000	2.163331
70.000000	0.100000	638.287449	29.500000	605.228004	29.900000	511.754396	26.600000	585.089950	11.216444	28.666667	1.800926
100.000000	25.000000	1107.424525	32.900000	924.900554	26.100000	1027.902589	27.500000	1020.075889	8.971229	28.833333	3.590729
100.000000	10.000000	849.890496	30.800000	728.993555	28.000000	817.394909	23.800000	798.759653	7.832862	27.533333	3.523256
100.000000	5.000000	638.624284	31.600000	564.923850	28.200000	672.707289	24.200000	625.418474	8.808799	28.000000	3.704052
100.000000	1.000000	372.186176	31.400000	344.169392	29.100000	414.364827	25.500000	376.906798	9.375000	28.666667	2.973774
100.000000	0.500000	285.011615	31.100000	279.056656	26.600000	341.591633	24.600000	301.886635	11.432837	27.433333	3.329164
100.000000	0.100000	172.087597	28.500000	190.105371	23.200000	229.925306	23.300000	197.372758	14.994875	25.000000	3.031501
130.000000	25.000000	274.037785	42.100000	274.584961	29.900000	416.245997	31.700000	321.622914	25.479046	34.566667	6.585843
130.000000	10.000000	198.529583	36.300000	224.772398	26.500000	314.333961	27.200000	245.878647	24.694608	30.000000	5.467175
130.000000	5.000000	159.531716	33.900000	189.390793	24.500000	252.691119	25.000000	200.537876	23.720978	27.800000	5.288667
130.000000	1.000000	106.083162	29.900000	132.733893	20.300000	165.332909	23.700000	134.716655	22.027414	24.633333	4.867580
130.000000	0.500000	77.983258	28.600000	114.854799	18.400000	135.194732	22.600000	109.344263	26.522728	23.200000	5.126402
130.000000	0.100000	72.813667	23.500000	92.412476	15.600000	98.520621	18.700000	87.915588	15.276587	19.266667	3.980368

Table D-24 Dynamic Modulus Summary Sheet for the Mix 24

Conditions		Specimen 1		Specimen 2		Specimen 3		Modulus		Phase Angle (Degrees)	
Temperature, °F	Frequency, Hz	Modulus, ksi	Phage Angle, degree	Modulus, ksi	Phage Angle, degree	Modulus, ksi	Phage Angle, degree	Avg. Modulus, ksi	CV, %	Avg. P. Angle, degree	Standard Dev, degree
14.000000	25.000000	7171.742429	0.600000	8142.735564	3.300000	8648.940161	0.800000	7987.806051	9.397910	1.566667	1.504438
14.000000	10.000000	7876.767604	5.200000	7821.794008	4.600000	7759.013586	4.800000	7819.191733	0.753532	4.866667	0.305505
14.000000	5.000000	7638.122158	5.300000	7451.497706	5.800000	7576.079088	5.400000	7555.232984	1.257970	5.500000	0.264575
14.000000	1.000000	6733.800600	7.900000	6796.931058	5.600000	6773.238296	10.400000	6767.989985	0.471200	7.966667	2.400694
14.000000	0.500000	6378.528997	4.200000	6595.797459	14.500000	6445.534799	122.200000	6473.287085	1.718773	46.966667	65.357198
14.000000	0.100000	5897.239023	7.800000	5954.471822	4.200000	5883.691495	8.800000	5911.800780	0.635507	6.933333	2.419366
40.000000	25.000000	6235.709347	4.400000	5790.447521	10.800000	6255.896239	7.300000	6094.017702	4.317237	7.500000	3.204684
40.000000	10.000000	5674.670705	8.700000	5675.169865	9.000000	5776.876203	10.100000	5708.905591	1.031105	9.266667	0.737111
40.000000	5.000000	5302.623934	10.300000	5379.026591	10.500000	5525.291475	10.500000	5402.314000	2.094392	10.433333	0.115470
40.000000	1.000000	4295.314702	14.500000	4355.948635	14.000000	4265.569644	17.300000	4305.610994	1.069786	15.266667	1.778576
40.000000	0.500000	4264.460352	16.200000	4212.758060	18.900000	4218.745077	17.300000	4231.987830	0.668265	17.466667	1.357694
40.000000	0.100000	2968.265031	20.700000	2902.288447	21.300000	2831.028835	22.000000	2900.527438	2.366295	21.333333	0.650641
70.000000	25.000000	2552.772633	20.800000	2876.000663	12.900000	2980.682232	11.300000	2803.151843	7.957560	15.000000	5.086256
70.000000	10.000000	2823.046918	19.100000	2667.289872	16.900000	2705.281150	18.800000	2731.872647	2.972761	18.266667	1.193035
70.000000	5.000000	2381.641432	19.700000	2464.630216	20.400000	2428.583355	19.200000	2424.951668	1.716051	19.766667	0.602771
70.000000	1.000000	1585.171058	24.500000	1600.424811	22.900000	1587.917816	25.000000	1591.171228	0.510986	24.133333	1.096966
70.000000	0.500000	1328.333039	21.800000	1279.118858	21.700000	1314.231662	24.900000	1307.227853	1.938730	22.800000	1.819341
70.000000	0.100000	827.504457	29.800000	811.583272	28.100000	797.401965	27.400000	812.163231	1.854261	28.433333	1.234234
100.000000	25.000000	1082.802493	34.700000	1032.544878	32.200000	1001.225893	29.800000	1038.857755	3.961376	32.233333	2.450170
100.000000	10.000000	783.689211	31.600000	769.359941	30.100000	749.223676	29.400000	767.424276	2.256133	30.366667	1.123981
100.000000	5.000000	604.083751	29.500000	613.117661	29.600000	579.426760	29.000000	598.876057	2.911909	29.366667	0.321455
100.000000	1.000000	365.759619	29.700000	379.320928	28.900000	354.702813	28.600000	366.594453	3.363464	29.066667	0.568624
100.000000	0.500000	290.327719	28.900000	301.230469	28.100000	278.078355	27.500000	289.878848	3.995663	28.166667	0.702377
100.000000	0.100000	196.793185	23.700000	189.736767	22.000000	178.825749	22.100000	188.451900	4.803543	22.600000	0.953939
130.000000	25.000000	255.899175	34.100000	253.420928	32.600000	252.543010	33.200000	253.954371	0.685364	33.300000	0.754983
130.000000	10.000000	202.899735	27.000000	202.006440	27.600000	198.740649	27.200000	201.215608	1.088097	27.266667	0.305505
130.000000	5.000000	166.580446	25.200000	163.250392	24.800000	160.967399	24.800000	163.599412	1.725405	24.933333	0.230940
130.000000	1.000000	113.016858	19.300000	110.976844	20.700000	107.647661	21.200000	110.547121	2.451688	20.400000	0.984886
130.000000	0.500000	93.397015	19.800000	92.690271	19.300000	90.188523	19.500000	92.091936	1.830622	19.533333	0.251661
130.000000	0.100000	73.667505	15.300000	70.291466	15.300000	68.995478	16.000000	70.984816	3.397841	15.533333	0.404145

Table D-25 Dynamic Modulus Summary Sheet for the Mix 25

Conditions		Specimen 1		Specimen 2		Specimen 3		Modulus		Phase Angle (Degrees)	
Temperature, °F	Frequency, Hz	Modulus, ksi	Phage Angle, degree	Modulus, ksi	Phage Angle, degree	Modulus, ksi	Phage Angle, degree	Avg. Modulus, ksi	CV, %	Avg. P. Angle, degree	Standard Dev, degree
14.000000	25.000000	7676.867471	13.100000	6430.938469	7.600000	8033.547775	10.300000	7380.451238	11.400646	10.333333	2.750152
14.000000	10.000000	6169.129594	5.900000	6179.440924	6.000000	6218.650292	6.000000	6189.073603	0.422161	5.966667	0.057735
14.000000	5.000000	5938.643476	6.100000	5916.768492	6.000000	6094.768691	4.800000	5983.393553	1.622354	5.633333	0.723418
14.000000	1.000000	5174.215369	8.400000	5256.336534	5.900000	5230.122151	7.900000	5220.224685	0.803523	7.400000	1.322876
14.000000	0.500000	5097.875669	4.200000	5221.675744	5.700000	5068.889868	8.600000	5129.480427	1.581996	6.166667	2.236813
14.000000	0.100000	4434.271049	9.900000	4388.548521	11.200000	4425.202034	11.100000	4416.007201	0.548196	10.733333	0.723418
40.000000	25.000000	4439.340837	13.300000	4207.290220	15.900000	4514.281409	13.800000	4386.970822	3.648436	14.333333	1.379613
40.000000	10.000000	3803.313026	15.100000	3748.289093	14.900000	3895.516612	13.100000	3815.706244	1.949628	14.366667	1.101514
40.000000	5.000000	3373.355580	16.700000	3389.280391	15.800000	3501.515943	14.900000	3421.383971	2.041619	15.800000	0.900000
40.000000	1.000000	2513.642904	19.200000	2569.363572	18.900000	2577.450804	18.000000	2553.485760	1.360534	18.700000	0.624500
40.000000	0.500000	2161.077007	19.200000	2187.372769	20.600000	2147.838316	20.900000	2165.429364	0.929302	20.233333	0.907377
40.000000	0.100000	1519.778061	24.200000	1557.040110	24.100000	1552.768166	23.800000	1543.195446	1.321428	24.033333	0.208167
70.000000	25.000000	1652.521093	22.700000	1280.955784	23.600000	1362.771012	23.800000	1432.082630	13.633222	23.366667	0.585947
70.000000	10.000000	1458.140586	23.300000	1073.761910	25.200000	1077.164786	25.200000	1203.022427	18.365855	24.566667	1.096966
70.000000	5.000000	1185.995431	24.700000	893.897514	26.500000	894.567558	26.400000	991.486834	16.989607	25.866667	1.011599
70.000000	1.000000	770.098164	29.000000	560.350901	28.500000	554.854774	29.400000	628.434613	19.527092	28.966667	0.450925
70.000000	0.500000	626.058538	27.900000	445.112557	29.400000	454.313723	30.100000	508.494939	20.042865	29.133333	1.123981
70.000000	0.100000	377.270760	26.900000	275.718914	28.200000	275.881094	27.900000	309.623589	18.921111	27.666667	0.680686
100.000000	25.000000	580.805578	36.800000	616.954273	35.500000	562.799990	33.700000	586.853280	4.699475	35.333333	1.556706
100.000000	10.000000	429.210229	35.100000	384.423935	32.900000	362.506448	31.200000	392.046871	8.672172	33.066667	1.955335
100.000000	5.000000	339.655194	34.000000	336.082886	32.700000	290.116508	30.000000	321.951529	8.581334	32.233333	2.040425
100.000000	1.000000	246.187533	28.100000	244.408197	26.500000	210.870772	26.000000	233.822167	8.509198	26.866667	1.096966
100.000000	0.500000	208.552383	26.000000	205.385670	24.500000	192.360947	23.800000	202.099667	4.246082	24.766667	1.123981
100.000000	0.100000	157.665633	20.000000	157.418446	18.300000	124.928082	18.100000	146.670720	12.838338	18.800000	1.044031
130.000000	25.000000	224.090894	34.100000	117.829305	33.700000	103.525276	33.800000	148.481825	44.361529	33.866667	0.208167
130.000000	10.000000	148.553824	26.500000	85.112353	27.400000	83.379001	27.200000	105.681726	35.141780	27.033333	0.472582
130.000000	5.000000	135.631370	24.000000	68.649504	24.600000	67.965390	24.700000	90.748755	42.833635	24.433333	0.378594
130.000000	1.000000	106.388954	19.500000	48.862694	20.700000	47.396113	20.600000	67.549254	49.806856	20.266667	0.665833
130.000000	0.500000	100.235840	17.100000	40.285441	19.700000	38.231357	19.400000	59.584213	59.110154	18.733333	1.422439
130.000000	0.100000	45.871361	16.200000	33.890943	16.300000	30.942693	15.400000	36.901666	21.426184	15.966667	0.493288

Table D-26 Dynamic Modulus Summary Sheet for the Mix 26

Conditions		Specimen 1		Specimen 2		Specimen 3		Modulus		Phase Angle (Degrees)	
Temperature, °F	Frequency, Hz	Modulus, ksi	Phage Angle, degree	Modulus, ksi	Phage Angle, degree	Modulus, ksi	Phage Angle, degree	Avg. Modulus, ksi	CV, %	Avg. P. Angle, degree	Standard Dev, degree
14.000000	25.000000	5439.566959	8.000000	4438.972523	4.300000	4147.028953	3.100000	4675.189478	14.499380	5.133333	2.554082
14.000000	10.000000	4674.499851	5.500000	4666.506620	5.000000	4618.000054	5.400000	4653.002175	0.657104	5.300000	0.264575
14.000000	5.000000	4510.955853	5.300000	4553.478302	4.600000	4508.714347	5.800000	4524.382834	0.557476	5.233333	0.602771
14.000000	1.000000	3994.438475	7.900000	4075.795596	8.100000	3997.035964	7.900000	4022.423345	1.149555	7.966667	0.115470
14.000000	0.500000	3932.262819	3.000000	3996.526650	11.400000	3859.480485	3.200000	3929.423318	1.744968	5.866667	4.793051
14.000000	0.100000	3504.305349	8.300000	3457.572897	7.500000	3479.705077	7.600000	3480.527774	0.671653	7.800000	0.435890
40.000000	25.000000	4665.773909	11.300000	3657.352773	5.700000	3267.719790	5.100000	3863.615491	18.673946	7.366667	3.419552
40.000000	10.000000	3603.122913	9.800000	3506.609956	10.700000	3424.101620	10.600000	3511.278163	2.551831	10.366667	0.493288
40.000000	5.000000	3372.348701	10.000000	3251.813401	10.900000	3216.099313	10.700000	3280.087138	2.496031	10.533333	0.472582
40.000000	1.000000	2869.422806	12.100000	2737.433809	12.600000	2662.208624	12.700000	2756.355080	3.805566	12.466667	0.321455
40.000000	0.500000	2692.714824	17.500000	2483.733636	18.300000	2333.949827	13.100000	2503.466096	7.197806	16.300000	2.800000
40.000000	0.100000	2043.861751	18.700000	1935.284095	19.000000	1871.757616	18.500000	1950.301154	4.462350	18.733333	0.251661
70.000000	25.000000	2695.496832	2.200000	2421.310358	5.200000	2253.699968	9.700000	2456.835719	9.077962	5.700000	3.774917
70.000000	10.000000	1896.525146	19.500000	1876.109200	19.600000	1777.715509	19.700000	1850.116618	3.433660	19.600000	0.100000
70.000000	5.000000	1644.552812	21.500000	1595.624114	21.400000	1599.536594	20.600000	1613.237840	1.685432	21.166667	0.493288
70.000000	1.000000	1096.674091	26.700000	1065.136061	27.200000	1074.564976	23.100000	1078.791709	1.500595	25.666667	2.236813
70.000000	0.500000	891.996471	30.800000	859.433430	31.000000	799.665665	25.900000	850.365189	5.506883	29.233333	2.888483
70.000000	0.100000	559.892213	29.900000	545.747028	28.900000	537.422764	28.400000	547.687335	2.074120	29.066667	0.763763
100.000000	25.000000	810.690702	20.900000	841.185298	17.000000	855.572738	16.600000	835.816246	2.741950	18.166667	2.375570
100.000000	10.000000	668.947270	28.600000	671.613083	29.000000	678.162508	28.900000	672.907620	0.704710	28.833333	0.208167
100.000000	5.000000	534.371520	29.600000	529.844120	28.900000	532.865771	28.700000	532.360470	0.433092	29.066667	0.472582
100.000000	1.000000	293.910037	29.600000	304.015523	27.900000	309.762753	29.200000	302.562771	2.652536	28.900000	0.888819
100.000000	0.500000	240.768435	29.500000	234.402659	27.900000	234.429206	29.800000	236.533433	1.550581	29.066667	1.021437
100.000000	0.100000	160.536419	24.200000	161.244904	23.900000	159.922079	23.100000	160.567801	0.412269	23.733333	0.568624
130.000000	25.000000	243.860732	17.600000	248.260186	21.700000	248.865241	20.800000	246.995386	1.105889	20.033333	2.154840
130.000000	10.000000	215.056694	27.800000	210.729771	27.400000	210.048993	27.500000	211.945153	1.281505	27.566667	0.208167
130.000000	5.000000	171.713481	24.800000	175.073998	25.700000	167.802162	25.100000	171.529880	2.121725	25.200000	0.458258
130.000000	1.000000	122.275179	21.900000	116.523888	22.300000	117.944630	21.500000	118.914566	2.519302	21.900000	0.400000
130.000000	0.500000	99.120019	20.400000	98.508001	19.400000	95.431661	20.400000	97.686560	2.023442	20.066667	0.577350
130.000000	0.100000	79.830193	16.600000	78.262938	16.900000	75.615258	16.300000	77.902796	2.734718	16.600000	0.300000

Table D-27 Dynamic Modulus Summary Sheet for the Mix 27

Conditions		Specimen 1		Specimen 2		Specimen 3		Modulus		Phase Angle (Degrees)	
Temperature, °F	Frequency, Hz	Modulus, ksi	Phage Angle, degree	Modulus, ksi	Phage Angle, degree	Modulus, ksi	Phage Angle, degree	Avg. Modulus, ksi	CV, %	Avg. P. Angle, degree	Standard Dev, degree
14.000000	25.000000	7837.631783	11.600000	5569.036221	11.000000	7073.421849	9.800000	6826.696618	16.907843	10.800000	0.916515
14.000000	10.000000	6798.247355	5.900000	7102.022364	6.900000	6142.205276	8.000000	6680.824998	7.342868	6.933333	1.050397
14.000000	5.000000	6818.185029	5.200000	6951.552990	6.900000	5875.315879	8.500000	6548.351299	8.959017	6.866667	1.650253
14.000000	1.000000	6113.322470	4.100000	6016.711451	11.800000	5115.488282	9.000000	5748.507401	9.573524	8.300000	3.897435
14.000000	0.500000	5643.834052	8.800000	5540.500839	7.700000	5137.138274	8.000000	5440.491055	4.921313	8.166667	0.568624
14.000000	0.100000	5255.015160	7.800000	5005.350769	12.200000	4300.575537	12.500000	4853.647155	10.197980	10.833333	2.631223
40.000000	25.000000	4131.699622	17.100000	3636.687030	17.500000	4796.120799	14.000000	4188.169150	13.890938	16.200000	1.915724
40.000000	10.000000	3718.337612	11.400000	3808.067593	16.100000	3909.961496	13.200000	3812.122234	2.515037	13.566667	2.371357
40.000000	5.000000	3465.940535	12.000000	3483.849801	16.600000	3619.398486	13.800000	3523.062941	2.381684	14.133333	2.318045
40.000000	1.000000	2787.212863	15.500000	2772.391832	18.500000	2870.457682	16.200000	2810.020792	1.881192	16.733333	1.569501
40.000000	0.500000	2629.284813	16.200000	2443.764141	21.100000	2699.239879	17.600000	2590.762944	5.095889	18.300000	2.523886
40.000000	0.100000	1948.707450	19.600000	1805.944809	23.100000	1930.027756	20.900000	1894.893338	4.094997	21.200000	1.769181
70.000000	25.000000	2450.100179	21.500000	1701.613566	23.200000	2311.416985	14.200000	2154.376910	18.482778	19.633333	4.781562
70.000000	10.000000	1919.021142	21.200000	1830.654168	24.000000	1731.146832	22.500000	1826.940714	5.144786	22.566667	1.401190
70.000000	5.000000	1671.305811	22.500000	1599.065431	25.400000	1479.293594	23.700000	1583.221612	6.125590	23.866667	1.457166
70.000000	1.000000	1125.554866	27.600000	1070.341918	30.800000	953.490624	26.600000	1049.795803	8.368571	28.333333	2.193931
70.000000	0.500000	908.520971	30.100000	916.835371	29.700000	744.032761	29.200000	856.463034	11.378913	29.666667	0.450925
70.000000	0.100000	562.503628	30.800000	546.491198	32.900000	471.000693	30.500000	526.665173	9.278603	31.400000	1.307670
100.000000	25.000000	986.359167	21.200000	901.733353	31.800000	727.066981	31.300000	871.719834	15.168407	28.100000	5.980803
100.000000	10.000000	662.305586	28.500000	704.909270	31.200000	535.357654	30.000000	634.190837	13.907957	29.900000	1.352775
100.000000	5.000000	529.577060	28.800000	564.850738	31.500000	425.183441	30.200000	506.537080	14.338199	30.166667	1.350309
100.000000	1.000000	311.243260	27.900000	334.789509	31.800000	249.378763	30.200000	298.470511	14.780252	29.966667	1.960442
100.000000	0.500000	250.054609	27.600000	270.451551	30.200000	197.647023	29.300000	239.384394	15.688919	29.033333	1.320353
100.000000	0.100000	162.025195	23.600000	176.955023	27.800000	130.583922	25.300000	156.521380	15.122802	25.566667	2.112660
130.000000	25.000000	305.622815	28.300000	387.367398	33.200000	241.307487	35.100000	311.432567	23.505271	32.200000	3.508561
130.000000	10.000000	211.246919	29.500000	278.913770	29.500000	195.113507	29.900000	228.424732	19.464910	29.633333	0.230940
130.000000	5.000000	167.344055	26.800000	220.159411	29.100000	165.137655	27.300000	184.213707	16.909401	27.733333	1.209683
130.000000	1.000000	119.330992	21.800000	159.380271	24.600000	120.546180	22.900000	133.085814	17.116604	23.100000	1.410674
130.000000	0.500000	97.300936	20.900000	135.339359	22.500000	108.991084	19.700000	113.877126	17.109877	21.033333	1.404754
130.000000	0.100000	74.636957	17.900000	105.243106	16.200000	100.389461	15.000000	93.423175	17.607350	16.366667	1.457166

Table D-28 Dynamic Modulus Summary Sheet for the Mix 28

Conditions		Specimen 1		Specimen 2		Specimen 3		Modulus		Phase Angle (Degrees)	
Temperature, °F	Frequency, Hz	Modulus, ksi	Phage Angle, degree	Modulus, ksi	Phage Angle, degree	Modulus, ksi	Phage Angle, degree	Avg. Modulus, ksi	CV, %	Avg. P. Angle, degree	Standard Dev, degree
14.000000	25.000000	5246.719328	20.800000	11705.496878	9.600000	6550.775438	15.600000	7834.330548	43.594610	15.333333	5.604760
14.000000	10.000000	5437.163129	10.500000	8055.022097	6.800000	5999.383885	11.600000	6497.189704	21.210680	9.633333	2.514624
14.000000	5.000000	5217.250759	10.900000	7703.309601	6.000000	5829.803112	11.900000	6250.121157	20.723290	9.600000	3.157531
14.000000	1.000000	4627.322493	13.100000	7071.617562	1.600000	5234.881505	14.000000	5644.607187	22.545693	9.566667	6.913995
14.000000	0.500000	4517.246196	12.300000	6262.693286	12.500000	5275.087597	12.900000	5351.675693	16.354510	12.566667	0.305505
14.000000	0.100000	3849.050494	11.700000	6051.089078	5.800000	4435.549049	16.400000	4778.562874	23.864688	11.300000	5.311309
40.000000	25.000000	3319.344473	16.900000	6760.485855	10.100000	4042.826816	13.900000	4707.552381	38.540631	13.633333	3.407834
40.000000	10.000000	3272.011898	13.900000	5115.638422	10.100000	3487.904732	18.400000	3958.518351	25.461361	14.133333	4.154917
40.000000	5.000000	3094.397566	14.600000	4674.014182	11.800000	3205.271561	19.200000	3657.894436	24.104850	15.200000	3.736308
40.000000	1.000000	2499.939579	16.300000	4043.991812	11.100000	2544.688302	21.400000	3029.539898	29.008563	16.266667	5.150081
40.000000	0.500000	2328.212897	18.900000	3616.356671	12.300000	2295.503343	19.500000	2746.690970	27.426826	16.900000	3.994997
40.000000	0.100000	1711.981470	19.600000	2893.505351	17.900000	1794.260028	23.700000	2133.248950	30.923975	20.400000	2.981610
70.000000	25.000000	1570.497990	26.400000	2362.774028	15.800000	1603.910952	23.600000	1845.727657	24.276975	21.933333	5.493026
70.000000	10.000000	1383.045667	22.700000	2273.974333	19.600000	1300.421716	24.700000	1652.480572	32.666799	22.333333	2.569695
70.000000	5.000000	1195.442624	24.100000	2122.087844	21.100000	1149.288681	25.700000	1488.939716	36.858965	23.633333	2.335237
70.000000	1.000000	815.026764	27.900000	1623.363538	22.900000	817.676475	28.500000	1085.355592	42.928828	26.433333	3.074627
70.000000	0.500000	753.752091	27.500000	1303.920767	28.100000	679.963169	30.500000	912.545342	37.361778	28.700000	1.587451
70.000000	0.100000	458.622369	29.100000	968.060698	26.400000	464.615479	31.900000	630.432849	46.382362	29.133333	2.750152
100.000000	25.000000	655.706114	31.200000	1019.296469	22.400000	773.044382	28.100000	816.015655	22.740378	27.233333	4.463556
100.000000	10.000000	504.622836	30.400000	740.858939	25.500000	593.429059	28.000000	612.970278	19.466558	27.966667	2.450170
100.000000	5.000000	407.700803	30.300000	616.311211	25.400000	492.248572	27.200000	505.420195	20.760368	27.633333	2.478575
100.000000	1.000000	249.295207	31.500000	403.817046	27.700000	318.158533	27.600000	323.756929	23.910807	28.933333	2.223361
100.000000	0.500000	202.510822	31.600000	332.225094	26.600000	258.786353	28.100000	264.507423	24.591411	28.766667	2.565801
100.000000	0.100000	137.898841	28.900000	231.001089	25.200000	167.337962	28.500000	178.745964	26.623237	27.533333	2.030599
130.000000	25.000000	207.546956	34.600000	367.578122	25.400000	262.769623	29.900000	279.298234	29.103604	29.966667	4.600362
130.000000	10.000000	159.502559	31.200000	269.559562	28.700000	201.053960	26.800000	210.038694	26.459836	28.900000	2.206808
130.000000	5.000000	141.584443	29.300000	224.922537	26.900000	166.505014	25.900000	177.670665	24.076184	27.366667	1.747379
130.000000	1.000000	109.003850	25.900000	160.591833	22.200000	111.214457	24.700000	126.936713	22.977702	24.266667	1.887679
130.000000	0.500000	96.755066	24.700000	134.676569	24.100000	93.399336	21.900000	108.276990	21.171803	23.566667	1.474223
130.000000	0.100000	85.383765	21.200000	109.247990	19.600000	71.353468	19.600000	88.661741	21.608809	20.133333	0.923760

Table D-29 Dynamic Modulus Summary Sheet for the Mix 29

Conditions		Specimen 1		Specimen 2		Specimen 3		Modulus		Phase Angle (Degrees)	
Temperature, °F	Frequency, Hz	Modulus, ksi	Phage Angle, degree	Modulus, ksi	Phage Angle, degree	Modulus, ksi	Phage Angle, degree	Avg. Modulus, ksi	CV, %	Avg. P. Angle, degree	Standard Dev, degree
14.000000	25.000000	5847.157804	8.400000	6218.827123	1.800000	7338.507540	4.100000	6468.164156	12.002020	4.766667	3.350124
14.000000	10.000000	5300.011649	7.100000	7172.420741	6.900000	7849.033982	5.900000	6773.822124	19.493153	6.633333	0.642910
14.000000	5.000000	5194.845427	6.600000	7077.778220	6.500000	7554.199608	6.600000	6608.941085	18.877387	6.566667	0.057735
14.000000	1.000000	4532.701296	8.300000	6159.020626	9.600000	7073.242262	8.400000	5921.654728	21.730345	8.766667	0.723418
14.000000	0.500000	4358.807671	10.000000	5857.381952	7.300000	7057.564636	5.000000	5757.918086	23.482881	7.433333	2.502665
14.000000	0.100000	3816.387650	9.000000	5239.090638	8.800000	5951.234463	8.200000	5002.237584	21.729340	8.666667	0.416333
40.000000	25.000000	3686.410815	10.200000	4987.542611	9.400000	5371.140996	8.000000	4681.698141	18.861229	9.200000	1.113553
40.000000	10.000000	3338.795899	12.500000	4725.316392	11.600000	5272.720178	10.000000	4445.610823	22.423040	11.366667	1.266228
40.000000	5.000000	3067.801089	13.100000	4333.940483	12.400000	4954.506957	11.400000	4118.749510	23.346520	12.300000	0.854400
40.000000	1.000000	2429.337534	16.000000	3591.090852	13.700000	4086.308418	12.300000	3368.912268	25.246591	14.000000	1.868154
40.000000	0.500000	2185.723119	19.200000	3099.524653	18.600000	3935.566907	13.200000	3073.604893	28.475026	17.000000	3.304542
40.000000	0.100000	1619.930200	21.600000	2403.654951	20.200000	2966.850817	16.300000	2330.145323	29.030915	19.366667	2.746513
70.000000	25.000000	1848.004944	21.100000	2855.285164	17.200000	2804.498796	16.700000	2502.596301	22.674899	18.333333	2.409011
70.000000	10.000000	1490.642266	23.700000	2340.554231	18.600000	2479.717872	17.900000	2103.638123	25.451652	20.066667	3.165965
70.000000	5.000000	1285.337976	24.900000	2055.696237	19.400000	2188.761887	19.100000	1843.265367	26.460569	21.133333	3.265476
70.000000	1.000000	823.538159	29.000000	1477.292893	23.900000	1588.784854	23.500000	1296.538635	31.885376	25.466667	3.066486
70.000000	0.500000	673.697341	28.600000	1247.270830	27.300000	1365.964127	20.900000	1095.644099	33.788749	25.600000	4.121893
70.000000	0.100000	391.356470	31.000000	766.072536	31.200000	920.084770	25.900000	692.504592	39.268051	29.366667	3.003886
100.000000	25.000000	535.401173	37.100000	1158.656814	29.100000	1083.908449	28.400000	925.988812	36.751771	31.533333	4.833563
100.000000	10.000000	360.531858	34.800000	818.474899	27.500000	819.057760	27.700000	666.021506	39.722735	30.000000	4.158125
100.000000	5.000000	279.060428	34.500000	670.035529	27.900000	674.129482	26.400000	541.075146	41.938839	29.600000	4.309292
100.000000	1.000000	158.471455	33.200000	379.780051	29.500000	415.467882	27.000000	317.906463	43.793702	29.900000	3.119295
100.000000	0.500000	123.098264	32.000000	293.542013	30.700000	325.051466	26.500000	247.230581	43.946853	29.733333	2.874601
100.000000	0.100000	69.661170	25.700000	186.193036	24.600000	209.977912	23.100000	155.277373	48.360864	24.466667	1.305118
130.000000	25.000000	123.357490	38.400000	209.261884	34.800000	313.834946	34.200000	215.484773	44.268131	35.800000	2.271563
130.000000	10.000000	90.072473	32.000000	144.838485	29.300000	235.175842	30.600000	156.695600	46.762487	30.633333	1.350309
130.000000	5.000000	72.544576	29.100000	116.645450	27.300000	190.054309	28.700000	126.414778	46.957232	28.366667	0.945163
130.000000	1.000000	48.370207	23.300000	73.706962	22.100000	134.722699	22.600000	85.599956	51.854853	22.666667	0.602771
130.000000	0.500000	40.980580	21.400000	61.314421	19.900000	118.165270	20.700000	73.486757	54.439968	20.666667	0.750555
130.000000	0.100000	34.087357	14.700000	47.769504	16.300000	91.923325	15.600000	57.926729	52.180158	15.533333	0.802081

Table D-30 Dynamic Modulus Summary Sheet for the Mix 30

Conditions		Specimen 1		Specimen 2		Specimen 3		Modulus		Phase Angle (Degrees)	
Temperature, °F	Frequency, Hz	Modulus, ksi	Phage Angle, degree	Modulus, ksi	Phage Angle, degree	Modulus, ksi	Phage Angle, degree	Avg. Modulus, ksi	CV, %	Avg. P. Angle, degree	Standard Dev, degree
14.000000	25.000000	6872.236608	12.400000	5208.837717	8.600000	5017.122298	14.900000	5699.398874	17.900494	11.966667	3.172276
14.000000	10.000000	6853.800620	6.000000	4940.110088	8.600000	5631.878294	9.000000	5808.596334	16.682294	7.866667	1.628906
14.000000	5.000000	6551.470142	6.400000	4690.146724	8.500000	5381.294788	9.500000	5540.970551	16.980402	8.133333	1.582193
14.000000	1.000000	6083.716237	6.300000	3977.706391	9.900000	5194.060059	7.800000	5085.160896	20.790291	8.000000	1.808314
14.000000	0.500000	5479.205276	4.500000	3819.391459	10.600000	4456.591664	10.700000	4585.062800	18.262161	8.600000	3.551056
14.000000	0.100000	5129.708320	8.300000	3299.072865	12.300000	3947.037431	11.900000	4125.272872	22.501338	10.833333	2.203028
40.000000	25.000000	4279.163592	9.900000	2922.056834	9.400000	3011.526718	14.400000	3404.249048	22.296185	11.233333	2.753785
40.000000	10.000000	4261.507895	8.800000	3010.976786	12.200000	3321.688393	12.900000	3531.391025	18.437650	11.300000	2.193171
40.000000	5.000000	3950.870706	9.800000	2721.015060	14.000000	3143.344251	13.600000	3271.743339	19.099933	12.466667	2.318045
40.000000	1.000000	3453.651568	10.500000	2237.662298	15.400000	2649.895577	15.600000	2780.403148	22.241759	13.833333	2.888483
40.000000	0.500000	3146.847365	10.200000	2013.854130	17.000000	2488.587281	19.400000	2549.762925	22.314569	15.533333	4.772141
40.000000	0.100000	2623.565725	15.400000	1519.734542	19.700000	1893.508427	19.200000	2012.269565	27.899688	18.100000	2.351595
70.000000	25.000000	2212.731428	23.800000	1560.693073	19.800000	1705.995032	12.300000	1826.473178	18.741472	18.633333	5.838093
70.000000	10.000000	2204.663199	17.400000	1685.598235	16.000000	1477.113886	20.700000	1789.125107	20.940980	18.033333	2.413158
70.000000	5.000000	1970.373979	17.300000	1555.720042	16.200000	1285.357124	22.100000	1603.817048	21.513171	18.533333	3.137409
70.000000	1.000000	1483.698996	18.900000	1098.825512	19.700000	1018.868534	26.100000	1200.464347	20.702406	21.566667	3.946306
70.000000	0.500000	1281.200504	16.400000	960.003783	18.300000	903.928148	24.700000	1048.377478	19.417693	19.800000	4.348563
70.000000	0.100000	1059.248411	22.500000	705.677376	22.400000	636.357538	26.100000	800.427775	28.335995	23.666667	2.107922
100.000000	25.000000	980.957766	19.000000	804.947099	23.800000	983.756601	22.200000	923.220489	11.095651	21.666667	2.444040
100.000000	10.000000	952.104117	22.200000	636.174469	25.200000	684.919808	27.600000	757.732798	22.446674	25.000000	2.705550
100.000000	5.000000	829.121178	19.200000	573.043431	21.700000	609.278728	26.800000	670.481112	20.668114	22.566667	3.873414
100.000000	1.000000	574.663489	23.100000	413.457897	22.000000	449.034755	28.000000	479.052047	17.678901	24.366667	3.194266
100.000000	0.500000	493.963211	25.700000	342.334062	22.300000	396.501256	28.200000	410.932843	18.698392	25.400000	2.961419
100.000000	0.100000	375.451097	27.300000	251.369890	24.200000	274.997228	28.700000	300.606072	21.917547	26.733333	2.302897
130.000000	25.000000	559.338800	24.100000	306.995396	27.800000	402.098055	26.700000	422.810750	30.141244	26.200000	1.900000
130.000000	10.000000	445.819301	23.600000	242.385011	25.700000	312.118422	26.100000	333.440911	31.003906	25.133333	1.342882
130.000000	5.000000	371.537892	23.800000	214.280900	25.600000	268.144768	24.500000	284.654520	28.075399	24.633333	0.907377
130.000000	1.000000	258.291980	25.300000	179.276023	24.200000	196.968421	23.200000	211.512141	19.605067	24.233333	1.050397
130.000000	0.500000	216.145243	26.700000	149.299300	20.600000	169.748900	22.600000	178.397814	19.199773	23.300000	3.109662
130.000000	0.100000	160.330140	27.000000	111.919460	18.500000	123.593217	19.600000	131.947606	19.146629	21.700000	4.622770

Table D-31 Dynamic Modulus Summary Sheet for the Mix 31

Conditions		Specimen 1		Specimen 2		Specimen 3		Modulus		Phase Angle (Degrees)	
Temperature, °F	Frequency, Hz	Modulus, ksi	Phage Angle, degree	Modulus, ksi	Phage Angle, degree	Modulus, ksi	Phage Angle, degree	Avg. Modulus, ksi	CV, %	Avg. P. Angle, degree	Standard Dev, degree
14.000000	25.000000	7822.894452	3.900000	5438.220489	14.000000	7704.342736	22.100000	6988.485892	19.229875	13.333333	9.118297
14.000000	10.000000	6157.611345	7.200000	4859.136222	8.000000	9213.920440	7.500000	6743.556002	33.153729	7.566667	0.404145
14.000000	5.000000	5805.467143	7.100000	4666.933393	8.200000	8839.718186	7.200000	6437.372907	33.506964	7.500000	0.608276
14.000000	1.000000	5284.430490	5.900000	4288.073039	9.300000	7943.219702	10.200000	5838.574410	32.362899	8.466667	2.267892
14.000000	0.500000	4872.384632	10.700000	4173.403339	8.700000	7784.821794	13.900000	5610.203255	34.141882	11.100000	2.622975
14.000000	0.100000	4452.771299	8.900000	3643.772606	9.500000	6588.475721	11.500000	4895.006542	31.079580	9.966667	1.361372
40.000000	25.000000	4378.538196	10.100000	3231.657262	7.000000	6354.367104	12.200000	4654.854187	33.934168	9.766667	2.615977
40.000000	10.000000	3392.667600	11.200000	2957.471368	12.600000	5845.737208	11.700000	4065.292059	38.304481	11.833333	0.709460
40.000000	5.000000	3100.947281	12.000000	2770.211108	12.900000	5408.803998	12.800000	3759.987462	38.230468	12.566667	0.493288
40.000000	1.000000	2568.420956	14.700000	2316.106564	14.800000	4560.612184	13.800000	3148.379901	39.052418	14.433333	0.550757
40.000000	0.500000	2442.169614	14.200000	2143.444519	14.000000	4076.067588	19.200000	2887.227240	36.032626	15.800000	2.946184
40.000000	0.100000	1830.237839	18.300000	1706.877302	18.400000	3190.338251	18.300000	2242.484464	36.708372	18.333333	0.057735
70.000000	25.000000	2158.980999	18.500000	1804.079451	17.100000	3189.227073	3.700000	2384.095841	30.178741	13.100000	8.170679
70.000000	10.000000	1649.019575	17.600000	1620.127775	18.800000	2538.445974	19.500000	1935.864441	26.967323	18.633333	0.960902
70.000000	5.000000	1462.394253	18.300000	1459.199397	19.500000	2235.333320	20.900000	1718.975657	26.014429	19.566667	1.301281
70.000000	1.000000	1070.371946	21.100000	1032.914497	22.200000	1622.231035	25.200000	1241.839159	26.570348	22.833333	2.122106
70.000000	0.500000	917.463346	21.900000	926.628248	23.600000	1440.387407	25.600000	1094.826334	27.337646	23.700000	1.852026
70.000000	0.100000	681.329077	24.300000	664.681854	24.600000	1002.978828	26.300000	782.996586	24.354124	25.066667	1.078579
100.000000	25.000000	756.228742	20.100000	972.029316	22.600000	1044.602180	24.600000	924.286746	16.228486	22.433333	2.254625
100.000000	10.000000	638.661710	21.900000	781.697648	21.400000	845.203093	26.800000	755.187484	14.008694	23.366667	2.983845
100.000000	5.000000	540.276577	22.600000	633.484576	22.300000	667.120789	26.700000	613.627314	10.708817	23.866667	2.458319
100.000000	1.000000	353.010369	25.000000	413.033734	23.200000	430.663030	28.400000	398.902378	10.205354	25.533333	2.640707
100.000000	0.500000	292.117645	25.900000	338.639902	23.400000	361.217713	28.600000	330.658420	10.655916	25.966667	2.600641
100.000000	0.100000	201.776951	26.400000	226.990983	22.800000	242.679923	26.600000	223.815952	9.219853	25.266667	2.138535
130.000000	25.000000	393.644686	22.000000	356.718166	27.000000	513.514874	28.300000	421.292575	19.457548	25.766667	3.326159
130.000000	10.000000	306.612576	27.600000	259.642222	25.400000	396.697670	28.300000	320.984156	21.698517	27.100000	1.513275
130.000000	5.000000	244.677143	27.200000	214.461648	25.200000	318.329706	26.700000	259.156166	20.615504	26.366667	1.040833
130.000000	1.000000	151.413586	27.800000	136.132271	24.500000	212.684198	25.100000	166.743352	24.296602	25.800000	1.757840
130.000000	0.500000	121.104235	27.300000	111.726237	23.100000	170.552982	23.500000	134.461151	23.505823	24.633333	2.318045
130.000000	0.100000	86.794932	23.300000	81.169990	20.000000	129.007383	19.200000	98.990768	26.413424	20.833333	2.173323

Table D-32 Dynamic Modulus Summary Sheet for the Mix 32

Conditions		Specimen 1		Specimen 2		Specimen 3		Modulus		Phase Angle (Degrees)	
Temperature, °F	Frequency, Hz	Modulus, ksi	Phage Angle, degree	Modulus, ksi	Phage Angle, degree	Modulus, ksi	Phage Angle, degree	Avg. Modulus, ksi	CV, %	Avg. P. Angle, degree	Standard Dev, degree
14.000000	25.000000	5968.377944	11.400000	6230.108050	3.000000	6005.604598	10.200000	6068.030197	2.333415	8.200000	4.543127
14.000000	10.000000	6113.115175	6.000000	5772.053456	7.700000	6136.187940	7.000000	6007.118857	3.394293	6.900000	0.854400
14.000000	5.000000	5865.618743	6.900000	5544.500936	7.900000	5971.917759	6.600000	5794.012479	3.840583	7.133333	0.680686
14.000000	1.000000	5378.096161	8.300000	4949.055219	8.300000	5302.386612	6.600000	5209.845997	4.395559	7.733333	0.981495
14.000000	0.500000	5208.366844	8.200000	4760.879180	9.100000	5236.792848	4.300000	5068.679624	5.266493	7.200000	2.551470
14.000000	0.100000	4407.761174	10.000000	4183.704225	11.000000	4558.150619	10.400000	4383.205339	4.298842	10.466667	0.503322
40.000000	25.000000	4324.154715	16.600000	4298.271800	8.400000	4369.161214	13.000000	4330.529243	0.828352	12.666667	4.110150
40.000000	10.000000	4034.687071	11.800000	3908.889050	11.900000	4232.430995	10.900000	4058.669039	4.018528	11.533333	0.550757
40.000000	5.000000	3728.077831	12.900000	3619.830337	12.100000	3904.754769	11.200000	3750.887646	3.834432	12.066667	0.850490
40.000000	1.000000	3066.980180	15.100000	2970.996267	13.700000	3281.952593	14.100000	3106.643013	5.125379	14.300000	0.721110
40.000000	0.500000	2805.521632	12.100000	2714.909671	17.900000	2989.752843	11.800000	2836.728049	4.937161	13.933333	3.438507
40.000000	0.100000	2094.644347	19.600000	2000.342723	19.800000	2352.700746	16.300000	2149.229272	8.487263	18.566667	1.965536
70.000000	25.000000	1765.304690	21.300000	1928.094654	19.300000	1983.190247	14.500000	1892.196530	5.987318	18.366667	3.494758
70.000000	10.000000	1480.720574	17.800000	1618.694413	20.200000	1684.980269	18.600000	1594.798419	6.534081	18.866667	1.222020
70.000000	5.000000	1300.312629	18.600000	1409.550754	21.500000	1441.142602	18.700000	1383.668662	5.340616	19.600000	1.646208
70.000000	1.000000	922.992982	22.500000	989.357318	25.600000	1047.502124	20.700000	986.617475	6.314481	22.933333	2.478575
70.000000	0.500000	766.833388	24.000000	835.018402	28.000000	887.618776	22.400000	829.823522	7.297941	24.800000	2.884441
70.000000	0.100000	524.783181	23.800000	569.712507	27.400000	629.175786	24.500000	574.557158	9.113916	25.233333	1.908752
100.000000	25.000000	740.681238	26.800000	960.098799	24.800000	862.101129	23.300000	854.293722	12.866411	24.966667	1.755942
100.000000	10.000000	572.464342	24.600000	743.889874	24.700000	663.323924	23.200000	659.892713	12.996697	24.166667	0.838650
100.000000	5.000000	475.649220	24.800000	624.885853	24.400000	533.239017	24.000000	544.591363	13.820125	24.400000	0.400000
100.000000	1.000000	294.001426	26.200000	403.513430	24.900000	350.102737	25.500000	349.205864	15.681727	25.533333	0.650641
100.000000	0.500000	238.266833	25.600000	328.472619	24.300000	283.838640	25.700000	283.526031	15.908136	25.200000	0.781025
100.000000	0.100000	161.548084	22.700000	225.436639	22.000000	213.276923	24.100000	200.087215	16.955162	22.933333	1.069268
130.000000	25.000000	268.351192	29.600000	326.108681	32.400000	383.418217	28.200000	325.959363	17.650561	30.066667	2.138535
130.000000	10.000000	204.092003	26.000000	274.247110	25.000000	338.278551	24.800000	272.205888	24.656542	25.266667	0.642910
130.000000	5.000000	169.142830	25.000000	225.914909	23.400000	278.028454	23.900000	224.362064	24.273007	24.100000	0.818535
130.000000	1.000000	130.791941	22.700000	161.021943	21.000000	156.529213	23.300000	149.447699	10.914707	22.333333	1.193035
130.000000	0.500000	120.712421	21.100000	135.244344	20.000000	117.538600	22.200000	124.498455	7.582861	21.100000	1.100000
130.000000	0.100000	96.611019	16.600000	107.356376	16.800000	87.152511	19.800000	97.039969	10.417110	17.733333	1.792577

Table D-33 Dynamic Modulus Summary Sheet for the Mix 33

Conditions		Specimen 1		Specimen 2		Specimen 3		Modulus		Phase Angle (Degrees)	
Temperature, °F	Frequency, Hz	Modulus, ksi	Phage Angle, degree	Modulus, ksi	Phage Angle, degree	Modulus, ksi	Phage Angle, degree	Avg. Modulus, ksi	CV, %	Avg. P. Angle, degree	Standard Dev, degree
14.000000	25.000000	7165.374477	9.600000	8523.389761	10.600000	7512.867541	19.500000	7733.877260	9.121792	13.233333	5.450076
14.000000	10.000000	7641.060253	6.600000	8042.273572	6.700000	7959.497306	8.100000	7880.943710	2.687849	7.133333	0.838650
14.000000	5.000000	7362.122693	6.800000	7637.783437	6.800000	7843.544819	7.500000	7614.483650	3.172314	7.033333	0.404145
14.000000	1.000000	6728.654799	8.000000	6977.045396	3.700000	7149.767787	10.800000	6951.822661	3.045050	7.500000	3.576311
14.000000	0.500000	6548.487223	8.400000	6186.605704	8.700000	6521.913666	6.300000	6419.002198	3.142223	7.800000	1.307670
14.000000	0.100000	5731.382149	7.200000	5783.187580	8.800000	5997.704932	10.400000	5837.424887	2.418922	8.800000	1.600000
40.000000	25.000000	5248.921376	11.900000	5457.418055	12.900000	4910.232878	22.000000	5205.524103	5.305170	15.600000	5.565070
40.000000	10.000000	4998.033528	10.700000	4878.777534	11.700000	4770.180149	13.100000	4882.330404	2.334300	11.833333	1.205543
40.000000	5.000000	4629.279675	11.000000	4465.484428	11.900000	4390.359336	14.100000	4495.041146	2.717922	12.333333	1.594783
40.000000	1.000000	3790.054897	13.000000	3595.114159	14.500000	3498.356047	15.400000	3627.841701	4.095488	14.300000	1.212436
40.000000	0.500000	3560.192113	16.600000	3058.113528	20.400000	3086.155117	15.000000	3234.820253	8.721625	17.333333	2.773686
40.000000	0.100000	2699.586868	17.400000	2357.202614	21.600000	2387.706349	19.400000	2481.498610	7.635902	19.466667	2.100794
70.000000	25.000000	2321.763710	19.500000	1949.458003	23.000000	2138.666017	26.400000	2136.629243	8.712846	22.966667	3.450121
70.000000	10.000000	1808.633106	21.700000	1623.059922	22.900000	1791.122181	19.500000	1740.938403	5.885362	21.366667	1.724336
70.000000	5.000000	1519.994059	22.400000	1370.703753	23.800000	1540.140334	20.300000	1476.946049	6.266870	22.166667	1.761628
70.000000	1.000000	1010.088049	27.400000	937.906854	28.500000	1098.231482	21.500000	1015.408795	7.907617	25.800000	3.764306
70.000000	0.500000	847.131698	26.400000	834.174429	27.100000	883.768238	25.900000	855.024788	3.008313	26.466667	0.602771
70.000000	0.100000	573.659656	28.200000	565.605934	27.900000	628.932516	25.000000	589.399369	5.848787	27.033333	1.767295
100.000000	25.000000	816.851795	23.300000	766.130561	25.900000	1102.246520	26.700000	895.076292	20.243884	25.300000	1.777639
100.000000	10.000000	624.069152	26.000000	578.218389	24.800000	833.513959	25.000000	678.600500	20.056523	25.266667	0.642910
100.000000	5.000000	489.390697	25.400000	478.050149	25.000000	668.964968	25.800000	545.468605	19.634713	25.400000	0.400000
100.000000	1.000000	288.403611	25.600000	294.891965	24.700000	405.365152	26.600000	329.553576	19.946636	25.633333	0.950438
100.000000	0.500000	223.369063	25.700000	231.729303	25.400000	318.755175	27.000000	257.951180	20.478084	26.033333	0.850490
100.000000	0.100000	144.640184	22.000000	154.706213	21.800000	204.770460	24.300000	168.038952	19.165864	22.700000	1.389244
130.000000	25.000000	205.875546	29.800000	217.504768	29.400000	275.104284	28.500000	232.828199	15.922047	29.233333	0.665833
130.000000	10.000000	156.479892	25.000000	166.474696	25.000000	199.930741	25.800000	174.295110	13.056367	25.266667	0.461880
130.000000	5.000000	122.756787	23.600000	132.200788	23.700000	156.771323	23.000000	137.242966	12.794023	23.433333	0.378594
130.000000	1.000000	85.625003	18.900000	92.379402	20.000000	111.039947	19.600000	96.348117	13.663033	19.500000	0.556776
130.000000	0.500000	74.792899	17.900000	82.619889	17.400000	94.879118	18.500000	84.097302	12.038773	17.933333	0.550757
130.000000	0.100000	58.980221	14.000000	66.167050	14.500000	74.223094	14.500000	66.456788	11.474473	14.333333	0.288675

Table D-34 Dynamic Modulus Summary Sheet for the Mix 34

Conditions		Specimen 1		Specimen 2		Specimen 3		Modulus		Phase Angle (Degrees)	
Temperature, °F	Frequency, Hz	Modulus, ksi	Phage Angle, degree	Modulus, ksi	Phage Angle, degree	Modulus, ksi	Phage Angle, degree	Avg. Modulus, ksi	CV, %	Avg. P. Angle, degree	Standard Dev, degree
14.000000	25.000000	6875.718107	2.400000	7210.385763	10.800000	7572.442953	7.200000	7219.515608	4.826531	6.800000	4.214262
14.000000	10.000000	5756.414417	8.900000	7083.017441	6.500000	7989.774597	6.100000	6943.068818	16.177832	7.166667	1.514376
14.000000	5.000000	5383.062229	10.000000	6869.914448	6.200000	7674.009885	6.200000	6642.328854	17.498481	7.466667	2.193931
14.000000	1.000000	4995.657695	10.600000	5918.687234	8.100000	7183.225574	6.200000	6032.523501	18.204948	8.300000	2.206808
14.000000	0.500000	4533.630856	9.600000	6004.072884	3.700000	6310.964415	6.200000	5616.222718	16.915747	6.500000	2.961419
14.000000	0.100000	4210.630283	10.100000	5075.627294	10.800000	5894.566102	6.800000	5060.274560	16.640854	9.233333	2.136196
40.000000	25.000000	3932.324615	9.800000	4375.475928	19.100000	5196.149828	12.200000	4501.316790	14.245639	13.700000	4.828043
40.000000	10.000000	3325.988189	12.700000	4051.048811	14.100000	4975.677517	10.800000	4117.571506	20.081110	12.533333	1.656301
40.000000	5.000000	3118.732374	12.400000	3688.337970	14.500000	4577.096066	11.600000	3794.722137	19.368458	12.833333	1.497776
40.000000	1.000000	2504.936256	14.300000	3004.787842	16.000000	3836.470823	12.600000	3115.398307	21.590282	14.300000	1.700000
40.000000	0.500000	2360.271846	16.200000	2590.699068	21.000000	3524.358493	16.800000	2825.109802	21.819677	18.000000	2.615339
40.000000	0.100000	1830.456158	17.000000	1913.817171	19.700000	2711.355641	16.200000	2151.876323	22.599475	17.633333	1.833939
70.000000	25.000000	1719.628873	21.100000	2070.570942	21.900000	1675.581527	25.500000	1821.927114	11.880564	22.833333	2.343786
70.000000	10.000000	1479.017831	18.500000	1499.508774	21.200000	1483.434402	27.000000	1487.320336	0.725064	22.233333	4.343194
70.000000	5.000000	1298.426236	19.600000	1291.950358	22.100000	1312.311470	25.300000	1300.896021	0.799666	22.333333	2.857155
70.000000	1.000000	940.526102	23.100000	890.038418	25.200000	888.827581	29.100000	906.464034	3.254936	25.800000	3.044667
70.000000	0.500000	822.231872	22.600000	782.101792	25.800000	735.926815	31.000000	780.086826	5.536281	26.466667	4.239497
70.000000	0.100000	588.099319	24.800000	526.933442	27.900000	517.250088	30.700000	544.094283	7.060506	27.800000	2.951271
100.000000	25.000000	754.558638	27.700000	671.540407	35.800000	874.645840	23.800000	766.914962	13.315029	29.100000	6.121274
100.000000	10.000000	594.458712	26.700000	544.409117	34.200000	669.670262	26.700000	602.846030	10.458785	29.200000	4.330127
100.000000	5.000000	487.988088	25.900000	494.503858	30.000000	555.634485	27.000000	512.708810	7.278441	27.633333	2.122106
100.000000	1.000000	307.543007	28.100000	346.139921	25.800000	343.135677	27.800000	332.272868	6.461347	27.233333	1.250333
100.000000	0.500000	253.854230	28.200000	282.801299	24.900000	268.099943	28.400000	268.251824	5.395726	27.166667	1.965536
100.000000	0.100000	176.449916	27.600000	195.497197	21.900000	180.500060	26.000000	184.149058	5.448981	25.166667	2.939955
130.000000	25.000000	275.224106	30.000000	246.378871	32.400000	251.754160	28.900000	257.785712	5.950439	30.433333	1.789786
130.000000	10.000000	204.941924	28.300000	194.924200	28.200000	184.048433	27.600000	194.638186	5.368773	28.033333	0.378594
130.000000	5.000000	172.201762	28.000000	179.893554	22.700000	141.649722	26.700000	164.581679	12.290928	25.800000	2.762245
130.000000	1.000000	115.789582	25.900000	137.145532	18.800000	92.635292	23.800000	115.190135	19.325591	22.833333	3.647373
130.000000	0.500000	98.755477	25.000000	117.791589	17.600000	80.756852	22.000000	99.101306	18.687736	21.533333	3.722007
130.000000	0.100000	76.978846	21.700000	96.462185	13.800000	60.033809	18.100000	77.824947	23.422979	17.866667	3.955165

Table D-35 Dynamic Modulus Summary Sheet for the Mix 35

Conditions		Specimen 1		Specimen 2		Specimen 3		Modulus		Phase Angle (Degrees)	
Temperature, °F	Frequency, Hz	Modulus, ksi	Phage Angle, degree	Modulus, ksi	Phage Angle, degree	Modulus, ksi	Phage Angle, degree	Avg. Modulus, ksi	CV, %	Avg. P. Angle, degree	Standard Dev, degree
14.000000	25.000000	6809.627940	9.800000	7857.082048	4.200000	6089.247759	6.000000	6918.652582	12.848537	6.666667	2.858904
14.000000	10.000000	6701.333155	8.200000	7699.744256	4.700000	5734.420482	7.200000	6711.832631	14.641366	6.700000	1.802776
14.000000	5.000000	6559.507473	7.900000	7478.495716	4.900000	5630.700822	7.000000	6556.234670	14.091957	6.600000	1.539480
14.000000	1.000000	6116.670801	8.200000	7154.409206	6.300000	5203.869327	6.800000	6158.316445	15.847458	7.100000	0.984886
14.000000	0.500000	5879.854158	9.800000	6511.827183	4.300000	4716.209226	8.800000	5702.630189	15.972161	7.633333	2.929733
14.000000	0.100000	5099.148301	9.600000	6136.723511	5.500000	4382.019115	9.500000	5205.963642	16.946246	8.200000	2.338803
40.000000	25.000000	5245.676764	12.900000	5934.990949	7.900000	3855.966782	11.700000	5012.211498	21.128246	10.833333	2.610236
40.000000	10.000000	4919.365576	11.000000	5531.591393	8.300000	3565.848968	12.600000	4672.268646	21.529089	10.633333	2.173323
40.000000	5.000000	4632.163372	10.800000	5263.590817	8.200000	3334.007967	12.800000	4409.920719	22.308836	10.600000	2.306513
40.000000	1.000000	3924.299325	14.400000	4468.625611	13.000000	2730.777908	14.900000	3707.900948	23.973233	14.100000	0.984886
40.000000	0.500000	3649.334881	9.500000	4306.527305	10.200000	2436.350144	16.400000	3464.070777	27.388391	12.033333	3.797806
40.000000	0.100000	2906.188452	16.600000	3329.731091	15.900000	1926.585134	20.700000	2720.834892	26.451529	17.733333	2.592939
70.000000	25.000000	3096.891480	17.800000	3332.563290	18.200000	2018.388638	20.600000	2815.947803	24.882774	18.866667	1.514376
70.000000	10.000000	2663.156607	17.800000	2690.696135	18.400000	1907.112965	20.900000	2420.321902	18.372152	19.033333	1.644182
70.000000	5.000000	2317.236021	19.100000	2438.617905	19.400000	1748.355737	19.800000	2168.069888	16.997380	19.433333	0.351188
70.000000	1.000000	1646.029838	22.100000	1714.377032	24.300000	1223.053958	24.100000	1527.820276	17.419492	23.500000	1.216553
70.000000	0.500000	1361.324304	24.700000	1469.194781	24.400000	1010.693104	26.800000	1280.404063	18.722432	25.300000	1.307670
70.000000	0.100000	913.908446	26.700000	1012.200013	28.900000	687.684118	27.900000	871.264192	19.099575	27.833333	1.101514
100.000000	25.000000	923.884681	32.000000	1110.204792	32.000000	963.057058	27.000000	999.048844	9.832973	30.333333	2.886751
100.000000	10.000000	698.614720	30.100000	849.906018	30.800000	734.217544	26.700000	760.912761	10.395352	29.200000	2.193171
100.000000	5.000000	562.882241	31.700000	685.982245	31.100000	580.200378	27.800000	609.688288	10.929764	30.200000	2.100000
100.000000	1.000000	340.630304	33.300000	409.915326	32.300000	333.400100	29.100000	361.315243	11.691695	31.566667	2.193931
100.000000	0.500000	267.858269	34.000000	317.701006	32.000000	254.331775	29.300000	279.963683	11.920815	31.766667	2.358672
100.000000	0.100000	176.447305	30.600000	197.426383	29.000000	159.306579	25.500000	177.726756	10.742379	28.366667	2.608320
130.000000	25.000000	398.634544	33.600000	305.152378	36.600000	294.833940	32.400000	332.873621	17.178845	34.200000	2.163331
130.000000	10.000000	283.006417	30.800000	214.582195	34.300000	212.391026	29.700000	236.659879	16.966217	31.600000	2.402082
130.000000	5.000000	224.361581	29.400000	166.837497	34.600000	160.760105	28.800000	183.986394	19.076262	30.933333	3.189566
130.000000	1.000000	139.780737	27.000000	102.316180	31.700000	101.743764	23.900000	114.613560	19.018075	27.533333	3.927255
130.000000	0.500000	117.502914	23.600000	88.412088	28.900000	86.363226	21.700000	97.426076	17.877354	24.733333	3.731398
130.000000	0.100000	87.560282	19.900000	64.370307	24.700000	63.126831	16.600000	71.685807	19.197316	20.400000	4.073082

Table D-36 Dynamic Modulus Summary Sheet for the Mix 36

Conditions		Specimen 1		Specimen 2		Specimen 3		Modulus		Phase Angle (Degrees)	
Temperature, °F	Frequency, Hz	Modulus, ksi	Phage Angle, degree	Modulus, ksi	Phage Angle, degree	Modulus, ksi	Phage Angle, degree	Avg. Modulus, ksi	CV, %	Avg. P. Angle, degree	Standard Dev, degree
14.000000	25.000000	4819.326876	17.000000	5958.378209	14.700000	5263.231642	6.400000	5346.978909	10.737375	12.700000	5.575841
14.000000	10.000000	5257.249412	12.400000	7463.967420	9.100000	5066.237256	6.900000	5929.151363	22.475670	9.466667	2.768273
14.000000	5.000000	5052.575998	12.400000	7063.980894	8.900000	4868.289373	6.900000	5661.615422	21.512846	9.400000	2.783882
14.000000	1.000000	4483.628261	15.200000	6437.373440	9.200000	4272.782730	6.100000	5064.594810	23.566075	10.166667	4.626374
14.000000	0.500000	4403.544353	14.200000	5876.966544	10.800000	4010.744657	8.300000	4763.751851	20.653344	11.100000	2.961419
14.000000	0.100000	3792.254624	13.200000	5226.320499	12.000000	3562.925234	10.300000	4193.833452	21.495422	11.833333	1.457166
40.000000	25.000000	3733.639381	10.100000	3801.858194	18.600000	3463.084690	11.100000	3666.194088	4.887209	13.266667	4.645787
40.000000	10.000000	3843.893669	13.800000	3969.316413	14.100000	3118.978400	11.600000	3644.062827	12.596936	13.166667	1.365040
40.000000	5.000000	3572.216340	14.700000	3759.673015	12.700000	2870.588963	12.600000	3400.826106	13.780969	13.333333	1.184624
40.000000	1.000000	2681.104460	20.800000	2991.976505	15.600000	2359.213180	14.000000	2677.431382	11.817209	16.800000	3.555278
40.000000	0.500000	2543.522290	18.500000	2834.067168	13.600000	2137.869624	13.700000	2505.153027	13.958475	15.266667	2.800595
40.000000	0.100000	1874.047572	21.800000	2120.639975	20.400000	1669.506166	17.600000	1888.064571	11.964279	19.933333	2.138535
70.000000	25.000000	1828.111803	19.600000	2072.903981	12.300000	1773.573250	17.100000	1891.529678	8.428324	16.333333	3.709897
70.000000	10.000000	1698.582776	21.100000	1810.723746	20.000000	1476.016633	17.600000	1661.774385	10.251838	19.566667	1.789786
70.000000	5.000000	1524.412807	21.700000	1590.929312	20.600000	1293.450449	18.500000	1469.597523	10.624080	20.266667	1.625833
70.000000	1.000000	1054.411594	25.300000	1187.326959	23.500000	948.679918	21.900000	1063.472824	11.244413	23.566667	1.700980
70.000000	0.500000	918.647346	26.800000	991.112283	27.900000	841.268128	20.600000	917.009252	8.171729	25.100000	3.935734
70.000000	0.100000	685.776692	29.400000	742.283743	27.100000	625.321186	21.100000	684.460540	8.545764	25.866667	4.285246
100.000000	25.000000	737.143599	24.700000	615.901265	14.500000	860.278564	20.700000	737.774476	16.561954	19.966667	5.139390
100.000000	10.000000	583.439477	23.800000	567.576172	28.100000	717.719736	21.000000	622.911795	13.242373	24.300000	3.576311
100.000000	5.000000	490.701481	24.500000	527.559967	27.900000	609.166885	20.500000	542.476111	11.175593	24.300000	3.704052
100.000000	1.000000	316.606219	26.000000	349.249770	27.200000	405.181938	22.800000	357.012642	12.547234	25.333333	2.274496
100.000000	0.500000	263.486957	27.500000	287.694836	27.500000	335.346258	23.700000	295.509350	12.372350	26.233333	2.193931
100.000000	0.100000	188.399146	27.200000	193.336637	27.300000	246.049144	22.900000	209.261642	15.270080	25.800000	2.511971
130.000000	25.000000	307.818626	26.600000	255.239431	27.100000	430.224506	21.200000	331.094188	27.117513	24.966667	3.271595
130.000000	10.000000	241.948953	24.400000	192.084313	26.400000	353.587573	21.500000	262.540280	31.498864	24.100000	2.463737
130.000000	5.000000	210.149086	25.500000	153.750832	26.300000	296.159375	20.600000	220.019764	32.595052	24.133333	3.085990
130.000000	1.000000	140.940656	25.000000	104.070131	27.600000	216.220240	20.500000	153.743676	37.179244	24.366667	3.592121
130.000000	0.500000	124.498552	25.600000	87.246367	27.000000	187.950323	20.600000	133.231747	38.216737	24.400000	3.364521
130.000000	0.100000	91.250526	23.800000	62.133443	23.800000	137.367623	19.500000	96.917197	39.142539	22.366667	2.482606

Table D-37 Dynamic Modulus Summary Sheet for the Mix 37

Conditions		Specimen 1		Specimen 2		Specimen 3		Modulus		Phase Angle (Degrees)	
Temperature, °F	Frequency, Hz	Modulus, ksi	Phage Angle, degree	Modulus, ksi	Phage Angle, degree	Modulus, ksi	Phage Angle, degree	Avg. Modulus, ksi	CV, %	Avg. P. Angle, degree	Standard Dev, degree
14.000000	25.000000	5208.837717	8.600000	5017.122298	14.900000	6181.414644	3.400000	5469.124886	11.414341	8.966667	5.758761
14.000000	10.000000	4940.110088	8.600000	5631.878294	9.000000	5904.406560	6.100000	5492.131647	9.051229	7.900000	1.571623
14.000000	5.000000	4690.146724	8.500000	5381.294788	9.500000	5625.446805	5.200000	5232.296106	9.271757	7.733333	2.250185
14.000000	1.000000	3977.706391	9.900000	5194.060059	7.800000	5092.370113	6.700000	4754.712188	14.192761	8.133333	1.625833
14.000000	0.500000	3819.391459	10.600000	4456.591664	10.700000	4905.413468	9.400000	4393.798864	12.420395	10.233333	0.723418
14.000000	0.100000	3299.072865	12.300000	3947.037431	11.900000	4371.040498	7.300000	3872.383598	13.941517	10.500000	2.778489
40.000000	25.000000	2922.056834	9.400000	3011.526718	14.400000	4337.969593	7.300000	3423.851048	23.158508	10.366667	3.647373
40.000000	10.000000	3010.976786	12.200000	3321.688393	12.900000	3869.566388	9.900000	3400.743856	12.783081	11.666667	1.569501
40.000000	5.000000	2721.015060	14.000000	3143.344251	13.600000	3598.392426	9.800000	3154.250579	13.911081	12.466667	2.318045
40.000000	1.000000	2237.662298	15.400000	2649.895577	15.600000	3085.817411	11.100000	2657.791762	15.958086	14.033333	2.542309
40.000000	0.500000	2013.854130	17.000000	2488.587281	19.400000	2742.288180	12.900000	2414.909864	15.311704	16.433333	3.286842
40.000000	0.100000	1519.734542	19.700000	1893.508427	19.200000	2282.892628	13.900000	1898.711866	20.098134	17.600000	3.214032
70.000000	25.000000	1560.693073	19.800000	1705.995032	12.300000	2469.434539	14.100000	1912.040881	25.530500	15.400000	3.915354
70.000000	10.000000	1685.598235	16.000000	1477.113886	20.700000	2050.764548	15.300000	1737.825556	16.708792	17.333333	2.936551
70.000000	5.000000	1555.720042	16.200000	1285.357124	22.100000	1812.335971	16.000000	1551.137712	16.988776	18.100000	3.465545
70.000000	1.000000	1098.825512	19.700000	1018.868534	26.100000	1344.774418	18.700000	1154.156155	14.716571	21.500000	4.014972
70.000000	0.500000	960.003783	18.300000	903.928148	24.700000	1195.185428	19.200000	1019.705786	15.154824	20.733333	3.464583
70.000000	0.100000	705.677376	22.400000	636.357538	26.100000	901.664159	20.700000	747.899691	18.398278	23.066667	2.761038
100.000000	25.000000	804.947099	23.800000	983.756601	22.200000	1182.859906	18.900000	990.521202	19.085628	21.633333	2.498666
100.000000	10.000000	636.174469	25.200000	684.919808	27.600000	936.069058	20.300000	752.387778	21.389101	24.366667	3.720663
100.000000	5.000000	573.043431	21.700000	609.278728	26.800000	799.177965	20.600000	660.500041	18.388719	23.033333	3.308071
100.000000	1.000000	413.457897	22.000000	449.034755	28.000000	543.900963	21.000000	468.797872	14.383565	23.666667	3.785939
100.000000	0.500000	342.334062	22.300000	396.501256	28.200000	454.787497	22.300000	397.874272	14.134940	24.266667	3.406367
100.000000	0.100000	251.369890	24.200000	274.997228	28.700000	324.189940	23.200000	283.519019	13.103335	25.366667	2.929733
130.000000	25.000000	306.995396	27.800000	402.098055	26.700000	543.518723	21.800000	417.537391	28.504065	25.433333	3.194266
130.000000	10.000000	242.385011	25.700000	312.118422	26.100000	427.282204	21.100000	327.261879	28.531943	24.300000	2.778489
130.000000	5.000000	214.280900	25.600000	268.144768	24.500000	361.587187	21.000000	281.337618	26.492741	23.700000	2.402082
130.000000	1.000000	179.276023	24.200000	196.968421	23.200000	240.236636	21.500000	205.493693	15.261660	22.966667	1.365040
130.000000	0.500000	149.299300	20.600000	169.748900	22.600000	219.012402	18.600000	179.353534	19.980237	20.600000	2.000000
130.000000	0.100000	111.919460	18.500000	123.593217	19.600000	161.778008	19.300000	132.430228	19.691534	19.133333	0.568624

Table D-38 Dynamic Modulus Summary Sheet for the Mix 38

Conditions		Specimen 1		Specimen 2		Specimen 3		Modulus		Phase Angle (Degrees)	
Temperature, °F	Frequency, Hz	Modulus, ksi	Phage Angle, degree	Modulus, ksi	Phage Angle, degree	Modulus, ksi	Phage Angle, degree	Avg. Modulus, ksi	CV, %	Avg. P. Angle, degree	Standard Dev, degree
14.000000	25.000000	7116.214695	2.500000	5412.577943	2.700000	7152.342646	1.300000	6560.378428	15.154438	2.166667	0.757188
14.000000	10.000000	7151.043902	6.500000	5610.358133	8.600000	6810.933502	5.300000	6524.111846	12.406284	6.800000	1.670329
14.000000	5.000000	6807.681057	5.700000	5278.053980	9.100000	6661.970892	4.400000	6249.235310	13.509129	6.400000	2.426932
14.000000	1.000000	6265.687955	8.700000	4863.673486	8.400000	5903.204717	5.700000	5677.522053	12.817978	7.600000	1.652271
14.000000	0.500000	5646.036681	5.300000	4395.995738	8.800000	5735.860952	7.500000	5259.297790	14.241241	7.200000	1.769181
14.000000	0.100000	5263.096734	9.500000	3960.757148	12.300000	5085.257555	7.500000	4769.703812	14.805717	9.766667	2.411086
40.000000	25.000000	5072.199613	10.500000	3827.650445	10.800000	4890.133169	9.500000	4596.661076	14.623128	10.266667	0.680686
40.000000	10.000000	4710.235118	10.900000	3611.777339	12.200000	4425.706416	10.300000	4249.239624	13.416389	11.133333	0.971253
40.000000	5.000000	4371.049056	12.700000	3383.498347	12.500000	4253.909959	10.100000	4002.819121	13.478899	11.766667	1.446836
40.000000	1.000000	3492.667133	14.800000	2802.953591	14.200000	3372.377859	13.600000	3222.666194	11.432279	14.200000	0.600000
40.000000	0.500000	3150.256332	15.300000	2403.343502	17.700000	3076.072115	13.100000	2876.557316	14.304959	15.366667	2.300725
40.000000	0.100000	2385.650523	21.600000	1868.280614	20.300000	2412.858439	19.100000	2222.263192	13.808428	20.333333	1.250333
70.000000	25.000000	2630.553819	16.800000	2072.006770	17.000000	2396.670193	17.800000	2366.410261	11.853412	17.200000	0.529150
70.000000	10.000000	2164.350776	19.200000	1742.562087	20.600000	1996.304764	19.800000	1967.739209	10.791081	19.866667	0.702377
70.000000	5.000000	1880.222881	20.500000	1516.844753	21.800000	1806.377240	20.400000	1734.481625	11.073140	20.900000	0.781025
70.000000	1.000000	1284.698105	23.800000	1013.728826	25.300000	1195.197323	24.700000	1164.541418	11.855423	24.600000	0.754983
70.000000	0.500000	1077.316666	25.200000	831.209642	27.300000	995.781844	27.200000	968.102717	12.949714	26.566667	1.184624
70.000000	0.100000	672.183179	28.400000	504.630234	30.600000	629.047840	30.000000	601.953751	14.452999	29.666667	1.137248
100.000000	25.000000	737.445039	31.500000	461.987528	33.000000	918.455719	27.700000	705.962762	32.559339	30.733333	2.731910
100.000000	10.000000	522.740412	33.000000	306.878911	34.000000	669.337633	28.800000	499.652319	36.491181	31.933333	2.759227
100.000000	5.000000	420.717403	33.000000	236.815193	35.200000	526.559471	28.700000	394.697356	37.145976	32.300000	3.306055
100.000000	1.000000	255.248280	30.500000	168.484681	32.300000	316.743303	28.400000	246.825421	30.178146	30.400000	1.951922
100.000000	0.500000	219.840564	27.400000	133.552045	30.200000	250.449759	27.300000	201.280789	30.116449	28.300000	1.646208
100.000000	0.100000	142.091727	22.500000	86.691938	24.700000	157.469073	24.600000	128.750913	28.913805	23.933333	1.242310
130.000000	25.000000	150.078721	34.600000	121.785448	36.000000	254.668465	30.300000	175.510878	39.881818	33.633333	2.970410
130.000000	10.000000	106.871287	29.500000	87.916265	36.000000	183.586554	27.400000	126.124702	40.164921	30.966667	4.483674
130.000000	5.000000	83.762692	26.900000	67.545144	35.000000	139.450865	25.600000	96.919567	38.913909	29.166667	5.093460
130.000000	1.000000	62.898938	20.700000	47.438471	27.700000	100.594869	18.800000	70.310759	38.887805	22.400000	4.687217
130.000000	0.500000	55.306659	19.500000	42.139339	26.300000	89.171345	17.000000	62.205781	39.004667	20.933333	4.812830
130.000000	0.100000	41.238647	15.900000	32.531562	22.700000	73.438451	12.100000	49.069553	43.914095	16.900000	5.370289

Table D-39 Dynamic Modulus Summary Sheet for the Mix 39

Conditions		Specimen 1		Specimen 2		Specimen 3		Modulus		Phase Angle (Degrees)	
Temperature, °F	Frequency, Hz	Modulus, ksi	Phage Angle, degree	Modulus, ksi	Phage Angle, degree	Modulus, ksi	Phage Angle, degree	Avg. Modulus, ksi	CV, %	Avg. P. Angle, degree	Standard Dev, degree
14.000000	25.000000	5124.143869	7.400000	7192.511312	4.100000	6226.837907	6.600000	6181.164363	16.743445	6.033333	1.721434
14.000000	10.000000	4984.735508	8.700000	6867.782175	6.000000	6065.904742	6.400000	5972.807475	15.821187	7.033333	1.457166
14.000000	5.000000	4807.886815	8.800000	6720.967069	6.400000	5741.963150	6.800000	5756.939011	16.616956	7.333333	1.285820
14.000000	1.000000	4204.232884	9.200000	6445.940538	6.100000	5498.138104	6.400000	5382.770509	20.905554	7.233333	1.709776
14.000000	0.500000	4184.950601	9.600000	5749.598802	6.600000	4957.428515	6.500000	4963.992639	15.760393	7.566667	1.761628
14.000000	0.100000	3570.777030	11.400000	5234.785184	9.100000	4540.868457	8.400000	4448.810224	18.787384	9.633333	1.569501
40.000000	25.000000	3769.790542	12.400000	5063.746388	7.800000	4197.609767	9.900000	4343.715566	15.176750	10.033333	2.302897
40.000000	10.000000	3444.031026	13.600000	4508.199086	10.700000	3932.783593	11.400000	3961.671235	13.445635	11.900000	1.513275
40.000000	5.000000	3147.696415	15.000000	4186.540341	11.000000	3639.998516	12.200000	3658.078424	14.205762	12.733333	2.052641
40.000000	1.000000	2544.272553	16.000000	3481.148883	12.200000	2971.357472	14.700000	2998.926303	15.640471	14.300000	1.931321
40.000000	0.500000	2271.444444	21.600000	2979.719163	18.000000	2675.661281	13.800000	2642.274963	13.447340	17.800000	3.903844
40.000000	0.100000	1716.436048	22.200000	2406.200072	19.500000	2033.731314	20.300000	2052.122478	16.824025	20.666667	1.386843
70.000000	25.000000	1682.406281	24.500000	2485.284934	16.200000	2199.217989	21.500000	2122.303068	19.173891	20.733333	4.202777
70.000000	10.000000	1240.608836	24.900000	2048.186063	19.600000	1785.987841	20.600000	1691.594247	24.354564	21.700000	2.816026
70.000000	5.000000	1058.207733	26.600000	1789.557103	20.900000	1541.252963	21.400000	1463.005933	25.420295	22.966667	3.156475
70.000000	1.000000	695.693742	29.400000	1254.948406	26.600000	1011.500377	28.400000	987.380842	28.399013	28.133333	1.418920
70.000000	0.500000	577.044834	30.600000	1012.942153	29.500000	825.652154	29.800000	805.213047	27.156324	29.966667	0.568624
70.000000	0.100000	370.998840	30.200000	639.852238	31.100000	542.359529	28.200000	517.736869	26.288928	29.833333	1.484363
100.000000	25.000000	517.472323	28.900000	715.681608	29.400000	609.721894	29.200000	614.291942	16.146010	29.166667	0.251661
100.000000	10.000000	386.128564	29.200000	515.078938	31.800000	461.636041	28.400000	454.281181	14.261882	29.800000	1.777639
100.000000	5.000000	300.205748	30.200000	454.602398	31.300000	364.384862	28.900000	373.064336	20.790892	30.133333	1.201388
100.000000	1.000000	178.808776	29.100000	310.895545	28.800000	221.223444	27.900000	236.975922	28.457588	28.600000	0.624500
100.000000	0.500000	143.115143	27.500000	269.286554	25.700000	178.904808	27.400000	197.102168	32.990167	26.866667	1.011599
100.000000	0.100000	96.686741	23.200000	187.499469	22.100000	118.754223	23.300000	134.313478	35.263437	22.866667	0.665833
130.000000	25.000000	138.350276	31.300000	231.975329	34.100000	212.028080	31.000000	194.117895	25.404792	32.133333	1.709776
130.000000	10.000000	107.312857	26.700000	183.771653	28.300000	163.078783	30.500000	151.387764	26.123247	28.500000	1.907878
130.000000	5.000000	84.711980	25.900000	175.829774	23.600000	135.040096	29.500000	131.860617	34.613845	26.333333	2.973774
130.000000	1.000000	61.801831	21.800000	132.107223	19.400000	88.582102	23.100000	94.163719	37.682759	21.433333	1.877054
130.000000	0.500000	56.646166	18.700000	116.883643	13.700000	75.619465	22.900000	83.049758	37.084351	18.433333	4.605793
130.000000	0.100000	47.986082	15.800000	100.989004	11.100000	60.670198	16.800000	69.881761	39.604198	14.566667	3.043572

Table D-40 Dynamic Modulus Summary Sheet for the Mix 40

Conditions		Specimen 1		Specimen 2		Specimen 3		Modulus		Phase Angle (Degrees)	
Temperature, °F	Frequency, Hz	Modulus, ksi	Phage Angle, degree	Modulus, ksi	Phage Angle, degree	Modulus, ksi	Phage Angle, degree	Avg. Modulus, ksi	CV, %	Avg. P. Angle, degree	Standard Dev, degree
14.000000	25.000000	5706.707895	8.700000	6294.912384	14.500000	6426.125877	22.600000	6142.582052	6.237393	15.266667	6.981643
14.000000	10.000000	5949.094211	9.300000	6707.394155	6.200000	7119.091574	7.200000	6591.859980	9.003430	7.566667	1.582193
14.000000	5.000000	5782.010688	9.600000	6587.136795	5.500000	6727.758313	7.800000	6365.635265	8.016493	7.633333	2.055075
14.000000	1.000000	5291.814024	10.100000	5854.129361	7.700000	5968.927586	13.800000	5704.956990	6.351796	10.533333	3.073001
14.000000	0.500000	5229.188964	12.300000	5781.156125	10.000000	6042.847064	8.600000	5684.397384	7.307181	10.300000	1.868154
14.000000	0.100000	4291.045949	13.700000	5114.772544	8.800000	5006.890317	12.500000	4804.236270	9.318803	11.666667	2.554082
40.000000	25.000000	4138.200161	12.800000	3041.499089	20.900000	2247.817105	4.100000	3142.505452	30.206172	12.600000	8.401786
40.000000	10.000000	3751.769142	14.000000	3075.084820	14.200000	4349.268653	13.800000	3725.374205	17.112425	14.000000	0.200000
40.000000	5.000000	3440.764800	15.000000	2858.879376	14.800000	4001.160380	14.100000	3433.601519	16.634842	14.633333	0.472582
40.000000	1.000000	2790.080313	17.900000	2297.135876	17.400000	3205.690501	16.900000	2764.302230	16.453538	17.400000	0.500000
40.000000	0.500000	2438.446151	20.600000	2148.206340	18.200000	2798.890681	18.300000	2461.847724	13.240981	19.033333	1.357694
40.000000	0.100000	1801.200396	22.600000	1580.454207	21.700000	2201.606588	20.500000	1861.087064	16.918970	21.600000	1.053565
70.000000	25.000000	2020.553840	23.400000	1591.996247	21.200000	934.460750	13.200000	1515.670279	36.093249	19.266667	5.367805
70.000000	10.000000	1606.902865	23.100000	1320.856229	22.400000	1901.128993	22.500000	1609.629362	18.025640	22.666667	0.378594
70.000000	5.000000	1383.260069	24.500000	1149.408212	23.200000	1610.426578	23.600000	1381.031620	16.691672	23.766667	0.665833
70.000000	1.000000	935.035778	28.000000	773.608240	26.900000	1076.079864	26.800000	928.241294	16.305053	27.233333	0.665833
70.000000	0.500000	787.653188	28.900000	642.356596	28.400000	903.754073	28.000000	777.921286	16.835919	28.433333	0.450925
70.000000	0.100000	500.152446	29.900000	412.028596	29.000000	580.472080	29.600000	497.551041	16.933312	29.500000	0.458258
100.000000	25.000000	609.256099	31.700000	621.562182	26.300000	766.654961	22.200000	665.824414	13.147360	26.733333	4.764801
100.000000	10.000000	480.862475	29.600000	438.815685	29.700000	707.882470	27.600000	542.520210	26.679715	28.966667	1.184624
100.000000	5.000000	385.044948	29.100000	344.276304	30.100000	565.517881	27.700000	431.613044	27.279745	28.966667	1.205543
100.000000	1.000000	240.322948	27.900000	207.647339	29.000000	359.892858	26.700000	269.287715	29.763404	27.866667	1.150362
100.000000	0.500000	201.932168	27.100000	166.613956	27.200000	296.577881	25.200000	221.708002	30.310567	26.500000	1.126943
100.000000	0.100000	146.423002	23.200000	111.098117	23.300000	205.513180	20.700000	154.344766	30.907057	22.400000	1.473092
130.000000	25.000000	274.511704	30.500000	212.922970	35.200000	306.677999	30.800000	264.704224	17.997731	32.166667	2.631223
130.000000	10.000000	206.035695	27.200000	161.323093	29.200000	230.877061	25.600000	199.411950	17.675421	27.333333	1.803700
130.000000	5.000000	169.588026	25.800000	126.429913	27.500000	188.441939	23.200000	161.486626	19.685775	25.500000	2.165641
130.000000	1.000000	120.484673	18.000000	84.280129	22.500000	137.543729	18.600000	114.102844	23.837477	19.700000	2.443358
130.000000	0.500000	100.860914	17.800000	72.636546	20.100000	127.226161	15.900000	100.241207	27.234392	17.933333	2.103172
130.000000	0.100000	84.764203	13.000000	54.814752	16.800000	106.261009	9.800000	81.946655	31.531001	13.200000	3.504283

Table D-41 Dynamic Modulus Summary Sheet for the Mix 41

Conditions		Specimen 1		Specimen 2		Specimen 3		Modulus		Phase Angle (Degrees)	
Temperature, °F	Frequency, Hz	Modulus, ksi	Phage Angle, degree	Modulus, ksi	Phage Angle, degree	Modulus, ksi	Phage Angle, degree	Avg. Modulus, ksi	CV, %	Avg. P. Angle, degree	Standard Dev, degree
14.000000	25.000000	7707.314776	1.800000	5512.483475	11.100000	7689.498204	1.100000	6969.765485	18.107850	4.666667	5.582413
14.000000	10.000000	7848.635641	4.400000	6537.989488	6.000000	7702.231352	4.200000	7362.952160	9.753955	4.866667	0.986577
14.000000	5.000000	7672.733191	5.000000	6175.021741	5.100000	7520.364369	4.100000	7122.706434	11.572110	4.733333	0.550757
14.000000	1.000000	7585.475364	2.500000	5819.751879	8.900000	6863.863167	8.100000	6756.363470	13.139564	6.500000	3.487119
14.000000	0.500000	6679.121046	5.900000	5861.328086	10.600000	6823.751221	0.500000	6454.733451	8.040102	5.666667	5.054041
14.000000	0.100000	6747.704982	124.900000	5239.752993	6.800000	6410.209333	6.700000	6132.555769	12.904737	46.133333	68.213953
40.000000	25.000000	6077.506258	1.600000	4264.716532	16.700000	6773.374800	3.800000	5705.199197	22.700462	7.366667	8.157410
40.000000	10.000000	5974.890959	6.800000	4565.318735	10.900000	6145.686775	6.700000	5561.965490	15.594052	8.133333	2.396525
40.000000	5.000000	5872.669504	6.700000	4405.476150	10.700000	6019.988992	6.500000	5432.711549	16.431137	7.966667	2.369247
40.000000	1.000000	5364.429101	6.500000	3899.851223	11.400000	5364.144634	9.700000	4876.141653	17.339372	9.200000	2.487971
40.000000	0.500000	5135.094344	12.900000	3898.729020	14.800000	5252.682265	5.500000	4762.168543	15.750564	11.066667	4.913587
40.000000	0.100000	4463.144716	8.900000	3193.417202	14.200000	4373.685277	9.000000	4010.082398	17.672102	10.700000	3.031501
70.000000	25.000000	3923.868780	11.400000	2965.719330	16.700000	4080.293983	8.700000	3656.627364	16.502476	12.266667	4.069808
70.000000	10.000000	3397.850972	14.000000	2815.147541	17.200000	3410.704666	13.100000	3207.901060	10.604917	14.766667	2.154840
70.000000	5.000000	3134.034868	14.800000	2645.307977	16.600000	3109.548469	14.000000	2962.963771	9.293745	15.133333	1.331666
70.000000	1.000000	2481.664900	17.900000	2092.605494	18.300000	2414.837526	16.400000	2329.702640	8.929598	17.533333	1.001665
70.000000	0.500000	2289.430593	17.200000	1911.560580	20.300000	2137.167522	16.800000	2112.719565	8.998716	18.100000	1.915724
70.000000	0.100000	1690.120992	22.400000	1392.809966	24.300000	1562.742806	22.400000	1548.557921	9.632331	23.033333	1.096966
100.000000	25.000000	1803.838357	22.400000	1742.061042	19.200000	1298.427687	24.800000	1614.775695	17.073654	22.133333	2.809508
100.000000	10.000000	1428.492430	25.400000	1492.233021	20.300000	979.140713	27.300000	1299.955388	21.512708	24.333333	3.619853
100.000000	5.000000	1413.094485	23.200000	1264.805690	21.200000	820.047666	28.800000	1165.982614	26.469264	24.400000	3.939543
100.000000	1.000000	939.485859	26.300000	824.072424	24.500000	499.354892	31.400000	754.304392	30.254276	27.400000	3.579106
100.000000	0.500000	741.624434	27.600000	650.265256	25.600000	383.938846	31.800000	591.942845	31.394635	28.333333	3.164385
100.000000	0.100000	483.527852	28.600000	412.846749	27.400000	234.025352	30.200000	376.799984	34.128937	28.733333	1.404754
130.000000	25.000000	884.603217	26.000000	560.327111	28.300000	430.567869	33.100000	625.166066	37.407521	29.133333	3.622614
130.000000	10.000000	465.825880	27.700000	418.005460	28.000000	316.629574	32.400000	400.153638	19.038520	29.366667	2.631223
130.000000	5.000000	461.931388	29.700000	333.124917	27.300000	254.583023	30.800000	349.879776	29.920183	29.266667	1.789786
130.000000	1.000000	301.610097	29.000000	201.596203	26.300000	158.820765	27.600000	220.675688	33.207905	27.633333	1.350309
130.000000	0.500000	240.039496	28.800000	152.995057	25.800000	125.238950	25.800000	172.757834	34.671396	26.800000	1.732051
130.000000	0.100000	131.368855	23.700000	103.380504	21.200000	87.382000	21.700000	107.377120	20.734500	22.200000	1.322876

Table D-42 Dynamic Modulus Summary Sheet for the Mix 42

Conditions		Specimen 1		Specimen 2		Specimen 3		Modulus		Phase Angle (Degrees)	
Temperature, °F	Frequency, Hz	Modulus, ksi	Phage Angle, degree	Modulus, ksi	Phage Angle, degree	Modulus, ksi	Phage Angle, degree	Avg. Modulus, ksi	CV, %	Avg. P. Angle, degree	Standard Dev, degree
14.000000	25.000000	7295.012157	0.300000	6275.852482	6.000000	5121.453976	9.000000	6230.772872	17.453374	5.100000	4.419276
14.000000	10.000000	7657.761149	5.500000	5874.324812	9.300000	5542.915984	9.300000	6358.333982	17.889457	8.033333	2.193931
14.000000	5.000000	7333.962443	5.700000	5570.254020	9.300000	5543.009984	9.800000	6149.075482	16.689218	8.266667	2.236813
14.000000	1.000000	6902.772836	6.400000	5155.877443	9.700000	4932.973015	7.800000	5663.874431	19.045102	7.966667	1.656301
14.000000	0.500000	6747.606485	7.400000	4543.605351	10.800000	4652.456885	12.300000	5314.556240	23.374496	10.166667	2.510644
14.000000	0.100000	5660.948666	9.400000	3968.114716	15.900000	4210.093407	12.200000	4613.052263	19.846612	12.500000	3.260368
40.000000	25.000000	5436.532542	9.900000	3965.273378	14.900000	3729.606644	13.500000	4377.137521	21.132508	12.766667	2.579406
40.000000	10.000000	5031.428503	10.400000	3299.300323	16.000000	3480.495812	12.900000	3937.074879	24.181874	13.100000	2.805352
40.000000	5.000000	4710.630849	10.300000	2984.567440	17.000000	3194.129168	12.800000	3629.775819	25.949102	13.366667	3.385754
40.000000	1.000000	3807.635452	14.000000	2321.731216	19.200000	2592.870218	13.500000	2907.412295	27.217179	15.566667	3.156475
40.000000	0.500000	3390.491083	15.200000	1990.316876	18.900000	2292.278604	14.000000	2557.695521	28.809366	16.033333	2.554082
40.000000	0.100000	2600.211684	20.300000	1400.548613	23.200000	1779.330054	19.000000	1926.696784	31.829511	20.833333	2.150194
70.000000	25.000000	2073.844856	22.000000	1577.266459	23.100000	1685.042646	18.800000	1778.717987	14.685098	21.300000	2.233831
70.000000	10.000000	1682.652161	21.500000	1222.123237	25.300000	1452.617913	20.600000	1452.464437	15.853366	22.466667	2.494661
70.000000	5.000000	1422.371520	22.700000	998.461583	26.200000	1278.540494	20.800000	1233.124532	17.481879	23.233333	2.739221
70.000000	1.000000	932.410437	26.500000	621.935863	29.400000	862.511800	24.100000	805.619367	20.216568	26.666667	2.653928
70.000000	0.500000	741.253074	27.600000	480.258145	31.000000	676.991129	27.900000	632.834116	21.488282	28.833333	1.882374
70.000000	0.100000	464.599377	28.300000	288.522997	30.100000	454.508687	26.300000	402.543687	24.562210	28.233333	1.900877
100.000000	25.000000	611.012950	30.500000	399.464446	32.700000	576.518838	26.200000	528.998745	21.455263	29.800000	3.306055
100.000000	10.000000	458.902339	30.100000	277.841903	32.500000	446.856352	27.200000	394.533531	25.659983	29.933333	2.653928
100.000000	5.000000	360.588867	28.700000	212.298767	32.100000	353.569875	27.700000	308.819170	27.091181	29.500000	2.306513
100.000000	1.000000	218.591431	27.600000	129.143742	28.600000	214.793986	27.700000	187.509720	26.975705	27.966667	0.550757
100.000000	0.500000	178.184573	26.300000	104.140921	27.100000	174.570632	27.100000	152.298709	27.409946	26.833333	0.461880
100.000000	0.100000	119.652885	22.100000	73.646761	22.100000	117.097610	25.300000	103.465752	24.989515	23.166667	1.847521
130.000000	25.000000	204.101142	30.900000	119.096861	34.300000	199.403729	30.600000	174.200577	27.427568	31.933333	2.055075
130.000000	10.000000	158.169290	27.600000	90.326623	28.000000	157.504033	28.500000	135.333315	28.801746	28.033333	0.450925
130.000000	5.000000	136.118635	24.400000	78.453696	24.800000	148.807103	28.700000	121.126478	30.956337	25.966667	2.375570
130.000000	1.000000	100.143000	19.600000	55.320005	19.700000	139.242845	21.400000	98.235283	42.748318	20.233333	1.011599
130.000000	0.500000	83.465459	19.200000	48.585625	18.000000	124.450971	20.900000	85.500685	44.413211	19.366667	1.457166
130.000000	0.100000	66.866977	15.100000	40.710619	13.400000	100.564406	15.800000	69.380667	43.248308	14.766667	1.234234

Table D-43 Dynamic Modulus Summary Sheet for the Mix 43

Conditions		Specimen 1		Specimen 2		Specimen 3		Modulus		Phase Angle (Degrees)	
Temperature, °F	Frequency, Hz	Modulus, ksi	Phage Angle, degree	Modulus, ksi	Phage Angle, degree	Modulus, ksi	Phage Angle, degree	Avg. Modulus, ksi	CV, %	Avg. P. Angle, degree	Standard Dev, degree
14.000000	25.000000	6938.615159	4.700000	6988.113807	5.200000	6339.938466	12.200000	6755.555811	5.340568	7.366667	4.193249
14.000000	10.000000	6933.726119	5.000000	6643.418708	6.200000	6601.729208	7.200000	6726.291345	2.688689	6.133333	1.101514
14.000000	5.000000	6734.260738	5.300000	6317.427093	5.500000	6361.471102	6.700000	6471.052978	3.538928	5.833333	0.757188
14.000000	1.000000	6021.698553	8.700000	5827.653721	6.000000	5673.593471	9.900000	5840.981915	2.986396	8.200000	1.997498
14.000000	0.500000	5709.390390	1.300000	5213.641170	8.600000	5402.503500	4.100000	5441.845020	4.597801	4.666667	3.682843
14.000000	0.100000	5242.454201	8.000000	4670.077187	12.300000	4942.211753	10.700000	4951.581047	5.782062	10.333333	2.173323
40.000000	25.000000	5074.306355	8.900000	4423.997145	11.400000	5060.686441	19.200000	4852.996647	7.656854	13.166667	5.372461
40.000000	10.000000	4569.913734	10.600000	4069.269236	14.700000	4176.238005	12.800000	4271.806992	6.171860	12.700000	2.051828
40.000000	5.000000	4326.400282	10.800000	3620.240863	16.100000	3949.836846	13.400000	3965.492664	8.910367	13.433333	2.650157
40.000000	1.000000	3520.662302	15.400000	2750.936223	19.000000	3177.528075	15.500000	3149.708867	12.242921	16.633333	2.050203
40.000000	0.500000	3215.435507	14.100000	2372.825406	20.800000	3073.444309	17.100000	2887.235074	15.624411	17.333333	3.356089
40.000000	0.100000	2389.310449	19.400000	1692.765191	24.900000	2267.446232	19.200000	2116.507291	17.575920	21.166667	3.234708
70.000000	25.000000	2479.542782	15.100000	2044.827722	20.900000	2490.332673	12.100000	2338.234392	10.869522	16.033333	4.473626
70.000000	10.000000	2002.652262	19.700000	1552.564208	26.700000	2205.162069	21.000000	1920.126180	17.396476	22.466667	3.723350
70.000000	5.000000	1723.326225	21.400000	1261.436324	27.900000	1903.502505	20.900000	1629.421685	20.324595	23.400000	3.905125
70.000000	1.000000	1133.916992	26.400000	764.109115	30.800000	1323.199858	25.400000	1073.741988	26.483212	27.533333	2.872862
70.000000	0.500000	933.598789	26.900000	578.231445	31.700000	1111.628290	24.500000	874.486175	31.054494	27.700000	3.666061
70.000000	0.100000	594.181643	27.000000	346.547982	29.000000	728.678624	26.700000	556.469416	34.833284	27.566667	1.250333
100.000000	25.000000	810.506183	28.500000	490.351881	33.200000	772.610065	21.200000	691.156043	25.309876	27.633333	6.046762
100.000000	10.000000	612.552788	26.600000	336.277995	32.100000	637.160749	29.600000	528.663844	31.601316	29.433333	2.753785
100.000000	5.000000	478.025923	25.800000	271.191660	31.700000	604.948614	25.400000	451.388732	37.321572	27.633333	3.527511
100.000000	1.000000	290.064286	28.800000	161.246790	27.800000	378.233105	26.100000	276.514727	39.464763	27.566667	1.365040
100.000000	0.500000	246.589356	25.200000	136.441834	26.200000	320.191003	24.700000	234.407398	39.451962	25.366667	0.763763
100.000000	0.100000	176.686513	18.600000	98.973361	22.000000	221.399695	21.300000	165.686523	37.389881	20.633333	1.795364
130.000000	25.000000	245.446845	32.800000	189.957407	26.300000	374.601176	29.100000	270.001809	35.088404	29.400000	3.260368
130.000000	10.000000	197.104489	28.600000	147.792827	23.900000	262.876970	25.000000	202.591429	28.499696	25.833333	2.458319
130.000000	5.000000	162.987684	25.900000	122.570381	21.400000	225.620433	23.800000	170.392833	30.472286	23.700000	2.251666
130.000000	1.000000	122.353948	19.100000	93.589223	16.500000	145.945456	19.000000	120.629542	21.736531	18.200000	1.473092
130.000000	0.500000	104.509380	18.800000	76.466195	15.000000	121.253069	21.300000	100.742881	22.462884	18.366667	3.172276
130.000000	0.100000	80.904526	13.000000	64.994655	11.400000	92.613242	15.900000	79.504141	17.436130	13.433333	2.281082

Table D-44 Dynamic Modulus Summary Sheet for the Mix 44

Conditions		Specimen 1		Specimen 2		Specimen 3		Modulus		Phase Angle (Degrees)	
Temperature, °F	Frequency, Hz	Modulus, ksi	Phage Angle, degree	Modulus, ksi	Phage Angle, degree	Modulus, ksi	Phage Angle, degree	Avg. Modulus, ksi	CV, %	Avg. P. Angle, degree	Standard Dev, degree
14.000000	25.000000	7287.067086	5.500000	7593.870854	4.400000	6879.112423	3.200000	7253.350121	4.943510	4.366667	1.150362
14.000000	10.000000	8051.489100	6.900000	7692.870907	5.900000	6978.645000	6.600000	7574.335002	7.210617	6.466667	0.513160
14.000000	5.000000	7678.450102	7.000000	7497.989645	5.900000	6755.058488	6.600000	7310.499412	6.694692	6.500000	0.556776
14.000000	1.000000	6770.331970	10.500000	6740.987430	6.800000	5963.037760	8.700000	6491.452387	7.053208	8.666667	1.850225
14.000000	0.500000	6632.925470	12.000000	6608.001999	10.700000	6020.347151	3.800000	6420.424873	5.399978	8.833333	4.407191
14.000000	0.100000	5774.286112	10.000000	5672.349125	10.400000	5277.548002	9.500000	5574.727746	4.706303	9.966667	0.450925
40.000000	25.000000	4395.520949	10.900000	5326.670358	7.500000	4919.193822	7.500000	4880.461710	9.564289	8.633333	1.962991
40.000000	10.000000	4313.646970	16.300000	5184.077875	10.500000	4570.518934	10.900000	4689.414593	9.537010	12.566667	3.239341
40.000000	5.000000	4022.104643	17.100000	4746.661318	11.100000	4122.319303	12.400000	4297.028421	9.136644	13.533333	3.156475
40.000000	1.000000	3087.361021	19.200000	3855.544070	13.700000	3332.876625	17.400000	3425.260572	11.454189	16.766667	2.804164
40.000000	0.500000	2750.019864	19.100000	3378.492241	13.200000	3037.952167	15.100000	3055.488091	10.296324	15.800000	3.011644
40.000000	0.100000	1970.769274	23.300000	2667.396638	18.000000	2163.191437	24.000000	2267.119116	15.868345	21.766667	3.280752
70.000000	25.000000	1621.674431	24.100000	2622.955157	11.700000	2337.388098	21.400000	2194.005895	23.509949	19.066667	6.520992
70.000000	10.000000	1595.877103	23.100000	2293.465215	19.800000	1878.515061	22.100000	1922.619126	18.250060	21.666667	1.692139
70.000000	5.000000	1347.695686	24.500000	2060.706114	21.300000	1607.084483	25.600000	1671.828761	21.586395	23.800000	2.233831
70.000000	1.000000	889.435393	28.000000	1310.473674	25.900000	1137.473198	31.100000	1112.460755	19.023649	28.333333	2.615977
70.000000	0.500000	730.924627	30.800000	1110.798097	28.500000	908.461931	32.000000	916.728218	20.733691	30.433333	1.778576
70.000000	0.100000	446.504866	30.800000	707.143087	29.200000	563.550979	33.000000	572.399644	22.806483	31.000000	1.907878
100.000000	25.000000	656.309139	30.200000	798.175438	28.400000	778.166393	27.900000	744.216990	10.317553	28.833333	1.209683
100.000000	10.000000	497.951848	30.700000	589.648006	29.200000	577.094010	30.900000	554.897955	8.959239	30.266667	0.929157
100.000000	5.000000	394.174744	29.000000	462.023648	30.000000	472.069804	31.000000	442.756065	9.569931	30.000000	1.000000
100.000000	1.000000	235.469884	27.800000	282.047409	29.800000	298.454118	30.700000	271.990470	12.013032	29.433333	1.484363
100.000000	0.500000	192.530235	26.100000	225.036266	28.600000	258.053643	29.400000	225.206715	14.547540	28.033333	1.721434
100.000000	0.100000	129.082525	21.400000	145.862626	24.600000	198.041303	24.700000	157.662151	22.809395	23.566667	1.877054
130.000000	25.000000	194.520492	29.200000	200.256261	32.700000	286.136430	36.600000	226.971061	22.610331	32.833333	3.701801
130.000000	10.000000	138.982168	27.800000	155.423692	26.000000	253.723383	29.700000	182.709748	33.959119	27.833333	1.850225
130.000000	5.000000	112.854968	24.800000	126.282965	23.900000	209.318748	28.200000	149.485560	34.953356	25.633333	2.267892
130.000000	1.000000	78.109462	20.600000	88.683210	19.900000	164.251468	21.800000	110.348047	42.574525	20.766667	0.960902
130.000000	0.500000	66.127158	19.800000	80.241881	16.400000	142.151202	17.400000	96.173414	42.047507	17.866667	1.747379
130.000000	0.100000	54.388849	15.200000	63.126106	15.100000	116.834757	12.900000	78.116571	43.287003	14.400000	1.300000

Table D-45 Dynamic Modulus Summary Sheet for the Mix 45

Conditions		Specimen 1		Specimen 2		Specimen 3		Modulus		Phase Angle (Degrees)	
Temperature, °F	Frequency, Hz	Modulus, ksi	Phage Angle, degree	Modulus, ksi	Phage Angle, degree	Modulus, ksi	Phage Angle, degree	Avg. Modulus, ksi	CV, %	Avg. P. Angle, degree	Standard Dev, degree
14.000000	25.000000	7818.050091	2.700000	9121.626770	3.400000	10525.293646	7.100000	9154.990169	14.788985	4.400000	2.364318
14.000000	10.000000	7899.619438	7.100000	9636.076572	7.200000	11112.914404	4.800000	9549.536805	16.842645	6.366667	1.357694
14.000000	5.000000	7855.275005	5.600000	9405.504287	9.100000	10728.922755	7.400000	9329.900682	15.416187	7.366667	1.750238
14.000000	1.000000	7368.820517	9.200000	9092.394944	6.800000	9854.616506	11.100000	8771.943989	14.517920	9.033333	2.154840
14.000000	0.500000	6805.604778	9.400000	8164.365248	6.900000	9914.553414	7.500000	8294.841147	18.789700	7.933333	1.305118
14.000000	0.100000	6374.567051	8.900000	8020.957369	8.600000	9049.370288	6.900000	7814.964903	17.264916	8.133333	1.078579
40.000000	25.000000	5442.844935	7.200000	6579.757902	3.400000	8449.157964	7.600000	6823.920267	22.244635	6.066667	2.318045
40.000000	10.000000	5412.895775	11.900000	6450.064084	9.900000	8104.523501	9.800000	6655.827787	20.396560	10.533333	1.184624
40.000000	5.000000	5130.481358	12.000000	6161.835708	10.500000	7754.331405	9.400000	6348.882824	20.820793	10.633333	1.305118
40.000000	1.000000	4264.210264	13.900000	5323.411530	11.900000	6266.485218	11.400000	5284.702337	18.954683	12.400000	1.322876
40.000000	0.500000	4168.042266	14.600000	4672.577484	17.400000	6565.968990	11.900000	5135.529580	24.617164	14.633333	2.750152
40.000000	0.100000	3281.100932	16.800000	3785.434948	18.000000	5182.545726	14.600000	4083.027202	24.125115	16.466667	1.724336
70.000000	25.000000	3233.149084	13.100000	3233.377993	12.000000	5102.762533	8.300000	3856.429870	27.988471	11.133333	2.514624
70.000000	10.000000	2702.078751	18.500000	2598.608164	18.700000	3704.235075	17.100000	3001.640663	20.344210	18.100000	0.871780
70.000000	5.000000	2385.067953	18.400000	2295.007955	19.900000	3338.984045	18.900000	2673.019984	21.642076	19.066667	0.763763
70.000000	1.000000	1681.541853	24.800000	1610.301969	24.200000	2431.891359	20.400000	1907.911727	23.857264	23.133333	2.386071
70.000000	0.500000	1548.589352	25.500000	1367.047453	26.600000	2305.639147	24.900000	1740.425317	28.604197	25.666667	0.862168
70.000000	0.100000	935.612256	29.600000	919.452008	30.000000	1506.731143	27.000000	1120.598469	29.849970	28.866667	1.628906
100.000000	25.000000	1336.822674	25.200000	1088.480673	32.200000	1840.242942	26.500000	1421.848763	26.938570	27.966667	3.723350
100.000000	10.000000	988.336513	27.700000	745.055886	32.900000	1275.741369	26.200000	1003.044589	26.484196	28.933333	3.516153
100.000000	5.000000	779.137006	29.100000	595.741644	32.500000	993.920402	27.100000	789.599684	25.240064	29.566667	2.730079
100.000000	1.000000	502.714539	30.300000	377.883939	31.500000	596.299990	29.800000	492.299489	22.258782	30.533333	0.873689
100.000000	0.500000	407.687457	29.800000	316.627689	30.200000	476.872532	30.500000	400.395893	20.072852	30.166667	0.351188
100.000000	0.100000	259.291316	26.800000	219.650532	24.600000	287.188858	27.700000	255.376902	13.289726	26.366667	1.594783
130.000000	25.000000	317.323698	37.400000	537.834886	33.200000	680.443615	36.700000	511.867400	35.741171	35.766667	2.250185
130.000000	10.000000	218.117657	32.200000	396.573642	28.500000	448.611173	31.300000	354.434157	34.106982	30.666667	1.929594
130.000000	5.000000	167.212483	29.300000	320.894411	27.000000	360.441339	30.600000	282.849411	36.089162	28.966667	1.823001
130.000000	1.000000	125.660067	25.200000	212.120630	22.400000	220.195677	29.700000	185.992125	28.175850	25.766667	3.682843
130.000000	0.500000	103.651045	22.800000	176.315588	20.600000	173.875492	26.200000	151.280708	27.278123	23.200000	2.821347
130.000000	0.100000	77.551697	18.700000	135.122201	17.300000	130.178037	22.400000	114.283978	27.919048	19.466667	2.635021

Table D-46 Dynamic Modulus Summary Sheet for the Mix 46

Conditions		Specimen 1		Specimen 2		Specimen 3		Modulus		Phase Angle (Degrees)	
Temperature, °F	Frequency, Hz	Modulus, ksi	Phage Angle, degree	Modulus, ksi	Phage Angle, degree	Modulus, ksi	Phage Angle, degree	Avg. Modulus, ksi	CV, %	Avg. P. Angle, degree	Standard Dev, degree
14.000000	25.000000	7981.012535	8.000000	6693.969640	5.200000	7521.522547	3.200000	7398.834907	8.815359	5.466667	2.411086
14.000000	10.000000	8234.440571	5.500000	7072.549153	4.900000	7460.151552	5.200000	7589.047092	7.795088	5.200000	0.300000
14.000000	5.000000	7681.045995	5.800000	7003.742547	3.800000	7029.317784	6.200000	7238.035442	5.303531	5.266667	1.285820
14.000000	1.000000	7330.687803	8.400000	6563.046707	4.400000	6724.171499	7.500000	6872.635336	5.889780	6.766667	2.098412
14.000000	0.500000	6942.751760	11.300000	5778.526288	6.900000	5856.571633	8.400000	6192.616560	10.509404	8.866667	2.236813
14.000000	0.100000	6254.511328	6.700000	5576.860600	5.200000	5635.890867	6.200000	5822.420932	6.446862	6.033333	0.763763
40.000000	25.000000	5283.416794	9.800000	5264.919009	6.400000	5602.796752	7.100000	5383.710852	3.528407	7.766667	1.795364
40.000000	10.000000	5441.577380	10.000000	5095.591515	8.800000	5223.172789	9.500000	5253.447228	3.330546	9.433333	0.602771
40.000000	5.000000	5111.866218	10.500000	4900.093738	8.500000	4837.436474	9.900000	4949.798810	2.905339	9.633333	1.026320
40.000000	1.000000	4123.698267	13.400000	3997.068893	12.300000	4121.924588	11.800000	4080.897249	1.779092	12.500000	0.818535
40.000000	0.500000	3645.073381	15.800000	3861.143916	12.000000	3595.140271	16.600000	3700.452523	3.820740	14.800000	2.457641
40.000000	0.100000	2924.832895	18.000000	3008.375526	14.800000	2917.663328	16.800000	2950.290583	1.709344	16.533333	1.616581
70.000000	25.000000	2253.588850	18.900000	2654.792596	19.000000	2880.719545	14.200000	2596.366997	12.233304	17.366667	2.742870
70.000000	10.000000	2016.942945	22.100000	2398.112549	20.000000	2345.487515	19.500000	2253.514336	9.166110	20.533333	1.379613
70.000000	5.000000	1693.202119	22.800000	2191.305848	19.700000	2030.470020	20.100000	1971.659329	12.893014	20.866667	1.686219
70.000000	1.000000	1207.973409	28.400000	1500.461834	24.900000	1435.294409	23.600000	1381.243217	11.117013	25.633333	2.482606
70.000000	0.500000	1036.628532	28.200000	1305.052254	24.300000	1178.677900	25.300000	1173.452895	11.443844	25.933333	2.025669
70.000000	0.100000	668.201794	31.300000	833.132735	26.900000	773.013484	28.000000	758.116004	11.010002	28.733333	2.289833
100.000000	25.000000	767.245366	30.000000	1151.500158	25.400000	801.508103	31.000000	906.751209	23.451857	28.800000	2.986637
100.000000	10.000000	577.197875	29.200000	831.494255	25.400000	554.698107	32.500000	654.463412	23.488769	29.033333	3.552933
100.000000	5.000000	440.553534	29.800000	670.745755	26.500000	418.186208	30.300000	509.828499	27.422253	28.866667	2.064784
100.000000	1.000000	264.385329	30.100000	417.780613	26.800000	241.942426	28.900000	308.036123	31.068329	28.600000	1.670329
100.000000	0.500000	213.388186	29.600000	338.146979	26.600000	190.908001	27.900000	247.481055	32.050708	28.033333	1.504438
100.000000	0.100000	135.275242	26.800000	222.931555	24.900000	124.172016	22.800000	160.792938	33.645275	24.833333	2.000833
130.000000	25.000000	220.970601	34.000000	384.120610	34.100000	211.107369	31.700000	272.066193	35.714544	33.266667	1.357694
130.000000	10.000000	158.763756	30.000000	292.797118	29.900000	154.708534	27.800000	202.089803	38.884200	29.233333	1.242310
130.000000	5.000000	126.097285	27.400000	235.067045	27.800000	125.909139	25.500000	162.357823	38.783535	26.900000	1.228821
130.000000	1.000000	82.583769	23.400000	152.911211	22.800000	84.889827	20.800000	106.794936	37.412361	22.333333	1.361372
130.000000	0.500000	71.870036	22.200000	128.946747	21.000000	71.811576	18.800000	90.876120	36.280316	20.666667	1.724336
130.000000	0.100000	59.896290	17.100000	94.196454	17.700000	55.412990	15.700000	69.835245	30.380336	16.833333	1.026320

Table D-47 Dynamic Modulus Summary Sheet for the Mix 47

Conditions		Specimen 1		Specimen 2		Specimen 3		Modulus		Phase Angle (Degrees)	
Temperature, °F	Frequency, Hz	Modulus, ksi	Phage Angle, degree	Modulus, ksi	Phage Angle, degree	Modulus, ksi	Phage Angle, degree	Avg. Modulus, ksi	CV, %	Avg. P. Angle, degree	Standard Dev, degree
14.000000	25.000000	6190.226608	3.600000	7974.000215	1.600000	7427.481310	7.600000	7197.236044	12.697995	4.266667	3.055050
14.000000	10.000000	5988.309817	6.000000	7641.113636	5.600000	6567.593545	5.600000	6732.338999	12.456702	5.733333	0.230940
14.000000	5.000000	5788.781479	5.700000	7354.676347	6.100000	6377.937433	5.000000	6507.131753	12.154379	5.600000	0.556776
14.000000	1.000000	5339.288471	7.800000	6533.362285	7.100000	5867.245619	8.300000	5913.298792	10.119014	7.733333	0.602771
14.000000	0.500000	4989.754234	6.300000	6514.726256	6.600000	5526.962450	4.200000	5677.147647	13.624793	5.700000	1.307670
14.000000	0.100000	4586.331033	7.600000	5659.160917	7.600000	4989.517927	9.000000	5078.336626	10.670852	8.066667	0.808290
40.000000	25.000000	4237.964113	6.400000	4529.694006	5.400000	4751.447799	7.500000	4506.368639	5.714919	6.433333	1.050397
40.000000	10.000000	3821.449315	10.100000	4107.752711	11.800000	4299.187579	9.900000	4076.129868	5.898583	10.600000	1.044031
40.000000	5.000000	3584.740453	11.100000	3816.649778	12.500000	4030.583979	10.000000	3810.658070	5.851539	11.200000	1.252996
40.000000	1.000000	3020.193620	13.900000	3155.847475	14.800000	3390.048787	10.600000	3188.696627	5.867693	13.100000	2.211334
40.000000	0.500000	2904.211105	11.200000	2836.130391	13.400000	2998.592949	10.600000	2912.978148	2.800753	11.733333	1.474223
40.000000	0.100000	2184.494440	18.100000	2153.112932	19.100000	2395.229143	17.800000	2244.278838	5.866699	18.333333	0.680686
70.000000	25.000000	2194.705386	14.500000	1818.462249	20.200000	2491.890353	12.600000	2168.352663	15.564193	15.766667	3.955165
70.000000	10.000000	1867.616518	18.900000	1525.379503	22.700000	1995.658801	18.100000	1796.218274	13.535859	19.900000	2.457641
70.000000	5.000000	1712.431019	19.200000	1337.489236	22.700000	1769.364988	20.100000	1606.428414	14.606402	20.666667	1.817507
70.000000	1.000000	1210.376224	22.300000	880.142402	27.400000	1261.274435	23.600000	1117.264354	18.520644	24.433333	2.650157
70.000000	0.500000	979.517876	25.900000	748.248856	27.000000	1054.865349	24.700000	927.544027	17.226046	25.866667	1.150362
70.000000	0.100000	640.075199	27.300000	454.668691	28.900000	668.453768	28.400000	587.732553	19.755069	28.200000	0.818535
100.000000	25.000000	778.486981	27.500000	667.654039	29.000000	788.980654	25.300000	745.040558	9.022833	27.266667	1.861003
100.000000	10.000000	566.801829	28.300000	452.684382	31.500000	580.682710	29.500000	533.389640	13.167964	29.766667	1.616581
100.000000	5.000000	446.608876	28.200000	355.785849	31.500000	442.427450	28.600000	414.940725	12.356529	29.433333	1.800926
100.000000	1.000000	276.749293	25.700000	207.607302	29.800000	269.211557	27.100000	251.189384	15.100517	27.533333	2.084067
100.000000	0.500000	222.921401	24.400000	173.569556	27.900000	214.334138	26.300000	203.608365	12.949527	26.200000	1.752142
100.000000	0.100000	154.172238	19.900000	119.868013	22.400000	143.776337	21.600000	139.272196	12.629991	21.300000	1.276715
130.000000	25.000000	200.692174	32.100000	203.209588	32.500000	237.059913	31.900000	213.653892	9.505679	32.166667	0.305505
130.000000	10.000000	143.268038	28.400000	145.437447	29.400000	170.059624	27.200000	152.921703	9.731424	28.333333	1.101514
130.000000	5.000000	115.932033	25.700000	117.149687	26.100000	136.702801	25.100000	123.261507	9.456653	25.633333	0.503322
130.000000	1.000000	77.403008	21.100000	81.215975	19.200000	92.537665	20.000000	83.718883	9.402478	20.100000	0.953939
130.000000	0.500000	65.124776	19.800000	70.487155	16.200000	81.891676	16.000000	72.501202	11.810803	17.333333	2.138535
130.000000	0.100000	50.079478	15.800000	57.272545	12.600000	67.072095	12.200000	58.141373	14.670381	13.533333	1.973153

Table D-48 Dynamic Modulus Summary Sheet for the Mix 48

Conditions		Specimen 1		Specimen 2		Specimen 3		Modulus		Phase Angle (Degrees)	
Temperature, °F	Frequency, Hz	Modulus, ksi	Phage Angle, degree	Modulus, ksi	Phage Angle, degree	Modulus, ksi	Phage Angle, degree	Avg. Modulus, ksi	CV, %	Avg. P. Angle, degree	Standard Dev, degree
14.000000	25.000000	6492.783238	1.600000	6564.022542	1.700000	6649.292578	2.100000	6568.699453	1.192921	1.800000	0.264575
14.000000	10.000000	6296.421904	5.300000	6337.045050	5.300000	6264.867482	5.200000	6299.444812	0.574394	5.266667	0.057735
14.000000	5.000000	6133.677779	5.100000	6136.340981	5.000000	6170.823924	4.800000	6146.947561	0.337084	4.966667	0.152753
14.000000	1.000000	5737.312157	4.700000	5698.499390	6.200000	5594.363256	4.200000	5676.724934	1.302162	5.033333	1.040833
14.000000	0.500000	5503.337722	7.800000	5435.090331	8.900000	5345.406045	7.100000	5427.944699	1.459262	7.933333	0.907377
14.000000	0.100000	4895.261417	6.600000	4917.357331	6.400000	4881.583622	7.700000	4898.067457	0.368537	6.900000	0.700000
40.000000	25.000000	4731.987379	5.300000	4656.633088	5.400000	4660.305780	5.600000	4682.975416	0.907229	5.433333	0.152753
40.000000	10.000000	4287.488437	9.600000	4222.578063	9.800000	4221.838970	9.500000	4243.968490	0.888112	9.633333	0.152753
40.000000	5.000000	3974.151925	10.100000	3950.071267	10.300000	3924.994174	10.500000	3949.739122	0.622334	10.300000	0.200000
40.000000	1.000000	3305.200303	13.200000	3289.951192	11.500000	3291.765634	11.500000	3295.639043	0.252754	12.066667	0.981495
40.000000	0.500000	3139.766141	12.700000	2969.775711	12.700000	2971.254913	12.300000	3026.932255	3.228345	12.566667	0.230940
40.000000	0.100000	2398.971319	17.800000	2392.741902	17.300000	2387.410566	17.300000	2393.041262	0.241792	17.466667	0.288675
70.000000	25.000000	2410.770410	12.400000	2402.586856	12.800000	2344.698375	13.400000	2386.018547	1.509523	12.866667	0.503322
70.000000	10.000000	2038.303538	18.500000	1984.527868	18.400000	1970.229787	18.800000	1997.687064	1.796780	18.566667	0.208167
70.000000	5.000000	1779.401570	19.700000	1733.347285	19.800000	1689.764139	19.800000	1734.170998	2.584773	19.766667	0.057735
70.000000	1.000000	1225.905015	22.800000	1182.358280	23.100000	1148.580631	23.500000	1185.614642	3.269604	23.133333	0.351188
70.000000	0.500000	1017.816977	24.400000	975.030804	24.500000	949.114090	24.900000	980.653957	3.537936	24.600000	0.264575
70.000000	0.100000	652.871158	26.000000	623.132338	24.900000	605.512036	25.000000	627.171844	3.816590	25.300000	0.608276
100.000000	25.000000	782.919074	26.900000	775.395990	28.400000	757.307717	29.400000	771.874260	1.705442	28.233333	1.258306
100.000000	10.000000	582.161042	28.200000	562.867154	28.100000	559.116709	28.400000	568.048302	2.176754	28.233333	0.152753
100.000000	5.000000	456.438018	28.500000	439.152810	28.500000	432.036916	28.400000	442.542581	2.835605	28.466667	0.057735
100.000000	1.000000	267.706679	27.000000	260.698131	26.800000	257.289599	26.500000	261.898136	2.027966	26.766667	0.251661
100.000000	0.500000	215.400492	25.600000	208.033785	25.800000	205.079878	25.700000	209.504718	2.537038	25.700000	0.100000
100.000000	0.100000	141.789852	21.000000	140.950520	19.100000	136.140830	20.600000	139.627067	2.183099	20.233333	1.001665
130.000000	25.000000	143.844372	38.900000	113.699232	39.900000	111.018622	38.900000	122.854075	14.836687	39.233333	0.577350
130.000000	10.000000	88.915020	33.100000	79.563133	33.500000	73.738730	32.400000	80.738961	9.482616	33.000000	0.556776
130.000000	5.000000	74.476083	29.800000	60.420546	31.200000	56.103487	29.900000	63.666705	15.089257	30.300000	0.781025
130.000000	1.000000	49.918024	22.800000	39.118269	26.600000	34.115064	24.600000	41.050452	19.675103	24.666667	1.900877
130.000000	0.500000	41.491345	21.000000	35.034615	24.800000	28.532481	23.400000	35.019480	18.502403	23.066667	1.921805
130.000000	0.100000	32.644711	15.700000	28.832615	18.600000	20.728120	19.300000	27.401815	22.209392	17.866667	1.908752

Table D-49 Dynamic Modulus Summary Sheet for the Mix 49

Conditions		Specimen 1		Specimen 2		Specimen 3		Modulus		Phase Angle (Degrees)	
Temperature, °F	Frequency, Hz	Modulus, ksi	Phage Angle, degree	Modulus, ksi	Phage Angle, degree	Modulus, ksi	Phage Angle, degree	Avg. Modulus, ksi	CV, %	Avg. P. Angle, degree	Standard Dev, degree
14.000000	25.000000	8597.682050	1.500000	8974.924378	1.900000	9029.695031	4.900000	8867.433820	2.652532	2.766667	1.858315
14.000000	10.000000	9699.924509	5.200000	9571.068136	5.700000	9582.085050	4.400000	9617.692565	0.742670	5.100000	0.655744
14.000000	5.000000	9328.910147	5.400000	9285.928140	5.000000	9231.878738	5.700000	9282.239008	0.523805	5.366667	0.351188
14.000000	1.000000	8330.117822	4.100000	8685.064050	5.700000	8465.658819	6.500000	8493.613564	2.108840	5.433333	1.222020
14.000000	0.500000	8285.686206	5.300000	8456.946512	7.600000	8542.358854	11.300000	8428.330524	1.550808	8.066667	3.027100
14.000000	0.100000	7440.194729	5.600000	7470.631155	6.300000	7590.011322	8.000000	7500.279069	1.055781	6.633333	1.234234
40.000000	25.000000	6233.337866	5.800000	6445.193757	10.100000	6963.319441	7.600000	6547.283688	5.735910	7.833333	2.159475
40.000000	10.000000	5685.572439	10.900000	6352.251223	11.500000	6160.449201	10.000000	6066.090954	5.657836	10.800000	0.754983
40.000000	5.000000	5336.352117	11.000000	5831.972811	12.800000	6141.877725	10.000000	5770.067551	7.041776	11.266667	1.418920
40.000000	1.000000	4366.257063	15.100000	4622.061222	14.700000	4860.337629	13.500000	4616.218638	5.352695	14.433333	0.832666
40.000000	0.500000	4476.044250	17.800000	4032.402917	10.000000	4101.149468	12.900000	4203.198878	5.680866	13.566667	3.942503
40.000000	0.100000	3336.914294	16.800000	3449.543690	19.300000	3616.346807	19.400000	3467.601597	4.054351	18.500000	1.473092
70.000000	25.000000	2862.037241	15.300000	3300.843642	15.700000	3275.515156	14.700000	3146.132013	7.830536	15.233333	0.503322
70.000000	10.000000	2418.496146	22.800000	2877.887636	19.800000	2823.553476	19.800000	2706.645753	9.274184	20.800000	1.732051
70.000000	5.000000	2240.738637	24.300000	2583.638298	20.800000	2619.083150	20.700000	2481.153362	8.421816	21.933333	2.050203
70.000000	1.000000	1581.149201	27.900000	1803.841693	22.400000	1798.269554	23.600000	1727.753483	7.350215	24.633333	2.891943
70.000000	0.500000	1343.957426	29.700000	1542.967746	25.000000	1526.545225	27.100000	1471.156799	7.508615	27.266667	2.354428
70.000000	0.100000	944.315859	33.100000	1005.222654	28.200000	972.106345	28.200000	973.881619	3.130995	29.833333	2.829016
100.000000	25.000000	1051.225732	23.100000	821.208746	23.800000	839.800676	26.300000	904.078385	14.132840	24.400000	1.682260
100.000000	10.000000	638.535216	30.300000	601.895194	30.300000	629.259777	31.400000	623.230062	3.056607	30.666667	0.635085
100.000000	5.000000	502.448349	31.200000	503.459435	32.100000	491.407065	32.300000	499.104950	1.339539	31.866667	0.585947
100.000000	1.000000	294.795643	33.200000	339.338958	32.300000	302.061242	33.200000	312.065281	7.657832	32.900000	0.519615
100.000000	0.500000	233.522855	33.400000	270.352473	31.200000	241.404824	32.800000	248.426717	7.806295	32.466667	1.137248
100.000000	0.100000	126.175619	29.500000	147.693749	28.700000	122.492048	28.700000	132.120472	10.302742	28.966667	0.461880
130.000000	25.000000	227.735879	37.800000	218.572863	38.600000	225.535426	39.000000	223.948056	2.135900	38.466667	0.611010
130.000000	10.000000	165.815822	33.900000	163.735771	33.700000	175.978173	34.400000	168.509922	3.887475	34.000000	0.360555
130.000000	5.000000	128.902358	31.800000	132.452616	31.800000	145.424972	32.000000	135.593315	6.414431	31.866667	0.115470
130.000000	1.000000	87.848231	27.500000	93.181887	26.300000	93.670458	25.800000	91.566859	3.527125	26.533333	0.873689
130.000000	0.500000	73.778187	26.000000	76.487954	24.200000	76.793166	23.500000	75.686436	2.192761	24.566667	1.289703
130.000000	0.100000	55.640303	19.200000	56.020656	18.300000	55.123155	18.400000	55.594705	0.810301	18.633333	0.493288

Table D-50 Dynamic Modulus Summary Sheet for the Mix 50

Conditions		Specimen 1		Specimen 2		Specimen 3		Modulus		Phase Angle (Degrees)	
Temperature, °F	Frequency, Hz	Modulus, ksi	Phage Angle, degree	Modulus, ksi	Phage Angle, degree	Modulus, ksi	Phage Angle, degree	Avg. Modulus, ksi	CV, %	Avg. P. Angle, degree	Standard Dev, degree
14.000000	25.000000	5362.064438	12.800000	5678.065457	12.400000	5972.027716	10.500000	5670.719204	5.379353	11.900000	1.228821
14.000000	10.000000	5319.356019	13.200000	5692.905491	11.700000	5956.079984	10.900000	5656.113831	5.656754	11.933333	1.167619
14.000000	5.000000	5117.650583	13.200000	5557.839285	11.800000	5806.536399	11.200000	5494.008756	6.349653	12.066667	1.026320
14.000000	1.000000	4594.537796	12.500000	4884.146586	13.700000	5088.292987	16.500000	4855.659123	5.109651	14.233333	2.052641
14.000000	0.500000	4494.291512	16.800000	4686.595885	15.000000	5111.444666	9.300000	4764.110688	6.628605	13.700000	3.915354
14.000000	0.100000	3999.692493	16.100000	4191.048302	17.300000	4511.248734	15.400000	4233.996510	6.104594	16.266667	0.960902
40.000000	25.000000	4161.755259	15.000000	4548.280424	11.100000	4674.300390	10.500000	4461.445358	5.986365	12.200000	2.443358
40.000000	10.000000	3863.366709	14.600000	4133.156195	12.500000	4238.042592	12.300000	4078.188499	4.739640	13.133333	1.274101
40.000000	5.000000	3683.826962	15.200000	3899.689478	12.900000	3951.845381	12.900000	3845.120607	3.695536	13.666667	1.327906
40.000000	1.000000	3009.952500	18.900000	3220.818775	15.800000	3303.530344	15.200000	3178.100540	4.763193	16.633333	1.985783
40.000000	0.500000	2844.590144	20.500000	2821.479663	18.400000	2934.228880	18.100000	2866.766229	2.077467	19.000000	1.307670
40.000000	0.100000	2102.067048	24.200000	2282.269585	21.700000	2439.542823	19.900000	2274.626485	7.423973	21.933333	2.159475
70.000000	25.000000	2668.402501	18.700000	2639.034606	17.200000	2596.156753	18.100000	2634.531287	1.379099	18.000000	0.754983
70.000000	10.000000	2255.298266	19.500000	2150.196307	19.500000	2111.103424	19.400000	2172.199332	3.433066	19.466667	0.057735
70.000000	5.000000	1984.433723	20.700000	1907.766761	20.800000	1833.262246	20.900000	1908.487577	3.960640	20.800000	0.100000
70.000000	1.000000	1403.106790	25.000000	1311.123409	22.600000	1316.350299	23.100000	1343.526833	3.845394	23.566667	1.266228
70.000000	0.500000	1159.715335	24.500000	1089.445048	22.900000	1050.149223	27.700000	1099.769869	5.047235	25.033333	2.444040
70.000000	0.100000	775.027241	27.200000	727.482004	25.500000	706.352786	25.200000	736.287344	4.777183	25.966667	1.078579
100.000000	25.000000	936.208463	29.600000	904.854227	29.000000	800.625253	28.000000	880.562648	8.060837	28.866667	0.808290
100.000000	10.000000	687.341190	28.700000	664.045320	28.600000	598.308090	28.200000	649.898200	7.104456	28.500000	0.264575
100.000000	5.000000	545.031870	29.700000	517.574592	28.600000	464.863971	28.500000	509.156811	8.001753	28.933333	0.665833
100.000000	1.000000	322.286575	29.300000	304.455207	29.200000	273.844707	28.400000	300.195496	8.161433	28.966667	0.493288
100.000000	0.500000	251.491307	29.900000	228.341224	30.700000	203.290098	29.400000	227.707543	10.586760	30.000000	0.655744
100.000000	0.100000	162.164165	26.100000	146.519904	26.100000	131.549167	23.700000	146.744412	10.432243	25.300000	1.385641
130.000000	25.000000	304.707471	35.500000	301.998865	35.800000	296.989278	34.700000	301.231871	1.299943	35.333333	0.568624
130.000000	10.000000	233.145693	33.400000	227.006359	32.500000	220.483916	32.800000	226.878656	2.790855	32.900000	0.458258
130.000000	5.000000	179.886736	31.100000	177.409214	31.700000	169.667811	31.400000	175.654587	3.034724	31.400000	0.300000
130.000000	1.000000	112.377858	28.200000	111.350670	27.400000	105.751550	27.600000	109.826693	3.247255	27.733333	0.416333
130.000000	0.500000	97.564804	26.400000	93.446771	27.400000	91.639583	25.300000	94.217053	3.223179	26.366667	1.050397
130.000000	0.100000	77.466255	21.800000	73.406247	22.700000	72.364264	21.500000	74.412255	3.622611	22.000000	0.624500

Table D-51 Dynamic Modulus Summary Sheet for the Mix 51

Conditions		Specimen 1		Specimen 2		Specimen 3		Modulus		Phase Angle (Degrees)	
Temperature, °F	Frequency, Hz	Modulus, ksi	Phage Angle, degree	Modulus, ksi	Phage Angle, degree	Modulus, ksi	Phage Angle, degree	Avg. Modulus, ksi	CV, %	Avg. P. Angle, degree	Standard Dev, degree
14.000000	25.000000	6816.070309	3.600000	6839.343115	1.300000	6827.567524	1.000000	6827.660316	0.170434	1.966667	1.422439
14.000000	10.000000	6831.150567	5.500000	6875.308451	5.500000	6902.354621	5.900000	6869.604546	0.523219	5.633333	0.230940
14.000000	5.000000	6587.306808	6.200000	6479.661903	6.600000	6811.525212	4.500000	6626.164641	2.555168	5.766667	1.115049
14.000000	1.000000	6109.240992	4.300000	6192.780433	5.100000	5942.483135	3.900000	6081.501520	2.095428	4.433333	0.611010
14.000000	0.500000	5490.485478	9.100000	5555.026959	8.900000	5711.786241	9.000000	5585.766226	2.037458	9.000000	0.100000
14.000000	0.100000	5063.394467	9.300000	5137.187595	6.600000	5111.799924	8.100000	5104.127329	0.734506	8.000000	1.352775
40.000000	25.000000	4950.646845	6.100000	4931.540088	6.800000	4874.821681	6.700000	4919.002871	0.801721	6.533333	0.378594
40.000000	10.000000	4478.157520	10.100000	4478.710788	9.900000	4443.034272	10.500000	4466.634193	0.457615	10.166667	0.305505
40.000000	5.000000	4164.182879	11.300000	4139.262744	11.000000	4153.793651	10.900000	4152.413091	0.301446	11.066667	0.208167
40.000000	1.000000	3431.705794	15.200000	3374.307044	14.900000	3435.454498	11.800000	3413.822445	1.003937	13.966667	1.882374
40.000000	0.500000	3253.916226	12.800000	3272.498002	13.200000	2950.348076	16.400000	3158.920768	5.725627	14.133333	1.973153
40.000000	0.100000	2436.525524	17.500000	2402.306595	18.400000	2382.498751	18.300000	2407.110290	1.135463	18.066667	0.493288
70.000000	25.000000	2405.520019	17.500000	2470.266617	15.900000	2482.345098	17.300000	2452.710578	1.684342	16.900000	0.871780
70.000000	10.000000	1970.489303	20.200000	1957.847690	19.700000	1938.432966	19.700000	1955.589986	0.825684	19.866667	0.288675
70.000000	5.000000	1690.561692	21.300000	1669.303079	21.000000	1666.260248	20.400000	1675.375006	0.790257	20.900000	0.458258
70.000000	1.000000	1183.398088	24.900000	1109.100432	23.600000	1102.187480	23.700000	1131.562000	3.978946	24.066667	0.723418
70.000000	0.500000	954.748461	25.100000	926.249925	26.500000	905.660774	26.000000	928.886387	2.653696	25.866667	0.709460
70.000000	0.100000	601.168866	27.100000	585.156582	25.900000	573.446124	25.200000	586.590524	2.372505	26.066667	0.960902
100.000000	25.000000	775.264563	28.900000	778.750705	28.600000	744.576455	30.200000	766.197241	2.454343	29.233333	0.850490
100.000000	10.000000	555.653923	28.800000	525.571451	30.500000	502.975216	30.500000	528.066863	5.004643	29.933333	0.981495
100.000000	5.000000	440.313745	28.400000	436.190635	28.200000	432.041558	28.300000	436.181979	0.948251	28.300000	0.100000
100.000000	1.000000	264.391712	26.800000	263.464908	26.400000	262.511267	26.300000	263.455962	0.356892	26.500000	0.264575
100.000000	0.500000	206.704433	26.100000	203.744433	26.000000	201.684546	26.200000	204.044471	1.236670	26.100000	0.100000
100.000000	0.100000	131.662606	21.100000	129.320718	21.300000	127.479440	21.000000	129.487588	1.619128	21.133333	0.152753
130.000000	25.000000	228.888835	31.900000	222.225971	32.500000	183.277135	33.800000	211.463980	11.650591	32.733333	0.971253
130.000000	10.000000	167.079606	27.600000	162.362030	27.700000	134.806835	28.400000	154.749490	11.264127	27.900000	0.435890
130.000000	5.000000	131.758493	25.000000	129.155492	24.900000	120.333808	25.300000	127.082598	4.711724	25.066667	0.208167
130.000000	1.000000	89.379945	18.100000	86.943041	19.200000	85.052152	18.700000	87.125046	2.490248	18.666667	0.550757
130.000000	0.500000	76.981747	16.500000	75.068228	16.000000	73.778913	16.400000	75.276296	2.140810	16.300000	0.264575
130.000000	0.100000	63.079106	11.700000	60.641911	12.200000	59.947642	12.400000	61.222886	2.686229	12.100000	0.360555

Table D-52 Dynamic Modulus Summary Sheet for the Mix 52

Conditions		Specimen 1		Specimen 2		Specimen 3		Modulus		Phase Angle (Degrees)	
Temperature, °F	Frequency, Hz	Modulus, ksi	Phage Angle, degree	Modulus, ksi	Phage Angle, degree	Modulus, ksi	Phage Angle, degree	Avg. Modulus, ksi	CV, %	Avg. P. Angle, degree	Standard Dev, degree
14.000000	25.000000	9501.689838	3.900000	9360.333723	3.700000	9509.364513	2.400000	9457.129358	0.887323	3.333333	0.814453
14.000000	10.000000	9723.112888	8.100000	9677.975833	7.500000	9651.168726	7.300000	9684.085816	0.375453	7.633333	0.416333
14.000000	5.000000	9325.454179	9.100000	9596.576499	7.600000	9357.754367	8.200000	9426.595015	1.570997	8.300000	0.754983
14.000000	1.000000	8505.038200	10.800000	7908.783324	11.900000	8681.006798	10.500000	8364.942774	4.838347	11.066667	0.737111
14.000000	0.500000	7624.292628	16.700000	7892.898404	11.200000	7840.990414	16.200000	7786.060482	1.829923	14.700000	3.041381
14.000000	0.100000	6716.163616	11.200000	6754.498547	12.800000	6728.585750	11.800000	6733.082638	0.290492	11.933333	0.808290
40.000000	25.000000	6693.342825	9.700000	5980.506472	12.400000	5835.056404	13.200000	6169.635234	7.445136	11.766667	1.833939
40.000000	10.000000	5600.120495	15.500000	5201.745468	15.900000	4958.233176	16.100000	5253.366380	6.168278	15.833333	0.305505
40.000000	5.000000	5131.695676	15.700000	4678.793265	16.900000	4394.290384	17.600000	4734.926442	7.854263	16.733333	0.960902
40.000000	1.000000	3870.420371	20.500000	3506.150398	21.000000	3389.333920	20.700000	3588.634896	6.992238	20.733333	0.251661
40.000000	0.500000	3375.568943	20.400000	3061.277485	20.100000	2833.250031	23.100000	3090.032153	8.812223	21.200000	1.652271
40.000000	0.100000	2212.832246	26.100000	2094.974509	25.600000	1996.353070	26.600000	2101.386608	5.157639	26.100000	0.500000
70.000000	25.000000	1765.195748	29.300000	1648.867404	29.400000	1619.959357	29.300000	1678.007503	4.581518	29.333333	0.057735
70.000000	10.000000	1288.141743	30.200000	1215.555824	30.500000	1203.542912	30.400000	1235.746826	3.703926	30.366667	0.152753
70.000000	5.000000	1024.765904	31.500000	978.807795	31.900000	964.569044	32.000000	989.380914	3.179810	31.800000	0.264575
70.000000	1.000000	582.929293	33.700000	546.667014	33.200000	546.345991	33.400000	558.647433	3.764328	33.433333	0.251661
70.000000	0.500000	467.253005	33.700000	407.812211	33.100000	396.799649	34.600000	423.954955	8.939473	33.800000	0.754983
70.000000	0.100000	265.735861	30.100000	235.084308	30.700000	231.285557	30.300000	244.035242	7.740286	30.366667	0.305505
100.000000	25.000000	396.749457	39.700000	382.915721	39.000000	373.439661	38.700000	384.368280	3.049833	39.133333	0.513160
100.000000	10.000000	271.307565	36.100000	263.018115	35.500000	252.149020	35.400000	262.158233	3.665029	35.666667	0.378594
100.000000	5.000000	206.482632	33.800000	207.787904	33.600000	189.344228	33.100000	201.204921	5.115369	33.500000	0.360555
100.000000	1.000000	126.688705	28.300000	137.999515	26.400000	121.241899	26.100000	128.643373	6.644802	26.933333	1.193035
100.000000	0.500000	108.895053	25.800000	112.848875	24.200000	109.240302	23.800000	110.328077	1.984889	24.600000	1.058301
100.000000	0.100000	88.360011	18.400000	86.405004	17.600000	82.986317	17.800000	85.917111	3.165687	17.933333	0.416333
130.000000	25.000000	139.938130	31.200000	127.038160	31.700000	121.088858	33.000000	129.355049	7.449154	31.966667	0.929157
130.000000	10.000000	104.550432	24.700000	97.697537	24.500000	92.792685	25.400000	98.346885	6.004978	24.866667	0.472582
130.000000	5.000000	87.425374	22.000000	82.448281	22.200000	75.237951	22.900000	81.703869	7.499912	22.366667	0.472582
130.000000	1.000000	68.577988	17.400000	63.313091	17.100000	61.130191	16.900000	64.340423	5.950698	17.133333	0.251661
130.000000	0.500000	62.833950	16.400000	58.615389	14.600000	54.598609	15.700000	58.682649	7.017547	15.566667	0.907377
130.000000	0.100000	58.956721	12.800000	51.309028	12.700000	25.728423	14.100000	45.331391	38.388375	13.200000	0.781025

Table D-53 Dynamic Modulus Summary Sheet for the Mix 53

Conditions		Specimen 1		Specimen 2		Specimen 3		Modulus		Phase Angle (Degrees)	
Temperature, °F	Frequency, Hz	Modulus, ksi	Phage Angle, degree	Modulus, ksi	Phage Angle, degree	Modulus, ksi	Phage Angle, degree	Avg. Modulus, ksi	CV, %	Avg. P. Angle, degree	Standard Dev, degree
14.000000	25.000000	10223.161324	8.600000	10164.119742	9.100000	10085.902788	8.800000	10157.727951	0.677830	8.833333	0.251661
14.000000	10.000000	10833.082099	4.900000	10812.427671	5.200000	10685.111571	6.000000	10776.873780	0.743598	5.366667	0.568624
14.000000	5.000000	10585.605540	4.800000	10615.735449	4.800000	10581.255988	5.500000	10594.198992	0.177243	5.033333	0.404145
14.000000	1.000000	9757.390713	3.800000	9922.618016	7.500000	9454.103693	7.900000	9711.370807	2.446856	6.400000	2.260531
14.000000	0.500000	9659.007756	3.900000	9700.605577	6.200000	9493.817878	7.000000	9617.810404	1.137228	5.700000	1.609348
14.000000	0.100000	8343.399451	7.700000	8459.969614	6.100000	8425.679895	5.900000	8409.682987	0.712380	6.566667	0.986577
40.000000	25.000000	7145.120131	13.700000	7022.631275	13.600000	7069.789050	13.300000	7079.180152	0.872729	13.533333	0.208167
40.000000	10.000000	7258.900598	11.400000	7055.863054	11.600000	6921.044469	11.700000	7078.602707	2.402622	11.566667	0.152753
40.000000	5.000000	6721.398340	11.900000	6332.186038	13.500000	6409.956054	12.200000	6487.846811	3.174635	12.533333	0.850490
40.000000	1.000000	5422.991252	15.600000	5274.513005	15.400000	5284.234511	13.600000	5327.246256	1.559154	14.866667	1.101514
40.000000	0.500000	5148.466202	18.800000	4710.126757	12.600000	4773.185698	20.900000	4877.259552	4.858849	17.433333	4.315476
40.000000	0.100000	3707.008524	21.300000	3608.970961	21.000000	3490.769716	21.500000	3602.249734	3.005788	21.266667	0.251661
70.000000	25.000000	3507.368343	20.800000	2797.179089	23.600000	3318.935542	22.600000	3207.827658	11.468842	22.333333	1.418920
70.000000	10.000000	3193.776812	21.100000	2461.497447	23.100000	2763.739146	23.100000	2806.337802	13.112946	22.433333	1.154701
70.000000	5.000000	2780.712469	22.600000	2299.237686	24.900000	2366.077971	24.600000	2482.009375	10.508999	24.033333	1.250333
70.000000	1.000000	1914.355933	23.800000	1533.913092	29.900000	1562.367094	28.500000	1670.212040	12.687786	27.400000	3.195309
70.000000	0.500000	1514.495902	25.400000	1396.291610	30.300000	1314.540790	28.800000	1408.442767	7.137659	28.166667	2.510644
70.000000	0.100000	988.334192	27.800000	834.350970	31.600000	805.924675	29.300000	876.203279	11.200923	29.566667	1.913984
100.000000	25.000000	1062.799685	34.600000	1032.530662	34.900000	1011.347046	35.500000	1035.559131	2.497169	35.000000	0.458258
100.000000	10.000000	761.799431	33.500000	735.042660	33.300000	711.558788	34.400000	736.133626	3.414880	33.733333	0.585947
100.000000	5.000000	589.027574	33.000000	571.080591	32.800000	549.614393	33.700000	569.907519	3.462449	33.166667	0.472582
100.000000	1.000000	337.897327	31.200000	334.791685	29.900000	324.949487	30.000000	332.546166	2.032707	30.366667	0.723418
100.000000	0.500000	271.876790	28.400000	268.324500	27.600000	258.432401	27.900000	266.211230	2.617047	27.966667	0.404145
100.000000	0.100000	178.689100	22.700000	177.448671	21.400000	174.855389	20.900000	176.997720	1.105231	21.666667	0.929157
130.000000	25.000000	195.234924	38.900000	186.377991	40.100000	158.269383	39.400000	179.960766	10.724681	39.466667	0.602771
130.000000	10.000000	144.865031	33.100000	131.547137	34.000000	108.213985	33.900000	128.208718	14.470299	33.666667	0.493288
130.000000	5.000000	117.207857	30.600000	110.288233	29.900000	83.809982	31.300000	103.768691	16.987413	30.600000	0.700000
130.000000	1.000000	85.085371	23.700000	75.988794	23.300000	53.209491	24.800000	71.427885	22.988346	23.933333	0.776745
130.000000	0.500000	79.320299	21.100000	68.947898	20.400000	47.381607	21.900000	65.216601	24.982907	21.133333	0.750555
130.000000	0.100000	74.450117	11.900000	63.114066	16.000000	40.722079	16.100000	59.428754	28.880582	14.666667	2.396525

Table D-54 Dynamic Modulus Summary Sheet for the Mix 54

Conditions		Specimen 1		Specimen 2		Specimen 3		Modulus		Phase Angle (Degrees)	
Temperature, °F	Frequency, Hz	Modulus, ksi	Phage Angle, degree	Modulus, ksi	Phage Angle, degree	Modulus, ksi	Phage Angle, degree	Avg. Modulus, ksi	CV, %	Avg. P. Angle, degree	Standard Dev, degree
14.000000	25.000000	9074.700660	7.400000	9324.769630	8.000000	9479.791644	8.400000	9293.087311	2.199435	7.933333	0.503322
14.000000	10.000000	9592.710875	6.100000	10023.358238	3.800000	9729.488819	5.200000	9781.852644	2.249545	5.033333	1.159023
14.000000	5.000000	9223.310333	5.000000	9636.015356	4.500000	9486.610595	5.400000	9448.645428	2.211486	4.966667	0.450925
14.000000	1.000000	8079.764385	8.700000	8534.763529	6.600000	8806.313638	3.800000	8473.613851	4.332441	6.366667	2.458319
14.000000	0.500000	7944.026104	5.300000	8481.882604	10.900000	8637.484724	6.000000	8354.464477	4.355336	7.400000	3.051229
14.000000	0.100000	7163.923272	6.600000	7537.419943	7.300000	7693.304353	8.500000	7464.882523	3.644303	7.466667	0.960902
40.000000	25.000000	6606.148391	13.400000	6433.877144	13.600000	6602.034564	10.700000	6547.353366	1.501291	12.566667	1.619671
40.000000	10.000000	6481.631561	10.100000	6392.873789	9.500000	6313.852174	11.100000	6396.119175	1.312308	10.233333	0.808290
40.000000	5.000000	6225.817973	10.700000	6028.423069	10.500000	5935.737730	11.100000	6063.326257	2.443483	10.766667	0.305505
40.000000	1.000000	5119.587457	15.800000	4900.226905	13.100000	4945.794070	10.500000	4988.536144	2.320481	13.133333	2.650157
40.000000	0.500000	4925.279047	12.200000	4974.316396	12.500000	4236.707001	16.700000	4712.100815	8.752626	13.800000	2.515949
40.000000	0.100000	3708.568816	16.900000	3703.168721	14.400000	3482.787944	17.900000	3631.508494	3.547398	16.400000	1.802776
70.000000	25.000000	3077.352437	22.200000	2948.203908	20.600000	2472.636938	23.700000	2832.731094	11.242371	22.166667	1.550269
70.000000	10.000000	2593.570290	20.100000	2480.821072	21.000000	2062.151661	23.400000	2378.847674	11.770433	21.500000	1.705872
70.000000	5.000000	2232.626019	21.900000	2077.655647	23.600000	1703.105968	24.700000	2004.462545	13.581803	23.400000	1.410674
70.000000	1.000000	1464.945031	25.500000	1254.448666	29.900000	1063.806999	29.000000	1261.066899	15.911201	28.133333	2.324507
70.000000	0.500000	1168.869647	27.100000	1012.792158	32.000000	847.440971	30.400000	1009.700925	15.919232	29.833333	2.498666
70.000000	0.100000	765.626033	28.700000	665.940416	31.900000	516.808517	30.900000	649.458322	19.281442	30.500000	1.637071
100.000000	25.000000	1056.415051	37.000000	1006.063436	36.700000	917.425340	36.800000	993.301276	7.084280	36.833333	0.152753
100.000000	10.000000	737.718047	32.600000	700.775715	34.700000	637.300444	34.600000	691.931402	7.340275	33.966667	1.184624
100.000000	5.000000	578.531579	32.600000	526.928510	33.900000	495.138652	34.600000	533.532914	7.888345	33.700000	1.014889
100.000000	1.000000	332.314018	30.500000	295.595953	32.300000	277.291246	32.600000	301.733739	9.286394	31.800000	1.135782
100.000000	0.500000	262.634715	28.500000	234.389458	30.800000	219.780363	31.100000	238.934845	9.117866	30.133333	1.422439
100.000000	0.100000	173.673275	22.900000	165.850637	22.700000	157.673031	23.500000	165.732314	4.827531	23.033333	0.416333
130.000000	25.000000	231.692602	41.100000	225.525707	39.800000	217.534796	39.300000	224.917702	3.156025	40.066667	0.929157
130.000000	10.000000	176.359977	34.000000	165.352347	33.600000	156.059936	33.300000	165.924087	6.124542	33.633333	0.351188
130.000000	5.000000	141.465782	31.600000	135.909745	30.700000	127.071089	30.300000	134.815539	5.384736	30.866667	0.665833
130.000000	1.000000	98.830910	24.500000	96.315962	23.300000	90.145005	23.100000	95.097292	4.699767	23.633333	0.757188
130.000000	0.500000	90.256268	21.100000	89.703144	18.900000	83.037524	19.600000	87.665645	4.582868	19.866667	1.123981
130.000000	0.100000	74.759390	14.000000	74.228606	12.500000	72.665558	12.800000	73.884518	1.473244	13.100000	0.793725

Appendix E

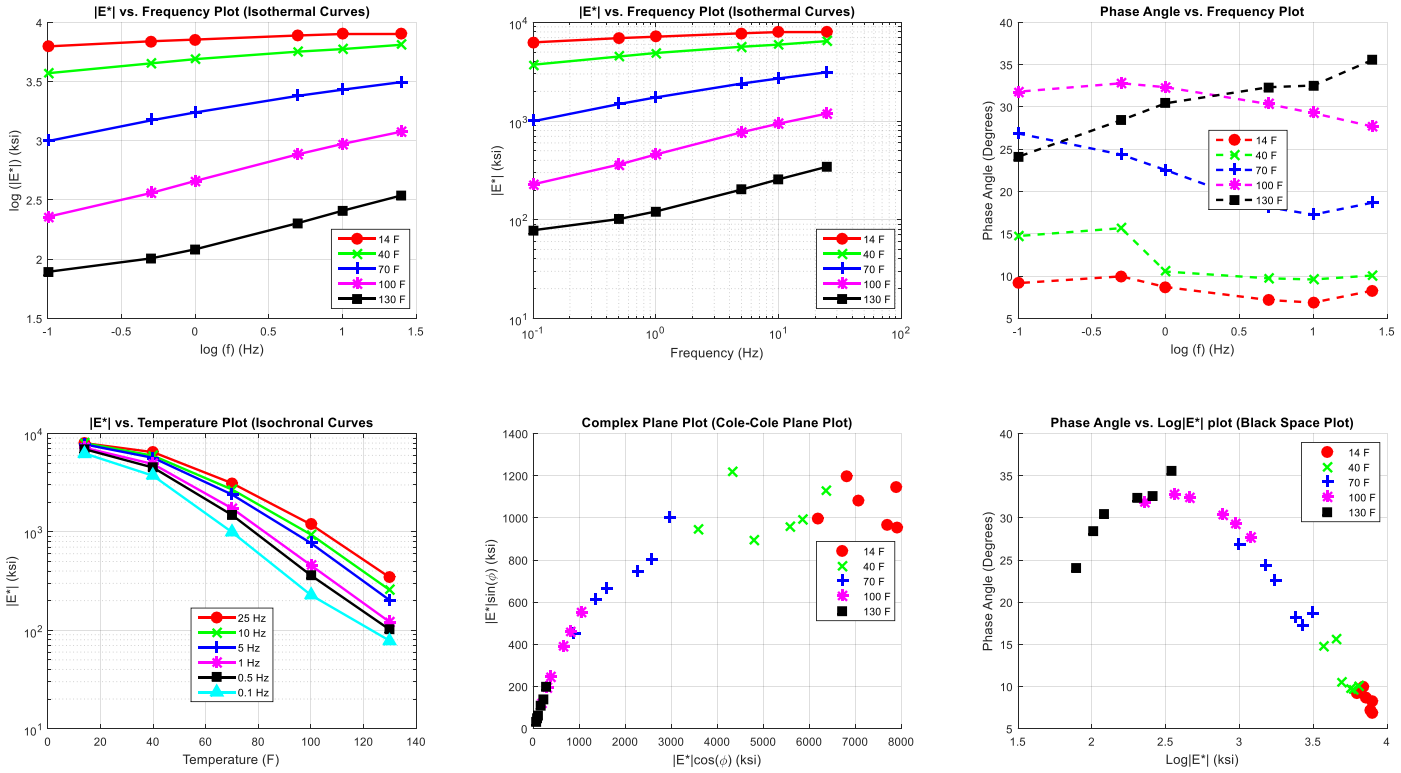

Figure E-1 (a) average log-|E*| versus log-f plot, (b) average |E*| versus f plot, (c) average ϕ versus log-f plot, (d) average |E*| versus temperature plot, (e) complex plane plot for average |E*|, and (f) black space plot for average |E*| for the AC Mix 1.

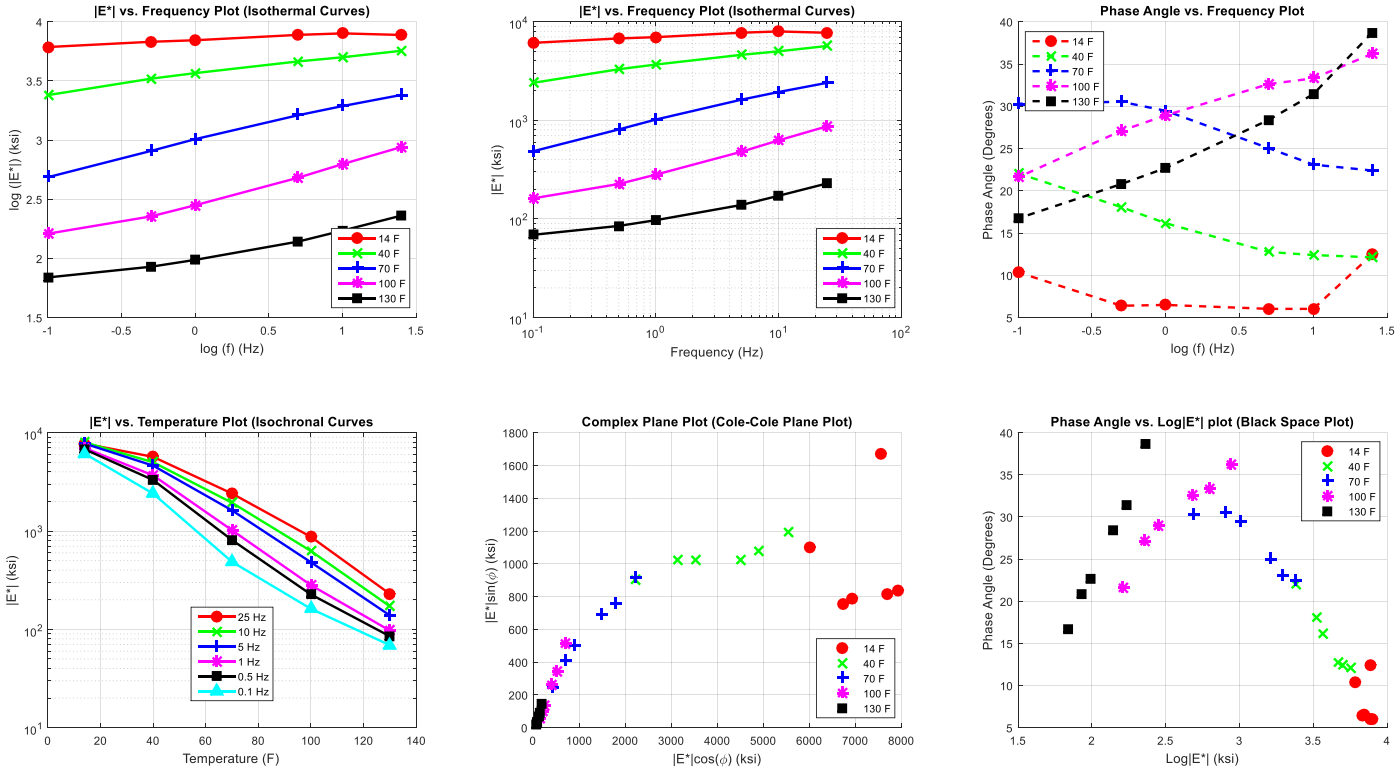

Figure E-2 (a) average log-|E*| versus log-f plot, (b) average |E*| versus f plot, (c) average ϕ versus log-f plot, (d) average |E*| versus temperature plot, (e) complex plane plot for average |E*|, and (f) black space plot for average |E*| for the AC Mix 2.

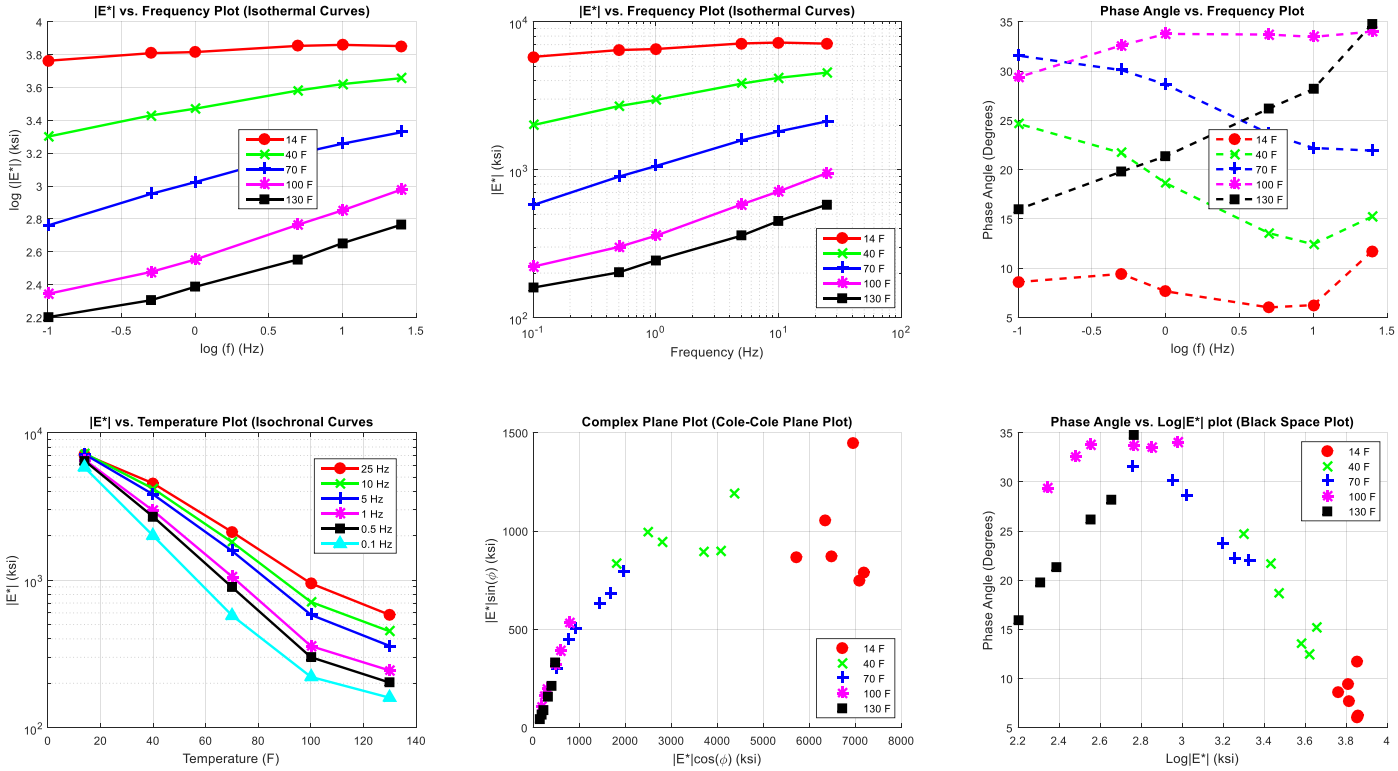

Figure E-3 (a) average log-|E*| versus log-f plot, (b) average |E*| versus f plot, (c) average ϕ versus log-f plot, (d) average |E*| versus temperature plot, (e) complex plane plot for average |E*|, and (f) black space plot for average |E*| for the AC Mix 3.

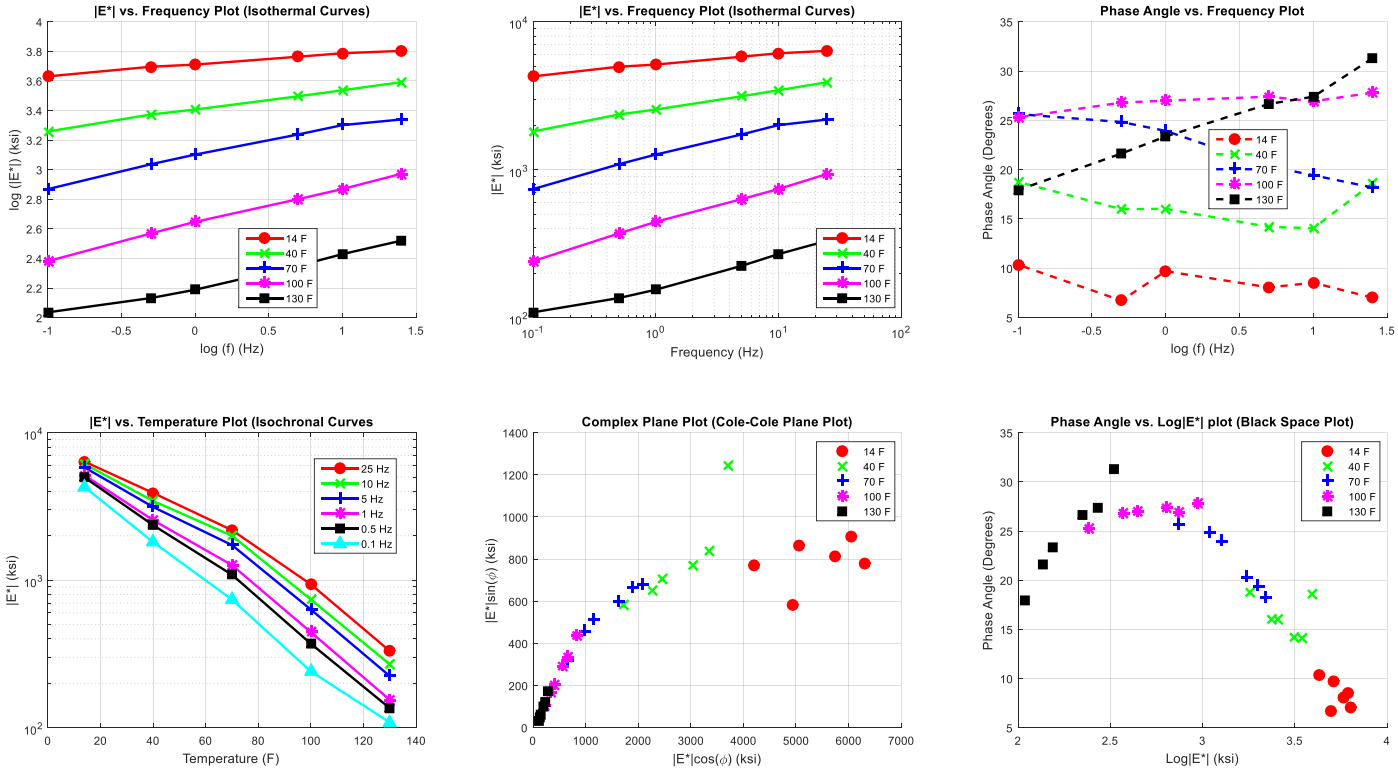

Figure E-4 (a) average log-|E*| versus log-f plot, (b) average |E*| versus f plot, (c) average ϕ versus log-f plot, (d) average |E*| versus temperature plot, (e) complex plane plot for average |E*|, and (f) black space plot for average |E*| for the AC Mix 4.

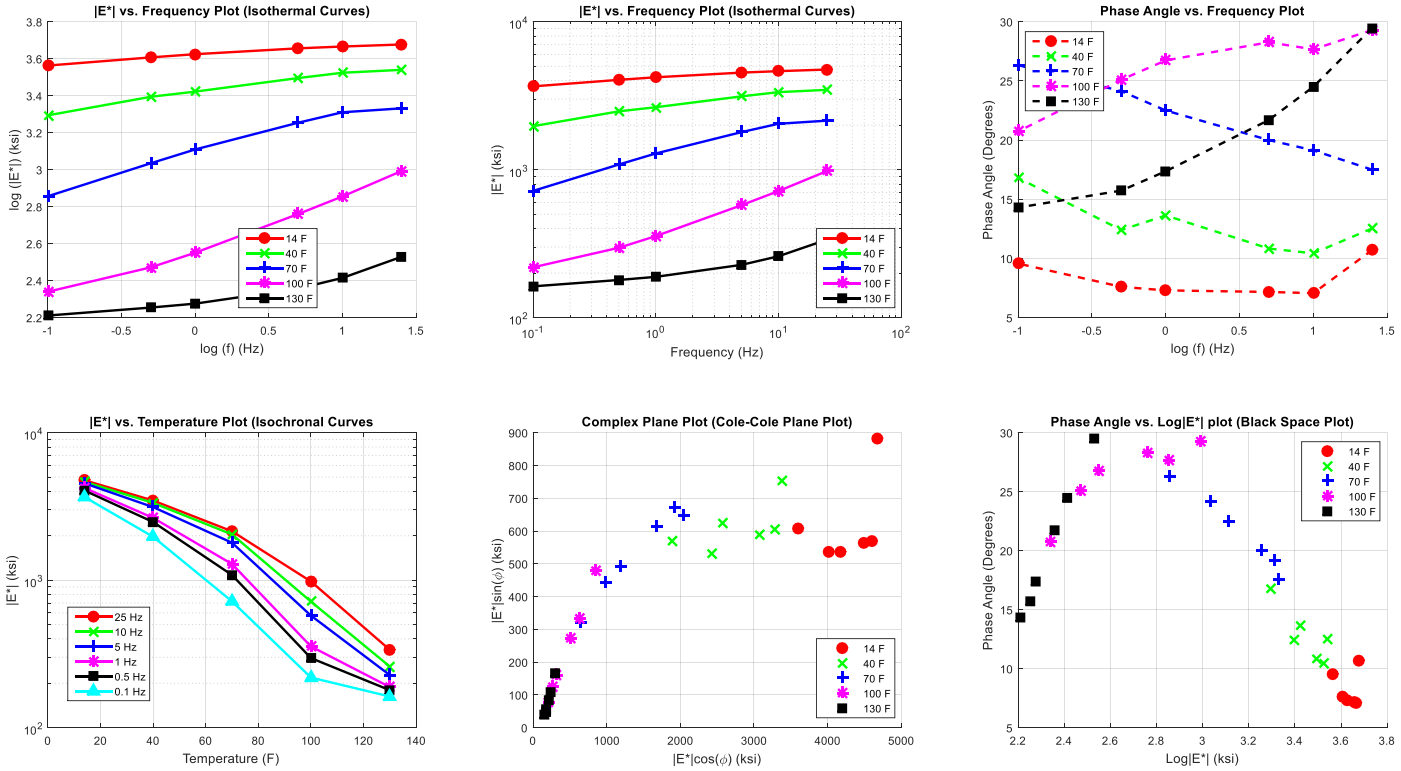

Figure E-5 (a) average log-|E*| versus log-f plot, (b) average |E*| versus f plot, (c) average ϕ versus log-f plot, (d) average |E*| versus temperature plot, (e) complex plane plot for average |E*|, and (f) black space plot for average |E*| for the AC Mix 5.

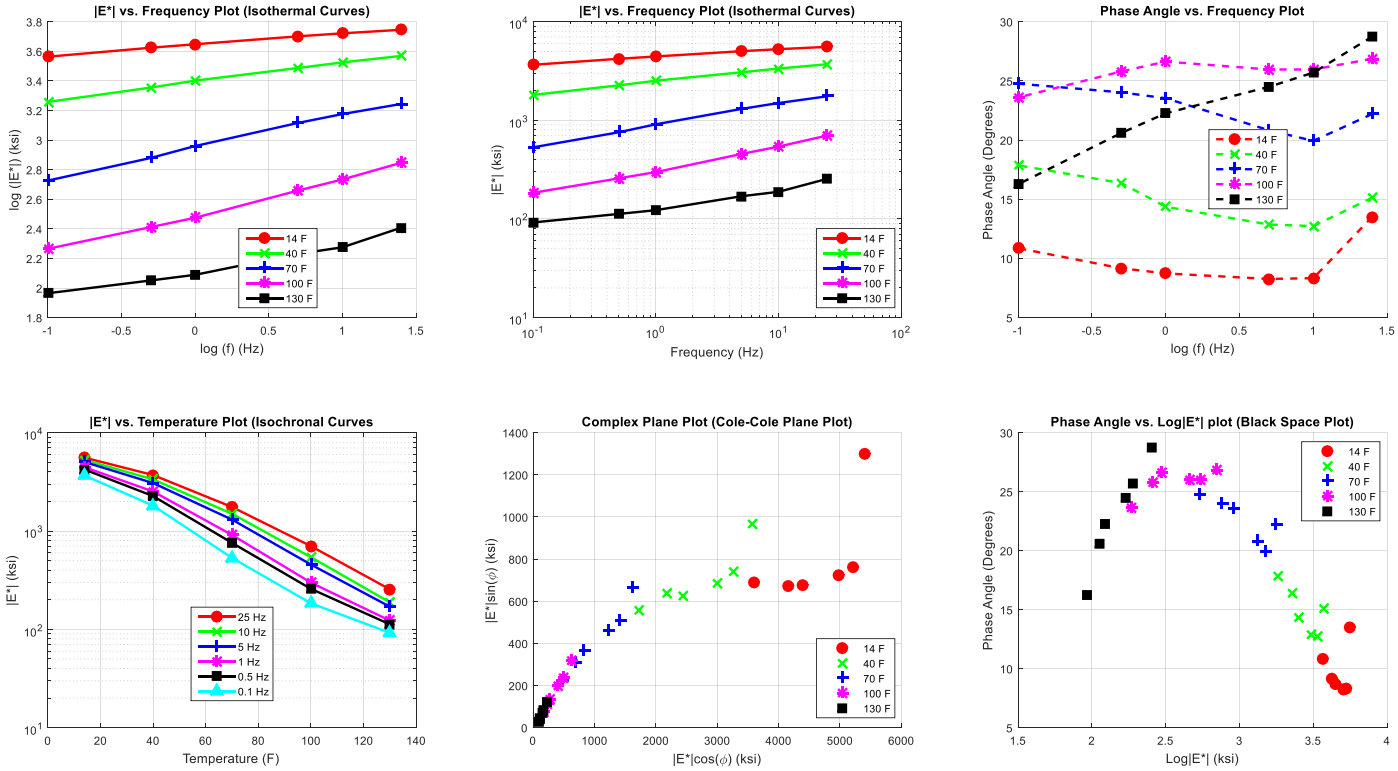

Figure E-6 (a) average log-|E*| versus log-f plot, (b) average |E*| versus f plot, (c) average ϕ versus log-f plot, (d) average |E*| versus temperature plot, (e) complex plane plot for average |E*|, and (f) black space plot for average |E*| for the AC Mix 6.

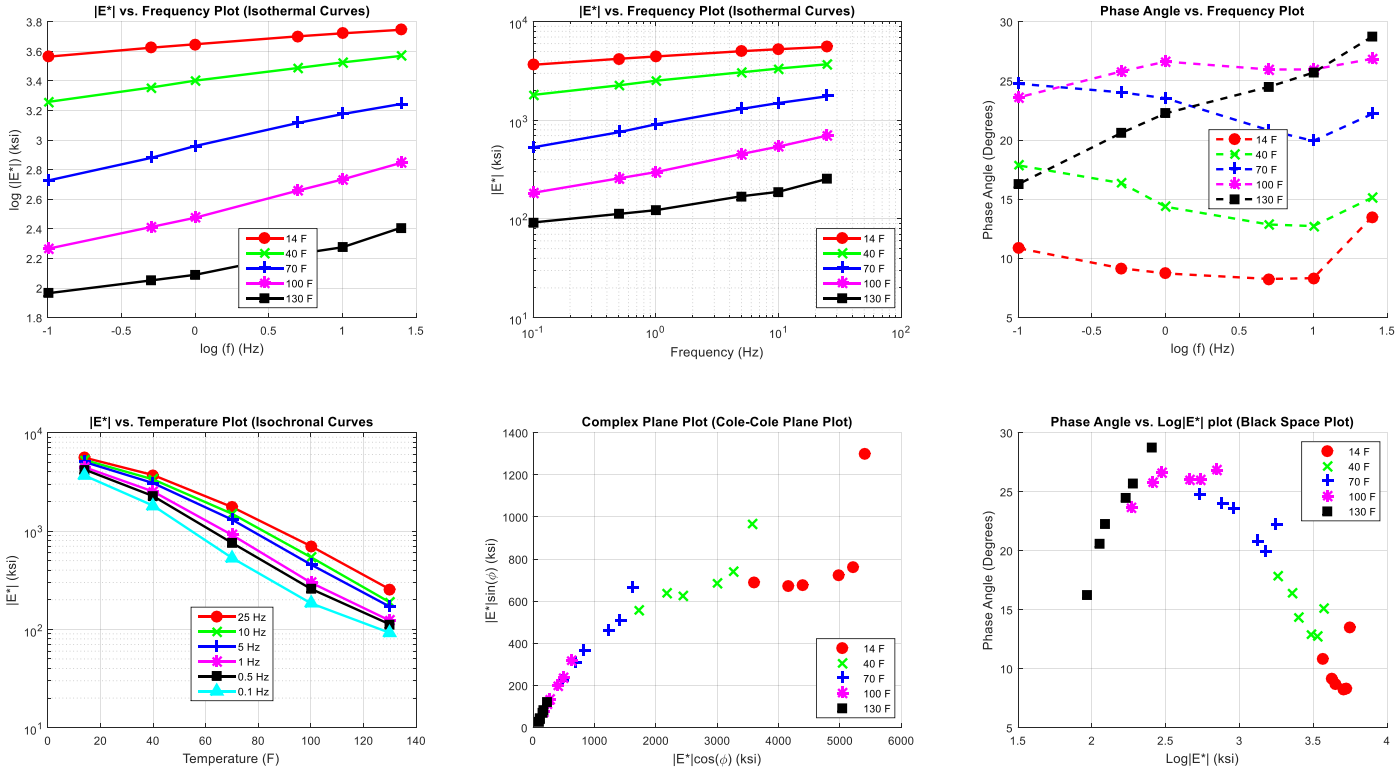

Figure E-7 (a) average log-|E*| versus log-f plot, (b) average |E*| versus f plot, (c) average ϕ versus log-f plot, (d) average |E*| versus temperature plot, (e) complex plane plot for average |E*|, and (f) black space plot for average |E*| for the AC Mix 7.

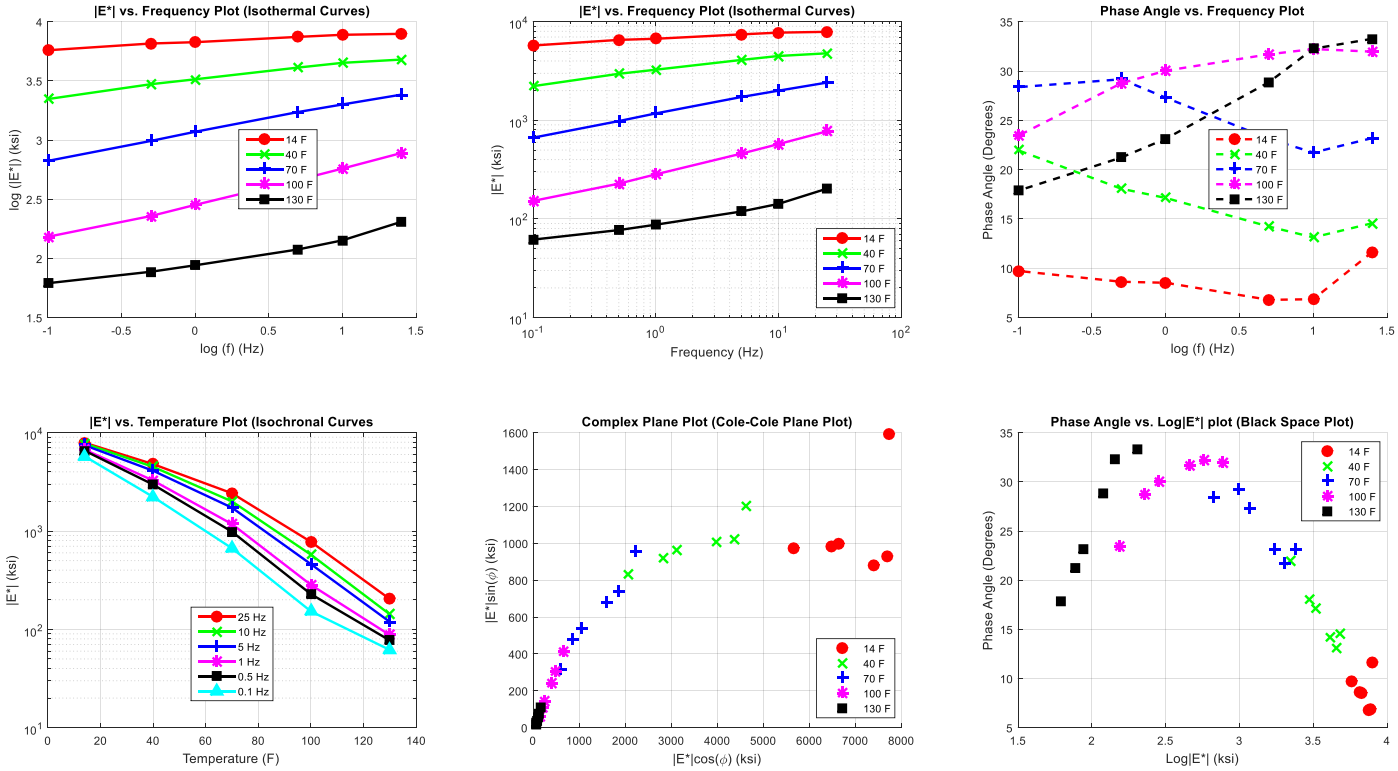

Figure E-8 (a) average log-|E*| versus log-f plot, (b) average |E*| versus f plot, (c) average ϕ versus log-f plot, (d) average |E*| versus temperature plot, (e) complex plane plot for average |E*|, and (f) black space plot for average |E*| for the AC Mix 8.

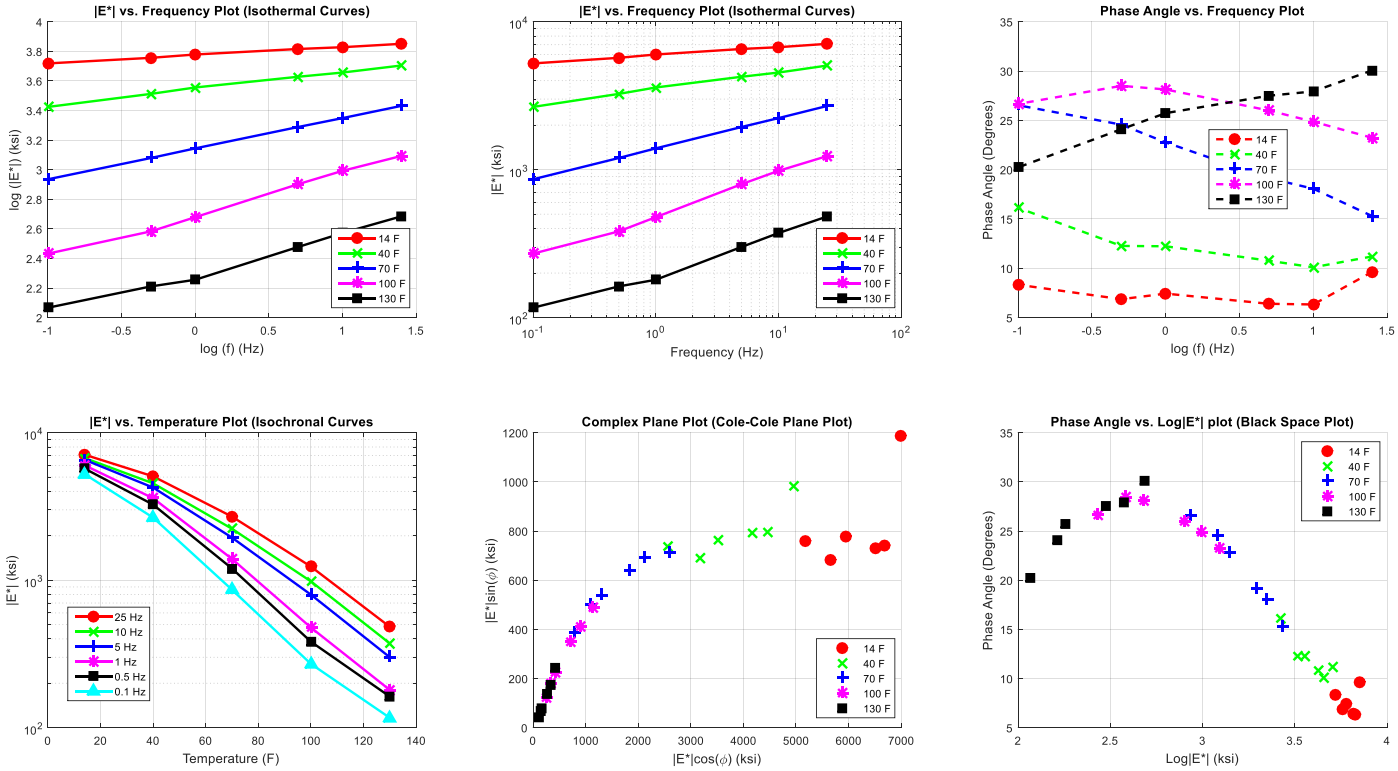

Figure E-9 (a) average log-|E*| versus log-f plot, (b) average |E*| versus f plot, (c) average ϕ versus log-f plot, (d) average |E*| versus temperature plot, (e) complex plane plot for average |E*|, and (f) black space plot for average |E*| for the AC Mix 9.

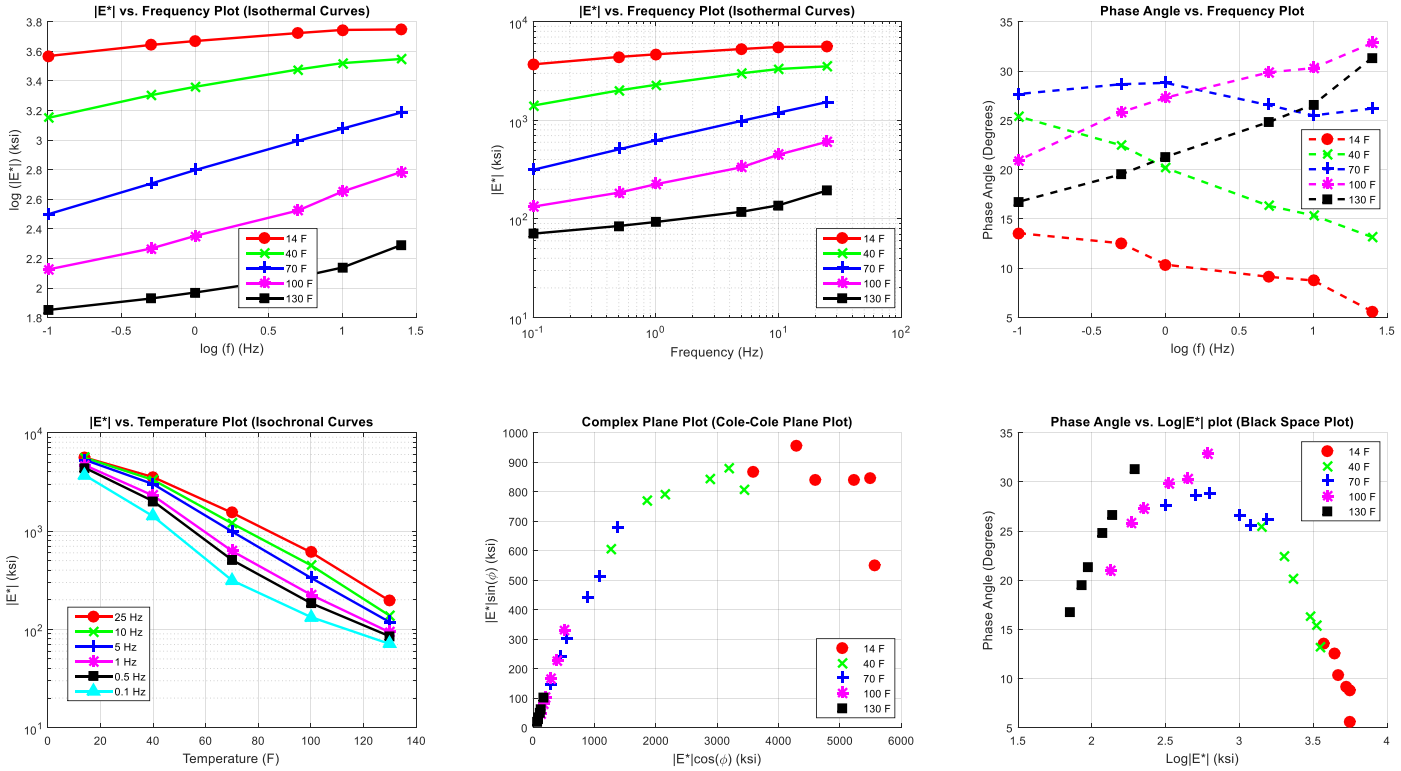

Figure E-10 (a) average log-|E*| versus log-f plot, (b) average |E*| versus f plot, (c) average ϕ versus log-f plot, (d) average |E*| versus temperature plot, (e) complex plane plot for average |E*|, and (f) black space plot for average |E*| for the AC Mix 10.

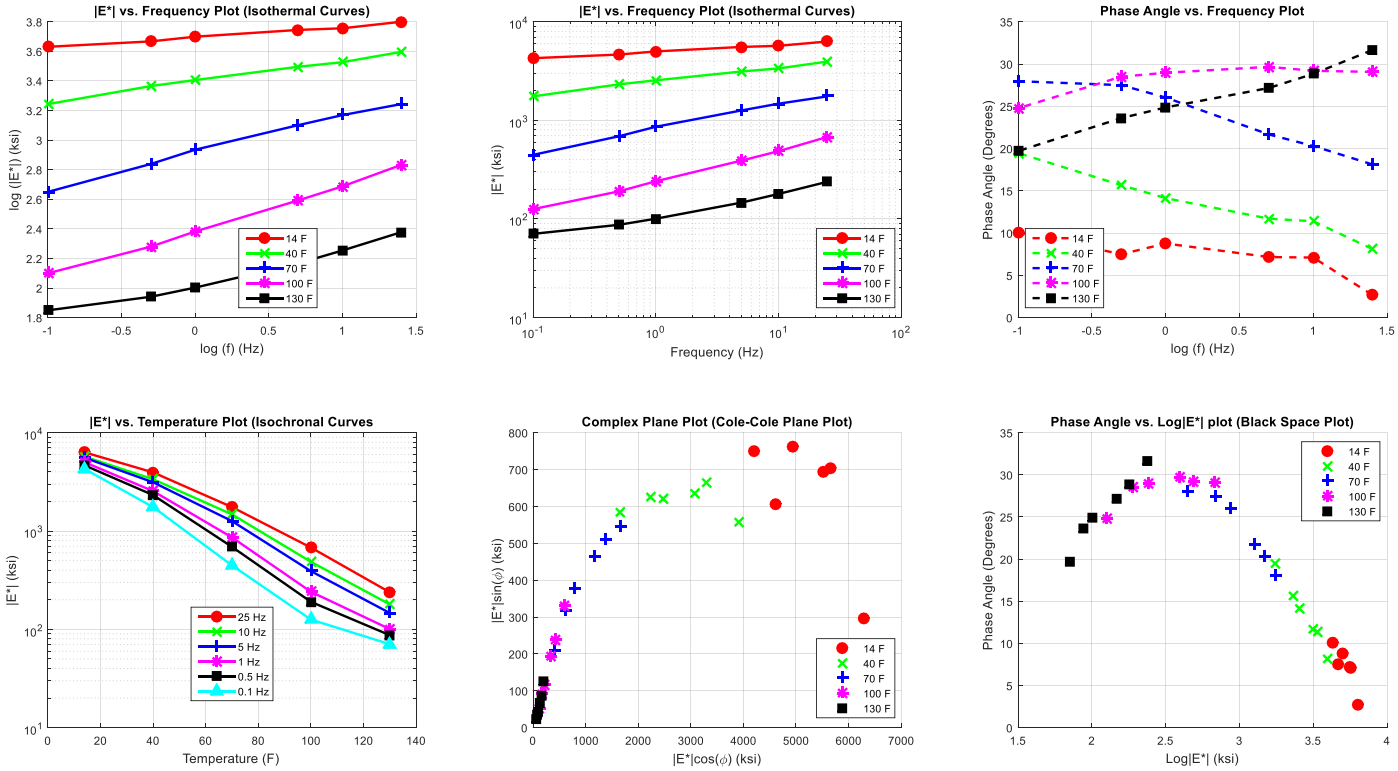

Figure E-11 (a) average log-|E*| versus log-f plot, (b) average |E*| versus f plot, (c) average ϕ versus log-f plot, (d) average |E*| versus temperature plot, (e) complex plane plot for average |E*|, and (f) black space plot for average |E*| for the AC Mix 11.

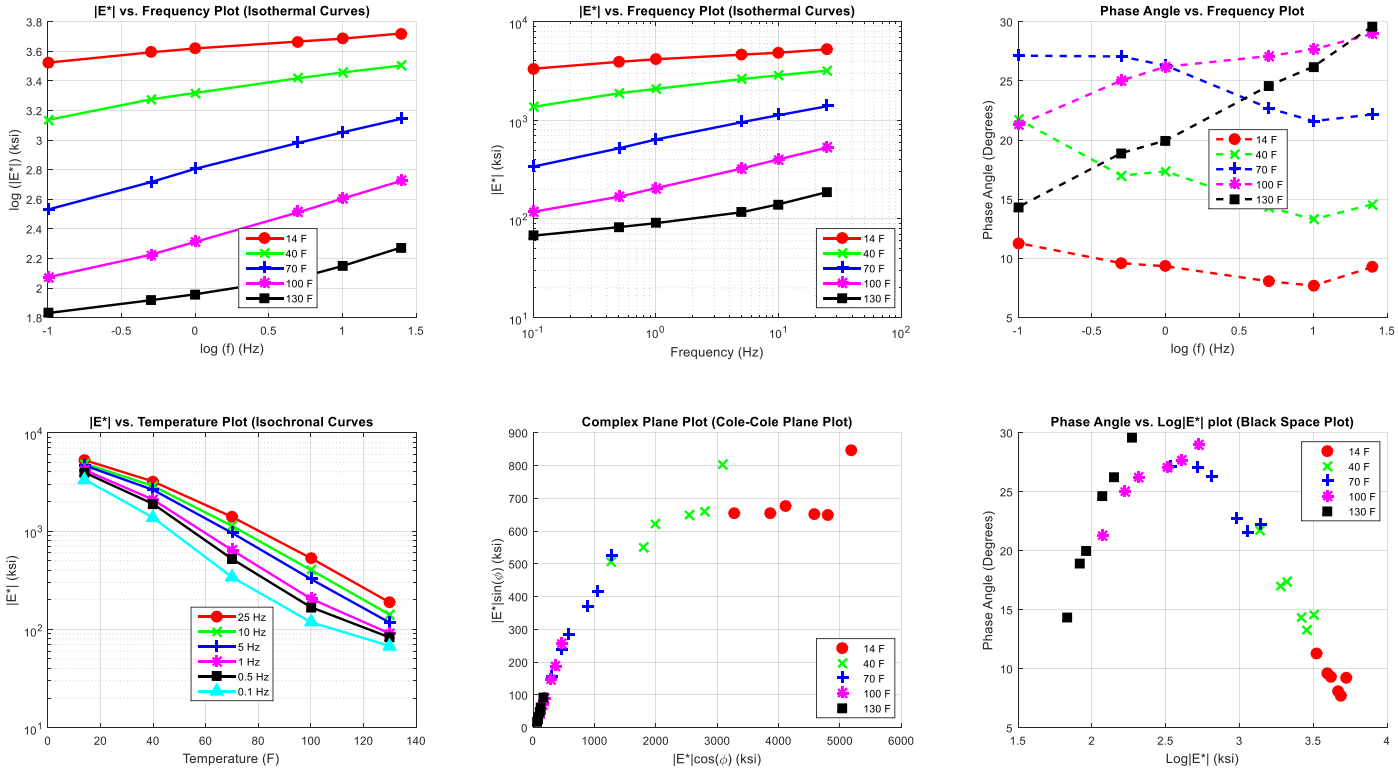

Figure E-12 (a) average log-|E*| versus log-f plot, (b) average |E*| versus f plot, (c) average ϕ versus log-f plot, (d) average |E*| versus temperature plot, (e) complex plane plot for average |E*|, and (f) black space plot for average |E*| for the AC Mix 12.

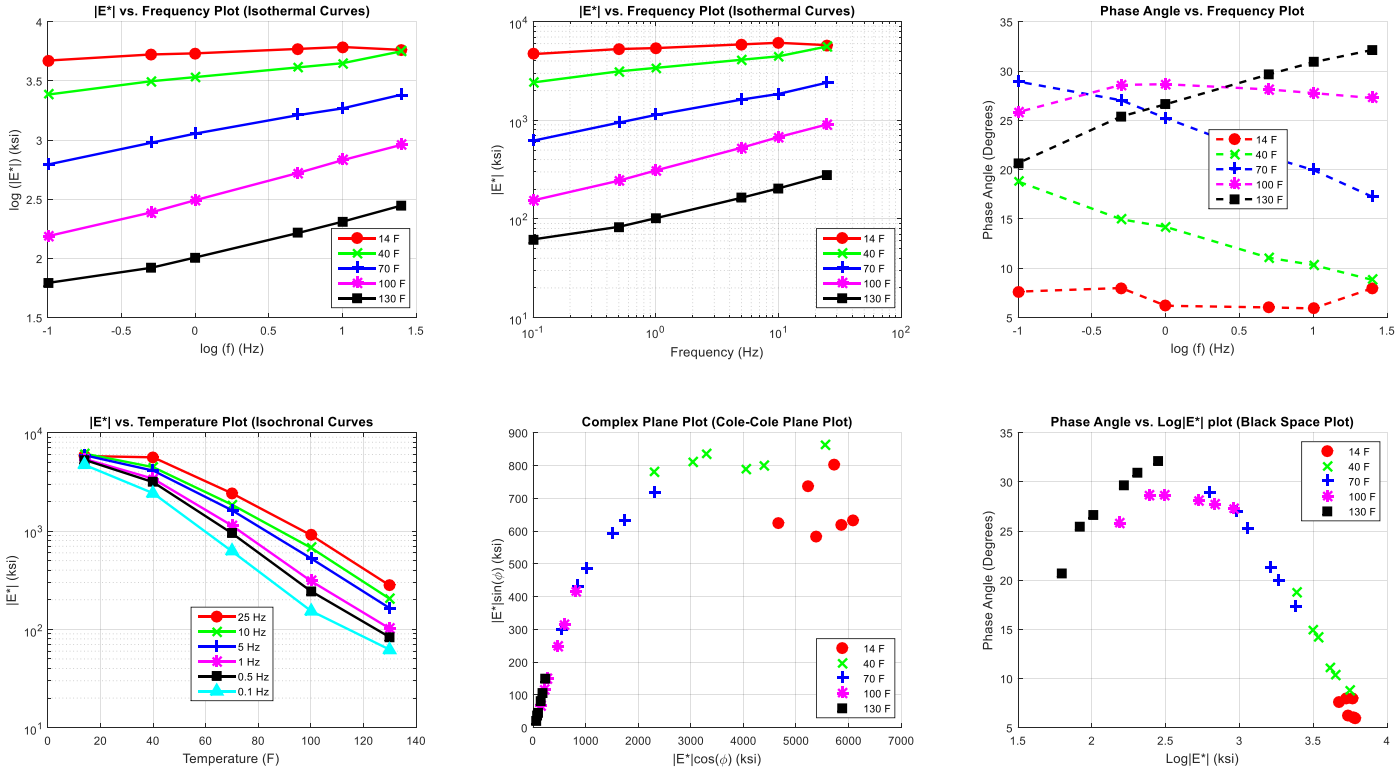

Figure E-13 (a) average log-|E*| versus log-f plot, (b) average |E*| versus f plot, (c) average ϕ versus log-f plot, (d) average |E*| versus temperature plot, (e) complex plane plot for average |E*|, and (f) black space plot for average |E*| for the AC Mix 13.

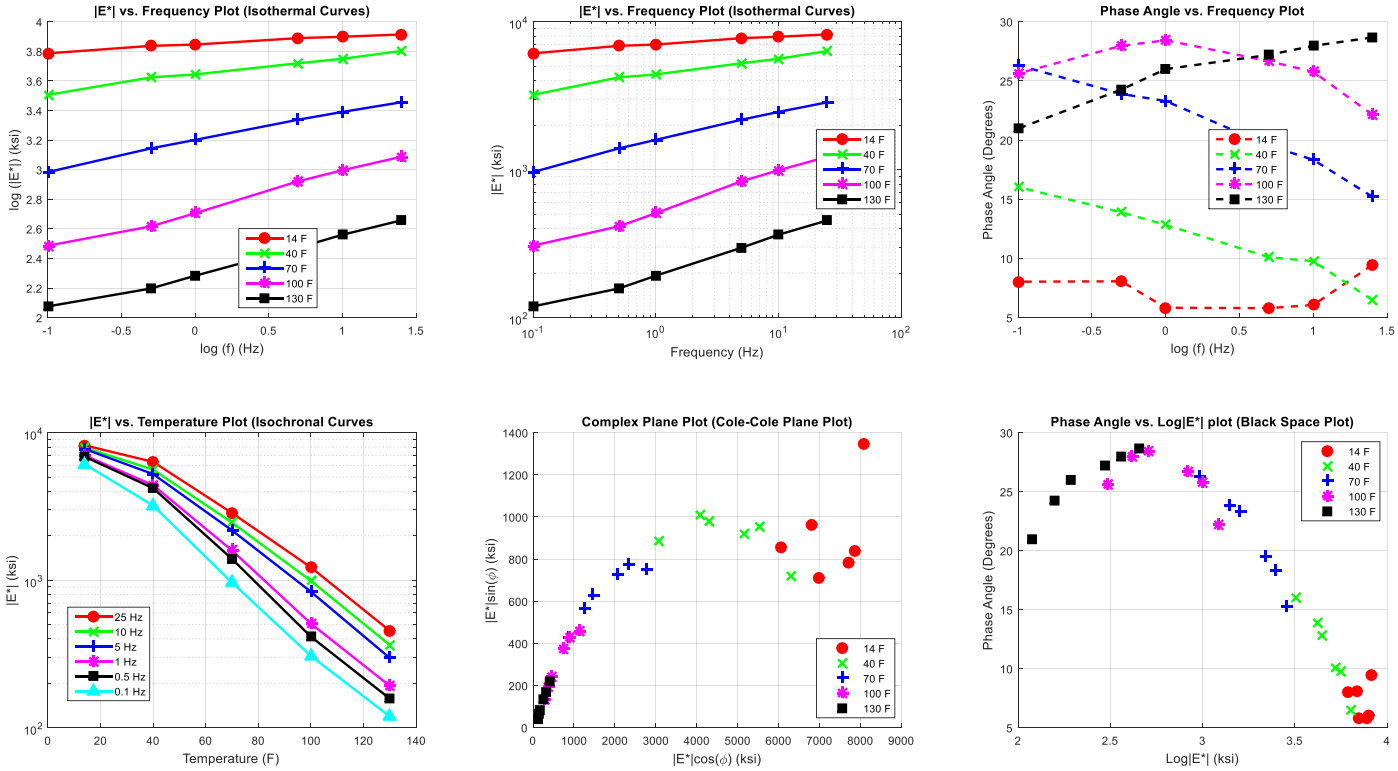

Figure E-14 (a) average log-|E*| versus log-f plot, (b) average |E*| versus f plot, (c) average ϕ versus log-f plot, (d) average |E*| versus temperature plot, (e) complex plane plot for average |E*|, and (f) black space plot for average |E*| for the AC Mix 14.

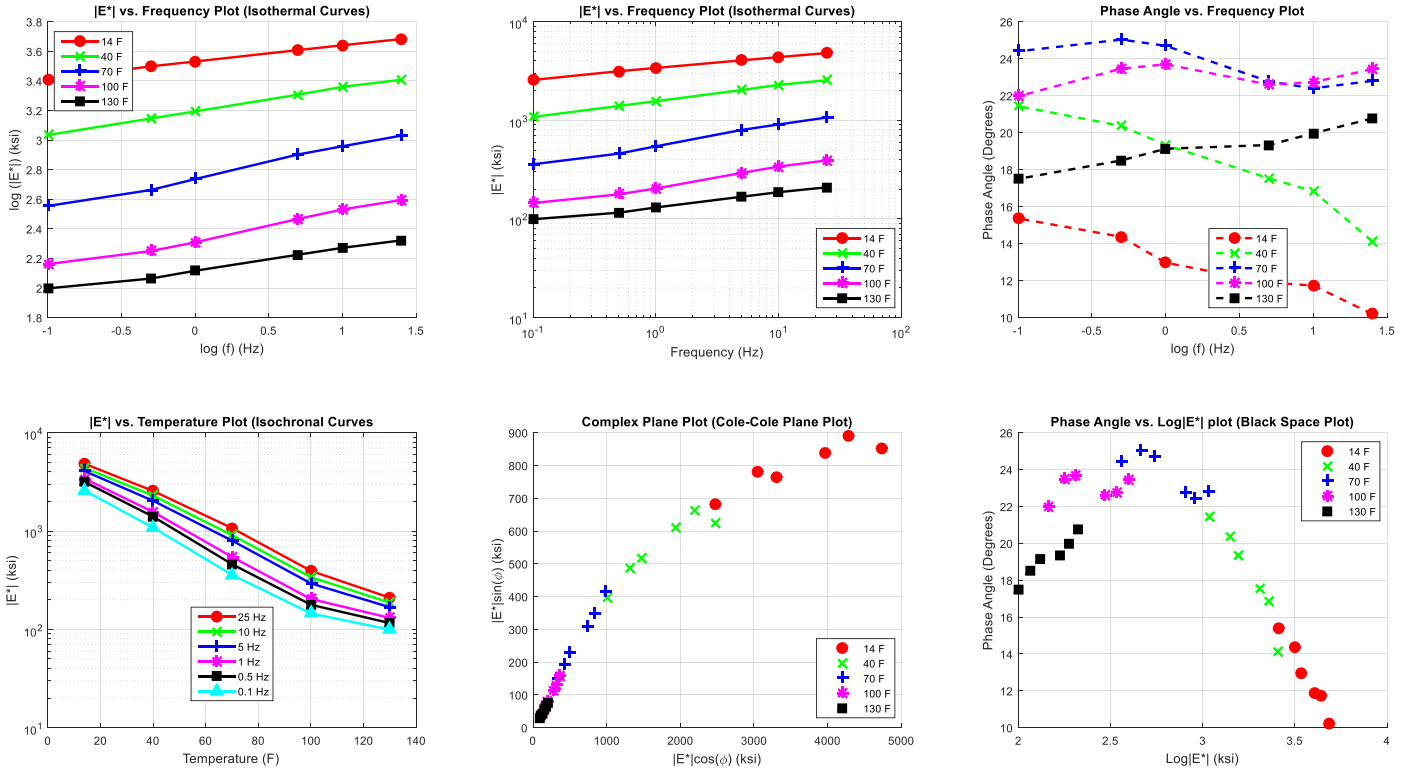

Figure E-15 (a) average log-|E*| versus log-f plot, (b) average |E*| versus f plot, (c) average ϕ versus log-f plot, (d) average |E*| versus temperature plot, (e) complex plane plot for average |E*|, and (f) black space plot for average |E*| for the AC Mix 15.

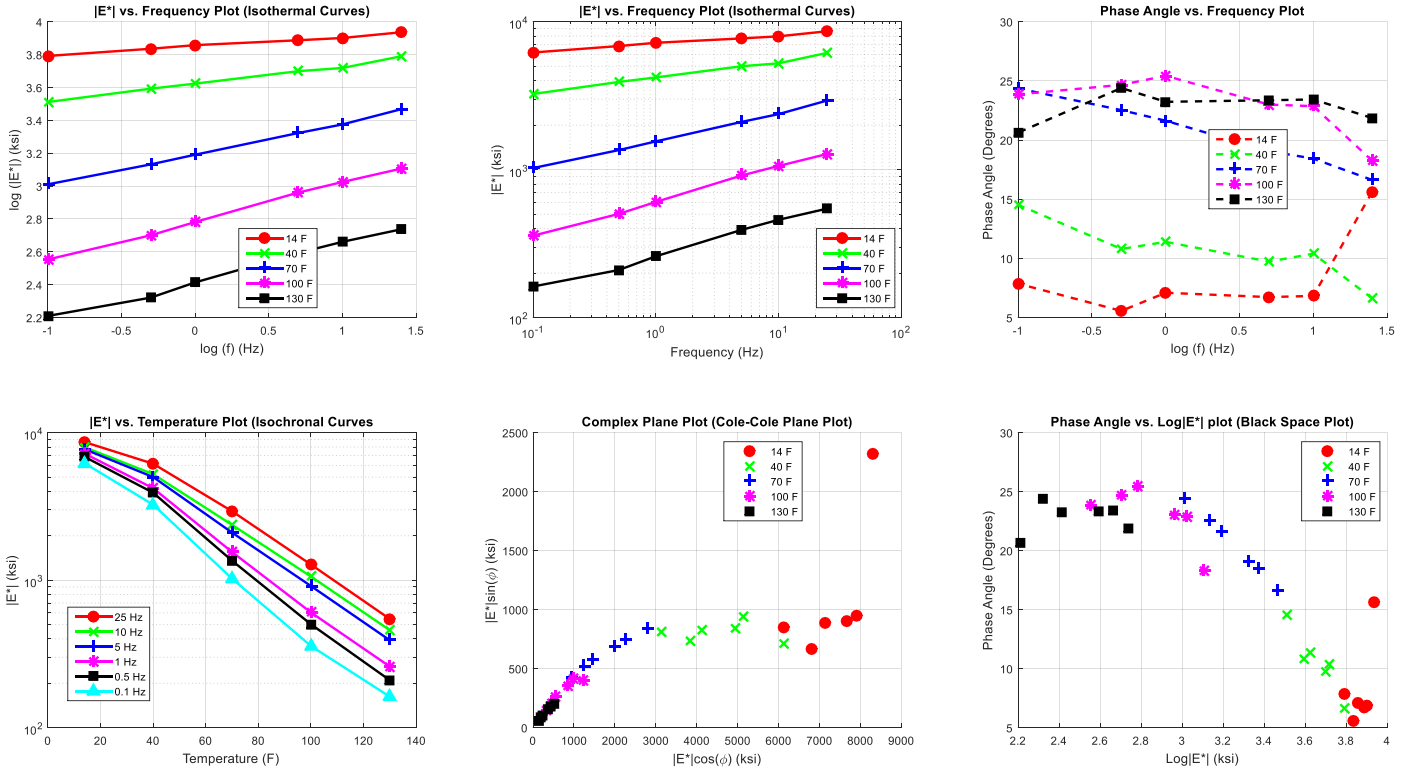

Figure E-16 (a) average log-|E*| versus log-f plot, (b) average |E*| versus f plot, (c) average ϕ versus log-f plot, (d) average |E*| versus temperature plot, (e) complex plane plot for average |E*|, and (f) black space plot for average |E*| for the AC Mix 16.

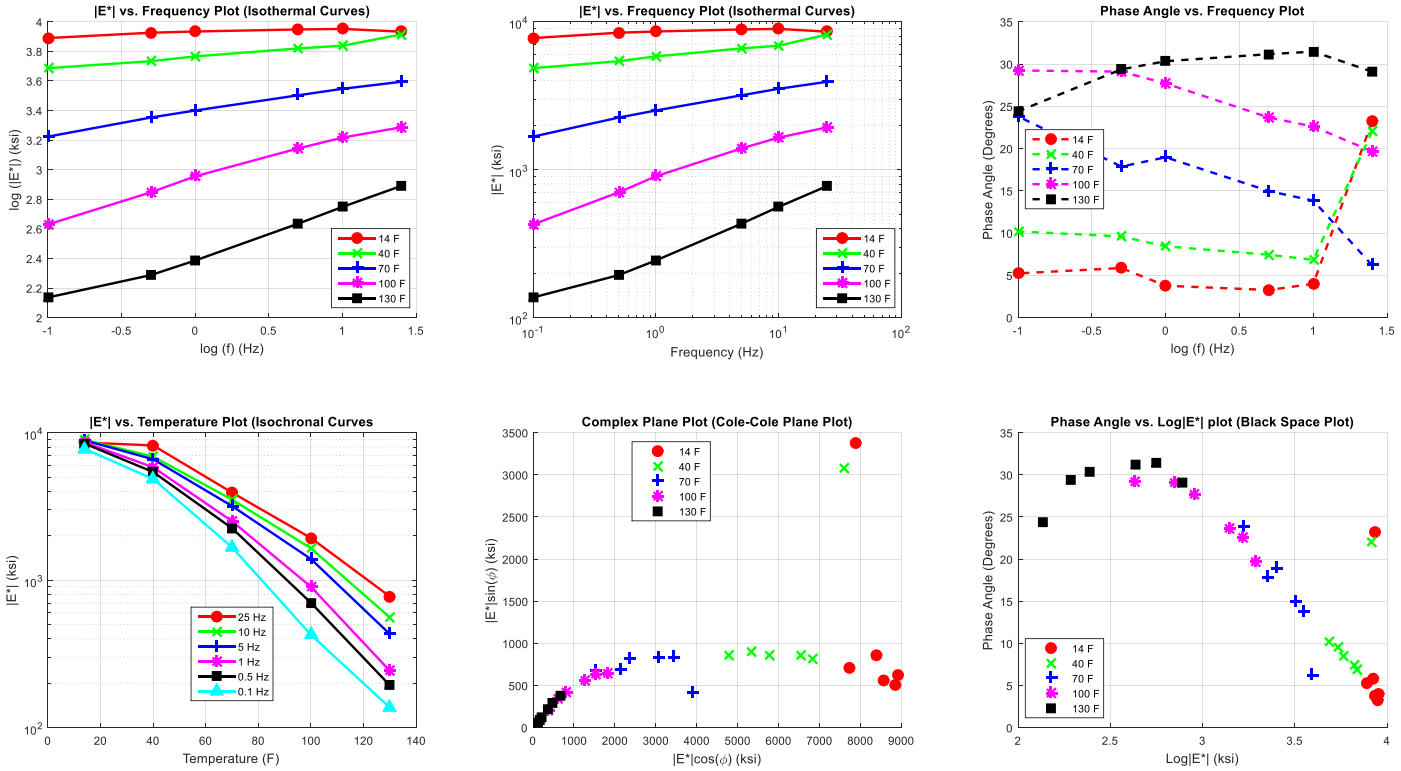

Figure E-17 (a) average log-|E*| versus log-f plot, (b) average |E*| versus f plot, (c) average ϕ versus log-f plot, (d) average |E*| versus temperature plot, (e) complex plane plot for average |E*|, and (f) black space plot for average |E*| for the AC Mix 17.

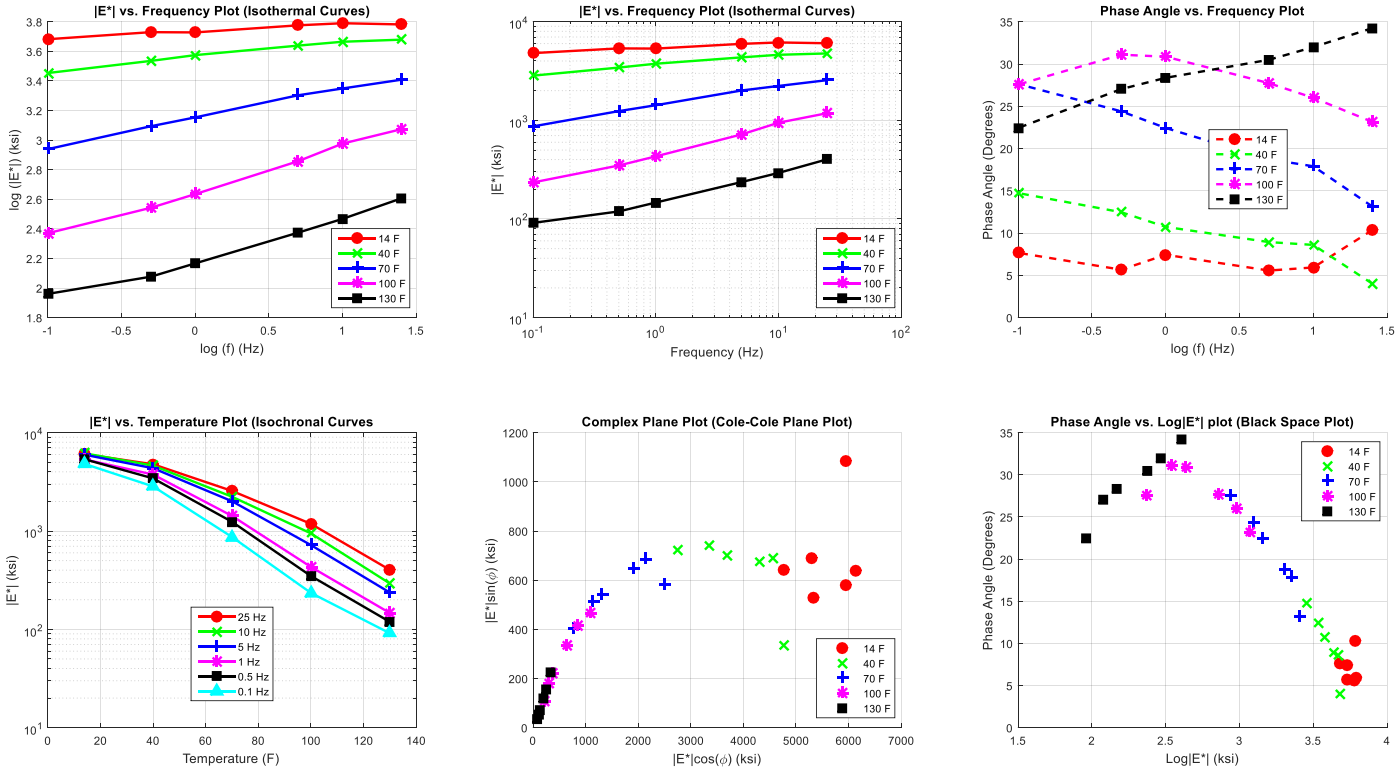

Figure E-18 (a) average log-|E*| versus log-f plot, (b) average |E*| versus f plot, (c) average ϕ versus log-f plot, (d) average |E*| versus temperature plot, (e) complex plane plot for average |E*|, and (f) black space plot for average |E*| for the AC Mix 18.

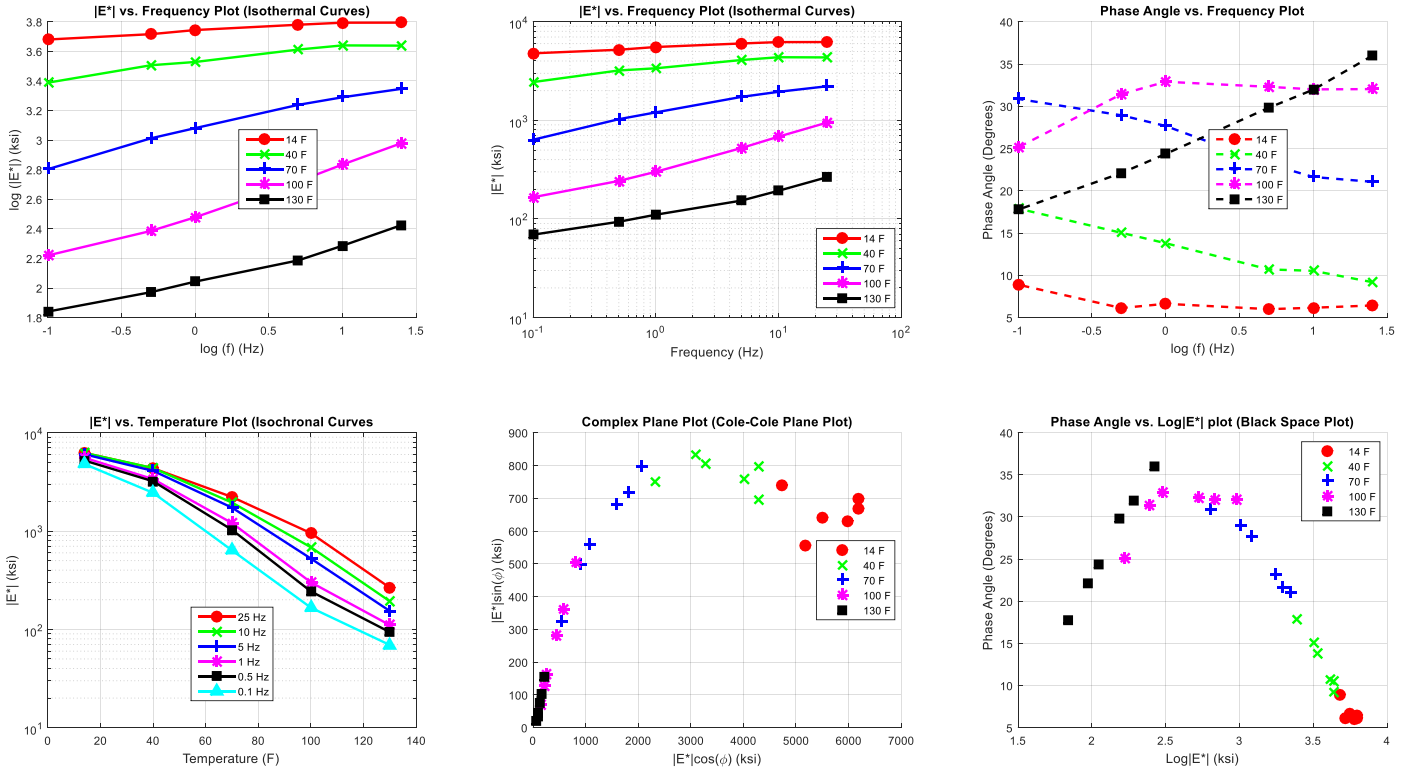

Figure E-19 (a) average log-|E*| versus log-f plot, (b) average |E*| versus f plot, (c) average ϕ versus log-f plot, (d) average |E*| versus temperature plot, (e) complex plane plot for average |E*|, and (f) black space plot for average |E*| for the AC Mix 19.

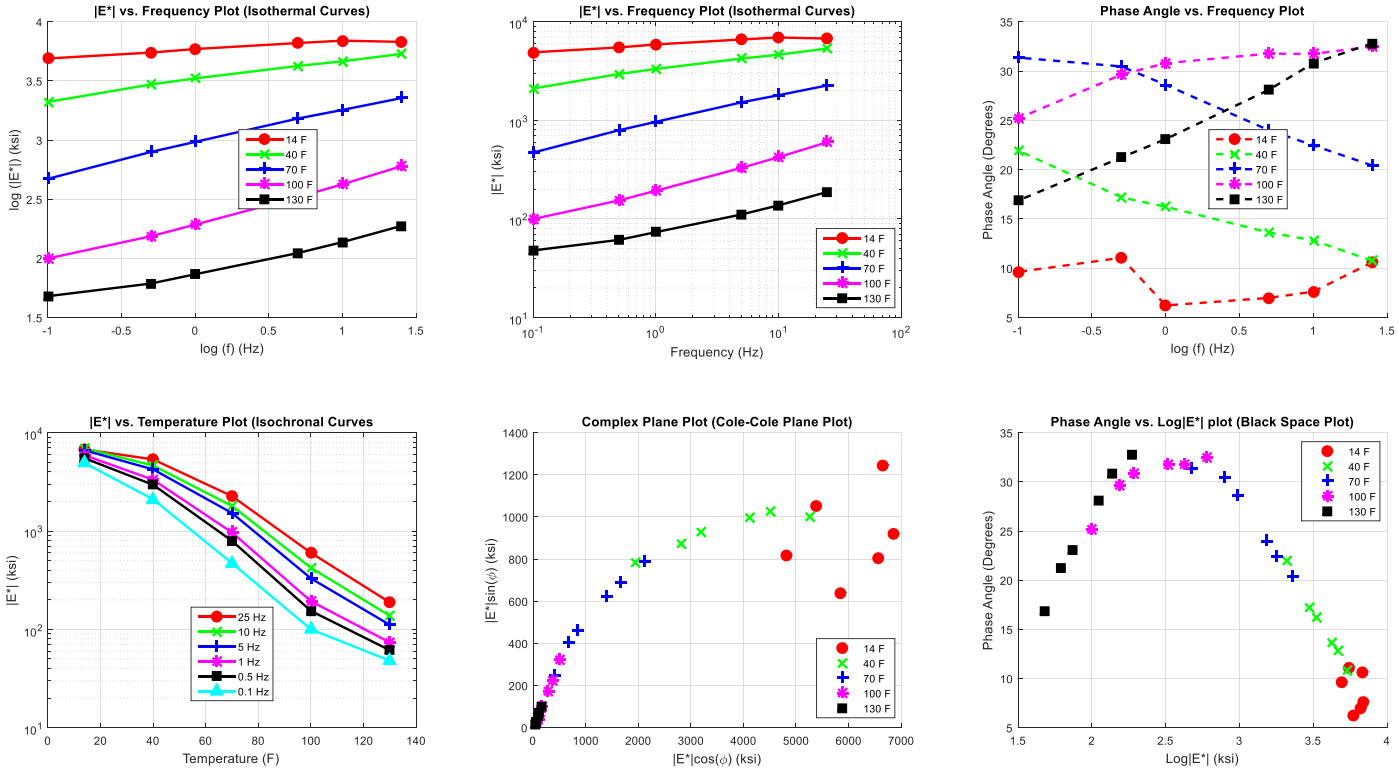

Figure E-20 (a) average log-|E*| versus log-f plot, (b) average |E*| versus f plot, (c) average ϕ versus log-f plot, (d) average |E*| versus temperature plot, (e) complex plane plot for average |E*|, and (f) black space plot for average |E*| for the AC Mix 20.

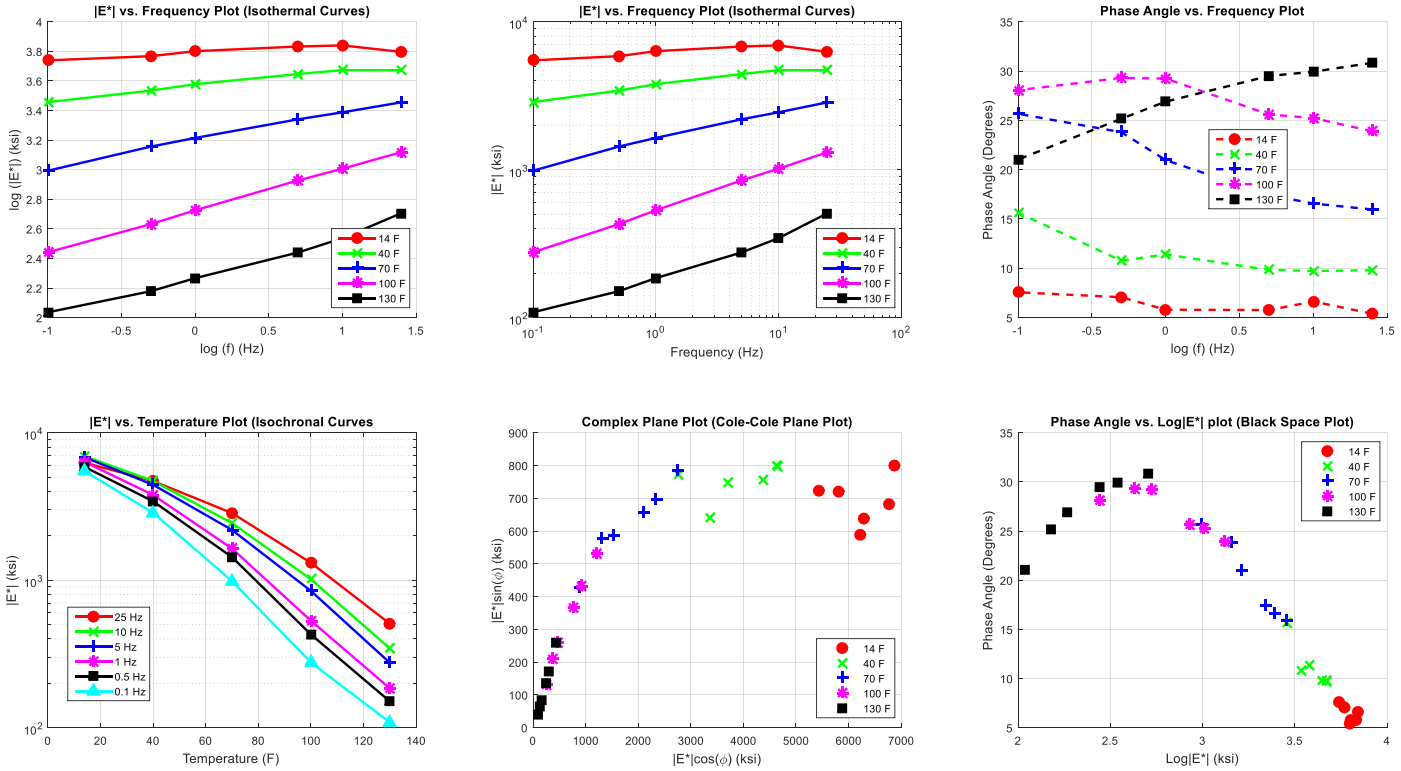

Figure E-21 (a) average log-|E*| versus log-f plot, (b) average |E*| versus f plot, (c) average ϕ versus log-f plot, (d) average |E*| versus temperature plot, (e) complex plane plot for average |E*|, and (f) black space plot for average |E*| for the AC Mix 21.

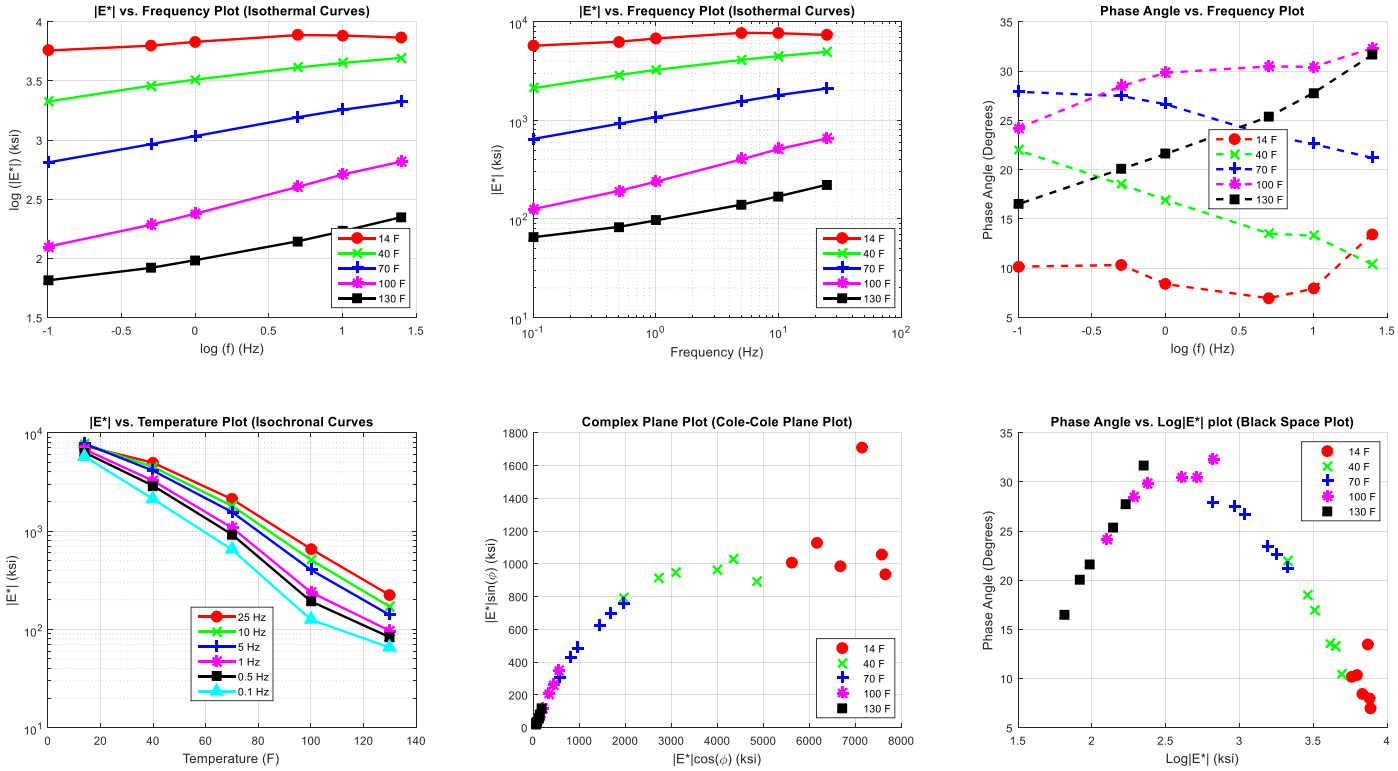

Figure E-22 (a) average log-|E*| versus log-f plot, (b) average |E*| versus f plot, (c) average ϕ versus log-f plot, (d) average |E*| versus temperature plot, (e) complex plane plot for average |E*|, and (f) black space plot for average |E*| for the AC Mix 22.

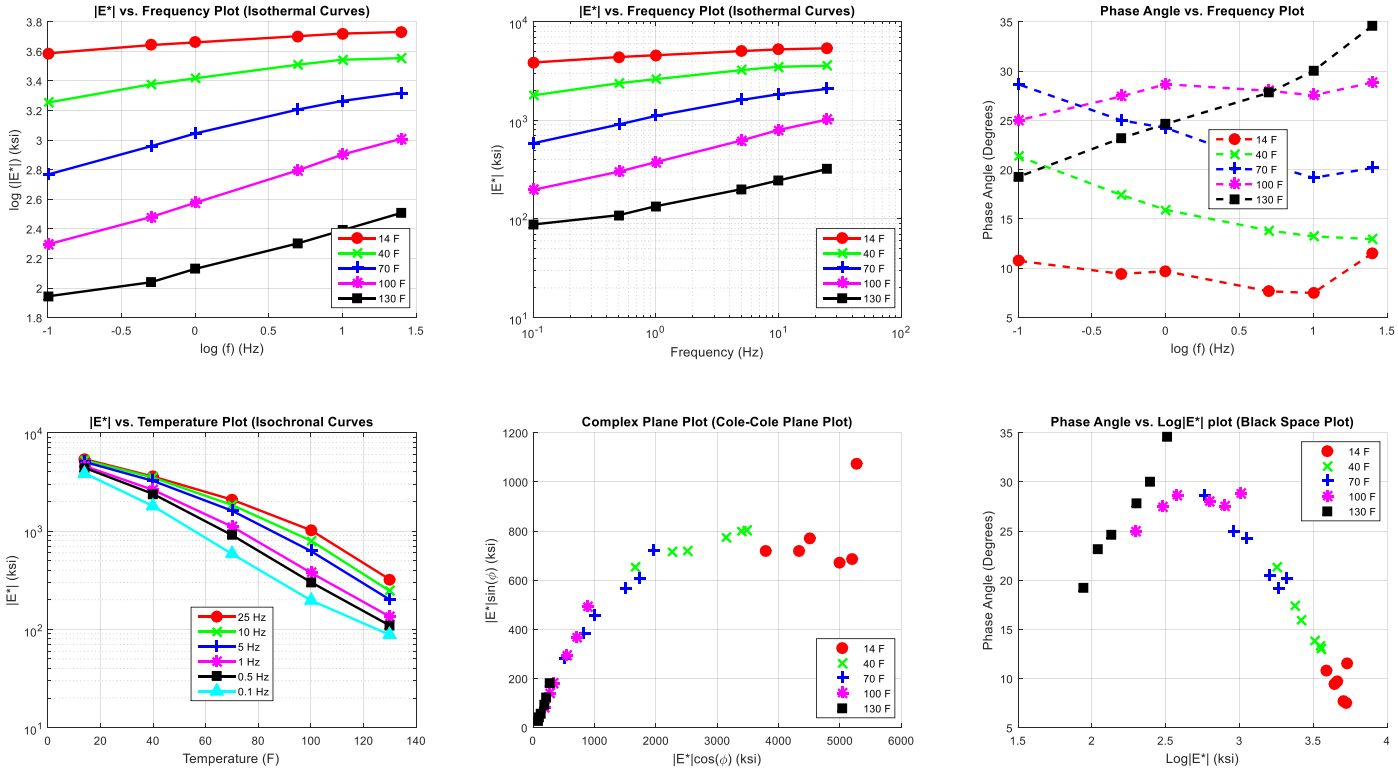

Figure E-23 (a) average log-|E*| versus log-f plot, (b) average |E*| versus f plot, (c) average ϕ versus log-f plot, (d) average |E*| versus temperature plot, (e) complex plane plot for average |E*|, and (f) black space plot for average |E*| for the AC Mix 23.

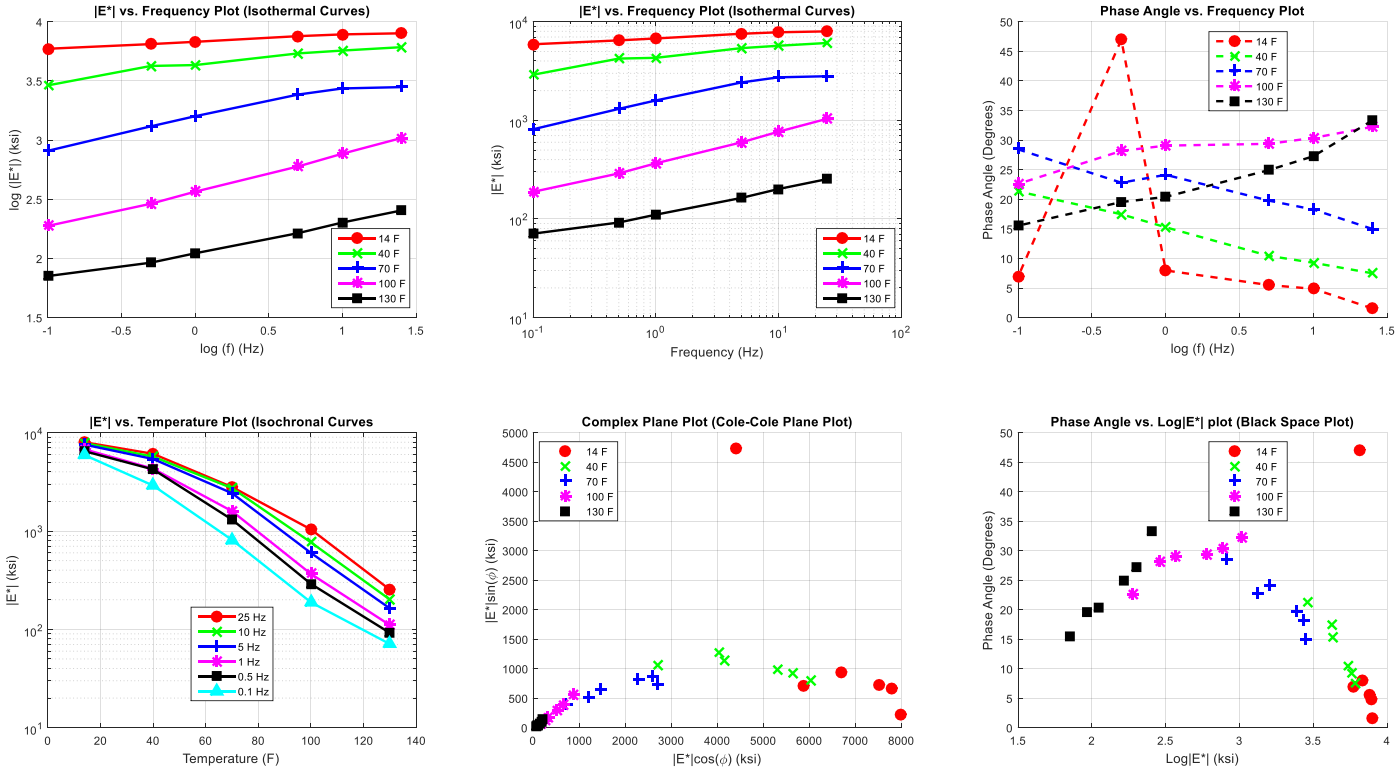

Figure E-24 (a) average log-|E*| versus log-f plot, (b) average |E*| versus f plot, (c) average ϕ versus log-f plot, (d) average |E*| versus temperature plot, (e) complex plane plot for average |E*|, and (f) black space plot for average |E*| for the AC Mix 24.

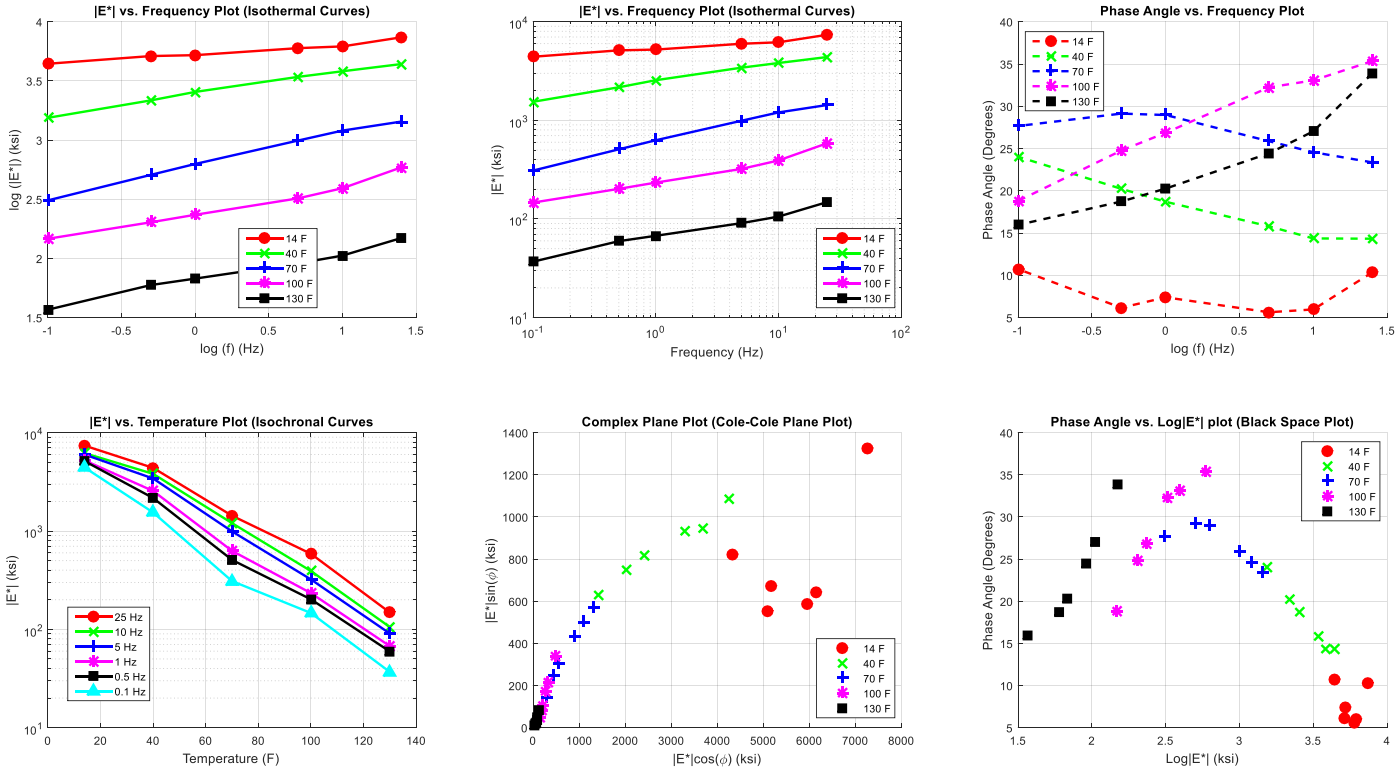

Figure E-25 (a) average log-|E*| versus log-f plot, (b) average |E*| versus f plot, (c) average ϕ versus log-f plot, (d) average |E*| versus temperature plot, (e) complex plane plot for average |E*|, and (f) black space plot for average |E*| for the AC Mix 25.

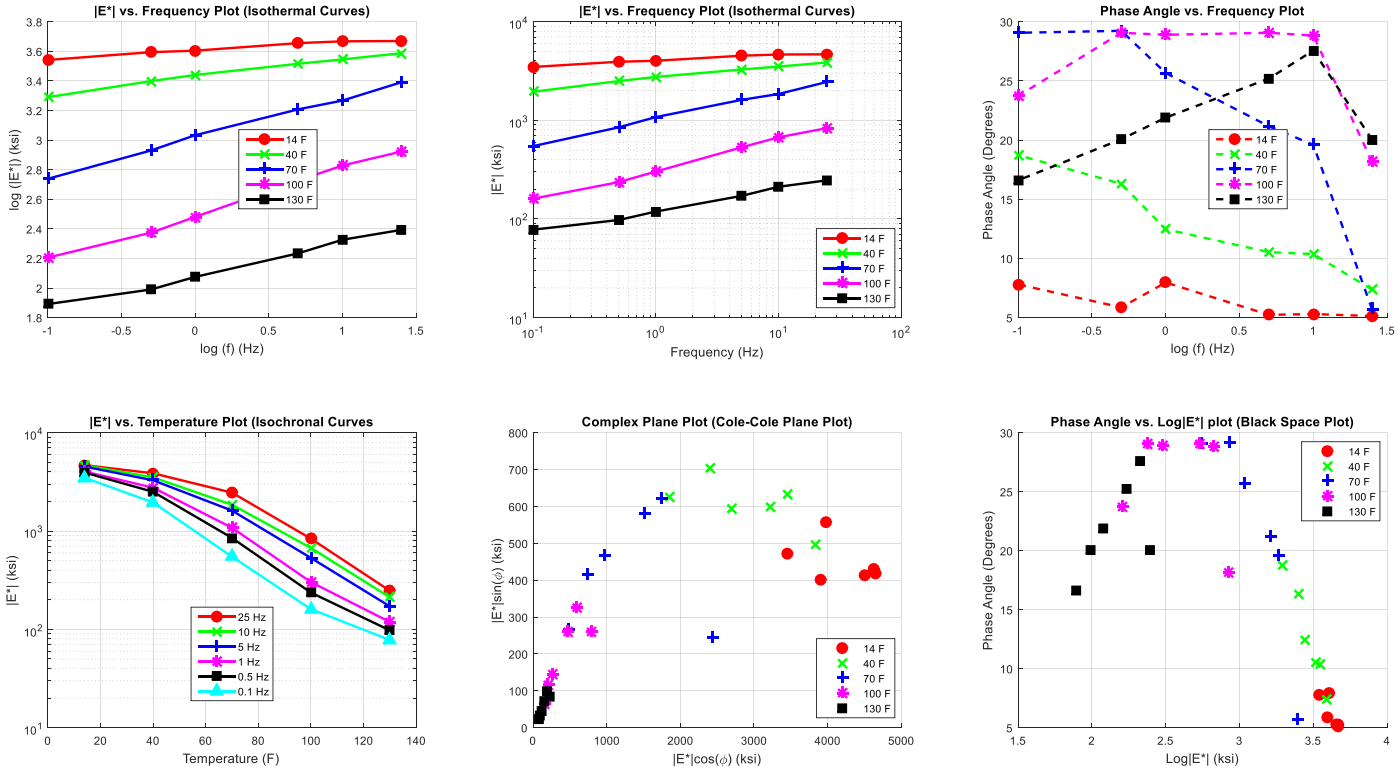

Figure E-26 (a) average log-|E*| versus log-f plot, (b) average |E*| versus f plot, (c) average ϕ versus log-f plot, (d) average |E*| versus temperature plot, (e) complex plane plot for average |E*|, and (f) black space plot for average |E*| for the AC Mix 26.

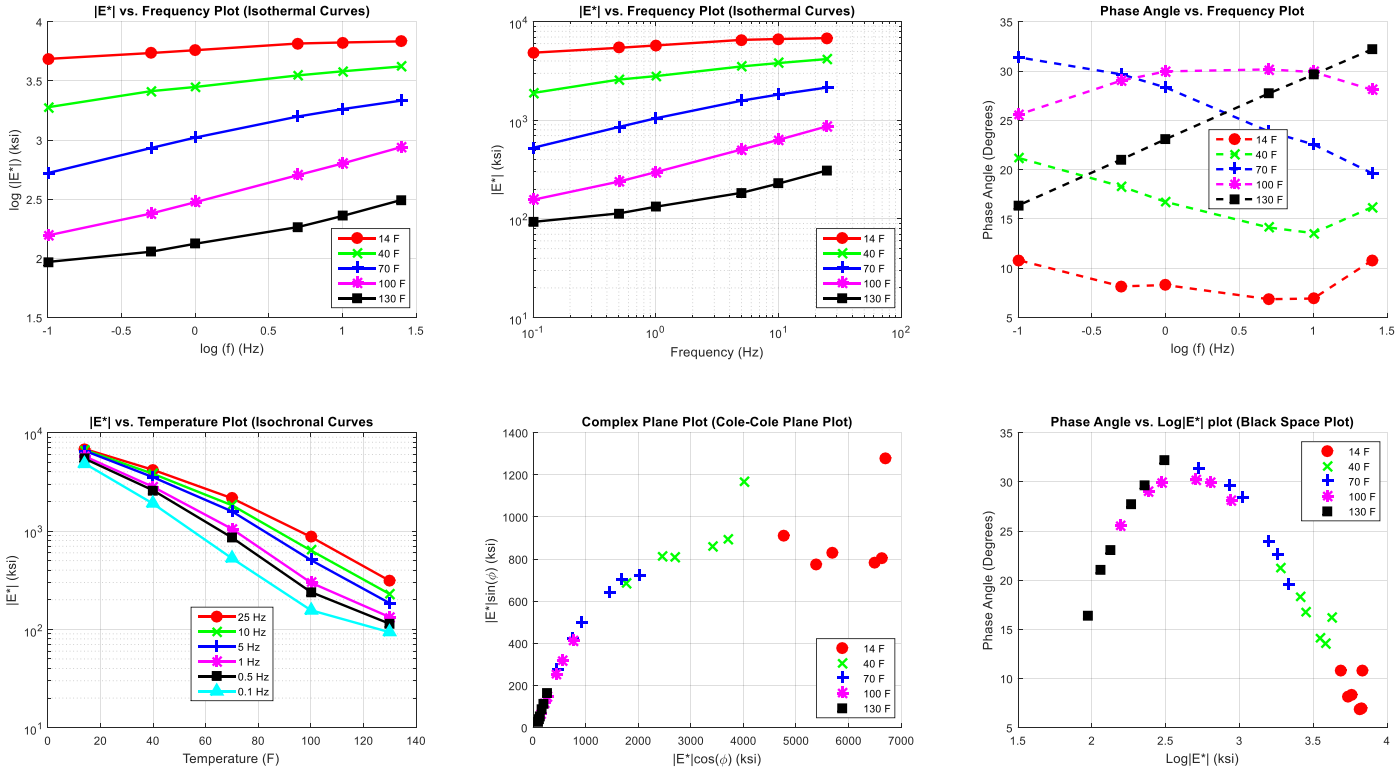

Figure E-27 (a) average log-|E*| versus log-f plot, (b) average |E*| versus f plot, (c) average ϕ versus log-f plot, (d) average |E*| versus temperature plot, (e) complex plane plot for average |E*|, and (f) black space plot for average |E*| for the AC Mix 27.

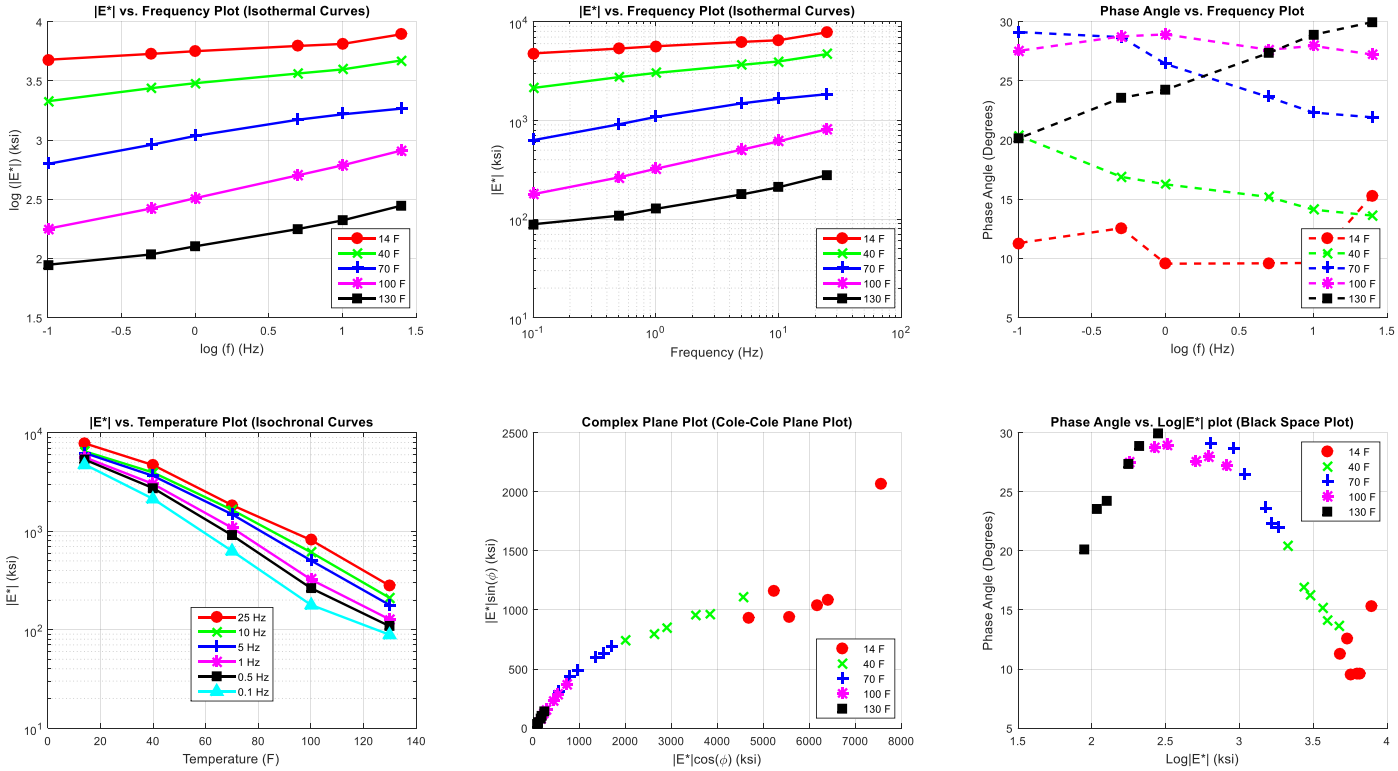

Figure E-28 (a) average log-|E*| versus log-f plot, (b) average |E*| versus f plot, (c) average ϕ versus log-f plot, (d) average |E*| versus temperature plot, (e) complex plane plot for average |E*|, and (f) black space plot for average |E*| for the AC Mix 28.

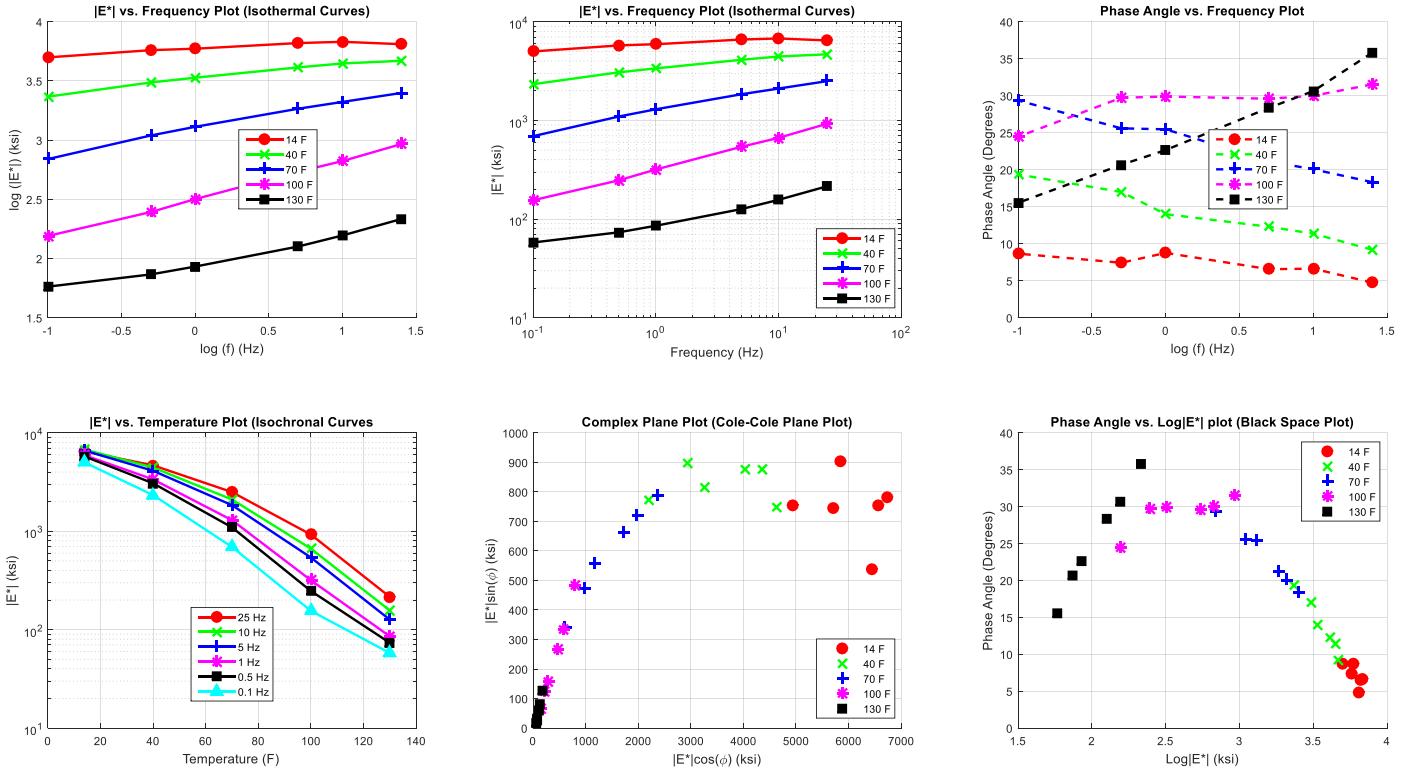

Figure E-29 (a) average log-|E*| versus log-f plot, (b) average |E*| versus f plot, (c) average ϕ versus log-f plot, (d) average |E*| versus temperature plot, (e) complex plane plot for average |E*|, and (f) black space plot for average |E*| for the AC Mix 29.

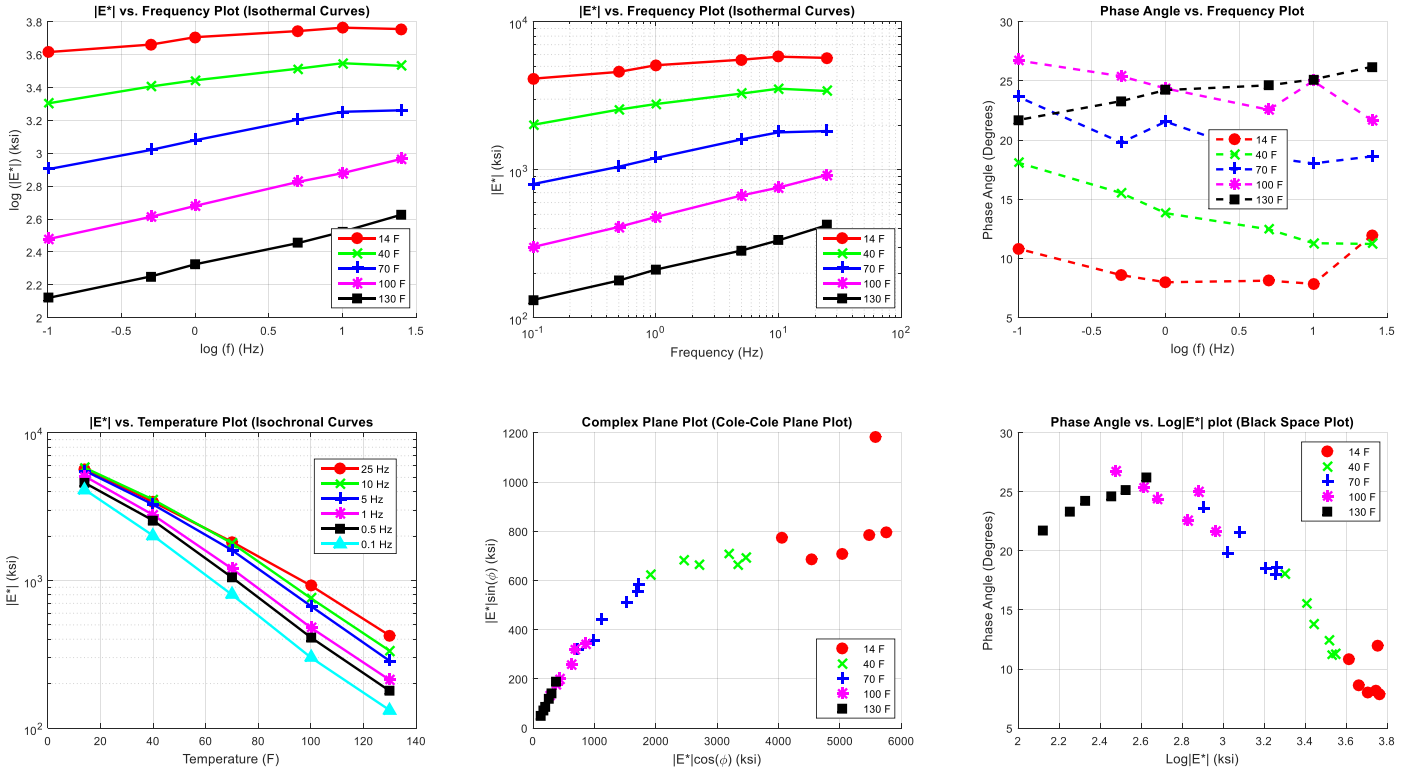

Figure E-30 (a) average log-|E*| versus log-f plot, (b) average |E*| versus f plot, (c) average ϕ versus log-f plot, (d) average |E*| versus temperature plot, (e) complex plane plot for average |E*|, and (f) black space plot for average |E*| for the AC Mix 30.

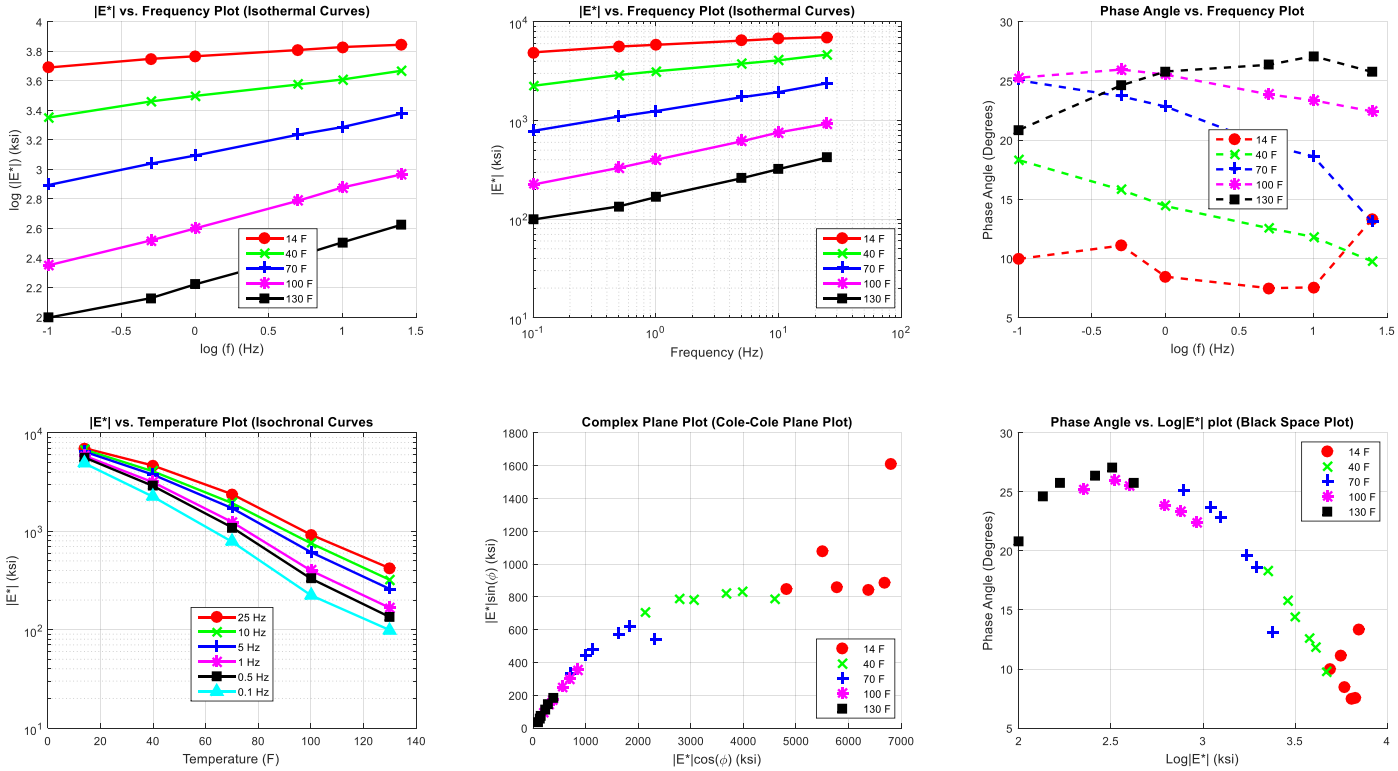

Figure E-31 (a) average log-|E*| versus log-f plot, (b) average |E*| versus f plot, (c) average ϕ versus log-f plot, (d) average |E*| versus temperature plot, (e) complex plane plot for average |E*|, and (f) black space plot for average |E*| for the AC Mix 31.

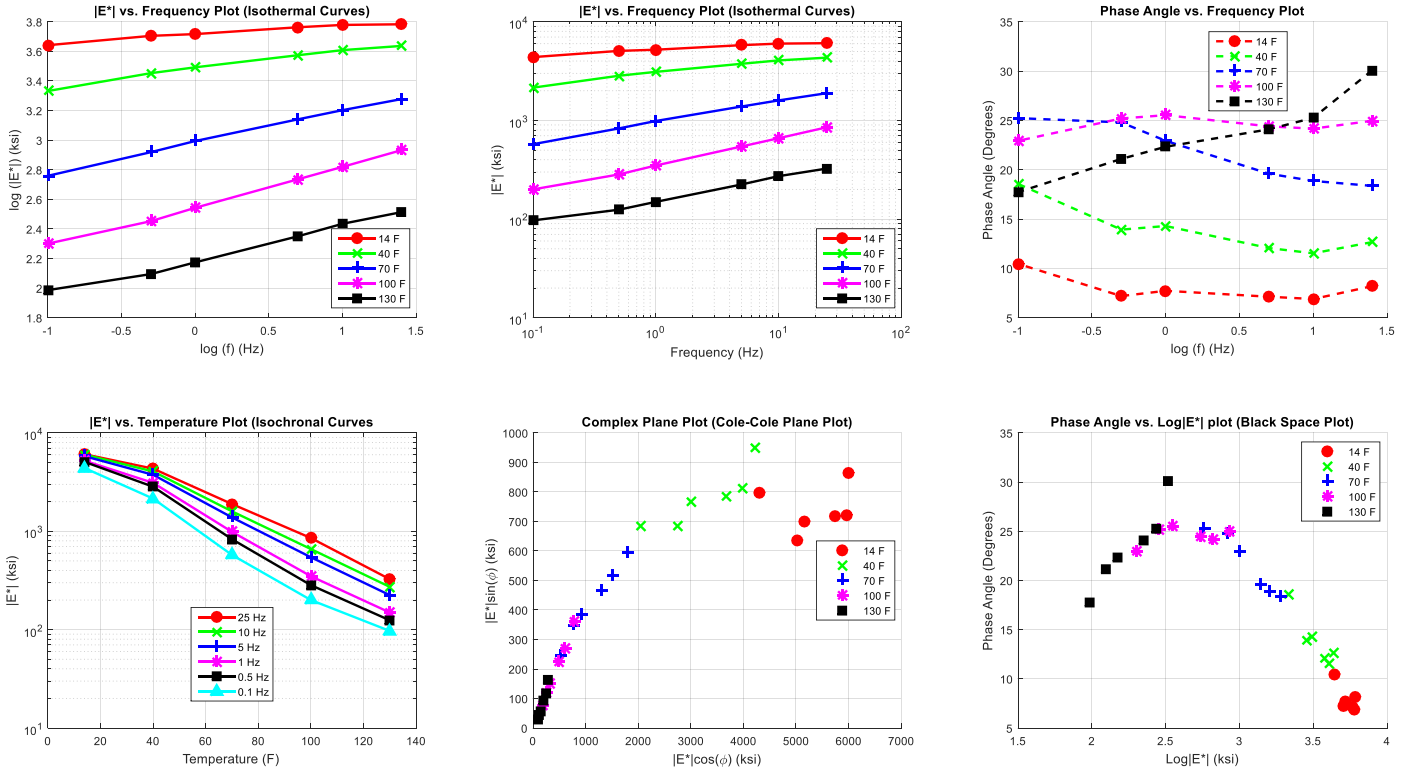

Figure E-32 (a) average log-|E*| versus log-f plot, (b) average |E*| versus f plot, (c) average ϕ versus log-f plot, (d) average |E*| versus temperature plot, (e) complex plane plot for average |E*|, and (f) black space plot for average |E*| for the AC Mix 32.

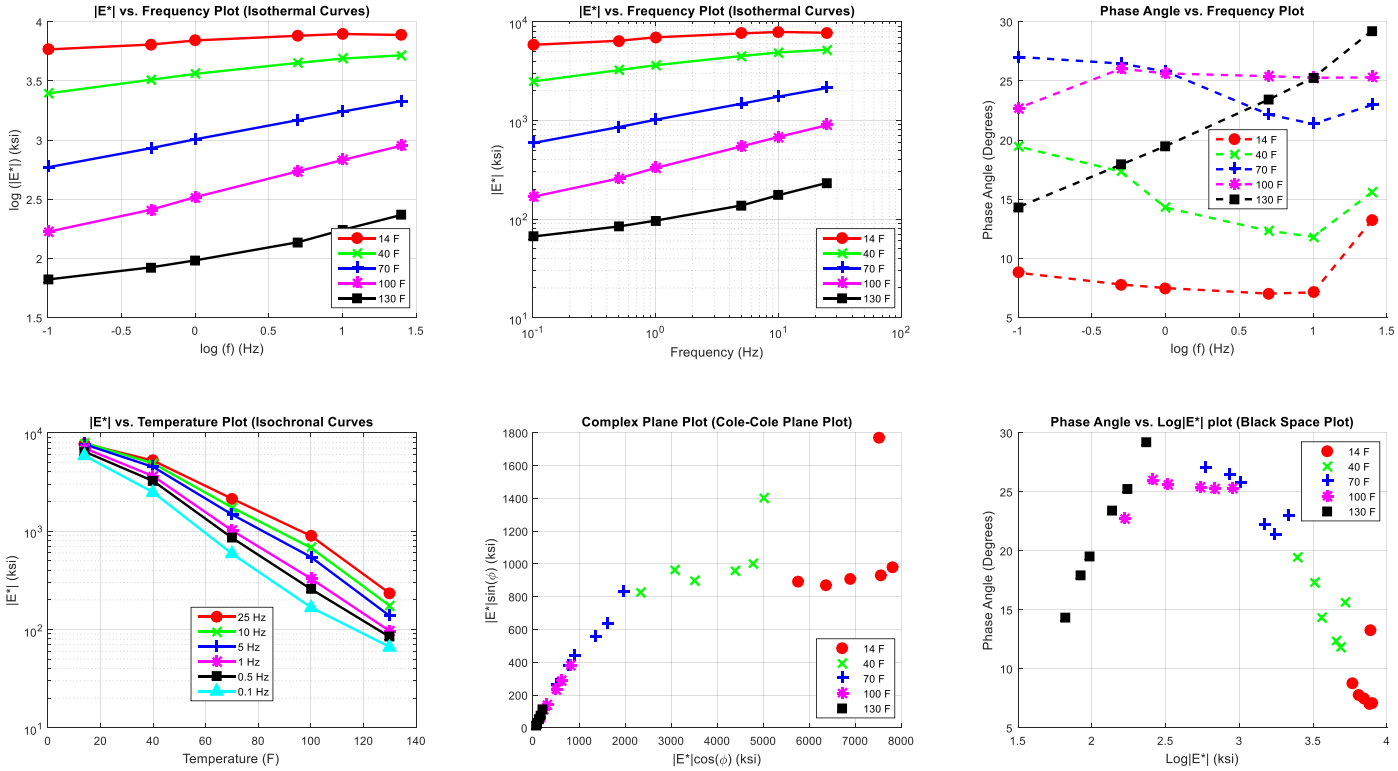

Figure E-33 (a) average log-|E*| versus log-f plot, (b) average |E*| versus f plot, (c) average ϕ versus log-f plot, (d) average |E*| versus temperature plot, (e) complex plane plot for average |E*|, and (f) black space plot for average |E*| for the AC Mix 33.

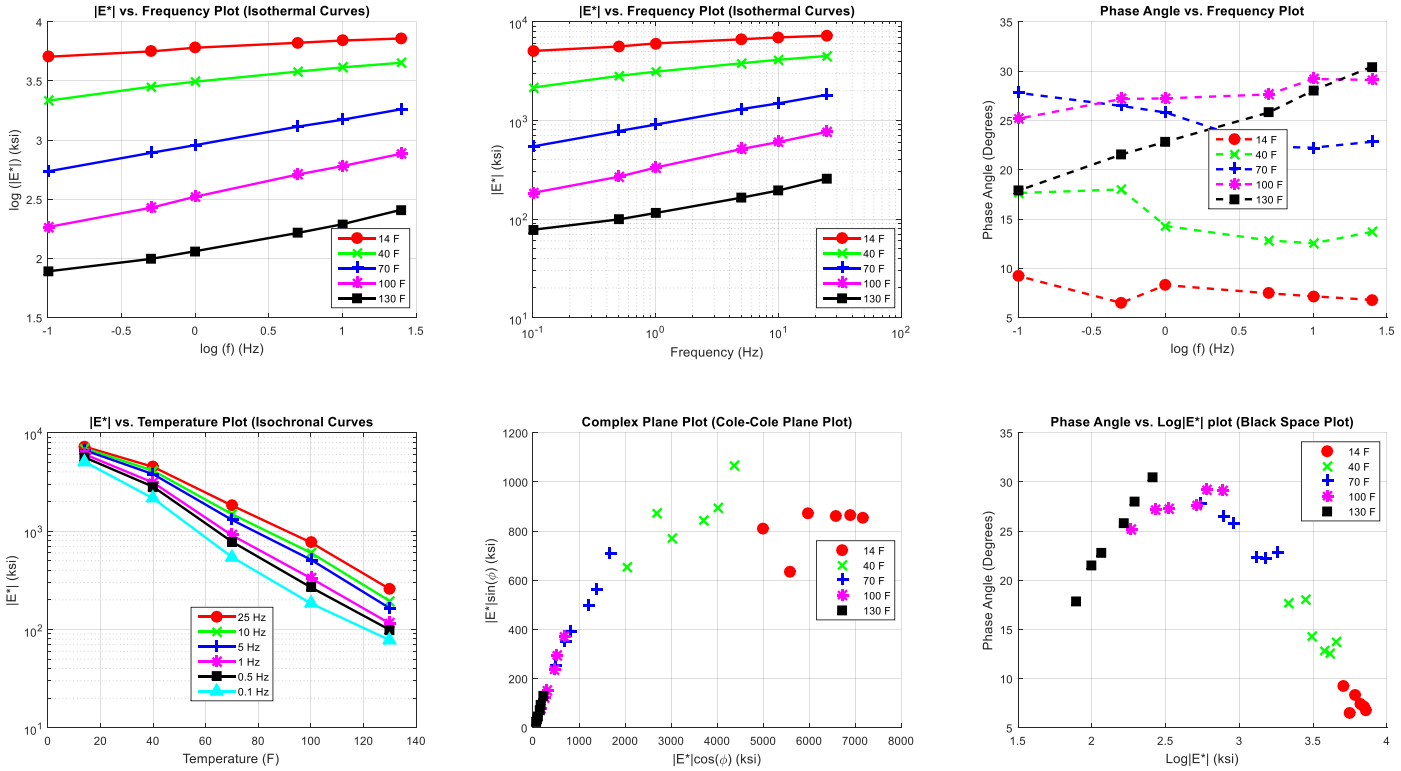

Figure E-34 (a) average log-|E*| versus log-f plot, (b) average |E*| versus f plot, (c) average ϕ versus log-f plot, (d) average |E*| versus temperature plot, (e) complex plane plot for average |E*|, and (f) black space plot for average |E*| for the AC Mix 34.

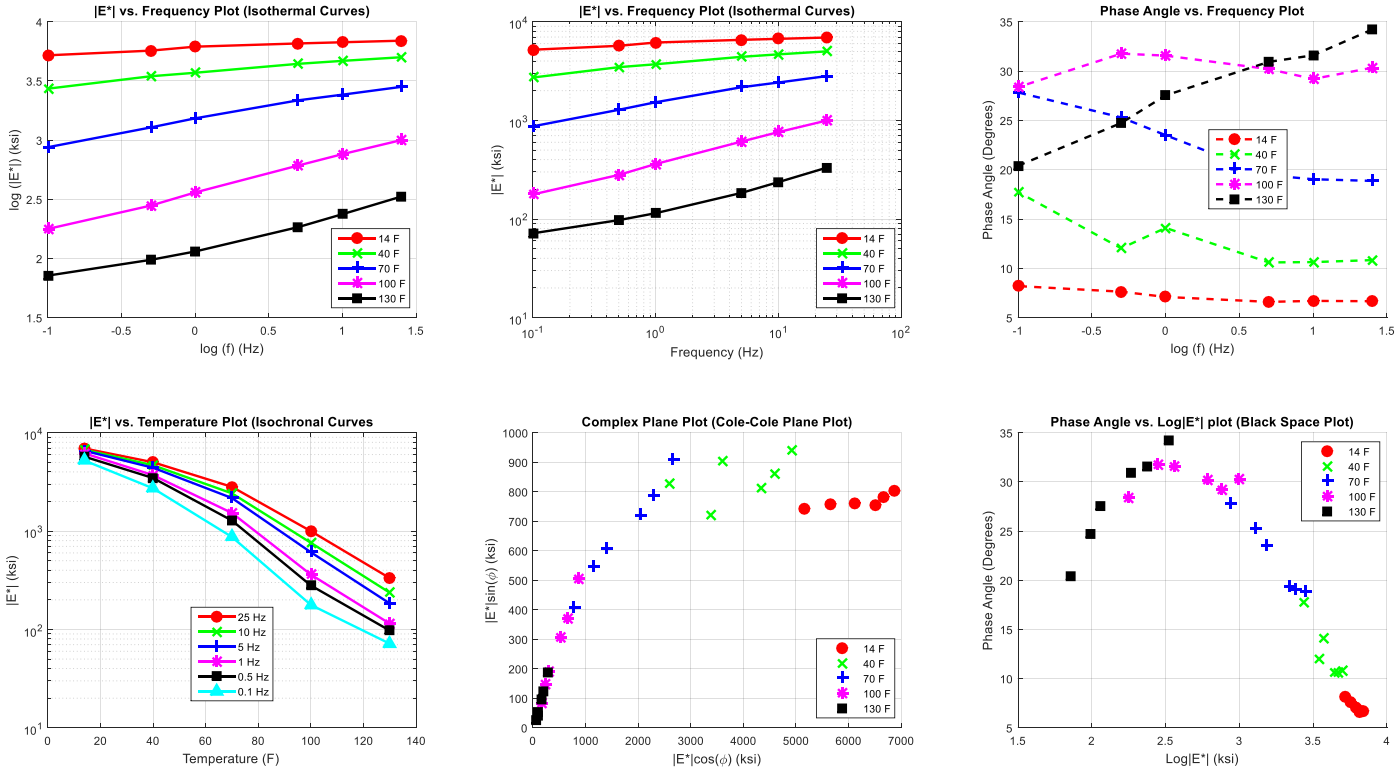

Figure E-35 (a) average log-|E*| versus log-f plot, (b) average |E*| versus f plot, (c) average ϕ versus log-f plot, (d) average |E*| versus temperature plot, (e) complex plane plot for average |E*|, and (f) black space plot for average |E*| for the AC Mix 35.

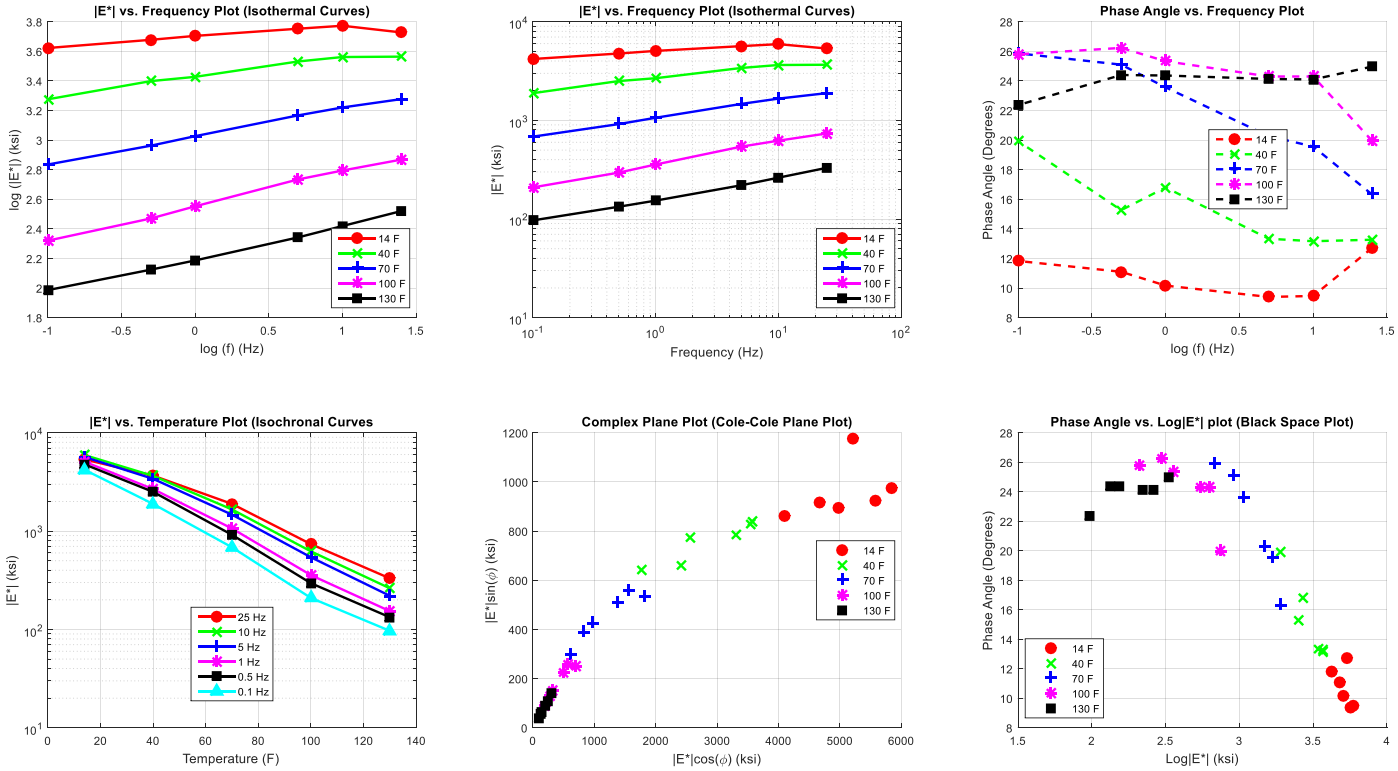

Figure E-36 (a) average log-|E*| versus log-f plot, (b) average |E*| versus f plot, (c) average ϕ versus log-f plot, (d) average |E*| versus temperature plot, (e) complex plane plot for average |E*|, and (f) black space plot for average |E*| for the AC Mix 36.

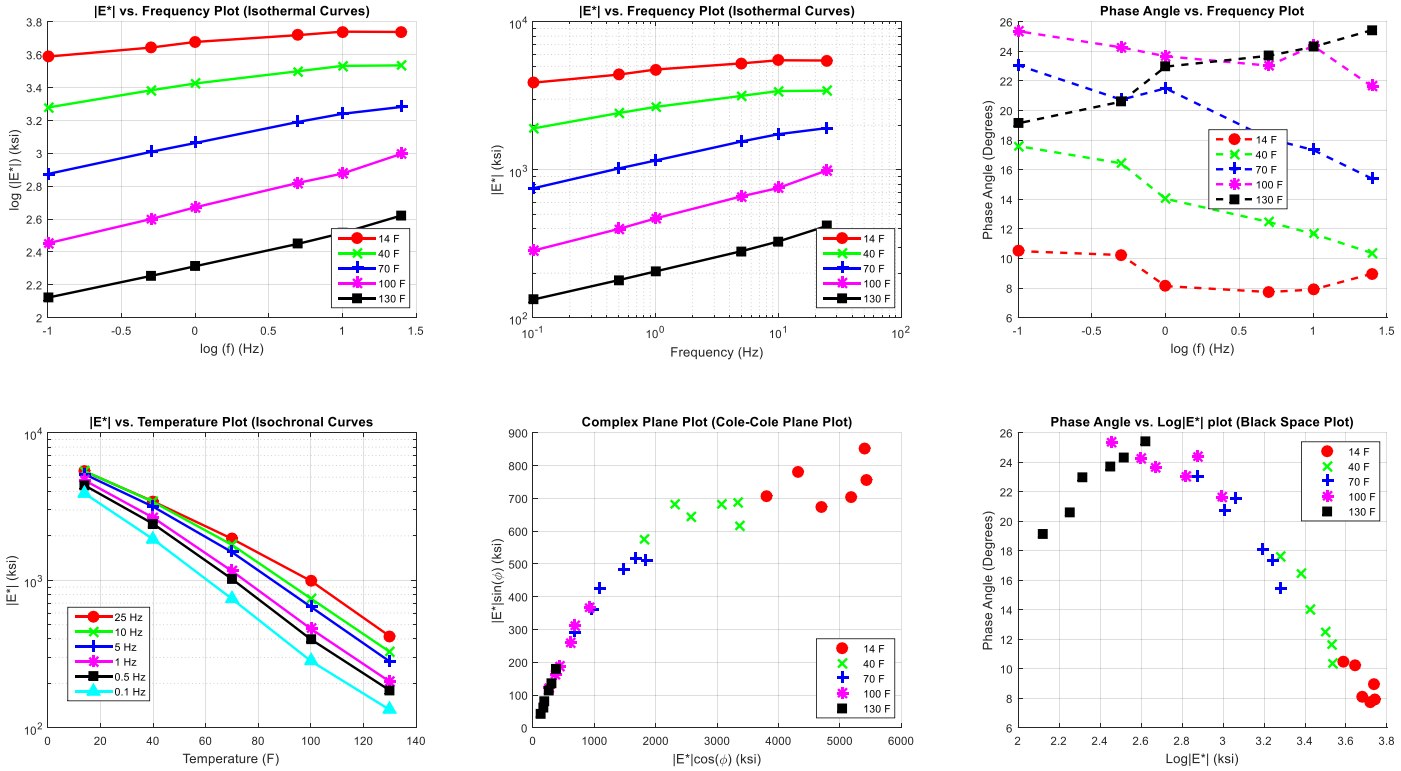

Figure E-37 (a) average log-|E*| versus log-f plot, (b) average |E*| versus f plot, (c) average ϕ versus log-f plot, (d) average |E*| versus temperature plot, (e) complex plane plot for average |E*|, and (f) black space plot for average |E*| for the AC Mix 37.

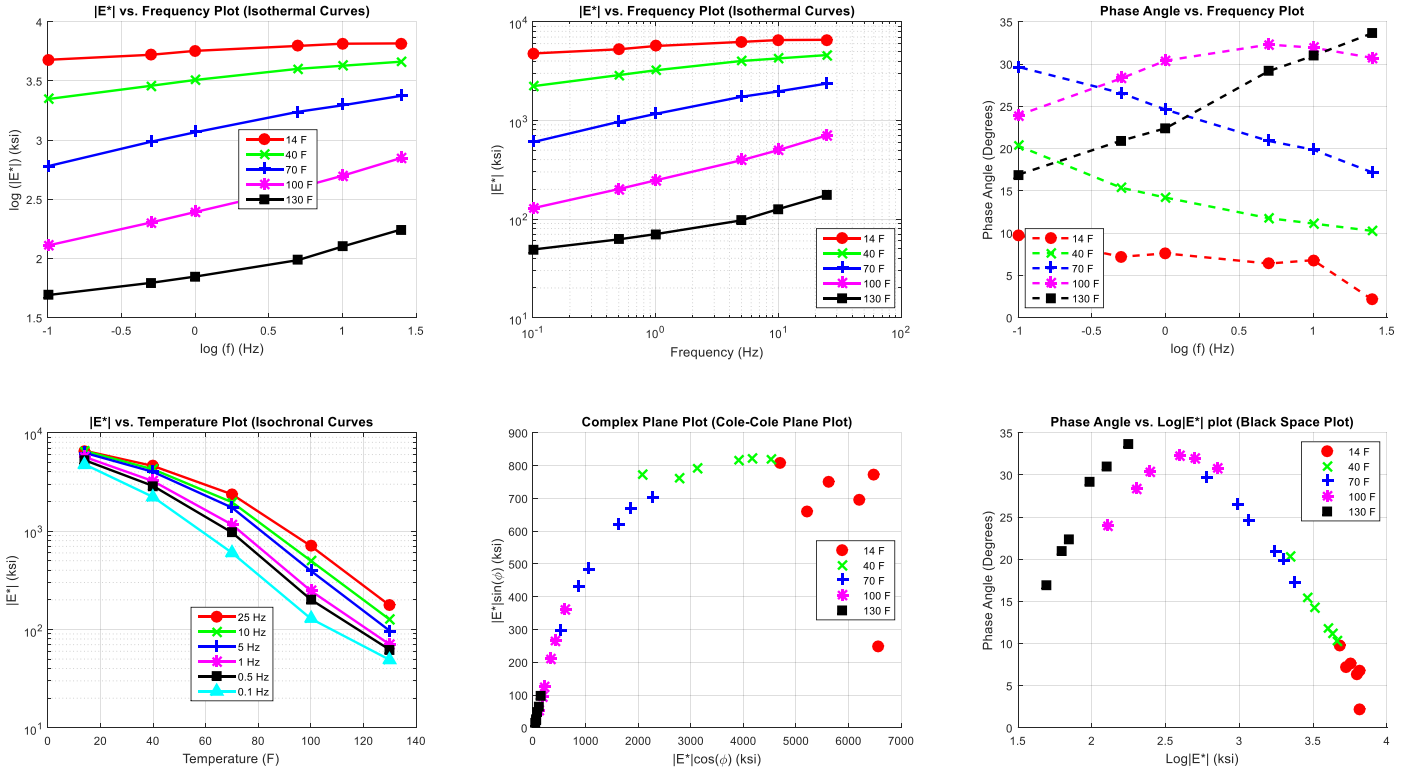

Figure E-38 (a) average log-|E*| versus log-f plot, (b) average |E*| versus f plot, (c) average ϕ versus log-f plot, (d) average |E*| versus temperature plot, (e) complex plane plot for average |E*|, and (f) black space plot for average |E*| for the AC Mix 38.

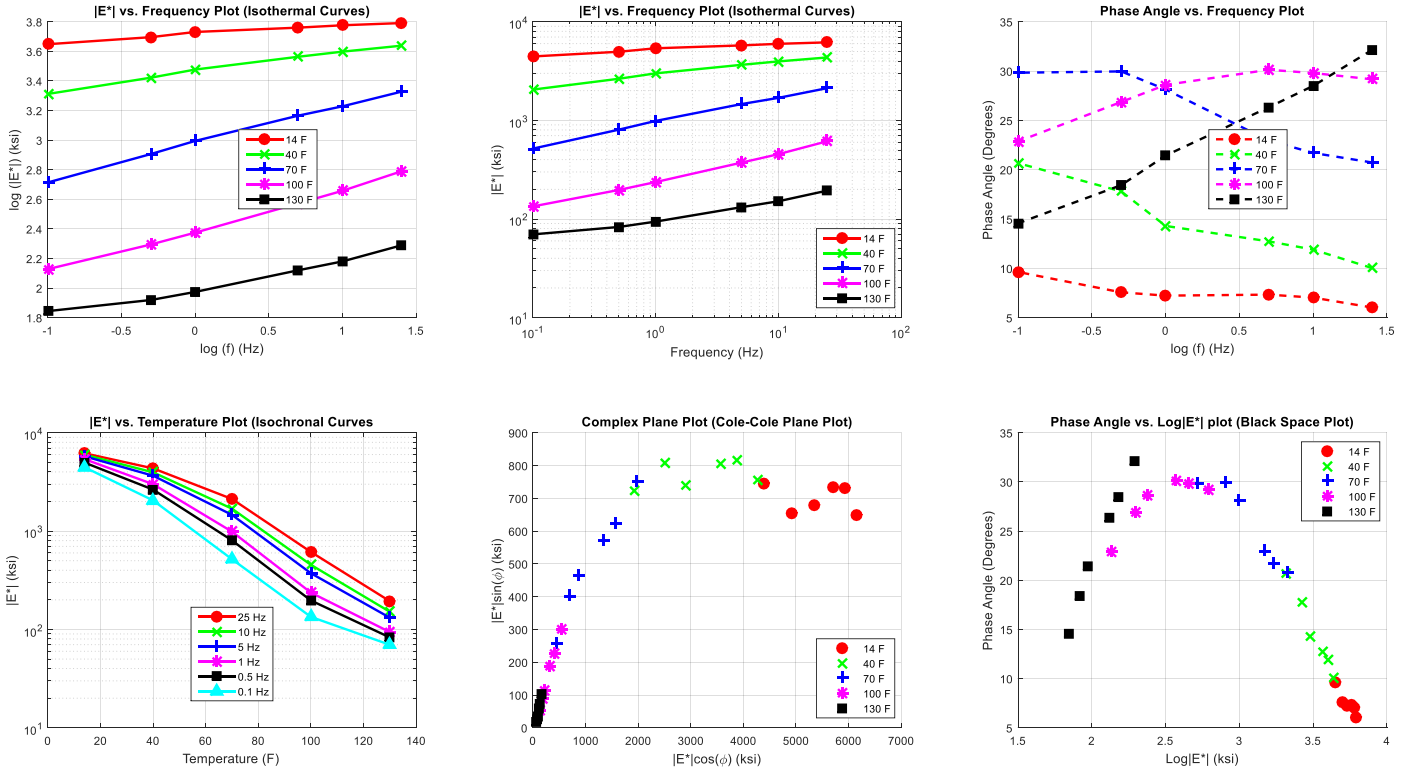

Figure E-39 (a) average log-|E*| versus log-f plot, (b) average |E*| versus f plot, (c) average ϕ versus log-f plot, (d) average |E*| versus temperature plot, (e) complex plane plot for average |E*|, and (f) black space plot for average |E*| for the AC Mix 39.

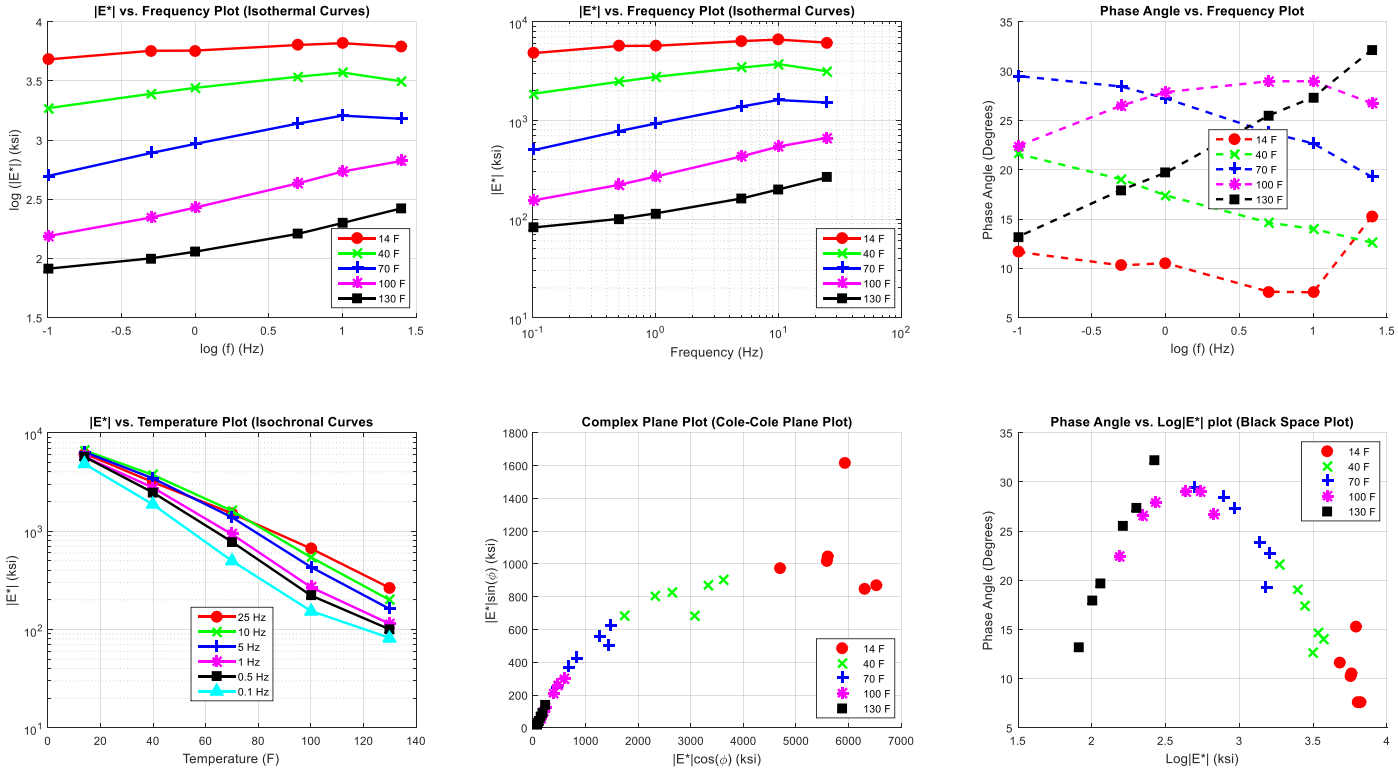

Figure E-40 (a) average log-|E*| versus log-f plot, (b) average |E*| versus f plot, (c) average ϕ versus log-f plot, (d) average |E*| versus temperature plot, (e) complex plane plot for average |E*|, and (f) black space plot for average |E*| for the AC Mix 40.

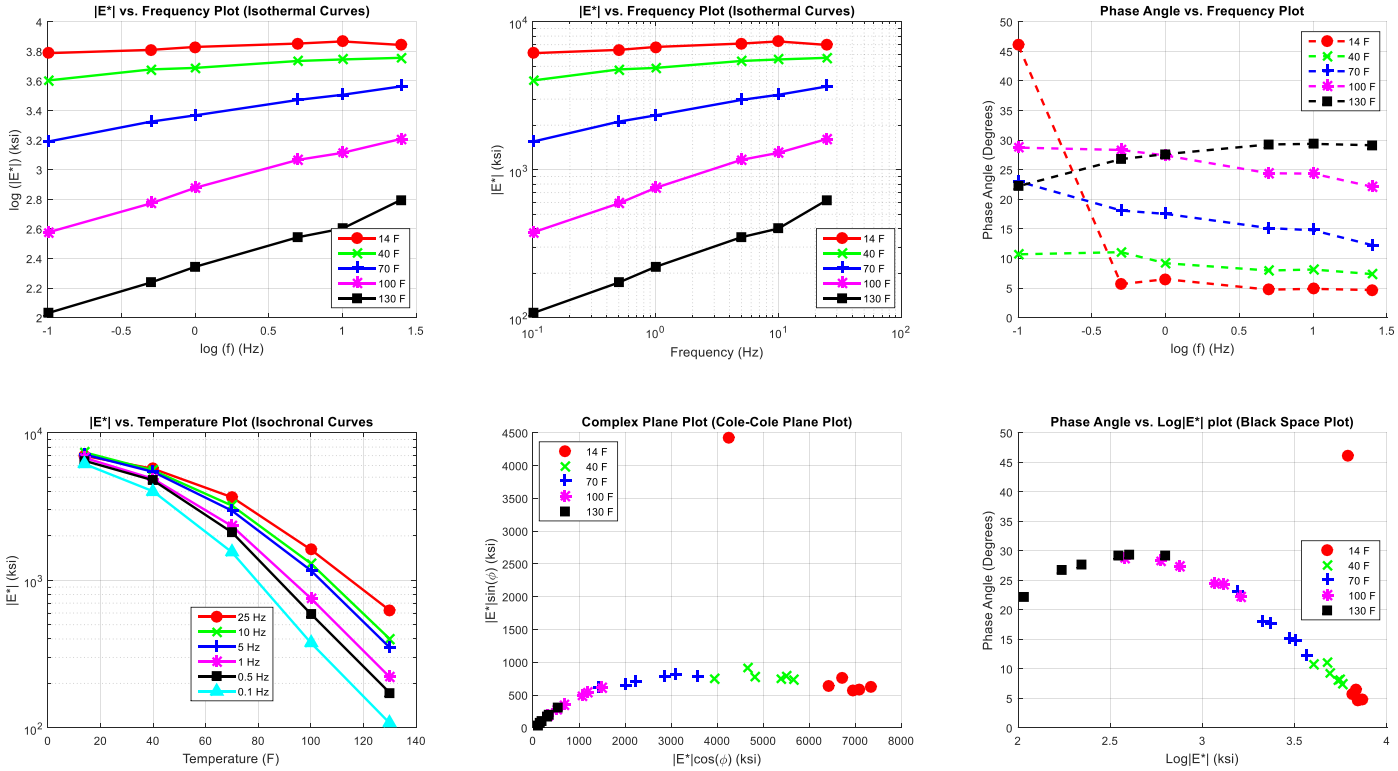

Figure E-41 (a) average log-|E*| versus log-f plot, (b) average |E*| versus f plot, (c) average ϕ versus log-f plot, (d) average |E*| versus temperature plot, (e) complex plane plot for average |E*|, and (f) black space plot for average |E*| for the AC Mix 41.

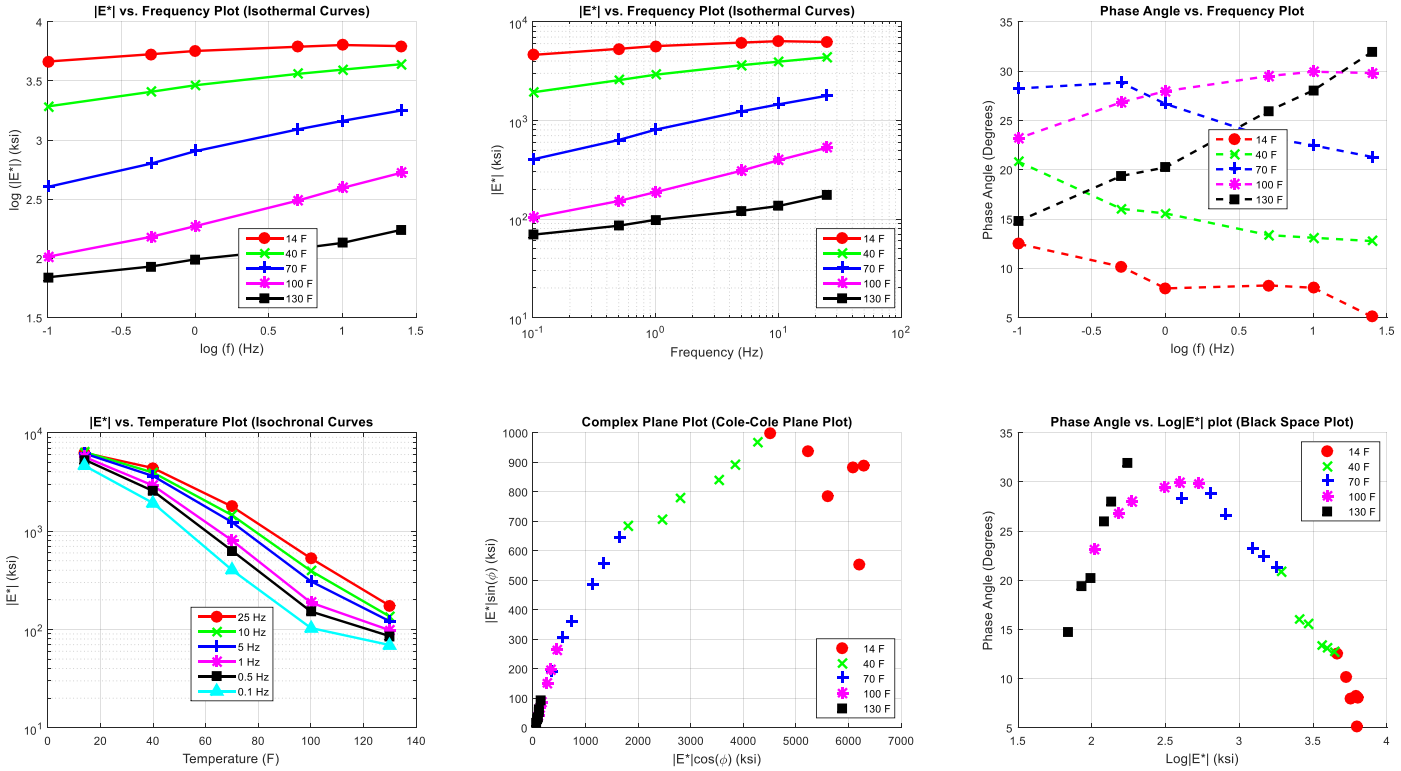

Figure E-42 (a) average log-|E*| versus log-f plot, (b) average |E*| versus f plot, (c) average ϕ versus log-f plot, (d) average |E*| versus temperature plot, (e) complex plane plot for average |E*|, and (f) black space plot for average |E*| for the AC Mix 42.

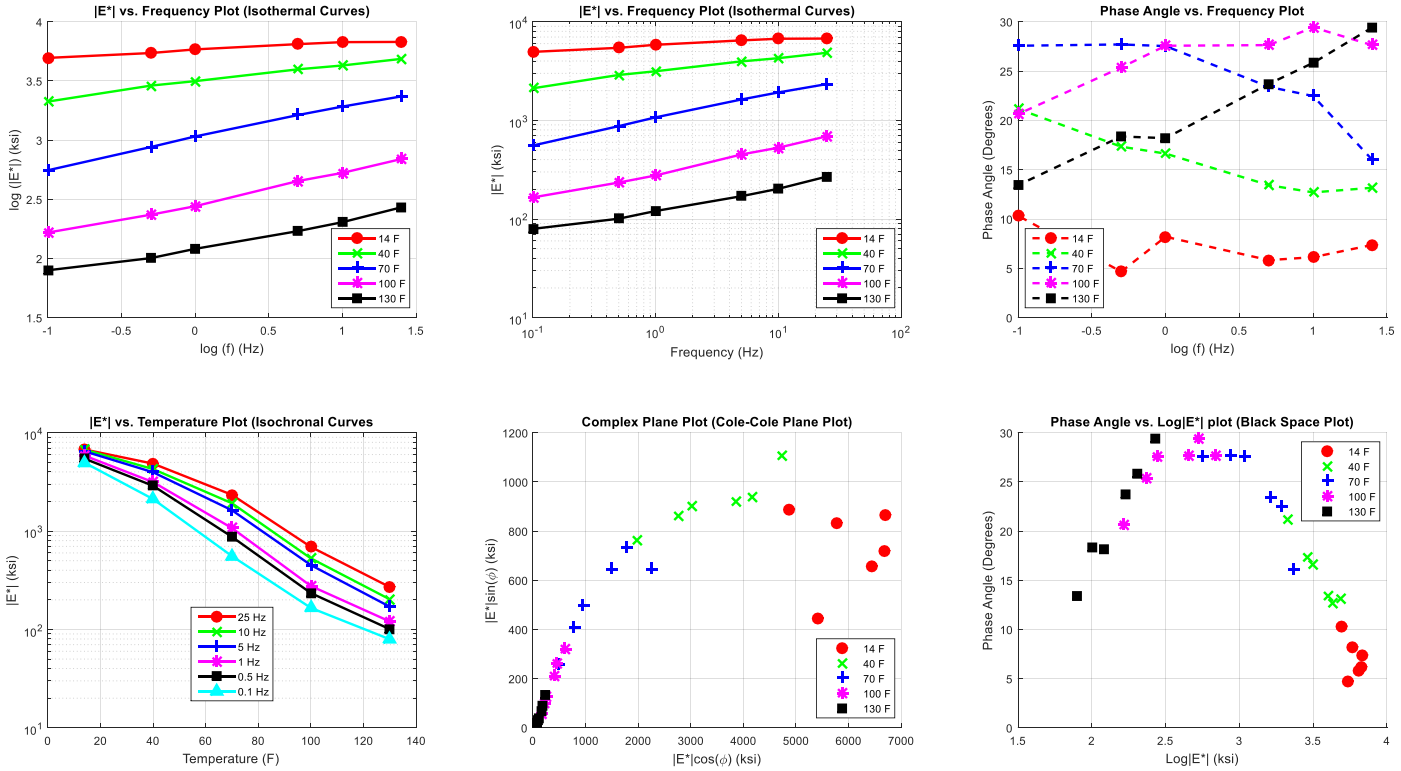

Figure E-43 (a) average log-|E*| versus log-f plot, (b) average |E*| versus f plot, (c) average ϕ versus log-f plot, (d) average |E*| versus temperature plot, (e) complex plane plot for average |E*|, and (f) black space plot for average |E*| for the AC Mix 43.

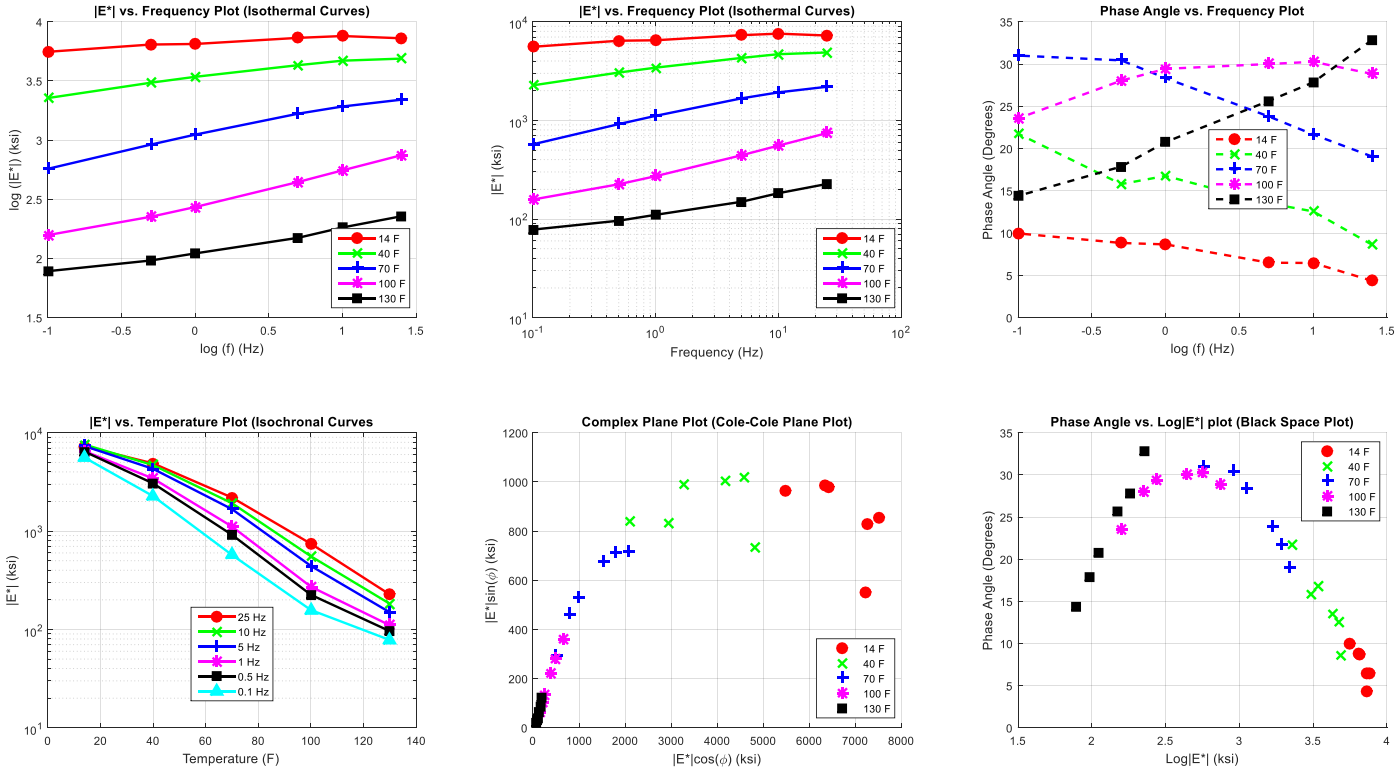

Figure E-44 (a) average log-|E*| versus log-f plot, (b) average |E*| versus f plot, (c) average ϕ versus log-f plot, (d) average |E*| versus temperature plot, (e) complex plane plot for average |E*|, and (f) black space plot for average |E*| for the AC Mix 44.

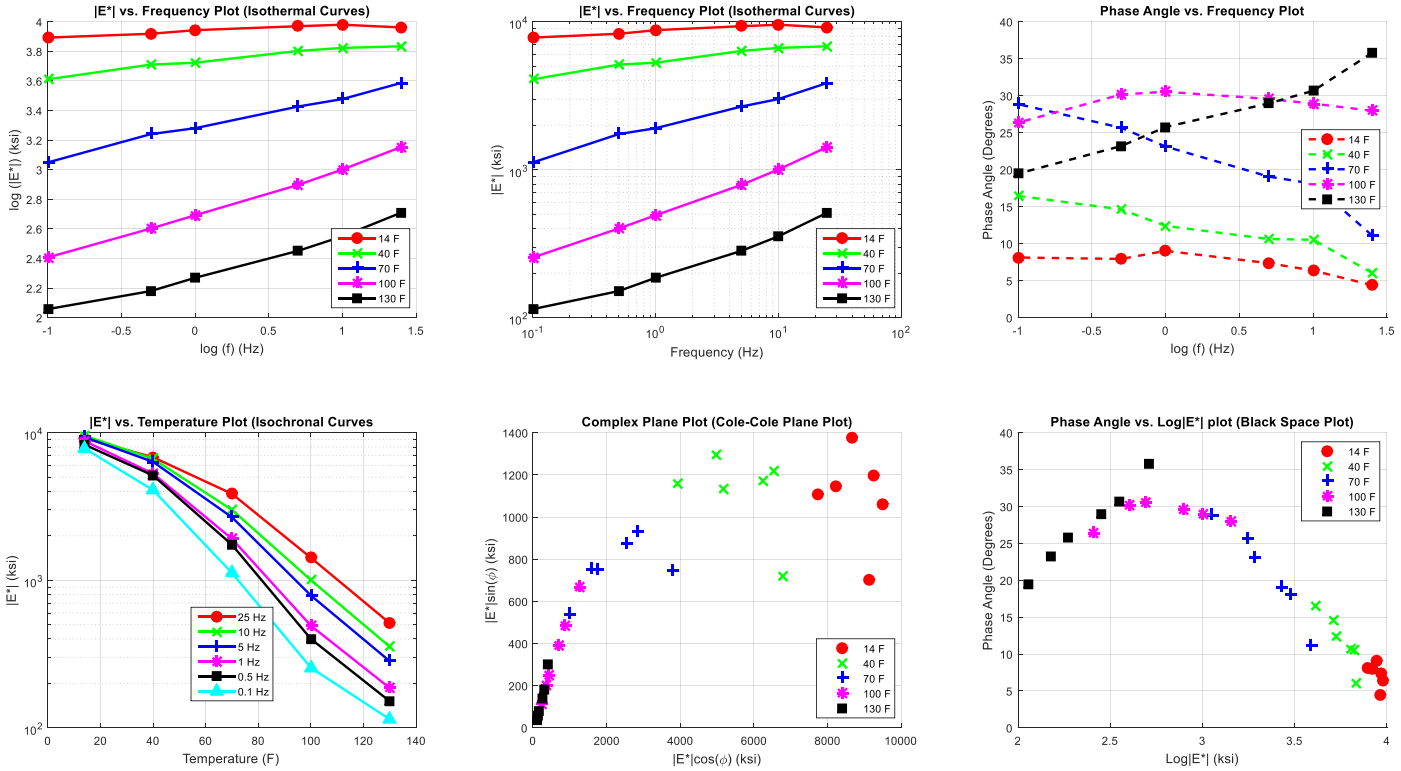

Figure E-45 (a) average log-|E*| versus log-f plot, (b) average |E*| versus f plot, (c) average ϕ versus log-f plot, (d) average |E*| versus temperature plot, (e) complex plane plot for average |E*|, and (f) black space plot for average |E*| for the AC Mix 45.

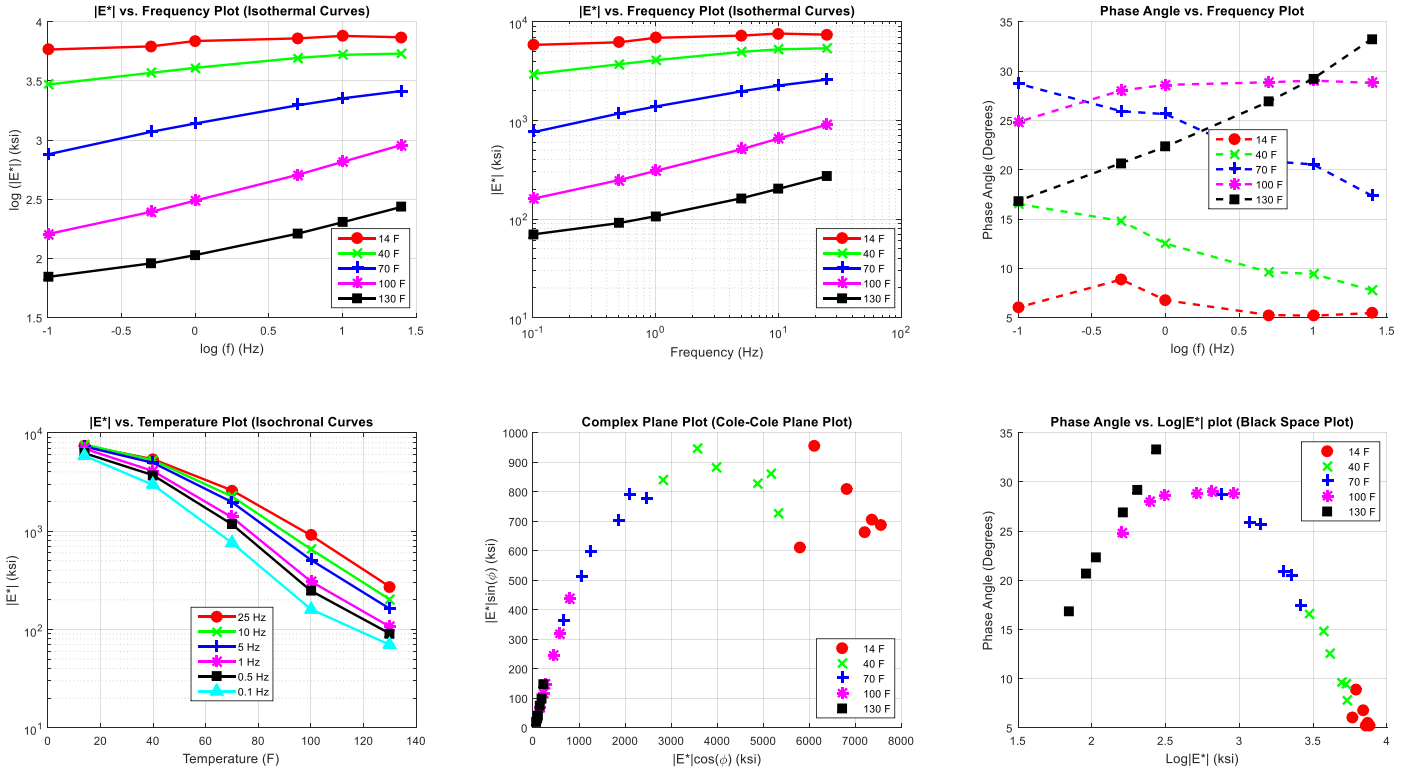

Figure E-46 (a) average log-|E*| versus log-f plot, (b) average |E*| versus f plot, (c) average ϕ versus log-f plot, (d) average |E*| versus temperature plot, (e) complex plane plot for average |E*|, and (f) black space plot for average |E*| for the AC Mix 46.

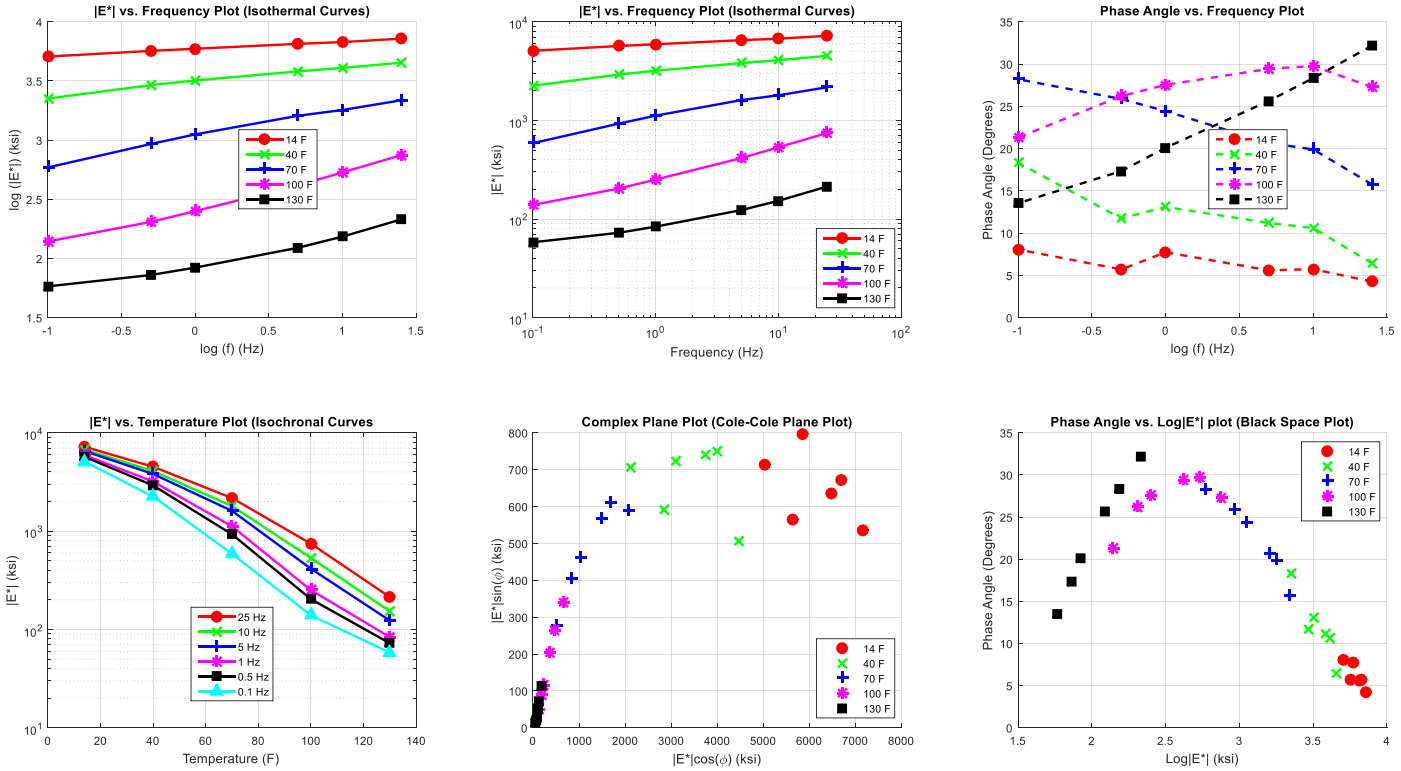

Figure E-47 (a) average log-|E*| versus log-f plot, (b) average |E*| versus f plot, (c) average ϕ versus log-f plot, (d) average |E*| versus temperature plot, (e) complex plane plot for average |E*|, and (f) black space plot for average |E*| for the AC Mix 47.

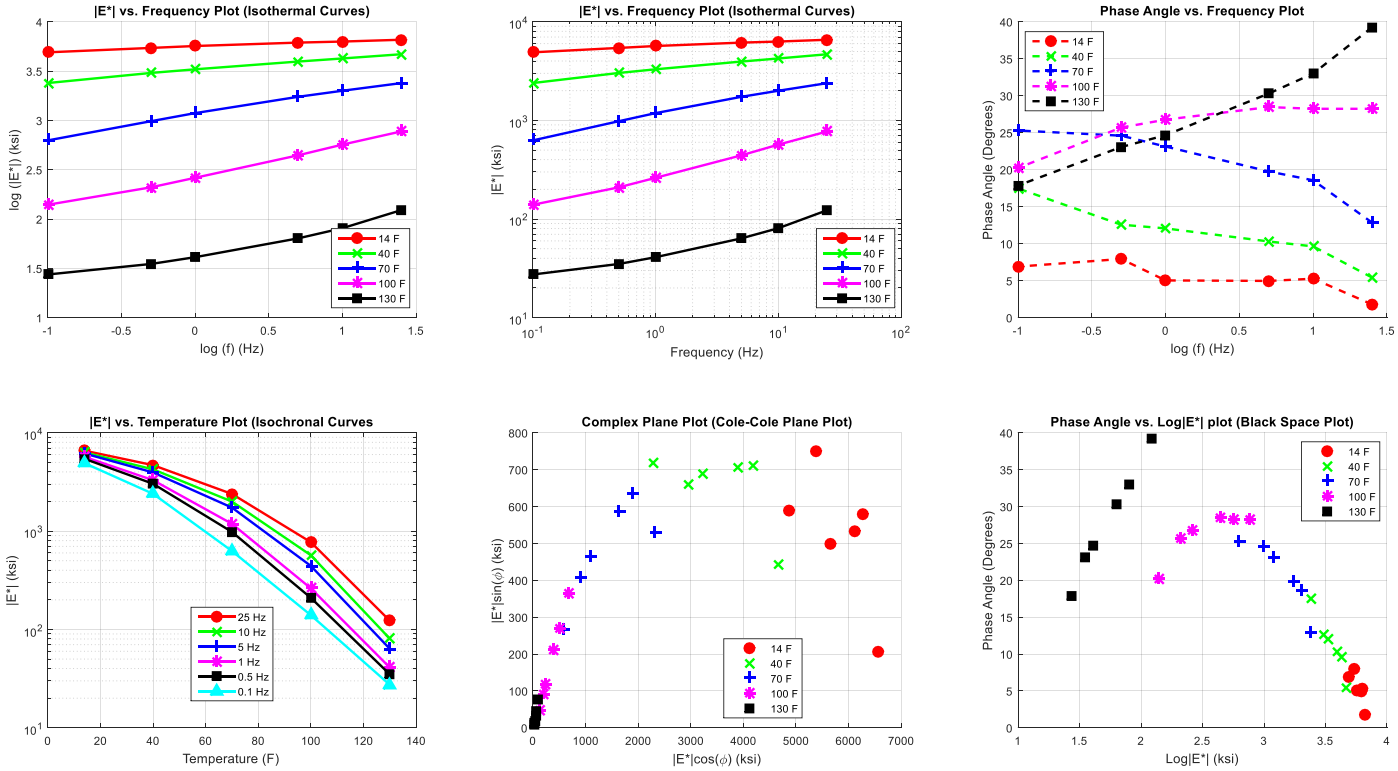

Figure E-48 (a) average log-|E*| versus log-f plot, (b) average |E*| versus f plot, (c) average ϕ versus log-f plot, (d) average |E*| versus temperature plot, (e) complex plane plot for average |E*|, and (f) black space plot for average |E*| for the AC Mix 48.

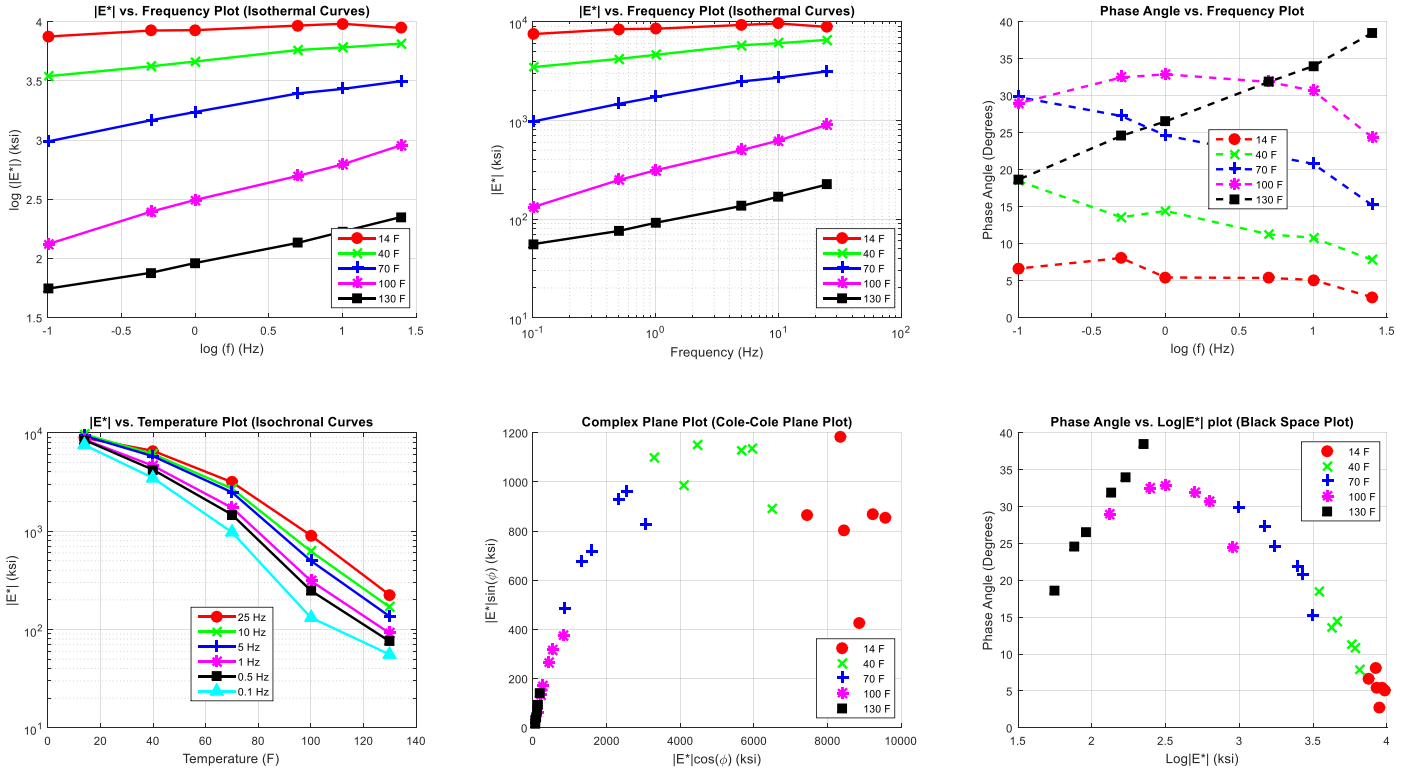

Figure E-49 (a) average log-|E*| versus log-f plot, (b) average |E*| versus f plot, (c) average ϕ versus log-f plot, (d) average |E*| versus temperature plot, (e) complex plane plot for average |E*|, and (f) black space plot for average |E*| for the AC Mix 49.

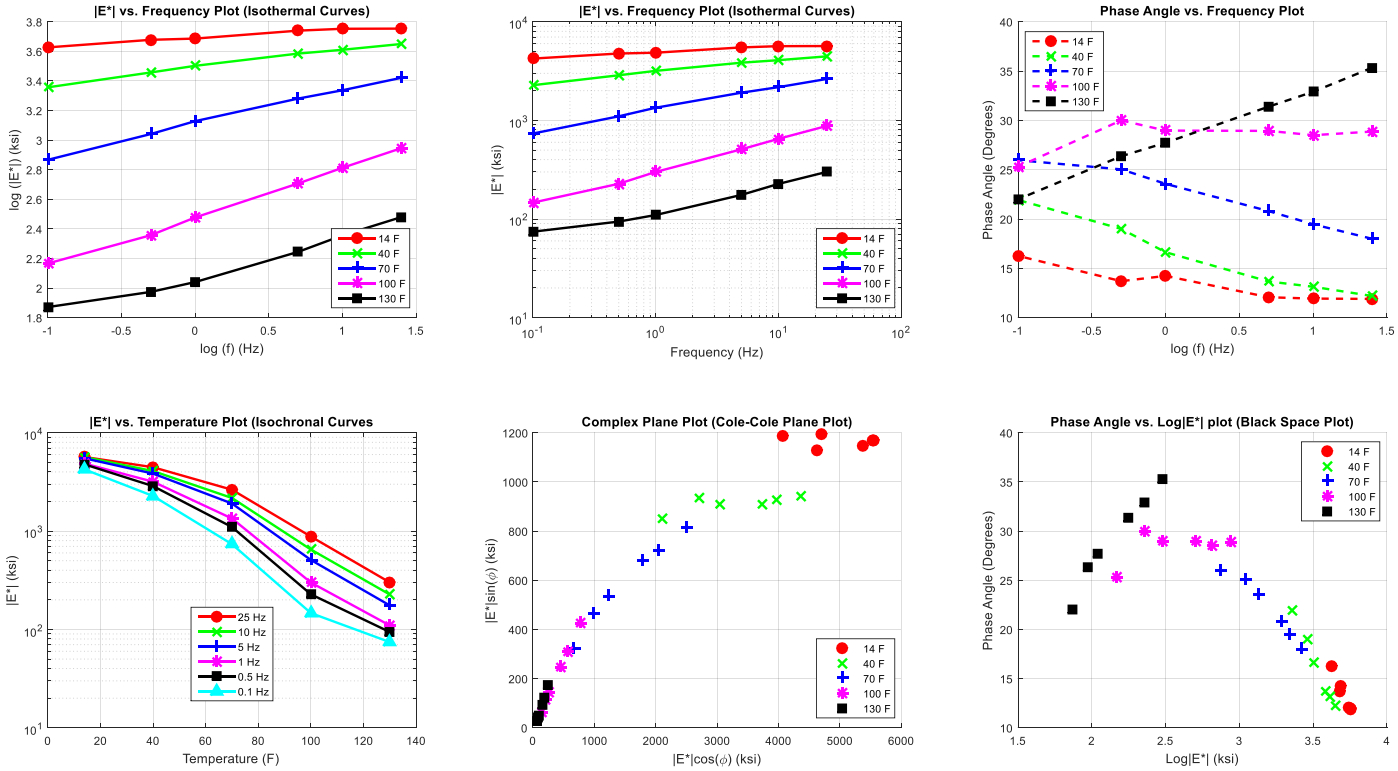

Figure E-50 (a) average log-|E*| versus log-f plot, (b) average |E*| versus f plot, (c) average ϕ versus log-f plot, (d) average |E*| versus temperature plot, (e) complex plane plot for average |E*|, and (f) black space plot for average |E*| for the AC Mix 50.

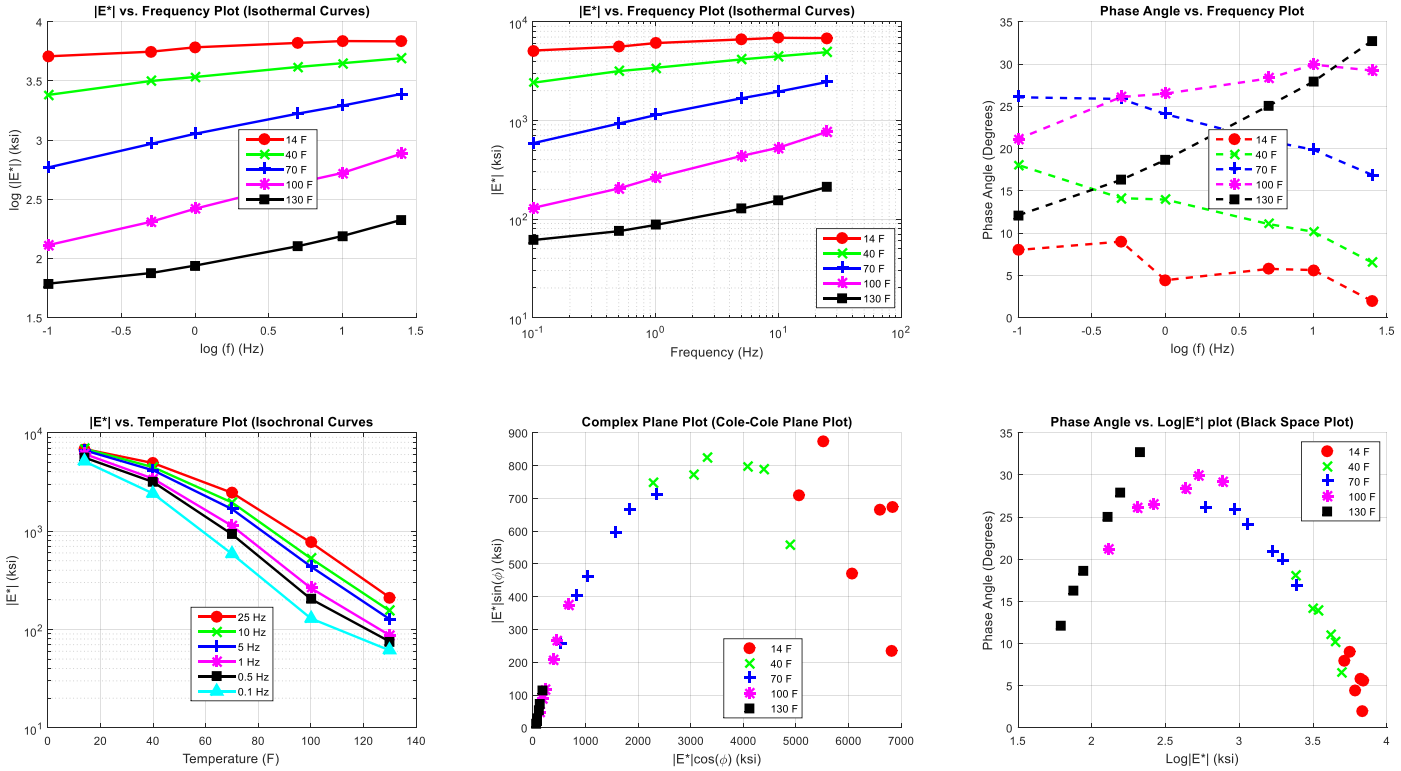

Figure E-51 (a) average log-|E*| versus log-f plot, (b) average |E*| versus f plot, (c) average ϕ versus log-f plot, (d) average |E*| versus temperature plot, (e) complex plane plot for average |E*|, and (f) black space plot for average |E*| for the AC Mix 51.

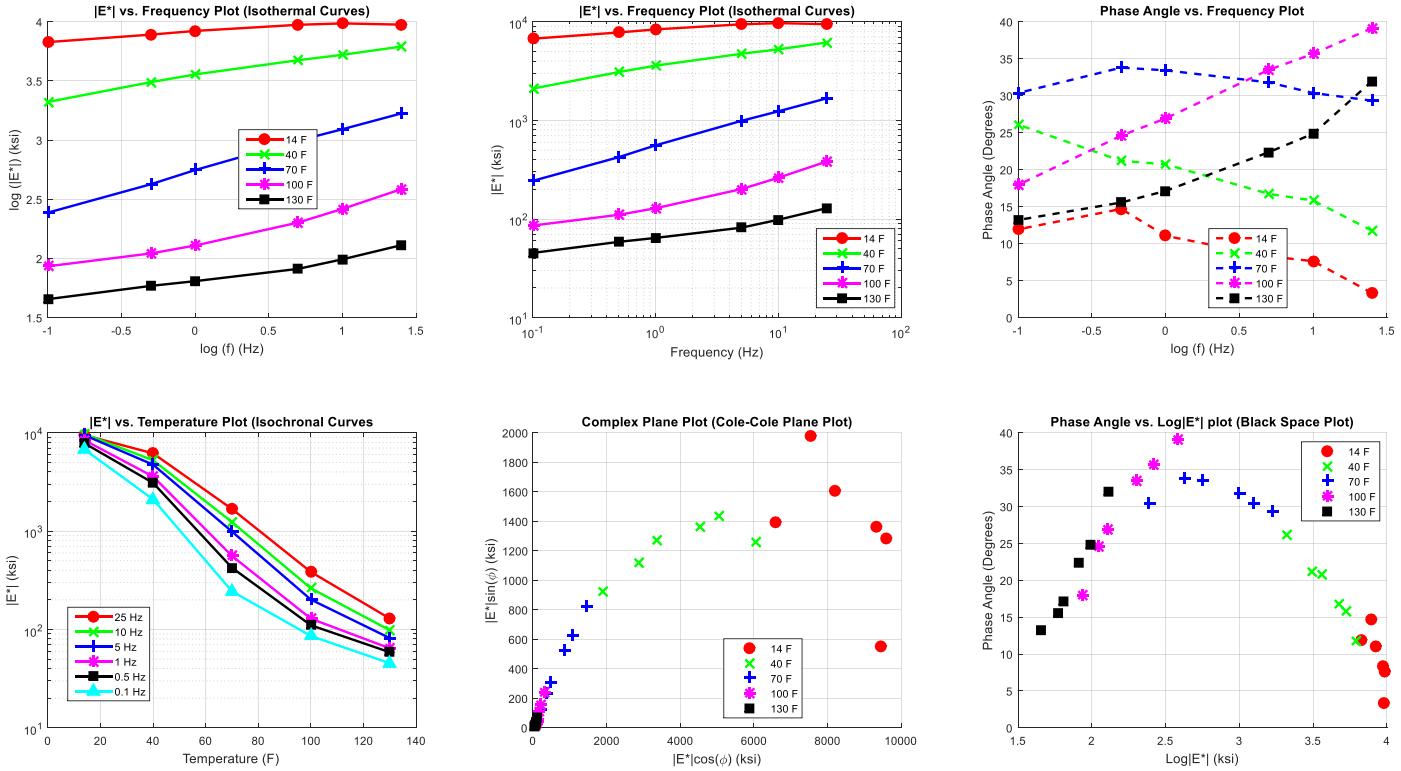

Figure E-52 (a) average log-|E*| versus log-f plot, (b) average |E*| versus f plot, (c) average ϕ versus log-f plot, (d) average |E*| versus temperature plot, (e) complex plane plot for average |E*|, and (f) black space plot for average |E*| for the AC Mix 52.

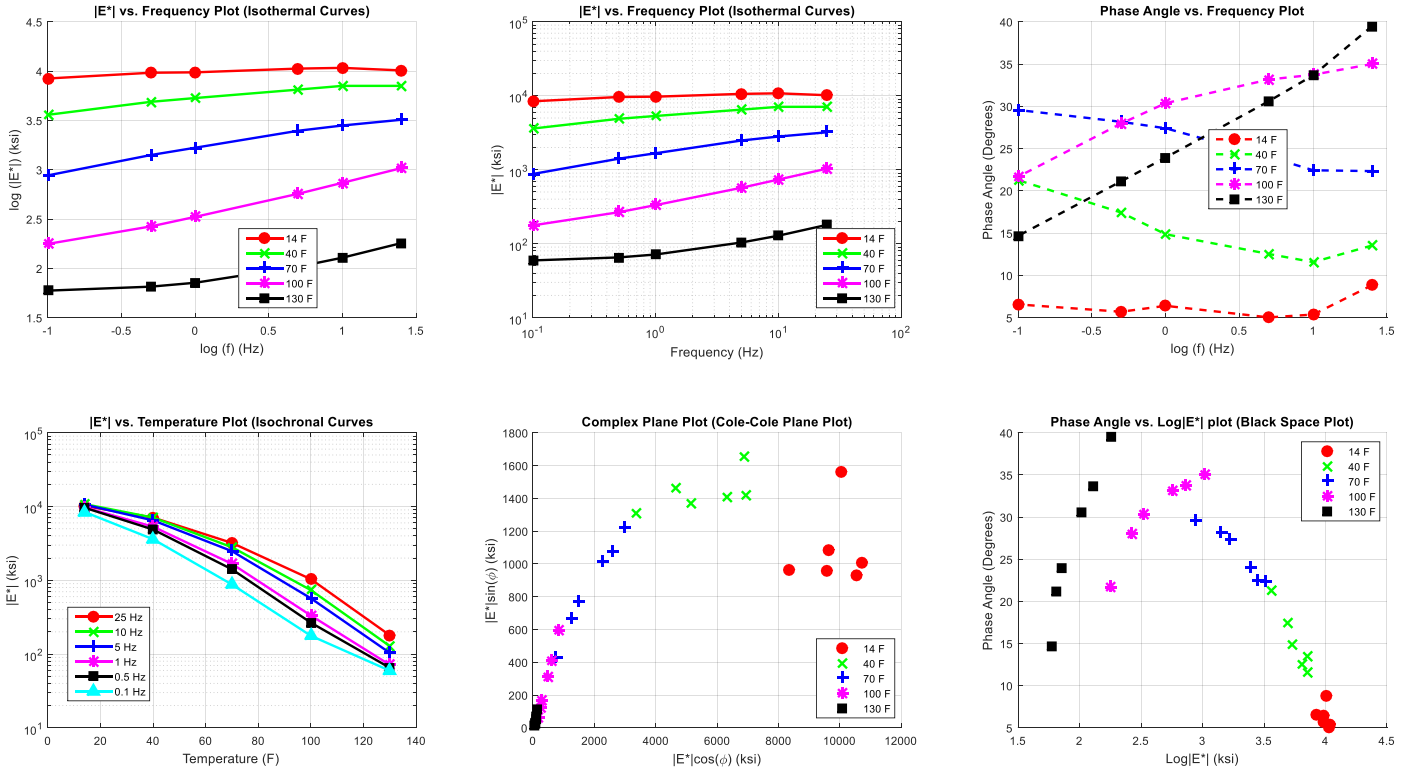

Figure E-53 (a) average log-|E*| versus log-f plot, (b) average |E*| versus f plot, (c) average ϕ versus log-f plot, (d) average |E*| versus temperature plot, (e) complex plane plot for average |E*|, and (f) black space plot for average |E*| for the AC Mix 53.

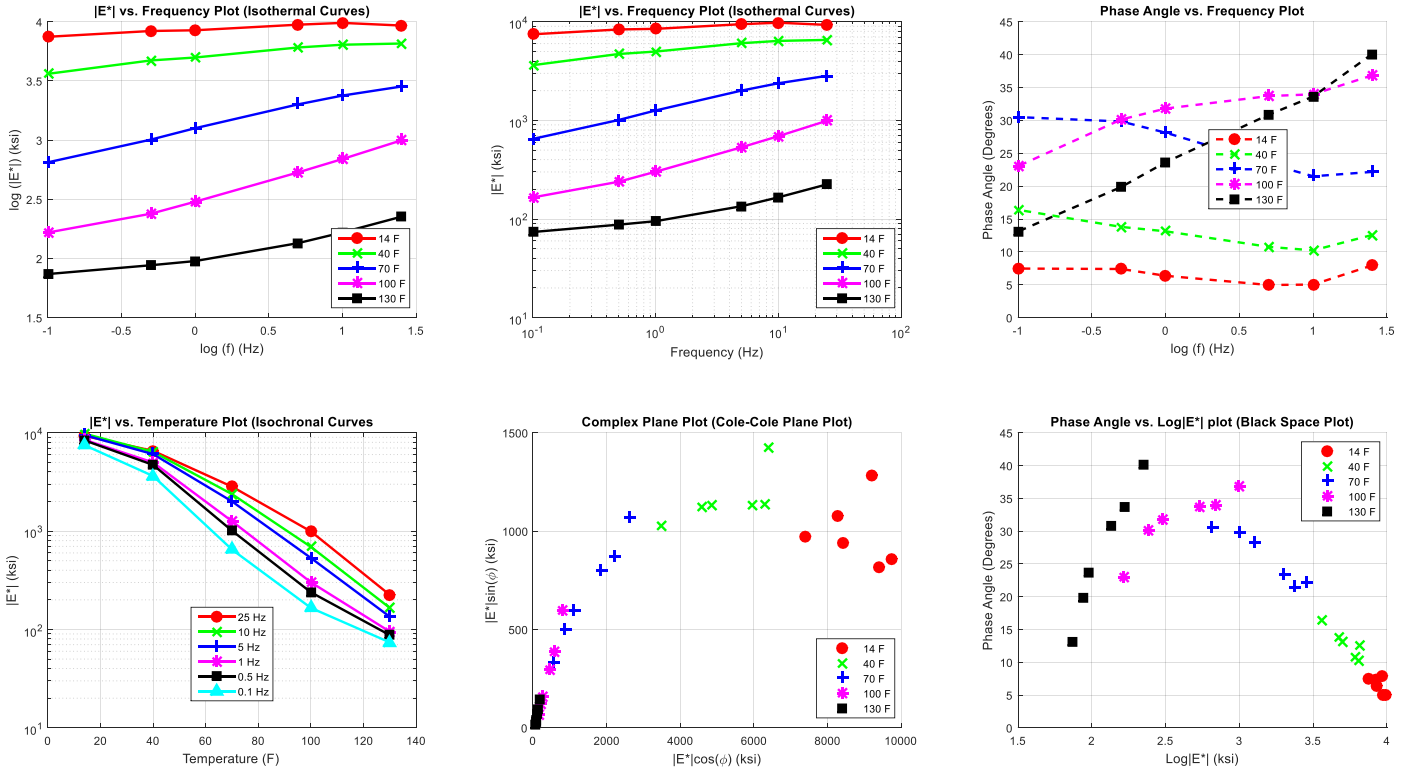

Figure E-54 (a) average log-|E*| versus log-f plot, (b) average |E*| versus f plot, (c) average ϕ versus log-f plot, (d) average |E*| versus temperature plot, (e) complex plane plot for average |E*|, and (f) black space plot for average |E*| for the AC Mix 54.

Appendix F

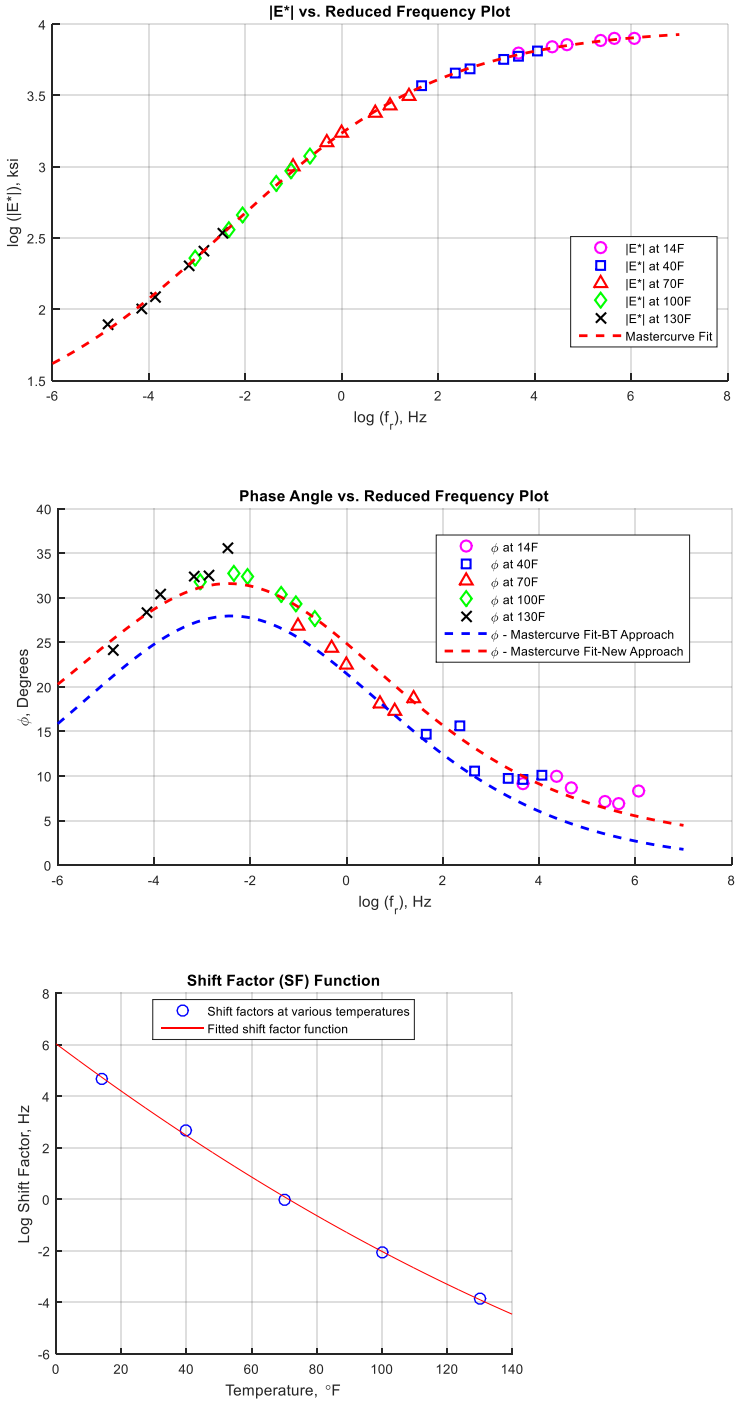

Figure F-1 |E*| and ϕ-mastercurves, and frequency temperature shift factor function for AC Mix 1.

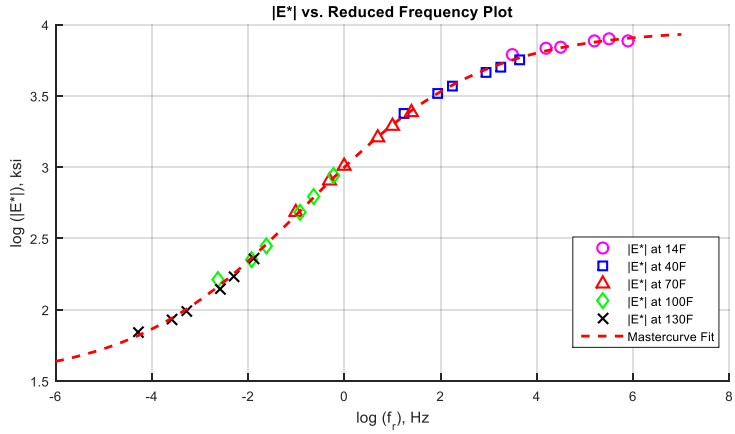

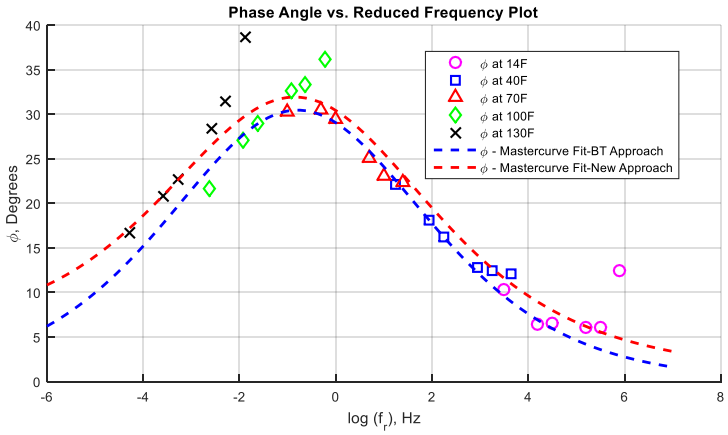

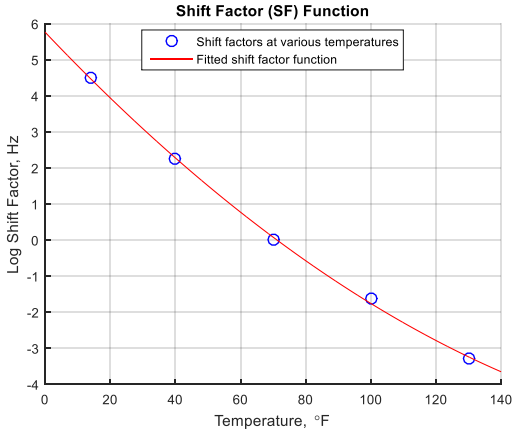

Figure F-2 |E*| and ϕ-mastercurves, and frequency temperature shift factor function for AC Mix 2.

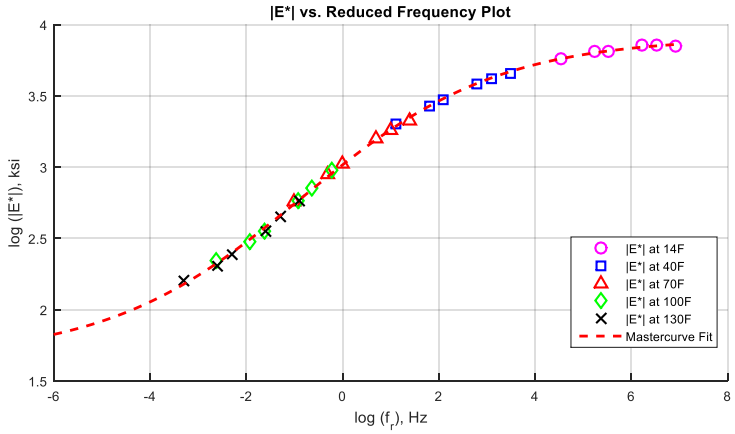

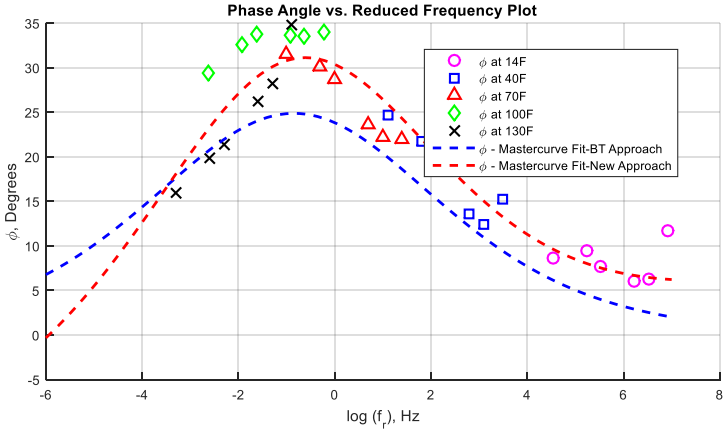

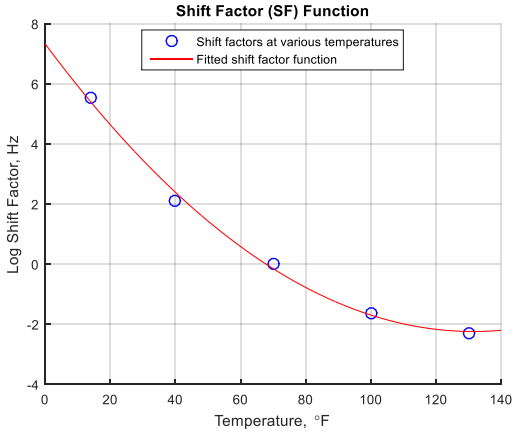

Figure F-3 |E*| and ϕ-mastercurves, and frequency temperature shift factor function for AC Mix 3.

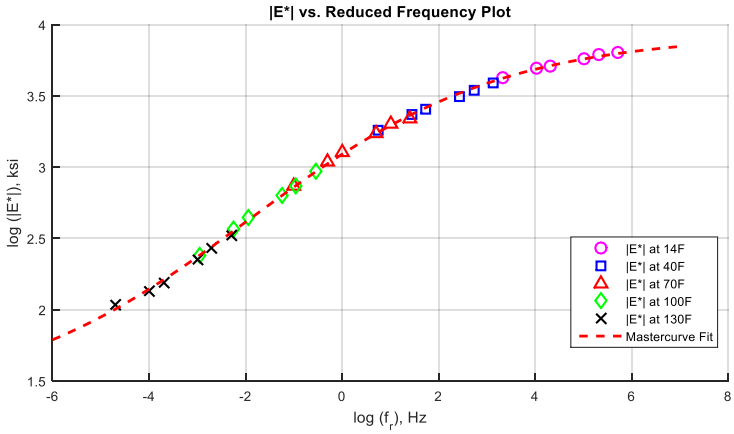

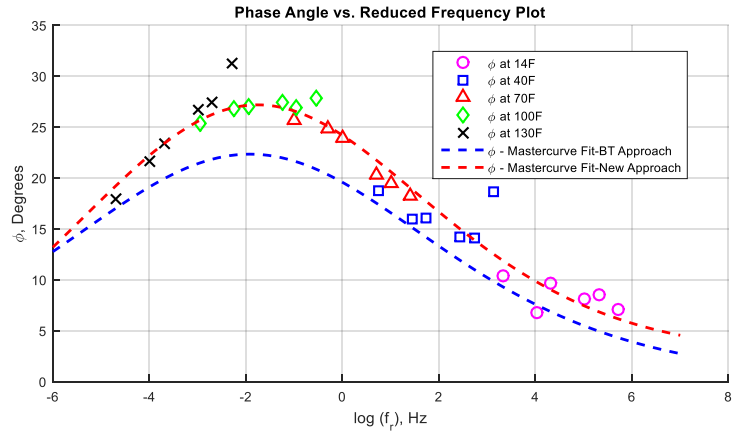

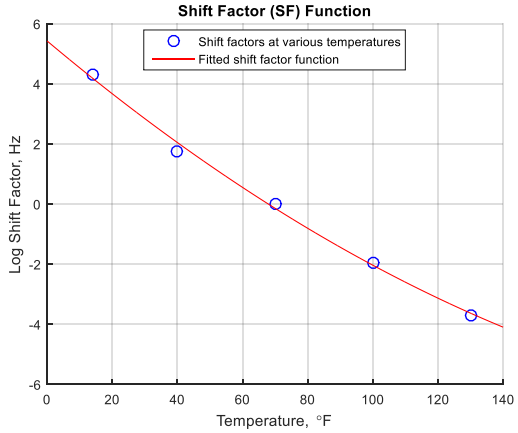

Figure F-4 |E*| and ϕ-mastercurves, and frequency temperature shift factor function for AC Mix 4.

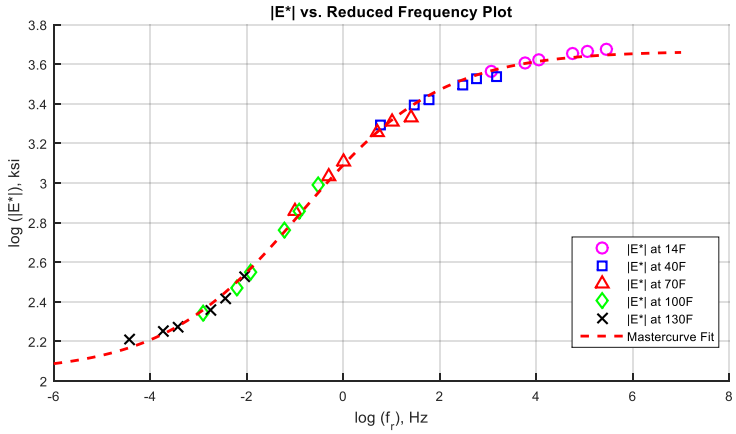

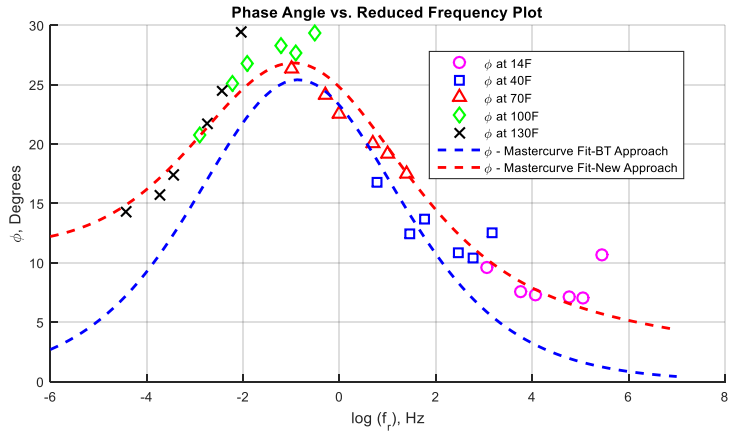

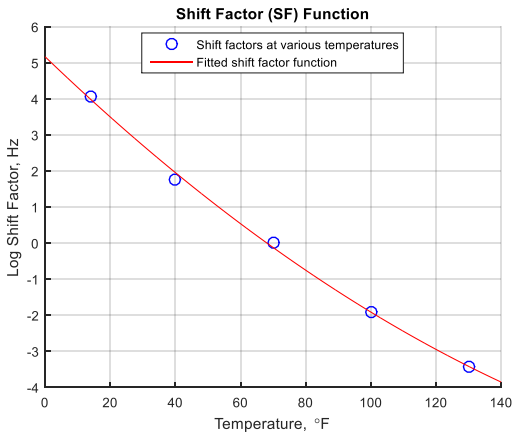

Figure F-5 |E*| and ϕ-mastercurves, and frequency temperature shift factor function for AC Mix 5.

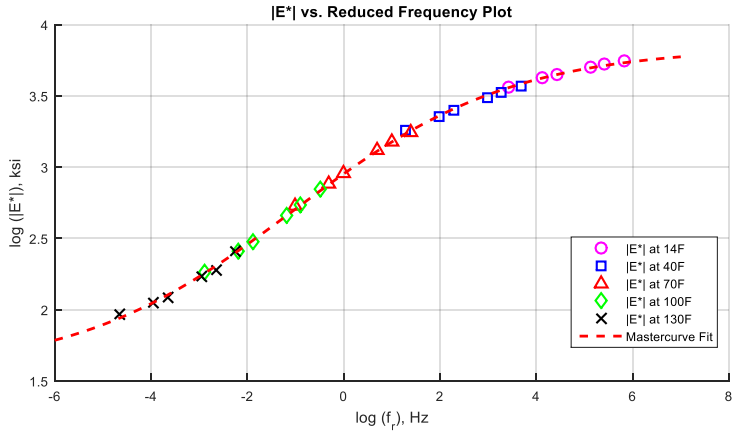

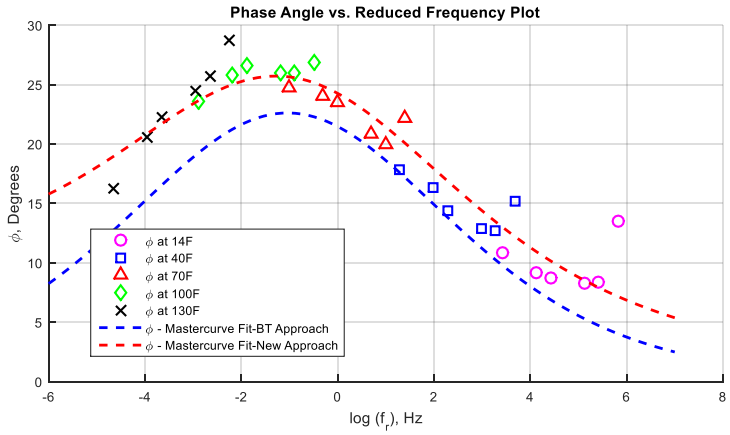

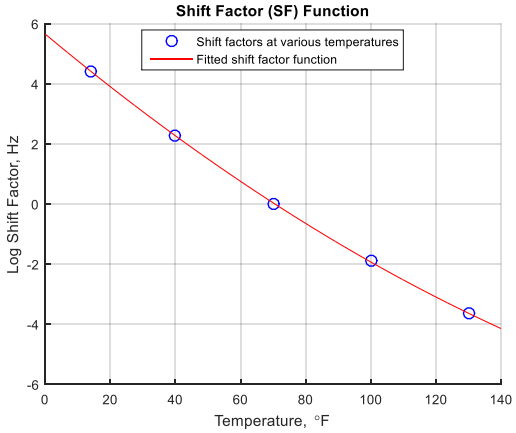

Figure F-6 |E*| and ϕ-mastercurves, and frequency temperature shift factor function for AC Mix 6.

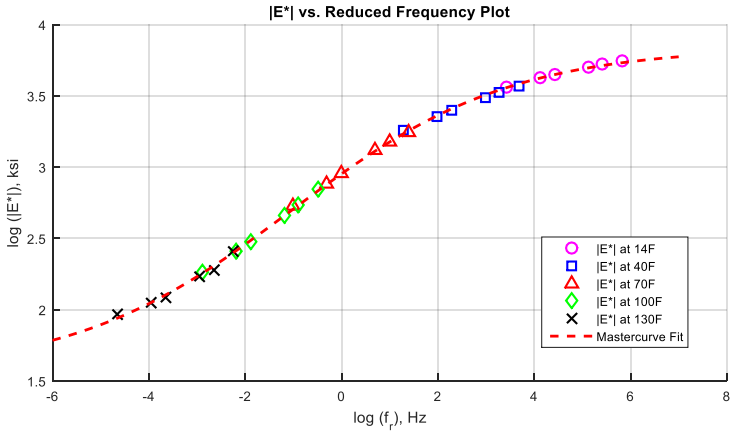

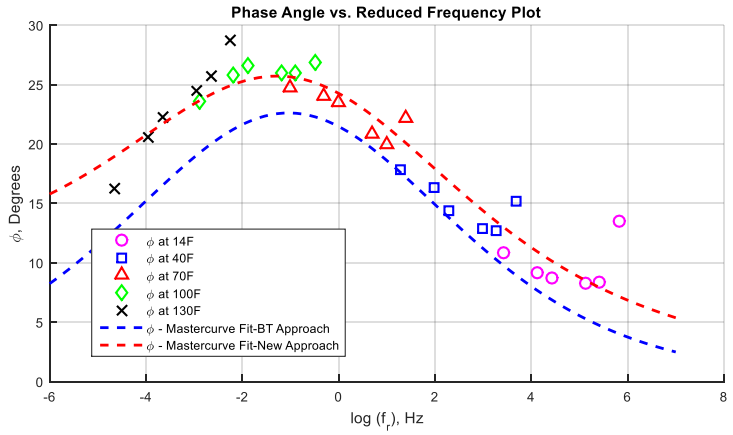

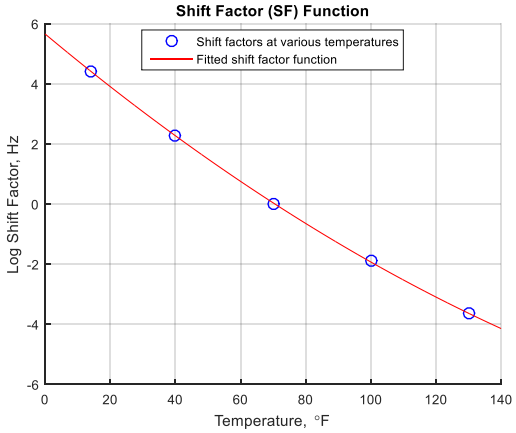

Figure F-7 |E*| and ϕ-mastercurves, and frequency temperature shift factor function for AC Mix 7.

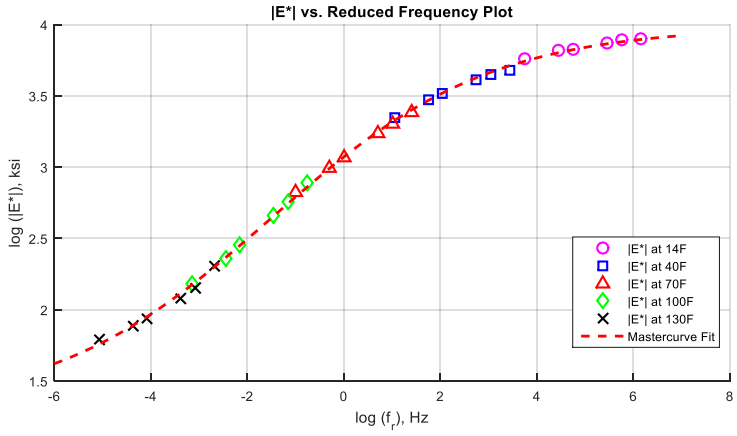

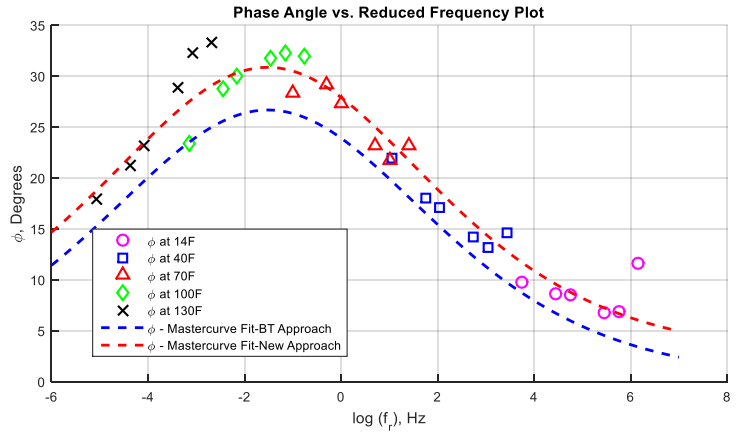

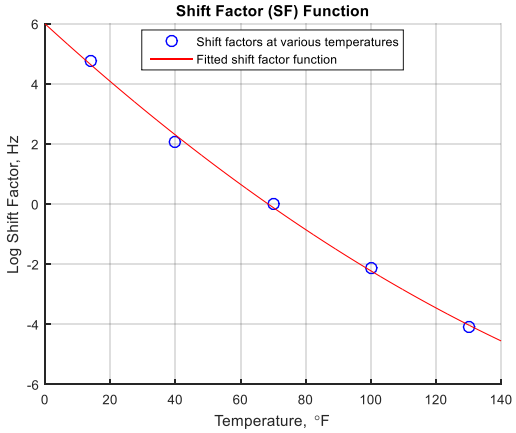

Figure F-8 |E*| and ϕ-mastercurves, and frequency temperature shift factor function for AC Mix 8.

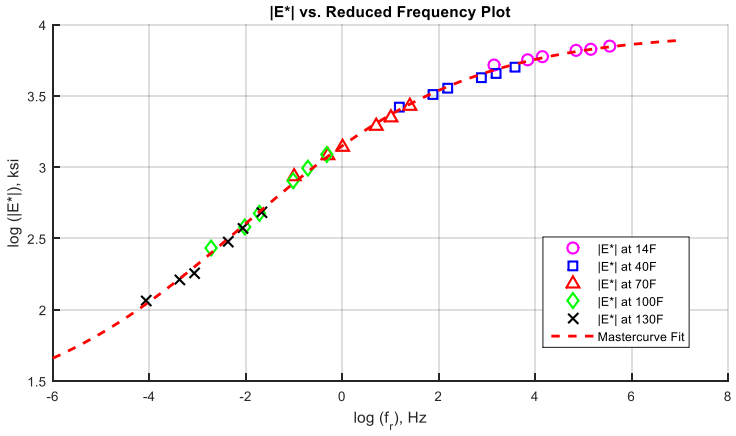

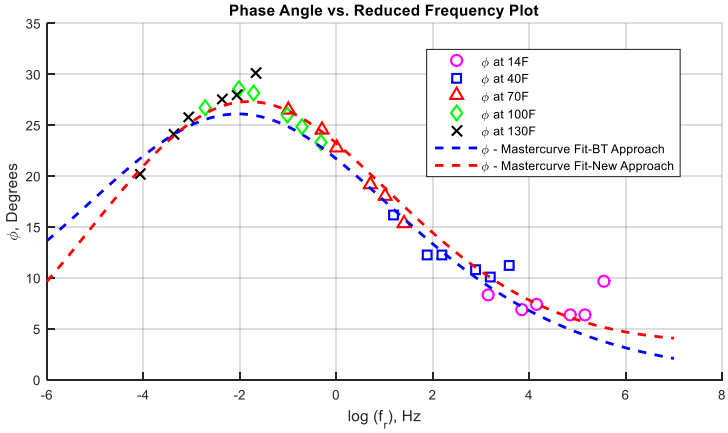

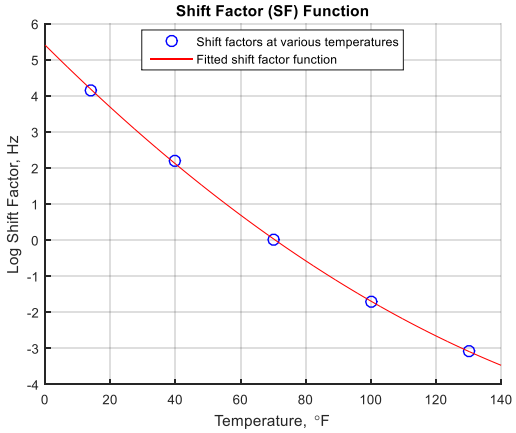

Figure F-9 |E*| and ϕ-mastercurves, and frequency temperature shift factor function for AC Mix 9.

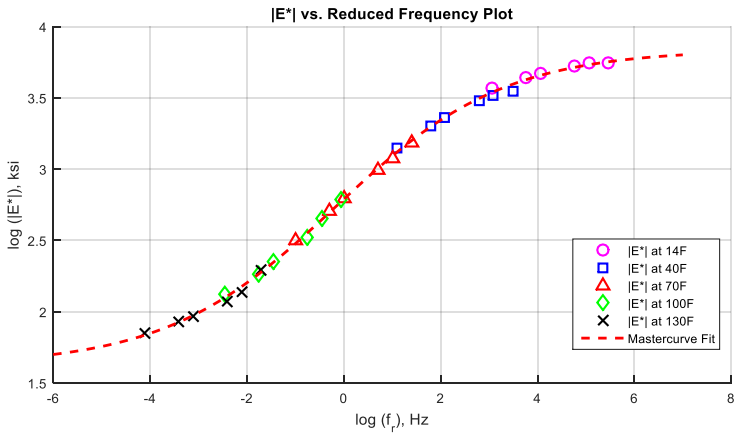

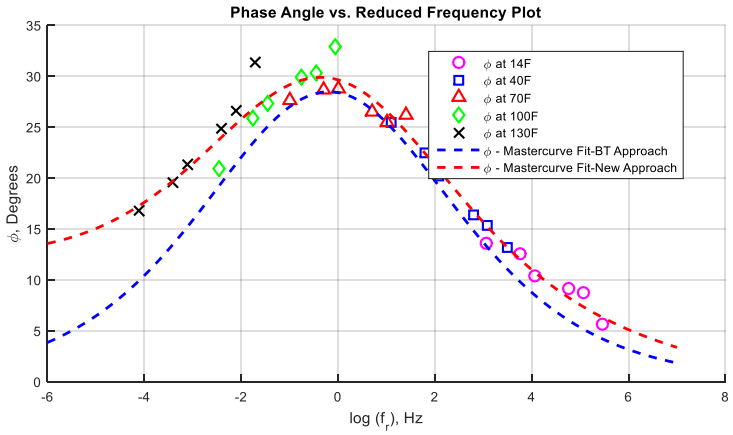

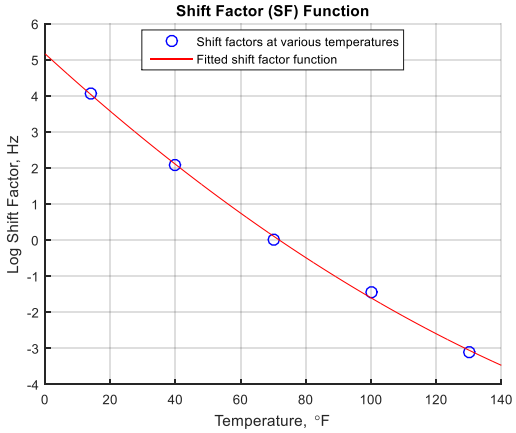

Figure F-10 |E*| and ϕ-mastercurves, and frequency temperature shift factor function for AC Mix 10.

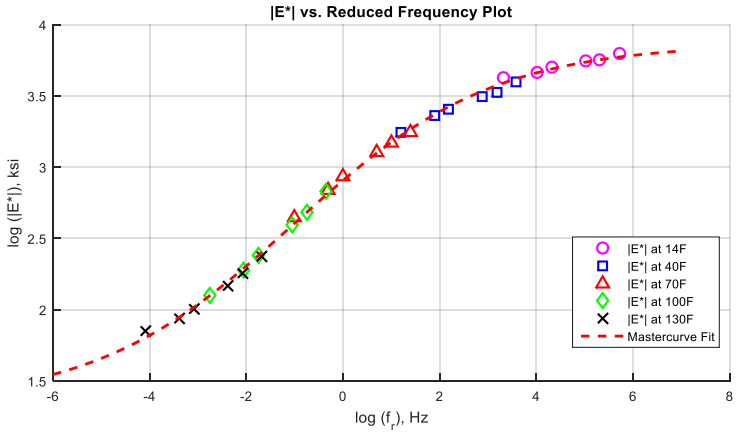

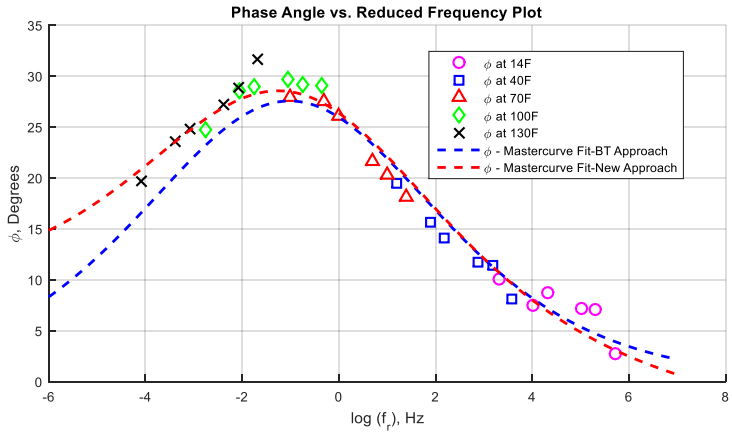

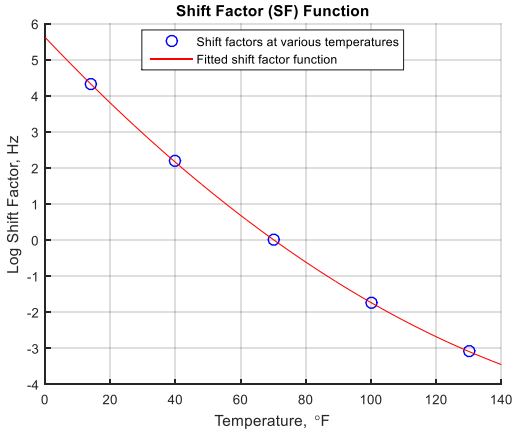

Figure F-11 |E*| and ϕ-mastercurves, and frequency temperature shift factor function for AC Mix 11.

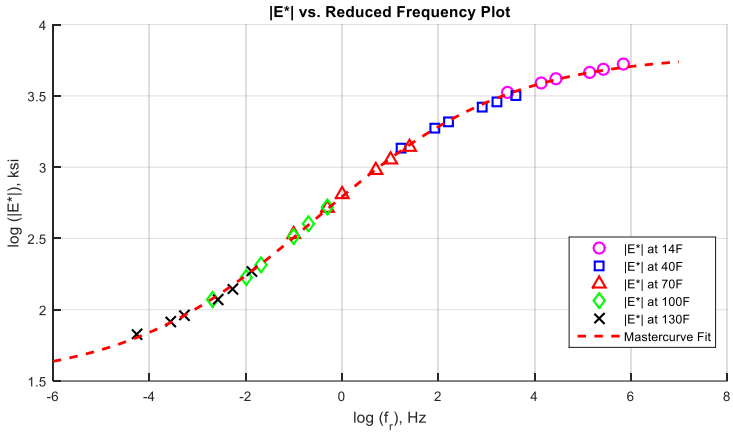

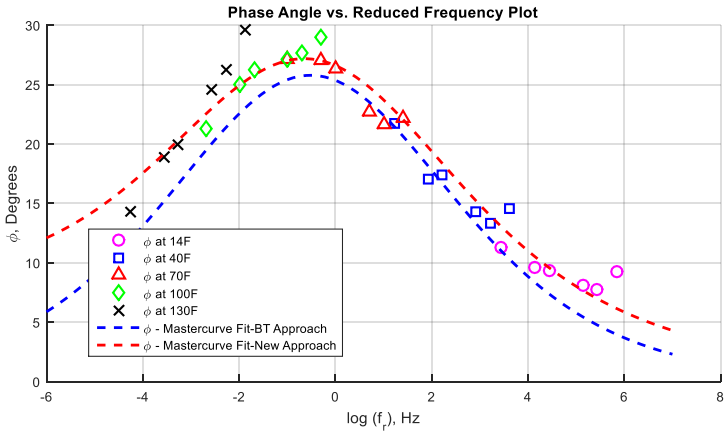

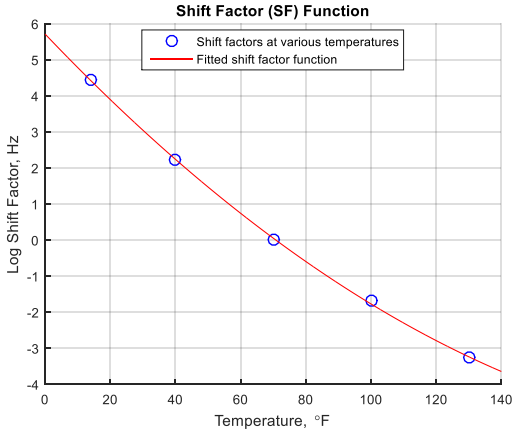

Figure F-12 |E*| and ϕ-mastercurves, and frequency temperature shift factor function for AC Mix 12.

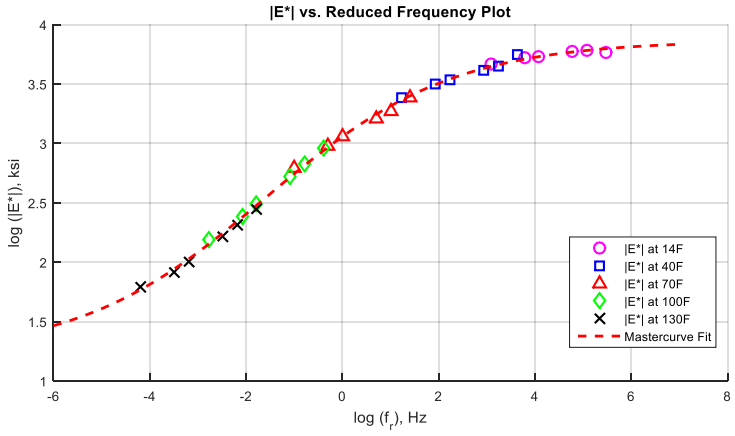

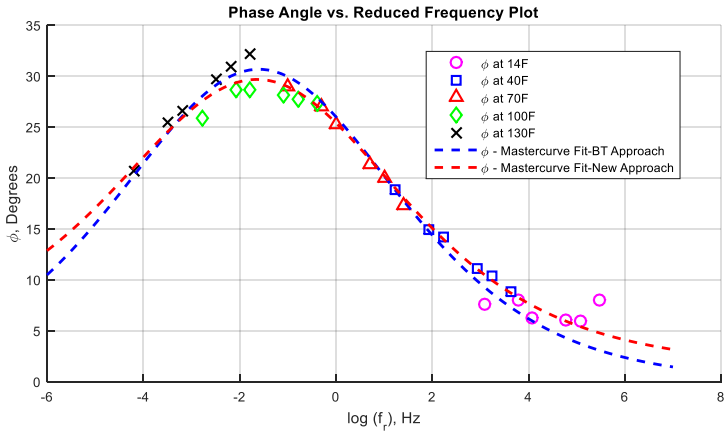

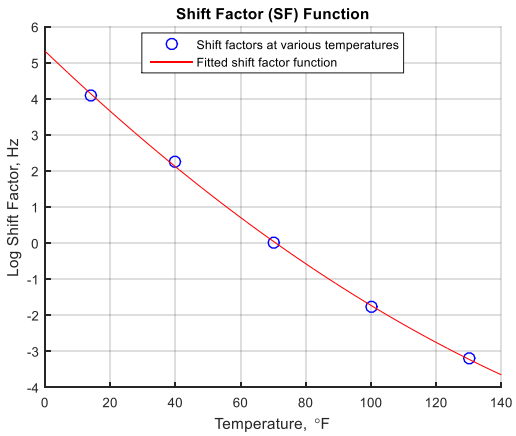

Figure F-13 |E*| and ϕ-mastercurves, and frequency temperature shift factor function for AC Mix 13.

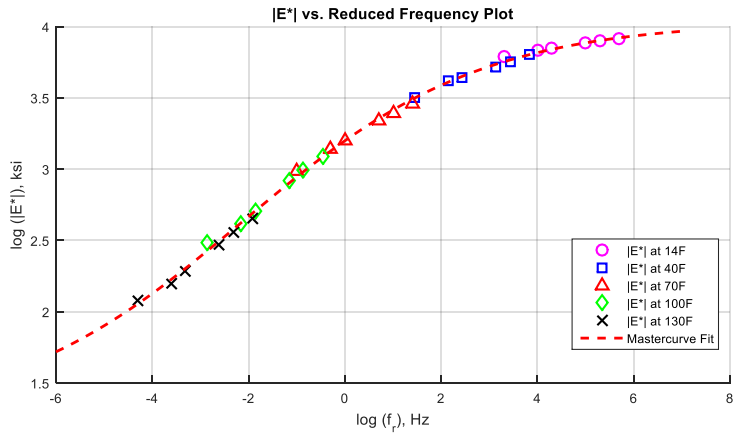

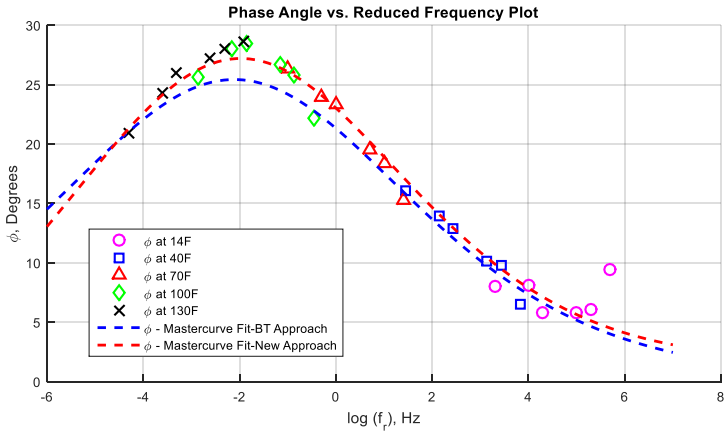

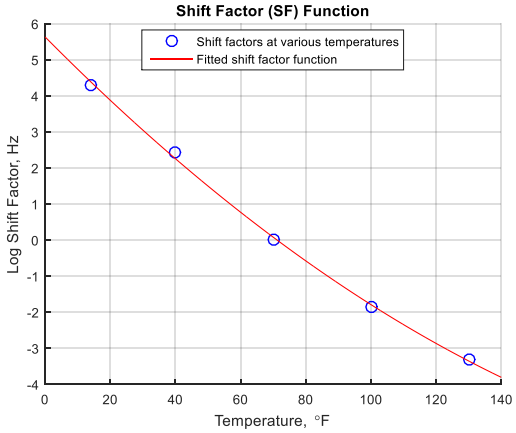

Figure F-14 |E*| and ϕ-mastercurves, and frequency temperature shift factor function for AC Mix 14.

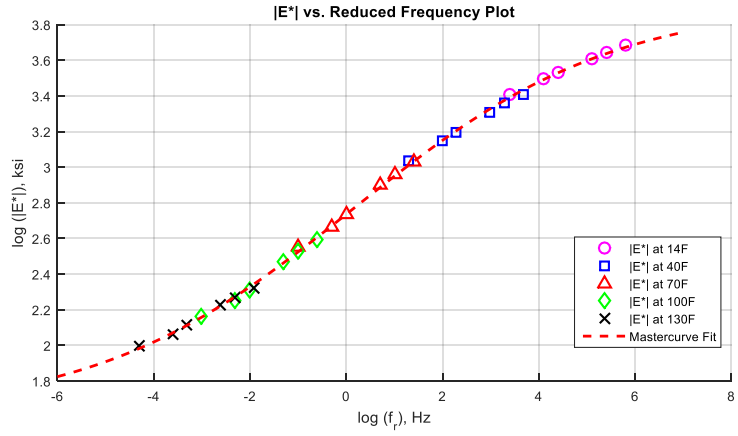

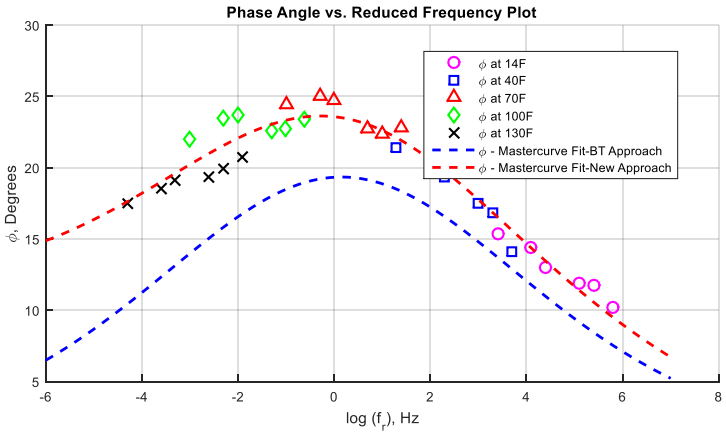

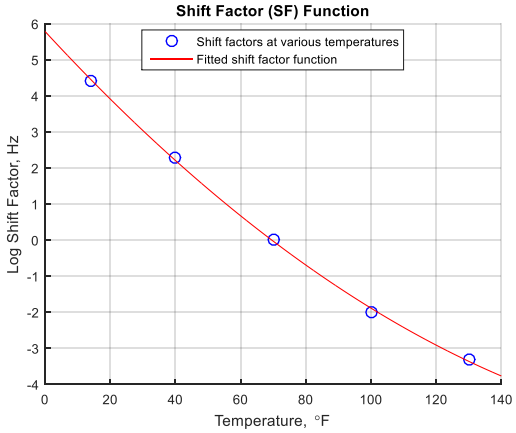

Figure F-15 |E*| and ϕ-mastercurves, and frequency temperature shift factor function for AC Mix 15.

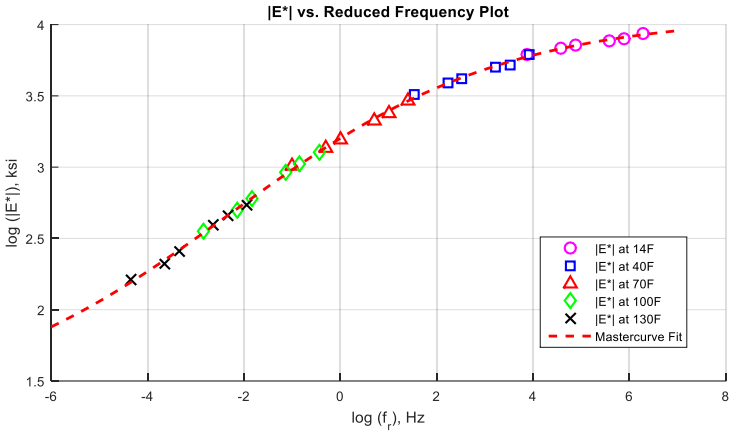

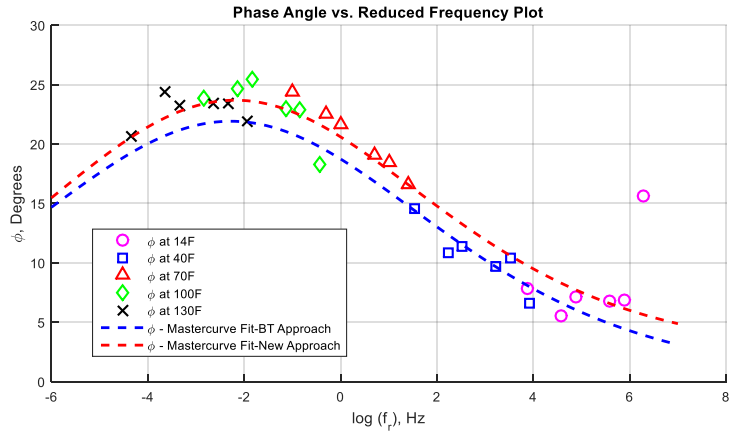

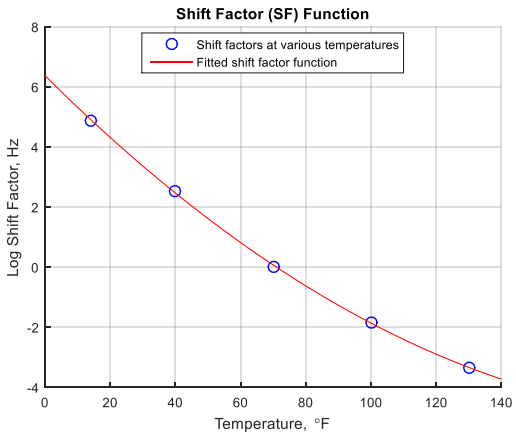

Figure F-16 |E*| and ϕ-mastercurves, and frequency temperature shift factor function for AC Mix 16.

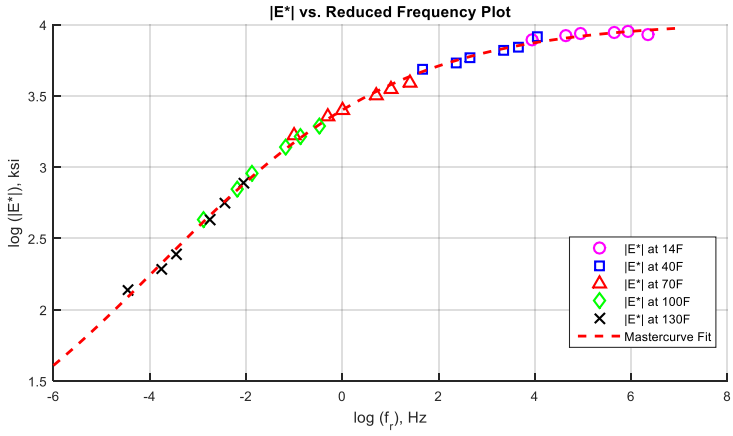

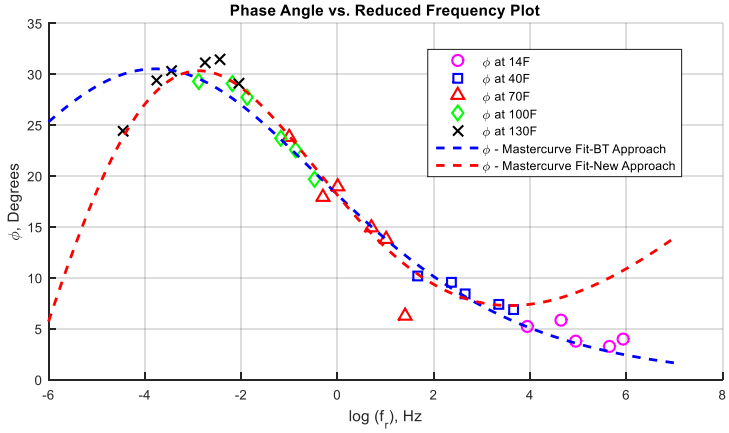

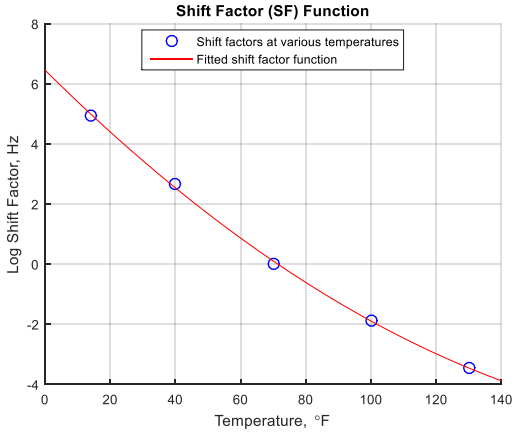

Figure F-17 |E*| and ϕ-mastercurves, and frequency temperature shift factor function for AC Mix 17.

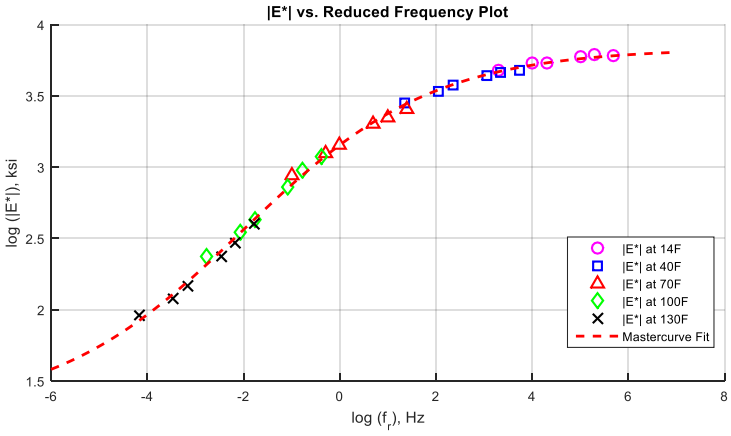

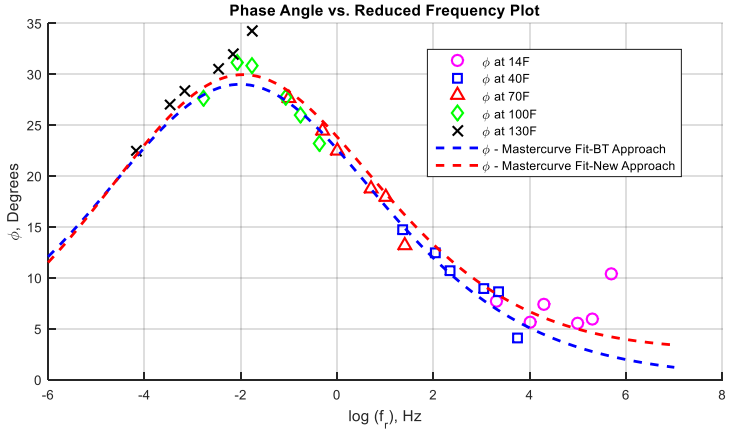

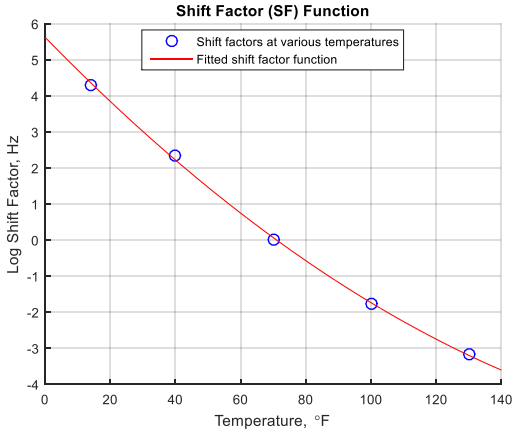

Figure F-18 |E*| and ϕ-mastercurves, and frequency temperature shift factor function for AC Mix 18.

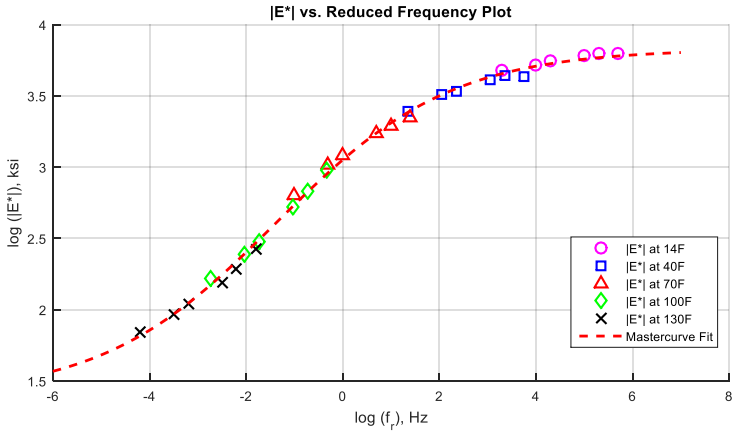

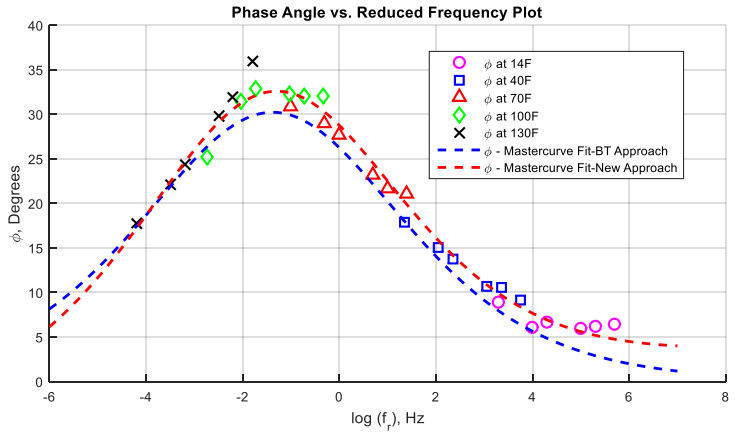

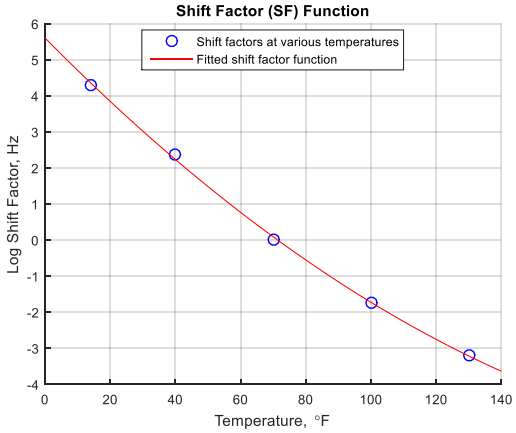

Figure F-19 |E*| and ϕ-mastercurves, and frequency temperature shift factor function for AC Mix 19.

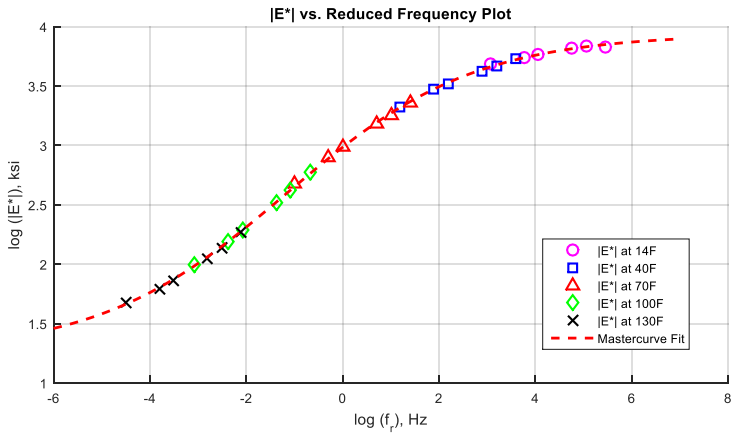

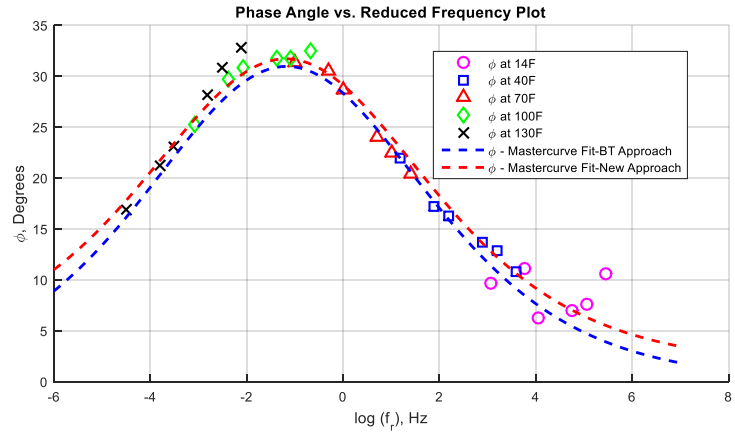

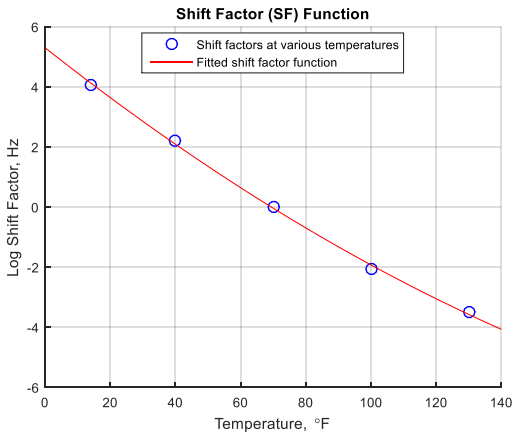

Figure F-20 |E*| and ϕ-mastercurves, and frequency temperature shift factor function for AC Mix 20.

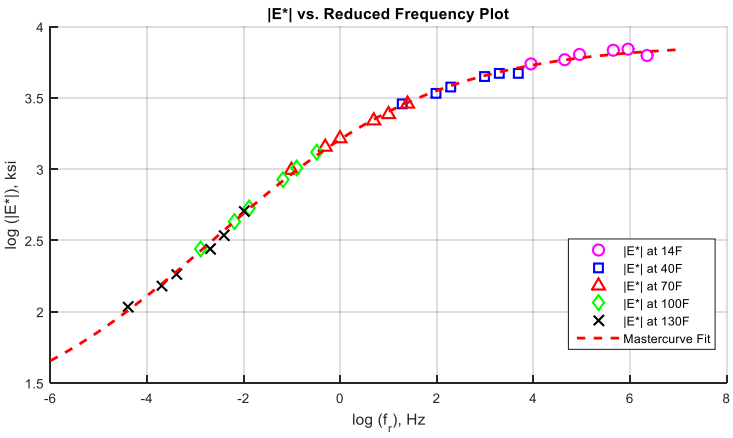

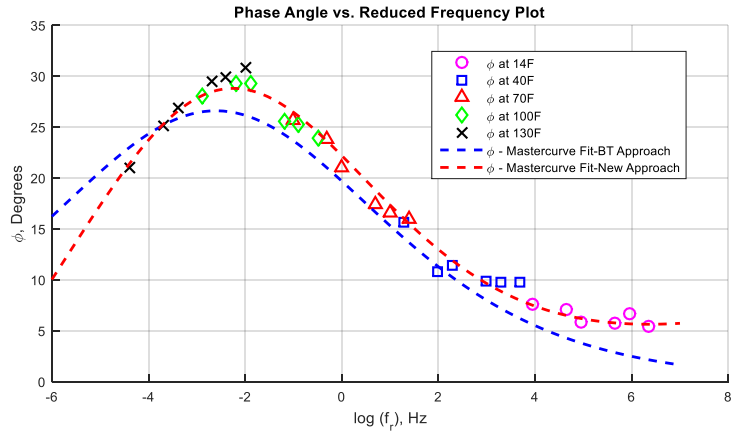

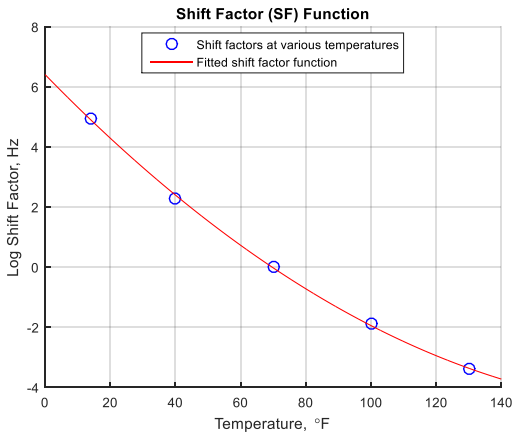

Figure F-21 |E*| and ϕ-mastercurves, and frequency temperature shift factor function for AC Mix 21.

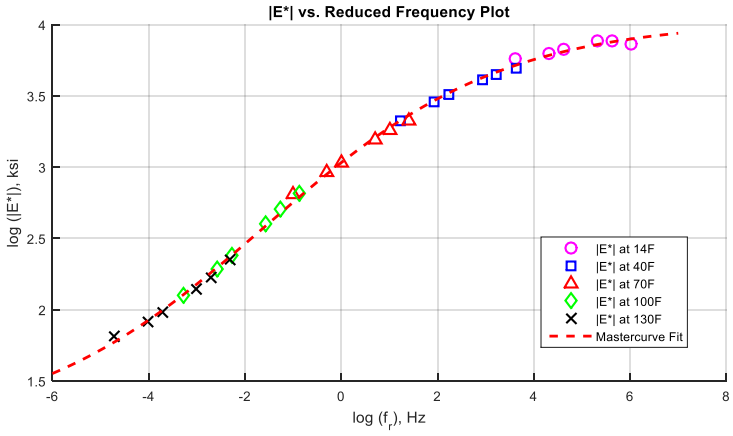

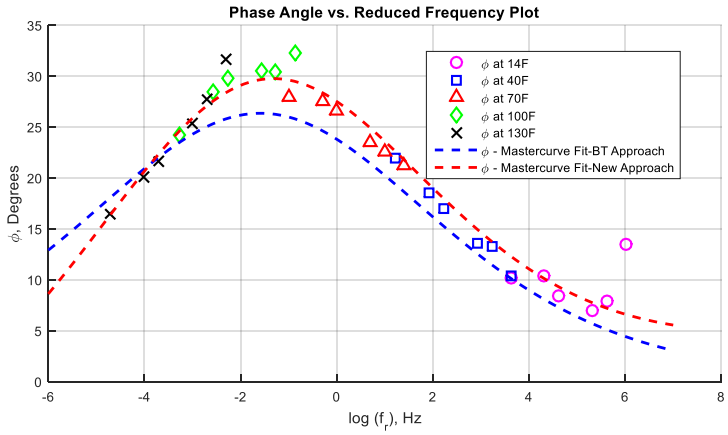

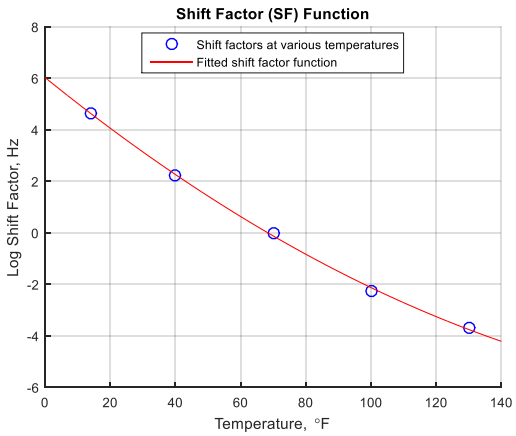

Figure F-22 |E*| and ϕ-mastercurves, and frequency temperature shift factor function for AC Mix 22.

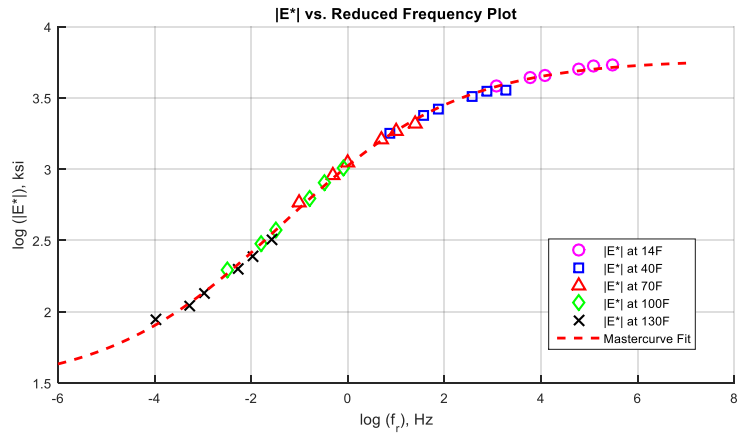

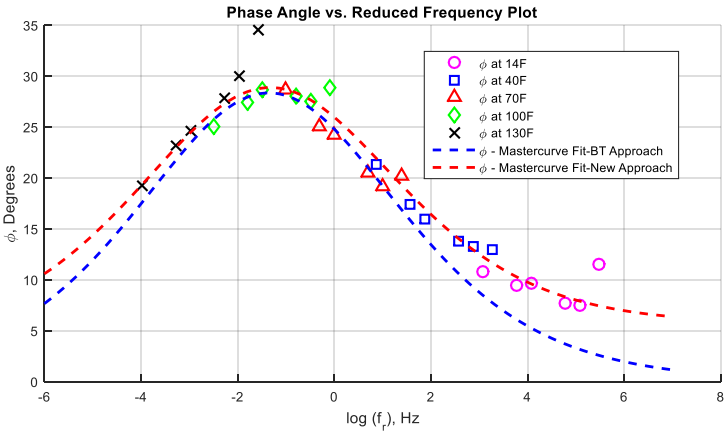

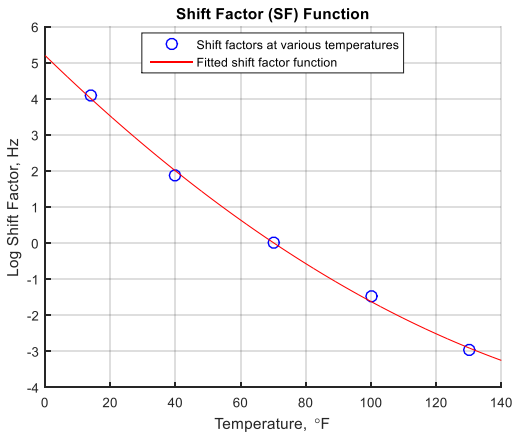

Figure F-23 |E*| and ϕ-mastercurves, and frequency temperature shift factor function for AC Mix 23.

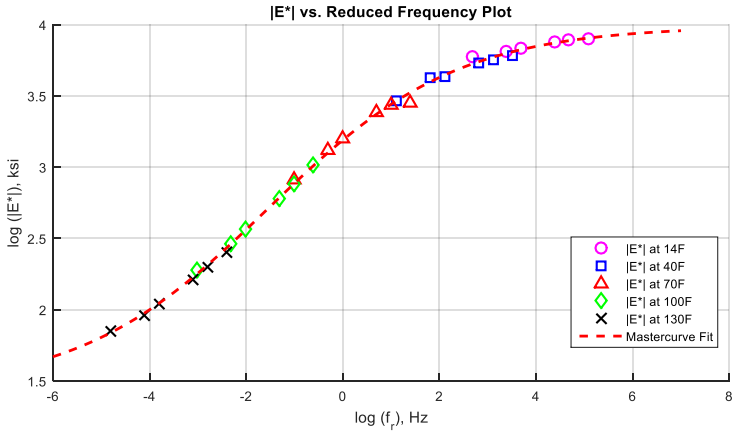

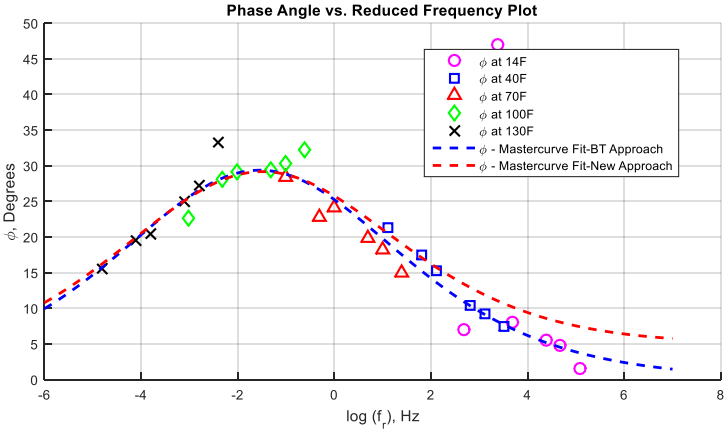

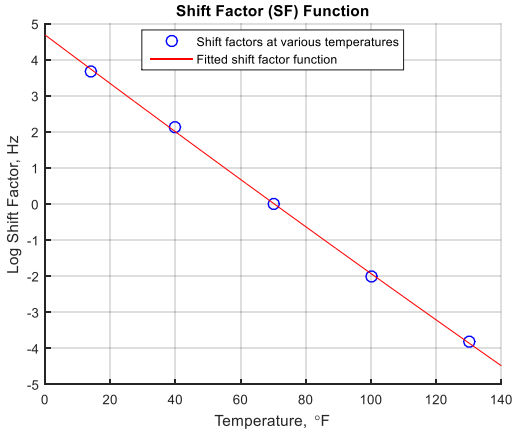

Figure F-24 |E*| and ϕ-mastercurves, and frequency temperature shift factor function for AC Mix 24.

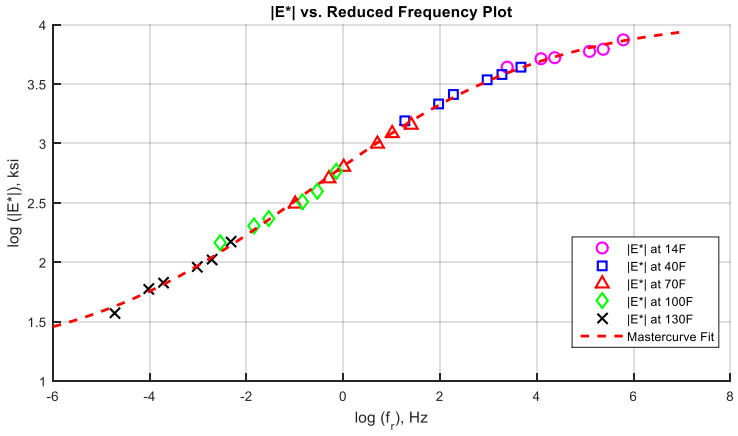

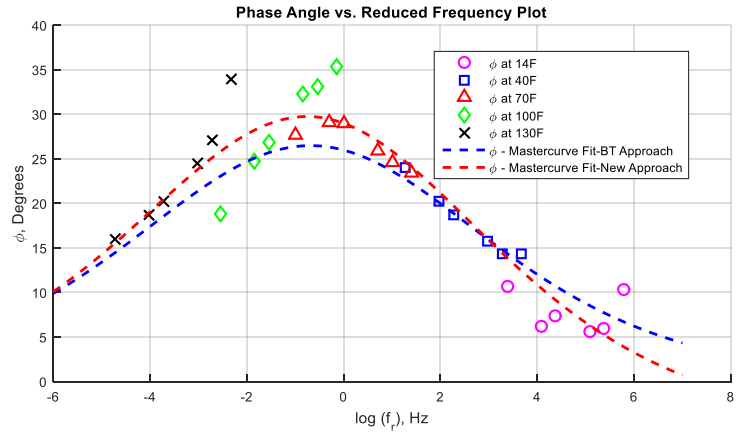

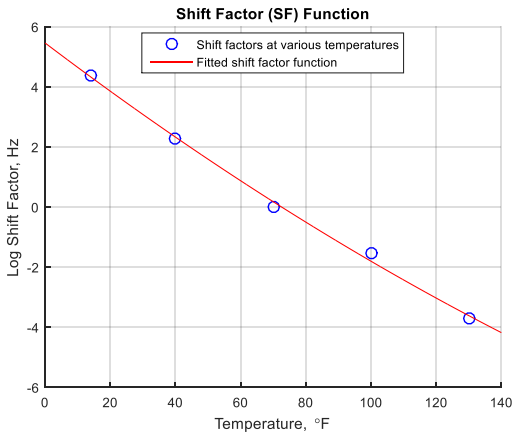

Figure F-25 |E*| and ϕ-mastercurves, and frequency temperature shift factor function for AC Mix 25.

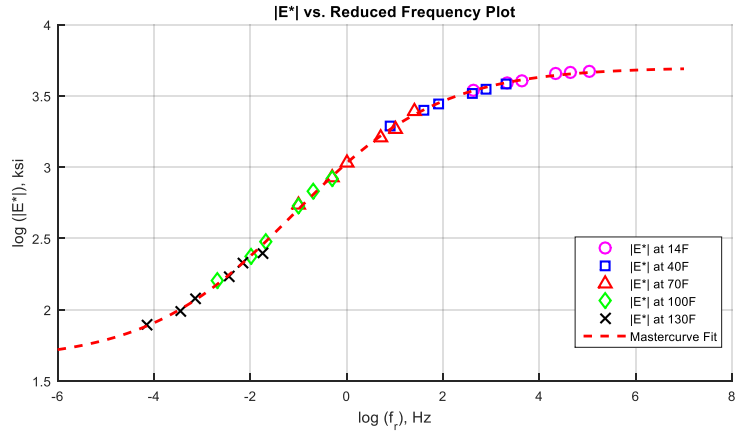

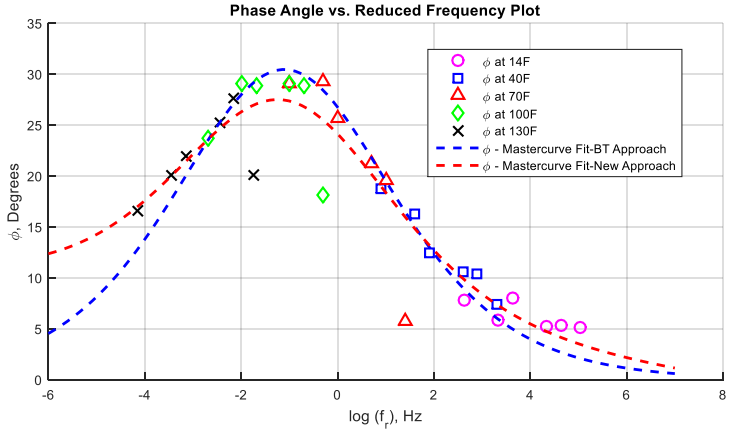

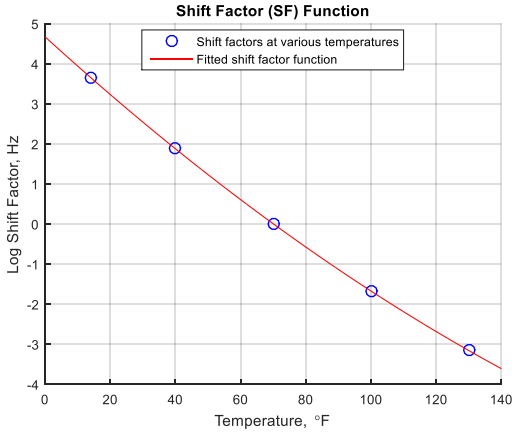

Figure F-26 |E*| and ϕ-mastercurves, and frequency temperature shift factor function for AC Mix 26.

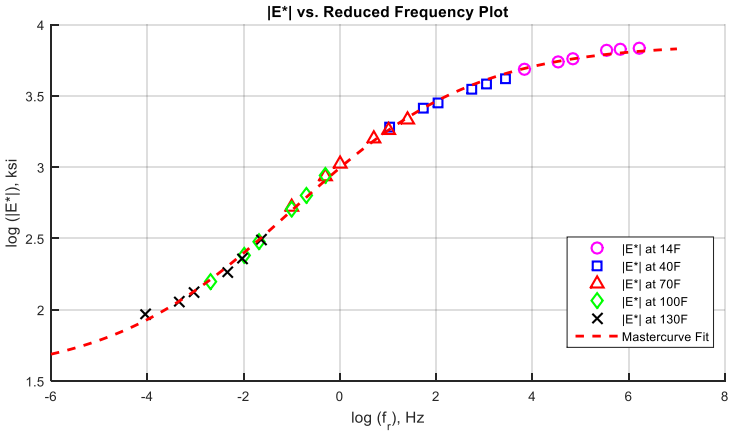

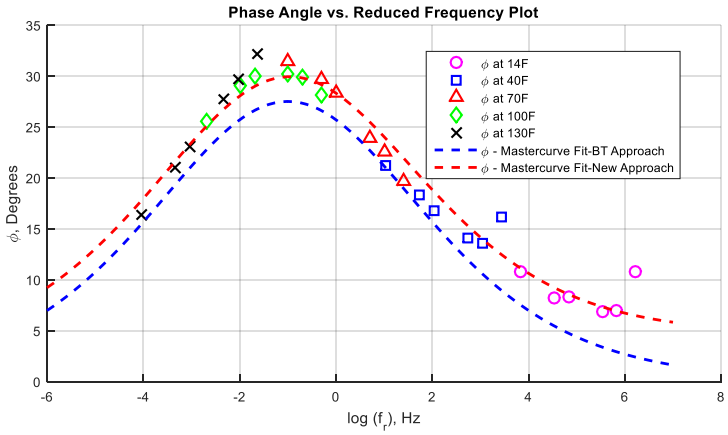

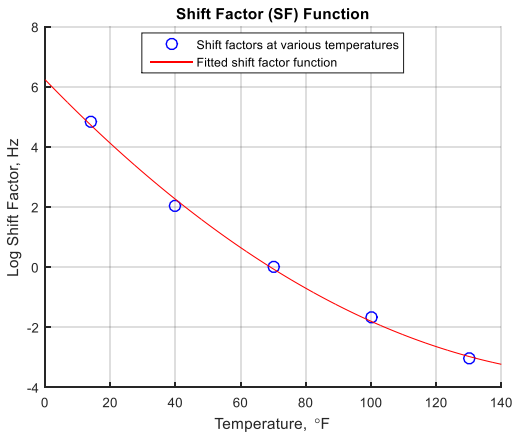

Figure F-27 |E*| and ϕ-mastercurves, and frequency temperature shift factor function for AC Mix 27.

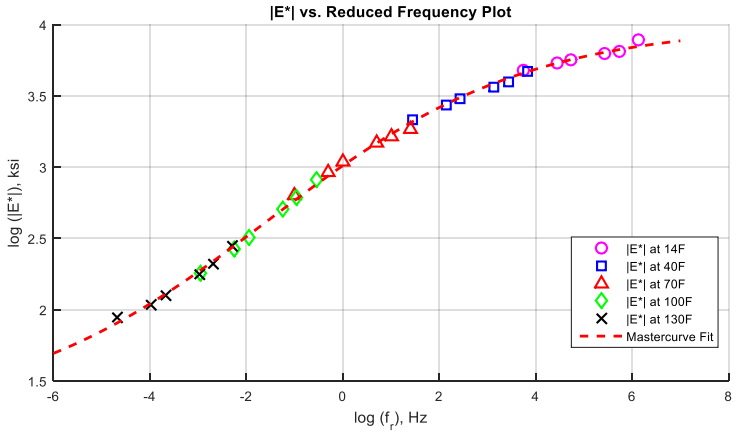

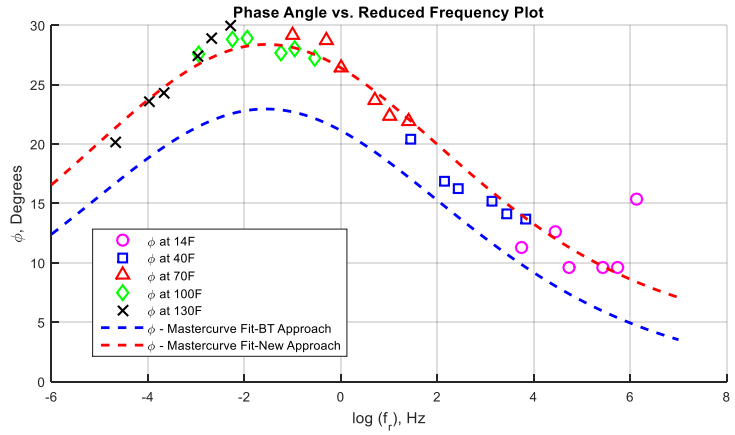

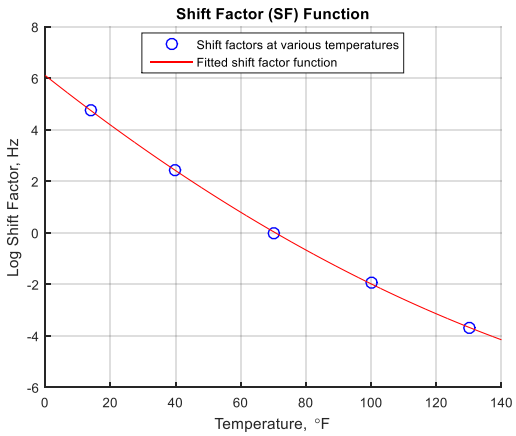

Figure F-28 |E*| and ϕ-mastercurves, and frequency temperature shift factor function for AC Mix 28.

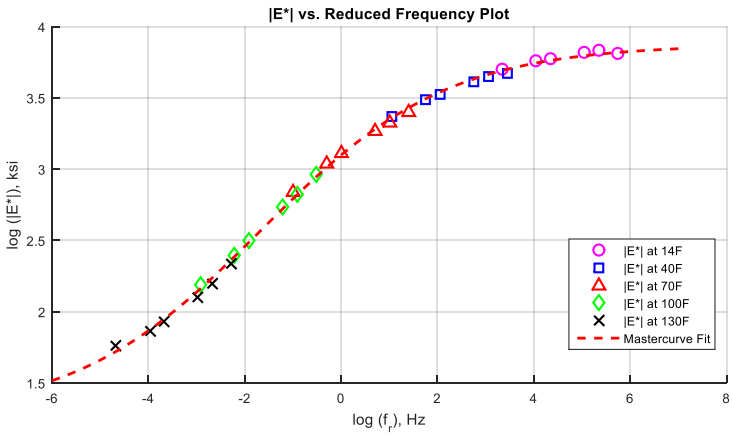

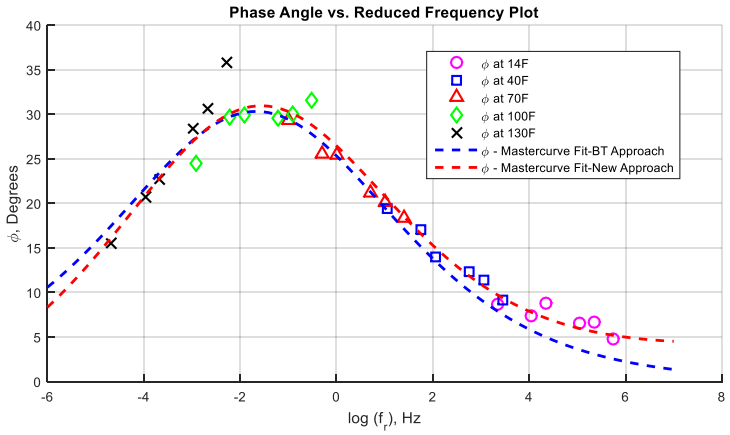

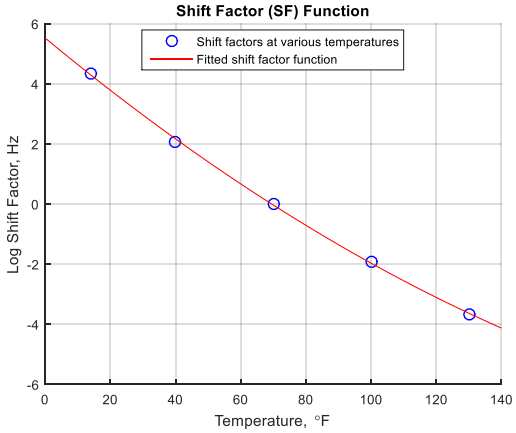

Figure F-29 |E*| and ϕ-mastercurves, and frequency temperature shift factor function for AC Mix 29.

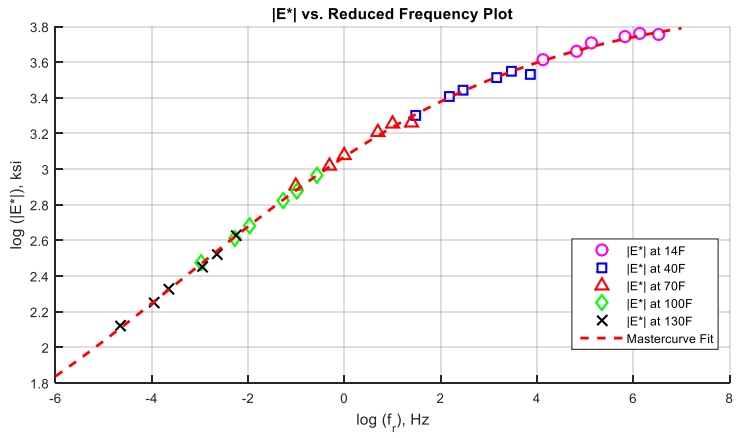

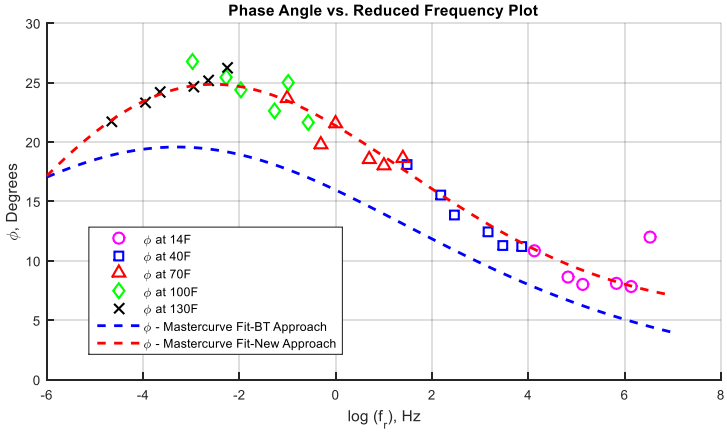

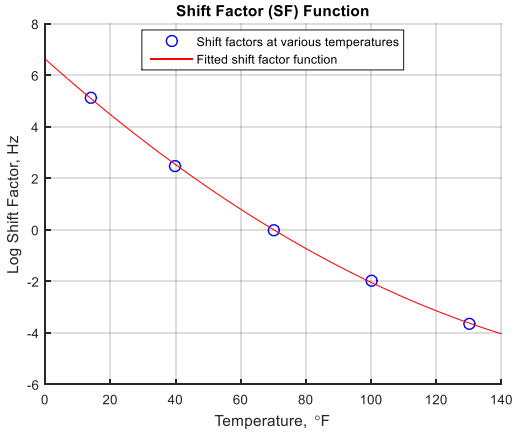

Figure F-30 |E*| and ϕ-mastercurves, and frequency temperature shift factor function for AC Mix 30.

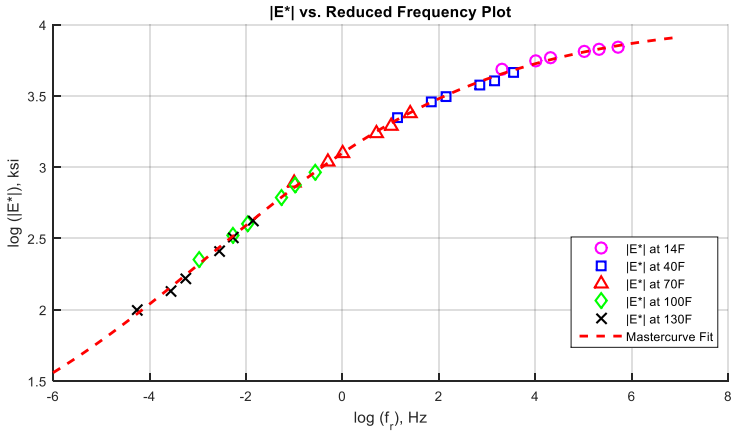

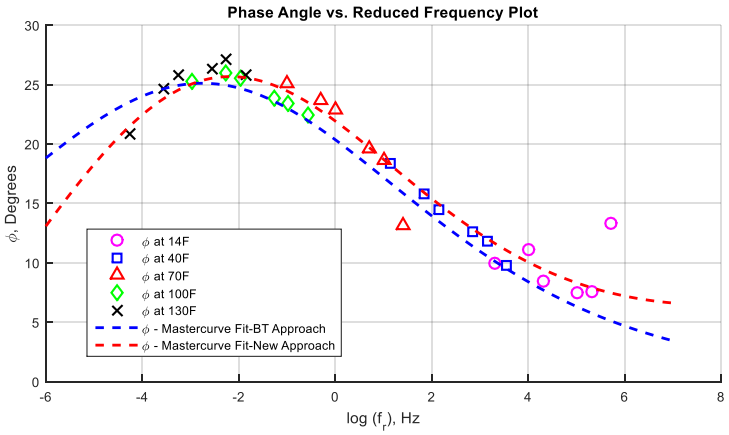

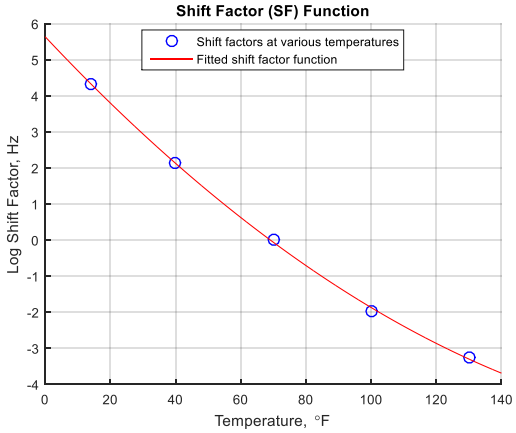

Figure F-31 |E*| and ϕ-mastercurves, and frequency temperature shift factor function for AC Mix 31.

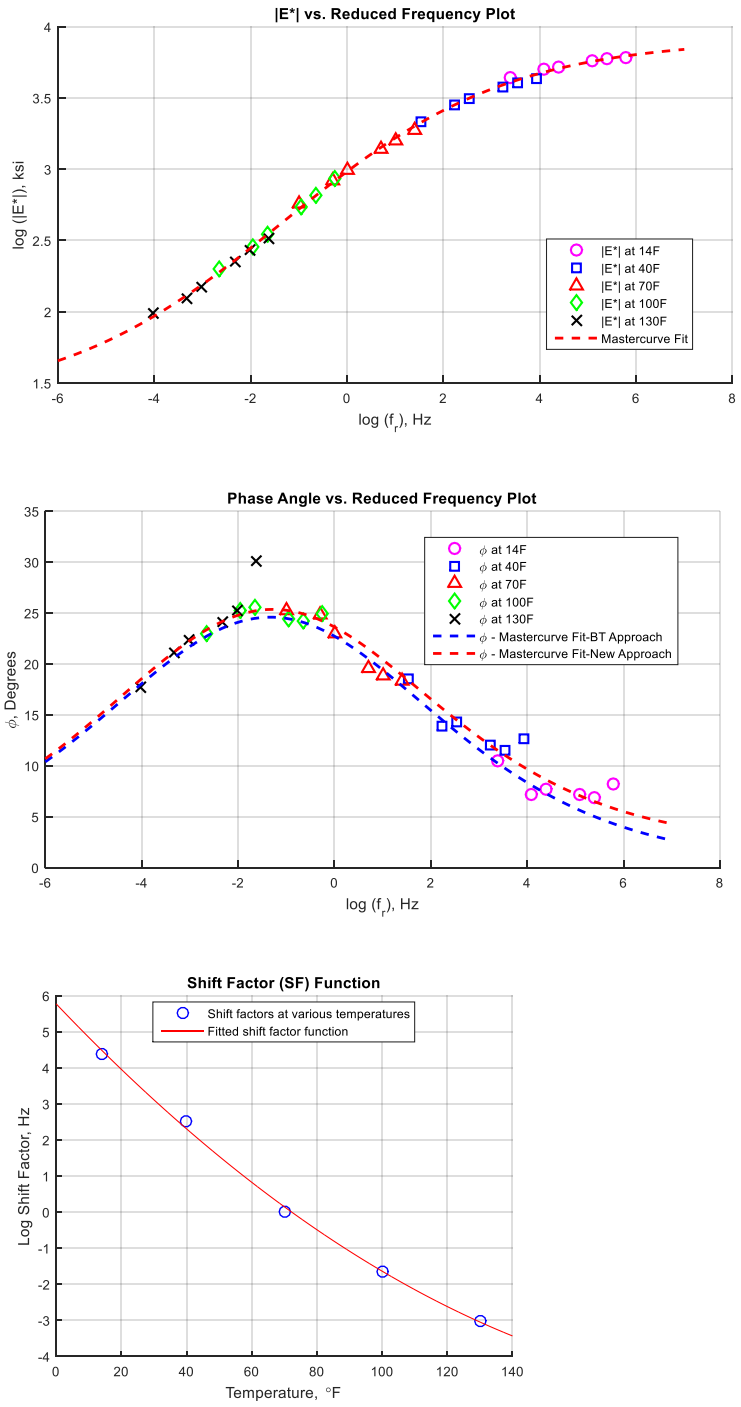

Figure F-32 |E*| and ϕ-mastercurves, and frequency temperature shift factor function for AC Mix 32.

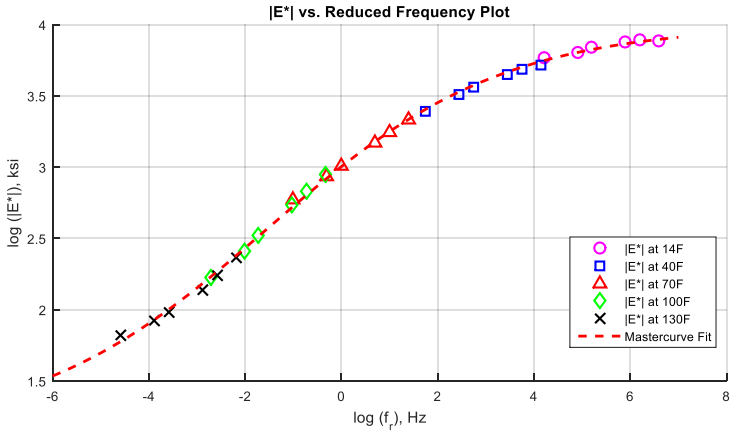

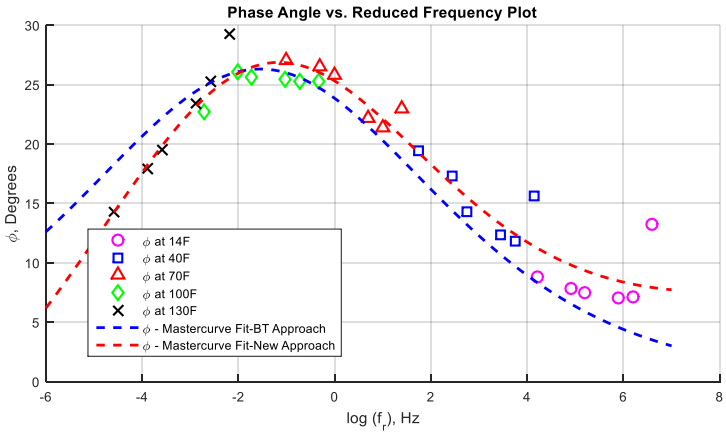

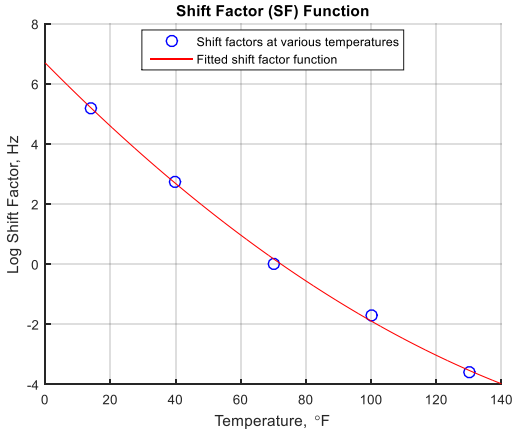

Figure F-33 |E*| and ϕ-mastercurves, and frequency temperature shift factor function for AC Mix 33.

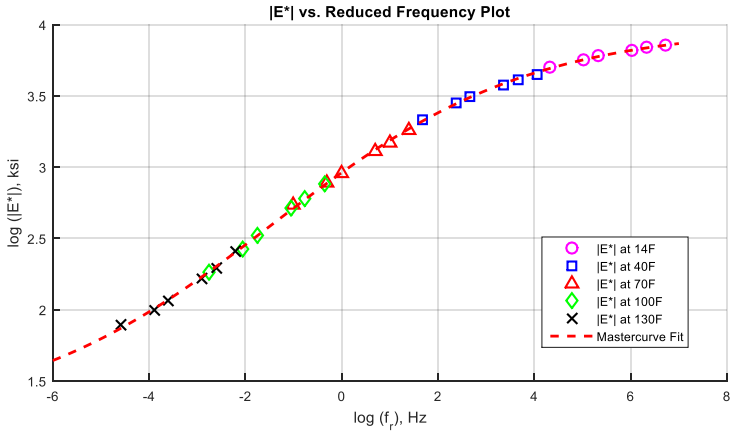

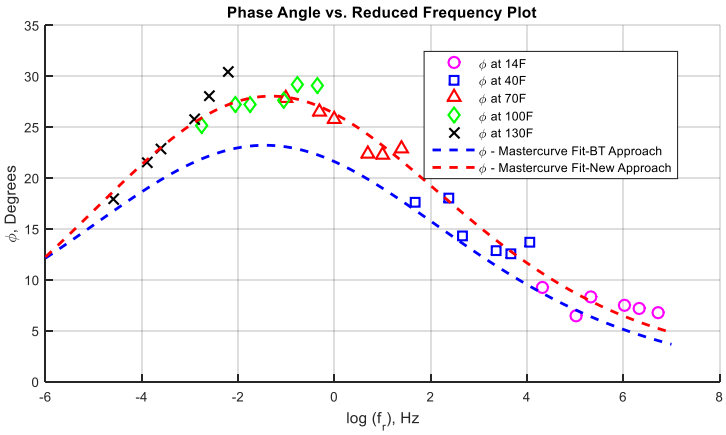

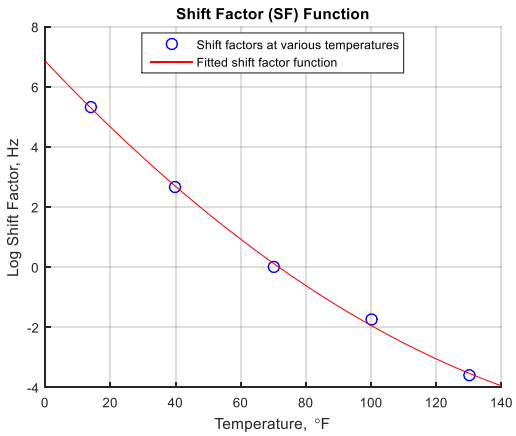

Figure F-34 |E*| and ϕ-mastercurves, and frequency temperature shift factor function for AC Mix 34.

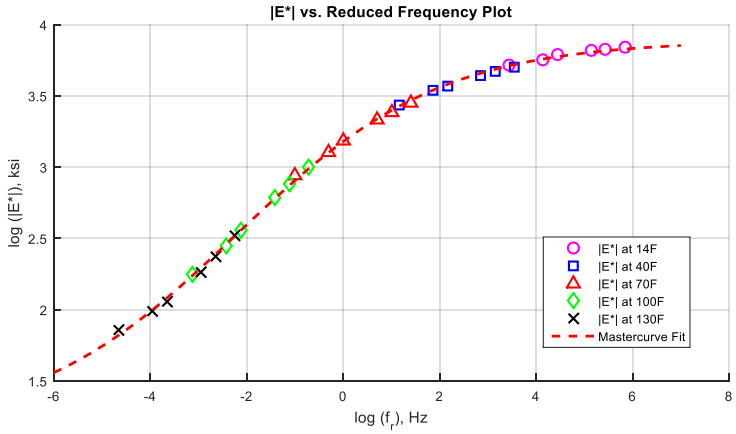

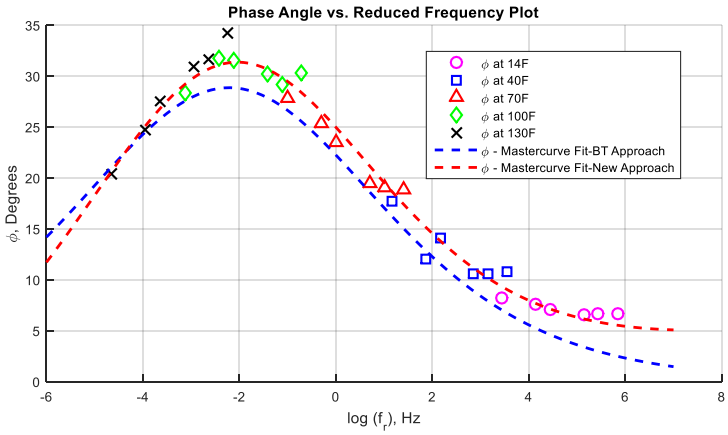

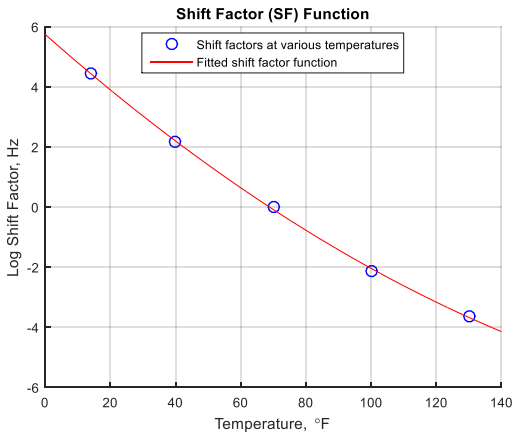

Figure F-35 |E*| and ϕ-mastercurves, and frequency temperature shift factor function for AC Mix 35.

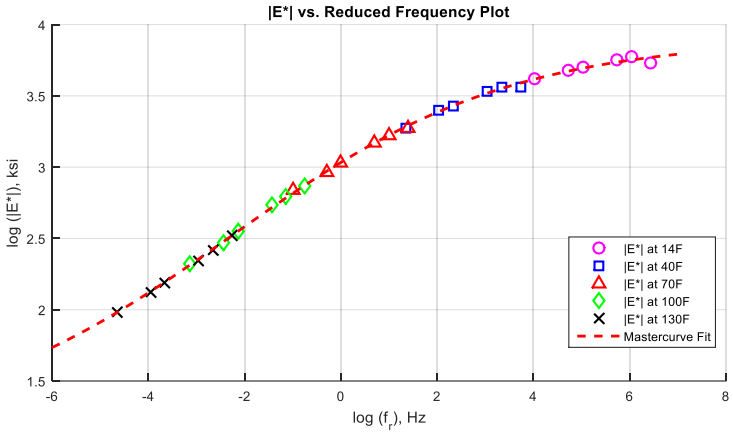

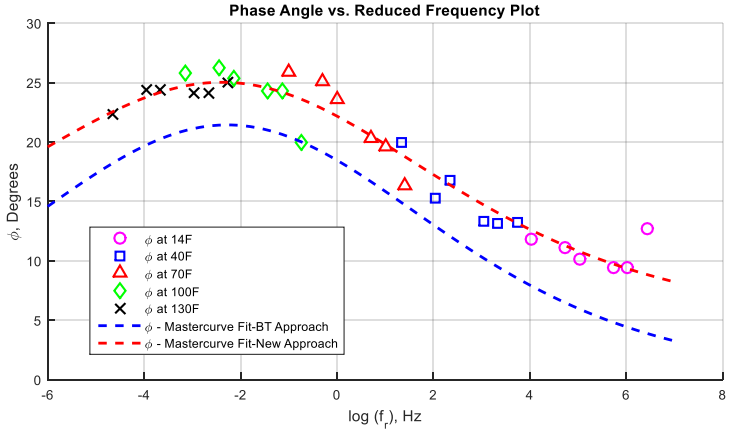

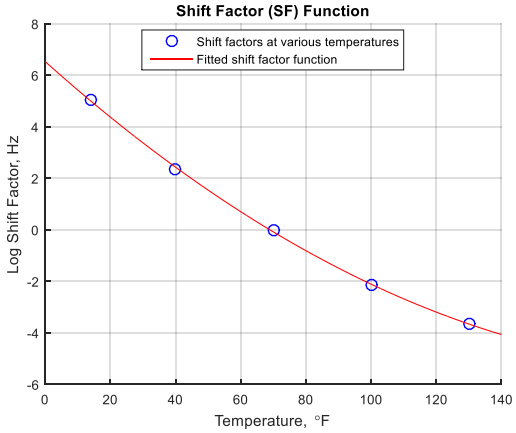

Figure F-36 |E*| and ϕ-mastercurves, and frequency temperature shift factor function for AC Mix 36.

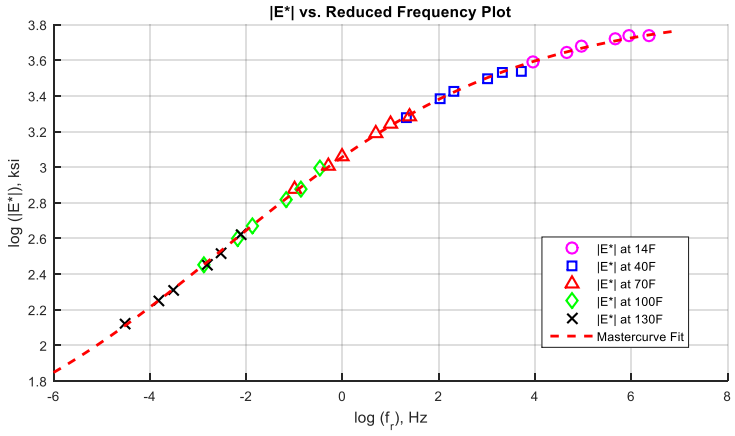

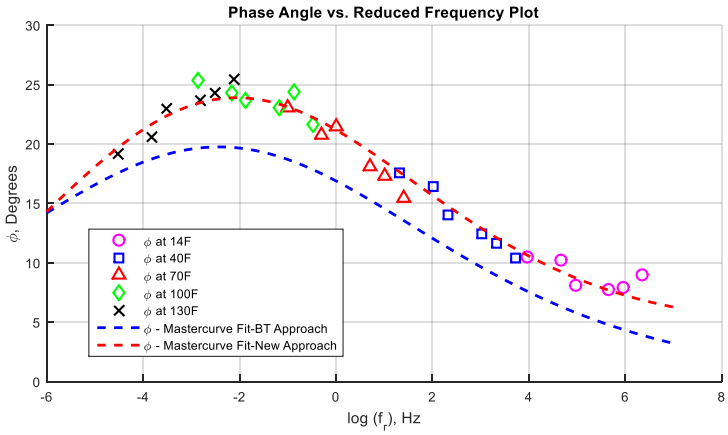

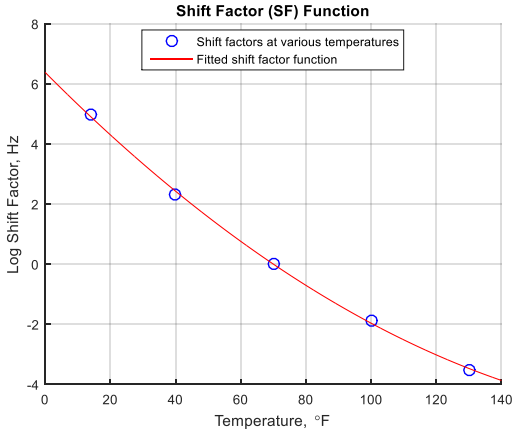

Figure F-37 |E*| and ϕ-mastercurves, and frequency temperature shift factor function for AC Mix 37.

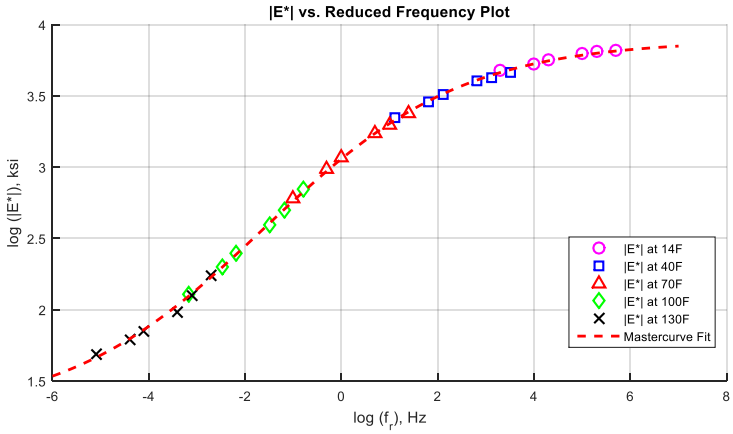

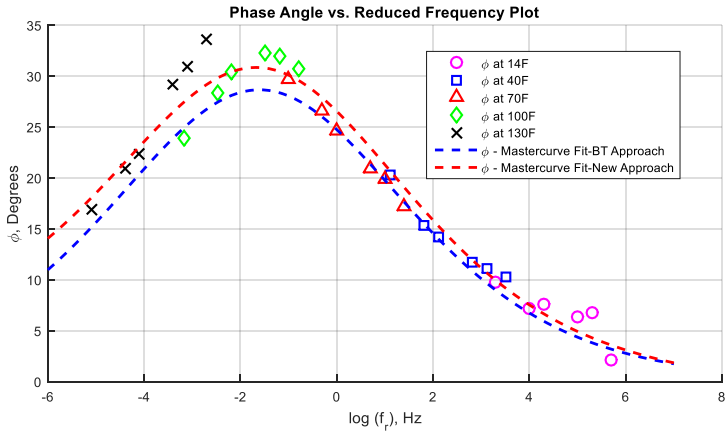

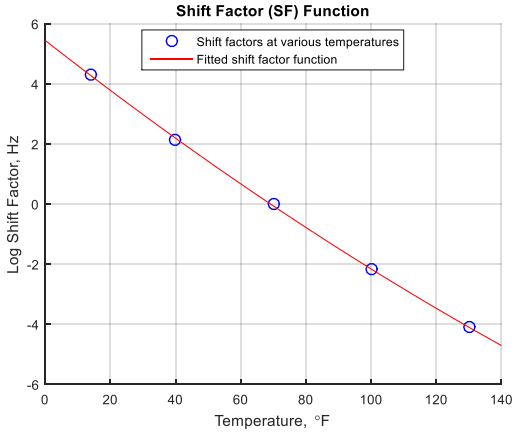

Figure F-38 |E*| and ϕ-mastercurves, and frequency temperature shift factor function for AC Mix 38.

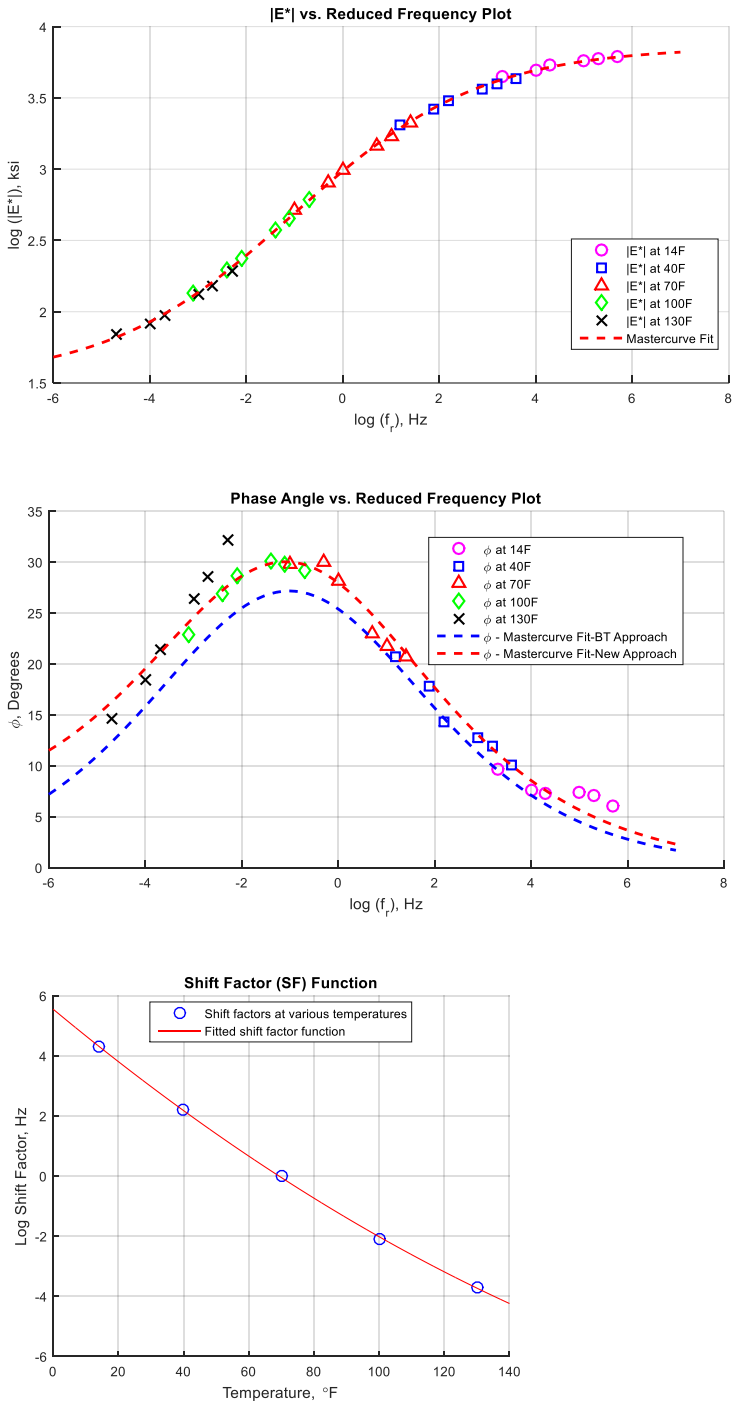

Figure F-39 |E*| and ϕ-mastercurves, and frequency temperature shift factor function for AC Mix 39.

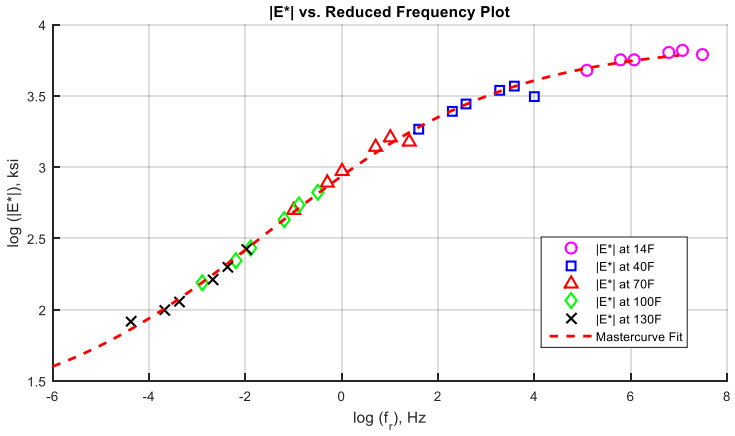

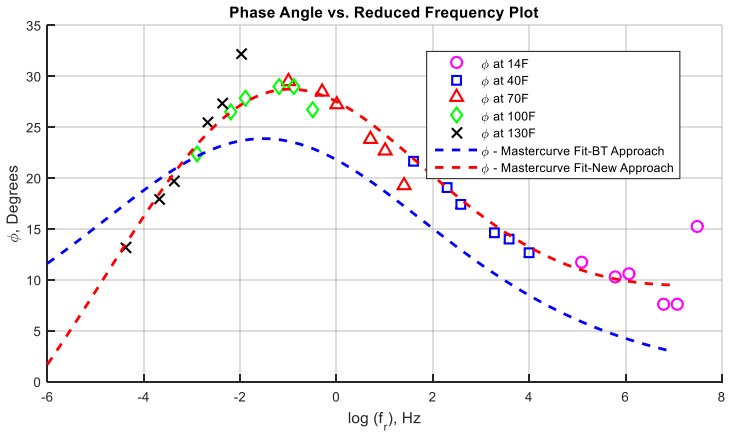

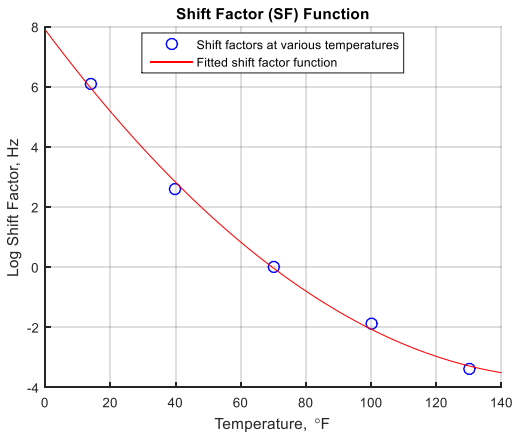

Figure F-40 |E*| and ϕ-mastercurves, and frequency temperature shift factor function for AC Mix 40.

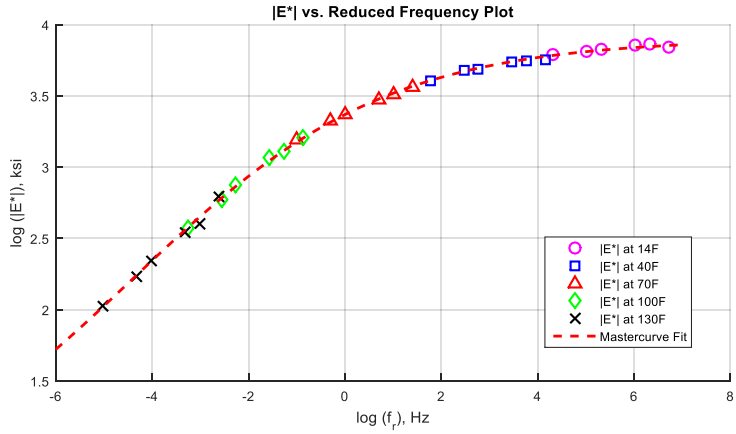

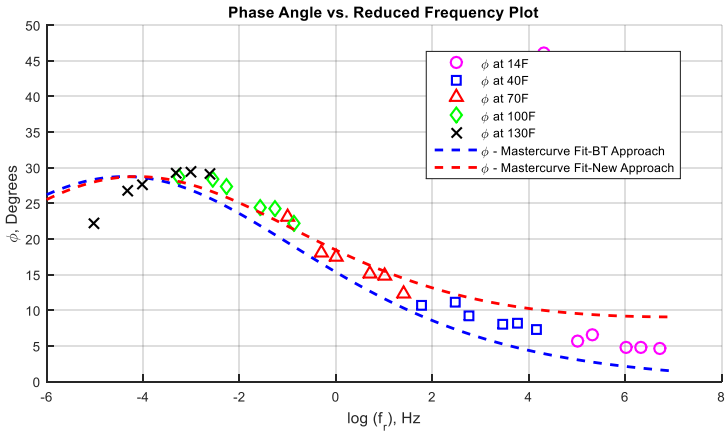

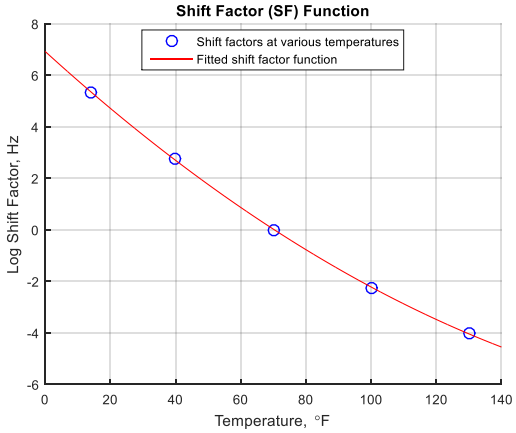

Figure F-41 |E*| and ϕ-mastercurves, and frequency temperature shift factor function for AC Mix 41.

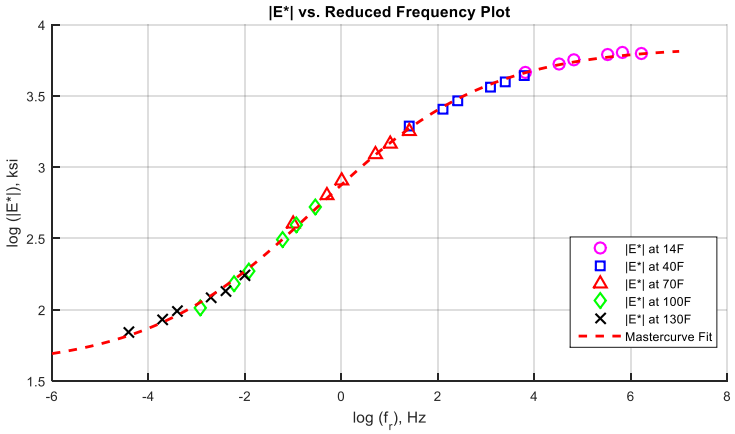

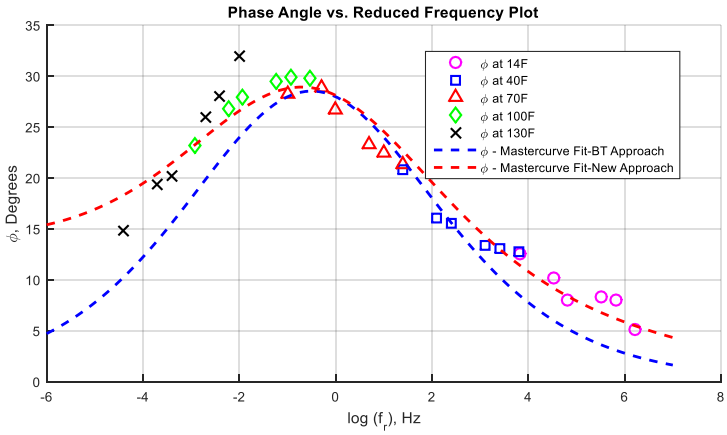

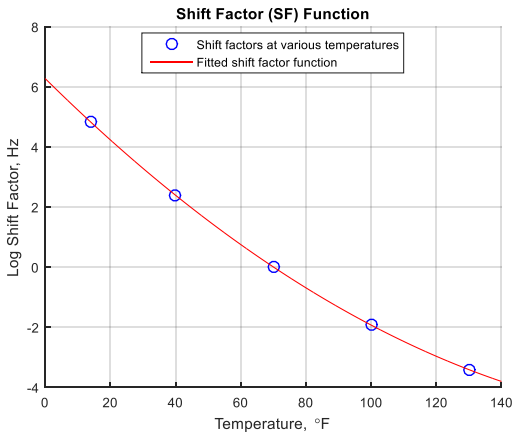

Figure F-42 |E*| and ϕ-mastercurves, and frequency temperature shift factor function for AC Mix 42.

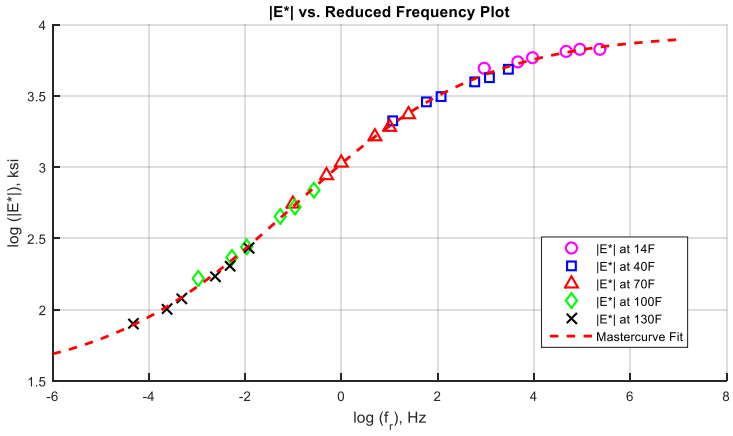

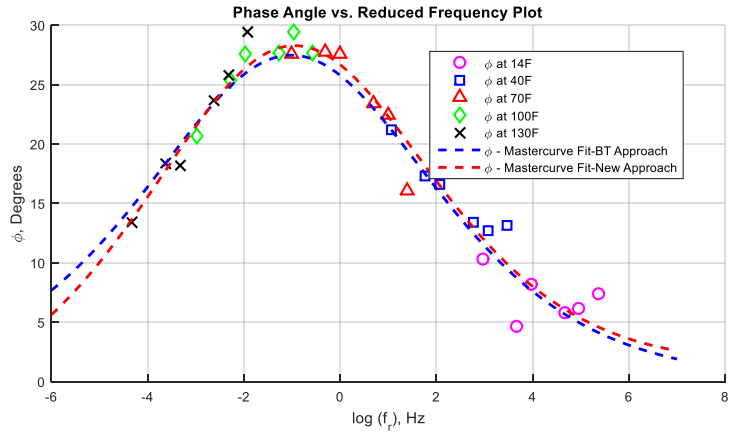

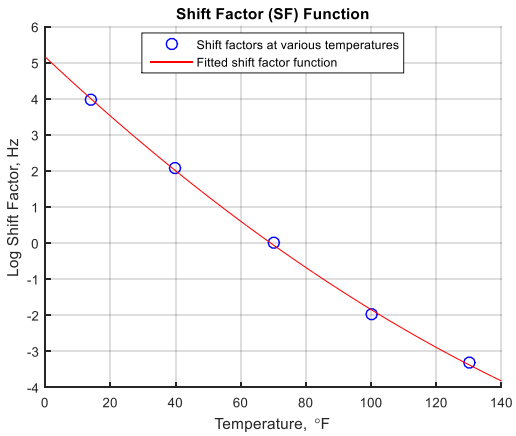

Figure F-43 |E*| and ϕ-mastercurves, and frequency temperature shift factor function for AC Mix 43.

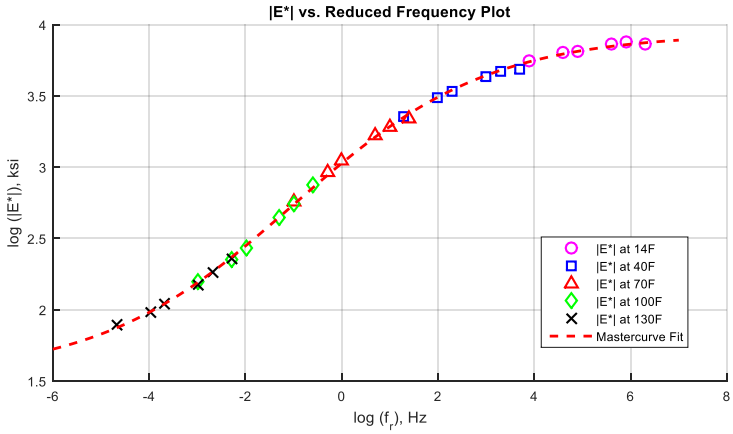

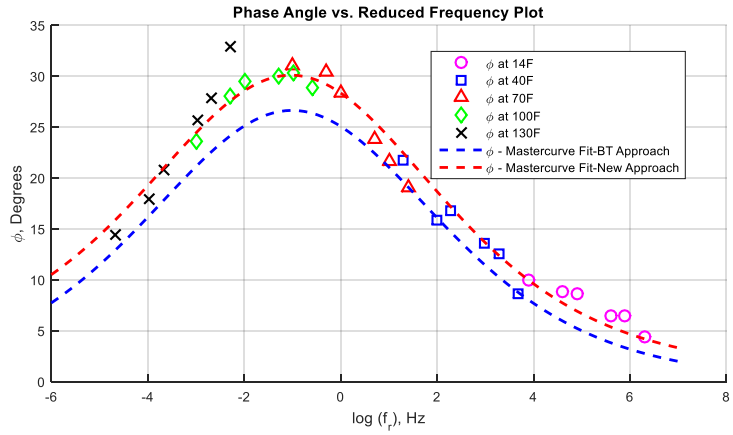

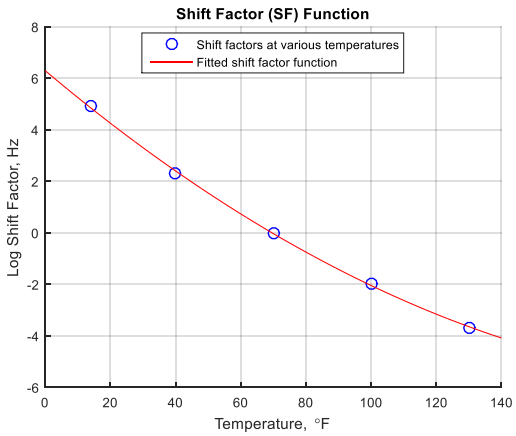

Figure F-44 |E*| and ϕ-mastercurves, and frequency temperature shift factor function for AC Mix 44.

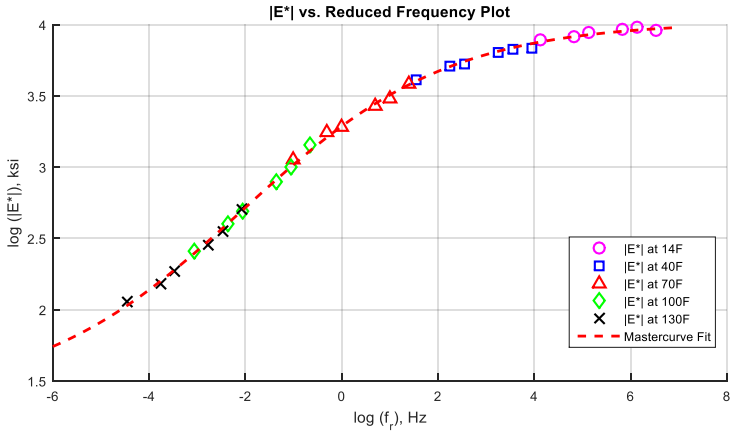

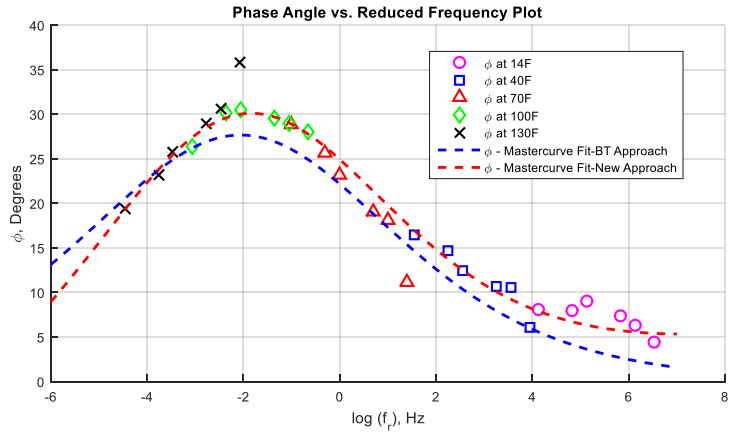

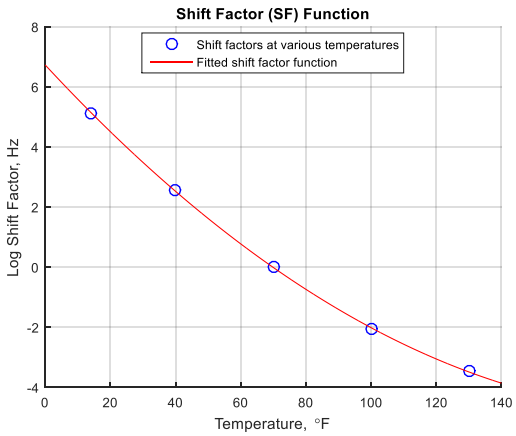

Figure F-45 |E*| and ϕ-mastercurves, and frequency temperature shift factor function for AC Mix 45.

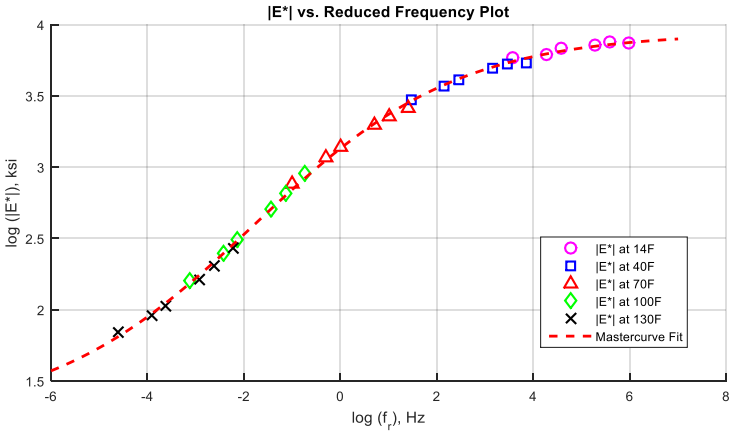

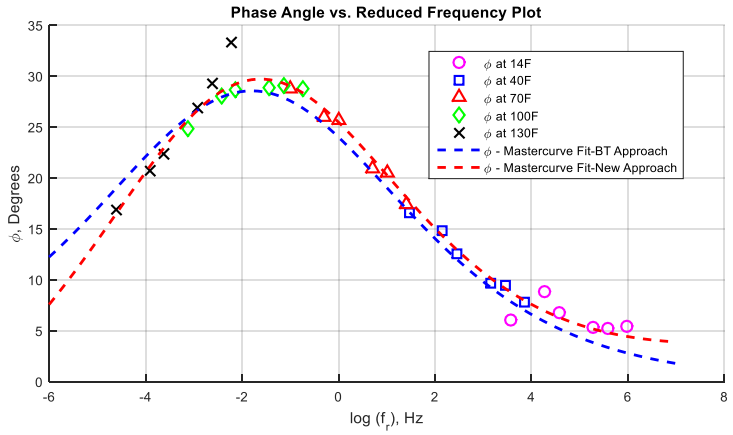

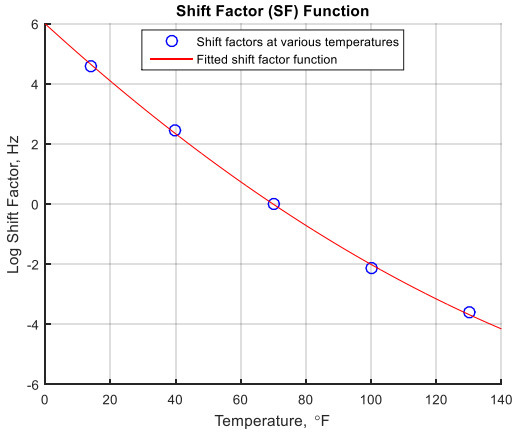

Figure F-46 |E*| and ϕ-mastercurves, and frequency temperature shift factor function for AC Mix 46.

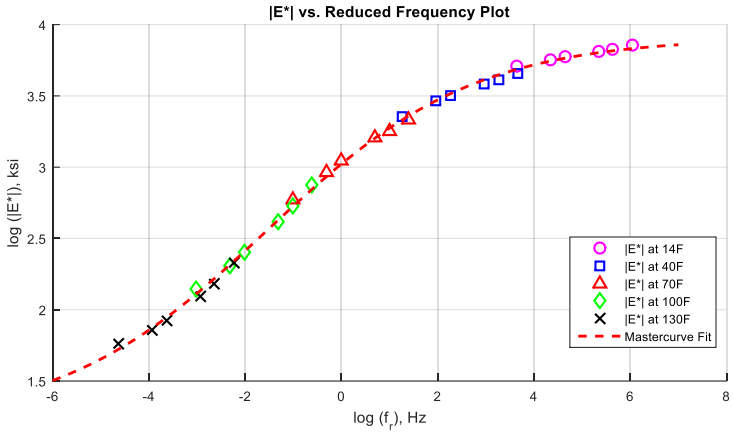

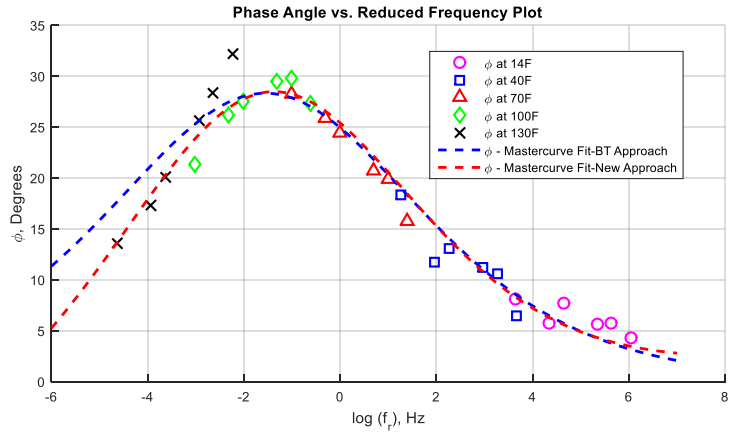

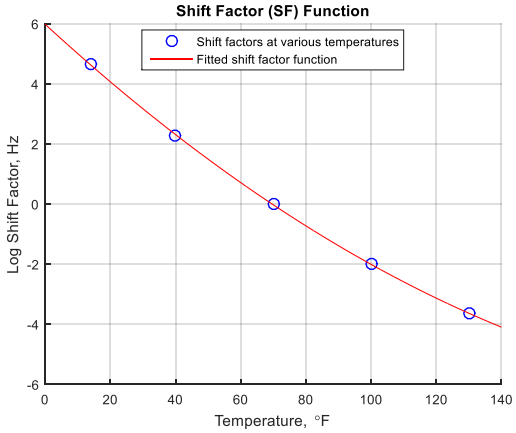

Figure F-47 |E*| and ϕ-mastercurves, and frequency temperature shift factor function for AC Mix 47.

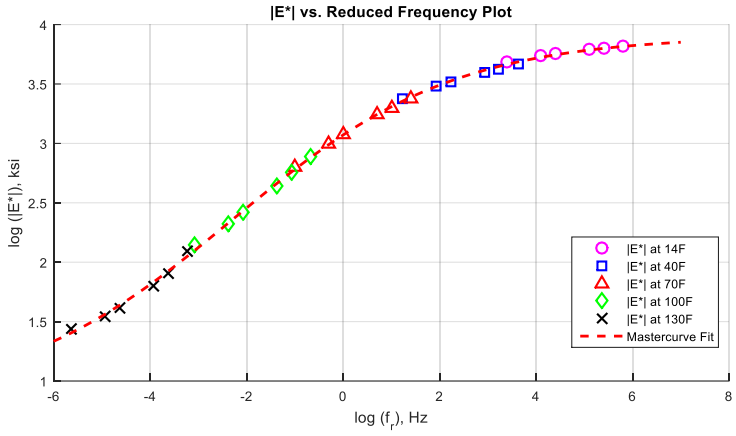

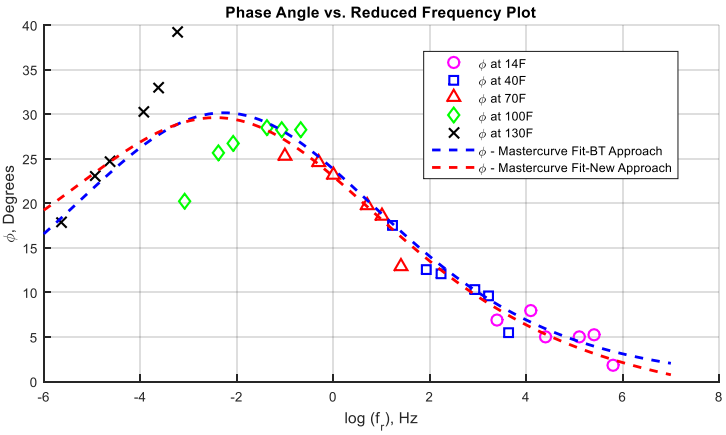

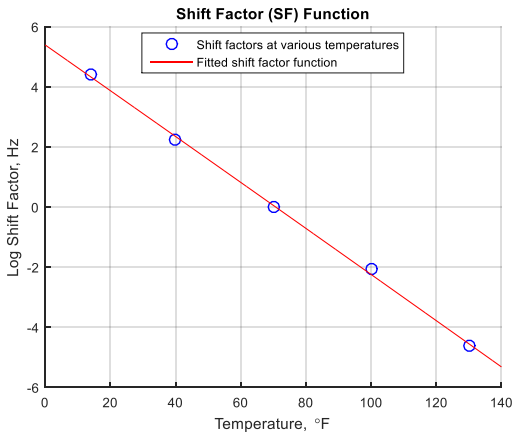

Figure F-48 |E*| and ϕ-mastercurves, and frequency temperature shift factor function for AC Mix 48.

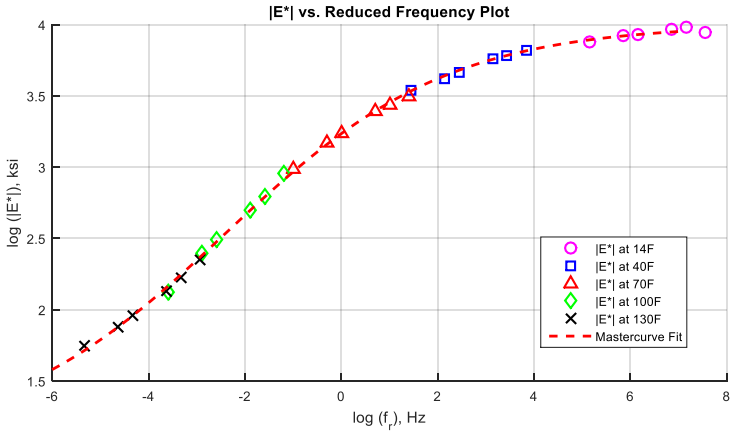

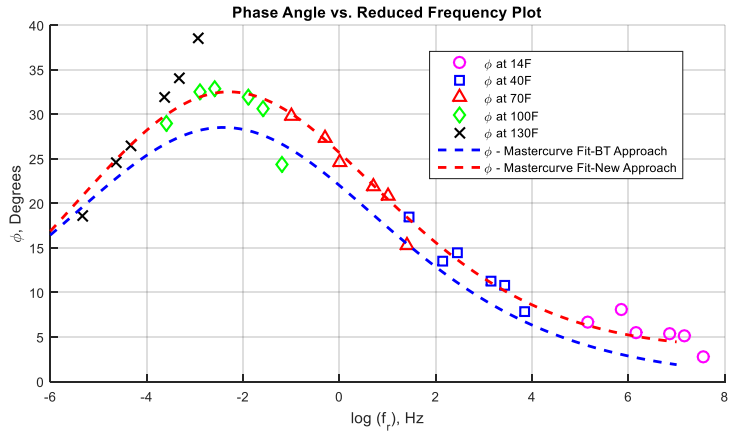

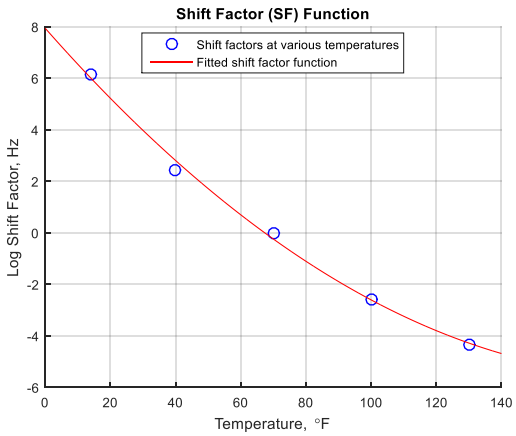

Figure F-49 |E*| and ϕ-mastercurves, and frequency temperature shift factor function for AC Mix 49.

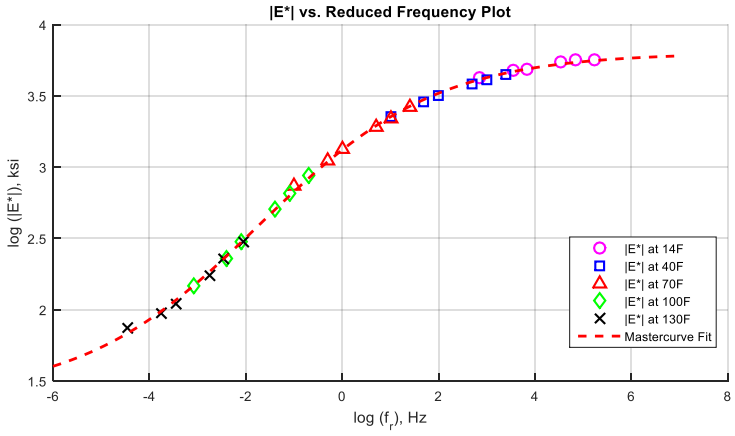

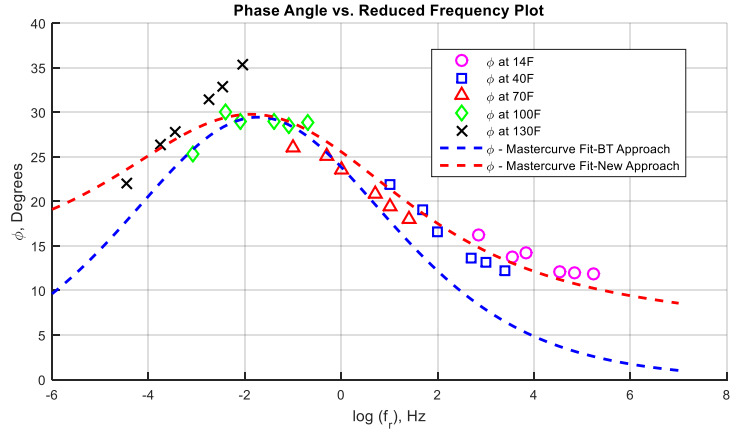

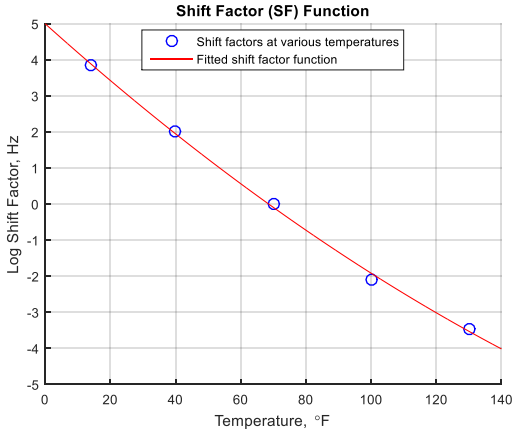

Figure F-50 |E*| and ϕ-mastercurves, and frequency temperature shift factor function for AC Mix 10.

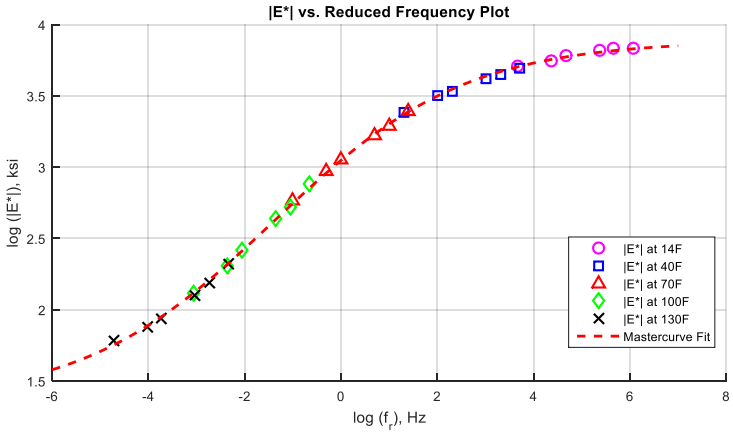

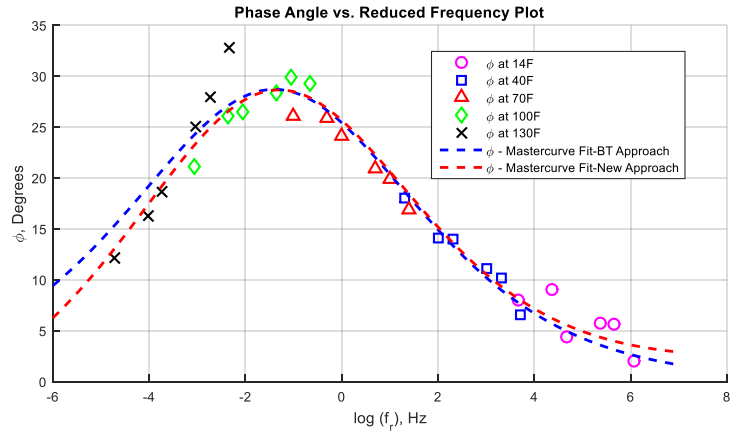

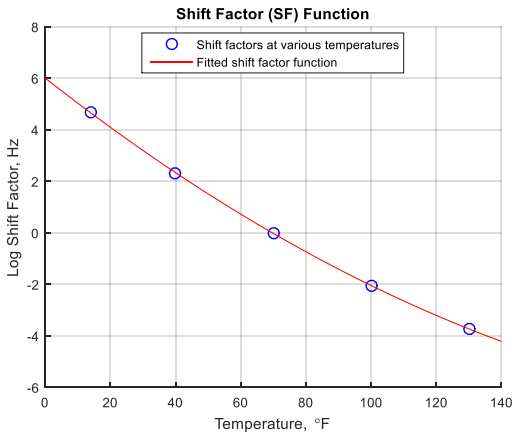

Figure F-51 |E*| and ϕ-mastercurves, and frequency temperature shift factor function for AC Mix 10.

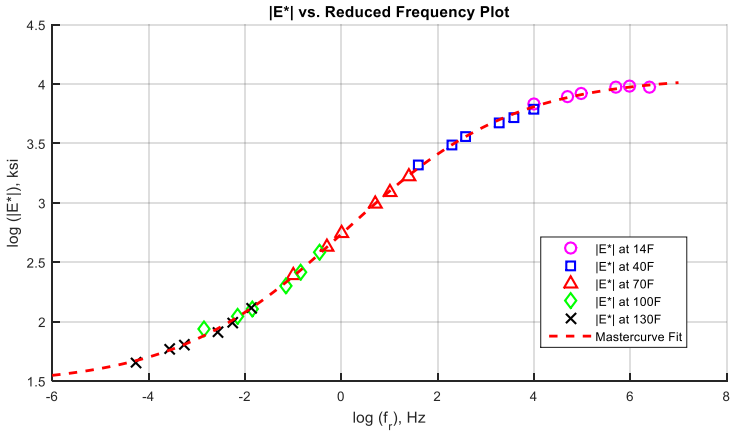

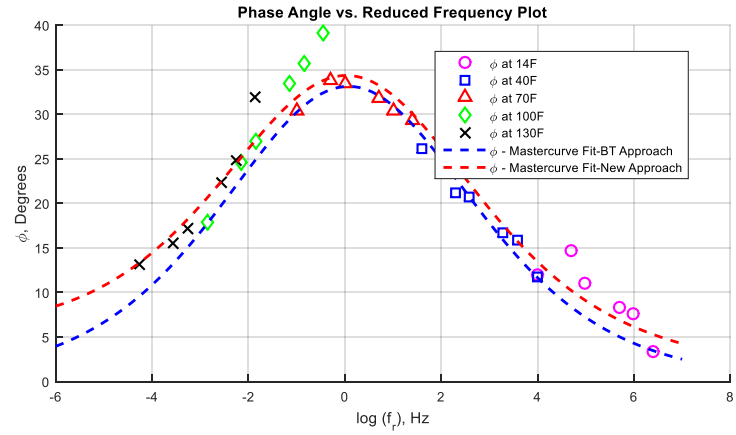

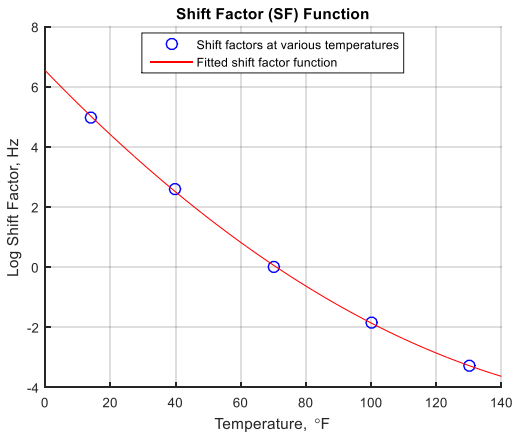

Figure F-52 |E*| and ϕ-mastercurves, and frequency temperature shift factor function for AC Mix 10.

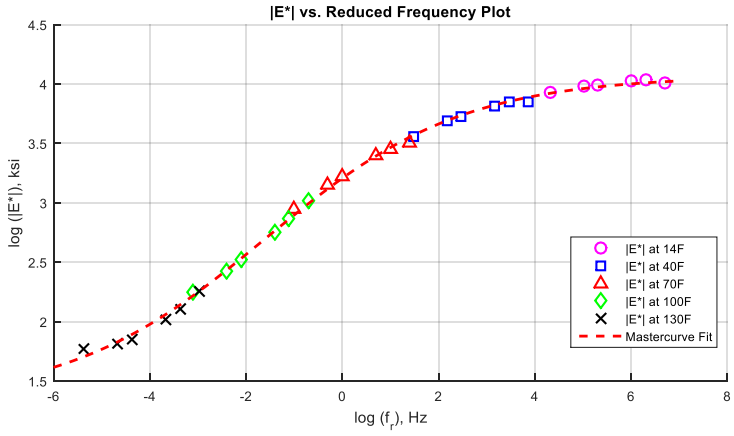

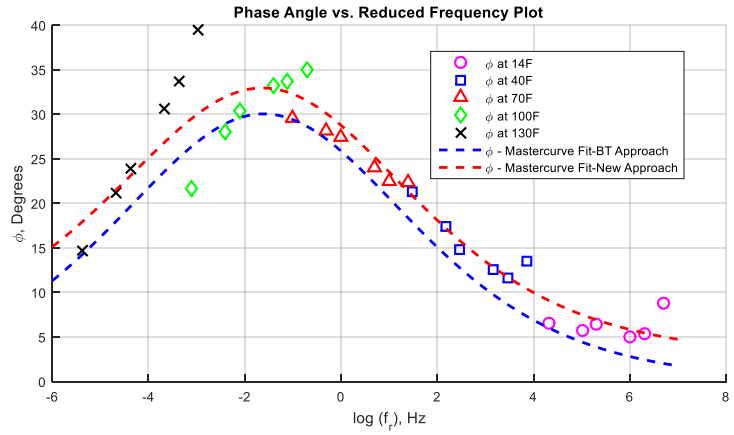

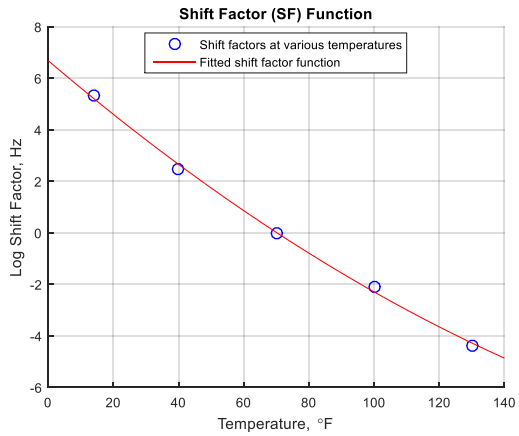

Figure F-53 |E*| and ϕ-mastercurves, and frequency temperature shift factor function for AC Mix 53.

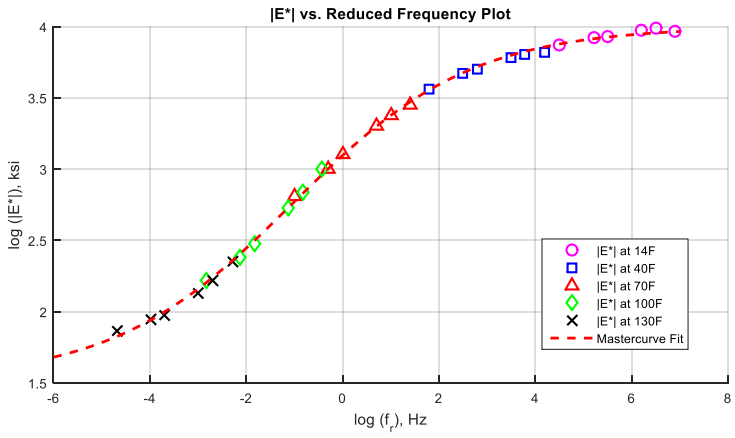

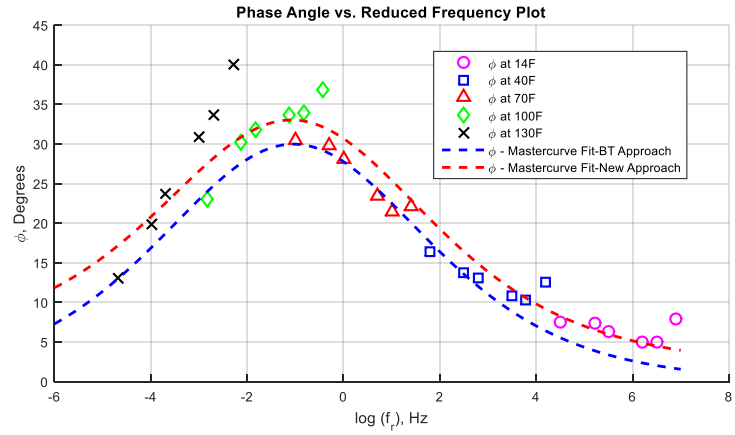

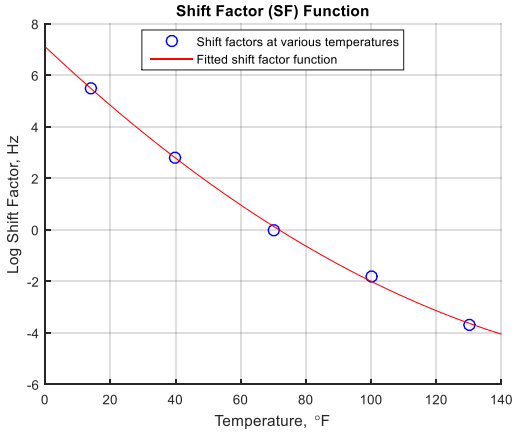

Figure F-54 |E*| and ϕ-mastercurves, and frequency temperature shift factor function for AC Mix 54.

Appendix G

Code G-1: MATLAB® Code for Processing Test Data of Individual Test Specimen from Machine Generated Test Data File

```
%% Load Data from file
clear;
close all;
clc;
test_data_info_14F = importdata('001 -10.csv','%s', 52);
test_num_data_14F = xlsread('001 -10.csv');
test_data_info_40F = importdata('002 4.4.csv','%s', 52);
test_num_data_40F = xlsread('002 4.4.csv');
test_data_info_70F = importdata('003 21.1.csv','%s', 52);
test_num_data_70F = xlsread('003 21.1.csv');
test_data_info_100F = importdata('004 37.8.csv','%s', 52);
test_num_data_100F = xlsread('004 37.8.csv');
test_data_info_130F = importdata('005 54.4.csv','%s', 52);
test_num_data_130F = xlsread('005 54.4.csv');
%% Temperatures (Celcious)
temperature_C_14F = -10*[1; 1; 1; 1; 1; 1];
temperature_C_40F = 4.4*[1; 1; 1; 1; 1; 1];
temperature_C_70F = 21.1*[1; 1; 1; 1; 1; 1];
temperature_C_100F = 37.8*[1; 1; 1; 1; 1; 1];
temperature_C_130F = 54.4*[1; 1; 1; 1; 1; 1];
%% Temperature (Farenhite)
temperature_F_14F = 14*[1; 1; 1; 1; 1; 1];
temperature_F_40F = 40*[1; 1; 1; 1; 1; 1];
temperature_F_70F = 70*[1; 1; 1; 1; 1; 1];
temperature_F_100F = 100*[1; 1; 1; 1; 1; 1];
temperature_F_130F = 130*[1; 1; 1; 1; 1; 1];
%% Frequencies (Hz)
frequency_14F = [25; 10; 5; 1; 0.5; 0.1];
frequency_40F = [25; 10; 5; 1; 0.5; 0.1];
frequency_70F = [25; 10; 5; 1; 0.5; 0.1];
frequency_100F = [25; 10; 5; 1; 0.5; 0.1];
frequency_130F = [25; 10; 5; 1; 0.5; 0.1];
%% Stress Amplitude (in kPa)
stress_amp_14F = zeros(6,1);
count = 0;
for i = 1:6
        stress_amp_14F(i,1) = test_num_data_14F(55+count,3);
        count = count+1;
end
stress_amp_40F = zeros(6,1);
count = 0;
for i = 1:6
        stress_amp_40F(i,1) = test_num_data_40F(55+count,3);
        count = count+1;
end
stress_amp_70F = zeros(6,1);
count = 0;
for i = 1:6
        stress_amp_70F(i,1) = test_num_data_70F(55+count,3);
        count = count+1;
end
stress_amp_100F = zeros(6,1);
count = 0;
for i = 1:6
        stress_amp_100F(i,1) = test_num_data_100F(55+count,3);
        count = count+1;
end
stress_amp_130F = zeros(6,1);
count = 0;
for i = 1:6
        stress_amp_130F(i,1) = test_num_data_130F(55+count,3);
        count = count+1;
end
stress_amp_neg_10C = 0.145062461.*stress_amp_14F;
stress_amp_4C = 0.145062461.*stress_amp_40F;
```

```
stress_amp_21C = 0.145062461.*stress_amp_70F;
stress_amp_37C = 0.145062461.*stress_amp_100F;
stress_amp_54C = 0.145062461.*stress_amp_130F;
%% Stress Standard Error (SE) in percentage
stress_std_err_14F = zeros(6,1);
count = 0;
for i = 1:6
        stress_std_err_14F(i,1) = test_num_data_14F(55+count,4);
        count = count+1;
end
stress_std_err_40F = zeros(6,1);
count = 0;
for i = 1:6
        stress_std_err_40F(i,1) = test_num_data_40F(55+count,4);
        count = count+1;
end
stress_std_err_70F = zeros(6,1);
count = 0;
for i = 1:6
        stress_std_err_70F(i,1) = test_num_data_70F(55+count,4);
        count = count+1;
end
stress_std_err_100F = zeros(6,1);
count = 0;
for i = 1:6
        stress_std_err_100F(i,1) = test_num_data_100F(55+count,4);
        count = count+1;
end
stress_std_err_130F = zeros(6,1);
count = 0;
for i = 1:6
        stress_std_err_130F(i,1) = test_num_data_130F(55+count,4);
        count = count+1;
end
%% Dynamic Modulus (MPa)
dyn_mod_14F = zeros(6,1);
count = 0;
for i = 1:6
        dyn_mod_14F(i,1) = test_num_data_14F(55+count,5);
        count = count+1;
end
dyn_mod_40F = zeros(6,1);
count = 0;
for i = 1:6
        dyn_mod_40F(i,1) = test_num_data_40F(55+count,5);
        count = count+1;
end
dyn_mod_70F = zeros(6,1);
count = 0;
for i = 1:6
        dyn_mod_70F(i,1) = test_num_data_70F(55+count,5);
        count = count+1;
end
dyn_mod_100F = zeros(6,1);
count = 0;
for i = 1:6
        dyn_mod_100F(i,1) = test_num_data_100F(55+count,5);
        count = count+1;
end
dyn_mod_130F = zeros(6,1);
count = 0;
for i = 1:6
        dyn_mod_130F(i,1) = test_num_data_130F(55+count,5);
        count = count+1;
end
dyn_mod_neg_10C = 0.145062461.*dyn_mod_14F;
dyn_mod_4C = 0.145062461.*dyn_mod_40F;
dyn_mod_21C = 0.145062461.*dyn_mod_70F;
dyn_mod_37C = 0.145062461.*dyn_mod_100F;
dyn_mod_54C = 0.145062461.*dyn_mod_130F;
%% Phase Angle (degree)
```

```
phase_angle_14F = zeros(6,1);
count = 0;
for i = 1:6
        phase_angle_14F(i,1) = test_num_data_14F(55+count,6);
        count = count+1;
end
phase_angle_40F = zeros(6,1);
count = 0;
for i = 1:6
        phase_angle_40F(i,1) = test_num_data_40F(55+count,6);
        count = count+1;
end
phase_angle_70F = zeros(6,1);
count = 0;
for i = 1:6
        phase_angle_70F(i,1) = test_num_data_70F(55+count,6);
        count = count+1;
end
phase_angle_100F = zeros(6,1);
count = 0;
for i = 1:6
        phase_angle_100F(i,1) = test_num_data_100F(55+count,6);
        count = count+1;
end
phase_angle_130F = zeros(6,1);
count = 0;
for i = 1:6
        phase_angle_130F(i,1) = test_num_data_130F(55+count,6);
        count = count+1;
end
%% Uniformity Coefficient (UC for phase angle in degree)
UC_phase_angle_14F = zeros(6,1);
count = 0;
for i = 1:6
        UC_phase_angle_14F(i,1) = test_num_data_14F(55+count,7);
        count = count+1;
end
UC_phase_angle_40F = zeros(6,1);
count = 0;
for i = 1:6
        UC_phase_angle_40F(i,1) = test_num_data_40F(55+count,7);
        count = count+1;
end
UC_phase_angle_70F = zeros(6,1);
count = 0;
for i = 1:6
        UC_phase_angle_70F(i,1) = test_num_data_70F(55+count,7);
        count = count+1;
end
UC_phase_angle_100F = zeros(6,1);
count = 0;
for i = 1:6
        UC_phase_angle_100F(i,1) = test_num_data_100F(55+count,7);
        count = count+1;
end
UC_phase_angle_130F = zeros(6,1);
count = 0;
for i = 1:6
        UC_phase_angle_130F(i,1) = test_num_data_130F(55+count,7);
        count = count+1;
end
%% (p-p) Recoverable Strain (microstrains)
pp_recov_strain_14F = zeros(6,1);
count = 0;
for i = 1:6
        pp_recov_strain_14F(i,1) = test_num_data_14F(55+count,8);
        count = count+1;
end
pp_recov_strain_40F = zeros(6,1);
count = 0;
for i = 1:6
```

```
        pp_recov_strain_40F(i,1) = test_num_data_40F(55+count,8);
        count = count+1;
end
pp_recov_strain_70F = zeros(6,1);
count = 0;
for i = 1:6
        pp_recov_strain_70F(i,1) = test_num_data_70F(55+count,8);
        count = count+1;
end
pp_recov_strain_100F = zeros(6,1);
count = 0;
for i = 1:6
        pp_recov_strain_100F(i,1) = test_num_data_100F(55+count,8);
        count = count+1;
end
pp_recov_strain_130F = zeros(6,1);
count = 0;
for i = 1:6
        pp_recov_strain_130F(i,1) = test_num_data_130F(55+count,8);
        count = count+1;
end
%% Permanent Strain (microstrains)
permanent_strain_14F = zeros(6,1);
count = 0;
for i = 1:6
        permanent_strain_14F(i,1) = test_num_data_14F(55+count,9);
        count = count+1;
end
permanent_strain_40F = zeros(6,1);
count = 0;
for i = 1:6
        permanent_strain_40F(i,1) = test_num_data_40F(55+count,9);
        count = count+1;
end
permanent_strain_70F = zeros(6,1);
count = 0;
for i = 1:6
        permanent_strain_70F(i,1) = test_num_data_70F(55+count,9);
        count = count+1;
end
permanent_strain_100F = zeros(6,1);
count = 0;
for i = 1:6
        permanent_strain_100F(i,1) = test_num_data_100F(55+count,9);
        count = count+1;
end
permanent_strain_130F = zeros(6,1);
count = 0;
for i = 1:6
        permanent_strain_130F(i,1) = test_num_data_130F(55+count,9);
        count = count+1;
end
%% Strain Standard Error (%)
dyn_mod_SE_14F = zeros(6,1);
count = 0;
for i = 1:6
        dyn_mod_SE_14F(i,1) = test_num_data_14F(55+count,10);
        count = count+1;
end
dyn_mod_SE_40F = zeros(6,1);
count = 0;
for i = 1:6
        dyn_mod_SE_40F(i,1) = test_num_data_40F(55+count,10);
        count = count+1;
end
dyn_mod_SE_70F = zeros(6,1);
count = 0;
for i = 1:6
        dyn_mod_SE_70F(i,1) = test_num_data_70F(55+count,10);
        count = count+1;
end
```

```
dyn_mod_SE_100F = zeros(6,1);
count = 0;
for i = 1:6
        dyn_mod_SE_100F(i,1) = test_num_data_100F(55+count,10);
        count = count+1;
end
dyn_mod_SE_130F = zeros(6,1);
count = 0;
for i = 1:6
        dyn_mod_SE_130F(i,1) = test_num_data_130F(55+count,10);
        count = count+1;
end
%% Uniformity coefficients for the LVDTs (%)
dyn_mod_UC_14F = zeros(6,1);
count = 0;
for i = 1:6
        dyn_mod_UC_14F(i,1) = test_num_data_14F(55+count,11);
        count = count+1;
end
dyn_mod_UC_40F = zeros(6,1);
count = 0;
for i = 1:6
        dyn_mod_UC_40F(i,1) = test_num_data_40F(55+count,11);
        count = count+1;
end
dyn_mod_UC_70F = zeros(6,1);
count = 0;
for i = 1:6
        dyn_mod_UC_70F(i,1) = test_num_data_70F(55+count,11);
        count = count+1;
end
dyn_mod_UC_100F = zeros(6,1);
count = 0;
for i = 1:6
        dyn_mod_UC_100F(i,1) = test_num_data_100F(55+count,11);
        count = count+1;
end
dyn_mod_UC_130F = zeros(6,1);
count = 0;
for i = 1:6
        dyn_mod_UC_130F(i,1) = test_num_data_130F(55+count,11);
        count = count+1;
end
%% Making column of 30 test data point for each parameter
temperature_C = [temperature_C_14F; temperature_C_40F; temperature_C_70F;...
    temperature_C_100F; temperature_C_130F];
temperature_F = [temperature_F_14F; temperature_F_40F; temperature_F_70F;...
    temperature_F_100F; temperature_F_130F];
frequency_hz = [frequency_14F; frequency_40F; frequency_70F;...
    frequency_100F; frequency_130F];
stress_amp_kpa = [stress_amp_14F; stress_amp_40F; stress_amp_70F; ...
    stress_amp_100F; stress_amp_130F];
stress_amp_psi = [stress_amp_neg_10C; stress_amp_4C; stress_amp_21C; ...
    stress_amp_37C; stress_amp_54C];
stress_std_err_percent = [stress_std_err_14F; stress_std_err_40F; ...
    stress_std_err_70F; stress_std_err_100F; stress_std_err_130F];
dyn_mod_mpa = [dyn_mod_14F; dyn_mod_40F; dyn_mod_70F; dyn_mod_100F;...
    dyn_mod_130F];
dyn_mod_ksi = [dyn_mod_neg_10C; dyn_mod_4C; dyn_mod_21C; dyn_mod_37C;...
    dyn_mod_54C];
phase_angle_deg = [phase_angle_14F; phase_angle_40F; phase_angle_70F; ...
    phase_angle_100F; phase_angle_130F];
UC_phase_angle_deg = [UC_phase_angle_14F; UC_phase_angle_40F; ...
    UC_phase_angle_70F; UC_phase_angle_100F; UC_phase_angle_130F];
pp_recov_strain = [pp_recov_strain_14F; pp_recov_strain_40F; ...
    pp_recov_strain_70F; pp_recov_strain_100F; pp_recov_strain_130F];
permanent_strain = [permanent_strain_14F; permanent_strain_40F;...
    permanent_strain_70F; permanent_strain_100F; permanent_strain_130F];
dyn_mod_SE_percent = [dyn_mod_SE_14F; dyn_mod_SE_40F; dyn_mod_SE_70F; ...
    dyn_mod_SE_100F; dyn_mod_SE_130F];
dyn_mod_UC_percent = [dyn_mod_UC_14F; dyn_mod_UC_40F; dyn_mod_UC_70F; ...
```

```
    dyn_mod_UC_100F; dyn_mod_UC_130F];
%% Summary Table
test_summary_SI = [temperature_C frequency_hz stress_amp_kpa ...
    stress_std_err_percent dyn_mod_mpa phase_angle_deg UC_phase_angle_deg ...
    pp_recov_strain permanent_strain dyn_mod_SE_percent dyn_mod_UC_percent];
test_summary_E = [temperature_F frequency_hz stress_amp_psi ...
    stress_std_err_percent dyn_mod_ksi phase_angle_deg UC_phase_angle_deg ...
    pp_recov_strain permanent_strain dyn_mod_SE_percent dyn_mod_UC_percent];
%% Export data to a text file
fid1 = fopen('dm_test_data_specimen_SI.txt', 'w');
fprintf(fid1, '%f %f %f %f %f %f %f %f %f %f %f\n', test_summary_SI');
fclose(fid1);
fid2 = fopen('dm_test_data_specimen_E.txt', 'w');
fprintf(fid2, '%f %f %f %f %f %f %f %f %f %f %f\n', test_summary_E');
fclose(fid2);
%% Plot tested data in x-y space in SI unit system
% dynamic modulus versus frequency plot
raw_dm_test_data_plots_SI = figure('Name','Test Data Plots (SI)');
subplot(2,2,1);
hold on;
grid on;
title('log |E*| versus log frequency plot (Isothermal Curves)');
xlabel('log (f), Hz');
ylabel('log (|E*|), MPa');
plot(log10(frequency_14F),log10(dyn_mod_14F),'-or','LineWidth',2,...
                        'MarkerEdgeColor','r',...
                        'MarkerFaceColor','r',...
                        'MarkerSize',8);
plot(log10(frequency_40F),log10(dyn_mod_40F),'-xg','LineWidth',2,...
                        'MarkerEdgeColor','g',...
                        'MarkerFaceColor','g',...
                        'MarkerSize',8);
plot(log10(frequency_70F),log10(dyn_mod_70F),'-+b','LineWidth',2,...
                        'MarkerEdgeColor','b',...
                        'MarkerFaceColor','b',...
                        'MarkerSize',8);
plot(log10(frequency_100F),log10(dyn_mod_100F),'-*m','LineWidth',2,...
                        'MarkerEdgeColor','m',...
                        'MarkerFaceColor','m',...
                        'MarkerSize',8);

plot(log10(frequency_130F),log10(dyn_mod_130F),'-sk','LineWidth',2,...
                        'MarkerEdgeColor','k',...
                        'MarkerFaceColor','k',...
                        'MarkerSize',8);
legend('-10 C','4.4 C','21.1 C','37.8 C','54.4 C','Location','Best')
hold off;
% Isochronal Plot
subplot(2,2,2);
temp_25 = zeros(1,5);
DM_25 = zeros(1,5);
phase_angle_25 = zeros(1,5);
count = 0;
for j = 1:30
    if frequency_hz(j,1) == 25
        temp_25(1+count) = temperature_C(j,1);
        DM_25(1+count) = dyn_mod_mpa(j,1);
        phase_angle_25(1+count) = phase_angle_deg(j,1);
        count = count+1;
    end
end
semilogy(temp_25,DM_25,'-or','LineWidth',2,...
                        'MarkerEdgeColor','r',...
                        'MarkerFaceColor','r',...
                        'MarkerSize',8);
hold on;
temp_10 = zeros(1,5);
DM_10 = zeros(1,5);
phase_angle_10 = zeros(1,5);
count = 0;
for j = 1:30
```

```
    if frequency_hz(j,1) == 10
        temp_10(1+count) = temperature_C(j,1);
        DM_10(1+count) = dyn_mod_mpa(j,1);
        phase_angle_10(1+count) = phase_angle_deg(j,1);
        count = count+1;
    end
end
semilogy(temp_10,DM_10,'-xg','LineWidth',2,...
                       'MarkerEdgeColor','g',...
                       'MarkerFaceColor','g',...
                       'MarkerSize',8);
temp_5 = zeros(1,5);
DM_5 = zeros(1,5);
phase_angle_5 = zeros(1,5);
count = 0;
for j = 1:30
    if frequency_hz(j,1) == 5
        temp_5(1+count) = temperature_C(j,1);
        DM_5(1+count) = dyn_mod_mpa(j,1);
        phase_angle_5(1+count) = phase_angle_deg(j,1);
        count = count+1;
    end
end
semilogy(temp_5,DM_5,'-+b','LineWidth',2,...
                       'MarkerEdgeColor','b',...
                       'MarkerFaceColor','b',...
                       'MarkerSize',8);
temp_1 = zeros(1,5);
DM_1 = zeros(1,5);
phase_angle_1 = zeros(1,5);
count = 0;
for j = 1:30
    if frequency_hz(j,1) == 1
        temp_1(1+count) = temperature_C(j,1);
        DM_1(1+count) = dyn_mod_mpa(j,1);
        phase_angle_1(1+count) = phase_angle_deg(j,1);
        count = count+1;
    end
end
semilogy(temp_1,DM_1,'-*m','LineWidth',2,...
                       'MarkerEdgeColor','m',...
                       'MarkerFaceColor','m',...
                       'MarkerSize',8);
temp_half = zeros(1,5);
DM_half = zeros(1,5);
phase_angle_half = zeros(1,5);
count = 0;
for j = 1:30
    if frequency_hz(j,1) == 0.5
        temp_half(1+count) = temperature_C(j,1);
        DM_half(1+count) = dyn_mod_mpa(j,1);
        phase_angle_half(1+count) = phase_angle_deg(j,1);
        count = count+1;
    end
end
semilogy(temp_half,DM_half,'-sk','LineWidth',2,...
                       'MarkerEdgeColor','k',...
                       'MarkerFaceColor','k',...
                       'MarkerSize',8);
temp_tenth = zeros(1,5);
DM_tenth = zeros(1,5);
phase_angle_tenth = zeros(1,5);
count = 0;
for j = 1:30
    if frequency_hz(j,1) == 0.1
        temp_tenth(1+count) = temperature_C(j,1);
        DM_tenth(1+count) = dyn_mod_mpa(j,1);
        phase_angle_tenth(1+count) = phase_angle_deg(j,1);
        count = count+1;
    end
end
```

```
semilogy(temp_tenth,DM_tenth,'-^c','LineWidth',2,...
                        'MarkerEdgeColor','c',...
                        'MarkerFaceColor','c',...
                        'MarkerSize',8);
grid on;
title('|E*| versus temperature plot (Isochronal Curves)');
xlabel('Temperature, C');
ylabel('|E*|, MPa');
legend('25 Hz','10 Hz','5 Hz','1 Hz','0.5 Hz','0.1 Hz','Location','Best')
hold off;
%Complex Plane plot
subplot(2,2,3);
hold on;
grid on;
title('Complex Plane Plot');
xlabel('|E*|cos(\phi), MPa');
ylabel('|E*|sin(\phi), MPa');
E_cos_phi_14 = zeros(1,6);
E_sin_phi_14 = zeros(1,6);
count = 0;
for j = 1:30
    if temperature_C(j,1) == -10
        E_cos_phi_14(1+count) = dyn_mod_mpa(j,1)*cosd(phase_angle_deg(j,1));
        E_sin_phi_14(1+count) = dyn_mod_mpa(j,1)*sind(phase_angle_deg(j,1));
        count = count+1;
    end
end
plot(E_cos_phi_14,E_sin_phi_14,'or','LineWidth',2,...
                        'MarkerEdgeColor','r',...
                        'MarkerFaceColor','r',...
                        'MarkerSize',8);
E_cos_phi_40 = zeros(1,6);
E_sin_phi_40 = zeros(1,6);
count = 0;
for j = 1:30
    if temperature_C(j,1) == 4.4
        E_cos_phi_40(1+count) = dyn_mod_mpa(j,1)*cosd(phase_angle_deg(j,1));
        E_sin_phi_40(1+count) = dyn_mod_mpa(j,1)*sind(phase_angle_deg(j,1));
        count = count+1;
    end
end
plot(E_cos_phi_40,E_sin_phi_40,'xg','LineWidth',2,...
                        'MarkerEdgeColor','g',...
                        'MarkerFaceColor','g',...
                        'MarkerSize',8);
E_cos_phi_70 = zeros(1,6);
E_sin_phi_70 = zeros(1,6);
count = 0;
for j = 1:30
    if temperature_C(j,1) == 21.1
        E_cos_phi_70(1+count) = dyn_mod_mpa(j,1)*cosd(phase_angle_deg(j,1));
        E_sin_phi_70(1+count) = dyn_mod_mpa(j,1)*sind(phase_angle_deg(j,1));
        count = count+1;
    end
end
plot(E_cos_phi_70,E_sin_phi_70,'+b','LineWidth',2,...
                        'MarkerEdgeColor','b',...
                        'MarkerFaceColor','b',...
                        'MarkerSize',8);
E_cos_phi_100 = zeros(1,6);
E_sin_phi_100 = zeros(1,6);
count = 0;
for j = 1:30
    if temperature_C(j,1) == 37.8
        E_cos_phi_100(1+count) = dyn_mod_mpa(j,1)*cosd(phase_angle_deg(j,1));
        E_sin_phi_100(1+count) = dyn_mod_mpa(j,1)*sind(phase_angle_deg(j,1));
        count = count+1;
    end
end
plot(E_cos_phi_100,E_sin_phi_100,'*m','LineWidth',2,...
                        'MarkerEdgeColor','m',...
```

```
                        'MarkerFaceColor','m',...
                        'MarkerSize',8);
E_cos_phi_130 = zeros(1,6);
E_sin_phi_130 = zeros(1,6);
count = 0;
for j = 1:30
    if temperature_C(j,1) == 54.4
        E_cos_phi_130(1+count) = dyn_mod_mpa(j,1)*cosd(phase_angle_deg(j,1));
        E_sin_phi_130(1+count) = dyn_mod_mpa(j,1)*sind(phase_angle_deg(j,1));
        count = count+1;
    end
end
plot(E_cos_phi_130, E_sin_phi_130,'sk','LineWidth',2,...
                        'MarkerEdgeColor','k',...
                        'MarkerFaceColor','k',...
                        'MarkerSize',8);
legend('-10 C','4.4 C','21.1 C','37.8 C','54.4 C','Location','Best')
hold off;
% Black Space Plot
subplot(2,2,4);
hold on;
grid on;
title('Phase angle versus log|E*| plot (Black Space Plot)');
xlabel('log|E*|, MPa');
ylabel('Phase angle, Degrees');
plot(log10(dyn_mod_14F), phase_angle_14F,'or','LineWidth',2,...
                        'MarkerEdgeColor','r',...
                        'MarkerFaceColor','r',...
                        'MarkerSize',8);
plot(log10(dyn_mod_40F), phase_angle_40F,'xg','LineWidth',2,...
                        'MarkerEdgeColor','g',...
                        'MarkerFaceColor','g',...
                        'MarkerSize',8);
plot(log10(dyn_mod_70F), phase_angle_70F,'+b','LineWidth',2,...
                        'MarkerEdgeColor','b',...
                        'MarkerFaceColor','b',...
                        'MarkerSize',8);
plot(log10(dyn_mod_100F), phase_angle_100F,'*m','LineWidth',2,...
                        'MarkerEdgeColor','m',...
                        'MarkerFaceColor','m',...
                        'MarkerSize',8);
plot(log10(dyn_mod_130F), phase_angle_130F,'sk','LineWidth',2,...
                        'MarkerEdgeColor','k',...
                        'MarkerFaceColor','k',...
                        'MarkerSize',8);
legend('-10 C','4.4 C','21.1 C','37.8 C','54.4 C','Location','Best')
hold off;
hold off;
%% Plot tested data in x-y space in English unit system
% dynamic modulus versus frequency plot
raw_dm_test_data_plots_E = figure('Name','Test Data Plots (E)');
subplot(2,2,1);
hold on;
grid on;
title('log |E*| versus log frequency plot (Isothermal Curves)');
xlabel('log (f), Hz');
ylabel('log (|E*|), ksi');
plot(log10(frequency_14F),log10(dyn_mod_neg_10C),'-or','LineWidth',2,...
                        'MarkerEdgeColor','r',...
                        'MarkerFaceColor','r',...
                        'MarkerSize',8);
plot(log10(frequency_40F),log10(dyn_mod_4C),'-xg','LineWidth',2,...
                        'MarkerEdgeColor','g',...
                        'MarkerFaceColor','g',...
                        'MarkerSize',8);
plot(log10(frequency_70F),log10(dyn_mod_21C),'-+b','LineWidth',2,...
                        'MarkerEdgeColor','b',...
                        'MarkerFaceColor','b',...
                        'MarkerSize',8);
plot(log10(frequency_100F),log10(dyn_mod_37C),'-*m','LineWidth',2,...
                        'MarkerEdgeColor','m',...
```

```
                        'MarkerFaceColor','m',...
                        'MarkerSize',8);

plot(log10(frequency_130F),log10(dyn_mod_54C),'-sk','LineWidth',2,...
                        'MarkerEdgeColor','k',...
                        'MarkerFaceColor','k',...
                        'MarkerSize',8);
legend('14 F','40 F','70 F','100 F','130 F','Location','Best')
hold off;
% Isochronal Plot
subplot(2,2,2);
temp_25 = zeros(1,5);
DM_25 = zeros(1,5);
phase_angle_25 = zeros(1,5);
count = 0;
for j = 1:30
    if frequency_hz(j,1) == 25
        temp_25(1+count) = temperature_F(j,1);
        DM_25(1+count) = dyn_mod_ksi(j,1);
        phase_angle_25(1+count) = phase_angle_deg(j,1);
        count = count+1;
    end
end
semilogy(temp_25,DM_25,'-or','LineWidth',2,...
                        'MarkerEdgeColor','r',...
                        'MarkerFaceColor','r',...
                        'MarkerSize',8);
hold on;
temp_10 = zeros(1,5);
DM_10 = zeros(1,5);
phase_angle_10 = zeros(1,5);
count = 0;
for j = 1:30
    if frequency_hz(j,1) == 10
        temp_10(1+count) = temperature_F(j,1);
        DM_10(1+count) = dyn_mod_ksi(j,1);
        phase_angle_10(1+count) = phase_angle_deg(j,1);
        count = count+1;
    end
end
semilogy(temp_10,DM_10,'-xg','LineWidth',2,...
                        'MarkerEdgeColor','g',...
                        'MarkerFaceColor','g',...
                        'MarkerSize',8);
temp_5 = zeros(1,5);
DM_5 = zeros(1,5);
phase_angle_5 = zeros(1,5);
count = 0;
for j = 1:30
    if frequency_hz(j,1) == 5
        temp_5(1+count) = temperature_F(j,1);
        DM_5(1+count) = dyn_mod_ksi(j,1);
        phase_angle_5(1+count) = phase_angle_deg(j,1);
        count = count+1;
    end
end
semilogy(temp_5,DM_5,'-+b','LineWidth',2,...
                        'MarkerEdgeColor','b',...
                        'MarkerFaceColor','b',...
                        'MarkerSize',8);
temp_1 = zeros(1,5);
DM_1 = zeros(1,5);
phase_angle_1 = zeros(1,5);
count = 0;
for j = 1:30
    if frequency_hz(j,1) == 1
        temp_1(1+count) = temperature_F(j,1);
        DM_1(1+count) = dyn_mod_ksi(j,1);
        phase_angle_1(1+count) = phase_angle_deg(j,1);
        count = count+1;
    end
```

```
end
semilogy(temp_1,DM_1,'-*m','LineWidth',2,...
                        'MarkerEdgeColor','m',...
                        'MarkerFaceColor','m',...
                        'MarkerSize',8);
temp_half = zeros(1,5);
DM_half = zeros(1,5);
phase_angle_half = zeros(1,5);
count = 0;
for j = 1:30
    if frequency_hz(j,1) == 0.5
        temp_half(1+count) = temperature_F(j,1);
        DM_half(1+count) = dyn_mod_ksi(j,1);
        phase_angle_half(1+count) = phase_angle_deg(j,1);
        count = count+1;
    end
end
semilogy(temp_half,DM_half,'-sk','LineWidth',2,...
                        'MarkerEdgeColor','k',...
                        'MarkerFaceColor','k',...
                        'MarkerSize',8);
temp_tenth = zeros(1,5);
DM_tenth = zeros(1,5);
phase_angle_tenth = zeros(1,5);
count = 0;
for j = 1:30
    if frequency_hz(j,1) == 0.1
        temp_tenth(1+count) = temperature_F(j,1);
        DM_tenth(1+count) = dyn_mod_ksi(j,1);
        phase_angle_tenth(1+count) = phase_angle_deg(j,1);
        count = count+1;
    end
end
semilogy(temp_tenth,DM_tenth,'-^c','LineWidth',2,...
                        'MarkerEdgeColor','c',...
                        'MarkerFaceColor','c',...
                        'MarkerSize',8);
grid on;
title('|E*| versus temperature plot (Isochronal Curves)');
xlabel('Temperature, F');
ylabel('|E*|, ksi');
legend('25 Hz','10 Hz','5 Hz','1 Hz','0.5 Hz','0.1 Hz','Location','Best')
hold off;
%Complex Plane plot
subplot(2,2,3);
hold on;
grid on;
title('Complex Plane Plot');
xlabel('|E*|cos(\phi), ksi');
ylabel('|E*|sin(\phi), ksi');
E_cos_phi_14 = zeros(1,6);
E_sin_phi_14 = zeros(1,6);
count = 0;
for j = 1:30
    if temperature_F(j,1) == 14
        E_cos_phi_14(1+count) = dyn_mod_ksi(j,1)*cosd(phase_angle_deg(j,1));
        E_sin_phi_14(1+count) = dyn_mod_ksi(j,1)*sind(phase_angle_deg(j,1));
        count = count+1;
    end
end
plot(E_cos_phi_14,E_sin_phi_14,'or','LineWidth',2,...
                        'MarkerEdgeColor','r',...
                        'MarkerFaceColor','r',...
                        'MarkerSize',8);
E_cos_phi_40 = zeros(1,6);
E_sin_phi_40 = zeros(1,6);
count = 0;
for j = 1:30
    if temperature_F(j,1) == 40
        E_cos_phi_40(1+count) = dyn_mod_ksi(j,1)*cosd(phase_angle_deg(j,1));
        E_sin_phi_40(1+count) = dyn_mod_ksi(j,1)*sind(phase_angle_deg(j,1));
```

```
        count = count+1;
    end
end
plot(E_cos_phi_40,E_sin_phi_40,'xg','LineWidth',2,...
                        'MarkerEdgeColor','g',...
                        'MarkerFaceColor','g',...
                        'MarkerSize',8);
E_cos_phi_70 = zeros(1,6);
E_sin_phi_70 = zeros(1,6);
count = 0;
for j = 1:30
    if temperature_F(j,1) == 70
        E_cos_phi_70(1+count) = dyn_mod_ksi(j,1)*cosd(phase_angle_deg(j,1));
        E_sin_phi_70(1+count) = dyn_mod_ksi(j,1)*sind(phase_angle_deg(j,1));
        count = count+1;
    end
end
plot(E_cos_phi_70,E_sin_phi_70,'+b','LineWidth',2,...
                        'MarkerEdgeColor','b',...
                        'MarkerFaceColor','b',...
                        'MarkerSize',8);
E_cos_phi_100 = zeros(1,6);
E_sin_phi_100 = zeros(1,6);
count = 0;
for j = 1:30
    if temperature_F(j,1) == 100
        E_cos_phi_100(1+count) = dyn_mod_ksi(j,1)*cosd(phase_angle_deg(j,1));
        E_sin_phi_100(1+count) = dyn_mod_ksi(j,1)*sind(phase_angle_deg(j,1));
        count = count+1;
    end
end
plot(E_cos_phi_100,E_sin_phi_100,'*m','LineWidth',2,...
                        'MarkerEdgeColor','m',...
                        'MarkerFaceColor','m',...
                        'MarkerSize',8);
E_cos_phi_130 = zeros(1,6);
E_sin_phi_130 = zeros(1,6);
count = 0;
for j = 1:30
    if temperature_F(j,1) == 130
        E_cos_phi_130(1+count) = dyn_mod_ksi(j,1)*cosd(phase_angle_deg(j,1));
        E_sin_phi_130(1+count) = dyn_mod_ksi(j,1)*sind(phase_angle_deg(j,1));
        count = count+1;
    end
end
plot(E_cos_phi_130, E_sin_phi_130,'sk','LineWidth',2,...
                        'MarkerEdgeColor','k',...
                        'MarkerFaceColor','k',...
                        'MarkerSize',8);
legend('14 F','40 F','70 F','100 F','130 F','Location','Best')
hold off;
% Black Space Plot
subplot(2,2,4);
hold on;
grid on;
title('Phase angle versus log|E*| plot (Black Space Plot)');
xlabel('log|E*|, ksi');
ylabel('Phase angle, Degrees');
plot(log10(dyn_mod_neg_10C), phase_angle_14F,'or','LineWidth',2,...
                        'MarkerEdgeColor','r',...
                        'MarkerFaceColor','r',...
                        'MarkerSize',8);
plot(log10(dyn_mod_4C), phase_angle_40F,'xg','LineWidth',2,...
                        'MarkerEdgeColor','g',...
                        'MarkerFaceColor','g',...
                        'MarkerSize',8);
plot(log10(dyn_mod_21C), phase_angle_70F,'+b','LineWidth',2,...
                        'MarkerEdgeColor','b',...
                        'MarkerFaceColor','b',...
                        'MarkerSize',8);
plot(log10(dyn_mod_37C), phase_angle_100F,'*m','LineWidth',2,...
```

```
                        'MarkerEdgeColor','m',...
                        'MarkerFaceColor','m',...
                        'MarkerSize',8);
plot(log10(dyn_mod_54C), phase_angle_130F,'sk','LineWidth',2,...
                        'MarkerEdgeColor','k',...
                        'MarkerFaceColor','k',...
                        'MarkerSize',8);
legend('14 F','40 F','70 F','100 F','130 F','Location','Best')
hold off;
hold off;
%EOP
```

Code G-2: MATLAB® Code for Generating Test Data Summary Table from the Test Results of Replicate Test Specimens

```
%% English (E) Unit System
%% Load Data from file
clear;
close all;
clc;
specimen1_E ='F:\10. QUARTERLY REPORTS AND REFERENCES\1. FINAL REPORT\DYNAMIC MODULUS TEST
DATA\1. D1 SP4 PG76-22 70-22 WMA 35%RAP\Sample 1 AV6.0\dm_test_data_specimen_E.txt';
specimen2_E ='F:\10. QUARTERLY REPORTS AND REFERENCES\1. FINAL REPORT\DYNAMIC MODULUS TEST
DATA\1. D1 SP4 PG76-22 70-22 WMA 35%RAP\Sample 2 AV6.0\dm_test_data_specimen_E.txt';
specimen3_E ='F:\10. QUARTERLY REPORTS AND REFERENCES\1. FINAL REPORT\DYNAMIC MODULUS TEST
DATA\1. D1 SP4 PG76-22 70-22 WMA 35%RAP\Sample 3 AV5.9\dm_test_data_specimen_E.txt';
test_data_specimen_1 = importdata(specimen1_E);
test_data_specimen_2 = importdata(specimen2_E);
test_data_specimen_3 = importdata(specimen3_E);
%% Summary Table Generation
avg_dyn_mod_ksi = (1/3)*(test_data_specimen_1(:,5)+ ...
    test_data_specimen_2(:,5)+ test_data_specimen_3(:,5));
avg_phase_angle_deg = (1/3)*(test_data_specimen_1(:,6)+ ...
    test_data_specimen_2(:,6)+ test_data_specimen_3(:,6));
CV_dyn_mod = zeros(length(test_data_specimen_1),1);
std_dyn_mod = zeros(length(test_data_specimen_1),1);
std_phase_angle = zeros(length(test_data_specimen_1),1);
for i = 1: length(test_data_specimen_1)
    std_dyn_mod (i,1) = std([test_data_specimen_1(i,5) ...
        test_data_specimen_2(i,5) test_data_specimen_3(i,5)]);
    CV_dyn_mod (i,1) = 100*(std_dyn_mod(i,1)/avg_dyn_mod_ksi(i,1));
    std_phase_angle (i,1) = std([test_data_specimen_1(i,6) ...
        test_data_specimen_2(i,6) test_data_specimen_3(i,6)]);
end
summary_table_of_all_specimens = [test_data_specimen_1(:,1) ...
    test_data_specimen_1(:,2) test_data_specimen_1(:,5) ...
    test_data_specimen_1(:,6) test_data_specimen_2(:,5) ...
    test_data_specimen_2(:,6) test_data_specimen_3(:,5) ...
    test_data_specimen_3(:,6) avg_dyn_mod_ksi CV_dyn_mod ...
    avg_phase_angle_deg std_phase_angle];
%% Export data to an external text file
fid1 = fopen('dm_test_summary_table_for_all_specimens_E.txt', 'w');
fid2 = fopen('dm_test_summary_table_for_all_specimens_E.csv', 'w');
fprintf(fid1, '%f %f %f %f %f %f %f %f %f %f %f %f\n', summary_table_of_all_specimens');
fprintf(fid2, '%f %f %f %f %f %f %f %f %f %f %f %f\n', summary_table_of_all_specimens');
fclose(fid1);
fclose(fid2);
%% Temperature
temperature_14F = zeros(6,1);
count = 1;
for i = 1:6
        temperature_14F(i,1) = summary_table_of_all_specimens(count,1);
        count = count+1;
end
temperature_40F = zeros(6,1);
for i = 1:6
        temperature_40F(i,1) = summary_table_of_all_specimens(count,1);
        count = count+1;
end
temperature_70F = zeros(6,1);
```

```
for i = 1:6
        temperature_70F(i,1) = summary_table_of_all_specimens(count,1);
        count = count+1;
end
temperature_100F = zeros(6,1);
for i = 1:6
        temperature_100F(i,1) = summary_table_of_all_specimens(count,1);
        count = count+1;
end
temperature_130F = zeros(6,1);
for i = 1:6
        temperature_130F(i,1) = summary_table_of_all_specimens(count,1);
        count = count+1;
end
%% Frequency
frequency_14F = zeros(6,1);
count = 1;
for i = 1:6
        frequency_14F(i,1) = summary_table_of_all_specimens(count,2);
        count = count+1;
end
frequency_40F = zeros(6,1);
for i = 1:6
        frequency_40F(i,1) = summary_table_of_all_specimens(count,2);
        count = count+1;
end
frequency_70F = zeros(6,1);
for i = 1:6
        frequency_70F(i,1) = summary_table_of_all_specimens(count,2);
        count = count+1;
end
frequency_100F = zeros(6,1);
for i = 1:6
        frequency_100F(i,1) = summary_table_of_all_specimens(count,2);
        count = count+1;
end
frequency_130F = zeros(6,1);
for i = 1:6
        frequency_130F(i,1) = summary_table_of_all_specimens(count,2);
        count = count+1;
end
%% Dynamic Modulus - Average
dyn_mod_14F = zeros(6,1);
count = 1;
for i = 1:6
        dyn_mod_14F(i,1) = summary_table_of_all_specimens(count,9);
        count = count+1;
end
dyn_mod_40F = zeros(6,1);
for i = 1:6
        dyn_mod_40F(i,1) = summary_table_of_all_specimens(count,9);
        count = count+1;
end
dyn_mod_70F = zeros(6,1);
for i = 1:6
        dyn_mod_70F(i,1) = summary_table_of_all_specimens(count,9);
        count = count+1;
end
dyn_mod_100F = zeros(6,1);
for i = 1:6
        dyn_mod_100F(i,1) = summary_table_of_all_specimens(count,9);
        count = count+1;
end
dyn_mod_130F = zeros(6,1);
for i = 1:6
        dyn_mod_130F(i,1) = summary_table_of_all_specimens(count,9);
        count = count+1;
end
%% Average Phase Angle
phase_angle_14F = zeros(6,1);
count = 1;
```

```
for i = 1:6
        phase_angle_14F(i,1) = summary_table_of_all_specimens(count,11);
        count = count+1;
end
phase_angle_40F = zeros(6,1);
for i = 1:6
        phase_angle_40F(i,1) = summary_table_of_all_specimens(count,11);
        count = count+1;
end
phase_angle_70F = zeros(6,1);
for i = 1:6
        phase_angle_70F(i,1) = summary_table_of_all_specimens(count,11);
        count = count+1;
end
phase_angle_100F = zeros(6,1);
for i = 1:6
        phase_angle_100F(i,1) = summary_table_of_all_specimens(count,11);
        count = count+1;
end
phase_angle_130F = zeros(6,1);
for i = 1:6
        phase_angle_130F(i,1) = summary_table_of_all_specimens(count,11);
        count = count+1;
end
%% Plot tested data in x-y space
% dynamic modulus versus frequency plot
avg_data_plots = figure('Name','Average Data Plots (English Unit System)');
H1 =  subplot(2,2,1);
hold on;
grid on;
title('Logarithm of average |E*| versus log frequency plot (Isothermal Curves)');
xlabel('log (f), Hz');
ylabel('log (average |E*|), ksi');
plot(log10(frequency_14F),log10(dyn_mod_14F),...
    '-or','LineWidth',2,'MarkerEdgeColor','r',...
                        'MarkerFaceColor','r',...
                        'MarkerSize',8);
plot(log10(frequency_40F),log10(dyn_mod_40F),'-xg','LineWidth',2,...
                        'MarkerEdgeColor','g',...
                        'MarkerFaceColor','g',...
                        'MarkerSize',8);
plot(log10(frequency_70F),log10(dyn_mod_70F),'-+b','LineWidth',2,...
                        'MarkerEdgeColor','b',...
                        'MarkerFaceColor','b',...
                        'MarkerSize',8);
plot(log10(frequency_100F),log10(dyn_mod_100F),'-*m','LineWidth',2,...
                        'MarkerEdgeColor','m',...
                        'MarkerFaceColor','m',...
                        'MarkerSize',8);

plot(log10(frequency_130F),log10(dyn_mod_130F),'-sk','LineWidth',2,...
                        'MarkerEdgeColor','k',...
                        'MarkerFaceColor','k',...
                        'MarkerSize',8);
legend('14 F','40 F','70 F','100 F','130 F','Location','Best')
hold off;
% Isochronal Plot
H2 =  subplot(2,2,2);
temp_25 = zeros(5,1);
DM_25 = zeros(5,1);
phase_angle_25 = zeros(5,1);
count = 0;
for j = 1:30
    if summary_table_of_all_specimens(j,2) == 25
        temp_25(1+count) = summary_table_of_all_specimens(j,1);
        DM_25(1+count) = summary_table_of_all_specimens(j,9);
        phase_angle_25(1+count) = summary_table_of_all_specimens(j,11);
        count = count+1;
    end
end
semilogy(temp_25,DM_25,'-or','LineWidth',2,...
```

```
                        'MarkerEdgeColor','r',...
                        'MarkerFaceColor','r',...
                        'MarkerSize',8);
hold on;
temp_10 = zeros(5,1);
DM_10 = zeros(5,1);
phase_angle_10 = zeros(5,1);
count = 0;
for j = 1:30
    if summary_table_of_all_specimens(j,2) == 10
        temp_10(1+count) = summary_table_of_all_specimens(j,1);
        DM_10(1+count) = summary_table_of_all_specimens(j,9);
        phase_angle_10(1+count) = summary_table_of_all_specimens(j,11);
        count = count+1;
    end
end
semilogy(temp_10,DM_10,'-xg','LineWidth',2,...
                        'MarkerEdgeColor','g',...
                        'MarkerFaceColor','g',...
                        'MarkerSize',8);
temp_5 = zeros(5,1);
DM_5 = zeros(5,1);
phase_angle_5 = zeros(5,1);
count = 0;
for j = 1:30
    if summary_table_of_all_specimens(j,2) == 5
        temp_5(1+count) = summary_table_of_all_specimens(j,1);
        DM_5(1+count) = summary_table_of_all_specimens(j,9);
        phase_angle_5(1+count) = summary_table_of_all_specimens(j,11);
        count = count+1;
    end
end
semilogy(temp_5,DM_5,'-+b','LineWidth',2,...
                        'MarkerEdgeColor','b',...
                        'MarkerFaceColor','b',...
                        'MarkerSize',8);
temp_1 = zeros(5,1);
DM_1 = zeros(5,1);
phase_angle_1 = zeros(5,1);
count = 0;
for j = 1:30
    if summary_table_of_all_specimens(j,2) == 1
        temp_1(1+count) = summary_table_of_all_specimens(j,1);
        DM_1(1+count) = summary_table_of_all_specimens(j,9);
        phase_angle_1(1+count) = summary_table_of_all_specimens(j,11);
        count = count+1;
    end
end
semilogy(temp_1,DM_1,'-*m','LineWidth',2,...
                        'MarkerEdgeColor','m',...
                        'MarkerFaceColor','m',...
                        'MarkerSize',8);
temp_half = zeros(5,1);
DM_half = zeros(5,1);
phase_angle_half = zeros(5,1);
count = 0;
for j = 1:30
    if summary_table_of_all_specimens(j,2) == 0.5
        temp_half(1+count) = summary_table_of_all_specimens(j,1);
        DM_half(1+count) = summary_table_of_all_specimens(j,9);
        phase_angle_half(1+count) = summary_table_of_all_specimens(j,11);
        count = count+1;
    end
end
semilogy(temp_half,DM_half,'-sk','LineWidth',2,...
                        'MarkerEdgeColor','k',...
                        'MarkerFaceColor','k',...
                        'MarkerSize',8);
temp_tenth = zeros(5,1);
DM_tenth = zeros(5,1);
phase_angle_tenth = zeros(5,1);
```

```
count = 0;
for j = 1:30
    if summary_table_of_all_specimens(j,2) == 0.1
        temp_tenth(1+count) = summary_table_of_all_specimens(j,1);
        DM_tenth(1+count) = summary_table_of_all_specimens(j,9);
        phase_angle_tenth(1+count) = summary_table_of_all_specimens(j,11);
        count = count+1;
    end
end
semilogy(temp_tenth,DM_tenth,'-^c','LineWidth',2,...
                        'MarkerEdgeColor','c',...
                        'MarkerFaceColor','c',...
                        'MarkerSize',8);
grid on;
title('Average |E*| versus temperature plot (Isochronal Curves)');
xlabel('Temperature, F');
ylabel('Average |E*|, ksi');
legend('25 Hz','10 Hz','5 Hz','1 Hz','0.5 Hz','0.1 Hz','Location','Best')
hold off;
%Complex Plane plot
H3 =  subplot(2,2,3);
hold on;
grid on;
title('Complex Plane Plot');
xlabel('|E*|cos(\phi), ksi');
ylabel('|E*|sin(\phi), ksi');
E_cos_phi_14 = zeros(6,1);
E_sin_phi_14 = zeros(6,1);
count = 0;
for j = 1:30
    if summary_table_of_all_specimens(j,1) == 14
        E_cos_phi_14(1+count) = summary_table_of_all_specimens(j,9)...
            *cosd(summary_table_of_all_specimens(j,11));
        E_sin_phi_14(1+count) = summary_table_of_all_specimens(j,9)...
            *sind(summary_table_of_all_specimens(j,11));
        count = count+1;
    end
end
plot(E_cos_phi_14,E_sin_phi_14,'or','LineWidth',2,...
                        'MarkerEdgeColor','r',...
                        'MarkerFaceColor','r',...
                        'MarkerSize',8);
E_cos_phi_40 = zeros(6,1);
E_sin_phi_40 = zeros(6,1);
count = 0;
for j = 1:30
    if summary_table_of_all_specimens(j,1) == 40
        E_cos_phi_40(1+count) = summary_table_of_all_specimens(j,9)...
            *cosd(summary_table_of_all_specimens(j,11));
        E_sin_phi_40(1+count) = summary_table_of_all_specimens(j,9)...
            *sind(summary_table_of_all_specimens(j,11));
        count = count+1;
    end
end
plot(E_cos_phi_40,E_sin_phi_40,'xg','LineWidth',2,...
                        'MarkerEdgeColor','g',...
                        'MarkerFaceColor','g',...
                        'MarkerSize',8);
E_cos_phi_70 = zeros(6,1);
E_sin_phi_70 = zeros(6,1);
count = 0;
for j = 1:30
    if summary_table_of_all_specimens(j,1) == 70
        E_cos_phi_70(1+count) = summary_table_of_all_specimens(j,9)...
            *cosd(summary_table_of_all_specimens(j,11));
        E_sin_phi_70(1+count) = summary_table_of_all_specimens(j,9)...
            *sind(summary_table_of_all_specimens(j,11));
        count = count+1;
    end
end
plot(E_cos_phi_70,E_sin_phi_70,'+b','LineWidth',2,...
```

```
                        'MarkerEdgeColor','b',...
                        'MarkerFaceColor','b',...
                        'MarkerSize',8);
E_cos_phi_100 = zeros(6,1);
E_sin_phi_100 = zeros(6,1);
count = 0;
for j = 1:30
    if summary_table_of_all_specimens(j,1) == 100
        E_cos_phi_100(1+count) = summary_table_of_all_specimens(j,9)...
            *cosd(summary_table_of_all_specimens(j,11));
        E_sin_phi_100(1+count) = summary_table_of_all_specimens(j,9)...
            *sind(summary_table_of_all_specimens(j,11));
        count = count+1;
    end
end
plot(E_cos_phi_100,E_sin_phi_100,'*m','LineWidth',2,...
                        'MarkerEdgeColor','m',...
                        'MarkerFaceColor','m',...
                        'MarkerSize',8);
E_cos_phi_130 = zeros(6,1);
E_sin_phi_130 = zeros(6,1);
count = 0;
for j = 1:30
    if summary_table_of_all_specimens(j,1) == 130
        E_cos_phi_130(1+count) = summary_table_of_all_specimens(j,9)...
            *cosd(summary_table_of_all_specimens(j,11));
        E_sin_phi_130(1+count) = summary_table_of_all_specimens(j,9)...
            *sind(summary_table_of_all_specimens(j,11));
        count = count+1;
    end
end
plot(E_cos_phi_130, E_sin_phi_130,'sk','LineWidth',2,...
                        'MarkerEdgeColor','k',...
                        'MarkerFaceColor','k',...
                        'MarkerSize',8);
legend('14 F','40 F','70 F','100 F','130 F','Location','Best')
hold off;
% Black Space Plot
H4 =  subplot(2,2,4);
hold on;
grid on;
title('Phase angle versus log|E*| plot (Black Space Plot)');
xlabel('log|E*|, ksi');
ylabel('Phase angle, Degrees');
plot(log10(dyn_mod_14F), phase_angle_14F,'or','LineWidth',2,...
                        'MarkerEdgeColor','r',...
                        'MarkerFaceColor','r',...
                        'MarkerSize',8);
plot(log10(dyn_mod_40F), phase_angle_40F,'xg','LineWidth',2,...
                        'MarkerEdgeColor','g',...
                        'MarkerFaceColor','g',...
                        'MarkerSize',8);
plot(log10(dyn_mod_70F), phase_angle_70F,'+b','LineWidth',2,...
                        'MarkerEdgeColor','b',...
                        'MarkerFaceColor','b',...
                        'MarkerSize',8);
plot(log10(dyn_mod_100F), phase_angle_100F,'*m','LineWidth',2,...
                        'MarkerEdgeColor','m',...
                        'MarkerFaceColor','m',...
                        'MarkerSize',8);
plot(log10(dyn_mod_130F), phase_angle_130F,'sk','LineWidth',2,...
                        'MarkerEdgeColor','k',...
                        'MarkerFaceColor','k',...
                        'MarkerSize',8);
legend('14 F','40 F','70 F','100 F','130 F','Location','Best')
hold off;
hold off;
%EOP
```

Code G-3: MATLAB® Code for Generating Mastercurves and Shift Factor Functions

```
%% Clear variables, closs all figures and clean command module
clear;
close all;
clc;
%% Input: Iterate shift factor to find best sigmoid shape of the mastercurve
log_shift_factor_14 = 0:0.01:10;
log_shift_factor_40 = 0:0.01:10;
log_shift_factor_70 = 0;
log_shift_factor_100 = 0:-0.01:-10;
log_shift_factor_130 = 0:-0.01:-10;
%% Input: Coeff. of Deter. (R^2) for MC fitting steps (Step 1,2,3, and 4)
% Step 1: considers data at 70 and 100 F
% Step 2: considers data at 40, 70, and 100 F
% Step 3: considers data at 40, 70, 100, and 130 F
% Step 4: considers data at 14, 40, 70, 100, and 130 F
% Please iterate with a lower value of R^2 and go higher
coef_or_determination = [0.9997 0.9995 0.9994 0.9995];
%% Import Data from External txt file generated in average_mix_dm script
avg_test_data = importdata('dm_test_summary_table_for_all_specimens_E.txt');
temperature = avg_test_data(:,1);
frequency = avg_test_data(:,2);
dynamic_modulus = avg_test_data(:,9);
phase_angle = avg_test_data(:,11);
%% Plot tested data in x-y space (to check any error with the data)
figure('Name','Average Data Plots');
hold on;
subplot(2,3,1);
hold on;
grid on;
title('|E*| vs. Frequency Plot (Isothermal Curves)');
xlabel('log (f) (Hz)');
ylabel('log (|E*|) (ksi)');
freq_14 = zeros(6,1);
DM_14 = zeros(6,1);
phase_angle_14 = zeros(6,1);
count = 0;
for j = 1:30
    if temperature(j,1) == 14
        freq_14(1+count) = frequency(j,1);
        DM_14(1+count) = dynamic_modulus(j,1);
        phase_angle_14(1+count) = phase_angle(j,1);
        count = count+1;
    end
end
plot(log10(freq_14),log10(DM_14),'-or','LineWidth',2,...
                        'MarkerEdgeColor','r',...
                        'MarkerFaceColor','r',...
                        'MarkerSize',8);
freq_40 = zeros(6,1);
DM_40 = zeros(6,1);
phase_angle_40 = zeros(6,1);
count = 0;
for j = 1:30
    if temperature(j,1) == 40
        freq_40(1+count) = frequency(j,1);
        DM_40(1+count) = dynamic_modulus(j,1);
        phase_angle_40(1+count) = phase_angle(j,1);
        count = count+1;
    end
end
plot(log10(freq_40),log10(DM_40),'-xg','LineWidth',2,...
                        'MarkerEdgeColor','g',...
                        'MarkerFaceColor','g',...
                        'MarkerSize',8);
freq_70 = zeros(6,1);
DM_70 = zeros(6,1);
phase_angle_70 = zeros(6,1);
count = 0;
```

```
for j = 1:30
    if temperature(j,1) == 70
        freq_70(1+count) = frequency(j,1);
        DM_70(1+count) = dynamic_modulus(j,1);
        phase_angle_70(1+count) = phase_angle(j,1);
        count = count+1;
    end
end
plot(log10(freq_70),log10(DM_70),'-+b','LineWidth',2,...
                        'MarkerEdgeColor','b',...
                        'MarkerFaceColor','b',...
                        'MarkerSize',8);
freq_100 = zeros(6,1);
DM_100 = zeros(6,1);
phase_angle_100 = zeros(6,1);
count = 0;
for j = 1:30
    if temperature(j,1) == 100
        freq_100(1+count) = frequency(j,1);
        DM_100(1+count) = dynamic_modulus(j,1);
        phase_angle_100(1+count) = phase_angle(j,1);
        count = count+1;
    end
end
plot(log10(freq_100),log10(DM_100),'-*m','LineWidth',2,...
                        'MarkerEdgeColor','m',...
                        'MarkerFaceColor','m',...
                        'MarkerSize',8);
freq_130 = zeros(6,1);
DM_130 = zeros(6,1);
phase_angle_130 = zeros(6,1);
count = 0;
for j = 1:30
    if temperature(j,1) == 130
        freq_130(1+count) = frequency(j,1);
        DM_130(1+count) = dynamic_modulus(j,1);
        phase_angle_130(1+count) = phase_angle(j,1);
        count = count+1;
    end
end
plot(log10(freq_130),log10(DM_130),'-sk','LineWidth',2,...
                        'MarkerEdgeColor','k',...
                        'MarkerFaceColor','k',...
                        'MarkerSize',8);
legend('14 F','40 F','70 F','100 F','130 F','Location','best')
hold off;
%% Plot in logarithminc space
subplot(2,3,2);
loglog(freq_14, DM_14,'-or','LineWidth',2,...
                        'MarkerEdgeColor','r',...
                        'MarkerFaceColor','r',...
                        'MarkerSize',8);
hold on;
loglog(freq_40, DM_40,'-xg','LineWidth',2,...
                        'MarkerEdgeColor','g',...
                        'MarkerFaceColor','g',...
                        'MarkerSize',8);
loglog(freq_70, DM_70,'-+b','LineWidth',2,...
                        'MarkerEdgeColor','b',...
                        'MarkerFaceColor','b',...
                        'MarkerSize',8);
loglog(freq_100, DM_100,'-*m','LineWidth',2,...
                        'MarkerEdgeColor','m',...
                        'MarkerFaceColor','m',...
                        'MarkerSize',8);
loglog(freq_130, DM_130,'-sk','LineWidth',2,...
                        'MarkerEdgeColor','k',...
                        'MarkerFaceColor','k',...
                        'MarkerSize',8);
legend('14 F','40 F','70 F','100 F','130 F','Location','best')
grid on;
```

```
title('|E*| vs. Frequency Plot (Isothermal Curves)');
xlabel('Frequency (Hz)');
ylabel('|E*| (ksi)');
hold off;
%% Phase angle plot
subplot(2,3,3);
hold on;
grid on;
title('Phase Angle vs. Frequency Plot');
xlabel('log (f) (Hz)');
ylabel('Phase Angle (Degrees)');
plot(log10(freq_14), phase_angle_14,'--or','LineWidth',2,...
                        'MarkerEdgeColor','r',...
                        'MarkerFaceColor','r',...
                        'MarkerSize',8);
plot(log10(freq_40), phase_angle_40,'--xg','LineWidth',2,...
                        'MarkerEdgeColor','g',...
                        'MarkerFaceColor','g',...
                        'MarkerSize',8);
plot(log10(freq_70), phase_angle_70,'--+b','LineWidth',2,...
                        'MarkerEdgeColor','b',...
                        'MarkerFaceColor','b',...
                        'MarkerSize',8);
plot(log10(freq_100), phase_angle_100,'--*m','LineWidth',2,...
                        'MarkerEdgeColor','m',...
                        'MarkerFaceColor','m',...
                        'MarkerSize',8);
plot(log10(freq_130), phase_angle_130,'--sk','LineWidth',2,...
                        'MarkerEdgeColor','k',...
                        'MarkerFaceColor','k',...
                        'MarkerSize',8);
legend('14 F','40 F','70 F','100 F','130 F','Location','best')
hold off;
%% Isochoronal Curves
subplot(2,3,4);
temp_25 = zeros(5,1);
DM_25 = zeros(5,1);
phase_angle_25 = zeros(5,1);
count = 0;
for j = 1:30
    if frequency(j,1) == 25
        temp_25(1+count) = temperature(j,1);
        DM_25(1+count) = dynamic_modulus(j,1);
        phase_angle_25(1+count) = phase_angle(j,1);
        count = count+1;
    end
end
semilogy(temp_25,DM_25,'-or','LineWidth',2,...
                        'MarkerEdgeColor','r',...
                        'MarkerFaceColor','r',...
                        'MarkerSize',8);
hold on;
temp_10 = zeros(5,1);
DM_10 = zeros(5,1);
phase_angle_10 = zeros(5,1);
count = 0;
for j = 1:30
    if frequency(j,1) == 10
        temp_10(1+count) = temperature(j,1);
        DM_10(1+count) = dynamic_modulus(j,1);
        phase_angle_10(1+count) = phase_angle(j,1);
        count = count+1;
    end
end
semilogy(temp_10,DM_10,'-xg','LineWidth',2,...
                        'MarkerEdgeColor','g',...
                        'MarkerFaceColor','g',...
                        'MarkerSize',8);
temp_5 = zeros(5,1);
DM_5 = zeros(5,1);
phase_angle_5 = zeros(5,1);
```

```
count = 0;
for j = 1:30
    if frequency(j,1) == 5
        temp_5(1+count) = temperature(j,1);
        DM_5(1+count) = dynamic_modulus(j,1);
        phase_angle_5(1+count) = phase_angle(j,1);
        count = count+1;
    end
end
semilogy(temp_5,DM_5,'-+b','LineWidth',2,...
                      'MarkerEdgeColor','b',...
                      'MarkerFaceColor','b',...
                      'MarkerSize',8);
temp_1 = zeros(5,1);
DM_1 = zeros(5,1);
phase_angle_1 = zeros(5,1);
count = 0;
for j = 1:30
    if frequency(j,1) == 1
        temp_1(1+count) = temperature(j,1);
        DM_1(1+count) = dynamic_modulus(j,1);
        phase_angle_1(1+count) = phase_angle(j,1);
        count = count+1;
    end
end
semilogy(temp_1,DM_1,'-*m','LineWidth',2,...
                      'MarkerEdgeColor','m',...
                      'MarkerFaceColor','m',...
                      'MarkerSize',8);
temp_half = zeros(5,1);
DM_half = zeros(5,1);
phase_angle_half = zeros(5,1);
count = 0;
for j = 1:30
    if frequency(j,1) == 0.5
        temp_half(1+count) = temperature(j,1);
        DM_half(1+count) = dynamic_modulus(j,1);
        phase_angle_half(1+count) = phase_angle(j,1);
        count = count+1;
    end
end
semilogy(temp_half,DM_half,'-sk','LineWidth',2,...
                      'MarkerEdgeColor','k',...
                      'MarkerFaceColor','k',...
                      'MarkerSize',8);
temp_tenth = zeros(5,1);
DM_tenth = zeros(5,1);
phase_angle_tenth = zeros(5,1);
count = 0;
for j = 1:30
    if frequency(j,1) == 0.1
        temp_tenth(1+count) = temperature(j,1);
        DM_tenth(1+count) = dynamic_modulus(j,1);
        phase_angle_tenth(1+count) = phase_angle(j,1);
        count = count+1;
    end
end
semilogy(temp_tenth,DM_tenth,'-^c','LineWidth',2,...
                      'MarkerEdgeColor','c',...
                      'MarkerFaceColor','c',...
                      'MarkerSize',8);
grid on;
title('|E*| vs. Temperature Plot (Isochronal Curves');
xlabel('Temperature (F)');
ylabel('|E*| (ksi)');
legend('25 Hz','10 Hz','5 Hz','1 Hz','0.5 Hz','0.1 Hz','Location','best')
hold off;
%% Complex Plane Plot
subplot(2,3,5);
hold on;
grid on;
```

```
title('Complex Plane Plot (Cole-Cole Plane Plot)');
xlabel('|E*|cos(\phi) (ksi)');
ylabel('|E*|sin(\phi) (ksi)');
E_cos_phi_14 = zeros(6,1);
E_sin_phi_14 = zeros(6,1);
count = 0;
for j = 1:30
    if temperature(j,1) == 14
        E_cos_phi_14(1+count) = dynamic_modulus(j,1)*cosd(phase_angle(j,1));
        E_sin_phi_14(1+count) = dynamic_modulus(j,1)*sind(phase_angle(j,1));
        count = count+1;
    end
end
plot(E_cos_phi_14,E_sin_phi_14,'or','LineWidth',2,...
                        'MarkerEdgeColor','r',...
                        'MarkerFaceColor','r',...
                        'MarkerSize',8);
E_cos_phi_40 = zeros(6,1);
E_sin_phi_40 = zeros(6,1);
count = 0;
for j = 1:30
    if temperature(j,1) == 40
        E_cos_phi_40(1+count) = dynamic_modulus(j,1)*cosd(phase_angle(j,1));
        E_sin_phi_40(1+count) = dynamic_modulus(j,1)*sind(phase_angle(j,1));
        count = count+1;
    end
end
plot(E_cos_phi_40,E_sin_phi_40,'xg','LineWidth',2,...
                        'MarkerEdgeColor','g',...
                        'MarkerFaceColor','g',...
                        'MarkerSize',8);
E_cos_phi_70 = zeros(6,1);
E_sin_phi_70 = zeros(6,1);
count = 0;
for j = 1:30
    if temperature(j,1) == 70
        E_cos_phi_70(1+count) = dynamic_modulus(j,1)*cosd(phase_angle(j,1));
        E_sin_phi_70(1+count) = dynamic_modulus(j,1)*sind(phase_angle(j,1));
        count = count+1;
    end
end
plot(E_cos_phi_70,E_sin_phi_70,'+b','LineWidth',2,...
                        'MarkerEdgeColor','b',...
                        'MarkerFaceColor','b',...
                        'MarkerSize',8);
E_cos_phi_100 = zeros(6,1);
E_sin_phi_100 = zeros(6,1);
count = 0;
for j = 1:30
    if temperature(j,1) == 100
        E_cos_phi_100(1+count) = dynamic_modulus(j,1)*cosd(phase_angle(j,1));
        E_sin_phi_100(1+count) = dynamic_modulus(j,1)*sind(phase_angle(j,1));
        count = count+1;
    end
end
plot(E_cos_phi_100,E_sin_phi_100,'*m','LineWidth',2,...
                        'MarkerEdgeColor','m',...
                        'MarkerFaceColor','m',...
                        'MarkerSize',8);
E_cos_phi_130 = zeros(6,1);
E_sin_phi_130 = zeros(6,1);
count = 0;
for j = 1:30
    if temperature(j,1) == 130
        E_cos_phi_130(1+count) = dynamic_modulus(j,1)*cosd(phase_angle(j,1));
        E_sin_phi_130(1+count) = dynamic_modulus(j,1)*sind(phase_angle(j,1));
        count = count+1;
    end
end
plot(E_cos_phi_130, E_sin_phi_130,'sk','LineWidth',2,...
                        'MarkerEdgeColor','k',...
```

```
                        'MarkerFaceColor','k',...
                        'MarkerSize',8);
legend('14 F','40 F','70 F','100 F','130 F','Location','best')
hold off;
%% Black space plot
subplot(2,3,6);
hold on;
grid on;
title('Phase Angle vs. Log|E*| plot (Black Space Plot)');
xlabel('Log|E*| (ksi)');
ylabel('Phase Angle (Degrees)');
plot(log10(DM_14), phase_angle_14,'or','LineWidth',2,...
                        'MarkerEdgeColor','r',...
                        'MarkerFaceColor','r',...
                        'MarkerSize',8);
plot(log10(DM_40), phase_angle_40,'xg','LineWidth',2,...
                        'MarkerEdgeColor','g',...
                        'MarkerFaceColor','g',...
                        'MarkerSize',8);
plot(log10(DM_70), phase_angle_70,'+b','LineWidth',2,...
                        'MarkerEdgeColor','b',...
                        'MarkerFaceColor','b',...
                        'MarkerSize',8);
plot(log10(DM_100), phase_angle_100,'*m','LineWidth',2,...
                        'MarkerEdgeColor','m',...
                        'MarkerFaceColor','m',...
                        'MarkerSize',8);
plot(log10(DM_130), phase_angle_130,'sk','LineWidth',2,...
                        'MarkerEdgeColor','k',...
                        'MarkerFaceColor','k',...
                        'MarkerSize',8);
legend('14 F','40 F','70 F','100 F','130 F','Location','best')
hold off;
hold off;
%% Iteration with data at 70 and 100 F
log_freq_70_shifted = log10(freq_70) + log_shift_factor_70;
for i = 1:length(log_shift_factor_100)
    log_freq_100_shifted = log10(freq_100) + log_shift_factor_100(i);
    master_log_freq_70 = [log_freq_70_shifted; log_freq_100_shifted];
    master_log_DM_70 = [log10(DM_70); log10(DM_100)];
    initialvals = [-10 -10 -10 -10];
    log_E =  @(p,x) (p(4) + (p(1)./(1 + exp(p(2) + p(3).* x))));
    trial_fit = nlinfit(master_log_freq_70, master_log_DM_70, log_E, initialvals);

    mean_DM = mean(master_log_DM_70);
    ss_total_sq = sum((master_log_DM_70-mean_DM).^2);
    SS_error_sq = sum((master_log_DM_70-log_E(trial_fit,master_log_freq_70)).^2);
    R_sq_1 = 1-(SS_error_sq/ss_total_sq);
    if R_sq_1 < coef_or_determination(1)
        continue
    else
        break
    end
end
log_shift_factor_100 = log_shift_factor_100(i);
%% Result plot with 70 and 100 F data
SF_fit_iteration = figure('name','Shift Factor and MC Iteration');
hold on;
P1 = subplot(2,2,1);
hold on;
grid on;
title('|E*| vs. Frequency Plot for 70 F and 100 F data');
xlabel('log (fr) (Hz)');
ylabel('log (|E*|) (ksi)');
plot(master_log_freq_70, master_log_DM_70, 'or','LineWidth',2);
log_E =  @(p,x) (p(4) + (p(1)./(1 + exp(p(2) + p(3).* x))));
startingVals = [-10 -10 -10 -10];
[coefEsts1,  a1,  b1,  c1,  d1]  =  nlinfit(master_log_freq_70,  master_log_DM_70,  log_E,
startingVals);
xgrid = linspace(-6,7,100);
line(xgrid, log_E(coefEsts1, xgrid), 'Color','r');
```

```
legend('Shifted Dynamic Modulus','Mastercurve Fit','Location','southeast');
hold off
%% Iteration with data at 40, 70 and 100 F
for j = 1:length(log_shift_factor_40)
    log_freq_40_shifted = log10(freq_40) + log_shift_factor_40(j);
    master_log_freq_70 = [log_freq_40_shifted; log_freq_70_shifted; log_freq_100_shifted];
    master_log_DM_70 = [log10(DM_40); log10(DM_70); log10(DM_100)];
    initialvals = [-10 -10 -10 -10];
    log_E =  @(p,x) (p(4) + (p(1)./(1 + exp(p(2) + p(3).* x))));
    trial_fit = nlinfit(master_log_freq_70, master_log_DM_70, log_E, initialvals);

    mean_DM = mean(master_log_DM_70);
    ss_total_sq = sum((master_log_DM_70-mean_DM).^2);
    SS_error_sq = sum((master_log_DM_70-log_E(trial_fit,master_log_freq_70)).^2);
    R_sq_2 = 1-(SS_error_sq/ss_total_sq);
    if R_sq_2 < coef_or_determination(2)
        continue
    else
        break
    end
end
log_shift_factor_40 = log_shift_factor_40(j);
%% Result plot with 40, 70 and 100 F data
P2 = subplot(2,2,2);
hold on;
grid on;
title('|E*| vs. Frequency Plot for 40 F, 70 F, and 100 F data');
xlabel('log (fr) (Hz)');
ylabel('log (|E*|) (ksi)');
plot(master_log_freq_70, master_log_DM_70, 'og','LineWidth',2);
log_E =  @(p,x) (p(4) + (p(1)./(1 + exp(p(2) + p(3).* x))));
startingVals = [-10 -10 -10 -10];
[coefEsts2,  a2,  b2,  c2,  d2]  =  nlinfit(master_log_freq_70,  master_log_DM_70,  log_E,
startingVals);
xgrid = linspace(-6,7,100);
line(xgrid, log_E(coefEsts2, xgrid), 'Color','r');
legend('Shifted Dynamic Modulus','Mastercurve Fit','Location','southeast');
hold off
%% Iteration with data at 40, 70, 100 and 130 F
for k = 1:length(log_shift_factor_130)
    log_freq_130_shifted = log10(freq_130) + log_shift_factor_130(k);
    master_log_freq_70 = [log_freq_40_shifted; log_freq_70_shifted; log_freq_100_shifted;
log_freq_130_shifted];
    master_log_DM_70 = [log10(DM_40); log10(DM_70); log10(DM_100); log10(DM_130)];
    initialvals = [-10 -10 -10 -10];
    log_E =  @(p,x) (p(4) + (p(1)./(1 + exp(p(2) + p(3).* x))));
    trial_fit = nlinfit(master_log_freq_70, master_log_DM_70, log_E, initialvals);

    mean_DM = mean(master_log_DM_70);
    ss_total_sq = sum((master_log_DM_70-mean_DM).^2);
    SS_error_sq = sum((master_log_DM_70-log_E(trial_fit,master_log_freq_70)).^2);
    R_sq_3 = 1-(SS_error_sq/ss_total_sq);
    if R_sq_3 < coef_or_determination(3)
        continue
    else
        break
    end
end
log_shift_factor_130 = log_shift_factor_130(k);
%% Result plot with 40, 70, 100 and 130 F data
P3 = subplot(2,2,3);
hold on;
grid on;
title('|E*| vs. Frequency Plot for 40 F, 70 F, 100 F, and 130 F data');
xlabel('log (fr) (Hz)');
ylabel('log (|E*|) (ksi)');
plot(master_log_freq_70, master_log_DM_70, 'ob','LineWidth',2);
log_E =  @(p,x) (p(4) + (p(1)./(1 + exp(p(2) + p(3).* x))));
startingVals = [-10 -10 -10 -10];
[coefEsts3,  a3,  b3,  c3,  d3]  =  nlinfit(master_log_freq_70,  master_log_DM_70,  log_E,
startingVals);
```

```
xgrid = linspace(-6,7,100);
line(xgrid, log_E(coefEsts3, xgrid), 'Color','r');
legend('Shifted Dynamic Modulus','Mastercurve Fit','Location','southeast');
hold off
%% Iteration with data at 14, 40, 70, 100 and 130 F
for l = 1:length(log_shift_factor_14)
    log_freq_14_shifted = log10(freq_14) + log_shift_factor_14(l);
    master_log_freq_70 = [log_freq_14_shifted; log_freq_40_shifted; log_freq_70_shifted;
log_freq_100_shifted; log_freq_130_shifted];
    master_log_DM_70   =   [log10(DM_14);   log10(DM_40);   log10(DM_70);   log10(DM_100);
log10(DM_130)];
    initialvals = [-10 -10 -10 -10];
    log_E =  @(p,x) (p(4) + (p(1)./(1 + exp(p(2) + p(3).* x))));
    trial_fit = nlinfit(master_log_freq_70, master_log_DM_70, log_E, initialvals);

    mean_DM = mean(master_log_DM_70);
    ss_total_sq = sum((master_log_DM_70-mean_DM).^2);
    SS_error_sq = sum((master_log_DM_70-log_E(trial_fit,master_log_freq_70)).^2);
    R_sq_4 = 1-(SS_error_sq/ss_total_sq);
    if R_sq_4 < coef_or_determination(4)
        continue
    else
        break
    end
end
log_shift_factor_14 = log_shift_factor_14(l);
%% Result plot with 14, 40, 70, 100 and 130 F data
P4 = subplot(2,2,4);
hold on;
grid on;
title('|E*| vs. f_{r} Plot for 14 F, 40 F, 70 F, 100 F, and 130 F data');
xlabel('log (f_{r}), Hz');
ylabel('log (|E*|), ksi');
plot(master_log_freq_70(1:6), master_log_DM_70(1:6), 'om','LineWidth',1);
plot(master_log_freq_70(7:12), master_log_DM_70(7:12), 'ob','LineWidth',1);
plot(master_log_freq_70(13:18), master_log_DM_70(13:18), 'ok','LineWidth',1);
plot(master_log_freq_70(19:24), master_log_DM_70(19:24), 'or','LineWidth',1);
plot(master_log_freq_70(25:30), master_log_DM_70(25:30), 'og','LineWidth',1);
log_E =  @(p,x) (p(4) + (p(1)./(1 + exp(p(2) + p(3).* x))));
startingVals = [-10 -10 -10 -10];
[coefEsts4,  a4,  b4,  c4,  d4]  =  nlinfit(master_log_freq_70,  master_log_DM_70,  log_E,
startingVals);
xgrid = linspace(-6,7,100);
line(xgrid, log_E(coefEsts4, xgrid), 'Color','r');
legend('Shifted |E*| at 14F','Shifted |E*| at 40F','|E*| at 70F (ref. temp.)',...
    'Shifted |E*| at 100F','Shifted |E*| at 130F','Mastercurve Fit','Location','best');
hold off
hold off
%% DM Mastercurve Final
figure('name','Final Mastercurve Fit');
subplot(1,2,1)
hold on;
grid on;
title('|E*| vs. Reduced Frequency Plot');
xlabel('log (f_{r}), Hz');
ylabel('log (|E*|), ksi');
plot(master_log_freq_70(1:6), master_log_DM_70(1:6), 'om','LineWidth',1.5,'MarkerSize',8);
plot(master_log_freq_70(7:12),                                    master_log_DM_70(7:12),
'sb','LineWidth',1.5,'MarkerSize',8);
plot(master_log_freq_70(13:18),                                   master_log_DM_70(13:18),
'^r','LineWidth',1.5,'MarkerSize',8);
plot(master_log_freq_70(19:24),                                   master_log_DM_70(19:24),
'dg','LineWidth',1.5,'MarkerSize',8);
plot(master_log_freq_70(25:30),                                   master_log_DM_70(25:30),
'xk','LineWidth',1.5,'MarkerSize',8);
log_E =  @(p,x) (p(4) + (p(1)./(1 + exp(p(2) + p(3).* x))));
startingVals = [-10 -10 -10 -10];
coefEsts = nlinfit(master_log_freq_70, master_log_DM_70, log_E, startingVals);
xgrid = linspace(-6,7,100);
line(xgrid, log_E(coefEsts, xgrid), 'Color','r','linestyle','--','linewidth', 2);
alpha1 = coefEsts(1);
```

```
beta1 = coefEsts(2);
gamma1 = coefEsts(3);
delta1 = coefEsts(4);
legend('|E*| at 14F','|E*| at 40F','|E*| at 70F','|E*| at 100F',...
    '|E*| at 130F','Mastercurve Fit','Location','best');
hold off
%% Statistics DM mastercurve fit
mean_DM = mean(master_log_DM_70);
S_error = sum(master_log_DM_70-log_E(coefEsts,master_log_freq_70));
SS_error_sq = sum((master_log_DM_70-log_E(coefEsts,master_log_freq_70)).^2);
S_total = sum(master_log_DM_70-mean_DM);
SS_total_sq = sum((master_log_DM_70-mean_DM).^2);
S_e = sqrt(SS_error_sq/(length(master_log_DM_70)-length(coefEsts)-1));
S_y = sqrt(SS_total_sq/(length(coefEsts)-1));
S_e_by_S_y = S_e/S_y;
R_sq_1 = 1-(SS_error_sq/SS_total_sq);
R_sq_2    =    1-(((length(master_log_DM_70)-length(coefEsts)-1))*S_e^2/((length(coefEsts)-
1)*S_y^2));
% Statistics summary: R^2, Se, Sy, Se/Sy, S_error, SS_error_sq, S_total,
% SS_total_sq
STAT_DM_MC_FIT = [R_sq_1;S_e;S_y;S_e_by_S_y;S_error;SS_error_sq;S_total;SS_total_sq];
%% Mastercurve for phase angle
master_phase_angle_70 = [phase_angle_14; phase_angle_40; phase_angle_70;...
                         phase_angle_100; phase_angle_130];
subplot(1,2,2);
hold on;
plot(master_log_freq_70(1:6),
master_phase_angle_70(1:6),'om','LineWidth',1.5,'MarkerSize',8);
plot(master_log_freq_70(7:12),
master_phase_angle_70(7:12),'sb','LineWidth',1.5,'MarkerSize',8);
plot(master_log_freq_70(13:18),
master_phase_angle_70(13:18),'^r','LineWidth',1.5,'MarkerSize',8);
plot(master_log_freq_70(19:24),
master_phase_angle_70(19:24),'dg','LineWidth',1.5,'MarkerSize',8);
plot(master_log_freq_70(25:30),
master_phase_angle_70(25:30),'xk','LineWidth',1.5,'MarkerSize',8);
phase_angle_fit_BT = @(z) (180./pi()).*(-pi()/2).*(alpha1.*gamma1).*...
    (exp(beta1+gamma1.*z))./((1+ exp(beta1+gamma1.*z)).^2);
phase_angle_fit = @(p,y) (180/pi()).*(p(1)+p(2).*y +( p(3).*...
    ((pi()/180)*((180./pi()).*(-pi()/2).*(alpha1.*gamma1).*...
    (exp(beta1+gamma1.*y))./((1+ exp(beta1+gamma1.*y)).^2)))));
startingVals = [-10 -10 -10];
coefEsts_pa    =    nlinfit(master_log_freq_70,    master_phase_angle_70,    phase_angle_fit,
startingVals);
line(xgrid, phase_angle_fit_BT(xgrid), 'Color','b','linestyle','--','linewidth',2);
line(xgrid,      phase_angle_fit(coefEsts_pa,      xgrid),      'Color','r','linestyle','--
','linewidth',2);
ekshy1 = coefEsts_pa(1);
ekshy2 = coefEsts_pa(2);
ekshy3 = coefEsts_pa(3);
grid on;
title('Phase Angle vs. Reduced Frequency Plot');
xlabel('log (f_{r}), Hz');
ylabel('\phi, Degrees');
legend('\phi at 14F','\phi at 40F','\phi at 70F','\phi at 100F',...
    '\phi at 130F','\phi - Mastercurve Fit-BT Approach',...
    '\phi - Mastercurve Fit-New Approach','Location','best')
hold off;
hold off;
%% Statistics PA mastercurve fit
mean_PA = mean(master_phase_angle_70);
S_error_pa = sum(master_phase_angle_70-phase_angle_fit(coefEsts_pa,master_log_freq_70));
SS_error_sq_pa                          =                          sum((master_phase_angle_70-
phase_angle_fit(coefEsts_pa,master_log_freq_70)).^2);
S_total_pa = sum(master_phase_angle_70-mean_PA);
SS_total_sq_pa = sum((master_phase_angle_70-mean_PA).^2);
S_e_pa = sqrt(SS_error_sq_pa/(length(master_phase_angle_70)-length(coefEsts_pa)-1));
S_y_pa = sqrt(SS_total_sq_pa/(length(coefEsts_pa)-1));
S_e_by_S_y_pa = S_e_pa/S_y_pa;
R_sq_3 = 1-(SS_error_sq_pa/SS_total_sq_pa);
```

```
R_sq_4              =              1-(((length(master_phase_angle_70)-length(coefEsts_pa)-
1))*S_e_pa^2/((length(coefEsts_pa)-1)*S_y_pa^2));
% Statistics summary: R^2, Se, Sy, Se/Sy, S_error, SS_error_sq, S_total,
% SS_total_sq
STAT_PA_MC_FIT                                                                    =
[R_sq_3;S_e_pa;S_y_pa;S_e_by_S_y_pa;S_error_pa;SS_error_sq_pa;S_total_pa;SS_total_sq_pa];
%% Plot the fitted data in logarithmic scale
figure('name','Dynamic Modulus and Phase Angle Mastercurves');
subplot(1,2,1);
xgrid1 = linspace(-8,8,100);
loglog(10.^master_log_freq_70, 10.^master_log_DM_70, 'o','LineWidth',1,...
    'MarkerEdgeColor','b','markersize',10);
hold on;
fitted_eq = @ (x) delta1 + (alpha1./(1+exp(beta1+gamma1*x)));
loglog(10.^xgrid1, 10.^fitted_eq(xgrid1), 'Color','k','linewidth', 1, 'linestyle','--');
hold on;
loglog(10.^master_log_freq_70, 10.^fitted_eq(master_log_freq_70), '*','LineWidth',1,...
    'MarkerEdgeColor','r','MarkerSize',6);
hold on;
grid on;
xlabel('Reduced Frequency,f_{r}, Hz');
ylabel('Dynamic Modulus, |E*|, ksi');
legend('TTSP Applied |E*| Mastercurve (30 discrete points: laboratory tested)',...
    '|E*| Mastercurve Fit (continuous sigmoid function)',...
    'Smoothened |E*| Data Points (30 discrete points: |E*| vs. f_{r})','Location','best');
hold off;
subplot(1,2,2);
semilogx(10.^master_log_freq_70, master_phase_angle_70, 'o','LineWidth',1,...
    'MarkerEdgeColor','b','markersize',10);
hold on;
semilogx(10.^xgrid1,  phase_angle_fit(coefEsts_pa,  xgrid1),  'Color','k','linewidth',  1,
'linestyle','--');
hold on;
semilogx(10.^master_log_freq_70,     phase_angle_fit(coefEsts_pa,     master_log_freq_70),
'*','LineWidth',1,...
    'MarkerEdgeColor','r','MarkerSize',6);
grid on;
xlabel('Reduced Frequency,f_{r}, Hz');
ylabel('Phase Angle, \delta, Degrees');
legend('\delta  -  Mastercurve  applying  |E*|  TTSP  shift  factors  (30  discrete  points:
laboratory tested)',...
    '\delta - Mastercurve Fit (New Approach)',...
    'Smoothened    \delta    Data    Points    (30    discrete    points:    \delta    vs.
f_{r})','Location','best');
hold off;
hold off;
%% Plot the shift factor function
test_temp = temp_25;
log_shift_factor = [log_shift_factor_14; log_shift_factor_40; ...
    log_shift_factor_70; log_shift_factor_100; log_shift_factor_130];
figure('name','Shift Factor (SF) Function');
hold on;
grid on;
title('Shift Factor (SF) Function');
plot(test_temp,log_shift_factor, 'o','LineWidth',1,'MarkerEdgeColor','b', 'markersize',8);
[curve1, goodness] = fit(test_temp, log_shift_factor, 'poly2');
curve1;
goodness;
plot(curve1, 'r');
xlabel('Temperature, \circF');
ylabel('Log Shift Factor, Hz');
legend('Shift     factors     at     various     temperatures','Fitted     shift     factor
function','Location','best')
hold off;
%% Statistics PA mastercurve fit
mean_SF = mean(log_shift_factor);
S_error_SF = sum(log_shift_factor-curve1(test_temp));
SS_error_sq_SF = sum((log_shift_factor-curve1(test_temp)).^2);
S_total_SF = sum(log_shift_factor-mean_SF);
SS_total_sq_SF = sum((log_shift_factor-mean_SF).^2);
S_e_SF = sqrt(SS_error_sq_SF/(length(log_shift_factor)-3-1));
```

```
S_y_SF = sqrt(SS_total_sq_SF/(3-1));
S_e_by_S_y_SF = S_e_SF/S_y_SF;
R_sq_5 = 1-(SS_error_sq_SF/SS_total_sq_SF);
R_sq_6 = 1-(((length(log_shift_factor)-3-1))*S_e_SF^2/((3-1)*S_y_SF^2));
% Statistics summary: R^2, Se, Sy, Se/Sy, S_error, SS_error_sq, S_total,
% SS_total_sq
STAT_SF_MC_FIT                                                                                                  =
[R_sq_3;S_e_pa;S_y_pa;S_e_by_S_y_pa;S_error_pa;SS_error_sq_pa;S_total_pa;SS_total_sq_pa];
%% Export Data Files for other analysis
mc_parameters = [alpha1; beta1; delta1; gamma1];
pa_mc_parameters = [ekshy1 ekshy2 ekshy3];
master_freq_70 = 10.^(master_log_freq_70);
data1 = [master_freq_70, 10.^log_E(coefEsts, log10(master_freq_70))];
data2 = [master_freq_70, phase_angle_fit(coefEsts_pa, master_log_freq_70)];
fid1 = fopen('Generated_1_data_freq_dynamic_modulus_E.txt','w');
fprintf(fid1, '%e %e\n', data1');
fid2 = fopen('Generated_2_data_freq_phase_angle_E.txt','w');
fprintf(fid2, '%e %e\n', data2');
fclose(fid1);
fclose(fid2);
%% End of Program
```

Appendix H

Code H-1: MATLAB® Code for Deploying ANN Model

```
function [Y,Xf,Af] = nn_function_script(X,~,~)

  % ===== NEURAL NETWORK CONSTANTS =====

  % Input 1
  x1_step1_xoffset = [-1;-1;-1;-1;-1;-1;-1;-1];
  x1_step1_gain = [1;1;1;1;1;1;1;1];
  x1_step1_ymin = -1;

  % Layer 1
  b1   =   [1.8227975841289059;-2.8397229653249432;-31.252594893114189;78.779277173179409;-
4.076454273497788;2.0726116560720622;-0.44163938737516983;-
1.1110618566386541;10.402450441179706;-
4.3220224219893897;1.39621846042036;6.5594107839870759];
  IW1_1 = [0.25131944576896043 0.40431434583963688 -1.9917363283899372 -1.3582216738681845
-0.61980268417459616               -1.9366836206601801               -0.041119023076559374
0.061118643623952432;3.5351365122209191     -4.1363676178839803     4.6142099489423059     -
1.455789294240087     2.8283965513958949     1.9433510463166883     -3.3854083348706872     -
0.031327893770023194;114.9615816244161     7.1006247133563072     -75.450607106560227     -
43.062047215911058     33.259379399194181     -66.42066395309773     2.1721023682925655     -
0.030911654345387188;0.0061966370223130885   0.00041623429421414884   -0.01010699179171206
0.0065830487811419629   0.023024337192427219   -0.0090583139602618736   78.855979979936848
0.0025249455530105599;-7.7892464981232408       11.591809071419355       -9.2664306554395814
0.7392465028934937      -2.342220487682428      4.8738445448453085      0.25183398156848419
0.011240496544538228;-1.5868902283282005      0.56103917712129081      -5.9341006694066385
0.19645504325808516   -6.7052096791053648   -2.3337086144387618   0.080887038592718327   -
0.01475390609580682;0.094882709962231387   0.27396652789349479   -0.34388358855896595   -
0.69874142614396828   -0.6137788542629361   0.30427684231349966   -0.65259446083076844   -
0.12673723913399265;0.10773191933045353    0.30069594687889356    -0.38599388281499319    -
0.76926705359354919    -0.61742934522713588    0.32275273362028561    -1.333412623437511    -
0.13727932294160264;0.024370847844438586     -0.02303326119415194     -0.015164037321837281
0.068426581507155373   0.011522150387922038   -0.0063444091662783484   0.058528635130423709
6.8380363732396567;-2.0574041199301893     1.4650638754519669     -0.32360930293196083     -
0.49363862640866951    2.1882509274827364    2.9982581656424396    0.02612375199713592    -
0.0070118468637203977;0.46171648096736645    -2.7697456599488945    5.0261414466357772    -
0.53337010673822893     -1.3165414182097153     1.7124560652172134     0.43521166538527112
0.023295112066930843;-5.7129900317258828       -13.428616139544966       13.167980228896425
3.7011618578706695     2.4294950959575696     -17.139936263599093     0.28573807224220221
0.014522101677969218];

  % Layer 2
  b2                                  =                                   [-58.88242310748187;-
8.3682014949416121;22.407845489249087;6.6892702359243428;178.75231105078066;6.09260744422
10663;-11.248476154845228;181.95765498726405;10.484202435356472;-8.2665918953890909;-
3.1926395704326227;1508.4182403404411];
  LW2_1 = [-11.965444458738794 -0.10752219688672796 6.2007603673056169 0.35410100892692281
-6.5837080290982213     -21.826039860050972     -5.7988097536368368     3.7239487826262776
55.33306321298182            4.1798421790210529            1.1447497225025498            -
4.429525087322677;6.4997064532507123     -2.3265318575770872     -0.17626994860170403     -
2.3851957494526679     -0.68772025003311976     -7.7122758917538174     -2.6014211646683907
2.6491090098853385    5.3449707701292297    2.7341117498283403    -1.9190079773802562    -
5.8793685333174501;0.016834879617963018    0.085052133841528405    0.27172079635632901    -
0.022486976180193685    -0.12474786011499846    0.57703641297765673    -0.60690912773575456
0.53193729790113065     -22.07284816278106     0.22098877036212292     -0.01746492515972203
0.34613805960653654;-0.43959400349205446   0.0004017077155759299   0.54552130641697216   -
0.067859986505662315   0.14730479754930989   0.027982164246911894   0.97916390505821482   -
0.83082081708226196     -5.2042787614727999     1.1514168935558167     -0.11993833350115274
0.020041003321048727;-0.30842354845372394   1.2309622449191058   0.038196748348433944   -
131.46057260902631     0.32498981120204468     0.80435538982068355     -54.939891435816925
49.155165710153803   -189.72136698449364   -1.5126286888000333   -0.67075338375854465   -
0.23315415766829142;-0.44610878794006031   0.0014339762495077526   0.56722916633682152   -
0.06436013197217437   0.15903584165301982   0.019538058178198956   0.95681906432660058   -
0.81218315523202855     -4.5904184614489258     1.1499128497952027     -0.12192437716355149
0.019854981682944056;0.25332956198416784     0.070418680403074807     0.019912352134986325
0.050347412039961494    -0.26744486308001653    0.82962450722496706    -0.51003337292674467
0.35818033442432451     10.951923657352376     0.22019577592885933     0.073772541710278333
```

```
0.37918941883918605;-0.32017298495702917    1.2350191919173907    0.044242766965704908    -
131.93348779459163     0.32461501876542281     0.81045027787736257     -55.269423469737887
49.469607657835574    -192.96433595150316    -1.5209963223057148    -0.67572501585028943    -
0.23129180674020097;-0.035253572404683249   -0.049432730336736626   -0.2629428456008856   -
0.10482667041318987   -0.14376285857453519   0.096653667709914168   1.0563287152407228   -
0.9077907583560838   -9.5664156700846412   0.51950641502556283   0.0015623727719184354   -
0.045265225897871124;6.5420864620744315    -2.3466241756283721    -0.2048922797741819    -
2.3903529146739806     -0.67821617476790708     -7.7781831567380193     -2.6683305314850672
2.7193052242436582    5.1770908328838905    2.7239257892449773    -1.9260970258445254    -
5.920078954718119;-2.1569110231418946        30.169277384684197        -17.377505734812182
55.812378320320569    10.044979692468182    8.8802343306404463    4.2894120287316975    -
2.9223543891675643     11.136165461751908     3.7633917048069478     -4.2614091551211626
7.8175358877757697;0.32206357733137148    -0.13979444284542611    1484.7861714897333    -
0.15676781841622392   0.81294668228118183   -0.22418425444424711   2.4432197399990288   -
2.0464352793570537   -18.796966887311395   -0.8540352521912703   -0.090334937663931872   -
1.4841461809952405];

  % Layer 3
  b3 = [221.21822768696157;-76.20647263562357];
  LW3_2 = [-0.30310149113327928 28.495331794527775 -6.5583645490823761 -77.410885659870814
-20.460623423910793    77.715026031696041    4.8498404167876918    18.819885442162636    -
0.89400999991663244    -28.423790350316775    0.59390252170949143    -222.43620135888278;-
0.13361149650612159     -92.822338545343428     3.3168701173625257     221.52265037443343
103.96087606931113    -219.0322061934956    -3.4312464006511916    -104.43311345667121    -
8.7491290652148734 92.542497589103789 -2.1299429997572532 81.52728716542687];

  % Output 1
  y1_step1_ymin = -1;
  y1_step1_gain = [1;1];
  y1_step1_xoffset = [-1;-1];

  % ===== SIMULATION ========

  % Format Input Arguments
  isCellX = iscell(X);
  if ~isCellX, X = {X}; end;

  % Dimensions
  TS = size(X,2); % timesteps
  if ~isempty(X)
    Q = size(X{1},2); % samples/series
  else
    Q = 0;
  end

  % Allocate Outputs
  Y = cell(1,TS);

  % Time loop
  for ts=1:TS

    % Input 1
    Xp1 = mapminmax_apply(X{1,ts},x1_step1_gain,x1_step1_xoffset,x1_step1_ymin);

    % Layer 1
    a1 = tansig_apply(repmat(b1,1,Q) + IW1_1*Xp1);

    % Layer 2
    a2 = tansig_apply(repmat(b2,1,Q) + LW2_1*a1);

    % Layer 3
    a3 = tansig_apply(repmat(b3,1,Q) + LW3_2*a2);

    % Output 1
    Y{1,ts} = mapminmax_reverse(a3,y1_step1_gain,y1_step1_xoffset,y1_step1_ymin);
  end

  % Final Delay States
  Xf = cell(1,0);
  Af = cell(3,0);
```

```
  % Format Output Arguments
  if ~isCellX, Y = cell2mat(Y); end
end

% ===== MODULE FUNCTIONS ========

% Map Minimum and Maximum Input Processing Function
function y = mapminmax_apply(x,settings_gain,settings_xoffset,settings_ymin)
  y = bsxfun(@minus,x,settings_xoffset);
  y = bsxfun(@times,y,settings_gain);
  y = bsxfun(@plus,y,settings_ymin);
end

% Sigmoid Symmetric Transfer Function
function a = tansig_apply(n)
  a = 2 ./ (1 + exp(-2*n)) - 1;
end

% Map Minimum and Maximum Output Reverse-Processing Function
function x = mapminmax_reverse(y,settings_gain,settings_xoffset,settings_ymin)
  x = bsxfun(@minus,y,settings_ymin);
  x = bsxfun(@rdivide,x,settings_gain);
  x = bsxfun(@plus,x,settings_xoffset);
end
```

Appendix I

Code I-1: MATLAB® Code for Prony Series Fit of Storage Modulus

```
% Import mastercurve data from text file generated in previous code
clear all;
close all;
clc;
data_E_w = importdata('Generated_1_data_freq_storage_modulus.txt');
freq_Ew = 2*pi().*data_E_w(:,1);
mod_Ew = data_E_w(:,2);
%% Plot storage modulus vs reduced frequency
storage_modulus_vs_freq_plot = figure('name','Storage Modulus vs Reduced Frequency
Plot');
loglog(freq_Ew,mod_Ew,'-or');
hold on;
title('Storage Modulus');
xlabel('Frequency (Hz)');
ylabel('E(w) (ksi)');
hold off;
%% Trial prony series fit to evaluate initial value for the nlinfit function
Ee = 1e1;
E_i = [1e4 1e3 1e2 1e2 1e2 9e2 8e2 3e2 1e1 1e2];
p_i = 0.1*[1e-5 1e-4 1e-3 1e-2 1e-1 1e0 1e1 1e2 1e3 1e4];
E_w_prony_fit = Ee + (p_i(1,1)^2*E_i(1,1))./(p_i(1,1)^2+(1./freq_Ew.^2))+...
                     (p_i(1,2)^2*E_i(1,2))./(p_i(1,2)^2+(1./freq_Ew.^2))+...
                     (p_i(1,3)^2*E_i(1,3))./(p_i(1,3)^2+(1./freq_Ew.^2))+...
                     (p_i(1,4)^2*E_i(1,4))./(p_i(1,4)^2+(1./freq_Ew.^2))+...
                     (p_i(1,5)^2*E_i(1,5))./(p_i(1,5)^2+(1./freq_Ew.^2))+...
                     (p_i(1,6)^2*E_i(1,6))./(p_i(1,6)^2+(1./freq_Ew.^2))+...
                     (p_i(1,7)^2*E_i(1,7))./(p_i(1,7)^2+(1./freq_Ew.^2))+...
                     (p_i(1,8)^2*E_i(1,8))./(p_i(1,8)^2+(1./freq_Ew.^2))+...
                     (p_i(1,9)^2*E_i(1,9))./(p_i(1,9)^2+(1./freq_Ew.^2))+...
                     (p_i(1,10)^2*E_i(1,10))./(p_i(1,10)^2+(1./freq_Ew.^2));
trial_prony_series_fit = figure('name','Trial Prony Series Fit');
loglog(freq_Ew,mod_Ew,'--or');
hold on;
grid on;
line(freq_Ew, E_w_prony_fit);
title('Storage Modulus');
xlabel('Frequency (Hz)');
ylabel('E(w) (ksi)');
legend('Storage Modulus','Trial Prony Fit', 'location','southeast');
hold off;
ini_val(1:(length(E_i))) = E_i(1:length(E_i));
ini_val(1,(length(E_i) + length(Ee))) = Ee;
%% Final Prony Series Fit
final_prony_series_fit = figure('name','Prony Series Fit');
loglog(freq_Ew, mod_Ew,'or');
hold on;
grid on;
prony_fit_eq = @(e,x) e(11) + (p_i(1,1)^2*e(1))./(p_i(1,1)^2+(1./x.^2))+...
                              (p_i(1,2)^2*e(2))./(p_i(1,2)^2+(1./x.^2))+...
                              (p_i(1,3)^2*e(3))./(p_i(1,3)^2+(1./x.^2))+...
                              (p_i(1,4)^2*e(4))./(p_i(1,4)^2+(1./x.^2))+...
                              (p_i(1,5)^2*e(5))./(p_i(1,5)^2+(1./x.^2))+...
                              (p_i(1,6)^2*e(6))./(p_i(1,6)^2+(1./x.^2))+...
                              (p_i(1,7)^2*e(7))./(p_i(1,7)^2+(1./x.^2))+...
                              (p_i(1,8)^2*e(8))./(p_i(1,8)^2+(1./x.^2))+...
                              (p_i(1,9)^2*e(9))./(p_i(1,9)^2+(1./x.^2))+...
                              (p_i(1,10)^2*e(10))./(p_i(1,10)^2+(1./x.^2));
options = statset('MaxIter',50000,'FunValCheck','off','TolX',1e-8,'TolFun', 1e-8,
'DerivStep', 1e-8);
startingVals = ini_val;
coefEsts = nlinfit(freq_Ew,mod_Ew, prony_fit_eq, startingVals, options);
xgrid = freq_Ew;
line(xgrid, prony_fit_eq(coefEsts, xgrid), 'Color','b');
legend('Storage Modulus','Prony Fit', 'location', 'southeast');
title('Storage Modulus');
xlabel('Frequency (rad/sec)');
```

```
ylabel('E(w) (ksi)');
legend('Storage Modulus','Prony Fit', 'location','southeast');
hold off;
%% Fourier Fit
try_fourier_fit = figure( 'Name', 'Fourier Fit');
hold on;
grid on;
log_freq_Ew = log10(freq_Ew);
log_mod_Ew = log10(mod_Ew);
plot(log_freq_Ew, log_mod_Ew, 'or');
% Set up fittype and options.
ft = fittype( 'fourier3' );
opts = fitoptions( ft );
opts.Display = 'Off';
opts.Lower = [-Inf -Inf -Inf -Inf -Inf -Inf -Inf -Inf];
opts.StartPoint = [0 0 0 0 0 0 0 0.25];
opts.Upper = [Inf Inf Inf Inf Inf Inf Inf Inf];
% Fit model to data.
[fourier_fit, gof] = fit( log_freq_Ew,log_mod_Ew, ft, opts );
% Plot fit with data.
plot(fourier_fit);
xlabel('log freq (s)');
ylabel('log E(w)');
hold off;
%% Export prony coefficients
row_i = p_i;
Ew_i = coefEsts(1:length(coefEsts)-1);
E_e = coefEsts(length(coefEsts));
y = [row_i; Ew_i];
fid = fopen('prony_series_coefficients_new_approach.txt', 'w');
fprintf(fid, '%f  %f\n', y);
fclose(fid);
fid1 = fopen('Equilibrium_modulus_new_apporach.txt', 'w');
fprintf(fid1, '%f  %f\n', E_e);
fclose(fid1);
```

Code I-2: MATLAB® Code for Relaxation Modulus and Creep Compliance from Storage Modulus

```
%% Import Data from text file
clear all;
close all;
clc;
data_prony_coef = importdata('prony_series_coefficients_new_approach.txt');
data_Eq_mod = importdata('Equilibrium_modulus_new_apporach.txt');
storage_freq_mod = importdata('Generated_1_data_freq_storage_modulus.txt');
storage_freq = 2*pi().*storage_freq_mod(:,1);
storage_mod = storage_freq_mod(:,2);
row_i = data_prony_coef(:,1);
Ew_i = data_prony_coef(:,2);
E_e = data_Eq_mod(:,1);
%% Computation of Relaxation Modulus
relax_time = logspace(-9,9)';
E_t = zeros(length(relax_time),1);
for j = 1:length(relax_time)
    sum_E = 0;
    for i = 1:length(row_i)
         sum_E = Ew_i(i,1)*exp(-(relax_time(j,1)/row_i(i,1)))+ sum_E;
    end
    E_t(j,1) = E_e + sum_E;
end
figure_1 = figure;
loglog(relax_time,E_t,'--or');
grid on;
title('Relaxation Modulus');
xlabel('Time (s)');
ylabel('E(t) (ksi)');
%% Comutation of retardation times for creep compliance curve
neg_1_over_s = (logspace(-8,8,10000))';
```

```
bar_Es = zeros(length(neg_1_over_s),1);
for j = 1:length(neg_1_over_s)
    sum_E = 0;
    for i = 1:length(row_i)
         sum_E = row_i(i)*Ew_i(i)/(row_i(i)-(neg_1_over_s(j)))+sum_E;
    end
    bar_Es(j) = abs(E_e + sum_E);
end
figure_2 = figure;
loglog(neg_1_over_s, bar_Es, 'r');
grid on;
title('Reterdation time estimation');
xlabel('-1/s');
ylabel('Operational Modulus (Es~) (ksi)');
%% Determination of the min value of Ew_s in each row_i range
%% Data group 1
n=0;
for i = 1:length(neg_1_over_s)
    if neg_1_over_s(i,1) > row_i(1,1) && neg_1_over_s(i,1) < row_i(2,1)
        n=1+n;
    end
end
bar_Es_gr1 = zeros(n,1);
neg_1_over_Es_gr1 = zeros(n,1);
count = 0;
for i = 1:length(neg_1_over_s)
    if neg_1_over_s(i,1) > row_i(1,1) && neg_1_over_s(i,1) < row_i(2,1)
        count = 1+count;
        bar_Es_gr1(count,1) = bar_Es(i,1);
        neg_1_over_Es_gr1(count,1) = neg_1_over_s(i,1);
    end
end
[bar_Es_gr1_min tj_gr_1] = min(bar_Es_gr1);
%% Data group 2
n=0;
for i = 1:length(neg_1_over_s)
    if neg_1_over_s(i,1) > row_i(2,1) && neg_1_over_s(i,1) < row_i(3,1)
        n=1+n;
    end
end
bar_Es_gr2 = zeros(n,1);
neg_1_over_Es_gr2 = zeros(n,1);
count = 0;
for i = 1:length(neg_1_over_s)
    if neg_1_over_s(i,1) > row_i(2,1) && neg_1_over_s(i,1) < row_i(3,1)
        count = 1+count;
        bar_Es_gr2(count,1) = bar_Es(i,1);
        neg_1_over_Es_gr2(count,1) = neg_1_over_s(i,1);
    end
end
[bar_Es_gr2_min tj_gr_2] = min(bar_Es_gr2);
%% Data group 3
n=0;
for i = 1:length(neg_1_over_s)
    if neg_1_over_s(i,1) > row_i(3,1) && neg_1_over_s(i,1) < row_i(4,1)
        n=1+n;
    end
end
bar_Es_gr3 = zeros(n,1);
neg_1_over_Es_gr3 = zeros(n,1);
count = 0;
for i = 1:length(neg_1_over_s)
    if neg_1_over_s(i,1) > row_i(3,1) && neg_1_over_s(i,1) < row_i(4,1)
        count = 1+count;
        bar_Es_gr3(count,1) = bar_Es(i,1);
        neg_1_over_Es_gr3(count,1) = neg_1_over_s(i,1);
    end
end
[bar_Es_gr3_min tj_gr_3] = min(bar_Es_gr3);
%% Data group 4
n=0;
```

```
for i = 1:length(neg_1_over_s)
    if neg_1_over_s(i,1) > row_i(4,1) && neg_1_over_s(i,1) < row_i(5,1)
        n=1+n;
    end
end
bar_Es_gr4 = zeros(n,1);
neg_1_over_Es_gr4 = zeros(n,1);
count = 0;
for i = 1:length(neg_1_over_s)
    if neg_1_over_s(i,1) > row_i(4,1) && neg_1_over_s(i,1) < row_i(5,1)
        count = 1+count;
        bar_Es_gr4(count,1) = bar_Es(i,1);
        neg_1_over_Es_gr4(count,1) = neg_1_over_s(i,1);
    end
end
[bar_Es_gr4_min tj_gr_4] = min(bar_Es_gr4);
%% Data group 5
n=0;
for i = 1:length(neg_1_over_s)
    if neg_1_over_s(i,1) > row_i(5,1) && neg_1_over_s(i,1) < row_i(6,1)
        n=1+n;
    end
end
bar_Es_gr5 = zeros(n,1);
neg_1_over_Es_gr5 = zeros(n,1);
count = 0;
for i = 1:length(neg_1_over_s)
    if neg_1_over_s(i,1) > row_i(5,1) && neg_1_over_s(i,1) < row_i(6,1)
        count = 1+count;
        bar_Es_gr5(count,1) = bar_Es(i,1);
        neg_1_over_Es_gr5(count,1) = neg_1_over_s(i,1);
    end
end
[bar_Es_gr5_min tj_gr_5] = min(bar_Es_gr5);
%% Data group 6
n=0;
for i = 1:length(neg_1_over_s)
    if neg_1_over_s(i,1) > row_i(6,1) && neg_1_over_s(i,1) < row_i(7,1)
        n=1+n;
    end
end
bar_Es_gr6 = zeros(n,1);
neg_1_over_Es_gr6 = zeros(n,1);
count = 0;
for i = 1:length(neg_1_over_s)
    if neg_1_over_s(i,1) > row_i(6,1) && neg_1_over_s(i,1) < row_i(7,1)
        count = 1+count;
        bar_Es_gr6(count,1) = bar_Es(i,1);
        neg_1_over_Es_gr6(count,1) = neg_1_over_s(i,1);
    end
end
[bar_Es_gr6_min tj_gr_6] = min(bar_Es_gr6);
%% Data group 7
n=0;
for i = 1:length(neg_1_over_s)
    if neg_1_over_s(i,1) > row_i(7,1) && neg_1_over_s(i,1) < row_i(8,1)
        n=1+n;
    end
end
bar_Es_gr7 = zeros(n,1);
neg_1_over_Es_gr7 = zeros(n,1);
count = 0;
for i = 1:length(neg_1_over_s)
    if neg_1_over_s(i,1) > row_i(7,1) && neg_1_over_s(i,1) < row_i(8,1)
        count = 1+count;
        bar_Es_gr7(count,1) = bar_Es(i,1);
        neg_1_over_Es_gr7(count,1) = neg_1_over_s(i,1);
    end
end
[bar_Es_gr7_min tj_gr_7] = min(bar_Es_gr7);
%% Data group 8
```

```
n=0;
for i = 1:length(neg_1_over_s)
    if neg_1_over_s(i,1) > row_i(8,1) && neg_1_over_s(i,1) < row_i(9,1)
        n=1+n;
    end
end
bar_Es_gr8 = zeros(n,1);
neg_1_over_Es_gr8 = zeros(n,1);
count = 0;
for i = 1:length(neg_1_over_s)
    if neg_1_over_s(i,1) > row_i(8,1) && neg_1_over_s(i,1) < row_i(9,1)
        count = 1+count;
        bar_Es_gr8(count,1) = bar_Es(i,1);
        neg_1_over_Es_gr8(count,1) = neg_1_over_s(i,1);
    end
end
[bar_Es_gr8_min tj_gr_8] = min(bar_Es_gr8);
%% Data group 9
n=0;
for i = 1:length(neg_1_over_s)
    if neg_1_over_s(i,1) > row_i(9,1) && neg_1_over_s(i,1) < row_i(10,1)
        n=1+n;
    end
end
bar_Es_gr9 = zeros(n,1);
neg_1_over_Es_gr9 = zeros(n,1);
count = 0;
for i = 1:length(neg_1_over_s)
    if neg_1_over_s(i,1) > row_i(9,1) && neg_1_over_s(i,1) < row_i(10,1)
        count = 1+count;
        bar_Es_gr9(count,1) = bar_Es(i,1);
        neg_1_over_Es_gr9(count,1) = neg_1_over_s(i,1);
    end
end
[bar_Es_gr9_min tj_gr_9] = min(bar_Es_gr9);
%% Data group 10
n=0;
for i = 1:length(neg_1_over_s)
    if neg_1_over_s(i,1) > row_i(10,1)
        n=1+n;
    end
end
bar_Es_gr10 = zeros(n,1);
neg_1_over_Es_gr10 = zeros(n,1);
count = 0;
for i = 1:length(neg_1_over_s)
    if neg_1_over_s(i,1) > row_i(10,1)
        count = 1+count;
        bar_Es_gr10(count,1) = bar_Es(i,1);
        neg_1_over_Es_gr10(count,1) = neg_1_over_s(i,1);
    end
end
[bar_Es_gr10_min tj_gr_10] = min(bar_Es_gr10);
%% Reterdation time vector
tou_j = [neg_1_over_Es_gr1(tj_gr_1);
          neg_1_over_Es_gr2(tj_gr_2);
          neg_1_over_Es_gr3(tj_gr_3);
          neg_1_over_Es_gr4(tj_gr_4);
          neg_1_over_Es_gr5(tj_gr_5);
          neg_1_over_Es_gr6(tj_gr_6);
          neg_1_over_Es_gr7(tj_gr_7);
          neg_1_over_Es_gr8(tj_gr_8);
          neg_1_over_Es_gr9(tj_gr_9);
          neg_1_over_Es_gr10(tj_gr_10)];
%% Reterdation strengths calculation
m = length(row_i);   %spread of E_i
n = length(tou_j);   %spread of D_j
p = 30;              %number of sampling points for tou_j, for collocation = m or n
i = 1:m;
j = 1:n;
k = 1:p;             %number of t_k
```

```
Akj = zeros(p,n);
Bk = zeros(p,1);
t_k = zeros(length(k),1);   %or can be the values identical to tou_j
for i = 1:length(k)
    if  n == p
        t_k(i) = 1*10^(k(i)-6);
    else
        t_k(i) = 10^(((k(i)-1)/2)-7);
    end
end
for k = 1:p
    for j = 1:n
        second_term_Akj = 0;
        for i = 1:m
            if row_i(i,1) ~= tou_j(j,1)
                second_term_1 = row_i(i)*Ew_i(i)*(exp(-(t_k(k)/row_i(i)))- ...
                                exp(-(t_k(k)/tou_j(j))))/(row_i(i)-tou_j(j));
            else
                second_term_1 = t_k(k)*Ew_i(i)*exp(-(t_k(k)/row_i(i)))/tou_j(j);
            end
            second_term_Akj = second_term_Akj + second_term_1;
        end
        Akj(k,j)= E_e*(1-exp(-(t_k(k)/tou_j(j))))+ second_term_Akj;
    end
end
sum_Ew_i = 0;
for i = 1:m
    sum_Ew_i_1 = Ew_i(i);
    sum_Ew_i = sum_Ew_i + sum_Ew_i_1;
end
D_g = 1/(E_e+sum_Ew_i);
for k = 1:p
    x_Bk = 0;
    y_Bk = 0;
    for i = 1:m
        x_Bk_1 = Ew_i(i)*exp(-(t_k(k)/row_i(i)));
        y_Bk_1 = Ew_i(i);
        x_Bk = x_Bk + x_Bk_1;
        y_Bk = y_Bk + y_Bk_1;
    end
    Bk(k,1) = 1 - ((E_e + x_Bk)/(E_e + y_Bk));
end

if n == p
    D_j = Akj\Bk;
else
    AA = Akj'*Akj;
    AB = Akj'*Bk;
    D_j = AA\AB;
end
%% Generation of creep curve
creep_time = relax_time;
D_t = zeros(length(creep_time),1);

for j = 1:length(creep_time)
    sum_D = 0;
    for i = 1:length(tou_j)
         sum_D = D_j(i,1)*(1-exp(-(creep_time(j,1)/tou_j(i,1))))+ sum_D;
    end
    D_t(j,1) = D_g + sum_D;
end
figure_3 = figure;
loglog(creep_time, D_t,'--ob');
grid on;
title('Creep Compliance');
xlabel('Time (s)');
ylabel('D(t) (1/ksi)');
%% Combined figure for relaxation modulus and creep compliance
figure_4 = figure;
[ax h1 h2] = plotyy(relax_time,E_t,creep_time,D_t,'loglog','loglog');
set(h1,'linestyle','--','linewidth',2);
```

```
set(h2,'linestyle','--','linewidth',2);
grid on;
title('Relaxation Modulus and Creep Compliance');
xlabel('Time (s)');
ylabel(ax(1),'E(t) (MPa)');
ylabel(ax(2),'D(t) (MPa)');
```

Code I-3: MATLAB® Code for Creep Compliance Mastercurve Fit

```
%% Load Data from text file
clear all;
close all;
clc;
%14F data
test_data_14F = importdata('14F_Creep.txt');
time_14F = test_data_14F(:,1);
creep_comp_14F = test_data_14F(:,2);
%40F data
test_data_40F = importdata('40F_Creep.txt');
time_40F = test_data_40F(:,1);
creep_comp_40F = test_data_40F(:,2);
%70F data
test_data_70F = importdata('70F_Creep.txt');
time_70F = test_data_70F(:,1);
creep_comp_70F = test_data_70F(:,2);
%100F data
test_data_100F = importdata('100F_Creep.txt');
time_100F = test_data_100F(:,1);
creep_comp_100F = test_data_100F(:,2);
%130F data
test_data_130F = importdata('130F_Creep.txt');
time_130F = test_data_130F(:,1);
creep_comp_130F = test_data_130F(:,2);
%% Plot tested data in log x-y space
Creep_comp_vs_time_plot = ...
    figure('Name','Creep Compliance at Different Test Temperatures');
loglog(time_14F,creep_comp_14F,'or','LineWidth',2,...
                        'MarkerEdgeColor','r',...
                        'MarkerFaceColor','r',...
                        'MarkerSize',8);
hold on;
loglog(time_40F,creep_comp_40F,'xg','LineWidth',2,...
                        'MarkerEdgeColor','g',...
                        'MarkerFaceColor','g',...
                        'MarkerSize',8);
hold on;
loglog(time_70F,creep_comp_70F,'+b','LineWidth',2,...
                        'MarkerEdgeColor','b',...
                        'MarkerFaceColor','b',...
                        'MarkerSize',8);
hold on;
loglog(time_100F,creep_comp_100F,'*m','LineWidth',2,...
                        'MarkerEdgeColor','m',...
                        'MarkerFaceColor','m',...
                        'MarkerSize',8);
hold on;
loglog(time_130F,creep_comp_130F,'sk','LineWidth',2,...
                        'MarkerEdgeColor','k',...
                        'MarkerFaceColor','k',...
                        'MarkerSize',8);
grid on;
title('D(t) vs. Time Plot');
xlabel('Time (sec)');
ylabel('D(t) (1/ksi)');
legend('14 F','40 F','70 F','100 F','130 F','Location','bestoutside')
hold off;
%% Plot log tested data in x-y space
log_time_14F = log10(time_14F);
log_creep_comp_14F = log10(creep_comp_14F);
log_time_40F = log10(time_40F);
```

```
log_creep_comp_40F = log10(creep_comp_40F);
log_time_70F = log10(time_70F);
log_creep_comp_70F = log10(creep_comp_70F);
log_time_100F = log10(time_100F);
log_creep_comp_100F = log10(creep_comp_100F);
log_time_130F = log10(time_130F);
log_creep_comp_130F = log10(creep_comp_130F);
log_creep_comp_vs_log_time_plot = ...
    figure('Name','Logarithm of Creep Compliance at Different Test Temperatures');
plot(log_time_14F,log_creep_comp_14F,'or','LineWidth',2,...
                        'MarkerEdgeColor','r',...
                        'MarkerFaceColor','r',...
                        'MarkerSize',8);
hold on;
plot(log_time_40F,log_creep_comp_40F,'xg','LineWidth',2,...
                        'MarkerEdgeColor','g',...
                        'MarkerFaceColor','g',...
                        'MarkerSize',8);
hold on;
plot(log_time_70F,log_creep_comp_70F,'+b','LineWidth',2,...
                        'MarkerEdgeColor','b',...
                        'MarkerFaceColor','b',...
                        'MarkerSize',8);
hold on;
plot(log_time_100F,log_creep_comp_100F,'*m','LineWidth',2,...
                        'MarkerEdgeColor','m',...
                        'MarkerFaceColor','m',...
                        'MarkerSize',8);
hold on;
plot(log_time_130F,log_creep_comp_130F,'sk','LineWidth',2,...
                        'MarkerEdgeColor','k',...
                        'MarkerFaceColor','k',...
                        'MarkerSize',8);
grid on;
title('log_D(t) vs. log_Time Plot');
xlabel('log Time (sec)');
ylabel('log D(t) (ksi)');
legend('14 F','40 F','70 F','100 F','130 F','Location','bestoutside')
hold off;
%% trial and error for smoothing
log_sf_14F = -5.4;
log_sf_40F = -3.05;
log_sf_70F = 0;
log_sf_100F = 2.45;
log_sf_130F = 3.75;
log_time_14F_shifted = log_time_14F + log_sf_14F;
log_time_40F_shifted = log_time_40F + log_sf_40F;
log_time_70F_shifted = log_time_70F + log_sf_70F;
log_time_100F_shifted = log_time_100F + log_sf_100F;
log_time_130F_shifted = log_time_130F + log_sf_130F;
master_log_time_70 = [log_time_14F_shifted; log_time_40F_shifted;...
    log_time_70F_shifted; log_time_100F_shifted; log_time_130F_shifted];
master_log_creep_70 = [log_creep_comp_14F; log_creep_comp_40F;...
    log_creep_comp_70F; log_creep_comp_100F; log_creep_comp_130F];
log_Creep_Comp_vs_log_Reduced_time_plot = ...
    figure('Name','Log Creep Compliance Mastercurve');
plot(master_log_time_70, master_log_creep_70, 'o','LineWidth',2);
hold on;
grid on;
title('log D(t) vs. log Tr Plot');
xlabel('log Tr (sec)');
ylabel('log D(t) (ksi)');
hold off;
%% Shift factor function
log_sf = [log_sf_14F log_sf_40F log_sf_70F log_sf_100F log_sf_130F];
test_temperatures = [14 40 70 100 130];
% test_temperatures = [14 40 70 100 130];
WLF_sf_function = figure('Name','Shift Factor Function');
plot(test_temperatures, log_sf, 'or','LineWidth',2);
hold on;
grid on;
```

```
initialvals_sf = [-5 400];
log_sf_fit =  @(p,x) -(p(1).*(x-70))./((p(2)+(x-70)));
trial_sf_fit = nlinfit(test_temperatures, log_sf, log_sf_fit, initialvals_sf);
xgrid_sf = linspace(0,150,150);
line(xgrid_sf, log_sf_fit(trial_sf_fit, xgrid_sf), 'Color','r');
legend('Shift Factor','WLF fit','Location','southeast');
title('Shift Factor Function');
xlabel('Temperature, F');
ylabel('log Shift Factor');
hold off;
%% Pre-smoothing the Relaxation Mastercurve
mc_smoothing = figure('Name','Mastercurve Smoothing');
hold on;
grid on;
smooth_ft = fittype( 'smoothingspline' );
opts_smooth = fitoptions( smooth_ft);
opts_smooth.SmoothingParam = 0.3;
[smooth_fitresult, gof] = fit(master_log_time_70, master_log_creep_70,smooth_ft,
opts_smooth);
smooth_xgrid = (linspace(master_log_time_70(1),
master_log_time_70(length(master_log_time_70)), 100))';
smooth_ygrid = smooth_fitresult(smooth_xgrid);
plot(master_log_time_70, master_log_creep_70, 'ob');
plot(smooth_xgrid, smooth_ygrid, '-r','linewidth',2);
legend('Unsmoothened Mastercurve', 'Smoothened Mastercurve','Location', 'NorthEast' );
xlabel( 'Log Time (sec)' );
ylabel( 'Log Creep Compliance (ksi)' );
%% Plot smoothened data in Logarithmic space
master_time_70 = 10 .^ master_log_time_70;
master_creep_70 = 10 .^ master_log_creep_70;
smooth_master_time_70 = 10 .^ smooth_xgrid;
smooth_master_creep_70 = 10 .^ smooth_ygrid;
mastercurve_log_space = figure('Name','Creep Compliance vs Time Plot');
loglog(master_time_70, master_creep_70, 'ob');
grid on;
hold on;
loglog(smooth_master_time_70, smooth_master_creep_70, 'or','LineWidth',3);
legend('Unsmoothened Mastercurve', 'Smoothened Mastercurve','Location', 'NorthEast' );
xlabel( 'Time (sec)' );
ylabel( 'Creep Compliance (1/ksi)' );
%% Export Data Files for other analysis
data1 = [master_time_70'; master_creep_70'];
data2 = [smooth_master_time_70'; smooth_master_creep_70'];
fid1 = fopen('Generated_1_Unsmoothened_Creep_Mastercurve.txt', 'w');
fprintf(fid1, '%e %e\n', data1);
fid2 = fopen('Generated_2_Smoothened_Creep_Mastercurve.txt', 'w');
fprintf(fid2, '%e  %e\n', data2);
fclose(fid1);
fclose(fid2);
%End of Program
```

Code I-4: MATLAB® Code for Prony Series Fit of Creep Compliance

```
%% Import mastercurve data from text file generated in previous code
clear all;
close all;
clc;
data_D_t = importdata('Generated_2_Smoothened_Creep_Mastercurve.txt');
time_D_t = data_D_t(:,1);
D_t = data_D_t(:,2);
%% Plot creep compliance vs reduced time
creep_comp_vs_time_plot = figure('name','Creep Compliance vs Reduced Time Plot');
loglog(time_D_t, D_t,'-or');
hold on;
title('Creep Compliance vs Reduced Time Plot');
xlabel('Reduced Time (sec)');
ylabel('D(t) (1/ksi)');
grid on;
hold off;
%% Trial prony series fit to evaluate initial value for the nlinfit function
```

```
Dg = 3e-5;
D_j = [7e-4 1e-4 3e-4 4e-4 1e-3 3e-3 6e-3 8e-3 1e-2 1e-2 2e-2];
t_j = [1e-5 1e-4 1e-3 1e-2 1e-1 1e0 1e1 1e2 1e3 1e4 1e5];
D_t_prony_fit = Dg + D_j(1,1).*(1-exp(-time_D_t./t_j(1,1)))+...
                D_j(1,2).*(1-exp(-time_D_t./t_j(1,2)))+...
                D_j(1,3).*(1-exp(-time_D_t./t_j(1,3)))+...
                D_j(1,4).*(1-exp(-time_D_t./t_j(1,4)))+...
                D_j(1,5).*(1-exp(-time_D_t./t_j(1,5)))+...
                D_j(1,6).*(1-exp(-time_D_t./t_j(1,6)))+...
                D_j(1,7).*(1-exp(-time_D_t./t_j(1,7)))+...
                D_j(1,8).*(1-exp(-time_D_t./t_j(1,8)))+...
                D_j(1,9).*(1-exp(-time_D_t./t_j(1,9)))+...
                D_j(1,10).*(1-exp(-time_D_t./t_j(1,10)))+...
                D_j(1,11).*(1-exp(-time_D_t./t_j(1,11)));
trial_prony_series_fit = figure('name','Trial Prony Series Fit');
loglog(time_D_t, D_t,'--or');
hold on;
grid on;
line(time_D_t, D_t_prony_fit);
title('Creep Mastercurve Prony Fit');
xlabel('Time (sec)');
ylabel('D(t) (1/ksi)');
legend('Creep Compliance','Trial Prony Fit', 'location','southeast');
hold off;
ini_val(1:(length(D_j))) = D_j(1:length(D_j));
ini_val(1,(length(D_j) + length(Dg))) = Dg;
%% Final Prony Series Fit
final_prony_series_fit = figure('name','Prony Series Fit');
loglog(time_D_t, D_t,'or');
hold on;
grid on;
prony_fit_eq = @(d,x) d(12) + d(1) .* (1-exp(-x/t_j(1,1)))+...
                        d(2) .* (1-exp(-x/t_j(1,2)))+...
                        d(3) .* (1-exp(-x/t_j(1,3)))+...
                        d(4) .* (1-exp(-x/t_j(1,4)))+...
                        d(5) .* (1-exp(-x/t_j(1,5)))+...
                        d(6) .* (1-exp(-x/t_j(1,6)))+...
                        d(7) .* (1-exp(-x/t_j(1,7)))+...
                        d(8) .* (1-exp(-x/t_j(1,8)))+...
                        d(9) .* (1-exp(-x/t_j(1,9)))+...
                        d(10) .* (1-exp(-x/t_j(1,10)))+...
                        d(11) .* (1-exp(-x/t_j(1,11)));
options = statset('MaxIter',50000,'FunValCheck','off','TolX',1e-8,'TolFun', 1e-8,
'DerivStep', 1e-8);
startingVals = ini_val;
coefEsts = nlinfit(time_D_t,D_t, prony_fit_eq, startingVals, options);
xgrid = time_D_t;
line(xgrid, prony_fit_eq(coefEsts, xgrid), 'Color','b');
legend('Creep MC','Prony Fit', 'location', 'southeast');
title('Creep Compliance');
xlabel('time (sec)');
ylabel('D(t) (1/ksi)');
hold off;
%% Export prony coefficients
tau_j = t_j;
D_j = coefEsts(1:length(coefEsts)-1);
Dg = coefEsts(length(coefEsts));
y = [tau_j; D_j];
fid = fopen('prony_series_coefficients_from_creep_compliance.txt', 'w');
fprintf(fid, '%f  %f\n', y);
fclose(fid);
fid1 = fopen('glassy_compliance_from_creep_compliance.txt', 'w');
fprintf(fid1, '%f  %f\n', Dg);
fclose(fid1);
```

Code I-5: MATLAB® Code for Relaxation Modulus from Prony Coefficients of Creep Compliance

```
%% Import Data from text file
clear all;
```

```
close all;
clc;
data_prony_coef = importdata('prony_series_coefficients_from_creep_compliance.txt');
data_glass_comp = importdata('glassy_compliance_from_creep_compliance.txt');
creep_data_unsmooth = importdata('Generated_1_Unsmoothened_Creep_Mastercurve.txt');
creep_data_smooth = importdata('Generated_2_Smoothened_Creep_Mastercurve.txt');
creep_time_unsmooth = creep_data_unsmooth(:,1);
creep_comp_unsmooth = creep_data_unsmooth(:,2);
time_D_t = creep_data_smooth(:,1);
D_t = creep_data_smooth(:,2);
tau_j = data_prony_coef(:,1);
D_j = data_prony_coef(:,2);
Dg = data_glass_comp(:,1);
%% Plot Relaxation Modulus
creep_mc_smooth_unsmooth = figure('name','Creep Compliance MC');
loglog( creep_time_unsmooth, creep_comp_unsmooth, 'ob');
hold on;
loglog(time_D_t,D_t,'-r','linewidth', 4);
grid on;
title('Creep Compliance');
xlabel('Time (s)');
ylabel('D(t) (1/ksi)');
legend('Unsmoothen','Smoothen','location','northeast');
hold off;
%% Plot smooth relaxation with prony fit
D_t_prony = zeros(length(time_D_t),1);
for j = 1:length(time_D_t)
    sum_D = 0;
    for i = 1:length(tau_j)
         sum_D_j = D_j(i)*(1-exp(-time_D_t(j)/tau_j(i)));
         sum_D = sum_D +sum_D_j;
    end
    D_t_prony(j) = Dg + sum_D;
end
creep_mc_prony_fit = figure('name','Creep Compliance MC Prony Fit');
loglog(time_D_t,D_t,'or');
hold on;
grid on;
line(time_D_t, D_t_prony, 'linewidth', 2);
title('Creep Compliance MC Prony Fit');
xlabel('Time (s)');
ylabel('D(t) (1/ksi)');
legend('Smoothened Creep MC','Prony Fit','location','northeast');
hold off;
%% Comutation of retardation times for creep compliance curve
neg_1_over_s = (logspace(-8,8,10000))';
bar_Ds = zeros(length(neg_1_over_s),1);
for j = 1:length(neg_1_over_s)
    sum_D = 0;
    for i = 1:length(tau_j)
         sum_D = -D_j(i)*neg_1_over_s(j)/(tau_j(i)-neg_1_over_s(j))+sum_D;
    end
    bar_Ds(j) = abs(Dg + sum_D);
end
figure_2 = figure;
loglog(neg_1_over_s, bar_Ds, 'r');
grid on;
title('Retardation time estimation');
xlabel('-1/s');
ylabel('Operational Compliance (Ds~) (1/ksi)');
%% Determination of the min value of D_s~ in each tau_j range
%% Data group 1
n=0;
for i = 1:length(neg_1_over_s)
    if neg_1_over_s(i,1) < tau_j(1,1)
        n=1+n;
    end
end
bar_Ds_gr1 = zeros(n,1);
neg_1_over_Ds_gr1 = zeros(n,1);
count = 0;
```

```
for i = 1:length(neg_1_over_s)
    if neg_1_over_s(i,1) < tau_j(1,1)
        count = 1+count;
        bar_Ds_gr1(count,1) = bar_Ds(i,1);
        neg_1_over_Ds_gr1(count,1) = neg_1_over_s(i,1);
    end
end
[bar_Ds_gr1_min pi_gr_1] = min(bar_Ds_gr1);
%% Data group 2
n=0;
for i = 1:length(neg_1_over_s)
    if neg_1_over_s(i,1) > tau_j(1,1) && neg_1_over_s(i,1) < tau_j(2,1)
        n=1+n;
    end
end
bar_Ds_gr2 = zeros(n,1);
neg_1_over_Ds_gr2 = zeros(n,1);
count = 0;
for i = 1:length(neg_1_over_s)
    if neg_1_over_s(i,1) > tau_j(1,1) && neg_1_over_s(i,1) < tau_j(2,1)
        count = 1+count;
        bar_Ds_gr2(count,1) = bar_Ds(i,1);
        neg_1_over_Ds_gr2(count,1) = neg_1_over_s(i,1);
    end
end
[bar_Ds_gr2_min pi_gr_2] = min(bar_Ds_gr2);
%% Data group 3
n=0;
for i = 1:length(neg_1_over_s)
    if neg_1_over_s(i,1) > tau_j(2,1) && neg_1_over_s(i,1) < tau_j(3,1)
        n=1+n;
    end
end
bar_Ds_gr3 = zeros(n,1);
neg_1_over_Ds_gr3 = zeros(n,1);
count = 0;
for i = 1:length(neg_1_over_s)
    if neg_1_over_s(i,1) > tau_j(2,1) && neg_1_over_s(i,1) < tau_j(3,1)
        count = 1+count;
        bar_Ds_gr3(count,1) = bar_Ds(i,1);
        neg_1_over_Ds_gr3(count,1) = neg_1_over_s(i,1);
    end
end
[bar_Ds_gr3_min pi_gr_3] = min(bar_Ds_gr3);
%% Data group 4
n=0;
for i = 1:length(neg_1_over_s)
    if neg_1_over_s(i,1) > tau_j(3,1) && neg_1_over_s(i,1) < tau_j(4,1)
        n=1+n;
    end
end
bar_Ds_gr4 = zeros(n,1);
neg_1_over_Ds_gr4 = zeros(n,1);
count = 0;
for i = 1:length(neg_1_over_s)
    if neg_1_over_s(i,1) > tau_j(3,1) && neg_1_over_s(i,1) < tau_j(4,1)
        count = 1+count;
        bar_Ds_gr4(count,1) = bar_Ds(i,1);
        neg_1_over_Ds_gr4(count,1) = neg_1_over_s(i,1);
    end
end
[bar_Ds_gr4_min pi_gr_4] = min(bar_Ds_gr4);
%% Data group 5
n=0;
for i = 1:length(neg_1_over_s)
    if neg_1_over_s(i,1) > tau_j(4,1) && neg_1_over_s(i,1) < tau_j(5,1)
        n=1+n;
    end
end
bar_Ds_gr5 = zeros(n,1);
neg_1_over_Ds_gr5 = zeros(n,1);
```

```
count = 0;
for i = 1:length(neg_1_over_s)
    if neg_1_over_s(i,1) > tau_j(4,1) && neg_1_over_s(i,1) < tau_j(5,1)
        count = 1+count;
        bar_Ds_gr5(count,1) = bar_Ds(i,1);
        neg_1_over_Ds_gr5(count,1) = neg_1_over_s(i,1);
    end
end
[bar_Ds_gr5_min pi_gr_5] = min(bar_Ds_gr5);
%% Data group 6
n=0;
for i = 1:length(neg_1_over_s)
    if neg_1_over_s(i,1) > tau_j(5,1) && neg_1_over_s(i,1) < tau_j(6,1)
        n=1+n;
    end
end
bar_Ds_gr6 = zeros(n,1);
neg_1_over_Ds_gr6 = zeros(n,1);
count = 0;
for i = 1:length(neg_1_over_s)
    if neg_1_over_s(i,1) > tau_j(5,1) && neg_1_over_s(i,1) < tau_j(6,1)
        count = 1+count;
        bar_Ds_gr6(count,1) = bar_Ds(i,1);
        neg_1_over_Ds_gr6(count,1) = neg_1_over_s(i,1);
    end
end
[bar_Ds_gr6_min pi_gr_6] = min(bar_Ds_gr6);
%% Data group 7
n=0;
for i = 1:length(neg_1_over_s)
    if neg_1_over_s(i,1) > tau_j(6,1) && neg_1_over_s(i,1) < tau_j(7,1)
        n=1+n;
    end
end
bar_Ds_gr7 = zeros(n,1);
neg_1_over_Ds_gr7 = zeros(n,1);
count = 0;
for i = 1:length(neg_1_over_s)
    if neg_1_over_s(i,1) > tau_j(6,1) && neg_1_over_s(i,1) < tau_j(7,1)
        count = 1+count;
        bar_Ds_gr7(count,1) = bar_Ds(i,1);
        neg_1_over_Ds_gr7(count,1) = neg_1_over_s(i,1);
    end
end
[bar_Ds_gr7_min pi_gr_7] = min(bar_Ds_gr7);
%% Data group 8
n=0;
for i = 1:length(neg_1_over_s)
    if neg_1_over_s(i,1) > tau_j(7,1) && neg_1_over_s(i,1) < tau_j(8,1)
        n=1+n;
    end
end
bar_Ds_gr8 = zeros(n,1);
neg_1_over_Ds_gr8 = zeros(n,1);
count = 0;
for i = 1:length(neg_1_over_s)
    if neg_1_over_s(i,1) > tau_j(7,1) && neg_1_over_s(i,1) < tau_j(8,1)
        count = 1+count;
        bar_Ds_gr8(count,1) = bar_Ds(i,1);
        neg_1_over_Ds_gr8(count,1) = neg_1_over_s(i,1);
    end
end
[bar_Ds_gr8_min pi_gr_8] = min(bar_Ds_gr8);
%% Data group 9
n=0;
for i = 1:length(neg_1_over_s)
    if neg_1_over_s(i,1) > tau_j(8,1) && neg_1_over_s(i,1) < tau_j(9,1)
        n=1+n;
    end
end
bar_Ds_gr9 = zeros(n,1);
```

```
neg_1_over_Ds_gr9 = zeros(n,1);
count = 0;
for i = 1:length(neg_1_over_s)
    if neg_1_over_s(i,1) > tau_j(8,1) && neg_1_over_s(i,1) < tau_j(9,1)
        count = 1+count;
        bar_Ds_gr9(count,1) = bar_Ds(i,1);
        neg_1_over_Ds_gr9(count,1) = neg_1_over_s(i,1);
    end
end
[bar_Ds_gr9_min pi_gr_9] = min(bar_Ds_gr9);
%% Data group 10
n=0;
for i = 1:length(neg_1_over_s)
    if neg_1_over_s(i,1) > tau_j(9,1) && neg_1_over_s(i,1) < tau_j(10,1)
        n=1+n;
    end
end
bar_Ds_gr10 = zeros(n,1);
neg_1_over_Ds_gr10 = zeros(n,1);
count = 0;
for i = 1:length(neg_1_over_s)
    if neg_1_over_s(i,1) > tau_j(9,1) && neg_1_over_s(i,1) < tau_j(10,1)
        count = 1+count;
        bar_Ds_gr10(count,1) = bar_Ds(i,1);
        neg_1_over_Ds_gr10(count,1) = neg_1_over_s(i,1);
    end
end
[bar_Ds_gr10_min pi_gr_10] = min(bar_Ds_gr10);
%% Data group 11
n=0;
for i = 1:length(neg_1_over_s)
    if neg_1_over_s(i,1) > tau_j(10,1) && neg_1_over_s(i,1) < tau_j(11,1)
        n=1+n;
    end
end
bar_Ds_gr11 = zeros(n,1);
neg_1_over_Ds_gr11 = zeros(n,1);
count = 0;
for i = 1:length(neg_1_over_s)
    if neg_1_over_s(i,1) > tau_j(10,1) && neg_1_over_s(i,1) < tau_j(11,1)
        count = 1+count;
        bar_Ds_gr11(count,1) = bar_Ds(i,1);
        neg_1_over_Ds_gr11(count,1) = neg_1_over_s(i,1);
    end
end
[bar_Ds_gr11_min pi_gr_11] = min(bar_Ds_gr11);
%% Reterdation time vector
row_i = [neg_1_over_Ds_gr1(pi_gr_1);
          neg_1_over_Ds_gr2(pi_gr_2);
          neg_1_over_Ds_gr3(pi_gr_3);
          neg_1_over_Ds_gr4(pi_gr_4);
          neg_1_over_Ds_gr5(pi_gr_5);
          neg_1_over_Ds_gr6(pi_gr_6);
          neg_1_over_Ds_gr7(pi_gr_7);
          neg_1_over_Ds_gr8(pi_gr_8);
          neg_1_over_Ds_gr9(pi_gr_9);
          neg_1_over_Ds_gr10(pi_gr_10);
          neg_1_over_Ds_gr11(pi_gr_11)];
%% Reterdation strengths calculation
m = length(row_i);    %spread of E_i
n = length(tau_j);    %spread of D_j
p = 11;               %number of sampling points for tou_j, for collocation = m or n
i = 1:m;
j = 1:n;
k = 1:p;              %number of t_k
Aki = zeros(p,m);
Bk = zeros(p,1);
t_k = zeros(length(k),1);   %or can be the values identical to tau_j
for i = 1:length(k)
    if  m == p
        t_k(i) = 1*10^(k(i)-6);
```

```
    else
        t_k(i) = 10^(((k(i)-1)/2)-7);
    end
end
for k = 1:p
    for i = 1:m
        second_term_Aki = 0;
        for j = 1:n
            if tau_j(j,1) ~= row_i(i,1)
                second_term_1 = row_i(i)*D_j(j)*(exp(-(t_k(k)/row_i(i)))- ...
                                exp(-(t_k(k)/tau_j(j))))/(row_i(i)-tau_j(j));
            else
                second_term_1 = t_k(k)*D_j(j)*exp(-(t_k(k)/row_i(i)))/tau_j(j);
            end
            second_term_Aki = second_term_Aki + second_term_1;
        end
        Aki(k,i)= Dg*exp(-(t_k(k)/row_i(i)))+ second_term_Aki;
    end
end
sum_D_j = 0;
for i = 1:n
    sum_D_j_1 = D_j(i);
    sum_D_j = sum_D_j + sum_D_j_1;
end
Ee = 1/(Dg+sum_D_j);
for k = 1:p
    x_Bk = 0;
    y_Bk = 0;
    for i = 1:n
        x_Bk_1 = D_j(i)*(1-exp(-(t_k(k)/tau_j(i))));
        y_Bk_1 = D_j(i);
        x_Bk = x_Bk + x_Bk_1;
        y_Bk = y_Bk + y_Bk_1;
    end
    Bk(k,1) = 1 - ((Dg + x_Bk)/(Dg + y_Bk));
end

if n == p
    E_i = Aki\Bk;
else
    AA = Aki'*Aki;
    AB = Aki'*Bk;
    E_i = AA\AB;
end
%% Generation of creep curve
time_E_t = time_D_t;
E_t = zeros(length(time_E_t),1);

for j = 1:length(time_E_t)
    sum_E = 0;
    for i = 1:length(row_i)
         sum_E = E_i(i,1)*exp(-(time_E_t(j,1)/row_i(i,1)))+ sum_E;
    end
    E_t(j,1) = Ee + sum_E;
end
figure_3 = figure;
loglog(time_E_t, E_t,'--ob');
grid on;
title('Relaxation Modulus');
xlabel('Time (s)');
ylabel('E(t) (ksi)');
%% Combined figure for relaxation modulus and creep compliance
figure_4 = figure;
[ax h1 h2] = plotyy(time_E_t,E_t,time_D_t,D_t,'loglog','loglog');
set(h1,'linestyle','--','linewidth',2);
set(h2,'linestyle','--','linewidth',2);
grid on;
title('Relaxation Modulus and Creep Compliance');
xlabel('Time (s)');
ylabel(ax(1),'E(t) (MPa)');
ylabel(ax(2),'D(t) (MPa)');
```

```
%% Export prony coefficients
y = [row_i'; E_i'];
fid = fopen('prony_series_coefficients_for_relaxation_modulus.txt', 'w');
fprintf(fid, '%f  %f\n', y);
fclose(fid);
fid1 = fopen('equilibrium_modulus_for_relaxation_modulus.txt', 'w');
fprintf(fid1, '%f  %f\n', Ee);
fclose(fid1);
```

Code I-6: MATLAB® Code for Dynamic Modulus and Phase Angle from Prony Coefficients of Creep Compliance

```
%% Import Data from text file
clear all;
close all;
clc;
data_prony_coef_compliance =
importdata('prony_series_coefficients_from_creep_compliance.txt');
data_glassy_compliance = importdata('glassy_compliance_from_creep_compliance.txt');
data_prony_coef_modulus =
importdata('prony_series_coefficients_for_relaxation_modulus.txt');
data_equilibrium_modulus = importdata('equilibrium_modulus_for_relaxation_modulus.txt');
tau_j = data_prony_coef_compliance(:,1);
D_j = data_prony_coef_compliance(:,2);
Dg = data_glassy_compliance;
row_i = data_prony_coef_modulus(:,1);
E_i = data_prony_coef_modulus(:,2);
Ee = data_equilibrium_modulus;
%% Storage Modulus and Loss Modulus
ang_freq = logspace(-5,5,50);
Ew_prime = zeros(1,length(ang_freq));
Ew_double_prime = zeros(1,length(ang_freq));
for p = 1:length(ang_freq)
    sum_Ew_prime = 0;
    sum_Ew_double_prime = 0;
    for i = 1:length (row_i)
        sum_Ew_prime = ang_freq(p)^2 *row_i(i)^2 * E_i(i)/(ang_freq(p)^2
*row_i(i)^2+1)+...
            sum_Ew_prime;
        sum_Ew_double_prime = ang_freq(p)*row_i(i)* E_i(i)/(ang_freq(p)^2
*row_i(i)^2+1)+...
            sum_Ew_double_prime;
    end
    Ew_prime(p) = Ee+sum_Ew_prime;
    Ew_double_prime(p) = sum_Ew_double_prime;
end
Ew_prime_ordinary_freq = (ang_freq ./ (2*pi()))';
Ew_prime = Ew_prime';
Ew_double_prime = Ew_double_prime';
loglog( Ew_prime_ordinary_freq, Ew_prime, 'ob');
hold on;
loglog( Ew_prime_ordinary_freq, Ew_double_prime, 'or');
grid on;
title('Storage and Loss Modulus');
xlabel('Ordinary Frequency (Hz)');
ylabel('Storage and Loss Modulus (ksi)');
legend('Storage Modulus','Loss Modulus','location','northeast');
hold off;
%% Dynamic Modulus
dyn_modulus = sqrt(Ew_prime.^2 + Ew_double_prime .^2);
loglog( Ew_prime_ordinary_freq, dyn_modulus, 'ob');
hold on;
grid on;
title('Dynamic Modulus');
xlabel('Ordinary Frequency (Hz)');
ylabel('Dynamic Modulus (ksi)');
legend('Dynamic Modulus','location','northeast');
hold off;
%EOP
```

Code I-7: MATLAB® Code for Relaxation Modulus Mastercurve Fit

```
%% Load Data from text file
clear all;
close all;
clc;
%14F data
test_data_14F = importdata('14F_Relaxation.txt');
time_14F = test_data_14F(:,1);
relax_mod_14F = test_data_14F(:,2);
%40F data
test_data_40F = importdata('40F_Relaxation.txt');
time_40F = test_data_40F(:,1);
relax_mod_40F = test_data_40F(:,2);
%55F data
test_data_55F = importdata('55F_Relaxation.txt');
time_55F = test_data_55F(:,1);
relax_mod_55F = test_data_55F(:,2);
%70F data
test_data_70F = importdata('70F_Relaxation.txt');
time_70F = test_data_70F(:,1);
relax_mod_70F = test_data_70F(:,2);
%85F data
test_data_85F = importdata('85F_Relaxation.txt');
time_85F = test_data_85F(:,1);
relax_mod_85F = test_data_85F(:,2);
%100F data
test_data_100F = importdata('100F_Relaxation.txt');
time_100F = test_data_100F(:,1);
relax_mod_100F = test_data_100F(:,2);
%130F data
test_data_130F = importdata('130F_Relaxation.txt');
time_130F = test_data_130F(:,1);
relax_mod_130F = test_data_130F(:,2);
%% Plot tested data in log x-y space
Relax_mod_vs_time_plot = ...
    figure('Name','Relaxation Modulus at Different Test Temperatures');
loglog(time_14F,relax_mod_14F,'or','LineWidth',2,...
                        'MarkerEdgeColor','r',...
                        'MarkerFaceColor','r',...
                        'MarkerSize',8);
hold on;
loglog(time_40F,relax_mod_40F,'xg','LineWidth',2,...
                        'MarkerEdgeColor','g',...
                        'MarkerFaceColor','g',...
                        'MarkerSize',8);
hold on;
loglog(time_55F,relax_mod_55F,'xk','LineWidth',2,...
                        'MarkerEdgeColor','k',...
                        'MarkerFaceColor','k',...
                        'MarkerSize',8);
hold on;
loglog(time_70F,relax_mod_70F,'+b','LineWidth',2,...
                        'MarkerEdgeColor','b',...
                        'MarkerFaceColor','b',...
                        'MarkerSize',8);
hold on;
loglog(time_85F,relax_mod_85F,'+k','LineWidth',2,...
                        'MarkerEdgeColor','k',...
                        'MarkerFaceColor','k',...
                        'MarkerSize',8);
hold on;
loglog(time_100F,relax_mod_100F,'*m','LineWidth',2,...
                        'MarkerEdgeColor','m',...
                        'MarkerFaceColor','m',...
                        'MarkerSize',8);
hold on;
loglog(time_130F,relax_mod_130F,'sk','LineWidth',2,...
                        'MarkerEdgeColor','k',...
                        'MarkerFaceColor','k',...
                        'MarkerSize',8);
```

```
grid on;
title('E(t) vs. Time Plot');
xlabel('Time (sec)');
ylabel('E(t) (ksi)');
legend('14 F','40 F','55 F','70 F','85 F','100 F','130 F','Location','bestoutside')
hold off;
%% Plot log tested data in x-y space
log_time_14F = log10(time_14F);
log_relax_mod_14F = log10(relax_mod_14F);
log_time_40F = log10(time_40F);
log_relax_mod_40F = log10(relax_mod_40F);
log_time_55F = log10(time_55F);
log_relax_mod_55F = log10(relax_mod_55F);
log_time_70F = log10(time_70F);
log_relax_mod_70F = log10(relax_mod_70F);
log_time_85F = log10(time_85F);
log_relax_mod_85F = log10(relax_mod_85F);
log_time_100F = log10(time_100F);
log_relax_mod_100F = log10(relax_mod_100F);
log_time_130F = log10(time_130F);
log_relax_mod_130F = log10(relax_mod_130F);
log_Relax_mod_vs_log_time_plot = ...
    figure('Name','Logarithm of Relaxation Modulus at Different Test Temperatures');
plot(log_time_14F,log_relax_mod_14F,'or','LineWidth',2,...
                        'MarkerEdgeColor','r',...
                        'MarkerFaceColor','r',...
                        'MarkerSize',8);
hold on;
plot(log_time_40F,log_relax_mod_40F,'xg','LineWidth',2,...
                        'MarkerEdgeColor','g',...
                        'MarkerFaceColor','g',...
                        'MarkerSize',8);
hold on;
plot(log_time_55F,log_relax_mod_55F,'xk','LineWidth',2,...
                        'MarkerEdgeColor','k',...
                        'MarkerFaceColor','k',...
                        'MarkerSize',8);
hold on;
plot(log_time_70F,log_relax_mod_70F,'+b','LineWidth',2,...
                        'MarkerEdgeColor','b',...
                        'MarkerFaceColor','b',...
                        'MarkerSize',8);
hold on;
plot(log_time_85F,log_relax_mod_85F,'+k','LineWidth',2,...
                        'MarkerEdgeColor','k',...
                        'MarkerFaceColor','k',...
                        'MarkerSize',8);
hold on;
plot(log_time_100F,log_relax_mod_100F,'*m','LineWidth',2,...
                        'MarkerEdgeColor','m',...
                        'MarkerFaceColor','m',...
                        'MarkerSize',8);
hold on;
plot(log_time_130F,log_relax_mod_130F,'sk','LineWidth',2,...
                        'MarkerEdgeColor','k',...
                        'MarkerFaceColor','k',...
                        'MarkerSize',8);
grid on;
title('log_E(t) vs. log_Time Plot');
xlabel('log Time (sec)');
ylabel('log E(t) (ksi)');
legend('14 F','40 F','70 F','100 F','130 F','Location','bestoutside')
hold off;
%% trial and error for smoothing
log_sf_14F = -4.9;
log_sf_40F = -2.8;
log_sf_55F = -1.4;
log_sf_70F = 0;
log_sf_85F = 0.7;
log_sf_100F = 2.1;
log_sf_130F = 2.8;
```

```
log_time_14F_shifted = log_time_14F + log_sf_14F;
log_time_40F_shifted = log_time_40F + log_sf_40F;
log_time_55F_shifted = log_time_55F + log_sf_55F;
log_time_70F_shifted = log_time_70F + log_sf_70F;
log_time_85F_shifted = log_time_85F + log_sf_85F;
log_time_100F_shifted = log_time_100F + log_sf_100F;
log_time_130F_shifted = log_time_130F + log_sf_130F;
master_log_time_70 = [log_time_14F_shifted; log_time_40F_shifted;...
    log_time_55F_shifted; log_time_70F_shifted; log_time_85F_shifted;...
    log_time_100F_shifted; log_time_130F_shifted];
master_log_relax_70 = [log_relax_mod_14F; log_relax_mod_40F;...
    log_relax_mod_55F; log_relax_mod_70F; log_relax_mod_85F;...
    log_relax_mod_100F; log_relax_mod_130F];
log_Relax_mod_vs_log_reduced_time_plot = ...
    figure('Name','Log Relaxation Modulus Mastercurve');
plot(master_log_time_70, master_log_relax_70, 'o','LineWidth',2);
hold on;
grid on;
title('log E(t) vs. log Tr Plot');
xlabel('log Tr (sec)');
ylabel('log E(t) (ksi)');
hold off;
%% Shift factor function
log_sf = [log_sf_14F log_sf_40F log_sf_55F log_sf_70F log_sf_85F log_sf_100F
log_sf_130F];
test_temperatures = [14 40 55 70 85 100 130];
WLF_sf_function = figure('Name','Shift Factor Function');
plot(test_temperatures, log_sf, 'or','LineWidth',2);
hold on;
grid on;
initialvals_sf = [-5 400];
log_sf_fit =  @(p,x) -(p(1).*(x-70))./((p(2)+(x-70)));
[trial_sf_fit R J COVB MSE] = nlinfit(test_temperatures, log_sf, log_sf_fit,
initialvals_sf);
xgrid_sf = test_temperatures;
line(xgrid_sf, log_sf_fit(trial_sf_fit, xgrid_sf), 'Color','r');
legend('Shift Factor','WLF fit','Location','southeast');
title('Shift Factor Function');
xlabel('Temperature, F');
ylabel('log Shift Factor');
hold off;
yresid_sf = log_sf - log_sf_fit(trial_sf_fit, xgrid_sf);
SSresid_sf = sum(yresid_sf.^2);
SStotal_sf = (length(log_sf)-1) * var(log_sf);
rsq_sf = 1 - SSresid_sf/SStotal_sf;
%% Pre-smoothing the Relaxation Mastercurve
pre_mc_smoothing = figure('Name','Mastercurve Smoothing');
hold on;
grid on;
smooth_ft = fittype( 'smoothingspline' );
opts_smooth = fitoptions( smooth_ft);
opts_smooth.SmoothingParam = 0.5;
[smooth_fitresult, gof] = fit(master_log_time_70, master_log_relax_70,smooth_ft,
opts_smooth);
smooth_xgrid = (linspace(master_log_time_70(1),
master_log_time_70(length(master_log_time_70)), 100))';
smooth_ygrid = smooth_fitresult(smooth_xgrid);
plot(master_log_time_70, master_log_relax_70, 'ob');
plot(smooth_xgrid, smooth_ygrid, '-r','linewidth',2);
legend('Unsmoothened Mastercurve', 'Smoothened Mastercurve','Location', 'NorthEast' );
xlabel( 'Log Time (sec)' );
ylabel( 'Log Relaxation Modulus (ksi)' );
mc_smoothing = figure('Name','Mastercurve Smoothing');
hold on;
grid on;
smooth_ft = fittype( 'smoothingspline' );
opts_smooth = fitoptions( smooth_ft);
opts_smooth.SmoothingParam = 0.5;
[smooth_fitresult, gof] = fit(smooth_xgrid, smooth_ygrid,smooth_ft, opts_smooth);
smooth_xgrid = (linspace(master_log_time_70(1),
master_log_time_70(length(master_log_time_70)), 100))';
```

```
smooth_ygrid = smooth_fitresult(smooth_xgrid);
plot(master_log_time_70, master_log_relax_70, 'ob');
plot(smooth_xgrid, smooth_ygrid, '-r','linewidth',2);
legend('Unsmoothened Mastercurve', 'Smoothened Mastercurve','Location', 'NorthEast' );
xlabel( 'Log Time (sec)' );
ylabel( 'Log Relaxation Modulus (ksi)' );

%% Plot smoothened data in Logarithmic space
master_time_70 = 10 .^ master_log_time_70;
master_relax_70 = 10 .^ master_log_relax_70;
smooth_master_time_70 = 10 .^ smooth_xgrid;
smooth_master_relax_70 = 10 .^ smooth_ygrid;
mastercurve_log_space = figure('Name','Relaxation Modulus vs Time Plot');
loglog(master_time_70, master_relax_70, 'ob');
grid on;
hold on;
loglog(smooth_master_time_70, smooth_master_relax_70, 'or','LineWidth',3);
legend('Unsmoothened Mastercurve', 'Smoothened Mastercurve','Location', 'NorthEast' );
xlabel( 'Time (sec)' );
ylabel( 'Relaxation Modulus (ksi)' );
%% Export Data Files for other analysis
data1 = [master_time_70'; master_relax_70'];
data2 = [smooth_master_time_70'; smooth_master_relax_70'];
fid1 = fopen('Generated_1_Unsmoothened_Relaxation_Mastercurve.txt', 'w');
fprintf(fid1, '%e %e\n', data1);
fid2 = fopen('Generated_2_Smoothened_Relaxation_Mastercurve.txt', 'w');
fprintf(fid2, '%e  %e\n', data2);
fclose(fid1);
fclose(fid2);
%End of Program
```

Code I-8: MATLAB® Code for Prony Series Fit of Relaxation Modulus

```
% Import mastercurve data from text file generated in previous code
clear all;
close all;
clc;
data_E_t = importdata('Generated_2_Smoothened_Relaxation_Mastercurve.txt');
time_E_t = data_E_t(:,1);
E_t = data_E_t(:,2);
%% Plot storage modulus vs reduced frequency
relax_mod_vs_time_plot = figure('name','Relaxation Modulus vs Reduced Time Plot');
loglog(time_E_t, E_t,'-or');
hold on;
title('Relaxation Modulus vs Reduced Time Plot');
xlabel('Reduced Time (sec)');
ylabel('E(t) (ksi)');
grid on;
hold off;
%% Trial prony series fit to evaluate initial value for the nlinfit function
Ee = 15.4902;
E_i = [1e3 1e3 1e2 1e2 1e2 9e2 8e2 3e2 1e1 1e2 1e2];
p_i = 2.*[1e-6 1e-5 1e-4 1e-3 1e-2 1e-1 1e0 1e1 1e2 1e3 1e4];
E_t_prony_fit = Ee + E_i(1,1).*exp(-time_E_t./p_i(1,1))+...
                     E_i(1,2).*exp(-time_E_t./p_i(1,2))+...
                     E_i(1,3).*exp(-time_E_t./p_i(1,3))+...
                     E_i(1,4).*exp(-time_E_t./p_i(1,4))+...
                     E_i(1,5).*exp(-time_E_t./p_i(1,5))+...
                     E_i(1,6).*exp(-time_E_t./p_i(1,6))+...
                     E_i(1,7).*exp(-time_E_t./p_i(1,7))+...
                     E_i(1,8).*exp(-time_E_t./p_i(1,8))+...
                     E_i(1,9).*exp(-time_E_t./p_i(1,9))+...
                     E_i(1,10).*exp(-time_E_t./p_i(1,10))+...
                     E_i(1,11).*exp(-time_E_t./p_i(1,11));
trial_prony_series_fit = figure('name','Trial Prony Series Fit');
loglog(time_E_t, E_t,'--or');
hold on;
grid on;
line(time_E_t, E_t_prony_fit);
title('Relaxation Mastercurve Prony Fit');
```

```
xlabel('Time (sec)');
ylabel('E(t) (ksi)');
legend('Relaxation Modulus','Trial Prony Fit', 'location','northeast');
hold off;
ini_val(1:(length(E_i))) = E_i(1:length(E_i));
ini_val(1,(length(E_i) + length(Ee))) = Ee;
%% Final Prony Series Fit
final_prony_series_fit = figure('name','Prony Series Fit');
loglog(time_E_t, E_t,'or');
hold on;
grid on;
prony_fit_eq = @(e,x) e(12) + e(1) .* exp(-x/p_i(1,1))+...
                            e(2) .* exp(-x/p_i(1,2))+...
                            e(3) .* exp(-x/p_i(1,3))+...
                            e(4) .* exp(-x/p_i(1,4))+...
                            e(5) .* exp(-x/p_i(1,5))+...
                            e(6) .* exp(-x/p_i(1,6))+...
                            e(7) .* exp(-x/p_i(1,7))+...
                            e(8) .* exp(-x/p_i(1,8))+...
                            e(9) .* exp(-x/p_i(1,9))+...
                            e(10) .* exp(-x/p_i(1,10))+...
                            e(11) .* exp(-x/p_i(1,11));
options = statset('MaxIter',50000,'FunValCheck','off','TolX',1e-8,'TolFun', 1e-8,
'DerivStep', 1e-8);
startingVals = ini_val;
coefEsts = nlinfit(time_E_t,E_t, prony_fit_eq, startingVals, options);
xgrid = time_E_t;
line(xgrid, prony_fit_eq(coefEsts, xgrid), 'Color','b');
legend('Relaxation MC','Prony Fit', 'location', 'northeast');
title('Relaxation Modulus');
xlabel('time (sec)');
ylabel('E(t) (ksi)');
hold off;
yresid_relax_prony = E_t - prony_fit_eq(coefEsts, time_E_t);
SSresid_relax_prony = sum(yresid_relax_prony.^2);
SStotal_relax_prony = (length(E_t)-1) * var(E_t);
rsq_relax_prony = 1 - SSresid_relax_prony/SStotal_relax_prony;
%% Export prony coefficients
row_i = p_i;
Ew_i = coefEsts(1:length(coefEsts)-1);
E_e = coefEsts(length(coefEsts));
y = [row_i; Ew_i];
fid = fopen('prony_series_coefficients_from_relaxation_modulus.txt', 'w');
fprintf(fid, '%f  %f\n', y);
fclose(fid);
fid1 = fopen('equilibrium_modulus_from_relaxation_modulus.txt', 'w');
fprintf(fid1, '%f  %f\n', E_e);
fclose(fid1);
```

Code I-9: MATLAB® Code for Dynamic Modulus from Prony Series Coefficients of Relaxation Modulus

```
%% Import Data from text file
clear all;
close all;
clc;
data_prony_coef_compliance =
importdata('prony_series_coefficients_for_creep_compliance.txt');
data_glassy_compliance = importdata('glassy_compliance_for_creep_compliance.txt');
data_prony_coef_modulus =
importdata('prony_series_coefficients_from_relaxation_modulus.txt');
data_equilibrium_modulus = importdata('equilibrium_modulus_from_relaxation_modulus.txt');
tau_j = data_prony_coef_compliance(:,1);
D_j = data_prony_coef_compliance(:,2);
Dg = data_glassy_compliance;
row_i = data_prony_coef_modulus(:,1);
E_i = data_prony_coef_modulus(:,2);
Ee = data_equilibrium_modulus;
%% Storage Modulus and Loss Modulus
ang_freq = logspace(-5,5,50);
```

```
Ew_prime = zeros(1,length(ang_freq));
Ew_double_prime = zeros(1,length(ang_freq));
for p = 1:length(ang_freq)
    sum_Ew_prime = 0;
    sum_Ew_double_prime = 0;
    for i = 1:length (row_i)
        sum_Ew_prime = ang_freq(p)^2 *row_i(i)^2 * E_i(i)/(ang_freq(p)^2
*row_i(i)^2+1)+...
            sum_Ew_prime;
        sum_Ew_double_prime = ang_freq(p)*row_i(i)* E_i(i)/(ang_freq(p)^2
*row_i(i)^2+1)+...
            sum_Ew_double_prime;
    end
    Ew_prime(p) = Ee+sum_Ew_prime;
    Ew_double_prime(p) = sum_Ew_double_prime;
end
Ew_prime_ordinary_freq = (ang_freq ./ (2*pi()))';
Ew_prime = Ew_prime';
Ew_double_prime = Ew_double_prime';
figure;
loglog( Ew_prime_ordinary_freq, Ew_prime, 'ob');
hold on;
loglog( Ew_prime_ordinary_freq, Ew_double_prime, 'or');
grid on;
title('Storage and Loss Modulus');
xlabel('Ordinary Frequency (Hz)');
ylabel('Storage and Loss Modulus (ksi)');
legend('Storage Modulus','Loss Modulus','location','northeast');
hold off;
%% Dynamic Modulus
dyn_modulus = sqrt(Ew_prime.^2 + Ew_double_prime .^2);
figure;
loglog( Ew_prime_ordinary_freq, dyn_modulus, 'ob');
hold on;
grid on;
title('Dynamic Modulus');
xlabel('Ordinary Frequency (Hz)');
ylabel('Dynamic Modulus (ksi)');
legend('Dynamic Modulus','location','northeast');
hold off;
%EOP
```

Code I-10: MATLAB® Code for Creep Compliance from Prony Series Coefficients of Relaxation Modulus

```
%% Import Data from text file
clear all;
close all;
clc;
data_prony_coef = importdata('prony_series_coefficients_from_relaxation_modulus.txt');
data_Eq_mod = importdata('equilibrium_modulus_from_relaxation_modulus.txt');
relax_data_unsmooth = importdata('Generated_1_Unsmoothened_Relaxation_Mastercurve.txt');
relax_data_smooth = importdata('Generated_2_Smoothened_Relaxation_Mastercurve.txt');
relax_time_unsmooth = relax_data_unsmooth(:,1);
relax_mod_unsmooth = relax_data_unsmooth(:,2);
time_E_t = relax_data_smooth(:,1);
E_t = relax_data_smooth(:,2);
row_i = data_prony_coef(:,1);
E_i = data_prony_coef(:,2);
Ee = data_Eq_mod(:,1);
%% Plot Relaxation Modulus
relaxation_mc_smooth_unsmooth = figure('name','Relaxation Modulus MC');
loglog( relax_time_unsmooth, relax_mod_unsmooth, 'ob');
hold on;
loglog(time_E_t,E_t,'-r','linewidth', 4);
grid on;
title('Relaxation Modulus');
xlabel('Time (s)');
ylabel('E(t) (ksi)');
legend('Unsmoothen','Smoothen','location','northeast');
```

```
hold off;
%% Plot smooth relaxation with prony fit
E_t_prony = zeros(length(time_E_t),1);
for j = 1:length(time_E_t)
    sum_E = 0;
    for i = 1:length(row_i)
         sum_E_i = E_i(i)*exp(-time_E_t(j)/row_i(i));
         sum_E = sum_E +sum_E_i;
    end
    E_t_prony(j) = Ee + sum_E;
end
relaxation_mc_prony_fit = figure('name','Relaxation Modulus MC Prony Fit');
loglog(time_E_t,E_t,'or');
hold on;
grid on;
line(time_E_t, E_t_prony, 'linewidth', 2);
title('Relaxation Modulus MC Prony Fit');
xlabel('Time (s)');
ylabel('E(t) (ksi)');
legend('Smoothened Relaxation MC','Prony Fit','location','northeast');
hold off;
%% Comutation of retardation times for creep compliance curve
neg_1_over_s = (logspace(-8,8,10000))';
bar_Es = zeros(length(neg_1_over_s),1);
for j = 1:length(neg_1_over_s)
    sum_E = 0;
    for i = 1:length(row_i)
         sum_E = row_i(i)*E_i(i)/(row_i(i)-(neg_1_over_s(j)))+sum_E;
    end
    bar_Es(j) = abs(Ee + sum_E);
end
figure_2 = figure;
loglog(neg_1_over_s, bar_Es, 'r');
grid on;
title('Reterdation time estimation');
xlabel('-1/s');
ylabel('Operational Modulus (Es~) (ksi)');
%% Determination of the min value of Ew_s in each row_i range
%% Data group 1
n=0;
for i = 1:length(neg_1_over_s)
    if neg_1_over_s(i,1) > row_i(1,1) && neg_1_over_s(i,1) < row_i(2,1)
        n=1+n;
    end
end
bar_Es_gr1 = zeros(n,1);
neg_1_over_Es_gr1 = zeros(n,1);
count = 0;
for i = 1:length(neg_1_over_s)
    if neg_1_over_s(i,1) > row_i(1,1) && neg_1_over_s(i,1) < row_i(2,1)
        count = 1+count;
        bar_Es_gr1(count,1) = bar_Es(i,1);
        neg_1_over_Es_gr1(count,1) = neg_1_over_s(i,1);
    end
end
[bar_Es_gr1_min tj_gr_1] = min(bar_Es_gr1);
%% Data group 2
n=0;
for i = 1:length(neg_1_over_s)
    if neg_1_over_s(i,1) > row_i(2,1) && neg_1_over_s(i,1) < row_i(3,1)
        n=1+n;
    end
end
bar_Es_gr2 = zeros(n,1);
neg_1_over_Es_gr2 = zeros(n,1);
count = 0;
for i = 1:length(neg_1_over_s)
    if neg_1_over_s(i,1) > row_i(2,1) && neg_1_over_s(i,1) < row_i(3,1)
        count = 1+count;
        bar_Es_gr2(count,1) = bar_Es(i,1);
        neg_1_over_Es_gr2(count,1) = neg_1_over_s(i,1);
```

```
    end
end
[bar_Es_gr2_min tj_gr_2] = min(bar_Es_gr2);
%% Data group 3
n=0;
for i = 1:length(neg_1_over_s)
    if neg_1_over_s(i,1) > row_i(3,1) && neg_1_over_s(i,1) < row_i(4,1)
        n=1+n;
    end
end
bar_Es_gr3 = zeros(n,1);
neg_1_over_Es_gr3 = zeros(n,1);
count = 0;
for i = 1:length(neg_1_over_s)
    if neg_1_over_s(i,1) > row_i(3,1) && neg_1_over_s(i,1) < row_i(4,1)
        count = 1+count;
        bar_Es_gr3(count,1) = bar_Es(i,1);
        neg_1_over_Es_gr3(count,1) = neg_1_over_s(i,1);
    end
end
[bar_Es_gr3_min tj_gr_3] = min(bar_Es_gr3);
%% Data group 4
n=0;
for i = 1:length(neg_1_over_s)
    if neg_1_over_s(i,1) > row_i(4,1) && neg_1_over_s(i,1) < row_i(5,1)
        n=1+n;
    end
end
bar_Es_gr4 = zeros(n,1);
neg_1_over_Es_gr4 = zeros(n,1);
count = 0;
for i = 1:length(neg_1_over_s)
    if neg_1_over_s(i,1) > row_i(4,1) && neg_1_over_s(i,1) < row_i(5,1)
        count = 1+count;
        bar_Es_gr4(count,1) = bar_Es(i,1);
        neg_1_over_Es_gr4(count,1) = neg_1_over_s(i,1);
    end
end
[bar_Es_gr4_min tj_gr_4] = min(bar_Es_gr4);
%% Data group 5
n=0;
for i = 1:length(neg_1_over_s)
    if neg_1_over_s(i,1) > row_i(5,1) && neg_1_over_s(i,1) < row_i(6,1)
        n=1+n;
    end
end
bar_Es_gr5 = zeros(n,1);
neg_1_over_Es_gr5 = zeros(n,1);
count = 0;
for i = 1:length(neg_1_over_s)
    if neg_1_over_s(i,1) > row_i(5,1) && neg_1_over_s(i,1) < row_i(6,1)
        count = 1+count;
        bar_Es_gr5(count,1) = bar_Es(i,1);
        neg_1_over_Es_gr5(count,1) = neg_1_over_s(i,1);
    end
end
[bar_Es_gr5_min tj_gr_5] = min(bar_Es_gr5);
%% Data group 6
n=0;
for i = 1:length(neg_1_over_s)
    if neg_1_over_s(i,1) > row_i(6,1) && neg_1_over_s(i,1) < row_i(7,1)
        n=1+n;
    end
end
bar_Es_gr6 = zeros(n,1);
neg_1_over_Es_gr6 = zeros(n,1);
count = 0;
for i = 1:length(neg_1_over_s)
    if neg_1_over_s(i,1) > row_i(6,1) && neg_1_over_s(i,1) < row_i(7,1)
        count = 1+count;
        bar_Es_gr6(count,1) = bar_Es(i,1);
```

```
        neg_1_over_Es_gr6(count,1) = neg_1_over_s(i,1);
    end
end
[bar_Es_gr6_min tj_gr_6] = min(bar_Es_gr6);
%% Data group 7
n=0;
for i = 1:length(neg_1_over_s)
    if neg_1_over_s(i,1) > row_i(7,1) && neg_1_over_s(i,1) < row_i(8,1)
        n=1+n;
    end
end
bar_Es_gr7 = zeros(n,1);
neg_1_over_Es_gr7 = zeros(n,1);
count = 0;
for i = 1:length(neg_1_over_s)
    if neg_1_over_s(i,1) > row_i(7,1) && neg_1_over_s(i,1) < row_i(8,1)
        count = 1+count;
        bar_Es_gr7(count,1) = bar_Es(i,1);
        neg_1_over_Es_gr7(count,1) = neg_1_over_s(i,1);
    end
end
[bar_Es_gr7_min tj_gr_7] = min(bar_Es_gr7);
%% Data group 8
n=0;
for i = 1:length(neg_1_over_s)
    if neg_1_over_s(i,1) > row_i(8,1) && neg_1_over_s(i,1) < row_i(9,1)
        n=1+n;
    end
end
bar_Es_gr8 = zeros(n,1);
neg_1_over_Es_gr8 = zeros(n,1);
count = 0;
for i = 1:length(neg_1_over_s)
    if neg_1_over_s(i,1) > row_i(8,1) && neg_1_over_s(i,1) < row_i(9,1)
        count = 1+count;
        bar_Es_gr8(count,1) = bar_Es(i,1);
        neg_1_over_Es_gr8(count,1) = neg_1_over_s(i,1);
    end
end
[bar_Es_gr8_min tj_gr_8] = min(bar_Es_gr8);
%% Data group 9
n=0;
for i = 1:length(neg_1_over_s)
    if neg_1_over_s(i,1) > row_i(9,1) && neg_1_over_s(i,1) < row_i(10,1)
        n=1+n;
    end
end
bar_Es_gr9 = zeros(n,1);
neg_1_over_Es_gr9 = zeros(n,1);
count = 0;
for i = 1:length(neg_1_over_s)
    if neg_1_over_s(i,1) > row_i(9,1) && neg_1_over_s(i,1) < row_i(10,1)
        count = 1+count;
        bar_Es_gr9(count,1) = bar_Es(i,1);
        neg_1_over_Es_gr9(count,1) = neg_1_over_s(i,1);
    end
end
[bar_Es_gr9_min tj_gr_9] = min(bar_Es_gr9);
%% Data group 10
n=0;
for i = 1:length(neg_1_over_s)
    if neg_1_over_s(i,1) > row_i(10,1) && neg_1_over_s(i,1) < row_i(11,1)
        n=1+n;
    end
end
bar_Es_gr10 = zeros(n,1);
neg_1_over_Es_gr10 = zeros(n,1);
count = 0;
for i = 1:length(neg_1_over_s)
    if neg_1_over_s(i,1) > row_i(10,1) && neg_1_over_s(i,1) < row_i(11,1)
        count = 1+count;
```

```
        bar_Es_gr10(count,1) = bar_Es(i,1);
        neg_1_over_Es_gr10(count,1) = neg_1_over_s(i,1);
    end
end
[bar_Es_gr10_min tj_gr_10] = min(bar_Es_gr10);
%% Data group 11
n=0;
for i = 1:length(neg_1_over_s)
    if neg_1_over_s(i,1) > row_i(11,1)
        n=1+n;
    end
end
bar_Es_gr11 = zeros(n,1);
neg_1_over_Es_gr11 = zeros(n,1);
count = 0;
for i = 1:length(neg_1_over_s)
    if neg_1_over_s(i,1) > row_i(11,1)
        count = 1+count;
        bar_Es_gr11(count,1) = bar_Es(i,1);
        neg_1_over_Es_gr11(count,1) = neg_1_over_s(i,1);
    end
end
[bar_Es_gr11_min tj_gr_11] = min(bar_Es_gr11);
%% Reterdation time vector
tou_j = [neg_1_over_Es_gr1(tj_gr_1);
          neg_1_over_Es_gr2(tj_gr_2);
          neg_1_over_Es_gr3(tj_gr_3);
          neg_1_over_Es_gr4(tj_gr_4);
          neg_1_over_Es_gr5(tj_gr_5);
          neg_1_over_Es_gr6(tj_gr_6);
          neg_1_over_Es_gr7(tj_gr_7);
          neg_1_over_Es_gr8(tj_gr_8);
          neg_1_over_Es_gr9(tj_gr_9);
          neg_1_over_Es_gr10(tj_gr_10);
          neg_1_over_Es_gr11(tj_gr_11)];
%% Reterdation strengths calculation
m = length(row_i);   %spread of E_i
n = length(tou_j);   %spread of D_j
p = 30;              %number of sampling points for tou_j, for collocation = m or n
i = 1:m;
j = 1:n;
k = 1:p;             %number of t_k
Akj = zeros(p,n);
Bk = zeros(p,1);
t_k = zeros(length(k),1);   %or can be the values identical to tou_j
for i = 1:length(k)
    if  n == p
        t_k(i) = 1*10^(k(i)-6);
    else
        t_k(i) = 10^(((k(i)-1)/2)-7);
    end
end
for k = 1:p
    for j = 1:n
        second_term_Akj = 0;
        for i = 1:m
            if row_i(i,1) ~= tou_j(j,1)
                second_term_1 = row_i(i)*E_i(i)*(exp(-(t_k(k)/row_i(i)))- ...
                                exp(-(t_k(k)/tou_j(j))))/(row_i(i)-tou_j(j));
            else
                second_term_1 = t_k(k)*E_i(i)*exp(-(t_k(k)/row_i(i)))/tou_j(j);
            end
            second_term_Akj = second_term_Akj + second_term_1;
        end
        Akj(k,j)= Ee*(1-exp(-(t_k(k)/tou_j(j))))+ second_term_Akj;
    end
end
sum_Ew_i = 0;
for i = 1:m
    sum_Ew_i_1 = E_i(i);
    sum_Ew_i = sum_Ew_i + sum_Ew_i_1;
```

```
end
D_g = 1/(Ee+sum_Ew_i);
for k = 1:p
    x_Bk = 0;
    y_Bk = 0;
    for i = 1:m
        x_Bk_1 = E_i(i)*exp(-(t_k(k)/row_i(i)));
        y_Bk_1 = E_i(i);
        x_Bk = x_Bk + x_Bk_1;
        y_Bk = y_Bk + y_Bk_1;
    end
    Bk(k,1) = 1 - ((Ee + x_Bk)/(Ee + y_Bk));
end

if n == p
    D_j = Akj\Bk;
else
    AA = Akj'*Akj;
    AB = Akj'*Bk;
    D_j = AA\AB;
end
%% Generation of creep curve
creep_time = time_E_t;
D_t = zeros(length(creep_time),1);
for j = 1:length(creep_time)
    sum_D = 0;
    for i = 1:length(tou_j)
         sum_D = D_j(i,1)*(1-exp(-(creep_time(j,1)/tou_j(i,1))))+ sum_D;
    end
    D_t(j,1) = D_g + sum_D;
end
figure_3 = figure;
loglog(creep_time, D_t,'--ob');
grid on;
title('Creep Compliance');
xlabel('Time (s)');
ylabel('D(t) (MPa)');
%% Combined figure for relaxation modulus and creep compliance
figure_4 = figure;
[ax h1 h2] = plotyy(time_E_t,E_t,creep_time,D_t,'loglog','loglog');
set(h1,'linestyle','--','linewidth',2);
set(h2,'linestyle','--','linewidth',2);
grid on;
title('Relaxation Modulus and Creep Compliance');
xlabel('Time (s)');
ylabel(ax(1),'E(t) (MPa)');
ylabel(ax(2),'D(t) (MPa)');
%% Export prony coefficients
y = [tou_j'; D_j'];
fid = fopen('prony_series_coefficients_for_creep_compliance.txt', 'w');
fprintf(fid, '%f  %f\n', y);
fclose(fid);
fid1 = fopen('glassy_compliance_for_creep_compliance.txt', 'w');
fprintf(fid1, '%f  %f\n', D_g);
fclose(fid1);
```